Université de Montréal

Design, Synthesis and Biomedical Applications of Azabicycloalkanone Amino Acid Peptidomimetics

Par

Nagavenkata Durga Prasad Atmuri

Département de chimie

Faculté des arts et des sciences

Thèse présentée à la Faculté des Études supérieures

en vue de l'obtention du grade de Philosophiae Doctor (Ph.D.)

en Chime

February, 2019

This Thesis entitled:

Design, Synthesis and Biomedical Applications of Azabicycloalkanone Amino Acid Peptidomimetics

Presented by:

Mr. Nagavenkata Durga Prasad Atmuri

Thesis was evaluated by a jury composed of the following persons:

Professor Richard Giasson, President of jury
Professor Stephen Hanessian, Member of jury
Professor William D. Lubell, Research director
Professor Graham Murphy, External examiner
Professor Jacques Bélair, Representative of the dean

Résumé

Conception, synthèse et applications biomédicales de mimes d'acides aminés azabicycloalkanones

Les molécules peptidomimétiques représentent des structures prometteuses ayant la capacité de mimer les fonctions et conformations des peptides. Elles offrent de nombreux avantages potentiels comme une meilleure reconnaissance moléculaire, un transport accru de part et d'autre des membranes biologiques et une résistance à la dégradation enzymatique. Parmi les différents types de mimes peptidiques, les azabicyclo[X.Y.0]alkanones présentent un intérêt particulier, notamment grâce à leur tendance à rigidifier les chaines peptidiques et les chaines latérales, ainsi que leur capacité à mimer certains éléments de structure secondaire tels que les repliements.

L'objectif de cette thèse est d'introduire des stratégies efficaces de synthèses d'acides aminés de type azabicycloalkanone possédant des cycles de différentes tailles. De plus, différentes stratégies pour introduire des substituants sur les différents cycles ont été développées dans le but de mimer les différentes chaines latérales des acides aminés naturels. Finalement, une série d'analogues d'un modulateur allostérique du récepteur prostaglandin-F2α (FP) contenant des acides aminés indolizidin-2-one (I^2aa) a été synthétisée pour tenter d'exploiter cette voie de signalisation pour le traitement des accouchements prématurés.

Une étude de cyclisation trans annulaire de lactames insaturées a permis l'obtention d'une série de systèmes bicycliques rigides en utilisant une stratégie commune, la synthèse des précurseurs cycliques par couplage d'acides aminés ω-insaturés énantiopurs suivi par la fermeture du cycle par métathèse croisée. L'iodo amidation et l'iodo acétoxylation trans annulaire de différent lactames insaturés ont été accomplies de manière régio- et diastéréosélective dépendant de la taille du cycle,

de la position de l'oléfine, du solvant, du groupe protecteur présent sur la portion amine, et de l'utilisation d'additifs d'iode (III) hypervalent. L'iodolactamisation trans annulaire de différents lactames insaturés de 8-, 9- et 10 chaînons ont fourni des bicycles 5,5-, 5,6-, 6,6-, et 7,5. Malgré le fait que certains lactames à 8 et 9 chaînons se sont avérés résistants à l'iodoamidation par l'iode moléculaire dans différents solvants, la cyclisation a été obtenue lors de l'ajout de diacétoxyiodobenzene dans le mélange réactionnel.

Les analyses spectroscopiques et de cristallographie par diffraction des rayons X des macrocycles à 8, 9 et 10 chaînons ainsi que des systèmes bicycliques 5,5, 5,6 et 7,5 ont démontré le potentiel de ces composés à mimer le résidu central des tour β de type I, II', II et VI. Différentes méthodes ont été utilisées pour introduire une variété de fonctionnalités sur les cycles dans le but de mimer les chaines latérales des acides aminés impliqués dans ce type de repliements. Par exemple, une réaction de type S_N2' catalysée au cuivre entre l'organozincate dérivé de la *N*-(Boc)iodo-alanine et le (*Z*)-1,4-dichlorobut-2-ène a permis l'obtention de la méthyle 2-*N*-(Boc)amino-4-(chlormethyl)hexanoate. Le déplacement intra et intermoléculaire du chlore de cet acide aminé ω-insaturé s'est avéré être une voie de synthèse efficace de la 4-vinyle-proline (Vyp) et de la 4-vinyle-ornithine (Von) sous forme énantiopure. De la diversité structurale a aussi été introduite par oxydation allylique et activation des liens C-H de résidus déhydro-indolizidin-2-one.

Dans le but de développer des agents pouvant retarder le travail lors de l'accouchement et ainsi aider à prévenir les accouchements prématurés (composé tocolytiques), une stratégie orientée vers la diversité a été employée pour préparer une série d'analogues I^2aa du modulateur du récepteur FP PDC113.824. Une série de dix différents analogues I^2aa a été synthétisée pour étudier la relation structure-activité pour la modulation du récepteur FP dans un essai de contraction myométrial. L'addition de substituants a été possible à la fois sur les cycles à cinq et six chaînons.

Certains de ces analogues I^2aa ont démontré de l'activité en inhibant les contractions myométriales, Probablement par modulation du récepteur FP.

Une méthodologie de synthèse efficace et avec une bonne économie atomique pour l'obtention de lactames et de composés peptidomimétiques bicycliques avec différentes tailles de cycles a été développée. Une grande quantité de données structurales provenant de rayons X ont été obtenus, indiquant le potentiel de ces structures à mimer divers repliements. Certains éléments mécanistiques des cyclisations trans annulaires menant aux différents bicycles pourraient avoir un impact au sein de la communauté de chimie organique impliquée dans la synthèse de produits naturel alcaloïdes. L'application d'acides aminés azabicycloalcanones spécifiques a été démontrée par la synthèse de modulateurs du récepteur FP de type I^2aa comportant des substituants sur les différents cycles dans le but de développer des composés tocolytiques pour la prévention des accouchements prématurés. Le contenu de cette thèse a, par conséquent, fait un apport à la chimie organique impliquant la synthèse d'hétérocycles, à la chimie peptidique en présentant de nouveaux mimes de structure secondaire et à la chimie médicinale en permettant de faire des avancées vers le traitement des accouchements prématurés.

Mot-clés : Cyclisation trans annulaire, peptidomimétisme, azabicycloalcanes (quinolozidinone, pyrrolizidinone, indolizidinone), iodolactamisation, inhibiteur allostérique, tocolytique, prostaglandine F2α, accouchements prématurés.

Abstract

Peptidomimetics are promising structures that replicate peptide function and conformation. They offer the potential to improve molecular-recognition, to enhance transport across biological membranes, and to resist metabolism. Among peptidomimetic classes, azabicyclo[X.Y.0]alkanone amino acids are particularly attractive, because of their capacity to rigidify backbone and side-chain geometry to replicate specific secondary structures such as turn conformations.

This thesis reveals an effective means for synthesizing azabicycloalkanone amino acids having different ring sizes. Strategies for adding ring substituents to the bicyclic ring system have been developed to mimic side-chain function. Finally, a set of indolizidin-2-one amino acid (I^2aa) analogs has been made based on a lead allosteric modulator of the prostaglandin-F2α (PGF2α) receptor (FP) with the goal to address the unmet biomedical need of preterm birth.

A study of transannular cyclization of unsaturated lactams has provided access to a series of constrained bicyclic peptide surrogates using a common synthetic strategy featuring preparation of the cyclic precursor by coupling of enantiomerically pure ω-unsaturated amino acids followed by ring closing metathesis. Transannular iodoamidation and iodoacetoxylation of different unsaturated lactams have been accomplished where regioselectivity and diastereoselectivity was contingent on ring size, olefin position, solvent, amine protection and the use of a hypervalent iodine(III) additive. Transannular iodolactamization of different 8-, 9- and 10-member unsaturated lactams gave access to fused 5,5-, 5,6-, 6,4-, 6,5-, 6,6- and 7,5-bicycles. Although 8- and certain 9-membered lactams were resistant to iodoamidation using iodine in different solvents, transannular cyclization was achieved by adding (diacetoxyiodo)benzene to the reaction mixture.

X-ray crystallographic and spectroscopic analyses of 8-, 9-, and 10-member macrocycles, and 5,5-, 5,6-, 6,5- and 7,5-bicycles have demonstrated the potential of these constrained

dipeptides to mimic the central residues of ideal type I, II', II and VI β-turn geometries. Different methods were investigated to introduce functionality onto these ring systems with the purpose of replicating side-chain presentation at such turn regions. For example, copper-catalyzed S_N2' reaction of the zincate from *N*-(Boc)iodo-alanine onto (*Z*)-1,4-dichlorobut-2-ene has provided methyl 2-*N*-(Boc)amino-4-(chloromethyl)hexenoate. Intra- and intermolecular displacement of the chloride from this ω-unsaturated amino acid building block has given effective entry to enantiomerically pure 4-vinylproline (Vyp) and 4-vinylornithine (Von) derivatives. Side-chain diversity has also been added by C-H bond activation and allylic oxidation of dehydro-indolizidin-2-one residues.

In the pursuit of agents to prolong labor and prevent preterm birth (so-called tocolytics), diversity-oriented methods were developed to prepare a series of analogues of the I^2aa FP modulator PDC113.824. A series of ten different I^2aa analogs was synthesized to study structure-activity relationships for FP modulation in a myometrial contraction assay. The addition of substituents was achieved on both the five and six membered rings. Certain I^2aa analogues exhibited activity and efficacy in inhibiting myometrial contractions likely by way of FP modulation.

An effective, atom-economical means for producing lactam and bicyclic peptidomimetics of different ring sizes has been developed using a common synthetic strategy. A wealth of X-ray structural data of the different peptidomimetics has been obtained indicating potential for turn mimicry. Mechanistic insights into the transannular cyclization to make the bicycles may have general utility for the organic chemistry community engaged in alkaloid natural product synthesis. The applications of specific azabicycloalkanone amino acids in medicinal chemistry was demonstrated by the synthesis of FP modulators possessing ring-substituted I^2aa residues with the

objective of developing therapeutics to delay labour and inhibit preterm birth. This thesis has thus addressed important issues in organic reactivity for the synthesis of heterocycles, in peptide science with respect to mimicry of secondary structure, and in medicinal chemistry towards treatment of the unmet medical need of preterm birth.

Keywords: Transannular cyclizations, Azabicyclo[X.Y.0]alkanone amino acid (Quinolozidinone, Pyrrolizidinone, Indolizidinone), Iodolactamization, Prostaglandin F2α, Allosterism, Tocolytic, Premature delivery.

Note

This thesis describes research on the design, synthesis and biomedical applications of heterocycles for peptide mimicry. The thesis is presented in the form of a series of publications and manuscripts submitted for publication. Author contributions in the research and writing of the respective publications and manuscripts is presented below. Unless specified otherwise, the following chapters were all written by myself and edited by Professor William D. Lubell:

Chapter 1 (Introduction).

Chapter 2 (Article 1) entitled "Peptidomimetic Synthesis by Way of Diastereoselective Iodoacetoxylation and Transannular Amidation of 7−9-Membered Lactams" was published in Organic Letters (*Org. Lett*. **2017**, 19, 5066−5069). The conception of this project and publication was designed by Professor Lubell and me. The experiments, and analysis and structural interpretation of all compounds in this publication, all were performed by me. The X-ray analyses on crystals that I obtained were performed by Ms. Francine Bélanger at the regional centre for X-ray crystallography of the Université de Montréal. Under my supervision, an undergraduate internship fellow, David J. Reilley from the laboratory of Professor Joshua Schrier, Haverford College, performed a 6-week stage, repeated the syntheses of allylglycine, homohomoallylglycine, and a bicyclic system, and contributed to the analysis of the data. I wrote the initial drafts of the manuscript, which were edited into the final publication with the assistance of Professor William D. Lubell.

Chapter 3 (Article 2) entitled "Stereo- and regiochemical transannular cyclization of a common hexahydro-1H-azonine to afford selectively three different indolizidinone dipeptide mimetics" has been submitted to the journal Organic Letters. The conception and design of the manuscript was done by Professor Lubell and me. The experiments, the analysis and the structural interpretation

of all compounds were performed by me. The X-ray analyses on crystals that I obtained were performed by Mr. Thierry Maris at the regional centre for X-ray crystallography of the Université de Montréal. I wrote the initial drafts of the manuscript, which were edited into the final publication with the assistance of Professor Lubell.

Chapter 4 (Article 3) entitled "4-Vinylproline" was published in The Journal of Organic Chemistry (*J. Org. Chem.*, **2018**, *83*, 13580–13586). The conception and design of this publication was done by Professor Lubell, with assistance from Ramakotaiah Mulamreddy and me. The experiments, and analysis and structural interpretation of all compounds in this publication, all were performed in a collaborative effort by Ramakotaiah Mulamreddy and me. Initial drafts of the manuscript were written by Ramakotaiah Mulamreddy and me, and were edited into the final publication with the assistance of Professor Lubell.

Chapter 5 (Article 4) entitled "Paired Utility of Aza-Amino Acyl Proline and Indolizidinone Amino Acid Residues for Peptide Mimicry: Conception of Prostaglandin F2α Receptor Allosteric Modulators that Delay Preterm Birth" has been submitted to the Journal of Medicinal Chemistry. The conception and design of this project was done by Professors Lubell and Sylvain Chemtob, with contributions from Fatemeh M. Mir, Dr. Carine B. Bourguet and me. The experiments, analysis and structural interpretation of all indolizidinone analogs in this manuscript were performed by me. Fatemeh Mir, Jennifer Rodon Fores and Dr. Carine B. Bourguet performed the syntheses and analyses of the azapeptides. The X-ray analyses on crystals that I obtained were performed by Ms. Francine Bélanger at the regional centre for X-ray crystallography of the Université de Montréal. Biological experiments were performed by Dr. Xin Hou under supervision of Professor Sylvain Chemtob in the Département de pédiatrie, Université de Montréal. Fatemeh

Mir and I wrote the initial drafts of the manuscript, which were edited into the final publication with the assistance of Professor Lubell

In Chapter 6, I have written the conclusion and perspectives of this thesis, both of which were edited by Professor Lubell.

Table of Contents

List of Figures

List of Schemes

List of Tables

List of Abbreviations

ACE/NEP	Angiotensin Converting Enzyme (ACE)
	Neutral Endopeptidase (NEP)
br	broad (spectral)
BQ	Benzoquinone
9-BBN	9-borabicyclo[3.3.1]nonane
BTD	β-Turn dipeptide
CD	Circular Dichroism
CBZ	Benzyl chloroformate
J	coupling constant
Dmb	2,4-dimethoxybenzyl
DIB	(Diacetoxyiodo)benzene
DIAD	Diisopropyl azodicarboxylate
DMF	*N*,*N*-dimethylformamide
DIPEA	diisopropylethylamine
DCM	Dichloromethane
DMSO-d_6	hexadeuterodimethyl sulfoxide
DMAP	4-Dimethylaminopyridine
ee	enantiomeric excess
Fmoc	9-fluorenylmethyloxycarbonyl
FP	prostaglandin F2α receptor
GPCR	G-protein-coupled receptor

HRMS	High-Resolution Mass Spectrometry
Hyp	Hydroxyproline
HATU	*O*-(7-azabenzotriazole-l-yl)-1,1,3,3-Tetramethyluronium hexafluorophosphate
Hgl	Hydroxy γ-Lactam
IR	Infrared
LHMDS	lithium hexamethyldisilazane
LPS	Lipopolysaccharide
LH-RH	luteinizing hormone-releasing hormone
lit.	literature
μ	micro
m	multiplet (spectral)
MS	mass spectrometry
MW	molecular weight
M	molar
Me	methyl
mg	milligram
μL	Microlitre
m-CPBA	meta-chloroperbenzoic acid
min	minutes
MHz	megahertz
mL	millilitre
mmol	millimole

mp	melting point
NMR	nuclear magnetic resonance
NBS	*N*-Bromosuccinimide
ORL1	Opioid Receptor Like-1
$[\alpha]_D$	Optical Rotation
ppm	part per milliom
PGF2α	prostaglandin F2α
PTB	Preterm Birth
Phth	Phthalimide
Qaa	Quinolizidinone amino acid
R_f	retention factor (in chromatography)
RCM	ring closing metathesis
s	singlet
SMAC	Second mitochondria-derive activator of caspase
t	triplet
TC	Transannular Cyclization
TBTU	*O*-(Benzotriazol-1-yl)-N,N,N′,N′-tetramethyluronium tetrafluoroborate
TFA	trifluoroacetic acid
THF	tetrahydrofuran
TBHP	tert-Butyl hydroperoxide
TLC	thin layer chromatography
Vyp	Vinylproline

Von vinylornithine

Acknowledgments

First, I am very grateful to my supervisor Professor William D. Lubell, who has provided me unlimited support, valuable advice and guidance during my Ph.D. study at the Université de Montréal. He helped me through difficulties in the research and encouraged me in my pursuit of advanced research in Organic and Medicinal chemistry. In addition, he assisted me to build up my abilities to become a more creative, open-minded, thoughtful and independent researcher. I appreciate very much the chance to work in cutting-edge and innovative research after my Master studies with him. The completion of my Ph.D. thesis research would not have been possible without his generous support.

I must also acknowledge the members of my graduate advisory committee, Professors Stephen Hanessian and Richard Giasson for their encouragement and guidance during my stay at the Université de Montréal.

My sincere gratitude extends to the staff of the Department of Chemistry. I thanks Dr. Alexandra Fürtös, Karine Gilbert, Marie-Christine Tang and Louiza Mahrouche for HRMS and LCMS analyses in the Regional Laboratory for Mass Spectrometry, Dr. Pedro Aguiar, Dr. Cedric Malveau, Sylvie Bilodeau and Antoine Hamel for NMR analyses in the Regional Laboratory for NMR Spectroscopy, and Tierry Maris and Francine Belanger-Gariepy for X-ray analyses in the Regional Laboratory for X-ray Diffractometry at the Université de Montréal.

I would like to thank my biological collaborators, especially Professor Sylvain Chemtob, Dr. Xin Hou and Dr. Christiane Quiniou for performing *ex vivo* and *in vivo* studies. I will never forget their kindness in examining my compounds and informing me of the assays and their results.

For their support and for creating a dynamic friendly work environment, I give special thanks to current and previous group members and visiting scholars, including Dr. Yésica Garcia-Ramos, Dr. Stéphane Turcotte, Dr. Mariam Traoré, Dr. Carine Bourguet, Dr. Mohamed Atfani, Dr. Antoine Douchez, Dr. Pradeep Chauhan, Dr. Ahsanullah, Azade Geranurimi, David J. Reilley and others.

A heart-felt thank you is offered to Julien Poupart and Cynthia Crifar for their assistance with the French language in helping me write my abstract.

I thank sincerely Pastor Raj Kumar Sajja for his friendship, encouragement and spiritual support.

I would like to acknowledge the funding agencies that supported my research including the Natural Sciences and Engineering Research Council of Canada (NSERC), the Canadian Institutes of Health Research, the Global Alliance to Prevent Prematurity and Stillbirth, an initiative of Seattle Children's, the Bill & Melinda Gates Foundation, the March of Dimes, and the Canadian Foundation for Innovation. The Shastri Indo-Canadian institute is specially thanked for providing me with a Quebec Tuition Fee Exemption grant to study at the Université de Montréal.

Finally, I thank my family for everything they have done for me over the years of my Ph.D. study. For their love, care, and moral support, I am especially grateful to my beloved parents, wife Arundhathi U., uncle V. Raghavaiah U., grandparents, and sisters. This thesis is a culmination of my Ph.D. study, which I dedicate to those I hold dear, especially my wife.

Chapter 1

Introduction

1 Introduction

1.1 Peptides and their applications

Peptides perform a wide range of essential functions in biology. Between 15–40% of all cellular interactions are estimated to be mediated through protein-peptide interactions.[1] Since the discovery of the peptide hormone insulin by Canadian physician Frederick Banting in 1921,[2] a wide range of naturally occurring peptides have been discovered which exert biological roles as enzyme inhibitors, neurotransmitters and regulators of physiological processes. Moreover, the significant prolongation of the life of fourteen-year-old diabetic Leonard Thompson, who Banting first injected with insulin in 1922, marked the potential of peptides as medicine.[3] Peptide -based drugs[4] have since found applications in various therapeutic areas,[5] including allergy,[6] oncology, infection,[7] diagnostics,[8] diabetes,[9] obesity,[10] cardiovascular disease,[11] and arthritis.[12] Peptides have also played key roles as components of cosmetics,[13] sensors,[14] and catalysts.[15] Extensive research of peptide structures is ongoing to understand their functions and to enhance their utility in diverse fields of study.[5]

1.2 Limitations of peptides in medicinal chemistry

Peptides possess physicochemical properties that may restrict their utility, such as limited chemical and metabolic stability. In the field of drug discovery, peptides exhibit promising advantages, such as high potency, selectivity, and minimal toxicity. Their intrinsic physicochemical properties and pharmacokinetic profiles have however, limited their clinical application. For example, their low oral bioavailability has necessitated delivery of peptide therapeutics by alternative routes: e.g., nasal, rectal, buccal, vaginal, and transdermal administration.[16,17] Their conformational flexibility may enable binding to more than one receptor or receptor subtype leading to undesirable side effects,[18] including a short half-life because of rapid

degradation by proteolytic enzymes.[19,20] The polyamide backbone possesses an abundance of hydrogen-bond donors and acceptors which may interfere with absorption and transportation. Peptides may also be quickly cleared from the blood circulation by the liver and kidneys. Compared with those for small molecules of similar molecular weight, peptides may have up to 10-fold higher production costs.[21] Challenges for using peptides entail devising structures with features that optimize properties such as enhanced selectivity and receptor binding, resistance to metabolism and clearance, and improved bioavailability.

To counteract these limitations, medicinal chemists have committed to design and synthesize non-peptide molecules, which display pharmacological activity like the native peptides at their receptors. These nonpeptidic compounds are referred to as peptidomimetics. Peptidomimetics can mimic the activity of the native peptides and function as receptor agonists, but may also serve as enzyme inhibitors and receptor antagonists. Peptide mimicry research has evolved as an interdisciplinary scientific endeavor combining organic chemistry, biochemistry and pharmacology.

1.3 Peptidomimetics

Peptidomimetics are molecular scaffolds that may improve the biological properties, mimic the structure, and replicate the activity of natural peptides.[22] The development of peptidomimetics is often pursued based on knowledge of the electronic and conformational interactions between the native peptide and the target protein. Peptidomimetics may be categorized in a number of different ways.[23] Functional mimetics binds to the peptide receptor and exhibit agonist or antagonist activities. They may be small non-peptide molecules that are synthesized based on insight from molecular modeling or obtained through high throughput screening. The opioid receptor ligand morphine may be considered an example of a functional mimetic.[24]

Topographical mimetics may appear unrelated to the original peptide. Instead, they may contain the essential pharmacophores positioned on a novel non-peptide scaffold, which may be synthesized by structure-based drug design.[25]

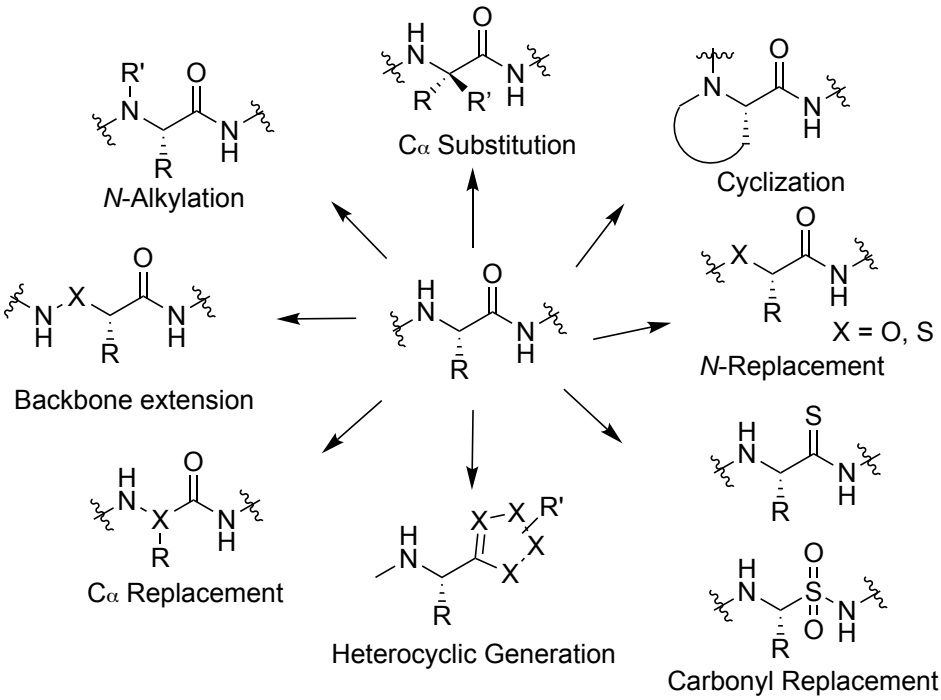

Figure 1.1. Peptidomimetic manipulations of native amino acids[26]

Peptidomimetics are often designed from their native peptides *via* modifications such as amine alkylation,[27] side-chain modification,[28] backbone modification,[29] and cyclization of neighbouring amino acids (Figure 1.1).[30] Such modifications may improve the pharmacokinetic properties of the peptide. In this context, heterocycle scaffolds have been frequently used to favor geometry of natural peptide secondary structures, such as sheets, helices and turns.

1.4 Peptide secondary structures

The rational design of peptide mimics entails restriction of the backbone and side-chain moieties into a bioactive conformation that may be a common secondary structure, such as a β-turn, γ-turn, α-helix, on β-strand.[31] Peptide secondary structures are defined by their backbone ϕ

(phi), ψ (psi) and ω (omega) dihedral angles and side-chain χ (chi) torsion angles (Figure 1.2).[32,33] Secondary structures typically favour hydrogen bonds between side residues within the peptide.

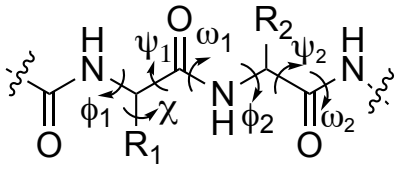

Figure 1.2. Representative peptide structure showing backbone ϕ, ψ, and ω dihedral angles and side-chain χ torsion angle

The α-helix is the most common peptide secondary structure constituting >40% of the residues in proteins.[34] The α-helix is characterised by a repetitive sequence featuring backbone hydrogen bonds between the first (*i*) residue carbonyl oxygen and fifth (*i+4*) residue NH hydrogen. β-Strands are the next most abundant peptide structural element and feature linear extended arrangements of amino acids.[35] Isolated β-strands are not common in proteins. Instead, β-strands arrange themselves into β-sheet structures featuring intermolecular hydrogen bonds. The strands orient in parallel or antiparallel alignments. β-Turns are the third most popular secondary structure after helices and β-strands. Often called reverse turns, β-turns can change the orientation of the peptide by 180 degrees and notably place the α-carbons of the first and fourth residues at a distance ≤ 7Å (Figure 1.3). Different types of β-turns are characterized by their ϕ (i+1), ψ (i+1), ϕ (i+2), and ψ (i+2) dihedral angles and classified into common types (Table 1.1).[36]

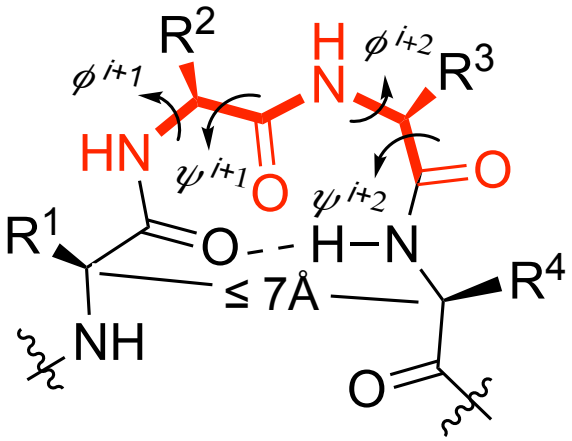

Figure 1.3. β-turn in peptide structure

Table 1.1. Ideal ϕ and ψ backbone torsional angles (in degrees) for type β-turns

Type of secondary structure		ϕ^{i+1}, deg	ψ^{i+1}, deg	ϕ^{i+2}, deg	ψ^{i+2}, deg
α-helix		-58	-47	-58	-47
β-turns	I	–60	–30	–90	0
	I’	60	30	90	0
	II	–60	120	80	0
	II’	60	–120	–80	0
	VIa	–60	120	–90	0
	VIb	–120	120	–60	0
	IV	–60	–1	–50	20
	VIII	–60	–30	–120	120
β-strand	parallel *β* -sheet	-	–139	135	-
	Anti-parallel *β* -sheet	-	–119	113	-

Certain secondary structures are more likely to bind specific receptors. For example, G protein-coupled receptors (GPCRs) recognize endogenous peptide ligands that adopt typically turn conformations.[37] For example, turn conformations have been suggested to be adopted by peptides that bind to pharmacologically important GPCRs, including bradykinin, dopamine, somatostatin, and opioid receptors.[37,38] Proteolytic enzymes are likely to recognize peptides with extended β-

strand conformations, and small-molecule β-strand mimetics have proven useful in the design of inhibitors of such enzymes.[39,40]

1.5 Covalent constraint in peptidomimetic design

Short linear peptides often exist in equilibrium between many different conformers, which may exhibit off-target effects and susceptibility to peptidase degradation limiting their efficacy and bioavailability. Elimination of conformers responsible for unwanted biological responses may enhance target specificity, cell permeability, and metabolic stability to improve linear peptide activity. Many strategies have thus been employed to generate peptides with reduced flexibility (Figure 1.4), among which the use of covalent constraints by way of heterocycles has proven particularly successful.

In the early 1980s, Freidinger and Veber prepared an analogue of luteinizing hormone releasing hormone (LHRH, Glu-His-Trp-Ser-Tyr-Gly-Leu-Arg-Pro-Gly-NH_2) in which G1y was replaced by an α-amino γ-lactam (Figure 1.4). The constrained analog **1.1** was predicted by modeling studies to adopt a β-turn conformation,[41] which resulted in an 8.9 fold improvement in potency relative to the native peptide. Subsequently, inspired by the natural azabicyclo[X.Y.0]alkanone amino acid structure of penicillin, bicyclic dipeptides were developed by the groups of Wyvratt,[42] and Nagai and Sato.[43] In the latter example, the thiaindolizidinone amino acid (Figure 1.4) was shown to induce a β-turn conformation.[44]

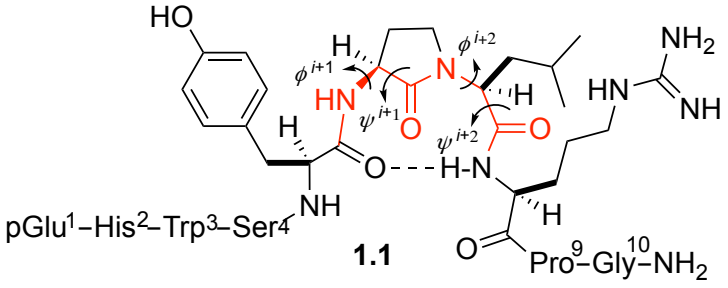

Figure 1.4. Representations of Freidinger's lactams with β turn

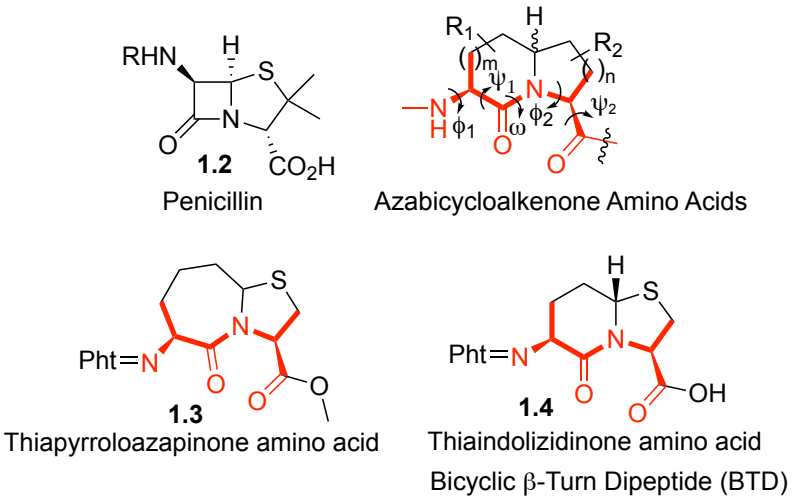

Figure 1.5. The first peptide mimics of the azabicycloalkanone type

Among applications, the thiaindolizidinone amino acid **1.4** was used to replace the D-Phe-Pro residues at the central type II' β-turn regions of gramicidin S [cyclo(Val-Orn-Leu-D-Phe-Pro)$_2$] (Figure 1.6), a naturally occurring cyclic peptide that exhibits potent antimicrobial effects against both Gram-negative and Gram-positive bacteria as well as fungi.[45,46] The resulting analog **1.5** was shown by circular dichroism (CD) to retain the conformation of the natural peptide in solution. Moreover, in spite of the lack of aromatic side-chains at the turn positions, thiaindolizidinone analog maintained antibiotic activity.

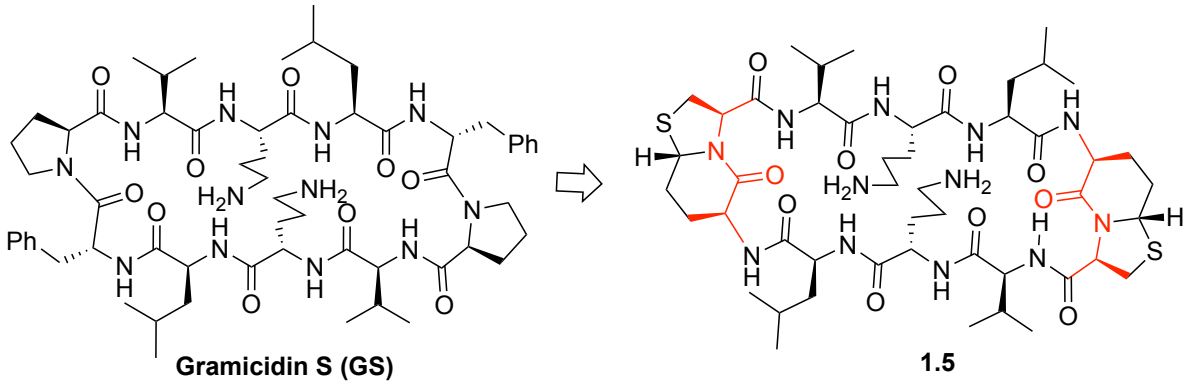

Figure 1.6. Gramicidin S and thiaindolizidinone analog **1.5**

1.6 Azabicyclo[X.Y.0]alkenone Amino Acids

Since the successful synthesis and application of thiaindolizidinone and thiapyrroloazepinone amino acids,[43,44,42b,42a] a variety of azabicycloalkanone amino acids possessing different ring sizes have attracted interest to develop probes for studying structure-activity relationships of various biologically relevant peptides. The bicyclic dipeptide mimetic has proven to be an important scaffold in several biologically active and pharmaceutically significant peptide analogs, due in great part to its ability to mimic and induce β-turn secondary structure (Figure 1.3), in which three contiguous ϕ, ψ and ω dihedral angles are restricted by the heterocycle. The dihedral angles in the bicyclic dipeptide system vary with ring size, substituents and configuration, as demonstrated using X-ray crystallography of their corresponding *N*-Boc(amino) esters.[47,48]

1.6.1 Synthesis and biomedical applications of azabicycloalkanone amino acids

The synthesis of azabicyclo[X.Y.0]alkenone amino acids poses several challenges, including the needs to introduce the amino acid and side-chain groups with stereochemical and regiochemical control on specific positions of the fused heterocycles with defined ring sizes.[49] Representative approaches discussed below the illustrate the issues in constructing different bicyclic ring systems with stereocontrol, and potential for adding side-chains onto ring carbons. In addition, interesting biological applications of azabicyclo[X.Y.0]alkenone amino acids are surveyed.[50]

1.6.2 Indolizidinone amino acids

Among the peptidomimetic scaffolds, indolizidinone amino acids are one of the most well studied as dipeptide surrogates, because their dihedral angles can closely resemble type II' β-turns. Since the advent of thiaindolizidinone **1.4**,[43] efforts have focused on the production of the oxa- and parent indolizidinone analogs,[47] in part due to the potential of the latter to exhibit improved physical and

pharmacokinetic properties. Biologically active indolizidinone peptidomimetics with therapeutic potential have included enzyme inhibitors (e.g., thrombin),[51] peptide hormone mimics (e.g., cholecystokinin), mitochondrial protein mimics [e.g., second mitochondria-derived activator of caspases (Smac)],[52] GPCR modulators [e.g., prostaglandin-F2α (PGF2α) receptor (FP)],[53] and integrin receptor ligands.[54]

Among effective routes to the parent indolizidine amino acid **1.9**, the diastereoselective reductive amination and lactamization of symmetric linear diamino carboxylate proved particularly efficient and cost effective due to the use of glutamic acid as the chiral building block (Scheme 1.1).[55] Claisen condensation of *N*-(PhF)glutamate **1.6** followed by hydrolysis of ester **1.7** and decarboxylation provided azelate **1.8**. Reduction of ester **1.7** and alkylation of ketone **1.8** were also shown to provide access to 5- and 7-substituted indolizidin-2-one amino acids.[56,57]

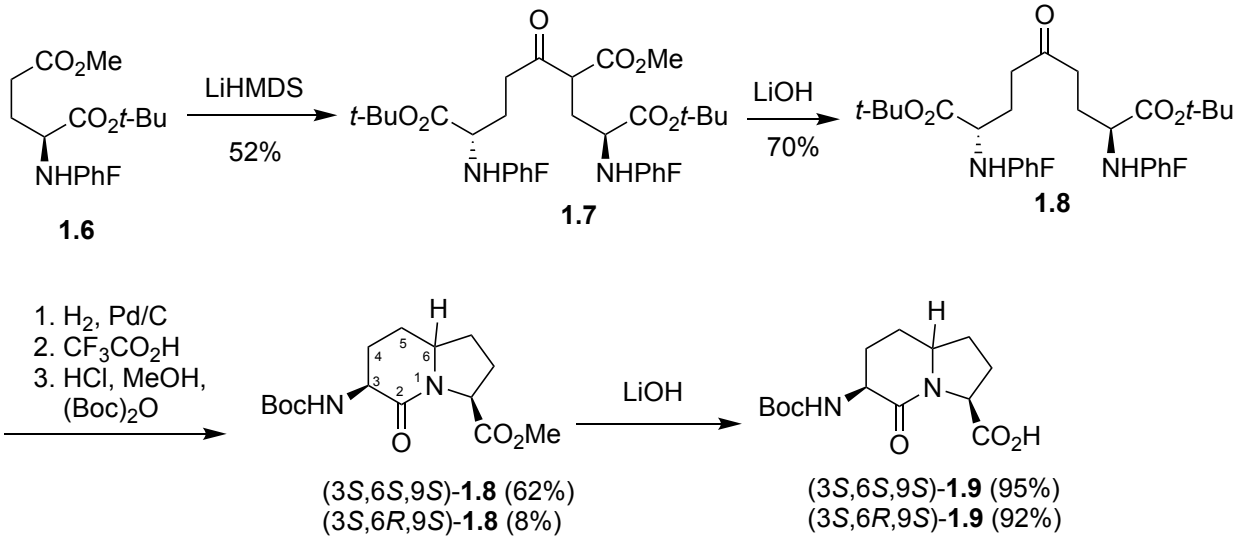

Scheme 1.1 Synthesis of protected azabicyclo[4.3.0]alkanone amino acid **1.9**

Relevant to the objectives of this thesis (Chapter 5), (3*S*,6*S*,9*S*)-indolizidin-2-one amino acid (I^2aa, **1.9**, Scheme 1.1) was introduced into the FP modulator PDC113.824 (Figure 1.7), which has been shown to delay labor in animal models by a allosteric mechanism featuring biased signalling.[53a,58]

Initially, the peptide PDC31 was conceived by modification of a sequence derived from the second extracellular loop of FP, and shown to selectively reduced PGF2α-induced uterine contractions *ex vivo*. From an effort to transform the peptide into a peptidomimetic,[58] PDC113.824 was produced employing an I^2aa residue to replace the Gly-D-His dipeptide residue, which was suspected to adopt the central positions of a β-turn based on earlier studies of bombesin.[59] Employing a phenylacetamide and pyridinylalaninyl-β-homophenylalanine to mimic respectively the *N*- and *C*-terminal residues, PDC113.824 was conceived and exhibited high efficacy in reducing PGF2α-induced uterine contractions and high potency.[53a]

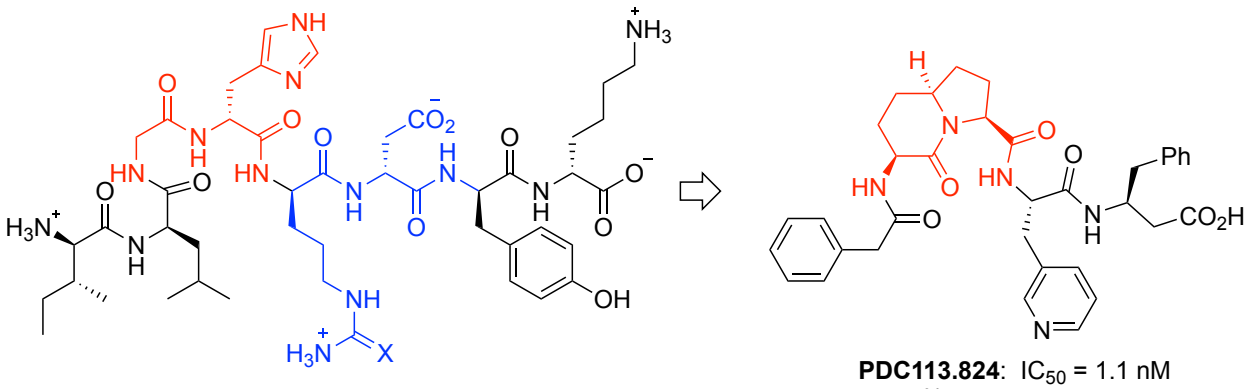

Figure 1.7 Peptide and (3*S*,6*S*,9*S*)-indolizidine-2-one amino acid inhibitors of myometrial contraction

1.6.3. Synthesis of indolizidinones with side-chains as thrombin and factor VIIa inhibitors

The importance of ring substituents for biological activity of an indolizidinone system was well illustrated by the synthesis of thrombin inhibitors.[60] Thrombin (Factor IIa) is a serine protease that plays a major role in thrombosis by catalyzing the conversion of fibrinogen to fibrin. The enzyme, Factor VII serves an earlier role in the production of thrombin from prothrombin. In the blood coagulation cascade, thrombosis can be inhibited by controlling the activity of Factors IIa and

VIIa. Chloromethyl ketone D-Phe-Pro-Arg **1.10** sequence has shown inhibitory activity against thrombin.[61] Co-crystallization of D-Phe-Pro-Arg-CH_2Cl **1.10** and human α-thrombin has revealed that the arginine residue fits into a specific pocket in which the guanidinium ion engages the carboxylate of Asp 189.[62] A hydrophobic pocket accommodates the proline and D-phenylalanine residues. Examination of a related peptide sequence in a human factor VIIa model indicated subtle differences with respect to thrombin binding. Employing 3-benzyl indolizidin-2-one amides, inhibitors **1.12**, **1.13** and **1.14** for factors IIa and VIIa were produced and their selectivity was increased for the latter upon addition of 5-methoxy and 7-ethyl ring substituents.[51]

Co-crystal strucutre of the Thrombin (FIIa) & Chloromethylketone analogue D-Phe-Pro-Arg

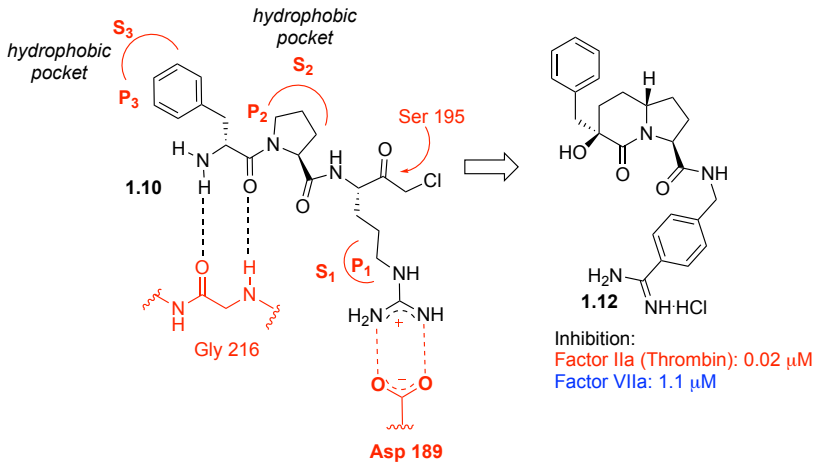

Co-crystal strucutre of the Factor VIIa & Chloromethylketone analogue D-Phe-Phe-Arg

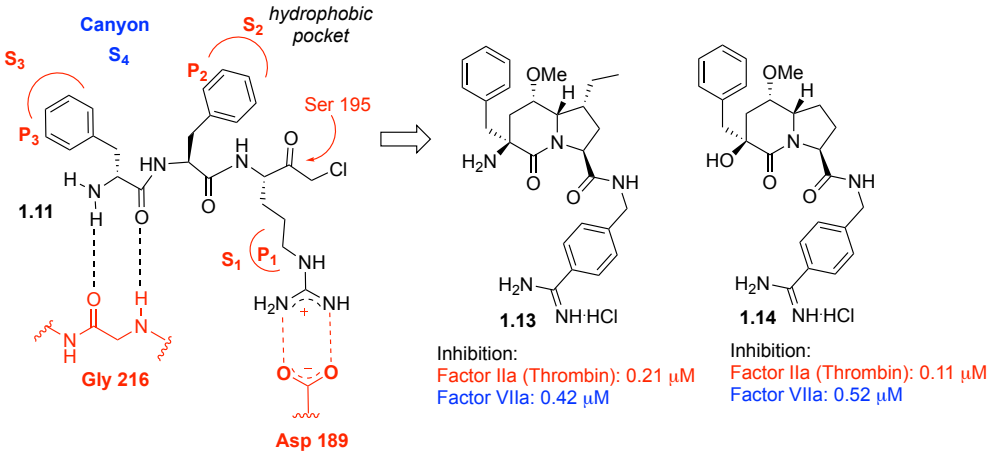

Figure 1.8. Design of indolizidinone inhibitors of Factors IIa and VIIa based on the X-ray crystal structures of peptide chloromethylketone analogs

Indolizidinone amino acid **1.20** was synthesized by an approach featuring acyl migration from lactone **1.15** to furnish lactam **1.16** after hydroxyl group methylation (Scheme 1.2). Sequential alkylation and azide addition onto lactam **1.17** proceeded diastereoselectively to afford indolizidinone **1.18**. Subsequent liberation and oxidation of the alcohol gave acid **1.19**, which was coupled to a protected 4-aminomethylbenzamidine. Azide reduction with concomitant removal of the Cbz protection provided desired indolizidinone amino amide inhibitor **1.20**.

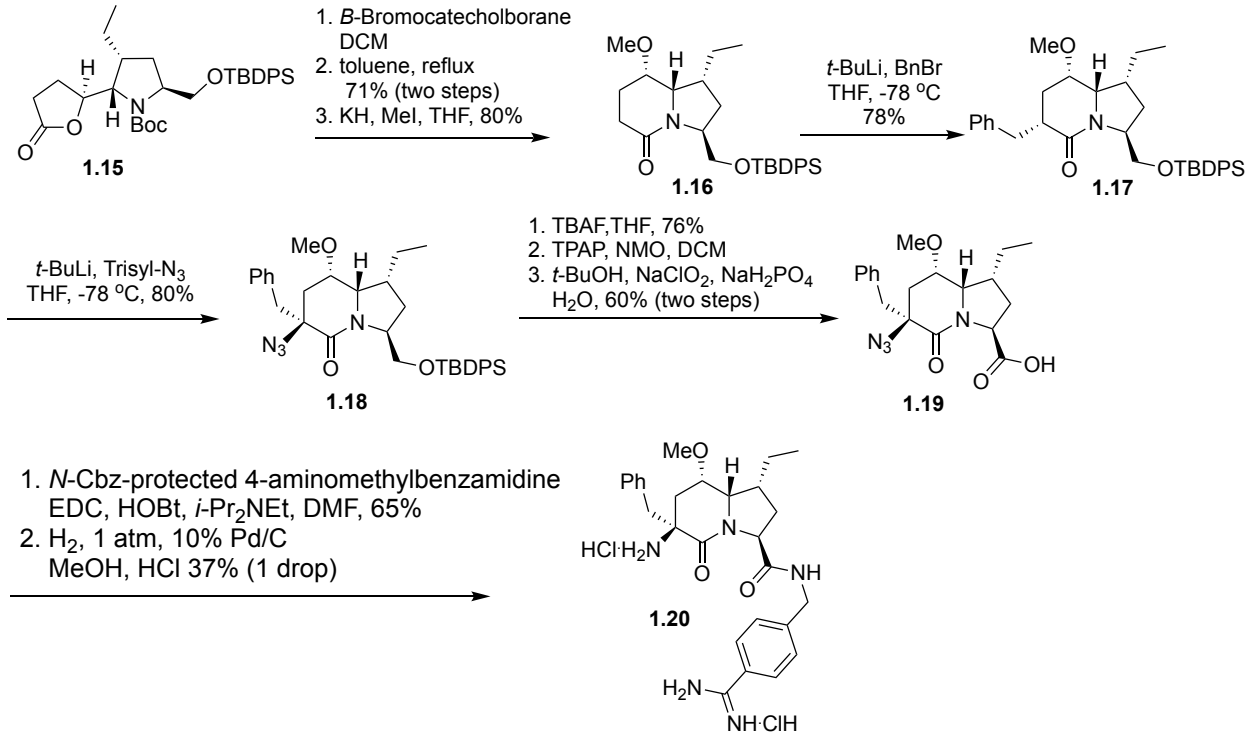

Scheme 1.2. Synthesis of thrombin inhibitor

1.6.4 Quinolizidinone amino acids (Qaa)

The first successful synthesis of a quinolizidinone amino acid (Qaa) was accomplished in seven steps and 40% overall yield from L-pyroglutamic acid.[63] Pyroglutamic acid **1.21** was protected with benzyl bromide in the presence of diisopropylethylamine (DIEA) in DCM, followed by di-

tert-butyl dicarbonate in presence of DMAP, and Et_3N in acetonitrile (Scheme 1.3). β-Ketophosphonate **1.23** was obtained by the addition of the lithium anion of dimethyl methylphosphonate to benzyl *N*-(Boc)pyroglutamate **1.22** in toluene in 74% yield. α,β-Unsaturated ketone **1.25** was obtained by the Horner-Wadsworth-Emmons olefination of *N*-(PhF)aspartate β-aldehyde **1.24** with β-ketophosphonate **1.23**. Ketone **1.25** underwent reductive amination on treatment with palladium-on-carbon to give pipecolate **1.26** as a single diastereomer. Without further purification pipecolate **1.26** was converted quantitatively to protected quinolizidinone amino acid **1.27** using diphenylphosphoryl azide and DIEA in CH_2Cl_2.[63] Notably, a pyrroloazepinone amino acid was also prepared from the same linear ketone precursor **1.25** using and alternative cyclization sequence.

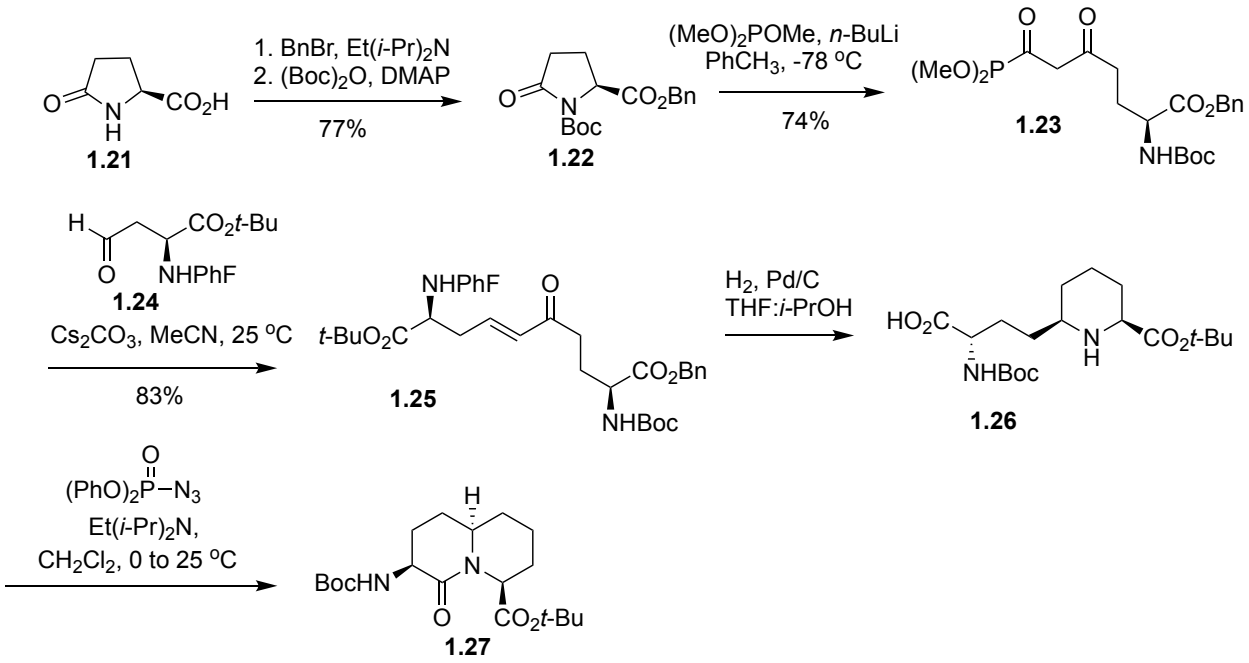

Scheme 1.3. Synthesis of azabicyclo[4.4.0]alkanone amino acid (Qaa)

The influences of azabicyclo[X.Y.0]alkanone amino acid ring size on dihedral angle geometry, peptide conformation and activity were explored using a combination of I^2aa, I^9aa and Qaa residues, which were respectively inserted in place of thiaindolizidinone amino acid **1.28** (Xaa) in

the opioid receptor-like receptor (ORL1R) antagonist sequence Ac-Arg-D-Cha-Xaa-D-Arg-D-*p*ClPhe-NH_2 (Figure 1.9).[64,65] In contrast to the thiaindolizidinone **1.28**, which exhibited high ORL1R antagonist activity (hORL1, K_i = 34 nM), but lacked selectivity and similarly antagonized the other opioid receptor subtypes, quinolizidinone **1.31** exhibited improved selectivity with high ORL1R antagonist potency.[65]

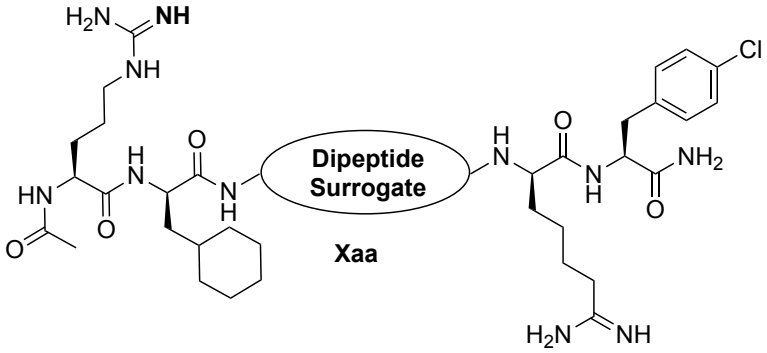

Different ring size azabicycloalkanone as dipetide surrogate

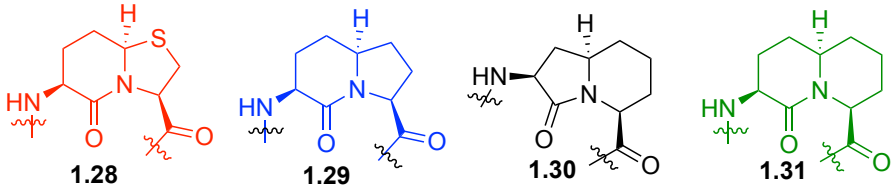

K_i (nM)	**1.28**	**1.29**	**1.30**	**1.31**
hKOR	78 ± 14	190 ± 1	1085 ± 5	441 ± 85
hMOR	53 ± 20	75 ± 21	2700 ± 20	496 ± 89
hDOR	222 ± 44	5200 ± 50	10900 ± 370	7050 ± 850
hORL1	34 ± 8	44 ± 2	2130 ± 10	35 ± 10

Figure 1.9. I^2aa, I^9aa and Qaa peptidomimetics as ORL1R antagonists

1.6.5 Pyrroloazepinone amino acids

Since the pioneering studies of thiapyrroloazepinone amino acid **1.3** (Figure 1.5) in the synthesis of enzyme inhibitors,[42a] considerable effort has been invested in the synthesis of the 7,5-fused bicyclic ring system. In an approach to the parent pyrroloazepinone amino acid **1.39**, glutamic acid served as a chiral building block to synthesize a precursor for an *N*-acylprolyl iminium ion

cyclization (Scheme 1.4). *N*-Phthaloyl-L-glutamate **1.32** was converted to γ-acetal acid **1.34** by an approach featuring thio ester reduction with triethylsilane to an aldehyde intermediate. Phthalimide removal and coupling to *N*-(phthaloyl)allylglycine provided dipeptide **1.35**. Using acidic conditions, *N*-acyl enamine **1.36** was first prepared and then induced to undergo an iminium ion cyclization to afford mixtures of chlo- and iodo-bicycles **1.37** and **1.38**. pyrroloazepinone amino ester **1.39** was obtained by free radical dehalogenation of halides **1.37** and **1.38**.

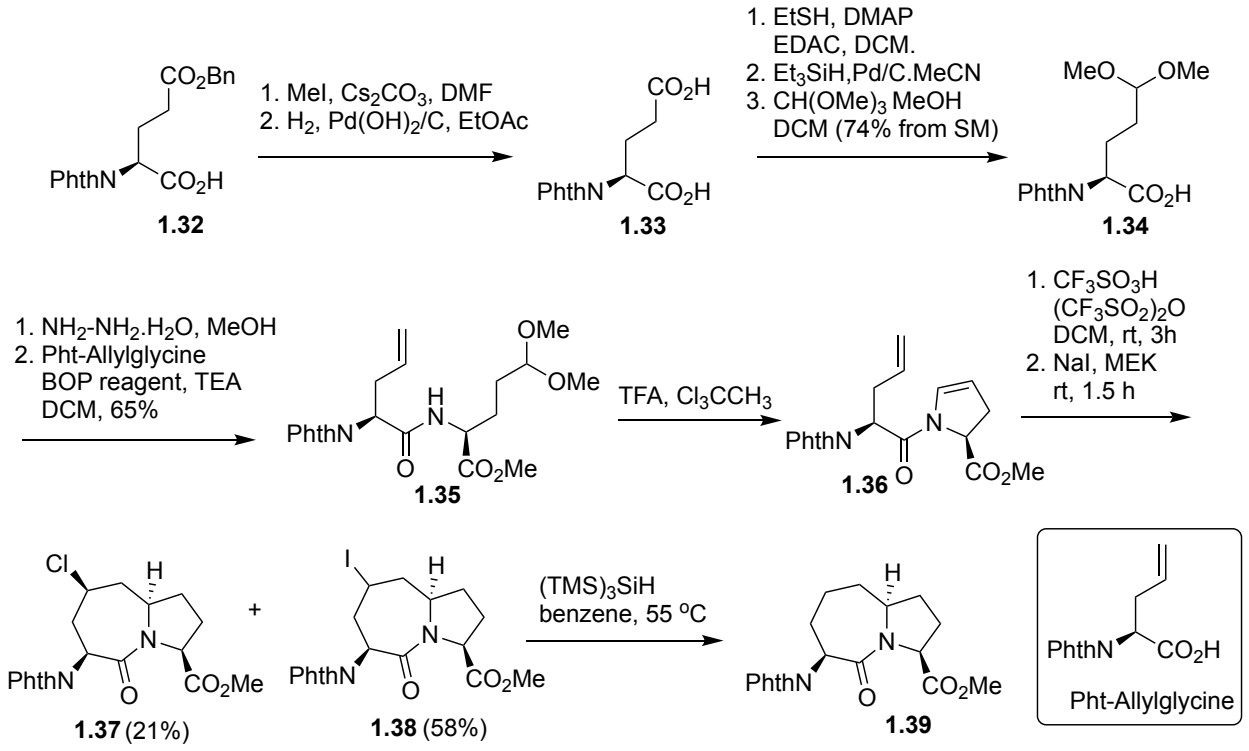

Scheme 1.4. Synthesis of Pyrroloazepinone amino acids

Pyrroloazepinone amino acids have served in the conception of dual ACE-NEP inhibitors for the treatment of cardiovascular disease.[66,67] The co-administration of selective inhibitors for both angiotensin-converting enzyme (ACE) and neutral endopeptidase (NEP) has demonstrated utility as an effective means for reducing hypertension and congestive heart failure in animal models. The zinc-containing carboxy-dipeptidase, ACE is largely responsible for converting the inactive decapeptide angiotensin I into the biologically active vasoconstrictive octapeptide angiotensin II.[68]

Found in high concentration within the brush border region of the kidney, the zinc containing endopeptidase NEP is in large part responsible for the degradation and inactivation of atrial natriuretic peptide, which causes a reduction in expanded extracellular fluid volume by increasing renal sodium excretion.[69,70]

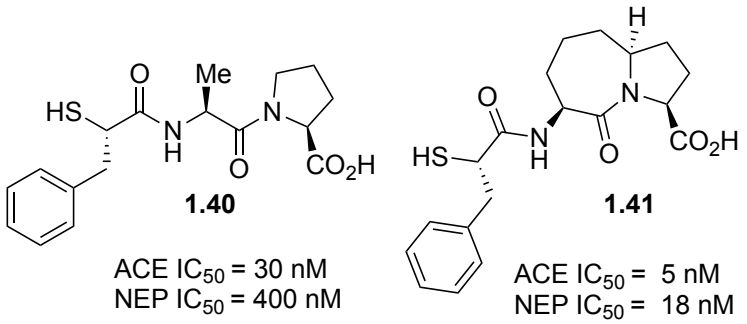

Figure 1.10. Pyrroloazepinone amino acid ACE and NEP inhibitors

N-Mercaptoacyl Ala-Pro dipeptide **1.40** had previously been developed as an ACE inhibitor, that was found to be marginally active against NEP *in vitro*.[71] Introducing conformational constraint by incorporation of the Ala-Pro residue of **1.40** within a pyrroloazepinone dipeptide gave inhibitor **1.41** which exhibited *in vitro* greater inhibitory potency against both ACE and NEP (Figure 1.10).[66]

1.6.6 Strategies for the synthesis of multiple azabicyclo[X.Y.0]alkanone amino acids from shared routes and common precursors

The many applications of azabicyclo[X.Y.0]alkanone amino acids having different ring sizes to explore biological systems indicates the advantage of having various scaffolds to study backbone orientation for activity. Among typical strategies for synthesizing azabicyclo[X.Y.0]alkane amino acids, each has been specific for the preparation of a unique ring system. A shared synthetic route to many bicycles was perceived as an ideal means to generate a spectrum of ring systems for parallel exploration of peptide conformation-activity relationships. In principle, two α-amino dicarboxylate components could be respectively derived from aspartate, glutamate or amino adipate, and employed in the Claisen condensation and olefination sequences mentioned above

(Scheme 1.3); however, attempts to generalize such routes have met with limited success. Instead, modifications of the linear ketone and its unsaturated counterparts by alkylation and 1,4-additions have proven effective for the synthesis of specific ring systems bearing various ring substituents with potential to mimic side-chains by routes featuring reductive amination and lactam ring formation (Scheme 1.5).[63,72]

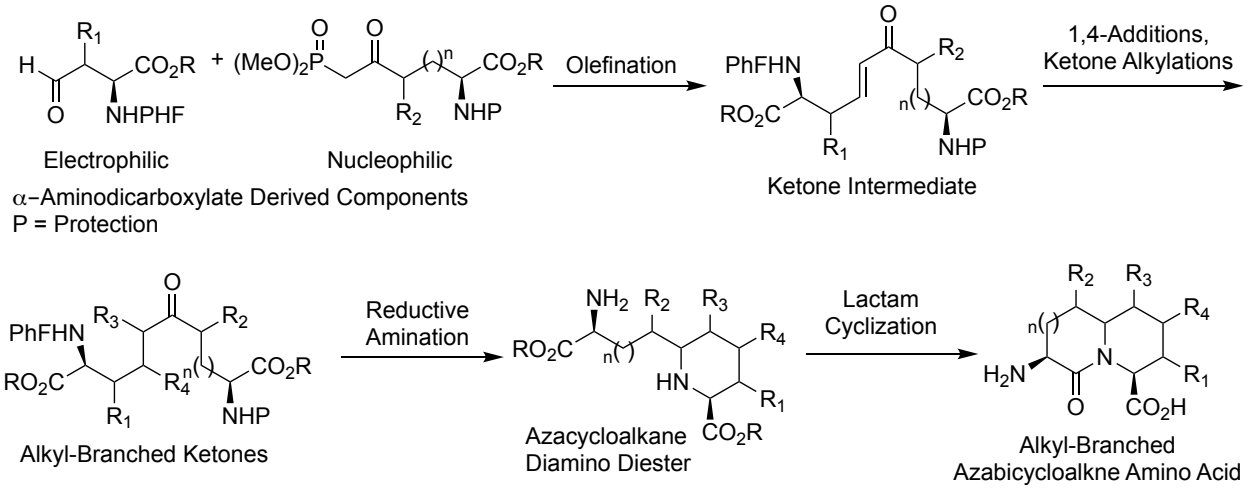

Scheme 1.5. Synthesis of alkyl-branched azabicyclo[X.Y.0]alkane amino acids

1.7 The ring-closing metathesis - transannular cyclization (RCM-TC) approach to bicycles of different ring size by way of a shared pathway

Transannular cyclization reactions have often been used for the synthesis of alkaloids, because of their high regiochemical and stereochemical selectivites.[73,74] Considering the potential of using transannular iodoamidation of unsaturated lactams to prepare azabicyclo[X.Y.0]alkanones of different ring sizes, our laboratory has pursued a route involving the coupling of various ω-unsaturated amino acids to give access to diverse dipeptides **1.44a**–**g**, which upon ring closure metathesis (RCM) would provide the desired olefin precursors **1.45a**–**g**.[75,76] In this route, the 2,4-dimethoxybenzyl (Dmb) group was employed to offset the isomer equilibrium in favor of the

dipeptide *cis* amide to promote cyclization in the case of unsaturated lactams having smaller ring sizes. Removal of the Dmb group with TFA afforded lactams **1.46a**–**g** (Scheme 1.6).

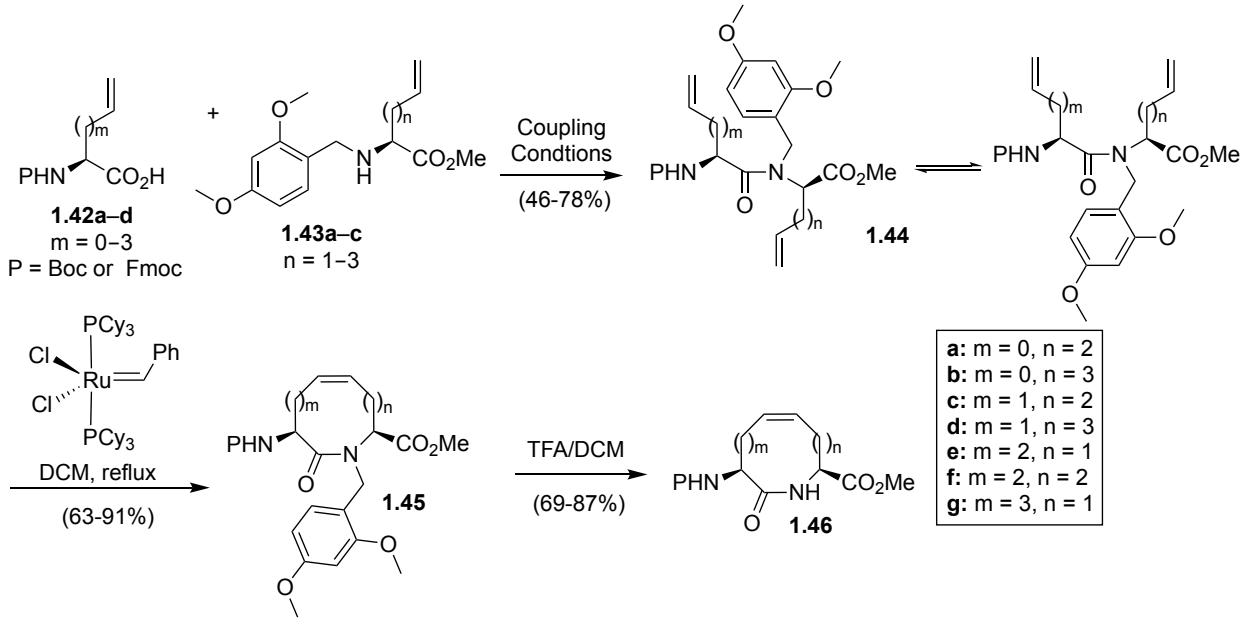

Scheme 1.6. Synthesis of unsaturated lactams of different ring sizes

The electrophilic transannular cyclization of *N*-(Fmoc)amino hexahydroazoninone carboxylate **1.45c** and **1.45d** using 4 equivalents of I_2 in THF at reflux gave diastereoselectively iodo indolizidinone and quinolizidinone **1.47** and **1.48** as a single product in 86% and 56% yields, respectively (Scheme 1.7).[76,77]On the other hand, two diastereomers (5*R*,6*R*)- and (5S,6S)-**1.47** were respectively obtained in 47% and 26% yields from treatment of lactam **1.46c** under identical conditions.[77] Iodo-pyrroloazepinone amino acids analog **1.49** was prepared from 10-membered lactam **1.46f** using similar cyclization conditions in 62% yield. Notably, the iodide of pyrroloazepinone **1.49** has served to functionalize the azabicyclic amino acid to add substituents for mimicry of peptide side-chains.[78]

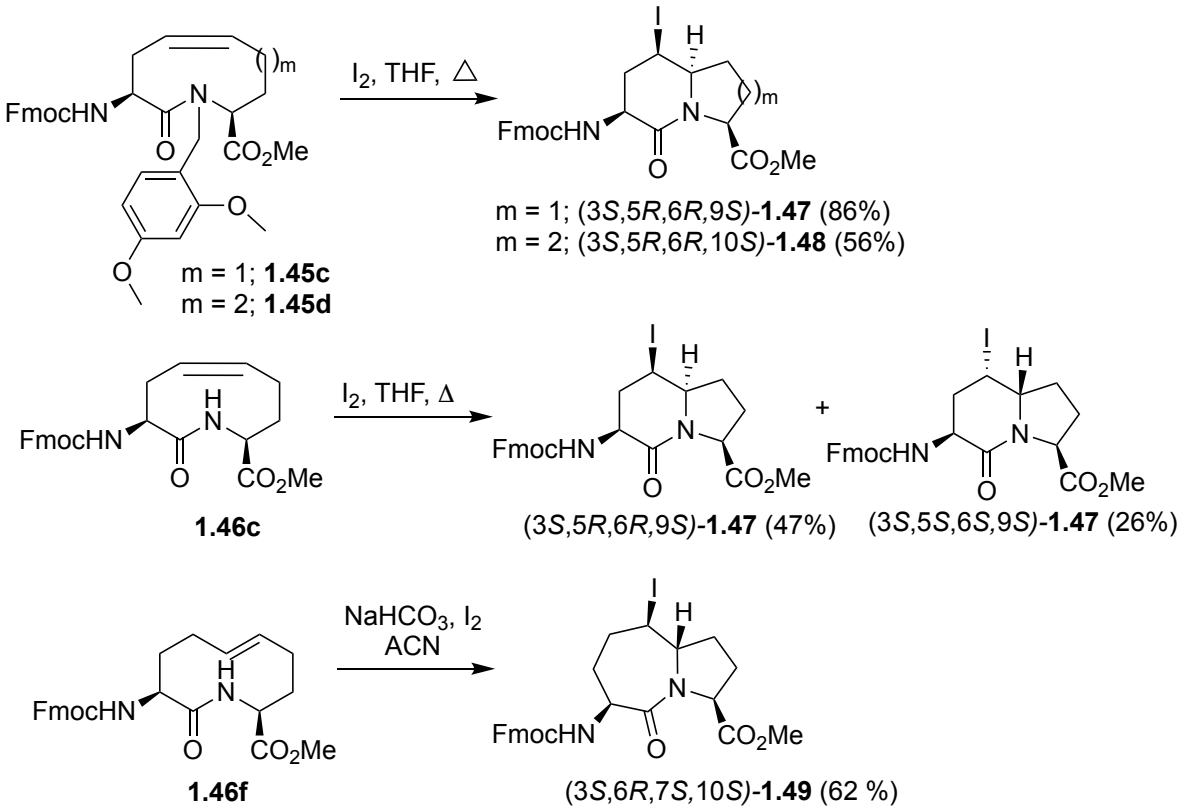

Scheme 1.7. Synthesis of indolizidinone, quinolizidinone and pyrroloazepinone amino acid analogs by way of a shared transannular cyclization approach

1.8 Synthesis of ω-unsaturated amino acids

Important starting materials for exploration of the RCM-TC approach were enantiomerically pure ω-unsaturated amino acids with 4−7 carbon chain lengths: e.g., vinyl-, allyl, homoallyl- and homohomoallylglycine. Many routes exist for the synthesis of such unsaturated amino acid building blocks;[75,79] however, they suffer often from long reaction sequences, especially in the cases of 2-aminopent-4-enoate (allylglycine) and 2-aminohept-6-enoate (homohomo-allylglycine).[80] Strategies to synthesize enantiomerically pure ω-unsaturated amino acids with chain lengths of 5−7 carbons were developed from a common sequence using L-serine as a chiral adduct (Scheme 1.8).[76]

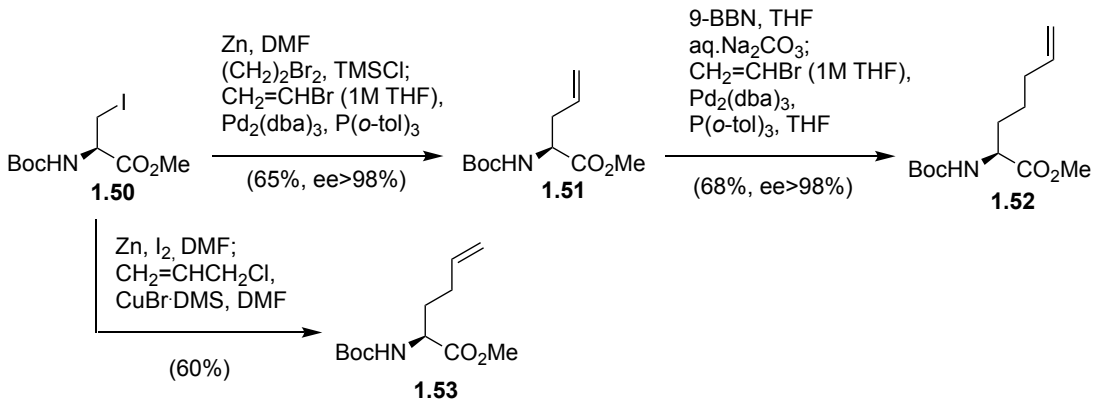

Scheme 1.8. Synthesis ω-unsaturated amino acids with chain lengths of 4−7

The copper-catalyzed cross-coupling of allyl chloride and the zincate derived from iodoalanine had previously been described for the synthesis of 2-(*N*-Boc-amino)hex-5-enoate **1.53** (Scheme 1.8).[81] Related transition-metal catalyzed methods were developed to make the higher and lower amino acid homologues using vinyl bromide. Methyl 2-(*N*-Boc-amino)pent-4-enoate **1.51** and methyl 2-(*N*-Boc-amino)hept-6-enoate **1.52** were prepared by Pd-catalyzed coupling of vinyl bromide and the zincate derived from iodoalanine, and the boronate derived from allylglycine, respectively.[82,76]

1.9. Aims and objectives of the thesis research

As mentioned, heterocyclic dipeptides have significant importance and utility for studying peptides to understand conformation-activity relationships. The aim of this thesis research was to develop an efficient general synthetic strategy for accessing sets of fused ring systems from shared routes featuring common precursors. Fundamental to this project has been a deeper investigation of the conditions and mechanism of the transannular iodo amidation reaction. As will be demonstrated in the following chapters, access has been achieved to 5,5-, 5,6-, 6,5-, 6,4-, 6,6-, and 7,5-fused bicyclic systems. As demonstrated by X-ray crystallographic analyses, the iodo-azabicyclo[X.Y.0]alkanone amino acid derivatives and their unsaturated lactam precursors, both

offer potential to explore various biological targets, because their different ring sizes offer potential to control backbone geometry and to mimic the central residues of different β-turn secondary structures. Moreover, the iodide ring substituent has provided an entry point for introducing various ring substituents onto the bicycle structure for side-chain mimicry.

The aims of this research built upon the previous successful enantioselective syntheses of iodo indolizidin-2-one, quinolizidinone and pyrroloazepinone systems by transannular cyclizations of 9- and 10- membered unsaturated lactams, respectively.[76-77] Moreover, my M.Sc. studies provided access to various chain length ω-unsaturated amino acids (e.g., vinylglycine, allylglycine, homoallylglycine and homohomoallylglycine) which underwent ring closing metathesis to provide various unsaturated lactams (Scheme 1.6).[76,82] My earlier studies of the scope and limitations of the transannular cyclization demonstrated the limitations of the original conditions for conversion of 8-membered and certain 9-membered unsaturated lactams into pyrrolizidinone and indolizidin-9-one ring systems.

In Chapter 2, diastereoselective transannular iodo amidation and iodoacetoxylation reactions of 7–9-membered unsaturated lactams have been achieved through addition of hypervalent(III)iodine reagents to the cyclization conditions contingent on reaction solvent. Electron-rich aromatic ligands and bulky carboxylates on the hypervalent(III)iodine gave higher yields in the transannular cyclization in acetonitrile to provide novel fused 5,5-, 5,6-, and 6,4-bicyclic ring systems. On the other hand, new 7- and 8-membered iodo acetoxy lactams were synthesized from their unsaturated lactam counterparts using similar conditions in toluene. The importance of an allylic carbamate directing group for diastereoselectivity was illustrated in the mechanisms of both the transannular iodoamidation and iodoacetoxylation reactions, which were demonstrated to proceed likely by way of a acetyl hypoiodite ($RCO_2^-I^+$) intermediate. X-ray

crystallographic and spectroscopic analyses of the 7–9-membered macrocycles demonstrated their potential to mimic the central residues of ideal type VI β-turns.

Chapter 3 builds upon the findings in Chapter 2 and examines cyclization of a 9-membered amino lactam carboxylate precursor possessing different nitrogen protection. Notably, regioselectivity and diastereoselectivity were altered in the transannular cyclization contingent on amine protection, solvent and (diacetoxyiodo)benzene (DIB) additive. Through control of such parameters, two different indolizidin-2-one diastereomers and one indolizidin-9-one isomer were prepared selectively from a common unsaturated lactam precursor. Moreover, elimination of the iodide from the bicycles and modification of the resulting olefin by palladium catalyzed arylation and selenium promoted allylic oxidation provided novel means for introducing ring substituents onto the indolizidinone systems for side-chain mimicry.

Furthering the goal to introduce a variety of side-chains onto azabicycloalkanone systems, Chapter 4 describes the copper-catalyzed S_N2' substitution of the zincate from *N*-(Boc)iodo-alanine onto (*Z*)-1,4-dichlorobut-2-ene to provide a separable diastereomeric mixture of (2*S*,4*S*)- and (2*S*,4*R*) 2-*N*-(Boc)amino-4-(chloromethyl)hexenoates. Subsequent intra- and intermolecular chloride displacements provided two unsaturated amino acid derivatives: 4-vinylproline (Vyp) and 4-vinylornithine (Von). Previously, application of Vyp in a RCM strategy has provided a tricyclic peptide mimic that induces α-helical geometry.[83] Conceptually, application of Von in our RCM-TC strategy may give access to various constrained ornithine and arginine containing bicycles.

Towards illustrating a biomedical application of our methodology, Chapter 5 describes the synthesis and activity of I^2aa analogues of the FP modulator PDC113.824. A variety of side-chains were added onto the I^2aa residue of PDC113.824 and used to explore the influences of ring modifications on potential to reduce myometrial contractions in collaboration with the laboratory

of Professor S. Chemtob in the Departments of Pediatrics of the Université de Montréal. In addition, the relationships of aza-amino acyl proline and indolizidinone residues are illustrated by the parallel development of azapeptide FP modulators as potential tocolytics for preventing premature birth.

In conclusion, effective methods have been developed for the synthesis of a variety of azabicycloalkanone amino acids from shared synthetic routes using common precursors. X-ray crystallographic analyses have illustrated that backbone dihedral angles vary with ring size and substituent indicating the potential to use sets of such heterocycle dipeptides to study conformation-activity relationships of biologically active peptides. In addition, substituents to mimic side-chains were introduced onto the various ring systems using novel approaches. Finally, the effectiveness of our methods was illustrated by the synthesis of a novel class of FP modulators with potential to delay labor to treat the unmet medical need of preterm birth. Considering the diversity of biologically active peptides and the wide range of contemporary applications of peptides in various areas of research, the described methods and heterocyclic peptidomimetics should have broad utility especially in medicinal chemistry for drug discovery.

1.10. References

1. Petsalaki, E.; Russell, R. B., Peptide-mediated interactions in biological systems: new discoveries and applications. *Curr. Opin. Biotechnol.* **2008**, *19*, 344–350.

2. Rendell, M., Insulin: moments in history. *Drug Dev. Res.* **2008**, *69*, 95–100.

3. Bliss, M., Rewriting medical history: Charles Best and the Banting and Best myth. *J. Hist. Med. Allied Sci.* **1993**, *48*, 253–274.

4. Vlieghe, P.; Lisowski, V.; Martinez, J.; Khrestchatisky, M., Synthetic therapeutic peptides: science and market. *Drug Discov. Today* **2010**, *15*, 4–56.

5. Lau, J. L.; Dunn, M. K., Therapeutic peptides: Historical perspectives, current development trends, and future directions. *Bioorg. Med. Chem.* **2018**, *26*, 2700–2707.

6. Calzada, D.; Baos, S.; Cremades, L.; Cardaba, B., New treatments for allergy: advances in peptide immunotherapy. *Curr. Med. Chem.* **2018**, *25*, 2215–2232.

7. Silva, O.; De La Fuente-núñez, C.; Haney, E.; Fensterseifer, I.; Ribeiro, S.; Porto, W.; Brown, P.; Faria-Junior, C.; Rezende, T.; Moreno, S., An anti-infective synthetic peptide with dual antimicrobial and immunomodulatory activities. *Sci. Rep.* **2016**, *6*, 35465.

8. (a) Kintzing, J. R.; Cochran, J. R., Engineered knottin peptides as diagnostics, therapeutics, and drug delivery vehicles. *Curr. Opin. Chem. Biol.* **2016**, *34*, 143–150; (b) Navalkar, K. A.; Johnston, S. A.; Stafford, P., Peptide based diagnostics: Are random-sequence peptides more useful than tiling proteome sequences? *J. Immunol. Methods* **2015**, *417*, 10–21.

9. Wang, F.; Carabino, J. M.; Vergara, C. M., Insulin glargine: a systematic review of a long-acting insulin analogue. *Clin. Ther.* **2003**, *25*, 1541–1577.

10. Greenwood, H. C.; Bloom, S. R.; Murphy, K. G., Peptides and their potential role in the treatment of diabetes and obesity. *Rev. Diabet. Stud. RDS* **2011**, *8*, 355.

11. Volpe, M.; Rubattu, S.; Burnett Jr, J., Natriuretic peptides in cardiovascular diseases: current use and perspectives. *Eur. Heart J.* **2013**, *35*, 419–425.

Holst-Jensen SE, Pfeiffer-Jensen M, Monsrud M, Tarp U, Buus A,Hessov I, Thorling E, Stengard-Pedersen K. Treatment of rheumatoidarthritis with a peptide diet: A randomized, controlled trial. *Scand J. Rheumatol*. **1998**, *27*, 329–336

12. Holst-Jensen, M. P.-J., M Monsrud, U Tarp, A Buus, I Hessov, E Thorling, K Stengaard-Pedersen, SE, Treatment of rheumatoid arthritis with a peptide diet: a randomized, controlled trial. *Scand. J. Rheumatol.* **1998**, *27*, 329–336.

13. (a) Lim, S. H.; Sun, Y.; Thiruvallur, T. M.; Rosa, V.; Kang, L., Enhanced Skin Permeation of Anti-wrinkle Peptides via Molecular Modification. *Sci. Rep.* **2018**, *8*, 1596; (b) Schagen, S. K., Topical peptide treatments with effective anti-aging results. *Cosmetics* **2017**, *4*, 16.

14. Piotto, S.; Di Biase, L.; Sessa, L., Transmembrane peptides as sensors of the membrane physical state. *Front. Phys.* **2018**, *6*, 48.

15. Davie, E. A. C.; Mennen, S. M.; Xu, Y.; Miller, S. J., Asymmetric catalysis mediated by synthetic peptides. *Chem. Rev.* **2007**, *107*, 5759–5812.

16. Pauletti, G. M.; Gangwar, S.; Siahaan, T. J.; Aubé, J.; Borchardt, R. T., Improvement of oral peptide bioavailability: Peptidomimetics and prodrug strategies. *Adv. Drug Deliv. Rev.* **1997**, *27*, 235–256.

17. Neurath, H., Proteolytic processing and physiological regulation. *Trends Biochem. Sci.* **1989**, *14*, 268–271.

18. Pichereau, C.; Allary, C., Therapeutic peptides under the spotlight. *Eur. Biopharm. Rev.* **2005**, *5*, 88–91.

19. Smith III, A. B.; Hirschmann, R.; Pasternak, A.; Akaishi, R.; Guzman, M. C.; Jones, D. R.; Keenan, T. P.; Sprengeler, P. A.; Darke, P. L., Design and synthesis of peptidomimetic inhibitors of HIV-1 protease and renin. Evidence for improved transport. *J. Med. Chem.* **1994**, *37*, 215-218.

20. Lee, V. H.; Yamamoto, A., Penetration and enzymatic barriers to peptide and protein absorption. *Adv. Drug Deliv. Rev.* **1989**, *4*, 171–207.

21. Bray, B. L., Large-scale manufacture of peptide therapeutics by chemical synthesis. *Nat. Rev. Drug Discov.* **2003**, *2*, 587.

22. (a) Farmer, P.; Ariens, E., Speculations on the design of nonpeptidic peptidomimetics. *Trends Pharmacol. Sci.* **1982**, *3*, 362-365; (b) Ko, E.; Liu, J.; Burgess, K., Minimalist and universal peptidomimetics. *Chem. Soc. Rev.* **2011**, *40*, 4411–4421.

23. Ripka, A. S.; Rich, D. H., Peptidomimetic design. *Curr. Opin. Chem. Biol.* **1998**, *2*, 441-452.

24. Gether, U., Uncovering molecular mechanisms involved in activation of G protein-coupled receptors. *Endocr. rev.* **2000**, *21*, 90–113.

25. Bursavich, M. G.; Rich, D. H., Designing non-peptide peptidomimetics in the 21st century: inhibitors targeting conformational ensembles. *J. Med. Chem.* **2002**, *45*, 541–558.

26. Avan, I.; Hall, C. D.; Katritzky, A. R., Peptidomimetics via modifications of amino acids and peptide bonds. *Chem. Soc. Rev.* **2014**, *43*, 3575–3594.

27. (a) Yoo, B.; Kirshenbaum, K., Peptoid architectures: elaboration, actuation, and application. *Curr. Opin. Chem. Biol.* **2008**, *12*, 714–721; (b) Yoo, B.; Shin, S. B. Y.; Huang, M. L.; Kirshenbaum, K., Peptoid macrocycles: making the rounds with peptidomimetic oligomers. *Chem. Eur. J.* **2010**, *16*, 5528–5537.

28. (a) Haskell-Luevano, C.; Toth, K.; Boteju, L.; Job, C.; Castrucci, A. M. d. L.; Hadley, M. E.; Hruby, V. J., β-Methylation of the Phe7 and Trp9 melanotropin side-chain pharmacophores affects ligand− receptor interactions and prolonged biological activity. *J. Med. Chem.* **1997**, *40*, 2740–2749; (b) Tourwé, D.; Mannekens, E.; Diem, T. N. T.; Verheyden, P.; Jaspers, H.; Tóth, G.; Péter, A.; Kertész, I.; Török, G.; Chung, N. N., Side-chain methyl substitution in the δ-opioid receptor antagonist TIPP has an important effect on the activity profile. *J. Med. Chem.* **1998**, *41*, 5167–5176.

29. (a) Yang, X.; Wang, M.; Fitzgerald, M. C., Analysis of protein folding and function using backbone modified proteins. *Bioorg. Chem.* **2004**, *32*, 438–449; (b) Gante, J., Peptidomimetics—tailored enzyme inhibitors. *Angew. Chem. Intl. Ed.* **1994**, *33*, 1699–1720.

30. (a) Freidinger, R. M., Design and synthesis of novel bioactive peptides and peptidomimetics. *J. Med. Chem.* **2003**, *46*, 5553-5566; (b) Su, T.; Yang, H.; Volkots, D.; Woolfrey, J.; Dam, S.; Wong, P.; Sinha, U.; Scarborough, R. M.; Zhu, B.-Y., Design, synthesis, and structure–Activity relationships of substituted piperazinone-Based transition state factor Xa inhibitors. *Bioorganic Med. Chem. Lett.* **2003**, *13*, 729–732.

31. Whitby, L. R.; Ando, Y.; Setola, V.; Vogt, P. K.; Roth, B. L.; Boger, D. L., Design, synthesis, and validation of a β-turn mimetic library targeting protein–protein and peptide–receptor interactions. *J. Am. Chem. Soc.* **2011**, *133*, 10184–10194.

32. Ramchandran, G.; Ramakrishnan, C.; Sasisekharan, V., Streochemistry of polypeptide chain configuration. *J. Mol. Biol.* **1963**, *7*, 95–99.

33. Stefanucci, A.; Pinnen, F.; Feliciani, F.; Cacciatore, I.; Lucente, G.; Mollica, A., Conformationally constrained histidines in the design of peptidomimetics: strategies for the χ-space control. *Int. J. Mol. Sci.* **2011**, *12*, 2853–2890.

34. Whitby, L. R.; Boger, D. L., Comprehensive peptidomimetic libraries targeting protein–protein interactions. *Acc. Chem. Res.* **2012**, *45*, 1698–1709.

35. Loughlin, W. A.; Tyndall, J. D.; Glenn, M. P.; Fairlie, D. P., Beta-strand mimetics. *Chem. Rev.* **2004**, *104*, 6085–6118.

36. (a) Wilmot, C.; Thornton, J., Analysis and prediction of the different types of β-turn in proteins. *J. Mol. Biol.* **1988**, *203*, 221–232; (b) Venkatachalam, C., Stereochemical criteria for polypeptides

and proteins. V. Conformation of a system of three linked peptide units. *Biopolymers: Original Research on Biomolecules* **1968**, *6*, 1425–1436.

37. Ruiz-Gomez, G.; Tyndall, J. D.; Pfeiffer, B.; Abbenante, G.; Fairlie, D. P., Update 1 of: Over one hundred peptide-activated G protein-coupled receptors recognize ligands with turn structure. *Chem. Rev.* **2010**, *110*, PR1–PR41.

38. Fairlie, D. P.; West, M. L.; Wong, A. K., Towards protein surface mimetics. *Curr. Med. Chem.* **1998**, *5*, 29–62.

39. Smith III, A. B.; Guzman, M. C.; Sprengeler, P. A.; Keenan, T. P.; Holcomb, R. C.; Wood, J. L.; Carroll, P. J.; Hirschmann, R., De Novo Design, Synthesis, and X-ray Crystal Structures of Pyrrolinone-Based. beta.-Strand Peptidomimetics. *J. Am. Chem. Soc.* **1994**, *116*, 9947–9962.

40. Glenn, M. P.; Pattenden, L. K.; Reid, R. C.; Tyssen, D. P.; Tyndall, J. D.; Birch, C. J.; Fairlie, D. P., β-Strand mimicking macrocyclic amino acids: templates for protease inhibitors with antiviral activity. *J. Med. Chem.* **2002**, *45*, 371–381.

41. (a) Freidinger, R. M.; Veber, D. F.; Perlow, D. S.; Saperstein, R., Bioactive conformation of luteinizing hormone-releasing hormone: evidence from a conformationally constrained analog. *Science* **1980**, *210*, 656-658; (b) Freidinger, R. M.; Perlow, D. S.; Veber, D. F., Protected lactam-bridged dipeptides for use as conformational constraints in peptides. *J. Org. Chem.* **1982**, *47*, 104–109.

42. (a) Wyvratt, M.; Tischler, M.; Ikeler, T.; Springer, J.; Tristram, E.; Patchett, A. In *Bicyclic inhibitors of angiotensin-converting enzyme*, Peptides: Structure and Function, Proceedings 8th American Peptide Symposium. Rockford, III, Pierce Chemical Co1983; pp 551–554; (b) Wyvratt, M. J.; Patchett, A. A., Recent developments in the design of angiotensin-converting enzyme inhibitors. *Med. Res. Rev.* **1985**, *5*, 483–531.

43. Nagai, U.; Sato, K., Synthesis of a bicyclic dipeptide with the shape of β-turn central part. *Tetrahedron Lett.* **1985**, *26*, 647–650.

44. Nagai, U.; Sato, K.; Nakamura, R.; Kato, R., Bicyclic turned dipeptide (BTD) as a β-turn mimetic; its design, synthesis and incorporation into bioactive peptides. *Tetrahedron* **1993**, *49*, 3577–3592.

45. Gause, G.; Brazhnikova, M., Gramicidin S and its use in the treatment of infected wounds. *Nature* **1944**, *154*, 703.

46. Sato, K.; Nagai, U., Synthesis and antibiotic activity of a gramicidin S analogue containing bicyclic β-turn dipeptides. *J. Chem. Soc., Perkin Transactions 1* **1986**, 1231–1234.

47. Cluzeau, J.; Lubell, W. D., Design, synthesis, and application of azabicyclo [XY 0] alkanone amino acids as constrained dipeptide surrogates and peptide mimics. *Peptide Science: Original Research on Biomolecules* **2005**, *80*, 98–150.

48. Halab, L.; Gosselin, F.; Lubell, W. D., Design, synthesis, and conformational analysis of azacycloalkane amino acids as conformationally constrained probes for mimicry of peptide secondary structures. *J. Pept. Sci.* **2000**, *55*, 101–122.

49. (a) Cordero, F. M.; Valenza, S.; Machetti, F.; Brandi, A., Design and synthesis of a new bicyclic dipeptide isostere. *Chem. Commun.* **2001**, 1590–1591; (b) Fustero, S.; Mateu, N.; Albert, L.; Aceña, J. L., Straightforward stereoselective access to cyclic peptidomimetics. *J. Org. Chem.* **2009**, *74*, 4429–4432; (c) Vartak, A. P.; Skoblenick, K.; Thomas, N.; Mishra, R. K.; Johnson, R. L., Allosteric Modulation of the Dopamine Receptor by Conformationally Constrained Type VI β-Turn Peptidomimetics of Pro-Leu-Gly-NH2. *J. Med. Chem.* **2007**, *50*, 6725–6729.

50. Khashper, A.; Lubell, W. D., Design, synthesis, conformational analysis and application of indolizidin-2-one dipeptide mimics. *Org. Biomol. Chem.* **2014**, *12*, 5052−5070.

51. Hanessian, S.; Therrien, E.; Granberg, K.; Nilsson, I., Targeting thrombin and factor VIIa: design, synthesis, and inhibitory activity of functionally relevant indolizidinones. *Bioorg. Med. Chem. Lett.* **2002**, *12*, 2907–2911.

52. Bourguet, C. B.; Boulay, P.-L.; Claing, A.; Lubell, W. D., Design and synthesis of novel azapeptide activators of apoptosis mediated by caspase-9 in cancer cells. *Bioorganic Med. Chem. Lett.* **2014**, *24*, 3361–3365.

53. (a) Bourguet, C. B.; Goupil, E.; Tassy, D.; Hou, X.; Thouin, E.; Polyak, F.; Hébert, T. E.; Claing, A.; Laporte, S. A.; Chemtob, S., Targeting the prostaglandin F2α receptor for preventing preterm labor with azapeptide tocolytics. *J. Med. Chem.* **2011**, *54*, 6085–6097;

54. Khashper, A.; Lubell, W. D., Design, synthesis, conformational analysis and application of indolizidin-2-one dipeptide mimics. *Org. Biomol. Chem.* **2014**, *12*, 5052–5070.

55. Lombart, H.-G.; Lubell, W. D., Synthesis of enantiopure α,ω-diamino dicarboxylates and azabicycloalkane amino acids by claisen condensation of α-[*N*-(Phenylfluorenyl)amino] dicarboxylates. *J. Org. Chem.* **1994,** *59*, 6147–6149.

56. Feng, Z.; Lubell, W. D., Synthesis of enantiopure 7-[3-azidopropyl]indolizidin-2-one amino acid. A constrained mimic of the peptide backbone geometry and heteroatomic side-chain functionality of the Ala-Lys dipeptide. *J. Org. Chem.* **2001**, *66*, 1181–1185.

57. Polyak, F.; Lubell, W. D., Mimicry of peptide backbone geometry and heteroatomic side-chain functionality: synthesis of enantiopure indolizidin-2-one amino acids possessing alcohol, acid, and azide functional groups. *J. Org. Chem.* **2001**, *66*, 1171–1180.

58. Bourguet, C. B.; Claing, A.; Laporte, S. A.; Hébert, T. E.; Chemtob, S.; Lubell, W. D., Synthesis of azabicycloalkanone amino acid and azapeptide mimics and their application as

modulators of the prostaglandin F2α receptor for delaying preterm birth. *Can. J. Chem.* **2014**, *92*, 1031–1040.

59. Gonzalez, N.; Moody, T. W.; Igarashi, H.; Ito, T.; Jensen, R. T., Bombesin-related peptides and their receptors: recent advances in their role in physiology and disease states. *Curr. Opin. Endocrinol. Diabetes Obes*. **2008**, *15*, 58.

60. Hanessian, S.; Balaux, E.; Musil, D.; Olsson, L.-L.; Nilsson, I., Exploring the chiral space within the active site of α-thrombin with a constrained mimic of d-Phe-Pro-Arg—design, synthesis, inhibitory activity, and X-ray structure of an enzyme–inhibitor complex. *Bioorg. Med. Chem. Lett.* **2000**, *10*, 243–247.

61. Sanderson, P.; Naylor-Olsen, A., Thrombin inhibitor design. *Curr. Med. Chem.* **1998**, *5*, 289–304.

62. Wiley, M. R.; Chirgadze, N. Y.; Clawson, D. K.; Craft, T. J.; Gifford-Moore, D. S.; Jones, N. D.; Olkowski, J. L.; Weir, L. C.; Smith, G. F., D-Phe-Pro-p-Amidinobenzylamine: A potent and highly selective thrombin inhibitor. *Bioorg. Med. Chem. Lett.* **1996**, *6*, 2387–2392.

63. Gosselin, F.; Lubell, W. D., Rigid dipeptide surrogates: Syntheses of enantiopure quinolizidinone and pyrroloazepinone amino acids from a common diaminodicarboxylate precursor. *J. Org. Chem.* **2000**, *65*, 2163–2171.

64. Halab, L.; Becker, J. A.; Darula, Z.; Tourwé, D.; Kieffer, B. L.; Simonin, F.; Lubell, W. D., Probing opioid receptor interactions with azacycloalkane amino acids. Synthesis of a potent and selective ORL1 antagonist. *J. Med. Chem.* **2002**, *45*, 5353–5357.

65. Van Cauwenberghe, S.; Simonin, F.; Cluzeau, J.; Becker, J. A.; Lubell, W. D.; Tourwé, D., Structure−Activity Study of the ORL1 Antagonist Ac-Arg-D-Cha-Qaa-D-Arg-D-*p*-ClPhe-NH_2. *J. Med. Chem.* **2004**, *47*, 1864–1867.

66. Robl, J. A.; Cimarusti, M. P.; Simpkins, L. M.; Brown, B.; Ryono, D. E.; Bird, J. E.; Asaad, M. M.; Schaeffer, T. R.; Trippodo, N. C., Dual metalloprotease inhibitors. 6. Incorporation of bicyclic and substituted monocyclic azepinones as dipeptide surrogates in angiotensin-converting enzyme/neutral endopeptidase inhibitors. *J. Med. Chem.* **1996**, *39*, 494–502.

67. Bralet, J.; Schwartz, J.-C., Vasopeptidase inhibitors: an emerging class of cardiovascular drugs. *Trends Pharmacol. Sci.* **2001**, *22*, 106–109.

68. Slusarchyk, W. A.; Robl, J. A.; Taunk, P. C.; Assad, M. M.; Bird, J. E.; DiMarco, J.; Pan, Y., Dual metalloprotease inhibitors. V. Utilization of bicyclic azepinonethiazolidines and azepinonetetrahydrothiazines in constrained peptidomimetics of mercaptoacyl dipeptides. *Bioorg. Med. Chem. Lett.* **1995**, *5*, 753–758.

69. Federico, C., Natriuretic peptide system and cardiovascular disease. *Heart views: the official journal of the Gulf Heart Association* **2010**, *11*, 10.

70. Curry, F.-R. E., Atrial natriuretic peptide: an essential physiological regulator of transvascular fluid, protein transport, and plasma volume. *J. Clin. Investig.* **2005**, *115*, 1458–1461.

71. Delaney, N. G.; Barrish, J. C.; Neubeck, R.; Natarajan, S.; Cohen, M.; Rovnyak, G. C.; Huber, G.; Murugesan, N.; Girotra, R.; Sieber-McMaster, E., Mercaptoacyl dipeptides as dual inhibitors of angiotensin-converting enzyme and neutral endopeptidase. Preliminary structure-activity studies. *Bioorg. Med. Chem. Lett.* **1994**, *4*, 1783–1788.

72. Gosselin, F.; Lubell, W. D., An olefination entry for the synthesis of enantiopure α, ω-diaminodicarboxylates and azabicyclo[X.Y.0]alkane amino acids. *J. Org. Chem.* **1998**, *63*, 7463–7471.

73. (a) White, J. D.; Hrnciar, P., Synthesis of polyhydroxylated pyrrolizidine alkaloids of the alexine family by tandem ring-closing metathesis− transannular cyclization.(+)-australine. *J. Org.*

Chem. **2000,** *65*, 9129-9142; (b) White, J. D.; Hrnciar, P.; Yokochi, A. F., Tandem ring-closing metathesis transannular cyclization as a route to hydroxylated pyrrolizidines. Asymmetric synthesis of (+)-Australine. *J. Am. Chem. Soc.* **1998**, *120*, 7359–7360.

74. Rizzo, A.; Harutyunyan, S. R., Azabicycles construction: the transannular ring contraction with *N*-protected nucleophiles. *Org. Biomol. Chem.* **2014**, *12*, 6570–6579.

75. Kaul, R.; Surprenant, S.; Lubell, W. D., Systematic study of the synthesis of macrocyclic dipeptide β-turn mimics possessing 8-, 9-, and 10-membered rings by ring-closing metathesis. *J. Org. Chem.* **2005**, *70*, 3838–3844.

76. Atmuri, N. P.; Lubell, W. D., Insight into transannular cyclization reactions to synthesize azabicyclo [X.Y.Z] alkanonea amino acid derivatives from 8-, 9-, and 10-membered macrocyclic dipeptide lactams. *J. Org. Chem.* **2015**, *80*, 4904–4918.

77. Surprenant, S.; Lubell, W. D., From macrocycle dipeptide lactams to azabicyclo[X.Y.0] alkanone Amino Acids: A transannular cyclization route for peptide mimic synthesis. *Org. Lett.* **2006**, *8*, 2851–2854.

78. Godina, T. A.; Lubell, W. D., Mimics of peptide turn backbone and side-chain geometry by a general approach for modifying azabicyclo[5.3.0]alkanone amino acids. *J. Org. Chem.* **2011**, *76*, 5846–5849.

79. Traoré, M.; Mietton, F.; Maubon, D. l.; Peuchmaur, M.; Francisco Hilário, F.; Pereira de Freitas, R.; Bougdour, A.; Curt, A. l.; Maynadier, M.; Vial, H., Flexible synthesis and evaluation of diverse anti-apicomplexa cyclic peptides. *J. Org. Chem.* **2013**, *78*, 3655–3675.

80. (a) Katagiri, N.; Okada, M.; Morishita, Y.; Kaneko, C., Synthesis of chiral spiro 3-oxazolin-5-one 3-oxides (chiral nitrones) via a nitrosoketene intermediate and their asymmetric 1, 3-dipolar cycloaddition reactions leading to the EPC synthesis of modified amino acids. *Tetrahedron* **1997**,

53, 5725–5746; (b) Myers, A. G.; Gleason, J. L., Asymmetric synthesis of alpha-amino acids by the alkylation of pseudoephedrine glycinamide: L-allylglycine and *N*-Boc-L-allylglycine. *Org. synth.* **1999**, *76*, 57–76; (c) Kitagawa, O.; Hanano, T.; Kikuchi, N.; Taguchi, T., Asymmetric synthesis of α-amino acids through α-iodination of chiral unsaturated carboxamides and stereoselective iodolactonization. *Tetrahedron Lett.* **1993**, *34*, 2165–2168; (d) Hanessian, S.; Yang, R.-Y., Enantioselective allylation of α-ketoester oximes with an external chiral ligand: Asymmetric synthesis of allylglycines and allylalanine. *Tetrahedron Lett.* **1996**, *37*, 8997–9000.

81. Rodríguez, A.; Miller, D. D.; Jackson, R. F., Combined application of organozinc chemistry and one-pot hydroboration–Suzuki coupling to the synthesis of amino acids. *Org. Biomol. Chem.* **2003**, *1*, 973–977.

82. Atmuri, N. P.; Lubell, W. D., Preparation of *N*-(Boc)-allylglycine methyl ester using a zinc-mediated, palladium-catalyzed cross-coupling reaction. *Org. Synth.* **2003**, *92*, 103–116.

83. Hack, V.; Reuter, C.; Opitz, R.; Schmieder, P.; Beyermann, M.; Neudörfl, J. M.; Kühne, R.; Schmalz, H. G., Efficient α-helix induction in a linear peptide chain by n-capping with a bridged-tricyclic diproline analogue. *Angew. Chem. Int. Ed.* **2013**, *52*, 9539 –9543

Chapter 2

Peptidomimetic Synthesis by way of Diastereoselective Iodoacetoxylation and Transannular Amidation of 7–9-Membered Lactams

2.01 Context

Constrained dipeptide surrogates are useful for mimicry of peptide geometry to study relationships between conformation and biological activity.[1] For example, bicyclic peptidomimetics such as azabicyclo[X.Y.0]alkanone ring skeletons have served as mimics secondary structures such as β-turns (Figure 2.01).[2,3,4] Their heterocycle framework can constrain the backbone dihedral angle geometry and side-chain conformations to specific orientations useful for investigating structure-activity relationships.[5,6]

Pyrrolizidinone and indolizidinone-9-one amino acid (Paa and I[9]aa) analogues have exhibited various activities (Figure 2.01). For example, thiapyrrolizidinone carbonitrile **2.01** has functioned as an prolyl oligopeptidase inhibitor (IC_{50} of 1.3 mM) in a cellular assay.[7] I[9]aa analog **2.04** is a potent cholecystokinin A receptor antagonist (IC_{50} 7.4 nM).[8]

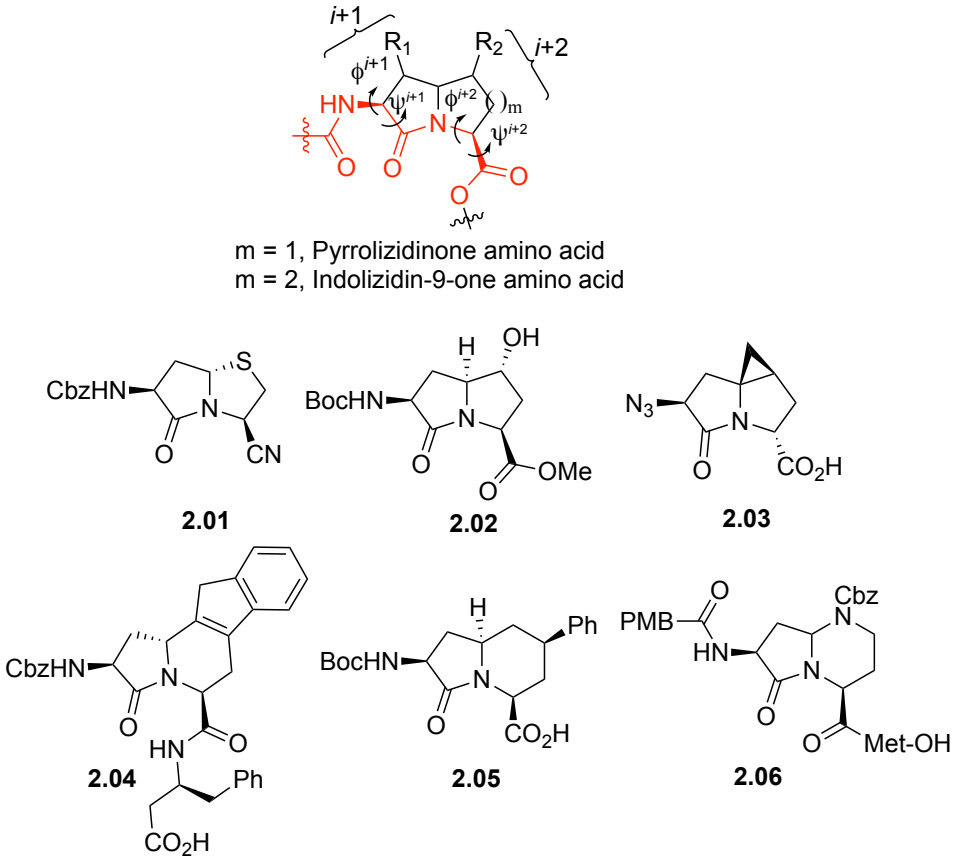

Figure 2.01. Constrained bicyclic γ-lactams

The synthesis of Paa and I[9]aa analogues has typically required multiple-step processes that furnish specific analogues.[9] For example, hydroxy pyrrolizidinone amino acid **2.02** was synthesized in seven steps from (2*S*)-α *tert*-butyl *N*-(PhF)aspartate β-aldehyde by way of a carbene-catalyzed acyloin condensation, which provided linear ketone precursors that were converted to the bicycle by diastereoselective reductive amination and lactam annulation.[10]

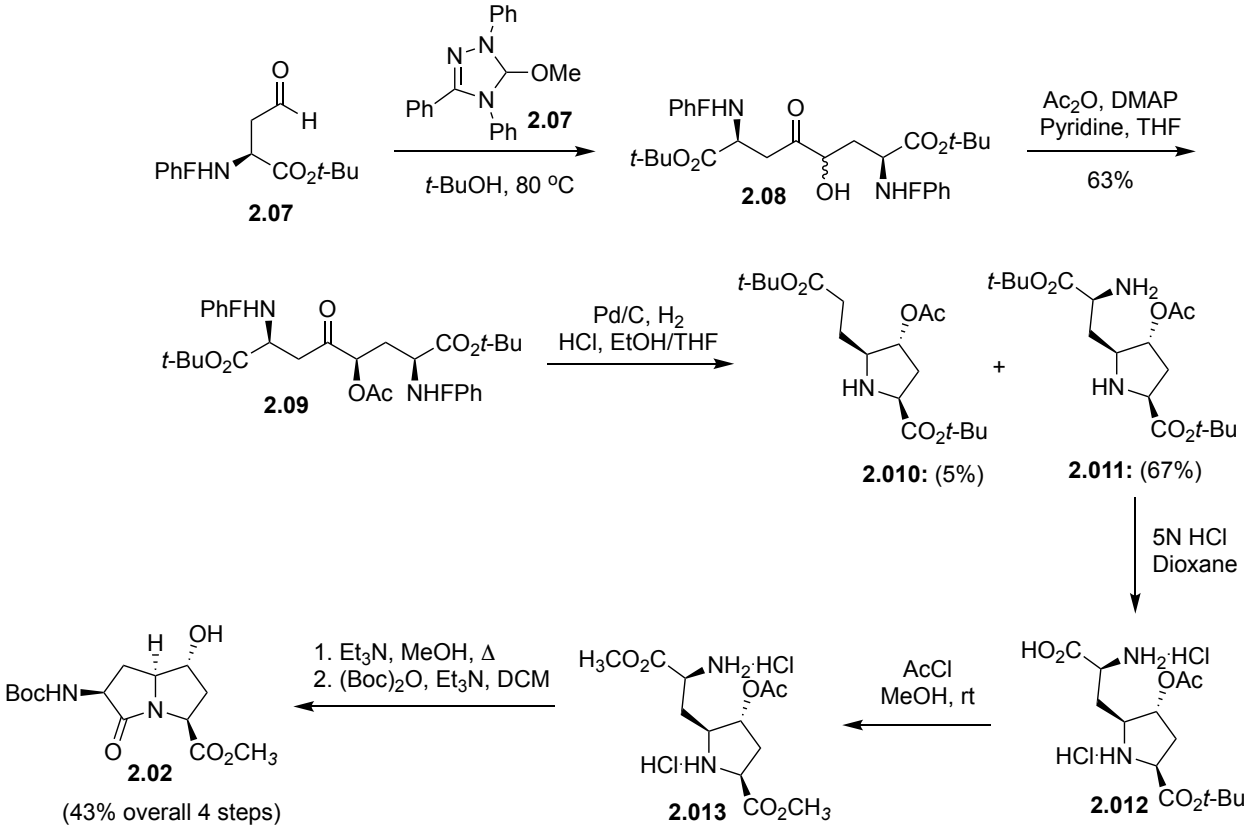

Scheme 2.01 Synthesis of azabicyclo[3.3.0]alkanone amino acid

Tricyclic pyrrolizidinone **2.03** was prepared as a single diastereoisomer from pyroglutamate *via* A intramolecular cyclopropanation mediated by a trimethylstannylmethyl group and an adjacent iminium ion in 13 steps.[11] 7-Amino-pyrrol[1,2-a]pyrimidin-6-one-4-carboxylate **2.06** was synthesized on 2-chlorotrityl chloride resin employing a strategy featuring a condensation between a diaminobutyric acid derivative and aspartate β–semialdehyde dimethyl acetal, followed by lactam formation. A shared route to Paa and I[9]aa analogues by way of common intermediates

remained an interesting goal to furnish a set of bicycles for systematic study of peptide conformation-activity relationships.

2.02 Halogen-induced cyclization for heterocycle synthesis

The cyclization of unsaturated acid derivatives induced by a halogen has been often used for the synthesis of heterocyclic compounds.[12] Relative to iodolactonization, iodolactamization has been less well investigated, in part because amide cyclization can produce cyclic imidate which on hydrolysis may give lactone instead of lactam. To achieve lactamization, methods employing *N*,*O*-bis-silylation, *N*-tosyl and *N*-alkoxycarbonyl substitution have been employed.[13] Strong bases have also been used to favour lactam formation.[13] On the other hand, in the synthesis of azabicycloalkanone amino acids, transannular iodolactamization has proven a stereoselective method for preparing bicycle with an iodide handle, that can be displaced stereoselectively to add various side-chains to the ring system.[15,16]

A variety of isomeric unsaturated lactams were previously made by the RCM-TC sequence using allyl- and homoallyl-building blocks.[14] Transannular iodolactamizations provided iodo-azabicyclo[4.3.0] and [5.3.0]alkanone amino acids (e.g., **1.47** and **1.49)** respectively from 9- and 10-membered lactams (e.g., **1.45c** and **1.46f)** using conditions such as I_2, THF, 80 °C, and I_2, $NaHCO_3$ in THF at rt.[14] During my M.Sc. degree studies, I explored vinylglycine and homohomoallylglycine to broaden the scope of the RCM-TC sequence.[15] Transannular cyclization using the above conditions failed however to induce cyclization of 7-, 8- and certain 9-membered lactams; instead, loss of the Dmb group occurred. Moreover, the resulting lactams were also resistant to transannular iodoamidation using I_2 in THF buffered with $NaHCO_3$, as well as using I_2 in acetonitrile at reflux (Introduction, Scheme 1.6 and 1.7).

Previously, diacetoxyiodobenzene (DIB) had been used in functionalization of alkenes and oxidative cyclization of *o*-hydroxystyrenes to benzofurans.[16] For example, alkenes reactive with

azide ion using a phenyliodine diacetate (PIDA)–trimethylsilylazide combination.[17] Functionalization of olefins is generally more difficult than that of alkynes due to the low polarizability of olefins. Unlike chlorination and bromination, iodination of alkenes is a considerably slower reaction due to the low electrophilicity of iodine. To activate elemental iodine for addition to alkenes, various methods have been studied to modify electrophilicity.[18] A few reports have explored the combination of hypervalent iodine reagents and I_2. For example, diacetoxyiodobenzene (DIB) and I_2 have been reported to combine to form an electrophilic "I^+" species, which may activate olefins by a cation–π interaction that leads to subsequent nucleophilic attack. The combination of DIB and I_2 has been used to generate anomeric alkoxy derivatives from unsaturated sugars.[19] Inspired by these precedents, a new invention in the transannular iodolactamization protocol was discovered by employing diacetoxyiodobenzene (DIB) as additive in the I_2 reaction conditions. This protocol, converted successfully 8-membered lactam **1.44a** in a single pyrrolizidinone diastereomer (Scheme 2.02).[15] Other 7–9 membered lactams were explored using these conditions.

This chapter reveals the influence of electron-rich aromatic substituents and bulky carboxylates as ligands on the reactivity of the hypervalent(III)iodine intermediates in the transannular cyclization. Moreover, solvent was also shown to influence the cyclization of the 8-membered lactams. Studying the mechanism of the latter, the importance of neighbouring group participation in the reaction of the olefin have been elucidated. In addition, X-ray crystallography of certain bicycles and substituted lactams has demonstrated further their potential for mimicry of peptide turn conformation. In summary, this chapter describes an effective new method for transannular cyclization that uses a hypervalent(III)iodine additive to provide bicycles from previously resistant unsaturated lactams. The method and the novel rigid dipeptide mimic products offer respectively interesting potential for heterocycle synthesis and peptide mimicry.

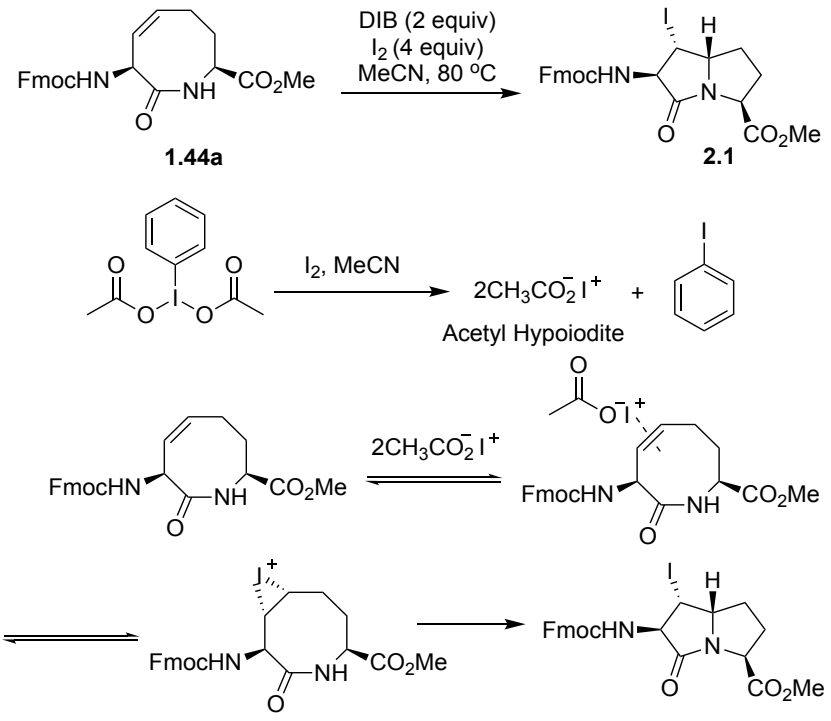

Scheme 2.02. Transannular cyclization with diacetoxyiodobenzene

2.03 References

1. St-Cyr, D. J.; García-Ramos, Y.; Doan, N.-D.; Lubell, W. D. Peptidomimetics I; Topics in Heterocyclic Chemistry, Vol. 48; Lubell, W. D., Ed.; Springer-Berlin Heidelberg; Germany, 2017; pp 125−176.

2. (a) Cluzeau, J.; Lubell, W. D., Design, synthesis, and application of azabicyclo [X.Y.0] alkanone amino acids as constrained dipeptide surrogates and peptide mimics. *J. Pept. Sci.* **2005**, *80*, 98–150; (b) Maison, W.; Prenzel, A. H., Stereoselective synthesis of aza-and diazabicyclo [X.Y.0] alkane dipeptide mimetics. *Synthesis* **2005**, *2005*, 1031–1048.

3. Hanessian, S.; McNaughton-Smith, G., A versatile synthesis of a β-turn peptidomimetic scaffold: an approach towards a designed model antagonist of the tachykinin NK-2 receptor. *Bioorg. Med. Chem. Lett.* **1996**, *6*, 1567–1572.

4. Venkatachalam, C., Stereochemical criteria for polypeptides and proteins. V. Conformation of a system of three linked peptide units. *Biopolymers* **1968**, *6*, 1425–1436.

5. (a) Nagai, U.; Sato, K.; Nakamura, R.; Kato, R., Bicyclic turned dipeptide (BTD) as a β-turn mimetic; its design, synthesis and incorporation into bioactive peptides. *Tetrahedron* **1993**, *49*, 3577–3592; (b) Haubner, R.; Schmitt, W.; Hölzemann, G.; Goodman, S. L.; Jonczyk, A.; Kessler, H., Cyclic RGD peptides containing β-turn mimetics. *J. Am. Chem. Soc.* **1996**, *118*, 7881–7891.

6. (a) Hanessian, S.; McNaughton-Smith, G.; Lombart, H.-G.; Lubell, W. D., Design and synthesis of conformationally constrained amino acids as versatile scaffolds and peptide mimetics. *Tetrahedron* **1997**, *53*, 12789–12854; (b) Falorni, M.; Giacomelli, G.; Nieddu, F.; Taddei, M., A new diketopiperazine tetra-carboxylic acid as template for the homogeneous phase synthesis of chemical libraries. *Tetrahedron Lett.* **1997**, *38*, 4663–4666.

7. Lawandi, J.; Toumieux, S.; Seyer, V.; Campbell, P.; Thielges, S.; Juillerat-Jeanneret, L.; Moitessier, N., Constrained peptidomimetics reveal detailed geometric requirements of covalent prolyl oligopeptidase inhibitors. *J. Med. Chem.* **2009**, *52*, 6672–6684.

8. Martín-Martínez, M.; De la Figuera, N.; Latorre, M.; Herranz, R.; García-López, M. T.; Cenarruzabeitia, E.; Del Río, J.; González-Muñiz, R., β-Turned dipeptoids as potent and selective CCK1 receptor antagonists. *J. Med. Chem.* **2000**, *43*, 3770–3777.

9. Vagner, J.; Qu, H.; Hruby, V. J., Peptidomimetics, a synthetic tool of drug discovery. *Curr. Opin. Chem. Biol.* **2008**, *12*, 292–296.

10. Rao, M. H. R.; Pinyol, E.; Lubell, W. D., Rigid dipeptide mimics: synthesis of enantiopure C6-functionalized pyrrolizidinone amino acids. *J. Org. Chem.* **2007**, *72*, 736–743.

11. Hanessian, S.; Buckle, R.; Bayrakdarian, M., Design and synthesis of a novel class of constrained tricyclic pyrrolizidinone carboxylic acids as carbapenem mimics. *J. Org. Chem.* **2002**, *67*, 3387–3397.

12. Shen, M.; Li, C., Asymmetric iodolactamization induced by chiral oxazolidine auxiliary. *J. Org. Chem.* **2004**, *69*, 7906–7909.

13. (a) Knapp, S.; Gibson, F. S.; Choe, Y. H., Radical based annulations of iodo lactams. *Tetrahedron Lett.* **1990**, *31*, 5397–5400; (b) Biloski, A. J.; Wood, R. D.; Ganem, B., A new. beta.-lactam synthesis. *J. Am. Chem. Soc.* **1982**, *104*, 3233–3235; (c) Rajendra, G.; Miller, M. J., Intramolecular electrophilic additions to olefins in organic syntheses. Stereoselective synthesis of 3, 4-substituted β-lactams by bromine-induced oxidative cyclization of *O*-acyl β,γ-unsaturated hydroxamic acid derivatives. *J. Org. Chem.* **1987**, *52*, 4471–4477.

14. Kaul, R.; Surprenant, S.; Lubell, W. D., Systematic study of the synthesis of macrocyclic dipeptide β-turn mimics possessing 8-, 9-, and 10-membered rings by ring-closing metathesis. *J. Org. Chem.* **2005**, *70*, 3838–3844.

15. Atmuri, N. P.; Lubell, W. D., Insight into transannular cyclization reactions to synthesize azabicyclo[X.Y.Z]alkanone amino acid derivatives from 8-, 9-, and 10-membered macrocyclic dipeptide lactams. *J. Org. Chem.* **2015**, *80*, 4904–4918.

16. Singh, F. V.; Wirth, T., Hypervalent iodine mediated oxidative cyclization of *o*-hydroxy stilbenes into benzo-and naphtho furans. *Synthesis* **2012**, *44*, 1171–1177.

17. Cech, F.; Zbiral, E., Zum verhalten konjugierter diene gegenüber $C_6H_5(OAc)_2$-$(CH_3)_3SiN_3$. *Tetrahedron* **1975**, *31*, 605–612.

18. Gottam, H.; Vinod, T. K., Versatile and iodine atom-economic co-iodination of alkenes. *J. Org. Chem.* **2010**, *76*, 974–977.

19. Courtneidge, J. L.; Lusztyk, J.; Pagé, D., Alkoxyl radicals from alcohols. spectroscopic detection of intermediate alkyl and acyl hypoiodites in the Suárez and Beebe reactions. *Tetrahedron Lett.* **1994**, *35*, 1003–1006.

Article 1

Peptidomimetic Synthesis by way of Diastereoselective Iodoacetoxylation and Transannular Amidation of 7–9-Membered Lactams

N. D. Prasad Atmuri, David J. Reilley, William D. Lubell*

Département de Chimie, Université de Montréal, P.O. Box 6128, Station Centre-ville, Montréal, Québec H3C 3J7, Canada.

Org. Lett. **2017**, 19, 5066−5069
Received: July 24, 2017; Published: September 26, 2017

2.1 Abstract

Azacyclo- and azabicycloalkanone peptidomimetics were synthesized regio- and diastereoselectively by iodoacetoxylation and transannular amidation reactions on unsaturated lactam precursors contingent on ring size, olefin position, solvent and hypervalent iodine(III) reagent. 4-Iodopyrrolizidinone **2.1**, 7-iodoindolizidinone **2.2** and 4-iodo-5-acetoxylactams (e.g., **2.6** and **2.7**) were made stereospecifically from 7–9-membered olefins **2.16** (Scheme **2.1**), iodine and hypervalent iodine(III) in acetonitrile or toluene, respectively. X-ray crystallography demonstrated potential for mimicry of natural peptide turn side-chain and backbone conformations.

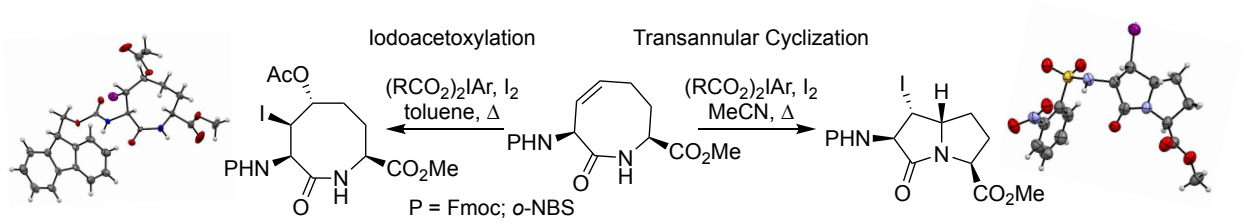

2.2 Introduction

Stereoselective synthesis and functionalization of ring systems are fundamental goals in organic and medicinal chemistry.[1] In peptide mimicry, stereo-controlled ring synthesis is desired to replicate precisely the side-chain and backbone orientations responsible for biological activity.[2] Constrained dipeptide lactam and azabicyclo[X.Y.0]alkanone rings have shown great utility for the mimicry of biologically active peptide secondary structures.[3,4] Although the stereoselective synthesis and functionalization of small ring lactams have been effectively accomplished, their introduction into bicyclic motifs, and the construction and modification of their larger 7–9-member ring counterparts remain two relatively unmet challenges.[5] Employing unsaturated 7–9-membered lactams, stereo–controlled means have now been conceived for their conversion to fused bicycles

composed of small ring systems (fused 5,5-, 5,6- and 6,4-bicycles **2.1**–**2.5**) as well as their functionalization (e.g., **2.6**–**2.8**, Figure 2.1). Exploring the scope and limitations of this method, a set of turn mimics bearing ring substituents has been made for replicating peptide geometry.

Recently,[6,7] a ring-closing metathesis (RCM)–transannular lactam cyclization strategy was disclosed for the synthesis of iodo substituted azabicyclo[X.Y.0]alkanone amino acid derivatives: e.g. fused 5,5-, 6,5-, 6,6- and 7,5-bicycles (**2.1, 2.9**–**2.11**, Scheme 2.1, Figure 2.1). Iodolactamization using iodine gave effectively 6,5-, 6,6- and 7,5-bicycles respectively from 9- and 10-membered lactams; however, similar conditions (i.e., I_2, THF, 80 °C or I_2, $NaHCO_3$, rt) failed to induce cyclization of 7- and 8-membered lactams **2.15** and **2.16,** as well as 9-membered lactam isomers **2.15c** and **2.16c**.

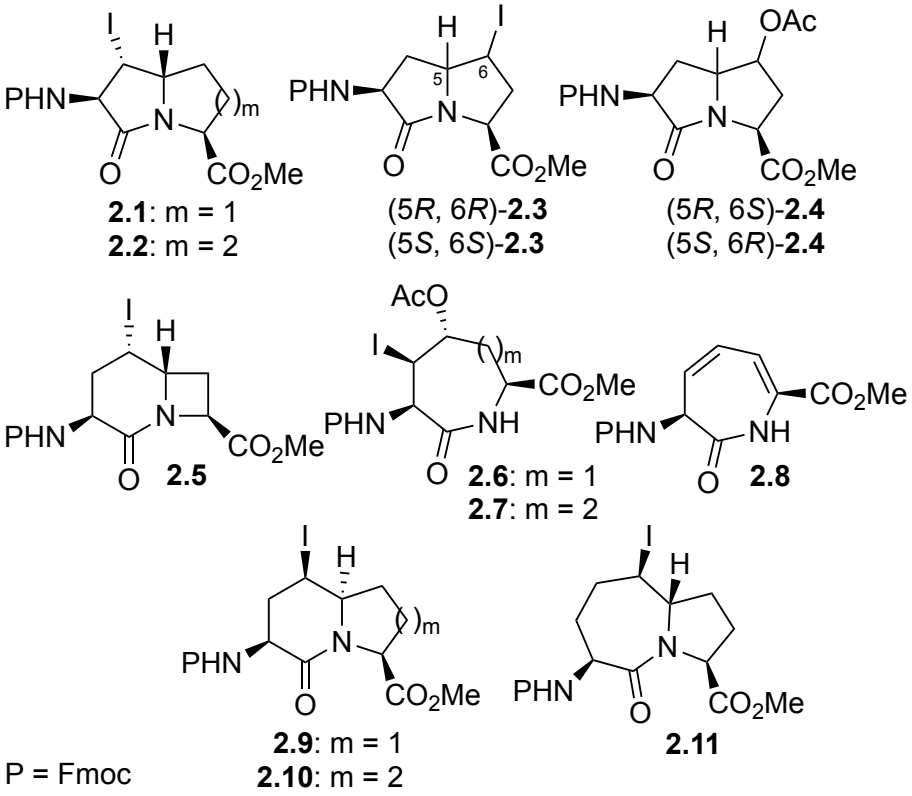

Figure 2.1: Novel bicycles (**2.2**–**2.5**) and lactams (**2.6**–**2.8**) and previously synthesized bicycles (**2.1** and **2.9**–**2.11**) from transannular lactamization and iodoacetoxylation reactions

A breakthrough in the transannular iodolactamization occurred on addition of diacetoxy iodobenzene (DIB) to the I_2 mixture, which converted **2.16b** diastereoselectively to pyrrolizidinone **2.1**.[6] Previously, DIB had been used in oxidative cyclization of *o*-hydroxystyrenes to benzofurans,[8] and *in situ* generation of hypervalent iodine species from DIB and I_2 has been employed in aromatic ring,[9] olefin[10] and alkyne[11] functionalization using halogen, oxygen and carbon nucleophiles. The nature of the hypervalent iodine reagent has, to our knowledge, yet to be examined in such chemistry, particularly with nitrogen nucleophiles. By studying the influence of sterically hindered carboxylate and aromatic ligands with varying electron densities, effective transannular iodolactamization as well as iodoacetoxylation of unsaturated lactams has now been achieved to provide stereoselectively novel 5,5-, 5,6- and 6,4-fused and 7- and 8-membered ring systems 2.2–2.8 (Figure 2.1).

2.3. Results and Discussion

Unsaturated lactams of 7- to 9-atoms were made by coupling 4–7-carbon chain length ω-olefin amino carboxylates[12] **2.12a**,**b** and **2.13a**–**c**, followed by RCM on the resulting dipeptides **2.14a**–**d** (Scheme 2.1).[6] *N*-(Fmoc)Vinylglycine **2.12a** was coupled as its acid chloride to 2-*N*-(Dmb)aminopent-4-enoate **2.13a**, hex-5-enoate **2.13b** and hept-6-enoate **2.13c** to afford dipeptides **2.14a**–**c** in 55%, 46% and 57% yields respectively.[6] Dipeptide **2.14d** was prepared in 71% yield by coupling of *N*-(Fmoc)allylglycine (**2.12b**) and 2-*N*-(Dmb)aminohex-5-enoate (**2.13b**) using HATU and *N*-ethylmorpholine in DCM. For RCM, less (10–12 mol% vs 30–35 mol%) second generation Grubb's catalyst in 1,2-dichloroethane at reflux gave higher yields in shorter reaction times (24 h vs 72 h) than first generation Grubb's catalyst in dichloromethane at reflux: e.g., 80% vs 68% yield of lactam **2.15c**. Lactams **2.15a**–**d** were converted to **2.16a**–**d** in 70–80% yields by Dmb group removal using 50% TFA in DCM. Attempts at transannular iodolactamization of 7–9-membered lactams failed using iodine in THF, MeCN or toluene at rt to reflux resulting in loss

of the Dmb group in the case of **2.15a**–**d** and recovered starting material from **2.16a**–**d**. The cyclization of **2.15b** was also unsuccessful using I_2 and DIB.

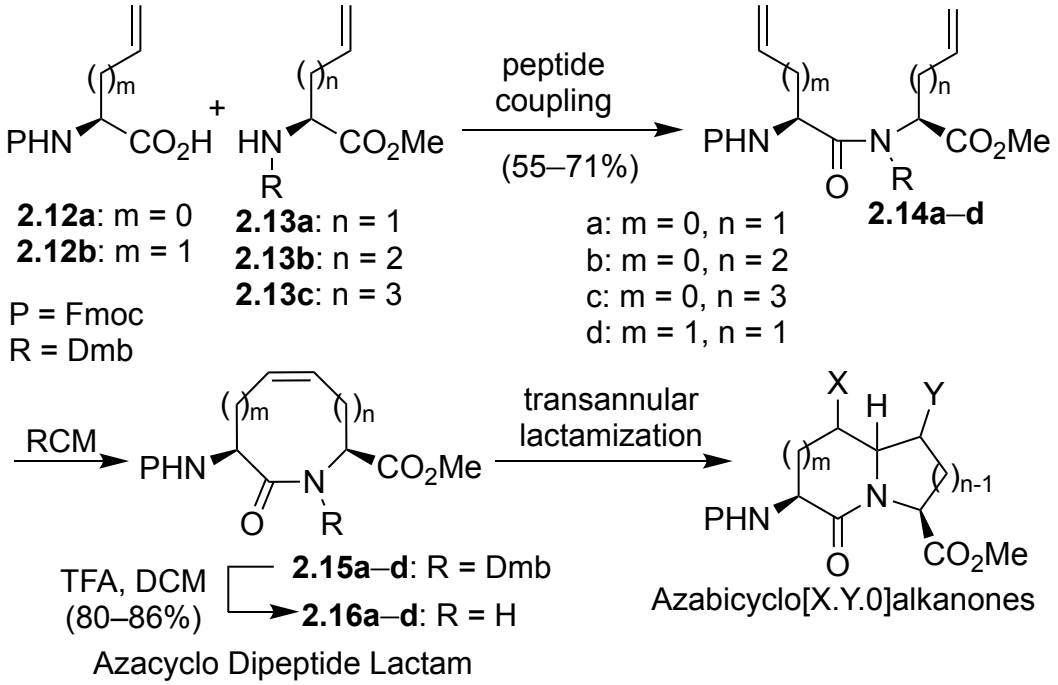

Scheme 2.1. Synthetic strategy to azacyclo- and azabicycloalkanones of different ring sizes

In acetonitrile, pyrrolizidinone **2.1** was prepared from 8-membered lactam **2.16b**, DIB and I_2 at reflux in 62% yield.[6] Moreover, iodoindolizidin-9-one **2.2** was prepared diastereoselectively in 52% yield using the same conditions on 9-membered lactam **2.16c** (entry 1, Table 2.1). The ligands on the hypervalent iodine were examined in the cyclization of lactams **2.16b** and **2.16c** using a set of iodonium reagents,[13] possessing different aryl substituents and carboxylates,[14] in MeCN at 80 °C (Table 2.1). Notably higher yields were typically obtained employing electron rich aromatic substituents and bulky carboxylates. The highest yields (78% and 75%) of pyrrolizidinone and indolizidinone **2.1** and **2.2** were obtained using 4-methoxy-iodosobenzene di-(adamantane-1-carboxylate) (MIDAd, entry 10, Table 2.1). Concurrent iodination of the Fmoc group using bis(trifluoroacetoxy)iodobenzene gave the corresponding bicycles as 2,7-diiodo-Fmoc derivatives

2.1a and **2.2a** (entry 11, Table 2.1, Experimental Section), which were characterized by X-ray crystallography and NMR spectroscopy.

Table 2.1. Influence of hypervalent(III)iodine on transannular iodolactamization

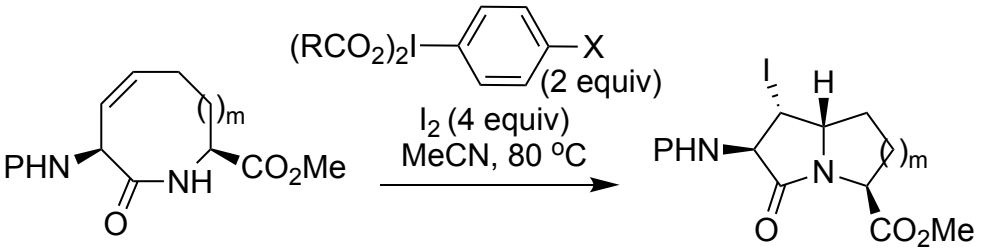

P = Fmoc **2.16b**: m = 1
2.16c: m = 2

2.1: m = 1
2.2: m = 2

entry	X	R	% yield **2.1** (m = 1)	% yield **2.2** (m = 2)
1	H	Me	62[6]	52
2	F	Me	51	52
3	Me	Me	52	60
4	OMe	Me	62	68
5	H	*t*-Bu	61	62
6	Me	*t*-Bu	59	61
7	OMe	*t*-Bu	71	70
8	CF_3	Ad[a]	61	57
9	H	Ad[b]	65	62
10	OMe	Ad[c]	78	75
11	H	CF_3	51[d]	35[d]

[a]8 equiv. of hypervalent iodine and 16 equiv. of I_2 employed. [b]6 equiv. of hypervalent iodine and 12 equiv. of I_2 employed. [c]3 equiv. of hypervalent iodine and 6 equiv. of I_2 employed. [d]Isolated as 2,7-diiodo- Fmoc derivatives **2.1a** and **2.2a**. Ad = 1-Adamantane

Using DIB and I_2 in MeCN at 80 °C, 8-membered lactam **2.16d** gave a mixture of 6-iodo- and 6-acetoxy pyrrolizidinones **2.3** and **2.4** and azetidinylpiperidine **2.5** (entry 1, Table 2.2). On the other hand, 7-membered lactam **2.16a** failed to react. Application of the MIDAd conditions on lactam **2.16d** increased slightly the yields of iodopyrrolizidinones **2.3** and azetidine **2.5** (entry 2, Table

2.2). On lactam **2.16a**, the MIDAd conditions caused dehydration yielding 35% of azepinone **2.8** (Figure 2.1), as ascertained by X-ray crystallography.

Table 2.2. Synthesis of azabicyclo[3.3.0]- and [4.2.0]alkanone amino esters **2.3**–**2.5**[a]

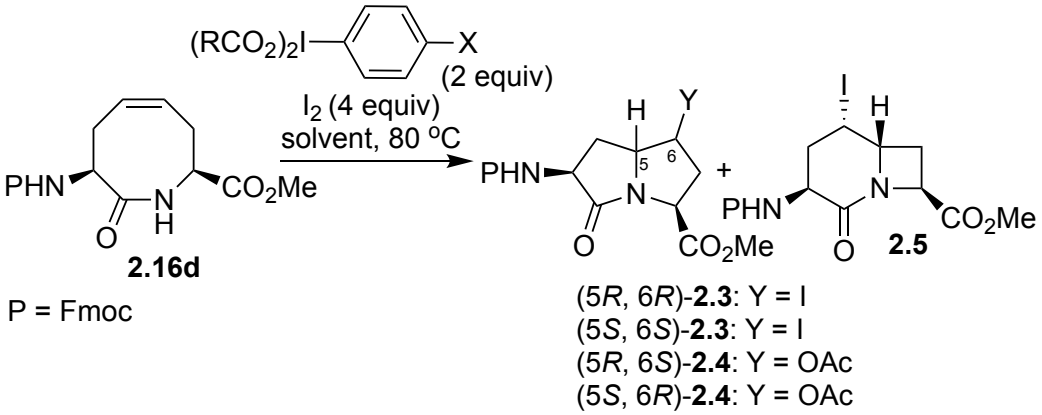

	X	R	isolated yield (%)				
			(5*R*,6*R*)-**2.3**	(5*S*,6*S*)-**2.3**	(5*R*,6*S*)-**2.4**	(5*S*,6*R*)-**2.4**	**2.5**
1	H	Me	20	18	5	-	4
2	OMe	Ad	21	19	-	-	8
3	H	Me	15	16	-	4	-

[a]Solvent = MeCN (entries 1 and 2); toluene (entry 3)

In toluene, 7- and 8-membered lactams **2.16a** and **2.16b** reacted with DIB and I_2 to give iodoacetoxylation products **2.6** and **2.7** in 59% and 70% yields, respectively (Scheme 2.2). On the other hand, lactam **2.16c** gave 45% yield of indolizidin-9-one **2.2** along with trace amounts of iodoacetoxylation product. Lactam **2.16d** gave (*S*,*S*)- and (*R*,*R*)-6-iodopyrrolizidinones **2.3** (15% and 16%) along with (*S*,*R*)-6-acetoxypyrrolizidinone **2.4** (4%) and trace amounts of iodoacetoxylation product (Table 2.2).

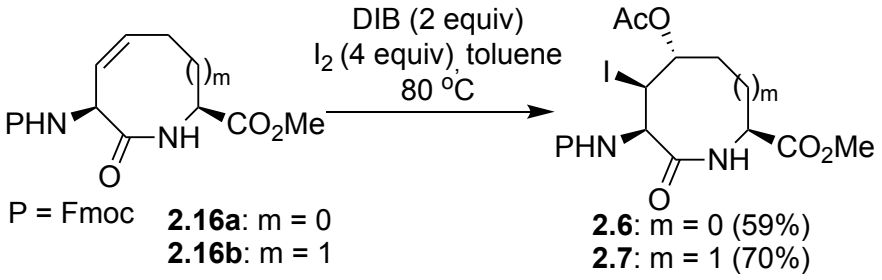

Scheme 2.2. Synthesis of iodoacetoxy lactams

Stereochemical assignments for the ring systems were made based on a combination of NMR spectroscopy and X-ray crystallography [Supporting Information (SI)]. The configurations of iodo acetates **2.6** and **2.7** were assigned based on analysis of dihedral angle coupling constants, which correlated with the X-ray structure of the latter.

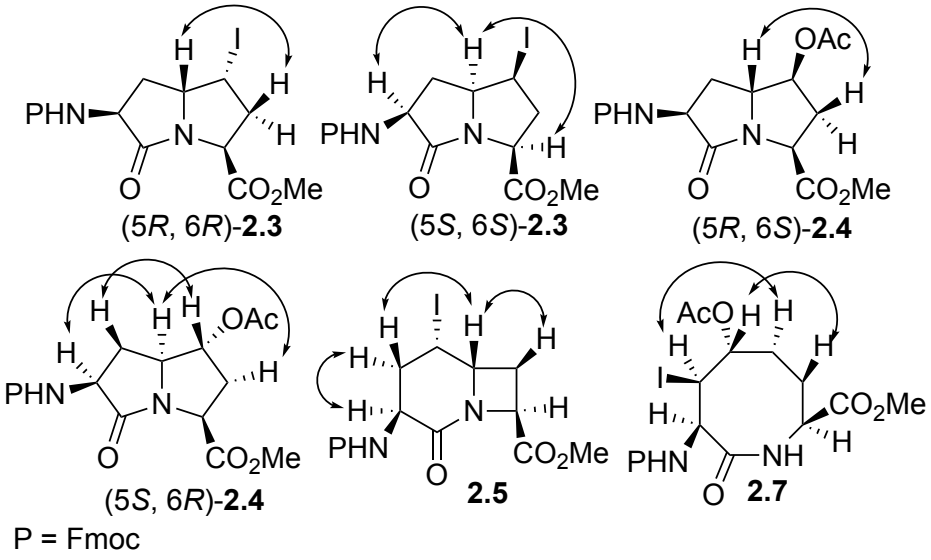

Figure 2.2. Representative NOESY correlations used to assign the relative configurations of ring systems **2.3**–**2.5** and **2.7**.

After through-bond correlations were made using COSY experiments to assign all protons in the bicycle, through-space nuclear Overhauser effects were measured to correlate the stereochemistry of the amino acid derived α-carbons with the newly generated ring fusion and iodide or acetate bearing carbons (Figure 2.2). The trans relationship of the ring fusion and iodide carbon bearing

protons was in certain cases inferred based on the reaction mechanism. In addition, in bicycles (5*R*, 6*R*)-**2.3,** (5*R*, 6*S*)-**2.4** and **2.5**, up-field shifting of the β-proton was observed due to anisotropy from the neighboring carboxylate.[15]

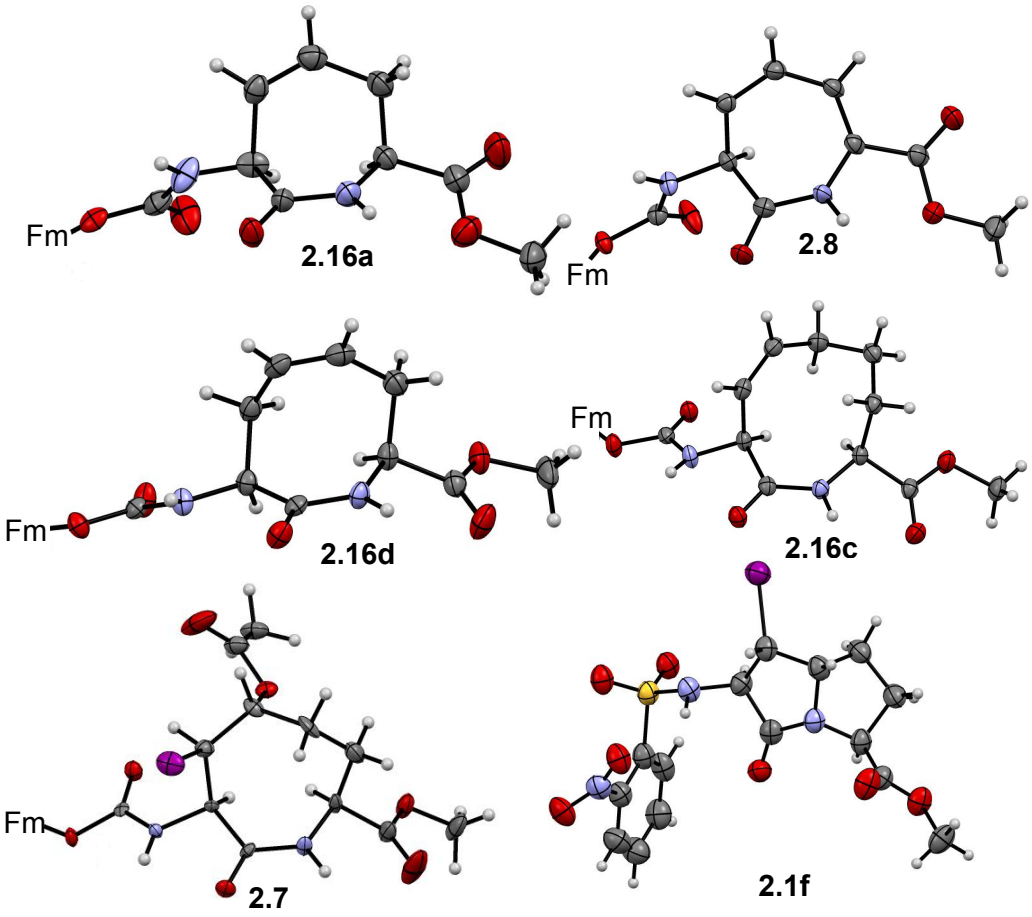

Figure 2.3 X-ray structures of lactams **2.7**, **2.8**, **2.16a,c,d** and **2.1f** (fluorenylmethyl group removed and represented as Fm for clarity; C, gray; H, off-white; N, blue; O, red; I, magenta; S, Yellow).

Type VI β-turn mimicry by 7–9-membered lactams was established using X-ray crystallography of **2.16a**, **2.16c** and **2.16d**, as well as 8-membered iodo acetate **2.7** (Figure 2.3, Table 2.3).[16] The dihedral angles of 8- and 9-membered lactams matched closely those of the central residues of an ideal type VI β-turn (except for ϕ^{i+2}); those of 7-membered lactam **2.16a** reflected values of an ideal type VI2 β-turn.

Table 2.3. Comparison of dihedral angles of lactams with ideal secondary structures

Type of β-turn	ϕ^{i+1}	ψ^{i+1}	ϕ^{i+2}	ψ^{i+2}
Ideal type VIb β-turn	–135°	135°	–75°	160°
Ideal type VI2 β-turn	–120°	120°	–60°	0°
7- membered lactam **2.16a**	−120°	178°	−158°	10°
7- membered lactam **2.8**	−89°	174°	−143°	0°
8- membered lactam **2.7**	–158°	155°	–146°	154°
8- membered lactam **2.16d**	–156°	176°	–154°	168°
9-membered lactam **2.16c**	–157°	160°	–151°	175°

2.4 Mechanistic studies

The literature offers two lines of thought on the reaction mechanism using DIB and I_2. Their combination has been suggested to rapidly provide iodobenzene and two equivalents of acetyl hypoiodite, that serves as iodinating agent.[10,17,18] On the other hand, exchange of iodide for one acetoxy group has been suggested to provide acetyl hypoiodite and an acetoxy iodobenzene iodide salt, which reacts with the olefin.[19] In our NMR experiments, DIB and I_2 reacted in CD_3CN to give rapidly iodobenzene and AcOI.[10b] Preparation of AcOI *in situ* from silver acetate (500 mol%) and I_2 (500 mol%) in MeCN, and reaction with lactam **2.16c** gave indolizidinone **2.2** in 45% yield; moreover, addition of 4-iodoanisole (300 mol%) to the reaction mixture increased the yield of **2.2** to 54%. Analysis by LCMS demonstrated that lactam **2.16b** reacted with AcOAg and I_2 to give pyrrolizidinone **2.1** and iodoacetate **2.7** in a 2:1 ratio, that reduced to 1.3:1 on addition of AgI (500 mol%) to the DIB condition indicating that the silver salt may interfere with lactamization, perhaps by amide coordination. Mixing AgOAc with I_2 in CD_3CN gave AcOI, the acetate carbonyl and methyl group ^{13}C NMR signals of which were respectively up- and downfield shifted on addition of anisole (50 mol%), which also caused an up-field shift of the methyl singlet in the ^1H NMR spectrum, indicating coordination between AcOI and the electron rich aromatic ring (SI).[20,21]

Iodination of the Fmoc group using ditrifluoroacetoxyiodobenzene and I_2 may also be explained by *in situ* formation of the iodinating reagent CF_3CO_2I.[22, 23]

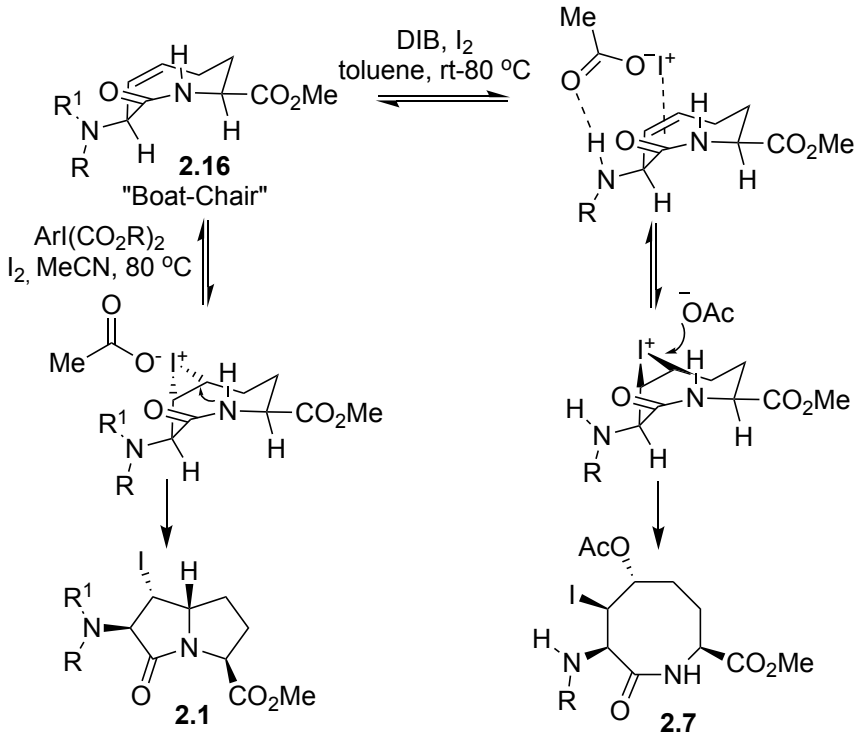

R	R^1	MeCN **2.1:2.7**	PhMe **2.1:2.7**
b: Fmoc	H	62%:NO	NO:70%
e: *o*-NBS	Me	57%:NO	42%:trace
f: *o*-NBS	H	54%:15%	trace:63%

Figure 2.4: Proposed mechanisms for iodoacetoxylation and transannular lactamization (NO = Not Observed).

The influences of hypoiodite, solvent and ring size on the products from iodoacetoxylation and transannular cyclization may be explained using RCO_2I as active reagent. The selectivity of facial attack of olefins **2.16a**–**c** by RCO_2I is directed by the allylic amine which may hydrogen bond with solvent or acyl hypoiodite respectively, in MeCN and toluene. (Figure 2.4). Iodonium ion formation is likely reversible.[24] In toluene, subsequent attack of the iodonium ion by acetate occurs from the opposite face to give **2.6** or **2.7**. In MeCN, the iodonium ion is opened by intramolecular attack of the amide to give bicycles **2.1** and **2.2**. The influences of the allylic amine and hydrogen

bonding were further demonstrated by the synthesis and reactivity of *o*-nitrobenzenesulfonamides (*o*-NBS) **2.16e** and **2.16f** (Figure 2.4). *N*-Methyl sulfonamide **2.16e** cannot hydrogen bond and gave predominantly bicycle **2.1e** in both solvents; sulfonamide **2.16f** behaved like carbamate **2.16b** and gave mainly bicycle **2.1f** and iodoacetate **2.7f** contingent on solvent. Stereochemical assignment for **2.1e**, **2.1f** and **2.7f** were based on NMR spectroscopy and analogy with their Fmoc counterparts. Favored formation of iodoacetate in the smaller ring systems may correlate with distance between the allylic amine and olefin, because a linear relationship between ring size and the acuteness of the allylic bond dihedral angle about the α- and vinyl-carbon C-C bond (**2.16a**, 175°; 2.16b, –154°;[6] 2.16c, –134°) was observed in the X-ray structures of 7–9-membered lactams.

2.5 Conclusions

In conclusion**,** we have shown that diastereoselective transannular iodolactamization and iodoacetoxylation of 7–9- membered lactams can be effectively achieved using the combination of iodine and hypervalent iodine(III). Contingent on solvent, an allylic carbamate appeared to serve as a key directing group for iodonium ion formation. In acetonitrile, subsequent intramolecular trans-annular cyclization provided stereoselectivity 4-iodopyrrolizidinone **2.1** and 4-iodoindolizidinone **2.2**. In toluene, intermolecular attack of acetate provided 7- and 8-membered iodoacetates **2.6** and **2.7**. Bulky carboxylates and electron-rich aromatic ligands on the hypervalent iodine improved yields in the formation of bicycles. X-ray crystallographic analysis has also shown the potential of 7–9-membered lactams to serve as β-turn mimics with complementary structures to those previously reported for azabicyclo[X.Y.0]alkanones. The fundamental findings and novel peptidomimetics from this study offer thus rich potential for the synthesis and functionalization of lactam ring systems for exploring peptide conformation−activity relationships.

2.6 Acknowledgment

This work was supported by NSERC, Canada. We thank Dr. A. Fürtös, K. Venne, M-C. Tang (mass spectrometry); S. Bilodeau, A. Hamel, C. Malveau (NMR spectroscopy), and F. Belanger-Gariepy (X-ray) from the U. de Montréal Laboratories for aid in analyses. Shastri Indo-Canadian Institute, India is thanked for a Quebec Tuition Fee Exemption grant to N.D.P.A.

2.7 References

1. Nicolaou, K. C. *Proc. R. Soc*. A **2014**, 470, 2163.

2. Hanessian, S.; Auzzas, L., *Acc. Chem. Res.* **2008**, *41*, 1241–1251.

3. St-Cyr, D. J.; García-Ramos, Y.; Doan, N.-D.; Lubell, W. D., *Peptidomimetics I*; Topics in Heterocyclic Chemistry, Vol. 48, 125–176, Lubell, W. D. (Ed.), Springer-Berlin Heidelberg, Germany, **2017**.

4. Khashper, A.; Lubell, W. D., *Org. Biomol. Chem.* **2014**, 12, 5052–5070.

5. Ballet, S.; Guillemyn, K.; Van der Poorten, O.; Schurgers, B.; Verniest, G.; Tourwé, D., *Peptidomimetics I*; Topics in Heterocyclic Chemistry, Vol. 48, 177–209, Lubell, W. D. (Ed.), Springer-Berlin Heidelberg, Germany, **2017**.

6. Atmuri, N. D. P.; Lubell, W. D., *J. Org. Chem.* **2015**, *80*, 4904–4918.

7. Surprenant, S.; Lubell, W. D., *Org. Lett.* **2006**, *8*, 2851–2854.

8. Singh, F. V.; Wirth, T., *Synthesis* **2012,** *44*, 1171–1177.

9. (a) Ogata, Y.; Aoki, K., *J. Am. Chem. Soc.* **1968**, *90*, 6187–6191; (b) Evans, P. A.; Brandt, T. A., *J. Org. Chem.* **1997**, *62*, 5321–5326; (c) Togo, H.; Muraki, T.; Hoshina, Y.; Yamaguchi, K.; Yokoyama, M., *J. Chem. Soc., Perkin Trans. 1* **1997**, 787–794.

10. (a) Gottam, H.; Vinod, T. K., *J. Org. Chem.* **2010,** *76*, 974–977; (b) Achar, T. K.; Maiti, S.; Mal, P., *Org. Biomol. Chem*. **2016**, *14*, 4654–4663.

11. Priebbenow, D. L.; Gable, R. W.; Baell, J., *J. Org. Chem.* **2015**, *80*, 4412–4418.

12. Atmuri, N. D. P.; Lubell, W. D. *Org. Synth.* **2015**, 92, 103−116.

13. (a) Chun, J.-H.; Pike, V. W., *J. Org. Chem.* **2012**, *77*, 1931–1938; (b) Wu, Y.; Izquierdo, S.; Vidossich, P.; Lledós, A.; Shafir, A., *Angew. Chem. Int. Ed.*, *128* , 7268–7272; (c) Wang, B.; Qin, L.; Neumann, K. D.; Uppaluri, S.; Cerny, R. L.; DiMagno, S. G., *Org. Lett.* **2010**, *12*, 3352–3355.

14. Stang, P. J.; Boehshar, M.; Wingert, H.; Kitamura, T., *J. Am. Chem. Soc.* **1988**, *110*, 3272–3278.

15. Mauger, A.; Irreverre, F.; Witkop, B., *J. Am. Chem. Soc.* **1966**, *88*, 2019–2024.

16. Creighton, C. J.; Leo, G. C.; Du, Y.; Reitz, A. B., *Biorg. Med. Chem.* **2004,** *12*, 4375–4385.

17. (a) Courtneidge, J. L.; Lusztyk, J.; Pagé, D., *Tetrahedron Lett.* **1994**, *35*, 1003–1006; (b) Chen, E.; Keefer, R.; Andrews, L., *J. Am. Chem. Soc.* **1967**, *89*, 428–430.

18.Radical intermediates may be possible. See: (a) Zard, S. Z., *Chem. Soc. Rev.* **2008**, *37*, 1603–1618; (b) Glover, S. A.; Goosen, A., *J. Chem. Soc., Perkin Trans. 1* **1977**, 1348–1356.

19. (a) Yuan, W.; Szabó, K. J., *Angew. Chem. Int. Ed.* **2015**, *127*, 8653–8657; (b) Geary, G. C.; Hope, E. G.; Stuart, A. M., *Angew. Chem. Int. Ed.* **2015**, *54* (49), 14911–14914; (c) Ilchenko, N. O.; Tasch, B. O.; Szabó, K. J., *Angew. Chem. Int. Ed.* **2014**, *53*, 12897–12901; (d) Ulmer, A.; Brunner, C.; Arnold, A. M.; Pöthig, A.; Gulder, T., *Chem. Eur. J.* **2016**, *22*, 3660–3664.; (e) Boye, A. C.; Meyer, D.; Ingison, C. K.; French, A. N.; Wirth, T., *Org. Lett.* **2003**, *5*, 2157–2159.

20. Heasley, V. L.; Holstein, L. S.; Moreland, R. J.; Rosbrugh, J. W.; Shellhamer, D. F., *J. Chem. Soc., Perkin Trans. 2* **1991**, 1271–1274.

21. Heasley, V. L.; Holstein, L. S.; Moreland, R. J.; Rosbrugh, J. W.; Shellhamer, D. F., *J. Chem. Soc., Perkin Trans. 2* **1991**, 1271–1274.

22. Carruthers, W.; Coggins, P.; Weston, J. B., *J. Chem. Soc., Perkin Trans. 1* **1991**, 611–616.

23. Lipshutz, B. H.; Barton, J. C., *J. Am. Chem. Soc.* **1992**, *114*, 1084–1086.

24. Brown, R., *Acc. Chem. Res.* **1997**, *30*, 131–137.

2.8 Experimental section

2.8.1 General Methods: Unless otherwise specified, all non-aqueous reactions were performed under an inert argon atmosphere. All glassware was dried with a flame under flushing argon gas or stored in the oven, and let cool under an inert atmosphere prior to use. Anhydrous solvents (THF, DCM, MeCN and DMF) were obtained by passage through solvent filtration systems (Glass Contour, Irvine, CA) and solvents were transferred by syringe. Reaction mixture solutions (after aqueous workup) were dried over anhydrous $MgSO_4$ or Na_2SO_4, filtered, and rotary-evaporated under reduced pressure. Flash chromatography[1] was performed on 230−400 mesh silica gel, and thin-layer chromatography was performed on a alumina plates coated with silica gel (Merck 60 F254 plates). Visualization of the developed chromatogram was performed by UV absorbance or staining with ceric ammonium molybdate or potassium permanganate solutions. Melting points were obtained on a Buchi melting point B-540 apparatus and are uncorrected. Specific rotations, $[\alpha]_D$ values, were calculated from optical rotations measured at 25 °C in $CHCl_3$ or MeOH at the specified concentrations (*c* in g/100 ml) using a 0.5-dm cell length (l) on a Anton Paar Polarimeter, MCP 200 at 589 nm, using the general formula: $[\alpha]_D^{25} = (100 \times \alpha)/(l \times c)$. Accurate mass measurements were performed on an LC-MSD instrument in electrospray ionization (ESI-TOF) mode at the Université de Montréal Mass Spectrometry facility. Sodium adducts $[M + Na]^+$ were used for empirical formula confirmation. Nuclear magnetic resonance spectra (^1H, ^{13}C, DEPT, COSY, HSQC, NOSEY) were recorded on Bruker 400, 500 and 700 MHz spectrometers. ^1H NMR spectra were referenced to $CDCl_3$ (7.26 ppm), CD_3OD (3.31 ppm), DMSO-d_6 (2.50 ppm) or $(CD_3)_2CO$ (2.05 ppm) and ^{13}C NMR spectra were measured in $CDCl_3$ (77.16 ppm), CD_3OD (49.0 ppm), DMSO-d_6 (39.52 ppm) or $(CD_3)_2CO$ (29.84 ppm) as specified below. ^1H and ^{13}C NMR spectra for the dipeptides **2.14a** and **2.14b** were recorded at 100 °C to coalesce signals due to conformational isomers. Coupling constant *J* values were measured in Hertz (Hz) and chemical

shift values in parts per million (ppm). Infrared spectra were recorded in the neat on a Perkin Elmer Spectrometer FT-IR instrument, and are reported in reciprocal centimeters (cm^{-1}). Crystallographic data for lactams **2.1a**, **2.7**, **2.8**, **2.16a,c,d** were acquired on a Bruker venture metaljet diffractometer at the Université de Montréal X-ray Regional Facility. Mixture of diastereomers (**5*R*, 6*S*)- 2.4**, (**5*S*, 6*R*)- 2.4** and **2.5** were separated by preparative reverse phase HPLC (Phenomenex Gemini 5 µm column, C18, 250 mm 21.2 mm) using a solvent gradient from 50% to 90% MeOH (containing 0.1% TFA) in water (containing 0.1% TFA) over 40-60 min at a flow rate of 10 mL/min.

2.8.2 Reagents: (*S*)-*N*-(Fmoc)Vinylglycine,[2] *N*-(Fmoc)Allylglycine,[3] *N*-(Dmb)amino ester[3a, 4] all were synthesized according to literature methods. The iodonium reagents with different aryl substituents and carboxylates were prepared according to literature procedure.[5] Iodine, Grubbs 1st Generation Catalyst (dichloro(benzylidene)bis(tricyclohexylphosphine)ruthenium(II)), Grubbs 2nd Generation Catalyst (dichloro[1,3-bis(2,4,6-trimethylphenyl)-2-imidazolidinylidene](benzylidene)(tricyclohexylphosphine)- ruthenium(II)), diisopropyl ethyl amine (DIEA), sodium triacetoxyborohydride, (diacetoxyiodo)benzene, thionyl chloride, all were purchased from Aldrich and used as received; [bis(trifluoroacetoxy)iodo]benzene was purchased from Alfa Aesar and used without further purification; HATU was purchased from Chem-Impex and used as received.

2.8.3 Synthetic experimental conditions and characterization data of compounds:

(*S*,*S*)-Methyl 2-[*N*-[2-(*N*-Fmoc-amino)but-3-enoyl]-*N*-(2,4-dimethoxybenzyl)amino]pent-4-enoate (2.14a)

(*S*)-*N*-(Fmoc)Vinylglycine (**2.12a**; 2.1 g, 6.51 mmol) was treated with thionyl chloride (0.97 mL, 13.02 mmol) in DCM (35 mL) at 0 °C. The resulting solution was then heated to reflux for 3 h and cooled. The volatiles were evaporated. The residue was dissolved and evaporated three times from DCM. Without further purification, acid chloride **2.12e** was dissolved in DCM (25 mL), cooled to

0 °C, and treated with *N*-(Dmb)allylglycine (**2.13a**; 1.3 g, 4.65 mmol, 30 mL DCM) at 0 °C. The resulting mixture was stirred at room temperature for 3 h. The volatiles were evaporated, and the residue was taken up in a minimum volume of DCM, applied onto a silica gel column, and eluted with 30−35% EtOAc/hexanes to give dipeptide **2.14a** (1.51 g, 2.58 mmol, 55%) as a colorless oil that solidified on standing: R_f = 0.62 (4:6 EtOAc/hexanes, visualized by UV); $[\alpha]_D^{25}$ –22.0 (*c* 0.5, $CHCl_3$); FT-IR (neat) ν_{max} 3406, 2949, 1718, 1646, 1611, 1588, 1506, 1437, 1290, 1206, 1156, 1032, 919, 759, 738, 533, 426 cm^{-1}; ^1H NMR (500 MHz, DMSO-d_6, 100°C) δ 7.84-7.85 (d, 2H, *J* = 7.5 Hz), 7.67-7.70 (t, 2H, *J* = 7.1 Hz), 7.38-7.42 (m, 2H), 7.29-7.32 (t, 2H, *J* = 7.5 Hz), 7.21(br s, 1H), 7.02 (br s, 1H), 6.55-6.56 (d, 1H, *J* = 1.9 Hz), 6.45-6.47 (m, 1H), 5.85-5.92 (m, 1H), 5.64-5.72 (m, 1H), 5.23-5.29 (m, 2H), 5.17-5.20 (t, 1H, *J* = 6.9 Hz), 4.94-4.97 (m, 2H), 4.55-4.58 (d, 1H, *J* = 16.1 Hz), 4.28-4.41 (m, 3H), 4.20-4.24 (m, 2H), 3.75 (s, 3H), 3.77 (s, 3H), 3.49 (s, 3H), 2.60-2.68 (m, 1H), 2.41-2.47 (m, 1H); ^{13}C NMR (125 MHz, DMSO-d_6, 100 °C) δ 169.6, 160.1, 158.1, 154.5, 143.4, 143.3, 140.2, 134.2, 133.6, 133.4, 129.8, 127.0, 126.4, 124.6, 124.7, 119.4, 117.1, 116.6, 104.4, 98.1, 78.5, 65.5, 57.9, 54.9, 54.8, 53.6, 50.9, 46.4, 32.5 ; HRMS (ESI-TOF) m/z $[M + H]^+$ calcd for $C_{34}H_{37}N_2O_7$ 585.2595, found 585.2575.

(*S*,*S*)-Methyl 2-[*N*-[2-(*N*-Fmoc-amino)pent-4-enoyl]-*N*-(2,4-dimethoxybenzyl)amino]pent-4-enoate (2.14d)

N-(Fmoc)Allylglycine (**2.12b**; 1.57 g, 4.65 mmol) and *N*-(Dmb)amino ester **2.13a** (1 g, 3.58 mmol) were dissolved in DCM (25 mL), treated with *N*-ethylmorpholine (0.68 mL, 5.37 mmol) and HATU (2.04 g, 5.37 mmol), stirred for 24 h, and diluted with water. The aqueous layer was extracted with DCM (3 × 50 mL). The combined organic layers were washed with brine (50 mL), dried over anhydrous sodium sulphate, filtered, and concentrated under reduced pressure. The residue was purified by chromatography on silica gel (30−35% EtOAc in hexane) to give dipeptide **2.14d** (1.52g, 2.54 mmol, 71%) as colorless gummy oil: R_f = 0.60 (4:6 EtOAc/hexanes, visualized

by UV); $[\alpha]_D^{25}$ –36.7 (*c* 0.83, $CHCl_3$); FT-IR (neat) ν_{max} 2948, 2841, 1718, 1638, 1612, 1588, 1506, 1437, 1206, 1156, 1117, 1032, 916, 758, 738, 537 cm^{-1}; ^1H NMR (400 MHz, DMSO-d_6, 100 °C) δ 7.84-7.86 (d, 2H, *J* = 7.4 Hz), 7.67-7.69 (m, 2H), 7.38-7.43 (m, 2H), 7.29-7.33 (m, 2H), 7.17-7.19 (d, 1H, *J* = 7.4 Hz), 6.92 (br s, 1H), 6.55-6.56 (d, 1H, *J* = 2.3 Hz), 6.45-6.47 (dd, 1H, *J* = 2.3 Hz), 5.58-5.79 (m, 2H), 5.02-5.12 (m, 2H), 4.87-4.96 (m, 2H), 4.50-4.73 (m, 2H), 4.41-4.45 (m, 1H), 4.30-4.32 (m, 2H), 4.19-4.23 (t, 2H, *J* = 7.0 Hz), 3.78 (s, 3H), 7.75 (s, 3H), 3.49 (s, 3H), 2.59-2.70 (m, 1H), 2.28-2.46 (m, 3H); ^{13}C NMR (100 MHz, DMSO-d_6, 100 °C) δ 171.1, 169.7, 160.0, 157.8, 154.8, 143.3, 140.3, 140.2, 133.4, 129.7, 127.0, 126.9, 126.4, 124.6, 124.5, 119.3, 116.9, 116.2, 104.4, 98.2, 78.5, 65.4, 57.9, 54.9, 54.8, 50.8, 50.4, 46.4 ,36.0, 32.6; HRMS (ESI-TOF) m/z $[M + H]^+$ calcd for $C_{35}H_{39}N_2O_7$ 599.2751, found 599.2778.

(3*S*,7*S*,*Z*)-Methyl 3-(*N*-Fmoc-amino)-1-(2,4-dimethoxybenzyl)-2-oxo-2,3,6,7-tetrahydro-1H-azepine-7-carboxylate (2.15a)

Dipeptide **2.14a** (1.2 g, 2.05 mmol) was dissolved in DCM (2 L), treated with the Grubbs first-generation catalyst (338 mg, 0.410 mmol), heated, and stirred at reflux for 2 days. After completion of the reaction was ascertained by TLC, the volatiles were removed under reduced pressure. The residue was taken up in a minimum volume of DCM, applied onto a silica gel column, and eluted with 35−40% EtOAc in hexanes. Evaporation of the collected fractions afforded macrocycle **2.15a** (950 mg, 1.70 mmol, 83% yield) as off-white solid: R_f = 0.46 (4:6 EtOAc/hexanes, visualized by UV); $[\alpha]_D^{25}$ 6.6 (*c* 1, $CHCl_3$); mp 91-93 °C, FT-IR (neat) ν_{max} cm^{-1}; ^1H NMR (500 MHz, $CDCl_3$) δ 7.76−7.77 (d, 2H, *J* = 7.5 Hz), 7.62−7.64 (d, 2H, *J* = 7.3 Hz), 7.39−7.42 (t, 2H, *J* = 7.4 Hz), 7.31−7.33 (t, 2H, *J* = 7.4 Hz), 7.08−7.09 (d, 1H, *J* = 8.3 Hz), 6.38−6.47 (m, 3H), 5.63−5.64 (m, 1H), 5.55−5.59 (m, 1H), 5.41−5.49 (m, 1H), 4.94−5.00 (m, 1H), 4.82−4.85 (d, 1H, *J* = 15.7 Hz), 4.44−4.50 (m, 1H), 4.33-4.44 (m, 2H), 4.23-4.26 (t, 1H, *J* = 7.2 Hz), 3.78 (s, 3H), 3.76 (s, 3H),

3.55 (s, 3H), 2.40-2.43 (m, 1H), 2.19-2.25 (m, 1H); ^{13}C NMR (125 MHz, $CDCl_3$) δ 171.4, 168.7, 160.4, 158.0, 144.0, 143.9, 141.4, 129.9, 129.6, 127.8, 127.5, 127.2, 125.3, 120.0, 117.3, 104.1, 98.1, 67.2, 57.4, 55.5, 55.4, 55.3, 52.4, 51.8, 47.2, 41.5, 29.8.; HRMS (ESI-TOF) m/z $[M + H]^+$ calcd for $C_{32}H_{33}N_2O_7$ 557.2282, found 557.2264.

(3*S*,10*S*,*Z*)-Methyl-3-(*N*-Fmoc-amino)-1-(2,4-dimethoxybenzyl)-2-oxo-1,2,3,6,7,8-hexahydroazocine-8-carboxylate (2.15d)

Dipeptide **2.14d** (1.4 g, 2.34 mmol) was dissolved in DCM (2 L), treated with the Grubbs first-generation catalyst (385 mg, 0.47 mmol), heated, and stirred at reflux for 2 days. After 2 days, TLC showed remaining **2.14d**, and more catalyst (193 mg, 0.23 mmol) was added to the reaction mixture, which was heated at reflux and stirred for 2 days. The volatiles were removed under reduced pressure. The residue was taken up in a minimum volume of DCM, applied onto a silica gel column, and eluted with 35−40% EtOAc in hexanes. Evaporation of the collected fractions afforded macrocycle **2.15d** (820 mg, 1.43 mmol, 61% yield) as off-white solid: R_f = 0.48 (4:6 EtOAc/hexanes, visualized by UV); mp 89-91 °C, $[\alpha]_D^{25}$ 11.8 (*c* 1, $CHCl_3$); FT-IR (neat) ν_{max} 3322, 2945, 1739, 1715, 1648, 1612, 1506, 1448, 1418, 1206, 1154, 1033, 759, 738, 620, 539 cm^{-1}; ^{1}H NMR (500 MHz, $CDCl_3$) δ 7.76−7.77 (d, 2H, *J* = 7.5 Hz), 7.62−7.63 (d, 2H, *J* = 7.4 Hz), 7.38−7.41 (t, 2H, *J* = 7.5 Hz), 7.30−7.33 (m, 2H), 7.10−7.12 (d, 1H, *J* = 8.3 Hz), 6.51−6.52 (d, 1H, *J* = 5.8 Hz), 6.39−6.42 (m, 2H), 5.69−5.75 (m, 1H), 5.43−5.46 (m, 1H), 4.98−5.01 (m, 1H), 4.89-4.92 (m, 1H), 4.57−4.61 (d, 1H, *J* = 15.7 Hz), 4.38-4.39 (d, 2H, *J* = 7.2 Hz), 4.31-4.34 (d, 1H, *J* = 15.7 Hz), 4.21-4.24 (t, 1H, *J* = 7.3 Hz), 3.78 (s, 3H), 3.77 (s, 3H), 3.45 (s, 3H), 2.98-3.05 (m, 1H), 2.56-2.72 (m, 2H), 2.37-2.43 (m, 1H); ^{13}C NMR (125 MHz, $CDCl_3$) δ 171.8, 169.4, 160.1, 157.7, 155.7, 144.10, 143.9, 141.4, 129.7, 127.8, 127.5, 127.2, 127.0, 125.4, 125.3, 120.1, 120.0, 117.2, 104.12, 98.1, 67.1, 57.6, 55.4, 55.3, 52.3, 52.1, 47.3, 41.0, 35.1, 28.4; HRMS (ESI-TOF) m/z $[M + H]^+$ calcd for $C_{33}H_{35}N_2O_7$ 571.2439, found 571.2463.

(3*S*,9*S*,*Z*)-Methyl-3-(*N*-Fmoc-amino)-1-(2,4-dimethoxybenzyl)-2-oxo-1,2,3,6,7,8,9-heptahydro-1H-azonine-9-carboxylate (2.15c)

Dipeptide **2.14c** (570 g, 0.93 mmol, prepared according to reference 3a) was dissolved in 1,2-dichloroethane (2 L), treated with the Grubbs second-generation catalyst (95 mg, 0.11 mmol), heated at reflux, and stirred for 24 h. After completion of the reaction, the volatiles were removed under reduced pressure. The residue was taken up in a minimum volume of DCM, applied onto a silica gel column, and eluted with 35−40% EtOAc in hexanes. Evaporation of the collected fractions afforded macrocycle **2.15c** (433 mg, 0.74 mmol, 80%). Spectroscopic data was in accordance with ref 3a.

(3*S*,7*S*,*Z*)-Methyl-3-(*N*-Fmoc-amino)-2-oxo-2,3,6,7-tetrahydro-1H-azepine-7-carboxylate (2.16a)

Lactam **2.15a** (1.1 g, 1.97 mmol) was treated with TFA (10 mL) in DCM (100 mL) overnight. The volatiles were removed under vacuum, and the residue was purified by chromatography on silica gel (40−50% EtOAc in hexane) to give tetrahydroazepine **2.16a** (751 mg, 1.85 mmol, 86%) as white solid: R_f = 0.22 (4:6 EtOAc/hexanes, visualized by UV); mp 187−190 °C, $[\alpha]_D^{25}$ 5.8 (*c* 1, $CHCl_3$); FT-IR (neat) ν_{max} 3324, 2958, 1734, 1672, 1541, 1421, 1361, 1254, 1202, 1101, 1087, 1048, 1031, 884, 762, 733, 646, 588 cm^{-1}; ^1H NMR (500 MHz, $CDCl_3$) δ 7.75−7.77 (d, 2H, J = 7.5 Hz), 7.60−7.63 (m, 2H), 7.38−7.41 (t, 2H, *J* = 7.5 Hz), 7.30−7.33 (m, 2H), 6.53−6.54 (d, 1H, *J* = 6.0 Hz), 6.19-6.20 (d, 1H, *J* = 6.2 Hz), 5.60−5.65 (m, 1H), 5.47−5.49 (m, 1H), 5.32−5.33 (m, 1H), 4.63-4.68 (m, 1H), 4.39−4.40 (d, 2H, J = 7.2), 4.22−4.25 (t, 1H, *J* = 7.1 Hz), 3.82 (s, 3H), 2.71-2.75 (m, 1H), 2.30-2.37 (m, 1H); ^{13}C NMR (125 MHz, $CDCl_3$) δ 170.7, 170.3, 156.0, 144.0, 143.8, 141.4, 128.7, 127.8, 127.2, 126.4, 125.2, 120.1, 67.3, 53.4, 52.0, 51.4, 47.2, 33.5; HRMS (ESI-TOF) m/z $[M + H]^+$ calcd for $C_{23}H_{23}N_2O_5$ 407.1601, found 407.1583.

(2*S*,7*S*,*Z*)-Methyl-3-(*N*-Fmoc-amino)-2-oxo-1,2,3,4,7,8-hexahydroazocine-8-carboxylate (2.16d)

Lactam **2.15d** (1.1, 1.92 mmol) was treated as described for the synthesis of tetrahydroazepine **2.16a** above with TFA (10 mL) in DCM overnight. Chromatography (30−40% EtOAc in hexane) gave hexahydroazocine **2.16d** (652 mg, 1.55 mmol, 80%) as white solid: R_f = 0.24 (4:6 EtOAc/hexanes, visualized by UV); mp 181-184 °C; $[\alpha]_D^{25}$ –19.6 (*c* 1, $CHCl_3$); FT-IR (neat) ν_{max} 3393, 3319, 1738, 1655, 1516, 1439, 1423, 1370, 1328, 1283, 1221, 1141, 1101, 1000, 967, 917, 881, 781, 736, 620, 572, 549 cm^{-1}; ^1H NMR (500 MHz, $CDCl_3$) δ 7.75−7.77 (d, 2H, *J* = 7.5 Hz), 7.59−7.60 (d, 2H, *J* = 6.5), 7.38−7.41 (m, 2H), 7.30− 7.33 (t, 2H, *J* = 7.45), 6.35−6.36 (d, 1H, *J* = 5.9 Hz), 6.06−6.07 (d, 1H, *J* = 6.6 Hz), 5.82−5.86 (m, 1H), 5.54−5.58 (m, 1H), 4.73-4.77 (q, 1H, *J* = 6.9), 4.48−4.52 (q, 1H, *J* = 6.6), 4.34-4.40 (m, 2H), 4.20-4.23 (t, 1H, *J* = 7.2), 3.83 (s, 3H), 2.88−3.00 (m, 2H), 2.51−2.57 (m, 1H), 2.34-2.40 (m, 1H); ^{13}C NMR (125 MHz, $CDCl_3$) δ 172.2, 171.4, 155.7, 144.0, 143.8, 141.4, 129.6, 127.8, 127.2, 125.4, 125.2, 120.1, 67.2, 53.3, 53.2, 52.4, 47.2, 34.7, 32.9; HRMS (ESI-TOF) m/z $[M + H]^+$ calcd for $C_{24}H_{25}N_2O_5$ 421.1758, found 421.1760.

(3*S*,4*S*,5*S*,8*S*)-Methyl 3-(*N*-Fmoc-amino)-4-iodo-pyrrolizidin-2-one-8-carboxylate (2.1)

In the dark, a solution of lactam **2.16b** (250 mg, 0.59 mmol, prepared according to reference 3a) in acetonitrile (12 mL) was treated with iodine (906 mg, 3.54 mmol) followed by 4-methoxy-iodosobenzene di-(adamantane-1-carboxylate) (**2.18b**, 1057 mg, 1.78 mmol). The resulting mixture was heated to 80 °C for 20-30 min and cooled to room temperature. The volatiles were evaporated under reduced pressure. The residue was chromatographed on silica gel (40−50% EtOAc in hexane) to give pyrrolizidinone **2.1** (255 mg, 0.47 mmol, 78%) as a light-sensitive white solid: spectroscopic data was in accordance with ref 3a.

(2*S*,6*S*,7*S*,8*S*)-8-(*N*-Fmoc-amino)-7-iodo-indolizidin-9-one-2-carboxylate (2.2)

Employing the protocol described for the synthesis of bicycle **2.1**, lactam **2.16c** (200 mg, 0.46 mmol) in acetonitrile (10 mL) was treated with iodine (700 mg, 2.76 mmol) followed by 4-methoxy-iodosobenzene di-(adamantane-1-carboxylate) (**2.18b,** 818 mg, 1.39 mmol). The resulting mixture was heated to 80 °C for 30 min and cooled to room temperature. The residue was chromatographed on silica gel (40−50% EtOAc in hexane) to give indolizidin-9-one **2** (193 mg, 0.34 mmol, 75%) as light-sensitive white solid: R_f = 0.46 (1:1 EtOAc/hexanes, visualized by UV); mp 95-98 °C; $[\alpha]_D^{25}$ −46.8 (*c* 1, $CHCl_3$); FT-IR (neat) ν_{max} 2949, 1694, 1519, 1445, 1199, 1043, 984, 759, 737, 620 cm^{-1}; ^1H NMR (700 MHz, CD_3COCD_3) δ 7.87−7.88 (d, 2H, *J* = 7.6 Hz), 7.74−7.75 (m, 2H), 7.42−7.44 (t, 2H, *J* = 7.5 Hz), 7.34−7.36 (t, 2H, *J* = 7.4 Hz) 7.09-7.10 (d, 1H, *J* = 8.6 Hz), 4.83−4.84 (d, 1H, *J* = 6.2 Hz), 4.69−4.72 (t, 1H, *J* = 7.9 Hz), 4.47−4.50 (t, 1H, *J* = 9.4 Hz), 4.38-4.39 (m, 2H), 4.28-4.31 (t, 1H, *J* = 7.3 Hz), 3.80−3.83 (m, 1H), 3.76 (s, 3H), 2.08-2.09 (m, 1H), 1.97-1.99 (m, 1H), 1.88-1.92 (m, 1H), 1.64-1.70 (m, 1H), 1.51-1.56 (m, 1H), 1.41-1.47 (m, 1H); ^{13}C NMR (175 MHz, CD_3COCD_3) δ 170.5, 168.0, 156.1, 144.1, 144.0, 141.2, 127.6, 127.1, 127.0, 125.3, 119.9, 66.5, 60.8, 54.6, 51.9, 51.7,47.0, 32.2, 25.9, 24.9, 21.1; HRMS (ESI-TOF) m/z $[M + H]^+$ calcd for $C_{25}H_{26}IN_2O_5$ 561.0880, found 561.0890.

Azabicyclo[3.3.0]- and [4.2.0]alkanone Amino Esters 2.3-2.5

Employing the protocol described for the synthesis of bicycle **2.1**, lactam **2.16d** (100 mg, 0.24 mmol) in acetonitrile (4 mL) was treated with iodine (243 mg, 0.96 mmol) followed by diacetoxyiodobenzene (154 mg, 0.48 mmol), and heated to 80 °C for 30 min. The residue was chromatographed on silica gel (40−50% EtOAc in hexane). First to elute was pyrrolizidinone (5*R*, 6*R*)**-3** (26 mg, 20%) as light-sensitive white solid. Second to elute was a mixture of pyrrolizidinone (5*R*, 6*S*)**-2.4** and **2.5**, which was further separated by preparative HPLC (Phenomenex Gemini 5 μm, C18, 250 mm 21.2 mm) using a gradient from 50% to 90% MeOH [containing 0.1% formic

acid (FA)] in water (containing 0.1% FA) to afford pyrrolizidinone (5*R*, 6*S*)-**2.4** (6 mg, 5%) as white solid and azetidine **2.5** (5.5 mg, 4%). Last to elute was pyrrolizidinone (5*S*, 6*S*)-**2.3** (23 mg, 18%) as light-sensitive white solid.

(3*S*,5*R*,6*R*,8*S*)-Methyl 3-(*N*-Fmoc-amino)-6-iodo-pyrrolizidin-2-one-8-carboxylate [(5*R*, 6*R*)-2.3]

R_f = 0.34 (6:4 EtOAc/hexanes, visualized by UV); mp 97-100 °C; $[\alpha]_D^{25}$ −48.0 (*c* 0.37, $CHCl_3$); FT-IR (neat) ν_{max} 2921, 1694, 1527, 1441, 1329, 1245, 1199, 1051, 1032, 1014, 758, 738, 673 cm^{-1}; ^1H NMR (700 MHz, C_6D_6) δ 7.57−7.58 (d, 2H, *J* = 7.1 Hz), 7.41−7.42 (d, 2H, *J* = 6.3 Hz), 7.21−7.23 (t, 2H, *J* = 7.1 Hz), 7.16-7.18 (m, 2H), 4.76−4.77 (d, 1H, *J* = 5.9 Hz), 4.66−4.69 (m, 1H), 4.54−4.57 (t, 1H, *J* = 8.4 Hz), 4.32−4.33 (d, 2H, *J* = 5.2 Hz), 3.95−3.97 (t, 1H, *J* = 6.6 Hz), 3.32−3.33 (m, 1H), 3.22 (s, 3H), 2.82-2.83 (m, 1H), 2.21-2.25 (m, 1H), 1.98-2.02 (m, 1H), 1.90−1.94 (t, 1H, *J* = 12.1 Hz), 1.53-1.57 (m, 1H); ^{13}C NMR (175 MHz, C_6D_6) δ 173.3, 171.1, 155.8, 144.2, 144.1, 141.4, 127.0, 125.1, 119.8, 77.3, 66.4, 64.1, 55.1, 52.5, 51.6, 47.2, 42.7, 32.8, 32.3; HRMS (ESI-TOF) m/z $[M + H]^+$ calcd for $C_{24}H_{24}IN_2O_5$ 547.0724, found 547.0732.

(3*S*,5*S*,6*S*,8*S*)-Methyl 3-(*N*-Fmoc-amino)-6-iodo-pyrrolizidin-2-one-8-carboxylate [(5*S*, 6*S*)-2.3]

R_f = 0.15 (6:4 EtOAc/hexanes, twice eluted and visualized by UV); mp 107-109 °C; $[\alpha]_D^{25}$ 24.9 (*c* 0.41, $CHCl_3$); FT-IR (neat) ν_{max} 2918, 2848, 1698, 1541, 1254, 1202, 1172, 1050, 1033, 758, 740 620, 426 cm^{-1}; ^1H NMR (700 MHz, C6D6) δ 7.55−7.56 (m, 2H), 7.41−7.43 (m, 2H), 7.20−7.22 (m, 2H), 7.13-7.14 (m, 2H), 5.25-5.26 (d, 1H, *J* = 7.1), 4.15−4.69 (m, 1H), 4.33−4.35 (m, 1H), 4.28-4.30 (m, 1H), 4.03-4.05 (t, 1H, *J* = 7.9 Hz), 3.66−3.68 (d, 1H, *J* = 9.4 Hz), 3.39 (s, 3H), 3.31-3.32 (t, 1H, *J* = 5.0 Hz), 2.31-2.33 (d, 1H, *J* = 14.9 Hz), 2.19-2.22 (m, 1H), 2.07−2.12 (m, 1H), 1.91−1.94 (m, 1H), 1.66−1.71 (m, 1H); ^{13}C NMR (175 MHz, C_6D_6) δ 168.7, 167.7, 156.1, 144.2, 144.0, 141.4, 141.3, 127.0, 127.1, 125.3, 125.2, 119.8, 67.0, 61.5, 57.1, 53.3, 51.7, 47.2,

43.9, 41.4, 25.0; HRMS (ESI-TOF) m/z [M + Na]$^+$ calcd for $C_{24}H_{23}IN_2O_5Na$ 569.0543, found 569.0519.

(3*S*,5*S*,6*S*,8*S*)-Methyl-3-(*N*-Fmoc-amino)-5-iodo-2-oxo-1-azabicyclo[4.2.0]octane-8-carboxylate (2.5)

R_f = 0.34 (6:4 EtOAc/hexanes, twice eluted and visualized by UV)); mp 117-120 °C; $[\alpha]_D^{25}$ −71.7 (*c* 0.13, CHCl); FT-IR (neat) ν_{max} 2922, 1702, 1690, 1527, 1448, 1234, 1032, 807, 757, 739, 539 cm^{-1}; ^{1}H NMR (700 MHz, DMSO-d_6) δ 7.89−7.90 (d, 2H, *J* = 7.5 Hz), 7.84−7.85 (d, 1H, *J* = 9.0 Hz), 7.69−7.70 (d, 2H, *J* = 7.3 Hz), 7.41−7.43 (t, 2H, *J* = 7.4 Hz), 7.32-7.34 (m, 2H), 4.82-4.83 (m, 1H), 4.62-4.63 (m, 1H), 4.27-4.32 (m, 3H), 4.21-4.23 (m, 2H), 3.71 (s, 3H), 2.55-2.59 (m, 1H), 2.48-2.49 (m, 1H), 2.34-2.38 (m, 1H), 2.18-2.22 (m, 1H); ^{13}C NMR (175 MHz, DMSO-d_6) δ 170.7, 167.6, 163.5, 156.4, 144.2, 141.2, 128.1, 127.5, 125.6, 120.6, 66.2, 65.7, 59.7, 52.7, 51.4, 47.0, 37.7, 35.9, 33.7; HRMS (ESI-TOF) m/z [M + H]$^+$ calcd for $C_{24}H_{24}IN_2O_5$ 547.0724, found 547.0749.

(3*S*,5*R*,6*S*,8*S*)-Methyl 3-(*N*-Fmoc-amino)-6-acetoxy-pyrrolizidin-2-one-8-carboxylate [(5*R*, 6*S*)- 2.4]

R_f = 0.42 (4:6 EtOAc/hexanes, twice eluted and visualized by UV); mp 92-94 °C; $[\alpha]_D^{25}$ –20.1 (*c* 0.4, $CHCl_3$); FT-IR (neat) ν_{max} 2915, 1707, 1532, 1448, 1364, 1232, 1047, 759, 741, 542 cm^{-1}; ^{1}H NMR (700 MHz, C_6D_6) δ 7.57−7.58 (d, 2H, *J* = 7.6 Hz), 7.41−7.43 (m, 2H), 7.21−7.23 (t, 2H, *J* = 7.3 Hz), 7.16-7.17 (m, 2H), 4.77-4.78 (d, 1H, *J* = 3.9 Hz), 4.34−4.38 (m, 3H), 4.24−4.27 (m, 1H), 4.12−4.15 (q, 1H, *J* = 7.5 Hz), 3.97-3.99 (t, 1H, *J* = 6.5 Hz), 3.76−3.78 (m, 1H), 3.23 (s, 3H), 2.26-2.30 (m, 1H), 1.96−1.99 (m, 1H), 1.81−1.84 (m, 1H), 1.70−1.73 (m, 1H), 1.51 (s, 3H); ^{13}C NMR (175 MHz, C_6D_6) δ 172.2, 171.0, 169.2, 155.8, 144.2, 144.0, 141.5, 141.4, 127.0, 125.1, 119.8, 77.3, 75.3, 66.4, 61.8, 54.52, 53.4, 51.6, 47.2, 36.1, 29.9, 19.7; HRMS (ESI-TOF) m/z [M + H]$^+$ calcd for $C_{26}H_{27}N_2O_7$ 479.1812, found 479.1810.

Azabicyclo[3.3.0]- and [4.2.0]alkanone Amino Esters 2.3-2.4

Employing the protocol described for the synthesis of bicycle **2.1**, lactam **2.16d** (100 mg, 0.24 mmol) in toluene (4 mL) was treated with iodine (243 mg, 0.96 mmol) followed by diacetoxyiodobenzene (154 mg, 0.48 mmol), and heated to 80 °C for 30 min. The residue was chromatographed on silica gel (40−50% EtOAc in hexane). First to elute was pyrrolizidinone (5*R*, 6*R*)**-3** (19 mg, 15%) as light-sensitive white solid. Second to elute was pyrrolizidinone (5*S*, 6*R*)**-2.4** contaminated with trace amounts of iodoacetoxy lactam, which were removed by preparative HPLC (Phenomenex Gemini 5 μm, C18, 250 mm 21.2 mm) using a gradient from 50% to 90% MeOH (containing 0.1% FA) in water (containing 0.1% FA) to afford pyrrolizidinone (5*S*, 6*R*)**-2.4** (5 mg, 4%) as white solid. Last to elute was pyrrolizidinone (5*S*, 6*S*)**-3** (21 mg, 16%) as light-sensitive white solid.

(3*S*,5*S*,6*R*,8*S*)-Methyl 3-(*N*-Fmoc-amino)-6-acetoxy-2- pyrrolizidine-2-one-8-carboxylate [(5*R*, 6*S*)- 2.4].

R_f = 0.4 (4:6 EtOAc/hexanes, twice eluted and visualized by UV)); mp 97−99 °C; $[\alpha]_D^{25}$ –4.3 (*c* 0.41, $CHCl_3$); FT-IR (neat) ν_{max} 2920, 2850, 1703, 1534, 1449, 1364, 1230, 1045, 758, 740, 620, 541 cm^{-1}; ^1H NMR (700 MHz, C_6D_6) δ 7.55−7.56 (d, 2H, *J* = 7.5 Hz), 7.39−7.42 (m, 2H), 7.19−7.22 (t, 2H, *J* = 7.6 Hz), 7.09-7.13 (m, 2H), 5.15-5.16 (d, 1H, *J* = 6.6 Hz), 4.83-4.86 (m, 1H), 4.52−4.58 (m, 1H), 4.27−4.35 (m, 2H), 4.01-4.03 (t, 1H, *J* = 7.1 Hz), 3.81-3.83 (d, 1H, *J* = 9.1), 3.31 (s, 3H), 2.91-2.94 (m, 1H), 2.63−2.66 (m, 1H), 2.04-2.07 (m, 1H), 1.79-1.84 (m, 1H), 1.66-1.70 (m, 1H), 1.52 (s, 3H); ^{13}C NMR (175 MHz, C_6D_6) δ 170.3, 169.8, 168.2, 155.0, 143.4, 143.2, 140.6, 140.5, 126.2, 124.4, 124.3, 118.9, 73.3, 66.0, 59.7, 54.8, 53.4, 51.0, 46.4, 36.9, 35.6, 18.8 ; HRMS (ESI-TOF) m/z $[M + Na]^+$ calcd for $C_{26}H_{26}N_2O_7Na$ 501.1632, found 501.1641.

(3*S*,4*R*,5*R*,8*S*)- Methyl 3-(*N*-Fmoc-amino)-5-Iodo-6-acetoxy-2-oxoazocane-8-carboxylate (2.7).

In the dark, a solution of lactam **2.16b** (90 mg, 0.21 mmol) in toluene (8 mL) was treated with iodine (213 mg, 0.84 mmol) followed by diacetoxyiodobenzene (135 mg, 0.42 mmol). The resulting mixture was heated to 80 °C for 30 min and cooled to room temperature. The volatiles were evaporated under reduced pressure. The residue was chromatographed on silica gel (40−50% EtOAc in hexane) to give iodide **2.7** (91 mg, 0.15 mmol, 70%) as light-sensitive white solid: R_f = 0.68 (6:4 EtOAc/hexanes, visualized by UV); mp 103-104 °C; $[\alpha]_D^{25}$ –2.1 (*c* 0.83, $CHCl_3$); FT-IR (neat) ν_{max} 3365, 2949, 1736, 1671, 1497, 1434, 1369, 1320, 1214, 1032, 1016, 953, 757, 738, 620, 543 cm^{-1}; ^1H NMR (700 MHz, C_6D_6) δ 7.53−7.54 (d, 2H, *J* = 7.4 Hz), 7.46−7.48 (d, 1H, *J* = 7.5 Hz), 7.44−7.45 (d, 1H, *J* = 7.1 Hz), 7.16− 7.21 (m, 2H), 7.12−7.16 (m, 2H), 6.39−6.40 (d, 1H, *J* = 6.7 Hz), 6.07-6.08 (d, 1H, *J* = 8.5), 5.29−5.31 (m, 1H), 4.82-4.83 (m, 1H), 4.34−4.36 (m, 1H,), 4.28-4.29 (m, 1H), 4.17-4.20 (m, 1H), 4.03-4.06 (t, 1H, *J* = 7.5 Hz) 3.85-3.89 (m, 1H), 3.12 (s, 3H), 1.89-1.94 (m, 1H), 1.71 (s, 3H), 1.60-1.64 (m, 1H), 1.49-1.55 (m, 1H) 1.02-1.07 (m, 1H); ^{13}C NMR (175 MHz, C_6D_6) δ 170.3, 168.4, 167.5, 154.8, 143.9, 143.8, 141.4, 141.3, 127.9, 127.1, 127.1, 125.3, 125.1, 119.9, 119.8, 73.9, 67.3, 53.08, 51.9, 50.4, 47.1, 38.1, 30.6, 25.3, 19.8; HRMS (ESI-TOF) m/z $[M + H]^+$ calcd for $C_{26}H_{28}IN_2O_7$ 607.0936, found 607.0949.

(3*S*,4*R*,5*R*,7*S*)-Methyl-3-(*N*-Fmoc-amino)-5-iodo-6-acetoxy-2-oxoazocane-7-carboxylate (2.6).

In the dark, a solution of macrocycle **2.16a** (100 mg, 0.25 mmol) in toluene (10 mL) was treated with iodine (250 mg, 1 mmol) followed by diacetoxyiodobenzene (161 mg, 0.50 mmol). The resulting mixture was heated to 80 °C for 30 min and cooled to room temperature. The volatiles were evaporated under reduced pressure. The residue was chromatographed on silica gel (40−50% EtOAc in hexane) to give iodide **6** (85 mg, 0.14 mmol, 59%) as light-sensitive white solid: R_f =

0.66 (6:4 EtOAc/hexanes, visualized by UV); mp 112-115 °C; $[\alpha]_D^{25}$ 13.0 (*c* 1, $CHCl_3$); FT-IR (neat) ν_{max} 3303, 2961, 1742, 1682, 1496, 1421, 1248, 1213, 1049, 1032, 761, 739, 620, 589, 426 cm^{-1}; ^1H NMR (700 MHz, C_6D_6) δ 7.53−7.54 (d, 2H, *J* = 7.5 Hz), 7.43−7.44 (d, 1H, *J* = 7.3 Hz), 7.38−7.39 (d, 1H, *J* = 7.5 Hz), 7.19-1.21 (t, 2H, *J* = 7.4 Hz), 7.12-7.16 (m, 2H), 6.41-6.42 (d, 2H, *J* = 4.9 Hz), 5.22-5.24 (m, 1H), 4.75-4.76 (m, 1H), 4.34-4.35 (m, 1H), 4.25-4.28 (m, 1H), 4.18-4.21 (m, 1H), 3.98-4.00 (t, 1H, *J* = 7.5 Hz), 3.65-3.67 (m, 1H), 3.09 (s, 3H), 2.03-2.07 (m, 1H), 2.91 (s, 3H), 1.76-1.79 (m, 1H); ^{13}C NMR (175 MHz, C_6D_6) δ 169.9, 168.4, 168.2, 155.0, 144.0, 143.8, 141.4, 141.3, 127.1, 127.0, 125.3, 125.1, 119.9, 119.8, 72.3, 67.1, 52.7, 52.1, 49.1, 47.0, 32.5, 29.2, 20.1; HRMS (ESI-TOF) m/z $[M + H]^+$ calcd for $C_{25}H_{26}IN_2O_7$ 593.0779, found 593.0759.

(3*S*)-Methyl 3-(*N*-Fmoc-amino)-2-oxo-2,3-dihydro-1H-azepine-7-carboxylate (2.8)

In the dark, a solution of macrocycle **2.16a** (50 mg, 0.12 mmol) in toluene (5 mL) was treated with iodine (122 mg, 0.48 mmol) followed by 4-methoxy-iodosobenzene di-(adamantane-1-carboxylate) (**2.18b**;148 mg, 0.25 mmol). The resulting mixture was heated to 80 °C for 30 min and cooled to room temperature. The volatiles were evaporated under reduced pressure. The residue was chromatographed on silica gel (40−50% EtOAc in hexane) to give dihydroazepine **2.8** (18 mg, 0.04 mmol, 36%) as white solid: R_f = 0.44 (1:1 EtOAc/hexanes, visualized by UV); mp 200-203 °C; $[\alpha]_D^{25}$ 15.0 (*c* 0.33, $CHCl_3$); FT-IR (neat) ν_{max} 3324, 2921, 1682, 1545, 1441, 1274, 1250, 1102, 1084, 1049, 1029, 732, 561 cm^{-1}; ^1H NMR (700 MHz, $CDCl_3$) δ 8.16 (br, s, 1H), 7.79−7.80 (d, 2H, *J* = 7.42 Hz), 7.64−7.65 (m, 2H), 7.42−7.44 (t, 2H, *J* = 7.7 Hz), 7.34−7.36 (t, 2H, *J* = 7.3 Hz), 7.11-7.12 (d, 1H, *J* = 5.2 Hz), 6.33−6.35 (t, 1H, *J* = 8.2 Hz), 6.27−6.28 (d, 1H, *J* = 5.2 Hz), 5.73−5.75 (m, 1H), 4.45-4.46 (d, 2H, *J* = 7.1 Hz), 4.26−4.28 (t, 2H, *J* = 6.4 Hz), 3.92 (s, 3H); ^{13}C NMR (125 MHz, $CDCl_3$) δ 165.4, 163.3, 155.7, 143.8, 143.7, 141.3, 141.4, 133.1,

127.9, 127.8, 127.7, 127.6, 127.1, 126.2, 125.1, 124.1, 120.9, 120.0, 67.2, 54.9, 53.3, 47.1; HRMS (ESI-TOF) m/z $[M + H]^+$ calcd for $C_{23}H_{21}N_2O_5$ 405.1445, found 405.1426.

(3*S*,8*S*,*Z*)-Methyl-3-*N*-2-nitrophenylsulfonamido-2-oxo-1,2,3,6,7,8-hexahydroazocine-8-carboxylate (2.16f)

Lactam **2.16b** (300 mg, 0.71 mmol) was treated with diethylamine (2 mL) in DCM (10 mL) for 2h. The volatiles were removed under vacuum. The residue used in the next step without further purification, dissolved in THF (4 mL), treated with *o*-nitrobenzenesulfonyl chloride (476mg, 2.14 mmol) and DIEA (523 µL, 2.84 mmol), and stirred overnight. The volatiles were evaporated. The residue was partitioned between EtOAc and water, and the aqueous phase was extracted with EtOAc (2 × 20 mL). The combined organic layers were dried over anhydrous sodium sulphate, filtered, and concentrated under reduced pressure. The residue was purified by chromatography on silica gel (60−70% EtOAc in hexane) to afford sulfonamide **2.16f** (81 mg, 0.21 mmol, 30%) as tan red solid: R_f = 0.44 (6:4 EtOAc/hexanes, twice eluted and visualized by UV), mp 175−178 °C, $[\alpha]_D^{25}$ 27.4 (*c* 0.83, $CHCl_3$); FT-IR (neat) ν_{max} 2941, 1739, 1666, 1520, 1416, 1326, 1161, 943, 913, 779, 732, 554 cm^{-1}; ^1H NMR (500 MHz, $CDCl_3$) δ 8.04−8.06 (m, 1H), 7.88−7.89 (m, 1H), 7.69−7.71 (m, 2H), 6.64−6.65 (d, 1H, *J* = 4.85 Hz), 5.97−5.98 (d, 1H, *J* = 8.2 Hz), 5.73−5.79 (m, 1H), 5.59−5.62 (dd, 1H, *J* = 6.2 Hz), 5.03 (brs, 1H), 4.37−4.41 (m, 1H), 3.80 (s, 3H), 2.39−2.43 (m, 2H), 2.11−2.17 (m, 1H), 1.52-1.57 (m, 1H); ^{13}C NMR (125 MHz, $CDCl_3$) δ 171.6, 170.5, 147.8, 134.9, 133.6, 132.9, 131.5, 130.4, 129.6, 125.5, 55.38, 55.01, 53.29, 32.7, 24.9 ; HRMS (ESI-TOF) m/z $[M + H]^+$ calcd for $C_{15}H_{18}N_3O_7S$ 384.0862, found 384.0868.

(3*S*,8*S*,*Z*)-Methyl-3-*N*-methyl-*N*-2-nitrophenylsulfonamido-2-oxo-1,2,3,6,7,8-hexa-hydroazocine-8-carboxylate (2.16e)

Sulfonamide **2.16f** (11 mg, 0.03 mmol) was treated with iodomethane (0.12 mmol, 8 µL) and K_2CO_3 in MeCN (2 mL) for 3h at 80 °C, quenched with water (5 mL) and extracted with ethyl

acetate (2 × 20 mL). The combined organic layers were dried over anhydrous sodium sulphate, filtered, and concentrated under reduced pressure. The residue was purified by chromatography on silica gel (60−70% EtOAc in hexane) to afford *N*-methyl sulfonamide **2.16e** (8.4 mg, 0.021 mmol, 73%) as tan red solid: R_f = 0.40 (6:4 EtOAc/hexanes, twice eluted and visualized by UV) mp 63−67 °C; $[\alpha]_D^{25}$ 62 (*c* 0.7, $CHCl_3$); FT-IR (neat) ν_{max} 2921, 2852, 1741, 1676, 1540, 1436, 1346, 1171, 977, 923, 779, 717, 575 cm^{-1}; ^1H NMR (500 MHz, $CDCl_3$) δ 8.12−8.13 (m, 1H), 7.68−7.72 (m, 2H), 7.63−7.65 (m, 1H), 5.90-5.96 (m, 1H), 5.79−5.81 (d, 1H, *J* = 10.45 Hz), 5.69-5.73 (m, 1H), 5.39−5.40 (m, 1H), 4.44−4.49 (m, 1H), 3.83 (s, 3H), 3.05 (s, 3H), 2.32-2.41 (m, 1H), 2.22−2.29 (m, 1H), 1.97-2.04 (m, 1H), 1.66-1.69 (m, 1H); ^{13}C NMR (125 MHz, $CDCl_3$) δ 171.6, 170.19, 147.8, 133.3, 132.9, 131.6, 131.0, 130.5, 129.0, 124.2, 59.8, 52.8, 52.4, 32.0, 31.7, 22.0 ; HRMS (ESI-TOF) m/z $[M + H]^+$ calcd for $C_{16}H_{20}N_3O_7S$ 398.1016, found 398.1018.

(3*R*,4*R*,5*S*,8*S*)-Methyl-3-*N*-2-nitrophenylsulfonamido-4-iodopyrrolizidin-2-one-8-carboxylate (2.1f)

Employing the protocol described for the synthesis of pyrrolizidinone **2.1**, a solution of lactam **2.16f** (10 mg, 0.03 mmol) in acetonitrile (4 mL) was treated with iodine (27 mg, 0.104mmol) followed by diacetoxyiodobenzene (20 mg, 0.06 mmol), heated to 80 °C for 30 min, cooled to room temperature, and the volatiles were evaporated. The residue was chromatographed on silica gel (50−60% EtOAc in hexane) to give pyrrolizidinone **2.1f** (7 mg, 0.014 mmol, 54%) as light-sensitive white solid: R_f = 0.62 (6:4 EtOAc/hexanes, twice eluted and visualized by UV); mp 175−178 °C; $[\alpha]_D^{25}$ −62.0 (*c* 0.16, $CHCl_3$); FT-IR (neat) ν_{max} 2920, 2850, 1720, 1538, 1350, 1162, 1113, 1055, 1006, 854, 809, 786, 654, 563, 540 cm^{-1}; ^1H NMR (500 MHz, $CDCl_3$) δ 8.21−8.22 (m, 1H), 7.96−7.98 (m, 1H), 7.77−7.82 (m, 2H), 6.42−6.43 (d, 1H, *J* = 2.5 Hz) 4.76−4.78 (dd, 1H, *J* = 3.5 Hz), 4.47−4.50 (m, 1H), 4.39−4.72 (brs, 1H), 3.99−4.04 (m, 1H), 3.76 (s, 3H), 2.48−2.54 (m, 1H) 2.12−2.19 (m, 2H), 1.73−1.79 (m, 1H); ^{13}C NMR (125 MHz, $CDCl_3$) δ 171.1, 168.1,

147.7, 134.0, 133.5, 133.2, 131.3, 125.8, 68.6, 62.9, 56.0, 52.7, 33.7, 30.9, 26.7; HRMS (ESI-TOF) m/z $[M + H]^+$ calcd for $C_{15}H_{17}IN_3O_7S$ 509.9826, found 509.9833.

(3*R*,4*R*,5*S*,8*S*)-Methyl-3-*N*-methyl-*N*-2-nitrophenylsulfonamido-4-iodo-pyrrolizidin-2-one-8-carboxylate (2.1e)

Employing the protocol described for the synthesis of pyrrolizidinone **2.1**, a solution of lactam **2.16e** (13 mg, 0.033 mmol) in acetonitrile (5 mL) was treated with iodine (34 mg, 0.132 mmol) followed by diacetoxyiodobenzene (21.1 mg, 0.07 mmol), heated to 80 °C for 30 min, cooled to room temperature, and the volatiles were evaporated. The residue was chromatographed on silica gel (50−60% EtOAc in hexane) to give pyrrolizidinone **2.1e** (9.6 mg, 0.02 mmol, 57%) as light-sensitive white solid: R_f = 0.58 (6:4 EtOAc/hexanes, twice eluted visualized UV); mp 69−72 °C; $[\alpha]_D^{25}$ −20 (*c* 0.5, $CHCl_3$); FT-IR (neat) ν_{max} 2921, 1707, 1540, 1436, 1347, 1163, 1123, 957, 883, 779, 576, 534 cm^{-1}; ^1H NMR (500 MHz, $CDCl_3$) δ 8.21−8.23 (m, 1H), 7.69−7.74 (m, 3H), 5.00−5.01 (d, 1H, *J* = 5.25 Hz), 4.65−4.76 (dd, 1H, *J* = 5.25) 4.56−4.59 (m, 1H) 3.93−3.98 (m, 1H), 3.76 (s, 3H), 3.04 (s, 3H), 2.55−2.61 (m, 1H), 2.12−2.20 (m, 2H), 1.69−1.78 (m, 1H); ^{13}C NMR (125 MHz, $CDCl_3$) δ 171.3, 167.8, 148.6, 143.4, 133.8, 132.0, 130.5, 124.5, 71.8, 63.5, 56.5, 52.9, 34.7, 32.1, 30.9, 21.1; HRMS (ESI-TOF) m/z $[M + H]^+$ calcd for $C_{16}H_{19}IN_3O_7S$ 523.9983 found 523.9993.

(3*S*,4*R*,5*R*,8*S*)-Methyl-3-*N*-2-nitrophenylsulfonamido-5-iodo-6-acetoxy-2-oxoazocane-8-carboxylate (2.7f).

Employing the protocol described for the synthesis of iodoacetate **2.7**, a solution of lactam **2.16f** (22 mg, 0.06 mmol) in acetonitrile (10 mL) was treated with iodine (60.7 mg, 0.24 mmol) followed by diacetoxy iododbenzene (39 mg, 0.12 mmol), stirred at room temperature overnight, quenched with 1M $Na_2S_2O_3$ (10 mL), and extracted with ethyl acetate (2 × 20 mL). The combined organic

layers were dried over anhydrous sodium sulphate, filtered, and concentrated under reduced pressure. The residue was purified by chromatography on silica gel (60−70% EtOAc in hexane, twice eluted and visualized by UV) to afford iodoacetate **2.7f** (20 mg, 0.04 mmol, 63%) as light-sensitive white solid: R_f = 0.5 (6:4 EtOAc/hexanes, visualized by UV); mp 80−84 °C; $[\alpha]_D^{25}$ 5.2 (*c* 1.6, $CHCl_3$); FT-IR (neat) ν_{max} 2922, 2853, 1737, 1677, 1539, 1437, 1371, 1290, 1219, 1168, 1120, 1033, 1015, 740, 580, 552 cm^{-1}; ^1H NMR (500 MHz, $CDCl_3$) δ 8.05−8.07 (m, 1H), 7.83−7.85 (m, 1H), 7.74−7.76 (m, 2H), 6.57−6.59 (d, 1H, *J* = 8.2 Hz) 6.24−6.26 (d, 1H, *J* = 8.9 Hz), 5.31−5.34 (dd, 1H, *J* = 6.4 Hz), 4.58−4.60 (dd, 1H, *J* = 3 Hz), 4.49−4.53 (m, 1H), 4.4−4.48 (dd, 1H, *J* = 1.5 Hz), 3.85 (s, 3H), 2.30-2.33 (m, 1H), 2.26 (s, 3H), 2.12-2.22 (m, 2H), 1.67-1.73 (m, 1H); ^{13}C NMR (125 MHz, $CDCl_3$) δ 170.8, 169.4, 167.2, 147.6, 134.4, 133.9, 132.8, 130.0, 125.1, 73.3, 53.3, 53.2, 52.6, 36.8, 30.9, 29.7, 20.84; HRMS (ESI-TOF) m/z $[M + H]^+$ calcd for $C_{17}H_{21}IN_3O_9S$ 570.0038, found 570.0048.

(3*R*,4*R*,5*S*,8*S*)-Methyl-3-(*N*-2,7-diiodofluorenylmethylcarbamato)-4-iodo-pyrrolizidin-2-one-8-carboxylate (2.1a).

In the dark, a solution of macrocycle **2.16b** (70 mg, 0.17 mmol) in acetonitrile (5 mL) was treated with iodine (173 mg, 0.68 mmol) followed by ditrifluroacetoxyiodobenzene (112 mg, 0.26 mmol). The resulting mixture was heated to 80 °C for 30 min and cooled to room temperature. The volatiles were evaporated under reduced pressure. The residue was chromatographed on silica gel (30−35% EtOAc in hexane) to give triiodide **2.1a** (68 mg, 0.08 mmol, 51%) as white solid: R_f = 0.54 (1:1 EtOAc/hexanes, visualized by UV); mp 150-155 °C; $[\alpha]_D^{25}$ –85.2 (*c* 1, $CHCl_3$); FT-IR (neat) ν_{max} 2947, 1698, 1523, 1449, 1411, 1214, 1121, 1053, 1033, 1000, 806, 747, 434 cm^{-1}; ^1H NMR (700 MHz, $CDCl_3$) δ 7.90-7.91 (d, 2H, *J* = 4.7 Hz), 7.71−7.73 (d, 2H, *J* = 8.1 Hz), 7.46−7.47 (d, 2H, *J* = 8.0 Hz), 5.78-5.79 (d, 1H, *J* = 4.1 Hz), 4.63-4.64 (m, 1H), 4.59-4.61 (m, 1H), 4.51-4.52 (m, 1H), 4.40-4.41 (m, 2H), 4.15-4.16 (m, 1H), 3.96-3.98 (m, 1H), 3.75 (s, 3H), 2.49-2.53 (m, 1H),

2.10-2.14 (m, 2H), 1.69-1.73 (m, 1H); ^{13}C NMR (175 MHz, $CDCl_3$) δ 171.6, 170.1, 155.7, 145.2, 140.1, 140.0, 137.0, 134.1, 121.7, 92.9, 66.4, 65.8, 62.9, 56.6, 52.7, 46.9, 33.7, 30.7, 25.1; HRMS (ESI-TOF) m/z $[M + H]^+$ calcd for $C_{24}H_{22}I_3N_2O_5$ 798.8657, found 798.8628.

(2*S*,6*S*,7*R*,8*S*)-8-(*N*-2,7-diiodofluorenylmethylcarbamato)-7-iodo-indolizidin-9-one-2-carboxylate (2.2a).

As described for the synthesis of triiodide **2.1a**, lactam **2.16c** (100 mg, 0.23 mmol) in acetonitrile (8 mL) was treated with iodine (233 mg, 0.92 mmol) followed by (ditrifluroacetoxyiodo)benzene (148 mg, 0.34 mmol), and heated to 80 °C for 30 min. The residue was chromatographed on silica gel (30−35% EtOAc in hexane) to give triiodide **2.2a** (66 mg, 0.08 mmol, 51%) as white solid: R_f = 0.62 (1:1 EtOAc/hexanes, visualized by UV); mp 147-150 °C; $[\alpha]_D^{25}$ –35.5 (*c* 1.1, $CHCl_3$); FT-IR (neat) ν_{max} 2922, 1693, 1528, 1444, 1202, 1052, 1032, 999, 870, 805, 731, 435 cm^{-1}; ^{1}H NMR (700 MHz, CD_3COCD_3) δ 8.12-8.13 (d, 2H, *J* = 5.2 Hz), 7.81−7.82 (m, 2H), 7.72−7.73 (d, 2H, *J* = 8.1 Hz), 7.10-7.12 (d, 1H, *J* = 8.4 Hz), 4.82-4.83 (d, 1H, *J* = 5.9 Hz), 4.65-4.68 (t, 1H, *J* = 8.3 Hz), 4.48-4.50 (m, 1H), 4.43-4.46 (m, 2H), 4.33-4.35 (t, 1H, *J* = 6.6 Hz), 3.37-3.79 (m, 1H), 3.75 (s, 3H), 2.08-2.10 (m, 1H), 1.96-1.98 (m, 1H), 1.88-1.91 (m, 1H), 1.64-1.69 (m, 1H), 1.50-1.56 (m, 1H), 1.41-1.46 (m, 1H); ^{13}C NMR (175 MHz, $CDCl_3$) δ 170.6, 169.6, 141.2, 139.6, 138.7, 137.8, 137.0, 136.8, 134.3, 130.4, 122.0, 111.7, 92.4, 70.9, 55.4, 51.8, 51.7, 51.6, 33.5, 32.2, 25.8, 20.6. HRMS (ESI-TOF) m/z $[M + H]^+$ calcd for $C_{25}H_{24}I_3N_2O_5$ 812.8814, found 812.8823.

2.8.4. Synthesis of iodosobenzene dicarboxylates:

Ditrimethylacetoxyiodobenzene (2.17a)

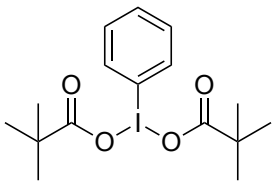

A solution of diacetoxyiodobenzene (1 g, 3.1 mmol) in chlorobenzene (30 mL) was treated with pivalic acid (888 mg, 8.7 mmol), heated at 50 °C, stirred for 30 min, cooled, and concentrated. Hexane was added and a precipitate appeared. The precipitate was filtered and washed with hexane to afford iodosobenzene **2.17a** (1.15 g 88%) as white solid: mp 108−111 °C; FT-IR (neat) ν_{max} 2977, 1641, 1475, 1439, 1475, 1393, 1282, 1168, 1012, 887, 746, 600, 544, 464 cm^{-1}; ^{1}H NMR (500 MHz, $CDCl_3$) δ 7.99-8.02 (m, 2H), 7.52−7.57 (m, 1H), 7.43−7.49 (m, 2H), 1.11 (s, 18H); ^{13}C NMR (125 MHz, $CDCl_3$) δ 183.7, 134.3, 131.3, 130.7, 122.2, 39.1, 27.8; HRMS (APPi-TOF) m/z $[M + Na]^+$ calcd for $C_{16}H_{23}IO_4Na$ 429.0533, found 429.0547.

4-Methyl-ditrimethylacetoxyiododobenzene (2.17b)

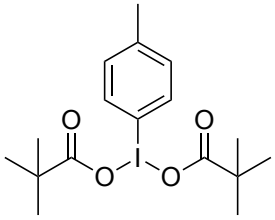

Employing the protocol described for the synthesis hypervalent iodine (III) **2.17a**, 4-methyl-diacetoxyiodobenzene (1 g, 2.97 mmol) in chlorobenzene (30 mL) was treated with pivalic acid (851 mg, 8.33 mmol), heated at 50 °C, and precipitated to afford iodosobenzene **2.17b** (1.11 g 85%): mp 142−145 °C;); FT-IR (neat) ν_{max} 2971, 1646, 1549, 1474, 1387, 1288, 1171, 1024, 888, 809, 715, 604, 550, 487 cm^{-1}; ^{1}H NMR (500 MHz, $CDCl_3$) δ 7.86-7.88 (m, 2H), 7.25−7.26 (m, 2H), 2.43 (s, 3H), 1.10 (s, 18H); ^{13}C NMR (125 MHz, $CDCl_3$) δ 183.5, 141.9, 134.2, 131.4, 118.8, 38.9, 27.7, 21.4; HRMS (APPi-TOF) m/z $[M + Na]^+$ calcd for $C_{17}H_{25}IO_4Na$ 443.0689, found 443.0703

4-Methoxy-ditrimethylacetoxyiodobenzene (2.17c)

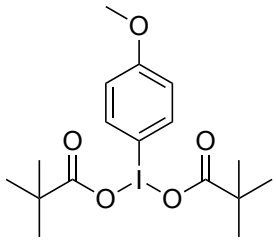

Employing the protocol described for the synthesis hypervalent iodine (III) **2.17a**, 4-methoxy-diacetoxyiodobenzene (1 g, 2.84 mmol) in chlorobenzene (30 mL) was treated with pivalic acid (812 mg, 7.95 mmol), heated at 50 °C, and precipitated to afford iodosobenzene **2.17c** (1.1 g, 85%): mp 147-149 °C; FT-IR (neat) ν_{max} 2972, 1629, 1578, 1486, 1461, 1287, 1252, 1167, 1018, 887, 828, 801, 780, 599, 515, 476 cm^{-1}; ^{1}H NMR (500 MHz, $CDCl_3$) δ 7.92-7.94 (m, 2H), 6.93-6.95 (m, 2H), 3.86 (s, 3H), 1.10 (s, 18H); ^{13}C NMR (125 MHz, $CDCl_3$) δ 183.6, 161.8, 136.4, 116.3, 112.3, 55.6, 39.1, 27.9; HRMS (APPi-TOF) m/z $[M + Na]^+$ calcd for $C_{17}H_{25}IO_5Na$ 459.0638, found 459.0651.

Iodosobenzene di-(adamantane-1-carboxylate) (2.18a)

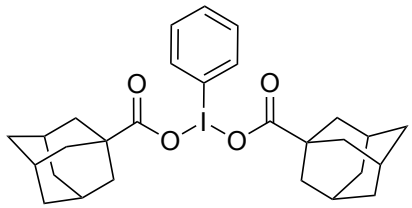

A solution of diacetoxyiodobenzene (1 g, 3.1 mmol) in chlorobenzene (30 mL) was treated with 1-adamantanecarboxylic acid (1566 mg, 8.7 mmol), heated at 50 °C, stirred for 30 min, cooled, and concentrated. After concentration, hexane was added and a precipitate appeared. The precipitate was filtered and washed with hexane to afford iodosobenzene **2.18a** (1.69 g, 93%) as white solid; mp 172−175 °C; FT-IR (neat) ν_{max} 2893, 2849, 1637, 1443, 1323, 1270, 1244, 1179, 1077, 993, 796, 763, 732, 678, 537, 480 cm^{-1}; ^{1}H NMR (500 MHz, $CDCl_3$) δ 7.98-8.00 (m, 2H),

7.52-7.55 (m, 1H), 7.45−7.48 (m, 2H), 1.91-1.94 (m, 6H), 1.79-1.80 (m, 11H), 1.62-1.74 (m, 13H); ^{13}C NMR (125 MHz, $CDCl_3$) δ 182.9, 134.3, 131.2, 130.7, 122.0, 41.2, 39.5, 36.6, 28.3; HRMS (ESI-TOF) m/z $[M + Na]^+$ calcd for $C_{28}H_{35}IO_4Na$ 585.1472, found 585.1449.

4-Methoxy-iodosobenzene di-(adamantane-1-carboxylate) (2.18b)

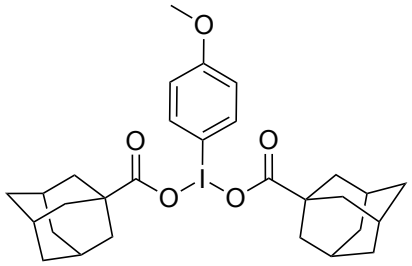

Employing the protocol described for the synthesis hypervalent iodine (III) **2.18a**, 4-methoxy-diacetoxyiodobenzene (1 g, 2.84 mmol) in chlorobenzene (30 mL) was treated with 1-adamantanecarboxylic acid (1432 mg, 7.95 mmol), and precipitated to afford iodosobenzene **2.18b** (1.71 g, 95%); mp 169−172 °C; $[\alpha]_D^{20}$ −70.8 (*c* 1, $CHCl_3$); FT-IR (neat) ν_{max} 2903, 2849, 1632, 1575, 1489, 1268, 1249, 1181, 1077, 1030, 821, 796, 678, 537, 480 cm^{-1}; ^{1}H NMR (500 MHz, $CDCl_3$) δ 7.92-7.95 (m, 2H), 6.95-6.99 (m, 2H), 3.89 (s, 3H), 1.92-1.96 (m, 6H), 1.79-180 (m, 11H), 1.63-1.73 (m, 13H); ^{13}C NMR (125 MHz, $CDCl_3$) δ 182.7, 161.6, 136.2, 116.2, 111.8, 55.5, 41.0, 39.3, 36.4, 28.1; HRMS (ESI-TOF) m/z $[M + Na]^+$ calcd for $C_{29}H_{37}IO_5Na$ 615.1578, found 615.1548.

4-Trifluoromethyl-iodosobenzene di-(adamantane-1-carboxylate) (2.18c)

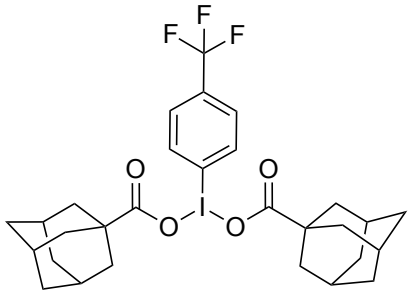

Employing the protocol described for the synthesis hypervalent iodine (III) **2.18a**, 4-trifluoromethyl-diacetoxyiodobenzene (1 g, 2.56 mmol) in chlorobenzene (30 mL) was treated with 1-adamantanecarboxylic acid (1293 mg, 7.95 mmol), and precipitated to afford iodosobenzene **2.18c** (1.65 g, 91%): mp 193−196 °C; FT-IR (neat) ν_{max} 2902, 2851, 1633, 1596, 1452, 1400, 1323, 1270, 1245, 1171, 1067, 1049, 842, 821, 677, 481 cm^{-1}; ^{1}H NMR (500 MHz, $CDCl_3$) δ 8.14-8.16 (d, 2H, *J* = 8.3 Hz), 7.74−7.76 (d, 2H, *J* = 8.4 Hz), 1.92-1.98 (m, 6H), 1.83-184 (m, 11H), 1.65-1.72 (m, 13H); ^{13}C NMR (125 MHz, $CDCl_3$) δ 182.9, 134.7, 132.7-132.9 (q, *J* = 33.10 Hz), 127.5-127.6 (q, *J* = 3.7 Hz), 124.7, 124.4, 41.3, 39.5, 36.6, 28.3; HRMS (ESI-TOF) m/z $[M + Na]^+$ calcd for $C_{29}H_{34}F_3IO_4Na$ 653.1346, found 653.1315.

2.9 References

1. Still, W. C.; Kahn, M.; Mitra, A., *J. Org. Chem.* **1978,** *43*, 2923–2925.

2. (a) Sicherl, F.; Cupido, T.; Albericio, F., *Chem. Commun.* **2010,** *46*, 1266–1268; (b) Organ, M. G.; Xu, J.; N'Zemba, B., *Tetrahedron Lett.* **2002,** *43*, 8177–8180.

3. (a) Atmuri, N. D. P.; Lubell, W. D., *J. Org. Chem.* **2015,** *80*, 4904–4918; (b) Atmuri, N. D. P.; Lubell, W. D. *Org. Synth*. **2015**, 92, 103−116.

4. Kaul, R.; Surprenant, S.; Lubell, W. D., *J. Org. Chem.* **2005,** *70*, 3838–3844.

5. (a) Wu, Y.; Izquierdo, S.; Vidossich, P.; Lledós, A.; Shafir, A., *Angew. Chem. Int. Ed.* **2016,** *128*, 7268–7272; (b) Wang, B.; Qin, L.; Neumann, K. D.; Uppaluri, S.; Cerny, R. L.; DiMagno, S. G., *Org. Lett.* **2010,** *12*, 3352–3355; (c) Stang, P. J.; Boehshar, M.; Wingert, H.; Kitamura, T., *J. Am. Chem. Soc.* **1988,** *110*, 3272–3278.

2.9. Crystallography data and Molecular structure for compounds

2.9.1. General Methods for making crystals:

Macro cyclic lactams **2.16a,c,d** crystallized by a common method featuring dissolving 5 mg of macrocycle in 1 mL of ethyl acetate and equilibrating hexane vapour into the mother liquor in a closed container to provide slow formation of crystals. Crystals of azabicyclo[X.Y.Z]alkanes **2.1a, 2.7** and **2.8** were grown respectively in dichloromethane-hexane using the liquid-vapour saturation method in the dark, because the iodides were light sensitive.

Compound 2.1a (LUB104):

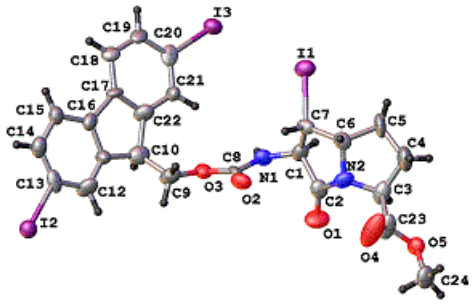

Table 1 Crystal data and structure refinement for LUB104.

Identification code	LUB104
Empirical formula	$C_{24}H_{21}I_3N_2O_5$
Formula weight	798.13
Temperature/K	100
Crystal system	orthorhombic
Space group	$P2_12_12_1$
a/Å	5.2720(5)
b/Å	14.4113(14)
c/Å	33.766(3)
α/°	90
β/°	90
γ/°	90
Volume/Å^3	2565.4(4)
Z	4
ρ_{calc}g/cm^3	2.066
μ/mm^{-1}	19.454
F(000)	1512.0
Crystal size/mm^3	0.22 × 0.14 × 0.04
Radiation	GaKα (λ = 1.34139)
2Θ range for data collection/°	4.554 to 109.93

Index ranges	$-6 \leq h \leq 6, -17 \leq k \leq 17, -36 \leq l \leq 41$
Reflections collected	19926
Independent reflections	4698 [$R_{int} = 0.0692$, $R_{sigma} = 0.0450$]
Data/restraints/parameters	4698/0/309
Goodness-of-fit on F^2	1.126
Final R indexes [I>=2σ (I)]	$R_1 = 0.0747$, $wR_2 = 0.1961$
Final R indexes [all data]	$R_1 = 0.0779$, $wR_2 = 0.1984$
Largest diff. peak/hole / e $Å^{-3}$	1.94/-1.64
Flack parameter	0.39(4)

Table 2 Fractional Atomic Coordinates ($\times 10^4$) and Equivalent Isotropic Displacement Parameters ($Å^2 \times 10^3$) for LUB104. U_{eq} is defined as 1/3 of of the trace of the orthogonalised U_{IJ} tensor.

Atom	*X*	*y*	*z*	U(eq)
I1	7197(3)	2481.6(9)	6032.6(4)	48.2(4)
I2	-1979(2)	5426.8(9)	8932.4(4)	42.4(3)
I3	12507(3)	2169.6(9)	7056.9(4)	46.3(4)
O1	4530(30)	6141(12)	5912(5)	57(4)
O2	2510(30)	4810(9)	6694(4)	44(3)
O3	5730(30)	5039(9)	7127(4)	39(3)
O4	-1560(30)	5500(20)	5261(6)	98(9)
O5	680(30)	6270(10)	4825(4)	40(3)
N1	6650(30)	4806(11)	6494(5)	37(3)
N2	3030(30)	4846(12)	5602(5)	40(4)
C1	6110(40)	4584(16)	6092(6)	43(5)
C2	4480(40)	5320(17)	5884(6)	41(5)
C3	2870(40)	5166(17)	5197(6)	48(5)
C4	3180(70)	4300(20)	4948(7)	74(8)
C5	4670(60)	3630(20)	5218(6)	62(7)
C6	3400(40)	3845(15)	5613(6)	38(4)
C7	4820(30)	3686(13)	6012(6)	35(4)
C8	4710(40)	4884(12)	6770(5)	36(4)
C9	3990(40)	4905(17)	7464(7)	51(6)
C10	5500(50)	4571(18)	7806(7)	54(6)
C11	3880(40)	4379(14)	8172(6)	38(4)
C12	2020(40)	4916(17)	8332(7)	51(5)
C13	890(40)	4571(19)	8670(6)	44(5)
C14	1470(50)	3742(18)	8831(6)	52(6)
C15	3340(50)	3170(17)	8659(5)	45(5)
C16	4450(40)	3506(14)	8312(6)	39(5)
C17	6490(40)	3042(12)	8062(6)	34(4)

C18	7810(40)	2197(12)	8108(6)	37(4)
C19	9520(50)	1974(14)	7820(6)	42(5)
C20	9860(40)	2544(16)	7500(6)	42(5)
C21	8570(40)	3380(14)	7460(6)	39(4)
C22	6950(40)	3655(15)	7759(7)	46(5)
C23	340(40)	5690(20)	5127(7)	56(7)
C24	-1540(40)	6770(20)	4709(7)	56(6)

Table 3 Anisotropic Displacement Parameters ($Å^2 \times 10^3$) for LUB104. The Anisotropic displacement factor exponent takes the form: $-2\pi^2[h^2a^{*2}U_{11}+2hka^*b^*U_{12}+\ldots]$.

Atom	U_{11}	U_{22}	U_{33}	U_{23}	U_{13}	U_{12}
I1	36.9(7)	44.0(7)	63.5(8)	5.3(6)	6.1(6)	1.1(5)
I2	35.2(6)	48.6(7)	43.4(6)	-1.0(5)	-0.5(5)	0.1(5)
I3	47.1(7)	41.1(7)	50.6(7)	-4.2(5)	1.0(6)	6.5(6)
O1	53(10)	34(9)	86(12)	-3(8)	-13(9)	-15(7)
O2	30(7)	40(7)	62(8)	-4(6)	12(7)	1(6)
O3	43(8)	29(7)	44(7)	-2(6)	2(6)	-1(6)
O4	27(8)	180(20)	90(14)	68(16)	6(9)	-2(12)
O5	31(7)	45(8)	44(8)	3(6)	9(6)	-3(6)
N1	22(7)	40(9)	48(8)	-3(7)	-3(7)	0(6)
N2	21(7)	41(9)	59(9)	11(7)	-2(7)	1(7)
C1	31(9)	56(13)	41(10)	8(10)	0(8)	12(9)
C2	26(9)	55(15)	42(10)	-5(10)	-2(8)	-2(9)
C3	23(9)	74(15)	46(10)	14(10)	-1(9)	-10(10)
C4	90(20)	100(20)	34(11)	-5(12)	7(13)	13(18)
C5	81(19)	83(19)	21(9)	-8(10)	8(11)	0(15)
C6	25(9)	44(11)	45(10)	-6(9)	2(8)	-6(8)
C7	28(9)	30(10)	47(11)	-2(8)	12(9)	-5(7)
C8	58(13)	18(9)	31(9)	-8(7)	10(9)	8(8)
C9	40(11)	49(14)	63(14)	14(11)	1(10)	10(10)
C10	51(13)	49(14)	64(14)	-1(12)	-14(11)	-7(12)
C11	49(11)	29(10)	35(9)	1(8)	6(8)	5(8)
C12	29(10)	58(13)	65(13)	18(11)	-3(10)	8(10)
C13	28(9)	73(16)	32(9)	-14(10)	-2(7)	-15(10)
C14	53(14)	70(16)	35(10)	2(10)	-4(9)	1(12)
C15	54(13)	51(13)	32(9)	-2(9)	0(9)	3(10)
C16	47(12)	41(12)	30(9)	1(8)	-9(8)	-7(9)
C17	42(10)	15(8)	45(10)	2(7)	-9(8)	5(7)
C18	35(10)	24(8)	52(10)	1(7)	-3(9)	-9(8)
C19	63(14)	19(10)	43(11)	-1(8)	-12(10)	-6(9)

C20	40(10)	47(12)	39(9)	-3(9)	-9(8)	-29(10)
C21	49(12)	35(11)	32(9)	5(8)	7(8)	6(9)
C22	30(10)	46(12)	61(12)	9(10)	-2(10)	3(9)
C23	23(10)	100(20)	45(11)	15(12)	-2(9)	-1(11)
C24	42(12)	83(18)	43(11)	1(12)	-14(9)	4(12)

Table 4 Bond Lengths for LUB104.

Atom	Atom	Length/Å	Atom	Atom	Length/Å
I1	C7	2.143(19)	C4	C5	1.54(4)
I2	C13	2.14(2)	C5	C6	1.52(3)
I3	C20	2.12(2)	C6	C7	1.56(3)
O1	C2	1.19(3)	C9	C10	1.48(3)
O2	C8	1.19(3)	C10	C11	1.53(3)
O3	C8	1.34(2)	C10	C22	1.53(3)
O3	C9	1.47(3)	C11	C12	1.36(3)
O4	C23	1.13(3)	C11	C16	1.38(3)
O5	C23	1.33(3)	C12	C13	1.38(3)
O5	C24	1.43(3)	C13	C14	1.35(3)
N1	C1	1.42(3)	C14	C15	1.41(3)
N1	C8	1.39(2)	C15	C16	1.40(3)
N2	C2	1.40(3)	C16	C17	1.52(3)
N2	C3	1.44(3)	C17	C18	1.41(3)
N2	C6	1.46(3)	C17	C22	1.37(3)
C1	C2	1.54(3)	C18	C19	1.37(3)
C1	C7	1.49(3)	C19	C20	1.37(3)
C3	C4	1.52(4)	C20	C21	1.39(3)
C3	C23	1.55(3)	C21	C22	1.38(3)

Table 5 Bond Angles for LUB104.

Atom	Atom	Atom	Angle/°	Atom	Atom	Atom	Angle/°
C8	O3	C9	115.0(17)	C11	C10	C22	101.9(18)
C23	O5	C24	114.5(17)	C12	C11	C10	128(2)
C8	N1	C1	120.7(16)	C12	C11	C16	123(2)
C2	N2	C3	121.3(17)	C16	C11	C10	108.8(18)
C2	N2	C6	113.2(17)	C11	C12	C13	116(2)
C3	N2	C6	110.3(18)	C12	C13	I2	116.0(19)
N1	C1	C2	113.2(17)	C14	C13	I2	120.3(16)
N1	C1	C7	117.4(17)	C14	C13	C12	124(2)

C7	C1	C2	105.2(17)	C13	C14	C15	121(2)
O1	C2	N2	124(2)	C16	C15	C14	116(2)
O1	C2	C1	130(2)	C11	C16	C15	121(2)
N2	C2	C1	106.2(19)	C11	C16	C17	111.4(17)
N2	C3	C4	104.7(19)	C15	C16	C17	127.6(19)
N2	C3	C23	110.5(17)	C18	C17	C16	131.7(18)
C4	C3	C23	114(2)	C22	C17	C16	104.8(16)
C3	C4	C5	103.8(19)	C22	C17	C18	123.4(19)
C6	C5	C4	100(2)	C19	C18	C17	116.7(18)
N2	C6	C5	103.5(18)	C18	C19	C20	120(2)
N2	C6	C7	103.4(16)	C19	C20	I3	119.3(18)
C5	C6	C7	121.1(18)	C19	C20	C21	122(2)
C1	C7	I1	115.5(13)	C21	C20	I3	118.3(15)
C1	C7	C6	104.4(16)	C22	C21	C20	118.6(19)
C6	C7	I1	115.3(13)	C17	C22	C10	112.8(19)
O2	C8	O3	126.9(18)	C17	C22	C21	118.0(19)
O2	C8	N1	124.5(18)	C21	C22	C10	129(2)
O3	C8	N1	108.6(19)	O4	C23	O5	125(2)
O3	C9	C10	108.1(18)	O4	C23	C3	126(3)
C9	C10	C11	113(2)	O5	C23	C3	107.9(17)
C9	C10	C22	118(2)				

Table 6 Torsion Angles for LUB104.

A	B	C	D	Angle/°	A	B	C	D	Angle/°
I2	C13	C14	C15	179.4(17)	C9	O3	C8	O2	14(3)
I3	C20	C21	C22	-176.1(16)	C9	O3	C8	N1	-165.3(16)
O3	C9	C10	C11	-178.4(18)	C9	C10	C11	C12	-46(3)
O3	C9	C10	C22	-60(3)	C9	C10	C11	C16	129(2)
N1	C1	C2	O1	38(3)	C9	C10	C22	C17	-129(2)
N1	C1	C2	N2	-149.2(17)	C9	C10	C22	C21	50(3)
N1	C1	C7	I1	-78.2(19)	C10	C11	C12	C13	-179(2)
N1	C1	C7	C6	154.1(16)	C10	C11	C16	C15	176.7(19)
N2	C3	C4	C5	-25(3)	C10	C11	C16	C17	1(2)
N2	C3	C23	O4	-37(4)	C11	C10	C22	C17	-5(2)
N2	C3	C23	O5	155.2(19)	C11	C10	C22	C21	174(2)
N2	C6	C7	I1	-152.8(12)	C11	C12	C13	I2	178.5(16)
N2	C6	C7	C1	-25.0(18)	C11	C12	C13	C14	-3(3)
C1	N1	C8	O2	-3(3)	C11	C16	C17	C18	174(2)
C1	N1	C8	O3	176.2(16)	C11	C16	C17	C22	-4(2)
C2	N2	C3	C4	136(2)	C12	C11	C16	C15	-8(3)

C2	N2	C3	C23	-101(2)	C12	C11	C16	C17	176(2)
C2	N2	C6	C5	-113.8(19)	C12	C13	C14	C15	1(3)
C2	N2	C6	C7	13(2)	C13	C14	C15	C16	-2(3)
C2	C1	C7	I1	154.9(13)	C14	C15	C16	C11	5(3)
C2	C1	C7	C6	27.2(19)	C14	C15	C16	C17	-180(2)
C3	N2	C2	O1	42(3)	C15	C16	C17	C18	-1(3)
C3	N2	C2	C1	-131.3(19)	C15	C16	C17	C22	-179(2)
C3	N2	C6	C5	26(2)	C16	C11	C12	C13	6(3)
C3	N2	C6	C7	153.0(15)	C16	C17	C18	C19	179(2)
C3	C4	C5	C6	40(3)	C16	C17	C22	C10	5(2)
C4	C3	C23	O4	80(4)	C16	C17	C22	C21	-174.0(19)
C4	C3	C23	O5	-87(3)	C17	C18	C19	C20	-2(3)
C4	C5	C6	N2	-40(2)	C18	C17	C22	C10	-172.9(18)
C4	C5	C6	C7	-155(2)	C18	C17	C22	C21	8(3)
C5	C6	C7	I1	-38(2)	C18	C19	C20	I3	-179.4(15)
C5	C6	C7	C1	90(2)	C18	C19	C20	C21	3(3)
C6	N2	C2	O1	177(2)	C19	C20	C21	C22	2(3)
C6	N2	C2	C1	3(2)	C20	C21	C22	C10	174(2)
C6	N2	C3	C4	0(2)	C20	C21	C22	C17	-7(3)
C6	N2	C3	C23	123(2)	C22	C10	C11	C12	-173(2)
C7	C1	C2	O1	168(2)	C22	C10	C11	C16	2(2)
C7	C1	C2	N2	-20(2)	C22	C17	C18	C19	-4(3)
C8	O3	C9	C10	148.2(19)	C23	C3	C4	C5	-146(2)
C8	N1	C1	C2	63(2)	C24	O5	C23	O4	9(4)
C8	N1	C1	C7	-60(2)	C24	O5	C23	C3	176.6(19)

Table 7 Hydrogen Atom Coordinates (Å×10^4) and Isotropic Displacement Parameters (Å^2×10^3) for LUB104.

Atom	*X*	*y*	*z*	U(eq)
H1	8227	4895	6569	44
H1A	7770	4564	5950	51
H3	4319	5596	5143	57
H4A	4136	4429	4702	89
H4B	1510	4029	4877	89
H5A	4448	2978	5140	74
H5B	6504	3787	5223	74
H6	1710	3530	5622	46
H7	3490	3605	6221	42
H9A	2672	4444	7394	61
H9B	3148	5498	7531	61

H10	6751	5065	7876	65
H12	1531	5491	8219	61
H14	613	3541	9063	63
H15	3809	2592	8772	55
H18	7512	1801	8328	44
H19	10495	1422	7842	50
H21	8797	3755	7231	46
H24A	-1051	7319	4558	84
H24B	-2488	6955	4946	84
H24C	-2612	6367	4544	84

Experimental

Single crystals of $C_{24}H_{21}I_3N_2O_5$ Compound **1a** (LUB104**)** were grown in dichloromethane-hexane mixture A suitable crystal was selected and mounted on the on a **Bruker Venture Metaljet** diffractometer. The crystal was kept at 100 K during data collection. Using Olex2 [1], the structure was solved with the ShelXT [2] structure solution program using Intrinsic Phasing and refined with the XL [3] refinement package using Least Squares minimisation.

1. Dolomanov, O.V., Bourhis, L.J., Gildea, R.J, Howard, J.A.K. & Puschmann, H. (2009), J. Appl. Cryst. 42, 339-341.
2. Sheldrick, G.M. (2015). Acta Cryst. A71, 3-8.
3. Sheldrick, G.M. (2008). Acta Cryst. A64, 112-122.

Crystal structure determination of [LUB104]

Crystal Data for $C_{24}H_{21}I_3N_2O_5$ (M =798.13 g/mol): orthorhombic, space group $P2_12_12_1$ (no. 19), a = 5.2720(5) Å, b = 14.4113(14) Å, c = 33.766(3) Å, V = 2565.4(4) Å^3, Z = 4, T = 100 K, μ(GaKα) = 19.454 mm^{-1}, *Dcalc* = 2.066 g/cm^3, 19926 reflections measured (4.554° ≤ 2Θ ≤ 109.93°), 4698 unique (R_{int} = 0.0692, R_{sigma} = 0.0450) which were used in all calculations. The final R_1 was 0.0747 (I > 2σ(I)) and wR_2 was 0.1984 (all data).

Refinement model description

Number of restraints - 0, number of constraints - unknown.

Details:

```
1. Twinned data refinement
 Scales: 0.61(4) 0.39(4)
2. Fixed Uiso
 At 1.2 times of:
  All C(H) groups, All C(H,H) groups, All N(H) groups
 At 1.5 times of:
  All C(H,H,H) groups
3.a Ternary CH refined with riding coordinates:
 C1(H1A), C3(H3), C6(H6), C7(H7), C10(H10)
3.b Secondary CH2 refined with riding coordinates:
 C4(H4A,H4B), C5(H5A,H5B), C9(H9A,H9B)
3.c Aromatic/amide H refined with riding coordinates:
 N1(H1), C12(H12), C14(H14), C15(H15), C18(H18), C19(H19), C21(H21)
3.d Idealised Me refined as rotating group:
 C24(H24A,H24B,H24C)
```

This report has been created with Olex2, compiled on 2016.09.09 svn.r3337 for OlexSys. Please let us know if there are any errors or if you would like to have additional features.

Compound 2.7 (lub105):

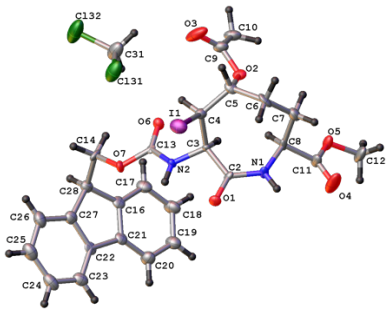

Table 1 Crystal data and structure refinement for lub105.

Identification code	lub105
Empirical formula	$C_{27}H_{29}Cl_2IN_2O_7$
Formula weight	691.32
Temperature/K	150
Crystal system	monoclinic
Space group	C2
a/Å	22.1529(11)
b/Å	9.8472(5)
c/Å	15.6753(8)
α/°	90
β/°	121.483(2)
γ/°	90
Volume/Å^3	2916.1(3)
Z	4
ρ_{calc}g/cm^3	1.575
μ/mm^{-1}	7.140
F(000)	1392.0
Crystal size/mm^3	0.4 × 0.03 × 0.02
Radiation	GaKα (λ = 1.34139)
2Θ range for data collection/°	5.752 to 109.894
Index ranges	-22 ≤ h ≤ 26, -11 ≤ k ≤ 12, -16 ≤ l ≤ 19
Reflections collected	8685
Independent reflections	4452 [R_{int} = 0.0551, R_{sigma} = 0.0867]
Data/restraints/parameters	4452/292/357
Goodness-of-fit on F^2	1.060
Final R indexes [I>=2σ (I)]	R_1 = 0.0650, wR_2 = 0.1419
Final R indexes [all data]	R_1 = 0.0800, wR_2 = 0.1517
Largest diff. peak/hole / e Å^{-3}	2.26/-1.40
Flack parameter	0.106(19)

Table 2 Fractional Atomic Coordinates ($\times 10^4$) and Equivalent Isotropic Displacement Parameters ($Å^2 \times 10^3$) for lub105. U_{eq} is defined as 1/3 of of the trace of the orthogonalised U_{IJ} tensor.

Atom	*x*	*y*	*z*	U(eq)
I1	5329.5(4)	2961.7(11)	3834.2(6)	33.8(3)
O1	7118(4)	2041(8)	4827(6)	19.8(17)
O2	6346(4)	6751(9)	5250(7)	21.8(19)
O3	5336(5)	7647(11)	4005(10)	64(4)
O4	8667(7)	3945(11)	8028(9)	65(4)
O5	8621(5)	6168(9)	7700(7)	31(2)
O6	6519(4)	6122(8)	2897(6)	21.1(18)
O7	6407(4)	4332(8)	1914(6)	19.4(17)
N1	7536(5)	3492(9)	6121(7)	19(2)
N2	6642(5)	3956(9)	3449(7)	14.6(18)
C2	7149(5)	3180(11)	5141(7)	14(2)
C3	6758(6)	4338(11)	4421(8)	13(2)
C4	6027(6)	4720(13)	4294(9)	22(2)
C5	6012(6)	5472(12)	5125(9)	22(2)
C6	6343(7)	4804(14)	6153(9)	28(3)
C7	7123(7)	5143(14)	6921(10)	31(3)
C8	7640(6)	4842(11)	6580(8)	19(2)
C9	5944(6)	7790(16)	4649(9)	31(3)
C10	6354(8)	9070(15)	4865(12)	34(3)
C11	8375(7)	4886(13)	7486(10)	29(3)
C12	9303(8)	6351(15)	8583(11)	43(4)
C13	6525(5)	4914(12)	2766(8)	13(2)
C14	6304(6)	5247(13)	1117(9)	21(2)
C16	7609(6)	5018(13)	1718(9)	23(2)
C17	7946(7)	6110(14)	2351(10)	30(3)
C18	8664(7)	5961(14)	3126(12)	36(3)
C19	9009(7)	4752(14)	3225(11)	32(3)
C20	8669(7)	3681(14)	2592(10)	32(3)
C21	7981(6)	3805(12)	1850(9)	23(2)
C22	7489(5)	2832(16)	1066(7)	20(2)
C23	7580(7)	1533(14)	864(10)	29(3)
C24	7043(8)	837(15)	89(11)	37(3)
C25	6387(9)	1482(15)	-518(11)	40(3)
C26	6275(7)	2811(19)	-324(9)	35(3)
C27	6835(7)	3488(13)	493(9)	25(2)
C28	6860(6)	4923(13)	844(9)	23(2)
Cl31	4643(2)	5821(4)	1758(3)	55.8(12)
Cl32	4340(3)	8145(6)	474(3)	74.1(15)

C31	4903(9)	7475(15)	1654(12)	47(4)

Table 3 Anisotropic Displacement Parameters ($Å^2 \times 10^3$) for lub105. The Anisotropic displacement factor exponent takes the form: $-2\pi^2[h^2a^{*2}U_{11}+2hka^*b^*U_{12}+\ldots]$.

Atom	U_{11}	U_{22}	U_{33}	U_{23}	U_{13}	U_{12}
I1	29.3(4)	27.1(4)	48.8(5)	-7.1(5)	23.1(4)	-10.0(4)
O1	25(4)	10(4)	24(4)	-1(3)	12(4)	-1(3)
O2	17(4)	22(4)	29(4)	2(3)	14(4)	1(3)
O3	35(4)	33(8)	80(7)	-4(5)	-1(5)	13(4)
O4	76(8)	21(5)	41(6)	6(4)	-10(6)	9(5)
O5	32(5)	20(4)	19(4)	-1(3)	-1(4)	-1(3)
O6	27(4)	16(4)	19(4)	-1(3)	11(4)	-2(3)
O7	27(4)	20(4)	9(3)	0(3)	9(3)	2(3)
N1	28(5)	7(4)	14(4)	1(3)	6(4)	0(3)
N2	20(5)	12(4)	12(4)	0(3)	9(4)	2(3)
C2	9(4)	12(5)	14(4)	1(3)	2(3)	-1(3)
C3	15(5)	10(4)	12(4)	0(3)	6(4)	3(3)
C4	23(5)	23(5)	22(5)	4(4)	14(4)	5(4)
C5	25(5)	23(5)	26(5)	-3(4)	20(5)	-4(4)
C6	46(6)	26(6)	27(5)	-9(4)	29(5)	-3(5)
C7	43(6)	27(7)	25(6)	-4(5)	19(5)	4(5)
C8	30(5)	10(5)	10(4)	1(4)	5(4)	2(4)
C9	29(5)	23(6)	38(6)	-1(5)	17(4)	6(4)
C10	34(7)	23(6)	48(9)	0(5)	23(7)	8(5)
C11	32(5)	16(5)	21(5)	-5(4)	2(4)	2(4)
C12	35(7)	30(7)	28(6)	-3(6)	-9(6)	4(5)
C13	4(5)	20(4)	13(4)	0(3)	4(4)	0(3)
C14	15(5)	29(6)	15(5)	12(4)	7(4)	9(4)
C16	28(5)	29(5)	23(5)	2(4)	21(4)	-1(4)
C17	28(5)	30(6)	40(6)	-4(5)	23(5)	0(4)
C18	36(6)	26(6)	47(7)	-9(5)	23(5)	-4(4)
C19	30(6)	31(6)	39(6)	-6(5)	20(5)	-1(4)
C20	33(5)	25(6)	34(6)	-1(5)	15(5)	-1(4)
C21	29(5)	26(5)	23(5)	1(4)	21(4)	0(4)
C22	33(4)	22(5)	18(4)	5(4)	21(4)	-2(4)
C23	40(6)	25(5)	35(6)	1(4)	28(5)	0(4)
C24	53(6)	32(6)	38(6)	-11(5)	33(5)	-11(5)
C25	54(7)	33(6)	37(7)	-9(5)	27(6)	-11(5)
C26	42(6)	41(7)	26(5)	-6(5)	21(5)	-7(5)
C27	32(5)	24(5)	24(5)	4(4)	18(4)	-1(4)

C28	29(5)	21(5)	23(5)	3(4)	16(4)	0(4)
Cl31	47(2)	40(2)	45(2)	3.8(17)	-0.2(19)	-10.6(17)
Cl32	76(3)	44(3)	45(2)	5(2)	-8(2)	-3(2)
C31	43(8)	27(6)	42(7)	-1(5)	2(6)	-3(5)

Table 4 Bond Lengths for lub105.

Atom	Atom	Length/Å	Atom	Atom	Length/Å
I1	C4	2.177(12)	C8	C11	1.501(17)
O1	C2	1.212(15)	C9	C10	1.48(2)
O2	C5	1.423(15)	C14	C28	1.533(17)
O2	C9	1.361(16)	C16	C17	1.388(19)
O3	C9	1.198(15)	C16	C21	1.404(17)
O4	C11	1.194(17)	C16	C28	1.504(17)
O5	C11	1.346(16)	C17	C18	1.42(2)
O5	C12	1.431(16)	C18	C19	1.379(19)
O6	C13	1.209(15)	C19	C20	1.372(19)
O7	C13	1.346(14)	C20	C21	1.356(18)
O7	C14	1.459(14)	C21	C22	1.489(18)
N1	C2	1.347(14)	C22	C23	1.36(2)
N1	C8	1.471(14)	C22	C27	1.402(17)
N2	C3	1.457(14)	C23	C24	1.36(2)
N2	C13	1.347(15)	C24	C25	1.41(2)
C2	C3	1.518(15)	C25	C26	1.39(2)
C3	C4	1.570(15)	C26	C27	1.402(18)
C4	C5	1.515(17)	C27	C28	1.506(18)
C5	C6	1.527(17)	Cl31	C31	1.764(15)
C6	C7	1.541(19)	Cl32	C31	1.733(16)
C7	C8	1.526(18)			

Table 5 Bond Angles for lub105.

Atom	Atom	Atom	Angle/°	Atom	Atom	Atom	Angle/°
C9	O2	C5	117.7(10)	O6	C13	O7	125.1(11)
C11	O5	C12	116.4(10)	O6	C13	N2	124.6(11)
C13	O7	C14	116.7(9)	N2	C13	O7	110.3(10)
C2	N1	C8	127.4(9)	O7	C14	C28	108.7(9)
C13	N2	C3	120.5(9)	C17	C16	C21	119.9(11)
O1	C2	N1	122.7(10)	C17	C16	C28	128.7(12)
O1	C2	C3	120.3(9)	C21	C16	C28	111.4(11)

N1	C2	C3	116.9(9)	C16	C17	C18	118.4(12)
N2	C3	C2	107.7(8)	C19	C18	C17	119.6(13)
N2	C3	C4	108.8(9)	C20	C19	C18	121.3(13)
C2	C3	C4	115.2(9)	C21	C20	C19	119.9(13)
C3	C4	I1	111.0(7)	C16	C21	C22	107.8(11)
C5	C4	I1	110.0(8)	C20	C21	C16	120.9(12)
C5	C4	C3	119.5(10)	C20	C21	C22	131.3(12)
O2	C5	C4	107.9(10)	C23	C22	C21	131.7(11)
O2	C5	C6	107.9(10)	C23	C22	C27	120.9(12)
C4	C5	C6	118.9(11)	C27	C22	C21	107.3(12)
C5	C6	C7	117.1(11)	C22	C23	C24	121.1(13)
C8	C7	C6	115.2(10)	C23	C24	C25	119.3(14)
N1	C8	C7	113.1(10)	C26	C25	C24	121.0(14)
N1	C8	C11	107.7(9)	C25	C26	C27	118.2(14)
C11	C8	C7	107.8(10)	C22	C27	C26	119.4(13)
O2	C9	C10	112.3(10)	C22	C27	C28	111.7(11)
O3	C9	O2	122.4(13)	C26	C27	C28	128.8(12)
O3	C9	C10	125.2(13)	C16	C28	C14	113.4(10)
O4	C11	O5	123.5(12)	C16	C28	C27	101.8(10)
O4	C11	C8	124.5(13)	C27	C28	C14	114.5(10)
O5	C11	C8	111.1(10)	Cl32	C31	Cl31	111.2(8)

Table 6 Hydrogen Bonds for lub105.

D	H	A	d(D-H)/Å	d(H-A)/Å	d(D-A)/Å	D-H-A/°
N1	H1	O6[1]	0.88	2.16	2.972(13)	153.1
N2	H2	O5[1]	0.88	2.34	3.166(13)	157.2

[1]3/2-X,-1/2+Y,1-Z

Table 7 Hydrogen Atom Coordinates (Å×10^4) and Isotropic Displacement Parameters (Å^2×10^3) for lub105.

Atom	*x*	*y*	*z*	U(eq)
H1	7752	2810	6534	30(30)
H2	6649	3094	3307	130(90)
H3	7068	5161	4662	15
H4	5798	5350	3708	26
H5	5504	5656	4889	26
H6A	6302	3808	6056	34
H6B	6057	5061	6447	34
H7A	7157	6119	7091	37
H7B	7271	4621	7540	37

H8	7593	5553	6093	23
H10A	6734	9085	5570	51
H10B	6039	9848	4725	51
H10C	6558	9123	4442	51
H12A	9478	7264	8583	65
H12B	9632	5674	8597	65
H12C	9266	6238	9175	65
H14A	6355	6201	1343	25
H14B	5823	5127	523	25
H17	7701	6939	2267	36
H18	8906	6689	3574	43
H19	9492	4659	3742	39
H20	8915	2855	2674	38
H23	8025	1103	1271	35
H24	7111	-75	-40	44
H25	6015	1006	-1069	48
H26	5832	3245	-735	42
H28	6800	5565	311	28
H31A	4901	8069	2163	57
H31B	5391	7450	1787	57

Experimental

Single crystals of $C_{27}H_{29}Cl_2IN_2O_7$ Compound **2.7** (LUB105) were grown in dichloromethane-hexane mixture A suitable crystal was selected and mounted on the on a **Bruker Venture Metaljet** diffractometer. The crystal was kept at 150 K during data collection. Using Olex2 [1], the structure was solved with the XT [2] structure solution program using Intrinsic Phasing and refined with the XL [3] refinement package using Least Squares minimisation.

1. Dolomanov, O.V., Bourhis, L.J., Gildea, R.J, Howard, J.A.K. & Puschmann, H. (2009), J. Appl. Cryst. 42, 339-341.
2. Sheldrick, G.M. (2015). Acta Cryst. A71, 3-8.
3. Sheldrick, G.M. (2008). Acta Cryst. A64, 112-122.

Crystal structure determination of [lub105]

Crystal Data for $C_{27}H_{29}Cl_2IN_2O_7$ (M =691.32 g/mol): monoclinic, space group C2 (no. 5), a = 22.1529(11) Å, b = 9.8472(5) Å, c = 15.6753(8) Å, β = 121.483(2)°, V = 2916.1(3) Å^3, Z = 4, T = 150 K, μ(GaKα) = 7.140 mm^{-1}, *Dcalc* = 1.575 g/cm^3, 8685 reflections measured (5.752° ≤ 2Θ ≤ 109.894°), 4452 unique (R_{int} = 0.0551, R_{sigma} = 0.0867) which were used in all calculations. The final R_1 was 0.0650 (I > 2σ(I)) and wR_2 was 0.1517 (all data).

Refinement model description

Number of restraints - 292, number of constraints - unknown.

Details:

```
1. Twinned data refinement
 Scales: 0.894(19)
 0.106(19)
2. Fixed Uiso
 At 1.2 times of:
  All C(H) groups, All C(H,H) groups
 At 1.5 times of:
  All C(H,H,H) groups
3. Rigid body (RIGU) restrains
```

```
 All non-hydrogen atoms
 with sigma for 1-2 distances of 0.004 and sigma for 1-3 distances of 0.004
4.a Ternary CH refined with riding coordinates:
 C3(H3), C4(H4), C5(H5), C8(H8), C28(H28)
4.b Secondary CH2 refined with riding coordinates:
 C6(H6A,H6B), C7(H7A,H7B), C14(H14A,H14B), C31(H31A,H31B)
4.c Aromatic/amide H refined with riding coordinates:
 N1(H1), N2(H2), C17(H17), C18(H18), C19(H19), C20(H20), C23(H23), C24(H24),
 C25(H25), C26(H26)
4.d Idealised Me refined as rotating group:
 C10(H10A,H10B,H10C), C12(H12A,H12B,H12C)
```

This report has been created with Olex2, compiled on 2017.03.28 svn.r3405 for OlexSys. Please let us know if there are any errors or if you would like to have additional features.

Compound 2.8 (LUB110):

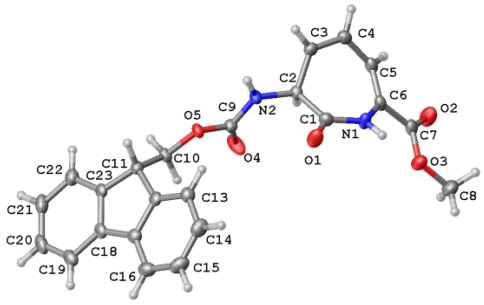

Table 1 Crystal data and structure refinement for lub110.

Identification code	lub110
Empirical formula	$C_{23}H_{20}N_2O_5$
Formula weight	404.41
Temperature/K	150
Crystal system	orthorhombic
Space group	$P2_12_12$
a/Å	11.5449(5)
b/Å	34.1483(14)
c/Å	4.9573(2)
α/°	90
β/°	90
γ/°	90
Volume/Å^3	1954.36(14)
Z	4
ρ_{calc}g/cm^3	1.374
μ/mm^{-1}	0.518
F(000)	848.0
Crystal size/mm^3	0.22 × 0.015 × 0.015
Radiation	GaKα (λ = 1.34139)
2Θ range for data collection/°	4.502 to 111.882

Index ranges	$-14 \leq h \leq 14$, $-42 \leq k \leq 42$, $-6 \leq l \leq 6$
Reflections collected	29195
Independent reflections	3855 [R_{int} = 0.0801, R_{sigma} = 0.0529]
Data/restraints/parameters	3855/0/272
Goodness-of-fit on F^2	1.050
Final R indexes [I>=2σ (I)]	R_1 = 0.0481, wR_2 = 0.0895
Final R indexes [all data]	R_1 = 0.0728, wR_2 = 0.0982
Largest diff. peak/hole / e $Å^{-3}$	0.19/-0.23
Flack parameter	0.26(14)

Table 2 Fractional Atomic Coordinates (×10^4) and Equivalent Isotropic Displacement Parameters ($Å^2$×10^3) for lub110. U_{eq} is defined as 1/3 of of the trace of the orthogonalised U_{IJ} tensor.

Atom	*x*	*y*	*z*	U(eq)
O1	4974(2)	5492.9(6)	9203(5)	37.4(6)
O2	8885(2)	4707.6(6)	4347(6)	40.7(6)
O3	6980.9(19)	4594.3(6)	4665(5)	33.9(6)
O4	5730(2)	6311.0(7)	4363(4)	41.5(7)
O5	4629.8(17)	6622.0(6)	7466(4)	21.6(5)
N1	6578(2)	5150.4(7)	8103(6)	25.8(6)
N2	5978(2)	6200.6(7)	8817(5)	21.8(6)
C1	6005(3)	5487.5(9)	8646(6)	25.3(7)
C2	6719(2)	5863.9(8)	8482(6)	20.1(7)
C3	7670(3)	5851.7(9)	10551(6)	21.8(7)
C4	8550(3)	5602.9(9)	10347(7)	26.3(7)
C5	8631(3)	5311.2(8)	8247(7)	25.4(7)
C6	7732(3)	5107.3(8)	7265(6)	23.4(7)
C7	7950(3)	4787.3(9)	5264(7)	26.8(8)
C8	7099(3)	4269.4(9)	2831(7)	37.6(9)
C9	5470(3)	6370.1(8)	6694(6)	21.8(7)
C10	4193(3)	6872.9(9)	5352(6)	22.3(7)
C11	3059(3)	7051.2(8)	6298(6)	21.4(7)
C12	2070(3)	6759.0(8)	6420(6)	22.7(7)
C13	1932(3)	6437.3(9)	8100(7)	26.9(8)
C14	948(3)	6208.4(10)	7832(7)	33.9(8)
C15	120(3)	6294.4(10)	5890(7)	35.3(9)
C16	250(3)	6613.5(10)	4207(7)	31.3(8)
C17	1228(3)	6850.8(9)	4496(6)	23.8(7)
C18	1572(3)	7213.9(9)	3122(6)	24.2(7)
C19	1031(3)	7431.4(9)	1089(6)	31.3(8)
C20	1551(3)	7771.2(10)	206(7)	34.4(9)

C21	2590(3)	7899.2(9)	1294(7)	33.9(9)
C22	3141(3)	7680.5(9)	3298(6)	28.7(8)
C23	2627(3)	7338.8(8)	4196(6)	22.5(7)

Table 3 Anisotropic Displacement Parameters ($Å^2×10^3$) for lub110. The Anisotropic displacement factor exponent takes the form: $-2\pi^2[h^2a^{*2}U_{11}+2hka^*b^*U_{12}+\ldots]$.

Atom	U_{11}	U_{22}	U_{33}	U_{23}	U_{13}	U_{12}
O1	18.1(13)	30.2(12)	64.0(16)	-9.6(12)	4.9(13)	-0.4(10)
O2	26.3(14)	34.8(13)	61.0(16)	-13.0(13)	8.0(13)	2.4(11)
O3	27.2(13)	30.4(12)	44.0(14)	-11.7(11)	-4.1(11)	1.6(11)
O4	50.0(16)	58.8(16)	15.7(11)	-2.9(12)	1.8(12)	31.6(13)
O5	23.4(12)	22.1(10)	19.3(10)	1.4(9)	-0.5(9)	8.9(9)
N1	16.0(14)	17.5(13)	44.0(17)	-1.5(12)	2.8(13)	-0.1(11)
N2	28.5(15)	21.3(13)	15.6(12)	-0.2(10)	-0.7(12)	7.2(12)
C1	20.5(18)	26.7(17)	28.6(16)	-1.3(14)	-1.7(15)	0.7(15)
C2	19.6(17)	20.6(15)	19.9(14)	0.6(13)	2.9(13)	3.1(13)
C3	21.4(17)	21.1(15)	23.0(15)	-0.7(13)	1.0(14)	-2.3(14)
C4	21.0(17)	26.0(17)	32.0(17)	1.3(14)	-4.3(15)	-0.3(15)
C5	16.8(17)	23.0(16)	36.3(18)	4.5(14)	1.0(15)	2.7(14)
C6	19.5(17)	19.0(15)	31.7(17)	4.3(13)	0.7(14)	3.2(13)
C7	24.2(19)	19.0(16)	37.3(19)	4.6(14)	-0.1(16)	1.7(15)
C8	41(2)	31.4(19)	40(2)	-10.4(16)	-8.0(18)	3.9(17)
C9	24.6(18)	21.5(16)	19.3(16)	0.1(13)	-0.9(14)	1.6(14)
C10	22.8(17)	22.8(15)	21.2(14)	3.5(13)	-0.9(14)	6.0(14)
C11	24.9(18)	19.3(15)	20.1(15)	-1.4(13)	-1.4(14)	2.5(14)
C12	25.4(18)	20.6(15)	22.1(15)	-5.8(13)	2.1(14)	5.6(14)
C13	29.1(19)	26.1(17)	25.5(17)	0.0(13)	0.1(16)	2.7(15)
C14	38(2)	29.6(17)	34.1(19)	-0.8(15)	8.6(18)	-6.0(17)
C15	30(2)	38(2)	38(2)	-9.6(17)	6.3(18)	-9.1(17)
C16	24.4(19)	37.9(19)	31.6(18)	-8.1(16)	-2.4(16)	2.9(16)
C17	22.4(18)	26.4(16)	22.7(14)	-4.6(14)	1.6(14)	3.8(14)
C18	23.1(18)	24.5(16)	25.0(17)	-3.3(14)	1.2(14)	10.8(15)
C19	33(2)	35.0(18)	25.6(18)	-3.2(14)	-2.4(16)	14.5(16)
C20	41(2)	33.0(19)	29.1(19)	2.7(16)	1.9(17)	20.6(18)
C21	45(2)	23.7(17)	32.9(18)	2.9(15)	6.7(18)	10.3(16)
C22	33(2)	23.7(17)	29.7(17)	-1.3(14)	2.1(16)	4.2(14)
C23	23.1(17)	21.0(15)	23.3(15)	-4.7(13)	0.1(14)	8.3(14)

Table 4 Bond Lengths for lub110.

Atom	Atom	Length/Å	Atom	Atom	Length/Å
O1	C1	1.222(4)	C10	C11	1.518(4)
O2	C7	1.202(4)	C11	C12	1.517(4)
O3	C7	1.332(4)	C11	C23	1.516(4)
O3	C8	1.441(4)	C12	C13	1.387(4)
O4	C9	1.211(4)	C12	C17	1.398(4)
O5	C9	1.352(4)	C13	C14	1.385(5)
O5	C10	1.444(3)	C14	C15	1.388(5)
N1	C1	1.354(4)	C15	C16	1.381(5)
N1	C6	1.404(4)	C16	C17	1.397(4)
N2	C2	1.443(4)	C17	C18	1.469(4)
N2	C9	1.337(4)	C18	C19	1.399(4)
C1	C2	1.529(4)	C18	C23	1.396(4)
C2	C3	1.502(4)	C19	C20	1.378(5)
C3	C4	1.329(4)	C20	C21	1.386(5)
C4	C5	1.444(4)	C21	C22	1.396(5)
C5	C6	1.341(4)	C22	C23	1.383(4)
C6	C7	1.497(4)			

Table 5 Bond Angles for lub110.

Atom	Atom	Atom	Angle/°	Atom	Atom	Atom	Angle/°
C7	O3	C8	116.2(3)	C12	C11	C10	113.4(2)
C9	O5	C10	115.0(2)	C23	C11	C10	109.3(2)
C1	N1	C6	127.7(3)	C23	C11	C12	101.9(2)
C9	N2	C2	121.0(2)	C13	C12	C11	129.1(3)
O1	C1	N1	122.2(3)	C13	C12	C17	120.4(3)
O1	C1	C2	121.6(3)	C17	C12	C11	110.4(3)
N1	C1	C2	116.1(3)	C14	C13	C12	118.9(3)
N2	C2	C1	110.1(2)	C13	C14	C15	120.8(3)
N2	C2	C3	112.1(2)	C16	C15	C14	120.7(3)
C3	C2	C1	109.5(2)	C15	C16	C17	118.9(3)
C4	C3	C2	121.6(3)	C12	C17	C18	108.5(3)
C3	C4	C5	123.1(3)	C16	C17	C12	120.1(3)
C6	C5	C4	124.7(3)	C16	C17	C18	131.3(3)
N1	C6	C7	115.6(3)	C19	C18	C17	131.4(3)
C5	C6	N1	124.9(3)	C23	C18	C17	108.5(3)
C5	C6	C7	119.3(3)	C23	C18	C19	120.1(3)
O2	C7	O3	123.9(3)	C20	C19	C18	118.8(3)
O2	C7	C6	124.5(3)	C19	C20	C21	121.3(3)

O3	C7	C6	111.6(3)	C20	C21	C22	120.2(3)
O4	C9	O5	123.7(3)	C23	C22	C21	119.0(3)
O4	C9	N2	124.8(3)	C18	C23	C11	110.6(3)
N2	C9	O5	111.6(2)	C22	C23	C11	128.8(3)
O5	C10	C11	108.3(2)	C22	C23	C18	120.6(3)

Table 6 Hydrogen Bonds for lub110.

D	H	A	d(D-H)/Å	d(H-A)/Å	d(D-A)/Å	D-H-A/°
N1	H1	O1[1]	0.88	2.02	2.886(3)	167.6
N2	H2	O4[2]	0.88	1.95	2.790(3)	159.2

[1]1-X,1-Y,+Z; [2]+X,+Y,1+Z

Table 7 Hydrogen Atom Coordinates (Å×10^4) and Isotropic Displacement Parameters (Å^2×10^3) for lub110.

Atom	*x*	*y*	*z*	U(eq)
H1	6179	4933	8299	31
H2	5859	6296	10443	26
H2A	7082	5878	6653	24
H3	7640	6026	12041	26
H4	9155	5618	11643	32
H5	9375	5260	7507	30
H8A	7348	4366	1062	56
H8B	6353	4135	2652	56
H8C	7678	4086	3533	56
H10A	4066	6719	3685	27
H10B	4761	7082	4954	27
H11	3162	7184	8080	26
H13	2503	6375	9412	32
H14	839	5990	8991	41
H15	-543	6132	5717	42
H16	-316	6671	2874	38
H19	318	7346	331	38
H20	1190	7921	-1175	41
H21	2928	8136	675	41
H22	3859	7765	4033	34

Experimental

Single crystals of $C_{23}H_{20}N_2O_5$ Compound **8** (LUB110**)** were grown in dichloromethane-hexane mixture A suitable crystal was selected and mounted on the on a **Bruker Venture Metaljet** diffractometer. The crystal was kept at 150

K during data collection. Using Olex2 [1], the structure was solved with the XT [2] structure solution program using Intrinsic Phasing and refined with the XL [3] refinement package using Least Squares minimisation.

1. Dolomanov, O.V., Bourhis, L.J., Gildea, R.J, Howard, J.A.K. & Puschmann, H. (2009), J. Appl. Cryst. 42, 339-341.
2. Sheldrick, G.M. (2015). Acta Cryst. A71, 3-8.
3. Sheldrick, G.M. (2008). Acta Cryst. A64, 112-122.

Crystal structure determination of [lub110]

Crystal Data for $C_{23}H_{20}N_2O_5$ (M =404.41 g/mol): orthorhombic, space group $P2_12_12$ (no. 18), a = 11.5449(5) Å, b = 34.1483(14) Å, c = 4.9573(2) Å, V = 1954.36(14) Å^3, Z = 4, T = 150 K, μ(GaKα) = 0.518 mm^{-1}, *Dcalc* = 1.374 g/cm^3, 29195 reflections measured (4.502° ≤ 2Θ ≤ 111.882°), 3855 unique (R_{int} = 0.0801, R_{sigma} = 0.0529) which were used in all calculations. The final R_1 was 0.0481 (I > 2σ(I)) and wR_2 was 0.0982 (all data).

Refinement model description

Number of restraints - 0, number of constraints - unknown.

Details:

```
1. Fixed Uiso
 At 1.2 times of:
  All C(H) groups, All C(H,H) groups, All N(H) groups
 At 1.5 times of:
  All C(H,H,H) groups
2.a Ternary CH refined with riding coordinates:
 C2(H2A), C11(H11)
2.b Secondary CH2 refined with riding coordinates:
 C10(H10A,H10B)
2.c Aromatic/amide H refined with riding coordinates:
 N1(H1), N2(H2), C3(H3), C4(H4), C5(H5), C13(H13), C14(H14), C15(H15),
 C16(H16), C19(H19), C20(H20), C21(H21), C22(H22)
2.d Idealised Me refined as rotating group:
 C8(H8A,H8B,H8C)
```

This report has been created with Olex2, compiled on 2017.03.28 svn.r3405 for OlexSys. Please let us know if there are any errors or if you would like to have additional features.

Compound (2.16a) lub106:

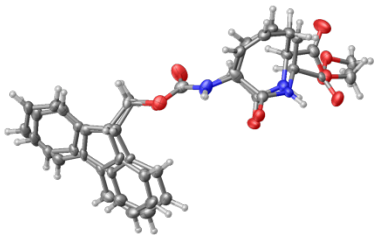

A big part of the molecule is disordered over 2 sites. Each model was refined anisotropically; to help to keep good geometry, SAME, SADI restraints were used.

Table 1 Crystal data and structure refinement for lub106.

Identification code	lub106
Empirical formula	$C_{23}H_{22}N_2O_5$
Formula weight	406.42
Temperature/K	150

Crystal system	orthorhombic
Space group	$P2_12_12$
a/Å	11.3495(5)
b/Å	36.3258(17)
c/Å	4.7864(2)
α/°	90
β/°	90
γ/°	90
Volume/Å^3	1973.34(15)
Z	4
ρ_{calc}g/cm^3	1.368
μ/mm^{-1}	0.513
F(000)	856.0
Crystal size/mm^3	0.4 × 0.04 × 0.04
Radiation	GaKα (λ = 1.34139)
2Θ range for data collection/°	4.232 to 109.94
Index ranges	-13 ≤ h ≤ 13, -44 ≤ k ≤ 44, -5 ≤ l ≤ 5
Reflections collected	51210
Independent reflections	3742 [R_{int} = 0.0550, R_{sigma} = 0.0232]
Data/restraints/parameters	3742/70/518
Goodness-of-fit on F^2	1.089
Final R indexes [I>=2σ (I)]	R_1 = 0.0312, wR_2 = 0.0754
Final R indexes [all data]	R_1 = 0.0350, wR_2 = 0.0771
Largest diff. peak/hole / e Å^{-3}	0.18/-0.12
Flack parameter	0.06(7)

Table 2 Fractional Atomic Coordinates (×10^4) and Equivalent Isotropic Displacement Parameters (Å^2×10^3) for lub106. U_{eq} is defined as 1/3 of of the trace of the orthogonalised U_{IJ} tensor.

Atom	*x*	*y*	*z*	U(eq)
O4	4337.7(14)	6351.5(4)	6386(3)	52.1(4)
N2	4284.7(16)	6127.6(4)	1987(3)	40.4(4)
C9	4652.9(17)	6358.6(5)	3966(4)	32.8(4)
N1	3527(10)	5179(2)	2660(20)	34.5(19)
O1	5111(2)	5462.1(7)	737(7)	41.4(8)
C1	4155(7)	5479(2)	1924(15)	28.5(16)
C2	3566(8)	5830(3)	2730(30)	28(3)
C3	2477(4)	5890.7(11)	765(10)	33.0(9)
C4	1586(3)	5654.2(11)	614(9)	35.9(9)
C5	1403(3)	5304.9(16)	2226(11)	36.9(10)
C6	2416(5)	5196.7(13)	4147(9)	30.2(9)

C7	2139(3)	4836.9(10)	5634(9)	37.1(10)
O2	1206(3)	4779.2(8)	6773(8)	65.4(11)
O3	3036(8)	4611(3)	5610(20)	48(3)
C8	2881(4)	4257.1(10)	7034(12)	45.0(11)
O5	5477(14)	6610(4)	3170(40)	26.7(19)
C10	5830(11)	6912(4)	4940(30)	37(4)
C11	6971(9)	7090(3)	4070(30)	24(2)
C12	7326(14)	7397(4)	5990(40)	26(2)
C13	6783(18)	7728(5)	6550(50)	39(3)
C14	7275(11)	7982(2)	8350(30)	40(2)
C15	8294(8)	7891(2)	9825(18)	39(2)
C16	8846(8)	7556(2)	9340(18)	33(2)
C17	8380(9)	7319(3)	7423(19)	26.2(18)
C18	8805(7)	6964(2)	6401(16)	26.4(17)
C19	9805(5)	6757.3(17)	7062(13)	37.5(14)
C20	10045(7)	6443(2)	5565(17)	44(2)
C21	9332(6)	6329.9(16)	3418(15)	42.0(14)
C22	8301(6)	6527.8(19)	2794(15)	37.7(15)
C23	8038(9)	6841(2)	4320(20)	30(2)
N31	3666(11)	5116(3)	1940(20)	29.8(17)
O31	4597(3)	5489.7(7)	-1103(6)	34.3(7)
C31	3999(8)	5447(3)	977(16)	30.0(19)
C32	3566(10)	5791(3)	2460(40)	45(5)
C33	2214(4)	5795.3(12)	2221(14)	41.1(12)
C34	1436(4)	5528.4(16)	2655(13)	43.9(13)
C35	1638(5)	5144.4(13)	3717(13)	36.6(10)
C36	2922(5)	5053.7(13)	4349(9)	28.3(10)
C37	3037(10)	4644(4)	5300(30)	25(2)
O32	3624(3)	4426.7(8)	4047(7)	44.4(8)
O33	2438(3)	4592.2(7)	7586(7)	36.0(8)
C38	2507(4)	4225.2(11)	8735(12)	40.1(11)
O50	5362(17)	6607(5)	2710(40)	35(3)
C40	5770(9)	6860(5)	4880(30)	27(3)
C41	6922(11)	7011(4)	3680(40)	30(3)
C42	7357(16)	7301(4)	5690(50)	31(3)
C43	6841(17)	7638(5)	6350(40)	36(3)
C44	7416(12)	7867(3)	8270(30)	40(2)
C45	8497(8)	7758(3)	9423(19)	38(3)
C46	9002(10)	7424(3)	8770(20)	37(2)
C47	8425(11)	7199(3)	6900(20)	28(2)
C48	8757(7)	6839(2)	5717(16)	25.6(16)
C49	9759(7)	6618(2)	6140(16)	41(2)

C50	9864(8)	6295(2)	4686(17)	43.5(17)
C51	9006(5)	6185.5(16)	2811(14)	40.1(14)
C52	8013(6)	6403.7(17)	2358(15)	32.8(14)
C53	7911(9)	6729(2)	3830(20)	23.7(18)

Table 3 Anisotropic Displacement Parameters ($Å^2×10^3$) for lub106. The Anisotropic displacement factor exponent takes the form: $-2\pi^2[h^2a^{*2}U_{11}+2hka^*b^*U_{12}+\ldots]$.

Atom	U_{11}	U_{22}	U_{33}	U_{23}	U_{13}	U_{12}
O4	65.3(10)	69.7(10)	21.4(7)	0.9(7)	5.3(6)	-23.1(8)
N2	66.6(11)	33.2(8)	21.5(8)	3.4(7)	7.8(8)	3.5(8)
C9	38.3(10)	36.1(9)	23.9(9)	7.0(8)	1.7(8)	8.1(8)
N1	29(3)	26(3)	49(5)	5(3)	0(3)	3(2)
O1	27.0(14)	31.3(13)	66(2)	9.8(13)	8.8(15)	-0.6(10)
C1	24(3)	24(3)	38(4)	6(3)	-1(3)	-1(2)
C2	31(5)	33(4)	20(4)	-14(3)	1(3)	10(3)
C3	36(2)	25(2)	37(2)	2.3(17)	6.7(19)	4.0(16)
C4	30.9(19)	37(2)	40(2)	-0.5(19)	-1.9(18)	4.9(16)
C5	24.4(19)	35(3)	51(3)	2(3)	1.9(19)	-2.3(19)
C6	23(3)	30(2)	38(2)	1.9(17)	1(2)	-3(2)
C7	33(2)	35.1(19)	43(2)	4.1(16)	-3.3(17)	-6.7(17)
O2	41.4(17)	55.9(18)	99(3)	30.0(18)	16.5(18)	-5.3(13)
O3	52(4)	38(3)	53(5)	8(3)	-1(4)	6(3)
C8	51(3)	32(2)	52(3)	5(2)	-8(2)	-8.1(18)
O5	38(3)	30(3)	12(4)	1(2)	1(3)	8(2)
C10	54(6)	29(4)	28(5)	-6(3)	-14(4)	3(3)
C11	28(3)	26(5)	18(4)	-1(4)	-3(2)	4(3)
C12	28(3)	25(6)	26(4)	-1(4)	6(3)	-2(4)
C13	36(4)	34(6)	47(5)	-9(4)	5(3)	3(4)
C14	41(4)	33(4)	47(3)	-15(4)	10(3)	-12(3)
C15	44(4)	43(5)	31(3)	-16(3)	10(3)	-21(3)
C16	33(5)	34(6)	33(4)	-2(4)	1(3)	-12(4)
C17	28(3)	24(5)	27(4)	1(3)	-1(3)	-9(4)
C18	29(2)	24(5)	26(3)	2(3)	0(2)	-14(3)
C19	29(2)	39(4)	44(3)	14(3)	-4(2)	-1(2)
C20	36(3)	39(5)	57(5)	10(4)	1(3)	9(3)
C21	43(4)	27(3)	56(4)	5(3)	10(3)	8(3)
C22	39(4)	33(4)	41(3)	-3(3)	2(2)	-4(3)
C23	41(4)	18(4)	30(4)	-1(3)	9(3)	0(3)
N31	22(3)	25(3)	42(5)	0(2)	5(3)	-4(2)
O31	39.2(16)	29.9(13)	33.7(17)	-1.7(12)	6.3(15)	-1.1(12)

C31	28(3)	29(3)	33(4)	1(3)	-5(3)	1(2)
C32	42(6)	62(8)	30(6)	0(5)	4(4)	-19(6)
C33	38(3)	21(2)	64(4)	2(2)	7(3)	9.3(18)
C34	25(2)	36(3)	71(4)	5(3)	9(2)	6(2)
C35	28(3)	32(2)	50(3)	1(2)	6(2)	-1(2)
C36	25(2)	29(2)	31(2)	-1.7(18)	6(2)	-3(2)
C37	19(4)	26(4)	29(4)	-7(3)	0(3)	-7(3)
O32	56.6(19)	27.6(14)	48.9(18)	1.1(13)	9.5(16)	2.1(13)
O33	41.0(16)	29.3(15)	37.9(18)	7.9(13)	3.9(15)	-5.1(12)
C38	48(3)	29(2)	43(3)	9(2)	-3(2)	-13.3(18)
O50	47(4)	41(4)	17(6)	4(3)	-4(3)	1(3)
C40	16(4)	36(6)	28(6)	7(4)	14(3)	2(3)
C41	37(4)	32(5)	22(4)	-6(4)	4(3)	-2(3)
C42	30(3)	35(8)	28(6)	3(5)	6(3)	0(5)
C43	36(6)	46(9)	25(4)	-5(5)	2(4)	-14(6)
C44	49(4)	31(5)	41(4)	-5(5)	15(3)	-9(4)
C45	41(6)	41(8)	31(4)	-20(5)	9(3)	-17(5)
C46	31(3)	40(6)	39(5)	-3(4)	7(3)	-8(4)
C47	34(4)	22(6)	28(4)	-7(4)	5(3)	-13(4)
C48	27(3)	26(4)	24(3)	-6(2)	-2(3)	-6(3)
C49	34(4)	48(6)	42(4)	-9(4)	2(3)	-4(4)
C50	41(4)	45(5)	45(4)	4(3)	9(3)	12(3)
C51	42(3)	31(3)	48(3)	-1(3)	15(3)	-3(2)
C52	36(3)	28(3)	34(3)	-3(3)	5(2)	-1(2)
C53	29(3)	21(5)	20(3)	-2(3)	6(2)	3(3)

Table 4 Bond Lengths for lub106.

Atom	Atom	Length/Å	Atom	Atom	Length/Å
O4	C9	1.212(2)	C20	C21	1.372(10)
N2	C9	1.333(3)	C21	C22	1.405(9)
N2	C2	1.400(11)	C22	C23	1.385(8)
N2	C32	1.489(12)	N31	C31	1.342(12)
C9	O5	1.361(11)	N31	C36	1.448(9)
C9	O50	1.348(14)	O31	C31	1.215(9)
N1	C1	1.348(10)	C31	C32	1.518(13)
N1	C6	1.450(9)	C32	C33	1.538(12)
O1	C1	1.226(9)	C33	C34	1.328(7)
C1	C2	1.492(11)	C34	C35	1.502(6)
C2	C3	1.569(12)	C35	C36	1.524(6)
C3	C4	1.330(6)	C36	C37	1.561(15)

C4	C5	1.499(6)	C37	O32	1.195(13)
C5	C6	1.524(7)	C37	O33	1.301(14)
C6	C7	1.521(5)	O33	C38	1.444(5)
C7	O2	1.209(5)	O50	C40	1.463(14)
C7	O3	1.308(10)	C40	C41	1.531(14)
O3	C8	1.465(11)	C41	C42	1.509(13)
O5	C10	1.445(13)	C41	C53	1.522(13)
C10	C11	1.507(12)	C42	C43	1.393(12)
C11	C12	1.502(12)	C42	C47	1.395(13)
C11	C23	1.517(11)	C43	C44	1.403(13)
C12	C13	1.375(12)	C44	C45	1.403(13)
C12	C17	1.408(12)	C45	C46	1.379(9)
C13	C14	1.381(13)	C46	C47	1.373(11)
C14	C15	1.395(13)	C47	C48	1.475(7)
C15	C16	1.386(8)	C48	C49	1.407(10)
C16	C17	1.367(10)	C48	C53	1.379(9)
C17	C18	1.461(8)	C49	C50	1.370(9)
C18	C19	1.397(9)	C50	C51	1.382(9)
C18	C23	1.395(9)	C51	C52	1.395(9)
C19	C20	1.374(8)	C52	C53	1.378(8)

Table 5 Bond Angles for lub106.

Atom	Atom	Atom	Angle/°	Atom	Atom	Atom	Angle/°
C9	N2	C2	119.2(6)	C18	C23	C11	111.4(7)
C9	N2	C32	125.5(7)	C22	C23	C11	128.3(8)
O4	C9	N2	124.97(18)	C22	C23	C18	120.3(8)
O4	C9	O5	119.0(7)	C31	N31	C36	125.3(7)
O4	C9	O50	127.9(8)	N31	C31	C32	119.0(9)
N2	C9	O5	115.9(7)	O31	C31	N31	123.5(8)
N2	C9	O50	107.0(8)	O31	C31	C32	117.4(9)
C1	N1	C6	123.5(7)	N2	C32	C31	115.2(9)
N1	C1	C2	112.7(8)	N2	C32	C33	121.7(9)
O1	C1	N1	123.3(8)	C31	C32	C33	107.3(9)
O1	C1	C2	124.0(8)	C34	C33	C32	130.0(6)
N2	C2	C1	109.5(8)	C33	C34	C35	129.0(4)
N2	C2	C3	101.4(8)	C34	C35	C36	114.5(4)
C1	C2	C3	108.5(9)	N31	C36	C35	111.4(7)
C4	C3	C2	122.8(5)	N31	C36	C37	109.5(7)
C3	C4	C5	128.6(4)	C35	C36	C37	110.1(5)
C4	C5	C6	115.1(3)	O32	C37	C36	122.0(11)

N1	C6	C5	111.8(6)	O32	C37	O33	128.1(13)
N1	C6	C7	111.8(6)	O33	C37	C36	109.9(8)
C7	C6	C5	110.4(4)	C37	O33	C38	115.2(7)
O2	C7	C6	122.7(4)	C9	O50	C40	107.1(13)
O2	C7	O3	125.2(6)	O50	C40	C41	103.2(10)
O3	C7	C6	112.0(6)	C42	C41	C40	106.8(14)
C7	O3	C8	116.9(7)	C42	C41	C53	101.5(10)
C9	O5	C10	122.3(12)	C53	C41	C40	111.8(11)
O5	C10	C11	113.7(10)	C43	C42	C41	128.3(12)
C10	C11	C23	114.0(10)	C43	C42	C47	120.2(12)
C12	C11	C10	112.3(12)	C47	C42	C41	111.5(11)
C12	C11	C23	100.4(8)	C42	C43	C44	118.4(12)
C13	C12	C11	130.4(11)	C43	C44	C45	119.8(9)
C13	C12	C17	117.6(12)	C46	C45	C44	121.5(8)
C17	C12	C11	112.0(9)	C47	C46	C45	118.2(9)
C12	C13	C14	121.6(13)	C42	C47	C48	107.1(9)
C13	C14	C15	119.4(10)	C46	C47	C42	121.9(9)
C16	C15	C14	119.9(8)	C46	C47	C48	130.9(9)
C17	C16	C15	119.5(8)	C49	C48	C47	131.0(7)
C12	C17	C18	107.3(8)	C53	C48	C47	109.5(7)
C16	C17	C12	121.8(9)	C53	C48	C49	119.4(7)
C16	C17	C18	130.9(8)	C50	C49	C48	119.1(7)
C19	C18	C17	131.8(7)	C49	C50	C51	121.0(7)
C23	C18	C17	108.4(6)	C50	C51	C52	120.4(6)
C23	C18	C19	119.8(7)	C53	C52	C51	118.3(7)
C20	C19	C18	119.3(6)	C48	C53	C41	110.3(8)
C21	C20	C19	121.5(6)	C52	C53	C41	127.9(9)
C20	C21	C22	119.8(6)	C52	C53	C48	121.7(7)
C23	C22	C21	119.2(7)				

Table 6 Hydrogen Bonds for lub106.

D	H	A	d(D-H)/Å	d(H-A)/Å	d(D-A)/Å	D-H-A/°
N2	H2B	O4[1]	0.88	1.96	2.802(2)	159.4
N1	H1	O1[2]	0.88	2.09	2.942(9)	162.9
N31	H31	O31[2]	0.88	2.47	3.293(9)	156.1

[1]+X,+Y,-1+Z; [2]1-X,1-Y,+Z

Table 7 Hydrogen Atom Coordinates (Å×10^4) and Isotropic Displacement Parameters (Å^2×10^3) for lub106.

Atom	*x*	*y*	*z*	U(eq)
H2A	4491	6162	233	49
H2B	4483	6179	252	49
H1	3807	4961	2213	41
H2	3344	5835	4753	34
H3	2455	6105	−366	40
H4	984	5715	−689	43
H5A	1267	5102	882	44
H5B	680	5331	3366	44
H6	2490	5392	5606	36
H8A	3503	4087	6445	68
H8B	2110	4154	6548	68
H8C	2925	4294	9059	68
H10A	5913	6820	6882	44
H10B	5200	7100	4938	44
H11	6903	7184	2113	29
H13	6052	7782	5680	47
H14	6922	8217	8586	48
H15	8610	8058	11158	47
H16	9542	7493	10332	40
H19	10314	6833	8529	45
H20	10720	6301	6030	53
H21	9534	6118	2355	50
H22	7791	6448	1342	45
H31	3920	4921	1027	36
H32	3704	5734	4481	54
H33	1885	6025	1676	49
H34	641	5589	2237	53
H35A	1342	4968	2308	44
H35B	1170	5109	5442	44
H36	3198	5216	5904	34
H38A	2140	4051	7439	60
H38B	2092	4218	10530	60
H38C	3335	4158	9017	60
H40A	5909	6729	6668	32
H40B	5192	7060	5198	32
H41	6817	7111	1747	36
H43	6118	7710	5513	43
H44	7074	8096	8791	48
H45	8890	7918	10686	45

H46	9729	7351	9578	44
H49	10355	6692	7415	50
H50	10536	6144	4970	52
H51	9094	5960	1826	48
H52	7422	6330	1069	39

Table 8 Atomic Occupancy for lub106.

Atom	***Occupancy***	**Atom**	***Occupancy***	**Atom**	***Occupancy***
H2A	0.523(3)	H2B	0.477(3)	N1	0.523(3)
H1	0.523(3)	O1	0.523(3)	C1	0.523(3)
C2	0.523(3)	H2	0.523(3)	C3	0.523(3)
H3	0.523(3)	C4	0.523(3)	H4	0.523(3)
C5	0.523(3)	H5A	0.523(3)	H5B	0.523(3)
C6	0.523(3)	H6	0.523(3)	C7	0.523(3)
O2	0.523(3)	O3	0.523(3)	C8	0.523(3)
H8A	0.523(3)	H8B	0.523(3)	H8C	0.523(3)
O5	0.523(3)	C10	0.523(3)	H10A	0.523(3)
H10B	0.523(3)	C11	0.523(3)	H11	0.523(3)
C12	0.523(3)	C13	0.523(3)	H13	0.523(3)
C14	0.523(3)	H14	0.523(3)	C15	0.523(3)
H15	0.523(3)	C16	0.523(3)	H16	0.523(3)
C17	0.523(3)	C18	0.523(3)	C19	0.523(3)
H19	0.523(3)	C20	0.523(3)	H20	0.523(3)
C21	0.523(3)	H21	0.523(3)	C22	0.523(3)
H22	0.523(3)	C23	0.523(3)	N31	0.477(3)
H31	0.477(3)	O31	0.477(3)	C31	0.477(3)
C32	0.477(3)	H32	0.477(3)	C33	0.477(3)
H33	0.477(3)	C34	0.477(3)	H34	0.477(3)
C35	0.477(3)	H35A	0.477(3)	H35B	0.477(3)
C36	0.477(3)	H36	0.477(3)	C37	0.477(3)
O32	0.477(3)	O33	0.477(3)	C38	0.477(3)
H38A	0.477(3)	H38B	0.477(3)	H38C	0.477(3)
O50	0.477(3)	C40	0.477(3)	H40A	0.477(3)
H40B	0.477(3)	C41	0.477(3)	H41	0.477(3)
C42	0.477(3)	C43	0.477(3)	H43	0.477(3)
C44	0.477(3)	H44	0.477(3)	C45	0.477(3)
H45	0.477(3)	C46	0.477(3)	H46	0.477(3)
C47	0.477(3)	C48	0.477(3)	C49	0.477(3)
H49	0.477(3)	C50	0.477(3)	H50	0.477(3)
C51	0.477(3)	H51	0.477(3)	C52	0.477(3)

H52 0.477(3) C53 0.477(3)

Experimental

Single crystals of $C_{23}H_{22}N_2O_5$ Compound **16a** (lub106) were grown in Ethyl acetate-hexane mixture A suitable crystal was selected and mounted on the on a **Bruker Venture Metaljet** diffractometer The crystal was kept at 150 K during data collection. Using Olex2 [1], the structure was solved with the XT [2] structure solution program using Intrinsic Phasing and refined with the XL [3] refinement package using Least Squares minimisation.

1. Dolomanov, O.V., Bourhis, L.J., Gildea, R.J, Howard, J.A.K. & Puschmann, H. (2009), J. Appl. Cryst. 42, 339-341.
2. Sheldrick, G.M. (2015). Acta Cryst. A71, 3-8.
3. Sheldrick, G.M. (2008). Acta Cryst. A64, 112-122.

Crystal structure determination of [lub106]

Crystal Data for $C_{23}H_{22}N_2O_5$ (M =406.42 g/mol): orthorhombic, space group $P2_12_12$ (no. 18), a = 11.3495(5) Å, b = 36.3258(17) Å, c = 4.7864(2) Å, V = 1973.34(15) Å^3, Z = 4, T = 150 K, μ(GaKα) = 0.513 mm^{-1}, *Dcalc* = 1.368 g/cm^3, 51210 reflections measured (4.232° ≤ 2Θ ≤ 109.94°), 3742 unique (R_{int} = 0.0550, R_{sigma} = 0.0232) which were used in all calculations. The final R_1 was 0.0312 (I > 2σ(I)) and wR_2 was 0.0771 (all data).

Refinement model description

Number of restraints - 70, number of constraints - unknown.

Details:

```
1. Fixed Uiso
 At 1.2 times of:
  All C(H) groups, All C(H,H) groups, All N(H) groups, All N(H,H) groups
 At 1.5 times of:
  All C(H,H,H) groups
2. Restrained distances
 N2-C32 ≈ N2-C2
 with sigma of 0.02
 O5-C9 ≈ O50-C9
 with sigma of 0.02
3. Same fragment restrains
{N1, O1, C1, C2, C3, C4, C5, C6, C7, O2, O3, C8, O5, C10, C11, C12, C13, C14,
C15, C16, C17, C18, C19, C20, C21, C22, C23} sigma for 1-2: 0.02, 1-3: 0.04
as
{N31, O31, C31, C32, C33, C34, C35, C36, C37, O32, O33, C38, O50, C40, C41,
C42, C43, C44, C45, C46, C47, C48, C49, C50, C51, C52, C53}
4. Others
 Sof(H2B)=Sof(N31)=Sof(H31)=Sof(O31)=Sof(C31)=Sof(C32)=Sof(H32)=Sof(C33)=
 Sof(H33)=Sof(C34)=Sof(H34)=Sof(C35)=Sof(H35A)=Sof(H35B)=Sof(C36)=Sof(H36)=
 Sof(C37)=Sof(O32)=Sof(O33)=Sof(C38)=Sof(H38A)=Sof(H38B)=Sof(H38C)=Sof(O50)=
 Sof(C40)=Sof(H40A)=Sof(H40B)=Sof(C41)=Sof(H41)=Sof(C42)=Sof(C43)=Sof(H43)=
 Sof(C44)=Sof(H44)=Sof(C45)=Sof(H45)=Sof(C46)=Sof(H46)=Sof(C47)=Sof(C48)=
 Sof(C49)=Sof(H49)=Sof(C50)=Sof(H50)=Sof(C51)=Sof(H51)=Sof(C52)=Sof(H52)=
 Sof(C53)=1-FVAR(1)
 Sof(H2A)=Sof(N1)=Sof(H1)=Sof(O1)=Sof(C1)=Sof(C2)=Sof(H2)=Sof(C3)=Sof(H3)=
 Sof(C4)=Sof(H4)=Sof(C5)=Sof(H5A)=Sof(H5B)=Sof(C6)=Sof(H6)=Sof(C7)=Sof(O2)=
 Sof(O3)=Sof(C8)=Sof(H8A)=Sof(H8B)=Sof(H8C)=Sof(O5)=Sof(C10)=Sof(H10A)=
 Sof(H10B)=Sof(C11)=Sof(H11)=Sof(C12)=Sof(C13)=Sof(H13)=Sof(C14)=Sof(H14)=
 Sof(C15)=Sof(H15)=Sof(C16)=Sof(H16)=Sof(C17)=Sof(C18)=Sof(C19)=Sof(H19)=
 Sof(C20)=Sof(H20)=Sof(C21)=Sof(H21)=Sof(C22)=Sof(H22)=Sof(C23)=FVAR(1)
5.a Ternary CH refined with riding coordinates:
 C2(H2), C6(H6), C11(H11), C32(H32), C36(H36), C41(H41)
5.b Secondary CH2 refined with riding coordinates:
 C5(H5A,H5B), C10(H10A,H10B), C35(H35A,H35B), C40(H40A,H40B)
5.c Aromatic/amide H refined with riding coordinates:
 N2(H2A), N2(H2B), N1(H1), C3(H3), C4(H4), C13(H13), C14(H14), C15(H15),
 C16(H16), C19(H19), C20(H20), C21(H21), C22(H22), N31(H31), C33(H33), C34(H34),
  C43(H43), C44(H44), C45(H45), C46(H46), C49(H49), C50(H50), C51(H51), C52(H52)
```

```
5.d Idealised Me refined as rotating group:
 C8(H8A,H8B,H8C), C38(H38A,H38B,H38C)
```

This report has been created with Olex2, compiled on 2017.03.28 svn.r3405 for OlexSys. Please let us know if there are any errors or if you would like to have additional features.

Compound 2.16c (LUB109)

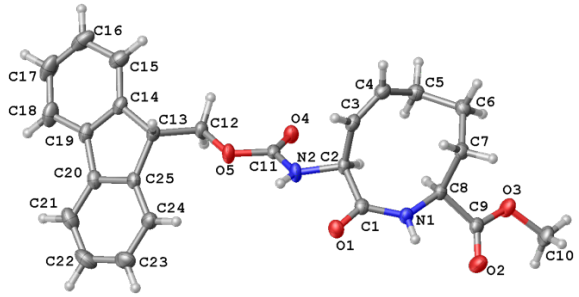

Table 1 Crystal data and structure refinement for LUB109.

Identification code	LUB109
Empirical formula	$C_{25}H_{26}N_2O_5$
Formula weight	434.48
Temperature/K	150
Crystal system	monoclinic
Space group	$P2_1$
a/Å	8.9667(2)
b/Å	7.6705(2)
c/Å	16.1715(4)
α/°	90
β/°	92.3380(10)
γ/°	90
Volume/Å^3	1111.33(5)
Z	2
ρ_{calc}g/cm^3	1.298
μ/mm^{-1}	0.477
F(000)	460.0
Crystal size/mm^3	0.1 × 0.08 × 0.04
Radiation	GaKα (λ = 1.34139)
2Θ range for data collection/°	4.758 to 121.31
Index ranges	$-11 \le h \le 11$, $-9 \le k \le 9$, $-20 \le l \le 20$
Reflections collected	29474
Independent reflections	5102 [R_{int} = 0.0265, R_{sigma} = 0.0192]
Data/restraints/parameters	5102/1/299
Goodness-of-fit on F^2	1.096
Final R indexes [I>=2σ (I)]	R_1 = 0.0339, wR_2 = 0.0820

Final R indexes [all data]	$R_1 = 0.0344$, $wR_2 = 0.0826$
Largest diff. peak/hole / e Å^{-3}	0.19/-0.29
Flack parameter	0.02(3)

Table 2 Fractional Atomic Coordinates (×10^4) and Equivalent Isotropic Displacement Parameters (Å^2×10^3) for LUB109. U_{eq} is defined as 1/3 of of the trace of the orthogonalised U_{IJ} tensor.

Atom	*x*	*y*	*z*	U(eq)
O1	3552.7(13)	2509.4(16)	5041.1(7)	28.3(3)
O2	6131.5(15)	4513(2)	2831.5(8)	38.7(3)
O3	8458.9(14)	5275.5(18)	3217.3(7)	33.7(3)
O4	5971.0(13)	5967.8(17)	7140.8(7)	29.3(3)
O5	3851.2(13)	4882.3(17)	7652.8(7)	29.3(3)
N1	5568.7(15)	3168.4(18)	4314.0(8)	23.6(3)
N2	4558.5(16)	3975(2)	6430.6(8)	26.5(3)
C1	4837.6(17)	3060(2)	5024.1(10)	22.5(3)
C2	5680.0(17)	3590(2)	5829.9(9)	22.6(3)
C3	6669.4(19)	2101(2)	6143.0(9)	25.7(3)
C4	8144.7(19)	2042(2)	6138.8(10)	28.3(3)
C5	9148.1(19)	3394(2)	5778.7(10)	29.2(3)
C6	9611.6(18)	2888(2)	4898.6(11)	28.4(3)
C7	8298.9(18)	2334(2)	4327(1)	25.9(3)
C8	7086.9(17)	3777(2)	4204.9(9)	21.9(3)
C9	7136.1(18)	4552(2)	3340.7(9)	23.8(3)
C10	8667(2)	5922(3)	2385.4(11)	35.4(4)
C11	4896.0(16)	5015(2)	7079.4(9)	22.2(3)
C12	4150.6(17)	5871(2)	8407.6(9)	25.3(3)
C13	2901.6(17)	5381(2)	8970.4(9)	23.1(3)
C14	3121.9(18)	6117(2)	9837.7(9)	26.5(3)
C15	4271(2)	5807(3)	10416.2(11)	36.1(4)
C16	4180(3)	6554(3)	11205.7(12)	45.0(5)
C17	2974(3)	7588(3)	11393.2(12)	46.8(5)
C18	1829(2)	7925(3)	10810.6(12)	39.8(4)
C19	1909(2)	7161(2)	10032.2(10)	28.5(3)
C20	833.7(19)	7184(2)	9320.5(10)	27.8(3)
C21	-554(2)	7977(3)	9208.4(13)	40.1(4)
C22	-1355(2)	7740(3)	8464.9(15)	44.5(5)
C23	-790(2)	6737(3)	7838.6(13)	38.7(4)
C24	593.5(19)	5922(2)	7947.3(10)	29.4(3)
C25	1400.8(17)	6141(2)	8693.2(9)	24.1(3)

Table 3 Anisotropic Displacement Parameters ($Å^2×10^3$) for LUB109. The Anisotropic displacement factor exponent takes the form: $-2\pi^2[h^2a^{*2}U_{11}+2hka^*b^*U_{12}+\ldots]$.

Atom	U_{11}	U_{22}	U_{33}	U_{23}	U_{13}	U_{12}
O1	24.0(5)	31.6(6)	29.6(6)	-1.5(5)	5.0(4)	-4.4(5)
O2	33.8(7)	54.6(9)	27.4(6)	9.6(6)	-0.5(5)	-4.4(6)
O3	32.4(6)	44.8(7)	24.0(5)	5.9(5)	3.6(4)	-9.9(5)
O4	24.5(5)	39.2(7)	24.4(5)	-3.8(5)	4.1(4)	-5.1(5)
O5	26.5(6)	38.5(6)	23.7(5)	-8.0(5)	9.6(4)	-4.3(5)
N1	23.2(6)	28.0(7)	19.8(6)	-3.3(5)	2.5(5)	-1.5(5)
N2	23.6(6)	31.1(7)	25.5(6)	-4.9(5)	10.2(5)	-5.0(5)
C1	24.6(7)	19.2(7)	23.9(7)	0.1(5)	4.2(5)	1.8(5)
C2	23.0(7)	25.0(7)	20.2(6)	-2.5(5)	6.6(5)	-1.5(6)
C3	31.8(8)	25.3(7)	20.1(6)	0.7(6)	4.6(6)	-1.1(6)
C4	31.8(8)	29.8(8)	23.3(7)	2.3(6)	0.8(6)	3.2(6)
C5	26.7(8)	33.0(8)	27.7(7)	0.1(6)	0.0(6)	-0.7(6)
C6	24.7(7)	29.4(8)	31.4(8)	0.8(6)	4.9(6)	2.4(6)
C7	28.1(7)	26.0(7)	24.1(7)	-0.8(6)	6.1(6)	4.7(6)
C8	23.9(7)	23.2(7)	18.8(6)	-1.8(5)	4.2(5)	0.0(6)
C9	28.0(7)	22.3(7)	21.5(7)	-1.7(5)	5.2(5)	2.5(6)
C10	39.4(9)	40.3(10)	27.0(8)	6.7(7)	8.5(7)	-6.9(8)
C11	21.5(7)	25.5(7)	19.8(6)	2.1(5)	3.3(5)	5.3(6)
C12	24.3(7)	31.2(8)	20.8(7)	-4.6(6)	4.9(5)	-0.8(6)
C13	25.9(7)	26.0(7)	17.7(6)	-0.9(5)	3.7(5)	-0.2(6)
C14	31.3(8)	29.1(8)	19.4(7)	-0.3(6)	4.1(6)	-6.0(7)
C15	40.7(10)	40.1(10)	27.3(8)	4.4(7)	-3.4(7)	-5.6(8)
C16	56.4(12)	52.6(12)	24.8(8)	3.7(8)	-10.4(8)	-19.5(10)
C17	64.2(13)	53.0(12)	23.7(8)	-11.7(8)	7.0(8)	-23.4(11)
C18	50.4(11)	39.9(10)	30.2(9)	-14.6(7)	13.8(7)	-10.6(9)
C19	34.9(8)	28.2(8)	22.9(7)	-4.3(6)	8.1(6)	-6.2(7)
C20	27.2(8)	27.6(8)	29.3(7)	-3.4(6)	8.6(6)	-1.4(6)
C21	31.5(9)	38.9(10)	50.8(11)	-6.3(9)	12.9(8)	5.4(8)
C22	23.5(8)	46.5(11)	63.3(13)	3.2(10)	1.4(8)	7.5(8)
C23	26.8(8)	47.8(11)	41.1(9)	6.9(8)	-4.5(7)	-4.9(8)
C24	26.3(8)	36.5(9)	25.7(7)	1.1(7)	2.1(6)	-4.0(7)
C25	22.7(7)	26.9(7)	23.2(7)	0.9(6)	5.8(5)	-1.3(6)

Table 4 Bond Lengths for LUB109.

Atom	Atom	Length/Å	Atom	Atom	Length/Å

O1	C1	1.228(2)	C8	C9	1.521(2)
O2	C9	1.196(2)	C12	C13	1.519(2)
O3	C9	1.332(2)	C13	C14	1.517(2)
O3	C10	1.4530(19)	C13	C25	1.517(2)
O4	C11	1.211(2)	C14	C15	1.384(2)
O5	C11	1.3486(17)	C14	C19	1.396(3)
O5	C12	1.4527(19)	C15	C16	1.405(3)
N1	C1	1.348(2)	C16	C17	1.385(4)
N1	C8	1.4565(19)	C17	C18	1.390(3)
N2	C2	1.4568(19)	C18	C19	1.393(2)
N2	C11	1.342(2)	C19	C20	1.471(2)
C1	C2	1.534(2)	C20	C21	1.390(3)
C2	C3	1.520(2)	C20	C25	1.404(2)
C3	C4	1.324(2)	C21	C22	1.387(3)
C4	C5	1.506(2)	C22	C23	1.384(3)
C5	C6	1.548(2)	C23	C24	1.394(3)
C6	C7	1.527(2)	C24	C25	1.391(2)
C7	C8	1.558(2)			

Table 5 Bond Angles for LUB109.

Atom	Atom	Atom	Angle/°	Atom	Atom	Atom	Angle/°
C9	O3	C10	115.44(13)	O5	C12	C13	104.99(12)
C11	O5	C12	115.38(12)	C14	C13	C12	112.98(13)
C1	N1	C8	127.77(13)	C25	C13	C12	113.25(12)
C11	N2	C2	120.13(13)	C25	C13	C14	102.16(13)
O1	C1	N1	121.97(15)	C15	C14	C13	128.76(16)
O1	C1	C2	120.12(14)	C15	C14	C19	120.77(16)
N1	C1	C2	117.87(13)	C19	C14	C13	110.39(14)
N2	C2	C1	106.91(12)	C14	C15	C16	118.34(19)
N2	C2	C3	109.86(13)	C17	C16	C15	120.51(19)
C3	C2	C1	110.14(13)	C16	C17	C18	121.36(17)
C4	C3	C2	126.42(15)	C17	C18	C19	118.1(2)
C3	C4	C5	126.25(15)	C14	C19	C20	108.80(14)
C4	C5	C6	111.70(14)	C18	C19	C14	120.95(17)
C7	C6	C5	113.39(13)	C18	C19	C20	130.20(18)
C6	C7	C8	113.31(13)	C21	C20	C19	131.45(16)
N1	C8	C7	114.07(13)	C21	C20	C25	120.26(16)
N1	C8	C9	107.38(12)	C25	C20	C19	108.26(14)
C9	C8	C7	110.36(12)	C22	C21	C20	118.98(18)
O2	C9	O3	123.90(15)	C23	C22	C21	121.02(18)

O2	C9	C8	125.01(15)	C22	C23	C24	120.48(18)
O3	C9	C8	111.09(13)	C25	C24	C23	118.97(17)
O4	C11	O5	124.21(14)	C20	C25	C13	110.39(14)
O4	C11	N2	125.18(14)	C24	C25	C13	129.33(15)
N2	C11	O5	110.60(13)	C24	C25	C20	120.27(15)

Table 6 Hydrogen Bonds for LUB109.

D	H	A	d(D-H)/Å	d(H-A)/Å	d(D-A)/Å	D-H-A/°
N1	H1	O4[1]	0.88(2)	2.34(3)	3.1662(18)	157(2)

[1]1-X,-1/2+Y,1-Z

Table 7 Hydrogen Atom Coordinates (Å×10^4) and Isotropic Displacement Parameters (Å^2×10^3) for LUB109.

Atom	*x*	*y*	*z*	U(eq)
H1	5050(30)	2860(30)	3867(15)	34(6)
H2	3780(30)	3320(30)	6444(15)	37(6)
H2A	6300	4649	5734	27
H3	6181	1116	6363	31
H4	8615	1051	6387	34
H5A	10054	3530	6144	35
H5B	8623	4529	5755	35
H6A	10116	3895	4649	34
H6B	10339	1918	4942	34
H7A	7833	1282	4559	31
H7B	8678	2018	3781	31
H8	7309	4725	4616	26
H10A	8560	4958	1990	53
H10B	9665	6431	2356	53
H10C	7914	6815	2249	53
H12A	4140	7139	8292	30
H12B	5135	5553	8664	30
H13	2821	4082	9001	28
H15	5101	5106	10283	43
H16	4952	6349	11614	54
H17	2929	8077	11931	56
H18	1015	8655	10939	48
H21	−948	8670	9635	48
H22	−2305	8274	8384	53

H23	−1349	6604	7331	46
H24	979	5229	7519	35

Experimental

Single crystals of $C_{25}H_{26}N_2O_5$ Compound **16c** (LUB109) were grown in Ethyl acetate-hexane mixture A suitable crystal was selected and mounted on the on a **Bruker Venture Metaljet** diffractometer The crystal was kept at 150 K during data collection. Using Olex2 [1], the structure was solved with the XT [2] structure solution program using Intrinsic Phasing and refined with the XL [3] refinement package using Least Squares minimisation.

1. Dolomanov, O.V., Bourhis, L.J., Gildea, R.J, Howard, J.A.K. & Puschmann, H. (2009), J. Appl. Cryst. 42, 339-341.
2. Sheldrick, G.M. (2015). Acta Cryst. A71, 3-8.
3. Sheldrick, G.M. (2008). Acta Cryst. A64, 112-122.

Crystal structure determination of [LUB109]

Crystal Data for $C_{25}H_{26}N_2O_5$ (M =434.48 g/mol): monoclinic, space group $P2_1$ (no. 4), a = 8.9667(2) Å, b = 7.6705(2) Å, c = 16.1715(4) Å, β = 92.3380(10)°, V = 1111.33(5) Å^3, Z = 2, T = 150 K, μ(GaKα) = 0.477 mm^{-1}, *Dcalc* = 1.298 g/cm^3, 29474 reflections measured (4.758° ≤ 2Θ ≤ 121.31°), 5102 unique (R_{int} = 0.0265, R_{sigma} = 0.0192) which were used in all calculations. The final R_1 was 0.0339 (I > 2σ(I)) and wR_2 was 0.0826 (all data).

Refinement model description

Number of restraints - 1, number of constraints - unknown.

Details:

```
1. Fixed Uiso
 At 1.2 times of:
  All C(H) groups, All C(H,H) groups
 At 1.5 times of:
  All C(H,H,H) groups
2.a Ternary CH refined with riding coordinates:
 C2(H2A), C8(H8), C13(H13)
2.b Secondary CH2 refined with riding coordinates:
 C5(H5A,H5B), C6(H6A,H6B), C7(H7A,H7B), C12(H12A,H12B)
2.c Aromatic/amide H refined with riding coordinates:
 C3(H3), C4(H4), C15(H15), C16(H16), C17(H17), C18(H18), C21(H21), C22(H22),
 C23(H23), C24(H24)
2.d Idealised Me refined as rotating group:
 C10(H10A,H10B,H10C)
```

This report has been created with Olex2, compiled on 2017.03.28 svn.r3405 for OlexSys. Please let us know if there are any errors or if you would like to have additional features.

Compound 2.16d (LUB108):

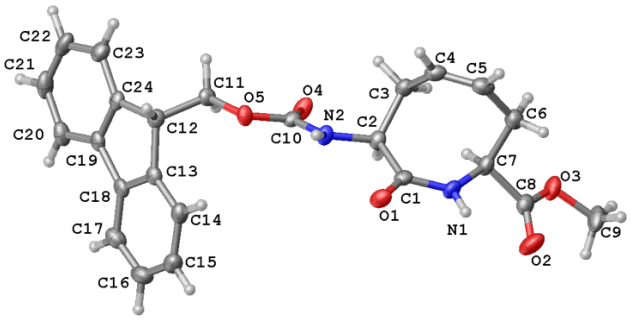

Table 1 Crystal data and structure refinement for lub108.

Identification code	lub108
Empirical formula	$C_{24}H_{24}N_2O_5$
Formula weight	420.45
Temperature/K	150
Crystal system	monoclinic
Space group	$P2_1$
a/Å	4.84660(10)
b/Å	11.7928(3)
c/Å	18.3146(5)
α/°	90
β/°	96.5347(15)
γ/°	90
Volume/Å^3	1039.97(4)
Z	2
ρ_{calc}g/cm^3	1.343
μ/mm^{-1}	0.499
F(000)	444.0
Crystal size/mm^3	0.36 × 0.02 × 0.02
Radiation	GaKα (λ = 1.34139)
2Θ range for data collection/°	4.224 to 117.476
Index ranges	$-5 \leq h \leq 5$, $-14 \leq k \leq 14$, $-23 \leq l \leq 23$
Reflections collected	24798
Independent reflections	4377 [R_{int} = 0.0501, R_{sigma} = 0.0424]
Data/restraints/parameters	4377/1/289
Goodness-of-fit on F^2	1.142
Final R indexes [I>=2σ (I)]	R_1 = 0.0440, wR_2 = 0.0811
Final R indexes [all data]	R_1 = 0.0615, wR_2 = 0.0861
Largest diff. peak/hole / e Å^{-3}	0.20/-0.24
Flack parameter	0.03(9)

Table 2 Fractional Atomic Coordinates (×10^4) and Equivalent Isotropic Displacement Parameters (Å^2×10^3) for lub108. U_{eq} is defined as 1/3 of of the trace of the orthogonalised U_{IJ} tensor.

Atom	*x*	*y*	*z*	U(eq)
O1	-2102(4)	4081.3(17)	6069.5(10)	29.7(5)
O2	1376(5)	2632(2)	4026.6(11)	46.3(6)
O3	5086(4)	1534.0(17)	4372.3(10)	35.1(5)
O4	5893(4)	4122.5(18)	7791(1)	30.6(5)
O5	2501(4)	4987.3(15)	8334.4(9)	24.2(4)

N1	327(5)	2927(2)	5412.7(12)	25.0(5)
N2	1403(5)	4030(2)	7292.0(12)	22.5(5)
C1	-78(6)	3471(2)	6040.9(14)	22.3(6)
C2	2133(6)	3328(2)	6694.8(14)	23.5(6)
C3	2722(6)	2081(2)	6933.5(15)	27.6(6)
C4	372(6)	1272(2)	6752.8(16)	29.7(7)
C5	-152(6)	738(2)	6120.0(16)	32.5(7)
C6	1409(7)	856(2)	5461.2(16)	32.9(7)
C7	2376(5)	2082(2)	5296.7(14)	25.7(6)
C8	2868(6)	2138(2)	4491.8(16)	29.1(6)
C9	5492(7)	1378(3)	3602.6(17)	42.2(8)
C10	3453(6)	4357(2)	7804.3(14)	21.4(6)
C11	4589(5)	5338(2)	8918.6(15)	23.3(6)
C12	3670(6)	6451(2)	9237.9(14)	23.7(6)
C13	3592(5)	7413(2)	8688.1(15)	23.4(6)
C14	1877(6)	7573(2)	8040.3(15)	29.7(7)
C15	2301(7)	8514(3)	7610.2(17)	36.0(7)
C16	4431(7)	9264(3)	7819.1(17)	38.7(8)
C17	6149(6)	9125(3)	8463.8(17)	34.3(7)
C18	5696(6)	8198(2)	8907.9(15)	23.7(6)
C19	7101(5)	7846(2)	9626.1(14)	24.5(6)
C20	9245(6)	8357(3)	10080.7(17)	32.4(7)
C21	10140(6)	7846(3)	10745.9(17)	38.4(8)
C22	8959(6)	6843(3)	10947.9(15)	36.9(8)
C23	6831(6)	6327(3)	10495.5(15)	31.3(7)
C24	5897(6)	6840(2)	9833.0(14)	23.1(6)

Table 3 Anisotropic Displacement Parameters ($Å^2×10^3$) for lub108. The Anisotropic displacement factor exponent takes the form: $-2\pi^2[h^2a^{*2}U_{11}+2hka^*b^*U_{12}+\ldots]$.

Atom	U_{11}	U_{22}	U_{33}	U_{23}	U_{13}	U_{12}
O1	25.2(10)	38.7(11)	25.5(10)	4.9(9)	5.0(8)	10.4(10)
O2	51.2(14)	64.6(16)	23.0(11)	7.5(11)	3.6(11)	10.9(12)
O3	38.5(13)	43.1(12)	25.3(11)	-9.9(9)	10.2(9)	0.5(10)
O4	16.4(10)	52.1(12)	23.4(10)	-5.6(10)	3.0(8)	4.0(9)
O5	19.3(10)	25.6(10)	27.4(10)	-7.5(8)	1.5(8)	-0.2(8)
N1	23.6(13)	32.6(13)	17.8(12)	-0.3(10)	-2.5(10)	3.0(11)
N2	15.4(12)	30.3(12)	22.1(12)	-4.5(10)	2.8(10)	-0.2(10)
C1	23.2(15)	23.8(13)	20.5(14)	4.7(11)	5.2(12)	-1.8(12)
C2	20.6(14)	28.6(15)	21.8(14)	-1.9(11)	4.8(11)	2.1(12)
C3	30.3(16)	31.0(15)	21.2(14)	1.1(12)	1.1(12)	6.2(14)

C4	30.4(17)	31.2(15)	27.8(16)	9.8(13)	4.3(13)	5.2(13)
C5	32.4(18)	27.9(15)	36.7(18)	8.1(13)	1.0(14)	-0.2(13)
C6	39.4(19)	29.3(15)	29.5(16)	-2.4(13)	1.2(14)	3.9(14)
C7	23.8(15)	32.9(15)	20.4(14)	-4.5(12)	2.2(12)	3.1(13)
C8	30.6(16)	31.3(16)	25.3(15)	-5.0(13)	3.3(13)	-4.1(14)
C9	56(2)	43.2(19)	31.1(17)	-13.3(14)	21.0(16)	-10.2(17)
C10	21.1(15)	24.2(14)	19.5(13)	2.8(11)	4.9(11)	-1.1(11)
C11	20.5(15)	23.2(13)	25.1(14)	-2.2(11)	-1.8(12)	-2.6(12)
C12	19.7(15)	28.0(14)	23.6(14)	-2.3(11)	3.6(12)	0.1(12)
C13	22.2(14)	22.6(13)	26.3(14)	-3.7(11)	6.5(12)	4.2(11)
C14	29.7(16)	30.1(15)	28.7(15)	-6.8(12)	0.4(13)	5.6(13)
C15	45.6(19)	33.4(16)	28.0(16)	-1.1(13)	0.0(14)	13.1(16)
C16	51(2)	26.8(16)	39.8(18)	7.9(14)	12.5(16)	10.3(15)
C17	35.3(17)	24.3(14)	44.5(18)	-0.3(14)	9.3(14)	3.3(14)
C18	24.5(15)	19.3(13)	28.4(15)	-4.7(11)	7.4(12)	5.6(11)
C19	23.5(15)	22.1(13)	28.3(15)	-7.5(12)	4.8(12)	5.5(12)
C20	27.3(16)	28.4(15)	40.7(18)	-13.0(13)	0.8(14)	0.7(13)
C21	30.7(17)	44.0(19)	38.1(18)	-20.6(15)	-6.7(14)	5.5(15)
C22	38.0(19)	51(2)	20.1(14)	-7.6(14)	-2.3(14)	15.8(16)
C23	34.4(17)	36.6(16)	23.4(15)	-1.3(12)	6.3(13)	3.3(14)
C24	21.7(15)	27.7(15)	20.7(13)	-5.7(11)	5.6(11)	3.7(11)

Table 4 Bond Lengths for lub108.

Atom	Atom	Length/Å	Atom	Atom	Length/Å
O1	C1	1.223(3)	C7	C8	1.521(4)
O2	C8	1.203(3)	C11	C12	1.523(4)
O3	C8	1.328(3)	C12	C13	1.514(4)
O3	C9	1.457(3)	C12	C24	1.515(4)
O4	C10	1.217(3)	C13	C14	1.382(4)
O5	C10	1.346(3)	C13	C18	1.402(4)
O5	C11	1.447(3)	C14	C15	1.389(4)
N1	C1	1.351(4)	C15	C16	1.381(5)
N1	C7	1.439(3)	C16	C17	1.375(4)
N2	C2	1.447(3)	C17	C18	1.395(4)
N2	C10	1.343(3)	C18	C19	1.470(4)
C1	C2	1.523(4)	C19	C20	1.393(4)
C2	C3	1.552(4)	C19	C24	1.393(4)
C3	C4	1.494(4)	C20	C21	1.384(5)
C4	C5	1.318(4)	C21	C22	1.383(5)
C5	C6	1.502(4)	C22	C23	1.388(4)

C6	C7	1.559(4)	C23	C24	1.385(4)		

Table 5 Bond Angles for lub108.

Atom	Atom	Atom	Angle/°	Atom	Atom	Atom	Angle/°
C8	O3	C9	115.3(2)	C13	C12	C11	112.1(2)
C10	O5	C11	115.0(2)	C13	C12	C24	102.3(2)
C1	N1	C7	128.6(2)	C24	C12	C11	108.7(2)
C10	N2	C2	117.8(2)	C14	C13	C12	129.8(3)
O1	C1	N1	120.7(2)	C14	C13	C18	120.2(3)
O1	C1	C2	121.8(2)	C18	C13	C12	110.0(2)
N1	C1	C2	117.4(2)	C13	C14	C15	118.9(3)
N2	C2	C1	108.7(2)	C16	C15	C14	120.6(3)
N2	C2	C3	112.5(2)	C17	C16	C15	121.4(3)
C1	C2	C3	114.6(2)	C16	C17	C18	118.3(3)
C4	C3	C2	115.6(2)	C13	C18	C19	108.5(2)
C5	C4	C3	124.5(3)	C17	C18	C13	120.5(3)
C4	C5	C6	126.7(3)	C17	C18	C19	131.0(3)
C5	C6	C7	115.6(2)	C20	C19	C18	130.6(3)
N1	C7	C6	112.7(2)	C20	C19	C24	120.9(3)
N1	C7	C8	107.4(2)	C24	C19	C18	108.6(2)
C8	C7	C6	108.2(2)	C21	C20	C19	118.4(3)
O2	C8	O3	125.1(3)	C22	C21	C20	120.7(3)
O2	C8	C7	124.0(3)	C21	C22	C23	121.2(3)
O3	C8	C7	110.8(2)	C24	C23	C22	118.5(3)
O4	C10	O5	123.6(2)	C19	C24	C12	110.4(2)
O4	C10	N2	124.3(2)	C23	C24	C12	129.3(3)
N2	C10	O5	112.0(2)	C23	C24	C19	120.3(3)
O5	C11	C12	108.7(2)				

Table 6 Hydrogen Bonds for lub108.

D	H	A	d(D-H)/Å	d(H-A)/Å	d(D-A)/Å	D-H-A/°
N2	H2	O4[1]	0.87(3)	2.06(3)	2.922(3)	169(3)

[1]-1+X,+Y,+Z

Table 7 Hydrogen Atom Coordinates (Å×10^4) and Isotropic Displacement Parameters (Å^2×10^3) for lub108.

Atom	*x*	*y*	*z*	U(eq)
H1	-900(60)	3040(30)	5041(17)	29(8)
H2	-310(70)	4100(30)	7386(17)	40(9)
H2A	3901	3640	6543	28
H3A	4336	1807	6697	33
H3B	3254	2067	7472	33
H4	-826	1133	7119	36
H5	-1675	225	6076	39
H6A	213	575	5025	40
H6B	3067	361	5532	40
H7	4145	2255	5613	31
H9A	5496	2119	3360	63
H9B	3982	913	3360	63
H9C	7272	998	3570	63
H11A	6395	5442	8724	28
H11B	4815	4750	9307	28
H12	1839	6364	9435	28
H14	432	7050	7892	36
H15	1114	8642	7168	43
H16	4717	9891	7511	46
H17	7608	9646	8603	41
H20	10072	9040	9938	39
H21	11580	8188	11067	46
H22	9616	6501	11404	44
H23	6033	5636	10637	38

Experimental

Single crystals of $C_{24}H_{24}N_2O_5$ compound **16d** (lub108) were grown in Ethyl acetate-hexane mixture A suitable crystal was selected and mounted on the on a **Bruker Venture Metaljet** diffractometer. The crystal was kept at 150 K during data collection. Using Olex2 [1], the structure was solved with the ShelXT [2] structure solution program using Intrinsic Phasing and refined with the XL [3] refinement package using Least Squares minimisation.

1. Dolomanov, O.V., Bourhis, L.J., Gildea, R.J, Howard, J.A.K. & Puschmann, H. (2009), J. Appl. Cryst. 42, 339-341.
2. Sheldrick, G.M. (2015). Acta Cryst. A71, 3-8.
3. Sheldrick, G.M. (2008). Acta Cryst. A64, 112-122.

Crystal structure determination of [lub108]

Crystal Data for $C_{24}H_{24}N_2O_5$ (M =420.45 g/mol): monoclinic, space group $P2_1$ (no. 4), a = 4.84660(10) Å, b = 11.7928(3) Å, c = 18.3146(5) Å, β = 96.5347(15)°, V = 1039.97(4) Å^3, Z = 2, T = 150 K, μ(GaKα) = 0.499 mm^{-1}, *Dcalc* = 1.343 g/cm^3, 24798 reflections measured (4.224° ≤ 2Θ ≤ 117.476°), 4377 unique (R_{int} = 0.0501, R_{sigma} = 0.0424) which were used in all calculations. The final R_1 was 0.0440 (I > 2σ(I)) and wR_2 was 0.0861 (all data).

Refinement model description

Number of restraints - 1, number of constraints - unknown.

Details:

```
1. Fixed Uiso
 At 1.2 times of:
```

```
  All C(H) groups, All C(H,H) groups
 At 1.5 times of:
  All C(H,H,H) groups
2.a Ternary CH refined with riding coordinates:
 C2(H2A), C7(H7), C12(H12)
2.b Secondary CH2 refined with riding coordinates:
 C3(H3A,H3B), C6(H6A,H6B), C11(H11A,H11B)
2.c Aromatic/amide H refined with riding coordinates:
 C4(H4), C5(H5), C14(H14), C15(H15), C16(H16), C17(H17), C20(H20), C21(H21),
 C22(H22), C23(H23)
2.d Idealised Me refined as rotating group:
 C9(H9A,H9B,H9C)
```

This report has been created with Olex2, compiled on 2017.03.28 svn.r3405 for OlexSys. Please let us know if there are any errors or if you would like to have additional features.

Compound 2.1f (lub116)

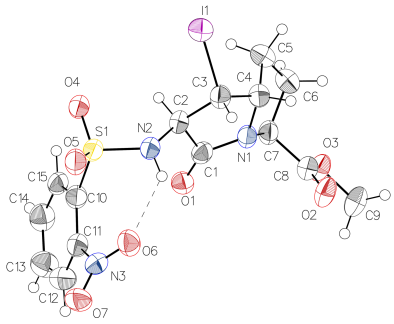

Table 1 Crystal data and structure refinement for lub116.

Identification code	lub116
Empirical formula	$C_{15}H_{16}IN_3O_7S$
Formula weight	509.27
Temperature/K	100
Crystal system	monoclinic
Space group	$P2_1$
a/Å	5.3844(4)
b/Å	21.4986(16)
c/Å	8.2956(6)
α/°	90
β/°	106.438(4)
γ/°	90
Volume/Å^3	921.02(12)
Z	2
ρ_{calc}g/cm^3	1.836
μ/mm^{-1}	15.130
F(000)	504.0

Crystal size/mm^3	0.2 × 0.02 × 0.02
Radiation	CuKα (λ = 1.54178)
2Θ range for data collection/°	8.226 to 144.352
Index ranges	-6 ≤ h ≤ 6, -26 ≤ k ≤ 26, -10 ≤ l ≤ 10
Reflections collected	17148
Independent reflections	3588 [R_{int} = 0.0653, R_{sigma} = 0.0490]
Data/restraints/parameters	3588/1/246
Goodness-of-fit on F^2	1.077
Final R indexes [I>=2σ (I)]	R_1 = 0.0712, wR_2 = 0.1855
Final R indexes [all data]	R_1 = 0.0732, wR_2 = 0.1874
Largest diff. peak/hole / e Å^{-3}	2.05/-0.71
Flack parameter	-0.006(18)

Table 2 Fractional Atomic Coordinates (×10^4) and Equivalent Isotropic Displacement Parameters (Å^2×10^3) for lub116. U_{eq} is defined as 1/3 of of the trace of the orthogonalised U_{ij}tensor.

Atom	*x*	*y*	*z*	U(eq)
I1	3484.5(16)	1113.7(5)	1006.1(11)	51.5(3)
O1	4090(20)	703(5)	7553(13)	47(2)
C1	3270(30)	908(7)	6167(19)	42(3)
S1	6437(6)	-433.9(15)	4916(5)	40.7(7)
N1	1740(20)	1419(5)	5685(16)	40(2)
N2	3850(20)	-9(5)	4410(17)	42(3)
C2	3930(20)	666(6)	4588(18)	39(3)
O2	-2226(19)	1794(6)	7052(17)	56(3)
O3	400(20)	2509(5)	8628(17)	50(3)
C3	2010(30)	988(6)	3117(18)	42(3)
N3	3640(20)	-1374(6)	6914(18)	47(3)
C4	1260(30)	1585(7)	3890(19)	44(3)
O4	8475(19)	-51(5)	4682(15)	47(2)
O5	5830(20)	-1006(5)	4027(16)	51(2)
C5	2810(30)	2188(7)	4020(20)	46(3)
O6	2130(20)	-1113(5)	5737(16)	55(3)
C6	2240(30)	2506(7)	5540(20)	48(3)
C7	2050(30)	1970(6)	6750(20)	43(3)
O7	3320(20)	-1901(5)	7378(18)	59(3)
C8	-210(30)	2063(7)	7474(18)	43(3)
C9	-1550(30)	2629(9)	9490(20)	57(4)

C10	7250(30)	-607(6)	7130(20)	45(3)
C11	5980(30)	-1035(7)	7890(20)	44(3)
C12	6760(40)	-1155(9)	9560(30)	58(4)
C13	8930(40)	-861(9)	10570(30)	62(4)
C14	10250(30)	-445(8)	9880(30)	58(4)
C15	9430(30)	-313(7)	8170(20)	49(4)

Table 3 Anisotropic Displacement Parameters ($Å^2 \times 10^3$) for lub116. The Anisotropic displacement factor exponent takes the form: $-2\pi^2[h^2a^{*2}U_{11}+2hka^*b^*U_{12}+\ldots]$.

Atom	$\mathbf{U_{11}}$	$\mathbf{U_{22}}$	$\mathbf{U_{33}}$	$\mathbf{U_{23}}$	$\mathbf{U_{13}}$	$\mathbf{U_{12}}$
I1	54.2(5)	52.9(5)	49.3(5)	5.1(5)	17.8(3)	1.6(5)
O1	52(6)	48(5)	43(6)	5(4)	19(4)	8(4)
C1	33(6)	40(7)	54(8)	-1(5)	15(6)	-3(4)
S1	36.0(14)	38.9(14)	49.4(18)	0.3(12)	15.9(13)	2.6(12)
N1	33(5)	38(5)	47(7)	0(5)	11(5)	4(4)
N2	33(6)	41(6)	54(8)	5(5)	14(5)	3(5)
C2	33(6)	43(6)	43(7)	-1(5)	10(5)	4(5)
O2	32(5)	61(6)	73(8)	-14(5)	13(5)	1(4)
O3	35(5)	52(5)	65(7)	-9(5)	17(5)	0(4)
C3	37(6)	42(8)	47(7)	0(5)	9(5)	3(5)
N3	40(6)	49(6)	56(8)	4(5)	21(5)	-2(5)
C4	40(7)	42(7)	51(9)	4(5)	13(6)	4(5)
O4	38(5)	43(5)	62(7)	5(4)	18(4)	5(4)
O5	40(5)	43(5)	69(7)	1(5)	13(5)	4(4)
C5	53(9)	41(7)	43(8)	5(6)	8(7)	-3(6)
O6	42(5)	47(5)	71(8)	6(5)	8(5)	1(4)
C6	56(8)	41(6)	45(8)	2(5)	10(6)	2(6)
C7	38(6)	38(6)	53(8)	-1(6)	14(6)	6(5)
O7	56(6)	47(6)	74(8)	13(5)	18(6)	-9(5)
C8	38(7)	45(7)	46(8)	-1(5)	12(6)	3(5)
C9	43(8)	67(10)	63(10)	-18(8)	19(7)	5(7)
C10	39(7)	40(7)	55(9)	1(6)	14(6)	1(5)
C11	37(6)	45(7)	51(8)	3(6)	12(6)	3(5)
C12	60(9)	58(9)	59(10)	9(8)	21(7)	-3(7)
C13	65(10)	63(10)	56(10)	6(8)	14(8)	-3(8)
C14	49(8)	53(8)	68(11)	-4(8)	11(7)	-4(7)

C15	34(6)	40(7)	75(12)	7(7)	20(7)	0(5)

Table 4 Bond Lengths for lub116.

Atom	Atom	Length/Å	Atom	Atom	Length/Å
I1	C3	2.136(15)	C3	C4	1.54(2)
O1	C1	1.194(18)	N3	O6	1.214(18)
C1	N1	1.363(17)	N3	O7	1.225(17)
C1	C2	1.54(2)	N3	C11	1.48(2)
S1	N2	1.620(12)	C4	C5	1.53(2)
S1	O4	1.428(11)	C5	C6	1.54(2)
S1	O5	1.423(12)	C6	C7	1.55(2)
S1	C10	1.804(17)	C7	C8	1.516(19)
N1	C4	1.48(2)	C10	C11	1.40(2)
N1	C7	1.458(18)	C10	C15	1.40(2)
N2	C2	1.457(18)	C11	C12	1.36(3)
C2	C3	1.526(19)	C12	C13	1.39(3)
O2	C8	1.192(19)	C13	C14	1.36(3)
O3	C8	1.329(18)	C14	C15	1.39(3)
O3	C9	1.448(19)			

Table 5 Bond Angles for lub116.

Atom	Atom	Atom	Angle/°	Atom	Atom	Atom	Angle/°
O1	C1	N1	127.5(14)	O7	N3	C11	117.1(13)
O1	C1	C2	125.5(13)	N1	C4	C3	103.1(11)
N1	C1	C2	106.8(12)	N1	C4	C5	101.4(12)
N2	S1	C10	108.9(7)	C5	C4	C3	122.3(12)
O4	S1	N2	106.1(6)	C4	C5	C6	101.7(13)
O4	S1	C10	106.5(7)	C5	C6	C7	105.4(12)
O5	S1	N2	107.4(7)	N1	C7	C6	103.2(12)
O5	S1	O4	119.9(7)	N1	C7	C8	112.4(12)
O5	S1	C10	107.7(7)	C8	C7	C6	111.5(12)
C1	N1	C4	114.1(12)	O2	C8	O3	125.4(13)
C1	N1	C7	121.3(12)	O2	C8	C7	125.8(14)
C7	N1	C4	111.8(11)	O3	C8	C7	108.7(12)
C2	N2	S1	122.4(10)	C11	C10	S1	125.9(12)

N2	C2	C1	114.5(12)	C11	C10	C15	117.0(15)
N2	C2	C3	112.1(12)	C15	C10	S1	117.0(12)
C3	C2	C1	104.9(11)	C10	C11	N3	121.8(14)
C8	O3	C9	114.7(12)	C12	C11	N3	115.6(14)
C2	C3	I1	112.7(9)	C12	C11	C10	122.6(15)
C2	C3	C4	104.1(11)	C11	C12	C13	119.5(16)
C4	C3	I1	116.0(9)	C14	C13	C12	119.8(18)
O6	N3	O7	124.0(13)	C13	C14	C15	120.7(16)
O6	N3	C11	118.9(12)	C14	C15	C10	120.3(14)

Table 6 Hydrogen Bonds for lub116.

D	H	A	d(D-H)/Å	d(H-A)/Å	d(D-A)/Å	D-H-A/°
N2	H2	O4[1]	0.86	2.25	2.966(16)	141.1
N2	H2	O6	0.86	2.24	2.877(17)	130.5

[1] -1+X,+Y,+Z

Table 7 Torsion Angles for lub116.

A	B	C	D	Angle/°	A	B	C	D	Angle/°
I1	C3	C4	N1	-149.7(9)	N3	C11	C12	C13	179.8(16)
I1	C3	C4	C5	-36.9(17)	C4	N1	C7	C6	-10.2(15)
O1	C1	N1	C4	174.4(14)	C4	N1	C7	C8	110.0(13)
O1	C1	N1	C7	36(2)	C4	C5	C6	C7	34.9(15)
O1	C1	C2	N2	45.6(19)	O4	S1	N2	C2	-28.8(14)
O1	C1	C2	C3	168.9(14)	O4	S1	C10	C11	-170.7(12)
C1	N1	C4	C3	17.1(14)	O4	S1	C10	C15	5.4(13)
C1	N1	C4	C5	-110.3(13)	O5	S1	N2	C2	-158.2(12)
C1	N1	C7	C6	129.1(13)	O5	S1	C10	C11	-40.9(14)
C1	N1	C7	C8	-110.7(14)	O5	S1	C10	C15	135.1(12)
C1	C2	C3	I1	151.5(9)	C5	C6	C7	N1	-16.0(15)
C1	C2	C3	C4	24.9(14)	C5	C6	C7	C8	-136.8(13)
S1	N2	C2	C1	-100.3(13)	O6	N3	C11	C10	-33(2)
S1	N2	C2	C3	140.4(11)	O6	N3	C11	C12	144.6(15)
S1	C10	C11	N3	-4(2)	C6	C7	C8	O2	103.7(18)
S1	C10	C11	C12	177.9(13)	C6	C7	C8	O3	-74.5(15)

S1	C10	C15	C14	-177.0(12)	C7	N1	C4	C3	159.5(11)
N1	C1	C2	N2	-138.6(11)	C7	N1	C4	C5	32.1(14)
N1	C1	C2	C3	-15.3(14)	O7	N3	C11	C10	147.8(14)
N1	C4	C5	C6	-39.7(13)	O7	N3	C11	C12	-34(2)
N1	C7	C8	O2	-12(2)	C9	O3	C8	O2	5(2)
N1	C7	C8	O3	170.2(12)	C9	O3	C8	C7	-177.2(13)
N2	S1	C10	C11	75.2(14)	C10	S1	N2	C2	85.5(13)
N2	S1	C10	C15	-108.7(12)	C10	C11	C12	C13	-2(3)
N2	C2	C3	I1	-83.6(12)	C11	C10	C15	C14	-1(2)
N2	C2	C3	C4	149.8(11)	C11	C12	C13	C14	1(3)
C2	C1	N1	C4	-1.3(15)	C12	C13	C14	C15	0(3)
C2	C1	N1	C7	-139.8(12)	C13	C14	C15	C10	0(3)
C2	C3	C4	N1	-25.2(13)	C15	C10	C11	N3	179.7(13)
C2	C3	C4	C5	87.6(16)	C15	C10	C11	C12	2(2)
C3	C4	C5	C6	-153.3(13)					

Table 8 Hydrogen Atom Coordinates (Å×10^{4}) and Isotropic Displacement Parameters (Å^{2}×10^{3}) for lub116.

Atom	***x***	***y***	***z***	**U(eq)**
H2	2695.74	-151.97	4847.02	51
H2A	5714.13	810.32	4630.79	47
H3	427.33	720.05	2752.79	51
H4	-624.87	1672.81	3383.55	53
H5A	2187.64	2443.47	2989.15	56
H5B	4680.45	2104.42	4227.17	56
H6A	597.57	2741.13	5188.62	58
H6B	3657.68	2795.58	6091.44	58
H7	3700.04	1939.61	7679.56	51
H9A	-3149.17	2770.5	8673.34	85
H9B	-926.17	2951.27	10341.37	85
H9C	-1894.29	2246.07	10028.18	85
H12	5809.36	-1438.91	10041.69	69
H13	9509.82	-948.39	11741.6	74
H14	11739.62	-243.34	10575.08	70
H15	10359.33	-21.23	7703.86	58

Experimental

Single crystals of $C_{15}H_{16}IN_5O_7S$ compound **1f** (LUB116) were grown from MeOH A suitable crystal was selected and mounted on a cryoloop on a Bruker Smart APEX diffractometer. The crystal was kept at 100 K during data collection. Using Olex2 [1], the structure was solved with the XT [2] structure solution program using Intrinsic Phasing and refined with the XL [3] refinement package using Least Squares minimisation.

1. Dolomanov, O.V., Bourhis, L.J., Gildea, R.J, Howard, J.A.K. & Puschmann, H. (2009), J. Appl. Cryst. 42, 339-341.
2. Sheldrick, G.M. (2015). Acta Cryst. A71, 3-8.
3. Sheldrick, G.M. (2015). Acta Cryst. C71, 3-8.

Crystal structure determination of [lub116]

Crystal Data for $C_{15}H_{16}IN_5O_7S$ (M =509.27 g/mol): monoclinic, space group $P2_1$ (no. 4), a = 5.3844(4) Å, b = 21.4986(16) Å, c = 8.2956(6) Å, β = 106.438(4)°, V = 921.02(12) Å^3, Z = 2, T = 100 K, μ(CuKα) = 15.130 mm^{-1}, $Dcalc$ = 1.836 g/cm^3, 17148 reflections measured (8.226° ≤ 2Θ ≤ 144.352°), 3588 unique (R_{int} = 0.0653, R_{sigma} = 0.0490) which were used in all calculations. The final R_1 was 0.0712 (I > 2σ(I)) and wR_2 was 0.1874 (all data).

Refinement model description

Number of restraints - 1, number of constraints - unknown.
Details:

```
1. Twinned data refinement
 Scales: 1.006(18)
 -0.006(18)
2. Fixed Uiso
 At 1.2 times of:
  All C(H) groups, All C(H,H) groups, All N(H) groups
 At 1.5 times of:
  All C(H,H,H) groups
3.a Riding coordinates:
 N2(H2)
3.b Ternary CH refined with riding coordinates:
 C2(H2A), C3(H3), C4(H4), C7(H7)
3.c Secondary CH2 refined with riding coordinates:
 C5(H5A,H5B), C6(H6A,H6B)
3.d Aromatic/amide H refined with riding coordinates:
 C12(H12), C13(H13), C14(H14), C15(H15)
3.e Idealised Me refined as rotating group:
 C9(H9A,H9B,H9C)
```

This report has been created with Olex2, compiled on 2017.08.10 svn.r3458 for OlexSys. Please let us know if there are any errors or if you would like to have additional features.

Chapter 3

Stereo- and regiochemical transannular cyclization of a common hexahydro-1H-azonine to afford three different indolizidinone dipeptide mimetics

3.01 Context

3.02 Transannular cyclization

Azabicyclo[X.Y.0]alkanone amino acids have been used as scaffolds for mimicry of turn structures and as rigid platforms for orienting pharmacophores in combinatorial libraries.[1] Transannular ring closure has provided an effective means to construct these heterocycles from unsaturated amino lactam carboxylates[2,3] Limited mechanistic understanding exists however to predict the factors that control the regioselectivity and stereoselectivity of such transannular cyclization reactions. Previously, relatively simple indolizidinones were synthesized by transannular cyclizations of unsaturated nine-membered lactams. For example, *cis*-9-methyl azon-5-en-2-one **3.01** reacted with mercuric acetate followed by $NaBH_4$ to obtain regioselectively azabicyclo[4.3.0]alkane **3.02** (Scheme 3.01).[4] Transannular cyclizations of *trans*-9- and 10-membered unsaturated lactams **3.03** and **3.04** gave respectively indolizidinone **3.05** and quinolizidinone **3.06** with regioselectivity and diastereoselectivity arising from anti-facial attack of an iodonium intermediate by the nitrogen lone pair to provide the iodide on the 6-membered lactam ring.[5]

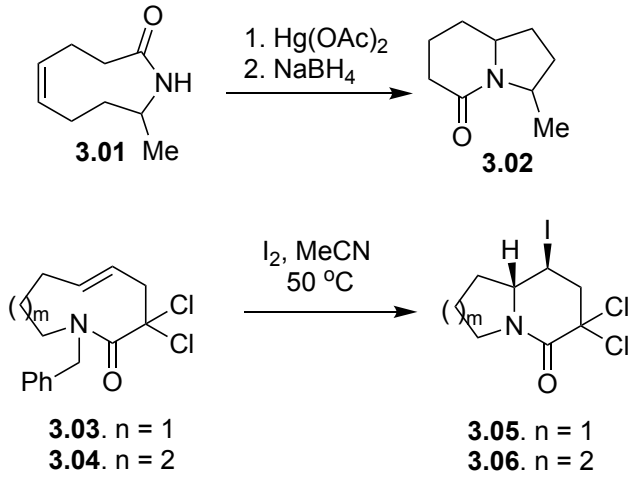

Scheme 3.01. Transannular cyclizations of lactams

Different conformers of lactam **3.07** underwent transannular cyclization to give regioselectively and diastereoselectively indolizidinones **3.08**–**3.010** (Scheme 3.02).[6] The barrier for isomerization of the conformers was higher than the activation energy for transannular cyclization. Electrophilic attack of the unhindered face of the olefin was predicted to provide the selenium ion which was attacked by the amide none pair to place the phenylselenide on the six-membered ring. The kinetically generated conformer **3.07a** afforded a 11:1 mixture of regioisomers **3.08** and **3.09**. After equilibration at rt over time, the thermodynamically stable conformer **3.07b** reacted to give a single isomer **3.010**. The conformation of the nine-membered lactam dictated the facial selectivity of the cyclization to afford different diastereomers.

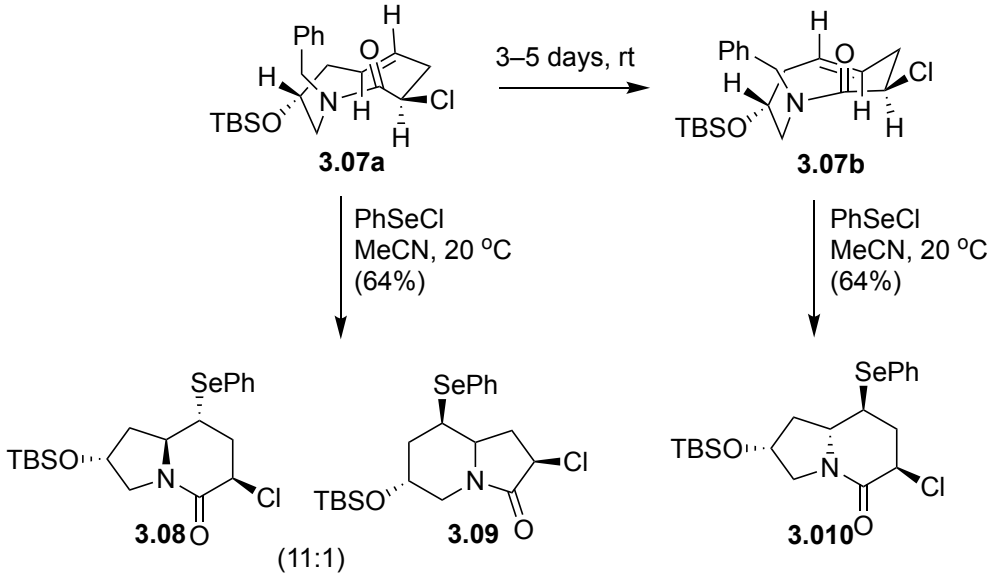

Scheme 3.02. Transannular cyclization of azoninones into indolizidinones

Tertiary amide **1.45c** was shown in our hands to react with iodine to give a single diastereomer (*R*,*R*)-**1.47**, which may be explained by a preferred conformer that minimizes allylic $A^{1,3}$ interactions between the amide dimethoxybenzyl (Dmb) group and exocyclic carbamate. After removal of the Dmb group, transannular cyclization of secondary amide **1.46c** afforded two diastereomeric products (*R*,*R*)- and (*S*,*S*)-**1.47**.[7] The diastereomeric mixture resulted likely from a

lack of facial preference in the addition of the iodine onto the *cis* double bond both to form cyclic iodonium ions, which underwent subsequent attack of the amide nitrogen to give respectively each diastereomer (*R*,*R*)- and (*S*,*S*)-**1.47**.

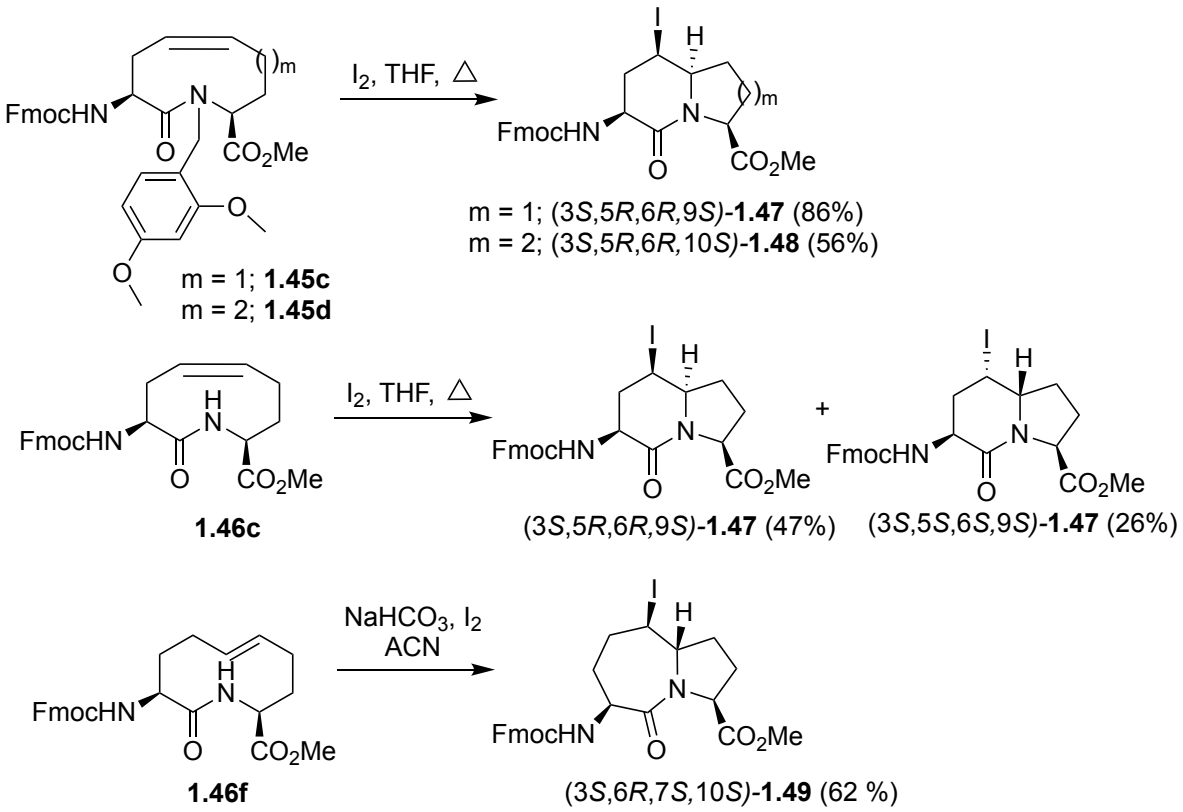

Scheme 1.7. Synthesis of indolizidinone, quinolizidinone and pyrroloazepinone amino acid analogs by way of a shared transannular cyclization approach

Finally, ring closure of 10-membered amide **1.46f** occurred with high regioselectivity and stereoselectivity likely by a mechanism featuring cyclic iodonium intermediate formation from attack of the least hindered face of the olefin. The *trans*-double bond reacted with similar anti-facial addition to place the iodide on the lactam ring of the pyrroloazepinone system **1.49**.

3.03 Side-chain modifications

Side-chains play important roles in recognition events of bioactive peptides. Methods for the synthesis of azabicycloalkanone amino acids have thus been pursued to prepare analogs with

substituents at different ring positions for side-chain mimicry. The iodide substituent from the transannular reaction has thus been studied as a handle to introduce functional groups onto the bicycle.

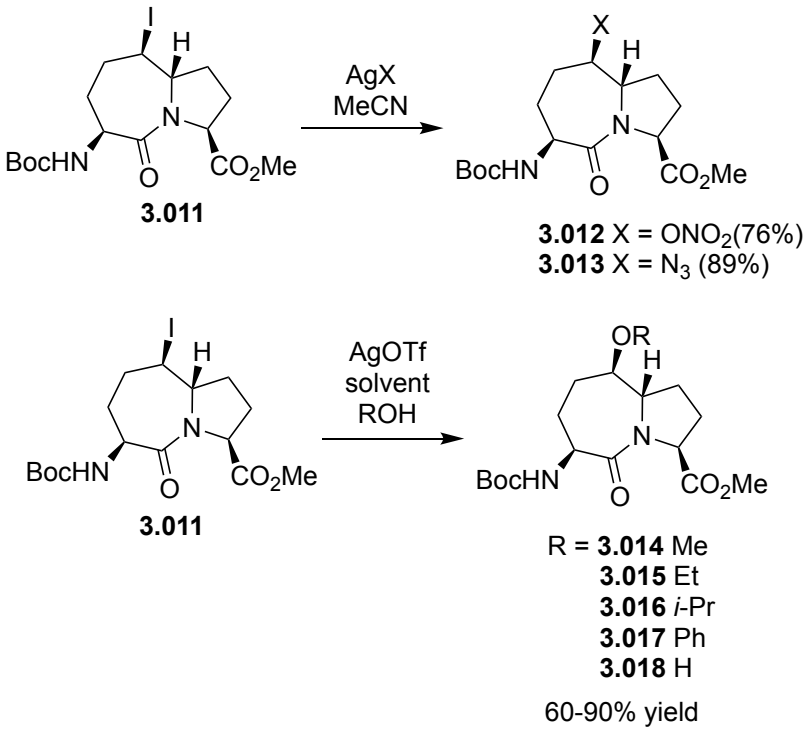

Scheme 3.03. Synthesis of substituted azabicyclo[5.3.0]alkanone amino acids

For example, 6-iodo-azabicyclo[5.3.0]alkanone **3.011** was successfully converted into a series of substituted analogs by nucleophilic displacements of the iodide using silver salts (Scheme 3.11).[8] Employing silver triflate to assist displacement of iodide **3.011** with alcohols and phenol a series of ethers (**3.014–3.018**) were produced diastereoselective S_N1 displacements in which the nucleophile added from the convex face of the cation intermediate. Similarly, silver azide gave the corresponding azide **3.013**, which may be employed for further diversification by reduction and acylations, or copper-catalyzed azide alkyne cycloaddition (CuAAC) reactions.

3.04 Objectives

In principle, the transannular iodo amidation of an unsaturated lactam could provide two azabicycloalkanone systems each possessing 4 different diastereomers. The ground state ring conformation and the cyclization conditions both may influence attack of the unsaturated lactam in this reaction. In related iodo lactamizations, regioselectivity has been considered to be a consequence of the unsaturated lactam conformation.[9] Moreover, ring strain may inhibit formation of certain products over others.[9] Inspired by our results in Chapter **2** and literature examples, the transannular iodo amidation of 9-memebered unsaturated lactams was further studied with the aim to develop stereoselective routes to I^2aa and I^9aa diastereomers by way of a common lactam precursor. Among conditions examined, nitrogen protection, solvent and the use of a hypervalent iodine additive, were are studied.

Finally, to examine the addition of substituents onto the I^2aa and I^9aa products, iodide elimination was examined to furnish olefin precursors. Arylation by palladium-catalyzed Heck coupling provide access to aromatic substitution of the I^2aa system. On the other hand, allylic oxidation, provided 7-hydroxy-I^9aa analogs, isomers of which were prepared by iodide displacement.

This chapter demonstrates effective methods for making multiple azabicyclo[X.Y.0]-alkanone amino acids from common unsaturated lactam precursors. Moreover, novel approaches for the functionalization of the azabicyclo[X.Y.0]alkanone have been developed by way of olefin precursors. This chapter offers thus considerable potential for the study of peptide mimicry by providing a set of useful dipeptide surrogates and methods for their procurement.

3.05 References

1. Cluzeau, J.; Lubell, W. D., Design, synthesis, and application of azabicyclo[X.Y.0]alkanone amino acids as constrained dipeptide surrogates and peptide mimics. *J. Pept. Sci.* **2005**, *80*, 98–150.

2. Robin, S., Electrophilic cyclization of unsaturated amides. *Tetrahedron* **1998**, *54*, 13681–13736.

3. Paquette, L. A.; Scott, M. K., Unsaturated heterocyclic systems. XXXIX. Transannular cyclizations in medium-sized unsaturated azalactams. *J. Org. Chem.* **1968**, *33*, 2379–2382.

4. Wilson, S. R.; Sawicki, R. A., Stereochemistry, conformational analysis, and transannular cyclizations of nine-membered ring azaolefins. *J. Org. Chem.* **1979**, *44*, 330–336.

5. Edstrom, E. D., New methodology for the synthesis of functionalized indolizidine and quinolizidine ring systems. *J. Am. Chem. Soc.* **1991**, *113*, 6690–6692.

6. Sudau, A.; Nubbemeyer, U., Unusual diastereoselection in the synthesis of nine-membered Ring lactams and conformation-controlled transannular reactions to generate optically active indolizidinones. *Angew. Chem. Int. Ed.* **1998**, *37*, 1140–1143.

7. Surprenant, S.; Lubell, W. D., From macrocycle dipeptide lactams to azabicyclo [X.Y.0] alkanone amino acids: A transannular cyclization route for peptide mimic synthesis. *Org. Lett.* **2006**, *8*, 2851–2854.

8. Godina, T. A.; Lubell, W. D., Mimics of peptide turn backbone and side-chain geometry by a general approach for modifying azabicyclo[5.3.0]alkanone amino acids. *J. Org. Chem.* **2011**, *76*, 5846–5849.

9. Sudau, A.; Münch, W.; Nubbemeyer, U.; Bats, J. W., Planar Chirality: Synthesis and Transannular Reactions of Unsaturated optically active azoninones bearing *E*-olefins. *J. Org. Chem.* **2000**, *65*, 1710–1720.

Article 2

Stereo- and regiochemical transannular cyclization of a common hexahydro-1H-azonine to afford three different indolizidinone dipeptide mimetics

N. D. Prasad Atmuri and William D. Lubell*

Département de Chimie, Université de Montréal, P.O. Box 6128, Station Centre-ville, Montréal, Québec H3C 3J7, Canada

3.1 Abstract

Three different indolizidin-2- and 9-one amino acid (I^2aa and I^9aa) analogs were synthesized from the same 9-membered unsaturated lactam precursor by stereo- and regiochemical transannular cyclizations. For example, (2*S*,5*R*,6*R*,9*S*)- and (2*S*,5*S*,6*S*,9*S*)-I^2aa **3.3** were diastereoselectively prepared from hexahydro-1H-azonines **3.5** and **3.6** using iodine in THF, and in MeCN with DIB as additive, respectively. The regioselectivity of the transannular cyclization was influenced by amine protection, such that I^9aa **3.8** could also be synthesized. Side-chains were added onto the I^2aa and I^9aa ring systems by way of olefin intermediates that underwent Pd-catalyzed C-H bond activation and allylic oxidation.

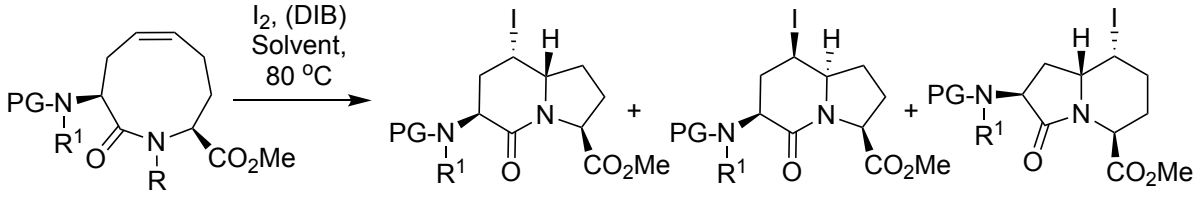

PG, R^1, R	Solvent/DIB	(5*S*,6*S*)-I^2aa	(5*R*,6*R*)-I^2aa	(5*R*,6*R*)-I^9aa
Fmoc, H, H	ACN, DIB	100%	–	–
Fmoc, H, Dmb	THF	–	94%	–
Phth, Dmb	ACN, DIB	63%	–	36%

3.2 Introduction

Constrained dipeptide lactams are commonly inserted into sequences to study biologically active conformers in peptide-based drug discovery.[1] For example, azabicyclo[X.Y.0]alkanone amino acids of different ring sizes have demonstrated utility for studying various targets, including metalloprotease inhibitors,[2] Smac mimetics,[3] and G-protein coupled receptor antagonists.[4,5] Among azabicyclo[X.Y.0]alkanones, indolizidin-2-one amino acids (e.g., **3.1** and **3.3**, Figure 1) have the longest history of applications in peptide mimicry, since a 7-thiaindolizidin-2-one amino acid was proven to serve as a type II' β-turn mimic.[6,7] On the other hand, the corresponding indolizidin-9-one amino acids (e.g., **3.2** and **3.4**) have been less well studied likely due to their

more challenging synthesis,[8] in spite their applications as enzyme inhibitors and receptor ligands.[9,10]

Ideal strategies for synthesizing azabicycloalkanones should provide specific ring sizes with stereocontrol and potential for ring substituent incorporation to mimic effectively both peptide backbone and side-chain conformation and function. For example, the ring closing metathesis-transannular cyclization (RCM-TC) approach to azabicycloalkanones has unambiguously provided 5,5-, 5,6-, 6,5-, 6,4-, 6,6- and 7,5-bicyclic systems by way of a shared synthetic route featuring diastereoselective iodo lactamization of various 8–10-membered unsaturated lactams.[11,12,13] Moreover, S_N1 displacement of the iodide from the resulting 7,5-bicyclic product gave access to a series of ring substituents to mimic different side-chains.[14]

In principle, contingent on olefin geometry and attack, the iodo lactamization can give rise to two different bicycles each having four possible diastereomers. Governing the transannular cyclization to provide specific isomers is challenging; however, the reward of preparing selectively various bicycles with condition control merits study considering the atom economy in synthesizing multiple ring systems from a common precursor.[15]

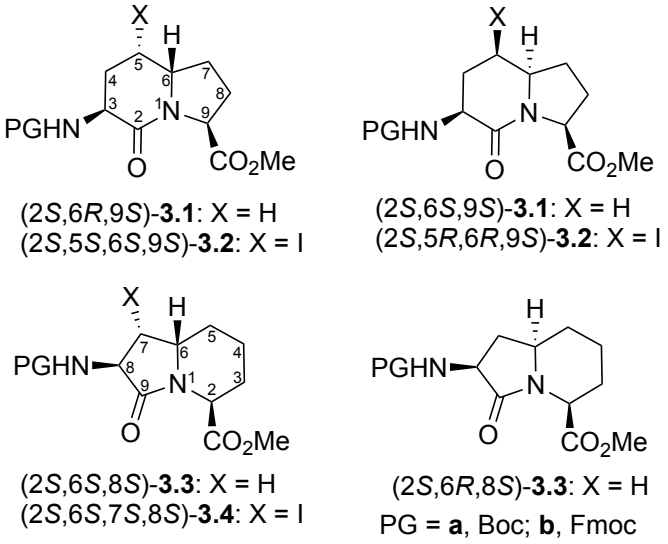

Figure 3.1. Representative Indolizidin-2- and 9-one Amino Acid (I^2aa and I^9aa) Derivatives

Earlier examinations of the RCM-TC strategy arrived at two effective and diastereoselective iodo lactamization conditions. Heating certain 9- and 10- membered lactams with iodine in THF gave diastereoselectively (2*S*,5*R*,6*R*,9*S*)-I^{2}aa **3.3**, as well as quinolizidinone and pyrroloazepinone systems,[11] but failed on 8-membered lactams.[12] In the case of the latter, as well as certain 9-membered lactams, employment of hypervalent iodine (e.g., diacetoxyiodobenzene, DIB) under the iodo lactamization conditions in acetonitrile provided access to pyrrolizidinones and (2*S*,6*S*,7*S*,8*R*)-I^{9}aa 3.4b.[13]

3.3 Results and discussions

Intrigued by the role of hypervalent iodine in halo aminations of unsaturated olefins,[16] the transannular amidation of 9-memebred unsaturated lactams possessing different amine protection has now been examined to develop stereoselective routes to I^{2}aa and I^{9}aa diastereomers by way of a common lactam precursor (e.g., **3.7**). Furthermore, methods to introduce substituents onto the I^{2}aa and I^{9}aa ring systems have been developed featuring iodide elimination, Heck arylation and allylic oxidation of olefin intermediates. In sum, insight gained in studying transannular iodo amidation has provided access to three indolizidinone isomers and their ring substituted variations. The electrophilic transannular cyclization of *N*-(Fmoc)amino hexahydroazoninone carboxylate **3.5b** (Dmb = dimethoxybenzyl) using 4 equivalents of I_2 in THF at reflux gave diastereoselectively (5*R*,6*R*)-**3.3b** as a single product in 86% yield (entry 1, Table 1).[11] On the other hand, two diastereomers (5*R*,6*R*)- and (5S,6S)-**3.3b** were respectively obtained in 46% and 27% yields from treatment of lactam **3.6b** under identical conditions.[11] Starting from this point of depart, a systematic study was performed to examine the influences of solvent and DIB additive on both *N*-(Fmoc)- and *N*-(*o*-NBS)amino lactam carboxylates **3.5b**, **3.5c**, **3.6b** and **3.6c** (Table 3.1).

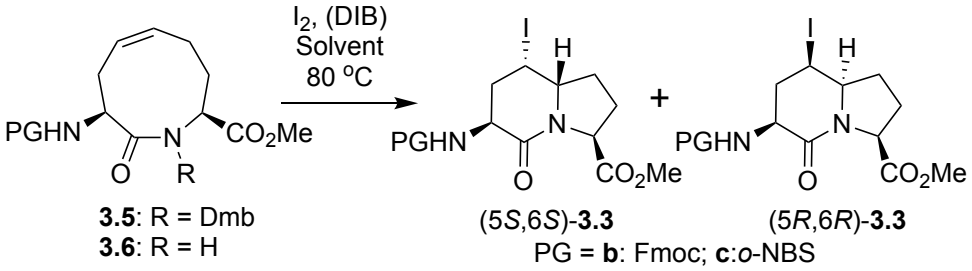

Scheme 3.1 Transannular cyclization of *N*-(Fmoc)- and *N*-(*o*-NBS)amino lactam carboxylates **3.5b**, **3.5c**, **3.6b** and **3.6c**

Table 3.1 Transannular cyclization of lactams **3.5b, 3.5c**, **3.6b** and **3.6c**

entry	#	solvent, (DIB)	% LC 254 nm (isolated yields)			
			(5*S*,6*S*)-**3.3b**	(5*R*,6*R*)-**3.3b**	(5*S*,6*S*)-**3.3c**	(5*R*,6*R*)-**3.3c**
1	**3.5**	THF	6	94 (86)	9	91 (75)
2		MeCN,	25	75	30 (21)	69 (59)
3		THF, DIB	19	81	20 (18)	80 (66)
4		MeCN, DIB	25	75	33	67
5	**3.6**	THF	42 (27)	58 (46)	42	57
6		MeCN,	52	48	40	60
7		THF, DIB	76	24	66	33
8		MeCN, DIB	100 (89)	0	92 (80)	8

Notably, the Fmoc and *o*-NBS protected amino lactams behaved similarly under all conditions with cyclization of the former showing a slight improvement in diastereoselectivity. Like Fmoc analog **3.5b**, *N*-(*o*-NBS)amino lactam **3.5c** reacted selectively with I_2 in THF at reflux to give (5*R*,6*R*)-**3c** in 75% yield. Lower selectivity was obtained subjecting **3.5b** and **3.5c** to the same conditions in MeCN and in the presence of DIB. On the other hand, without Dmb protection, hexahydro-1H-azoninones **3.6b** and **3.6c** reacted with I_2 and DIB in MeCN at 80°C to give selectively (5*S*,6*S*)-**3.3b** and **3.3c** in 89% and 80% yields. The presence of the Dmb group, solvent composition and the DIB additive, all were responsible for the reversal of facial selectivity in the transannular cyclization to go from (5*R*,6*R*)- to (5S,6S)-bicycles **3.3** (entries 1 and 8, Table 3.1).

Considering the NH of carbamates and sulfonamides **3.5** and **3.6** may play roles in the transannular cyclization,[13] *N*-alkyl sulfonamides **3.5d**, **3.5e**, **3.6d** and **3.6e** as well as phthalimido lactams **3.5f** and **3.6f**, all were prepared to examine further the influence of the exocyclic amine component on the iodo amidation (Scheme 3.2). Commencing with amine hydrochloride **7**,[17] *N*-(*o*-NBS)- and *N*-(Phth)amino lactam carboxylates **3.5c** and **3.5f** were respectively prepared using 2-nitrobenzenesulfonyl chloride and *N*-carbethoxyphthalimide and a tertiary amine in THF and MeCN in 80% and 85% yields. Alkylation of sulfonamide **3.5c** with methyl iodide and benzyl bromide using K_2CO_3 in MeCN at 80°C gave respectively *N*-methyl and *N*-benzyl sulfonamides **3.5d** and **3.5e** in 90% and 86% yields. The Dmb group was removed from **3.5c**–**f** using 50% TFA in DCM to afford **3.6**c–**f** in 85−92% yields.

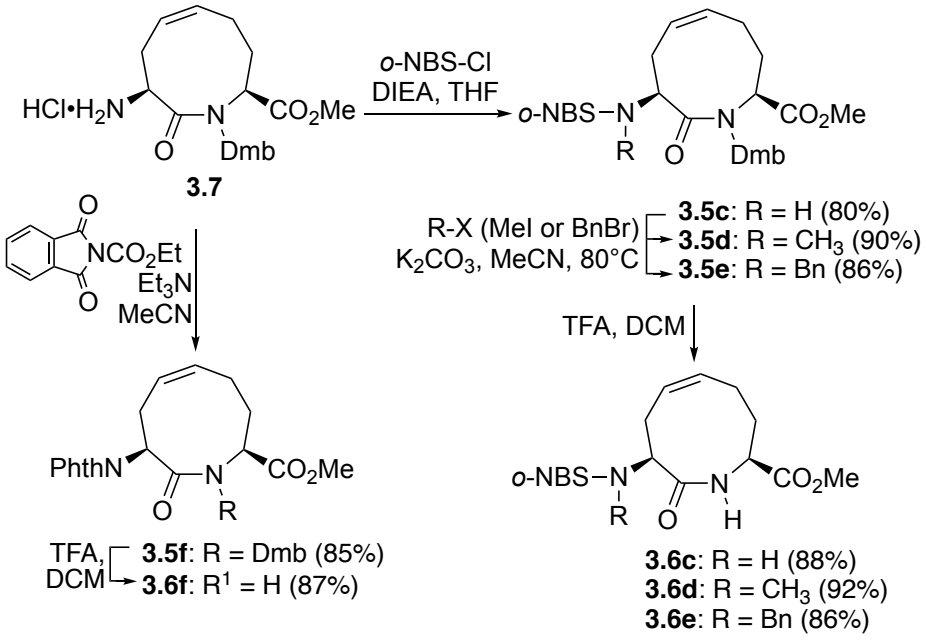

Scheme 3.2. Exocyclic amine modification of lactams **3.5** and **3.6**

With *N*-methyl and *N*-benzyl sulfonamides and *N*-phthalimides **3.5d–f** and **3.6d–f** in hand, transannular cyclization was performed to study the relevance of the exocyclic amine in the iodo amidation (Scheme 3.3, Table 3.2, Table S1, see supporting information (SI). *N*-Methylation of

sulfonamide **3.5c** did not influence the selectivity of the reaction with iodine in THF, which provide stereoselectively (5*R*,6*R*)-**3.3d** from **3.5d** (entry 1). On the other hand, iodine in THF destroyed *N*-benzyl sulfonamide **3.5e** leaving multiple products as observed by LC and TLC, but caused phthalimide **3.5f** to provide a 1:1:1 ratio of (5*S*,6*S*)- and (5*R*,6*R*)-I^2aa **3.3f** and I^9aa **3.8**. Formation of I^9aa **3.8** had never been previously observed and necessitated an alternative iodo amidation mechanism.

Using conditions that transformed respectively hexahydroazoninones **3.6b** and **3.6c** selectively into (5*S*,6*S*)-I^2aa **3.3b** and **3.3c**, lactams **3.6d**–**f** were treated with iodine and DIB in MeCN. Although *N*-alkyl sulfonamides **3.6d** and **3.6e** gave respectively 2:1 and 3:2 mixtures of (5*S*,6*S*)- and (5*R*,6*R*)-I^2aa **3.3d** and **3.3e**, phthalimide **3.6f** reacted selectively to furnish (5*S*,6*S*)-I^2aa **3.3f** in 78% isolated yield (Table 3.2). Finally, lactams **3.5d**–**f** were reacted with iodine and DIB in MeCN. In the cases of *N*-methyl sulfonamide **3.5d** and phthalimide **3.5f**, these conditions gave 4:1 and 2:1 ratios of (5*S*,6*S*)-I^2aa **3** and I^9aa **8**. *N*-Benzyl sulfonamide **3.5e** reacted to give an 8:1:1 ratio of (5*S*,6*S*)-**3.3e**, (5*R*,6*R*)- **3.3e** and **3.8**.

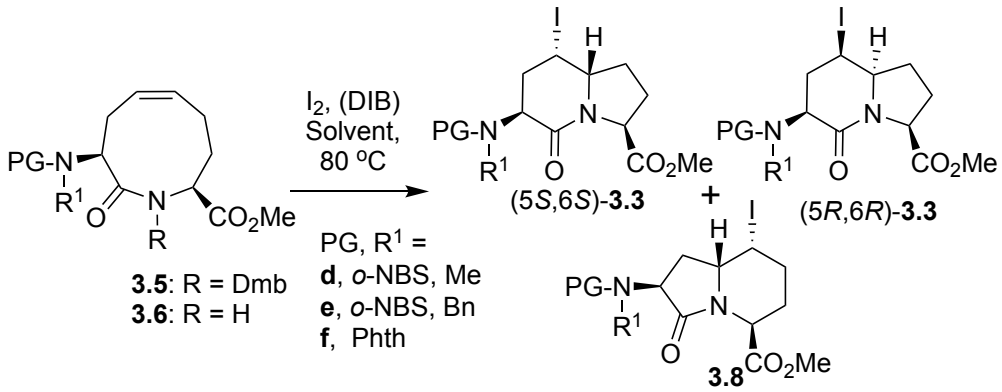

Scheme 3.3: Transannular cyclization of *N*-alkyl sulfonamido-and *N*-phthalimido lactam carboxylates **3.5d**–**f** and **3.6d**–**f**

Table 3.2: Transannular cyclization of lactams **3.5d–f** and **3.6d–f**

entry	#	solvent, (DIB)	% LC 254 nm (isolated yields)		
			(5*S*,6*S*)- **3.3**	(5*R*,6*R*)- **3.3**	**3.8**
1	**3.5d**	THF	0	100 (79)	0
2	**3.5d**	MeCN, DIB	80 (44)	0	20 (15)
3	**3.6d**	MeCN, DIB	70 (54)	30 (20)	0
4	**3.5e**	THF	0	0	0
5	**3.5e**	MeCN, DIB	75 (35)	12 (9)	12 (8)
6	**3.6e**	MeCN, DIB	60 (53)	40 (33)	0
7	**3.5f**	THF	36 (24)	34 (20)	30 (29)
8	**3.5f**	MeCN, DIB	63 (52)	0	36 (20)
9	**3.6f**	MeCN, DIB	100 (78)	0	0

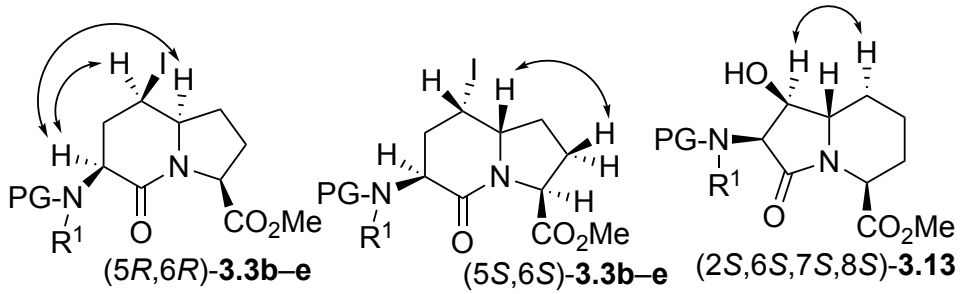

PG, R^1 = (b) Fmoc, H; (**c**) *o*-NBS, H; (**d**) *o*-NBS, Me; (**e**) *o*-NBS, Bn; (**f**) Phth

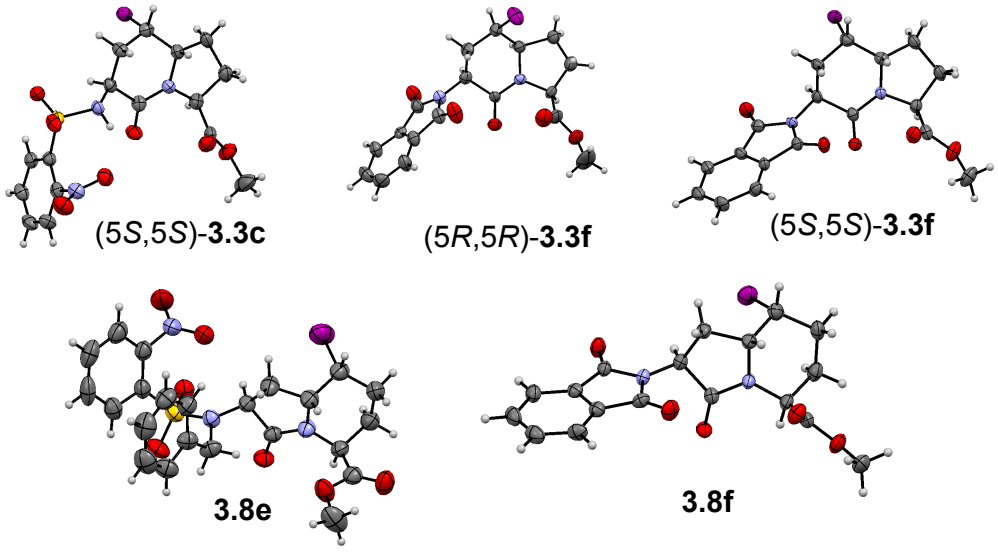

Figure 3.2. NOE correlations and X-ray structures used to assign relative configurations of (5*R*,6*R*)- and (5*S*,6*S*)-**3.3**, and **3.8**.

The structural assignments of I^2aa **3.3b–f** and I^9aa **3.8d–f** were made based on a combination of NMR experiments and X-ray crystallography (Figure 3.2). The configuration of (5*R*,6*R*)-I^2aa **3.3b–f** was assigned based consistently on observed magnetization transfers between the C3, C5 and C6 protons in the NOSEY spectra,[11] and confirmed by the X-ray structure of (5*R*,6*R*)-**3.3f**. Assignment of configuration of (5*S*,6*S*)-I^2aa **3.3b–f** was made based on the observed transfer of magnetisation between the ring fusion C6 and β–C8 protons; the latter appeared consistently up-field of the α–C8 proton due to an anisotropic effect caused by the C9 carboxylate.[18] The iodide 5*S*-configuration was assigned based on anti-facial addition to the *cis* olefin, and confirmed by X-ray structural analyses of (5*S*,6*S*)- **3.3c** and **3.3f**. No significant long range NOE were detected for I^9aa **3.8**; instead, configuration was assigned by X-ray crystallography of **3.8e** and **3.8f**. The C7 stereochemistry of alcohols **3.12** and **3.13b** were respectively assigned based on attach of the least hindered face of the allylic system, and long range NOSEY interactions between the C7 and Cα5 protons (Figure 3.2). The X-ray determined backbone dihedral angle values within bicycles **3.3** and **3.8** demonstrated (5*S*,6*S*)- and (5*R*,6*R*)-I^2aa, and I^9aa all resemble the central residues of an ideal type II'β-turn with subtle differences contingent on ring system and configuration (Table 3.3).

Table 3.3. Backbone Dihedral Angle Values of Bicycles **3.3** and **3.8** and Ideal Type II' β-Turn

Type of β-turn	ϕ^{i+1}, °	ψ^{i+1}, °	ϕ^{i+2}, °	ψ^{i+2}, °
Ideal type II' β-turn	60	–120	–80	0
I^2aa- (*S*,*S*)- **3.3c**	–128 –119	–127 –134	–65 –64	162 154
I^2aa- (*S*,*S*)- **3.3f**	54 (−132)	–150	−69	161
I^2aa-(*R*,*R*)- **3.3f**	54 (−109) 63 (−111) 56 (−110) 71 (−77)	–159 –166 –164 –178	−58 −78 –79 –44	149 156 155 137
I^9aa-**3.8e**	57(−102)	–136	−109	35
I^9aa-**3.8f**	54(−129)	–141	−109	170

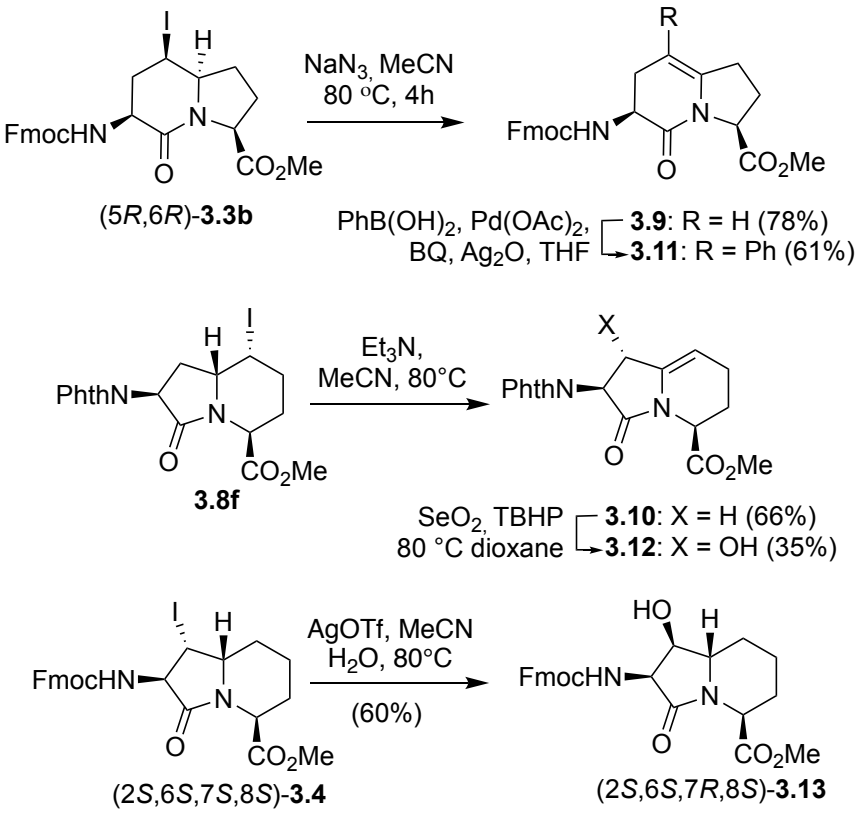

Scheme 3.4. Side-chain installation onto I^2aa and I^9aa analogs

The introduction of ring substituents on to the bicycle offers opportunity for side-chain mimicry. Iodide displacement has previously opened access to diverse 7,5-bicyclic systems.[14] Iodide elimination is now reported to functionalize 5,6- and 6,5-bicyclic systems (Scheme 3.4). Treatment of (5*R*,6*R*)-I^2aa **3.3b** and I^9aa **3.8f** with sodium azide and triethylamine, respectively, in MeCN at 80 °C gave selective elimination of the bridge head proton to provide Δ^5-I^2aa **3.9** and Δ^5-I^9aa **3.10**. Arylation of **3.9** was performed using phenyl boronic acid, $Pd(OAc)_2$, 1,4-benzoquinone and silver oxide in THF at 80°C to provide 5-phenyl-Δ^5-I^2aa **3.11** in 75% yield (Scheme 3.4). Hydroxylation of **3.10** with selenium dioxide and *tert*-butyl hydroperoxide in dioxane at 80 °C afforded the *trans* α-amino-β-hydroxy-γ-lactam (Hgl) analog, 7-hydroxy-Δ^5-I^9aa **3.12** in 35% yield. For comparison, (2*R*,6*S*,7*S*,8*S*)-iodide **3.4b** was displaced with silver triflate in wet acetonitrile to obtain the *cis* Hgl analog, 7-hydroxy-I^9aa **3.13** in 60% yield. Considering the value of Hgl residues as rigid Ser/Thr

residues,[19,20] variants such as 7-hydroxy-I^{9}aas **3.12** and **3.13** offer interesting potential to constrain their *C*-terminal residue for further examination of biologically active peptide conformation.

3.4 Conclusions

Novel diastereoselective routes to indolizidinone amino acids were accessed by way of transannular iodo amidations from a common entry point, hexahydro-1H-azonine **3.7**. Amine protection, solvent and DIB additive, all influenced the stereo- and regio-chemical outcomes of the cyclization to afford (5*R*,6*R*)- and (5*S*,6*S*)-I^{2}aa **3.3**, and I^{9}aa **3.8**, both of which were demonstrated by X-ray crystallography to possess potential for β-turn mimicry. In addition, by employing routes featuring iodide elimination and olefin functionalization, substituents were added to the indolizidinone rings for side-chain mimicry. Intrigued by the results of this preliminary investigation, further study is ongoing to better understand the mechanism for the formation of **3.3** and **3.8**, the optimization of the synthesis of the latter, and the application of this method to other ring systems. The reported I^{2}aa and I^{9}aa systems offer notable potential for exploring structure−activity relationships in peptide chemical biology and utility for biomedical research.

3.5 Acknowledgments

This work was supported by NSERC, Canada. We thank Dr. A. Fürtös, K. Venne, M-C. Tang (mass spectrometry); S. Bilodeau, A. Hamel, C. Malveau (NMR spectroscopy), and F. Belanger-Gariepy (X-ray) from the U. de Montréal Laboratories for aid in analyses. Shastri Indo-Canadian Institute, India is thanked for a Quebec Tuition Fee Exemption grant to N.D.P.A.

3.6 References

1. (a) Hruby, V. J., *Nat. rev. Drug Discov.* **2002,** *1*, 847; (b) Perdih, A.; Kikelj, D., *Curr. Med. Chem.* **2006**, *13*, 1525–1556; (c) Hanessian, S.; Auzzas, L., *Acc. Chem. Res.* **2008**, *41*, 1241–1251.

2. Robl, J. A.; Cimarusti, M. P.; Simpkins, L. M.; Brown, B.; Ryono, D. E.; Bird, J. E.; Asaad, M. M.; Schaeffer, T. R.; Trippodo, N. C., *J. Med. Chem.* **1996**, *39*, 494–502.

3. Sun, H.; Lu, J.; Liu, L.; Yi, H.; Qiu, S.; Yang, C.-Y.; Deschamps, J. R.; Wang, S., *J. Med. Chem.* **2010**, *53*, 6361–6367.

4. Van Cauwenberghe, S.; Simonin, F.; Cluzeau, J.; Becker, J. A.; Lubell, W. D.; Tourwé, D., *J. Med. Chem.* **2004**, *47*, 1864–1867.

5. Martín-Martínez, M.; De la Figuera, N.; Latorre, M.; Herranz, R.; García-López, M. T.; Cenarruzabeitia, E.; Del Río, J.; González-Muñiz, R., *J. Med. Chem.* **2000**, *43*, 3770–3777.

6. Khashper, A.; Lubell, W. D., *Org. Biomol. Chem.* **2014**, *12*, 5052–5070.

7. (a) Nagai, U.; Sato, K.; Nakamura, R.; Kato, R., *Tetrahedron* **1993**, *49*, 3577–3592; (b) Sato, K.; Nagai, U., *J. Chem. Soc. Perkin Trans. 1* **1986**, 1231–1234.

8. (a) Gosselin, F.; Lubell, W. D., *J. Org. Chem.* **1998**, *63*, 7463–7471; (b) De la Figuera, N.; Alkorta, I.; García-López, M. T.; Herranz, R.; González-Muñiz, R., *Tetrahedron* **1995**, *51*, 7841–7856; (c) De la Figuera, N.; Rozas, I.; García-López, M. T.; González-Muñiz, R., *J. Chem. Soc., Chem. Commun.* **1994**, 613–614; (d) Martín-Martínez, M.; De la Figuera, N.; Latorre, M.; García-López, M. T.; Cenarruzabeitia, E.; Del Río, J.; González-Muñiz, R., *J. Med. Chem.* **2005**, *48*, 7667–7674.

9. D'Alessio, S.; Gallina, C.; Gavuzzo, E.; Giordano, C.; Gorini, B.; Mazza, F.; Paradisi, M. P.; Panini, G.; Pochetti, G., *Eur. J. Med. Chem.* **2001**, *36*, 43–53.

10. Gosselin, F.; Lubell, W. D. ; Tourwé, D.; Ceusters, M.; Meert, T.; Heylen, L.; Jurzak, M., *J. Pept. Res.* **2001**, *57*, 337–344.

11. Surprenant, S.; Lubell, W. D., *Org. Lett.* **2006**, *8*, 2851–2854.

12. Atmuri, N. P.; Lubell, W. D., *J. Org. Chem.* **2015**, *80*, 4904–4918.

13. Atmuri, N. P.; Reilley, D. J.; Lubell, W. D., *Org. Lett.* **2017**, *19*, 5066–5069.

14. Godina, T. A.; Lubell, W. D., *J. Org. Chem.* **2011**, *76*, 5846–5849.

15. Gosselin, F.; Lubell, W. D., *J. Org. Chem.* **2000**, *65*, 2163–2171.

16. (a) Tellitu, I.; Dominguez, E., *Synlett* **2012**, *23*, 2165–2175; (b) Muñiz, K., *Pure Appl. Chem.* **2013**, *85*, 755-761; (c) Romero, R. M.; Woeste, T. H.; Muniz, K., *Chem. Asian J.* **2014**, *9*, 972–983.

17. Kaul, R.; Surprenant, S.; Lubell, W. D., *J. Org. Chem.* **2005**, *70*, 3838–3844.

18. Mauger, A.; Irreverre, F.; Witkop, B., *J. Am. Chem. Soc.* **1966**, *88*, 2019–2024.

19. Geranurimi, A.; Lubell, W. D., *Org. Lett.* **2018**, *20*, 6126–6129.

20. Geranurimi, A.; Cheng, C. W.; Quiniou, C.; Hou, X.; Zhu, T.; Rivera, J. C.; St-Cyr, D. J.; Beauregard, K.; Bernard-Gauthier, V.; Chemtob, S., *Front. Chem.* **2019**, *7*, 23.

3.7 Experimental section

3.7.1 General Methods:. ^{1}H and ^{13}C NMR spectra for lactam **3.6f** was recorded at 100 °C to coalesce signals due to conformational isomers. Coupling constant *J* values were measured in Hertz (Hz) and chemical shift values in parts per million (ppm). Infrared spectra were recorded in the neat on a Perkin Elmer Spectrometer FT-IR instrument, and are reported in reciprocal centimeters (cm^{-1}). Crystallographic data for lactams (5*S*,6*S*)-**3.3c**, (5*R*,6*R*)-**3.3f**, (5*S*,6*S*)-**3.3f**, **3.8e** and **3.8f** were acquired on a Bruker venture metal jet diffractometer at the Université de Montréal X-ray Regional Facility. The isomeric mixture of (5*S*, 6*S*)-**3.3f**, was (5*R*, 6*R*)-**3.3f** was separated by preparative reverse phase HPLC (Phenomenex Gemini 5 µm column, C18, 250 mm 21.2 mm) using a solvent gradient from 20% to 90% MeOH (containing 0.1% TFA) in water (containing 0.1% TFA) over 60 min at a flow rate of 10 mL/min.

3.7.2 Reagents: Iodine, Grubbs 1st generation catalyst [dichloro(benzylidene)-bis(tricyclohexylphosphine)-ruthenium(II)], 2-nitrobenzenesulfonyl chloride, diisopropyl ethyl amine (DIEA), sodium triacetoxyborohydride, (diacetoxyiodo)benzene, thionyl chloride, all were purchased from Aldrich and used as received without further purification; HATU and L-serine were purchased from Chem-Impex and used as received.

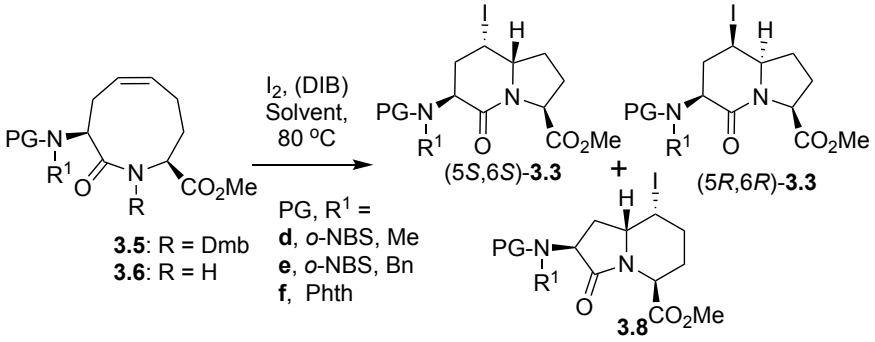

Scheme 3.3: Transannular cyclization of *N*-phthalimido lactam carboxylates **3.5f** and **3.6f**

Table S1: Solvent effects in transannular cyclization of lactams **3.5f** and **3.6f**

entry	#	solvent, (DIB)	% LC 254 nm		
			(5*S*,6*S*)- **3.3**	(5*R*,6*R*)- **3.3**	**3.8**
1	**3.5f**	MeCN	58	13	23
2		toluene	46	43	10
3		EtOH	41	29	29
4		DCM	15	76	11
5		THF, DIB	69	18	12
6		MeCN, MIDAD	66	10	23
7		THF, MIDAD	69	18	12
8		tolune, DIB	55	24	19
9	**3.6f**	THF	61	36	2
10		ACN	36	63	-
11		THF, DIB	73	-	26
12		Toluene, DIB	82	-	1

3.7.3 Synthetic experimental conditions and compound characterization data:

(3*S*,9*S*,*Z*)-Methyl-1-(2,4-dimethoxybenzyl)-3-((2-nitrophenyl)sulfonamido)-2-oxo-2,3,4,7,8,9-hexahydro-1*H*-azonine-9-carboxylate (3.5c)

Hydrochloride salt **3.7** (600 mg, 1.50 mmol) was treated with *o*-nitrobenzenesulfonyl chloride (835 mg, 3.76 mmol) and DIEA (692 μL, 3.76 mmol) in THF, and stirred overnight. The volatiles were evaporated. The residue was partitioned between EtOAc and water. The aqueous phase was extracted with EtOAc (2 × 20 mL). The combined organic layers were dried over anhydrous sodium sulphate, filtered, and concentrated under reduced pressure. The residue was purified by chromatography on silica gel (60−70% EtOAc in hexane) to afford sulfonamide **3.5c** (660 mg, 80%) as off white solid: R_f = 0.28 (2:3 EtOAc/hexanes, twice eluted and visualized by UV), mp 150−153 °C, $[\alpha]_D^{25}$ –114.4 (*c* 1, $CHCl_3$); FT-IR (neat) ν_{max} 3306, 2942, 1744, 1653, 1618, 1154, 776 cm^{-1}; ^1H NMR (500 MHz, $CDCl_3$) δ 8.06−8.08 (m, 1H), 7.94−7.96 (m, 1H), 7.70−7.77 (m, 2H), 7.12–7.14 (d, 1H, *J* = 8.7 Hz), 6.86–6.88 (d, 1H, *J* = 8.5 Hz), 6.35–6.36 (d, 1H, *J* = 2.4), 6.27–6.29 (dd, 1H, *J* = 2.4, 8.4 Hz), 6.02–6.08 (m, 1H), 5.61–5.66 (m, 1H), 4.40–4.46 (m, 3H), 4.27−4.30 (d, 1H, *J* = 15.4), 3.78 (s, 3H), 3.76 (s, 3H), 3.46 (s, 3H), 2.63–2.69 (m, 1H), 2.46–2.50 (m, 1H), 2.06–2.13 (m, 1H), 1.76–1.89 (m, 2H), 1.67–1.74 (m,1H); ^{13}C NMR (125 MHz, $CDCl_3$) δ 172.7, 170.3, 160.1, 157.6, 147.8, 134.3, 133.2, 132.6, 131.7, 130.5, 130.4, 128.0, 125.6, 117.5, 104.5, 97.7, 57.1, 55.3, 55.2, 54.6, 52.2, 39.4, 34.7, 27.8, 22.2 ; HRMS (ESI-TOF) m/z $[M + Na]^+$ calcd for $C_{25}H_{29}N_3O_9S$ Na 570.1516, found 570.1501.

(3*S*,9*S*,*Z*)-Methyl-1-(2,4-dimethoxybenzyl)-3-(*N*-methyl-*N*-(2-nitrophenyl)sulfonamido)-2-oxo-2,3,4,7,8,9-hexahydro-1*H*-azonine-9-carboxylate (3.5d)

Sulfonamide **3.5c** (300 mg, 0.54 mmol) was treated with iodomethane (2.2 mmol, 136 µL) and K_2CO_3 (1.08 mmol, 149 mg) in MeCN (2 mL), stirred overnight at 80 °C, cooled to rt, quenched with water (5 mL) and extracted with ethyl acetate (2 × 30 mL). The combined organic layers were dried over anhydrous sodium sulphate, filtered, and concentrated under reduced pressure. The residue was purified by chromatography on silica gel (60−70% EtOAc in hexane) to afford *N*-methyl sulfonamide **3.5d** (275 mg, 90%) as tan red solid: R_f = 0.46 (2:3 EtOAc/hexanes, twice eluted and visualized by UV); mp 170−175 °C; $[\alpha]_D^{25}$ –47 (*c* 1, $CHCl_3$); FT-IR (neat) ν_{max} 3106, 1742, 1661, 1545, 1285, 852 cm^{-1}; ^1H NMR (500 MHz, $CDCl_3$) δ 8.07−8.08 (m, 1H), 7.64−7.72 (m, 3H), 7.16−7.18 (m, 1H), 6.38–6.40 (m, 2H), 6.00−6.05 (m, 1H), 5.65-5.71 (m, 1H), 5.03−5.05 (d, 1H, *J* = 7.3 Hz), 4.43−4.57 (m, 3H), 3.80 (s, 3H), 3.79 (s, 3H), 3.52 (s, 3H), 3.26 (s, 3H), 2.59-2.65 (m, 1H), 2.39−2.43 (m, 1H), 2.15–2.22 (m, 1H), 1.86–1.98 (m, 2H), 1.74–1.80 (m, 1H); ^{13}C NMR (125 MHz, $CDCl_3$) δ 173.9, 170.8, 159.8, 157.6, 148.2, 133.3, 132.5, 131.9, 131.6, 131.1, 130.0, 127.9, 124.1, 117.9, 104.2, 97.9, 57.4, 56.4, 55.3, 55.2, 52.2, 39.7, 32.1, 30.0, 28.2, 22.5; HRMS (ESI-TOF) m/z $[M + Na]^+$ calcd for $C_{26}H_{31}N_3O_9SNa$ 584.1673, found 584.1660.

(3*S*,9*S*,*Z*)-Methyl-3-(*N*-benzyl-*N*-(2-nitrophenyl)sulfonamido)-1-(2,4-dimethoxybenzyl)-2-oxo-2,3,4,7,8,9-hexahydro-1*H*-azonine-9-carboxylate (3.5e)

Sulfonamide **3.5c** (240 mg, 0.43 mmol) was treated with benzyl bromide (1.32 mmol, 156 µL) and K_2CO_3 (1.32, 182 mg) in MeCN (2 mL), stirred for 3h at 80 °C, quenched with water (5 mL) and extracted with ethyl acetate (2 × 20 mL). The combined organic layers were dried over anhydrous sodium sulphate, filtered, and concentrated under reduced pressure. The residue was purified by chromatography on silica gel (60−70% EtOAc in hexane) to afford *N*-benzyl sulfonamide **3.5e** (240 mg, 86%) as tan red solid: R_f = 0.40 (3:2 EtOAc/hexanes, twice eluted and visualized by UV); mp 87−91 °C; $[\alpha]_D^{25}$ 62 (*c* 0.7, $CHCl_3$); FT-IR (neat) ν_{max} 2951, 1740, 1653, 1613, 1289, 1058,

786 cm^{-1}; ^1H NMR (500 MHz, $CDCl_3$) δ 7.55–7.56 (dd, 1H, *J* = 1.3, 7.9 Hz), 7.48−7.52 (m, 1H), 7.44−7.56 (dd, 1H, *J* = 1.2, 8.0 Hz), 7.29–7.31 (m, 2H), 7.27–7.28 (m, 1H), 7.24–7.25 (m, 1H), 7.09–7.11 (m, 3H), 6.40−6.44 (m, 2H), 6.12–6.18 (m, 1H), 5.68–5.73 (m, 1H), 5.31–5.34 (dd, 1H, *J* = 16.5), 5.20–5.21 (d, 1H, *J* = 6.9), 4.78-4.81 (d, 1H, *J* = 16.7), 465–4.68 (dd, 1H, *J* = 2.4, 12.2 Hz), 4.57–4.60 (d, 1H, *J* = 15.7), 4.48–4.51 (d, 1H, *J* = 15.7), 3.81 (s, 3H), 3.79 (s, 3H), 3.54 (s, 3H), 2.63-2.69 (m, 1H), 2.54-2.58 (m, 1H), 2.16-2.23 (m, 1H), 1.90-1.97 (m, 2H), 1.78-1.84 (m, 1H); ^{13}C NMR (125 MHz, $CDCl_3$) δ 174.4, 170.9, 159.8, 157.5, 147.3, 137.3, 134.5, 132.7, 131.7, 131.4, 131.2, 129.8, 128.2, 128.1, 127.9, 127.2, 123.7, 118.0, 104.1, 98.0, 57.9, 57.6, 55.3, 55.3, 52.2, 50.6, 40.0, 30.7, 28.4, 22.5; HRMS (ESI-TOF) m/z $[M + Na]^+$ calcd for $C_{32}H_{35}N_3O_9SNa$ 660.1986, found 660.1987.

(3*S*,9*S*,*Z*)-Methyl-1-(2,4-dimethoxybenzyl)-3-(1,3-dioxoisoindolin-2-yl)-2-oxo-2,3,4,7,8,9-hexahydro-1*H*-azonine-9-carboxylate (3.5f)

Hydrochloride salt **3.7** (1.0 g, 2.59 mmol) was dissolved in MeCN (20 mL), treated with *N*-carbethoxypthalimide (770 mg, 3.51 mmol) and Et_3N (905 μL, 6.2 mmol), and stirred overnight. The volatiles were evaporated. The residue was purified by chromatography on silica gel (60−70% EtOAc in hexane) to afford phthalimide **3.5f** (1.05 g, 85%) as white foam: R_f = 0.46 (2:3 EtOAc/hexanes, twice eluted and visualized by UV), $[\alpha]_D^{25}$ –54.6 (*c* 1, $CHCl_3$); FT-IR (neat) ν_{max} 2944, 1710, 1652, 1611, 1506, 1328, 1205, 1033 cm^{-1}; ^1H NMR (500 MHz, $CDCl_3$) δ 7.88–7.90 (dd, 2H, *J* = 3.0, 5.5 Hz), 7.73−7.74 (dd, 2H, *J* = 3.0, 5.5), 7.21−7.23 (d, 1H, *J* = 8.4 Hz), 6.42−6.45 (dd, 1H, *J* = 2.4, 8.5 Hz), 6.39–6.40 (d, 1H, *J* = 2.4 Hz), 5.99−6.04 (m, 1H), 5.68–5.73 (m, 1H), 5.22–5.23 (d, 1H, *J* = 7.8), 4.73−4.76 (d, 1H, *J* = 15.6), 4.61–4.64 (dd, 1H, *J* = 2.5, 12.2), 4.33–4.36 (d, 1H, *J* = 15.6), 3.81 (s, 3H), 3.78 (s, 3H), 3.54 (s, 3H), 3.23–3.30 (m, 1H), 2.82–2.87 (dd, 1H, *J* = 8.2, 15.2), 2.17–2.24 (m, 1H), 2.07–2.13 (m, 1H), 1.97–1.99 (m, 1H), 1.72–1.78 (m, 1H);

^{13}C NMR (125 MHz, $CDCl_3$) δ 171.7, 171.0, 168.2, 159.9, 157.6, 133.9, 132.1, 131.9, 130.2, 129.0, 123.4, 117.9, 104.3, 98.0, 61.1, 57.7, 55.3, 55.2, 52.4, 52.1, 40.5, 29.5, 27.4, 22.2. HRMS (ESI-TOF) m/z $[M + Na]^+$ calcd for $C_{27}H_{28}N_2O_7Na$ 515.1788, found 515.1793.

(3*S*,9*S*,*Z*)-Methyl-3-((2-nitrophenyl)sulfonamido)-2-oxo-2,3,4,7,8,9-hexahydro-1*H*-azonine-9-carboxylate (3.6c)

Lactam **3.5c** (150 mg, 0.27mmol) was treated with TFA (1.5 mL) in DCM (5 mL) overnight. The volatiles were removed under vacuum, and the residue was purified by chromatography on silica gel (40−50% EtOAc in hexane) to give macrocycle **3.6c** (95 mg, 0.23 mmol, 88%) as a white solid: R_f = 0.18 (3:2 EtOAc/hexanes, visualized by UV); mp 182−187 °C, $[\alpha]_D^{24}$ –114 (*c* 1, $CHCl_3$); FT-IR (neat) ν_{max} 3308, 2951, 1740, 1506, 1375, 1258, 1167, 1080 cm^{-1}. ^{1}H NMR (500 MHz, $CDCl_3$) (1:1 mixture of ring conformational isomers, peaks of major isomers in brackets) δ 8.14−8.16 (m, 1H) [8.02−8.03 (m, 1H)], 7.92−7.94 (m, 1H) [7.85−7.87 (m, 1H)], 7.75−7.78 (m, 2H) [7.68−7.74 (m, 2H)], 6.79–6.81 (d, 1H, *J* = 8.26) [6.47–6.49 (d, 1H), *J* = 11.0], 6.01–6.06 (m, 1H) [5.89−5.84 (m, 1H)], 5.82−5.84 (d, 1H, *J* = 11.5) [5.74–5.75 (d, 1H, *J* = 2.7)], 5.66−5.72 (m, 1H) [5.51−5.57 (m, 1H)], 4.94−4.99 (m, 1H) [4.16− 4.21 (m, 1H)], 4.11–4.16 (m, 1H) [4.06–4.08 (m, 1H)], 3.78 (s, 3H) [3.69 (s, 3H)], 2.66–2.72 (m, 1H) [2.74–2.78 (m, 1H)], 2.39–2.42 (m, 1H) [2.44–2.49 (m, 1H)], 2.29–2.35 (m, 1H) [2.19–2.24 (m, 1H)], 2.13–2.17 (m, 1H) [2.04–2.06 (m, 1H)], 1.98–2.01 (m, 1H) [1.88–1.91 (m, 1H)], 1.70–1.74 (m, 1H) [1.65–1.68 (m, 1H)]; ^{13}C NMR (175 MHz, $CDCl_3$): δ 172.2/(171.7), 171.6/(171.5), 147.9/(141.7), 141.5/(134.1), 134.0/(133.7), 133.3/(132.6), 132.5/(131.6), 131.0/(130.2), 127.9/(126.2), 125.4/(119.7), 56.6/(54.3), 53.4/(52.7), 52.4/(52.3), 34.2/(33.9), 33.8/(30.8), 24.3/(22.9); HRMS (ESI-TOF) m/z $[M + Na]^+$ calcd for $C_{16}H_{19}N_3O_7SNa$ 420.0835, found 420.0830.

(3*S*,9*S*,*Z*)-Methyl-3-(*N*-methyl-(*N*-2-nitrophenyl)sulfonamido)-2-oxo-2,3,4,7,8,9-hexahydro-1*H*-azonine-9-carboxylate (3.6d)

Lactam **3.5d** (210 mg, 0.37 mmol) was treated under the same conditions used to prepare macrocycle **3.6c** using TFA (3 mL) in DCM (8 mL). Purification by chromatography on silica gel (40−50% EtOAc in hexane) to give macrocycle **3.6d** (141 mg, 92 %) as a white solid: R_f = 0.16 (3:2 EtOAc/hexanes, visualized by UV); mp 80−87 °C; $[\alpha]_D^{24}$ 127 (c 0.5, $CHCl_3$); FT-IR (neat) ν_{max} 3271, 2950, 1776, 1741, 1714, 1616, 1437, 1032 cm^{-1}. ^1H NMR (500 MHz, $CDCl_3$) δ 8.02–8.04 (m, 1H), 7.68−7.70 (m, 2H), 7.59−7.61 (m, 1H), 6.01–6.07 (m, 1H), 5.70–5.75 (m, 2H), 4.68–4.69 (d, 1H, *J* = 7.43), 4.28–4.33 (m, 1H), 3.80 (s, 3H), 3.24 (s, 3H), 2.66–2.72 (m, 1H), 2.39–2.43 (m, 1H), 2.28–2.36 (m, 1H), 2.13–2.18 (m, 1H), 1.87–1.94 (m, 1H), 1.65–1.72 (m, 1H); ^{13}C NMR (125 MHz, $CDCl_3$) δ 173.3, 172.6, 147.8, 133.4, 132.2, 131.7, 131.1, 130.9, 127.9, 124.3, 56.5, 52.6 (2C), 33.8, 32.4, 30.1, 22.9; HRMS (ESI-TOF) m/z $[M + Na]^+$ calcd for $C_{17}H_{21}N_3O_7SNa$ 434.0992, found 434.0986.

(3*S*,9*S*,*Z*)-Methyl-3-(*N*-benzyl-(*N*-(2-nitrophenyl)sulfonamido)-2-oxo-2,3,4,7,8,9-hexahydro-1*H*-azonine-9-carboxylate (3.6e)

Lactam **3.5e** (160 mg, 0.25 mmol) was treated under the same conditions used to prepare macrocycle **3.6c** using TFA (2 mL) in DCM (5 mL). Purification by chromatography on silica gel (40−50% EtOAc in hexane) gave macrocycle **3.6e** (105 mg, 86%) as white solid: R_f = 0.20 (3:2 EtOAc/hexanes, visualized by UV); mp 84−89 °C; $[\alpha]_D^{24}$ 26 (*c* 0.5, $CHCl_3$); FT-IR (neat) ν_{max} 3021, 2929, 1740, 1669, 1590, 1345, 1222, 892 cm^{-1}. ^1H NMR (500 MHz, $CDCl_3$) δ 7.52–7.53 (m, 2H), 7.39−7.40 (m, 3H), 7.29−7.33 (m, 1H), 7.15–7.16 (m, 3H), 6.03–6.08 (m, 1H), 5.82–5.84 (d, 1H, *J* = 11.2), 5.69–5.75 (m, 1H), 5.19−5.22 (d, 1H, *J* = 15.8), 4.84–4.85 (d, 1H, *J* = 7.05), 4.79–4.82 (d, 1H, *J* = 15.9), 4.36–4.41 (m, 1H), 3.82 (s, 3H), 2.61–2.68 (m, 1H), 2.50–2.55 (m,

1H), 2.28–2.36 (m, 1H), 2.15–2.19 (m, 1H), 1.92–1.91 (m, 1H), 1.73-1.75 (m, 1H); ^{13}C NMR (125 MHz, $CDCl_3$) δ 173.2, 172.5, 147.2, 137.3, 132.9, 131.3, 131.2, 130.9, 128.4, 128.2, 127.8, 127.3, 123.8, 57.3, 52.8, 52.7, 50.9, 33.9, 30.1, 23.1, 22.6; HRMS (ESI-TOF) m/z $[M + Na]^+$ calcd for $C_{23}H_{25}N_3O_7SNa$ 510.1305, found 510.1297.

(3*S*,9*S*,*Z*)-Methyl-3-(1,3-dioxoisoindolin-2-yl)-2-oxo-2,3,4,7,8,9-hexahydro-1*H*-azonine-9-carboxylate 3.6f.

Lactam **3.5f** (200 mg, 0.40 mmol) was treated under the same conditions used to prepare macrocycle **3.6c** using TFA (2 mL) in DCM (8 mL). Purification by chromatography on silica gel (40−50% EtOAc in hexane) gave macrocycle **3.6f** (121 mg, 87%) as a white solid: R_f = 0.36 (3:2 EtOAc/hexanes, visualized by UV); mp 226−228 °C; $[\alpha]_D^{25}$ 104 (c 0.5, $CHCl_3$); FT-IR (neat) ν_{max} 3276, 2950, 1741, 1663, 1615, 1438, 1118, 716 cm^{-1}; ^{1}H NMR (500 MHz, DMSO-d_6, 100 °C) δ 7.86−7.87 (m, 4H), 7.55 (s, 1H), 5.91 (s, 1H), 5.68−5.73 (m, 1H), 4.79 (brs, 1H), 4.29−4.32 (m, 1H), 3.70 (s, 3H), 3.07 (brs, 1H), 2.83 (brs, 1H), 2.23−2.31 (m, 1H), 2.15 (brs, 1H), 1.91–1.93 (m, 2H); ^{13}C NMR (125 MHz, DMSO-d_6, 100 °C) δ 172.2, 170.4, 168.1, 134.9, 132.1, 126.5, 123.5, 117.5, 79.6, 53.0, 52.5, 31.8, 28.7, 22.9; HRMS (ESI-TOF) m/z $[M + Na]^+$ calcd for $C_{18}H_{18}N_2O_5Na$ 365.1107, found 365.1104.

(3*S*,5*R*,6*R*,9*S*)-Methyl-5-iodo-3-((2-nitrophenyl)sulfonamido)-indolizidin-2-one-9-carboxylate [(5*R*,6*R*)- 3.3c]

In the dark, a solution of macrocycle **3.5c** (70 mg, 0.28 mmol) in THF (10 mL) was treated with iodine (130 mg, 1.12 mmol), heated to 80 °C for 1 h, and cooled to room temperature. The volatiles were removed under reduced pressure to give a residue, that was chromatographed on silica gel (70−80% EtOAc in hexane as eluent) to provide (5*R*,6*R*)- **3.3c** (36 mg, 75%) as off white solid: R_f = 0.25 (4:1 EtOAc/hexanes, visualized by UV); mp 170−172 °C; $[\alpha]_D^{25}$ –32.4 (*c* 1, $CHCl_3$); FT-

IR (neat) ν_{max} 2939, 2843, 1704, 161, 1432, 1396, 1293, 1274, 714 cm^{-1}. ^1H NMR (700 MHz, DMSO-d_6) δ 8.26–8.27 (d, 1H, *J* = 7.7 Hz), 8.16–8.18 (m, 1H), 7.97–7.98 (m, 1H), 7.83–7.87 (m, 2H), 4.84–4.87 (m, 1H), 4.25–4.26 (m, 1H), 4.09–4.13 (m, 1H), 3.61 (s, 3H), 3.18–3.20 (m, 1H), 2.92–2.96 (m, 1H), 2.43-2.47 (m, 1H), 2.16–2.22 (m, 1H), 2.01–2.06 (m, 2H), 1.71–1.77 (m, 1H); ^{13}C NMR (175 MHz, $CDCl_3$) δ 171.5, 167.1, 147.8, 134.4, 134.0, 133.1, 130.4, 124.9, 59.4, 58.2, 52.6, 52.2, 41.9, 35.9, 28.6, 28.4; HRMS (ESI-TOF) m/z $[M + H]^+$ calcd for $C_{16}H_{19}N_3O_7SI$ 523.9982, found 523.9992.

(3*S*,5*S*,6*S*,9*S*)-Methyl-5-iodo-3-((2-nitrophenyl)sulfonamido)-indolizidin-2-one-9-carboxylate [(5*S*,6*S*)- 3.3c]

In the dark, a solution of macrocycle **3.6c** (50 mg, 0.12 mmol) in acetonitrile (5 mL) was treated with iodine (127 mg, 0.50 mmol) followed by (diacetoxyiodo)benzene (77 mg, 0.24 mmol). The resulting mixture was heated to 80 °C for 30 min and cooled to room temperature. The volatiles were evaporated under reduced pressure. The residue was chromatographed on silica gel (50−70% EtOAc in hexane as eluent) to provide (5*S*,6*S*)- **3.3c** (38 mg, 80%) as a light-sensitive off-white foam: R_f = 0.21 (4:1 EtOAc/hexanes, visualized by UV); $[\alpha]_D^{25}$ –56.4 (*c* 1, $CHCl_3$); ^1H NMR (700 MHz, $CDCl_3$) δ 8.18–8.19 (m, 1H), 7.97–7.98 (m, 1H), 7.74–7.78 (m, 2H), 7 6.54–6.55 (d, 1H, *J* = 3.9 Hz), 4.76-4.77 (m, 1H), 4.39–4.41 (t, 1H, *J* = 7.64), 4.33–4.36 (m, 1H), 3.74 (s, 3H), 3.32–3.34 (m, 1H), 3.01–3.04 (m, 1H), 2.43-2.47 (m, 1H), 2.33–2.38 (m, 1H), 2.08–2.13 (m, 1H), 1.91–1.96 (m, 1H), 1.76–1.82 (m, 1H); ^{13}C NMR (175 MHz, $CDCl_3$) δ 170.9, 163.8, 146.9, 132.7, 132.1, 131.8, 130.3, 124.9, 61.7, 57.3, 53.5, 51.5, 38.4, 33.9, 29.0, 26.0. HRMS (ESI-TOF) m/z $[M + H]^+$ calcd for $C_{16}H_{19}N_3O_7SI$ 523.9982, found 523.9988.

(3*S*,5*S*,6*S*,9*S*)-Methyl 3-(*N*-methyl-*N*-(2-nitrophenyl)sulfonamide)-5-iodo-indolizidin-2-one-9-carboxylate [(5*S*, 6*S*)-3.3d] and (2*S*,5*R*,6*R*,9*S*)-methyl 8-(*N*-methyl-*N*-(2-nitrophenyl)sulfonamide)-5-iodo-indolizidin-9-one-2-carboxylate (3.8d)

In the dark, a solution of macrocycle **3.5d** (50 mg, 0.09 mmol) in acetonitrile (4 mL) was treated with iodine (90 mg, 0.35 mmol) followed by (diacetoxyiodo)benzene (58 mg, 0.18 mmol). The resulting mixture was heated to 80 °C for 30 min and cooled to room temperature. The volatiles were evaporated under reduced pressure. The residue was chromatographed on silica gel (50−70% EtOAc in hexane as eluent). First to elute was (5*S*,6*S*)-**3.3d** (21 mg, 44%) as a light-sensitive off white foam: R_f = 0.28 (4:1 EtOAc/hexanes, visualized by UV); $[\alpha]_D^{25}$ –49.2 (*c* 0.5, $CHCl_3$); ^{1}H NMR (700 MHz, $CDCl_3$) δ 8.38–8.39 (m, 1H), 7.68–7.73 (m, 3H), 5.13–5.15 (dd, 1H, *J* = 6.8, 11.2 Hz), 4.73–4.74 (m, 1H), 4.56–4.59 (t, 1H, *J* = 7.9), 3.74 (s, 3H), 3.75–3.78 (m, 1H), 2.92 (s, 3H), 2.75–2.78 (m, 1H), 2.41–2.49 (m, 2H), 2.09–2.13 (m, 1H), 1.91–1.96 (m, 1H), 1.81–1.86 (m, 1H); ^{13}C NMR (175 MHz, $CDCl_3$) δ 172.0, 163.9, 148.4, 133.3, 131.9, 130.7, 132.9, 124.3, 62.6, 58.6, 58.4, 52.5, 36.8, 34.8, 31.9, 29.8, 26.9. HRMS (ESI-TOF) m/z $[M + H]^+$ calcd for $C_{17}H_{21}N_3O_7SI$ 538.0139, found 538.0147. Second to elute was bicycle **3.8d** (7 mg, 15%) as off white solid: R_f = 0.25 (4:1 EtOAc/hexanes, visualized by UV); $[\alpha]_D^{25}$ –87.9 (*c* 0.2, $CHCl_3$); ^{1}H NMR (700 MHz, $CDCl_3$) δ 8.30–8.32 (m, 1H), 7.68–7.73 (m, 3H), 5.11–5.13 (dd, 1H, *J* = 6.5, 10.9 Hz), 4.84–4.85 (d, 1H, J = 6.7), 4.58–4.59 (m, 1H), 3.76 (s, 3H), 3.42–3.44 (dt, 1H, J = 2.8 Hz), 2.89 (s, 3H), 2.35–2.39 (m, 1H), 2.20–2.27 (m, 2H), 2.14–2.19 (m, 2H), 1.75–1.80 (m, 1H); ^{13}C NMR (175 MHz, $CDCl_3$) δ 170.0, 168.9, 148.4, 133.5, 132.8, 131.8, 130.6, 124.2, 56.8, 56.8, 52.8, 50.7, 39.2, 31.4, 31.1, 30.7, 22.1; HRMS (ESI-TOF) m/z $[M + H]^+$ calcd for $C_{17}H_{21}N_3O_7SI$ 538.0139, found 538.0144.

(3*S*,5*S*,6*S*,9*S*)- and (3*S*,5*R*,6*R*,9*S*)- Methyl 3-(*N*-methyl-*N*-(2-nitrophenyl)sulfonamide)-5-iodo-indolizidin-2-one-9-carboxylates [(5*S*, 6*S*)- and (5*R*, 6*R*)-3.3d]

Using the protocol to prepare bicycle (5*S*,6*S*)-**3.3d**, macrocycle **3.6d** (100 mg, 0.24 mmol) in acetonitrile (5 mL) was treated with iodine (246 mg, 0.97 mmol) and (diacetoxyiodo)benzene (155 mg, 0.48 mmol). The residue was chromatographed on silica gel (50−70% EtOAc in hexane as eluent). First to elute was (5*S*,6*S*)-**3.3d** (70 mg, 54%) as a light-sensitive off white foam: R_f = 0.28 (4:1 EtOAc/hexanes, visualized by UV). Second to elute was (5*R*,6*R*)-**3.3d** (32 mg, 20%) as a light-sensitive off white foam: R_f = 0.2 (4:1 EtOAc/hexanes, visualized by UV); $[\alpha]_D^{25}$ 19.2 (*c* 0.2, $CHCl_3$); ^{1}H NMR (700 MHz, C_6D_6) δ 7.97–7.98 (d, 1H, *J* = 7.9), 6.71–6.76 (m, 2H), 6.50–6.52 (t, 1H, *J* = 7.6 Hz), 4.66–4.69 (t, 1H, *J* = 8.3), 4.19–4.20 (d, 1H, *J* = 9.3), 3.70–3.73 (m, 1H), 3.25 (s, 3H), 2.78 (s, 3H), 2.45–2.49 (m, 1H), 2.38–2.42 (m, 1H), 1.91–1.93 (m, 1H), 1.57–1.62 (m, 2H), 1.33–1.38 (m, 1H), 1.17–1.21 (m, 1H); ^{13}C NMR (175 MHz, C_6D_6) δ 169.8, 164.9, 147.5, 132.1, 129.9, 129.5, 127.4, 122.8, 57.9, 57.1, 55.4, 50.4, 38.6, 34.9, 30.2, 26.9, 24.7. HRMS (ESI-TOF) m/z $[M + H]^+$ calcd for $C_{17}H_{21}N_3O_7SI$ 538.0139, found 538.0144.

(3*S*,5*S*,6*S*,9*S*)- and (3*S*,5*R*,6*R*,9*S*)-Methyl 3-(*N*-benzyl-*N*-(2-nitrophenyl)sulfonamido)-5-iodo-indolizidin-2-one-9-carboxylates [(5*S*, 6*S*)- and (5*R*, 6*R*)-3.3e], and (2*S*,5*R*,6*R*,9*S*)-methyl 8-(*N*-benzyl-*N*-(2-nitrophenyl)sulfonamido)-5-iodo-indolizidin-9-one-2-carboxylate (3.8e)

Using the protocol to prepare bicycle (5*S*,6*S*)–**3.3c**, macrocycle **3.5e** (50 mg, 0.08 mmol) in acetonitrile (5 mL) was treated with iodine (79 mg, 0.32 mmol) and (diacetoxyiodo)benzene (52 mg, 0.16 mmol). The residue was chromatographed on silica gel (50−70% EtOAc in hexane as eluent. First to elute was (5*S*,6*S*)-**3.3e** (15 mg, 35%) as a light-sensitive off white foam: R_f = 0.60 (3:2 EtOAc/hexanes, visualized by UV); $[\alpha]_D^{25}$ –16.8 (*c* 0.5, $CHCl_3$); ^{1}H NMR (700 MHz,

CD_3OD) δ 8.14–8.15 (d, 1H, *J* = 7.8), 7.69–7.81 (m, 3H), 7.51–7.52 (d, 2H, *J* = 7.2), 7.26–7.34 (m, 3H), 5.12–5.16 (m, 1H), 4.87–4.90 (m, 1H), 4.71–4.72 (m, 1H), 4.42–4.44 (t, 1H, *J* = 8.5 Hz), 4.15–4.17 (d, 1H, *J* = 14.1), 3.79 (s, 3H), 2.93–2.99 (m, 1H), 2.38–2.45 (m, 2H), 2.05–2.12.(m, 1H), 1.92–1.99 (m, 1H), 1.86 (brs, 1H), 1.72–1.78 (m, 1H); ^{13}C NMR (175 MHz, $CDCl_3$) δ 172.1, 164.8, 148.2, 136.8, 133.6, 132.7, 131.5, 130.6, 128.9, 128.4, 127.8, 123.9, 62.8, 59.2, 59.1, 51.5, 50.2, 37.8, 34.6, 31.3, 26.9; HRMS (ESI-TOF) m/z $[M + H]^+$ calcd for $C_{23}H_{25}N_3O_7SI$ 614.0452, found 614.0460. Second to elute was **3.8e** (5 mg, 8%) as a light-sensitive off white foam: R_f = 0.54 (4:1 EtOAc/hexanes, visualized by UV); $[\alpha]_D^{25}$ –24 (*c* 0.3, $CHCl_3$); ^{1}H NMR (700 MHz, $CDCl_3$) δ 8.25–8.26 (m, 1H), 7.65–7.70 (m, 3H), 7.48–7.49 (m, 2H), 7.28–7.33 (m, 3H), 5.09–5.12 (dd, 1H, *J* = 7.5, 11.1), 4.90–4.91 (d, 1H, *J* = 6.7), 4.86–4.88 (d, 1H, *J* = 15.5 Hz), 4.43–4.44 (s, 1H), 4.23–4.25 (d, 1H, *J* = 15.5), 3.82 (s, 3H), 3.17–3.19 (m, 1H), 2.19–2.27 (m, 1H), 2.03–2.15.(m, 3H), 1.80–1.85 (m, 1H), 1.72–1.77 (m, 1H); ^{13}C NMR (175 MHz, $CDCl_3$) δ 169.2, 168.3, 147.2, 135.4, 132.7, 132.3, 130.8, 129.6, 127.9, 127.6, 127.1, 123.3, 56.2, 55.5, 51.7, 49.6, 49.3, 38.3, 31.4, 29.9, 21.3. HRMS (ESI-TOF) m/z $[M + H]^+$ calcd for $C_{23}H_{25}N_3O_7SI$ 614.0452, found 614.0458; Third to elute was (5*R*,6*R*)-**3.1e** (5 mg, 9%) as a light-sensitive off white foam: R_f = 0.40 (4:1 EtOAc/hexanes, visualized by UV); $[\alpha]_D^{25}$ –17.2 (*c* 0.3, $CHCl_3$); H NMR (700 MHz, $CDCl_3$) δ 7.62–7.63 (d, 1H, *J* = 7.9), 7.54–7.57 (m, 2H), 7.537–7.40 (m, 1H), 7.34–7.36 (m, 2H), 7.17–7.18 (m, 3H), 4.93–4.95 (d, 1H, *J* = 15.7), 4.88–4.90 (dd, 1H, *J* = 7.1, 11.0), 4.71–4.74 (m, 1H), 4.54–4.56 (m, 1H), 4.42–4.45 (d, 1H, *J* = 15.7), 3.77 (s, 3H), 3.23–3.26 (m, 1H), 3.11–3.19 (m, 1H), 2.60–2.65 (m, 1H), 2.25–2.29 (m, 2H), 2.13–2.16 (m, 1H), 2.01–2.06 (m, 1H); ^{13}C NMR (175 MHz, $CDCl_3$) δ 170.2, 166.0, 146.4, 135.3, 133.3, 131.2, 130.5, 130.1, 127.7, 127.3, 126.6, 122.9, 58.4, 57.2, 57.1, 51.4, 49.4, 39.3, 35.2, 27.6, 24.1. HRMS (ESI-TOF) m/z $[M + H]^+$ calcd for $C_{23}H_{25}N_3O_7SI$ 614.0452, found 614.0456.

(3*S*,5*S*,6*S*,9*S*)- and (3*S*,5*R*,6*R*,9*S*)-Methyl 3-(1,3-dioxoisoindolin-2-yl)-5-iodo-indolizidin-2-one-9-carboxylates [(5*S*, 6*S*)- and (5*R*, 6*R*)-3f], and (2*S*,5*R*,6*R*,9*S*)-methyl 8-(1,3-dioxoisoindolin-2-yl)-5-iodo-indolizidin-9-one-2-carboxylate (3.8f)

Using the protocol to prepare bicycle (5*R*,6*R*)–**3.3c**, macrocycle **3.5f** (100 mg, 0.20 mmol) in THF (10 mL) was treated with iodine (205 mg, 0.81 mmol). Purification was performed by chromatography on silica gel (40−70% EtOAc in hexane as eluent). First to elute was **3.8f** (30 mg, 29%) as off white solid: R_f = 0.42 (3:2 EtOAc/hexanes, visualized by UV); mp 200−205 °C; $[\alpha]_D^{25}$ –47.4 (*c* 0.5, $CHCl_3$); FT-IR (neat) ν_{max} 2939, 2843, 1704, 161, 1432, 1396, 1293, 1274, 714 cm^{-1}; ^1H NMR (700 MHz, $CDCl_3$) δ 7.86−7.87 (m, 2H), 7.73−7.74 (m, 2H), 5.20−5.23 (dd, 2H, *J* = 7.4 , 11.2 Hz), 4.91−4.95 (d, 1H, *J* = 6.56), 4.64−4.65 (m, 1H),3.84 (s, 3H,), 3.72−3.74 (dt, 1H, *J* = 2.4), 2.44−2.49 (m, 1H), 2.25−2.35 (m, 2H), 2.15−2.22 (m, 1H), 1.92−1.97 (m, 1H); ^{13}C NMR (175 MHz, $CDCl_3$) δ 169.3, 167.7, 166.2, 133.1, 130.9, 122.5, 55.8, 51.6, 49.7, 46.4, 39.0, 30.9, 30.2, 21.3. HRMS (ESI-TOF) m/z $[M + H]^+$ calcd for $C_{18}H_{18}N_2O_5$ 469.0254, found 469.0263. Second eluent was a mixture of (5*S*, 6*S*)- and (5*R*, 6*R*)-**3.3f** [R_f = 0.4 (3:2 EtOAc/hexanes, visualized by UV)], which was evaporated to a residue and purified by preparative HPLC (Phenomenex Gemini 5 µm, C18, 250 mm X 21.2 mm) using a gradient from 20% to 90% MeOH (containing 0.1% FA) in water (containing 0.1% FA). First to elute was (5*S*, 6*S*)-**3.3f** (21 mg, 24%) as white solid: (Rt = 6.0 min); $[\alpha]_D^{25}$ –3.7 (*c* 0.83 MeOH); ^1H NMR (700 MHz, $CDCl_3$) δ 7.87−7.88 (m, 2H), 7.72−7.73 (m, 2H), 5.28−5.30 (dd, 1H, *J* = 6.9 , 11.4 Hz), 4.80−4.82 (q, 1H, *J* = 3.09, 6.02), 4.56−4.58 (t, 1H, *J* = 7.8),3.76 (s, 3H,), 3.53−3.55 (m, 1H), 2.91−2.95 (m, 1H), 2.52−2.56 (m, 1H), 2.40−2.45 (m, 1H), 2.10−2.22 (m, 1H), 2.02–2.07 (m, 1H), 1,87–1.92 (m, 1H); ^{13}C NMR (175 MHz, $CDCl_3$) δ 170.7, 166.3, 162.9, 133.0, 131.0, 122.5, 61.2, 57.8, 51.3, 47.7, 35.2, 33.7, 30.4, 26.0; HRMS (ESI-TOF) m/z $[M + H]^+$ calcd for $C_{18}H_{18}N_2O_5I$ 469.0254, found

469.0263. Second to elute was (5*R*, 6*R*)-**3.3f** (19 mg, 20%) as white solid: (Rt = 6.30 min); $[\alpha]_D^{25}$ 13.6 (*c* 0.33, $CHCl_3$); ^1H NMR (700 MHz, $CDCl_3$) δ 7.86−7.87 (m, 2H), 7.73−7.74 (m, 2H), 4.84−4.86 (dd, 1H, *J* = 6.6 , 11.9 Hz), 4.75−4.78 (m, 1H), 4.58−4.60 (dd, 1H, *J* = 1.5, 8.7), 3.83 (s, 3H,), 3.48−3.53 (m, 1H), 3.33−3.36 (m, 1H), 2.91−2.95 (m, 1H), 2.32−2.35 (m, 1H), 2.23−2.28 (m, 1H), 2.14–2.22 (m, 2H); ^{13}C NMR (175 MHz, $CDCl_3$) δ 170.0, 164.5, 133.2, 132.9, 122.6, 122.4, 58.6, 57.3, 51.4, 48.2, 36.4, 35.7, 27.6, 22.4; HRMS (ESI-TOF) m/z $[M + H]^+$ calcd for $C_{18}H_{18}N_2O_5I$ 469.0254, found 469.0262.

(3*S*,9*S*)-Methyl 3-(Fmoc)amino-2-oxo-1,2,3,6,7,8-hexahydroindolizine-9-carboxylate (3.9)

Iodide (5*R*,6*R*)-**3.3b** (100 g, 0.23 mmol) was treated with sodium azide (30 mg, 0.46 mmol) in acetonitrile (20 mL) at 70 °C for 5h. The reaction mixture was partitioned between ethyl acetate (40 mL) and water (20 mL). The organic layer was separated. The aqueous layer was extracted with ethyl acetate (2 x 20 mL). The organic layers were combined, washed with brine (30 mL), dried over anhydrous sodium sulfate, filtered, and concentrated under reduced pressure. The residue was purified by column chromatography using 30-40 % EtOAc in hexanes (R_f = 0.6 in 3:2 EtOAc/hexanes) as eluent. Evaporation of the collected fractions afforded olefin **3.9** as colorless gum (61 mg, 78%). $[\alpha]_D^{25}$ –43.2 (*c* 0.5, $CHCl_3$); ^1H NMR (500 MHz, $CDCl_3$) δ 7.77-7.79 (m, 2H), 7.62–7.64 (m, 2H), 7.40–7.43 (m, 2H), 7.32–7.35 (m, 2H), 5.73–5.74 (br d, 1H, *J* = 4.1 Hz), 5.02–5.03 (d, 1H, *J* = 2.8) 4.65–4.67 (dd, 1H, *J* = 4.1, 8.6), 4.34–4.40 (m, 3H,), 4.24–4.27 (t, 1H, *J* = 7.3), 3.80 (s, 3H), 2.90–2.96 (m, 1H), 2.65-2.67 (m, 2H), 2.28–2.41 (m, 2H), 2.09–2.15 (m, 1H); ^{13}C NMR (125 MHz, $CDCl_3$) δ 171.2, 166.3, 156.1, 144.4, 141.4, 141.3, 139.3, 127.0, 125.3, 125.1, 119.8, 95.0, 66.8, 58.2, 51.5, 50.1, 47.3, 27.8, 27.0, 26.6; HRMS (ESI-TOF) m/z $[M + H]^+$ calcd for $C_{25}H_{25}N_2O_5$ 433.1758, found 433.1746.

(3*S*,9*S*)-Methyl-2-oxo-5-phenyl-3-(Fmoc)amino-1,2,3,4,7,8,9-hexahydroindolizine-9-carboxylate (3.11)

Olefin **3.9** (100 mg, 0.23 mmol) was treated with phenyl boronic acid (143 mg, 0.92 mmol), 1,4-benzoquinone (25 mg, 0.23 mmol), Ag_2O (53 mg, 0.23 mmol) and $Pd(OAc)_2$ (10 mg, 0.05mmol) in dry THF (10 mL), heated to 80 °C, stirred overnight, cooled to room temperature, diluted with ethyl acetate (30 mL) and water (30 mL), and filtered through a pad of Celite™. The filter-cake was washed with EtOAc (30 mL). The filtrate and washings were combined and transferred to a separating funnel. The organic layer was separated. The aqueous layer was extracted with ethyl acetate (2 x 30 mL). The organic layers were combined, washed with brine (50 mL), dried over anhydrous sodium sulfate, filtered, and concentrated under reduced pressure. The residue was purified by column chromatography using 60-70% EtOAc in hexanes as eluent. Evaporation of the collected fractions afforded styrene **3.11** (72 mg, 61%) as off white solid: R_f = 0.50 (3:2 EtOAc/hexanes); mp 90−95 °C; $[\alpha]_D^{25}$ 90.4 (*c* 0.5, MeOH); FT-IR (neat) ν_{max} 3306, 3030, 2922, 1743, 1651, 1495, 1407, 1324, 1172, 1031, 736, 695, 498 cm^{-1}; ^1H NMR (500 MHz, $CDCl_3$) δ 7.78–7.79 (m, 2H), 7.63–7.64 (m, 2H), 7.32–7.44 (m, 5H), 7.24–7.29 (m, 4H), 5.80–5.81 (d, 1H, *J* = 4.8 Hz), 4.68-4.71 (m, 1H), 4.53–4.56 (m, 1H), 4.40–4.41(m, 2H), 4.24–4.27 (t, 1H, *J* = 7.04), 3.83 (s, 3H), 3.21–3.25 (dd, 1H, *J* = 6.4, 14.8), 2.79-2.95 (m, 3H), 2.35–2.43 (m, 1H), 2.06–2.10 (m, 1H); ^{13}C NMR (125 MHz, $CDCl_3$) δ 171.6, 166.5, 156.2, 143.9, 143.8, 141.3, 138.8, 135.6, 128.3, 127.7, 127.0, 126.9, 126.6, 125.2, 119.9, 67.1, 58.3, 52.7, 51.4, 47.1, 31.6, 28.0, 27.3; HRMS (ESI-TOF) m/z $[M + H]^+$ calcd for $C_{31}H_{29}N_2O_5$ 509.2071, found 509.2054.

(2*S*,8*S*)-Methyl-8-(1,3-dioxoisoindolin-2-yl)-3-oxo-,2,3,4,5,6,7-hexahydroindolizine-2-carboxylate (3.10)

Iodide **3.8f** (300 mg, 0.64 mmol) was treated with Et_3N (185 μL, 1.3 mmol) in acetonitrile (10 mL) at 70 °C overnight. The reaction mixture was partitioned between ethyl acetate (50 mL) and water (20 mL). The organic layer was separated. The aqueous layer was extracted with EtOAc (2 x 20 mL). The organic layers were combined, washed with brine (50 mL), dried over anhydrous sodium sulfate, filtered, and concentrated under reduced pressure. The residue was purified by column chromatography using 30-40 % EtOAc in hexanes as eluent. Evaporation of the collected fractions afforded olefin **3.10** as a white solid (140 mg, 66%): R_f = 0.5 (3:2 EtOAc/hexanes); $[\alpha]_D^{25}$ –81.6 (*c* 1, $CHCl_3$); FT-IR (neat) ν_{max} 2947, 1719, 1647, 1612, 1588, 1506, 1207, 1156, 1032, 759, 738 cm^{-1}; ^1H NMR (700 MHz, $CDCl_3$) δ 7.41-7.42 (dd, 2H, *J* = 3.1, 5.4), 6.86–6.87 (dd, 2H, *J* = 2.96, 5.4), 5.01–5.04 (t, 1H, *J* = 9.4 Hz), 4.85–4.86 (m, 1H), 4.45–4.46 (d, 1H, *J* = 5.7 Hz), 3.49 (s, 3H), 3.02–3.06 (s, 1H), 2.42–2.45 (s, 1H), 2.13-2.16 (m, 1H), 1.98–2.04 (m, 1H), 1.72–1.76 (m, 1H), 1.33–1.39 (m, 1H); ^{13}C NMR (125 MHz, $CDCl_3$) δ 168.7, 167.5, 165.8, 132.2 (2C), 130.8, 121.8, 96.3, 50.7, 50.0, 47.1, 27.3, 21.2, 17.7; HRMS (ESI-TOF) m/z $[M + H]^+$ calcd for $C_{18}H_{17}N_2O_5Na$ 341.1132, found 341.1136.

(2*S*,7S,8S)-Methyl-8-(1,3-dioxoisoindolin-2-yl)-7-hydroxy-3-oxo-,2,3,4,5,6,7 hexahydroindolizine-2-carboxylate (3.12)

A solution of olefin **3.10** (50 mg, 0.37 mmol) in dioxane (100 mL) was treated with SeO_2 (61 mg, 0.55 mmol) and a 70 wt % solution of *tert*-butyl hydroperoxide in water (0.15 mL) at room temperature, stirred for 2 h, and evaporated to a residue that was partitioned between H_2O (100 mL) and EtOAc (25 mL). The aqueous phase was separated and extracted with EtOAc (25 mL). The organic layers were combined, washed with brine, dried over Na_2SO_4, filtered, and concentrated under reduced pressure. The residue was purified by column chromatography using 60-80 % EtOAc in hexanes to give **3.12** (40 mg, 22%) as colorless gum: R_f = 0.45 (9:1

EtOAc/hexanes, twice eluted, visualized under UV light); $[\alpha]_D^{25}$ –92.2 (*c* 1, MeOH); FT-IR (neat) ν_{max} 3306, 3031, 2928, 1742, 1643, 1530, 1495, 1454, 1275, 1730, 695 cm^{-1}; ^1H NMR (700 MHz, $CDCl_3$) δ 7.89-7.90 (dd, 2H, *J* = 3.0, 5.4), 7.59–7.77 (dd, 2H, *J* = 3.0, 5.4), 5.31–5.33 (m, 1H), 5.19–5.20 (m, 1H), 4.97–4.98 (d, 1H, *J* = 7.1 Hz), 4.92-4.93 (m, 1H), 3.83 (s, 3H), 2.43–2.46 (m 1H), 2.24–2.28 (m, 1H), 2.14-2.20 (m, 1H), 1.83–1.88 (m, 1H); ^{13}C NMR (125 MHz, $CDCl_3$) δ 168.7, 167.5, 165.8, 132.2 (2C), 130.8, 121.8, 96.3, 50.7, 50.0, 47.1, 27.3, 21.2, 17.7; HRMS (ESI-TOF) m/z $[M + H]^+$ calcd for $C_{18}H_{17}N_2O_6$ 357.1081, found 357.1090.

(2*S*,6*S*,7*R*,8*S*)-Methyl 2-(Fmoc)amino)-7-hydroxy-indolizidin-9-one-2-carboxylate

Silver trifluoromethanesulfonate (219 mg, 0.85 mmol) was flame-dried in a round-bottom flask under argon flow, allowed to cool to room temperature, and treated with a solution of iodide (2*S*,6*S*,7*S*,8*S*)-**3.4** (120 mg, 0.21 mmol) in acetonitrile (4 mL), followed by distilled H_2O (1.00 mL). The mixture was stirred at room temperature for 2 days, concentrated to dryness, taken up in EtOAc, and filtered through a plug of Celite™. The filtrate was transferred to a separating funnel and washed with water and brine. The organic phase was dried over $MgSO_4$, filtered, and concentrated to a residue, which was purified by flash column chromatography using a gradient of 50% to 100% EtOAc in hexanes as eluant to give (2*R*,6*R*,7*R*,8R)-**3.13** (58 mg, 60% yield) as white foam: R_f 0.15 (60% EtOAc in hexanes as eluent); mp 100–103 °C; $[\alpha]_D^{25}$ 30.6 (*c* 0.2, MeOH); ^1H NMR (700 MHz, $CDCl_3$) δ 7.58-7.77 (d, 2H, *J* = 7.5), 7.60–7.61 (d, 2H, *J* = 7.4), 7.39–7.41 (m, 2H), 7.31–7.33 (m, 2H), 5.38 (brs, 1H), 4.92 (brs, 1H), 4.45–4.46 (m, 2H), 4.33–4.34 (m, 1H), 4.22–4.24 (t, 1H, *J* = 6.73), 4.18 (brs, 1H), 3.76 (s, 3H), 3.70–3.72 (brd, 1H, *J* = 12.0), 2.58 (brs, 1H), 2.19–2.21 (d, 1H, J = 14.3), 1.96–1.98 (m, 1H), 1.82–1.84 (m 1H), 1.45–1.50 (m, 1H), 1.52–1.21 (m, 1H); ^{13}C NMR (175 MHz, $CDCl_3$) δ 170.6, 168.9, 157.2, 143.7, 143.6, 141.4, 141.3, 127.2, 127.,1, 125.2, 125.1, 120.1, 120.0, 70.1, 67.5, 61.3, 55.4, 52.6, 51.6, 47.1, 28.5, 26.4, 20.8;

(700 MHz, DMSO-d_6) δ 7.89–7.90 (d, 2H, *J* = 7.5), 7.78–7.81 (m, 2H), 7.41–7.45 (m, 3H), 7.32–7.34 (m, 2H), 5.45 (brs, 1H), 4.75–4.76 (d, 1H, *J* = 5.84Hz), 4.35–4.37 (m, 1H), 4.24–4.27 (m, 3H), 3.90 (brs, 1H), 3.69 (s, 3H), 3.49–3.51 (m, 1H), 1.98–2.0 (m, 1H), 1.78–1.80 (m, 1H), 1.70–1.72 (m, 1H), 1.48–1.53 (m 1H), 1.34–1.40 (m, 1H), 1.20–1.26 (m, 1H); ^{13}C NMR (175 MHz, DMSO-d_6) δ 171.1, 170.0, 156.9, 144.3, 144.2, 141.2, 141.1, 128.1, 127.5, 126.0 (2C), 120.5 (2C), 68.8, 66.5, 61.6, 54.5, 52.6, 51.3, 47.0, 28.2, 26.4, 20.8; HRMS (ESI-TOF) m/z $[M + H]^+$ calcd for $C_{25}H_{27}N_2O_6$ 451.1863, found 451.1842.

3.8 Crystallography data and Molecular structure for compounds

3.8.1 General Methods for making crystals:

Bicycles **(*S*,*S*)-3.3c**, **(*S*,*S*)-3.3f**, **(*R*,*R*)-3.3f**, **3.8e** and **3.8f** crystallized by a common method featuring dissolving 2–5 mg of bicycle in 1 mL of ethyl acetate and equilibrating hexane vapour into the mother liquor in a closed container to provide slow formation of crystals.

(3*S*,5*S*,6*S*,9*S*)-Methyl-5-iodo-3-((2-nitrophenyl)sulfonamido)-indolizidin-2-one-9-carboxylate

[(5*S*,6*S*)-3.3c, LUB131(2)]

Table 1 Crystal data and structure refinement for lub131(2).

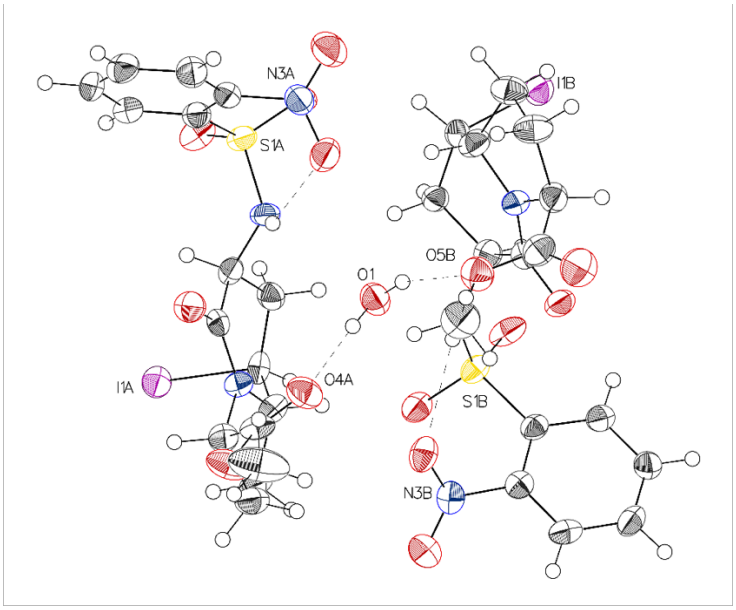

Identification code	lub131(2)
Empirical formula	$C_{32}H_{38}I_2N_6O_{15}S_2$
Formula weight	1064.60
Temperature/K	150
Crystal system	monoclinic
Space group	C2
a/Å	20.3654(7)
b/Å	10.6860(4)
c/Å	18.0155(7)
α/°	90
β/°	91.228(2)
γ/°	90
Volume/Å^3	3919.7(3)
Z	4
ρ_{calc}g/cm^3	1.804
μ/mm^{-1}	9.747
F(000)	2120.0
Crystal size/mm^3	0.33 × 0.09 × 0.08
Radiation	GaKα (λ = 1.34139)
2Θ range for data collection/°	4.268 to 109.934
Index ranges	$-24 \leq h \leq 24$, $-13 \leq k \leq 13$, $-21 \leq l \leq 21$
Reflections collected	29942
Independent reflections	7155 [R_{int} = 0.0473, R_{sigma} = 0.0465]
Data/restraints/parameters	7155/1/520
Goodness-of-fit on F^2	1.056
Final R indexes [I>=2σ (I)]	R_1 = 0.0390, wR_2 = 0.0818

Final R indexes [all data]	R_1 = 0.0460, wR_2 = 0.0861
Largest diff. peak/hole / e Å^{-3}	1.44/-0.95
Flack parameter	0.092(10)

Table 2 Fractional Atomic Coordinates (×10^4) and Equivalent Isotropic Displacement Parameters (Å^2×10^3) for lub131(2). U_{eq} is defined as 1/3 of of the trace of the orthogonalised U_{ij} tensor.

Atom	*x*	*y*	*z*	U(eq)
I1A	7607.1(3)	758.1(5)	8498.9(3)	38.80(16)
S1A	7050.5(10)	3577(2)	5756.4(11)	33.5(5)
O1A	7621(3)	2834(8)	5813(3)	44.8(17)
O2A	7087(3)	4865(6)	5530(3)	42.8(16)
O3A	5805(3)	1643(6)	6925(3)	41.5(15)
O4A	4818(3)	3192(7)	7862(4)	47.5(17)
O5A	4359(3)	1397(8)	8201(4)	54.1(19)
O6A	5671(3)	4903(7)	5606(4)	47.1(17)
O7A	5805(4)	5553(7)	4474(4)	58.8(19)
N1A	6703(4)	3565(7)	6551(3)	33.6(16)
N2A	6071(3)	2129(7)	8107(4)	31.3(15)
N3A	5818(4)	4743(8)	4951(4)	39.7(18)
C1A	6524(4)	2849(9)	5085(4)	32.9(19)
C2A	6001(4)	3479(9)	4726(5)	35(2)
C3A	5636(5)	2932(10)	4165(5)	42(2)
C4A	5788(5)	1720(10)	3947(5)	44(2)
C5A	6298(4)	1092(9)	4278(5)	38(2)
C6A	6671(4)	1645(9)	4852(5)	36(2)
C9A	6838(4)	2647(8)	7138(4)	32.1(18)
C10A	7260(4)	3266(8)	7763(5)	36(2)
C11A	7197(4)	2659(8)	8512(5)	33.4(19)
C12A	6494(4)	2646(9)	8709(5)	36(2)
C13A	6191(4)	2096(8)	7385(5)	31.3(18)
C14A	6274(5)	1921(10)	9400(5)	42(2)
C15A	5541(5)	1707(11)	9247(5)	43(2)
C16A	5484(4)	1522(9)	8395(5)	38(2)
C17A	4864(4)	2155(10)	8114(5)	38(2)
C18A	3715(5)	1906(17)	8013(7)	84(5)
I1B	7499.7(3)	9248.0(5)	6476.9(3)	40.60(16)
S1B	6999.8(10)	6551(2)	9210.3(11)	32.6(5)
O1B	7546(3)	7381(8)	9148(3)	44.1(18)
O2B	7088(3)	5300(6)	9479(3)	40.7(15)
O3B	5705(3)	8355(6)	8161(3)	41.3(16)

O4B	4148(3)	8786(8)	7101(4)	58(2)
O5B	4684(3)	6953(7)	7058(4)	46.9(16)
O6B	5679(3)	5072(7)	9390(3)	43.4(16)
O7B	5811(3)	4582(7)	10563(4)	51.4(18)
N1B	6669(3)	6443(7)	8398(3)	32.1(16)
N2B	5869(4)	8109(7)	6928(4)	33.2(16)
N3B	5816(3)	5338(7)	10047(4)	36.9(18)
C1B	6454(4)	7276(9)	9834(4)	30.7(18)
C2B	5963(4)	6661(9)	10213(5)	31.7(19)
C3B	5590(4)	7218(10)	10746(5)	38(2)
C4B	5700(4)	8475(9)	10906(5)	39(2)
C5B	6188(4)	9102(9)	10554(4)	37.1(19)
C6B	6567(4)	8527(9)	10021(4)	33.4(19)
C9B	6726(4)	7386(9)	7810(4)	33.9(19)
C10B	7026(4)	6752(8)	7128(4)	31.0(18)
C11B	6941(4)	7497(8)	6420(5)	35(2)
C12B	6219(4)	7704(10)	6261(5)	40(2)
C13B	6051(4)	7985(9)	7644(5)	32.7(19)
C14B	5983(5)	8608(11)	5671(5)	45(2)
C15B	5261(5)	8782(11)	5866(5)	48(3)
C16B	5266(4)	8782(9)	6724(5)	38(2)
C17B	4642(5)	8195(10)	6988(5)	42(2)
C18B	4066(5)	6358(13)	7237(7)	60(3)
O1	5706(3)	5033(7)	7454(4)	43.4(15)

Table 3 Anisotropic Displacement Parameters ($Å^2 \times 10^3$) for lub131(2). The Anisotropic displacement factor exponent takes the form: $-2\pi^2[h^2a^{*2}U_{11}+2hka^*b^*U_{12}+\ldots]$.

Atom	U_{11}	U_{22}	U_{33}	U_{23}	U_{13}	U_{12}
I1A	40.7(3)	38.4(4)	37.1(3)	-1.0(3)	-4.7(2)	4.3(3)
S1A	34.1(10)	39.9(12)	26.7(10)	-4.3(9)	5.7(8)	-8.2(9)
O1A	35(3)	61(5)	39(4)	-8(3)	0(3)	2(3)
O2A	54(4)	40(4)	34(3)	1(3)	8(3)	-21(3)
O3A	44(4)	43(4)	37(3)	-5(3)	-4(3)	-13(3)
O4A	41(4)	50(5)	52(4)	14(3)	1(3)	3(3)
O5A	34(3)	71(5)	58(4)	23(4)	3(3)	-11(3)
O6A	52(4)	44(4)	45(4)	-10(3)	4(3)	0(3)
O7A	77(5)	48(5)	52(4)	10(4)	-5(4)	0(4)
N1A	38(4)	39(4)	24(3)	5(3)	6(3)	2(3)
N2A	32(4)	36(4)	26(3)	-1(3)	1(3)	-1(3)
N3A	47(5)	34(4)	38(4)	2(4)	-2(3)	-3(3)
C1A	34(4)	35(5)	29(4)	0(4)	4(3)	-4(4)
C2A	42(5)	31(5)	33(5)	0(4)	8(4)	-6(4)

C3A	48(5)	41(6)	36(5)	1(4)	-7(4)	1(4)
C4A	52(6)	49(6)	30(5)	-8(4)	-3(4)	-12(5)
C5A	52(5)	29(5)	34(4)	-7(4)	5(4)	-4(4)
C6A	40(5)	39(5)	30(4)	1(4)	5(4)	0(4)
C9A	37(4)	30(5)	29(4)	-5(4)	3(3)	3(4)
C10A	44(5)	31(5)	33(4)	0(4)	-1(4)	-10(4)
C11A	35(4)	25(5)	40(5)	-10(4)	-3(4)	4(4)
C12A	35(4)	42(5)	31(4)	-7(4)	2(3)	3(4)
C13A	37(4)	21(4)	36(5)	-1(4)	5(4)	-4(4)
C14A	47(5)	54(7)	25(4)	1(4)	6(4)	13(5)
C15A	42(5)	52(7)	36(5)	6(5)	9(4)	4(5)
C16A	37(5)	38(5)	39(5)	0(4)	6(4)	-1(4)
C17A	32(4)	55(6)	29(4)	1(4)	8(3)	-3(4)
C18A	36(6)	140(15)	77(8)	46(9)	-1(6)	-13(7)
I1B	41.9(3)	37.7(4)	42.6(3)	-6.3(3)	8.0(2)	-7.0(3)
S1B	29.5(10)	41.1(13)	27.1(10)	-6.1(9)	-1.8(8)	4.7(9)
O1B	35(3)	67(5)	31(3)	-15(3)	6(3)	-11(3)
O2B	46(3)	46(4)	29(3)	-1(3)	-5(3)	17(3)
O3B	48(4)	45(4)	32(3)	1(3)	10(3)	13(3)
O4B	46(4)	61(5)	67(5)	1(4)	4(3)	10(4)
O5B	43(4)	46(4)	52(4)	-1(3)	1(3)	-4(3)
O6B	47(4)	41(4)	41(4)	-13(3)	-8(3)	2(3)
O7B	59(4)	42(4)	54(4)	4(3)	6(3)	-6(3)
N1B	36(4)	36(4)	23(3)	-1(3)	-4(3)	1(3)
N2B	41(4)	34(4)	25(3)	-1(3)	3(3)	-1(3)
N3B	31(4)	34(4)	45(4)	-5(4)	-1(3)	0(3)
C1B	32(4)	36(5)	24(4)	0(4)	-2(3)	6(4)
C2B	29(4)	37(5)	29(4)	0(4)	-4(3)	3(4)
C3B	35(4)	50(6)	29(4)	3(4)	7(4)	2(4)
C4B	44(5)	42(6)	31(4)	-7(4)	1(4)	14(4)
C5B	47(5)	33(5)	31(4)	1(4)	-1(4)	-2(4)
C6B	34(4)	37(5)	30(4)	1(4)	2(3)	2(4)
C9B	35(4)	35(5)	32(4)	-2(4)	-3(3)	-3(4)
C10B	30(4)	32(5)	31(4)	2(4)	5(3)	3(3)
C11B	45(5)	28(5)	31(4)	-5(4)	2(4)	-9(4)
C12B	44(5)	47(6)	29(4)	-7(4)	3(4)	-6(4)
C13B	36(5)	28(5)	34(5)	1(4)	3(4)	1(4)
C14B	47(5)	56(7)	32(5)	8(5)	-6(4)	-5(5)
C15B	47(5)	67(7)	29(5)	8(5)	-8(4)	0(5)
C16B	46(5)	34(5)	34(4)	0(4)	-4(4)	6(4)
C17B	40(5)	49(6)	37(5)	-6(4)	-3(4)	-1(4)
C18B	45(6)	67(8)	68(7)	-6(7)	6(5)	-14(6)

O1	45(4)	35(4)	51(4)	3(3)	3(3)	-2(3)

Table 4 Bond Lengths for lub131(2).

Atom	Atom	Length/Å	Atom	Atom	Length/Å
I1A	C11A	2.196(9)	I1B	C11B	2.191(9)
S1A	O1A	1.409(7)	S1B	O1B	1.430(7)
S1A	O2A	1.438(7)	S1B	O2B	1.432(7)
S1A	N1A	1.610(7)	S1B	N1B	1.601(6)
S1A	C1A	1.777(8)	S1B	C1B	1.775(8)
O3A	C13A	1.230(10)	O3B	C13B	1.244(10)
O4A	C17A	1.200(12)	O4B	C17B	1.209(12)
O5A	C17A	1.322(11)	O5B	C17B	1.336(12)
O5A	C18A	1.454(13)	O5B	C18B	1.453(12)
O6A	N3A	1.236(10)	O6B	N3B	1.242(9)
O7A	N3A	1.219(10)	O7B	N3B	1.233(10)
N1A	C9A	1.465(11)	N1B	C9B	1.469(11)
N2A	C12A	1.477(10)	N2B	C12B	1.473(11)
N2A	C13A	1.328(11)	N2B	C13B	1.342(11)
N2A	C16A	1.465(11)	N2B	C16B	1.464(11)
N3A	C2A	1.461(12)	N3B	C2B	1.474(12)
C1A	C2A	1.407(13)	C1B	C2B	1.389(12)
C1A	C6A	1.389(13)	C1B	C6B	1.396(13)
C2A	C3A	1.372(13)	C2B	C3B	1.372(12)
C3A	C4A	1.389(15)	C3B	C4B	1.391(14)
C4A	C5A	1.365(13)	C4B	C5B	1.367(13)
C5A	C6A	1.400(12)	C5B	C6B	1.388(12)
C9A	C10A	1.550(11)	C9B	C10B	1.541(11)
C9A	C13A	1.518(12)	C9B	C13B	1.539(12)
C10A	C11A	1.504(12)	C10B	C11B	1.510(12)
C11A	C12A	1.483(12)	C11B	C12B	1.509(13)
C12A	C14A	1.541(13)	C12B	C14B	1.507(13)
C14A	C15A	1.530(13)	C14B	C15B	1.531(13)
C15A	C16A	1.550(12)	C15B	C16B	1.546(12)
C16A	C17A	1.510(12)	C16B	C17B	1.503(13)

Table 5 Bond Angles for lub131(2).

Atom	Atom	Atom	Angle/°	Atom	Atom	Atom	Angle/°
O1A	S1A	O2A	120.8(4)	O1B	S1B	O2B	120.9(4)
O1A	S1A	N1A	108.0(4)	O1B	S1B	N1B	106.6(4)
O1A	S1A	C1A	106.7(4)	O1B	S1B	C1B	106.1(4)
O2A	S1A	N1A	106.6(4)	O2B	S1B	N1B	106.8(4)
O2A	S1A	C1A	105.1(4)	O2B	S1B	C1B	105.7(4)

N1A	S1A	C1A	109.4(4)	N1B	S1B	C1B	110.7(4)
C17A	O5A	C18A	116.3(9)	C17B	O5B	C18B	113.6(8)
C9A	N1A	S1A	124.6(6)	C9B	N1B	S1B	124.9(6)
C13A	N2A	C12A	127.7(7)	C13B	N2B	C12B	128.8(8)
C13A	N2A	C16A	120.3(7)	C13B	N2B	C16B	120.1(7)
C16A	N2A	C12A	111.8(6)	C16B	N2B	C12B	111.0(7)
O6A	N3A	C2A	117.4(8)	O6B	N3B	C2B	117.0(7)
O7A	N3A	O6A	124.9(9)	O7B	N3B	O6B	124.3(8)
O7A	N3A	C2A	117.6(8)	O7B	N3B	C2B	118.7(7)
C2A	C1A	S1A	123.0(7)	C2B	C1B	S1B	124.9(7)
C6A	C1A	S1A	118.7(7)	C2B	C1B	C6B	116.8(8)
C6A	C1A	C2A	118.0(8)	C6B	C1B	S1B	118.0(7)
C1A	C2A	N3A	120.6(8)	C1B	C2B	N3B	119.9(8)
C3A	C2A	N3A	117.5(8)	C3B	C2B	N3B	116.4(8)
C3A	C2A	C1A	121.9(9)	C3B	C2B	C1B	123.6(9)
C2A	C3A	C4A	119.1(9)	C2B	C3B	C4B	118.4(9)
C5A	C4A	C3A	120.4(9)	C5B	C4B	C3B	119.4(8)
C4A	C5A	C6A	120.8(9)	C4B	C5B	C6B	121.7(9)
C1A	C6A	C5A	119.8(8)	C5B	C6B	C1B	120.0(8)
N1A	C9A	C10A	109.3(7)	N1B	C9B	C10B	108.2(7)
N1A	C9A	C13A	108.8(7)	N1B	C9B	C13B	110.0(7)
C13A	C9A	C10A	115.0(7)	C13B	C9B	C10B	113.4(7)
C11A	C10A	C9A	114.2(7)	C11B	C10B	C9B	113.6(7)
C10A	C11A	I1A	110.5(6)	C10B	C11B	I1B	111.2(6)
C12A	C11A	I1A	111.3(6)	C12B	C11B	I1B	112.8(6)
C12A	C11A	C10A	108.6(7)	C12B	C11B	C10B	109.3(7)
N2A	C12A	C11A	112.2(7)	N2B	C12B	C11B	112.0(7)
N2A	C12A	C14A	103.4(7)	N2B	C12B	C14B	103.6(8)
C11A	C12A	C14A	119.8(8)	C14B	C12B	C11B	121.4(8)
O3A	C13A	N2A	122.8(8)	O3B	C13B	N2B	122.7(8)
O3A	C13A	C9A	120.1(8)	O3B	C13B	C9B	120.3(8)
N2A	C13A	C9A	117.1(7)	N2B	C13B	C9B	117.0(7)
C15A	C14A	C12A	103.2(7)	C12B	C14B	C15B	102.0(8)
C14A	C15A	C16A	104.4(7)	C14B	C15B	C16B	104.2(7)
N2A	C16A	C15A	104.5(7)	N2B	C16B	C15B	103.7(7)
N2A	C16A	C17A	111.4(7)	N2B	C16B	C17B	115.3(8)
C17A	C16A	C15A	108.6(7)	C17B	C16B	C15B	109.2(8)
O4A	C17A	O5A	123.8(9)	O4B	C17B	O5B	123.8(9)
O4A	C17A	C16A	126.8(8)	O4B	C17B	C16B	123.1(10)
O5A	C17A	C16A	109.4(8)	O5B	C17B	C16B	113.1(8)

Table 6 Hydrogen Bonds for lub131(2).

D	H	A	d(D-H)/Å	d(H-A)/Å	d(D-A)/Å	D-H-A/°
N1A	H1A	O6A	0.86	2.42	3.035(10)	129.0
N1A	H1A	O1	0.86	2.61	3.061(10)	114.3
N1B	H1B	O6B	0.86	2.45	3.092(10)	132.3
N1B	H1B	O1	0.86	2.47	2.978(9)	118.7
O1	H1C	O4A	0.85	1.94	2.782(10)	176.0
O1	H1D	O5B	0.85	2.18	2.997(10)	160.1

Table 7 Torsion Angles for lub131(2).

A	B	C	D	Angle/°	A	B	C	D	Angle/°
I1A	C11A	C12A	N2A	-71.4(8)	I1B	C11B	C12B	N2B	-78.2(8)
I1A	C11A	C12A	C14A	50.0(10)	I1B	C11B	C12B	C14B	44.7(10)
S1A	N1A	C9A	C10A	105.5(8)	S1B	N1B	C9B	C10B	122.2(7)
S1A	N1A	C9A	C13A	-128.1(7)	S1B	N1B	C9B	C13B	-113.5(7)
S1A	C1A	C2A	N3A	-6.8(12)	S1B	C1B	C2B	N3B	-7.1(11)
S1A	C1A	C2A	C3A	174.3(7)	S1B	C1B	C2B	C3B	173.5(7)
S1A	C1A	C6A	C5A	-174.5(7)	S1B	C1B	C6B	C5B	-174.6(6)
O1A	S1A	N1A	C9A	-17.5(8)	O1B	S1B	N1B	C9B	-23.9(8)
O1A	S1A	C1A	C2A	-161.5(7)	O1B	S1B	C1B	C2B	-160.6(7)
O1A	S1A	C1A	C6A	12.2(8)	O1B	S1B	C1B	C6B	12.2(7)
O2A	S1A	N1A	C9A	-148.7(7)	O2B	S1B	N1B	C9B	-154.4(7)
O2A	S1A	C1A	C2A	-32.1(8)	O2B	S1B	C1B	C2B	-31.1(8)
O2A	S1A	C1A	C6A	141.6(7)	O2B	S1B	C1B	C6B	141.7(6)
O6A	N3A	C2A	C1A	-57.5(11)	O6B	N3B	C2B	C1B	-55.5(10)
O6A	N3A	C2A	C3A	121.5(9)	O6B	N3B	C2B	C3B	124.0(9)
O7A	N3A	C2A	C1A	124.6(9)	O7B	N3B	C2B	C1B	127.4(9)
O7A	N3A	C2A	C3A	-56.5(12)	O7B	N3B	C2B	C3B	-53.2(10)
N1A	S1A	C1A	C2A	81.9(8)	N1B	S1B	C1B	C2B	84.1(8)
N1A	S1A	C1A	C6A	-104.3(7)	N1B	S1B	C1B	C6B	-103.1(7)
N1A	C9A	C10A	C11A	155.5(7)	N1B	C9B	C10B	C11B	164.0(7)
N1A	C9A	C13A	O3A	53.1(10)	N1B	C9B	C13B	O3B	47.4(11)
N1A	C9A	C13A	N2A	-127.0(8)	N1B	C9B	C13B	N2B	-134.1(8)
N2A	C12A	C14A	C15A	-33.2(9)	N2B	C12B	C14B	C15B	-37.4(10)
N2A	C16A	C17A	O4A	-19.4(13)	N2B	C16B	C17B	O4B	153.6(9)
N2A	C16A	C17A	O5A	162.0(7)	N2B	C16B	C17B	O5B	-28.5(11)
N3A	C2A	C3A	C4A	-178.7(8)	N3B	C2B	C3B	C4B	-178.2(7)
C1A	S1A	N1A	C9A	98.2(7)	C1B	S1B	N1B	C9B	91.1(7)
C1A	C2A	C3A	C4A	0.2(14)	C1B	C2B	C3B	C4B	1.2(13)
C2A	C1A	C6A	C5A	-0.4(12)	C2B	C1B	C6B	C5B	-1.2(11)
C2A	C3A	C4A	C5A	-1.1(15)	C2B	C3B	C4B	C5B	-2.5(13)
C3A	C4A	C5A	C6A	1.2(14)	C3B	C4B	C5B	C6B	1.9(13)
C4A	C5A	C6A	C1A	-0.4(14)	C4B	C5B	C6B	C1B	0.0(13)

C6A	C1A	C2A	N3A	179.4(8)	C6B	C1B	C2B	N3B	−179.9(7)
C6A	C1A	C2A	C3A	0.5(13)	C6B	C1B	C2B	C3B	0.6(12)
C9A	C10A	C11A	I1A	66.5(8)	C9B	C10B	C11B	I1B	66.4(8)
C9A	C10A	C11A	C12A	−55.9(10)	C9B	C10B	C11B	C12B	−58.8(9)
C10A	C9A	C13A	O3A	176.1(8)	C10B	C9B	C13B	O3B	168.7(8)
C10A	C9A	C13A	N2A	−4.0(12)	C10B	C9B	C13B	N2B	−12.9(11)
C10A	C11A	C12A	N2A	50.5(10)	C10B	C11B	C12B	N2B	46.0(10)
C10A	C11A	C12A	C14A	171.9(8)	C10B	C11B	C12B	C14B	168.9(8)
C11A	C12A	C14A	C15A	−159.0(8)	C11B	C12B	C14B	C15B	−164.3(9)
C12A	N2A	C13A	O3A	−179.9(9)	C12B	N2B	C13B	O3B	−179.0(9)
C12A	N2A	C13A	C9A	0.2(13)	C12B	N2B	C13B	C9B	2.6(13)
C12A	N2A	C16A	C15A	1.4(10)	C12B	N2B	C16B	C15B	−0.4(10)
C12A	N2A	C16A	C17A	118.5(8)	C12B	N2B	C16B	C17B	118.9(8)
C12A	C14A	C15A	C16A	34.5(10)	C12B	C14B	C15B	C16B	37.6(11)
C13A	N2A	C12A	C11A	−24.9(13)	C13B	N2B	C12B	C11B	−20.0(13)
C13A	N2A	C12A	C14A	−155.3(9)	C13B	N2B	C12B	C14B	−152.5(9)
C13A	N2A	C16A	C15A	177.2(8)	C13B	N2B	C16B	C15B	176.6(8)
C13A	N2A	C16A	C17A	−65.7(11)	C13B	N2B	C16B	C17B	−64.1(11)
C13A	C9A	C10A	C11A	32.8(11)	C13B	C9B	C10B	C11B	41.8(10)
C14A	C15A	C16A	N2A	−22.6(10)	C14B	C15B	C16B	N2B	−23.2(10)
C14A	C15A	C16A	C17A	−141.6(8)	C14B	C15B	C16B	C17B	−146.5(9)
C15A	C16A	C17A	O4A	95.2(11)	C15B	C16B	C17B	O4B	−90.2(11)
C15A	C16A	C17A	O5A	−83.4(10)	C15B	C16B	C17B	O5B	87.7(10)
C16A	N2A	C12A	C11A	150.5(8)	C16B	N2B	C12B	C11B	156.7(8)
C16A	N2A	C12A	C14A	20.1(9)	C16B	N2B	C12B	C14B	24.2(10)
C16A	N2A	C13A	O3A	5.0(13)	C16B	N2B	C13B	O3B	4.5(13)
C16A	N2A	C13A	C9A	−174.8(7)	C16B	N2B	C13B	C9B	−173.9(8)
C18A	O5A	C17A	O4A	−3.5(14)	C18B	O5B	C17B	O4B	3.9(14)
C18A	O5A	C17A	C16A	175.1(9)	C18B	O5B	C17B	C16B	−173.9(8)

Table 8 Hydrogen Atom Coordinates (Å×10⁴) and Isotropic Displacement Parameters (Å²×10³) for lub131(2).

Atom	*x*	*y*	*z*	U(eq)
H1A	6286.17	3624.26	6485.18	40
H3A	5285.4	3374.71	3928.98	50
H4A	5533.96	1326.79	3564.41	53
H5A	6402.37	270.15	4117.62	46
H6A	7023.9	1197.23	5081.36	44
H9A	7102.11	1954.93	6920.51	39
H10A	7726.28	3241.09	7621.07	43
H10B	7130.83	4156.54	7804.2	43
H11A	7446.67	3167.44	8888.44	40

H12A	6358.59	3536.77	8778.72	43
H14A	6511.53	1116.88	9451.02	50
H14B	6347.28	2420.94	9857.55	50
H15A	5280.53	2439.6	9405.06	52
H15B	5384.82	955.64	9512.43	52
H16A	5478.62	611.5	8267.16	45
H18A	3698.79	2143.77	7487.05	127
H18B	3633.38	2645.57	8319.15	127
H18C	3377.98	1273.46	8104.68	127
H1B	6262.93	6256.48	8445.73	38
H3B	5265.16	6756.14	10998.28	45
H4B	5437.23	8894.08	11258.28	47
H5B	6269.75	9953.6	10676.07	45
H6B	6903.21	8983.7	9783.81	40
H9B	7033.27	8055.46	7988.99	41
H10C	7500.72	6617.53	7227.05	37
H10D	6819.26	5921	7056.65	37
H11B	7118.64	6985.69	6005.37	42
H12B	6032.17	6869.34	6121.44	48
H14C	6027.76	8248.92	5167.73	54
H14D	6226.64	9409	5700.72	54
H15C	4989.37	8086.96	5665.27	57
H15D	5088.48	9583.02	5666.81	57
H16B	5295.56	9662.74	6909.93	46
H18D	3735.93	6554.71	6850.34	89
H18E	3916.65	6670.03	7716.52	89
H18F	4127.39	5450.03	7264.8	89
H1C	5432.28	4464.72	7556.07	65
H1D	5476.38	5603.24	7248	65

Experimental

A suitable crystal of $C_{32}H_{38}I_2N_6O_{15}S_2$ lub131(2), was selected and mounted on a cryoloop on a Bruker Venture Metaljet diffractometer. The crystal was kept at 150 K during data collection. Using Olex2 [1], the structure was solved with the XT [2] structure solution program using Intrinsic Phasing and refined with the XL [3] refinement package using Least Squares minimisation.

1. Dolomanov, O.V., Bourhis, L.J., Gildea, R.J, Howard, J.A.K. & Puschmann, H. (2009), J. Appl. Cryst. 42, 339-341.
2. Sheldrick, G.M. (2015). Acta Cryst. A71, 3-8.
3. Sheldrick, G.M. (2015). Acta Cryst. C71, 3-8.

Crystal structure determination of lub131(2)

Crystal Data for $C_{32}H_{38}I_2N_6O_{15}S_2$ (M =1064.60 g/mol): monoclinic, space group C2 (no. 5), a = 20.3654(7) Å, b = 10.6860(4) Å, c = 18.0155(7) Å, β = 91.228(2)°, V = 3919.7(3) Å^3, Z = 4, T = 150 K, μ(GaKα) = 9.747 mm^{-1}, *Dcalc* = 1.804 g/cm^3, 29942 reflections measured (4.268° ≤ 2Θ ≤ 109.934°), 7155 unique (R_{int} = 0.0473, R_{sigma} = 0.0465) which were used in all calculations. The final R_1 was 0.0390 (I > 2σ(I)) and wR_2 was 0.0861 (all data).

Refinement model description

Number of restraints - 1, number of constraints - unknown.

Details:

```
1. Twinned data refinement
 Scales: 0.908(10)
 0.092(10)
2. Fixed Uiso
 At 1.2 times of:
  All C(H) groups, All C(H,H) groups, All N(H) groups
 At 1.5 times of:
  All C(H,H,H) groups, All O(H,H) groups
3.a Riding coordinates:
 N1A(H1A), N1B(H1B)
3.b Free rotating group:
 O1(H1C,H1D)
3.c Ternary CH refined with riding coordinates:
 C9A(H9A), C11A(H11A), C12A(H12A), C16A(H16A), C9B(H9B), C11B(H11B),
 C12B(H12B), C16B(H16B)
3.d Secondary CH2 refined with riding coordinates:
 C10A(H10A,H10B), C14A(H14A,H14B), C15A(H15A,H15B), C10B(H10C,H10D), C14B(H14C,
 H14D), C15B(H15C,H15D)
3.e Aromatic/amide H refined with riding coordinates:
 C3A(H3A), C4A(H4A), C5A(H5A), C6A(H6A), C3B(H3B), C4B(H4B), C5B(H5B), C6B(H6B)
3.f Idealised Me refined as rotating group:
 C18A(H18A,H18B,H18C), C18B(H18D,H18E,H18F)
```

This report has been created with Olex2, compiled on 2018.05.29 svn.r3508 for OlexSys. Please let us know if there are any errors or if you would like to have additional features.

(3*S*,5*R*,6*R*,9*S*)-Methyl-3-(1,3-dioxoisoindolin-2-yl)-5-iodo-indolizidin-2-one-9-carboxylates
[(5*R*, 6*R*)-3.3f, lub130(3)]

Table 1 Crystal data and structure refinement for lub130(3).

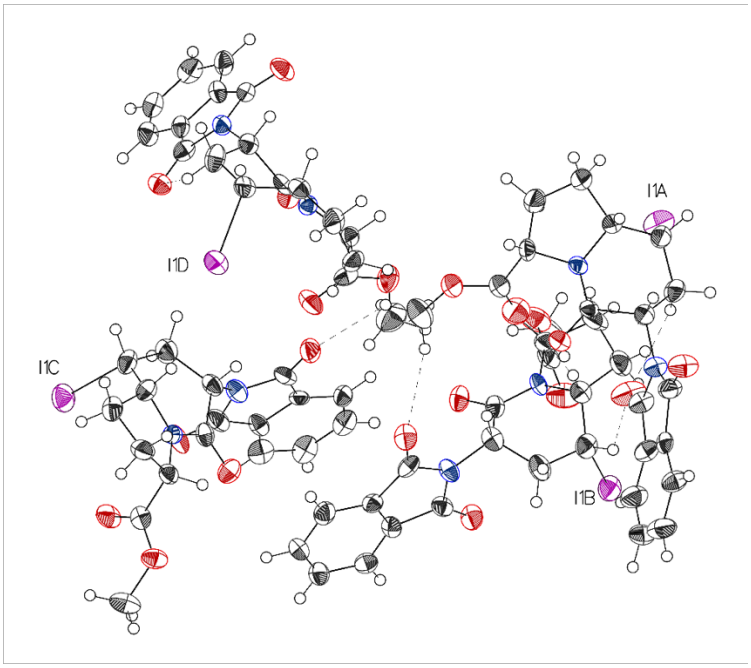

Identification code	lub130(3)
Empirical formula	$C_{18}H_{17}IN_2O_5$
Formula weight	468.23
Temperature/K	150
Crystal system	triclinic
Space group	P1
a/Å	10.4928(3)
b/Å	10.9595(3)
c/Å	18.3029(6)
α/°	73.120(2)
β/°	78.857(2)
γ/°	64.829(2)
Volume/Å^3	1816.90(10)
Z	4
ρ_{calc}g/cm^3	1.712
μ/mm^{-1}	9.682
F(000)	928.0
Crystal size/mm^3	0.25 × 0.09 × 0.09
Radiation	GaKα (λ = 1.34139)
2Θ range for data collection/°	4.404 to 109.944
Index ranges	$-12 \leq h \leq 12$, $-13 \leq k \leq 13$, $-22 \leq l \leq 22$
Reflections collected	28778
Independent reflections	12189 [R_{int} = 0.0525, R_{sigma} = 0.0791]
Data/restraints/parameters	12189/21/942

Goodness-of-fit on F^2	1.062
Final R indexes [I>=2σ (I)]	R_1 = 0.0493, wR_2 = 0.0951
Final R indexes [all data]	R_1 = 0.0733, wR_2 = 0.1070
Largest diff. peak/hole / e $Å^{-3}$	0.94/-0.88
Flack parameter	0.059(10)

Table 2 Fractional Atomic Coordinates (×10⁴) and Equivalent Isotropic Displacement Parameters (Å²×10³) for lub130(3). U_{eq} is defined as 1/3 of of the trace of the orthogonalised U_{ij} tensor.

Atom	*x*	*y*	*z*	U(eq)
I1A	3374.4(9)	12142.6(9)	7878.3(5)	53.9(3)
O1A	-2398(9)	10167(9)	9275(5)	48(2)
O2A	2287(10)	7931(9)	8646(6)	59(3)
O3A	316(9)	9507(8)	7351(5)	40(2)
O4A	3326(11)	9252(9)	6499(6)	60(3)
O5A	2208(11)	9915(8)	5447(5)	58(2)
N1A	-35(10)	9371(9)	8866(5)	31(2)
N2A	901(9)	11367(8)	7077(5)	27(2)
C1A	-1260(15)	9214(12)	9234(7)	39(3)
C2A	-894(12)	7698(11)	9530(6)	28(3)
C3A	-1707(14)	6975(12)	9939(7)	40(3)
C4A	-1074(17)	5532(14)	10083(8)	53(4)
C5A	332(17)	4899(13)	9829(8)	53(4)
C6A	1193(16)	5599(14)	9448(8)	51(4)
C7A	532(14)	7017(13)	9314(7)	40(3)
C8A	1112(13)	8082(12)	8901(7)	35(3)
C9A	4(12)	10652(11)	8351(6)	32(3)
C10A	991(14)	11135(12)	8595(7)	39(3)
C11A	1157(13)	12412(12)	8029(6)	37(3)
C12A	571(13)	12683(11)	7267(6)	34(3)
C13A	396(12)	10442(10)	7536(6)	28(3)
C14A	1030(14)	13560(12)	6527(6)	40(3)
C15A	1866(15)	12565(13)	6016(7)	45(3)
C16A	1281(13)	11432(11)	6257(6)	33(3)
C17A	2391(18)	10073(14)	6109(8)	55(3)
C18A	3340(20)	8743(16)	5179(10)	99(7)
I1B	7176.7(8)	4071.6(7)	8972.4(5)	46.9(2)
O1B	3835(9)	5367(9)	5828(5)	42(2)
O2B	7605(9)	2584(8)	7251(5)	43(2)
O3B	7369(9)	5634(9)	6262(4)	43(2)
O4B	9315(10)	5663(10)	7669(6)	62(3)

O5B	9573(11)	7420(10)	6745(6)	59(3)
N1B	5621(11)	4217(10)	6639(6)	33(2)
N2B	6493(10)	6606(9)	7277(5)	30(2)
C1B	4868(13)	4347(13)	6056(6)	32(3)
C2B	5616(12)	3032(11)	5800(6)	29(3)
C3B	5299(15)	2641(13)	5205(7)	42(3)
C4B	6241(16)	1339(13)	5087(7)	44(3)
C5B	7388(14)	488(13)	5520(7)	40(3)
C6B	7669(13)	900(12)	6097(7)	36(3)
C7B	6762(13)	2192(12)	6213(6)	30(3)
C8B	6793(13)	2945(11)	6777(7)	32(3)
C9B	5329(12)	5310(12)	7029(7)	34(3)
C10B	4887(14)	4910(13)	7889(7)	41(3)
C11B	5267(13)	5572(12)	8386(7)	42(3)
C12B	5430(13)	6891(12)	7931(6)	35(3)
C13B	6524(13)	5826(12)	6823(6)	32(3)
C14B	5911(15)	7684(13)	8280(7)	46(3)
C15B	6562(16)	8501(13)	7610(8)	50(4)
C16B	7262(13)	7516(12)	7068(7)	35(3)
C17B	8821(14)	6709(13)	7199(8)	40(3)
C18B	11022(15)	6878(14)	6897(12)	73(5)
I1C	4465.9(9)	4635.5(8)	789.8(5)	52.4(2)
O1C	4269(9)	7035(8)	3898(5)	42(2)
O2C	6564(10)	3533(9)	2645(5)	48(2)
O3C	3732(9)	3712(9)	3613(5)	43(2)
O4C	3285(10)	2124(8)	2252(5)	45(2)
O5C	1720(9)	1670(8)	3204(5)	41(2)
N1C	5149(11)	5417(10)	3146(6)	36(2)
N2C	2419(10)	4754(9)	2587(5)	29(2)
C1C	5214(14)	6013(12)	3711(7)	35(3)
C2C	6583(13)	5136(11)	4041(6)	29(3)
C3C	7197(14)	5220(12)	4628(6)	38(3)
C4C	8495(14)	4186(14)	4821(7)	43(3)
C5C	9182(14)	3129(14)	4444(7)	46(3)
C6C	8593(13)	3029(14)	3854(7)	42(3)
C7C	7285(13)	4068(12)	3656(7)	33(3)
C8C	6348(14)	4255(12)	3070(7)	39(3)
C9C	3883(13)	5809(12)	2779(7)	34(3)
C10C	4081(15)	6412(14)	1905(7)	46(3)
C11C	3139(14)	6214(13)	1447(7)	40(3)
C12C	1936(13)	5905(12)	1923(6)	34(3)
C13C	3363(12)	4640(12)	3027(6)	33(3)

C14C	968(13)	5537(12)	1592(6)	39(3)
C15C	309(14)	4799(12)	2306(7)	41(3)
C16C	1545(13)	3959(11)	2817(7)	32(3)
C17C	2328(12)	2492(12)	2721(7)	31(3)
C18C	2208(15)	260(12)	3095(9)	52(4)
I1D	6678.1(9)	8206.3(8)	1949.9(5)	50.4(2)
O1D	10191(9)	12510(8)	1490(5)	44(2)
O2D	10615(9)	8887(8)	575(4)	37.8(19)
O3D	10476(9)	9191(8)	2451(4)	35.1(19)
O4D	9851(10)	6752(9)	3501(5)	48(2)
O5D	10075(10)	7646(9)	4406(5)	48(2)
N1D	9961(11)	10864(9)	1039(5)	30(2)
N2D	8141(10)	9700(9)	2809(5)	29(2)
C1D	10709(13)	11617(11)	1136(6)	31(3)
C2D	12107(14)	11118(12)	724(6)	37(3)
C3D	13185(13)	11592(13)	596(6)	38(3)
C4D	14394(14)	10907(14)	164(7)	44(3)
C5D	14510(12)	9828(12)	-117(6)	34(3)
C6D	13440(13)	9349(12)	27(7)	38(3)
C7D	12220(13)	10020(12)	446(6)	30(3)
C8D	10906(12)	9782(12)	678(6)	33(3)
C9D	8729(12)	10839(11)	1553(6)	32(3)
C10D	7645(14)	10619(14)	1202(7)	43(3)
C11D	6525(13)	10319(12)	1829(7)	37(3)
C12D	6683(12)	10491(11)	2594(6)	35(3)
C13D	9238(13)	9816(11)	2306(7)	30(3)
C14D	5797(14)	10056(13)	3308(7)	43(3)
C15D	6835(13)	8832(12)	3844(7)	40(3)
C16D	8234(13)	9061(11)	3611(6)	32(3)
C17D	9499(13)	7676(12)	3814(7)	36(3)
C18D	11192(17)	6363(16)	4706(9)	65(4)

Table 3 Anisotropic Displacement Parameters (Å^2×10^3) for lub130(3). The Anisotropic displacement factor exponent takes the form: -2π^2[h^{2}a*^{2}U$_{11}$+2hka*b*U$_{12}$+…].

Atom	U_{11}	U_{22}	U_{33}	U_{23}	U_{13}	U_{12}
I1A	41.1(5)	59.8(6)	60.8(6)	3.1(4)	-14.6(4)	-26.7(5)
O1A	27(5)	36(5)	65(6)	-8(4)	12(4)	-5(4)
O2A	26(5)	43(5)	72(7)	5(5)	8(5)	2(4)
O3A	50(6)	30(4)	40(5)	-10(4)	-6(4)	-14(4)
O4A	53(6)	43(5)	59(6)	-12(5)	-3(5)	2(5)
O5A	88(6)	37(4)	40(4)	-16(3)	4(4)	-14(4)

N1A	18(5)	27(5)	38(5)	-5(4)	1(4)	-2(4)
N2A	24(5)	23(4)	31(5)	-9(4)	0(4)	-6(4)
C1A	42(9)	31(6)	38(7)	-2(5)	-2(6)	-13(6)
C2A	28(7)	35(6)	24(5)	-7(5)	-10(5)	-10(5)
C3A	33(8)	38(7)	40(7)	-1(5)	0(6)	-13(6)
C4A	63(10)	43(8)	56(9)	8(7)	-16(8)	-31(8)
C5A	68(11)	25(6)	52(8)	-4(6)	-17(8)	-4(7)
C6A	52(9)	41(8)	49(8)	-3(6)	9(7)	-17(7)
C7A	39(8)	39(7)	36(7)	1(5)	-9(6)	-14(6)
C8A	19(7)	35(6)	41(7)	-1(5)	-3(5)	-6(5)
C9A	28(7)	28(6)	32(6)	-8(5)	-1(5)	-2(5)
C10A	42(8)	41(7)	32(6)	-2(5)	-14(6)	-15(6)
C11A	42(8)	40(7)	32(6)	-7(5)	-3(6)	-19(6)
C12A	42(8)	29(6)	30(6)	-5(5)	-7(5)	-13(5)
C13A	29(7)	19(5)	30(6)	-8(5)	6(5)	-6(5)
C14A	47(8)	34(6)	34(6)	-7(5)	-6(6)	-12(6)
C15A	50(9)	44(7)	34(7)	-10(6)	2(6)	-15(7)
C16A	40(7)	35(6)	24(6)	-13(5)	0(5)	-10(6)
C17A	85(6)	35(4)	39(4)	-15(4)	4(5)	-16(4)
C18A	139(16)	49(9)	73(11)	-38(8)	25(11)	-2(10)
I1B	43.9(5)	44.4(5)	40.5(4)	-12.6(4)	-1.4(4)	-5.4(4)
O1B	31(5)	46(5)	43(5)	-14(4)	-11(4)	-4(5)
O2B	39(6)	42(5)	41(5)	-12(4)	-17(4)	-2(4)
O3B	44(6)	52(5)	31(4)	-15(4)	4(4)	-16(4)
O4B	39(6)	45(6)	89(8)	-4(6)	-10(6)	-10(5)
O5B	56(7)	51(6)	81(7)	-25(5)	14(5)	-33(5)
N1B	27(6)	32(5)	42(6)	-18(4)	-5(5)	-6(4)
N2B	27(5)	31(5)	34(5)	-19(4)	3(4)	-8(4)
C1B	23(7)	43(7)	25(6)	0(5)	2(5)	-15(6)
C2B	25(7)	25(6)	30(6)	-3(5)	-6(5)	-4(5)
C3B	50(9)	53(8)	33(6)	-9(6)	2(6)	-32(7)
C4B	65(10)	38(7)	40(7)	-15(6)	-4(7)	-26(7)
C5B	44(8)	39(7)	36(7)	-15(6)	6(6)	-15(6)
C6B	34(7)	37(7)	37(7)	-5(5)	1(5)	-20(6)
C7B	28(7)	38(6)	34(6)	-11(5)	-3(5)	-19(6)
C8B	27(7)	28(6)	38(7)	-11(5)	1(6)	-8(5)
C9B	20(7)	36(6)	46(7)	-16(5)	-8(6)	-3(5)
C10B	29(7)	45(7)	49(7)	-25(6)	4(6)	-8(6)
C11B	35(8)	43(7)	38(7)	-14(6)	6(6)	-7(6)
C12B	32(7)	36(6)	40(6)	-13(5)	-1(5)	-14(5)
C13B	26(7)	35(6)	32(6)	-12(5)	-2(5)	-7(5)
C14B	48(8)	40(7)	46(7)	-22(6)	-1(6)	-8(6)

C15B	56(10)	30(7)	66(9)	-22(6)	9(8)	-17(7)
C16B	38(8)	31(6)	36(6)	-9(5)	7(6)	-16(6)
C17B	37(8)	33(7)	49(8)	-20(6)	4(6)	-8(6)
C18B	30(9)	45(8)	154(17)	-56(10)	19(10)	-15(7)
I1C	50.8(6)	58.3(5)	47.6(5)	-24.4(4)	9.7(4)	-18.9(5)
O1C	46(6)	40(5)	35(4)	-14(4)	-4(4)	-7(4)
O2C	45(6)	51(5)	57(6)	-36(5)	-4(5)	-14(5)
O3C	44(6)	45(5)	36(5)	-1(4)	-13(4)	-14(4)
O4C	39(6)	36(5)	54(6)	-21(4)	14(5)	-9(4)
O5C	39(5)	35(4)	52(5)	-7(4)	2(4)	-22(4)
N1C	29(6)	36(6)	45(6)	-18(5)	0(5)	-11(5)
N2C	32(6)	28(5)	29(5)	-5(4)	-8(4)	-13(4)
C1C	36(8)	25(6)	46(7)	-15(6)	10(6)	-15(6)
C2C	37(7)	20(5)	30(6)	-3(4)	2(5)	-16(5)
C3C	49(9)	41(7)	28(6)	-11(5)	7(6)	-25(6)
C4C	38(8)	60(8)	36(7)	-5(6)	-4(6)	-27(7)
C5C	30(8)	63(9)	44(7)	-10(7)	-2(6)	-20(7)
C6C	25(7)	50(8)	48(8)	-10(6)	7(6)	-17(6)
C7C	28(7)	37(6)	41(7)	-18(5)	4(6)	-18(6)
C8C	34(7)	35(7)	50(7)	-23(6)	10(6)	-14(6)
C9C	34(7)	32(6)	42(7)	-14(5)	-12(6)	-12(6)
C10C	54(9)	52(8)	43(7)	-15(6)	-2(7)	-29(7)
C11C	41(8)	45(7)	28(6)	-6(5)	-8(6)	-11(6)
C12C	34(7)	37(6)	30(6)	-3(5)	-7(5)	-12(6)
C13C	27(7)	39(7)	32(6)	-17(5)	3(5)	-10(6)
C14C	33(7)	42(7)	34(6)	-11(5)	-10(6)	-2(6)
C15C	46(9)	28(6)	47(7)	-10(5)	-2(6)	-13(6)
C16C	33(7)	27(6)	34(6)	-11(5)	-4(5)	-7(5)
C17C	18(7)	34(6)	38(7)	-11(5)	-13(5)	0(5)
C18C	48(9)	34(7)	77(10)	-11(7)	-4(7)	-21(6)
I1D	63.8(6)	42.8(5)	51.1(5)	-15.7(4)	-8.3(4)	-22.5(4)
O1D	45(5)	35(4)	55(5)	-23(4)	10(4)	-15(4)
O2D	37(5)	33(4)	45(5)	-10(4)	-9(4)	-12(4)
O3D	26(5)	39(5)	38(4)	-11(4)	-1(4)	-10(4)
O4D	50(6)	36(5)	61(6)	-23(4)	-13(5)	-7(4)
O5D	46(6)	55(6)	37(5)	-9(4)	-15(4)	-12(5)
N1D	35(6)	32(5)	29(5)	-10(4)	2(4)	-17(5)
N2D	30(6)	31(5)	27(5)	-6(4)	-3(4)	-14(4)
C1D	38(7)	29(6)	26(6)	-5(5)	-4(5)	-14(5)
C2D	44(8)	36(6)	31(6)	-15(5)	4(6)	-15(6)
C3D	38(8)	48(7)	33(6)	-17(6)	6(6)	-20(6)
C4D	39(8)	61(8)	42(7)	-5(6)	-2(6)	-33(7)

C5D	20(7)	47(7)	30(6)	−10(5)	0(5)	−10(6)
C6D	30(7)	38(6)	37(7)	−16(5)	3(6)	−4(6)
C7D	29(7)	35(6)	26(6)	−9(5)	−6(5)	−9(5)
C8D	26(7)	37(6)	31(6)	−5(5)	3(5)	−13(6)
C9D	28(7)	32(6)	34(6)	−12(5)	5(5)	−11(5)
C10D	35(8)	59(8)	33(6)	−10(6)	−10(6)	−13(6)
C11D	35(7)	33(6)	40(7)	−15(5)	11(6)	−12(6)
C12D	29(7)	27(6)	41(7)	−10(5)	−4(5)	−4(5)
C13D	28(8)	27(6)	40(7)	−19(5)	0(6)	−11(6)
C14D	35(8)	51(8)	39(7)	−18(6)	11(6)	−15(6)
C15D	43(8)	38(7)	30(6)	−4(5)	6(5)	−15(6)
C16D	35(7)	28(6)	26(6)	−9(5)	0(5)	−7(5)
C17D	36(7)	34(6)	35(6)	1(5)	1(6)	−18(6)
C18D	53(10)	59(9)	59(9)	−2(8)	−13(8)	−5(8)

Table 4 Bond Lengths for lub130(3).

Atom	Atom	Length/Å	Atom	Atom	Length/Å
I1A	C11A	2.189(13)	I1C	C11C	2.212(12)
O1A	C1A	1.214(15)	O1C	C1C	1.226(14)
O2A	C8A	1.189(14)	O2C	C8C	1.191(13)
O3A	C13A	1.208(13)	O3C	C13C	1.236(14)
O4A	C17A	1.195(17)	O4C	C17C	1.197(14)
O5A	C17A	1.333(16)	O5C	C17C	1.345(14)
O5A	C18A	1.466(16)	O5C	C18C	1.468(14)
N1A	C1A	1.386(16)	N1C	C1C	1.400(15)
N1A	C8A	1.407(14)	N1C	C8C	1.377(15)
N1A	C9A	1.458(14)	N1C	C9C	1.446(15)
N2A	C12A	1.464(13)	N2C	C12C	1.459(14)
N2A	C13A	1.343(13)	N2C	C13C	1.338(15)
N2A	C16A	1.464(13)	N2C	C16C	1.447(15)
C1A	C2A	1.488(14)	C1C	C2C	1.475(18)
C2A	C3A	1.379(16)	C2C	C3C	1.399(17)
C2A	C7A	1.394(18)	C2C	C7C	1.397(15)
C3A	C4A	1.394(17)	C3C	C4C	1.380(18)
C4A	C5A	1.39(2)	C4C	C5C	1.379(18)
C5A	C6A	1.39(2)	C5C	C6C	1.393(19)
C6A	C7A	1.373(17)	C6C	C7C	1.390(18)
C7A	C8A	1.490(17)	C7C	C8C	1.507(18)
C9A	C10A	1.528(17)	C9C	C10C	1.553(17)
C9A	C13A	1.525(15)	C9C	C13C	1.518(16)
C10A	C11A	1.535(16)	C10C	C11C	1.527(18)
C11A	C12A	1.532(16)	C11C	C12C	1.495(17)

C12A	C14A	1.541(16)	C12C	C14C	1.512(16)
C14A	C15A	1.516(16)	C14C	C15C	1.533(17)
C15A	C16A	1.529(17)	C15C	C16C	1.535(17)
C16A	C17A	1.512(17)	C16C	C17C	1.509(15)
I1B	C11B	2.208(12)	I1D	C11D	2.199(11)
O1B	C1B	1.213(14)	O1D	C1D	1.205(12)
O2B	C8B	1.198(14)	O2D	C8D	1.216(13)
O3B	C13B	1.224(13)	O3D	C13D	1.224(14)
O4B	C17B	1.190(15)	O4D	C17D	1.194(14)
O5B	C17B	1.347(15)	O5D	C17D	1.325(14)
O5B	C18B	1.429(18)	O5D	C18D	1.432(16)
N1B	C1B	1.388(15)	N1D	C1D	1.421(14)
N1B	C8B	1.405(15)	N1D	C8D	1.424(14)
N1B	C9B	1.463(14)	N1D	C9D	1.449(14)
N2B	C12B	1.477(14)	N2D	C12D	1.467(15)
N2B	C13B	1.341(14)	N2D	C13D	1.356(14)
N2B	C16B	1.461(14)	N2D	C16D	1.433(14)
C1B	C2B	1.483(16)	C1D	C2D	1.466(17)
C2B	C3B	1.419(16)	C2D	C3D	1.389(17)
C2B	C7B	1.367(16)	C2D	C7D	1.390(15)
C3B	C4B	1.398(18)	C3D	C4D	1.394(17)
C4B	C5B	1.390(19)	C4D	C5D	1.373(17)
C5B	C6B	1.385(17)	C5D	C6D	1.382(17)
C6B	C7B	1.380(16)	C6D	C7D	1.385(16)
C7B	C8B	1.508(15)	C7D	C8D	1.470(17)
C9B	C10B	1.540(17)	C9D	C10D	1.539(17)
C9B	C13B	1.527(17)	C9D	C13D	1.523(16)
C10B	C11B	1.512(17)	C10D	C11D	1.547(17)
C11B	C12B	1.505(16)	C11D	C12D	1.514(16)
C12B	C14B	1.496(16)	C12D	C14D	1.533(16)
C14B	C15B	1.526(18)	C14D	C15D	1.534(18)
C15B	C16B	1.535(16)	C15D	C16D	1.552(17)
C16B	C17B	1.522(18)	C16D	C17D	1.534(16)

Table 5 Bond Angles for lub130(3).

Atom	Atom	Atom	Angle/°	Atom	Atom	Atom	Angle/°
C17A	O5A	C18A	114.8(13)	C17C	O5C	C18C	116.5(9)
C1A	N1A	C8A	111.5(9)	C1C	N1C	C9C	124.1(10)
C1A	N1A	C9A	124.3(9)	C8C	N1C	C1C	112.4(10)
C8A	N1A	C9A	122.6(9)	C8C	N1C	C9C	122.6(10)
C12A	N2A	C16A	112.4(8)	C13C	N2C	C12C	122.6(10)
C13A	N2A	C12A	120.7(9)	C13C	N2C	C16C	123.2(9)

C13A	N2A	C16A	122.5(9)	C16C	N2C	C12C	112.7(9)
O1A	C1A	N1A	124.3(11)	O1C	C1C	N1C	125.0(12)
O1A	C1A	C2A	128.7(11)	O1C	C1C	C2C	128.5(12)
N1A	C1A	C2A	106.9(10)	N1C	C1C	C2C	106.5(10)
C3A	C2A	C1A	131.1(10)	C3C	C2C	C1C	131.6(11)
C3A	C2A	C7A	121.5(11)	C7C	C2C	C1C	107.6(11)
C7A	C2A	C1A	107.5(10)	C7C	C2C	C3C	120.8(11)
C2A	C3A	C4A	117.3(12)	C4C	C3C	C2C	117.0(11)
C5A	C4A	C3A	119.2(13)	C5C	C4C	C3C	122.1(12)
C6A	C5A	C4A	124.7(12)	C4C	C5C	C6C	121.9(12)
C7A	C6A	C5A	114.5(13)	C7C	C6C	C5C	116.4(12)
C2A	C7A	C8A	108.3(10)	C2C	C7C	C8C	107.9(10)
C6A	C7A	C2A	122.7(12)	C6C	C7C	C2C	121.8(12)
C6A	C7A	C8A	128.9(12)	C6C	C7C	C8C	130.2(11)
O2A	C8A	N1A	124.9(11)	O2C	C8C	N1C	126.7(12)
O2A	C8A	C7A	129.3(11)	O2C	C8C	C7C	127.8(11)
N1A	C8A	C7A	105.7(10)	N1C	C8C	C7C	105.5(9)
N1A	C9A	C10A	112.3(9)	N1C	C9C	C10C	110.9(10)
N1A	C9A	C13A	108.6(8)	N1C	C9C	C13C	110.1(9)
C13A	C9A	C10A	112.5(10)	C13C	C9C	C10C	117.3(9)
C9A	C10A	C11A	113.8(9)	C11C	C10C	C9C	112.5(10)
C10A	C11A	I1A	109.9(8)	C10C	C11C	I1C	109.1(9)
C12A	C11A	I1A	112.1(8)	C12C	C11C	I1C	112.8(8)
C12A	C11A	C10A	110.6(9)	C12C	C11C	C10C	113.7(10)
N2A	C12A	C11A	110.0(9)	N2C	C12C	C11C	111.5(10)
N2A	C12A	C14A	104.3(8)	N2C	C12C	C14C	103.1(9)
C11A	C12A	C14A	120.9(10)	C11C	C12C	C14C	121.8(9)
O3A	C13A	N2A	125.2(10)	O3C	C13C	N2C	123.5(11)
O3A	C13A	C9A	122.8(10)	O3C	C13C	C9C	121.9(11)
N2A	C13A	C9A	111.9(9)	N2C	C13C	C9C	114.4(10)
C15A	C14A	C12A	105.6(9)	C12C	C14C	C15C	102.9(9)
C14A	C15A	C16A	105.2(10)	C14C	C15C	C16C	103.0(10)
N2A	C16A	C15A	102.0(9)	N2C	C16C	C15C	103.6(9)
N2A	C16A	C17A	112.1(10)	N2C	C16C	C17C	112.7(10)
C17A	C16A	C15A	110.9(11)	C17C	C16C	C15C	112.5(9)
O4A	C17A	O5A	123.2(12)	O4C	C17C	O5C	124.6(11)
O4A	C17A	C16A	127.3(12)	O4C	C17C	C16C	125.5(11)
O5A	C17A	C16A	109.5(12)	O5C	C17C	C16C	109.7(10)
C17B	O5B	C18B	115.0(12)	C17D	O5D	C18D	116.0(11)
C1B	N1B	C8B	112.5(9)	C1D	N1D	C8D	108.8(9)
C1B	N1B	C9B	124.8(10)	C1D	N1D	C9D	119.4(9)
C8B	N1B	C9B	122.5(10)	C8D	N1D	C9D	125.7(9)

C13B	N2B	C12B	122.8(9)	C13D	N2D	C12D	120.4(9)
C13B	N2B	C16B	123.0(9)	C13D	N2D	C16D	125.0(10)
C16B	N2B	C12B	112.7(8)	C16D	N2D	C12D	113.5(9)
O1B	C1B	N1B	124.1(12)	O1D	C1D	N1D	122.4(11)
O1B	C1B	C2B	130.6(12)	O1D	C1D	C2D	130.1(11)
N1B	C1B	C2B	105.3(10)	N1D	C1D	C2D	107.5(9)
C3B	C2B	C1B	128.3(11)	C3D	C2D	C1D	129.8(10)
C7B	C2B	C1B	109.8(10)	C3D	C2D	C7D	122.5(11)
C7B	C2B	C3B	121.8(11)	C7D	C2D	C1D	107.7(11)
C4B	C3B	C2B	114.5(12)	C2D	C3D	C4D	116.1(11)
C5B	C4B	C3B	123.0(12)	C5D	C4D	C3D	121.8(12)
C6B	C5B	C4B	121.1(12)	C4D	C5D	C6D	121.6(11)
C7B	C6B	C5B	116.7(12)	C5D	C6D	C7D	117.9(11)
C2B	C7B	C6B	122.9(11)	C2D	C7D	C8D	108.9(10)
C2B	C7B	C8B	107.4(10)	C6D	C7D	C2D	120.2(12)
C6B	C7B	C8B	129.7(11)	C6D	C7D	C8D	130.9(11)
O2B	C8B	N1B	125.3(10)	O2D	C8D	N1D	124.6(10)
O2B	C8B	C7B	129.7(10)	O2D	C8D	C7D	128.9(10)
N1B	C8B	C7B	105.0(10)	N1D	C8D	C7D	106.5(9)
N1B	C9B	C10B	112.4(10)	N1D	C9D	C10D	114.2(9)
N1B	C9B	C13B	110.1(9)	N1D	C9D	C13D	108.0(9)
C13B	C9B	C10B	116.5(10)	C13D	C9D	C10D	115.0(10)
C11B	C10B	C9B	114.5(10)	C9D	C10D	C11D	110.6(9)
C10B	C11B	I1B	110.1(8)	C10D	C11D	I1D	109.9(7)
C12B	C11B	I1B	112.2(9)	C12D	C11D	I1D	109.8(7)
C12B	C11B	C10B	111.4(10)	C12D	C11D	C10D	112.0(10)
N2B	C12B	C11B	109.8(9)	N2D	C12D	C11D	111.1(9)
N2B	C12B	C14B	102.2(9)	N2D	C12D	C14D	103.6(9)
C14B	C12B	C11B	121.7(10)	C11D	C12D	C14D	119.6(10)
O3B	C13B	N2B	122.9(11)	O3D	C13D	N2D	123.7(11)
O3B	C13B	C9B	123.2(10)	O3D	C13D	C9D	124.9(11)
N2B	C13B	C9B	113.7(9)	N2D	C13D	C9D	111.5(10)
C12B	C14B	C15B	105.5(10)	C12D	C14D	C15D	106.6(10)
C14B	C15B	C16B	103.3(9)	C14D	C15D	C16D	103.4(9)
N2B	C16B	C15B	103.9(9)	N2D	C16D	C15D	102.5(9)
N2B	C16B	C17B	111.7(9)	N2D	C16D	C17D	115.4(9)
C17B	C16B	C15B	109.8(11)	C17D	C16D	C15D	110.0(9)
O4B	C17B	O5B	123.9(13)	O4D	C17D	O5D	126.1(11)
O4B	C17B	C16B	126.2(12)	O4D	C17D	C16D	124.1(11)
O5B	C17B	C16B	109.7(11)	O5D	C17D	C16D	109.7(10)

Table 6 Hydrogen Bonds for lub130(3).

D	H	A	d(D-H)/Å	d(H-A)/Å	d(D-A)/Å	D-H-A/°
C9A	H9A	O2B[1]	1.00	2.47	3.134(14)	123.7
C10A	H10A	O2A	0.99	2.53	3.160(15)	120.9
C11A	H11A	O4B[1]	1.00	2.43	3.183(15)	131.8
C12A	H12A	O2B[1]	1.00	2.38	3.166(16)	134.9
C14A	H14B	I1A	0.99	2.89	3.383(13)	111.6
C18A	H18A	O1C	0.98	2.47	3.173(16)	128.8
C18A	H18B	O1B	0.98	2.46	3.381(19)	156.0
C11B	H11B	O2A	1.00	2.46	3.154(15)	126.2
C12B	H12B	O2A	1.00	2.56	3.144(15)	117.5
C12B	H12B	O4A	1.00	2.59	3.447(16)	144.2
C14B	H14C	I1B	0.99	2.95	3.508(13)	116.7
C18B	H18D	O3A[2]	0.98	2.16	2.980(15)	140.4
C18B	H18E	O1B[2]	0.98	2.38	3.283(17)	153.7
C11C	H11C	O2D[3]	1.00	2.36	3.235(15)	145.7
C14C	H14E	I1C	0.99	2.96	3.504(12)	115.6
C15C	H15E	O1D[4]	0.99	2.42	3.324(14)	152.1
C10D	H10G	O2D	0.99	2.40	3.080(15)	125.6
C11D	H11D	O4C[5]	1.00	2.38	3.197(15)	137.9
C12D	H12D	O2C[5]	1.00	2.35	3.311(14)	161.6

[1]-1+X,1+Y,+Z; [2]1+X,+Y,+Z; [3]-1+X,+Y,+Z; [4]-1+X,-1+Y,+Z; [5]+X,1+Y,+Z

Table 7 Torsion Angles for lub130(3).

A	B	C	D	Angle/°	A	B	C	D	Angle/°
I1A	C11A	C12A	N2A	85.1(10)	I1C	C11C	C12C	N2C	73.2(10)
I1A	C11A	C12A	C14A	-36.5(13)	I1C	C11C	C12C	C14C	-49.0(13)
O1A	C1A	C2A	C3A	-2(2)	O1C	C1C	C2C	C3C	-1(2)
O1A	C1A	C2A	C7A	177.5(14)	O1C	C1C	C2C	C7C	178.1(12)
N1A	C1A	C2A	C3A	179.6(12)	N1C	C1C	C2C	C3C	-178.8(11)
N1A	C1A	C2A	C7A	-1.0(13)	N1C	C1C	C2C	C7C	0.8(13)
N1A	C9A	C10A	C11A	175.1(9)	N1C	C9C	C10C	C11C	153.3(10)
N1A	C9A	C13A	O3A	17.1(16)	N1C	C9C	C13C	O3C	19.4(15)
N1A	C9A	C13A	N2A	-159.6(9)	N1C	C9C	C13C	N2C	-164.5(9)
N2A	C12A	C14A	C15A	-11.1(13)	N2C	C12C	C14C	C15C	33.6(11)
N2A	C16A	C17A	O4A	-33(2)	N2C	C16C	C17C	O4C	-29.5(16)
N2A	C16A	C17A	O5A	149.0(11)	N2C	C16C	C17C	O5C	155.2(9)
C1A	N1A	C8A	O2A	-178.1(13)	C1C	N1C	C8C	O2C	178.5(12)
C1A	N1A	C8A	C7A	1.5(13)	C1C	N1C	C8C	C7C	0.7(13)
C1A	N1A	C9A	C10A	125.1(12)	C1C	N1C	C9C	C10C	117.7(12)
C1A	N1A	C9A	C13A	-109.9(12)	C1C	N1C	C9C	C13C	-110.8(12)
C1A	C2A	C3A	C4A	174.9(11)	C1C	C2C	C3C	C4C	177.6(12)

C1A	C2A	C7A	C6A	-175.2(12)	C1C	C2C	C7C	C6C	-177.6(11)
C1A	C2A	C7A	C8A	1.9(13)	C1C	C2C	C7C	C8C	-0.3(13)
C2A	C3A	C4A	C5A	1.7(19)	C2C	C3C	C4C	C5C	1.5(18)
C2A	C7A	C8A	O2A	177.4(13)	C2C	C7C	C8C	O2C	-178.0(12)
C2A	C7A	C8A	N1A	-2.2(13)	C2C	C7C	C8C	N1C	-0.2(13)
C3A	C2A	C7A	C6A	4.3(19)	C3C	C2C	C7C	C6C	2.0(17)
C3A	C2A	C7A	C8A	-178.6(10)	C3C	C2C	C7C	C8C	179.3(10)
C3A	C4A	C5A	C6A	1(2)	C3C	C4C	C5C	C6C	-1(2)
C4A	C5A	C6A	C7A	-2(2)	C4C	C5C	C6C	C7C	1.2(19)
C5A	C6A	C7A	C2A	-1(2)	C5C	C6C	C7C	C2C	-1.6(17)
C5A	C6A	C7A	C8A	-177.6(13)	C5C	C6C	C7C	C8C	-178.2(12)
C6A	C7A	C8A	O2A	-6(2)	C6C	C7C	C8C	O2C	-1(2)
C6A	C7A	C8A	N1A	174.7(13)	C6C	C7C	C8C	N1C	176.7(12)
C7A	C2A	C3A	C4A	-4.4(18)	C7C	C2C	C3C	C4C	-1.9(16)
C8A	N1A	C1A	O1A	-179.0(12)	C8C	N1C	C1C	O1C	-178.4(12)
C8A	N1A	C1A	C2A	-0.4(13)	C8C	N1C	C1C	C2C	-0.9(13)
C8A	N1A	C9A	C10A	-70.6(13)	C8C	N1C	C9C	C10C	-74.0(14)
C8A	N1A	C9A	C13A	54.5(14)	C8C	N1C	C9C	C13C	57.6(14)
C9A	N1A	C1A	O1A	-13.1(19)	C9C	N1C	C1C	O1C	-9.0(19)
C9A	N1A	C1A	C2A	165.5(9)	C9C	N1C	C1C	C2C	168.5(10)
C9A	N1A	C8A	O2A	15.8(19)	C9C	N1C	C8C	O2C	9(2)
C9A	N1A	C8A	C7A	-164.6(10)	C9C	N1C	C8C	C7C	-168.9(10)
C9A	C10A	C11A	I1A	-137.8(9)	C9C	C10C	C11C	I1C	-108.9(10)
C9A	C10A	C11A	C12A	-13.4(14)	C9C	C10C	C11C	C12C	17.9(15)
C10A	C9A	C13A	O3A	142.0(12)	C10C	C9C	C13C	O3C	147.5(11)
C10A	C9A	C13A	N2A	-34.7(13)	C10C	C9C	C13C	N2C	-36.4(15)
C10A	C11A	C12A	N2A	-37.9(13)	C10C	C11C	C12C	N2C	-51.8(13)
C10A	C11A	C12A	C14A	-159.5(10)	C10C	C11C	C12C	C14C	-173.9(11)
C11A	C12A	C14A	C15A	113.1(12)	C11C	C12C	C14C	C15C	159.5(10)
C12A	N2A	C13A	O3A	161.3(11)	C12C	N2C	C13C	O3C	176.2(10)
C12A	N2A	C13A	C9A	-22.1(14)	C12C	N2C	C13C	C9C	0.2(15)
C12A	N2A	C16A	C15A	26.9(12)	C12C	N2C	C16C	C15C	-7.0(11)
C12A	N2A	C16A	C17A	145.5(11)	C12C	N2C	C16C	C17C	114.9(10)
C12A	C14A	C15A	C16A	27.4(13)	C12C	C14C	C15C	C16C	-38.1(11)
C13A	N2A	C12A	C11A	61.9(14)	C13C	N2C	C12C	C11C	44.4(14)
C13A	N2A	C12A	C14A	-167.1(10)	C13C	N2C	C12C	C14C	176.7(10)
C13A	N2A	C16A	C15A	-176.7(10)	C13C	N2C	C16C	C15C	159.3(10)
C13A	N2A	C16A	C17A	-58.1(15)	C13C	N2C	C16C	C17C	-78.8(13)
C13A	C9A	C10A	C11A	52.2(13)	C13C	C9C	C10C	C11C	25.6(16)
C14A	C15A	C16A	N2A	-32.5(12)	C14C	C15C	C16C	N2C	27.7(11)
C14A	C15A	C16A	C17A	-152.0(11)	C14C	C15C	C16C	C17C	-94.3(11)
C15A	C16A	C17A	O4A	80.6(17)	C15C	C16C	C17C	O4C	87.2(15)

C15A	C16A	C17A	O5A	-97.8(13)	C15C	C16C	C17C	O5C	-88.1(12)
C16A	N2A	C12A	C11A	-141.2(10)	C16C	N2C	C12C	C11C	-149.2(9)
C16A	N2A	C12A	C14A	-10.2(13)	C16C	N2C	C12C	C14C	-16.9(12)
C16A	N2A	C13A	O3A	6.8(18)	C16C	N2C	C13C	O3C	11.3(16)
C16A	N2A	C13A	C9A	-176.6(10)	C16C	N2C	C13C	C9C	-164.8(9)
C18A	O5A	C17A	O4A	-7(2)	C18C	O5C	C17C	O4C	-5.0(17)
C18A	O5A	C17A	C16A	171.1(13)	C18C	O5C	C17C	C16C	170.3(10)
I1B	C11B	C12B	N2B	67.7(10)	I1D	C11D	C12D	N2D	70.9(10)
I1B	C11B	C12B	C14B	-51.3(13)	I1D	C11D	C12D	C14D	-49.7(12)
O1B	C1B	C2B	C3B	0(2)	O1D	C1D	C2D	C3D	-4(2)
O1B	C1B	C2B	C7B	178.1(12)	O1D	C1D	C2D	C7D	176.7(12)
N1B	C1B	C2B	C3B	-178.5(12)	N1D	C1D	C2D	C3D	174.6(12)
N1B	C1B	C2B	C7B	-0.8(13)	N1D	C1D	C2D	C7D	-4.8(13)
N1B	C9B	C10B	C11B	150.9(10)	N1D	C9D	C10D	C11D	168.9(9)
N1B	C9B	C13B	O3B	18.7(16)	N1D	C9D	C13D	O3D	3.4(14)
N1B	C9B	C13B	N2B	-166.5(9)	N1D	C9D	C13D	N2D	-177.9(8)
N2B	C12B	C14B	C15B	32.6(12)	N2D	C12D	C14D	C15D	-10.0(12)
N2B	C16B	C17B	O4B	-29.4(17)	N2D	C16D	C17D	O4D	-46.6(16)
N2B	C16B	C17B	O5B	156.0(10)	N2D	C16D	C17D	O5D	136.6(10)
C1B	N1B	C8B	O2B	-179.7(11)	C1D	N1D	C8D	O2D	173.6(11)
C1B	N1B	C8B	C7B	-0.1(13)	C1D	N1D	C8D	C7D	-8.5(12)
C1B	N1B	C9B	C10B	116.8(12)	C1D	N1D	C9D	C10D	153.0(10)
C1B	N1B	C9B	C13B	-111.5(12)	C1D	N1D	C9D	C13D	-77.8(11)
C1B	C2B	C3B	C4B	177.9(11)	C1D	C2D	C3D	C4D	-178.8(12)
C1B	C2B	C7B	C6B	-179.5(10)	C1D	C2D	C7D	C6D	179.7(10)
C1B	C2B	C7B	C8B	0.7(13)	C1D	C2D	C7D	C8D	-0.4(13)
C2B	C3B	C4B	C5B	0.6(18)	C2D	C3D	C4D	C5D	-0.1(18)
C2B	C7B	C8B	O2B	179.2(12)	C2D	C7D	C8D	O2D	-176.8(12)
C2B	C7B	C8B	N1B	-0.4(12)	C2D	C7D	C8D	N1D	5.5(13)
C3B	C2B	C7B	C6B	-1.6(18)	C3D	C2D	C7D	C6D	0.2(18)
C3B	C2B	C7B	C8B	178.6(11)	C3D	C2D	C7D	C8D	-179.9(11)
C3B	C4B	C5B	C6B	-1(2)	C3D	C4D	C5D	C6D	-1.1(19)
C4B	C5B	C6B	C7B	-0.4(18)	C4D	C5D	C6D	C7D	1.9(18)
C5B	C6B	C7B	C2B	1.5(17)	C5D	C6D	C7D	C2D	-1.4(17)
C5B	C6B	C7B	C8B	-178.7(11)	C5D	C6D	C7D	C8D	178.7(11)
C6B	C7B	C8B	O2B	-1(2)	C6D	C7D	C8D	O2D	3(2)
C6B	C7B	C8B	N1B	179.8(11)	C6D	C7D	C8D	N1D	-174.6(12)
C7B	C2B	C3B	C4B	0.5(17)	C7D	C2D	C3D	C4D	0.6(18)
C8B	N1B	C1B	O1B	-178.4(11)	C8D	N1D	C1D	O1D	-173.1(10)
C8B	N1B	C1B	C2B	0.5(13)	C8D	N1D	C1D	C2D	8.3(12)
C8B	N1B	C9B	C10B	-68.8(14)	C8D	N1D	C9D	C10D	-57.8(15)
C8B	N1B	C9B	C13B	62.9(14)	C8D	N1D	C9D	C13D	71.5(13)

C9B	N1B	C1B	O1B	-3.5(18)	C9D	N1D	C1D	O1D	-19.1(15)
C9B	N1B	C1B	C2B	175.4(10)	C9D	N1D	C1D	C2D	162.3(9)
C9B	N1B	C8B	O2B	5.2(19)	C9D	N1D	C8D	O2D	21.7(18)
C9B	N1B	C8B	C7B	-175.2(10)	C9D	N1D	C8D	C7D	-160.4(10)
C9B	C10B	C11B	I1B	-101.3(10)	C9D	C10D	C11D	I1D	-115.4(9)
C9B	C10B	C11B	C12B	23.8(15)	C9D	C10D	C11D	C12D	6.9(14)
C10B	C9B	C13B	O3B	148.3(11)	C10D	C9D	C13D	O3D	132.1(11)
C10B	C9B	C13B	N2B	-36.9(14)	C10D	C9D	C13D	N2D	-49.1(12)
C10B	C11B	C12B	N2B	-56.2(13)	C10D	C11D	C12D	N2D	-51.4(13)
C10B	C11B	C12B	C14B	-175.3(11)	C10D	C11D	C12D	C14D	-172.0(10)
C11B	C12B	C14B	C15B	155.4(11)	C11D	C12D	C14D	C15D	114.4(12)
C12B	N2B	C13B	O3B	177.0(10)	C12D	N2D	C13D	O3D	179.7(10)
C12B	N2B	C13B	C9B	2.2(15)	C12D	N2D	C13D	C9D	0.9(13)
C12B	N2B	C16B	C15B	-3.2(13)	C12D	N2D	C16D	C15D	28.1(11)
C12B	N2B	C16B	C17B	115.1(11)	C12D	N2D	C16D	C17D	147.6(10)
C12B	C14B	C15B	C16B	-35.3(14)	C12D	C14D	C15D	C16D	26.0(12)
C13B	N2B	C12B	C11B	45.2(14)	C13D	N2D	C12D	C11D	49.8(13)
C13B	N2B	C12B	C14B	175.6(10)	C13D	N2D	C12D	C14D	179.5(9)
C13B	N2B	C16B	C15B	162.8(11)	C13D	N2D	C16D	C15D	-164.0(9)
C13B	N2B	C16B	C17B	-79.0(13)	C13D	N2D	C16D	C17D	-44.5(15)
C13B	C9B	C10B	C11B	22.4(15)	C13D	C9D	C10D	C11D	43.2(13)
C14B	C15B	C16B	N2B	23.1(14)	C14D	C15D	C16D	N2D	-32.0(11)
C14B	C15B	C16B	C17B	-96.5(12)	C14D	C15D	C16D	C17D	-155.2(10)
C15B	C16B	C17B	O4B	85.4(16)	C15D	C16D	C17D	O4D	68.7(14)
C15B	C16B	C17B	O5B	-89.3(12)	C15D	C16D	C17D	O5D	-108.1(11)
C16B	N2B	C12B	C11B	-148.8(10)	C16D	N2D	C12D	C11D	-141.6(9)
C16B	N2B	C12B	C14B	-18.4(12)	C16D	N2D	C12D	C14D	-11.9(12)
C16B	N2B	C13B	O3B	12.4(17)	C16D	N2D	C13D	O3D	12.5(16)
C16B	N2B	C13B	C9B	-162.4(10)	C16D	N2D	C13D	C9D	-166.3(9)
C18B	O5B	C17B	O4B	-4.0(18)	C18D	O5D	C17D	O4D	-2.2(18)
C18B	O5B	C17B	C16B	170.8(11)	C18D	O5D	C17D	C16D	174.6(11)

Table 8 Hydrogen Atom Coordinates (Å×10^4) and Isotropic Displacement Parameters (Å^2×10^3) for lub130(3).

Atom	*x*	*y*	*z*	U(eq)
H3A	-2660.44	7440.54	10116.59	48
H4A	-1598.8	4989.24	10350.45	64
H5A	734.87	3915.33	9923.13	63
H6A	2159.66	5134.96	9292.15	61
H9A	-971.3	11388.84	8367.52	39
H10A	1933.77	10364.75	8652.09	47
H10B	624.19	11354.44	9101.76	47

H11A	594.65	13234.49	8254.25	45
H12A	-481.55	13138.14	7345.59	41
H14A	195.08	14316.07	6277.78	47
H14B	1623.49	13972.98	6641.04	47
H15A	2885.87	12165.67	6092.11	54
H15B	1732.34	13043.21	5470.22	54
H16A	422.85	11719.99	5984.45	40
H18A	3251.94	8833.12	4640.98	149
H18B	3280.89	7874.3	5489.65	149
H18C	4260.9	8739.42	5226.31	149
H3B	4511.05	3216.1	4911.06	50
H4B	6090.59	1023.26	4692.12	53
H5B	7988.36	-391.19	5418.58	48
H6B	8446.92	322.37	6398.48	43
H9B	4481.58	6108.59	6801.42	41
H10C	3851.6	5174.97	7954.34	49
H10D	5340.15	3889.32	8070.61	49
H11B	4470.06	5819.49	8788.6	50
H12B	4504	7541.55	7717.89	42
H14C	6619.03	7044.33	8650.51	55
H14D	5102.6	8319.02	8547.92	55
H15C	7268.51	8711.51	7781.91	60
H15D	5827.24	9379.36	7360.07	60
H16B	7142.73	8048.22	6522.87	42
H18D	11256.08	7627.19	6941.89	110
H18E	11623.35	6472.14	6476.46	110
H18F	11180.76	6161.64	7377	110
H3C	6741.15	5956.94	4883.42	45
H4C	8928.04	4202.51	5226.14	52
H5C	10082.69	2448.97	4589.44	55
H6C	9059.36	2290.28	3600.99	50
H9C	3142.92	6592.32	2990.83	41
H10E	3860.51	7414.43	1812.47	55
H10F	5080.99	5952.62	1722.08	55
H11C	2719.39	7111.14	1065.72	48
H12C	1320.78	6742.57	2126.75	41
H14E	1506.57	4913.99	1242.85	47
H14F	236.02	6378.84	1311.28	47
H15E	-37.43	4183.81	2175.49	49
H15F	-482.43	5475.36	2558.85	49
H16C	1178.86	3940.17	3365.31	38
H18G	1566.9	-174.32	3396.71	78

H18H	3163	-289.09	3264.54	78
H18I	2221.44	301.27	2551.72	78
H3D	13103.5	12337.83	791.25	45
H4D	15159.29	11195.74	61.01	53
H5D	15344.78	9399.47	-416.35	41
H6D	13539.66	8583.48	-156.89	45
H9D	8240.08	11777.03	1668.41	38
H10G	8136.53	9831.24	952.5	52
H10H	7174.17	11459.09	806.8	52
H11D	5567.08	10989.23	1664.53	45
H12D	6470.46	11493.64	2532.52	42
H14G	5113.69	9773.78	3168.36	52
H14H	5266.17	10834.75	3561.98	52
H15G	6947.18	7935.78	3762.15	47
H15H	6515.9	8851	4387.25	47
H16D	8240.48	9722.5	3887.47	38
H18J	11161.82	6220.6	5261.84	98
H18K	12103.2	6391.79	4469.24	98
H18L	11075.97	5597.63	4591.5	98

Experimental

A suitable crystal of $C_{18}H_{17}IN_2O_5$ lub130(3), was selected and mounted on a cryoloop on a Bruker Venture Metaljet diffractometer. The crystal was kept at 150 K during data collection. Using Olex2 [1], the structure was solved with the XT [2] structure solution program using Intrinsic Phasing and refined with the XL [3] refinement package using Least Squares minimisation.

1. Dolomanov, O.V., Bourhis, L.J., Gildea, R.J, Howard, J.A.K. & Puschmann, H. (2009), J. Appl. Cryst. 42, 339-341.
2. Sheldrick, G.M. (2015). Acta Cryst. A71, 3-8.
3. Sheldrick, G.M. (2015). Acta Cryst. C71, 3-8.

Crystal structure determination of lub130(3)

Crystal Data for $C_{18}H_{17}IN_2O_5$ (M =468.23 g/mol): triclinic, space group P1 (no. 1), a = 10.4928(3) Å, b = 10.9595(3) Å, c = 18.3029(6) Å, α = 73.120(2)°, β = 78.857(2)°, γ = 64.829(2)°, V = 1816.90(10) Å^3, Z = 4, T = 150 K, μ(GaKα) = 9.682 mm^{-1}, $Dcalc$ = 1.712 g/cm^3, 28778 reflections measured (4.404° ≤ 2Θ ≤ 109.944°), 12189 unique (R_{int} = 0.0525, R_{sigma} = 0.0791) which were used in all calculations. The final R_1 was 0.0493 (I > 2σ(I)) and wR_2 was 0.1070 (all data).

Refinement model description

Number of restraints - 21, number of constraints - unknown.

Details:

```
1. Twinned data refinement
 Scales: 0.941(10)
 0.059(10)
2. Fixed Uiso
 At 1.2 times of:
  All C(H) groups, All C(H,H) groups
 At 1.5 times of:
  All C(H,H,H) groups
3. Uiso/Uaniso restraints and constraints
```

```
C17A ≈ O4A ≈ O5A ≈ C18A: within 2A with sigma of 0.002 and sigma
for terminal atoms of 0.02
4.a Ternary CH refined with riding coordinates:
 C9A(H9A), C11A(H11A), C12A(H12A), C16A(H16A), C9B(H9B), C11B(H11B),
 C12B(H12B), C16B(H16B), C9C(H9C), C11C(H11C), C12C(H12C), C16C(H16C), C9D(H9D),
  C11D(H11D), C12D(H12D), C16D(H16D)
4.b Secondary CH2 refined with riding coordinates:
 C10A(H10A,H10B), C14A(H14A,H14B), C15A(H15A,H15B), C10B(H10C,H10D), C14B(H14C,
 H14D), C15B(H15C,H15D), C10C(H10E,H10F), C14C(H14E,H14F), C15C(H15E,H15F),
 C10D(H10G,H10H), C14D(H14G,H14H), C15D(H15G,H15H)
4.c Aromatic/amide H refined with riding coordinates:
 C3A(H3A), C4A(H4A), C5A(H5A), C6A(H6A), C3B(H3B), C4B(H4B), C5B(H5B),
 C6B(H6B), C3C(H3C), C4C(H4C), C5C(H5C), C6C(H6C), C3D(H3D), C4D(H4D), C5D(H5D),
  C6D(H6D)
4.d Idealised Me refined as rotating group:
 C18A(H18A,H18B,H18C), C18B(H18D,H18E,H18F), C18C(H18G,H18H,H18I), C18D(H18J,
 H18K,H18L)
```

This report has been created with Olex2, compiled on 2018.05.29 svn.r3508 for OlexSys. Please let us know if there are any errors or if you would like to have additional features.

(3*S*,5*S*,6*S*,9*S*)-Methyl-3-(1,3-dioxoisoindolin-2-yl)-5-iodo-indolizidin-2-one-9-carboxylates
[(5*S*, 6*S*)-3.3f, lub129(2)]

Table 1 Crystal data and structure refinement for lub129(2).

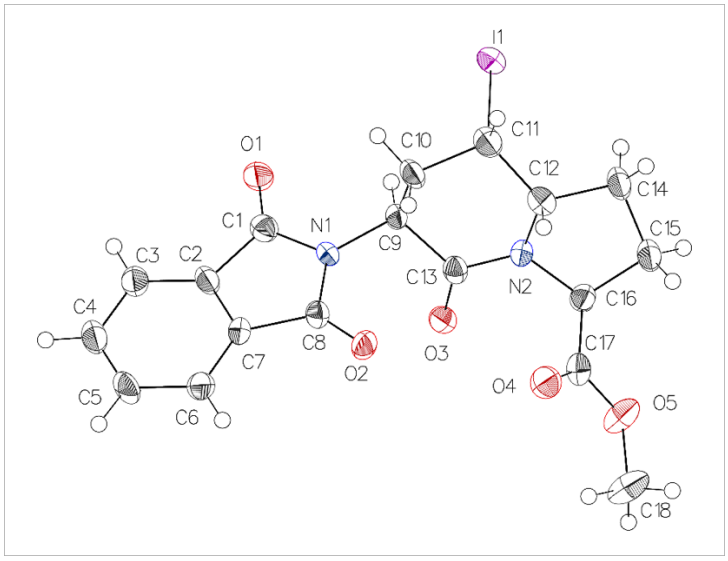

Identification code	lub129(2)
Empirical formula	$C_{18}H_{17}IN_2O_5$
Formula weight	468.23
Temperature/K	150
Crystal system	monoclinic
Space group	$P2_1$
a/Å	8.4719(2)
b/Å	11.2069(3)

c/Å	9.3465(3)
α/°	90
β/°	92.1070(10)
γ/°	90
Volume/Å^3	886.79(4)
Z	2
ρ_{calc}g/cm^3	1.754
μ/mm^{-1}	9.919
F(000)	464.0
Crystal size/mm^3	0.11 × 0.09 × 0.07
Radiation	GaKα (λ = 1.34139)
2Θ range for data collection/°	8.236 to 109.848
Index ranges	-10 ≤ h ≤ 10, -13 ≤ k ≤ 12, -11 ≤ l ≤ 11
Reflections collected	14061
Independent reflections	3320 [R_{int} = 0.0316, R_{sigma} = 0.0260]
Data/restraints/parameters	3320/1/236
Goodness-of-fit on F^2	1.065
Final R indexes [I>=2σ (I)]	R_1 = 0.0476, wR_2 = 0.1195
Final R indexes [all data]	R_1 = 0.0507, wR_2 = 0.1231
Largest diff. peak/hole / e Å^{-3}	0.70/-1.33
Flack parameter	-0.021(17)

Table 2 Fractional Atomic Coordinates (×10^4) and Equivalent Isotropic Displacement Parameters (Å^2×10^3) for lub129(2). U_{eq} is defined as 1/3 of of the trace of the orthogonalised U_{ij} tensor.

Atom	*x*	*y*	*z*	U(eq)
I1	2155.1(6)	3420.8(7)	1034.3(5)	38.7(2)
O1	7524(9)	2679(6)	3010(8)	37.3(16)
O2	6544(8)	6293(6)	5079(7)	32.2(15)
O3	6546(8)	6354(6)	1734(7)	30.2(14)
O4	4395(8)	8491(11)	3265(6)	38.6(15)
O5	4575(11)	9452(7)	1150(8)	42.2(18)
N1	6744(8)	4540(7)	3783(8)	24.5(15)
N2	3874(9)	6356(7)	1816(8)	25.7(16)
C1	7697(9)	3521(17)	3792(8)	29(2)
C2	8942(10)	3740(8)	4953(10)	28(2)
C3	10192(12)	3037(9)	5410(11)	33(2)
C4	11187(10)	3473(15)	6524(9)	36(2)
C5	10875(12)	4568(11)	7152(10)	37(2)
C6	9581(12)	5284(9)	6696(10)	34(2)
C7	8637(11)	4834(8)	5584(9)	25.8(18)

C8	7206(11)	5360(9)	4854(9)	27.1(18)
C9	5322(10)	4671(8)	2866(9)	24.9(18)
C10	3849(10)	4409(10)	3715(10)	31(2)
C11	2348(12)	4686(10)	2823(10)	33(2)
C12	2359(11)	5974(9)	2375(9)	29.2(19)
C13	5324(12)	5897(9)	2117(10)	26(2)
C14	1182(12)	6419(10)	1213(11)	35(2)
C15	1898(13)	7613(10)	736(12)	37(2)
C16	3708(12)	7485(9)	1062(10)	28(2)
C17	4292(10)	8499(14)	1977(8)	29.3(18)
C18	5045(19)	10552(12)	1880(15)	52(3)

Table 3 Anisotropic Displacement Parameters (Å²×10³) for lub129(2). The Anisotropic displacement factor exponent takes the form: $-2\pi^2[h^2a^{*2}U_{11}+2hka^*b^*U_{12}+\ldots]$.

Atom	U_{11}	U_{22}	U_{33}	U_{23}	U_{13}	U_{12}
I1	36.5(3)	33.4(3)	44.7(3)	2.3(4)	-16.6(2)	-6.8(4)
O1	40(4)	30(4)	41(4)	-13(3)	-11(3)	4(3)
O2	38(4)	23(4)	35(3)	-4(3)	-7(3)	8(3)
O3	28(3)	30(4)	32(3)	3(3)	-3(3)	-3(3)
O4	48(3)	37(4)	30(3)	0(4)	-6(2)	0(5)
O5	68(5)	26(4)	33(4)	2(3)	8(4)	3(4)
N1	21(3)	23(4)	29(4)	-1(3)	-8(3)	0(3)
N2	26(4)	22(4)	29(4)	2(3)	-5(3)	4(3)
C1	26(4)	31(7)	29(4)	1(5)	1(3)	-2(5)
C2	22(4)	34(7)	27(4)	3(3)	-5(3)	-1(3)
C3	27(4)	33(6)	38(5)	8(4)	0(4)	0(3)
C4	26(4)	45(5)	38(4)	14(7)	-4(3)	0(6)
C5	36(5)	48(6)	26(4)	7(4)	-14(4)	-5(5)
C6	42(5)	29(5)	29(4)	6(4)	-9(4)	-6(4)
C7	26(4)	23(5)	28(4)	3(3)	-4(3)	4(4)
C8	27(4)	28(5)	26(4)	6(4)	-5(3)	0(4)
C9	27(4)	22(5)	25(4)	1(3)	-9(3)	2(4)
C10	24(4)	39(5)	28(4)	6(4)	-8(3)	-3(4)
C11	29(5)	39(6)	31(4)	4(4)	-2(4)	-3(4)
C12	25(4)	34(5)	28(4)	-2(4)	0(4)	0(4)
C13	26(5)	28(6)	22(4)	0(4)	-3(3)	3(4)
C14	28(5)	38(6)	37(5)	2(4)	-10(4)	7(4)
C15	35(5)	34(6)	41(5)	-1(4)	-14(4)	8(4)
C16	33(5)	23(5)	27(4)	2(4)	-4(4)	1(4)
C17	28(4)	33(5)	27(3)	1(5)	-1(3)	9(5)

C18	77(10)	26(6)	55(8)	0(5)	10(7)	-4(6)

Table 4 Bond Lengths for lub129(2).

Atom	Atom	Length/Å	Atom	Atom	Length/Å
I1	C11	2.194(10)	C2	C7	1.389(13)
O1	C1	1.199(18)	C3	C4	1.403(15)
O2	C8	1.209(12)	C4	C5	1.39(2)
O3	C13	1.221(12)	C5	C6	1.412(15)
O4	C17	1.204(10)	C6	C7	1.383(13)
O5	C17	1.345(15)	C7	C8	1.490(12)
O5	C18	1.457(16)	C9	C10	1.531(12)
N1	C1	1.398(18)	C9	C13	1.541(13)
N1	C8	1.404(12)	C10	C11	1.527(13)
N1	C9	1.460(11)	C11	C12	1.503(15)
N2	C12	1.468(12)	C12	C14	1.531(13)
N2	C13	1.352(12)	C14	C15	1.542(16)
N2	C16	1.453(12)	C15	C16	1.559(14)
C1	C2	1.505(12)	C16	C17	1.495(16)
C2	C3	1.375(13)			

Table 5 Bond Angles for lub129(2).

Atom	Atom	Atom	Angle/°	Atom	Atom	Atom	Angle/°
C17	O5	C18	117.0(9)	N1	C8	C7	105.6(8)
C1	N1	C8	112.6(8)	N1	C9	C10	110.3(7)
C1	N1	C9	123.3(8)	N1	C9	C13	110.0(7)
C8	N1	C9	123.7(7)	C10	C9	C13	114.9(8)
C13	N2	C12	127.9(7)	C11	C10	C9	110.9(7)
C13	N2	C16	120.3(8)	C10	C11	I1	108.7(7)
C16	N2	C12	110.9(8)	C12	C11	I1	114.2(6)
O1	C1	N1	125.6(8)	C12	C11	C10	109.5(8)
O1	C1	C2	129.4(12)	N2	C12	C11	113.2(8)
N1	C1	C2	105.1(12)	N2	C12	C14	102.0(7)
C3	C2	C1	129.9(10)	C11	C12	C14	120.0(9)
C3	C2	C7	121.8(9)	O3	C13	N2	123.6(9)
C7	C2	C1	108.3(10)	O3	C13	C9	121.5(9)
C2	C3	C4	117.8(11)	N2	C13	C9	114.7(8)
C5	C4	C3	120.1(10)	C12	C14	C15	103.6(8)
C4	C5	C6	122.1(9)	C14	C15	C16	104.9(8)

C7	C6	C5	116.1(10)	N2	C16	C15	104.6(8)
C2	C7	C8	108.4(8)	N2	C16	C17	111.1(8)
C6	C7	C2	122.0(9)	C17	C16	C15	110.1(9)
C6	C7	C8	129.6(9)	O4	C17	O5	124.9(13)
O2	C8	N1	124.8(8)	O4	C17	C16	125.2(12)
O2	C8	C7	129.6(9)	O5	C17	C16	109.7(7)

Table 6 Torsion Angles for lub129(2).

A	B	C	D	Angle/°	A	B	C	D	Angle/°
I1	C11	C12	N2	-76.0(9)	C8	N1	C9	C10	-73.2(11)
I1	C11	C12	C14	44.5(11)	C8	N1	C9	C13	54.6(11)
O1	C1	C2	C3	0.1(18)	C9	N1	C1	O1	4.6(15)
O1	C1	C2	C7	-178.9(10)	C9	N1	C1	C2	-176.1(8)
N1	C1	C2	C3	-179.1(9)	C9	N1	C8	O2	-4.8(14)
N1	C1	C2	C7	1.8(10)	C9	N1	C8	C7	175.9(8)
N1	C9	C10	C11	173.2(8)	C9	C10	C11	I1	67.0(9)
N1	C9	C13	O3	35.2(12)	C9	C10	C11	C12	-58.4(11)
N1	C9	C13	N2	-150.3(8)	C10	C9	C13	O3	160.4(8)
N2	C12	C14	C15	-36.6(9)	C10	C9	C13	N2	-25.1(11)
N2	C16	C17	O4	-23.1(14)	C10	C11	C12	N2	46.2(10)
N2	C16	C17	O5	161.5(8)	C10	C11	C12	C14	166.7(8)
C1	N1	C8	O2	-178.3(9)	C11	C12	C14	C15	-162.6(8)
C1	N1	C8	C7	2.4(10)	C12	N2	C13	O3	-171.2(9)
C1	N1	C9	C10	99.6(10)	C12	N2	C13	C9	14.4(13)
C1	N1	C9	C13	-132.7(9)	C12	N2	C16	C15	-17.9(10)
C1	C2	C3	C4	179.6(9)	C12	N2	C16	C17	100.9(9)
C1	C2	C7	C6	179.9(9)	C12	C14	C15	C16	26.6(10)
C1	C2	C7	C8	-0.4(10)	C13	N2	C12	C11	-26.1(13)
C2	C3	C4	C5	1.5(14)	C13	N2	C12	C14	-156.4(9)
C2	C7	C8	O2	179.6(9)	C13	N2	C16	C15	172.3(8)
C2	C7	C8	N1	-1.1(10)	C13	N2	C16	C17	-68.9(11)
C3	C2	C7	C6	0.7(14)	C13	C9	C10	C11	48.2(11)
C3	C2	C7	C8	-179.6(9)	C14	C15	C16	N2	-6.4(10)
C3	C4	C5	C6	-0.8(15)	C14	C15	C16	C17	-125.8(9)
C4	C5	C6	C7	0.0(14)	C15	C16	C17	O4	92.4(12)
C5	C6	C7	C2	0.1(14)	C15	C16	C17	O5	-83.1(10)
C5	C6	C7	C8	-179.6(9)	C16	N2	C12	C11	165.1(8)
C6	C7	C8	O2	-0.7(17)	C16	N2	C12	C14	34.8(10)
C6	C7	C8	N1	178.5(9)	C16	N2	C13	O3	-3.3(14)
C7	C2	C3	C4	-1.5(14)	C16	N2	C13	C9	-177.7(8)

C8	N1	C1	O1	178.1(10)	C18	O5	C17	O4	0.2(15)
C8	N1	C1	C2	-2.7(10)	C18	O5	C17	C16	175.7(10)

Table 7 Hydrogen Atom Coordinates (Å×10^4) and Isotropic Displacement Parameters (Å^2×10^3) for lub129(2).

Atom	*x*	*y*	*z*	U(eq)
H3	10375.07	2281.97	4985.12	40
H4	12076.09	3018.06	6849.57	43
H5	11554.41	4843.41	7913.43	45
H6	9370.43	6032.09	7128.45	40
H9	5372.6	4050.63	2100.88	30
H10A	3847.82	3557.71	3998.56	37
H10B	3873.15	4897.53	4597.44	37
H11	1423.56	4559.28	3441.22	40
H12	2182.59	6459.92	3252.47	35
H14A	122.92	6539.02	1601.62	42
H14B	1096.51	5848.23	404.66	42
H15A	1459.68	8286.52	1280.85	44
H15B	1676.72	7750.31	-298.25	44
H16	4287.66	7459.68	149.67	34
H18A	5437.87	10367.11	2853.7	79
H18B	4132.15	11086.32	1921.82	79
H18C	5880.97	10942.33	1353.57	79

Experimental

A suitable crystal of $C_{18}H_{17}IN_2O_5$ lub129(2) was selected and mounted on a cryoloop on a Bruker Venture Metaljet diffractometer. The crystal was kept at 150 K during data collection. Using Olex2 [1], the structure was solved with the XT [2] structure solution program using Intrinsic Phasing and refined with the XL [3] refinement package using Least Squares minimisation.

1. Dolomanov, O.V., Bourhis, L.J., Gildea, R.J, Howard, J.A.K. & Puschmann, H. (2009), J. Appl. Cryst. 42, 339-341.
2. Sheldrick, G.M. (2015). Acta Cryst. A71, 3-8.
3. Sheldrick, G.M. (2015). Acta Cryst. C71, 3-8.

Crystal structure determination of lub129(2)

Crystal Data for $C_{18}H_{17}IN_2O_5$ (M =468.23 g/mol): monoclinic, space group $P2_1$ (no. 4), a = 8.4719(2) Å, b = 11.2069(3) Å, c = 9.3465(3) Å, β = 92.1070(10)°, V = 886.79(4) Å^3, Z = 2, T = 150 K, μ(GaKα) = 9.919 mm^{-1}, $Dcalc$ = 1.754 g/cm^3, 14061 reflections measured (8.236° ≤ 2Θ ≤ 109.848°), 3320 unique (R_{int} = 0.0316, R_{sigma} = 0.0260) which were used in all calculations. The final R_1 was 0.0476 (I > 2σ(I)) and wR_2 was 0.1231 (all data).

Refinement model description

Number of restraints - 1, number of constraints - unknown.

Details:

```
1. Fixed Uiso
 At 1.2 times of:
```

```
  All C(H) groups, All C(H,H) groups
 At 1.5 times of:
  All C(H,H,H) groups
2.a Ternary CH refined with riding coordinates:
 C9(H9), C11(H11), C12(H12), C16(H16)
2.b Secondary CH2 refined with riding coordinates:
 C10(H10A,H10B), C14(H14A,H14B), C15(H15A,H15B)
2.c Aromatic/amide H refined with riding coordinates:
 C3(H3), C4(H4), C5(H5), C6(H6)
2.d Idealised Me refined as rotating group:
 C18(H18A,H18B,H18C)
```

This report has been created with Olex2, compiled on 2018.05.29 svn.r3508 for OlexSys. Please let us know if there are any errors or if you would like to have additional features.

(2*S*,5*R*,6*R*,9*S*)-methyl 8-(*N*-benzyl-*N*-(2-nitrophenyl)sulfonamido)-5-iodo-indolizidin-9-one-2-carboxylate **(3.8e, lub134)**

Table 1 Crystal data and structure refinement for lub134.

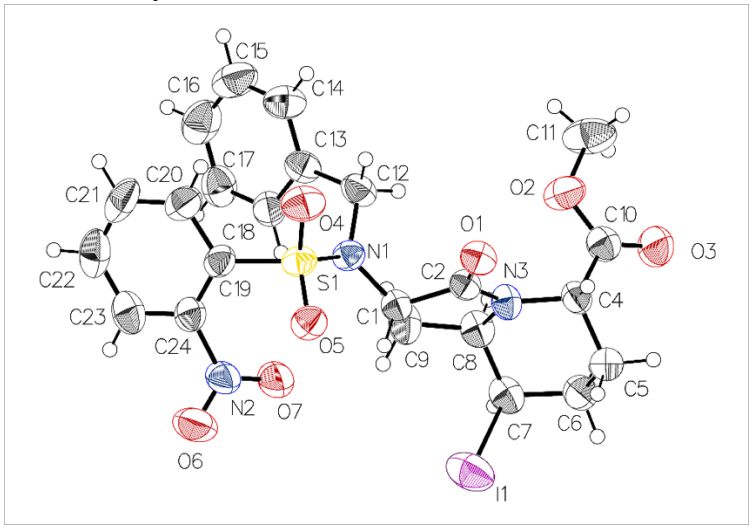

Identification code	lub134
Empirical formula	$C_{23}H_{24}IN_3O_7S$
Formula weight	613.41
Temperature/K	295
Crystal system	orthorhombic
Space group	$P2_12_12_1$
a/Å	7.8514(4)
b/Å	11.5391(6)
c/Å	27.4981(12)
α/°	90
β/°	90
γ/°	90

Volume/Å^3	2491.3(2)
Z	4
ρ_{calc}g/cm^3	1.635
μ/mm^{-1}	7.716
F(000)	1232.0
Crystal size/mm^3	0.12 × 0.11 × 0.06
Radiation	GaKα (λ = 1.34139)
2Θ range for data collection/°	5.592 to 110.014
Index ranges	$-9 \leq h \leq 9$, $-14 \leq k \leq 14$, $-32 \leq l \leq 33$
Reflections collected	19664
Independent reflections	4694 [R_{int} = 0.0504, R_{sigma} = 0.0393]
Data/restraints/parameters	4694/0/318
Goodness-of-fit on F^2	1.059
Final R indexes [I>=2σ (I)]	R_1 = 0.0431, wR_2 = 0.1035
Final R indexes [all data]	R_1 = 0.0555, wR_2 = 0.1122
Largest diff. peak/hole / e Å^{-3}	0.52/-0.63
Flack parameter	-0.033(6)

Table 2 Fractional Atomic Coordinates (×10^4) and Equivalent Isotropic Displacement Parameters (Å^2×10^3) for lub134. U_{eq} is defined as 1/3 of of the trace of the orthogonalised U_{ij} tensor.

Atom	*x*	*y*	*z*	U(eq)
I1	9349.0(7)	3590.8(6)	2470.6(2)	86.5(3)
S1	3814.1(19)	6212.8(14)	3519.8(5)	45.0(4)
O5	3612(6)	5745(4)	3043.9(16)	52.7(11)
O4	2509(6)	6037(5)	3871(2)	66.7(14)
O1	5204(5)	3239(4)	3811.3(16)	49.5(11)
O2	8708(7)	2751(5)	4640.9(18)	67.3(14)
N1	5619(7)	5762(4)	3739.5(17)	43.1(11)
O7	6741(7)	6918(5)	2805(2)	74.6(16)
N3	8097(6)	3261(4)	3710(2)	46.0(12)
N2	5707(9)	7648(5)	2697(2)	59.1(15)
O3	10364(7)	1261(5)	4436(2)	73.7(15)
C2	6507(7)	3702(5)	3688(2)	41.6(13)
O6	5329(10)	7893(7)	2282(2)	98(2)
C4	8477(8)	2069(5)	3839(2)	45.8(14)
C24	4895(8)	8301(6)	3091(2)	50.3(15)
C13	6310(9)	7124(6)	4425(2)	48.7(15)
C1	6665(8)	4935(5)	3475(2)	43.2(14)
C8	9477(8)	4038(5)	3576(3)	50.2(15)
C12	5896(10)	5891(6)	4269(2)	52.6(16)
C18	7348(10)	7841(6)	4148(3)	53.2(16)

C10	9313(9)	1981(6)	4333(2)	51.1(15)
C7	10580(9)	3515(6)	3179(2)	54.7(15)
C19	4026(8)	7740(5)	3463(2)	47.3(15)
C17	7694(10)	8946(6)	4299(3)	64.1(19)
C5	9558(10)	1524(6)	3435(2)	56.8(16)
C6	11067(10)	2273(6)	3301(3)	58.1(18)
C14	5658(12)	7548(7)	4854(3)	63.2(19)
C9	8604(9)	5195(6)	3491(3)	59.1(18)
C23	5034(10)	9487(7)	3057(3)	66(2)
C20	3257(9)	8448(7)	3814(3)	59.0(18)
C22	4297(13)	10161(7)	3426(4)	74(2)
C16	7040(12)	9357(8)	4724(3)	78(2)
C21	3424(11)	9642(7)	3792(3)	74(2)
C15	6024(12)	8649(8)	5004(3)	78(2)
C11	9321(14)	2660(10)	5143(3)	88(3)

Table 3 Anisotropic Displacement Parameters ($Å^2 \times 10^3$) for lub134. The Anisotropic displacement factor exponent takes the form: $-2\pi^2[h^2a^{*2}U_{11}+2hka^*b^*U_{12}+\ldots]$.

Atom	U_{11}	U_{22}	U_{33}	U_{23}	U_{13}	U_{12}
I1	73.1(4)	126.6(6)	59.7(3)	20.7(3)	-2.6(3)	10.2(3)
S1	37.8(7)	53.5(8)	43.6(8)	-3.2(7)	2.0(6)	-1.0(6)
O5	53(3)	58(3)	48(2)	-7(2)	-9(2)	1(2)
O4	47(2)	84(4)	69(3)	-1(3)	20(2)	-8(3)
O1	41(2)	54(3)	54(3)	3(2)	3.1(19)	-11(2)
O2	61(3)	89(4)	51(3)	-14(3)	-4(2)	19(3)
N1	41(3)	48(3)	41(3)	-4(2)	-1(2)	2(2)
O7	77(4)	80(3)	67(3)	20(3)	22(3)	26(3)
N3	38(3)	42(3)	57(3)	8(2)	0(2)	-3(2)
N2	55(3)	69(4)	54(3)	16(3)	15(3)	14(3)
O3	79(3)	75(3)	67(3)	1(3)	-14(3)	26(3)
C2	41(3)	43(3)	41(3)	2(3)	-1(2)	-3(3)
O6	113(5)	132(6)	50(3)	20(3)	12(3)	51(5)
C4	47(3)	44(3)	46(4)	8(3)	2(3)	0(3)
C24	48(4)	51(4)	51(4)	2(3)	-5(3)	9(3)
C13	48(3)	57(4)	41(3)	-1(3)	-8(3)	-7(3)
C1	37(3)	45(3)	48(3)	5(3)	2(3)	0(3)
C8	36(3)	54(4)	61(4)	7(3)	0(3)	-5(3)
C12	64(4)	54(4)	40(3)	5(3)	-7(3)	-8(3)
C18	59(4)	48(4)	52(4)	1(3)	-3(3)	1(3)
C10	46(3)	53(4)	55(4)	5(3)	2(3)	-4(3)
C7	41(3)	61(4)	62(4)	14(3)	1(3)	-3(3)
C19	45(4)	50(3)	47(3)	-4(3)	-3(3)	11(3)

C17	68(5)	53(4)	71(5)	4(4)	-9(4)	-7(4)
C5	69(4)	52(4)	50(4)	1(3)	5(3)	6(3)
C6	53(4)	63(4)	58(4)	8(3)	7(3)	11(3)
C14	65(5)	76(5)	48(4)	-7(3)	1(4)	-10(4)
C9	42(3)	49(4)	86(5)	14(4)	6(4)	-4(3)
C23	60(4)	63(5)	76(5)	16(4)	-10(4)	9(4)
C20	57(4)	66(5)	54(4)	-12(4)	-3(3)	12(3)
C22	76(5)	49(4)	96(6)	-1(4)	-28(5)	14(4)
C16	85(6)	66(5)	82(6)	-21(5)	-22(5)	3(5)
C21	70(5)	66(5)	85(6)	-28(5)	-22(5)	34(4)
C15	81(6)	96(6)	57(4)	-24(5)	-5(4)	12(5)
C11	69(5)	141(9)	55(5)	-24(5)	-14(5)	11(6)

Table 4 Bond Lengths for lub134.

Atom	Atom	Length/Å	Atom	Atom	Length/Å
I1	C7	2.175(7)	C4	C5	1.533(9)
S1	O5	1.425(5)	C24	C19	1.389(9)
S1	O4	1.421(5)	C24	C23	1.376(11)
S1	N1	1.626(5)	C13	C12	1.522(9)
S1	C19	1.777(6)	C13	C18	1.390(10)
O1	C2	1.203(7)	C13	C14	1.375(10)
O2	C10	1.317(8)	C1	C9	1.552(9)
O2	C11	1.465(9)	C8	C7	1.520(10)
N1	C1	1.454(8)	C8	C9	1.519(9)
N1	C12	1.479(8)	C18	C17	1.368(10)
O7	N2	1.208(8)	C7	C6	1.521(10)
N3	C2	1.350(8)	C19	C20	1.402(9)
N3	C4	1.451(8)	C17	C16	1.363(12)
N3	C8	1.453(8)	C5	C6	1.512(10)
N2	O6	1.211(8)	C14	C15	1.367(12)
N2	C24	1.466(9)	C23	C22	1.403(12)
O3	C10	1.205(8)	C20	C21	1.386(12)
C2	C1	1.543(8)	C22	C21	1.356(13)
C4	C10	1.512(9)	C16	C15	1.377(13)

Table 5 Bond Angles for lub134.

Atom	Atom	Atom	Angle/°	Atom	Atom	Atom	Angle/°
O5	S1	N1	108.5(3)	N1	C1	C2	111.7(5)
O5	S1	C19	107.8(3)	N1	C1	C9	114.4(5)
O4	S1	O5	119.3(3)	C2	C1	C9	104.3(5)
O4	S1	N1	109.3(3)	N3	C8	C7	111.2(5)
O4	S1	C19	105.6(3)	N3	C8	C9	104.2(5)

N1	S1	C19	105.5(3)	C9	C8	C7	119.7(6)
C10	O2	C11	116.0(6)	N1	C12	C13	113.8(5)
C1	N1	S1	121.1(4)	C17	C18	C13	120.3(7)
C1	N1	C12	118.3(5)	O2	C10	C4	112.1(6)
C12	N1	S1	117.5(4)	O3	C10	O2	124.1(6)
C2	N3	C4	124.0(5)	O3	C10	C4	123.8(6)
C2	N3	C8	116.5(5)	C8	C7	I1	112.0(4)
C4	N3	C8	119.5(5)	C8	C7	C6	111.0(6)
O7	N2	O6	123.9(6)	C6	C7	I1	110.4(5)
O7	N2	C24	118.0(6)	C24	C19	S1	124.9(5)
O6	N2	C24	118.0(6)	C24	C19	C20	116.6(6)
O1	C2	N3	127.3(6)	C20	C19	S1	118.5(5)
O1	C2	C1	125.8(6)	C16	C17	C18	120.7(8)
N3	C2	C1	106.9(5)	C6	C5	C4	112.0(6)
N3	C4	C10	111.9(5)	C5	C6	C7	113.3(6)
N3	C4	C5	109.0(5)	C15	C14	C13	120.8(8)
C10	C4	C5	112.5(6)	C8	C9	C1	106.1(5)
C19	C24	N2	121.3(6)	C24	C23	C22	118.0(8)
C23	C24	N2	115.2(7)	C21	C20	C19	120.5(8)
C23	C24	C19	123.5(7)	C21	C22	C23	120.0(7)
C18	C13	C12	121.8(6)	C17	C16	C15	119.4(8)
C14	C13	C12	119.7(6)	C22	C21	C20	121.3(7)
C14	C13	C18	118.5(7)	C14	C15	C16	120.3(8)

Table 6 Hydrogen Bonds for lub134.

D	H	A	d(D-H)/Å	d(H-A)/Å	d(D-A)/Å	D-H-A/°
C1	H1	O5	0.98	2.32	2.833(8)	111.4
C7	H7	O5[1]	0.98	2.59	3.526(8)	159.4
C6	H6A	O7[2]	0.97	2.61	3.518(9)	156.4
C9	H9A	O7	0.97	2.60	3.107(9)	113.1
C23	H23	O5[3]	0.93	2.62	3.522(10)	164.5
C11	H11A	O2[4]	0.96	2.59	3.528(12)	166.5

[1]1+X,+Y,+Z; [2]2-X,-1/2+Y,1/2-Z; [3]1-X,1/2+Y,1/2-Z; [4]1/2+X,1/2-Y,1-Z

Table 7 Torsion Angles for lub134.

A	B	C	D	Angle/°	A	B	C	D	Angle/°
I1	C7	C6	C5	-73.4(7)	C4	N3	C2	C1	-172.9(5)
S1	N1	C1	C2	-102.6(5)	C4	N3	C8	C7	52.3(8)
S1	N1	C1	C9	139.2(5)	C4	N3	C8	C9	-177.4(6)
S1	N1	C12	C13	-76.2(7)	C4	C5	C6	C7	-52.9(8)

S1	C19	C20	C21	178.4(6)	C24	C19	C20	C21	-2.1(10)
O5	S1	N1	C1	-4.9(5)	C24	C23	C22	C21	-2.4(12)
O5	S1	N1	C12	-164.8(4)	C13	C18	C17	C16	0.5(12)
O5	S1	C19	C24	-37.4(7)	C13	C14	C15	C16	0.7(13)
O5	S1	C19	C20	142.1(5)	C1	N1	C12	C13	123.4(6)
O4	S1	N1	C1	126.6(5)	C8	N3	C2	O1	-174.8(6)
O4	S1	N1	C12	-33.3(5)	C8	N3	C2	C1	4.8(7)
O4	S1	C19	C24	-165.9(6)	C8	N3	C4	C10	72.8(7)
O4	S1	C19	C20	13.6(6)	C8	N3	C4	C5	-52.3(8)
O1	C2	C1	N1	43.5(9)	C8	C7	C6	C5	51.4(8)
O1	C2	C1	C9	167.6(6)	C12	N1	C1	C2	57.1(7)
N1	S1	C19	C24	78.4(6)	C12	N1	C1	C9	-61.1(7)
N1	S1	C19	C20	-102.1(5)	C12	C13	C18	C17	180.0(7)
N1	C1	C9	C8	137.1(6)	C12	C13	C14	C15	179.5(7)
O7	N2	C24	C19	-56.2(9)	C18	C13	C12	N1	-38.7(9)
O7	N2	C24	C23	125.0(7)	C18	C13	C14	C15	-0.1(12)
N3	C2	C1	N1	-136.1(5)	C18	C17	C16	C15	0.1(13)
N3	C2	C1	C9	-12.0(7)	C10	C4	C5	C6	-74.6(7)
N3	C4	C10	O2	35.8(8)	C7	C8	C9	C1	112.9(7)
N3	C4	C10	O3	-146.7(7)	C19	S1	N1	C1	-120.3(5)
N3	C4	C5	C6	50.2(8)	C19	S1	N1	C12	79.9(5)
N3	C8	C7	I1	75.6(6)	C19	C24	C23	C22	1.8(12)
N3	C8	C7	C6	-48.3(8)	C19	C20	C21	C22	1.5(12)
N3	C8	C9	C1	-12.1(8)	C17	C16	C15	C14	-0.7(13)
N2	C24	C19	S1	1.2(9)	C5	C4	C10	O2	159.0(6)
N2	C24	C19	C20	-178.3(6)	C5	C4	C10	O3	-23.5(9)
N2	C24	C23	C22	-179.4(7)	C14	C13	C12	N1	141.8(7)
C2	N3	C4	C10	-109.6(7)	C14	C13	C18	C17	-0.5(11)
C2	N3	C4	C5	125.2(7)	C9	C8	C7	I1	-46.0(7)
C2	N3	C8	C7	-125.4(6)	C9	C8	C7	C6	-169.9(6)
C2	N3	C8	C9	4.8(8)	C23	C24	C19	S1	179.9(6)
C2	C1	C9	C8	14.7(8)	C23	C24	C19	C20	0.4(10)
O6	N2	C24	C19	125.4(8)	C23	C22	C21	C20	0.8(13)
O6	N2	C24	C23	-53.4(11)	C11	O2	C10	O3	-3.2(11)
C4	N3	C2	O1	7.5(10)	C11	O2	C10	C4	174.3(7)

Table 8 Hydrogen Atom Coordinates (Å×10^4) and Isotropic Displacement Parameters (Å^2×10^3) for lub134.

Atom	*x*	*y*	*z*	U(eq)
H4	7396.66	1645.79	3853.51	55
H1	6294.99	4920.35	3134.98	52
H8	10199.99	4127.54	3864.09	60

H12A	6823.44	5386.36	4366.34	63
H12B	4879.16	5636.6	4438.64	63
H18	7809.71	7569.11	3857.83	64
H7	11631	3969.92	3159.59	66
H17	8382.28	9421.62	4109.51	77
H5A	9961.23	771.1	3541.48	68
H5B	8853.99	1407.23	3148.84	68
H6A	11642.22	1931.89	3023.74	70
H6B	11863.19	2279.23	3570.98	70
H14	4960.11	7079.64	5044.15	76
H9A	8977.82	5534.37	3186.82	71
H9B	8863.58	5729.99	3753.2	71
H23	5599.57	9831.98	2797.86	80
H20	2629.79	8112.83	4064.59	71
H22	4407.07	10963.1	3420.3	89
H16	7278.4	10109.72	4824.82	93
H21	2927.74	10096.79	4032.68	88
H15	5584.19	8921.9	5296.65	94
H11A	10535	2562.29	5142.22	132
H11B	8797.64	2003.87	5297.23	132
H11C	9030.97	3352.27	5317.44	132

Experimental

A suitable crystal of $C_{23}H_{24}IN_3O_7S$ lub134, was selected and mounted on a cryoloop on a Bruker Venture Metaljet diffractometer. The crystal was kept at 295 K during data collection. Using Olex2 [1], the structure was solved with the ShelXT [2] structure solution program using Intrinsic Phasing and refined with the XL [3] refinement package using Least Squares minimisation.

1. Dolomanov, O.V., Bourhis, L.J., Gildea, R.J, Howard, J.A.K. & Puschmann, H. (2009), J. Appl. Cryst. 42, 339-341.
2. Sheldrick, G.M. (2015). Acta Cryst. A71, 3-8.
3. Sheldrick, G.M. (2015). Acta Cryst. C71, 3-8.

Crystal structure determination of lub134

Crystal Data for $C_{23}H_{24}IN_3O_7S$ (M =613.41 g/mol): orthorhombic, space group $P2_12_12_1$ (no. 19), a = 7.8514(4) Å, b = 11.5391(6) Å, c = 27.4981(12) Å, V = 2491.3(2) Å^3, Z = 4, T = 295 K, μ(GaKα) = 7.716 mm^{-1}, $Dcalc$ = 1.635 g/cm^3, 19664 reflections measured (5.592° ≤ 2Θ ≤ 110.014°), 4694 unique (R_{int} = 0.0504, R_{sigma} = 0.0393) which were used in all calculations. The final R_1 was 0.0431 (I > 2σ(I)) and wR_2 was 0.1122 (all data).

Refinement model description

Number of restraints - 0, number of constraints - unknown.

Details:

```
1. Fixed Uiso
 At 1.2 times of:
  All C(H) groups, All C(H,H) groups
 At 1.5 times of:
  All C(H,H,H) groups
2.a Ternary CH refined with riding coordinates:
 C4(H4), C1(H1), C8(H8), C7(H7)
```

```
2.b Secondary CH2 refined with riding coordinates:
 C12(H12A,H12B), C5(H5A,H5B), C6(H6A,H6B), C9(H9A,H9B)
2.c Aromatic/amide H refined with riding coordinates:
 C18(H18), C17(H17), C14(H14), C23(H23), C20(H20), C22(H22), C16(H16),
 C21(H21), C15(H15)
2.d Idealised Me refined as rotating group:
 C11(H11A,H11B,H11C)
```

This report has been created with Olex2, compiled on 2018.05.29 svn.r3508 for OlexSys. Please let us know if there are any errors or if you would like to have additional features.

(2*S*,5*R*,6*R*,9*S*)-methyl 8-(1,3-dioxoisoindolin-2-yl)-5-iodo-indolizidin-9-one-2-carboxylate **(3.8f, lub 129)**

Table 1 Crystal data and structure refinement for lub129.

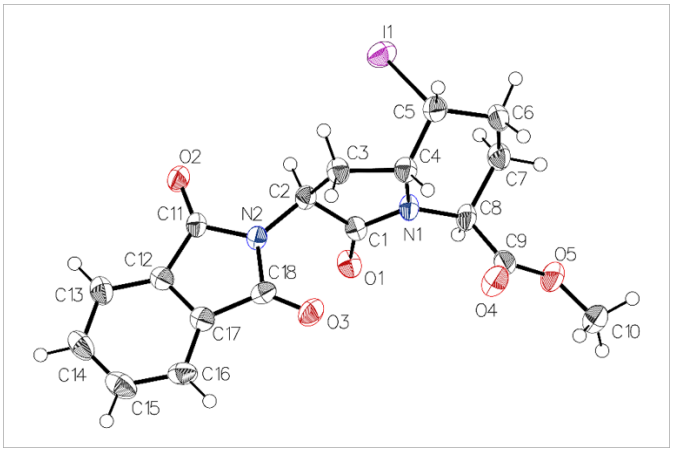

Identification code	lub129
Empirical formula	$C_{18}H_{17}IN_2O_5$
Formula weight	468.23
Temperature/K	150
Crystal system	orthorhombic
Space group	$P2_12_12_1$
a/Å	9.4104(6)
b/Å	13.1390(8)
c/Å	14.3976(9)
α/°	90
β/°	90
γ/°	90
Volume/Å^3	1780.17(19)
Z	4
ρ_{calc}g/cm^3	1.747
μ/mm^{-1}	9.882
F(000)	928.0
Crystal size/mm^3	0.17 × 0.13 × 0.08
Radiation	GaKα (λ = 1.34139)

2Θ range for data collection/°	7.926 to 121.58
Index ranges	$-10 \leq h \leq 12$, $-17 \leq k \leq 16$, $-16 \leq l \leq 18$
Reflections collected	11595
Independent reflections	3923 [R_{int} = 0.0478, R_{sigma} = 0.0442]
Data/restraints/parameters	3923/0/237
Goodness-of-fit on F^2	1.069
Final R indexes [I>=2σ (I)]	R_1 = 0.0319, wR_2 = 0.0813
Final R indexes [all data]	R_1 = 0.0333, wR_2 = 0.0827
Largest diff. peak/hole / e $Å^{-3}$	0.51/-1.02
Flack parameter	-0.031(5)

Table 2 Fractional Atomic Coordinates (×10^4) and Equivalent Isotropic Displacement Parameters (Å^2×10^3) for lub129. U_{eq} is defined as 1/3 of of the trace of the orthogonalised U_{ij} tensor.

Atom	*x*	*y*	*z*	U(eq)
I1	6423.6(4)	3249.4(3)	1758.5(2)	43.89(15)
O1	8377(3)	3723(3)	4811(2)	32.2(7)
O2	6892(4)	557(3)	4488(3)	36.8(8)
O3	5457(4)	3377(3)	6090(3)	41.2(8)
O4	5609(4)	6205(3)	4770(3)	43.3(9)
O5	7474(5)	7091(3)	4206(3)	44.1(9)
N1	6618(4)	4438(3)	3919(3)	27.7(8)
N2	6268(4)	2122(3)	5105(3)	25.0(7)
C1	7248(5)	3674(3)	4391(3)	26.0(9)
C2	6342(5)	2718(3)	4269(3)	26.7(8)
C3	4899(5)	3131(4)	3907(4)	30.2(9)
C4	5213(5)	4214(4)	3548(4)	29.3(10)
C5	5174(6)	4397(4)	2503(4)	35.0(11)
C6	5735(6)	5459(4)	2276(4)	36.6(11)
C7	7218(6)	5639(4)	2671(4)	36.8(11)
C8	7311(5)	5406(3)	3721(4)	30.0(10)
C9	6670(5)	6259(4)	4306(3)	32.1(10)
C10	7053(8)	7996(4)	4704(5)	47.5(14)
C11	6548(5)	1077(3)	5148(3)	26.6(8)
C12	6347(5)	784(3)	6136(3)	27.5(9)
C13	6522(6)	-142(4)	6571(4)	35.9(10)
C14	6233(6)	-197(5)	7524(4)	40.8(12)
C15	5778(6)	651(5)	8005(4)	44.1(13)
C16	5619(6)	1594(4)	7571(3)	37.1(11)
C17	5904(5)	1640(4)	6623(3)	29.8(9)
C18	5825(5)	2507(4)	5964(3)	29.6(9)

Table 3 Anisotropic Displacement Parameters ($Å^2 \times 10^3$) for lub129. The Anisotropic displacement factor exponent takes the form: $-2\pi^2[h^2a^{*2}U_{11}+2hka^*b^*U_{12}+\ldots]$.

Atom	U_{11}	U_{22}	U_{33}	U_{23}	U_{13}	U_{12}
I1	54.0(2)	39.4(2)	38.3(2)	-9.28(14)	4.41(15)	0.97(16)
O1	22.5(15)	34.1(16)	40.1(18)	7.7(14)	-4.7(14)	-2.0(13)
O2	53(2)	23.7(16)	33.8(19)	-2.2(14)	5.9(15)	5.6(14)
O3	52(2)	29.1(18)	42(2)	-7.9(16)	6.2(16)	7.4(16)
O4	46(2)	32.4(19)	51(2)	-6.1(17)	7.9(19)	-2.7(16)
O5	57(2)	26.9(17)	49(2)	-1.0(16)	1.4(19)	-11.2(16)
N1	26.3(18)	20.1(16)	37(2)	4.5(15)	-2.9(16)	-1.4(14)
N2	26.0(17)	20.5(15)	28.3(18)	0.6(13)	3.3(15)	0.7(14)
C1	24(2)	26(2)	28(2)	3.2(18)	3.2(17)	2.3(16)
C2	28(2)	22.9(19)	29(2)	0.7(17)	1.9(19)	-1.9(18)
C3	25.9(19)	28(2)	36(2)	5(2)	-2.9(17)	-2.6(18)
C4	26(2)	28(2)	34(2)	1.7(19)	-2.4(18)	0.4(17)
C5	39(3)	30(3)	36(3)	-1(2)	-4(2)	4(2)
C6	51(3)	28(2)	31(3)	6(2)	3(2)	4(2)
C7	47(3)	28(2)	36(3)	4(2)	7(2)	-5(2)
C8	30(2)	21(2)	39(3)	3.9(19)	-2.5(18)	-4.3(17)
C9	38(3)	28(2)	30(2)	5.9(18)	-7(2)	-2.3(19)
C10	64(4)	30(3)	49(3)	-5(2)	-10(3)	-2(2)
C11	27(2)	22.0(19)	31(2)	2.6(16)	0.1(19)	-1.6(17)
C12	24.2(19)	31(2)	27(2)	2.3(17)	0.2(18)	-4.0(18)
C13	37(2)	31(2)	39(3)	8(2)	-1(2)	-3(2)
C14	40(3)	46(3)	36(3)	17(2)	0(2)	-8(2)
C15	43(3)	59(3)	31(3)	11(2)	0(2)	-10(3)
C16	42(2)	45(3)	25(2)	-6(2)	4.5(19)	-4(2)
C17	27.2(18)	33(2)	30(2)	1(2)	0.8(16)	-2.1(17)
C18	30(2)	30(2)	29(2)	-6.5(19)	1.1(18)	-3.7(18)

Table 4 Bond Lengths for lub129.

Atom	Atom	Length/Å	Atom	Atom	Length/Å
I1	C5	2.192(5)	C3	C4	1.543(7)
O1	C1	1.224(6)	C4	C5	1.524(8)
O2	C11	1.215(6)	C5	C6	1.527(7)
O3	C18	1.209(6)	C6	C7	1.526(8)
O4	C9	1.203(6)	C7	C8	1.544(7)
O5	C9	1.337(6)	C8	C9	1.526(7)
O5	C10	1.443(7)	C11	C12	1.485(6)
N1	C1	1.350(6)	C12	C13	1.379(7)
N1	C4	1.456(6)	C12	C17	1.389(7)
N1	C8	1.458(6)	C13	C14	1.400(8)

N2	C2	1.438(6)	C14	C15	1.380(9)
N2	C11	1.399(6)	C15	C16	1.396(8)
N2	C18	1.399(6)	C16	C17	1.392(7)
C1	C2	1.529(6)	C17	C18	1.484(7)
C2	C3	1.553(6)			

Table 5 Bond Angles for lub129.

Atom	Atom	Atom	Angle/°	Atom	Atom	Atom	Angle/°
C9	O5	C10	117.7(5)	N1	C8	C7	109.8(4)
C1	N1	C4	115.7(4)	N1	C8	C9	110.9(4)
C1	N1	C8	123.5(4)	C9	C8	C7	111.9(4)
C4	N1	C8	120.7(4)	O4	C9	O5	125.3(5)
C11	N2	C2	124.2(4)	O4	C9	C8	126.2(4)
C18	N2	C2	123.9(4)	O5	C9	C8	108.5(4)
C18	N2	C11	111.8(4)	O2	C11	N2	124.6(4)
O1	C1	N1	126.2(4)	O2	C11	C12	129.6(4)
O1	C1	C2	125.8(4)	N2	C11	C12	105.8(4)
N1	C1	C2	108.0(4)	C13	C12	C11	130.5(4)
N2	C2	C1	112.2(4)	C13	C12	C17	121.4(4)
N2	C2	C3	115.5(4)	C17	C12	C11	108.1(4)
C1	C2	C3	103.8(4)	C12	C13	C14	117.9(5)
C4	C3	C2	105.5(4)	C15	C14	C13	120.8(5)
N1	C4	C3	103.8(4)	C14	C15	C16	121.6(5)
N1	C4	C5	110.6(4)	C17	C16	C15	117.2(5)
C5	C4	C3	118.1(4)	C12	C17	C16	121.2(5)
C4	C5	I1	111.2(3)	C12	C17	C18	108.3(4)
C4	C5	C6	110.3(4)	C16	C17	C18	130.6(5)
C6	C5	I1	109.8(4)	O3	C18	N2	124.1(5)
C7	C6	C5	112.2(4)	O3	C18	C17	130.1(5)
C6	C7	C8	112.7(4)	N2	C18	C17	105.8(4)

Table 6 Hydrogen Atom Coordinates (Å×10^4) and Isotropic Displacement Parameters (Å^2×10^3) for lub129.

Atom	*x*	*y*	*z*	U(eq)
H2	6769.61	2298.28	3780.61	32
H3A	4537.68	2705.41	3409.6	36
H3B	4202.2	3150.11	4403.07	36
H4	4534.04	4681.05	3839.99	35
H5	4185.2	4352.22	2293.52	42
H6A	5761.5	5544.96	1607.27	44
H6B	5088.82	5963.58	2527.71	44
H7A	7484.94	6342.79	2566.1	44

H7B	7892.34	5212.18	2342.14	44
H8	8316.7	5342.8	3886.52	36
H10A	6737.19	8502.35	4269.96	71
H10B	7849.2	8253.34	5048.21	71
H10C	6294.38	7832.98	5123.58	71
H13	6822.81	-712.19	6242.43	43
H14	6349.55	-811.06	7835.22	49
H15	5571.31	592.16	8634.82	53
H16	5334.52	2167.41	7900.48	44

Experimental

A suitable crystal of $C_{18}H_{17}IN_2O_3$, lub129, was selected and mounted on a Cryoloop on a Bruker Venture Metaljet diffractometer. The crystal was kept at 150 K during data collection. Using Olex2 [1], the structure was solved with the XT [2] structure solution program using Intrinsic Phasing and refined with the XL [3] refinement package using Least Squares minimisation.

1. Dolomanov, O.V., Bourhis, L.J., Gildea, R.J, Howard, J.A.K. & Puschmann, H. (2009), J. Appl. Cryst. 42, 339-341.
2. Sheldrick, G.M. (2015). Acta Cryst. A71, 3-8.
3. Sheldrick, G.M. (2015). Acta Cryst. C71, 3-8.

Crystal structure determination of lub129

Crystal Data for $C_{18}H_{17}IN_2O_3$ (M =468.23 g/mol): orthorhombic, space group $P2_12_12_1$ (no. 19), a = 9.4104(6) Å, b = 13.1390(8) Å, c = 14.3976(9) Å, V = 1780.17(19) Å^3, Z = 4, T = 150 K, μ(GaKα) = 9.882 mm^{-1}, $Dcalc$ = 1.747 g/cm^3, 11595 reflections measured (7.926° ≤ 2Θ ≤ 121.58°), 3923 unique (R_{int} = 0.0478, R_{sigma} = 0.0442) which were used in all calculations. The final R_1 was 0.0319 (I > 2σ(I)) and wR_2 was 0.0827 (all data).

Refinement model description

Number of restraints - 0, number of constraints - unknown.

Details:

```
1. Fixed Uiso
 At 1.2 times of:
  All C(H) groups, All C(H,H) groups
 At 1.5 times of:
  All C(H,H,H) groups
2.a Ternary CH refined with riding coordinates:
 C2(H2), C4(H4), C5(H5), C8(H8)
2.b Secondary CH2 refined with riding coordinates:
 C3(H3A,H3B), C6(H6A,H6B), C7(H7A,H7B)
2.c Aromatic/amide H refined with riding coordinates:
 C13(H13), C14(H14), C15(H15), C16(H16)
2.d Idealised Me refined as rotating group:
 C10(H10A,H10B,H10C)
```

This report has been created with Olex2, compiled on 2018.05.29 svn.r3508 for OlexSys. Please let us know if there are any errors or if you would like to have additional features.

Chapter 4

4-Vinylproline

4.01 Context

4.02 ω-Unsaturated amino acids

ω-Unsaturated amino acids are non-proteinogenic analogues commonly used as starting materials for organic synthesis,[1,2] due to the orthogonal reactivity of the olefin function. In peptides, ω-unsaturated amino acid residues have been used in different cyclization strategies featuring Diels-Alder, cycloaddition, hydroformylation and metathesis reactions.[3] Certain ω-unsaturated amino acids, such as (*S*)-allylglycine and (*S*)-homoallylglycine have been isolated from Amanita mushrooms.[4]

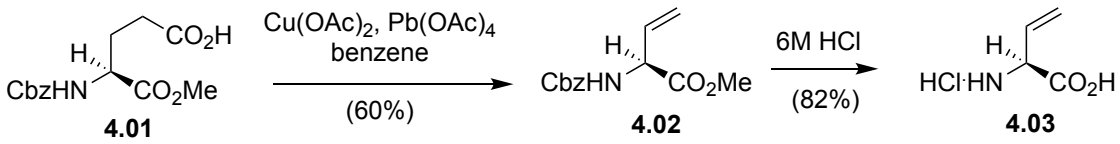

Scheme 4.01. Hanessian synthesis of L-vinylglycine from L-Glu

A variety of methods have been developed to synthesize enantiomerically enriched forms of ω-unsaturated amino acid. For example, vinylglycine has been synthesized using routes featuring thermal elimination of the sulfoxide derived from methionine,[5] and oxidative γ-decarboxylation of glutamic acid (Scheme 4.01).[6] Enantiomers of allylglycine are commercially available and commonly prepared by enzymatic resolution.[7] As mentioned in the introduction, homoallylglycine has been prepared by copper-catalyzed coupling of allyl chloride and the zincate derived from iodoalanine.[8] Various ω-unsaturated amino acids have been prepared by enantioselective and diastereoselective alkylation of glycine derivatives.[9] Moreover, in my M.Sc. degree studies, I prepared allylglycine and homohomoallylglycine by Pd-catalyzed coupling of vinyl bromide to the zincate derived from iodoalanine and the boronate derived from allylglycine, respectively.[10]

With the interest in using substituted ω-unsaturated amino acids in our RCM-TC strategy to azabicycloalkanone amino acids, the copper-catalyzed S_N2' substitution of the zincate from *N*-(Boc)iodo-alanine onto (*Z*)-1,4-dichlorobut-2-ene was pursued to provide 2-*N*-(Boc)amino-4-(chloromethyl)hexenoate in one-step from the commercially available iodide.[11] A diastereomeric mixture of chlorides were prepared by this reaction and readily separated by column chromatography. Intramolecular chloride displacement was used to provide 4-vinylproline (Vyp). Intermolecular chloride displacement has provided 2-amino-4-(azidomethyl)hexenoate, which is a 4-vinylornithine (Von) equivalent.

4.03. Copper-Catalyzed Allylic Substitution

Among various synthetic methods involving the formation of a new C-C bond, allylic substitutions reactions have been used with considerable success.[12] For example, copper(I)-catalyzed allylic substitutions have been effective for reacting hard nucleophiles including Grignard and organozinc reagents onto allylic systems (Figure 4.01).[13]

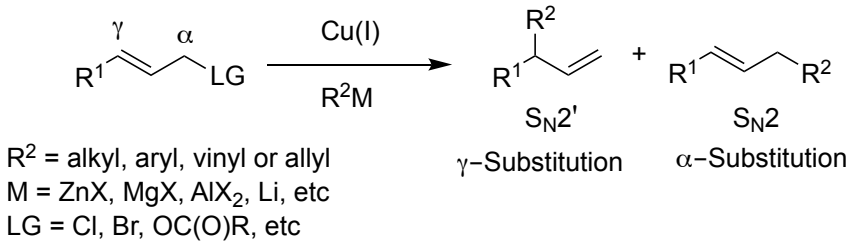

Figure 4.01. Allylic substitution reaction

In the allylic substitution reaction mechanism (Figure 4.02), the control of regioselectivity depends on the ligands of the copper catalyst. Electron withdrawing ligands favor rapid reductive elimination from the corresponding Cu(III) intermediate to form the γ-substituted product. Electron donating ligands may enable equilibration of the allylic electrophile to favor substitution at the least sterically hindered carbon.[14]

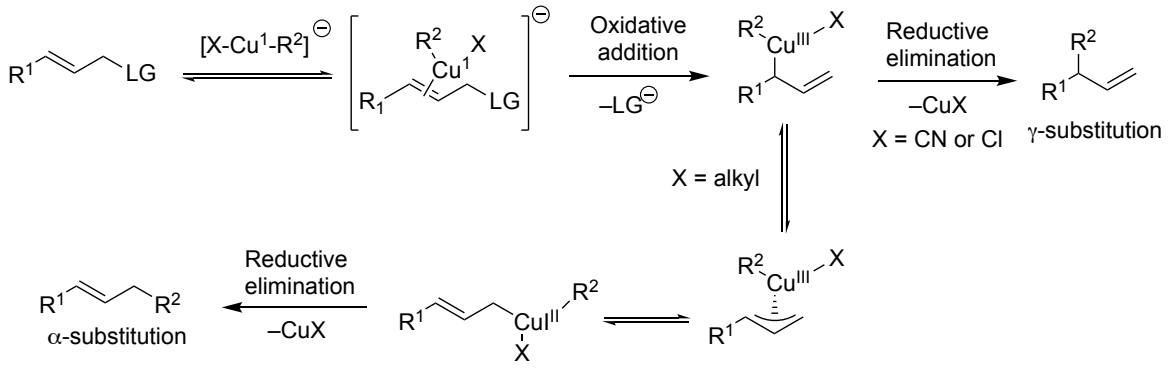

Figure 4.02. Mechanism of the copper-mediated allylic substitution.

4.04 Perspectives

The described atom-economical way for producing Vyp and Von analogs offers interesting potential for the synthesis of peptidomimetics. For example, Vyp was found in natural products active against some Gram-positive bacteria and potent mycelium-inducing activity.[15] An α-helix inducing *N*-capped bridged-tricyclic diproline analogue was also prepared by incorporating (2*S*,4*R*)-Boc-Vyp-OH into a peptide followed by olefin metathesis.[16] α-Vinylornithine (Von) may be a potential enzyme-activated inhibitor of mammalian ornithine decarboxylase.[17] This method and the unsaturated amino acids (e.g., Vyp and Von) offer important utility for studies of medicinal chemistry and peptide science.

4.05. References:

1. (a) Kazmaier, U.; Deska, J.; Watzke, A., Highly stereoselective allylic alkylations of peptides. *Angew. Chem. Int. Ed.* **2006**, *45*, 4855–4858; (b) Caplan, J. F.; Sutherland, A.; Vederas, J. C., The first stereospecific synthesis of L-tetrahydrodipicolinic acid; a key intermediate of diaminopimelate metabolism. *J. Chem. Soc. Perkin Transactions 1* **2001**, 2217–2220; (c) Nair, L. G.; Bogen, S.; Bennett, F.; Chen, K.; Vibulbhan, B.; Huang, Y.; Yang, W.; Doll, R. J.; Shih, N.-Y.; Njoroge, F. G., Design and synthesis of novel fluoro amino acids: synthons for potent macrocyclic HCV NS3 protease inhibitors. *Tetrahedron Lett.* **2010**, *51*, 3057–3061.

2. Hruby, V. J., Designing peptide receptor agonists and antagonists. *Nat. rev. Drug discov.* **2002**, *1*, 847.

3. Kaul, R.; Surprenant, S.; Lubell, W. D., Systematic study of the synthesis of macrocyclic dipeptide β-turn mimics possessing 8-, 9-, and 10-membered rings by ring-closing metathesis. *J. Org. Chem.* **2005**, *70*, 3838–3844.

4. Dardenne, G.; Casimir, J.; Marlier, M.; Larsen, P. O., Acide 2(*R*)-amino-3-butenoique (vinylglycine) dans les carpophores de rhodophyllus nidorosus. *Phytochemistry* **1974**, *13*, 1897–1900.

5. Afzali-Ardakani, A.; Rapoport, H., l-Vinylglycine. *J. Org. Chem.* **1980**, *45*, 4817–4820.

6. Hanessian, S.; Sahoo, S. P., A novel and efficient synthesis of L-vinylglycine. *Tetrahedron Lett.* **1984**, *25*, 1425–1428.

7. Cox, R. J.; Sherwin, W. A.; Lam, L. K.; Vederas, J. C., Synthesis and evaluation of novel substrates and inhibitors of N-succinyl-LL-diaminopimelate aminotransferase (DAP-AT) from Escherichia coli. *J. Am. Chem. Soc.* **1996**, *118*, 7449–7460.

8. Rodríguez, A.; Miller, D. D.; Jackson, R. F., Combined application of organozinc chemistry and one-pot hydroboration–Suzuki coupling to the synthesis of amino acids. *Org. Biomol. Chem.* **2003**, *1*, 973–977.

9. Belokon, Y. N.; Maleyev, V. I.; Vitt, S. V.; Ryzhov, M. G.; Kondrashov, Y. D.; Golubev, S. N.; Vauchskii, Y. P.; Kazika, A. I.; Novikova, M. I.; Krasutskii, P. A., Enantioselectivity of nickel (II) and copper (II) complexes of Schiff bases derived from amino acids and (*S*)-*o*-[(*N*-benzylprolyl) amino]-acetophenone or (*S*)-*o*-[(*N*-benzylprolyl) amino] benzaldehyde. Crystal and molecular structures of [Ni{(*S*)-bap-(*S*)-Val}] and [Cu {(*S*)-bap-(*S*)-Val}]. *J. Chem. Soc., Dalton Trans.* **1985**, 17–26.

10. Atmuri, N. P.; Lubell, W. D., Insight into transannular cyclization reactions to synthesize azabicyclo[X.Y.Z]alkanone amino acid derivatives from 8-, 9-, and 10-membered macrocyclic dipeptide lactams. *J. Org. Chem.* **2015**, *80*, 4904–4918.

11. Dunn, M. J.; Jackson, R. F.; Pietruszka, J.; Turner, D., Synthesis of enantiomerically pure unsaturated. α-amino acids using serine-derived zinc/copper reagents. *J. Org. Chem.* **1995**, *60*, 2210–2215.

12. Trost, B. M.; Van Vranken, D. L., Asymmetric transition metal-catalyzed allylic alkylations. *Chem. Rev.* **1996**, *96*, 395–422.

13. Yorimitsu, H.; Oshima, K., Recent progress in asymmetric allylic substitutions catalyzed by chiral copper complexes. *Angew. Chem. Int. Ed.* **2005**, *44*, 4435–4439.

14. Baeckvall, J. E.; Sellen, M.; Grant, B., Regiocontrol in copper-catalyzed Grignard reactions with allylic substrates. *J. Am. Chem. Soc.* **1990**, *112*, 6615–6621.

15. Mauger, A. B., Naturally occurring proline analogues. *J. Nat. Prod.* **1996**, *59*, 1205–1211.

16. Hack, V.; Reuter, C.; Opitz, R.; Schmieder, P.; Beyermann, M.; Neudörfl, J. M.; Kühne, R.; Schmalz, H. G., Efficient α-helix induction in a linear peptide chain by n-capping with a bridged-tricyclic diproline analogue. *Angew. Chem. Int. Ed.* **2013**, *125*, 9718–9722.

17. Danzin, C.; Casara, P.; Claverie, N.; Metcalf, B. W., α-Ethynyl and α-vinyl analogs of ornithine as enzyme-activated inhibitors of mammalian ornithine decarboxylase. *J. Med. Chem.* **1981**, *24*, 16–20.

Article 3.

4-Vinylproline

Ramakotaiah Mulamreddy, N. D. Prasad Atmuri, William D. Lubell*

Département de Chimie, Université de Montréal, P.O. Box 6128, Station Centre-ville, Montréal, Québec H3C 3J7, Canada

J. Org. Chem. **2018**, 83, 13580−13586

4.1 Abstract

Enantiomerically pure 4-vinylproline (Vyp) was synthesized by a five-step approach from *N*-(Boc)iodo-alanine (**4.2**) featuring copper-catalyzed S_N2' substitution of the corresponding zincate onto (*Z*)-1,4-dichlorobut-2-ene to prepare methyl 2-*N*-(Boc)amino-4-(chloromethyl)hexenoate (**4.3**). Intra- and intermolecular displacement of the chloride provided respectively Vyp and methyl 2-*N*-(Boc)amino-4-(azidomethyl)hexenoate (**4.7**) suitable for the synthesis of constrained peptide analogs.

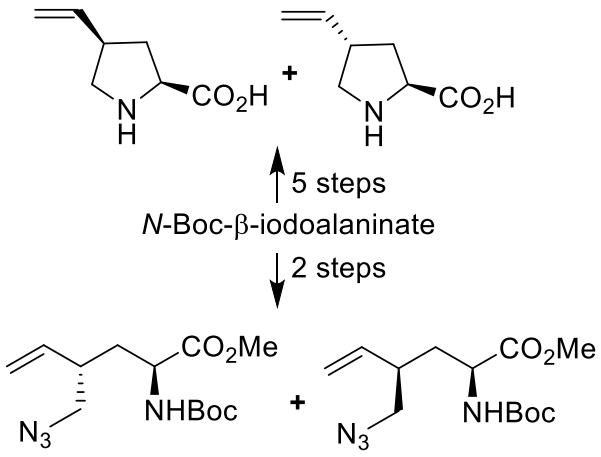

4.2 Introduction

4-Substituted prolines are natural products, peptide components and useful building blocks for a variety of applications (Figure 4.1).[1] For example, prolines with methyl, hydroxymethyl, carboxy and methylene 4-position substituents have been isolated from various fruits and seeds.[2] 4-Hydroxyproline is a key component of collagen.[3] Moreover, various peptides exhibiting antibiotic, anticancer and immunosuppressant activities contain prolines bearing alkyl,[4] alkenyl,[5] aryl,[6] amine,[7] and thio[8,9] 4-position substituents. 4-Cyclohexylproline is a component of the angiotensin converting enzyme (ACE) inhibitor Fosinopril, which is used to treat hypertension and chronic heart failure.[6] In addition, synthetic peptides possessing prolines with fluoride, amine, guanidine

and various alkyl oxide 4-position substituents have exhibited improved activity, cellular uptake and cell-penetrating ability.[10]

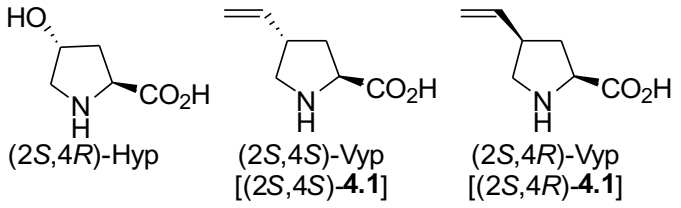

Figure 4.1. 4-Substituted proline derivatives

Natural (*2S*,4*R*)-4-hydroxproline (Hyp) is the principle starting material for the synthesis of enantiopure 4-substituted prolines.[11] Unnatural Hyp stereoisomers are however relatively unavailable and expensive, dictating more laborious synthetic routes to procure 4-substituted analogs. In the light of modern methods for olefin modification, 4-vinylproline (Vyp) offers an interesting but rarely used alternative starting material for 4-substituted proline assembly. For example, incorporation of (2*S*,4*R*)-Boc-Vyp-OH into a peptide and olefin metathesis was used to prepare an α-helix inducing *N*-cap bridged-tricyclic diproline analogue.[12] The traditional strategy for the synthesis of (2*S*,4*R*)-Boc-Vyp-OH from (2*S*,4*R*)-Hyp demanded however seven steps to deliver the target in 12% overall yield.[12] Herein, (2*S*,4*S*)- and (2*S*,4*R*)-Vyp-OH were obtained in five steps in 22% and 31% overall yields respectively.

Considering copper catalyzed coupling of various organometallic reagents with allylic halides has given selective S_N2' reactions,[13] the reaction of (*Z*)-1,4-dichlorobut-2-ene with the zincate of *N*-(Boc)iodo-alanine **4.2** has now been explored to provide 2-(Boc)amino-4-(chloromethyl)hexenoate **4.3**. The resulting chloride **4.3** has proven to be an effective precursor for the synthesis of enantiopure (2*S*,4*S*)- and (2*S*,4*R*)-Vyp [(2*S*,4*S*)- and (2*S*,4*R*)-**4.1**]. Moreover, chloride displacement with azide has provided (2*S*,4*S*)- and (2*S*,4*R*)-2-*N*-(Boc)amino-4-(azidomethyl)hexenoates [(2*S*,4*S*)- and (2*S*,4*R*)-**4.7**]. In the context of our program in peptide

mimicry, Vyp (**4.1**) and **4.7**, both represent readily assembled ω-olefin amino acids for the synthesis and application of constrained frameworks.[14]

4.3 Results and discussion

(*2S*)-*N*-(Boc)Iodoalanine **4.2** is a commercially available enantiopure precursor, which can be prepared on multiple-gram scale from L-serine in three steps.[15] Treatment of iodide **4.2** with zinc and iodine in DMF provided the corresponding zincate which was reacted with (*Z*)-1,4-dichlorobut-2-ene in the presence of catalytic copper(I) bromide dimethyl sulfide complex (Scheme 1). After aqueous workup and chromatography on silica gel, (2*S*,4*S*)- and (2*S*,4*R*)-2-*N*-(Boc) amino-4-(chloromethyl)hex-5-enoates [(2*S*,4*S*)- and (2*S*,4*R*)-**4.3**] were obtained respectively in 30 and 42% yields on 2 g scale. Although various conditions and chiral catalysts have been employed to achieve stereoselectivity in the Cu-catalyzed addition of organometallic reagents to allylic halides, sulfonates and phosphates,[16] no attempts were made to improve diastereoselectivity, because both isomeric chlorides are expected to have value in our research program using ω-unsaturated amino acids for the synthesis of peptide mimics.[14, 17] In addition, in contrast to routes from Hyp, effective access to the enantiomeric series is expected by employing D-serine in the sequence.

4-Vinylprolines (**4.1**) were respectively synthesized from chlorides **4.3** by intramolecular cyclization. Although attempts to cyclize carbamate **4.3** to methyl *N*-Boc-4-vinylprolinate **4.4** failed using bases such as sodium hydride and K_2CO_3, after Boc group removal with HCl gas in DCM, cyclization of amine hydrochloride was achieved effectively using K_2CO_3 and silver nitrate. Subsequent, protection with di-*tert*-butyldicarbonate delivered respectively (2*S*,4*S*)- and (2*S*,4*R*)-Boc-Vyp-OMe (2*S*,4*S*)- and (2*S*,4*R*)-**4.4** in 80% and 82% yields from **4.3** in a one-pot synthesis. Finally, (2*S*,4*S*)- and (2*S*,4*R*)-Vyp [(2*S*,4*S*)- and (2*S*,4*R*)-**4.1**] were respectively prepared as the

hydrochloride salts by hydrolysis of Boc-Vyp-OMe (**4.4**) using 6N HCl in 1,4 dioxane in 90% yields. Ion exchange chromatography provided the respective zwitterions as crystalline solids.

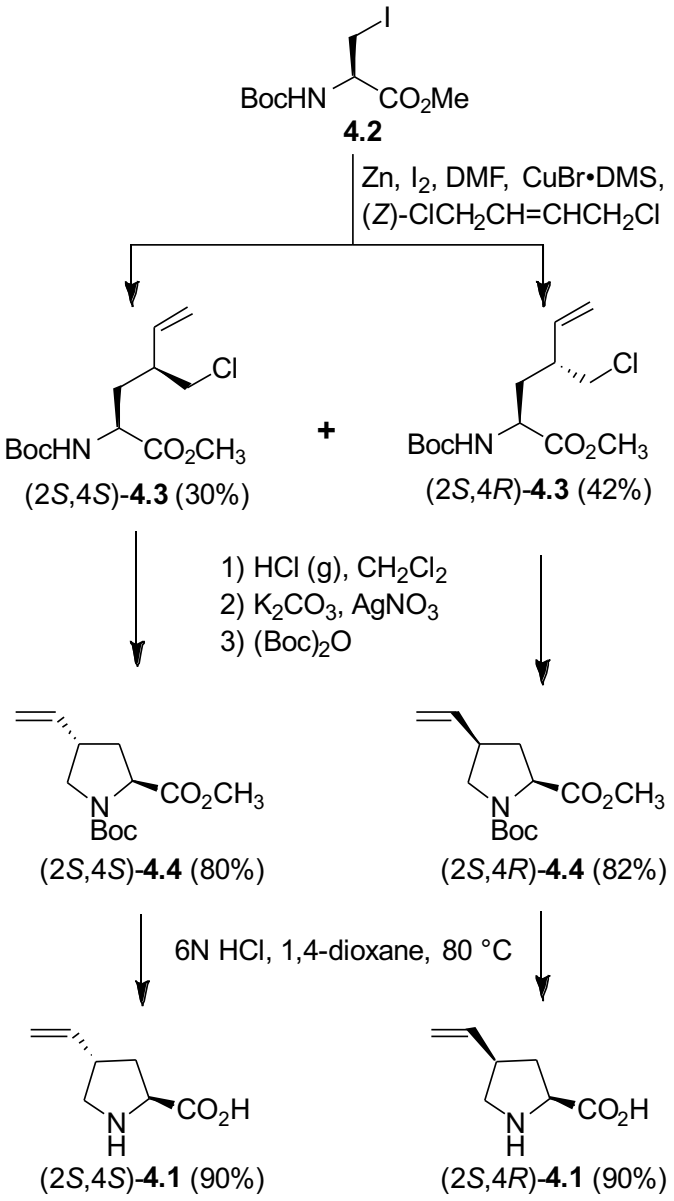

Scheme 4.1. Synthetic strategy to make 4-vinylproline

The enantiomeric purity of aminohexenoates **4.3** was ascertained after conversion to diastereomeric dipeptides by coupling respectively to L- and D-*N*-(Boc)alanine using TBTU, HOBt and *N*-ethylmorpholine in DCM (Scheme 4.2). Although clean dipeptides

were obtained using the above conditions, employment of HBTU under similar coupling conditions gave trace amounts of Boc-Ala-Vyp-OMe due to acylation after intramolecular cyclization. Examination of the diastereotopic methyl ester singlets at 3.208 and 3.222 ppm in the ^{1}H NMR spectra of (2'*S*, 4*S*)- and (2'*R*, 4*S*)-**4.6** in C_6D_6 and incremental additions of the opposite diastereomer to determine the limits of detection demonstrated a >99:1 dr for both peptides. Hence aminohexenoates **4.3** are assumed to be of >98% enantiomeric purity.

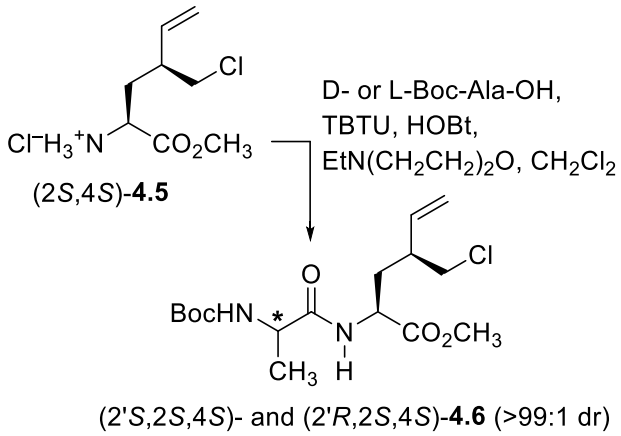

Scheme 4.2. Enantiomeric purity analysis of (2*S*,4*S*)-**4.5** by synthesis and analysis of diastereomeric dipeptides.

With enantiopure aminohexenoates **4.3** in hand, chloride displacement was briefly explored to demonstrate potential for preparing novel ω-unsaturated amino acids. (2*S*,4*S*)- and (2*S*,4*R*)-Methyl 2-*N*-(Boc)amino-4-(azidomethyl)hex-5-enoates [(2*S*,4*S*)- and (2*S*,4*R*)-**4.7**] were respectively synthesized by treating the corresponding chlorides **4.3** with sodium azide at 80 °C (Scheme 4.3). Considering the orthogonal azide and olefin functionality, amino acids **4.7** represent intriguing building blocks for exploring peptide cyclization by approaches such as copper-catalyzed azide alkyne cycloaddition (CuACC) reactions,[18] and olefin metathesis.[19] The application of azido olefin **4.7** in such chemistry may be feasible considering ω-unsaturated azides have been employed in sequential CuACC / ring closing metathesis protocols for constructing fused and bridged

triazoles,[20] and that olefin metathesis has been used to release azide-containing sugars from solid supports,[21] and to prepare azido sphingolipid analogs.[21b]

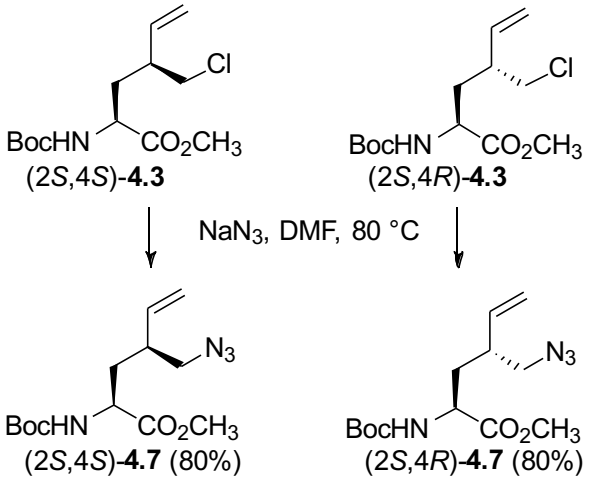

Scheme 4.3. Synthesis of azides **4.7**

The relative stereochemistry of the *cis* and *trans* Vyp diastereomers (2*S*,4*R*)- and (2*S*,4*S*)-**4.8** (Supporting information) were assigned using NOESY spectroscopy, which indicated a long-range transfer of magnetization between the C2 (4.54 ppm) and C4 (3.17 ppm) proton signals of the *cis*-isomer. In contrast, the NOESY spectrum of the *trans* diastereomer exhibited transfer of magnetization only between neighboring protons on the same face of the pyrrolidine ring. Furthermore, hydrolysis of methyl ester (2*S*,4*R*)-**4.4** gave (2*S*,4*R*)-Boc-Vyp-OH, which exhibited identical spectroscopic properties as previously reported.[12]

4.4 Conclusion

Enantiomerically pure vinylprolines **4.1** and 4-azidomethyl-2-aminohex-5-enoates **4.7** were respectively prepared in five and two steps from commercially available L-iodoalanine **4.2**. Copper catalyzed S_N2' reaction of the zincate from **2** onto (*Z*)-1,4-dichlorobut-2-ene provided effective access to separable 4-chloromethyl-2-aminohex-5-enoate diastereomers **4.3**, which may serve in the synthesis of various ω-olefin amino acids by way of chloride displacement chemistry.

Application of ω-unsaturated amino acids **4.1**, **4.3** and **4.7** offers potential for synthesizing constrained peptide analogs presently under investigation.

4.5 Experimental Section

4.5.1 General Methods: Unless otherwise specified, non-aqueous reactions were performed under an inert argon atmosphere, glassware was flame dried under argon or stored in the oven and cooled under inert atmosphere prior to use. Anhydrous solvents (DCM and DMF) were obtained by passage through solvent filtration systems (Glass Contour, Irvine, CA) and transferred by syringe. After aqueous workup, organic reaction mixtures were dried over anhydrous Na_2SO_4, filtered, and rotary-evaporated under reduced pressure. Flash chromatography was performed on 230−400 mesh silica gel.[22] Thin-layer chromatography (TLC) was performed on alumina plates coated with silica gel (Merck 60 F254 plates), and visualized by UV absorbance or staining with potassium permanganate solutions. Melting points were obtained on a Buchi melting point B-540 apparatus and are uncorrected. Specific rotations, $[\alpha]_D$ values, were calculated from optical rotation measurements at 25 °C in $CHCl_3$ or MeOH at the specified concentrations (*c* in g/100 ml) using a 0.5-dm cell length (l) on a Anton Paar Polarimeter, MCP 200 at 589 nm, and calculated by the general formula: $[\alpha]_D^{25} = (100 \times \alpha)/(l \times c)$. Accurate mass measurements were performed on an LC-MSD instrument in electrospray ionization (ESI-TOF) mode at the Université de Montréal Mass Spectrometry facility. Sodium adducts $[M + Na]^+$ were used for empirical formula confirmation. Nuclear magnetic resonance spectra (^1H, ^{13}C, COSY, HSQC, NOESY) were recorded on Bruker 400, 500 and 700 MHz spectrometers. ^1H NMR spectra were referenced to $CDCl_3$ (7.26 ppm), CD_3OD (3.31 ppm) or C_6D_6 (7.16 ppm) and ^{13}C NMR spectra were measured in $CDCl_3$ (77.16 ppm), CD_3OD (49.0 ppm), or C_6D_6 (128.06 ppm) as specified below. Coupling constant *J* values were measured in Hertz (Hz) and chemical shift values in parts per million (ppm).

In cases of carbamate isomers, ^{1}H and ^{13}C NMR signals of the minor isomers are respectively presented in brackets and parentheses. Infrared spectra were recorded in the neat on a Perkin Elmer Spectrometer FT-IR instrument, and are reported in reciprocal centimeters (cm^{-1}).

(2*S*,4*R*)- and (2*S*,4*S*)-Methyl 2-*N*-(Boc)amino-4-(chloromethyl)hex-5-enoates (4.3)

In a 100-mL round bottom flask, fitted with three-way tap, CuBr•DMS (160 mg, 0.8 mmol, 0.13 equiv) was weighed, dried gently with a heat gun under vacuum until the powder changed color from white to light green, placed under argon, treated with dry DMF (4 mL), followed by *cis*-2-butene-1,4-dichloride (980 mg, 7.8 mmol, 1.3 equiv, pre-filtered through a plug of silica gel), and cooled to –15 °C. In a second 100-mL round bottom flask with side arm and 3-way tap, zinc dust (1.2 g, 18.2 mmol, 3 equiv) was weighed, treated with iodine (50 mg, 0.18 mmol, 0.03 equiv) and heated with a heat gun under vacuum for 10 min. The flask was allowed to cool, flushed with nitrogen, evacuated, and flushed again with nitrogen (3 x), cooled to 0 °C, treated dropwise with a solution of *N*-(Boc)-3-iodo-L-alanine methyl ester (**4.2**, 2 g, 6.1 mmol, prepared from serine according to ref. 15b) in dry DMF (4 mL), allowed to warm to rt, and stirred for 1 h, when TLC analysis indicated full consumption of the iodide ((R_f = 0.7) and organozinc reagent (R_f = 0.2), 2:1 petroleum ether/EtOAc). Stirring was stopped, the excess zinc powder was let settle and the supernatant was transferred dropwise via syringe (care being taken to minimize the transfer of zinc) into the flask containing the copper catalyst at –15°C. The cooling bath was removed, and the mixture was stirred at rt overnight, diluted with ethyl acetate (35 mL) and stirred for 15 min. The reaction mixture was transferred to a separating funnel and diluted with ethyl acetate (50 mL). The organic phase was washed successively with 1 M $Na_2S_2O_3$ (35 mL), water (2 × 35 mL) and brine (70 mL), and dried. The volatiles were

removed to afford a residue that was purified by chromatography using 4-6% EtOAc in hexane as eluent. First to elute was (2*S*,4*S*)-**4.3** (530 mg, 30%) as light green liquid. (2*S*,4*S*)-**4.3**:R_f = 0.52 (1:9 EtOAc/hexanes, 3 times eluted, visualized with $KMnO_4$); $[\alpha]_D^{25}$ –20.4 (*c* 1, $CHCl_3$); ^{1}H NMR (700 MHz, $CDCl_3$) δ 5.68–5.74 (m, 1H), 5.19–5.20 (d, 1H, *J* = 1.4), 5.17–5.18 (d, 1H, *J* = 3.2), 5.09–5.10 (br, d, 1H, *J* = 6.7), 4.37–4.38 (d, 1H, *J* = 6.9), 3.75 (s, 3H), 3.59–3.62 (m, 1H), 3.51–3.54 (m, 1H), 2.55–2.58 (m, 1H), 2.11–2.15 (m, 1H), 1.72–1.76 (m, 1H), 1.46 (s, 9H); $^{13}C\{^1H\}$ NMR (175 MHz, $CDCl_3$) δ 173.0, 155.3, 137.7, 117.8, 80.2, 52.4, 51.5, 48.1, 42.0, 34.9, 28.1; FT-IR (neat) ν_{max} 3368, 2979, 1742, 1707, 1502, 1438, 1391, 1365,1160, 1032 cm^{-1}. HRMS (ESI-TOF) m/z $[M+Na]^+$ calcd for $C_{13}H_{22}ClNO_4Na$ 314.1130 found 314.1130. Second to elute was (2*S*,4*R*)**- 4.3** (740 mg, 42%), which solidified on standing: R_f = 0.45 (1:9 EtOAc/hexanes, 3 times eluted, visualized with $KMnO_4$); $[\alpha]_D^{25}$ –0.2 (*c* 1, $CHCl_3$); ^{1}H NMR (700 MHz, $CDCl_3$) δ 5.66–5.71 (m, 1H), 5.25–5.26 (d, 1H, *J* = 10.3), 5.22–5.25 (d, 1H, *J* = 17.2), 4.91–4.93 (m, 1H), 4.33–4.34 (d, 1H, *J* = 6.5), 3.75 (s, 3H), 3.55–3.56 (m, 1H), 3.46–3.48 (m, 1H), 2.55–2.56 (m, 1H), 1.87–1.89 (m, 2H), 1.46 (s, 9H); $^{13}C\{^1H\}$ NMR (175 MHz, $CDCl_3$) δ 173.4, 155.4, 137.0, 119.0, 80.1, 52.5, 51.6, 48.5, 42.7, 35.1, 28.4; FT-IR (neat) ν_{max} 3392, 2979, 1735, 1712, 1516, 1438, 1392, 1366, 1304, 1285, 1223 cm^{-1}; HRMS (ESI-TOF) m/z $[M+Na]^+$ calcd for $C_{13}H_{22}ClNO_4Na$ 314.1130 found 314.1140.

(2*S*,4*S*)-*N*-Boc-4-Vinylproline [(2*S*,4*S*)-4.4]

A solution of (2*S*,4*S*)-methyl 2-(Boc)amino-4-(chloromethyl)hex-5-enoate [(2*S*,4*S*)-**4.3**, 2.0 g, 6.87 mmol] in DCM (20 mL) was treated with HCl gas bubbles for 3 h, when TLC showed complete conversion of starting material (R_f = 0.45 (100% EtOAc visualized with $KMnO_4$). Argon was bubbled into the mixture to purge excess HCl for 15 min. The reaction mixture was treated with K_2CO_3 (4.74 g, 34.3 mmol, 5 equiv) and $AgNO_3$ (0.93 g, 5.5 mmol, 0.8 equiv), stirred for 36

h, treated with $(Boc)_2O$ (1.8 g, 8.2 mmol, 1.2 equiv), and stirred for 2 h. The reaction mixture was filtered through a pad of silica gel (0.5 cm height x 7 cm diameter), which was washed with DCM. Evaporation of the filtrate and washings under reduced pressure gave a residue that was purified by chromatography using 5-7% EtOAc in hexane as eluent. Evaporation of the collected fractions afforded (2*S*,4*S*)-Boc-Vyp-OMe [(2*S*,4*S*)-**4.4**, 1.4 g, 80%] as pale-yellow liquid: R_f = 0.25 (1:9 EtOAc/hexanes, visualized with $KMnO_4$); $[\alpha]_D^{25}$ –34.8 (*c* 0.54, $CHCl_3$); ^1H NMR (700 MHz, $CDCl_3$): (1:2 mixture of carbamate isomers) δ 5.69–5.75 (m, 1H), 5.05–5.14 (m, 2H), [4.39–4.40 (m, 1H)], 4.28–4.30 (m, 1H), 3.77–3.79 (m, 1H) [3.75 (s, 3H,)], 3.74 (s, 3H), [3.70–3.72 (m, 1H)], 3.17–3.20 (t, 1H, *J* = 8.9) [3.10–3.13 (t, 1H, *J* = 9.3)], 2.93–3.01 (m, 1H), 2.07–2.13 (m, 2H), [2.00–2.05 (m, 1H)], [1.47 (s, 9H)], 1.42 (s, 9H); $^{13}C\{^1H\}$ NMR (175 MHz, $CDCl_3$): δ 173.5/(173.3), (154.3)/153.6, 137.5, 116.1, 80.5, 58.9/(58.6), (52.2)/52.0, (51.3)/50.9, (41.3)/40.3, 36.5/(35.7), (28.4)/28.3; FT-IR (neat) ν_{max} 2976, 1747, 1697, 1390, 1198, 1178, 1160 cm^{-1}; HRMS (ESI-TOF) m/z $[M+Na]^+$ calcd for $C_{13}H_{21}NO_4Na$ 278.1363, found 278.1356.

(2*S*,4*R*)-*N*-Boc-4-Vinylproline [(2*S*,4*R*)-4.4]

(2*S*,4*R*)-Boc-Vyp-OMe [(2*S*,4*R*)-**4.4**] was synthesized as described for (2*S*,4*S*)-**4.4** using (2*S*,4*R*)-**4.3** (4.0 g, 13.7 mmol), and purified by chromatography on silica gel (5–7% EtOAc in hexane), which gave a pale-yellow liquid (2.9 g, 82%). R_f = 0.25 (1:9 EtOAc/hexanes, visualized with $KMnO_4$); $[\alpha]_D^{25}$ –104.0 (*c* 0.54, $CHCl_3$); ^1H NMR (500 MHz, $CDCl_3$): (1:2 mixture of carbamate isomers) δ 5.70–5.79 (m, 1H), 5.12–5.15 (d, 1H, *J* = 16.9), 5.06–5.09 (dd, 1H, *J* = 4.6, 10.3), [4.29–4.32 (t, 1H, *J* = 8.5)], 4.22–4.25 (m, 1H), 3.78–3.84 (m, 1H), [3.75 (s, 3H)], 3.74 (s, 3H), , [3.69–3.73 (m, 1H)], 3.17–3.22 (m, 1H), 2.74–2.88 (m, 1H), 2.40–2.46 (m,1H), 1.74–1.83 (m, 1H), [1.47 (s, 9H)], 1.42 (s, 9H); $^{13}C\{^1H\}$ NMR (125 MHz, $CDCl_3$): δ 173.5/(173.3), (154.1)/153.4, (137.2)/137.0, 116.3 /(116.2), 80.1/(80.0), 59.3/(58.8), (52.1)/51.9, (51.6)/51.1,

(42.5)/41.7, 36.9 /(36.0), (28.4)/28.2; FT-IR (neat) ν_{max} 2977, 1750, 1697, 1393, 1157, 1113 cm^{-1}. HRMS (ESI-TOF) m/z $[M+Na]^+$ calcd for $C_{13}H_{21}NO_4Na$ 278.1363, found 278.1356.

(2*S*,4*S*)-4-Vinylproline [(2*S*,4*S*)-4.1]

A solution of (2*S*,4*S*)-Boc-Vyp-OMe [(2*S*,4*S*)-**4.1**, 250 mg, 0.98 mmol] in 1,4-dioxane was treated with 6N HCl, heated to 80 °C for 2 h, cooled, and washed with ethyl acetate. The aqueous layer was lyophilized to provide hydrochloride salt (170 mg, 98%) as a pale-yellow gum. $[\alpha]_D^{25}$ – 4.4 (*c* 0.5, $CHCl_3$); ^1H NMR (400 MHz, CD_3OD) δ 5.79–5.88 (m, 1H), 5.22–5.29 (d,1H, *J* = 17.2), 5.19–5.22 (d, 1H, *J* = 10.4), 4.50–4.53 (m, 1H), 3.57–3.62 (m, 1H), 3.11–3.16 (t, 1H, *J* = 9.7), 3.02–3.16 (m, 1H), 2.40–2.46 (m, 1H), 2.24–2.32 (m, 1H); $^{13}C\{^1H\}$ NMR (125 MHz, CD_3OD) δ 171.7, 136.7, 118.1, 60.2, 51.1, 42.0, 35.3; FT-IR (neat) ν_{max} 3377, 2938, 1727, 1644, 1216, 1143 cm^{-1}; HRMS (ESI-TOF) m/z $[M+H]^+$ calcd for $C_7H_{12}NO_2$ 142.0863, found 142.0856. The hydrochloride salt was purified by ion-exchange chromatography on Dowex-50WX8 resin hydrogen form (prewashed with 2M HCl, followed by water until neutral effluent), eluting with ammonia. Freeze-drying of the collected fractions gave 126 mg (91% yield) as off white solid: mp = 228–230 °C, R_f = 0.64 (3:1:1 *tert*-BuOH/AcOH/H_2O, visualized with $KMnO_4$); $[\alpha]_D^{25}$ – 54.2 (*c* 0.7, MeOH); ^1H NMR (500 MHz, CD_3OD) δ 5.74–5.81 (m, 1H), 5.20–5.24 (dt, 1H, *J* = 1.2, *J* = 17.2), 5.13–5.16 (dt, 1H, *J* = 1, *J* = 10.4), 4.04–4.07 (dd, 1H, *J* = 4.1, *J* = 9.3), 3.52–3.55 (m, 1H), 2.88–3.01 (m, 2H), 2.32–2.36 (m, 1H), 2.09–2.15 (m, 1H); $^{13}C\{^1H\}$ NMR (125 MHz, CD_3OD) δ 173.9, 137.0, 117.6, 62.2, 51.0, 42.4, 36.4.

(2*S*,4*R*)-4-Vinylproline [(2*S*,4*R*)-4.1] Synthesized as described for (2*S*,4*S*)-**4.1**, which gave hydrochloride salt (165 mg, 95% yield) as gum: $[\alpha]_D^{25}$ –6.1 (*c* 0.5, $CHCl_3$); ^1H NMR (400 MHz, CD_3OD) δ 5.77–5.86 (m, 1H), 5.25–5.30 (d, 1H, *J* = 17.1), 5.18–5.20 (d, 1H, *J* = 10.4), 4.45–4.49 (m, 1H), 3.51–3.59 (m, 1H), 3.11–3.18 (m, 2H), 2.62–2.69 (m, 1H), 1.94–2.02 (m, 1H); $^{13}C\{^1H\}$

NMR (125 MHz, CD_3OD) δ 169.9, 135.2, 116.9, 59.4, 49.6, 41.9, 34.4; FT-IR (neat) ν_{max} 3388, 2922, 1731, 1645, 1453, 1420, 1223 cm^{-1}; HRMS (ESI-TOF) m/z $[M+H]^+$ calcd for $C_7H_{12}NO_2$ 142.0863, found 142.0862. Purified by Ion-exchange chromatography as described for (2*S*,4*S*)-**4.1** above gave (2*S*,4*R*)-**4.1** (125 mg , 91% yield) as off white solid: mp = 218–220 °C, R_f = 0.64 (3:1:1 *tert*-BuOH/AcOH/H_2O, visualized with $KMnO_4$); $[\alpha]_D^{25}$ – 12.4 (*c* 0.5, MeOH); ^1H NMR (500 MHz, CD_3OD) δ 5.75–5.82 (m, 1H), 5.17–5.21 (dt, 1H, *J* = 1.1, *J* = 17.1), 5.08–5.10 (dt, 1H, *J* = 1.0, *J* = 10.4), 3.93–3.96 (m, 1H), 3.33–3.36 (m, 1H), 3.01–3.10 (m, 1H), 2.91–2.99 (m, 1H), 2.47–2.53 (m, 1H), 1.77–1.83 (m, 1H); $^{13}C\{^1H\}$ NMR (125 MHz, CD_3OD) δ 174.9, 137.8, 117.2, 62.8, 51.2, 44.3, 37.1

(2*S*,4*S*-Methyl 2-amino-4-(chloromethyl)hex-5-enoate hydrochloride [(2*S*,4*S*)-4.5]

A solution of carbamate (2*S*,4*S*)- **4.3** (200 mg, 0.69 mmol) in DCM (5 mL) was treated with HCl gas bubbles for 3 h, and concentrated under reduced pressure to afford hydrochloride (2*S*,4*R*)- **4.5** (156 mg, 100%) as off-white solid: mp 146-148 °C; $[\alpha]_D^{25}$ –15.2 (*c* 0.5, $CHCl_3$); ^1H NMR (500 MHz, $CDCl_3$) δ 8.87 (br, s, 3H), 5.70–5.77 (m, 1H), 5.34–5.37 (d, 1H, *J* = 17.1), 5.24–5.26 (d, 1H, *J* = 11.0), 4.18–4.21 (m, 1H), 3.83 (s, 3H), 3.65–3.69 (m, 1H), 3.56–3.59 (m, 1H), 2.89–2.95 (m, 1H), 2.38–2.43 (m, 1H), 2.15–2.23 (m, 1H); $^{13}C\{^1H\}$ NMR (125 MHz, $CDCl_3$) δ 169.7, 136.7, 119.5, 53.3, 51.3, 48.3, 41.5, 32.4. FT-IR (neat) ν_{max} 2847, 1743, 1644, 1583, 1504, 1437, 1222 cm^{-1}; HRMS (ESI-TOF) m/z $[M+H]^+$ calcd for $C_8H_{15}ClNO_2$ 192.0786, found 192.0794.

(2*S*,4*R*)-Methyl 2-amino-4-(chloromethyl)hex-5-enoate hydrochloride [(2*S*,4*R*)-4.5] was prepared from carbamate (2*S*,4*R*)- **4.3** (200 mg, 0.687 mmol) as described for hydrochloride (2*S*,4*R*)-**5** to afford hydrochloride (2*S*,4*S*)- **4.5** as off-white solid (156 mg, 100%): mp 150-152 °C; $[\alpha]_D^{25}$ –24 (*c* 0.5, $CHCl_3$); ^1H NMR (500 MHz, $CDCl_3$) δ 8.98 (br, s, 3H), 5.71–5.77 (m, 1H), 5.57–5.60 (dd, 1H, *J* = 1.0, 17.1), 5.33–5.35 (dd, 1H, *J* = 1.3, 10.3), 4.06–4.07 (m, 1H), 3.85 (s,

3H), 3.62–3.70 (m, 2H), 3.07–3.12 (m, 1H), 2.31–2.37 (m, 1H), 2.19–2.20 (m, 1H); $^{13}C\{^{1}H\}$ NMR (125 MHz, $CDCl_3$) δ 170.0, 136.1, 120.8, 53.5, 51.6, 48.9, 41.4, 33.1; FT-IR (neat) ν_{max} 2860, 1747, 1581, 1505, 1438, 1283, 1214 cm^{-1}; HRMS (ESI-TOF) m/z $[M+H]^+$ calcd for $C_8H_{15}ClNO_2$ 192.0786, found 192.0793.

(2'*S*,2*S*,4*S*)-Methyl *N*-(Boc)alaninyl-2-amino-4-(chloromethyl)hex-5-enoate [(2'*S*,2*S*,4*S*)-4.6]

A stirred solution of *N*-Boc-L-alanine (83 mg, 0.44 mmol, 1 equiv) in DCM (5 mL) was treated with TBTU (141 mg, 0.44 mmol, 1 equiv) and HOBt (60 mg, 0.44 mmol, 1 equiv), stirred for 10-15 min, treated with *N*-ethylmorpholine (76 mg, 0.66 mmol, 1.5 equiv) and hydrochloride (2*S*,4*S*)-**4.5** (100 mg, 0.44 mmol), and stirred overnight. The reaction mixture was partitioned between water and DCM. The organic layer was separated, dried over Na_2SO_4 and concentrated under reduced pressure to a residue which was examined for diastereomeric purity by evaluation of the methyl ester singlet (3.208 ppm) with that of the (2'*R*)-diastereomer (3.222 ppm). Incremental additions of the (2'*R*)- into the (2'*S*)-isomer established the limits of detection at 1%. Subsequent purification by column chromatography using 14-16% EtoAc in hexane eluent to afforded peptide **4.6** (125 mg, 78%) as colourless liquid. R_f = 0.50 (3:7 EtOAc/hexanes, 3 times eluted, visualized with $KMnO_4$); $[\alpha]_D^{25}$ –11.8 (*c* 1, $CHCl_3$); ^{1}H NMR (400 MHz, C_6D_6) δ 6.54–6.56 (d, 1H, *J* = 7.84), 5.49–5.58 (m, 1H), 5.04–5.08 (d, 1H, *J* = 17.2), 4.97–4.99 (d, 1H, *J* = 10.4), 4.91 (br, s, 1H), 4.71–4.77 (m, 1H), 4.03–4.10 (m, 1H), 3.35–3.40 (m, 1H), 3.21–3.22 (d, 1H, *J* = 5.16), 3.20 (s, 3H), 2.41–2.49 (m, 1H), 2.07–2.04 (m, 1H), 1.52–1.59 (m, 1H), 1.40 (s, 9H), 1.06–1.08 (d, 3H); $^{13}C\{^{1}H\}$ NMR (100 MHz, C_6D_6) δ 172.0, 171.9, 155.0, 137.4, 116.6, 79.2, 51.4, 49.8, 47.7, 41.5, 34.2, 29.8, 28.0, 17.5; FT-IR (neat) ν_{max} 3307, 2979, 1742, 1659, 1163 cm^{-1}; HRMS (ESI-TOF) m/z $[M+Na]^+$ calcd for $C_{16}H_{27}ClN_2O_5Na$ 385.1501, found 385.1504

(2'*R*,2*S*,4*S*)-Methyl *N*-(Boc)alaninyl-2-amino-4-(chloromethyl)hex-5-enoate [(2'*R*,2*S*,4*S*)-4.6]

(2'*R*,2*S*,4*S*)- **4.6** was synthesized, analyzed and later purified as described for (2'*S*,2*S*,4*S*)- **4.6** from hydrochloride (2*S*,4*R*)- **4.5** (100 mg, 0.44 mmol): off-white solid (122 mg, 76%); R_f = 0.50 (3:7 EtOAc/hexanes, 3 times eluted, visualized with $KMnO_4$); $[\alpha]_D^{25}$ –41.4 (*c* 1, $CHCl_3$); ^{1}H NMR (400 MHz, C_6D_6) δ 7.07–7.09 (br d, 1H, *J* = 5.2), 5.49–5.58 (m, 1H), 5.17–5.18 (brd, 1H, *J* = 3.2), 5.02–5.07 (d, 1H, *J* = 17.1), 4.97–5.00 (d, 1H, *J* = 10.3), 4.74–4.80 (m, 1H), 4.27–4.30 (br, t, 1H, *J* = 7.1), 3.34–3.38 (m, 1H), 3.25 (s, 3H), 3.15–3.23 (m, 1H), 2.42–2.50 (m, 1H), 2.09–2.18 (m, 1H), 1.57–1.66 (m, 1H), 1.42 (s, 9H), 1.16–1.18 (d, 3H, *J* = 6.9); ^{13}C{^{1}H} NMR (100 MHz, C_6D_6) δ 172.7, 172.6, 155.9, 138.2, 117.4, 79.6, 51.8, 50.4, 48.1, 42.1, 34.5, 30.2, 28.4, 18.1; FT-IR (neat) ν_{max} 3380, 2980, 1748, 1703, 1663, 1570, 1527, 1207, 1161 cm^{-1}; HRMS (ESI-TOF) m/z $[M+Na]^+$ calcd for $C_{16}H_{27}ClN_2O_5Na$ 385.1506, found 385.1501.

Methyl (2*S*,4*S*)-4-(azidomethyl)-2-((tert-butoxycarbonyl)amino)hex-5-enoate [(2*S*,4*S*)-4.7]

A solution of methyl (2*S*,4*S*)-2-((tert-butoxycarbonyl)amino)-4-(chloromethyl)hex-5-enoate **4.3** (50 mg, 0.171 mmol) in *N*,*N*-dimethylformamide (2.5 mL) was treated with sodium azide (33 mg, 0.515 mmol, 3 equiv), heated at 80 °C overnight, cooled, and poured into water. The mixture was extracted with ethyl acetate. The combined organic layer was washed with water (4 X 5 mL), dried with sodium sulfate, and evaporated to a residue that was purified by column chromatography using 6-8% EtOAc in hexane as eluent to provide azide (2*S*,4*R*)-**4.7** (41 mg, 80%) as a colourless liquid. R_f = 0.44 (1:9 EtOAc/hexanes, 3 times eluted, visualized with $KMnO_4$); $[\alpha]_D^{25}$ –1.39 (*c* 0.6, $CHCl_3$); ^{1}H NMR (500 MHz, $CDCl_3$) δ 5.64–5.71 (m, 1H), 5.18–5.22 (m, 2H), 5.10–5.11 (d, 1H, *J* = 7.4), 4.35–4.39 (m, 1H), 3.75 (s, 3H), 3.30–3.47 (m, 2H), 2.44–2.51 (m, 1H), 1.96–2.01 (m, 1H), 1.68–1.73 (m, 1H), 1.46 (s, 9H); ^{13}C{^{1}H} NMR (125 MHz, $CDCl_3$) δ 173.0, 155.3, 138.0,

117.9, 80.2, 55.1, 52.5, 51.6, 40.3, 34.9, 28.1; FT-IR (neat) ν_{max} 3358, 2978, 2095, 1742, 1708, 1503, 1365, 1159 cm^{-1}; HRMS (ESI-TOF) m/z $[M+Na]^+$ calcd for $C_{13}H_{22}N_4O_4Na$ 321.1533, found 321.1537.

Methyl (2*S*,4*R*)-4-(azidomethyl)-2-((tert-butoxycarbonyl)amino)hex-5-enoate [(2*S*,4*R*)-4.7]

Azide (2*S*,4*R*)- **4.7** was synthesized from (2*S*,4*R*)-**4.3** (50 mg, 0.171 mmol) using the protocol for (2*S*,4*R*)-**4.7** to provide colourless liquid (41 mg, 80%): R_f = 0.34 (1:9 EtOAc/hexanes, 3 times eluted, visualized with $KMnO_4$); $[\alpha]_D^{25}$ –13.09 (*c* 0.8, $CHCl_3$); ^1H NMR (500 MHz, $CDCl_3$) δ 5.63–5.68 (m, 1H), 5.23–5.27 (m, 2H), 4.92–4.94 (m, 1H), 4.26–4.34 (m, 1H), 3.76 (s, 3H), 3.31–3.35 (m, 1H), 3.24–3.28 (m, 1H), 2.43–2.50 (m, 1H), 1.81–1.90 (m, 1H), 1.72–1.77 (m, 1H), 1.46 (s, 9H); $^{13}C\{^1H\}$ NMR (125 MHz, $CDCl_3$) δ 173.3, 155.3, 137.2, 118.9, 80.1, 55.5, 52.4, 51.5, 40.7, 35.0, 28.3; FT-IR (neat) ν_{max} 3357, 2978, 2096, 1707, 1510, 1437, 1391, 1365, 1159 cm^{-1}; HRMS (ESI-TOF) m/z $[M+Na]^+$ calcd for $C_{13}H_{22}N_4O_4Na$ 321.1533, found 321.1536.

(2*S*,4*S*)-Methyl 4-vinylprolinate hydrochloride [(2*S*,4*S*)-4.8]

A solution of (2*S*,4*S*)-methyl *N*-Boc-4-vinylprolinate **4.4** (50mg, 0.196 mmol) in DCM (20 mL) was treated with HCl gas bubbles for 2h and concentrated under reduced pressure to afford hydrochloride (2*S*,4*S*)-**4.8** as off-white solid (38 mg, 100%). $[\alpha]_D^{25}$ –1.53 (*c* 0.8, $CHCl_3$); ^1H NMR (500 MHz, $CDCl_3$) δ 10.99 (br, s, 1H), 9.31 (br, s, 1H), 5.71–5.78 (m, 1H), 5.20–5.23 (d, 1H, *J* = 17.0), 5.16–5.18 (d, 1H, *J* = 10.3), 4.59–4.60 (m, 1H), 3.83 (s, 3H), 3.81–3.82 (m, 1H), 3.18–3.22 (m, 1H), 3.01–3.09 (m, 1H), 2.39–2.44 (m, 1H), 2.18–2.27 (m, 1H); $^{13}C\{^1H\}$ NMR (125 MHz, $CDCl_3$) δ 169.2, 134.8, 118.1, 58.9, 53.6, 49.6, 40.7, 34.6; FT-IR (neat) ν_{max} 2954, 2825, 2673, 2541, 2446, 1744, 1644, 1595, 1443, 1388, 1353, 1330, 1289, cm^{-1}; HRMS (ESI-TOF) m/z $[M+H]^+$ calcd for $C_8H_{14}NO_2$ 156.1019, found 156.1023.

(2*S*,4*R*)-Methyl 4-vinylprolinate hydrochloride [(2*S*,4*R*)- 4.8]

Hydrochloride (2*S*,4*R*)-**4.8** was synthesized from (2*S*,4*R*)-**4.4** (50mg, 0.196 mmol) using the protocol for (2*S*,4*S*)-**4.8** to afford off-white solid (38 mg, 100%): $[\alpha]_D^{25}$ –16.5 (*c* 0.8, $CHCl_3$); ^1H NMR (500 MHz, $CDCl_3$) δ 5.68–5.75 (m, 1H), 5.20–5.23 (d, 1H, *J* = 17.1), 5.15–5.17 (d, 1H, *J* = 10.3), 4.53–4.56 (t, 1H, *J* = 8.7), 3.85 (s, 3H), 3.68–3.72 (m, 1H), 3.28–3.30 (t, 1H, *J* = 10.9), 3.12–3.22 (m, 1H), 2.58–2.64 (m, 1H), 1.93–2.00 (m, 1H); $^{13}C\{^1H\}$ NMR (125 MHz, $CDCl_3$) δ 169.0, 134.5, 118.2, 58.8, 53.5, 50.0, 41.9, 34.8; FT-IR (neat) ν_{max} 3388, 2920, 2852, 2695, 2527, 2418, 1745, 1647, 1583, 1483, 1411, 1381, 1356, 1265 cm^{-1}; HRMS (ESI-TOF) m/z $[M+H]^+$ calcd for $C_8H_{14}NO_2$ 156.1019, found 156.1021.

4.6 Acknowledgment

This work was supported by NSERC Canada. For aid in analyses, we thank Dr. A. Fürtös, K. Venne, M-C. Tang (mass spectrometry); S. Bilodeau, C. Malveau (NMR spectroscopy) from the U. de Montréal Regional Laboratories. Shastri Indo-Canadian Institute, India is thanked for a Quebec Tuition Fee Exemption grant to N.D.P.A.

4.7 References

1. (a) Koskinen, A. M.; Rapoport, H. Synthesis of 4-substituted prolines as conformationally constrained amino acid analogs. *J. Org. Chem.* **1989**, *54*, 1859–1866; (b) Mothes, C.; Caumes, C.; Guez, A.; Boullet, H.; Gendrineau, T.; Darses, S.; Delsuc, N.; Moumné, R.; Oswald, B.; Lequin, O. 3-Substituted prolines: from synthesis to structural applications, from peptides to foldamers. *Molecules* **2013**, *18*, 2307–2327; (c) Nevalainen, M.; Kauppinen, P. M.; Koskinen, A. M. Synthesis of Fmoc-Protected trans-4-methylproline. *J. Org. Chem.* **2001**, *66*, 2061–2066; (d) Koivisto, J. J.; Kumpulainen, E. T.; Koskinen, A. M. Conformational ensembles of flexible β-turn mimetics in DMSO-d6. *Org. Bimol. Chem.* **2010**, *8*, 2103–2116; (e) Zwick III, C. R.; Renata, H.

Remote C–H Hydroxylation by an α-Ketoglutarate-Dependent Dioxygenase Enables Efficient Chemoenzymatic Synthesis of Manzacidin C and Proline Analogs. *J. Am. Chem. Soc.* **2018**, *140*, 1165–1169; (f) Johnston, H. J.; McWhinnie, F. S.; Landi, F.; Hulme, A. N. Flexible, phase-transfer catalyzed approaches to 4-substituted prolines. *Org. Lett.* **2014**, *16*, 4778–4781.

2. Mauger, A. B. Naturally occurring proline analogues. *J. Nat. Prod.* **1996**, *59*, 1205–1211.

3. (a) Bulleid, N.; John, D.; Kadler, K., Recombinant expression systems for the production of collagen. *Biochem. Soc. Trans*., 2**000**, 28, 350; (b) Myllyharju, J. Prolyl 4-hydroxylases, key enzymes in the synthesis of collagens and regulation of the response to hypoxia, and their roles as treatment targets. *Ann. Med.* **2008**, *40*, 402–417; (c) Kang, Y. K.; Shin, K. J.; Yoo, K. H.; Seo, K. J.; Hong, C. Y.; Lee, C.-S.; Park, S. Y.; Kim, D. J.; Park, S. W. Synthesis and antibacterial activity of new carbapenems containing isoxazole moiety. *Bioorg. Med. Chem. Lett.* **2000**, *10*, 95–99.

4. Jiraskova, P.; Gazak, R.; Kamenik, Z.; Steiningerova, L.; Najmanova, L.; Kadlcik, S.; Novotna, J.; Kuzma, M.; Janata, J. New concept of the biosynthesis of 4-alkyl-L-proline precursors of lincomycin, hormaomycin, and pyrrolobenzodiazepines: Could a γ-glutamyltransferase cleave the C–C Bond. *Front Microbiol.* **2016**, *7*, 276.

5. Höfer, I.; Crüsemann, M.; Radzom, M.; Geers, B.; Flachshaar, D.; Cai, X.; Zeeck, A.; Piel, J. Insights into the biosynthesis of hormaomycin, an exceptionally complex bacterial signaling metabolite. *Chem. Biol.* **2011**, *18*, 381–391.

6. Krapcho, J.; Turk, C.; Cushman, D. W.; Powell, J. R.; DeForrest, J. M.; Spitzmiller, E. R.; Karanewsky, D. S.; Duggan, M.; Rovnyak, G. Angiotensin-converting enzyme inhibitors. Mercaptan, carboxyalkyl dipeptide, and phosphinic acid inhibitors incorporating 4-substituted prolines. *J. Med. Chem.* **1988**, *31*, 1148–1160.

7. Mollica, A.; Pinnen, F.; Stefanucci, A.; Feliciani, F.; Campestre, C.; Mannina, L.; Sobolev, A. P.; Lucente, G.; Davis, P.; Lai, J. The cis-4-amino-L-proline residue as a scaffold for the synthesis of cyclic and linear endomorphin-2 analogues. *J. Med. Chem.* **2012**, *55*, 3027–3035.

8. Enomoto, H.; Morikawa, Y.; Miyake, Y.; Tsuji, F.; Mizuchi, M.; Suhara, H.; Fujimura, K.-i.; Horiuchi, M.; Ban, M. Synthesis and biological evaluation of *N*-mercaptoacylproline and *N*-mercaptoacylthiazolidine-4-carboxylic acid derivatives as leukotriene A 4 hydrolase inhibitors. *Bioorg. Med. Chem. Lett.* **2008**, *18*, 4529–4532.

9. Krogsgaard-Larsen, N.; Delgar, C. G.; Koch, K.; Brown, P. M.; Møller, C.; Han, L.; Huynh, T. H.; Hansen, S. W.; Nielsen, B.; Bowie, D. Design and synthesis of a series of l-trans-4-substituted prolines as selective antagonists for the ionotropic glutamate receptors including functional and X-ray crystallographic studies of new subtype selective kainic acid receptor subtype 1 (GluK1) antagonist (2*S*,4*R*)-4-(2-carboxyphenoxy) pyrrolidine-2-carboxylic acid. *J. Med. Chem.* **2017**, *60*, 441–457.

10. (a) Yamashita, H.; Kato, T.; Oba, M.; Misawa, T.; Hattori, T.; Ohoka, N.; Tanaka, M.; Naito, M.; Kurihara, M.; Demizu, Y. Development of a cell-penetrating peptide that exhibits responsive changes in its secondary structure in the cellular environment. *Sci Rep.* **2016**, *6*, 33003; (b) Fillon, Y. A.; Anderson, J. P.; Chmielewski, J. Cell penetrating agents based on a polyproline helix scaffold. *J. Am. Chem. Soc.* **2005**, *127*, 11798–11803; (c) Crespo, L.; Sanclimens, G.; Montaner, B.; Pérez-Tomás, R.; Royo, M.; Pons, M.; Albericio, F.; Giralt, E. Peptide dendrimers based on polyproline helices. *J. Am. Chem. Soc.* **2002**, *124*, 8876–8883; (d) Newberry, R. W.; Raines, R. T., 4-Fluoroprolines: Conformational analysis and effects on the stability and folding of peptides and proteins. In *Peptidomimetics I*, Springer **2016**; pp 1–25.

11. (a) Bhagwat, S. S.; Fink, C. A.; Gude, C.; Chan, K.; Qiao, Y.; Sakane, Y.; Berry, C.; Ghai, R. D. 4-Substituted proline derivatives that inhibit angiotensin converting enzyme and neutral endopeptidase 24.11. *Bioorg. Med. Chem. Lett.* **1994**, *4*, 2673–2676; (b) Arasappan, A.; Chen, K. X.; Njoroge, F. G.; Parekh, T. N.; Girijavallabhan, V. Novel Dipeptide macrocycles from 4-oxo-thio, and-amino-substituted proline derivatives. *J. Org. Chem.* **2002**, *67*, 3923–3926; (c) Pandey, A. K.; Naduthambi, D.; Thomas, K. M.; Zondlo, N. J. Proline editing: a general and practical approach to the synthesis of functionally and structurally diverse peptides. Analysis of steric versus stereoelectronic effects of 4-substituted prolines on conformation within peptides. *J. Am. Chem. Soc.* **2013**, *135*, 4333–4363; (d) Del Valle, J. R.; Goodman, M. Asymmetric hydrogenations for the synthesis of Boc-protected 4-alkylprolinols and prolines. *J. Org. Chem.* **2003**, *68*, 3923–3931; (e) Murphy, A. C.; Mitova, M. I.; Blunt, J. W.; Munro, M. H. Concise, stereoselective route to the four diastereoisomers of 4-methylproline. *J. Nat. Prod.* **2008**, *71*, 806–809.

12. Hack, V.; Reuter, C.; Opitz, R.; Schmieder, P.; Beyermann, M.; Neudörfl, J. M.; Kühne, R.; Schmalz, H. G. Efficient α-helix induction in a linear peptide chain by *N*-capping with a bridged-tricyclic diproline analogue. *Angew. Chem. Int. Ed.* **2013**, *52*, 9539–9543.

13. Dunn, M. J.; Jackson, R. F.; Pietruszka, J.; Turner, D. Synthesis of enantiomerically pure unsaturated. α-amino acids using serine-derived zinc/copper reagents. *J. Org. Chem.* **1995**, *60*, 2210–2215.

14. (a) Surprenant, S.; Lubell, W. D. From macrocycle dipeptide lactams to azabicyclo[X.Y.0] alkanone amino acids: A transannular cyclization route for peptide mimic synthesis. *Org. Lett.* **2006**, *8*, 2851–2854; (b) Atmuri, N. D. P.; Lubell, W. D. Insight into transannular cyclization reactions to synthesize azabicyclo[X.Y.Z]alkanone amino acid derivatives from 8-, 9-, and 10-membered macrocyclic dipeptide lactams. *J. Org. Chem.* **2015,** *80*, 4904–4918; (c) Atmuri, N. D.

P.; Reilley, D. J.; Lubell, W. D. Peptidomimetic synthesis by way of diastereoselective iodoacetoxylation and transannular amidation of 7–9-membered lactams. *Org. Lett.* **2017**, *19*, 5066–5069.

15. (a) Atmuri, N. D. P.; Lubell, W. D. Preparation of *N*-(Boc)-allylglycine methyl ester using a zinc-mediated, palladium-catalyzed cross-coupling reaction. *Org. Synth.* **2015**, *92*, 103–116; (b) Trost, B. M.; Rudd, M. T. Chemoselectivity of the ruthenium-catalyzed hydrative diyne cyclization: total synthesis of (+)-cylindricine C, D, and E. *Org. Lett.* **2003**, *5*, 4599–4602.

16. (a) Falciola, C. A.; Alexakis, A. 1,4-dichloro- and 1,4-dibromo-2-butenes as substrates for Cu-catalyzed asymmetric allylic substitution. *Angew. Chem. Int. Ed.* **2007**, *119*, 2673–2676; (b) Börner, C.; Gimeno, J.; Gladiali, S.; Goldsmith, P. J.; Ramazzotti, D.; Woodward, S. Asymmetric chemo-and regiospecific addition of organozinc reagents to Baylis–Hillman derived allylic electrophiles. *Chem. Commun.* **2000**, 2433–2434; (c) Belelie, J. L.; Chong, J. M. Stereoselective reactions of acyclic allylic phosphates with organocopper reagents. *J. Org. Chem.* **2001**, *66*, 5552–5555.

17. Godina, T. A.; Lubell, W. D. Mimics of peptide turn backbone and side-chain geometry by a general approach for modifying azabicyclo[5.3.0]alkanone amino acids. *J. Org. Chem.* **2011**, *76*, 5846–5849.

18. Diness, F.; Schoffelen, S.; Meldal, M., Advances in merging triazoles with peptides and proteins. In *Peptidomimetics I*, Springer **2015**; pp 267–304.

19. Brik, A. Metathesis in peptides and peptidomimetics. *Adv. Synth. Catal.* **2008**, *350*, 1661–1675.

20. Zhang, X.; Hsung, R. P.; Li, H. A triazole-templated ring-closing metathesis for constructing novel fused and bridged triazoles. *Chem. Commun.* **2007**, 2420–2422.

21. (a) Kanemitsu, T.; Seeberger, P. H. Use of olefin cross-metathesis to release azide-containing sugars from solid support. *Org. Lett.* **2003**, *5*, 4541–4544; (b) Rai, A. N.; Basu, A. Sphingolipid Synthesis via Olefin Cross Metathesis: Preparation of a differentially protected building block and application to the synthesis of D-erythro-Ceramide. *Org. Lett.* **2004**, *6*, 2861–2863.

22. Still, W. C.; Kahn, M.; Mitra, A. Rapid chromatographic technique for preparative separations with moderate resolution. *J. Org. Chem.* **1978**, *43*, 2923–2925.

Chapter 5

Paired Utility of Aza-Amino Acyl Proline and Indolizidinone Amino Acid Residues for Peptide Mimicry: Conception of Prostaglandin F2α Receptor Allosteric Modulators that Delay Preterm Birth

5.01 Context

Preterm birth (PTB) is characterized by uterine contractions that cause the cervix to open early (< 37 weeks' gestation) leading to premature delivery and associated health problems.[1] The leading cause of perinatal mortality and morbidity, PTB is an unmet healthcare need rising in incidence over the past 25 years in North America.[2] Labor delaying therapy with so-called tocolytic drugs may inhibit PTB; however, contemporary agents are only effective for a couple of days and risk complications with side effects for mother and neonatal.[3]

Targeting improved tocolytics, the prostaglandin F2α (PGF2α) receptor (FP) has been considered an important point of intervention, because of roles in the stimulation of uterine contractions leading to preterm birth. In a collaborative effort with the laboratory of Professor Sylvain Chemtob (Saint-Justine Hospital), FP modulators were conceived based on the second extracellular loop of this G protein-coupled receptor (GPCR) such as the short D-peptide PDC113 (H-ile-leu-Gly-his-arg-asp-tyr-lys-NH_2), which exhibited inhibitory activity (IC_{50} of 340 nmol/L) against PGF2α-induced contractions in a porcine eye vessel microvascular assay.[4] Furthermore, PDC113 blocked spontaneous uterine contractions and reduced PGF2α-induced contractions in an *ex vivo* mouse uterine strip assay.[5] The indolizidin-2-one amino acid (I^2aa) analog PDC113.824 was subsequently developed using a peptide mimicry approach, exhibited improved tocolytic activity (IC_{50} = 1.1 nmol/L with 98.6% inhibition),[6] delayed preterm labor in a mouse model,[7] and served as a probe in cell culture to establish an allosteric mechanism of action featuring biased signalling.[8] In addition, replacement of the I^2aa residue of PDC113.824 with aza-amino acyl proline counterparts led to a second series of small-molecule FP modulators that exhibited inhibitory potency in a murine myometrium contraction assay.[6]

5.02 Exploring the influence of substituents on the activity of PDC113.824 by modification of the indolizidin-2-one amino acid residue

Earlier studies of PDC113.824 examined the relationship between backbone geometry and activity by replacing the I^2aa residue with related heterocycles: e.g., (2*S*,6*R*,8*S*)-I^9aa, (3*R*,6*R*,9*R*)-I^2aa, and (2*S*,6*R*,8*S*)-Qaa residues.[9,10,11,12] In these studies, activity was typically abolished, likely due to significant changes in backbone dihedral angles.[13] A strategy to explore more subtle effects on the I^2aa residue was thus pursued using the ring fusion stereoisomer and the corresponding unsaturated Δ^5-I^2aa residue.

Although diversification of indolizidinone residues have proven challenging,[14] methods described in this chapter indicated that Δ^5-I^2aa analogs were accessible by way of the RCM-TC strategy and iodide elimination. With Δ^5-I^2aa in hand, olefin reduction gave access to the ring fusion stereoisomer. Moreover, olefin arylation and allylic oxidation offered respectively means to add substituents to the 6- and 5-membered rings of the I^2aa system.

5.03 Palladium(II)-Catalyzed-Oxidative Heck reactions

Employing Heck reaction conditions related to those described in this chapter, the six-membered ring of a Δ^5-I^2aa moiety was coupled with various aryl boronic acid at C5. The Heck reaction features typically palladium-catalyzed arylation of olefins.[15] Aryl boronic acids undergo trans-metalation with a Pd(II) catalyst under mild conditions (Scheme 5.01). After olefin carbopalladation, β-hydride elimination provides the substituted double bond and releases a Pd(0) species which must be oxidized to restart the catalytic cycle. Several oxidants have been used to oxidize Pd(0) to Pd(II): e.g., O_2, air, benzoquinone and $Cu(OAc)_2$.[16]

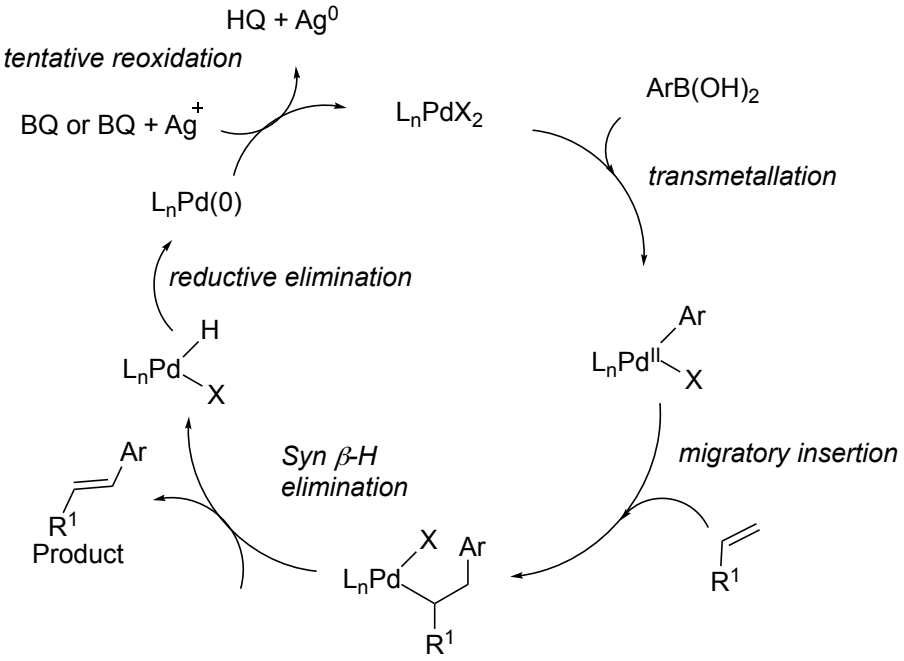

Scheme 5.01. General mechanism for the oxidative palladium-catalyzed arylation of olefins.

5.04 Allylic oxidation

Employing oxidative reaction conditions related to those described in Chapter 5, allylic oxidation of the Δ^5-I^{2}aa residue were pursued to obtain the corresponding allylic alcohols. Selenium dioxide (SeO_2) is commonly used in allylic oxidations,[17] due in part to greater selectivity compared to chromium reagents. Allylic oxidation with selenium dioxide has been suggested to proceed by a mechanism featuring a pericyclic reaction similar to the carbonyl ene-reaction followed by a [2,3]-sigmatropic rearrangement to afford the allyl selenite ester, which undergoes hydrolysis to yield the allylic alcohol (Figure 5.01).

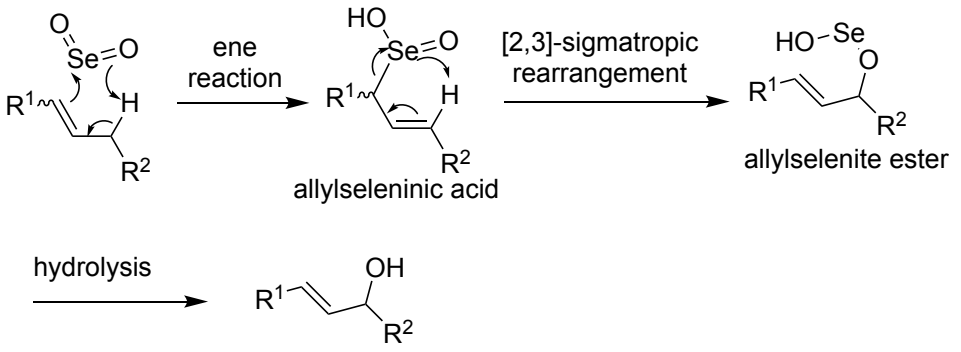

Figure 5.01. The mechanism for allylic oxidation by selenium dioxide proposed by Sharpless[18]

5.05 Examination of the phenylacetyl moiety

In the interest of preparing a potential photo-affinity labeling agent, modification of the phenylacetyl component of PDC113.824 was explored. Protocols were developed for the synthesis of the *p*-azido- and *p*-aminophenylacetyl counterparts.

5.06 Perspectives

This chapter provides methods for the modifications of the azabicycloalkanone residue of the FP modulator PDC113.824. Analogs were synthesized featuring modification of the ring fusion, and the six and five membered rings of the I^2aa system. Moreover, the phenylacetyl moiety was also modified by the addition of *p*-azido and *p*-amino substituents. Examination of the structure-activity relationships of the different indolizidinone analogs in a murine myometrium contraction assay demonstrated the sensitivity of the activity of PDC113.824 to structural modifications. In addition, a parallel investigation of related aza-amino acyl proline derivatives of PDC113.824 has indicated both relationships with the I^2aa analogs as well as novel prototypes with promising capacity to delay labor in an animal model towards the development of improved tocolytic agents for preventing preterm labor.

5.07 References

1. Mikkola, K.; Ritari, N.; Tommiska, V.; Salokorpi, T.; Lehtonen, L.; Tammela, O.; Pääkkönen, L.; Olsen, P.; Korkman, M.; Fellman, V., Neurodevelopmental outcome at 5 years of age of a national cohort of extremely low birth weight infants who were born in 1996–1997. *Pediatrics* **2005**, *116*, 1391–1400.

2. Goldenberg, R. L.; Culhane, J. F.; Iams, J. D.; Romero, R., Epidemiology and causes of preterm birth. *The Lancet* **2008**, *371*, 75–84.

3. Hernandez, W. R.; Francisco, R. P.; Bittar, R. E.; Gomez, U. T.; Zugaib, M.; Brizot, M. L., Effect of vaginal progesterone in tocolytic therapy during preterm labor in twin pregnancies: Secondary analysis of a placebo-controlled randomized trial. *J. Obstet. Gynaecol. Res.* **2017**, *43*, 1536–1542.

4. Peri, K. G.; Quiniou, C.; Hou, X.; Abran, D.; Varma, D. R.; Lubell, W. D.; Chemtob, S. In *THG113: a novel selective FP antagonist that delays preterm labor*, Seminars in perinatology **2002** Elsevier; pp 389–397.

5. Goupil, E.; Tassy, D.; Bourguet, C.; Quiniou, C.; Wisehart, V.; Pétrin, D.; Le Gouill, C.; Devost, D.; Zingg, H. H.; Bouvier, M., A novel biased allosteric compound inhibitor of parturition selectively impedes the prostaglandin F2α-mediated Rho/ROCK signaling pathway. *J. Biol. Chem.* **2010**, *285*, 25624–25636.

6. Bourguet, C. B.; Goupil, E.; Tassy, D.; Hou, X.; Thouin, E.; Polyak, F.; Hébert, T. E.; Claing, A.; Laporte, S. A.; Chemtob, S., Targeting the prostaglandin F2α receptor for preventing preterm labor with azapeptide tocolytics. *J. Med. Chem.* **2011**, *54*, 6085–6097.

7. Bourguet, C. B.; Claing, A.; Laporte, S. A.; Hebert, T. E.; Chemtob, S.; Lubell, W. D., Synthesis of azabicycloalkanone amino acid and azapeptide mimics and their application as modulators of the prostaglandin F2α receptor for delaying preterm birth. *Can. J. Chem.* **2014,** *92*, 1031-1040.

8. Goupil, E.; Tassy, D.; Bourguet, C.; Quiniou, C.; Wisehart, V.; Pétrin, D.; LeGouill, C.; Devost, D.; Zingg, H. H.; Bouvier, M., A novel biased allosteric compound inhibitor of parturition, selectively impedes the PGF2α-mediated rho/rock signaling pathway. *J. Med. Chem.* **2011**, *54*, 6085–6097.

9. Lombart, H.-G.; Lubell, W. D., Rigid dipeptide mimetics: efficient synthesis of enantiopure indolizidinone amino acids. *J. Org. Chem.* **1996**, *61*, 9437–9446.

10. Halab, L.; Becker, J. A.; Darula, Z.; Tourwé, D.; Kieffer, B. L.; Simonin, F.; Lubell, W. D., Probing opioid receptor interactions with azacycloalkane amino acids. Synthesis of a potent and selective ORL1 antagonist. *J. Med. Chem.* **2002**, *45*, 5353–5357.

11. Polyak, F.; Lubell, W. D., Rigid dipeptide mimics: Synthesis of enantiopure 5-and 7-benzyl and 5, 7-dibenzyl indolizidinone amino acids *via* enolization and alkylation of δ-oxo α, ω-di-[*N*-(9-(9-phenylfluorenyl)) amino] azelate Esters. *J. Org. Chem.* **1998**, *63*, 5937–5949.

12. Gosselin, F.; Lubell, W. D., Rigid dipeptide surrogates: Syntheses of enantiopure quinolizidinone and pyrroloazepinone amino acids from a common diaminodicarboxylate precursor. *J. Org. Chem.* **2000**, *65*, 2163–2171.

13. Boukanoun, M. K.; Hou, X.; Nikolajev, L.; Ratni, S.; Olson, D.; Claing, A.; Laporte, S. A.; Chemtob, S.; Lubell, W. D., Investigation of the active turn geometry for the labour delaying activity of indolizidinone and azapeptide modulators of the prostaglandin F2α receptor. *Org. Biomol. Chem.* **2015**, *13*, 7750–7761.

14. Hanessian, S.; McNaughton-Smith, G.; Lombart, H.-G.; Lubell, W. D., Design and synthesis of conformationally constrained amino acids as versatile scaffolds and peptide mimetics. *Tetrahedron* **1997**, *53*, 12789–12854.

15. Lee, A.-L., Enantioselective oxidative boron Heck reactions. *Org. Biomol. Chem.* **2016**, *14*, 5357–5366.

16. Koley, M.; Dastbaravardeh, N.; Schnürch, M.; Mihovilovic, M. D., Palladium(II)-catalyzed regioselective ortho arylation of sp^2 C-H Bonds of *N*-aryl-2-amino pyridine derivatives. *Chem. Cat. Chem.* **2012**, *4*, 1345–1352.

17. Riley, H. L.; Morley, J. F.; Friend, N. A. C., 255. Selenium dioxide, a new oxidising agent. Part I. Its reaction with aldehydes and ketones. *J. Chem. Soc. (Resumed)* **1932**, 1875–1883.

18. Nakamura, A.; Nakada, M., Allylic oxidations in natural product synthesis. *Synthesis* **2013**, *45*, 1421–1451.

Article 4

Paired Utility of Aza-Amino Acyl Proline and Indolizidinone Amino Acid Residues for Peptide Mimicry: Conception of Prostaglandin F2α Receptor Allosteric Modulators that Delay Preterm Birth

Fatemeh M. Mir [†§], N. D. Prasad Atmuri [†§], Jennifer Rodon Fores [†], Xin Hou[‡], Sylvain Chemtob[‡], William D. Lubell [†*]

†Département de Chimie, Université de Montréal, C.P. 6128 Succursale Centre-Ville, Montréal H3C 3J7 QC, Canada

‡Centre Hospitalier Universitaire Sainte-Justine Research Center, Montréal H3T 1C5, QC, Canada

§Equal contribution

J. Med. Chem. **2019**, *62*, 4500–4525

5.1 Abstract

Peptide mimicry employing a combination of aza-amino acyl proline and indolizidinone residues has been used to develop allosteric modulators of the prostaglandin F2α receptor. Systematic study of the *N*-terminal phenylacetyl moiety, and the conformation and side-chain functions of the central turn dipeptide residue has demonstrated the sensitive relationships between modulator activity and topology. Examination of aza-Gly-Pro and aza-Phe-Pro analogs **5.2a** and **5.2b** in a murine preterm labor model featuring treatment with lipopolysaccharide demonstrated their capacity to extend significantly (>20 h) the average time of delivery offering new prototypes for delaying premature birth.

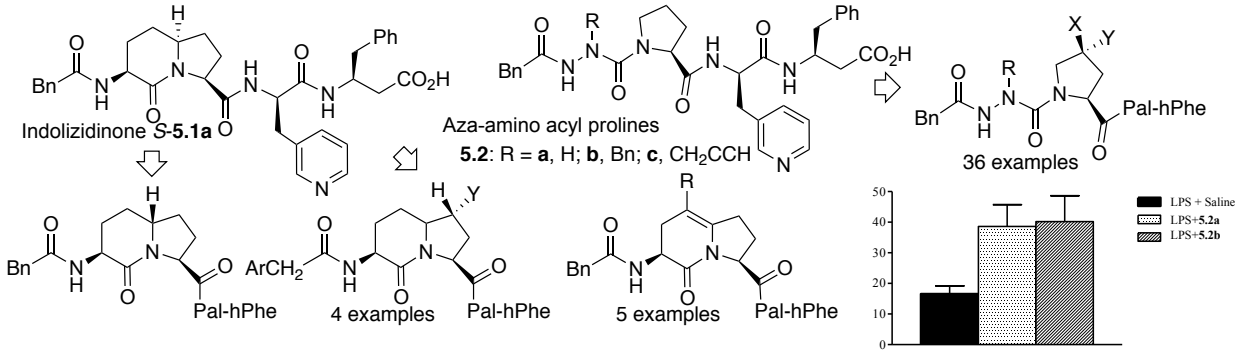

5.2 Introduction

Complementary methods to mimic relevant secondary structures offer potential for parallel investigation of structure-activity relationships in peptide-based drug discovery. Paired utility for type II′ β-turn mimicry has specifically been exhibited by aza-amino acyl proline and indolizidin-2-one amino acid (I^2aa) scaffolds in several biologically active peptides.[1] For example, 10- and 7-fold greater potency was observed respectively on replacement of the Gly-Pro dipeptide by aza-Gly-Pro and I^2aa in calcitonin gene-related peptide antagonists.[1a] Moreover, increased caspase-9 mediated apoptotic cell death has been exhibited relative to the parent Ala-Val-Pro-Ile SMAC (second mitochondria-derived activator of caspase) protein mimic by analogs in which the Val-Pro

dipeptide was swapped for aza-amino acyl proline and I^2aa residues.[1b, 1c] Pertinent to the present study, similar activity and efficacy in inhibiting myometrial contractions by way of modulation of the prostaglandin-F2α (PGF2α) receptor (FP) has been exhibited by the I^2aa analog PDC113.824 (*S*-**5.1a**) and its aza-amino acyl proline counterparts **5.2a**–**c** (Figure 5.1).[1d] To better seize the advantages of the paired utility of aza-amino acyl proline and I^2aa peptide derivatives, a series of diversity-oriented methods are now presented for synthesizing analogs of the related turn mimics in *S*-**5.1a** and **5.2** to conceive novel FP modulators.[2]

In a program targeted on the development of novel tocolytic (labor suppressing) agents that can delay labor and inhibit preterm birth, modulators *S*-**5.1a** and **5.2a**–**c** have been valuable prototypes and probes for mediating FP signalling and myometrial contractions. For example, I^2aa analog *S*-**5.1a** inhibited selectively PGF2*α*-induced myometrial contractions in a mouse model delaying labor up to 42 h.[3] Examination of the action of *S*-**5.1a** has revealed an allosteric mechanism implicating biased signalling.[3] In the absence of the endogenous agonist PGF2α, *S*-**5.1a** is inactive. Without competing for the binding site of the orthosteric ligand, *S*-**5.1a** modulated the exchange rate of PGF2α with tritium-labeled PGF2α. Downstream of the FP receptor, *S*-**5.1a** potentiated PGF2*α*-mediated activation of protein kinase C and mitogen-activated protein kinase (ERK1/2) signalling, but reduced Gα12-dependent activation of RhoA/ROCK signalling leading to actin remodeling and contraction of human myometrial cells.[3]

Replacement of the I^2aa scaffold with aza-amino acyl-L-proline analogs gave azapeptides **5.2a**–**c**, which exhibited similar effects on myometrial contraction and ERK1/2 signalling; however, varying influences on RhoA/ROCK signalling contingent on the aza-residue side-chain.[1d] The latter result was particularly interesting for two reasons. In the first place, the complementarity of aza-amino acyl-L-proline and I^2aa residues was highlighted because earlier attempts failed to provide active analogs from replacement of the I^2aa scaffold with alternative indolizidin-9-one and

quinolizidinone amino acid residues. Furthermore, modification of the aza-amino acid side-chain offered the potential to modulate biased signalling to ideally create alternative probes for studying FP receptor signalling towards the development of improved tocolytic agents.

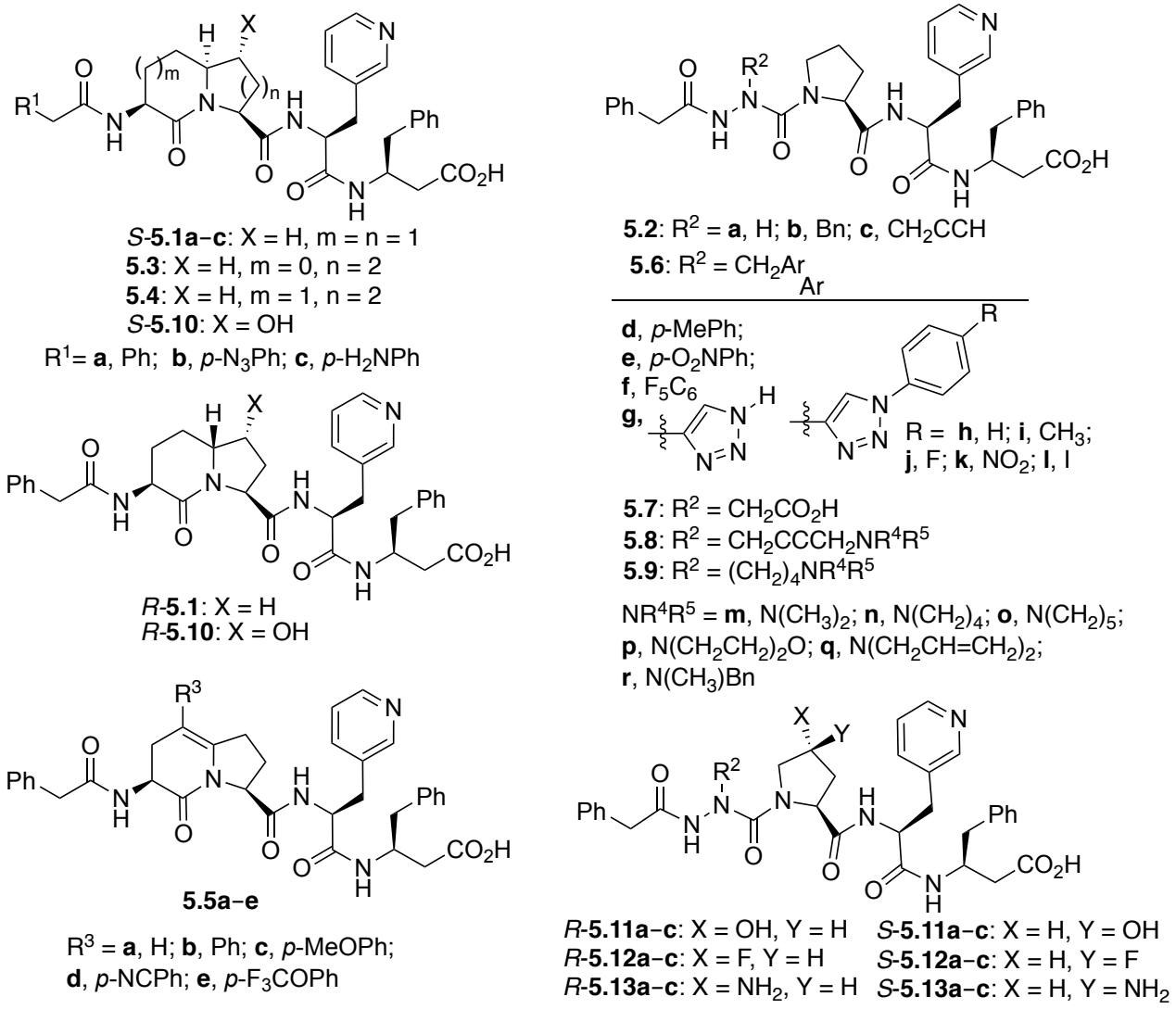

Figure 5.1. I[2]aa and aza-amino acyl proline FP modulators *S*-**5.1a** and **5.2a**–**c**, and related counterparts

The healthcare drivers for developing tocolytic prototypes such as *S*-**5.1a** and **5.2a**–**c** include the growing significance of preterm birth before 37 weeks of pregnancy, and the associated socioeconomic consequences. Preterm birth is correlated with 60-80% of all perinatal deaths,[4] and

long-term neonatal and infant healthcare outcomes, including neurodevelopmental handicap, chronic respiratory illness, infections, and long-term impairment.[5] In spite of advances in knowledge of risk factors and medical interventions to reduce perinatal death, success has been limited in the prediction and prevention of preterm labor, the rate of which has risen globally, such that 15 million babies are estimated to be born prematurely per year.[6] Healthcare costs connected to preterm birth are significant: >$26.2 billion in 2005 in the USA alone amounting to $51,600 per premature birth.[7] Tocolytic drugs currently used in the clinical setting to block uterine contractions have marginal efficacy and at times are associated with significant adverse effects to either the mother and/or fetus.[8] Although they may extend gestation for the 48 hours needed to administer corticosteroids to the parturient for fetal surfactant maturation, for many patients, gestation needs to be prolonged for longer periods. Prevention of preterm birth remains a major health concern associated with serious short- and long-term complications to infants in industrialized and agrarian countries worldwide.

In the pursuit of improved tocolytics to inhibit preterm labor and probes to better understand the importance of FP mediated signalling pathways in labor, a set of diversity-oriented methods for making azapeptide and indolizidin-2-one amino acids have been developed and used to prepare a series of analogues of *S*-**5.1a** and **5.2a**–**c**. In the case of the I^2aa scaffold found in *S*-**5.1a**, methods have been conceived that illustrate the value of 5-iodoindolizidin-2-ones, which were prepared by transannular cyclization of unsaturated macrocycles.[9] In contrast to the corresponding 6-iodopyrroloazepinone counterpart,[9a] which served effectively in S_N1 chemistry to install a variety of side-chains onto the seven membered cycle,[10] attempts to perform substitution chemistry on the 5-iodoindolizidin-2-ones **5.16** and **5.17** resulted in elimination to the corresponding unsaturated indolizidin-2-ones **5.18** and **5.19** (Scheme 5.1). The latter have however provided valuable intermediates for the synthesis of indolizidin-2-ones having different ring fusion stereochemistry

(e.g., *R*- and *S*-**5.1a**) and substituents on both the five (e.g., *R*- and *S*-**5.10**) and six (e.g., **5.5b**-**e**) membered rings. In parallel, the aza-amino acyl proline dipeptide of **5.2a–c** has been elaborated on the aza-residue using a combination of submonomer chemistry in which side-chains were introduced by alkylation of an aza-glycine residue (e.g., **5.6c**–**f**),[11] as well as diversification of the acetylene of an aza-propargylglycine (azaPra) residue in solution (e.g., **5.6g–l** and **5.7**–**9**). In addition, to explore modification of the proline ring system, a solid-phase approach has been introduced for the assembly of modulators in which hydroxyproline has served to prepare a diverse set of analogs (e.g., **5.11**–**13**) using so called proline editing.[12]

The influences of analogs **5.1**–**5.13** have been studied on spontaneous and PGF2α-induced contractions of the myometrium in mouse tissue removed immediately after parturition. The limited activity of many of the analogs reflects significantly the relevance of conformation and the impact of substituents on biological activity. Moreover, the significant potency of the aza-Gly-Pro and aza-Phe-Pro derivatives **5.2a** and **5.2b** as effective counterparts of *S*-**5.1a** has been further demonstrated in a mouse model for preterm labor. In sum, the reported study has highlighted novel methods for using the dual combination of aza-amino acyl proline and I^2aa scaffolds as complementary tools for studying peptide-based drug design and further illustrates the promise of aza-Gly-Pro 5.2a and aza-Phe-Pro 5.2b as prototypes for delaying preterm birth.

5.3 Results and discussion

Parallel development of methods to study the I^2aa and aza-amino acyl proline components of *S*-**5.1a** and **5.2a**–**c** has focused on both the conformation and substituents of theses dipeptide mimics. Initially, methods were developed for the modification of the I^2aa ring fusion and six-membered ring system. Considering that the I^2aa six-membered ring would occupy the same position as the aza-residue of the aza-amino acyl proline dipeptide, methods were also employed to diversify the

semicarbazide side-chain. Finally, approaches were used for modifying the five-membered rings of the I^2aa and Pro components.

5-Iodoindolizidine-2-ones **5.16** and **5.17** were respectively synthesized via transannular cyclizations of 9-membered unsaturated lactams **5.14** and **5.15** (Scheme 5.1).[9a,13] Phenylacetamide benzyl ester **5.14** was prepared from the corresponding *N*-(Boc)amino methyl ester[13] by a sequence featuring treatment with HCl gas in dichloromethane, acylation using phenylacetyl chloride and Hünig's base, saponification with LiOH, and carboxylate alkylation with benzyl bromide and $NaHCO_3$ (Experimental Section). In spite of changes to an *N*-terminal amide and larger ester, transannular cyclization of **5.14** with iodine in THF proceeded in the same fashion as carbamate **5.15** with regiocontrol and diastereoselectivity to afford the (3*S*,5*R*,6*R*,9*S*)-indolizidin-2-one **5.16** in 76% yield.[9a] Attempts to add side-chain diversity by displacement of iodides **5.16** and **5.17** were unsuccessful using various nucleophiles; instead, elimination of the bridge head proton occurred to form enamine. Enamines **5.18** and **5.19** were effectively prepared by iodide elimination with triethylamine at 80 °C in acetonitrile; however, concomitant loss of the Fmoc group necessitated protection with di-*tert*-butyldicarbonate. Olefin reduction provided access to different ring fusion stereochemistry. For example, hydride reduction of enamine **5.18** with sodium cyanoborohydride and catalytic acetic acid in EtOH gave a 2:1 diasteroisomeric ratio in favor of the convex over the concave isomers (e.g., *R*- and *S*-**5.21**: 57% and 21% yields). Alternatively, hydrogenation of enamine **5.19** with palladium-on-carbon in EtOH furnished selectively concave isomer *S*-**5.20** in 86% yield. Indolizidinone ring fusion stereochemistry was ascertained by NOESY NMR experiments based on the observed transfer of magnetization between the ring fusion and C3 protons in *S*-**5.21**, and confirmed by X-ray crystallography (Figure 5.2).

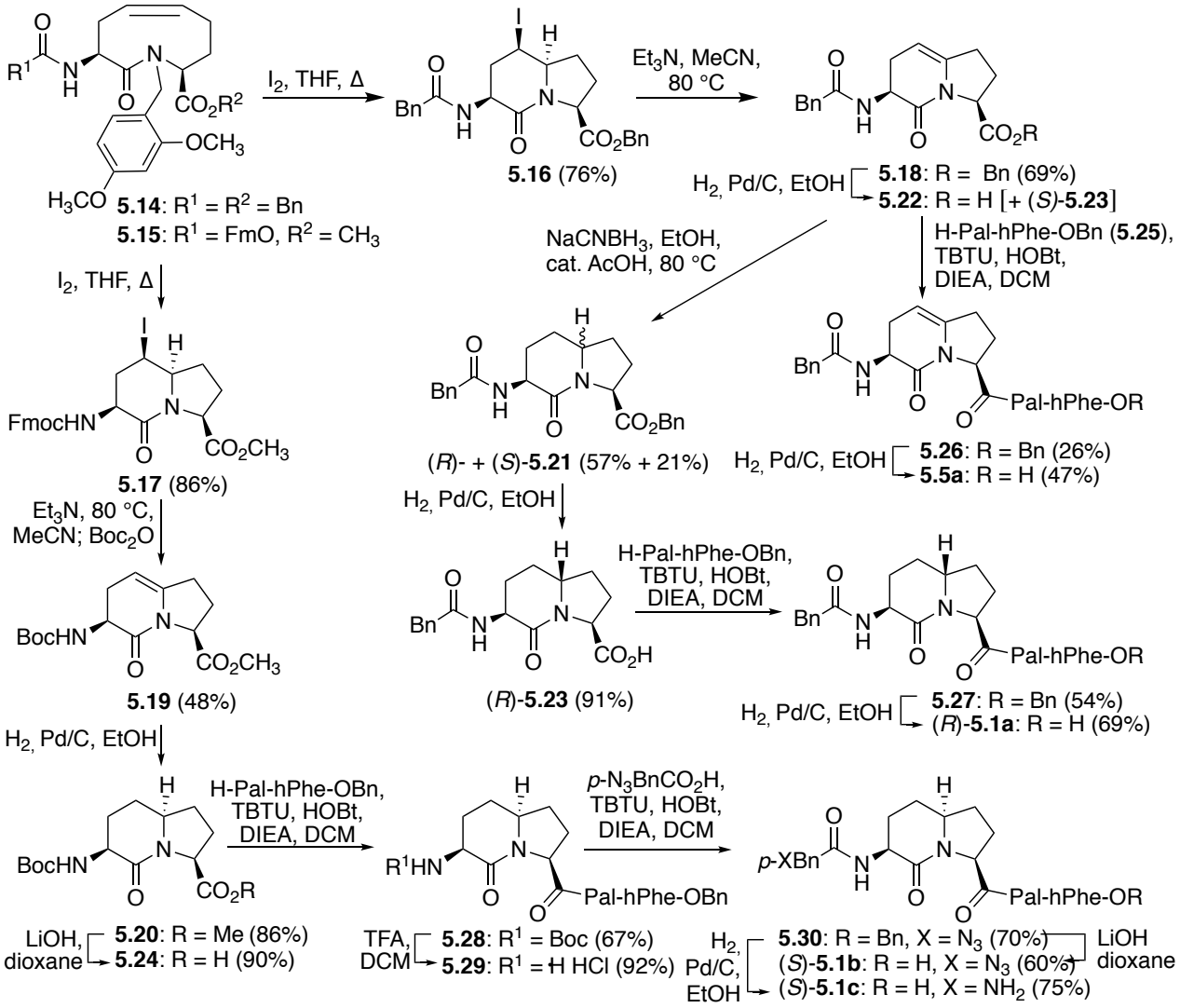

Scheme 5.1: Synthesis of indolizidin-2-one analogs *R*-**5.1a**, *S*-**5.1b**, *S*-**5.1c** and **5.5a**

Analogs of modulator *S*-**5.1a** were synthesized from unsaturated Δ^5-indolizidinone **5.18** and ring fusion stereoisomers **5.20** and **5.21**. Hydrogenolysis of benzyl ester **5.18** using palladium-on-carbon in EtOH under a balloon of hydrogen for <10 min occurred with concomitant olefin reduction to give a 1:1 mixture of acids **5.22** and *S*-**5.23**, which was used in the subsequent peptide coupling step. Benzyl ester *R*-**5.21** was converted to acid *R*-**5.23** under similar hydrogenolytic conditions. Saponification of methyl ester **5.20** with LiOH in dioxane gave carboxylic acid **5.24**. The four acids **5.22**, *S*-**5.23**, *R*-**5.23** and **5.24** were coupled to (*S*,*S*)-pyridinylalaninyl-β-

homophenylalanine benzyl ester (**5.25**)[1d] using TBTU, HOBt, and DIEA to give protected peptides **5.26**–**5.28** in 26–67% yields.

In the interest of exploring diversity at the phenylacetamide component as well as preparing a potential photoaffinity labeling agent, *p*-azido- and *p*-aminophenylacetamide analogs *S*-**5.1b** and *S*-**5.1c** were prepared by routes commencing with removal of the Boc group from peptide **5.28** using HCl gas and acylation of the resulting hydrochloride salt **5.29** using 2-(4-azidophenyl)acetic acid, TBTU, HOBt, and DIEA in CH_2Cl_2 to provide 4-azidophenylacetamide **5.30**. Hydrolysis of benzyl ester **5.30** with LiOH in dioxane gave acid *S*-**5.1b**. Hydrogenolytic cleavages of benzyl esters **5.26**, **5.27** and **5.30** using palladium-on-carbon in ethanol under a balloon of hydrogen furnished respectively modulator analogs **5.5a**, *R*-**5.1a** and *S*-**5.1c**, which were purified by preparative reverse-phase HPLC (Table 5.1).

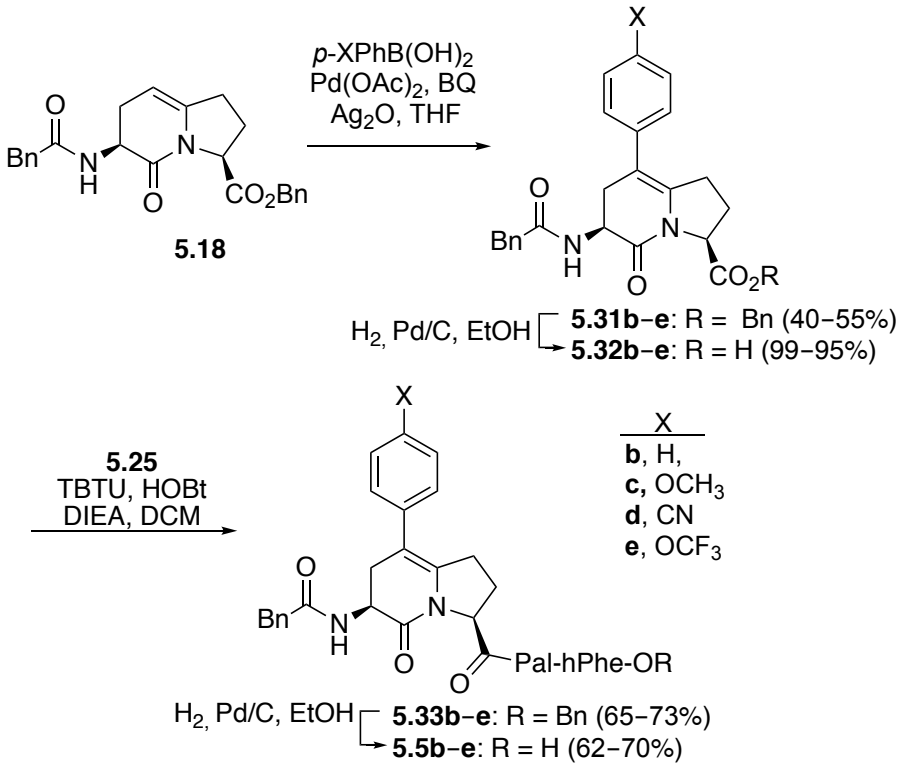

Scheme 5.2. Synthesis of 5-aryl-indolizidinone analogs **5.5b**–**e**

The modification of the six-membered ring of the I[2]aa moiety was next explored by C-H bond activation and arylation at C5 using palladium-catalysis (Scheme 5.2). Four aryl boronates were coupled to enamine **5.18** using $Pd(OAc)_2$, 1,4-benzoquinone (BQ) and silver oxide in THF at 80 °C to provide **5.31b**–**e** in 40–55% yields. Hydrogenolytic cleavages of benzyl esters **5.31b**–**e**, respective couplings of the resulting acids **5.32b**–**e** to dipeptide **5.25**, and benzyl ester cleavages as discussed for the synthesis of **5.5a** gave the 5-aryl analogs **5.5b**–**e**, which were purified by preparative reverse-phase HPLC (Table 5.1).

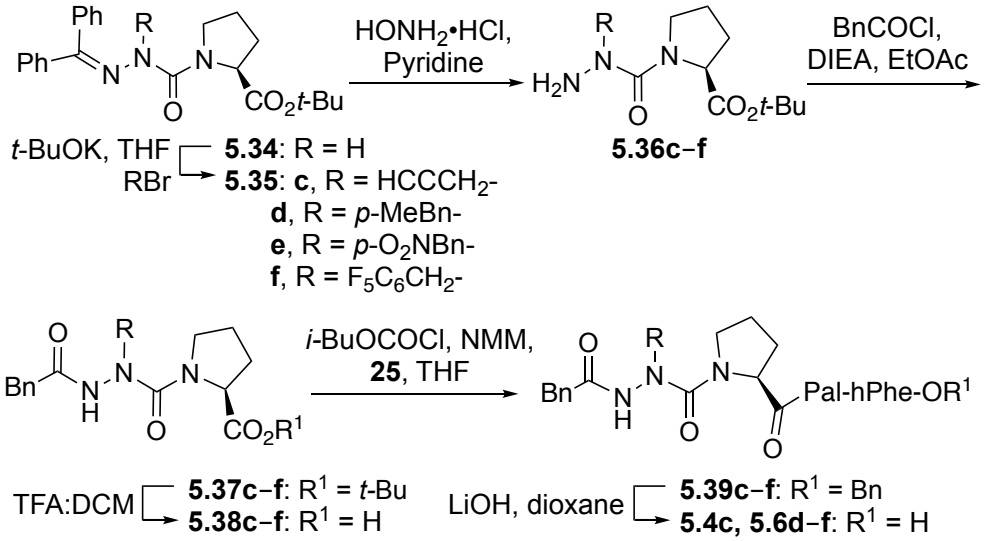

Scheme 5.3. Synthesis of aza-Pra-Pro and aza-Phe-Pro peptides **5.2c** and **5.6d**–**f**

In parallel to efforts to modify the six-membered ring of the I[2]aa residue, a set of methods was employed to append a series of side-chains on the aza-residue to make analogs of azapeptides **5.2a**–**c**. Modification of the aza-residue side-chain was first explored by the synthesis and alkylation of aza-glycinyl proline *t*-butyl ester **5.34** using propargyl bromide, as well as *p*-methyl-, *p*-nitro- and pentafluoro benzyl bromides (Scheme 5.3).[11a] The propargyl side-chain was selected for further diversification as discussed below. The three benzyl groups were chosen to contrast the influences of aromatic electron-density and hydrophobicity for activity with those of 5-arylindolizidinones **5.5b**–**e**. Aza-dipeptides **5.38c**–**f**, all were prepared from the respective azaPra

and azaPhe analogs **5.35c** and **5.35d**–**f** by benzhydrylidene removal using hydroxylamine hydrochloride in pyridine, acylation of the resulting semicarbazide with phenylacetyl chloride, and *tert*-butyl ester removal in a TFA/DCM solution. They were then coupled to dipeptide **5.25** using *iso*-butyl chloroformate and *N*-methylmorpholine to furnish azapeptide benzyl esters **5.39c**–**f**, which after saponification with LiOH in dioxane and RP-HPLC purification afforded aza-amino acyl prolyl peptides **5.6d**–**f** (Table 5.1).

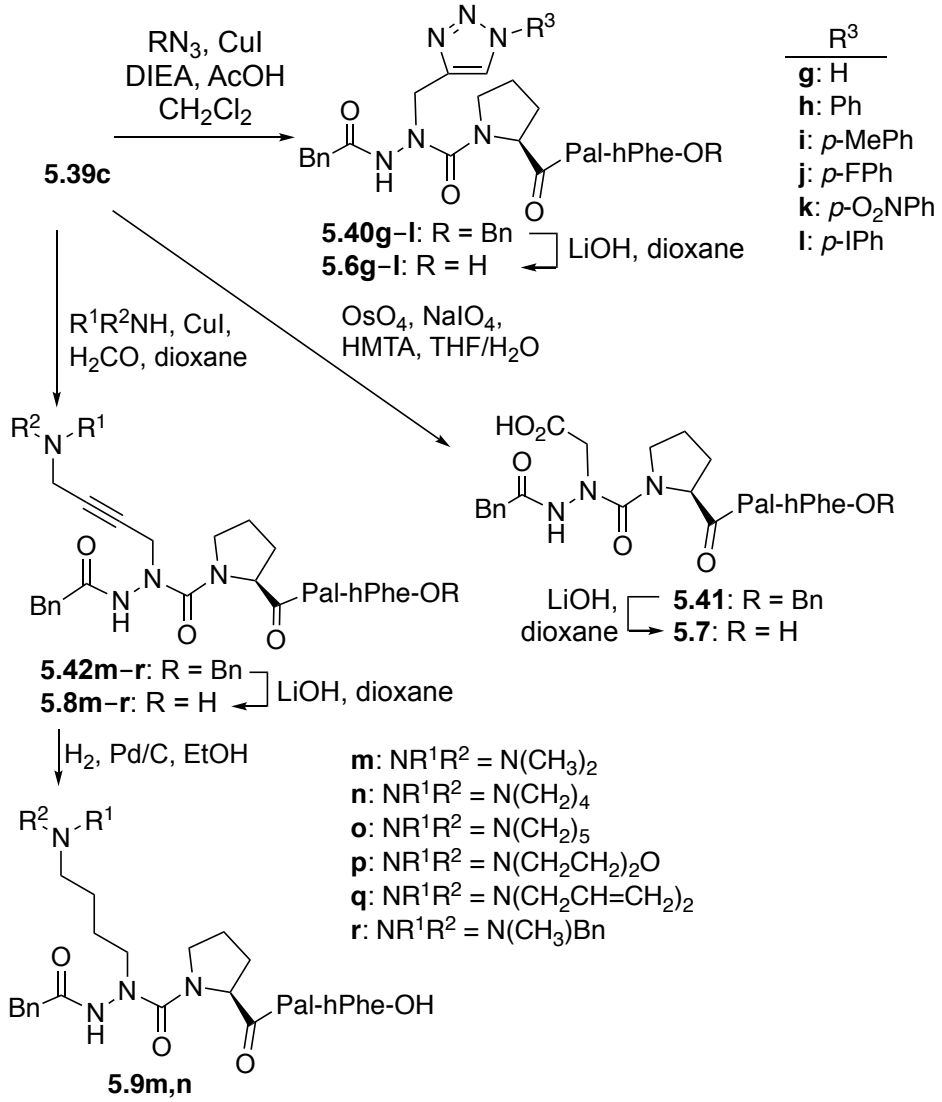

Scheme 5.4. Aza-triazole-alanine, aza-Asp and aza-Lys analog synthesis by azaPra diversification

With azaPra peptide **5.39c** in hand, diversity-oriented routes were used to prepare a broader group of side-chain analogs including aza-1,2,3-triazole-3-alanine, aza-aspartate and aza-lysine analogs **5.6**–**5.9** to study the influences of charge and hydrogen-bonding at the side-chain for activity (Scheme 5.4). A set of six aza-1,2,3-triazole-3-alanines **5.40g–l** was synthesized from azaPra peptide **5.39c** by copper-catalyzed azide-alkyne cycloadditions. Among various methods explored, 1,3-dipolar cycloadditions were best accomplished with sodium azide and aryl azides using CuI and DIPEA in AcOH.[14] After benzyl ester saponification, triazole-alanine peptides **5.6g–l** were purified by HPLC (Table 5.1). The azaPra peptide **5.39c** was converted to aza-aspartate **5.41** in 89% yield using an OsO_4/$NaIO_4$/hexamethylenetetramine-mediated oxidation.[15] Hydrolysis of benzyl ester **5.41** and HPLC purification gave aza-Asp peptide **5.7**. Finally, in Mannich-like additions on the acetylene moiety,[16] azaPra peptide **5.39c** reacted in dioxane at 80 °C with copper iodide, formaldehyde and a set of six secondary amines: dimethylamine, pyrrolidine, piperidine, morpholine, diallylamine and methylbenzylamine. After saponification as described above, the set of aza-lysines **5.8m**–**r** was isolated by HPLC in 40 to 80% yields. Acetylenes **5.8m** and **5.8n** were reduced using catalytic hydrogenation with palladium-on-carbon to afford more flexible aza-Lys analogs **5.9m** and **5.9n**.

The five-membered ring of the I^2aa residue was modified by allylic oxidation of 5,6-dehydroindolizidin-2-one **5.18** with selenium dioxide and TBHP (tert-Butyl hydroperoxide) in dioxane to give a separable mixture of 5- and 7-hydroxy-dehydroindolizidin-2-ones **5.43** and **5.44** (Scheme 5.5). Olefin **5.43** was reduced using sodium cyanoborohydride and catalytic acetic acid in EtOH at 80 °C to give a 3:1 mixture of convex and concave diastereomers (e.g., *R*- and *S*-**5.45**, 44% and 26% yields) after chromatography. The regio- and stereochemistry of 5- and 7-hydroxyindolizidin-2-ones **5.43**–**5.45** were assigned using COSY and NOESY NMR spectroscopic

experiments and X-ray crystallography of *R*-**5.45** (Figure 5.2). Employing a similar sequence of benzyl ester hydrogenolysis and couplings to dipeptide **5.25**, 7-hydroxindolizidinones *R*-**5.46** and *S*-**5.46** were respectively converted to acids *R*-**5.10** and *S*-**5.10**, which were purified by preparative reverse-phase HPLC (Table 5.1).

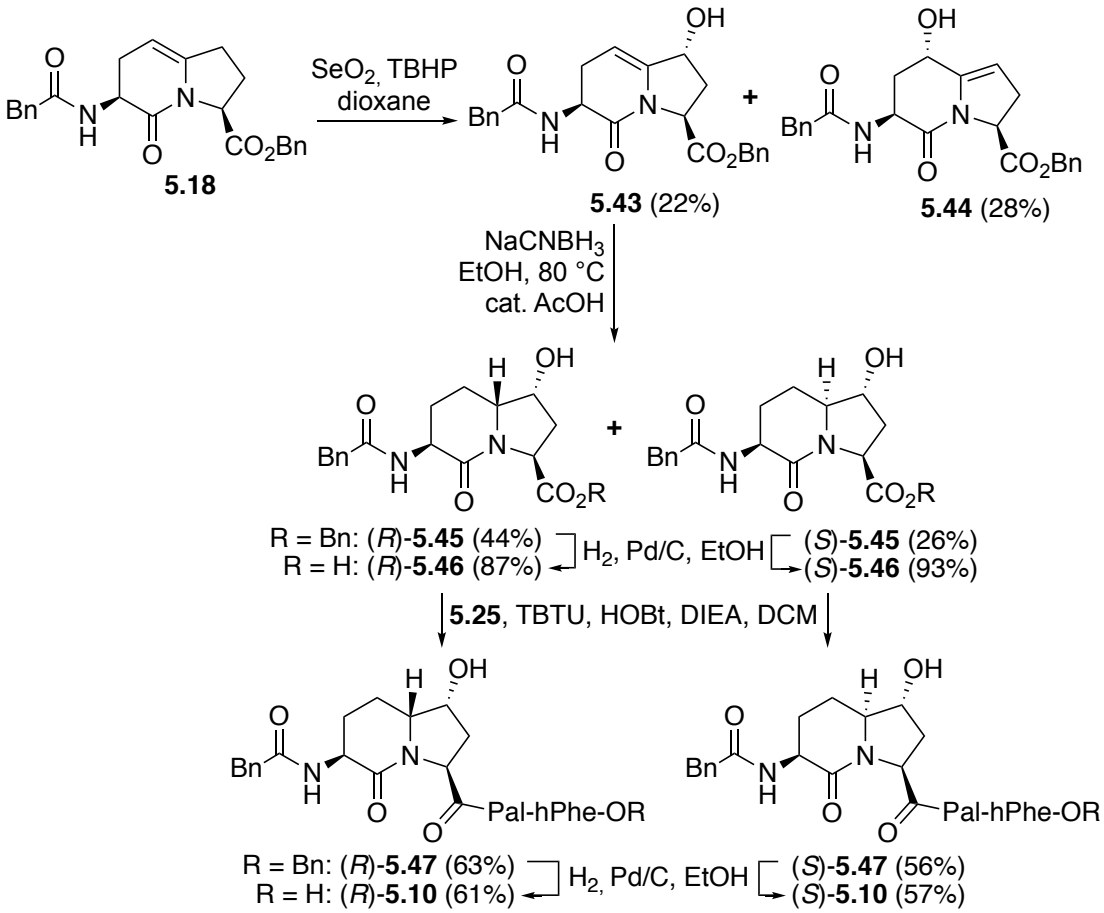

Scheme 5.5. Synthesis of 7-hydroxy-indolizidinones *R*- and *S*-**5.10**

In parallel, a set of proline residue analogs of azapeptides **5.2a**–**c** was prepared using 4-hydroxyproline. The related 4-hydroxy (Hyp), 4-fluoro- (Flp) and 4-aminoproline (Amp) analogs were generated to study influences of the ring pucker, hydrophobicity and substituents on activity.[12,17] A solid-phase route was developed featuring modification of Hyp azapeptides (*R*)-**5.54b**–**d** (Scheme 5.6).

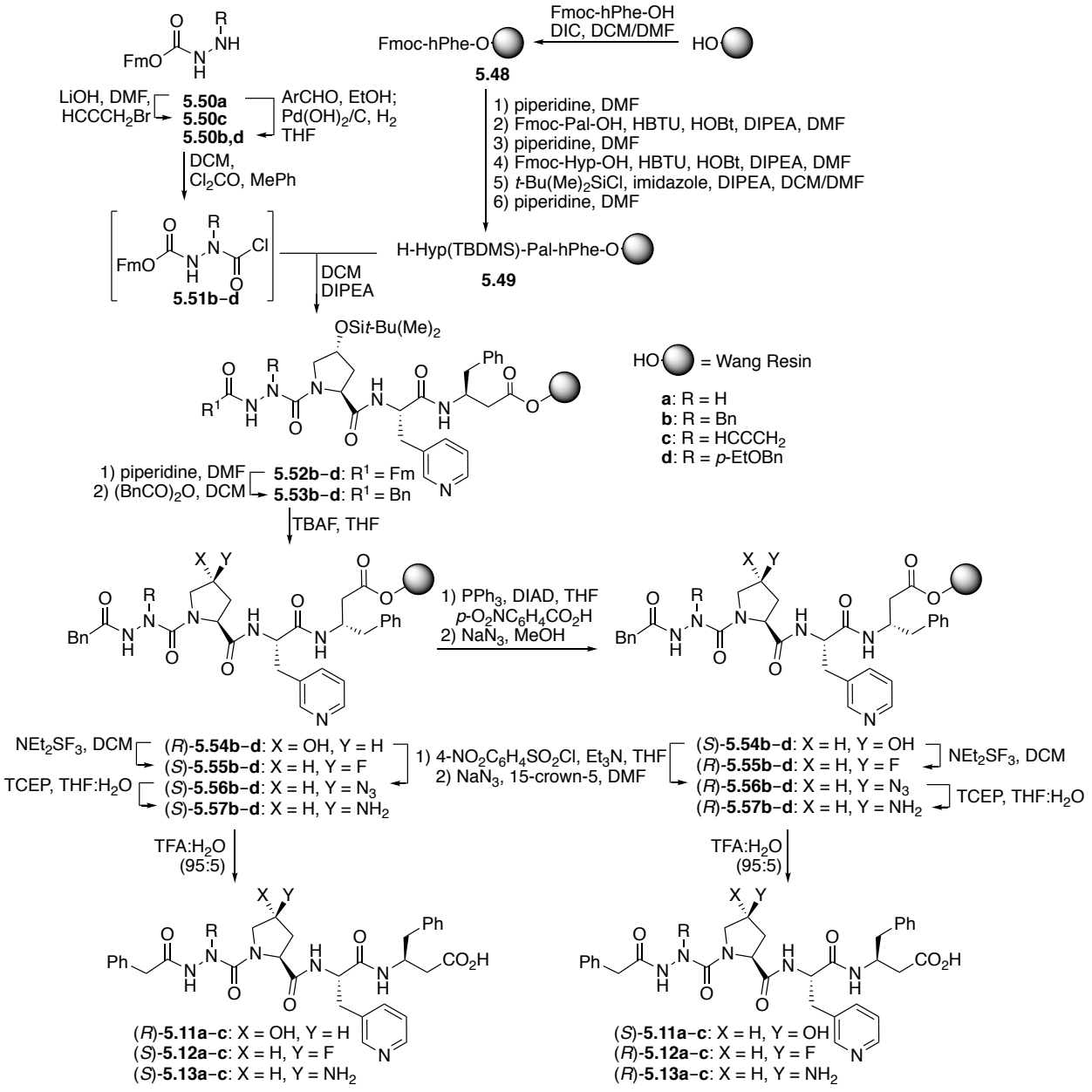

Scheme 5.6. Solid-phase synthesis of 4*R*- and 4*S*-Hyp-, Flp- and Amp-azapeptides **5.11**–**5.13**

N-Fmoc-β–Homophenylalanine (Fmoc-hPhe-OH) was coupled to Wang resin by way of its symmetrical anhydride to provide β-amino ester resin **5.48**. After capping unreactive sites with acetic anhydride, linear tripeptide resin **5.49** was synthesized by Fmoc removals, couplings of *N*-(Fmoc)pyridylalanine and (4*R*)-Fmoc-Hyp-OH, and hydroxyl group silylation. Central to the success of the solid-phase synthesis of azapeptides was the effective introduction of the aza-residue

using different *N*-Fmoc-aza-amino acid chlorides.[18] To avoid formation of oxadiazolone in the synthesis of the aza-glycinyl-proline analogs,[19] the 4-ethoxybenzyl side-chain was employed as a temporary protecting group, which was removed during cleavage of the azapeptide from the resin with TFA. The benzyl and 4-ethoxybenzyl side-chains were added to the aza-residue by reductive aminations of semicarbazones formed from the corresponding aldehydes and fluorenylmethyl carbazate **5.50a** in EtOH, using palladium hydroxide-on-carbon in THF.[18] Propargyl carbazate **5.50b** was synthesized by alkylation of **5.50a** with propargyl bromide and lithium hydroxide in DMF.[20] Activation of carbazates **5.50b**–**d** with phosgene in toluene gave the corresponding *N*-Fmoc-aza-amino acid chlorides, which were coupled to tripeptide resin **5.49**.[18] After aza-amino acylation, the Fmoc group was removed from **5.52b**–**d** and the aza-residues were phenylacetylated using the corresponding anhydride in dichloromethane. The 4*R*-hydroxyl group was liberated from resins **5.53b**–**d** using tetra-n-butylammonium fluoride (TBAF) in THF and converted to the 4*S*-alcohol *S*-**5.54b**–**d** employing a two-step process featuring Mitsunobu reaction with 4-nitrobenzoic acid, PPh_3 and diisopropyl azodicarboxylate (DIAD) in THF, followed by nitrobenzoate removal without Fmoc cleavage using NaN_3 in MeOH.[12]

With 4*R*- and 4*S*-hyroxyproline azapeptides *R*- and *S*-**5.54b**–**d** in hand, syntheses were pursued to make the diasteromeric 4*S*- and 4*R*-Flp and Amp azapeptides *R*- and *S*-**5.55b**–**d** and **5.57b**–**d** (Scheme 5.6). Fluorination of 4*R*- and 4*S*-hydroxyprolines *R*- and *S*-**5.54b**–**d** was accomplished using diethylaminosulfur trifluoride (DAST) in dichloromethane via S_N2 chemistry with inversion of stereochemistry. Aminoprolines *S*- and *R*-**5.57b**–**c** were prepared from alcohols *R*- and *S*-**5.54b**–**c** by activation as the corresponding *p*-nitrophenylsulfonates,[12] followed by S_N2 displacement using NaN_3. Attempts to synthesize aza-*p*-ethoxyphenylalaninyl azidoprolines *S*- and *R*-**5.56d** using the same protocol were however unsuccessful, likely due to interactions between the electron

rich aromatic ring of the *p*-ethoxybenzyl group and Hyp ring. Prolyl amide-π interactions are known to favor *cis*-amide bond isomers,[21] which in the case of **5.56d** may have prevented activation of the hydroxyl group as a *p*-nitrophenylsulfonate. To circumvent this obstacle, the 4*S*- and 4*R*-*N*-Fmoc-azidoprolines were synthesized in solution, coupled onto the resin and elongated with *N*-Fmoc-aza-4-ethoxyphenylalaninyl chloride and phenyl acetic anhydride to obtain azidoproline peptides *S*- and *R*-**5.56d**. Azides *S*- and *R*-**5.56b**–**d** were reduced with tris(2-carboxyethyl)phosphine (TCEP) to provide the corresponding amines *S*- and *R*-**5.57b**–**d**. Finally, resin cleavage was performed using 95:5 TFA/H_2O to provide Hyp, Flp and Amp azapeptides *R*- and *S*-**5.11**–**5.13a**–**c** after HPLC purification (Table 5.1).

The stereochemical assignments of bicycles **5.16**, **5.21** and **5.43**–**5.45** were made using 2D NMR spectroscopy and X-ray crystallography [Supporting Information (SI)]. After the ring protons in the bicycle were assigned using COSY experiments to ascertain through-bond correlations, configuration assignments at the amino acid derived α-carbons were correlated to the newly generated ring fusion, iodide and alcohol bearing carbons using NOESY experiments to determine through-space nuclear Overhauser effects (Figure 5.2).

Table 5.1. Purity, retention times and mass spectrometric analyses of I^2aa and aza-Xaa-Pro analogs

entry	Compounds	RT (min) in		Purity at 214/254 nm (%)	MS [M+1]/[M+Na]	
		CH_3OH	CH_3CN		m/z (calc.)	m/z (obs.)
1	Phenylacetyl-(3*S*,6*R*,9*S*)-I^2aa-Pal-hPhe (*R*-**5.1**)	5.1 [h]	4.7 [d]	≥ 96	626.2973	626.2981
2	4-Azidophenylacetyl-(3*S*,6*S*,9*S*)-I^2aa-Pal-hPhe (*S*-**5.1b**)	5.7 [c]	5.3 [d]	≥ 96	689.2807	689.2817
3	4-Aminophenylacetyl-(3*S*,6*S*,9*S*)-I^2aa-Pal-hPhe (*S*-**5.1c**)	6.4 [c]	-	≥ 96	663.2902	663.2903
4	Phenylacetyl-(3*S*,9*S*)-5-Δ^5-I^2aa-Pal-hPhe (**5.5a**)	6.1 [b]	5.0 [d]	≥ 96	646.2636	646.2641
5	Phenylacetyl-(3*S*,9*S*)-5-Ph-Δ^5-I^2aa-Pal-hPhe (**5.5b**)	6.7 [c]	6.0 [d]	≥ 96	722.2949	722.2951
6	Phenylacetyl-(3*S*,9*S*)-5-(4-methoxyphenyl)-Δ^5-I^2aa-Pal-hPhe (**5.5c**)	5.9 [f]	8.1 [d]	≥ 96	730.3235	730.3262
7	Phenylacetyl-(3*S*,9*S*)-5-(4-cyanophenyl)-Δ^5-I^2aa-Pal-hPhe (**5.5d**)	6.0 [h]	6.7 [h]	≥ 96	725.3082	725.3104
8	Phenylacetyl-(3*S*,9*S*)-5-(4-trifloromethylphenyl)-Δ^5-I^2aa-Pal-hPhe (**5.5e**)	10.7 [c]	8.9 [d]	≥ 96	784.2952	784.2964
9	Phenylacetyl-aza-(4-Me)Phe-Pro-Pal-hPhe (**5.6d**)	9.5 [g]	5.1 [b]	≥ 96	705.3395	705.3394
10	Phenylacetyl-aza-(4-O_2N)Phe-Pro-Pal-hPhe (**5.6e**)	7.3 [c]	6.3 [d]	≥ 99	736.3086	736.3091
11	Phenylacetyl-aza-(pentafluoro)Phe-Pro-Pal-hPhe (**5.6f**)	10.3 [a]	5.4 [b]	≥ 99	787.2768	787.2780
12	Phenylacetyl-aza-(triazole)Ala-Pro-Pal-hPhe (**5.6g**)	5.8 [e]	5.0 [d]	≥ 99	682.3096	682.3111
13	Phenylacetyl-aza-(1-phenyltriazole)Ala-Pro-Pal-hPhe (**5.6h**)	4.4 [f]	6.0 [d]	≥ 99	758.3409	758.3408
14	Phenylacetyl-aza-(1-toluyltriazole)Ala-Pro-Pal-hPhe (**5.6i**)	6.7 [g]	6.3 [d]	≥ 97	772.3566	772.3581
15	Phenylacetyl-aza-[1-(4-fluorophenyl)triazole]Ala-Pro-Pal-hPhe (**5.6j**)	8.9 [b]	4.7 [d]	≥ 97	776.3315	776.3331
16	Phenylacetyl-aza-[1-(4-nitrophenyl)triazole]Ala-Pro-Pal-hPhe (**5.6k**)	7.7 [g]	6.1 [d]	≥98	803.3259	803.3276
17	Phenylacetyl-aza-[1-(4-iodophenyl)]triazole-Ala-Pro-Pal-hPhe (**5.6l**)	6.5 [h]	5.9 [h]	≥ 99	884.2376	884.2383
18	Phenylacetyl-aza-Asp-Pro-Pal-hPhe (**5.7**)	7.6 [b]	5.0 [d]	≥ 99	659.2824	659.2836
19	Phenylacetyl-aza-[(*N*,*N*-dimethylamino)but-2ynyl]Gly-Pro-Pal-hPhe (**5.8m**)	5.4 [b]	4.2 [d]	≥ 98	696.3504	696.3509
20	Phenylacetyl-aza-[(pyrrolidinyl)but-2-ynyl]Gly -Pro-Pal-hPhe (**5.8n**)	6.3 [d]	4.4 [d]	≥ 99	722.3661	722,3652
21	Phenylacetyl-aza-[(piperidinyl)but-2-ynyl]Gly-Pro-Pal-hPhe (**5.8o**)	5.8 [b]	4.4 [i]	≥ 99	736.3817	736.3822
22	Phenylacetyl-aza-[(morpholino)but-2-ynyl]Gly-Pro-Pal-hPhe (**5.8p**)	7.1 [j]	4.4 [i]	≥ 99	738.3610	738.3620
23	Phenylacetyl-aza-[(*N*,*N*-diallylamino)but-2-ynyl]Gly-Pro-Pal-hPhe (**5.8q**)	2.2 [e]	4.6 [i]	≥ 99	748.3817	748.3821
24	Phenylacetyl-aza-[(*N*-methyl,*N*-benzyl)but-2-ynyl]Gly-Pro-Pal-hPhe (**5.8r**)	6.6 [b]	4.9 [d]	≥ 99	772.3817	772.3840
25	Phenylacetyl-aza-(*N*,*N*-dimethyl)Lys-Pro-Pal-hPhe (**5.9m**)	5.7 [b]	4.4 [d]	≥ 99	700.3817	700.3814
26	Phenylacetyl-aza-[(pyrrolidinyl)butyl]Gly-Pro-Pal-hPhe (**5.9n**)	5.7 [b]	6.6 [d]	> 99	726.3974	726.3980
27	Phenylacetyl-(3S,6S,7R,9S)-7-hydroxy-I^2aa-Pal-hPhe (*R*-**5.10**)	5.6 [b]	4.5 [d]	≥ 96	664.2742	664.2712
28	Phenylacetyl-(3S,6S,7S,9S)-7-hydroxy-I^2aa-Pal-hPhe (*S*-**5.10**)	5.2 [b]	4.4 [d]	≥ 96	664.2742	664.2748
29	Phenylacetyl-aza-Gly-(4*R*)-Hyp-Pal-hPhe (*R*-**5.11a**)	6.7 [d]	4.4 [d]	> 99	617.2718	617.2698
30	Phenylacetyl-aza-Phe-(4*R*)-Hyp-Pal-hPhe (*R*-**5.11b**)	6.5 [e]	5.8 [d]	≥ 96	707.3188	707.3208
31	Phenylacetyl-aza-Pra-(4*R*)-Hyp-Pal-hPhe (*R*-**5.11c**)	5.6 [k]	5.2 [d]	≥ 99	655.2875	655.2892
32	Phenylacetyl-aza-Gly-(4*S*)-Hyp-Pal-hPhe (*S*-**5.11a**)	6.9 [d]	4.5 [d]	≥ 99	617.2718	617.2728
33	Phenylacetyl-aza-Phe-(4*S*)-Hyp-Pal-hPhe (*S*-**5.11b**)	6.7 [c]	5.8 [d]	≥ 99	707.3188	707.3217
34	Phenylacetyl-aza-Pra-(4*S*)-Hyp-Pal-hPhe (*S*-**5.11c**)	8.1 [d]	5.2 [d]	≥ 99	655.2875	655.2878
35	Phenylacetyl-aza-Gly-(4*S*)-Flp-Pal-hPhe (*S*-**5.12a**)	7.6 [d]	6.2 [d]	~82	619.2675	619.2697
36	Phenylacetyl-aza-Phe-(4*S*)-Flp-Pal-hPhe (*S*-**5.12b**)	7.6 [d]	6.0 [d]	≥ 99	709.3144	709.3162
37	Phenylacetyl-aza-Pra-(4*S*)-Flp-Pal-hPhe (S-**5.12c**)	5.4 [d]	5.3 [d]	≥ 99	657.2831	657.2857
38	Phenylacetyl-aza-Gly-(4*R*)-Flp-Pal-hPhe (*R*-**5.12a**)	6.8 [d]	4.6 [d]	≥ 95	619.2675	619.2678
39	Phenylacetyl-aza-Phe-(4*R*)-Flp-Pal-hPhe (*R*-**5.12b**)	9.5 [d]	6.2 [d]	≥ 97	709.3144	709.3146
40	Phenylacetyl-aza-Pra-(4*R*)-Flp-Pal-hPhe (*R*-**5.12c**)	8.3 [d]	5.5 [d]	≥ 95	657.2831	657.2834
41	Phenylacetyl-aza-Gly-(4*S*)-Amp-Pal-hPhe (*S*-**5.13a**)	5.2 [d]	4.9 [d]	≥ 99	616.2878	616.285
42	Phenylacetyl-aza-Phe-(4*S*)-Amp-Pal-hPhe (*S*-**5.13b**)	8.4 [d]	5.2 [d]	≥ 95	706.3348	706.3349
43	Phenylacetyl-aza-Pra-(4*S*)-Amp-Pal-hPhe (*S*-**5.13c**)	7.7 [d]	6.1 [l]	~91	654.3035	654.3038
44	Phenylacetyl-aza-Gly-(4*R*)-Amp-Pal-hPhe (*R*-**5.13a**)	5.6 [d]	5.0 [d]	≥ 95	616.2878	616.2852
45	Phenylacetyl-aza-Phe-(4*R*)-Amp-Pal-hPhe (*R*-**5.13b**)	8.4 [d]	5.2 [d]	≥ 99	706.3348	706.3356
46	Phenylacetyl-aza-Pra-(4*R*)-Amp-Pal-hPhe (*R*-**5.13c**)	7.2 [d]	4.6 [d]	≥ 99	654.3035	654.3039

Isolated purity determined by LC-MS analysis using gradients of X-Y% A [MeOH (0.1% FA)/B H_2O (0.1% FA)/] or B [MeCN (0.1% FA)/H_2O (0.1% FA)/] over Z min: [a]70-90% A or B /20; [b]20-80% A or B/14; [c]30-95% A or B /14; [d]10-90% A or B/14/15; [e]40-90% A or B /12; [f]50-90% A or B

/14; [g]50-80% A or B /14, [h]30-90% A or B /14; [i]5-80% A or B /14; [j]30-80% A or B /12; [k]40-70% A or B/15; [l]5-90% A or B/15.

Previously, 3-*N*-(Fmoc)amino-5-iodo-indolizidinone-9-carboxylate **5.17** (Scheme 5.1) was assigned based on observation of magnetization transfer between the C3, C5 and C6 protons.[9a] 3-Phenylacetamide **5.16** exhibited similar long range nuclear Overhauser effects indicating that such modification at the 3-position nitrogen had no effect on the regio- and diastereoselectivity of the transannular cyclization. Similarly, magnetization transfer between the C3 and C6 protons was observed in the NOSEY spectrum of indolizidinone (6*S*)-**5.21**, the stereochemical assignment of which was confirmed by X-ray crystallography.

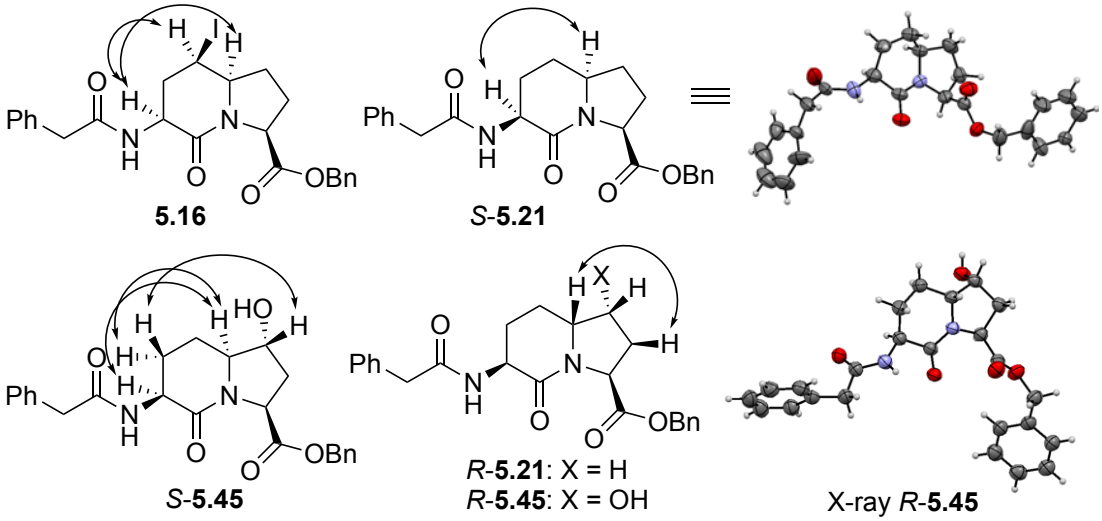

Figure 5.2. Assignment of relative stereochemistry by NOSEY correlations and X-ray structures

The protons on carbons bearing hydroxyl groups were consistently up-field of those on nitrogen bearing carbons. Similar to the C3-protons of proline analogs,[22] the β–C8 proton appeared consistently up-field of the β–C8 proton due to an anisotropic effect caused by the C9 carboxylate. The *R*-configuration of the ring fusion C6-protons in (6*R*)-**5.21** and (6*R*)-**5.45** were assigned based on the observed transfer of magnetisation with the β–C8 proton. The assignment of alcohol (6*R*)-**5.45** was consistent with allylic oxidation from the less sterically hindered face of olefin **5.18** and

confirmed by X-ray crystallography; the alcohol stereochemistry of (5*S*)-**5.44** is based similarly on the facial selectivity of the oxidation. In their X-ray crystal structures, the dihedral angle values of the backbone within bicycles *S*-**5.21** and *R*-**5.45**, both resembled those of the central residues of an ideal type II′ β-turn (Table 5.2).

Table 5.2. Comparison of dihedral angles from X-ray analysis and ideal type I and II′ β-turns

Type β-turn	ϕ^{i+1}, °	ψ^{i+1}, °	ϕ^{i+2}, °	ψ^{i+2}, °
Boc-(3*S*,6*S*,9*S*)-I^{2}aa-OMe[23]	–158	–176	–78	179
PhAc-(3S,6S,9S)-I^{2}aa-OBn (*S*-**5.21**)	–139 –120	–175 –173	–71 –75	144 148
PhAc-7-OH-(3*S*,6*R*,7*S*,9*S*)-I^{2}aa-OBn (*R*-**5.45**)	–134	–142	–64	157
Boc-aza-Ala-Pro-NH*i*-Pr[24]	–68	–18	–58	–25
Pivaloyl-D-Ala-Pro-NH*i*-Pr[25]	60	–140	–89	9
Ideal type I β-turn[26]	–60	–30	–90	0
Ideal type II′ β-turn [26]	60	–120	–80	0

5.4 Structure activity relationship studies

Previously, the indolizidinone peptide mimic *S*-**5.1a** (PDC113.824) exhibited high efficacy (98% inhibition) and potency (IC_{50} = 1.1 nmol/L) in a porcine ocular micro-vessel assay, and delayed labor significantly in murine models induced respectively with lipopolysaccharide and PGF2α.[1d,27b] Modifications of *S*-**5.1a** by replacement of the (3*S*,6*S*,9*S*)-I^{2}aa residue by its D-enantiomer [(3*R*,6*R*,9*R*)-I^{2}aa], and related indolizidin-9-one, quinolizidinone, and pyrroloazepinone, 5,6-, 6,6- and 7,5-fused bicycles (e.g., **5.3a** and **5.4a**),[1d,27] and a ten-membered macrocycle system,[27a] as well as examination of the enantiomer of *S*-**5.1a**,[1d,27b] all gave analogs that exhibited no inhibition of myometrial contractions. On the other hand, aza-amino acyl proline analogs **5.2a**–**c** displayed activity contingent on the nature of the aza-amino acid side-chain, and reduced the tension and duration of PGF2α-induced myometrial contractions with similar efficacy

as *S*-**5.1a**.[1d,27b] Moreover, modulators possessing Gly-Pro and D-Ala-Pro residues were previously shown to have lower activity than aza-Gly-Pro **5.2a**.[27a] Further investigation of the turn regions of *S*-**5.1a** and **5.2** was thus pursued in parallel to provide more detailed structure activity relationships for guiding development of novel modulators of FP as potential tocolytic agents for inhibiting preterm labor.

The activity of *S*-**5.1a** in the myometrial contraction assay proved to be very sensitive to structural modifications (Figure 5.3). For example, replacement of the phenyl acetyl moiety by *p*-azido and *p*-amino counterparts (e.g., *S*-**5.1b** and *S*-**5.1c**) diminished activity, respectively. Changing the ring fusion stereochemistry from the (3*S*,6*S*,9*S*)-I^2aa residue in *S*-**5.1a** to the (3*S*,6*R*,9*S*)-I^2aa isomer in *R*-**5.1a** reduced significantly the activity, which was one third that of *S*-**5.1a** at 10 μM (Figure S2, SI). Flattening the ring in Δ^5-I^2aa analog **5.5a** improved activity relative to *R*-**5.1a,** but gave only half the activity of *S*-**5.1a** at 1 μ M. A concave I^2aa residue was thus shown to be a prerequisite for high activity.

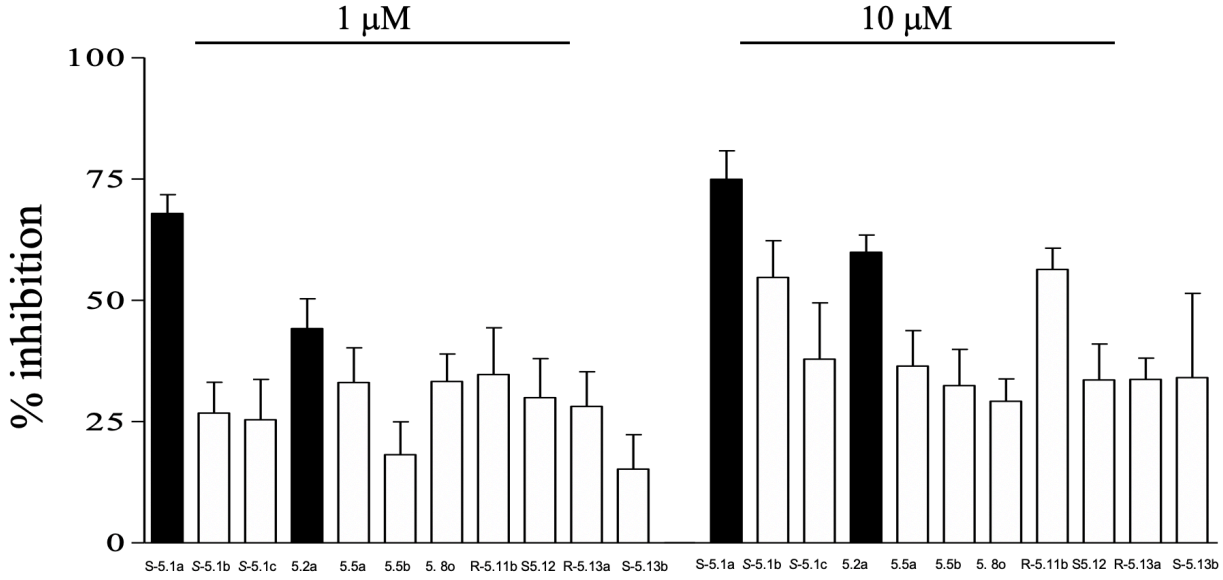

Figure 5.3. Effects of *S*-**5.1a**, **5.2a** and analogs on mean tension induced by PGF2α. Results are expressed as % inhibition, calculated as (A-B)/A, where A is the increase in mean tension induced

by PGF2α in the absence of a 20-min pre-treatment with FP inhibitor and B is the increase in mean tension induced by PGF2α in the presence of a 20-min pre-treatment with FP inhibitor.

The addition of aromatic rings to the 5-position of Δ^5-I^{2}aa analog **5.5a** demonstrated tolerance for the phenyl group in **5.5b**, but not for larger substituents (e.g., 4-methoxy, 4-cyano and 4-trifluoromethoxyphenyl analogs **5.5c**–**5.5e**), which caused a complete loss of activity. In contrast to our previously reported FP modulators, which do not typically exhibit effect in the absence of exogenous PGF2α, 5-(4-trifluoromethoxyphenyl)-Δ^5-I^{2}aa **5e** exhibited activity in the presence of the endogenous orthosteric ligand (Figure S3, SI).

The influence of substitution on the 6-membered lactam of **5.5a** may be compared with the effects of different side-chains on azapeptide **5.2a**, on which benzyl and propargyl residues were tolerated.[1d] Attempts to introduce larger and less electron rich aromatic side-chains onto azapeptide **5.2a** (e.g., **5.6d**–**l**) resulted in loss of activity correlating with the inactivity of **5.5c**–**e**. In the cases of **5.6f** and **5.6k**, the analogs were insoluble as the zwitterion and examined as the sodium salts, which exhibited half the activity of **5.2a** at 10 μM (Figure S2, SI). Examination of the activity of azapeptides **5.7**–**5.9** featuring carboxylate and basic amine side-chains yielded aza-4-piperidinobutynylglycine **5.8o**, which exhibited similar activity as **5.5a**, and aza-4-(*N*,*N*-dimethylamino)butynylglycine **5.8m**, which was inactive at 1 μM but showed about half the activity of **5.2a** at 10 μM (Figure S2, SI), demonstrating further the restrictive size requirement and need for a lyophilic moiety at this residue.

The conformational preferences of aza-amino acyl proline residues have been examined to a limited extent in dipeptide models by X-ray crystallographic and spectroscopic methods.[24,28] For example, X-ray crystallographic analyses of *N*-Cbz-azaAsn(Me)-Pro-NH*i*-Pr, *N*-Cbz-azaAsp(Et)-Pro-NH*i*-Pr, *N*-Boc-azaAla-Pro-NH*i*-Pr (Table 5.2), and *N*-*i*-Pr-azaAla-Pro-O*t*-Bu, all indicated

that in the solid state, the aza-residue exhibited *R*-like chirality and the aza-amino acyl proline dipeptide adopted respectively ϕ and ψ dihedral angle values indicative of the $i + 1$ and $i + 2$ residues of an ideal type I β-turn.[24, 28] Although the type I β -turn has been described as an energy minimum adopted by model azapeptides (e.g., Ac-aza-Gly-Ala-NHMe and Ac-aza-Ala-Ala-NHMe) in computational analyses, the corresponding type II β -turn was less than one kcal higher in energy.[29] Examination of *N*-*i*-Pr-azaAla-Pro-O*t*-Bu in solution at low temperature (–90°C in CD_2Cl_2) by NMR spectroscopy indicated four methyl singlets corresponding to two pairs of prolyl amide *cis* and *trans* isomers with one major *trans* amide conformer representing two-thirds of the total population.[28] At ambient temperature, *N*-*i*-Pr-azaAla-Pro-O*t*-Bu exhibited infrared spectra in hexane and CH_2Cl_2 exhibiting strong concentration independent absorptions at 3260 cm^{-1} corresponding to an intramolecular hydrogen bond involving the azaAla NH and semicarbazide carbonyl oxygen indicating a more extended conformation.[28] Potential for conformational liberty and adoptive chirality may both account for the activity of **5.2a**–**c** and related aza-amino acyl proline analogs, which may assume backbone geometry similar to the I^2aa residue in *S*-**5.1a**.

The influence of a ring substituent on the proline residue in *S*-**5.1a** and **5.2** was next explored typically with limited success. For example, neither (6*R*,7*R*)- nor (6*S*,7*R*)-7-hydroxyl-I^2aa analogs *R*- and *S*-**10a** exhibited activity in the myometrial contraction assay. Similarly, among the (2*S*,4*R*)- and (2*S*,4*R*)-4-hydroxyproline analogs *R*- and *S*-**5.11a**–**c**, only aza-Pra-4*R*-Hyp *R*-**5.11c** exhibited activity, which was comparable to azapeptide **5.2a**. Among the (2*S*,4*R*)- and (2*S*,4*R*)-4-fluoroproline analogs *R*- and *S*-**5.12a**–**c**, only aza-Gly-4*S*-Flp *S*-**5.12a** exhibited activity. Moreover, aza-Gly-4*R*-Amp *R*-**5.13a** and aza-Phe-4*S*-Amp *S*-**5.13b** retained activity among the 4-aminoproline analogs.

4-Position substituents on proline have been shown to influence both the ring pucker and prolyl amide isomer equilibrium.[30,31] (2*S*,4*R*)-Hydroxy- and fluoroprolines exhibit C$^{\gamma}$-*exo* puckers and higher *trans*-amide populations than their (2*S*,4*S*)-counterparts which favor a C$^{\gamma}$-*endo* pucker.[30] (4*S*)-Aminoproline has been shown to fluctuate between ring puckers contingent on pH with amine protonation favoring the C$^{\gamma}$-*endo* pucker.[31] Considering that active analogs were observed with both (2*S*,4*R*)- and (2*S*,4*S*)-stereochemistry contingent on the aza-residue side-chain, the 4-position substituent may influence factors other than receptor engagement, such as cell permeability, which may influence performance in the *ex vivo* myometrial contraction assay.

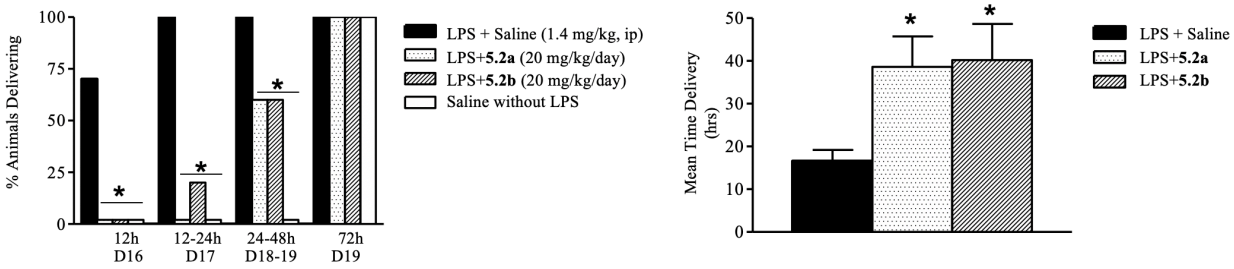

Figure 5.4. Tocolytic action of azapeptides **5.2a** and **5.2b** in LPS-induced preterm labor in mice. Left) Percentage of animals delivered following injection of LPS (B, 1.4 mg/kg by intraperitoneal injection) in the presence or absence of azapeptides **5.2a** and **5.2b** (20 mg/kg/day). Pregnant mice were treated with azapeptides **5.2a** and **5.2b** (20 mg/kg/day) starting on day 16 of gestation. Control mice were injected with saline. Bars are presented at 12, 15–24, 24–48 h, and 72 h. The time in hours refers to time of delivery following LPS treatment. Right) Average delivery time after LPS treatment.

Finally, the tocolytic effects of azapeptides **5.2a** and **5.2b** were examined in a preterm labor model in which mice near term were treated with azapeptide and lipopolysaccharide (LPS) *Escherichia coli* endotoxin, which is known to promote a general inflammatory state resulting in prostaglandin synthesis, and induced premature delivery.[32] Following LPS injection into mice at gestational day

16, all the animals tested delivered within 12–24 h (Figure 5.4). Pretreatment with azapeptide prior to LPS injection significantly delayed delivery, such that by gestational day 17, <20% of treated animals delivered. Azapeptide-treated mice did not deliver until day 19 even after treatment with LPS. Azapeptides **5.2a** and **5.2b** extended significantly (>20 h) the average time of delivery following LPS treatment compared with untreated animals (Figure 5.4b). Considering the results with azapeptides **5.2a** and **5.2b** in the *ex vivo* myometrial contraction assay and *in vivo* preterm LPS model, their ability to delay preterm labor is due in part through the inhibition of uterine contraction.

5.5 Conclusion

The relationships between structure and function of novel modulators of FP has been studied towards the development of potential tocolytics for delaying premature birth. Commencing from the understanding that indolizidin-2-one amino acids and aza-amino acyl proline derivatives share a common preference for mimicry of the central residues of type II' β-turns,[1] diversity-oriented methods were developed in parallel for the synthesis of analogs of lead indolizidin-2-one *S*-**5.1a** and azapeptides **2**. Peptides *S*-**5.1a** and azapeptides **5.2** had previously exhibited similar activity and efficacy in inhibiting myometrial contractions by way of modulation of the prostaglandin-F2α receptor; moreover, *S*-**5.1a** delayed labor for up to 42 h in mice. Parallel study on structural modifications of *S*-**5.1a** and **5.2** demonstrated that activity in the myometrial contraction assay was sensitive to the conformation, size, nature and lipophilicity of the modified analogs. The significance of the conformation of the I^2aa was demonstrated by the significant loss of activity of the convex bridge-head isomer *R*-**5.1a** and the regaining of activity in its flatter counterpart Δ^5-I^2aa **5.5a**. Substitution on the six-membered lactam of the I^2aa residue and the aza-amino acid side-chain indicated a limited tolerance for aromatic and lipophilic residues, with a limited set of

analogs retaining activity including 5-phenyl Δ^5-I^2aa **5.5b**, aza-Phe-Pro **5.2b** and aza-4-piperidinobutynylglycine **5.8o**. Although hydroxylation of the proline moiety of the I^2aa residue in **5.10a** abolished inhibitory activity on uterine contractions, certain replacements of the proline residue in the more flexible azapeptide **5.2** by Hyp, Flp and Amp analogs retained activity, contingent on aza-residue side-chain: e.g. *R*-**5.11c**, *S*-**15.2a**, *R*-**5.13a** and *S*-**5.13b**. Although the structure-activity profile indicated high sensitivity to changes of the ligand at the turn region, the potential for the azapeptides to serve as alternative prototypes for developing tocolytic agents was further evidenced by the ability of aza-Gly-Pro **5.2a** and aza-Phe-Pro **5.2b** to delay labor from 12-24 h in a LPS-induced mouse model of preterm birth. Effective synthetic methods for employing the parallel utility of I^2aa and azapeptide residues have thus revealed a sensitive structure-activity relationship profile from which active ligands have emerged exhibiting promise for delaying preterm labor.

5.6 Experimental section

5.6.1 Ex *Vivo* Myometrial Contraction Assay

Ex vivo myometrial contraction was measured as previously described.[32] Briefly, uteri from mice were obtained from animals immediately following term delivery. Myometrial strips (2–3 mm wide and 1–2 cm long) from both were suspended in organ baths containing Krebs buffer equilibrated with 95% oxygen at 37 °C with an initial tension at 2 g. After 1 h of equilibration, changes in mean basal tension, as well as peak, duration, and frequency of spontaneous contraction in the absence or presence of PGF2α and azapeptide or I^2aa analog were recorded with a Biopac digital polygraph system.

5.6.2 Murine Preterm Labor Model

Timed-pregnant CD-1 mice at 16 days gestational (normal term is 19.2 days) were anesthetized with isoflurane (2%). Primed osmotic pumps (Alzet pump, Alzet, Cupertino, CA) containing either saline or azapeptide **2a** and **2b** (20 mg/day/animal) were subcutaneously implanted on the backs of the animals; infusion of azapeptide was immediately preceded by bolus injection of azapeptide (0.1 mg/animal intraperitoneally). Within 15 min after placement of the pumps, animals were injected with lipopolysaccharide (LPS) *Escherichia coli* endotoxin (35 μg/animal intraperitoneally) to mimic the inflammatory/infectious component of human preterm labor. Animals were inspected every hour for the first 18 h and every 2 h thereafter to document the timing of birth. All experiments were approved by the Animal Care Committee of Centre Hospitalier Universitaire Sainte-Justine (Montreal, Quebec, Canada).

Note: This section provides only Indolizidinone syntheses part.

5.6.3 Materials and Methods

Anhydrous solvents (THF, DMF, CH_2Cl_2, and CH_3OH) were obtained by passage through solvent filtration systems (GlassContour, Irvine, CA). All reagents from commercial sources were used as received. Wang resin (1.1 mmol/g, 75-100 mesh) was purchased from Advanced Chemtech™; amino acids and coupling reagents such as HBTU and diisopropylcarbodiimide (DIC) were purchased from GL Biochem™; solvents were obtained from VWR international. (2*S*)-(3-Pyridyl)alaninyl-(3S)-β-homophenylalanine benzyl ester hydrochloride (**5.25**) was prepared according to the literature procedure and exhibited ^{1}H NMR spectral data and R_f value identical to the reported literature.[1d] Purification by silica gel chromatography was performed on 230-400 mesh silica gel; analytical thin-layer chromatography (TLC) was performed on Silica gel 60 F254 (Aluminium Sheet) and visualised by UV absorbance or staining with iodine. Melting points are uncorrected and were obtained on sample that was placed in a capillary tube using a Mel-Temp

melting point apparatus equipped with a thermometer and reported in degree Celsius (°C). ^{1}H and ^{13}C NMR spectra were recorded at room temperature (298 K) in $CDCl_3$ (7.26 ppm/77.16 ppm), DMSO (d6) (2.50 ppm/39.52 ppm) or CD_3OD (3.31 ppm/ 49.0 ppm) on Brucker AV (300/75, 500/125 and 700/175 MHz) instruments and referenced to internal solvent. Chemicals shifts are reported in parts per million (ppm); coupling constant (*J*) values in Hertz; abbreviations for peak multiplicities are s (singlet), d (doublet), t (triplet), q (quadruplet), qu (quintuplet), m (multiplet) and br (broad). Certain ^{13}C NMR chemical shifts values were extracted from HSQC spectra. High Resolution Mass Spectrometry (HRMS) data were obtained by the Centre Régional de Spectrométrie de Masse de l'Université de Montréal. Either protonated molecular ions $[M + H]^+$, $[M + 2H]/2^+$ or sodium adducts $[M + Na]^+$ were used for empirical formula confirmation. X-ray structures were solved on a Brucker Venture Metaljet diffractometer by the Laboratoire de diffraction des rayons X de Université de Montréal. Specific rotations, $[\alpha]_D$ were measured at 25 °C at the specified concentrations (*c* in g/100 mL) using a 0.5 dm cell on a Perkin Elmer Polarimeter 589 and expressed using the general formula: $[\alpha]_D^{25} = (100 \times \alpha)/(d \times c)$.

Phenylacetyl-(3*S*,6*R*,9*S*)-I^{2}aa-(2*S*)-(3-pyridyl)alaninyl-(3*S*)-*β*-homophenylalanine [(*R*)-5.1a]

Benzyl ester **5.27** (15 mg, 0.02 mmol) and palladium-on-carbon (10% by wt, 10 mg) in EtOH (5 mL) were stirred under a balloon of hydrogen (1 atm) for 3-4 h. The catalyst was filtered onto Celite™ and washed with methanol. The filtrate and washings were combined and evaporated to a residue, which was purified by preparative HPLC (Phenomenex Gemini 5 μm, C18, 250 mm X 21.2 mm) using a gradient from 20% to 80% acetonitrile (containing 0.1% FA) in water (containing 0.1% FA) to afford peptide (*R*)- **5.1a** (8 mg, 68 %) as white solid: $[\alpha]_D^{25}$ –30.1 (*c* 0.16, MeOH); FT-IR (neat) *v*max 3270, 2922, 2864, 2844, 1633, 1539, 1496, 1441, 1966, 1128, 1054, 1032, 1013, 752, 699, 625 cm^{-1}; ^{1}H NMR (700 MHz, CD_3OD) δ 8.63–8.66 (m, 2H), 8.41-8.42 (d, 1H, *J* = 6.2

Hz), 7.91-7.92 (t, 1H, *J* = 6.6 Hz), 7.30-7.34 (m, 4H), 7.21-7.25 (m, 5H), 7.15-7.17 (m, 1H), 4.41-4.50 (m, 3H), 4.07-4.10 (m, 1H), 3.62-3.66 (m, 1H), 3.58-3.60 (d, 1H, *J* = 15.0 Hz), 3.49-3.51 (d, 1H, *J* = 15.0 Hz) 3.17-3.20 (dd, 1H, *J* = 4.7, 14.3 Hz), 2.91-2.95 (m, 2H), 2.86-2.89 (m, 1H), 2.51-2.52 (d, 2H, *J* = 6.4 Hz), 2.30-2.34 (m, 1H), 2.17-2.20 (m, 2H), 2.08-2.11 (m, 1H), 1.93-1.98 (m, 1H), 1.49-1.62 (m, 3H); ^{13}C NMR (175 MHz, CD_3OD) δ 173.1, 172.8, 170.0, 169.2, 166.8, 160.9, 146.7, 142.5, 140.1, 138.1, 137.9, 135.2, 129.1, 128.9, 128.3, 128.2, 126.6, 126.3, 60.7, 60.1, 54.1, 50.8, 48.1, 42.0, 39.9, 37.3, 33.4, 32.3, 27.9, 27.6, 27.3; HRMS calcd for $C_{35}H_{40}N_5O_6$ $[M+H]^+$, 626.2973; found 626.2981.

4-Azidophenylacetyl-(3S,6S,9S)-I^{2}aa-(2*S*)-(3-pyridyl)alaninyl-(3*S*)-β-homophenylalanine [(*S*)- 5.1b]

Benzyl ester **5.30** (17 mg, 0.022 mmol) was dissolved in 1 mL of dioxane, cooled to 0 ^{o}C, treated with 1 N LiOH (35 μL) and stirred for 1 h. The volatiles were evaporated under reduced pressure. The remaining aqueous phase was acidified with 1N HCl to pH 3 and extracted with ethyl acetate (2×10 mL). The organic extractions were combined, dried with Na_2SO_4, filtered and concentrated under vacuum. Analysis by LCMS showed two peaks with desired mass. Purification by preparative HPLC using a C18 reverse phase column with using a gradient from 20% to 90% methanol (0.1% FA) in water (0.1% FA) as eluent. First to elute (Rt = 7.40 min) was peptide (3*S*,6*S*,9*R*)-I^{2}aa **5.1b**: (3 mg, 20%): $[\alpha]_D^{25}$ –119.2 (*c* 0.16, MeOH); ^{1}H NMR (700 MHz, CD_3OD) δ 8.51-8.55 (m, 2H), 8.18 (brs, 1H), 7.69 (brs, 2H), 7.35-7.37 (d, 2H), 7.26-7.29 (m, 2H), 7.19-7.22 (m, 2H), 7.01-7.03 (m, 2H), 4.53-4.55 (m, 1H), 4.41-4.42 (m, 1H), 4.31-4.32 (d, 1H, *J* = 9.6 Hz), 4.21-4.24 (dd, 1H, *J* = 6.1, 11.4 Hz), 3.61-3.66 (m, 1H), 3.56-3.57 (d, 2H, *J* = 5.0 Hz), 3.24-3.27 (m, 1H), 3.07-3.10 (m, 1H), 2.79-2.87 (m, 2H), 2.41-2.48 (m, 2H), 2.06-2.22 (m, 3H), 2.00-2.03 (m, 1H), 1.86-1.92 (m, 1H), 1.77-1.79 (dd, 1H, *J* = 6.8, 13.0 Hz), 1.65-1.74 (m, 2H); ^{13}C

NMR (175 MHz, CD_3OD) δ 173.2, 172.7, 172.4, 169.8, 168.5, 143.8, 143.5, 142.7, 138.7, 137.9, 136.1, 132.3, 130.5, 129.1, 128.0, 127.3, 126.2, 118.7, 60.5, 59.3, 53.8, 50.4, 48.1, 41.6, 39.8, 37.3, 34.6, 31.3, 28.5, 27.9, 27.3 HRMS calcd for $C_{35}H_{39}N_8O_6Na$ $[M+H]^+$, 667.2987; found 667.2974. Next to elute (Rt = 8.78 min) was peptide (3*S*,6*S*,9*S*)-I^2aa *S*-**5.1b**: (9 mg, 60%): $[\alpha]_D^{25}$ –55 (*c* 0.4, MeOH); FT-IR (neat) *ν*max 3271, 2927, 2113, 1638, 1505, 1439, 1285, 1128, 701 cm^{-1}; ^1H NMR (700 MHz, CD_3OD) δ: 8.39-8.41 (m, 2H), 7.75-7.76 (d, 1H, *J* = 7.6 Hz), 7.35-7.37 (m, 1H), 7.26-7.31 (m, 6H), 7.20-7.22 (m, 1H), 6.97-6.99 (m, 2H), 4.44-4,48 (m, 2H), 4.35-4.37 (d, 1H, *J* = 9.4 Hz), 4.29-4.31 (m, 1H), 3.63-3.67 (m, 1H), 3.55-3.57 (d, 1H, *J* = 14.8 Hz), 3.48-3.50 (d, 1H, *J* = 14.8 Hz), 3.08-3.11 (dd, 1H, *J* = 5.3, 14.1 Hz), 2.83-2.94 (m, 3H), 2.43-2.44 (d, 2H, *J* = 6.3 Hz), 2.01-2.21 (m, 4H), 1.81-1.87 (m, 2H), 1.67-1.73 (m, 1H), 1.40-1.46 (m, 1H); ^{13}C NMR (175 MHz, CD_3OD) δ 173.4, 172.5, 172.4, 170.9, 168.9, 149.5, 146.8, 138.7, 138.0, 137.8, 134.0, 132.3, 130.5, 129.0, 128.1, 126.2, 123.8, 118.7, 59.7, 59.3, 54.7, 48.6, 48.1, 41.4, 39.7, 37.6, 33.9, 31.2, 28.5, 28.4, 25.7. HRMS calcd for $C_{35}H_{38}N_8O_6Na$ [M+Na]+, 689.2807; found 689.2817.

4-Aminophenylacetyl-(3*S*,6*S*,9*S*)-I^2aa-(2*S*)-(3-pyridyl)alaninyl-(3*S*)-*β*-homophenylalanine [(*S*)- 5.1c)]

Amine **5.1c** was synthesized from ester **5.30** (10 mg, 0.013 mmol) and purified using the protocols described for the preparation of acid (*R*)- **5.1a**, and isolated as white solid (6 mg, 75%): $[\alpha]_D^{25}$ –38.5 (*c* 0.3, MeOH); FT-IR (neat) *ν*max 3269, 2922, 2864, 2844, 1636, 1515, 1323, 1054, 1032, 1014, 701 cm^{-1}; ^1H NMR (700 MHz, CD_3OD) δ 8.34-8.42 (m, 3H), 7.75-7.76 (d, 1H, *J* = 6.2), 7.35-7.36 (m, 1H), 7.25-7.32 (m, 3H), 7.20-7.22 (m, 1H), 7.00-7.01 (d, 2H, *J* = 8.25 Hz), 6.66-6.67 (d, 2H, *J* = 8.3 Hz), 4.43-4.48 (m, 2H), 4.35-4.36 (d, 1H, *J* = 9.2 Hz), 4.25-4.27 (m, 1H), 3.63-3.66 (m, 1H), 3.41-3.43 (d, 1H, *J* = 14.8 Hz), 3.36-3.38 (d, 1H, *J* = 14.8 Hz), 3.09-3,12 (m, 1H), 2.93-2.96 (m, 1H), 2.84-2.90 (m, 2H), 2.42-2.43 (d, 2H, *J* = 5.8 Hz), 2.15-2.20 (m, 1H), 2.07-2.13

(m, 1H), 2.00-2.05 (m, 2H), 1.84-1.87 (dd, 1H, *J* = 6.6, 13.0 Hz), 1.77-1.80 (m, 1H), 1.67-1.73 (m, 1H), 1.38-1.44 (m, 1H); ^{13}C NMR (175 MHz, CD_3OD) δ 173.2, 172.5, 170.8, 169.1, 167.1, 149.5, 146.8, 146.1, 138.1, 137.8, 134.1, 129.6, 129.1, 128.1, 126.2, 124.6, 123.8, 115.4, 59.7, 59.3, 54.7, 48.5, 48.2, 41.5, 39.8, 37.8, 33.8, 31.2, 28.5, 28.4, 25.7; HRMS calcd for $C_{35}H_{40}N_6O_6Na$ $[M+Na]^+$, 663.2902; found 663.2903.

Phenylacetyl-(3*S*,9*S*)-2-oxo-1,2,3,4,7,8-hexahydroindolizine-9-carbonyl-(2*S*)-(3-pyridyl)alaninyl-(3*S*)-*β*-homophenylalanine (5.5a)

Peptide **5.5a** was synthesized from ester **5.26** (12 mg, 0.017 mmol) using the protocol described for the synthesis of acid (*R*)- **5.1a**, and isolated by preparative HPLC (Phenomenex Gemini 5 μm, C18, 250 mm X 21.2 mm) using a gradient from 20% to 90% acetonitrile in water (containing 10 mmol ammonium acetate) as white solid (5 mg, 48%): $[\alpha]_D^{25}$ –81.9 (*c* 0.16, MeOH); FT-IR (neat) *ν*max 2922, 2865, 2844, 1645, 1540, 1418, 1055, 1032, 1013, 698, 600 cm^{-1}; ^{1}H NMR (700 MHz, CD_3OD) δ 8.42 (br s, 1H), 8.38 (br s, 1H), 7.75-7.76 (d, 1H, *J* = 7.6 Hz), 7.17-7.35 (m, 12H), 4.99-5.0 (m, 1H), 4.53-4.60 (m, 3H, *J* = 8.8 Hz), 4.35-4.37 (m, 1H), 3.63-3.65 (d, 1H, *J* = 14.6 Hz), 3.60-3.62 (d, 1H, *J* = 14.7 Hz), 3.13-3.16 (dd, 1H, *J* = 5.2, 14.2 Hz), 2.93-2.97 (dd, 1H, *J* = 8.8, 14.2 Hz), 2.87-2.88 (m, 2H), 2.58-2.62 (m, 1H), 2.51-2.56 (m, 2H), 2.37-2.44 (m, 3H), 2.12-2.17 (m, 1H), 1.93-1.98 (m, 1H); ^{13}C NMR (175 MHz, CD_3OD) δ 172.7, 171.6, 170.2, 167.7, 149.5, 146.8, 140.1, 138.4, 137.9, 135.3, 133.7, 129.2, 129.1, 128.8, 128.2, 128.0, 127.9, 126.5, 126.0, 123.8, 95.2, 59.8, 54.2, 49.1, 48.8, 42.3, 39.7, 34.6, 27.3, 27.0, 26.8; HRMS calcd for $C_{35}H_{37}N_5O_6Na$ $[M+Na]^+$, 646.2636; found 646.2641.

Phenylacetyl-(3*S*,9*S*)-2-oxo-5-phenyl-1,2,3,7,8,9-hexahydroindolizine-carbonyl-(2*S*)-(3-pyridyl)alaninyl-(3*S*)- β-homophenylalanine (5.5b)

Acid **5.5b** was synthesized from ester **5.33b** (12 mg, 0.015 mmol) and purified using the protocols described for the preparation of peptide (*R*)-**5.1a**, and isolated as white solid (7 mg, 74%): $[\alpha]_D^{25}$ –112.5 (*c* 0.25, MeOH); FT-IR (neat) *ν*max 3280, 2980, 2864, 2844, 1643, 1538, 1390, 1353, 1247, 1054, 1032, 1013, 847, 697, 674, 565 cm^{-1}; ^1H NMR (700 MHz, CD_3OD) δ 8.44 (br s, 2H), 8.38-8.39 (d, 1H, *J* = 4.4), 7.77-7.78 (d, 1H, *J* = 7.7), 7.32-7.36 (m, 5H), 7.21-7.30 (m, 9H), 7.16-7.18 (m, 1H), 4.73-4,76 (dd, 1H, *J* = 7.3, 13.3 Hz), 4.56-4.60 (m, 2H), 4.39-4.41 (m, 1H), 3.63-3.65 (d, 1H, *J* = 14.7), 3.61-3.63 (d, 1H, *J* = 14.7 Hz), 3.14-3.17 (dd, 1H, *J* = 5.8, 12.2 Hz), 2.97-3.00 (dd, 1H, *J* = 8.6, 14.1 Hz), 2.81-2.94 (m, 5H), 2.67-2.72 (m, 1H), 2.38-2.45 (m, 2H), 2.18-2.23 (m, 1H), 1.89-1.03 (m, 1H); ^{13}C NMR (175 MHz, CD_3OD) δ 174.1, 172.7, 171.8, 170.4, 167.3, 167.1, 149.5, 146.9, 139.1, 138.1, 137.9, 136.4, 135.3, 133.7, 129.1, 128.9, 128.2, 128.0, 127.9, 126.8, 126.5, 126.1, 126.0, 123.8, 109.8, 59.7, 54.3, 49.6, 42.3, 39.7, 38.0, 34.5, 32.5, 27.6,. 27.1; HRMS calcd for $C_{41}H_{41}N_5O_6Na$ $[M+Na]^+$, 722.2949; found 722.2951.

Phenylacetyl-(3*S*,9*S*)-2-oxo-5-(4-methoxyphenyl)-1,2,3,7,8,9-hexahydroindolizine-carbonyl-(2*S*)-(3-pyridyl)alaninyl-(3*S*)-β-homophenylalanine (5.5c)

Acid **5.5c** was synthesized from ester **5.33c** (15 mg, 0.018 mmol) and purifed using the protocols for the preparation of peptide (*R*)- **5.1a**, and isolated as white solid (8 mg, 62%): $[\alpha]_D^{25}$ –110.8 (*c* 0.16, MeOH); FT-IR (neat) *ν*max 2972, 2865, 2843, 1645, 1509, 1243, 1054, 1032, 1013 cm^{-1}; ^1H NMR (700 MHz, CD_3OD) δ 8.42-8.43 (m, 2H), 8.38-8.39 (m, 1H), 7.60-7.77 (m, 1H), 7.31-7.35 (m, 3H), 7.20-7.30 (m, 8H), 7.16-7.18 (m, 1H), 6.91-6.92 (d, 2H, *J* = 8.8), 4.70-4.73 (dd, 1H, *J* = 7.5, 12.9 Hz), 4.56-4.59 (m, 2H), 4.40-4.42 (m, 1H), 3.81 (s, 3H), 3.62-3.63 (d, 1H, *J* = 2.5 Hz), 3.13-3.16 (dd, 1H, *J* = 5.5, 12.3 Hz), 2.97-3.00 (dd, 1H, *J* = 8.4, 14.1 Hz), 2.76-2.89 (m, 5H), 2.68-2.72 (m, 1H), 2.37-2.51 (m, 3H), 2.14-2.22 (m, 1H), 1.89-1.94 (m, 1H); ^{13}C NMR (175 MHz, CD_3OD) δ 172.7, 171.8, 170.4, 167.2, 167.1, 158.4, 149.5, 146.9, 138.0, 137.9, 135.3, 135.2,

133.6, 131.3, 129.1, 128.8, 128.2, 128.0, 127.9, 126.5, 126.1, 123.7, 113.3, 109.6, 59.7, 54.3, 54,2, 49.6, 42.3, 39.7, 37.9, 34.5, 32.6, 29.0, 27.6, 27.1; HRMS calcd for $C_{42}H_{44}N_5O_7$ $[M+H]^+$, 730.3235; found 730.3262.

Phenylacetyl-(3*S*,9*S*)-2-oxo-5-(4-cyanophenyl)-1,2,3,7,8,9-hexahydroindolizine-carbonyl-(2*S*)-(3-pyridyl)alaninyl-(3*S*)-β-homophenylalanine (5.5d)

Acid **5.5d** was synthesized from ester **5.33d** (14 mg, 0.017 mmol) and purified using the protocols for the preparation of peptide (*R*)- **5.1a**, and isolated as white solid (8 mg, 65%): $[\alpha]_D^{25}$ –122.8 (*c* 0.16, MeOH); ^{1}H NMR (700 MHz, CD_3OD) δ: 8.47 (br s, 1H), 8.38 (br s, 1H), 7.78-7.79 (d, 1H, *J* = 7.9 Hz), 7.69-7.70 (d, 2H, *J* = 8.4 Hz), 7.46-7.48 (d, 2H, *J* = 8.4 Hz), 7.33-7.36 (m, 3H), 7.28-7.30 (m, 2H), 7.22-7.25 (m, 5H), 7.14-7.16 (m, 1H), 4.76-4.79 (dd, 1H, *J* = 6.9, 13.5 Hz), 4.59-4.63 (m, 2H), 4.29-4.31 (m, 1H), 3.64-3.65 (d, 2H, *J* = 2.3 Hz), 3.16-3.19 (dd, 1H, *J* = 5.1, 14.3 Hz), 2.94-2.99 (m, 2H), 2.88-2.92 (m, 3H), 2.83-2.86 (dd, 1H, *J* = 7.2, 15.3 Hz), 2.75-2.78 (m, 1H), 2.25-2.36 (m, 3H), 1.90-1.95 (m, 1H); ^{13}C NMR (175 MHz, CD_3OD) δ 177.8, 172.8, 171.7, 170.1, 168.9, 167.2, 149.5, 146.8, 144.3, 139.6, 138.7, 137.8, 135.4, 133.8, 131.8, 129.2, 128.8, 127.5, 127.4, 127.3, 125.8, 123.8, 118.5, 108.9, 108.2, 59.9, 54.2, 49.3, 49.3, 42.3, 40.3, 39.7, 34.6, 31.8, 28.1, 27.1; HRMS calcd for $C_{42}H_{41}N_6O_6Na$ $[M+H]^+$, 725.3082; found 725.3104.

Phenylacetyl-(3*S*,9*S*)-2-oxo-5-(4-trifluoromethoxyphenyl)-1,2,3,7,8,9-hexahydroindolizine-carbonyl-(2*S*)-(3-pyridyl)alaninyl-(3*S*)-β-homophenylalanine (5.5e)

Acid **5.5e** was synthesized from ester **5.33e** (12 mg, 0.014 mmol) and purifed using the protocols for the preparation of peptide (*R*)- **5.1a**, and isolated as white solid (7 mg, 65%): $[\alpha]_D^{25}$ –80 (*c* 0.16, MeOH); FT-IR (neat) *ν*max 3680, 3286, 2972, 2865, 2843, 1645, 1557, 1455, 1255, 1054, 1032, 1013, 698 cm^{-1}; ^{1}H NMR (700 MHz, CD_3OD) δ: 8.38-8.44 (m, 2H), 7.76-7.77 (d, 1H, *J* = 7.7 Hz), 7.37-7.38 (m, 2H), 7.32-7.35 (m, 3H), 7.21-7.29 (m, 9H), 7.16-7.18 (m, 1H), 4.73-4.76

(dd, 1H, *J* = 7.1, 13.2 Hz), 4.56-4.61 (m, 2H), 4.39-4.41 (m, 1H), 3.63-3.65 (d, 1H, *J* = 14.7 Hz), 3.60-3.62 (d, 1H, *J* = 14.7 Hz), 3.13-3.16 (dd, 1H, *J* = 5.7, 14.3 Hz), 2.97-3.00 (dd, 1H, *J* = 8.5, 14.2 Hz), 2.80-2.94 (m, 5H), 2.67-2.72 (m, 1H), 2,38-2,45 (m, 2H), 2.19-2.24 (m, 1H), 1.90-1.94 (m, 1H); ^{13}C NMR (175 MHz, CD_3OD) δ 174.1, 172.7, 171.7, 170.4, 167.1, 149.5, 147.4, 147.3, 146.9, 138.3, 138.1, 137.9, 137.4, 135.3, 133.7, 129.1, 128.9, 128.4, 128.2, 128.0, 126.5, 126.1, 123.8, 120.6, 108.4, 59.8, 54.3, 49.5, 48.3, 42.3, 39.7, 37.9, 34.5, 32.3, 27.7, 27.0; HRMS calcd for $C_{42}H_{41}N_5O_7F_3$ $[M+H]^+$, 784.2952; found 784.2964.

Phenylacetyl-(3*S*,6*R*,7*R*,9*S*)-7-hydroxy-I^{2}aa-(2*S*)-(3-pyridyl)alaninyl-(3*S*)-*β*-homophenyl alanine [(*R*)-5.10]

Acid (*R*)-**5.10** was prepared from ester (*R*)-**5.47** (15 mg, 0.02 mmol) and purified using the protocols described for the synthesis of peptide (*R*)-**5.1a**, and isolated as white solid (8 mg, 61%): $[\alpha]_D^{25}$ 8.0 (*c* 0.2, MeOH); FT-IR (neat) *ν*max 3279, 2922, 2865, 2844, 1633, 1541, 1496, 1441, 1207, 1054, 1032, 1016, 698, 631 cm^{-1}; ^{1}H NMR (700 MHz, CD_3OD) δ 8.40-8.42 (m, 1H), 8.36-8.37 (m, 1H), 7.72-7.74 (m, 1H), 7.32-7.36 (m, 5H), 7.18-7.28 (m, 6H), 4.51-4.54 (t, 1H, *J* = 9.4 Hz), 4.45-4.49 (m, 1H), 4.39-4.37 (dd, 1H, *J* = 4.5, 11.0 Hz), 4.12-4.13 (t, 1H, *J* = 3.3 Hz), 3.93-3.96 (dd, 1H, *J* = 6.8, 11.1 Hz), 3.58-3.61 (dt, 1H, *J* = 3.1 Hz), 3.56-3.58 (d, 1H, *J* = 15.1 Hz), 3.43-3.46 (dd, 1H, *J* = 15.1 Hz), 3.04-3.06 (dd, 1H, *J* = 4.5, 14.1 Hz), 2.93-2.96 (dd, 1H, *J* = 7.0, 13.9 Hz), 2.87-2.90 (dd, 1H, *J* = 7.8, 13.9 Hz), 2.82-2.85 (dd, 1H, *J* = 11.0, 14.1 Hz), 2.49-2.53 (dd, 1H, *J* = 7.2, 16.0 Hz), 2.42-2.46 (dd, 1H, *J* = 6.1, 16.0 Hz), 2.22-2.25 (dd, 1H, *J* = 8.5, 13.7 Hz), 2.17-2.20 (m, 1H), 1.96-2.05 (m, 1H), 1.91-1.94 (m, 1H), 1.79-1.1.85 (m, 1H), 1.56-1.60 (m, 1H); ^{13}C NMR (175 MHz, CD_3OD) δ 173.5, 172.7, 172.5, 171.1, 170.3, 167.1, 149.6, 146.8, 138.2, 137.6, 135.1, 134.5, 129.1, 128.9, 128.2, 128.1, 126.5, 126.2, 123.7, 70.7, 64.7, 58.7, 55.1, 51.0,

42.0, 39.8, 37.7, 36.9, 33.1, 27.1, 21.3; HRMS calcd for $C_{35}H_{39}N_5O_7Na$ $[M+Na]^+$, 664.2742; found 664.2712.

Phenylacetyl-(3*S*,6*S*,9*S*,7*R*)-7-hydroxy-I^{2}aa-(2*S*)-(3-pyridyl)alaninyl-(3*S*)-*β*-homophenyl alanine [(*S*)-5.10]

Acid (*S*)- **5.10** was synthesized from ester (*S*)- **5.47** (10 mg, 0.014 mmol) and purified using the protocols described for the preparation of peptide (*R*)-5.**1a**, and isolated as white solid (5 mg, 57%): $[\alpha]_D^{25}$ –34.4 (*c* 0.25, MeOH); FT-IR (neat) *ν*max 3269, 2922, 2863, 1637, 1542, 1454, 1438, 1258, 1054, 1032, 1015, 698 cm^{-1}; ^1H NMR (700 MHz, CD_3OD) δ 8.36-8.39 (m, 2H), 7.72-7.73 (d, 1H, *J* = 7.6 Hz), 7.33-7.34 (m, 1H), 7.24-7.30 (m, 8H), 7.19-7.21 (m, 2H), 4.41-4.44 (m, 2H), 4.37-4.39 (d, 1H, *J* = 9.5 Hz), 4.29-4.3 (t, 1H, *J* = 6.4 Hz), 3.76-3.79 (m, 1H), 3.53-3.55 (d, 1H, *J* = 14.7 Hz), 3.47-3.49 (d, 1H, *J* = 14.7 Hz), 3.32-3.33 (m, 1H), 3.05-3.07 (dd, 1H, *J* = 5.4, 14.0 Hz), 2.88-2.89 (m, 1H), 2.84-2.85 (d, 2H, *J* = 6.4 Hz), 2.39-2.40 (d, 2H, *J* = 6.2 Hz), 2.10-2.16 (m, 2H), 2.03-2.05 (m, 1H), 1.96-2.01 (m, 1H), 1.81-1.84 (m, 1H), 1.68-1.74 (m, 1H); ^{13}C NMR (175 MHz, CD_3OD) δ 175.1, 173.8, 173.6, 172, 170.4, 168.4, 150.8, 148.3, 139.5, 139.2, 136.7, 135.4, 130.5, 130.3, 130.2, 129.6, 127.8, 127.6, 125.2, 74.9, 64.9, 59.1, 56.2, 50.1, 43.6, 41.1, 39.3, 37.3, 35.3, 29.5, 25.0. HRMS calcd for $C_{35}H_{39}N_5O_7Na$ $[M+Na]^+$, 664.2742; found 664.2748.

(3*S*,9*S*,*Z*)-Benzyl-1-(2,4-dimethoxybenzyl)-2-oxo-3-(phenylacetamido)-2,3,4,7,8,9-hexahydro-1H-azonine-2-carboxylate (5.14)

(3*S*,9*S*,*Z*)-Methyl-1-(2,4-dimethoxybenzyl)-2-oxo-3-*N*-(Boc)amino-2,3,4,7,8,9-hexahydro-1*H*-azonine-2-carboxylate (2.2 g, 4.76 mmol, prepared according to the procedure described in reference[13] was treated with HCl gas bubbles for 3 h, when TLC showed complete conversion of starting material [R_f = 0.45 (4:6 EtOAc/hexanes, visualized by UV)]. The volatiles were evaporated and the residue was dissolved and evaporated from DCM (20 mL) three times. Without further

purification, amine HCl salt was dissolved 30 mL of dichloromethane, treated with phenyl acetyl chloride (957 mg, 6.19 mmol) and DIEA (1.22 g, 9.5 mmol), stirred for 12 h, washed with 100 mL of brine, dried over Na_2SO_4, filtered and evaporated. The residue was purified by column chromatography using 50-60 % EtOAc in hexanes as the eluent. Evaporation of the collected fractions gave the phenyl acetamide (1.82 g, 80%) as colorless oil: TLC R_f = 0.46 (5:5 EtOAc/hexanes, visualized by UV); $[\alpha]_D^{25}$ –72.0 (*c* 0.5, MeOH); FT-IR (neat) *v*max 3324, 2947, 1739, 1630, 1587, 1505, 1450, 1417, 1287, 1206, 1122, 1031, 831, 710 cm^{-1}; ^1H NMR (500 MHz, $CDCl_3$) δ: 7.30-7.39 (m, 5H), 7.25-2.27 (d, 1H, *J* = 6.3 Hz), 7.17-7.19 (d, 1H, *J* = 8.3 Hz), 6.40-6.44 (m, 2H), 6.06-6.15 (q, 1H, *J* = 9.1 Hz), 5.57-5.63 (m, 1H), 4.65-4.70 (m, 2H), 4.54-4.57 (dd, 1H, *J* = 2.6, 12.2 Hz), 4.40-4.44 (d, 1H, *J* = 15.5 Hz), 3.80 (s, 3H), 3.79 (s, 3H), 3.62 (s, 2H), 3.50 (s, 3H), 2.55-2.61 (m, 1H), 2.11-2.91 (m, 2H), 1.87-1.91 (m, 2H), 1.72-1.91 (m, 1H); ^{13}C NMR (125 MHz, $CDCl_3$) δ 173.5, 170.7, 169.8, 160.0, 157.6, 134.7, 130.8, 129.9, 129.4, 129.3, 128.9, 127.2, 117.7, 104.2, 98.1, 57.2, 55.4, 55.3, 52.3, 50.6, 43.7, 40.1, 34.8, 28.0, 22.2 ; HRMS calcd for $C_{27}H_{33}N_2O_6$ $[M+H]^+$, 481.2348; found 481.2310.

A solution of phenyl acetamide (3.5 g, 7.3 mmol) in 1:1 H2O/dioxane (100 mL) was treated with 1M LiOH (11 mL, 10.9 mmol) at 0 °C, stirred for 3 h, and evaporated to a residue that was partitioned between H_2O (100 mL) and EtOAc (50 mL). The aqueous phase was acidified with 1 M HCl to pH 4 and extracted with EtOAc (2 X 70 mL). The combined organic extracts were washed with brine, dried over Na_2SO_4, filtered, and concentrated to afford the acid (3.25 g, 96%) as colorless oil, that was taken to the next step without further purification: $[\alpha]_D^{25}$ –58.0 (*c* 0.5, MeOH); FT-IR (neat) *v*max 2947, 1719, 1647, 1612, 1588, 1506, 1207, 1156, 1032, 759, 738 cm^{-1}; ^1H NMR (500 MHz, $CDCl_3$) δ 7.45-7.47 (d, 1H, *J* = 6.6 Hz) 7.31-7.35 (m, 2H), 7.26-7.28 (m, 2H), 7.25 (s, 1H), 7.19-7.21 (d, 1H, *J* = 8.4 Hz), 6.37-6.39 (m, 2H), 6.03-6.09 (dd, 1H, *J* = 8.8, 10.2

Hz), 5.44-5.59 (dd, 1H, *J* = 8.3, 9.8 Hz), 4.78-4.81 (d, 1H, *J* = 15.7 Hz), 4.70-4.73 (t, 1H, *J* = 7.1 Hz), 4.54-4.58 (dd, 1H, *J* = 2.4, 12.5 Hz), 4.33-4.36 (d, 1H), 3.75 (s, 6H), 3.56 (s, 2H), 2.51-2.57 (m, 1H), 2.08-2.12 (dd, 1H, *J* = 8.1, 14.1 Hz), 1.99-2.05 (m, 1H), 1.72-1.82 (m, 3H); ^{13}C NMR (125 MHz, $CDCl_3$) δ 173.4, 172.9, 171.1, 160.0, 157.4, 134.3, 131.0, 130.0, 129.3, 129.2, 128.9, 127.3, 118.1, 104.1, 98.2, 57.8, 55.3, 55.2, 50.6, 43.3, 40.9, 34.6, 28.3, 22.4; HRMS calcd for $C_{26}H_{31}N_2O_6$ $[M+H]^+$, 467.2176; found 467.2191.

The acid (3.2 g, 6.9 mmol) was treated with sodium bicarbonate (1.16 g, 13.8) and benzyl bromide (1.77 g, 10.3 mmol) at 0 ºC, stirred overnight at room temperature, and quenched with cold water (60 mL). After extraction of the aqueous phase with EtOAc (2 X 60 mL), the combined organic layers were washed with 100 mL of brine, dried over Na_2SO_4, filtered and evaporated. The residue was purified by column chromatography using 50-60 % EtOAc in hexanes (R_f = 0.52 in 5:5 EtOAc/hexanes) as eluent. Evaporation of the collected fractions yielded ester **5.14** as white foam (3.2 g, 84%): $[\alpha]_D^{25}$ –48.8 (*c* 0.5, MeOH); FT-IR (neat) *ν*max 3306, 2938, 2842, 1737, 1632, 1587, 1505, 1452, 1288, 1256, 1206, 1154, 1032, 831, 695 cm^{-1}; ^{1}H NMR (500 MHz, $CDCl_3$) δ: 7.30-7.39 (m, 8H), 7.28-2.24 (m, 3H,), 7.15-7.17 (d, 1H, *J* = 8.4 Hz), 6.35-6.39 (m, 2H), 6.10-6.16 (q, 1H, *J* = 9.1, 9.8 Hz), 5.57-5.62 (m, 1H), 5.00-5.02 (d, 1H, *J* = 12.3 Hz), 4.89-4.91 (d, 1H, *J* = 12.3 Hz), 4.68-4.73 (m, 2H), 4.60-4.63 (dd, 1H, *J* = 2.6, 12.1 Hz), 4.33-4.37 (d, 1H, *J* = 15.6 Hz), 3.78 (s, 3H), 3.74 (s, 3H), 3.61 (s, 2H), 2.52-2.61 (m, 1H), 2.07-2.22 (m, 2H), 1.83-1.92 (m, 2H), 1.72-1.79 (m, 1H); ^{13}C NMR (125 MHz, $CDCl_3$) δ 173.6, 170.2, 169.8, 160.0, 157.5, 135.2, 134.8, 130.8, 129.9, 129.4, 129.3, 128.9, 128.5, 128.3, 128.2, 127.2, 117.9, 104.1, 98.2, 67.2, 57.7, 55.3, 55.2, 50.6, 43.6, 40.4, 34.7, 28.2, 22.2; HRMS calcd for $C_{33}H_{36}N_2O_6$ $[M+Na]^+$, 579.2465; found 579.2473.

(3*S*,5*R*,6*R*,9*S*)-Benzyl 5-iodo-2-oxo-3-(phenylacetamido)-indolizine-9-carboxylate (5.16)

Lactam **5.14** (3.2 g, 5.75 mmol) in THF (100 mL) was treated with iodine (5.8 g, 23 mmol), and heated to 80 °C for 3 h, when complete consumption of the starting material was observed by TLC (R_f = 0.6 in 6:4 EtOAc/hexanes). The mixture was cooled to room temperature. The volatiles were removed by evaporation on a rotary evaporator. The residue was dissolved in a minimal volume of DCM, applied onto a silica gel column and eluted with 0-100 % EtOAc in hexanes (TLC R_f = 0.26, EtOAc) to obtain brownish oil that solidified on standing to afford bicycle **5.16** as brownish gummy solid (2.32 g, 76 %): $[\alpha]_D^{25}$ –125.2 (*c* 0.5, MeOH); FT-IR (neat) *v*max 3305, 3030, 2950, 1738, 1645, 1495, 1450, 1269, 1164, 1032, 1164, 1002, 729, 695, 577 cm^{-1}; ^1H NMR (500 MHz, C_6D_6) δ 7.18-7.23 (m, 4H), 7.07-7.13 (m, 4H), 7.00-7.04 (m, 2H), 6.52-6.54 (d, 1H, *J* = 6.0 Hz), 5.07-5.09 (d, 1H, *J* = 12.3 Hz), 4.99-5.01 (d, 1H, *J* = 12.3 Hz), 4.27-4.32 (m, 1H), 4.24-4.26 (m, 1H), 3.66-3.68 (m, 1H), 3.25-3.28 (d, 1H, *J* = 14.8), 3.19-3.22 (d, 1H, *J* = 14.8), 2.67-2.73 (m, 1H), 2.18-2.24 (m, 1H), 1.82-1.85 (m, 1H), 1.64-1.73 (m, 2H), 1.31-1.39 (m, 1H), 1.12-1.8 (m, 1H); ^{13}C NMR (125 MHz, C_6D_6) δ 170.1, 169.8, 167.2, 136.0, 135.4, 129.3, 128.5, 128.4, 128.3, 128.0, 126.7, 66.5, 59.1, 57.9, 49.0, 43.1, 40.4, 35.7, 27.7, 25.5; HRMS calcd for $C_{24}H_{26}IN_2O_4I$ $[M+H]^+$, 533.0931; found 533.0939.

(3*S*,9*S*)-Benzyl-2-oxo-3-(phenylacetamido)-1,2,3,7,8,9-hexahydroindolizine-9-carboxylate (5.18)

Bicycle **5.16** (1 g, 1.88 mmol) was treated with Et_3N (542 μL, 3.76 mmol) in acetonitrile (20 mL) at 60 °C overnight. The reaction mixture was partitioned between ethyl acetate (25 mL) and water (20 mL). The organic layer was separated. The aqueous layer was extracted with ethyl acetate (2 x 20 mL). The organic layers were combined, washed with brine (50 mL), dried over anhydrous sodium sulfate, filtered, and concentrated under reduced pressure. The residue was purified by column chromatography using 30-40 % EtOAc in hexanes (R_f = 0.42 in 7:3 EtOAc/hexanes) as

eluent. Evaporation of the collected fractions afforded olefin **5.18** as colorless oil (574 mg, 69%). $[\alpha]_D^{25}$ –164.4 (*c* 0.5, $CHCl_3$); FT-IR (neat) *ν*max 2947, 1719, 1647, 1612, 1588, 1506, 1207, 1156, 1032, 759, 738 cm^{-1}; ^1H NMR (500 MHz, C_6D_6) δ 7.19-7.20 (m, 2H), 7.01-7.14 (m, 8H), 6.27-6.28 (d, 1H, *J* = 5.6 Hz), 4.99-5.01 (d, 1H, *J* = 12.4), 4.89-4.92 (d, 1H, *J* = 12.3 Hz), 4.58-4.64 (m, 1H), 4.42-4.38 (m, 1H), 4.36-4.39 (dd, 1H, *J* = 4.2, 8.6 Hz), 3.29-3.32 (d, 1H, *J* = 14.8 Hz), 3.24-3.27 (d, 1H, *J* = 15 Hz), 2.78-2.84 (m, 1H), 1.94-2.03 (m, 2H), 1.77-1.83 (m, 1H), 1.45-1.51 (m, 1H), 1.36-1.43 (m, 1H); ^{13}C NMR (125 MHz, C_6D_6) δ 170.9, 170.2, 166.6, 140.3, 136.3, 136.2, 129.2, 128.4, 128.2, 128.0, 127.8, 126.4, 94.6, 66.2, 58.4, 49.1, 42.6, 27.5, 27.2, 26.8; HRMS calcd for $C_{24}H_{25}N_2O_4$ $[M+H]^+$, 405.1808; found 405.1812.

(3*S*,9*S*)-Methyl 3-*N*-(Boc)amino-2-oxo-1,2,3,7,8,9-hexahydroindolizine-9-carboxylate (5.19)

Bicycle **5.17** (400 mg, 0.72 mmol, prepared according to the procedures in reference[9a]) was treated with Et_3N (206 μL, 1.4 mmol) in acetonitrile (20 mL) at 60 °C overnight. The mixture was cooled to room temperature, treated with $(Boc)_2O$ (327 mg, 1.5 mmol), and stirred for 2 h. After the volatiles were removed under reduced pressure, the residue was purified by chromatography using 30-40% EtOAc in hexane (R_f = 0.42 in 5:5 EtOAc/hexanes) as eluent). Evaporation of the collected fractions afforded olefin **19** as colorless oil (105 mg, 48%): $[\alpha]_D^{25}$ –164.4 (*c* 0.5, MeOH); FT-IR (neat) *ν*max 3399, 2973, 1744, 1672, 1497, 1437, 1394, 1277, 1160, 1049, 1032, 868, 776 cm^{-1}; ^1H NMR (500 MHz, $CDCl_3$) δ 5.35 (br, 1H), 4.97-5.00 (m, 1H), 4.62-4.65 (dd, 1H, *J* = 4.1, 8.7 Hz), 4.27-4.35 (m, 1H), 3.77 (s, 3H), 2.81-2.86 (m, 1H), 2.59-2.69 (m, 2H), 2.24-2.35 (m, 2H), 2.06-2.12 (m, 1H), 1.46 (s, 9H); ^{13}C NMR (125 MHz, $CDCl_3$) δ 171.6, 167.2, 155.8, 139.3, 96.3, 79.7, 58.3, 52.5, 50.7, 28.3, 28.1, 27.5, 27.2; HRMS calcd for $C_{15}H_{22}N_2O_5$ [M+Na]+, 333.1418; found 333.1420

(3*S*,6*S*,9*S*)-Methyl 3-*N*-(Boc)amino-indolizidin-2-one-9-carboxylate (5.20)

Alkene **5.19** (50 mg, 0.16 mmol) was stirred with palladium-on-activated carbon (10% by wt, 20 mg) in EtOH (15 mL) under a balloon of hydrogen (1 atm) for 3-4 h. The catalyst was filtered onto Celite™ and washed with methanol. The filtrate and washings were combined and evaporated to provide ester (*S*)-**5.20** (43 mg, 86 %) as colorless gum, which exhibited identical characterization as reported.[23]

(3*S*,6*S*,9*S*)- and (3*S*,6*R*,9*S*)-Benzyl-2-oxo-3-phenlacetamido-1-azabicyclo[4.3.0]nonane-9-carboxylates [(*R*)- and (*S*)-5.21]

Bicycle **5.18** (280 mg, 0.69 mmol) was treated with sodium cyanoborohydride (131 mg, 2.08 mmol) and AcOH (100 μL) in EtOH (10 mL), heated to 80 ^{o}C and stirred overnight. The reaction mixture was cooled to room temperature. The volatiles were evaporated, and the residue was partitioned between ethyl acetate (50 mL) and water (40 mL). The organic layer was separated. The aqueous layer was extracted with ethyl acetate (2 x 200 mL). The organic layers were combined, washed with brine (50 mL), dried over anhydrous sodium sulfate, filtered, and concentrated under reduced pressure. The residue was purified by column chromatography using 1-2 % MeOH in DCM as eluent. First to elute was bicycle *S*-**5.21** (60 mg, 21%) as colorless gum: R_f = 0.54 (EtOAc, visualized with UV); $[\alpha]_D^{25}$ –36.4(*c* 0.5, $CHCl_3$); FT-IR (neat) *ν*max 3318, 3066, 2929, 1739, 1673, 1653, 1540, 1465, 1248, 1167, 960, 751, 724, 693, 528, 505 cm^{-1}; ^{1}H NMR (500 MHz, CDCl3) δ: 7.28-7.38 (m, 10H), 6.64-6.65 (d, 1H, *J* = 5.4), 5.19-5.22 (d, 1H, *J* = 12.2), 5.09-5.12 (d, 1H, *J* = 12.2), 4.54-4.56 (d, 1H, *J* = 8.2), 4.33-4.38 (m, 1H), 3.70-3.77 (m, 1H), 3.61 (s, 2H), 2.52-2.60 (m, 1H), 2.15-2.23 (m, 2H), 2.06-2.12 (m, 2H), 1.60-1.70 (m, 2H), 1.46-1.53 (m, 1H); ^{13}C NMR (125 MHz, $CDCl_3$) δ 171.5, 171.1, 169.1, 135.5, 134.8, 129.4, 129.0, 128.7, 128.5, 128.2, 127.3, 67.2, 58.4, 56.4, 49.3, 43.8, 32.2, 29.2, 27.0, 26.5. HRMS calcd for $C_{24}H_{26}N_2O_4Na$ $[M+Na]^+$, 429.1785; found 429.1801. Second to elute was bicycle *R*-**5.21** (159 mg,

57%) as a colorless gum: R_f = 0.48 (EtOAc, visualized with UV); $[\alpha]_D^{25}$ –66.4 (*c* 0.5, $CHCl_3$); FT-IR (neat) *ν*max 3295, 3062, 2944, 1741, 1630, 1539, 1443, 1167, 728, 696 cm^{-1}; ^1H NMR (500 MHz, $CDCl_3$) δ 7.29-7.39 (m, 10H), 6.28-6.29 (d, 1H, *J* = 5.6), 5.22-5.24 (d, 1H *J* = 12.3), 5.13-5.15 (d, 1H, *J* = 12.3), 4.51-4.55 (t, 1H, *J* = 8.5), 4.33-4.37 (m, 1H), 3.68-3.74 (m, 1H), 3.61 (s, 2H), 2.58-2.63 (m, 1H), 2.37-2.43 (m, 1H), 2.07-2.17 (m, 2H), 1.76-1.84 (m, 1H), 1.47-1.69 (m, 3H); ^{13}C NMR (125 MHz, $CDCl_3$) δ 172.0, 171.5, 167.7, 135.5, 134.8, 129.3, 128.8, 128.5, 128.3, 128.0, 127.1, 66.8, 60.1, 57.8, 51.3, 43.6, 32.8, 27.9, 27.8, 27.4; HRMS calcd for $C_{24}H_{26}N_2O_4Na$ $[M+Na]^+$, 429.1785; found 429.1781.

(3*S*,6*S*,9*S*)-2-Oxo-3-phenylacetamido-1-azabicyclo[4.3.0]nonane-9-carboxylic acid (*S*)-5.23

Benzyl ester (*S*)- **5.21** (30 mg, 0.07 mmol) and palladium-on-activated carbon (10% by wt, 12 mg) in EtOH (15 mL) were stirred under a balloon of hydrogen (1 atm) for 3-4 h. The catalyst was filtered onto Celite™ and washed with methanol. The filtrate and washings were combined and evaporated to acid (*S*)- **5.23** (21 mg, 91%) as white solid: mp 85–89 °C; $[\alpha]_D^{25}$ –29.2 (*c* 0.5, MeOH); FT-IR (neat) *ν*max 3294, 2944, 1733, 1624, 1544, 1494, 1440, 1169, 985, 725, 695 cm^{-1}; ^1H NMR (500 MHz, CD_3OD) δ 7.30-7.35 (m, 4H), 7.23-7.26 (m, 1H), 4.51-4.54 (t, 1H, *J* = 7.8 Hz), 4.43-4.45 (d, 1H, *J* = 9.06 Hz), 3.73-3.80 (m, 1H), 3.59 (s, 2H), 2.19-2.30 (m, 3H), 2.07-2.13 (m, 2H), 1.64-1.79 (m, 3H); ^{13}C NMR (125 MHz, CD_3OD) δ 173.8, 172.4, 169.1, 135.4, 128.8, 128.1, 126.4, 58.4, 57.6, 48.1, 42.2, 31.4, 28.5, 26.5, 26.1; HRMS calcd for $C_{17}H_{20}N_2O_4$ $[M+Na]^+$, 339.1315; found 339.1316.

(3*S*,6*R*,9*S*)-2-Oxo-3-phenylacetamido-1-azabicyclo[4.3.0]nonane-9-carboxylic acid [(*R*)-23]

Benzyl ester (*R*)-**5.21** (45 mg, 0.11 mmol) was hydrogenated under the same conditions used to provide acid (*S*)-**5.23** above. Evaporation of the filtrate and washings gave acid (*R*)-**23** (31 mg, 88 %) as a white solid: mp 68–70 °C; $[\alpha]_D^{25}$ –108.4 (*c* 0.3, MeOH); FT-IR (neat) *ν*max 3242, 3066,

2943, 1735, 1625, 1445, 1317, 1199, 1084, 978726, 696 cm^{-1}; ^1H NMR (500 MHz, CD_3OD) δ 7.30-7.35 (m, 4H), 7.23-7.27 (m, 1H), 4.44-4.52 (m, 2H), 3.71-3.79 (m, 1H, *J* = 12.4 Hz), 3.57-3.58 (d, 2H, *J* = 3.2 Hz), 2.39-2.48 (m, 1H), 2.13-2.20 (m, 3H), 1.77-1.89 (m, 2H), 1.52-1.61 (m, 2H); ^{13}C NMR (125 MHz, CD_3OD) δ 173.1, 172.5, 168.4, 135.3, 128.8, 128.1, 126.4, 60.4, 58.4, 49.7, 42.4, 32.4, 27.8, 27.7, 27.3; HRMS calcd for $C_{17}H_{20}N_2O_4Na$ $[M+Na]^+$, 339.1315; found 339.1312.

(3*S*,6*S*,9*S*)-3-*N*-(Boc)amino-indolizidin-2-one-9-carboxylic acid (5.24)

Methyl ester **5.20** (40 mg, 0.13 mmol) was dissolved in 1 mL of dioxane, cooled to 0 °C, treated with 1 N LiOH (180 μL) and stirred for 1 h. The volatiles were evaporated under reduced pressure. The remaining aqueous phase was acidified with 1N HCl to pH 3 and extracted with ethyl acetate (2×10 mL). The organic extractions were combined, dried with Na_2SO_4, filtered and concentrated under vacuum to afford acid **5.24** (35 mg, 92%) as pale brown gum, which exhibited identical characterization as previously reported.[23]

Phenylacetyl-(3*S*,9*S*)-2-oxo-1,2,3,4,7,8-hexahydroindolizine-9-carbonyl-(2*S*)-(3-pyridyl)alaninyl-(3*S*)-*β*-homophenylalanine benzyl ester (5.26).

Benzyl ester **5.18** (30 mg, 0.07 mmol) and palladium-on-activated carbon (10% by wt, 12 mg) in MeOH (5 mL) was stirred under a balloon of hydrogen (1 atm) for 8-10 minutes. The catalyst was filtered onto Celite™ and washed with methanol. The filtrate and washings were combined and evaporated to give a 1:1 mixture of bicycle (*S*)- **5.23** and olefin **5.22**, which was reacted with dipeptide hydrochloride **5.25** using the protocol described for the synthesis of ester **5.27**. The residue was purified by flash chromatography on silica gel using 2-4% MeOH in DCM. First to elute was peptide **5.26** (14 mg, 26%) as colorless foam: R_f = 0.44 (1:9 MeOH/$CHCl_3$); $[\alpha]_D^{25}$ –6.1 (*c* 0.5, $CHCl_3$); FT-IR (neat) *ν*max 3680, 3337, 2936, 2843, 1739, 1693, 1650, 1527, 1385, 1363,

1269, 1189, 1054, 998, 772, 731 cm^{-1}; ^1H NMR (400 MHz, $CDCl_3$) δ 8.33-8.34 (d, 1H, *J* = 4.3 Hz), 8.29 (br s, 1H), 7.77-7.79 (d, 1H, *J* = 7.9 Hz), 7.52-7.54 (d, 1H, *J* = 7.9 Hz), 7.33-7.43 (m, 9H), 7.20-7.29 (m, 5H), 7.13-7.18 (m, 3H), 6.99-7.01 (d, 1H, *J* = 8.6 Hz), 5.15-5.18 (d, 1H, *J* = 12.2 Hz), 5.09-5.12 (d, 1H, *J* = 12.2 Hz), 4.83-4.85 (m, 1H), 4.65-4.73 (m, 1H), 4.51-4.57 (m, 2H), 4.38-4.44 (m, 1H), 3.75 (s, 2H), 3.10-3.15 (dd, 1H, *J* = 4.3, 14.6 Hz), 2.82-2.92 (m, 3H), 2.49-2.62 (m, 5H), 2.34-2.39 (m, 1H), 1.91-2.01 (m,1H), 1.77-1.87 (m, 1H); ^{13}C NMR (125 MHz, CD_2Cl_2) δ 171.2, 170.0, 169.9, 169.5, 169.5, 168.9, 150.9, 147.8, 139.0, 137.6, 136.9, 135.9, 135.6, 132.9, 129.3, 129.2, 128.6, 128.5, 128.4, 128.3, 128.2, 126.8, 126.6, 123.7, 96.0, 66.4, 59.7, 55.1, 48.5, 47.4, 43.5, 39.9, 37.7, 33.7, 27.6, 24.1; HRMS calcd for $C_{42}H_{43}N_5O_6Na$ $[M+Na]^+$, 736.3106; found 736.3108.; Second to elute was (*S*)- **5.27** (11 mg, 44%) as white foam: R_f = 0.40 (0.5:9.5 MeOH/$CHCl_3$, twice eluted), which exhibited identical characterization as reported.[1d]

Benzyl-phenylacetyl-(3*S*,6*R*,9*S*)-I^{2}aa-(2*S*)-(3-pyridyl)alaninyl-(3*S*)-*β*-homophenylalaninate (5.27)

A solution of phenylacetyl-I^{2}aa (*R*-**5.23**, 30 mg, 0.09 mmol) in dichloromethane (5 mL) was treated with HOBt (12 mg, 1 equiv) and TBTU (29 mg, 1 equiv), stirred for 15 min, treated with dipeptide hydrochloride **5.25** (41 mg, 1 equiv, 0.09 mmol), followed by DIEA (33 μL, 2 equiv, 0.18 mmol), and stirred at room temperature for 6 h. Evaporation of the volatiles gave a residue, which was purified by flash chromatography on silica gel using 2% MeOH in $CHCl_3$ as eluant. Evaporation of the collected fractions afforded benzyl ester **5.27** (36 mg, 54%) as white foam: R_f = 0.6 (10% MeOH/$CHCl_3$); $[\alpha]_D^{25}$ –65.8 (*c* 1, $CHCl_3$); FT-IR (neat) *ν*max 3294, 3029, 2930, 1732, 1631, 1517, 1496, 1438, 1197, 1147, 1028, 747, 697 cm^{-1}; ^1H NMR (500 MHz, $CDCl_3$) δ: 8.50-8.49 (d, 1H, *J* = 1.5 Hz), 8.41-8.42 (m, 1H), 7.62-7.66 (m, 2H), 7.29-7.36 (m, 9H), 7.20-7.27 (m, 8H), 7.05-7.07 (d, 1H, *J* = 7.3 Hz), 5.05-5.11 (q, 2H, *J* = 12.3, 7.0 Hz), 4.55-4.59 (m, 1H), 4.44-4.55 (m, 2H),

3.84-3.89 (m, 1H), 3.58 (s, 2H), 3.41-3.46 (m, 1H), 3.27-3.30 (dd, 1H, *J* = 3.6, 14.2 Hz), 3.02-3.06 (dd, 1H, *J* = 6.0, 13.6 Hz), 2.83-2.90 (m, 2H), 2.58-2.60 (d, 2H, *J* = 6.23 Hz), 2.19-2.25 (m, 1H), 2.07-2.14 (m, 2H), 1.92-2.04 (m, 2H), 1.60-1.69 (m, 1H), 1.31-1.44 (m, 2H) ; ^{13}C NMR (125 MHz, $CDCl_3$) δ 171.9, 171.2, 171.1, 170.4, 168.9, 151.1, 147.7, 137.9, 136.7, 136.1, 134.5, 134.2, 129.6, 129.5, 129.0, 128.7, 128.6, 128.5, 128.2, 127.5, 126.8, 123.6, 66.4, 60.2, 60.1, 55.2, 51.6, 48.0, 43.3, 40.1, 37.8, 33.5, 32.9, 28.1, 27.9, 27.1; HRMS calcd for $C_{42}H_{46}N_5O_6$ $[M+H]^+$, 716.3442; found 716.3453.

4-Azidophenylacetyl-(3*S*,6*R*,7*R*,9*S*)-I^{2}aa-(2*S*)-(3-pyridyl)alaninyl-(3*S*)-β-homophenyl alanine benzyl ester (5.30).

A solution of HCl salt **5.29** (35 mg, 0.06 mmol, synthesized from Boc-I^{2}aa **5.24** as previously described in reference[1d]) in dichloromethane (5 mL) was treated with HOBt (8 mg, 1 equiv) and TBTU (20 mg, 1 equiv), stirred for 15 min, treated with 4-azidophenyl acetic acid (11 mg, 0.06 mmol), followed by DIEA (22 μL, 0.12 mmol), and stirred at room temperature for 6 h. Evaporation of the volatiles gave a residue, which was purified by flash chromatography on silica gel using 2-3% MeOH in $CHCl_3$ as eluant. Evaporation of the collected fractions afforded azide **5.30** (29 mg, 70%) as white foam: R_f = 0.64 (10% MeOH in $CHCl_3$); $[\alpha]_D^{25}$ –45.2 (*c* 0.5, $CHCl_3$); FT-IR (neat) *ν*max 3297, 3030, 2928, 2111, 1732, 1635, 1504, 1436, 1284, 1190, 1031, 800, 745, 698, cm^{-1}; ^{1}H NMR (500 MHz, $CDCl_3$) δ 8.38-8.39 (m, 2H), 7.72-7.73 (d, 1H, *J* = 7.6), 7.54-7.56 (dt, 1H, *J* = 1.8 Hz), 7.32-7.40 (m, 8H), 7.25-7.27 (m, 2H), 7.14-7.23 (m, 4H), 7.08-7.10 (d, 1H, *J* = 8.7 Hz), 6.99-7.012 (m, 2H), 5.13-5.16 (d, 1H, *J* = 12.3 Hz), 5.07-5.10 (d, 1H, *J* = 12.3 Hz), 4.45-4.55 (m, 2H), 4.35-4.39 (m, 2H), 3.65 (s, 2H), 3.48-3.55 (m, 1H), 3.13-3.17 (dd, 1H, *J* = 4.4, 14.1 Hz), 2.82-2.93 (m, 3H), 2.55-2.56 (d, 2H, *J* = 5.5 Hz), 2.18-2.33 (m, 2H), 1.95-2.07 (m, 2H), 1.78-1.86 (m, 1H), 1.37-1.45 (m, 1H), 1.22-1.30 (m, 2H); ^{13}C NMR (125 MHz, $CDCl_3$) δ 171.4,

171.2, 170.9, 170.5, 169.8, 151.2, 147.9, 138.9, 137.4, 136.6, 135.6, 132.9, 131.8, 130.8, 129.2, 128.6, 128.5, 128.4, 128.3, 126.7, 123.6, 119.4, 66.5, 59.4, 57.6, 54.8, 48.7, 47.4, 42.8, 39.9, 37.3, 33.8, 32.2, 27.1, 26.9, 26.6; HRMS calcd for $C_{42}H_{44}N_8O_6Na$ $[M+Na]^+$, 779.3276; found 779.3281.

(3*S*,9*S*)-Benzyl-2-oxo-5-phenyl-3-phenylacetamido-1,2,3,4,7,8,9-hexahydroindolizine-9-carboxylate (5.31b)

Olefin **5.18** (280 mg, 0.69 mmol) was treated with phenyl boronic acid (169 mg, 1.38 mmol), 1,4-benzoquinone (37 mg, 0.35 mmol), Ag_2O (158 mg, 0.69 mmol) and $Pd(OAc)_2$ (31 mg, 0.13 mmol) in dry THF (10 mL), heated to 80 °C, stirred overnight, cooled to room temperature, diluted with ethyl acetate (50 mL) and water (30 mL), and filtered through a pad of Celite™. The pad was washed with ethyl acetate (50 mL). The filtrate and washing were combined and transferred to a separating funnel. The organic layer was separated. The aqueous layer was extracted with ethyl acetate (2 x 200 mL). The organic layers were combined, washed with brine (50 mL), dried over anhydrous sodium sulfate, filtered, and concentrated under reduced pressure. The residue was purified by column chromatography using 60-70% EtOAc in hexanes (R_f = 0.23 in 5:5 EtOAc/hexanes) as eluent. Evaporation of the collected fractions afforded styrene **5.31b** (172 mg, 52%) as colorless gum: $[\alpha]_D^{25}$ –79.0 (*c* 1, MeOH); FT-IR (neat) *v*max 3306, 3030, 2922, 1743, 1651, 1495, 1407, 1324, 1172, 1031, 736, 695, 498 cm^{-1}; ^1H NMR (500 MHz, $CDCl_3$) δ 7.31-7.38 (m, 12H), 7.20-7.22 (m, 3H), 6.39-6.40 (d, 1H, *J* = 5.5 Hz), 5.23-5.26 (d, 1H, *J* = 12.3 Hz), 5.16-5.19 (d, 1H, *J* = 12.3 Hz), 4.67-4.73 (m, 2H), 3.64 (s, 2H), 3.19-3.23 (dd, 1H, *J* = 6.8, 15.4 Hz), 2.84-2.91 (m, 1H), 2.65-2.80 (m, 2H), 2.31-2.38 (m, 1H), 2.01-2.07 (m, 1H); ^{13}C NMR (125 MHz, $CDCl_3$) δ 171.2, 170.8, 166.6, 138.7, 135.4, 135.3, 134.5, 129.4, 128.9, 128.6, 128.5, 128.3, 128.1, 127.3, 127.0, 126.6, 111.1, 67.3, 58.4, 50.1, 43.7, 32.6, 27.8, 27.2; HRMS calcd for $C_{30}H_{28}N_2O_4Na$ $[M+Na]^+$, 503.1951; found 503.1941.

(3*S*,9*S*)-Benzyl-2-oxo-5-(4-methoxyphenyl)-3-phenylacetamido-1,2,3,4,7,8-hexahydro indolizine-9-carboxylate (5.31c)

Bicycle **5.31c** was synthesized from olefin **5.8** (200 mg, 0.50 mmol) using the protocol for styrene **5.31b**, which provide colourless gum (101 mg, 40%): R_f = 0.32 (5:5 EtOAc/hexanes, visualized under UV light); $[\alpha]_D^{25}$ –79.0 (*c* 1, $CHCl_3$); FT-IR (neat) *v*max 3304, 2922, 1734, 1671, 1497, 1380, 11290, 1210, 1110, 796, 710, 498 cm^{-1}; ^1H NMR (500 MHz, $CDCl_3$) δ 7.31-7.39 (m, 10H), 7.13-7.15 (d, 2H, *J* = 8.8 Hz), 6.86-6.87 (d, 2H *J* = 8.8 Hz), 6.43-6.45 (d, 1H, *J* = 5.6 Hz), 5.23-5.25 (d, 1H, *J* = 12.4 Hz), 5.16-5.19 (d, 1H, *J* = 12.3 Hz), 4.66-4.72 (m, 2H), 3.82 (s, 3H), 3.64 (s, 2H), 3.15-3.20 (dd, 1H, *J* = 6.9, 15.5 Hz), 2.71-2.86 (m, 2H), 2.61-2.68 (m, 1H), 2.29-2.36 (m, 1H), 2.01-2.07 (m, 1H); ^{13}C NMR (125 MHz, $CDCl_3$) δ 171.3, 170.9, 166.5, 158.2, 135.3, 134.6, 134.3, 131.1, 129.4, 128.9, 128.6, 128.4, 128.2, 128.0, 127.3, 113.7, 110.7, 67.2, 58.3, 55.3, 50.1, 43.7, 32.7, 27.7, 27.2; HRMS calcd for $C_{31}H_{30}N_2O_5Na$ $[M+Na]^+$, 533.2047; found 533.2053.

(3*S*,9*S*)-Benzyl-2-oxo-5-(4-cyanophenyl)-3-phenylacetamido-1,2,3,4,7,8,9-hexahydro indolizine-9-carboxylate (5.31d)

Bicycle **5.31d** was synthesized from olefin **5.18** (100 mg, 0.25 mmol) using the protocol for the synthesis of styrene **5.31b** to provide as pale yellow foam (67 mg, 54%): R_f = 0.44 (7:3 EtOAc/hexanes, visualized under UV light): $[\alpha]_D^{25}$ –164 (*c* 0.5, MeOH); FT-IR (neat) *v*max 3304, 2922, 2223, 1742, 1652, 1600, 1495, 1399, 1322, 1250, 1744, 1032, 909, 729, 695, 537 cm^{-1}; ^1H NMR (500 MHz, $CDCl_3$) δ 7.60-7.62 (d, 2H, *J* = 8.2), 6.28-6.40 (m, 12H), 6.41-6.42 (d, 1H *J* = 5.2), 5.23-5.25 (d, 1H, *J* = 12.3), 5.17-5.19 (d, 1H, *J* = 12.3), 4.72-4.73 (dd, 1H, *J* = 5.4, 8.6), 4.66-4.70 (m, 1H), 3.64 (s, 2H), 3.19-3.22(dd, 1H, *J* = 6.8, 15.2), 2.89-2.94 (m, 1H), 2.68-2.77 (m, 2H), 2.35-2.42 (m, 1H), 2.02-2.09 (m, 1H); ^{13}C NMR (700 MHz, $CDCl_3$) δ 171.3, 170.6, 166.6, 143.6, 138.1, 135.1, 134.4, 132.1, 129.4, 129.0, 128.7, 128.6, 128.2, 127.4, 127.4, 118.8, 109.8, 109.6,

67.4, 58.4, 49.9, 43.7, 32.1, 28.2, 27.0 HRMS calcd for $C_{31}H_{27}N_3O_4$ $[M+Na]^+$, 528.1894; found 528.1905

(3*S*,9*S*)-Benzyl-2-oxo-5-(4-trifluoromethoxyphenyl)-3-phenylacetamido-1,2,3,4,7,8,9-hexahydroindolizine-9-carboxylate (5.31e)

Bicycle **31e** was synthesized from olefin **5.18** (100 mg, 0.25 mmol) using the protocol for described for the synthesis of styrene **5.31b** to provide a colorless gum (61 mg, 44%): R_f = 0.40 (7:3 EtOAc/hexanes, visualized with UV); $[\alpha]_D^{25}$ –107.0 (*c* 0.6, $CHCl_3$); ^{1}H NMR (500 MHz, $CDCl_3$) δ 7.31-7.40 (m, 10H), 7.21-7.24 (d, 2H, *J* = 8.8 Hz), 6.86-6.87 (d, 2H, *J* = 8.4 Hz), 6.43-6.45 (d, 1H, *J* = 5.4 Hz), 5.23-5.25 (d, 1H, *J* = 12.2 Hz), 5.16-5.19 (d, 1H, *J* = 12.3 Hz), 4.65-4.73 (m, 2H), 3.64 (s, 2H), 3.15-3.20 (dd, 1H, *J* = 6.8, 15.3 Hz), 2.82-2.89 (m, 1H), 2.64-2.77 (m, 2H), 2.30-2.39 (m, 1H), 2.02-2.11 (m, 1H); ^{13}C NMR (125 MHz, $CDCl_3$) δ 171.3, 170.8, 166.5, 147.6, 137.5, 136.1, 135.2, 134.5, 129.3, 129.0, 128.6, 128.5, 128.4, 128.1, 127.4, 121.5, 120.9, 109.8, 67.3, 58.4, 50.1, 43.7, 32.6, 27.8, 27.1; HRMS calcd for $C_{31}H_{27}F_3N_2O_5Na$ $[M+Na]^+$, 587.1764; found 587.1781

(3*S*,9*S*)-3-Phenylacetamido-2-oxo-5-phenyl-1,2,3,4,7,8-hexahydroindolizine-3-carboxylic acid (5.32b)

Acid **5.32b** was synthesized from ester **5.31b** (35 mg, 0.07 mmol) using the protocol for the preparation of acid (*S*)- **5.23** as white solid (25 mg, 89 %): $[\alpha]_D^{25}$ –141.8 (*c* 0.3, MeOH); FT-IR (neat) *ν*max 2922, 2864, 1733, 1647, 1495, 1409, 1322, 1201, 1054, 1032, 1011, 763, 695, 695 cm^{-1}; ^{1}H NMR (700 MHz, CD_3OD) δ 7.27-7.33 (m, 8H), 7.18-7.23 (m, 2H), 4.77-4.80 (dd, 1H, *J* = 7.1, 13.5 Hz), 4.60-4.62 (dd, 1H, *J* = 4.9, 4.6 Hz), 3.60 (s, 2H), 2.85-2.92 (m, 2H), 2.75-2.83 (m, 2H), 2.33-2.38 (m, 1H), 2.03-2.07 (m, 1H); ^{13}C NMR (175 MHz, CD_3OD) δ 174.1, 172.7, 166.7,

139.1, 136.4, 135.3, 128.8, 128.2, 127.9, 126.8, 126.5, 126.1, 109.6, 59.2, 49.4, 42.3, 32.4, 27.5, 27.2.; HRMS calcd for $C_{23}H_{23}N_2O_4$ $[M+H]^+$, 391.1652; found 391.1665.

(3*S*,9*S*)-3-Phenylacetamido-2-oxo-5-(4-methoxyphenyl)-1,2,3,4,7,8-hexahydroindolizine-3-carboxylic acid (5.32c)

Acid **32c** was synthesized from ester **5.31c** (41 mg, 0.08 mmol) using the protocol for the preparation of acid (*S*)- **5.23** as pale yellow foam (31 mg, 94%): mp 112–115 ºC; $[\alpha]_D^{25}$ –129 (*c* 0.8, MeOH); FT-IR (neat) *ν*max 2937, 2842, 1734, 2645, 1501, 1410, 1243, 1177, 1032, 831, 642, 491 cm^{-1}; ^1H NMR (700 MHz, CD_3OD) δ 7.29-7.34 (m, 4H), 7.21-7.24 (m, 3H), 6.90-6.91 (m, 2H), 4.71-4.80 (dd, 1H, *J* = 7.1, 13.4 Hz), 4.61-4.63 (dd, 1H, *J* = 4.9, 8.8 Hz), 3.80 (s, 3H), 3.62 (s, 2H), 2.75-2.89 (m, 4H), 2.33-2.38 (m, 1H), 2.04-2.09 (m, 1H); ^{13}C NMR (175 MHz, CD_3OD) δ 174.0, 172.8, 166.8, 158.3, 135.3, 135.2, 131.4, 128.9, 128.2, 127.9, 126.4, 113.4, 109.4, 59.1, 54.3, 49.4, 42.3, 32.5, 27.5, 27.2. HRMS calcd for $C_{24}H_{25}N_2O_5$ $[M+H]^+$, 421.1758; found 421.1766.

(3*S*,9*S*)-3-Phenylacetamido-2-oxo-5-(4-cyanophenyl)-1,2,3,4,7,8-hexahydroindolizine-3-carboxylic acid (5.32d).

Acid **5.32d** was synthesized from ester **5.31d** (26 mg, 0.05 mmol) using the protocol for the preparation of acid (*S*)- **5.23** as white solid (20 mg, 95%): $[\alpha]_D^{25}$ –43.0 (*c* 0.5, MeOH); FT-IR (neat) *ν*max 2922, 2860, 2223, 1647, 1598, 1541, 1400, 1324, 1054, 1032, 1011, 839, 725, 695, 538 cm^{-1}; ^1H NMR (700 MHz, CD_3OD) δ 7.68-7.70 (d, 2H, *J* = 8.3 Hz), 7.21-7.24 (d, 2H, *J* = 8.3 Hz), 7.29-7.34 (m, 4H), 7.23-7.25 (m, 1H), 4.79-4.82 (dd, 1H, *J* = 6.7, 13.4 Hz), 4.79-4.82 (dd, 1H, *J* = 5.1, 8.8 Hz), 3.62 (s, 2H), 2.93-2.99 (m, 2H), 2.79-2.87 (m, 2H), 2.37-2.42 (m, 1H), 2.06-2.11 (m, 1H); ^{13}C NMR (175 MHz, CD_3OD) δ 174.9, 172.7, 166.8, 144.3, 139.6, 135.3, 131.8, 128.8, 128.2,

127.4, 126.5, 118.5, 108.9, 108.0, 59.6, 49.3, 42.3, 31.8, 27.9, 27.1.; HRMS calcd for $C_{24}H_{22}N_3O_4$ $[M+H]^+$, 416.1604; found 416.1616.

(3*S*,9*S*)-3-Phenylacetamido)-2-oxo-5-(4-trifluoromethoxyphenyl)-1,2,3,4,7,8-hexahydro-indolizine-3-carboxylic acid (5.32e)

Acid **5.32e** was synthesized from ester **5.31e** (32 mg, 0.06 mmol) using the protocol for the preparation of acid (*S*)-**23** as white solid (25 mg, 93%): $[\alpha]_D^{25}$ –108.8 (*c* 0.5, MeOH); FT-IR (neat) *ν*max 2922, 2864, 2843, 1733, 1651, 1508, 1407, 1249, 1205, 1153, 1055, 1205, 1153, 1055, 1032, 1014, 850, 725 cm^{-1}; ^1H NMR (700 MHz, CD_3OD) δ 7.39-7.40 (m, 2H), 7.29-7.34 (m, 4H), 7.24-7.26 (m, 3H), 4.79-4.82 (dd, 1H, *J* = 6.9, 13.5 Hz), 4.64-4.66 (dd, 1H, *J* = 5.1, 8.7 Hz), 3.62 (s, 2H), 2.89-2.95 (m, 2H), 2.77-2.84 (m, 2H), 2.37-2.43 (m, 1H), 2.06-2.11 (m, 1H); ^{13}C NMR (175 MHz, CD_3OD) δ 173.8, 172.7, 166.8, 147.4, 147.3, 138.4, 137.3, 135.3, 128.8, 128.4, 128.2, 126.5, 120.5, 108.3, 59.0, 49.3, 42.3, 32.3, 27.5, 27.0; HRMS calcd for $C_{24}H_{22}N_2O_5F_3$ $[M+H]^+$, 475.1475; found 475.1486.

(3*S*,9*S*)-Benzyl-2-oxo-3-(phenylacetamido)-5-phenyl-1,2,3,4,7,8-hexahydroindolizine-carbonyl-(2S)-(3-pyridyl)alaninyl-(3S)-β-homophenylalaninate (5.33b)

Peptide **5.33b** was synthesized from acid **5.2b** (27 mg, 0.07 mmol) using the protocol for the synthesis of ester **5.27** as white solid (35 mg, 65%): $[\alpha]_D^{25}$ –106 (*c* 0.5, $CHCl_3$); FT-IR (neat) *ν*max 2947, 1719, 1647, 1612, 1588, 1506, 1207, 1156, 1032, 759, 738 cm^{-1}; ^1H NMR (500 MHz, $CDCl_3$) δ 8.35 (br s, 2H), 7.89-7.91 (d, 1H, *J* = 7.7 Hz), 7.54-7.57 (m, 1H), 7.30-7.44 (m, 12H), 7.26-7.28 (m, 2H), 7.14-7.21 (m, 8H), 7.01-7.03 (d, 1H, *J* = 8.8 Hz), 5.16-5.18 (d, 1H, *J* = 12.3 Hz), 5.10-5.13 (d, 1H, *J* = 12.3 Hz), 4.86-4.92 (m, 1H), 4.63-4.65 (dd, 1H, *J* = 1.6, 8.3 Hz), 4.51-4.56 (m, 1H), 4.41-4.45 (m, 1H), 3.78 (s, 2H), 3.14-3.18 (dd, 1H, *J* = 4.2, 14.4 Hz), 2.83-2.95 (m, 4H), 2.67-2.72 (m, 2H), 2.57-2.58 (m, 2H), 2.29-2.40 (m, 2H), 1.77-1.93 (m, 1H),; ^{13}C NMR (125

MHz, $CDCl_3$) δ 171.7, 171.5, 170.1, 169.5, 168.7, 150.9, 147.9, 138.2, 137.3, 136.9, 135.6, 135.2, 134.9, 129.4, 129.2, 128.7, 128.7, 128.6, 128.5, 128.4, 128.3, 127.4, 127.0, 126.8, 126.7, 123.8, 110.6, 66.6, 59.7, 54.9, 48.9, 47.2, 43.8, 39.9, 37.3, 33.8, 33.2, 29.7, 28.0, 24.3; HRMS calcd for $C_{48}H_{47}N_5O_6Na$ $[M+Na]^+$, 812.3419; found 812.3432.

(3*S*,9*S*)-Benzyl-2-oxo-3-(phenylacetamido)-5-(4-methoxyphenyl)-1,2,3,4,7,8-hexahydroindolizine-carbonyl-(2S)-(3-pyridyl)alaninyl-(3S)-β-homophenylalaninate (5.33c)

Peptide **5.33c** was synthesized from acid **5.32c** (25 mg, 0.06 mmol) using the protocol for the synthesis of ester **5.27** as white solid (31 mg, 65%): $[\alpha]_D^{25}$ –95.7 (*c* 1, $CHCl_3$); ^{1}H NMR (500 MHz, $CDCl_3$) δ 8.32-8.34 (m, 2H), 7.88-7.90 (d, 1H, *J* = 8.0 Hz), 7.54-7.56 (m, 1H), 7.43-7.45 (m, 2H), 7.33-7.40 (m, 9H), 7.23-7.30 (m, 3H), 7.11-7.17 (m, 5H), 7.02-7.04 (d, 1H, *J* = 8.8 Hz), 6.85-6.86 (m, 2H), 5.16-5.18 (d, 1H, *J* = 12.2 Hz), 5.10-5.13 (d, 1H, *J* = 12.2 Hz), 4.84-4.90 (m, 1H), 4.63-4.65 (m, 1H), 4.52-4.56 (m, 1H), 4.41-4.45 (m, 1H), 3.82 (s, 3H), 3.78 (s, 2H), 3.14-3.17 (dd, 1H, *J* = 4.3, 14.4 Hz), 2.82-2.93 (m, 4H), 2.63-2.72 (m, 2H), 2.57-2.58 (d, 2H, *J* = 6.04 Hz), 2.35-2.40 (m, 1H), 2.25-2.32 (m, 1H), 1.80-1.88 (m, 1H); ^{13}C NMR (125 MHz, $CDCl_3$) δ 171.7, 171.5, 170.2, 169.5, 168.5, 158.4, 150.9, 147.9, 137.3, 136.9, 135.6, 135.2, 133.9, 132.6, 130.5, 129.4, 129.2, 128.8, 128.7, 128.6, 128.5, 128.4, 128.3, 127.0, 126.7, 123.8, 113.7, 110.2, 66.6, 59.7, 55.3, 54.9, 48.9, 47.2, 43.7, 39.9, 37.3, 33.8, 33.4, 27.9, 24.2; HRMS calcd for $C_{49}H_{50}N_5O_7$ $[M+H]^+$, 820.3704; found 820.3713**.**

(3*S*,9*S*)-Benzyl-2-oxo-3-(phenylacetamido)-5-(4-cyanophenyl)-1,2,3,4,7,8-hexahydroindolizine-carbonyl-(2S)-(3-pyridyl)alaninyl-(3S)-β-homophenylalaninate (5.33d)

Peptide **5.33d** was synthesized from acid **5.32d** (35 mg, 0.08 mmol) using the protocol for the synthesis of ester **5.27** as white color foam (45 mg, 66%): $[\alpha]_D^{25}$–98.2 (*c* 0.5, $CHCl_3$); ^{1}H NMR (500 MHz, $CDCl_3$) δ 8.32-8.34 (m, 2H), 7.90-7.92 (d, 1H, *J* = 7.9 Hz), 7.59-7.61 (m, 2H), 7.54-

7.57 (dt, 1H, *J* = 1.8 Hz), 7.34-7.43 (m, 9H), 7.29-7.30 (m, 2H), 7.21-7.27 (m, 5H), 7.17-7.19 (dd, 1H, *J* = 4.8, 7.7 Hz), 7.13-7.15 (m, 2H), 6.96-6.98 (d, 1H, *J* = 8.7 Hz), 5.16-5.18 (d, 1H, *J* = 8.2 Hz), 5.10-5.13 (d, 1H, *J* = 12.2 Hz), 4.84-4.90 (m, 1H), 4.64-4.66 (dd, 1H, *J* = 1.9, 8.4 Hz), 4.51-4.57 (m, 1H), 4.40-4.45 (m, 1H), 3.77 (s, 2H), 3.13-3.17 (dd, 1H, *J* = 4.4, 14.3 Hz), 2.83-2.95 (m, 4H), 2.72-2.74 (m, 2H), 2.56-2.58 (m, 2H), 2.34-2.50 (m, 2H), 1.87-1.95 (m, 1H); ^{13}C NMR (125 MHz, $CDCl_3$) δ 171.8, 171.5, 169.7, 169.3, 168.5, 150.9, 147.8, 143.1, 137.5, 137.3, 137.1, 135.5, 135.0, 132.6, 132.1, 129.4, 129.2, 128.8, 128.7, 128.6, 128.5, 128.4, 127.9, 127.1, 126.8, 123.8, 118.7, 110.1, 109.1, 66.6, 59.7, 54.9, 48.8, 47.3, 43.7, 39.8, 37.2, 34.0, 32.6, 28.4, 24.4.; $C_{49}H_{47}N_6O_6$ $[M+H]^+$, 815.3801; found 815.3809.

(3*S*,9*S*)-Benzyl-2-oxo-3-(phenylacetamido)-5-(4-(trifluoromethoxy)phenyl)-1,2,3,4,7,8-hexahydroindolizine-carbonyl-(2S)-(3-pyridyl)alaninyl-(3S)-β-homophenylalaninate (5.33e)

Peptide **5.33e** was synthesized from acid **5.32e** (21 mg, 0.04 mmol) using the protocol for the synthesis of ester **5.27** as white solid (28 mg, 73%): $[\alpha]_D^{25}$–167.2 (*c* 1, $CHCl_3$); ^{1}H NMR (500 MHz, $CDCl_3$) δ 8.33-8.34 (m, 2H), 7.90-7.91 (d, 1H, *J* = 7.9 Hz), 7.54-7.57 (m, 1H), 7.33-7.43 (m, 10H), 7.29-7.30 (m, 1H), 7.27-7.14 (m, 10H), 7.01-7.03 (d, 1H, *J* = 8.7 Hz), 5.16-5.18 (d, 1H, *J* = 12.3 Hz), 5.10-5.13 (d, 1H, *J* = 12.3 Hz), 4.85-4.91 (m, 1H), 4.63-4.65 (m, 1H), 4.52-4.56 (m, 1H), 4.41-4.45 (m, 1H), 3.77 (s, 2H), 3.14-3.17 (dd, 1H, *J* = 4.2, 14.4 Hz), 2.84-2.93 (m, 4H), 2.67-2.72 (m, 2H), 2.57-2.58 (m, 2H), 2.30-2.40 (m, 2H), 1.83-1.91 (m, 1H); ^{13}C NMR (125 MHz, $CDCl_3$) δ 171.8, 171.5, 170.0, 169.4, 168.5, 150.1, 147.9, 147.7, 137.3, 137.0, 135.7, 135.6, 135.1, 132.6, 129.3, 129.2, 128.9, 128.8, 128.7, 128.6, 128.5, 128.4, 127.1, 126.8, 123.8, 121.5, 120.8, 119.4, 109.3, 66.6, 59.8, 54.9, 48.9, 47.3, 43.7, 39.9, 37.2, 33.9, 33.2, 28.1, 24.3; HRMS calcd for $C_{49}H_{47}N_5O_7F_3$ $[M+H]^+$, 874.3421; found 874.3428.

(3*S*,7*R*,9*S*)-Benzyl-7-hydroxy-2-oxo-3-phenylacetamido-1,2,3,4,7,8,9-heptahydro indolizine-3-carboxylate (5.43) and (3*S*,5*S*,9*S*)-benzyl 5-hydroxy-2-oxo-3-phenylacetamido-1,2,3,4,5,8,9-heptahydroindolizine-3-carboxylate (5.44)

A solution of olefin **5.18** (150 mg, 0.37 mmol) in dioxane (100 mL) was treated with SeO_2 (61 mg, 0.55 mmol) and a 70 wt% solution of *tert*-butyl hydroperoxide in water (0.15 mL) at room temperature, stirred for 2 h, and evaporated to a residue that was partitioned between H_2O (100 mL) and EtOAc (25 mL). The aqueous phase was separated and extracted with EtOAc (25 mL). The organic layers were combined, washed with brine, dried over Na_2SO_4, filtered, and concentrated under reduced pressure. The residue was purified by column chromatography using 60-80 % EtOAc in hexanes. First to elute was alcohol **5.43** (35 mg, 22%) as colorless gum: R_f = 0.4 (9:1 EtOAc, visualized under UV light); $[\alpha]_D^{25}$–191.2 (*c* 0.5, MeOH); FT-IR (neat) *ν*max 3306, 3031, 2928, 1742, 1643, 1530, 1495, 1454, 1275, 1730, 695 cm^{-1}; ^1H NMR (700 MHz, C_6D_6) δ 7.14-7.15 (m, 4H), 7.07-7.12 (m, 4H), 7.00-7.04 (m, 2H), 6.20-6.21 (d, 1H, *J* = 6.3), 5.01-5.02 (d, 1H, *J* = 12.4), 4.95-4.97 (d, 1H, *J* = 12.4), 4.87-4.88 (m, 1H), 4.68-4.71 (t, 1H, *J* = 7.5), 4.53-4.59 (m, 1H), 4.33-4.34 (m, 1H), 3.52 (br, 1H), 3.18-3.23 (q, 2H, *J* = 15.0, 10.5), 2.62-2.66 (m, 1H), 1.97-2.00 (m, 1H), 1.91-1.95 (m, 1H), 1.84-1.87 (m, 1H); ^{13}C NMR (175 MHz, C_6D_6) δ 170.4, 169.9, 165.9, 142.6, 134.9, 134.2, 128.5, 127.7, 127.5, 127.2, 127.1, 126.1, 97.5, 69.1, 65.9, 56.2, 48.9, 42.3, 36.0, 25.8; HRMS calcd for $C_{24}H_{24}N_2O_5Na$ $[M+Na]^+$, 443.1577; found 443.1584. Second to elute was alcohol **5.44** (45 mg, 28%) as colorless gum: R_f = 0.3 (EtOAc, visualized under UV light); $[\alpha]_D^{25}$ –6.1 (*c* 0.5, $CHCl_3$); FT-IR (neat) *ν*max 2947, 1719, 1647, 1612, 1588, 1506, 1207, 1156, 1032, 759, 738 cm^{-1}; ^1H NMR (700 MHz, CD_3COCD_3) δ 7.34-7.42 (m, 8H), 7.30-7.32 (m, 3H), 7.22-7.24 (m, 1H), 65.16-5.22 (m, 2H), 5.10-5.11 (t, 1H, *J* = 2.5), 4.97-5.0 (m, 1H), 4.79-4.81 (dd, 1H, *J* = 4.1, 11.7), 4.72-4.73 (m, 1H), 3.61 (s, 2H), 3.02-3.07 (m, 1H), 2.54-

2.57 (m, 1H), 2.31-2.34 (m, 1H), 1.78-1.82 (m, 1H); ^{13}C NMR (175 MHz, CD_3COCD_3) δ 170.2, 170.1, 165.8, 143.1, 136.4, 136.2, 129.2, 128.5, 128.2, 128.1, 127.9, 126.4, 105.3, 97.1, 66.3, 57.6, 45.6, 42.7, 34.7, 32.8; HRMS calcd for $C_{24}H_{24}N_2O_5Na$ $[M+Na]^+$, 443.1577; found 443.1580.

(3*S*,6*R*,7*R*,9*S*)- and (3*S*,6*S*,7*R*,9*S*)-Benzyl 7-hydroxy-2-oxo-3-phenylacetamido-octahydroindolizine-9-carboxylate [(*R*)- and (*S*)-5.45]

Hydroxy indolizidinones (*R*)- and (*S*)-**5.45** were synthesized from olefin **5.43** (80 mg, 0.19 mmol) using the same protocol described for the synthesis of (*R*)- and (*S*)-**5.21** using sodium cyanoborohydride (48 mg, 0.76 mmol) and AcOH (100 μL) in EtOH (10 mL). The residue was purified by column chromatography using 60-80 % EtOAc in hexanes. First to elute was bicycle (*S*)-**5.45** (21 mg, 26%) as a colorless gum: R_f = 0.28 (EtOAc, visualized under UV light)); $[\alpha]_D^{25}$ –74 (*c* 0.25, $CHCl_3$); FT-IR (neat) *ν*max 3373, 3066, 2939, 2862, 1766, 1656, 1623, 1518, 1463, 1421, 1330, 1276, 987, 921, 762, 696, 477 cm^{-1}; ^{1}H NMR (700 MHz, $CDCl_3$) δ 7.37-7.32 (m, 8H), 7.29-7.30 (m, 2H), 6.59-6.60 (d, 1H, *J* = 5.7 Hz), 5.19-5.21 (d, 1H, *J* = 12.2 Hz), 5.09-5.10 (d, 1H, *J* = 12.3 Hz), 4.53-4.54 (d, 1H, *J* = 8.9 Hz), 4.29-4.32 (m, 1H), 4.08-4.12 (m, 1H), 3.59 (s, 2H), 3.48-3.51 (m, 1H), 2.84 (brs, 1H), 2.48-2.53 (m, 1H), 2.25-2.28 (m, 1H), 2.20-2.24-2.0 (m, 1H), 2.13-2.18 (m, 1H), 1.67-1.74 (m, 1H), 143-1.54 (m, 1H); ^{13}C NMR (175 MHz, $CDCl_3$) δ 171.2, 171.1, 169.0, 135.2, 134.5, 129.3, 128.9, 128.6, 128.5, 128.2, 127.3, 75.8, 67.3, 61.5, 56.7, 49.4, 43.6, 36.5, 25.9, 24.7; HRMS calcd for $C_{24}H_{26}N_2O_5Na$ $[M+Na]^+$, 445.1731; found 445.1734.

Second to elute was bicycle (*R*)-**5.45** (35 mg, 44%) as colorless gum: R*f* = 0.16 (EtOAc, visualized under UV light); $[\alpha]_D^{25}$ –6.1 (*c* 0.5, $CHCl_3$); FT-IR (neat) *ν*max 2947, 1719, 1647, 1612, 1588, 1506, 1207, 1156, 1032, 759, 738 cm^{-1}; ^{1}H NMR (700 MHz, $CDCl_3$) δ 7.32-7.37 (m, 7H), 7.28-7.30 (m, 2H), 7.26-7.27 (m, 1H), 6.20-6.21 (d, 1H, *J* = 6.3 Hz), 5.21-5.22 (d, 1H, *J* = 12.3 Hz), 5.11-5.13 (d, 1H, *J* = 12.3 Hz), 4.63-4.66 (t, 1H, *J* = 8.9 Hz), 4.36-4.40 (m, 1H), 4.17-4.18 (m,

1H), 3.69-3.73 (dt, 1H, *J* = 3.6 Hz), 3.59 (s, 2H), 3.09 (br s, 1H), 2.48-2.52 (m, 1H), 2.30-2.33 (dd, 1H, *J* = 8.9, 14.1 Hz), 1.92-2.0 (m, 2H), 1.87-1.91 (m, 1H), 1.63-1.69 (m, 1H); ^{13}C NMR (175 MHz, $CDCl_3$) δ 172.3, 171.9, 168.6, 135.7, 134.8, 129.5, 128.9, 128.7, 128.4, 128.2, 127.3, 71.4, 67.0, 64.4, 56.6, 51.1, 43.7, 37.6, 27.6, 21.3. HRMS calcd for $C_{24}H_{26}N_2O_5Na$ $[M+Na]^+$, 445.1734; found 445.1733.

(3*S*,6*R*,7*R*,9*S*)-2-Oxo-5-hydroxy-3-phenylacetamido-1-azabicyclo[4.3.0]-nonane-9-carboxylic acid [(*R*)-5.46]

Acid (*R*)-**5.46** was synthesized from ester (*R*)-**5.45** (32 mg, 0.075 mmol) using the protocol for the preparation of acid (*S*)-**5.23** as white solid (22 mg, 87%): $[\alpha]_D^{25}$ –114.8 (*c* 0.8, $CHCl_3$); ^{1}H NMR (500 MHz, CD_3OD) δ 7.30-7.34 (m, 4H), 7.23-7.26 (m, 1H), 4.51-4.55 (t, 1H, *J* = 8.9 Hz), 4.46-4.49 (dd, 1H, *J* = 6.2, 11.4 Hz), 4.21-4.23 (t, 1H, *J* = 3.5 Hz), 3.76-3.79 (m, 1H), 3.57 (s, 2H), 2.33-2.38 (dd, 1H, *J* = 8.6, 13.8 Hz), 2.18-2.22 (m, 1H), 2.03-2.08 (m, 1H), 1.80-1.91 (m, 3H); ^{13}C NMR (125 MHz, CD_3OD) δ 174.3, 172.6, 169.1, 135.3, 128.9, 128.2, 126.5, 70.9, 64.4, 56.9, 49.7, 42.4, 36.9, 27.4, 21.2; HRMS calcd for $C_{17}H_{20}N_2O_5Na$ $[M+Na]^+$, 355.1264; found 355.1271

(3*S*,6*S*,7*R*,9*S*)-2-Oxo-5-hydroxy-3-phenylacetamido-1-azabicyclo[4.3.0]-nonane-9-carboxylic acid [(*S*)-5.46]

Acid (*S*)-**5.46** was synthesized from ester (*S*)-**5.45** (19 mg, 0.05 mmol) using the protocol for the preparation of acid (*S*)-**5.23** as white solid (14 mg, 93%): $[\alpha]_D^{25}$ –3.75 (*c* 0.5, MeOH); ^{1}H NMR (500 MHz, CD_3OD) δ 7.30-7.34 (m, 4H), 7.23-7.26 (m, 1H), 4.50-4.53 (t, 1H, *J* = 7.1 Hz), 4.43-4.45 (d, 1H, *J* = 9.6 Hz), 4.01-4.06 (m, 1H), 3.59 (s, 2H), 3.41-3.45 (m, 1H), 2.14-2.30 (m, 4H), 1.70-1.82 (m, 2H); ^{13}C NMR (125 MHz, CD_3OD) δ 173.5, 172.3, 169.2, 135.4, 128.8, 128.2, 126.5, 74.4, 62.4, 56.6, 48.3, 42.2, 35.8, 26.4, 24.0.; HRMS calcd for $C_{17}H_{20}N_2O_5Na$ $[M+Na]^+$, 355.1264; found 355.1273.

Phenylacetyl-(3*S*,6*R*,7*R*,9S)-7-hydroxy-I^{2}aa-(2*S*)-(3-pyridyl)alaninyl-(3*S*)-β-homophenylalanine benzyl ester [(*R*)-5.47]

Peptide (*R*)-**5.47** was synthesized from acid (*R*)-**5.46** (22 mg, 0.068 mmol) using the protocol for the synthesis of ester **5.27** as white solid (30 mg, 63%): m.p. 122–125 ^{o}C; $[\alpha]_D^{25}$ –134.4 (*c* 0.3, MeOH); FT-IR (neat) *ν*max 3280, 2922, 2864, 1731, 1632, 1496, 1442, 1198, 1151, 1032, 746, 697, 633 cm^{-1}; ^{1}H NMR (700 MHz, $CDCl_3$) δ 8.40-8.46 (m, 2H), 7.83-7.84, (d, 1H, *J* = 8.2 Hz), 7.67 (s, 1H), 7.33-7.42 (m, 5H), 7.29-7.32 (m, 6H), 7.20-7.25 (m, 7H), 5.08-5.10 (d, 1H, *J* = 12.3 Hz), 5.04-5.06 (d, 1H, *J* = 12.2 Hz), 4.60-4.62 (t, 1H, *J* = 8.9 Hz), 4.50-4.56 (m, 1H), 4.46-4.48 (m, 1H), 4.12 (s, 1H), 3.99-4.02 (m, 1H), 3.58 (s, 2H), 3.47-3.48 (d, 1H, *J* = 7.6 Hz), 3.27 (br s, 1H), 3.00-3.03 (dd, 1H, *J* = 6.2, 13.7 Hz), 2.84-2.91 (m, 3H), 2.57-2.58 (m, 2H), 2.10-2.19 (m, 2H), 1.83-1.92 (m, 4H); ^{13}C NMR (175 MHz, $CDCl_3$) δ 172.0, 171.3, 171.1, 170.2, 170.0, 137.7, 135.8, 134.5, 129.5, 129.4, 129.3, 129.2, 128.9, 128.8, 128.6, 128.5, 128.4, 128.3, 128.2, 128.1, 127.3, 126.7, 71.3, 66.5, 64.1, 58.2, 55.2, 51.2, 47.9, 43.2, 40.4, 37.5, 36.5, 33.7, 27.1, 21.3; HRMS calcd for $C_{42}H_{45}N_5O_7Na$ $[M+Na]^+$, 754.3211; found 754.3215.

Phenylacetyl-(3S,6S,7*R*,9S)-7-hydroxy-I^{2}aa-(2*S*)-(3-pyridyl)alaninyl-(3*S*)-β-homophenylalanine Benzyl Ester [(*S*)-5.47]

Peptide (*S*)-**5.47** was synthesized from acid (*S*)-**5.46** (14 mg, 0.043 mmol) using the protocol for the synthesis of ester **5.27** as white foam (18 mg, 56%): $[\alpha]_D^{25}$ –80.0 (*c* 0.4, $CHCl_3$); FT-IR (neat) *ν*max 3679, 2919, 2805, 1733, 1646, 1541, 1461, 1376, 1054, 1032, 1015, 719 cm^{-1}; ^{1}H NMR (700 MHz, $CDCl_3$) δ 8.35-8.38 (m, 2H), 7.68-7.69 (d, 1H, *J* = 8.08 Hz), 7.59-7.60 (d, 1H, *J* = 7.6 Hz), 7.38-7.28 (m, 10H), 7.18-7.27 (m, 6H), 7.13-7.15 (m, 1H), 6.98-6.99 (d, 1H, *J* = 7.3 Hz), 5.11-5.13 (d, 1H, *J* = 12.2 Hz), 5.06-5.08 (d, 1H, *J* = 12.2 Hz), 4.50-4.53 (m, 1H), 4.44-4.47 (m, 1H), 4.37-4.39 (d, 1H, *J* = 9.2 Hz), 4.17-4.20 (dd, 1H, *J* = 7.5, 14.9 Hz), 3.75-3.79 (m, 1H) 3.63

(s, 2H), 3.27-3.30 (m, 1H), 3.20-3.22 (dd, 1H, *J* = 3.9, 14.3), 2.94-2.97 (dd, 1H, *J* = 6.5, 13.6 Hz), 2.83-2.89 (m, 2H), 2.56-2.57 (d, 2H, *J* = 5.8 Hz), 2.34-2.36 (dd, 1H, *J* = 6.2, 12.4 Hz), 2.19-2.34 (m, 1H), 2.13-2.15 (m, 1H), 1.86-1.91 (m, 1H), 1.46-1.58 (m, 2H); ^{13}C NMR (175 MHz, $CDCl_3$) δ 170.7, 170.2, 169.5, 168.8, 168.7, 149.3, 146.3, 136.5, 136.2, 134.7, 133.5, 132.7, 128.4, 128.3, 127.9, 127.6, 127.5, 127.3, 127.3, 126.3, 125.7, 122.8, 73.5, 65.4, 61.6, 56.6, 54.0, 48.1, 46.6, 42.4, 39.1, 36.3, 34.2, 32.6, 26.8, 23.6; HRMS calcd for $C_{42}H_{45}N_5O_7Na$ $[M+Na]^+$, 754.3238; found 754.3211.

5.7 Author Contributions

§ These authors contributed equally to this paper and are listed alphabetically.

5.8 Acknowledgment

We thank the Canadian Institutes of Health Research (CIHR) and the Natural Sciences and Engineering Research Council of Canada (NSERC) for funding for a Discovery Research Project, and for the Collaborative Health Research Project "Treatment of Preterm Birth with ProstaglandinF2alpha Receptor Modulators" No. 337381. We acknowledge the assistance of members of the Université de Montreal facilities: Dr. A. Fürtös, K. Gilbert, M.-C. Tang and L. Mahrouche (mass spectroscopy), C. Malveau, Dr. P. Aguiar and S. Bilodeau (NMR spectroscopy) and Mr. T. Maris (X-ray). F. M. Mir, individually would like to thank A. Geranurimi for her kind supports. Shastri Indo-Canadian Institute, India is thanked for a Quebec Tuition Fee Exemption grant to N.D.P.A.

5.9 Abbreviations

Boc, *tert*-butyloxycarbonyl; Fmoc, Fluorenylmethyloxycarbonyl; DMF, dimethylformamide; FA, formic acid; IC50, inhibitor concentration; TFA, trifluoroacetic acid; FP, prostaglandin F2α receptor; PGF2α , prostaglandin F2α; LPS, Lipopolysaccharides; SI, Supporting Information;

TLC, thin layer chromatography; Smac, second mitochondria-derived activator of caspase; I^2aa, indolizidin-2-one amino acid.

5.10 References

1. (a) Boeglin, D.; Hamdan, F. F.; Melendez, R. E.; Cluzeau, J.; Laperriere, A.; Héroux, M.; Bouvier, M.; Lubell, W. D., Calcitonin gene-related peptide analogs with aza and indolizidinone amino acid residues reveal conformational requirements for antagonist activity at the human calcitonin gene-related peptide 1 receptor. *J. Med. Chem.* **2007**, *50*, 1401–1408; (b) Bourguet, C. B.; Boulay, P.-L.; Claing, A.; Lubell, W. D., Design and synthesis of novel azapeptide activators of apoptosis mediated by caspase-9 in cancer cells. *Bioorg. Med. Chem. Lett.* **2014**, *24*, 3361–3365; (c) Chingle, R.; Ratni, S.; Claing, A.; Lubell, W. D., Application of constrained aza-valine analogs for Smac mimicry. *J. Pept. Sci.* **2016**, *106*, 235–244; (d) Bourguet, C. B.; Goupil, E.; Tassy, D.; Hou, X.; Thouin, E.; Polyak, F.; Hébert, T. E.; Claing, A.; Laporte, S. A.; Chemtob, S.; Lubell, W. D., Targeting the prostaglandin F2α receptor for preventing preterm labor with azapeptide tocolytics. *J. Med. Chem.* **2011**, *54*, 6085–6097.

2. (a) Proulx, C.; Sabatino, D.; Hopewell, R.; Spiegel, J.; Garcıa-Ramos, Y.; Lubell, W., Future Med. Chem., **2011**, *3*, 1139–1164; (b) Vagner, J.; Qu, H.; Hruby, V.J. *Curr. Opin. Chem. Biol* **2008,** *12*, 292-296; (b) Khashper, A.; Lubell, W. D., Design, synthesis, conformational analysis and application of indolizidin-2-one dipeptide mimics. *Org. Biomol. Chem.* **2014**, *12*, 5052–5070.

3. Goupil, E.; Tassy, D.; Bourguet, C.; Quiniou, C.; Wisehart, V.; Pétrin, D.; LeGouill, C.; Devost, D.; Zingg, H. H.; Bouvier, M.; Saragovi H. U.; Chemtob, S.; Lubell, W. D.; Claing, A.; Hébert, T. E.; Laporte S. A., A novel biased allosteric compound inhibitor of parturition, selectively impedes the PGF2α-mediated rho/rock signalling pathway. *J. Biol. Chem.* **2010**, *285*, 25624–25636.

4. (a) Sebayang, S. K.; Dibley, M. J.; Kelly, P. J.; Shankar, A. V.; Shankar, A. H.; Group, S. S., Determinants of low birthweight, small-for-gestational-age and preterm birth in Lombok, Indonesia: analyses of the birthweight cohort of the SUMMIT trial. *Tropical Medicine & International Health* **2012,** *17*, 938-950; (b) Petrini, J. R.; Callaghan, W. M.; Klebanoff, M.; Green, N. S.; Lackritz, E. M.; Howse, J. L.; Schwarz, R. H.; Damus, K., Estimated effect of 17 alpha-hydroxyprogesterone caproate on preterm birth in the United States. *Obstet. Gynecol.* **2005**, *105*, 267–272.

5. Berkowitz, G. S.; Papiernik, E., Epidemiology of preterm birth. *Epidemiol. Rev.* **1993**, *15*, 414–443.

6. Purisch, S. E.; Gyamfi-Bannerman, C. In Epidemiology of preterm birth, *Seminars in perinatology* **2017**, *41*, 387–391.

7. Behrman, R. E.; Butler, A. S., Preterm birth: causes, consequences, and prevention. Obstet. Gynaecol. **2008**, *10*, 280.

8. (a) Haas, D. M.; Caldwell, D. M.; Kirkpatrick, P.; McIntosh, J. J.; Welton, N. J., Tocolytic therapy for preterm delivery: systematic review and network meta-analysis. *BMJ* **2012**, *345*: e6226; (b) Olson, D. M.; Christiaens, I.; Gracie, S.; Yamamoto, Y.; Mitchell, B. F., Emerging tocolytics: challenges in designing and testing drugs to delay preterm delivery and prolong pregnancy. *Expert Opin. Emerg. Drugs* **2008**, *13*, 695-707; (c) Hernandez, W. R.; Francisco, R. P.; Bittar, R. E.; Gomez, U. T.; Zugaib, M.; Brizot, M. L., Effect of vaginal progesterone in tocolytic therapy during preterm labor in twin pregnancies: Secondary analysis of a placebo-controlled randomized trial. *Obstet. Gynecol. Research* **2017**, *43*, 1536–1542.

9. (a) Surprenant, S.; Lubell, W. D., From macrocycle dipeptide lactams to azabicyclo [X.Y.0] alkanone amino acids: a transannular cyclization route for peptide mimic synthesis. *Org. Lett.*

2006, *8*, 2851–2854; (b) Atmuri, N. D. P.; Lubell, W. D., Insight into transannular cyclization reactions to synthesize azabicyclo[X.Y.Z]alkanone amino acid aerivatives from 8-, 9-, and 10-membered macrocyclic dipeptide lactams. *J. Org. Chem.* **2015**, *80*, 4904–4918.

10. Godina, T. A.; Lubell, W. D., Mimics of peptide turn backbone and side-chain geometry by a general approach for modifying azabicyclo[5.3.0]alkanone amino acids. *J. Org. Chem.* **2011**, *76*, 5846–5849.

11. (a) Bourguet, C. B.; Proulx, C.; Klocek, S.; Sabatino, D.; Lubell, W. D., Solution-phase submonomer diversification of aza-dipeptide building blocks and their application in aza-peptide and aza-DKP synthesis. *J. Peptide Sci.* **2010**, *16*, 284–296; (b) Garcia-Ramos, Y.; Proulx, C.; Lubell, W. D., Synthesis of hydrazine and azapeptide derivatives by alkylation of carbazates and semicarbazones. *Can. J. Chem.* **2012**, *90*, 985–993.

12. Pandey, A. K.; Naduthambi, D.; Thomas, K. M.; Zondlo, N. J., Proline editing: a general and practical approach to the synthesis of functionally and structurally diverse peptides. Analysis of steric versus stereoelectronic effects of 4-substituted prolines on conformation within peptides. *J. Am. Chem. Soc*. **2013**, *135*, 4333–4363.

13. Kaul, R.; Surprenant, S.; Lubell, W. D., Systematic study of the synthesis of macrocyclic dipeptide β-turn mimics possessing 8-, 9-, and 10-membered rings by ring-closing metathesis. *J. Org. Chem.* **2005**, *70*, 3838–3844.

14. Shao, C.; Wang, X.; Zhang, Q.; Luo, S.; Zhao, J.; Hu, Y., Acid–base jointly promoted copper (I)-catalyzed azide–alkyne cycloaddition. *J. Org. Chem.* **2011**, *76*, 6832–6836.

15. Le Quement, S. T.; Nielsen, T. E.; Meldal, M., Divergent pathway for the solid-phase conversion of aromatic acetylenes to carboxylic acids, α-ketocarboxylic acids, and methyl ketones. *J. Comb. Chem.* **2008**, *10*, 546–556.

16. Zhang, J.; Proulx, C.; Tomberg, A.; Lubell, W. D., Multicomponent diversity-oriented synthesis of aza-lysine-peptide mimics. *Org. Lett.* **2013**, *16*, 298–301.

17. Kang, Y. K.; Choi, H. Y., Cis–trans isomerization and puckering of proline residue. *Biophys. Chem.* **2004**, *111*, 135-142.

18. Boeglin, D.; Lubell, W. D., Aza-amino acid scanning of secondary structure suited for solid-phase peptide synthesis with Fmoc chemistry and aza-amino acids with heteroatomic side-chains. *J. Comb. Chem.* **2005**, *7*, 864–878.

19. Gibson, C.; Goodman, S. L.; Hahn, D.; Hölzemann, G.; Kessler, H., Novel solid-phase synthesis of azapeptides and azapeptoides via Fmoc-strategy and its application in the synthesis of RGD-mimetics. *J. Org. Chem.* **1999**, *64*, 7388–7394.

20. Ahsanullah; Chingle, R.; Ohm, R. G.; Chauhan, P. S.; Lubell, W. D., Aza-propargylglycine installation by aza-amino acylation: Synthesis and Ala-scan of an azacyclopeptide CD36 modulator. *J. Pept. Sci*. **2019**; 111: e24102.

21. Thomas, K. M.; Naduthambi, D.; Zondlo, N. J., Electronic control of amide cis− trans isomerism via the aromatic− prolyl interaction. *J. Am. Chem. Soc.* **2006**, *128*, 221–2217.

22. Mauger, A.; Irreverre, F.; Witkop, B., The stereochemistry of 3-methylproline. *J. Am. Chem. Soc.* **1966**, *88*, 2019–2024.

23. Lombart, H.-G.; Lubell, W. D., Rigid dipeptide mimetics: efficient synthesis of enantiopure indolizidinone amino acids. *J. Org. Chem.* **1996**, *61*, 9437–9446.

24. André, F.; Boussard, G.; Bayeul, D.; Didierjean, C.; Aubry, A.; Marraud, M., Aza-peptides II. X-Ray structures of aza-alanine and aza-asparagine-containing peptides. *J. Peptide Res.* **1997**, *49*, 556–562.

25. Nair, C.; Vijayan, M., Structural characteristics of prolyl residues—a review. *J. Indian I. Sci.* **2013**, *63*, 81.

26. Venkatachalam, C., Stereochemical criteria for polypeptides and proteins. V. Conformation of a system of three linked peptide units. *Biopolymers* **1968**, *6*, 1425–1436.

27. (a) Boukanoun, M. K.; Hou, X.; Nikolajev, L.; Ratni, S.; Olson, D.; Claing, A.; Laporte, S. A.; Chemtob, S.; Lubell, W. D., Investigation of the active turn geometry for the labor delaying activity of indolizidinone and azapeptide modulators of the prostaglandin F2α receptor. *Org. Biomol. Chem.* **2015**, *13*, 7750–7761; (b) Bourguet, C. B.; Claing, A.; Laporte, S. A.; Hébert, T. E.; Chemtob, S.; Lubell, W. D., Synthesis of azabicycloalkanone amino acid and azapeptide mimics and their application as modulators of the prostaglandin F2α receptor for delaying preterm birth. *Can. J. Chem.* **2014**, *92*, 1031–1040.

28. Greenlee, W.; Thorsett, E.; Springer, J.; Patchett, A.; Ulm, E.; Vassil, T., Azapeptides: a new class of angiotensin-converting enzyme inhibitors. *Biochem. Biophys. Res. Commun.* **1984**, *122*, 791–797.

29. Thormann, M.; Hofmann, H.-J., Conformational properties of azapeptides. *J. Mol. Struct.: THEOCHEM* **1999**, *469*, 63–76.

30. Newberry, R. W.; Raines, R. T., 4-Fluoroprolines: Conformational analysis and effects on the stability and folding of peptides and proteins. In *Peptidomimetics I*, Springer **2016**; pp 1–25.

31. Siebler, C.; Trapp, N.; Wennemers, H., Crystal structure of (4S)-aminoproline: conformational insight into a pH-responsive proline derivative. *J. Pept. Sci.* **2015**, *21*, 208–211.

32. Peri, K. G.; Quiniou, C.; Hou, X.; Abran, D.; Varma, D. R.; Lubell, W. D.; Chemtob, S. In *THG113: a novel selective FP antagonist that delays preterm labor*, Seminars in perinatology2002 Elsevier; pp 389–397.

33. Conroy, T.; Jolliffe, K. A.; Payne, R. J., Efficient use of the Dmab protecting group: applications for the solid-phase synthesis of N-linked glycopeptides. *Org. Biomol. Chem.* **2009**, *7*, 2255–2258.

34. (a) Tietze, L. F.; Brasche, G.; Grube, A.; Böhnke, N.; Stadler, C., Synthesis of Novel Spinosyn A Analogues by Pd-Mediated Transformations. *Chem. Eur. J.* **2007**, *13*, 8543–8563; (b) Williams, M. A.; Rapoport, H., Synthesis of conformationally constrained DTPA analogs. Incorporation of the ethylenediamine units as aminopyrrolidines. *J. Org. Chem.* **1994**, *59*, 3616–3625.

5.11 Biological Data

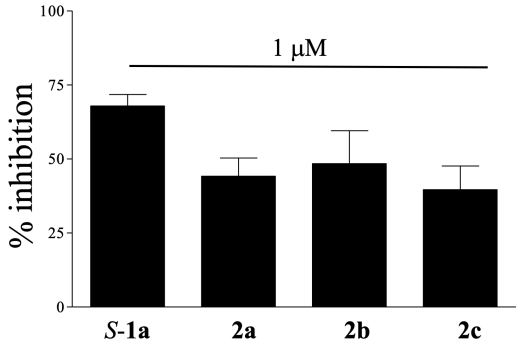

Figure S1. Effects of indolizidinone and azapeptide modulators on mean tension induced by PGF2α. At the beginning of each experiment, mean tension of spontaneous myometrial contractions was considered as the basal response.

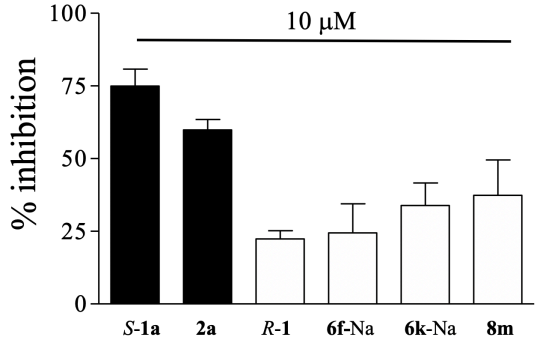

Figure S2. Effects of indolizidinone and azapeptide modulators on mean tension induced by PGF2α. At the beginning of each experiment, mean tension of spontaneous myometrial contractions was considered as the basal response.

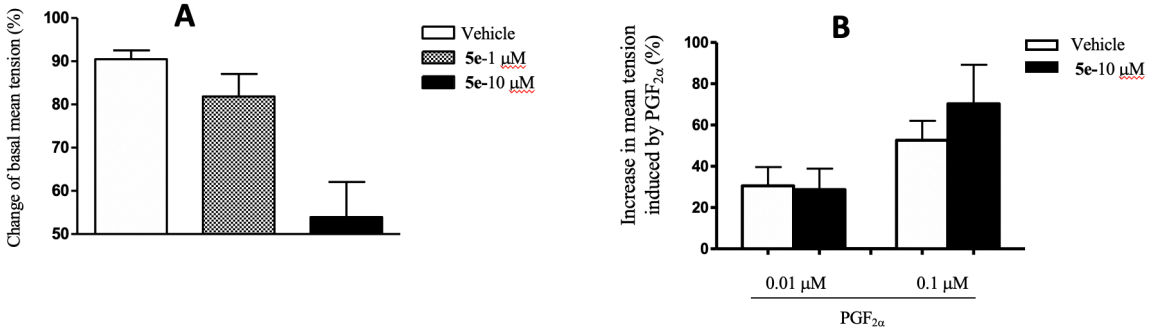

Figure S3. 5e at 10 μM caused a significant decrease in mean tension of spontaneous myometrial contraction (A), but PGF2α-induced increased mean tension of contractions was not inhibited by **5e** (B)

Table S1. Effects of indolizidinone and azapeptide modulator candidates (1 μM and 10μM) on mean tension induced by PGF2α. At the beginning of each experiment, mean tension of spontaneous myometrial contractions was considered as the basal response.

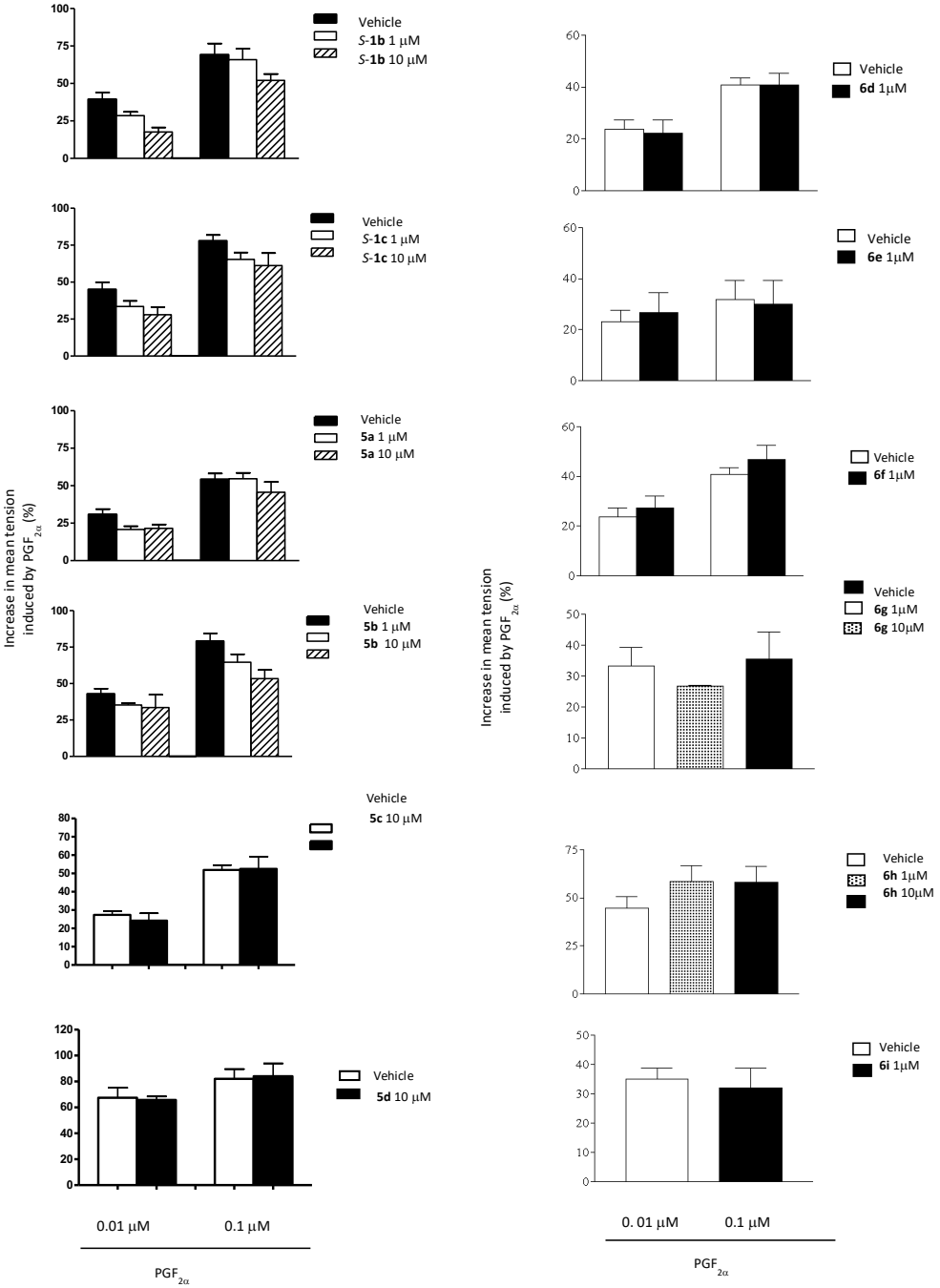

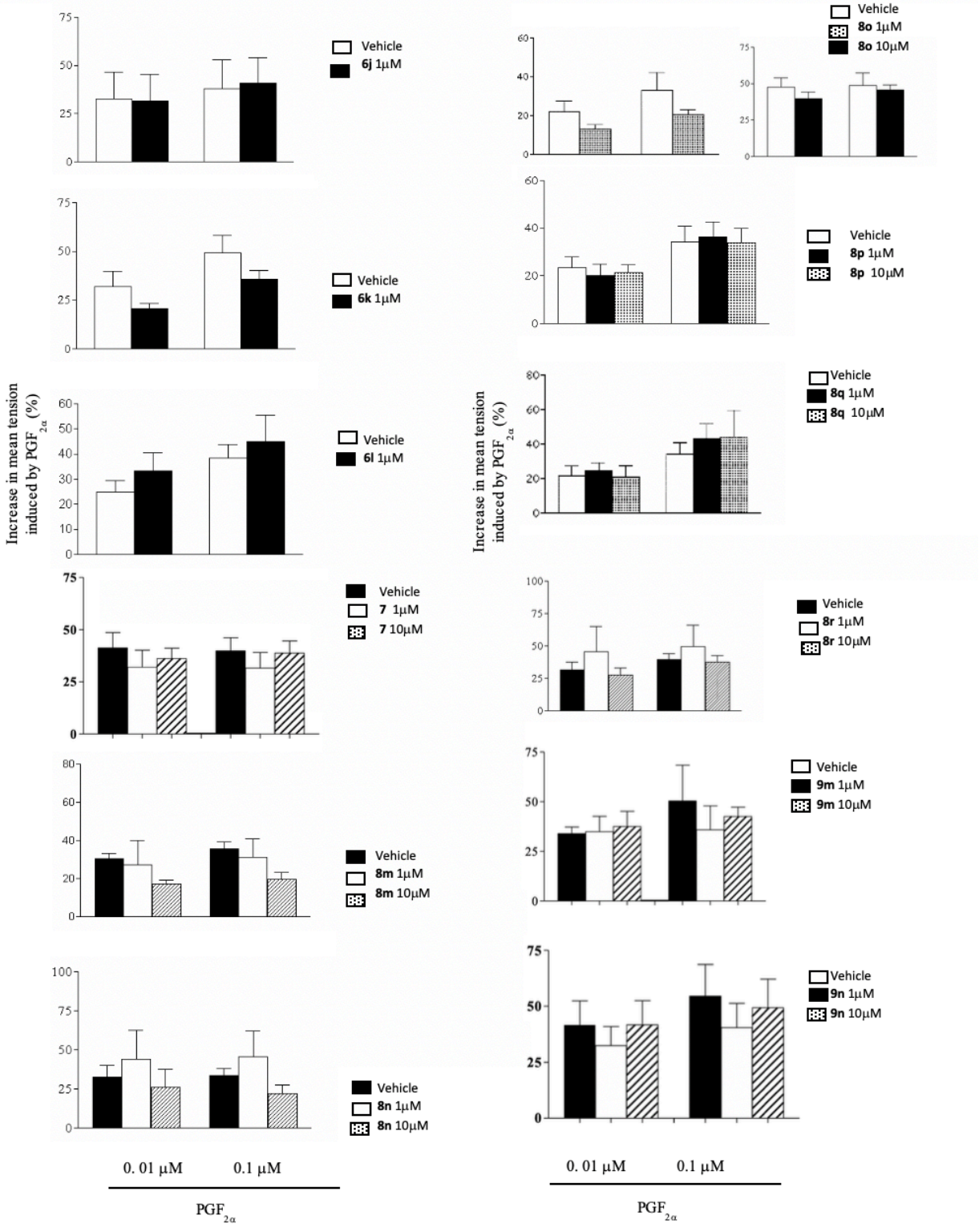
Increase in mean tension induced by PGF2α (%)
Vehicle
6j 1μM
Vehicle
6k 1μM
Vehicle
6l 1μM
Vehicle
7 1μM
7 10μM
Vehicle
8m 1μM
8m 10μM
Vehicle
8n 1μM
8n 10μM
0. 01 μM
0.1 μM
PGF2α
Vehicle
8o 1μM
8o 10μM
Vehicle
8p 1μM
8p 10μM
Vehicle
8q 1μM
8q 10μM
Vehicle
8r 1μM
8r 10μM
Vehicle
9m 1μM
9m 10μM
Vehicle
9n 1μM
9n 10μM
0. 01 μM
0.1 μM
PGF2α

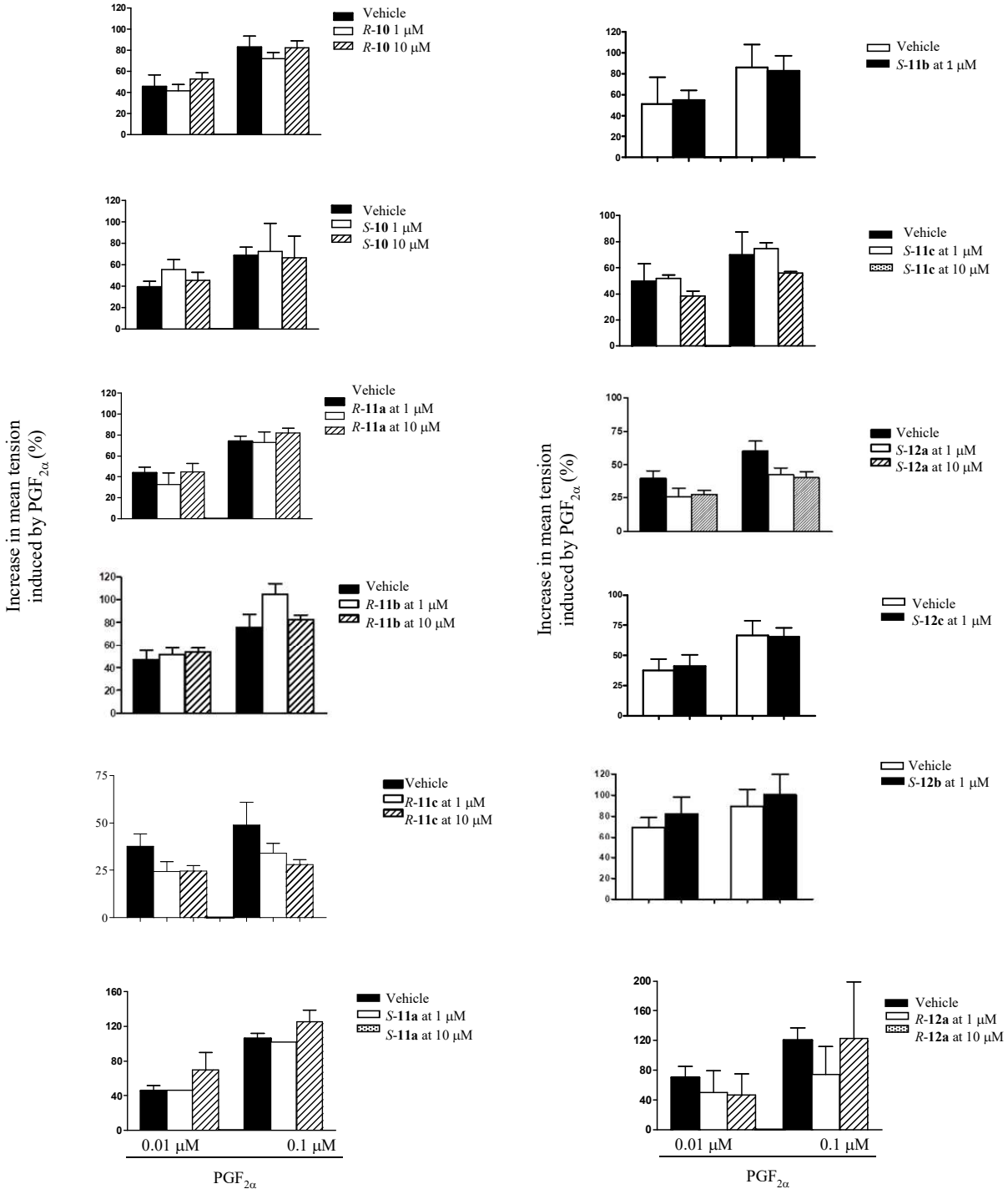
Increase in mean tension induced by PGF2α (%)
Vehicle
R-10 1 μM
R-10 10 μM
Vehicle
S-10 1 μM
S-10 10 μM
Vehicle
R-11a at 1 μM
R-11a at 10 μM
Vehicle
R-11b at 1 μM
R-11b at 10 μM
Vehicle
R-11c at 1 μM
R-11c at 10 μM
Vehicle
S-11a at 1 μM
S-11a at 10 μM
0.01 μM
0.1 μM
PGF2α
Vehicle
S-11b at 1 μM
Vehicle
S-11c at 1 μM
S-11c at 10 μM
Vehicle
S-12a at 1 μM
S-12a at 10 μM
Vehicle
S-12c at 1 μM
Vehicle
S-12b at 1 μM
Vehicle
R-12a at 1 μM
R-12a at 10 μM
0.01 μM
0.1 μM
PGF2α

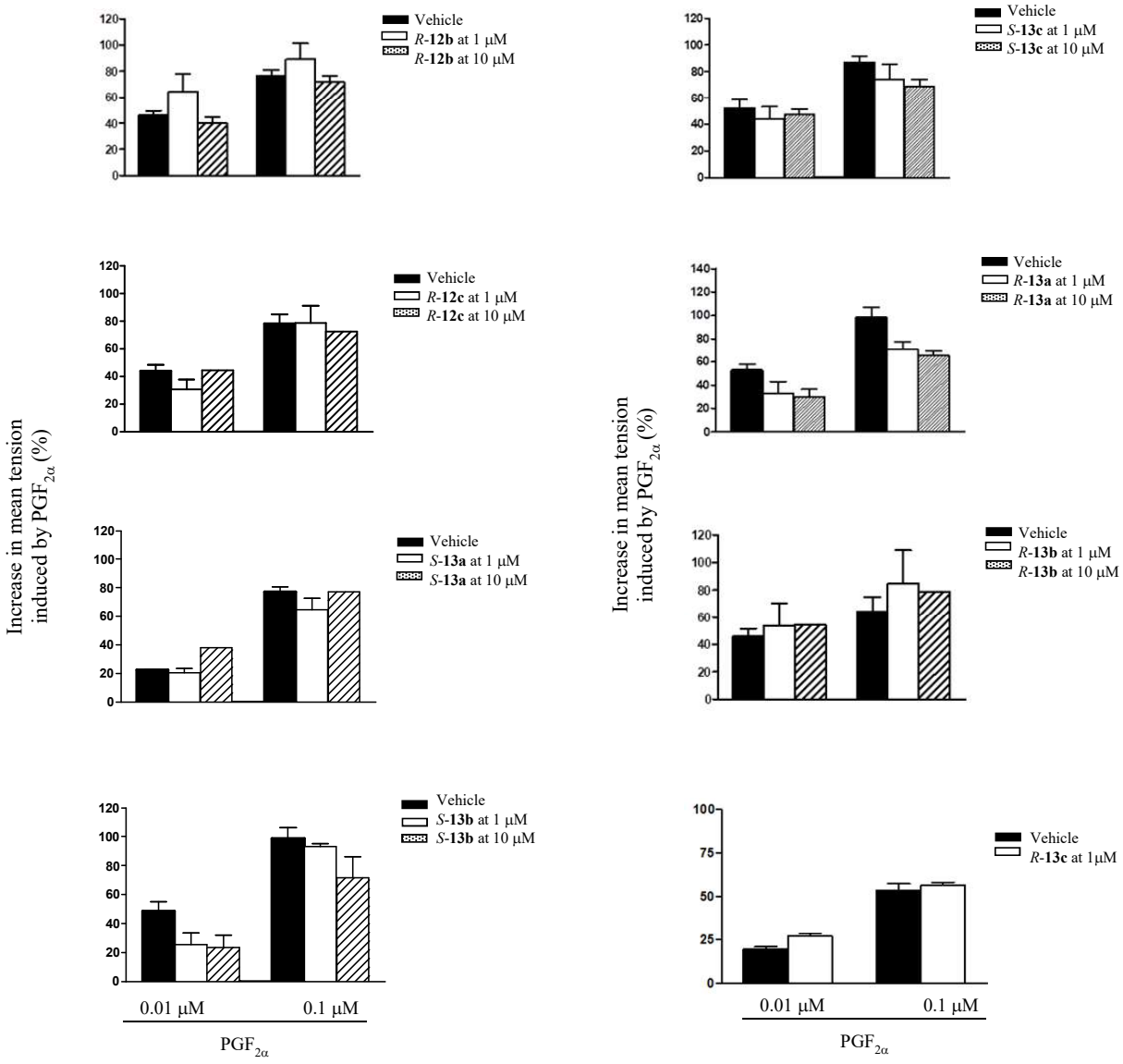
Increase in mean tension induced by $PGF_{2\alpha}$ (%)
Vehicle
R-**12b** at 1 μM
R-**12b** at 10 μM
Vehicle
S-**13c** at 1 μM
S-**13c** at 10 μM
Vehicle
R-**12c** at 1 μM
R-**12c** at 10 μM
Vehicle
R-**13a** at 1 μM
R-**13a** at 10 μM
Vehicle
S-**13a** at 1 μM
S-**13a** at 10 μM
Vehicle
R-**13b** at 1 μM
R-**13b** at 10 μM
Vehicle
S-**13b** at 1 μM
S-**13b** at 10 μM
Vehicle
R-**13c** at 1μM
0.01 μM
0.1 μM
$PGF_{2\alpha}$

5.12. X-ray data

(3*S*,6*S*,9*S*)-Benzyl 2-oxo-3-phenlacetamido-1-azabicyclo[4.3.0]nonane-9-carboxylates [(*S*)-**5.21, LUB1032]**

Table 1 Crystal data and structure refinement for LUB1032

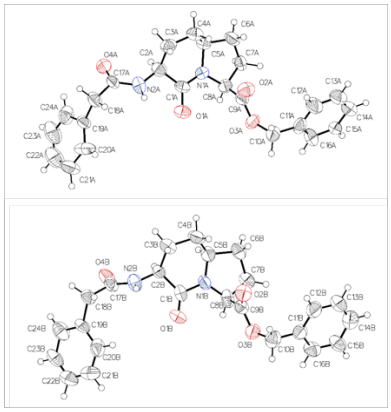

Identification code	
Empirical formula	$C_{24}H_{26}N_2O_4$
Formula weight	406.47
Temperature/K	150
Crystal system	monoclinic
Space group	$P2_1$
a/Å	11.4081(12)
b/Å	16.2769(16)
c/Å	12.6451(18)
α/°	90
β/°	116.589(4)
γ/°	90
Volume/Å^3	2099.7(4)
Z	4
ρ_{calc}g/cm^3	1.286
μ/mm^{-1}	0.456
F(000)	864.0
Crystal size/mm^3	0.37 × 0.13 × 0.1
Radiation	GaKα (λ = 1.34139)
2Θ range for data collection/°	4.724 to 108.218
Index ranges	$-13 \leq h \leq 13$, $-19 \leq k \leq 19$, $-15 \leq l \leq 15$
Reflections collected	27430
Independent reflections	7671 [R_{int} = 0.0661, R_{sigma} = 0.0574]
Data/restraints/parameters	7671/1/544

Goodness-of-fit on F^2	1.571
Final R indexes [I>=2σ (I)]	R_1 = 0.1453, wR_2 = 0.3377
Final R indexes [all data]	R_1 = 0.1570, wR_2 = 0.3547
Largest diff. peak/hole / e $Å^{-3}$	1.32/-0.43
Flack parameter	?

Table 2 Fractional Atomic Coordinates ($\times 10^4$) and Equivalent Isotropic Displacement Parameters ($Å^2 \times 10^3$) for LUB1032. U_{eq} is defined as 1/3 of of the trace of the orthogonalised U_{IJ} tensor.

Atom	*x*	*y*	*z*	U(eq)
O1A	-4398(9)	-3947(5)	-4968(7)	60.3(18)
O1B	-3423(8)	-6029(5)	-4982(6)	57.9(18)
O2B	-2833(9)	-6039(5)	-7614(8)	66(2)
O3B	-1008(8)	-6591(6)	-6177(7)	69(2)
O4B	-6824(10)	-6301(6)	-4431(7)	72(2)
N1B	-4258(9)	-6873(6)	-6585(8)	53(2)
N2B	-5872(11)	-5539(6)	-5319(9)	60(2)
C1B	-4364(12)	-6325(6)	-5797(10)	53(2)
C2B	-5797(10)	-6192(8)	-6083(9)	58(3)
C3B	-6623(13)	-5951(8)	-7382(10)	62(3)
C4B	-6347(13)	-6495(8)	-8242(11)	70(3)
C5B	-5389(12)	-7206(8)	-7589(11)	61(3)
C6B	-4802(14)	-7644(8)	-8316(12)	69(3)
C7B	-3387(12)	-7876(6)	-7353(10)	56(2)
C8B	-3042(13)	-7167(7)	-6470(10)	59(3)
C9B	-2315(11)	-6504(6)	-6831(9)	53(2)
C10B	-169(14)	-6160(8)	-6628(15)	72(3)
C11B	146(11)	-6775(9)	-7343(10)	63(3)
C12B	-462(14)	-6777(13)	-8559(13)	88(5)
C13B	-153(18)	-7382(16)	-9167(14)	103(6)
C14B	784(17)	-7962(13)	-8615(16)	91(4)
C15B	1471(15)	-7935(8)	-7397(11)	67(3)
C16B	1129(13)	-7369(9)	-6759(11)	67(3)
C17B	-6380(12)	-5648(8)	-4572(9)	58(2)
C18B	-6357(13)	-4877(8)	-3845(9)	64(3)
C19B	-5282(12)	-4968(7)	-2552(8)	57(3)
C20B	-3984(15)	-4754(9)	-2249(13)	72(3)
C21B	-3092(16)	-4810(15)	-1075(16)	99(6)
C22B	-3401(16)	-5003(8)	-225(12)	74(4)
C23B	-4605(17)	-5232(9)	-503(11)	73(3)
C24B	-5601(17)	-5208(8)	-1685(12)	75(3)
O2A	-7439(9)	-3894(6)	-7490(8)	67(2)

O3A	-7762(7)	-3283(6)	-6068(7)	63(2)
O4A	-266(9)	-3961(8)	-4690(10)	94(4)
N1A	-4958(8)	-3095(5)	-6547(8)	46.0(17)
N2A	-2258(10)	-4501(6)	-5172(9)	60(2)
C1A	-4185(11)	-3638(6)	-5784(9)	50(2)
C2A	-3005(12)	-3853(7)	-5972(10)	55(2)
C3A	-3411(12)	-4060(8)	-7270(10)	62(3)
C4A	-4531(13)	-3543(7)	-8147(10)	60(3)
C5A	-4812(11)	-2784(7)	-7582(9)	51(2)
C6A	-6098(13)	-2352(8)	-8294(11)	64(3)
C7A	-6549(10)	-2055(6)	-7386(10)	53(2)
C8A	-6083(10)	-2743(6)	-6448(9)	50(2)
C9A	-7146(10)	-3386(6)	-6754(9)	48(2)
C10A	-8967(11)	-3745(10)	-6381(14)	74(4)
C11A	-10109(11)	-3201(8)	-7110(15)	72(4)
C12A	-10756(16)	-3313(12)	-8353(12)	84(4)
C13A	-11783(17)	-2850(11)	-9064(13)	83(4)
C14A	-12208(15)	-2194(10)	-8533(12)	78(4)
C15A	-11582(10)	-2088(7)	-7336(9)	50(2)
C16A	-10571(12)	-2600(8)	-6628(11)	67(3)
C17A	-945(11)	-4511(8)	-4615(8)	59(3)
C18A	-323(13)	-5257(9)	-3848(9)	64(3)
C19A	157(11)	-5064(7)	-2558(8)	52(2)
C20A	-150(20)	-5504(15)	-1791(17)	105(6)
C21A	560(20)	-5275(12)	-531(14)	94(5)
C22A	1520(20)	-4736(13)	-205(16)	99(6)
C24A	1207(13)	-4514(9)	-2074(13)	75(3)
C23A	1840(20)	-4327(13)	-917(16)	100(6)

Table 3 Anisotropic Displacement Parameters ($Å^2×10^3$) for LUB1032. The Anisotropic displacement factor exponent takes the form: $-2\pi^2[h^2a^{*2}U_{11}+2hka^*b^*U_{12}+\ldots]$.

Atom	U_{11}	U_{22}	U_{33}	U_{23}	U_{13}	U_{12}
O1A	75(5)	66(4)	44(4)	-3(3)	31(4)	-1(4)
O1B	69(4)	55(4)	37(3)	-6(3)	13(3)	-7(3)
O2B	75(5)	62(4)	65(5)	16(4)	34(4)	8(4)
O3B	59(4)	95(6)	53(4)	16(4)	26(4)	18(4)
O4B	92(6)	83(5)	51(4)	-16(4)	39(4)	-32(5)
N1B	59(5)	60(5)	46(4)	-14(4)	29(4)	-8(4)
N2B	82(6)	53(4)	56(5)	3(4)	41(5)	0(4)
C1B	72(6)	47(4)	50(5)	-2(4)	38(5)	2(5)
C2B	50(5)	93(8)	33(4)	6(5)	19(4)	0(5)
C3B	73(7)	58(6)	49(6)	-3(5)	22(5)	-7(5)

C4B	65(7)	77(7)	49(6)	-16(6)	9(5)	0(6)
C5B	65(6)	65(6)	56(6)	-5(5)	31(5)	-1(5)
C6B	79(8)	61(6)	65(7)	-25(5)	31(6)	-3(6)
C7B	75(7)	35(4)	54(5)	-2(4)	27(5)	1(4)
C8B	88(8)	53(5)	53(6)	17(5)	46(6)	19(5)
C9B	56(5)	54(5)	47(5)	-5(4)	21(4)	-5(4)
C10B	71(7)	66(7)	89(9)	-8(6)	45(7)	-8(6)
C11B	54(6)	86(8)	50(6)	17(6)	26(5)	11(5)
C12B	63(7)	141(14)	61(7)	16(8)	30(6)	25(8)
C13B	89(10)	170(18)	49(7)	-13(10)	31(7)	-1(12)
C14B	83(9)	115(12)	83(10)	-1(9)	45(8)	10(9)
C15B	91(8)	57(6)	46(6)	4(5)	24(6)	7(6)
C16B	73(7)	79(7)	45(5)	20(5)	22(5)	1(6)
C17B	67(6)	71(6)	36(5)	5(4)	23(5)	7(5)
C18B	69(7)	79(7)	37(5)	10(5)	18(5)	23(6)
C19B	71(7)	62(6)	29(4)	3(4)	14(5)	4(5)
C20B	83(8)	82(8)	62(7)	21(6)	42(7)	26(7)
C21B	60(7)	147(16)	67(9)	-12(10)	8(7)	-10(9)
C22B	83(9)	72(7)	47(6)	-1(5)	10(6)	5(7)
C23B	111(11)	70(7)	39(5)	4(5)	34(6)	1(7)
C24B	108(10)	62(6)	60(7)	4(6)	43(7)	-7(7)
O2A	74(5)	73(5)	58(5)	-15(4)	34(4)	-19(4)
O3A	46(4)	94(5)	56(4)	-8(4)	28(3)	-9(4)
O4A	53(4)	139(9)	84(7)	49(7)	26(5)	-8(5)
N1A	48(4)	47(4)	48(4)	-2(3)	27(4)	-3(3)
N2A	52(4)	58(5)	56(5)	2(4)	12(4)	8(4)
C1A	64(6)	52(5)	35(4)	-1(4)	23(4)	-2(4)
C2A	61(6)	56(5)	48(5)	-2(4)	24(5)	1(4)
C3A	66(6)	76(7)	51(6)	-8(5)	34(5)	-5(5)
C4A	75(7)	61(6)	47(5)	0(4)	31(5)	-6(5)
C5A	58(5)	62(5)	37(5)	3(4)	24(4)	1(4)
C6A	67(6)	67(6)	47(5)	16(5)	16(5)	-4(5)
C7A	44(4)	51(5)	54(6)	7(4)	14(4)	7(4)
C8A	52(5)	56(5)	46(5)	-6(4)	25(4)	5(4)
C9A	50(5)	52(5)	39(4)	1(4)	18(4)	3(4)
C10A	49(6)	89(8)	83(9)	25(7)	29(6)	3(6)
C11A	44(5)	65(6)	108(10)	36(7)	37(6)	4(5)
C12A	84(9)	114(11)	46(6)	-7(7)	24(7)	19(8)
C13A	87(9)	111(11)	50(6)	5(7)	31(7)	13(8)
C14A	74(7)	99(9)	58(7)	22(7)	29(6)	18(7)
C15A	47(4)	59(5)	43(5)	3(4)	20(4)	0(4)
C16A	57(6)	67(6)	53(6)	1(5)	4(5)	0(5)

C17A	51(5)	88(7)	32(4)	11(5)	13(4)	17(5)
C18A	61(6)	84(7)	38(5)	-1(5)	13(5)	16(5)
C19A	53(5)	62(6)	32(4)	4(4)	11(4)	-7(4)
C20A	123(14)	138(15)	78(10)	29(10)	67(10)	-10(12)
C21A	114(12)	112(12)	62(8)	35(9)	44(9)	17(11)
C22A	108(13)	101(11)	58(8)	-15(8)	9(8)	2(10)
C24A	55(6)	87(8)	73(8)	-22(7)	19(6)	-10(6)
C23A	95(11)	100(11)	64(9)	-23(9)	-2(8)	9(9)

Table 4 Bond Lengths for LUB1032.

Atom	Atom	Length/Å	Atom	Atom	Length/Å
O1A	C1A	1.265(13)	C23B	C24B	1.42(2)
O1B	C1B	1.206(14)	O2A	C9A	1.176(13)
O2B	C9B	1.175(14)	O3A	C9A	1.348(12)
O3B	C9B	1.350(14)	O3A	C10A	1.457(15)
O3B	C10B	1.490(16)	O4A	C17A	1.214(17)
O4B	C17B	1.226(15)	N1A	C1A	1.315(13)
N1B	C1B	1.383(13)	N1A	C5A	1.481(13)
N1B	C5B	1.450(16)	N1A	C8A	1.462(12)
N1B	C8B	1.412(15)	N2A	C2A	1.445(15)
N2B	C2B	1.464(15)	N2A	C17A	1.340(15)
N2B	C17B	1.322(15)	C1A	C2A	1.510(15)
C1B	C2B	1.524(15)	C2A	C3A	1.530(15)
C2B	C3B	1.535(15)	C3A	C4A	1.517(18)
C3B	C4B	1.541(18)	C4A	C5A	1.532(15)
C4B	C5B	1.551(18)	C5A	C6A	1.508(16)
C5B	C6B	1.534(16)	C6A	C7A	1.531(18)
C6B	C7B	1.572(19)	C7A	C8A	1.542(14)
C7B	C8B	1.529(15)	C8A	C9A	1.515(15)
C8B	C9B	1.548(15)	C10A	C11A	1.502(17)
C10B	C11B	1.496(19)	C11A	C12A	1.42(2)
C11B	C12B	1.37(2)	C11A	C16A	1.38(2)
C11B	C16B	1.412(18)	C12A	C13A	1.34(2)
C12B	C13B	1.39(3)	C13A	C14A	1.46(2)
C13B	C14B	1.36(3)	C14A	C15A	1.365(18)
C14B	C15B	1.38(2)	C15A	C16A	1.380(16)
C15B	C16B	1.392(19)	C17A	C18A	1.517(16)
C17B	C18B	1.548(17)	C18A	C19A	1.503(14)
C18B	C19B	1.551(14)	C19A	C20A	1.375(18)
C19B	C20B	1.40(2)	C19A	C24A	1.398(17)
C19B	C24B	1.357(18)	C20A	C21A	1.48(3)
C20B	C21B	1.38(2)	C21A	C22A	1.32(3)

C21B	C22B	1.31(3)	C22A	C23A	1.30(3)
C22B	C23B	1.31(2)	C24A	C23A	1.34(2)

Table 5 Bond Angles for LUB1032.

Atom	Atom	Atom	Angle/°	Atom	Atom	Atom	Angle/°
C9B	O3B	C10B	116.1(10)	C9A	O3A	C10A	117.5(10)
C1B	N1B	C5B	122.8(10)	C1A	N1A	C5A	125.1(8)
C1B	N1B	C8B	122.9(10)	C1A	N1A	C8A	121.8(8)
C8B	N1B	C5B	114.4(9)	C8A	N1A	C5A	113.1(8)
C17B	N2B	C2B	123.2(10)	C17A	N2A	C2A	123.1(10)
O1B	C1B	N1B	122.8(10)	O1A	C1A	N1A	123.8(10)
O1B	C1B	C2B	126.5(10)	O1A	C1A	C2A	123.1(10)
N1B	C1B	C2B	110.6(10)	N1A	C1A	C2A	113.1(8)
N2B	C2B	C1B	108.7(9)	N2A	C2A	C1A	110.3(9)
N2B	C2B	C3B	109.3(10)	N2A	C2A	C3A	113.0(9)
C1B	C2B	C3B	111.7(9)	C1A	C2A	C3A	110.9(9)
C2B	C3B	C4B	112.8(11)	C4A	C3A	C2A	114.4(10)
C3B	C4B	C5B	111.8(10)	C3A	C4A	C5A	113.0(9)
N1B	C5B	C4B	109.0(10)	N1A	C5A	C4A	105.5(8)
N1B	C5B	C6B	104.0(9)	N1A	C5A	C6A	102.9(8)
C6B	C5B	C4B	114.8(11)	C6A	C5A	C4A	116.7(10)
C5B	C6B	C7B	102.6(10)	C5A	C6A	C7A	105.3(9)
C8B	C7B	C6B	103.0(8)	C6A	C7A	C8A	103.4(8)
N1B	C8B	C7B	105.0(10)	N1A	C8A	C7A	103.4(8)
N1B	C8B	C9B	111.4(9)	N1A	C8A	C9A	109.9(8)
C7B	C8B	C9B	108.0(8)	C9A	C8A	C7A	110.1(9)
O2B	C9B	O3B	125.7(10)	O2A	C9A	O3A	123.4(10)
O2B	C9B	C8B	124.3(10)	O2A	C9A	C8A	126.8(10)
O3B	C9B	C8B	109.7(9)	O3A	C9A	C8A	109.8(8)
O3B	C10B	C11B	106.6(10)	O3A	C10A	C11A	108.5(11)
C12B	C11B	C10B	122.7(12)	C12A	C11A	C10A	118.8(14)
C12B	C11B	C16B	117.9(13)	C16A	C11A	C10A	123.1(14)
C16B	C11B	C10B	119.4(11)	C16A	C11A	C12A	118.0(12)
C11B	C12B	C13B	119.7(15)	C13A	C12A	C11A	122.4(14)
C14B	C13B	C12B	122.9(15)	C12A	C13A	C14A	118.3(13)
C13B	C14B	C15B	118.3(16)	C15A	C14A	C13A	119.2(12)
C14B	C15B	C16B	120.0(13)	C14A	C15A	C16A	120.9(11)
C15B	C16B	C11B	120.9(11)	C11A	C16A	C15A	121.1(12)
O4B	C17B	N2B	124.2(11)	O4A	C17A	N2A	123.5(11)
O4B	C17B	C18B	121.0(10)	O4A	C17A	C18A	120.5(11)
N2B	C17B	C18B	114.7(11)	N2A	C17A	C18A	116.0(11)
C17B	C18B	C19B	110.1(9)	C19A	C18A	C17A	111.4(10)

C20B	C19B	C18B	120.4(11)	C20A	C19A	C18A	125.0(14)
C24B	C19B	C18B	120.5(12)	C20A	C19A	C24A	117.8(14)
C24B	C19B	C20B	119.0(12)	C24A	C19A	C18A	115.7(11)
C21B	C20B	C19B	117.5(14)	C19A	C20A	C21A	116.1(18)
C22B	C21B	C20B	124.0(16)	C22A	C21A	C20A	118.8(16)
C23B	C22B	C21B	118.9(13)	C23A	C22A	C21A	125.4(16)
C22B	C23B	C24B	121.7(13)	C23A	C24A	C19A	124.1(18)
C19B	C24B	C23B	118.8(15)	C22A	C23A	C24A	117(2)

Table 6 Hydrogen Bonds for LUB1032.

D	H	A	d(D-H)/Å	d(H-A)/Å	d(D-A)/Å	D-H-A/°
N2B	H2B	O1A	0.88	2.16	3.011(13)	163.8
N2A	H2A	O1B	0.88	2.02	2.880(13)	163.8

Table 7 Torsion Angles for LUB1032.

A	B	C	D	Angle/°	A	B	C	D	Angle/°
O1A	C1A	C2A	N2A	5.3(14)	C22B	C23B	C24B	C19B	2(2)
O1A	C1A	C2A	C3A	131.3(11)	C24B	C19B	C20B	C21B	1(2)
O1B	C1B	C2B	N2B	9.1(15)	O3A	C10A	C11A	C12A	102.1(15)
O1B	C1B	C2B	C3B	129.8(12)	O3A	C10A	C11A	C16A	-78.5(15)
O3B	C10B	C11B	C12B	103.1(15)	O4A	C17A	C18A	C19A	76.3(16)
O3B	C10B	C11B	C16B	-78.5(15)	N1A	C1A	C2A	N2A	-175.2(9)
O4B	C17B	C18B	C19B	73.4(15)	N1A	C1A	C2A	C3A	-49.3(12)
N1B	C1B	C2B	N2B	-173.5(8)	N1A	C5A	C6A	C7A	29.1(11)
N1B	C1B	C2B	C3B	-52.8(13)	N1A	C8A	C9A	O2A	-37.4(14)
N1B	C5B	C6B	C7B	26.9(12)	N1A	C8A	C9A	O3A	144.4(9)
N1B	C8B	C9B	O2B	-37.4(15)	N2A	C2A	C3A	C4A	161.4(10)
N1B	C8B	C9B	O3B	147.7(9)	N2A	C17A	C18A	C19A	-102.9(12)
N2B	C2B	C3B	C4B	166.4(10)	C1A	N1A	C5A	C4A	44.2(13)
N2B	C17B	C18B	C19B	-105.7(12)	C1A	N1A	C5A	C6A	167.0(10)
C1B	N1B	C5B	C4B	47.0(14)	C1A	N1A	C8A	C7A	171.4(9)
C1B	N1B	C5B	C6B	169.9(10)	C1A	N1A	C8A	C9A	-71.1(11)
C1B	N1B	C8B	C7B	168.6(9)	C1A	C2A	C3A	C4A	37.0(13)
C1B	N1B	C8B	C9B	-74.8(13)	C2A	N2A	C17A	O4A	3.3(19)
C1B	C2B	C3B	C4B	46.1(14)	C2A	N2A	C17A	C18A	-177.5(10)
C2B	N2B	C17B	O4B	0.8(18)	C2A	C3A	C4A	C5A	14.0(14)
C2B	N2B	C17B	C18B	179.8(10)	C3A	C4A	C5A	N1A	-51.8(12)
C2B	C3B	C4B	C5B	5.2(15)	C3A	C4A	C5A	C6A	-165.2(10)
C3B	C4B	C5B	N1B	-49.5(14)	C4A	C5A	C6A	C7A	143.9(9)
C3B	C4B	C5B	C6B	-165.7(11)	C5A	N1A	C1A	O1A	-173.5(9)
C4B	C5B	C6B	C7B	145.9(10)	C5A	N1A	C1A	C2A	7.0(13)
C5B	N1B	C1B	O1B	-177.8(10)	C5A	N1A	C8A	C7A	-9.3(11)

C5B	N1B	C1B	C2B	4.7(14)	C5A	N1A	C8A	C9A	108.2(9)
C5B	N1B	C8B	C7B	-10.5(12)	C5A	C6A	C7A	C8A	-35.2(11)
C5B	N1B	C8B	C9B	106.2(12)	C6A	C7A	C8A	N1A	26.8(10)
C5B	C6B	C7B	C8B	-32.9(12)	C6A	C7A	C8A	C9A	-90.6(9)
C6B	C7B	C8B	N1B	26.8(11)	C7A	C8A	C9A	O2A	75.9(13)
C6B	C7B	C8B	C9B	-92.1(11)	C7A	C8A	C9A	O3A	-102.3(10)
C7B	C8B	C9B	O2B	77.4(13)	C8A	N1A	C1A	O1A	5.7(15)
C7B	C8B	C9B	O3B	-97.5(11)	C8A	N1A	C1A	C2A	-173.8(9)
C8B	N1B	C1B	O1B	3.3(16)	C8A	N1A	C5A	C4A	-135.1(9)
C8B	N1B	C1B	C2B	-174.3(9)	C8A	N1A	C5A	C6A	-12.3(11)
C8B	N1B	C5B	C4B	-134.0(10)	C9A	O3A	C10A	C11A	-96.2(14)
C8B	N1B	C5B	C6B	-11.1(13)	C10A	O3A	C9A	O2A	-9.4(17)
C9B	O3B	C10B	C11B	-94.9(12)	C10A	O3A	C9A	C8A	168.9(9)
C10B	O3B	C9B	O2B	-11.0(16)	C10A	C11A	C12A	C13A	-179.9(15)
C10B	O3B	C9B	C8B	163.9(10)	C10A	C11A	C16A	C15A	176.7(11)
C10B	C11B	C12B	C13B	-177.9(16)	C11A	C12A	C13A	C14A	2(3)
C10B	C11B	C16B	C15B	-178.3(12)	C12A	C11A	C16A	C15A	-3.9(19)
C11B	C12B	C13B	C14B	-3(3)	C12A	C13A	C14A	C15A	-2(2)
C12B	C11B	C16B	C15B	0(2)	C13A	C14A	C15A	C16A	-1(2)
C12B	C13B	C14B	C15B	-1(3)	C14A	C15A	C16A	C11A	4.1(19)
C13B	C14B	C15B	C16B	5(3)	C16A	C11A	C12A	C13A	1(2)
C14B	C15B	C16B	C11B	-5(2)	C17A	N2A	C2A	C1A	-139.4(11)
C16B	C11B	C12B	C13B	4(2)	C17A	N2A	C2A	C3A	95.9(13)
C17B	N2B	C2B	C1B	-120.5(12)	C17A	C18A	C19A	C20A	127.5(16)
C17B	N2B	C2B	C3B	117.3(12)	C17A	C18A	C19A	C24A	-67.0(14)
C17B	C18B	C19B	C20B	84.7(15)	C18A	C19A	C20A	C21A	172.5(15)
C17B	C18B	C19B	C24B	-99.4(14)	C18A	C19A	C24A	C23A	-173.7(15)
C18B	C19B	C20B	C21B	176.8(15)	C19A	C20A	C21A	C22A	-7(3)
C18B	C19B	C24B	C23B	-175.9(12)	C19A	C24A	C23A	C22A	6(3)
C19B	C20B	C21B	C22B	-4(3)	C20A	C19A	C24A	C23A	-7(2)
C20B	C19B	C24B	C23B	0.0(19)	C20A	C21A	C22A	C23A	6(3)
C20B	C21B	C22B	C23B	7(3)	C21A	C22A	C23A	C24A	-6(3)
C21B	C22B	C23B	C24B	-5(2)	C24A	C19A	C20A	C21A	7(3)

Table 8 Hydrogen Atom Coordinates (Å×10^4) and Isotropic Displacement Parameters (Å^2×10^3) for LUB1032.

Atom	*x*	*y*	*z*	U(eq)
H2B	-5564.91	-5049.71	-5359.12	72
H2BA	-6155.16	-6710.59	-5918.37	70
H3BA	-6438.63	-5370.77	-7491.14	74
H3BB	-7563.35	-5992.84	-7576.15	74
H4BA	-5965.67	-6153.34	-8658.39	84

H4BB	-7182.21	-6727.2	-8842.2	84
H5B	-5839.96	-7615.63	-7307.09	73
H6BA	-4766.51	-7274.37	-8922.81	83
H6BB	-5313.35	-8140.74	-8708	83
H7BA	-3389.61	-8407.19	-6972.44	67
H7BB	-2764.03	-7907.91	-7699.32	67
H8B	-2483.09	-7363.33	-5646.18	71
H10C	644.97	-5958.46	-5961.37	87
H10D	-642.66	-5685.47	-7125.21	87
H12B	-1091.83	-6367.31	-8980.43	105
H13B	-615.69	-7391.61	-10006.13	123
H14B	961.02	-8373.69	-9056.07	109
H15B	2177.35	-8304.64	-6994.46	81
H16B	1561.56	-7381.35	-5918.92	81
H18C	-7222.92	-4806.45	-3853.51	76
H18D	-6178.63	-4383.08	-4207.1	76
H20B	-3728.03	-4576.63	-2830.48	86
H21B	-2196.7	-4702.38	-869.14	119
H22B	-2762.84	-4977.75	578.86	89
H23B	-4815.15	-5417.92	103.59	88
H24B	-6476.66	-5356.74	-1868.1	90
H2A	-2686.15	-4908.58	-5045.45	72
H2AA	-2431.62	-3355.35	-5771.74	66
H3AA	-2641.78	-3988.68	-7428.1	74
H3AB	-3670.17	-4645.9	-7404.72	74
H4AA	-5331.54	-3885.44	-8506.87	71
H4AB	-4315.65	-3364.22	-8788.28	71
H5A	-4067.89	-2385.72	-7325.34	61
H6AA	-6748.41	-2733.56	-8866.36	76
H6AB	-5978.36	-1881.23	-8732.19	76
H7AA	-7514.33	-1994.02	-7750.23	63
H7AB	-6137.74	-1523.11	-7035.93	63
H8A	-5818.31	-2514.04	-5638.37	60
H10A	-9022.05	-3921.67	-5655.87	89
H10B	-8977.06	-4240.56	-6838.7	89
H12A	-10452.75	-3729.81	-8695.7	100
H13A	-12220.99	-2949.27	-9891.74	99
H14A	-12912.99	-1844.13	-9013.67	93
H15A	-11845.2	-1654.36	-6986.33	60
H16A	-10187.22	-2537.38	-5793.12	80
H18A	-974.07	-5706.85	-4075.16	77
H18B	421.87	-5447.33	-3985.19	77

H20A	-787.69	-5931.83	-2056.17	126
H21A	321.08	-5510.31	35.84	113
H22A	2022.91	-4639.92	618.52	119
H24A	1488.55	-4255.57	-2594.47	90
H23A	2498.96	-3912.61	-633.63	120

Experimental

A suitable crystal of $C_{24}H_{26}N_2O_4$ [LUB1032] *S*-**5.21** was selected and mounted on a Mylar Cryoloop on a Bruker Venture Metaljet diffractometer. The crystal was kept at 150 K during data collection. Using Olex2 [1], the structure was solved with the XT [2] structure solution program using Intrinsic Phasing and refined with the XL [3] refinement package using Least Squares minimisation.

1. Dolomanov, O.V., Bourhis, L.J., Gildea, R.J, Howard, J.A.K. & Puschmann, H. (2009), J. Appl. Cryst. 42, 339-341.
2. Sheldrick, G.M. (2015). Acta Cryst. A71, 3-8.
3. Sheldrick, G.M. (2015). Acta Cryst. C71, 3-8.

Crystal structure determination of LUB1032

Crystal Data for $C_{24}H_{26}N_2O_4$ (M =406.47 g/mol): monoclinic, space group $P2_1$ (no. 4), a = 11.4081(12) Å, b = 16.2769(16) Å, c = 12.6451(18) Å, β = 116.589(4)°, V = 2099.7(4) Å^3, Z = 4, T = 150 K, μ(GaKα) = 0.456 mm^{-1}, *Dcalc* = 1.286 g/cm^3, 27430 reflections measured (4.724° ≤ 2Θ ≤ 108.218°), 7671 unique (R_{int} = 0.0661, R_{sigma} = 0.0574) which were used in all calculations. The final R_1 was 0.1453 (I > 2σ(I)) and wR_2 was 0.3547 (all data).

Refinement model description

Number of restraints - 1, number of constraints - unknown.
Details:
1. Twinned data refinement
Scales: 0.5(9)
-0.11(12) 0.3(9) 0.30(12)
2. Fixed Uiso
At 1.2 times of:
All C(H) groups, All C(H,H) groups, All N(H) groups
3.a Ternary CH refined with riding coordinates:
C2B(H2BA), C5B(H5B), C8B(H8B), C2A(H2AA), C5A(H5A), C8A(H8A)
3.b Secondary CH2 refined with riding coordinates:
C3B(H3BA,H3BB), C4B(H4BA,H4BB), C6B(H6BA,H6BB), C7B(H7BA,H7BB), C10B(H10C,
H10D), C18B(H18C,H18D), C3A(H3AA,H3AB), C4A(H4AA,H4AB), C6A(H6AA,H6AB),
C7A(H7AA,H7AB), C10A(H10A,H10B), C18A(H18A,H18B)
3.c Aromatic/amide H refined with riding coordinates:
N2B(H2B), C12B(H12B), C13B(H13B), C14B(H14B), C15B(H15B), C16B(H16B),
C20B(H20B), C21B(H21B), C22B(H22B), C23B(H23B), C24B(H24B), N2A(H2A),
C12A(H12A), C13A(H13A), C14A(H14A), C15A(H15A), C16A(H16A), C20A(H20A),
C21A(H21A), C22A(H22A), C24A(H24A), C23A(H23A)
This report has been created with Olex2, compiled on 2018.05.18 svn.r3508 for OlexSys.
Please let us know if there are any errors or if you would like to have additional features.

(3*S*,6*R*,7*R*,9*S*)-Benzyl 7-hydroxy-2-oxo-3-phenylacetamido-octahydroindolizine-9-carboxylate [(*R*)-**5.45,** lub121**]**

Table 1 Crystal data and structure refinement for lub121.

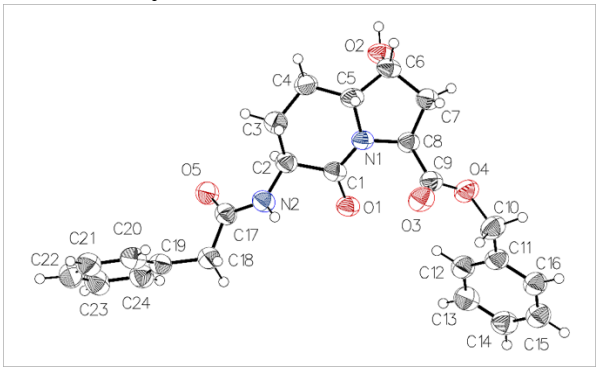

Identification code	
Empirical formula	$C_{24}H_{26}N_2O_5$
Formula weight	422.47
Temperature/K	150
Crystal system	orthorhombic
Space group	$P2_12_12_1$
a/Å	5.3744(4)
b/Å	13.8340(10)
c/Å	28.1059(19)
α/°	90
β/°	90
γ/°	90
Volume/Å^3	2089.7(3)
Z	4
ρ_{calc}g/cm^3	1.343
μ/mm^{-1}	0.496
F(000)	896.0
Crystal size/mm^3	0.5 × 0.2 × 0.05
Radiation	GaKα (λ = 1.34139)
2Θ range for data collection/°	5.472 to 121.734
Index ranges	$-6 \le h \le 6$, $-17 \le k \le 17$, $-36 \le l \le 36$
Reflections collected	24918
Independent reflections	4789 [R_{int} = 0.0680, R_{sigma} = 0.0471]
Data/restraints/parameters	4789/0/282
Goodness-of-fit on F^2	1.088
Final R indexes [I>=2σ (I)]	R_1 = 0.0620, wR_2 = 0.1591
Final R indexes [all data]	R_1 = 0.0737, wR_2 = 0.1702

Largest diff. peak/hole / e Å^{-3}	0.21/-0.26
Flack parameter	-0.2(3)

Table 2 Fractional Atomic Coordinates (×10^4) and Equivalent Isotropic Displacement Parameters (Å^2×10^3) for lub121. U_{eq} is defined as 1/3 of of the trace of the orthogonalised U_{IJ} tensor.

Atom	*x*	*y*	*z*	U(eq)
O1	7445(5)	6483.6(17)	7470.0(9)	46.7(6)
O2	5018(5)	3188.3(19)	7680.3(11)	52.7(7)
O3	12520(5)	5570(2)	7711.7(11)	59.1(7)
O4	11027(6)	5441(2)	8456.6(10)	56.9(7)
O5	2714(5)	7062.9(19)	6248.5(11)	53.6(7)
N1	7904(5)	4880(2)	7365.0(10)	42.3(6)
N2	6615(6)	6671(2)	6480.6(12)	49.1(7)
C1	7183(7)	5752(2)	7216.9(13)	43.0(7)
C2	5864(8)	5812(3)	6736.4(13)	45.8(8)
C3	6069(9)	4898(3)	6434.5(15)	54.2(9)
C4	5709(8)	4004(3)	6737.9(15)	50.7(9)
C5	7746(7)	3956(2)	7106.2(14)	44.3(8)
C6	7489(7)	3218(3)	7505.6(14)	45.8(8)
C7	9179(7)	3641(3)	7885.8(15)	48.0(8)
C8	8661(7)	4736(3)	7858.7(13)	43.9(8)
C9	10958(7)	5306(3)	7981.7(14)	46.0(8)
C10	13092(8)	5981(3)	8652.1(17)	60.2(11)
C11	12096(8)	6808(3)	8942.0(15)	52.3(9)
C12	9983(8)	7307(3)	8816.7(17)	56.7(10)
C13	9207(9)	8107(3)	9076.5(17)	60.5(11)
C14	10589(9)	8417(3)	9461.9(17)	60.4(11)
C15	12702(9)	7927(3)	9591.3(17)	61.0(11)
C16	13465(8)	7118(3)	9336.9(15)	56.1(10)
C17	4944(7)	7244(3)	6262.5(14)	47.5(8)
C18	6075(9)	8166(3)	6052.0(15)	55.8(10)
C19	4640(8)	8584(3)	5640.4(14)	50.4(9)
C20	5393(9)	8432(3)	5173.0(16)	59.7(11)
C21	4053(11)	8838(3)	4800.1(17)	66.2(12)
C22	1957(10)	9372(4)	4884.9(18)	70.5(13)
C23	1207(9)	9542(3)	5346.6(19)	67.2(12)
C24	2535(9)	9146(3)	5721.0(16)	57.7(10)

Table 3 Anisotropic Displacement Parameters (Å^2×10^3) for lub121. The Anisotropic displacement factor exponent takes the form: $-2\pi^2[h^2a^{*2}U_{11}+2hka^*b^*U_{12}+\ldots]$.

Atom	U_{11}	U_{22}	U_{33}	U_{23}	U_{13}	U_{12}
O1	45.0(14)	37.5(12)	57.8(15)	-2.8(10)	-0.3(12)	1.4(11)
O2	39.3(14)	42.6(13)	76.1(18)	2.6(12)	6.9(13)	-4.1(11)
O3	38.2(14)	69.2(18)	70.0(17)	0.9(14)	4.3(14)	-10.6(13)
O4	50.3(15)	60.0(16)	60.4(16)	-2.8(13)	-3.6(13)	-13.8(13)
O5	44.6(15)	50.1(15)	66.2(16)	3.8(12)	-4.3(13)	0.9(12)
N1	39.4(15)	34.8(14)	52.7(16)	-2.2(12)	-0.6(12)	0.2(12)
N2	43.6(17)	44.2(16)	59.6(18)	5.5(13)	-0.2(14)	0.4(13)
C1	33.6(17)	37.1(16)	58.3(19)	1.0(14)	3.2(15)	-0.3(13)
C2	42.5(19)	40.0(17)	54.9(19)	1.9(15)	-2.5(16)	1.6(15)
C3	58(2)	45(2)	59(2)	-1.7(16)	-5.9(19)	2.4(19)
C4	49(2)	41.6(19)	62(2)	-3.6(16)	-6.4(18)	-3.1(15)
C5	37.9(18)	36.4(16)	59(2)	-5.7(14)	0.5(16)	0.7(14)
C6	35.1(18)	34.7(16)	68(2)	0.5(14)	3.1(16)	2.1(14)
C7	37.1(18)	42.4(18)	64(2)	3.8(16)	0.1(16)	2.0(15)
C8	38.1(17)	41.8(17)	51.7(19)	0.2(14)	0.0(15)	-2.4(15)
C9	38.2(18)	38.3(17)	61(2)	0.2(15)	-2.7(16)	0.7(15)
C10	47(2)	61(3)	73(3)	-7(2)	-8.9(19)	-5.5(18)
C11	44(2)	48(2)	65(2)	1.5(17)	-4.2(17)	-8.7(16)
C12	45(2)	54(2)	71(3)	2.8(19)	-9.1(19)	-4.5(18)
C13	45(2)	56(2)	81(3)	7(2)	-1(2)	1.2(18)
C14	54(3)	55(2)	72(3)	1(2)	4(2)	-3.7(19)
C15	55(3)	61(2)	67(2)	-0.6(19)	-4(2)	-5(2)
C16	50(2)	55(2)	64(2)	-0.7(18)	-5.9(19)	-2.2(18)
C17	48(2)	44.2(18)	50.4(19)	1.4(15)	-1.4(17)	2.4(16)
C18	52(2)	50(2)	66(2)	7.3(18)	-11(2)	-6.0(18)
C19	50(2)	42.6(19)	58(2)	5.2(16)	-3.7(17)	-5.7(17)
C20	63(3)	47(2)	69(3)	0.5(18)	2(2)	-3.9(19)
C21	81(3)	59(2)	58(2)	6.1(19)	-1(2)	-15(3)
C22	67(3)	69(3)	76(3)	21(2)	-19(2)	-15(2)
C23	49(2)	64(3)	89(3)	17(2)	-4(2)	2(2)
C24	53(2)	55(2)	66(2)	6.1(18)	-1(2)	-2.6(19)

Table 4 Bond Lengths for lub121.

Atom	Atom	Length/Å	Atom	Atom	Length/Å
O1	C1	1.245(4)	C7	C8	1.542(5)
O2	C6	1.417(4)	C8	C9	1.505(5)
O3	C9	1.189(5)	C10	C11	1.503(6)
O4	C9	1.348(5)	C11	C12	1.375(6)
O4	C10	1.446(5)	C11	C16	1.399(6)
O5	C17	1.225(5)	C12	C13	1.389(6)
N1	C1	1.334(4)	C13	C14	1.382(7)

N1	C5	1.474(4)	C14	C15	1.371(7)
N1	C8	1.460(5)	C15	C16	1.390(6)
N2	C2	1.446(5)	C17	C18	1.532(6)
N2	C17	1.345(5)	C18	C19	1.506(6)
C1	C2	1.527(5)	C19	C20	1.391(6)
C2	C3	1.527(5)	C19	C24	1.391(6)
C3	C4	1.515(6)	C20	C21	1.391(7)
C4	C5	1.508(5)	C21	C22	1.367(8)
C5	C6	1.524(5)	C22	C23	1.379(7)
C6	C7	1.520(5)	C23	C24	1.384(6)

Table 5 Bond Angles for lub121.

Atom	Atom	Atom	Angle/°	Atom	Atom	Atom	Angle/°
C9	O4	C10	118.0(3)	O3	C9	C8	126.4(4)
C1	N1	C5	127.9(3)	O4	C9	C8	108.8(3)
C1	N1	C8	120.1(3)	O4	C10	C11	109.0(4)
C8	N1	C5	111.5(3)	C12	C11	C10	122.5(4)
C17	N2	C2	121.6(3)	C12	C11	C16	118.9(4)
O1	C1	N1	121.6(3)	C16	C11	C10	118.4(4)
O1	C1	C2	120.9(3)	C11	C12	C13	120.9(4)
N1	C1	C2	117.4(3)	C14	C13	C12	119.9(4)
N2	C2	C1	110.8(3)	C15	C14	C13	120.0(4)
N2	C2	C3	112.6(3)	C14	C15	C16	120.4(4)
C3	C2	C1	114.4(3)	C15	C16	C11	120.0(4)
C4	C3	C2	110.8(3)	O5	C17	N2	123.2(4)
C5	C4	C3	109.2(3)	O5	C17	C18	123.1(4)
N1	C5	C4	110.0(3)	N2	C17	C18	113.7(4)
N1	C5	C6	102.9(3)	C19	C18	C17	114.4(3)
C4	C5	C6	118.0(3)	C20	C19	C18	121.2(4)
O2	C6	C5	111.1(3)	C24	C19	C18	120.4(4)
O2	C6	C7	109.1(3)	C24	C19	C20	118.4(4)
C7	C6	C5	101.9(3)	C21	C20	C19	120.0(5)
C6	C7	C8	103.7(3)	C22	C21	C20	120.9(5)
N1	C8	C7	103.4(3)	C21	C22	C23	119.8(4)
N1	C8	C9	112.1(3)	C22	C23	C24	119.8(5)
C9	C8	C7	110.8(3)	C23	C24	C19	121.1(4)
O3	C9	O4	124.8(4)				

Table 6 Hydrogen Bonds for lub121.

D	H	A	d(D-H)/Å	d(H-A)/Å	d(D-A)/Å	D-H-A/°
O2	H2	O1[1]	0.84	1.90	2.737(4)	170.8
N2	H2A	O5[2]	0.88	2.52	3.385(4)	166.9

[1]1-X,-1/2+Y,3/2-Z; [2]1+X,+Y,+Z

Table 7 Torsion Angles for lub121.

A	B	C	D	Angle/°	A	B	C	D	Angle/°
O1	C1	C2	N2	41.9(5)	C6	C7	C8	N1	-27.7(4)
O1	C1	C2	C3	170.4(3)	C6	C7	C8	C9	-147.9(3)
O2	C6	C7	C8	-77.3(4)	C7	C8	C9	O3	89.6(5)
O4	C10	C11	C12	-35.7(6)	C7	C8	C9	O4	-87.9(4)
O4	C10	C11	C16	148.4(4)	C8	N1	C1	O1	9.8(5)
O5	C17	C18	C19	-28.1(6)	C8	N1	C1	C2	-166.4(3)
N1	C1	C2	N2	-142.0(3)	C8	N1	C5	C4	147.3(3)
N1	C1	C2	C3	-13.5(5)	C8	N1	C5	C6	20.7(4)
N1	C5	C6	O2	79.1(4)	C9	O4	C10	C11	125.0(4)
N1	C5	C6	C7	-37.0(3)	C10	O4	C9	O3	2.8(6)
N1	C8	C9	O3	-25.4(5)	C10	O4	C9	C8	-179.7(3)
N1	C8	C9	O4	157.2(3)	C10	C11	C12	C13	-175.9(4)
N2	C2	C3	C4	170.0(4)	C10	C11	C16	C15	175.1(4)
N2	C17	C18	C19	154.4(4)	C11	C12	C13	C14	1.0(7)
C1	N1	C5	C4	-24.4(5)	C12	C11	C16	C15	-0.9(6)
C1	N1	C5	C6	-151.0(3)	C12	C13	C14	C15	-0.9(7)
C1	N1	C8	C7	176.7(3)	C13	C14	C15	C16	0.0(7)
C1	N1	C8	C9	-63.9(4)	C14	C15	C16	C11	1.0(7)
C1	C2	C3	C4	42.4(5)	C16	C11	C12	C13	0.0(6)
C2	N2	C17	O5	-3.0(6)	C17	N2	C2	C1	-134.5(4)
C2	N2	C17	C18	174.5(3)	C17	N2	C2	C3	96.0(4)
C2	C3	C4	C5	-62.4(4)	C17	C18	C19	C20	-100.3(5)
C3	C4	C5	N1	51.6(4)	C17	C18	C19	C24	80.5(5)
C3	C4	C5	C6	169.2(3)	C18	C19	C20	C21	-179.1(4)
C4	C5	C6	O2	-42.2(4)	C18	C19	C24	C23	179.5(4)
C4	C5	C6	C7	-158.3(3)	C19	C20	C21	C22	-1.5(7)
C5	N1	C1	O1	-179.2(3)	C20	C19	C24	C23	0.3(6)
C5	N1	C1	C2	4.7(5)	C20	C21	C22	C23	2.5(7)
C5	N1	C8	C7	4.3(4)	C21	C22	C23	C24	-2.0(7)
C5	N1	C8	C9	123.7(3)	C22	C23	C24	C19	0.6(7)
C5	C6	C7	C8	40.1(4)	C24	C19	C20	C21	0.1(6)

Table 8 Hydrogen Atom Coordinates (Å×10^4) and Isotropic Displacement Parameters (Å^2×10^3) for lub121.

Atom	*x*	*y*	*z*	U(eq)
H2	4418.48	2635.04	7635.15	79
H2A	8203.98	6822.66	6467.21	59
H2B	4054.52	5894.98	6808.53	55

H3A	4793.3	4912.59	6180.56	65
H3B	7726.7	4874.89	6281.19	65
H4A	4065.85	4028.83	6896.82	61
H4B	5759.73	3419.04	6534.98	61
H5	9364.15	3841.67	6939.87	53
H6	8068.22	2563.08	7402.88	55
H7A	10947.39	3498.68	7816.54	58
H7B	8756.5	3381.92	8204.06	58
H8	7268.59	4912.26	8078.14	53
H10A	14150.67	6230.37	8391.4	72
H10B	14120.49	5554.03	8855.28	72
H12	9041.07	7102.93	8549.03	68
H13	7730.1	8439.81	8989.28	73
H14	10076.03	8969.34	9637.23	73
H15	13649.87	8142.17	9856.32	73
H16	14916.15	6775.81	9431.18	67
H18A	6185.31	8659.84	6306.12	67
H18B	7789.77	8022.49	5944.73	67
H20	6822.73	8049.72	5108.58	72
H21	4600.32	8743.82	4482.05	79
H22	1021.23	9624.2	4626.51	85
H23	-217.74	9929.05	5407.54	81
H24	2000.74	9260.23	6038.2	69

Experimental

Single crystals of $C_{24}H_{26}N_2O_5$ [lub121] (*R*-**5.45**) were crystallized from EtOAc. A suitable crystal was selected and mounted on a mylar cryollop on a Bruker Venture Metaljet diffractometer. The crystal was kept at 150 K during data collection. Using Olex2 [1], the structure was solved with the XT [2] structure solution program using Intrinsic Phasing and refined with the XL [3] refinement package using Least Squares minimisation.

Crystal structure determination of lub121

Crystal Data for $C_{24}H_{26}N_2O_5$ (M =422.47 g/mol): orthorhombic, space group $P2_12_12_1$ (no. 19), a = 5.3744(4) Å, b = 13.8340(10) Å, c = 28.1059(19) Å, V = 2089.7(3) Å^3, Z = 4, T = 150 K, μ(GaKα) = 0.496 mm^{-1}, *Dcalc* = 1.343 g/cm^3, 24918 reflections measured (5.472° ≤ 2Θ ≤ 121.734°), 4789 unique (R_{int} = 0.0680, R_{sigma} = 0.0471) which were used in all calculations. The final R_1 was 0.0620 (I > 2σ(I)) and wR_2 was 0.1702 (all data).

Refinement model description

Number of restraints - 0, number of constraints - unknown.
Details:
1. Fixed Uiso
 At 1.2 times of:
  All C(H) groups, All C(H,H) groups, All N(H) groups
 At 1.5 times of:
  All O(H) groups
2.a Ternary CH refined with riding coordinates:
 C2(H2B), C5(H5), C6(H6), C8(H8)
2.b Secondary CH2 refined with riding coordinates:

C3(H3A,H3B), C4(H4A,H4B), C7(H7A,H7B), C10(H10A,H10B), C18(H18A,H18B)
2.c Aromatic/amide H refined with riding coordinates:
N2(H2A), C12(H12), C13(H13), C14(H14), C15(H15), C16(H16), C20(H20), C21(H21), C22(H22), C23(H23), C24(H24)
2.d Idealised tetrahedral OH refined as rotating group:
O2(H2)
This report has been created with Olex2, compiled on 2018.04.26 svn.r3504 for OlexSys. Please let us know if there are any errors or if you would like to have additional features.

References:

1. Dolomanov, O.V., Bourhis, L.J., Gildea, R.J, Howard, J.A.K. & Puschmann, H. (2009), J. Appl. Cryst. 42, 339-341.
2. Sheldrick, G.M. (2015). Acta Cryst. A71, 3-8.
3. Sheldrick, G.M. (2015). Acta Cryst. C71, 3-8.

Chapter 6

Conclusions and perspectives

6.1 Resume

A shared synthetic route for the synthesis of iodo azabicyclo[X.Y.0]alkanones of different ring size has been developed by employing the RCM-TC strategy. Novel iodo substituted pyrrolizidinone, indolizidin-2-one, indolizidin-9-one, quinolizidinone and pyrroloazepinone amino acid analogs, all were successfully synthesized using this approach starting from various ω-unsaturated amino acids of 4–7-carbon chain lengths (Figure 6.1). The use of a hypervalent(III)iodine additive in the iodo lactamization conditions proved essential to synthesize pyrrolizidinone and indolizidin-9-ones from the respective 8- and 9-membered unsaturated lactams (Chapter 2). Bulky carboxylates and electron-rich aromatic ligands on the hypervalent iodine improved yields in the formation of such bicycles in acetonitrile. Moreover, the allylic carbamate acted as a directing group in toluene to favour intermolecular iodoacetoxylation of 7- and 8-membered unsaturated lactams. Subsequently, two I^2aa diastereomers and one I^9aa isomer were prepared for a common 9-membered unsaturated lactam precursor using transannular iodo amidation contingent on amine protection, solvent, and hypervalent iodine additive (Chapter 3).

With the interest in adding ring substituents for side-chain mimicry, routes were developed featuring iodide elimination and functionalization of the resulting olefin by Pd-catalyzed arylation and allylic oxidation. Moreover, copper-catalyzed S_N2' substitution of the zincate from *N*-(Boc)iodo-alanine onto (*Z*)-1,4-dichlorobut-2-ene provided an effective entry to enantiomerically pure 4-vinylproline (Vyp) and 4-vinylornithine (Von) analogs, which may be employed in RCM-TC strategies to make substituted ring systems (Chapter 4). Employing such methods, ring substituted indolizidin-2-one systems were generated and applied in a biomedical application.

Notably, the indolizidin-2-one residue was modified in the FP modulator PDC113.824 to examine effects on activity from changes of ring fusion stereochemistry and addition of ring

substituents (Chapter 5). Modifications of the indolizidin-2-one system caused typically a reduction in the inhibitory effect of PDC113.824 on myometrium contraction. Towards the development of labor delaying (tocolytic) agents for the treatment of preterm birth, this study has demonstrated that the activity of PDC113.824 is particularly sensitive to structural modifications at the indolizidin-2-one residue.

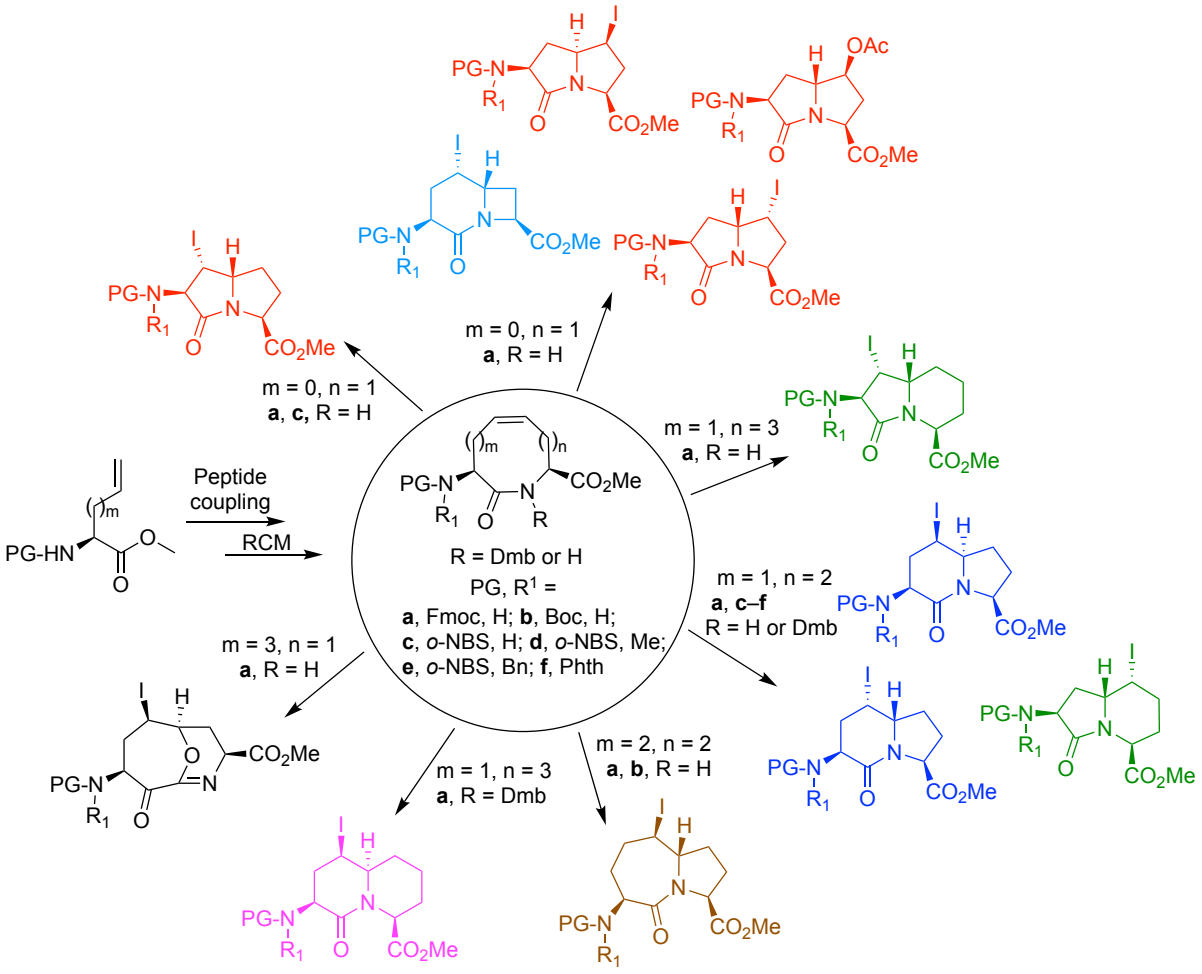

Figure 6.1. Syntheses of the different ring size azabicycloalkanone amino acid with common precursor

Other applications of our methods are merited for studying peptides due in part to the strong potential for our constrained dipeptide products to mimic β-turn conformations. X-ray crystallographic and spectroscopic analyses of the lactams and bicycles has demonstrated their

capacity to mimic the central residues of ideal type I, II', II and VI β-turns (Chapter 2 & 3). The subtle differences in dihedral angle caused by modification of the lactam and bicycle structure suggest their systematic use for exploring conformation-activity relationships. With our methods to prepare such systems by shared synthetic routes featuring common intermediates, opportunity exists for targeting a broad spectrum of biologically active peptide targets.

6.2 Perspectives

Introduction of our constrained lactams and bicycles into other peptides may have interesting utility for enhancing selectivity and potency. Inspired by the pioneering research of Freidinger and Veber on the use of α-amino-γ-lactam (Agl) residues to constrain peptide structure as described in my introduction,[1] Agl and β-hydroxy-α-amino-γ-lactam[2,3] (Hgl) residues have recently been used to study peptide **6.1** (101.10, H-D-Arg-D-Tyr-D-Thr-D-Val-D-Glu-D-Leu-Ala-NH_2), which is an allosteric modulator of the interleukin-1 receptor (IL-1R). Peptide **6.1** exhibits functional selectivity and conserves NF-kB signaling while inhibiting other IL-1-activated pathways (Figure 6.2).[4] Similar to the parent peptide **6.1**, Agl and Hgl analogs **6.2** and **6.3** have exhibited capacity to delay labour in murine models of preterm birth as well as to prevent vaso-obliteration in a murine model of retinopathy of prematurity.[3,5] Considering the activity of Agl and Hgl peptides **6.2** and **6.3**, the employment of indolizidin-9-one amino acid (I^9aa) residues and their 7-hydroxy counterparts (7-HO-I^9aa) merits exploration to examine further constraint of the D-Thr-D-Val residue in peptide **6.1** (Figure 6.3).

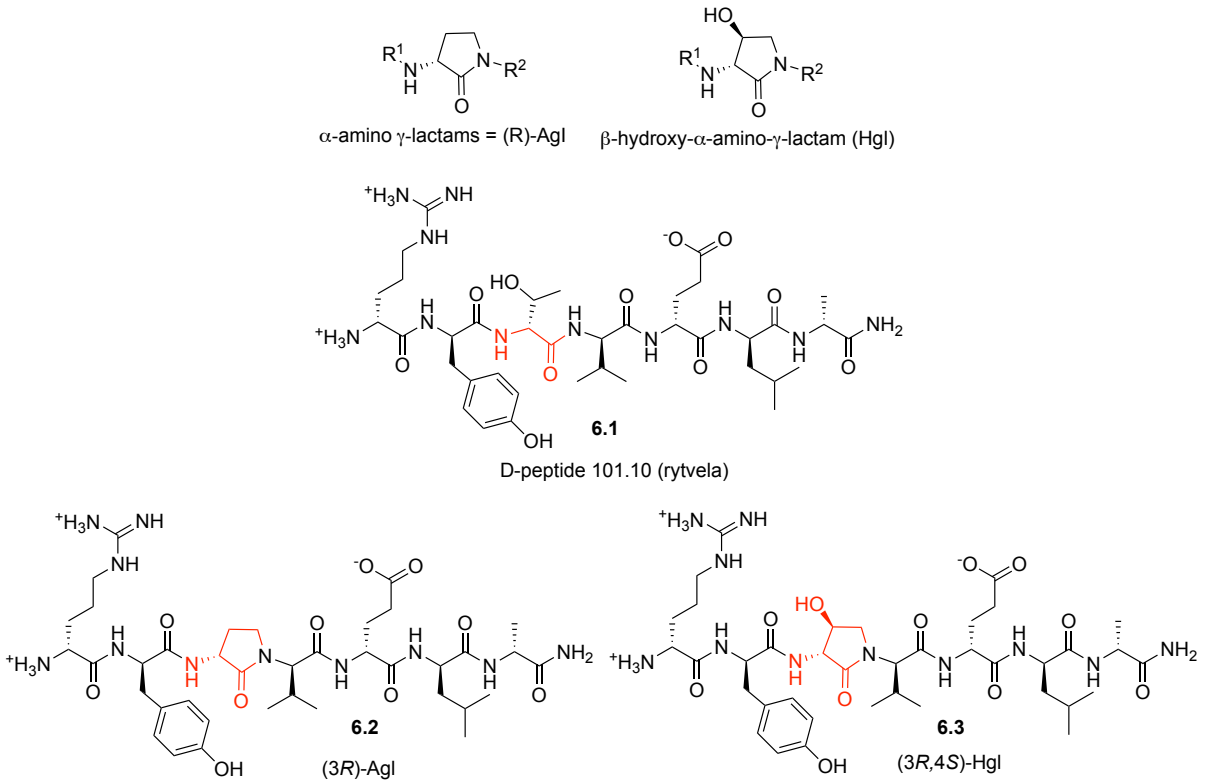

Figure 6.2. Constrained peptides analogues to rytvela (101.10)

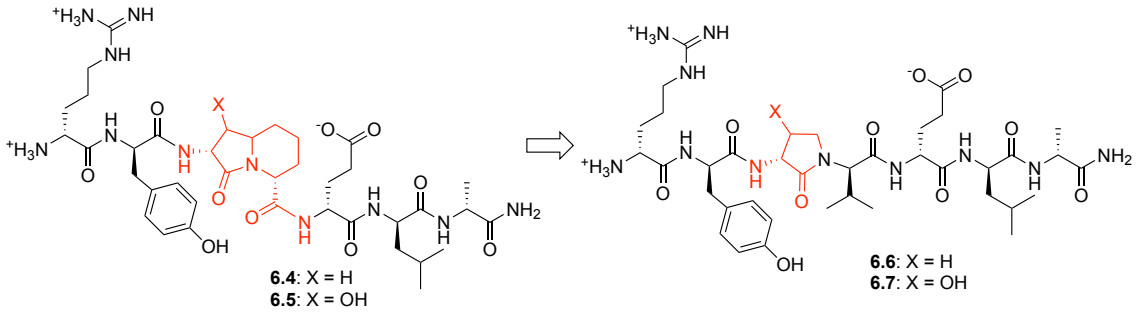

Figure 6.3. Proposed I[9]aa peptide for IL-1R target

With the goal of exploring various I[9]aa and 7-HO-I[9]aa stereoisomers in peptide **6.1**, the synthesis of peptide **6.5** was first performed using (2*S*,6*S*,7*R*,8*S*)-7-HO-I[9]aa **3.13** (Scheme 6.1).

Initially, linear precursor **6.9** was prepared by standard Fmoc-based solid-phase synthesis on Rink amide resin (Scheme 6.1).[2] The D-enantiomer of *N*-(Fmoc)-7-HO-I[9]aa-OMe **3.13** of was prepared from D-Ser using the protocols described in Chapter 3. Ester **3.13b** was hydrolyzed with 6N HCl and coupled to *O*-*tert*-butyl-D-glutamyl-D-leucinyl-D-alanine Rink amide resin **6.9** using

HBTU, DIEA, and DMF to give the corresponding resin-bound pentapeptide **6.10**. Subsequent removals of the Fmoc protection using 20% piperidine in DMF, and peptide elongation by sequential couplings of *N*-Fmoc-*O*-*tert*-butyl-tyrosine and *N*-Boc-*N*-(Pmc)arginine as described above gives protected heptapeptide resin **6.11**. Resin cleavage was performed using a cocktail of 95:2.5:2.5 TFA/H_2O/TES to furnish peptides **6.5** in 20% crude purity. Purification by HPLC provided in 6% overall yield peptide **6.5**, which has been submitted for biological testing.

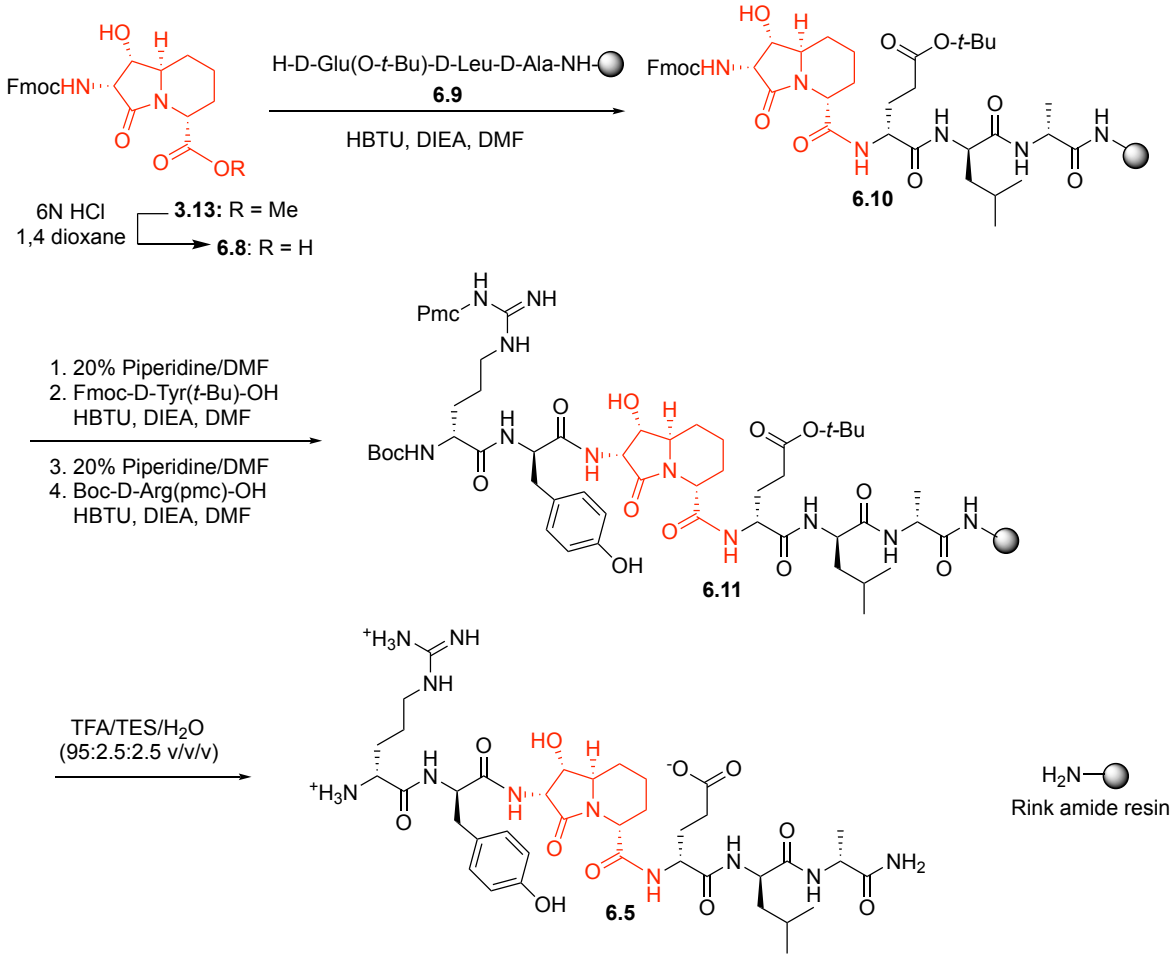

Scheme 6.1. Solid-phase synthesis of Hydroxy-I[9]aa peptide **6.5**

In the light of earlier investigation of 101.10 with Agl residues,[5] a systematic scan of the 101.10 sequence using I[9]aa and substituted analogs may provide significant insight into the conformational requirements for IL-1R modulation. In such studies, CD and NMR spectroscopic

investigations of effective analogs may demonstrate conformational requirements for biological activity.

Several other investigations may be launched based on the methods and molecules described in this thesis. For example, by extending the iodo transannular cyclization to lactams having other ring sizes and olefin positions using conditions explored in Chapter 3, an expanded range of peptide surrogates may be obtained. Further mechanistic insight into the transannular cyclization may be obtained by computational analysis, and is now being pursued in collaboration with the laboratory of Professor Gino DiLabio in the Department of Chemistry, at The University of British Columbia, Okanagan. Different biological targets may also be explored using the described methods and novel bicycles. On another note, Vyp and Von (Chapter 4) may be used as synthetic intermediates in the RCM-TC strategy to make peptidomimetics with proline and arginine residues. Finally, the *p*-azido residue that was attached to PDC113.824 (Chapter 5) exhibited activity in reducing PGF2α-induced myometrial contractions, and would be worth interesting to develop into a photo-labelling probe to tag FP to identify the site of allosteric interaction.[6]

6.3 Conclusion

Study of the transannular cyclization has begun to provide mechanic understanding of stereochemical and regiochemical outcomes of this reaction, which offers potential for preparing a verity of bicyclic heterocycle structures. Already, an effective, atom-economical means for producing lactam and bicycle peptidomimetics has been developed to provide different ring sizes using a common synthetic strategy. Potential for these peptidomimetics to replicate secondary structures has also been established by our X-ray data which has shown capacity for mimicry of different β-turn conformations. The transannular cyclization method may have general utility for

the organic community engaged in alkaloid natural product synthesis, because pyrrolizidines, indolizidines and quinolizidines are abundant in nature. As demonstrated by our efforts to synthesize FP modulators possessing ring-substituted I^2aa residues to develop therapeutics to delay labour and inhibit preterm birth, our methods to prepare azabicycloalkanone amino acids may have many biomedical applications. This thesis has thus addressed important issues in organic reactivity, in the synthesis of heterocycles, in peptide mimicry, and in medicinal chemistry opening a new horizon for research in peptide science towards drug discovery.

6.4 Experimental section

_N_-Fmoc-[(2*S*,6*S*,7*R*,8*S*)-7-HO-I^9aa]-D-Glu(*t*-Bu)-D-Leu-D-Ala-NH-Rink amide resin (6.10)

A solution of acid (2*S*,6*S*,7*R*,8*S*)-**6.9** (1 eq., 55 mg, 0.13 mmol) and 2-(1H-benzotriazol-1-yl)-1,1,3,3-tetramethyluronium hexafluorophosphate (HBTU, 1 eq., 95 mg, 0.26 mmol) in dimethylformamide (DMF, 2 mL) was stirred for 1 min, treated with *N*,*N*-diisopropylethylamine (DIEA, 2 eq., 34 mg, 0.26 mmol), stirred for 5 min and added to H-D-Glu(*t*-Bu)-D-Leu-D-Ala-NH-Rink amide resin **6.6** (312 mg, 0.5 mmol/g, 0.16 mmol, prepared according to the procedure in reference 4), which was swollen in DMF (2 mL) in a 3-mL plastic filtration tube equipped with a polyethylene filter. The resin mixture was shaken at rt for 12 h. The liquid phase was removed by filtration. The resin was repeatedly (3x per solvent) washed (20 s per wash) with DMF and DCM, and dried under vacuum to afford resin **6.7**. To assess resin-bound peptide purity, a resin aliquot (5 mg) was placed into a 1-mL plastic filtration tube equipped with a polyethylene filter, treated with 0.5 mL of a 95:2.5:2.5 cocktail of TFA:H_2O:triethylsilane (TES) at rt for 1 h, and filtered. The filtrate was collected in a 1.5 mL tube and concentrated by purging with a stream of air. The residue was treated with Et_2O (1 mL), and centrifuged for 2 min. After decantation, the precipitate was dissolved in H_2O (1 mL) and analyzed by LCMS of *N*-Fmoc-[(2*S*,6*S*,7*R*,8*S*)-7-

HO-I^{9}aa]-D-Glu-D-Leu-D-Ala-NH_2 [10–90% MeCN (0.1% FA)/ water (0.1% FA), 14 min, RT 7.58 min].

H-D-Arg-D-Tyr-[2*S*,6*S*,7*R*,8*S*-7-HO-I^{9}aa]-D-Glu(*t*-Bu)-D-Leu-D-Ala-NH_2 (6.11)

Resin **6.10** was swollen in DMF (2 mL), treated with piperidine (1 mL), shaken for 1 h, filtered and washed by shaking (1 min/wash) with DMF (3 × 7 mL) and DCM (3 × 7 mL), and then dried in vacuo. The resulting resin was swollen in DMF (3 mL) and coupled with Fmoc-D-Tyr(*t*-Bu)-OH, HBTU (1 eq., 190 mg, 0.52 mmol) and (DIEA, 4 eq., 68 mg, 0.52 mmol) for overnight.

The Fmoc group was removed and Boc-D-Arg(Pmc)-OH was coupled using the conditions described above. The resin was cleaved from the peptide by shaking in a cocktail of TFA/H_2O/TES (7 mL, 95/2.5/2.5, v/v/v) for 2 h, filtered, and washed with TFA (7 mL). The combined filtrate and washings were concentrated in vacuo. The residue was dissolved in a minimum volume of TFA (~1 mL), transferred to a centrifuge tube and precipitated by the addition of ice-cold diethyl ether (40 mL). The mixture was centrifuged. The diethyl ether was decanted from the tube. The precipitated peptide was triturated twice with cold diethyl ether. The resulting white solid was dissolved in water (10 mL) and freeze-dried to give a white fluffy solid that was purified by preparative RP-HPLC, using the specified conditions. Crude peptide was purified by preparative HPLC (Phenomenex Gemini 5 μm C18 column, 250 mm X 21.2 mm) using a gradient from 20% to 80% acetonitrile (containing 0.1% FA) in water (containing 0.1% FA). Free-drying of the collected fractions afforded peptide **6.11**. Analytical HPLC demonstrated the peptide to be of X% purity: 5 to 50% MeCN (0.1% FA) in water (0.1% FA) over 14 min, flow rate of 0.8 mL/min on a on XTerra TM C18 column C18 (3.5 μm, 2.1 mm X 50mm). HRMS calcd for $C_{38}H_{59}N_{11}O_{11}$ $[M+H]^+$, 846.4468; found 846.4430.

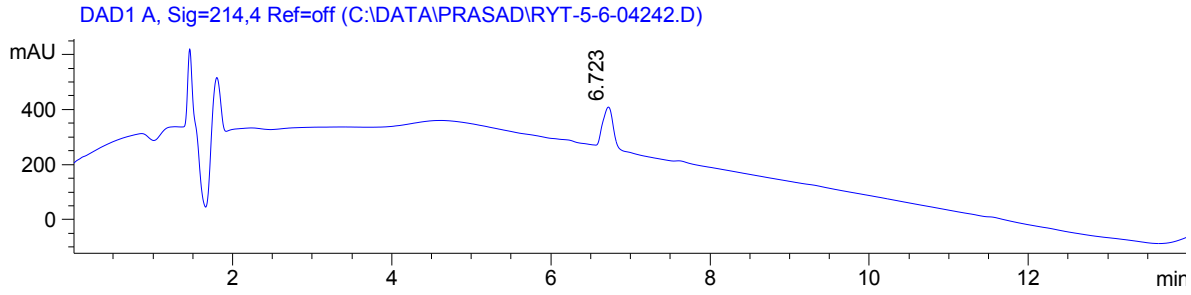

Figure 6.4. LCMS chromatogram for the purity of the peptide **6.5**

6.5 References:

1. (a) Freidinger, R. M.; Veber, D. F.; Perlow, D. S.; Saperstein, R., Bioactive conformation of luteinizing hormone-releasing hormone: evidence from a conformationally constrained analog. *Science* **1980**, *210*, 656–658; (b) Freidinger, R. M.; Perlow, D. S.; Veber, D. F., Protected lactam-bridged dipeptides for use as conformational constraints in peptides. *J. Org. Chem.* **1982**, *47*, 104–109.

2. Boutard, N.; Turcotte, S.; Beauregard, K.; Quiniou, C.; Chemtob, S.; Lubell, W. D., Examination of the active secondary structure of the peptide 101.10, an allosteric modulator of the interleukin-1 receptor, by positional scanning using β-amino γ-lactams. *J. Pept. Sci.* **2011**, *17*, 288–296.

3. (a) Ede, N.; Lim, N.; Rae, I.; Ng, F.; Hearn, M., Synthesis and evaluation of constrained peptide analogues related to the N-terminal region of human growth hormone. *J. Pept. Res.* **1991**, *4*, 171–176; (b) EDE, N. J.; RAE, I. D.; HEARN, M. T., Synthesis and conformation of constrained peptides with hypoglycaemic activity derived from human growth hormone. *Int. J. Pept. Protein Res.* **1994**, *44*, 568–581; (c) Elliott, R. L.; Kopecka, H.; Tufano, M. D.; Shue, Y.-K.; Gauri, A. J.; Lin, C.-W.; Bianchi, B. R.; Miller, T. R.; Witte, D. G., Novel Asp32-replacement tetrapeptide analogs as potent and selective CCK-A agonists. *J. Med. Chem.* **1994**, *37*, 1562–1568.

4. Geranurimi, A.; Cheng, C. W.; Quiniou, C.; Hou, X.; Zhu, T.; Rivera, J. C.; St-Cyr, D. J.; Beauregard, K.; Bernard-Gauthier, V.; Chemtob, S., Probing anti-inflammatory properties independent of NF-κB through conformational constraint of peptide-based interleukin-1β receptor biased ligands. *Front. Chem.* **2019**, *7*, 23.

5. Jamieson, A. G.; Boutard, N.; Beauregard, K.; Bodas, M. S.; Ong, H.; Quiniou, C.; Chemtob, S.; Lubell, W. D., Positional scanning for peptide secondary structure by systematic solid-phase synthesis of amino lactam peptides. *J. Am. Chem. Soc.* **2009**, *131*, 7917–7927.

6. Bourguet, C. B.; Goupil, E.; Tassy, D.; Hou, X.; Thouin, E.; Polyak, F.; Hébert, T. E.; Claing, A.; Laporte, S. A.; Chemtob, S., Targeting the prostaglandin F2α receptor for preventing preterm labor with azapeptide tocolytics. *J. Med. Chem.* **2011**, *54*, 6085–6097.

Spectral data for Article 1.

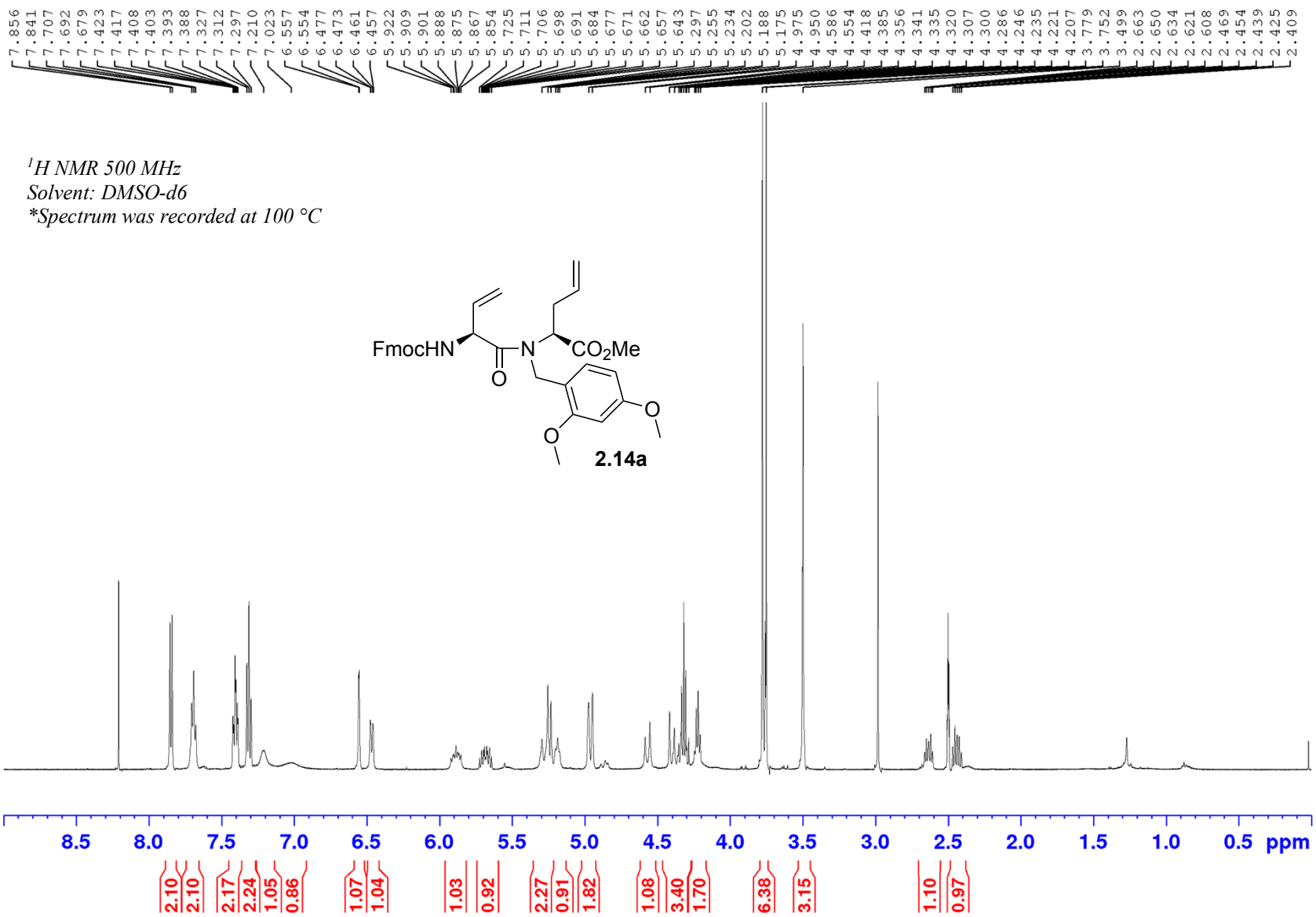
7.856 7.841 7.707 7.692 7.679 7.423 7.417 7.408 7.403 7.393 7.388 7.327 7.312 7.297 7.210 7.023 6.557 6.554 6.477 6.473 6.461 6.457 5.922 5.909 5.901 5.888 5.875 5.867 5.854 5.725 5.711 5.706 5.698 5.691 5.684 5.677 5.671 5.662 5.657 5.643 5.297 5.255 5.234 5.202 5.188 5.175 4.975 4.950 4.586 4.554 4.418 4.385 4.356 4.341 4.335 4.320 4.307 4.300 4.286 4.246 4.235 4.221 4.207 3.779 3.752 3.499 2.663 2.650 2.634 2.621 2.608 2.469 2.454 2.439 2.425 2.409
1H NMR 500 MHz
Solvent: DMSO-d6
*Spectrum was recorded at 100 °C
FmocHN
N
CO2Me
O
O
O
2.14a
8.5 8.0 7.5 7.0 6.5 6.0 5.5 5.0 4.5 4.0 3.5 3.0 2.5 2.0 1.5 1.0 0.5 ppm
2.10 2.10 2.17 2.24 1.05 0.86 1.07 1.04 1.03 0.92 2.27 0.91 1.82 1.08 3.40 1.70 6.38 3.15 1.10 0.97

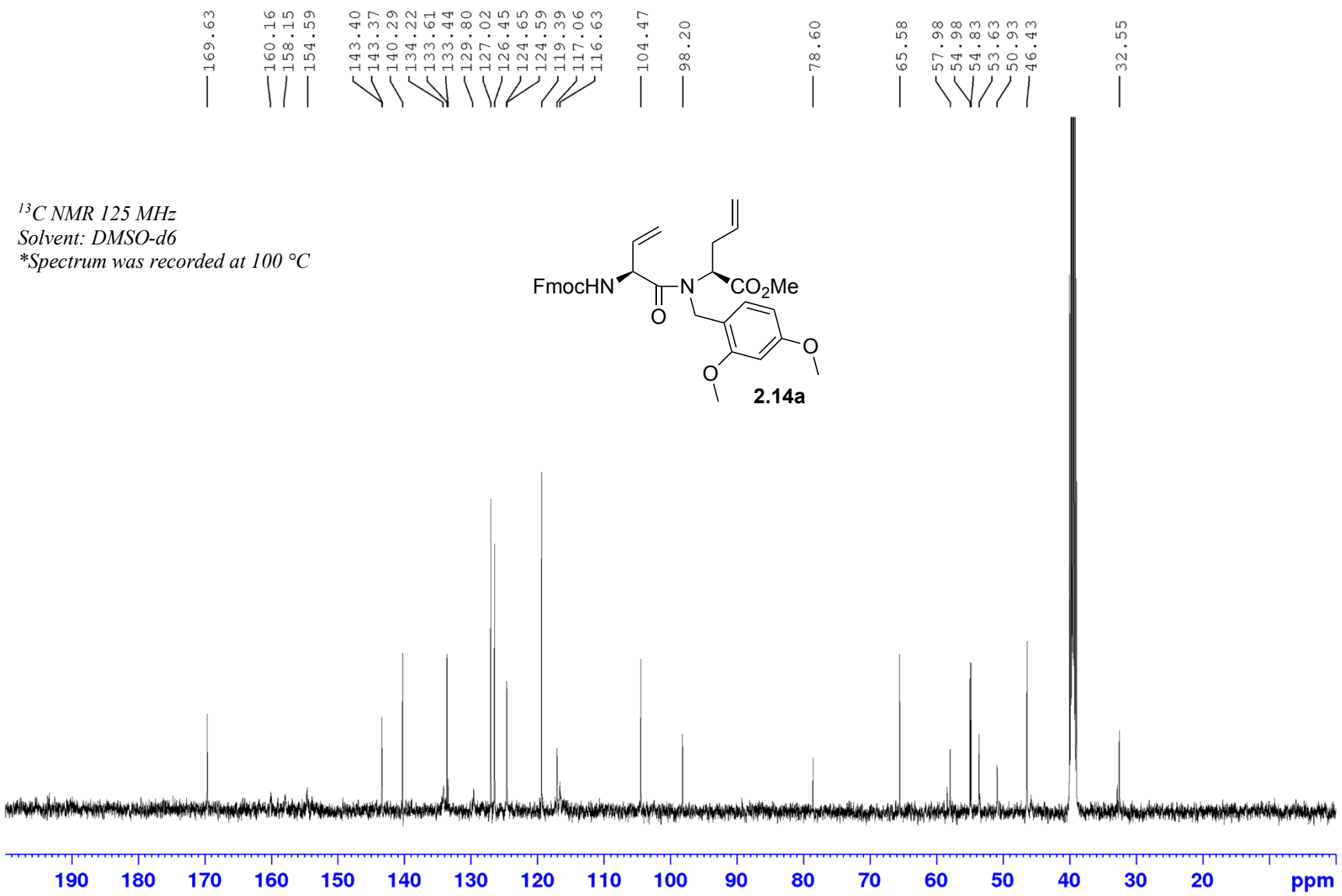
169.63
160.16
158.15
154.59
143.40
143.37
140.29
134.22
133.61
133.44
129.80
127.02
126.45
124.65
124.59
119.39
117.06
116.63
104.47
98.20
78.60
65.58
57.98
54.98
54.83
53.63
50.93
46.43
32.55
13C NMR 125 MHz
Solvent: DMSO-d6
*Spectrum was recorded at 100 °C
FmocHN
N
CO2Me
O
O
O
2.14a
190
180
170
160
150
140
130
120
110
100
90
80
70
60
50
40
30
20
ppm

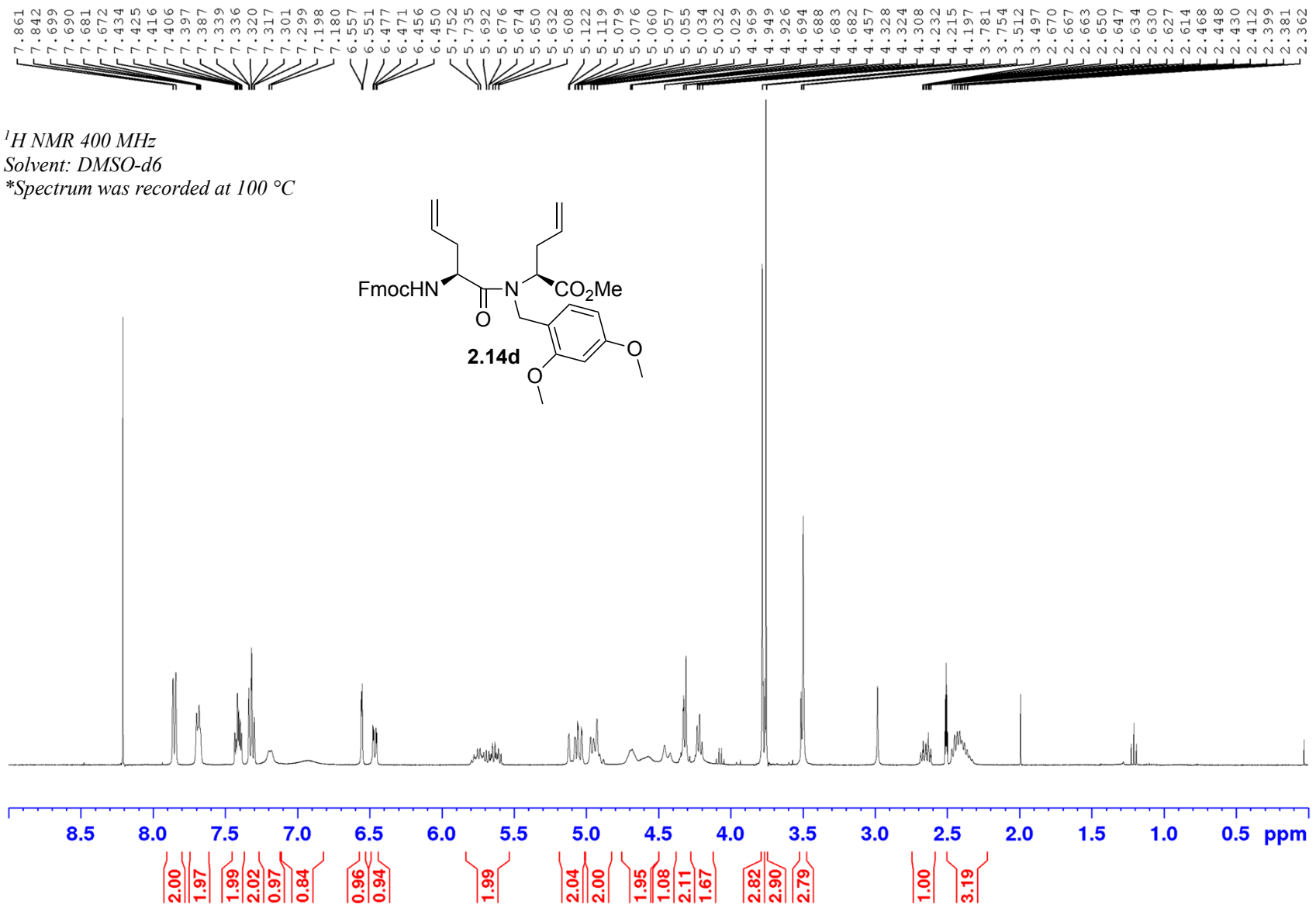
7.861
7.842
7.699
7.690
7.681
7.672
7.434
7.425
7.416
7.406
7.397
7.387
7.339
7.336
7.320
7.317
7.301
7.299
7.198
7.180
6.557
6.551
6.477
6.471
6.456
6.450
5.752
5.735
5.692
5.676
5.674
5.650
5.632
5.608
5.122
5.119
5.079
5.076
5.060
5.057
5.055
5.034
5.032
5.029
4.969
4.949
4.926
4.694
4.688
4.683
4.682
4.457
4.328
4.324
4.308
4.232
4.215
4.197
3.781
3.754
3.512
3.497
2.670
2.667
2.663
2.650
2.647
2.634
2.630
2.627
2.614
2.468
2.448
2.430
2.412
2.399
2.381
2.362
1H NMR 400 MHz
Solvent: DMSO-d6
*Spectrum was recorded at 100 °C
FmocHN
N
CO2Me
O
O
O
2.14d
8.5
8.0
7.5
7.0
6.5
6.0
5.5
5.0
4.5
4.0
3.5
3.0
2.5
2.0
1.5
1.0
0.5
ppm
2.00
1.97
1.99
2.02
0.97
0.84
0.96
0.94
1.99
2.04
2.00
1.95
1.08
2.11
1.67
2.82
2.90
2.79
1.00
3.19

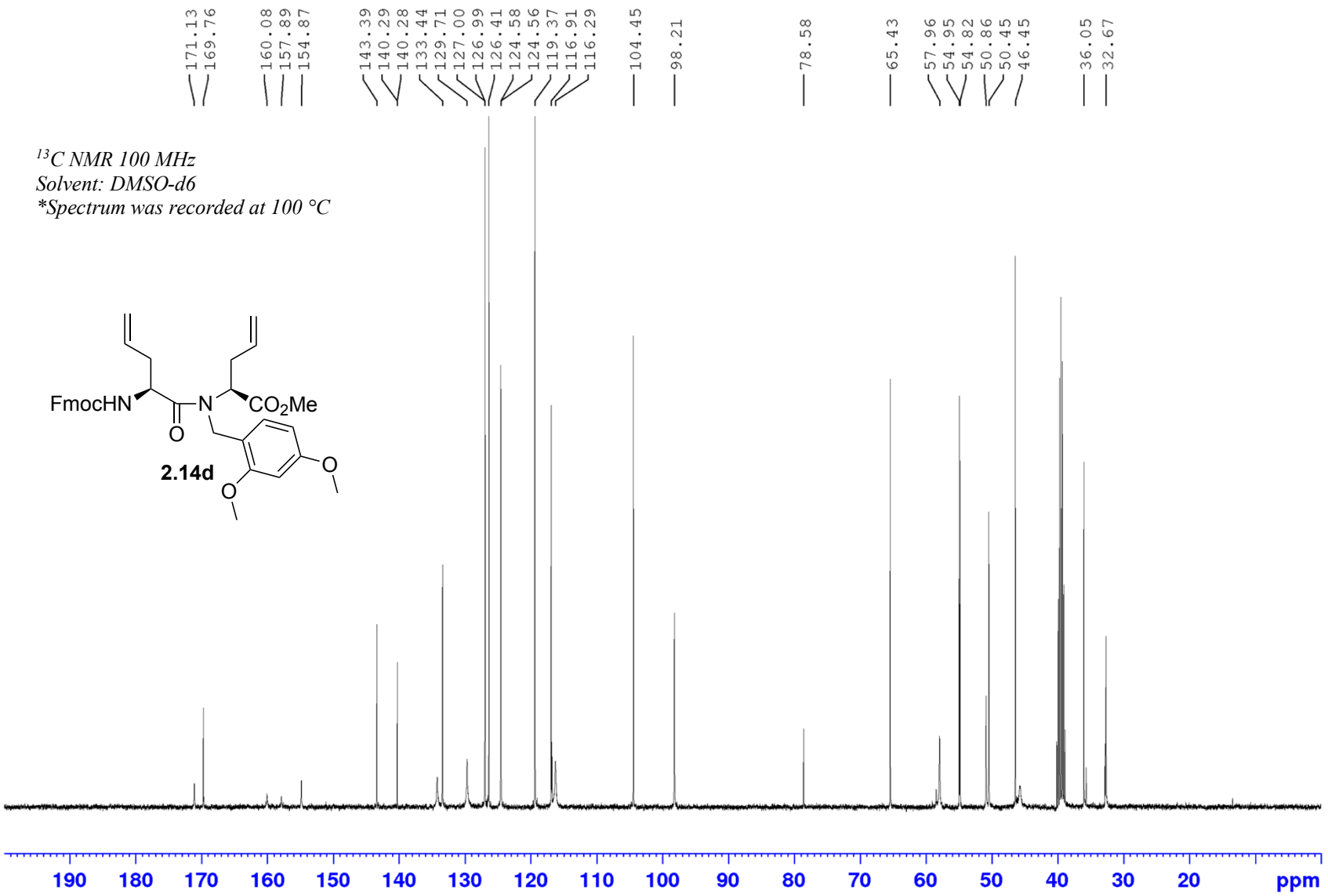
171.13
169.76
160.08
157.89
154.87
143.39
140.29
140.28
133.44
129.71
127.00
126.99
126.41
124.58
124.56
119.37
116.91
116.29
104.45
98.21
78.58
65.43
57.96
54.95
54.82
50.86
50.45
46.45
36.05
32.67
13C NMR 100 MHz
Solvent: DMSO-d6
*Spectrum was recorded at 100 °C
FmocHN
N
CO2Me
O
O
O
2.14d
190
180
170
160
150
140
130
120
110
100
90
80
70
60
50
40
30
20
ppm

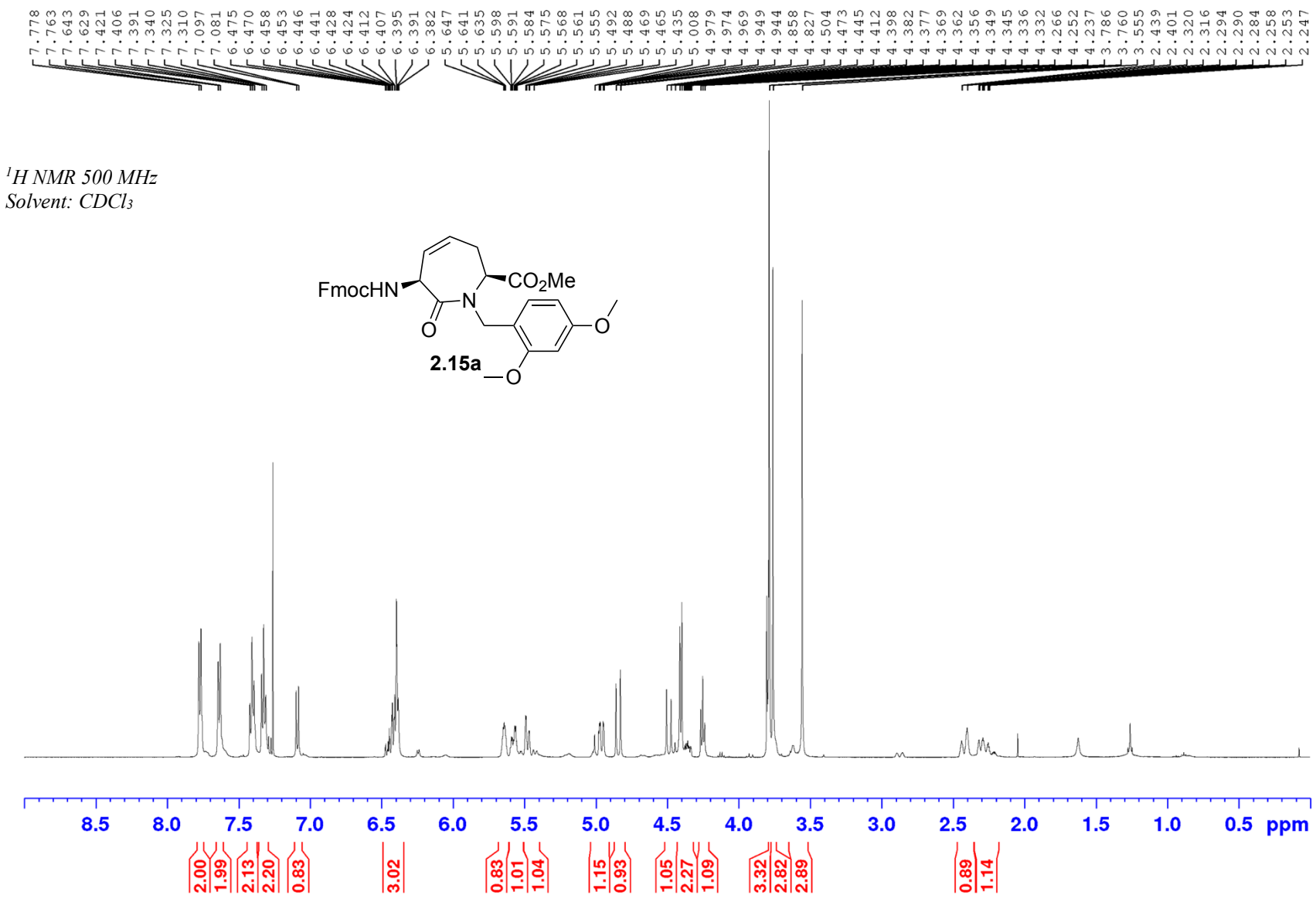

[1]H NMR 500 MHz
Solvent: $CDCl_3$

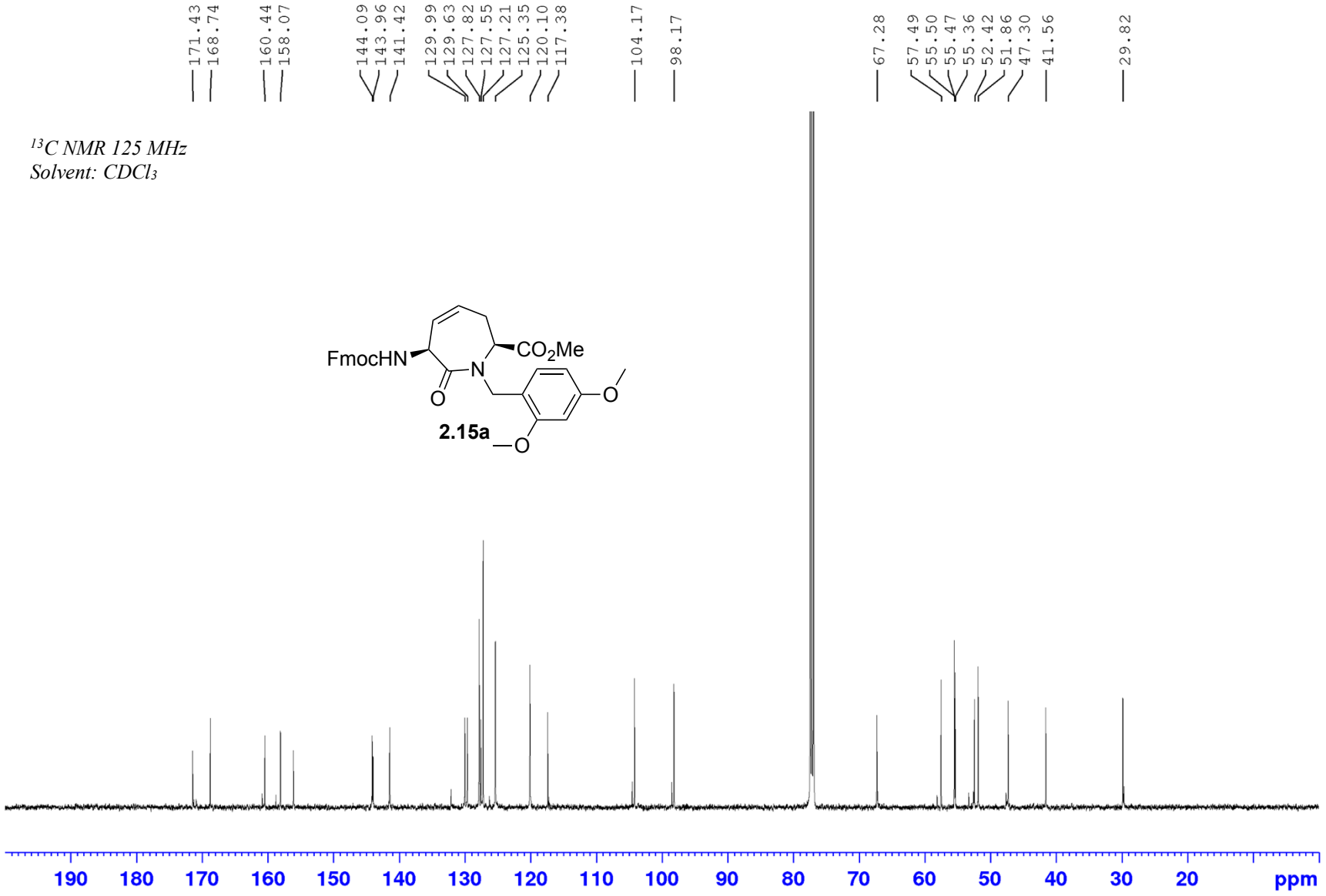
171.43
168.74
160.44
158.07
144.09
143.96
141.42
129.99
129.63
127.82
127.55
127.21
125.35
120.10
117.38
104.17
98.17
67.28
57.49
55.50
55.47
55.36
52.42
51.86
47.30
41.56
29.82
13C NMR 125 MHz
Solvent: CDCl3
FmocHN
CO2Me
N
O
O
O
2.15a
190
180
170
160
150
140
130
120
110
100
90
80
70
60
50
40
30
20
ppm

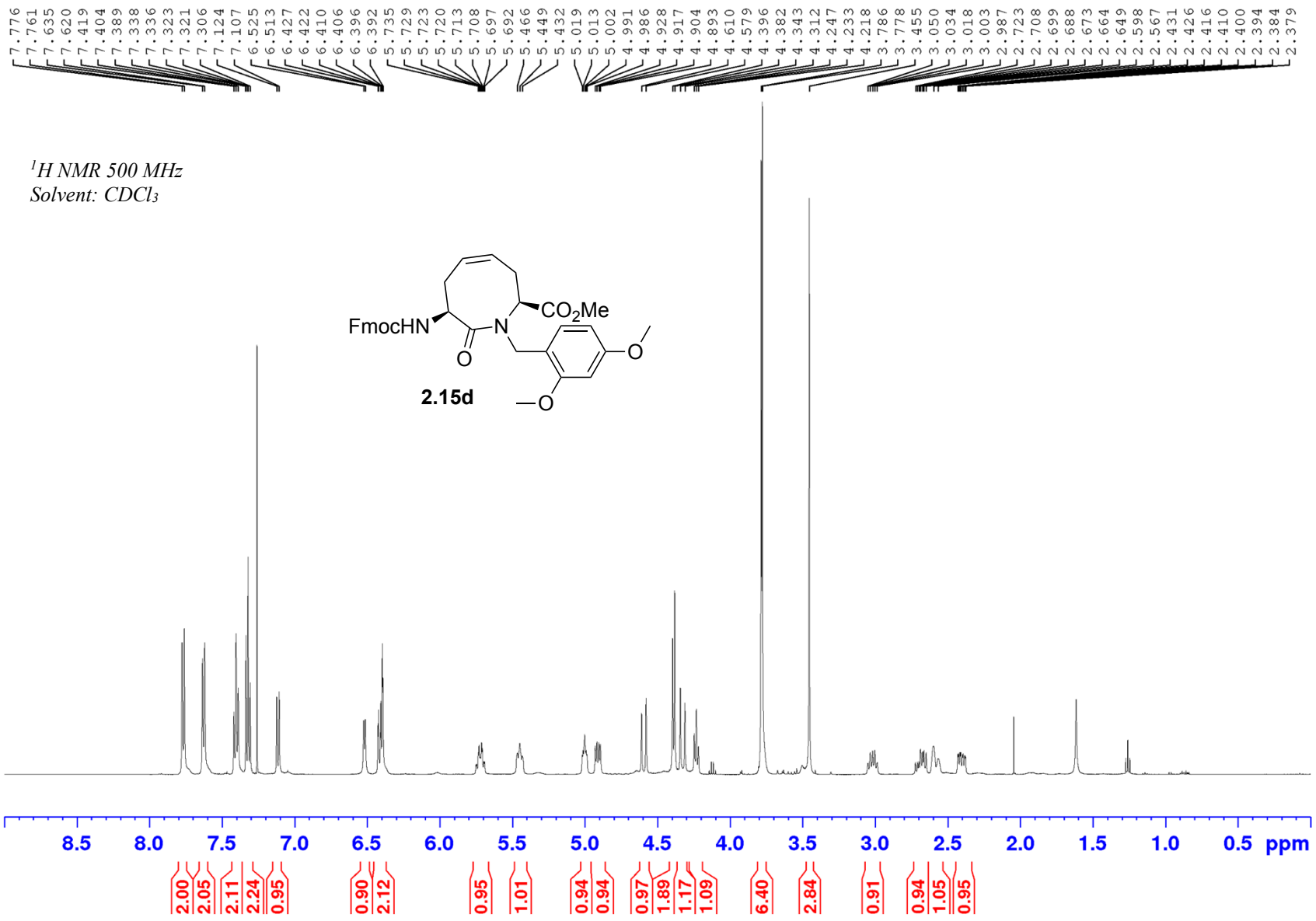
7.776
7.761
7.635
7.620
7.419
7.404
7.389
7.338
7.336
7.323
7.321
7.306
7.124
7.107
6.525
6.513
6.427
6.422
6.410
6.406
6.396
6.392
5.735
5.729
5.723
5.720
5.713
5.708
5.697
5.692
5.466
5.449
5.432
5.019
5.013
5.002
4.991
4.986
4.928
4.917
4.904
4.893
4.610
4.579
4.396
4.382
4.343
4.312
4.247
4.233
4.218
3.786
3.778
3.455
3.050
3.034
3.018
3.003
2.987
2.723
2.708
2.699
2.688
2.673
2.664
2.649
2.598
2.567
2.431
2.426
2.416
2.410
2.400
2.394
2.384
2.379
1H NMR 500 MHz
Solvent: CDCl3
FmocHN
N
CO2Me
O
O
O
2.15d
8.5
8.0
7.5
7.0
6.5
6.0
5.5
5.0
4.5
4.0
3.5
3.0
2.5
2.0
1.5
1.0
0.5
ppm
2.00
2.05
2.11
2.24
0.95
0.90
2.12
0.95
1.01
0.94
0.94
0.97
1.89
1.17
1.09
6.40
2.84
0.91
0.94
1.05
0.95

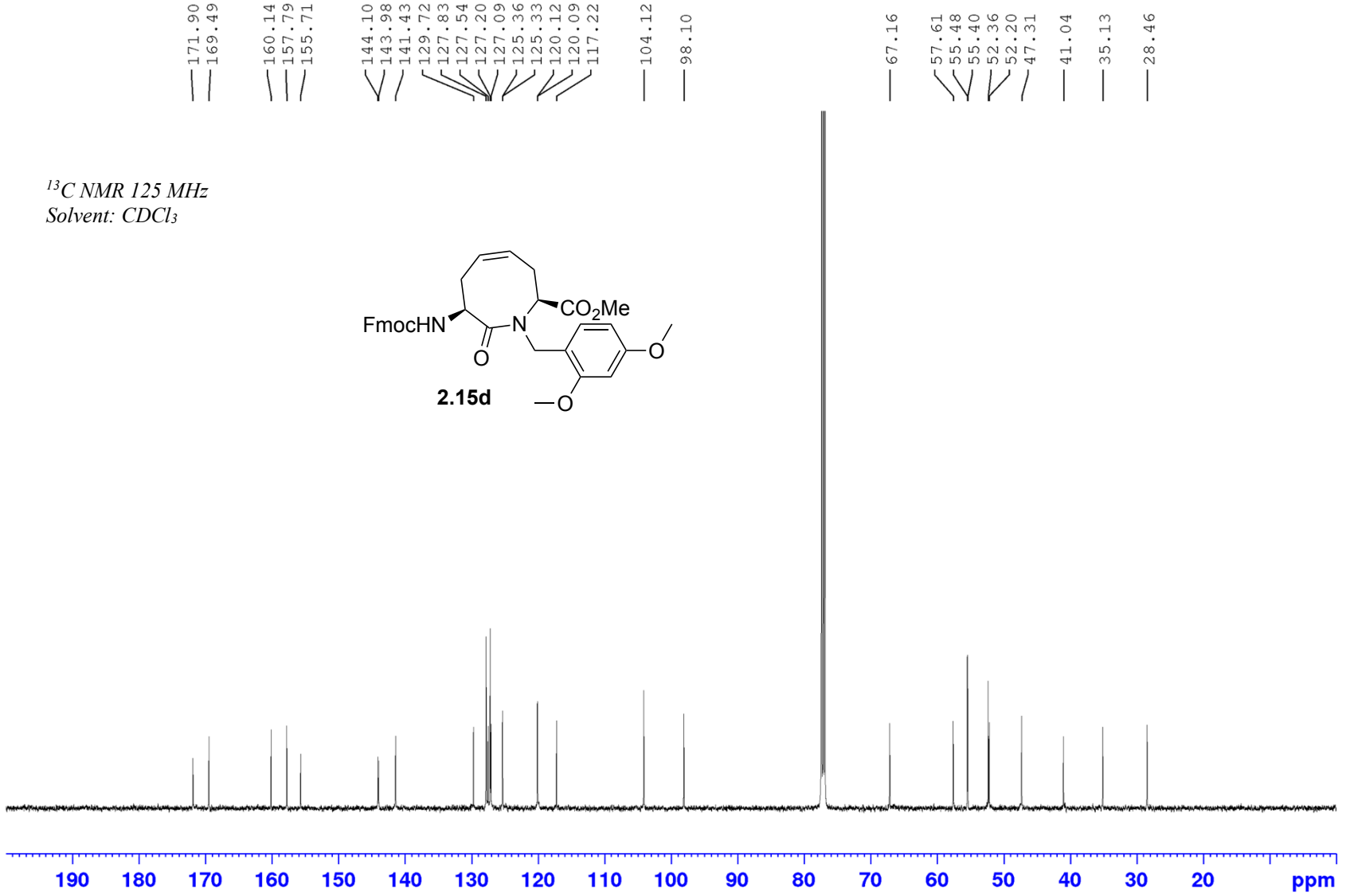
171.90
169.49
160.14
157.79
155.71
144.10
143.98
141.43
129.72
127.83
127.54
127.20
127.09
125.36
125.33
120.12
120.09
117.22
104.12
98.10
67.16
57.61
55.48
55.40
52.36
52.20
47.31
41.04
35.13
28.46
13C NMR 125 MHz
Solvent: CDCl3
FmocHN
N
CO2Me
O
O
O
2.15d
190
180
170
160
150
140
130
120
110
100
90
80
70
60
50
40
30
20
ppm

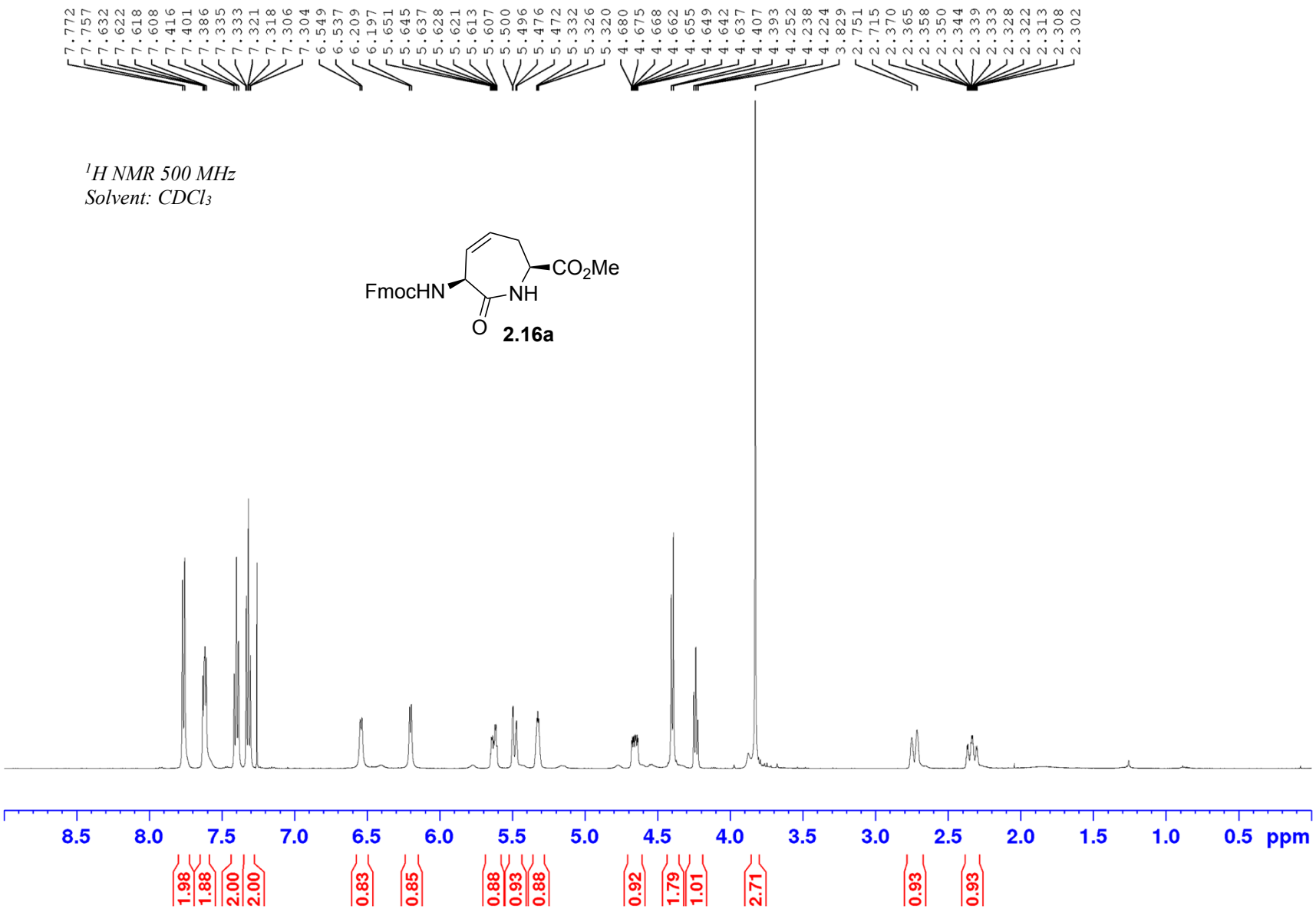
7.772
7.757
7.632
7.622
7.618
7.608
7.416
7.401
7.386
7.335
7.333
7.321
7.318
7.306
7.304
6.549
6.537
6.209
6.197
5.651
5.645
5.637
5.628
5.621
5.613
5.607
5.500
5.496
5.476
5.472
5.332
5.326
5.320
4.680
4.675
4.668
4.662
4.655
4.649
4.642
4.637
4.407
4.393
4.252
4.238
4.224
3.829
2.751
2.715
2.370
2.365
2.358
2.350
2.344
2.339
2.333
2.328
2.322
2.313
2.308
2.302
1H NMR 500 MHz
Solvent: CDCl3
FmocHN
NH
CO2Me
O
2.16a
8.5
8.0
7.5
7.0
6.5
6.0
5.5
5.0
4.5
4.0
3.5
3.0
2.5
2.0
1.5
1.0
0.5
ppm
1.98
1.88
2.00
2.00
0.83
0.85
0.88
0.93
0.88
0.92
1.79
1.01
2.71
0.93
0.93

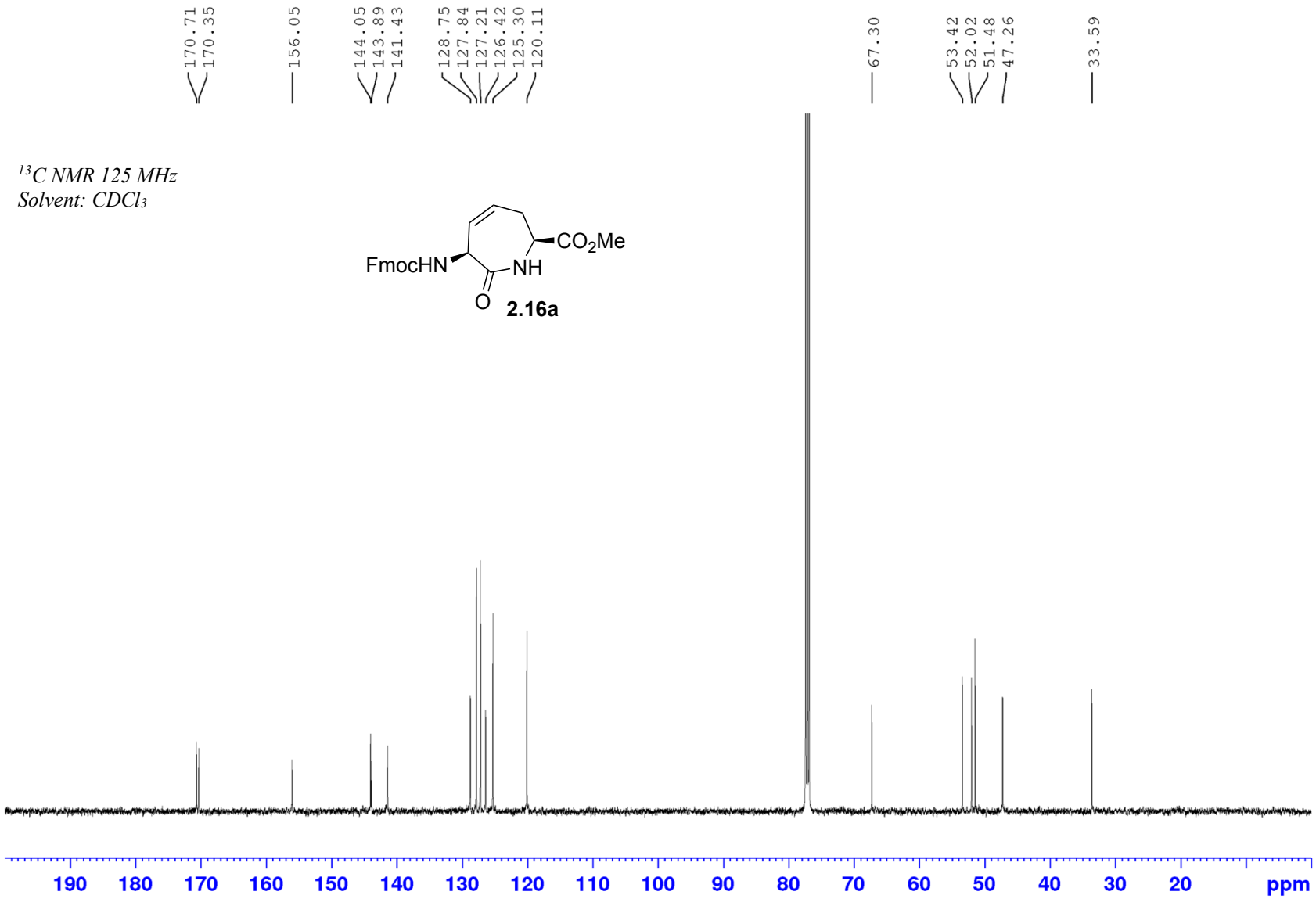
170.71
170.35
156.05
144.05
143.89
141.43
128.75
127.84
127.21
126.42
125.30
120.11
67.30
53.42
52.02
51.48
47.26
33.59
13C NMR 125 MHz
Solvent: CDCl3
CO2Me
FmocHN
NH
O
2.16a
190
180
170
160
150
140
130
120
110
100
90
80
70
60
50
40
30
20
ppm

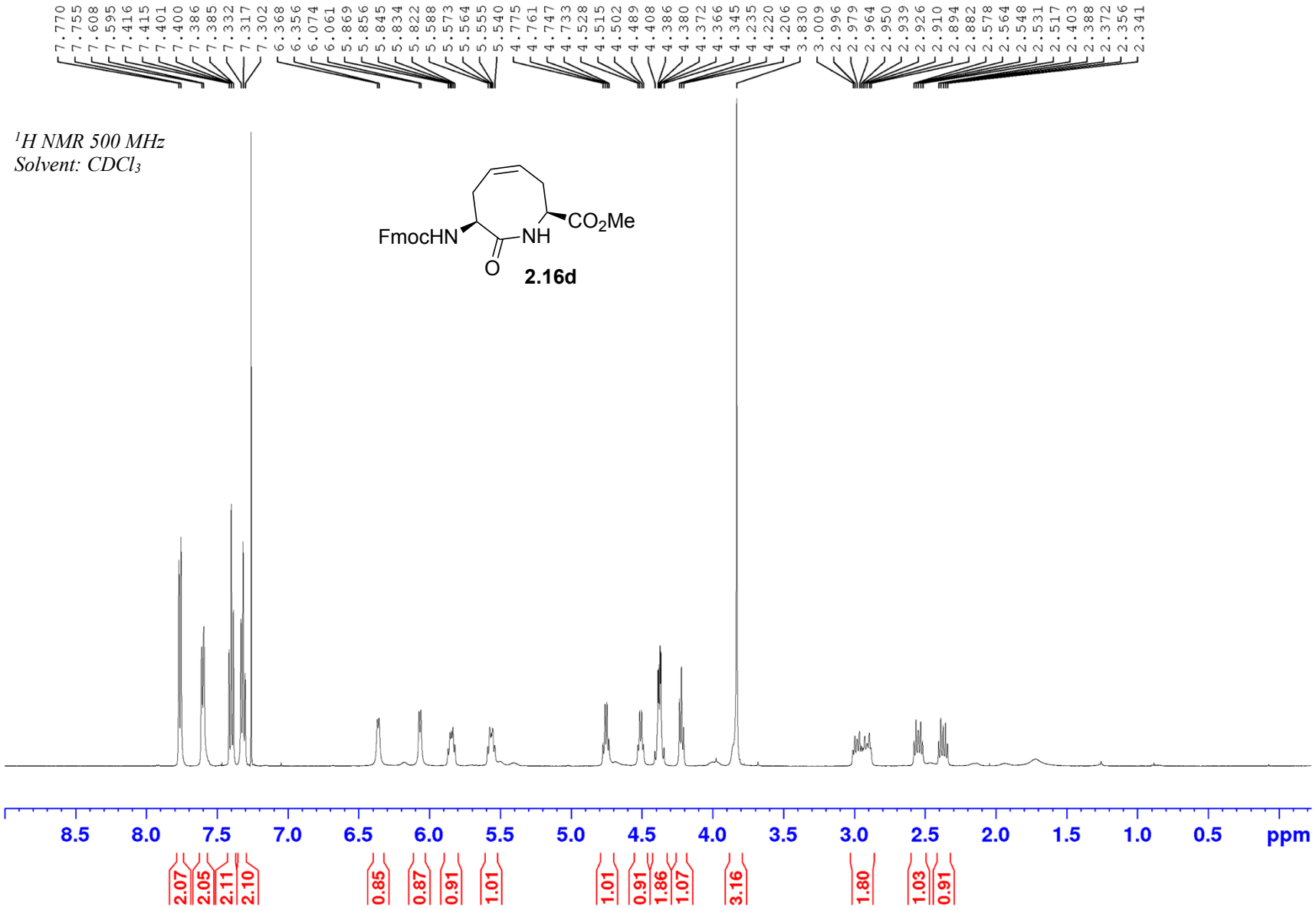
7.770
7.755
7.608
7.595
7.416
7.415
7.401
7.400
7.386
7.385
7.332
7.317
7.302
6.368
6.356
6.074
6.061
5.869
5.856
5.845
5.834
5.822
5.588
5.573
5.564
5.555
5.540
4.775
4.761
4.747
4.733
4.528
4.515
4.502
4.489
4.408
4.386
4.380
4.372
4.366
4.345
4.235
4.220
4.206
3.830
3.009
2.996
2.979
2.964
2.950
2.939
2.926
2.910
2.894
2.882
2.578
2.564
2.548
2.531
2.517
2.403
2.388
2.372
2.356
2.341
1H NMR 500 MHz
Solvent: CDCl3
FmocHN
NH
CO2Me
O
2.16d
8.5
8.0
7.5
7.0
6.5
6.0
5.5
5.0
4.5
4.0
3.5
3.0
2.5
2.0
1.5
1.0
0.5
ppm
2.07
2.05
2.11
2.10
0.85
0.87
0.91
1.01
1.01
0.91
1.86
1.07
3.16
1.80
1.03
0.91

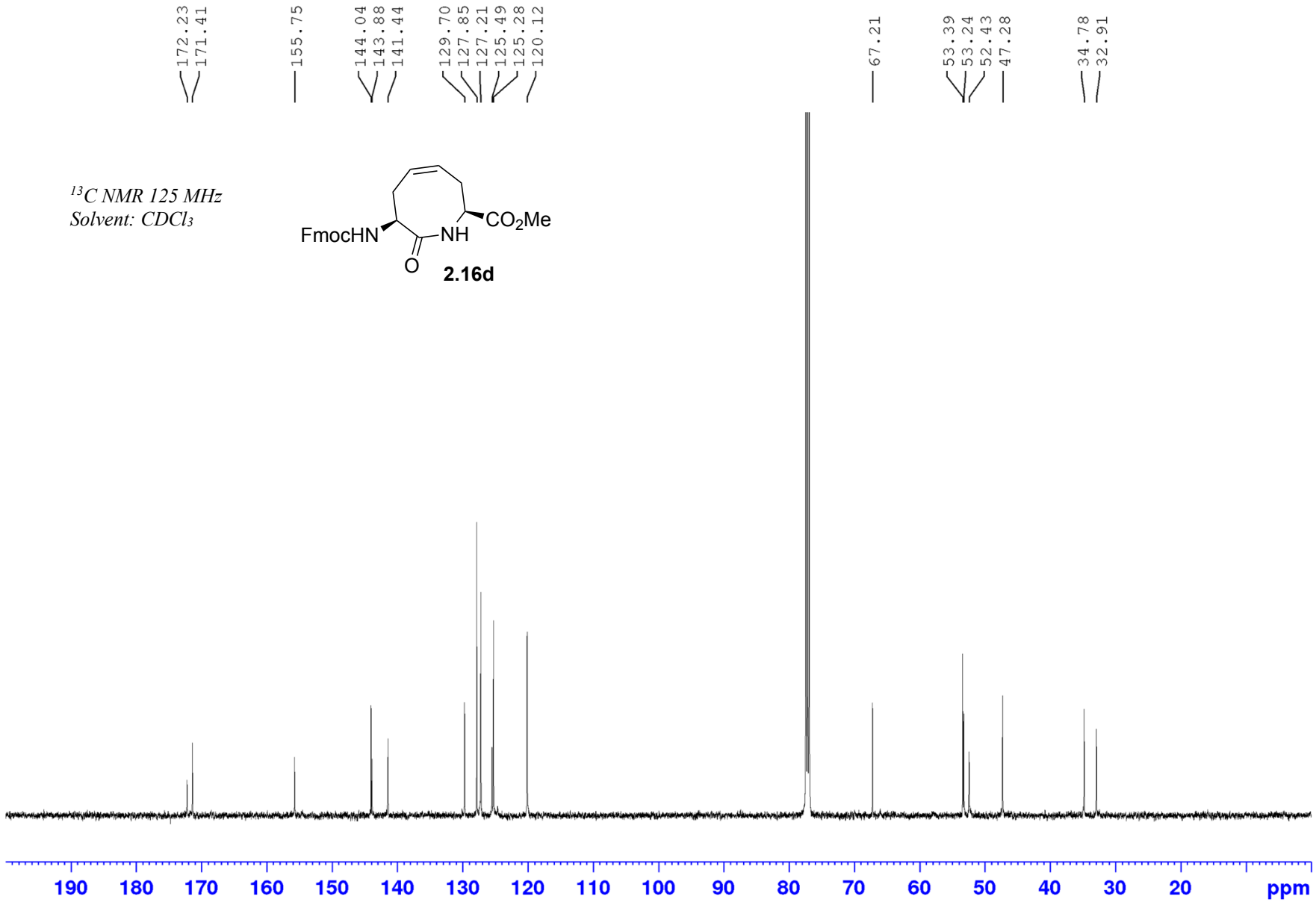
172.23
171.41
155.75
144.04
143.88
141.44
129.70
127.85
127.21
125.49
125.28
120.12
67.21
53.39
53.24
52.43
47.28
34.78
32.91
13C NMR 125 MHz
Solvent: CDCl3
FmocHN
NH
CO2Me
O
2.16d
190
180
170
160
150
140
130
120
110
100
90
80
70
60
50
40
30
20
ppm

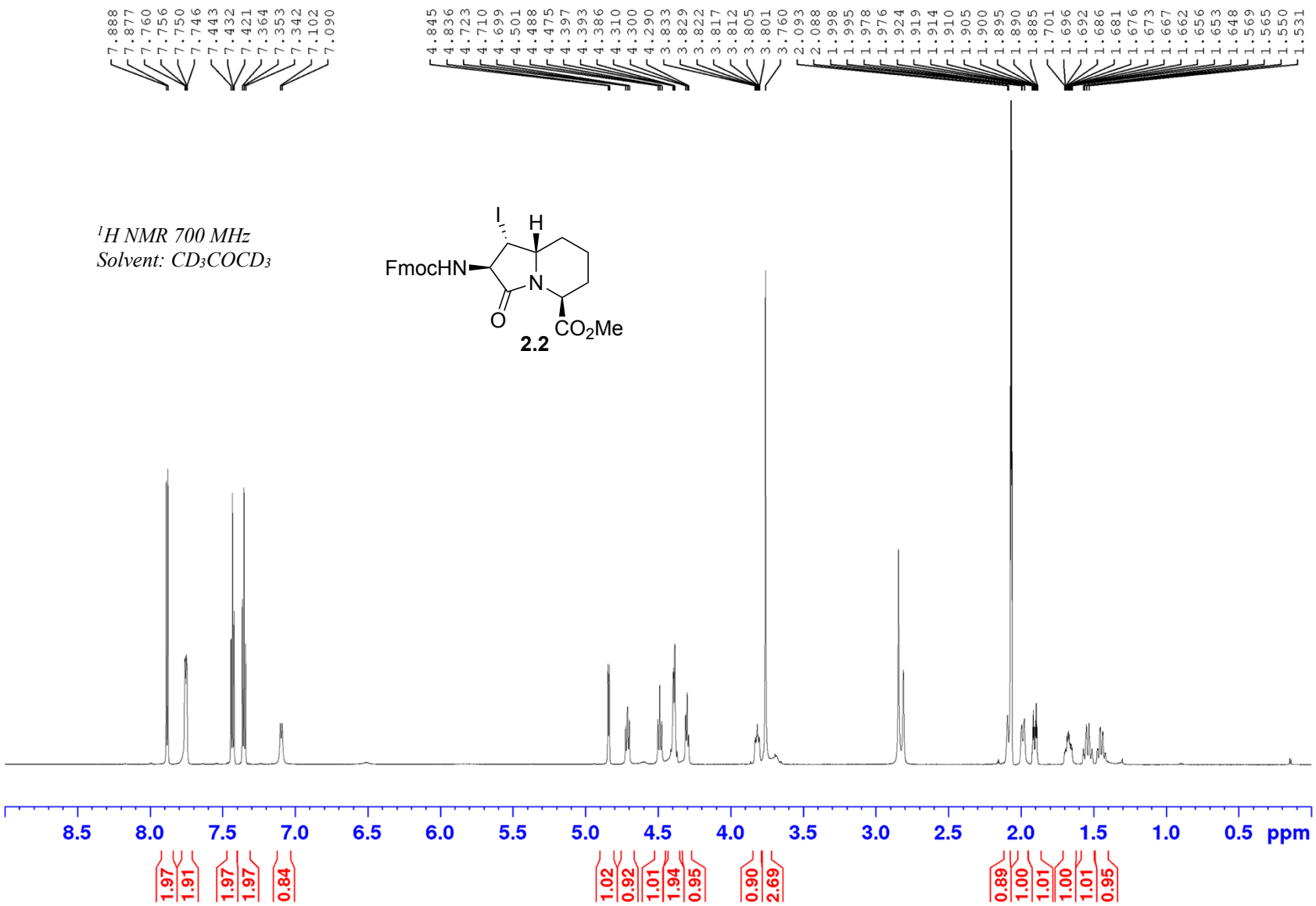
7.888
7.877
7.760
7.756
7.750
7.746
7.443
7.432
7.421
7.364
7.353
7.342
7.102
7.090
4.845
4.836
4.723
4.710
4.699
4.501
4.488
4.475
4.397
4.393
4.386
4.310
4.300
4.290
3.833
3.829
3.822
3.817
3.812
3.805
3.801
3.760
2.093
2.088
1.998
1.995
1.978
1.976
1.924
1.919
1.914
1.910
1.905
1.900
1.895
1.890
1.885
1.701
1.696
1.692
1.686
1.681
1.676
1.673
1.667
1.662
1.656
1.653
1.648
1.569
1.565
1.550
1.531
1H NMR 700 MHz
Solvent: CD3COCD3
I
H
FmocHN
N
O
CO2Me
2.2
8.5
8.0
7.5
7.0
6.5
6.0
5.5
5.0
4.5
4.0
3.5
3.0
2.5
2.0
1.5
1.0
0.5
ppm
1.97
1.91
1.97
1.97
0.84
1.02
0.92
1.01
1.94
0.95
0.90
2.69
0.89
1.00
1.01
1.00
1.01
0.95

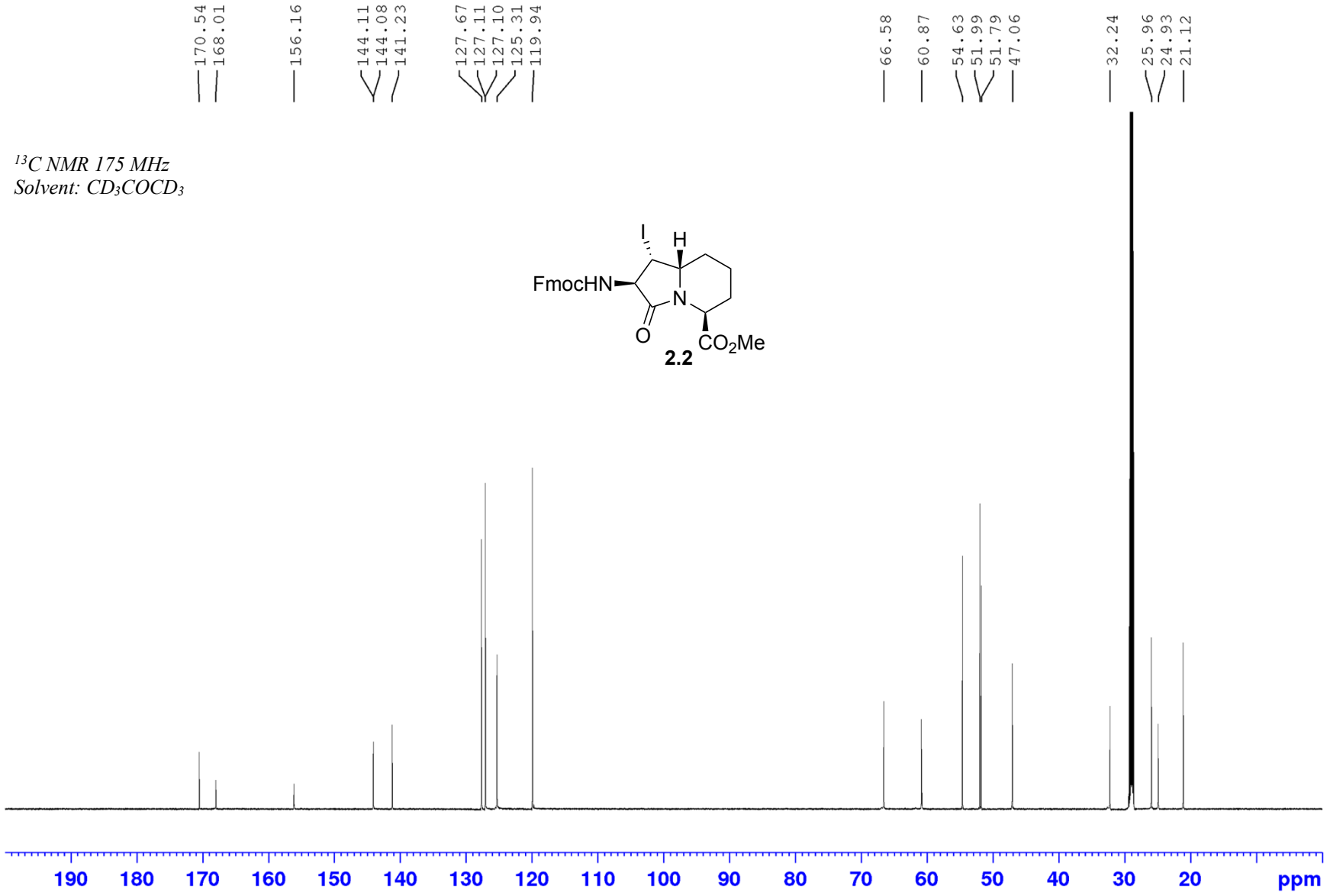
170.54
168.01
156.16
144.11
144.08
141.23
127.67
127.11
127.10
125.31
119.94
66.58
60.87
54.63
51.99
51.79
47.06
32.24
25.96
24.93
21.12
13C NMR 175 MHz
Solvent: CD3COCD3
I
H
FmocHN
N
O
CO2Me
2.2
190
180
170
160
150
140
130
120
110
100
90
80
70
60
50
40
30
20
ppm

DEPT 175 MHz
Solvent: CD_3COCD_3

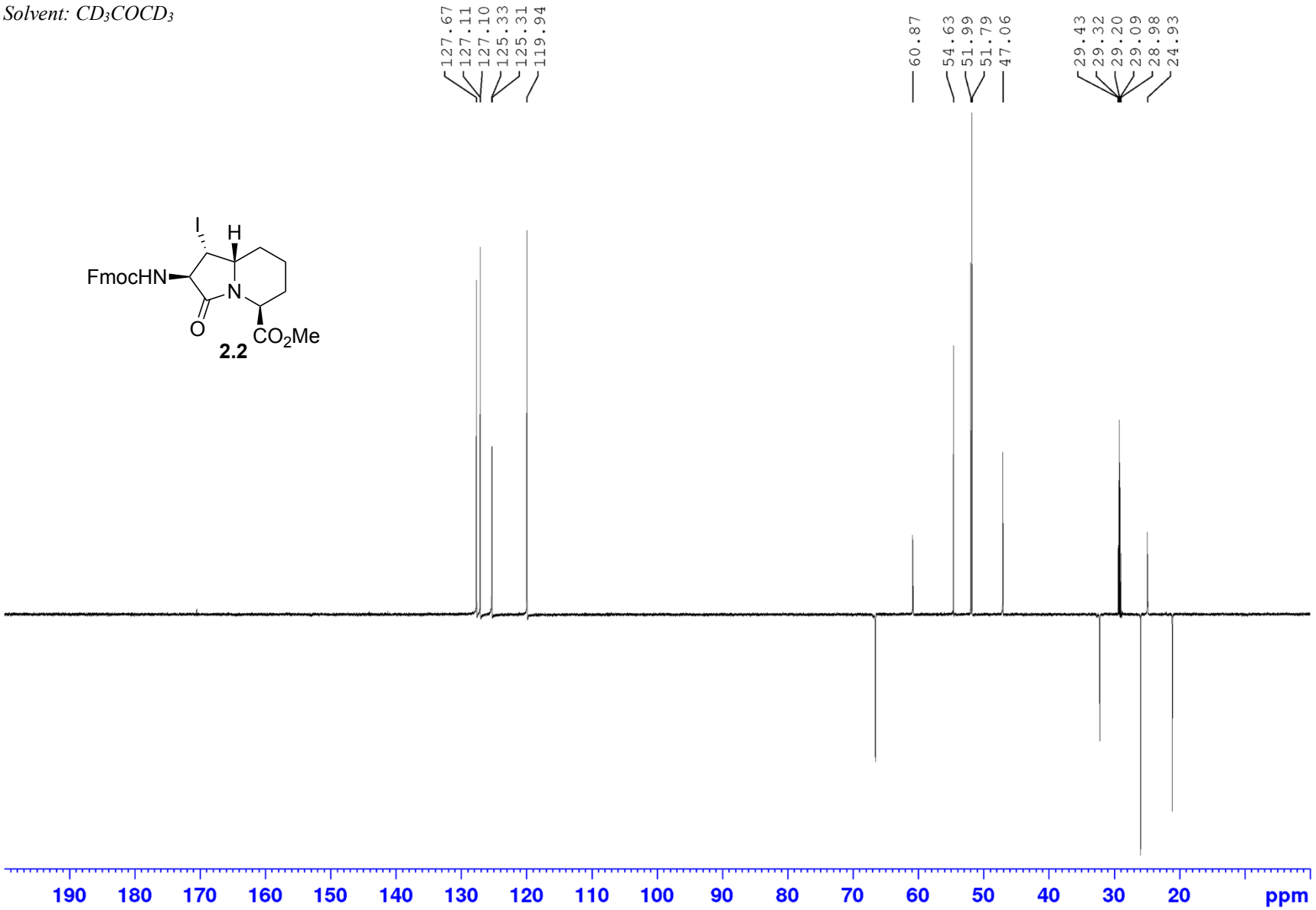

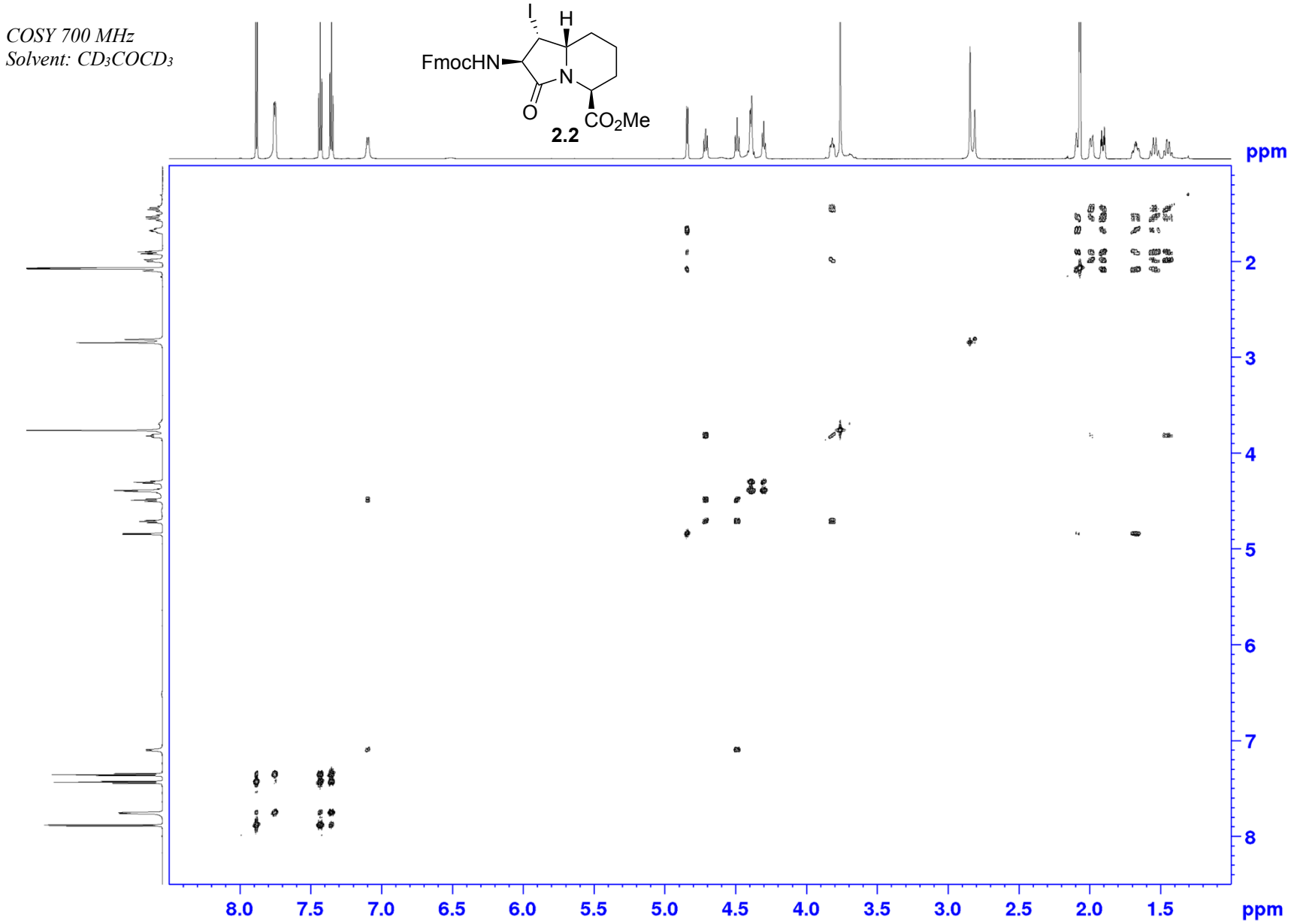
COSY 700 MHz
Solvent: CD3COCD3
I
H
FmocHN
N
O
CO2Me
2.2
ppm
2
3
4
5
6
7
8
8.0
7.5
7.0
6.5
6.0
5.5
5.0
4.5
4.0
3.5
3.0
2.5
2.0
1.5
ppm

HSQC 175 MHz
Solvent: CD_3COCD_3

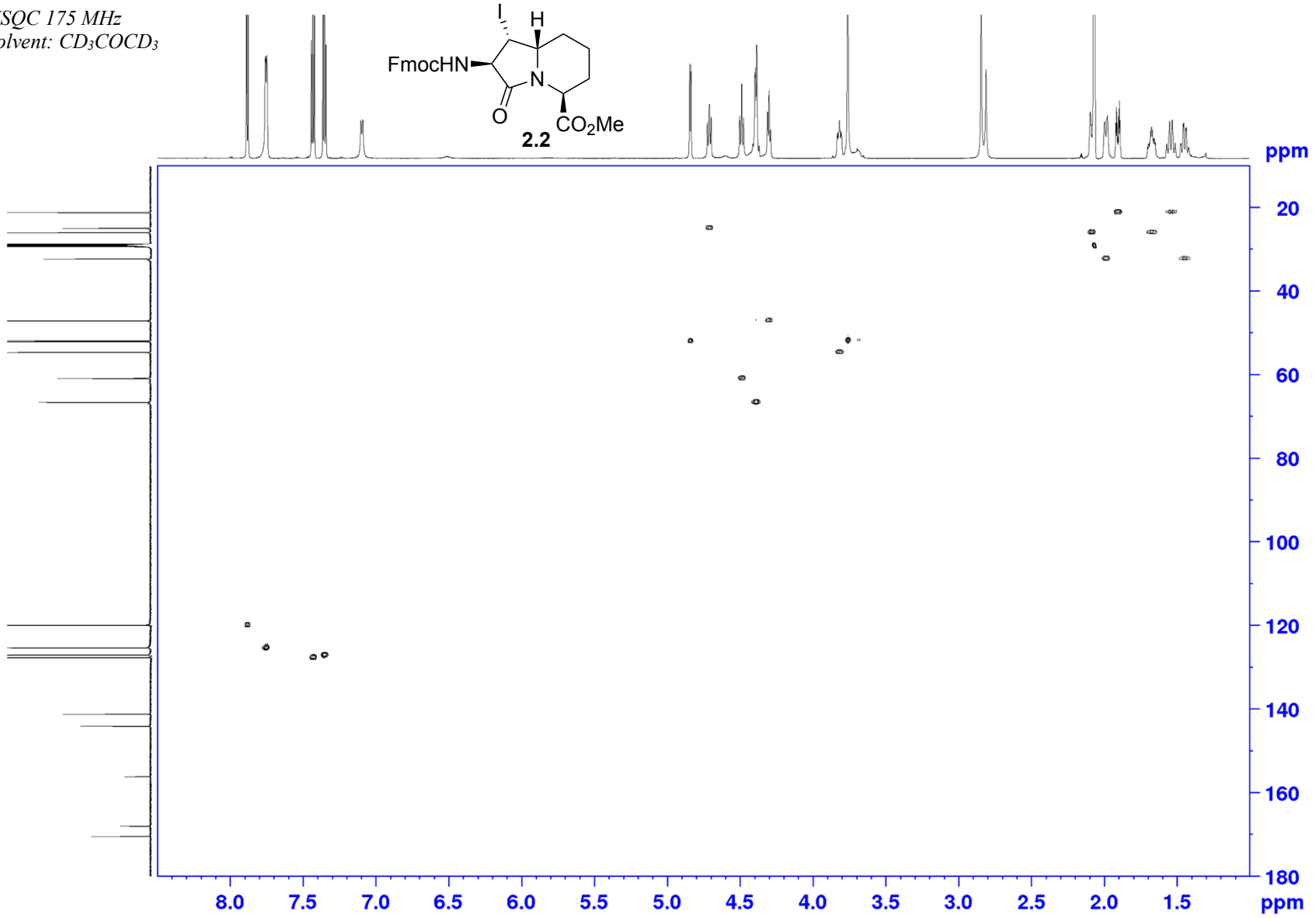

NOESY 700 MHz
Solvent: CD_3COCD_3

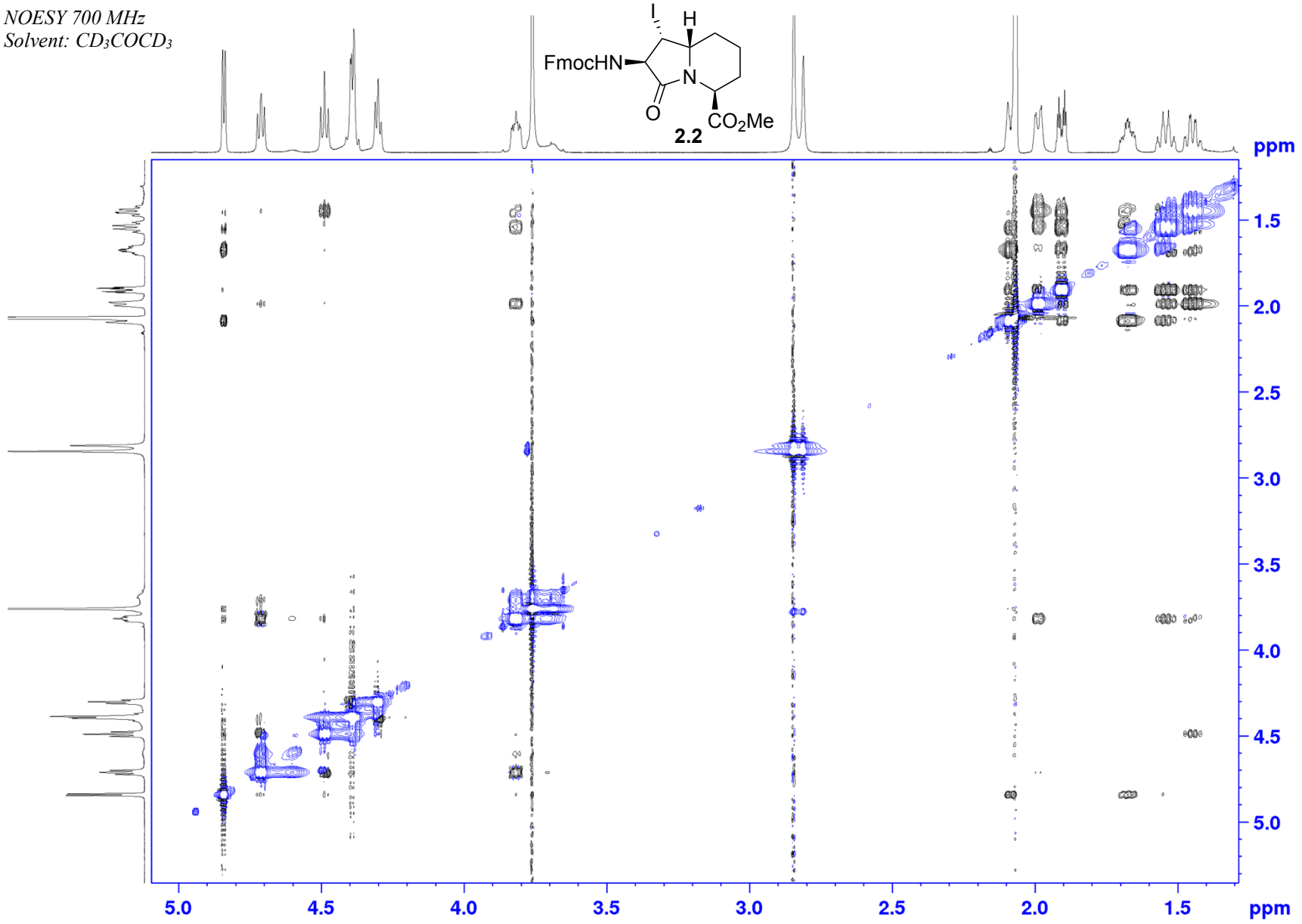

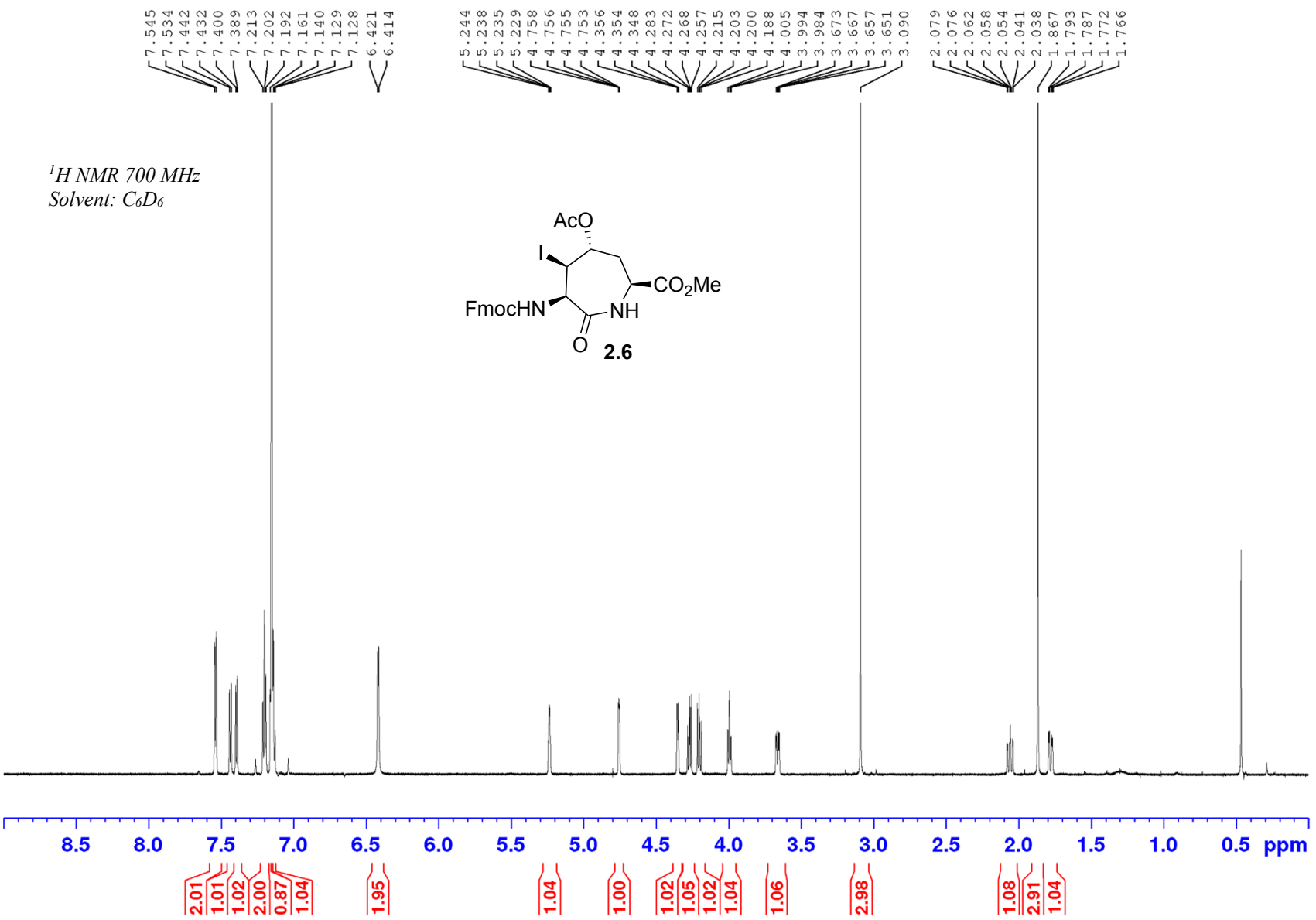
7.545
7.534
7.442
7.432
7.400
7.389
7.213
7.202
7.192
7.161
7.140
7.129
7.128
6.421
6.414
5.244
5.238
5.235
5.229
4.758
4.756
4.755
4.753
4.356
4.354
4.348
4.283
4.272
4.268
4.257
4.215
4.203
4.200
4.188
4.005
3.994
3.984
3.673
3.667
3.657
3.651
3.090
2.079
2.076
2.062
2.058
2.054
2.041
2.038
1.867
1.793
1.787
1.772
1.766
1H NMR 700 MHz
Solvent: C6D6
AcO
I
CO2Me
FmocHN
NH
O
2.6
8.5
8.0
7.5
7.0
6.5
6.0
5.5
5.0
4.5
4.0
3.5
3.0
2.5
2.0
1.5
1.0
0.5
ppm
2.01
1.01
1.02
2.00
0.87
1.04
1.95
1.04
1.00
1.02
1.05
1.02
1.04
1.06
2.98
1.08
2.91
1.04

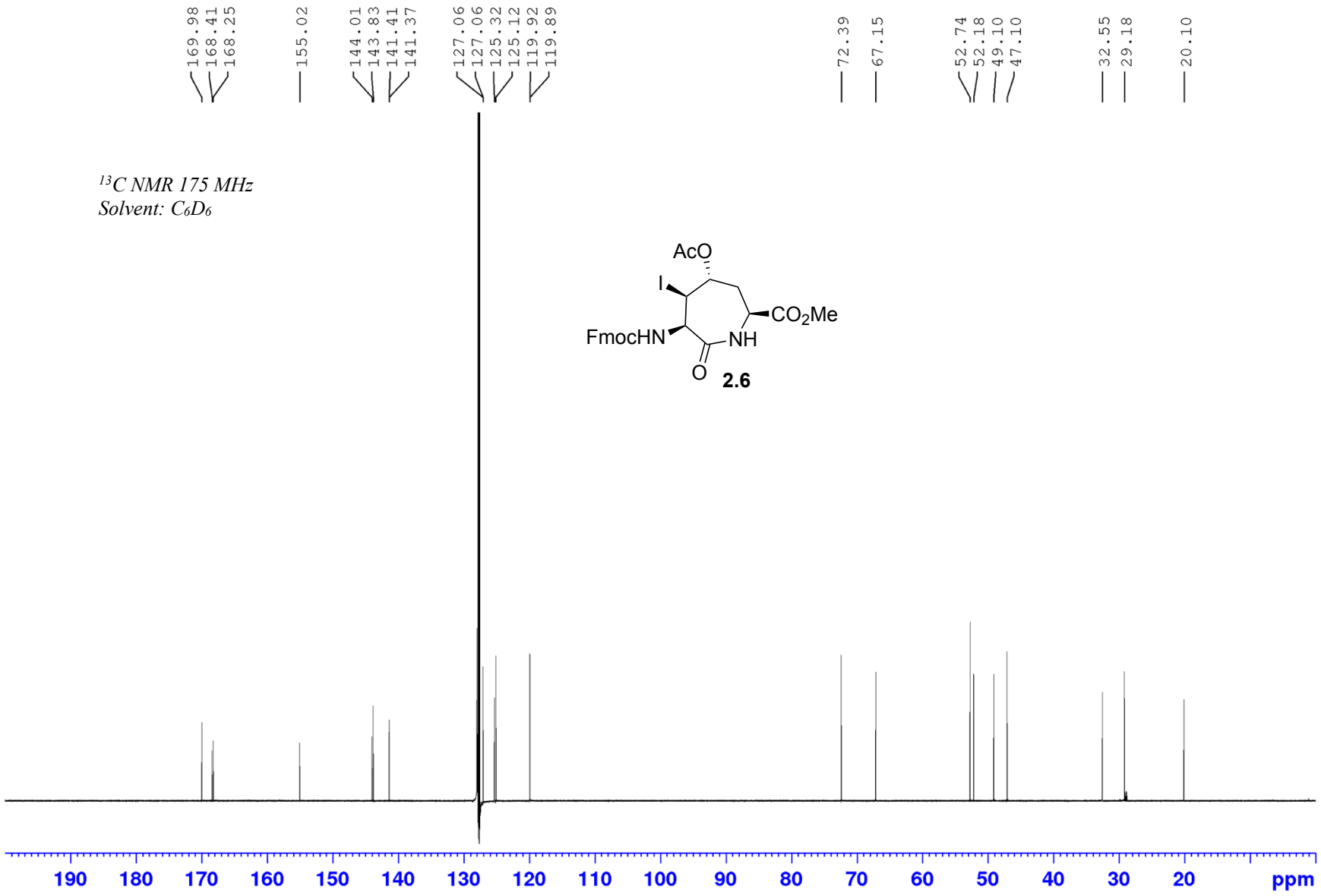
169.98
168.41
168.25
155.02
144.01
143.83
141.41
141.37
127.06
127.06
125.32
125.12
119.92
119.89
72.39
67.15
52.74
52.18
49.10
47.10
32.55
29.18
20.10
13C NMR 175 MHz
Solvent: C6D6
AcO
I
CO2Me
FmocHN
NH
O
2.6
190
180
170
160
150
140
130
120
110
100
90
80
70
60
50
40
30
20
ppm

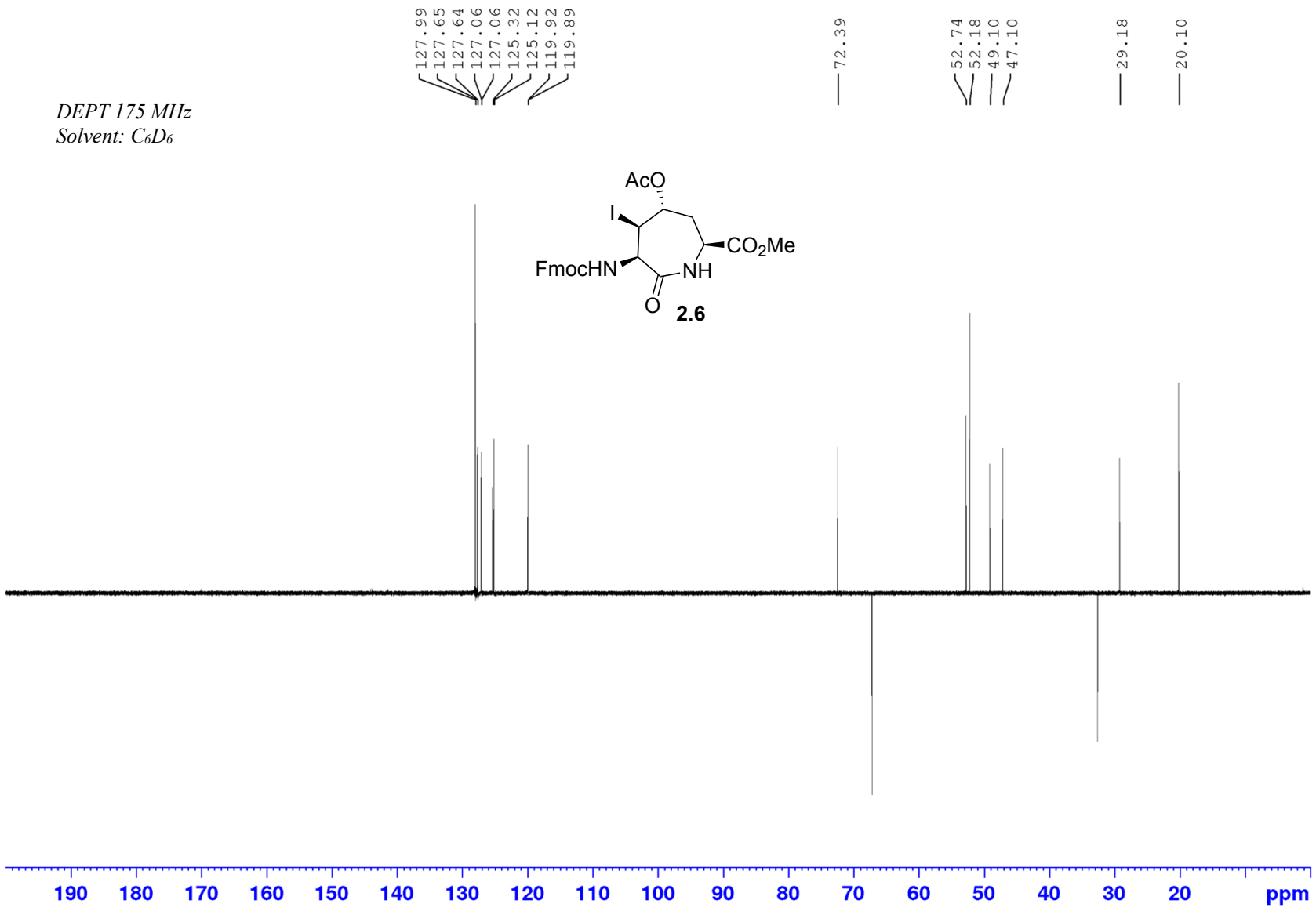
127.99
127.65
127.64
127.06
127.06
125.32
125.12
119.92
119.89
72.39
52.74
52.18
49.10
47.10
29.18
20.10
DEPT 175 MHz
Solvent: C6D6
AcO
I
CO2Me
FmocHN
NH
O
2.6
190
180
170
160
150
140
130
120
110
100
90
80
70
60
50
40
30
20
ppm

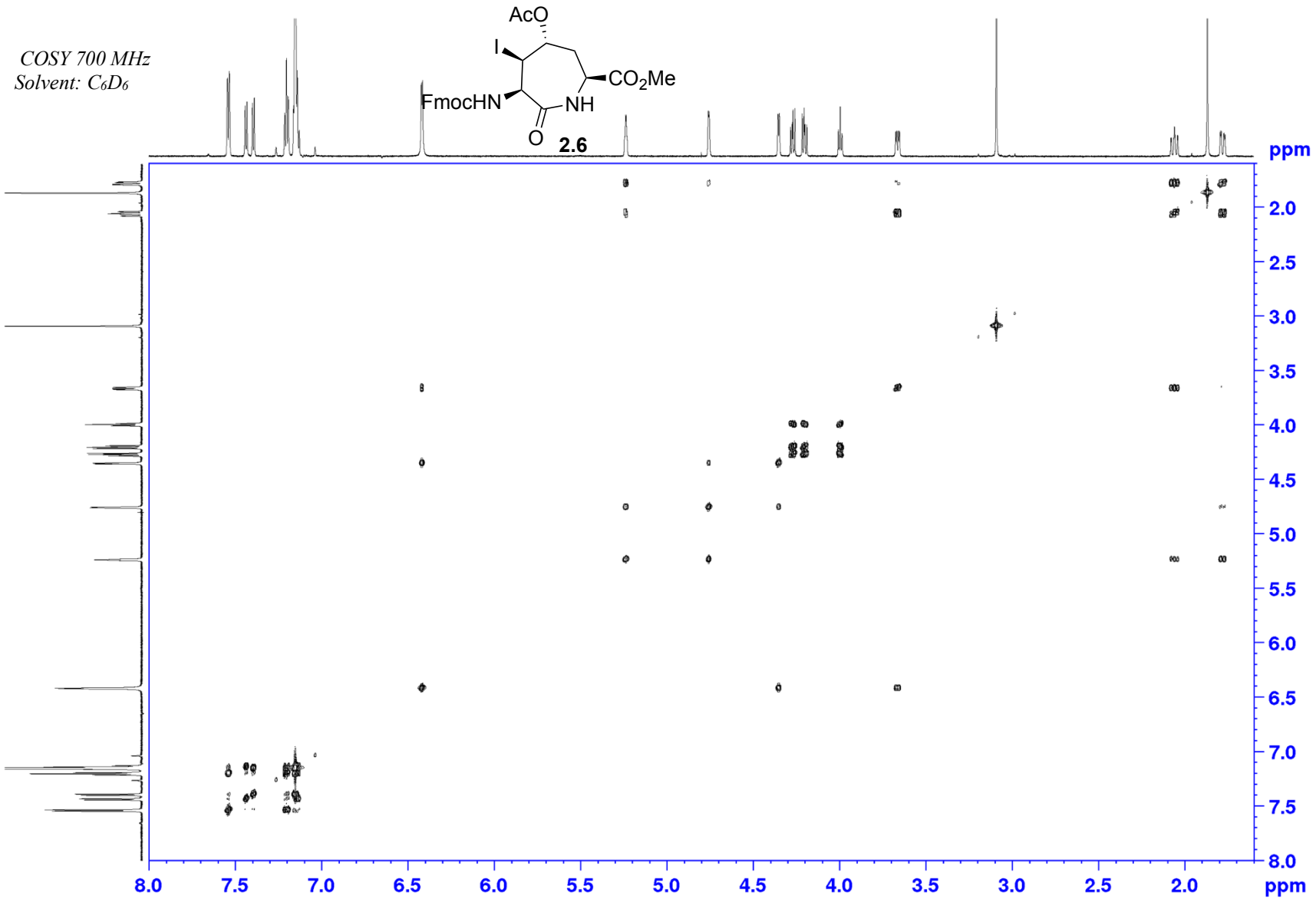
COSY 700 MHz
Solvent: C6D6
AcO
I
CO2Me
FmocHN
NH
O
2.6
ppm
8.0
7.5
7.0
6.5
6.0
5.5
5.0
4.5
4.0
3.5
3.0
2.5
2.0

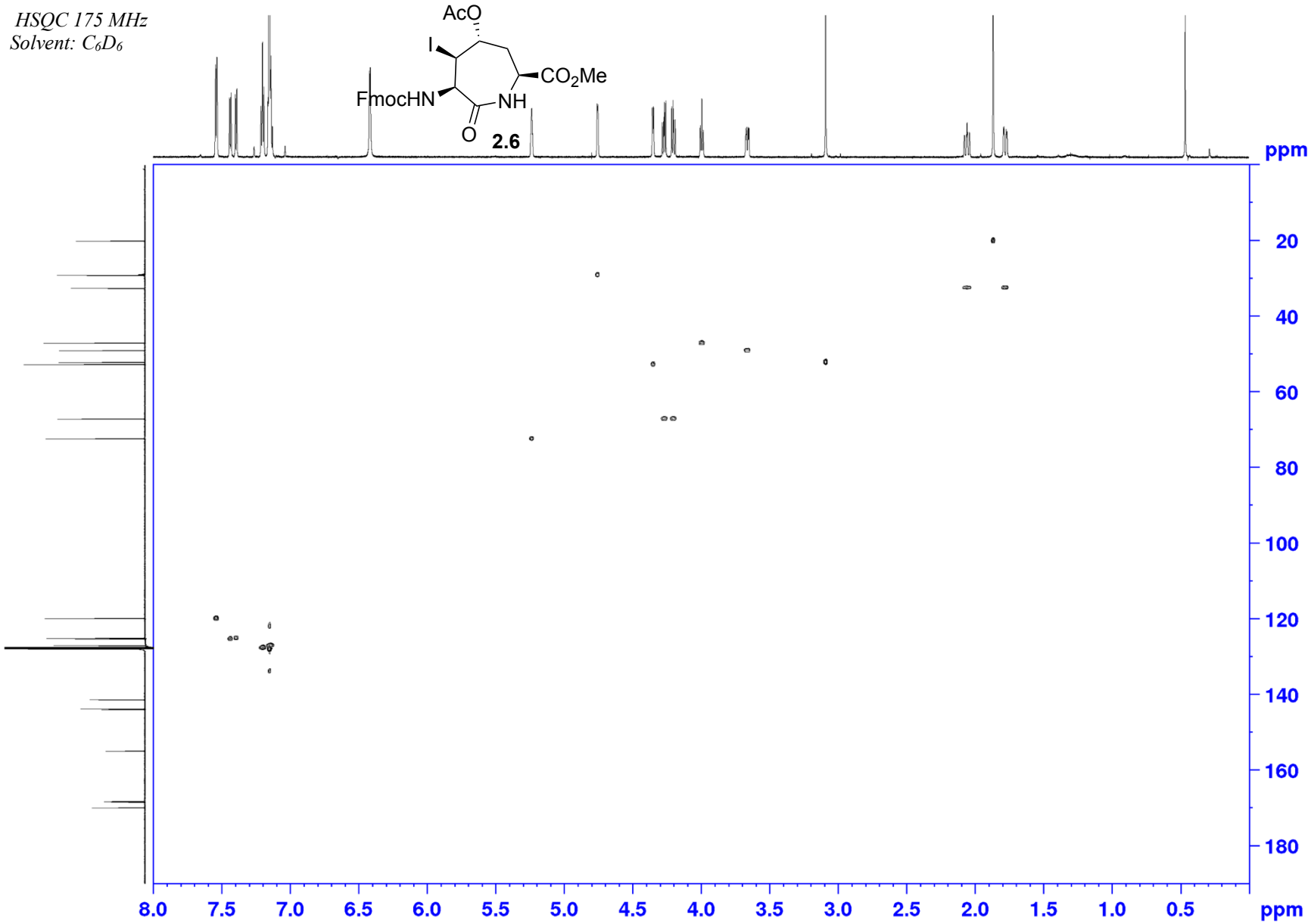
HSQC 175 MHz
Solvent: C6D6
AcO
I
CO2Me
FmocHN
NH
O
2.6
ppm
20
40
60
80
100
120
140
160
180
8.0
7.5
7.0
6.5
6.0
5.5
5.0
4.5
4.0
3.5
3.0
2.5
2.0
1.5
1.0
0.5
ppm

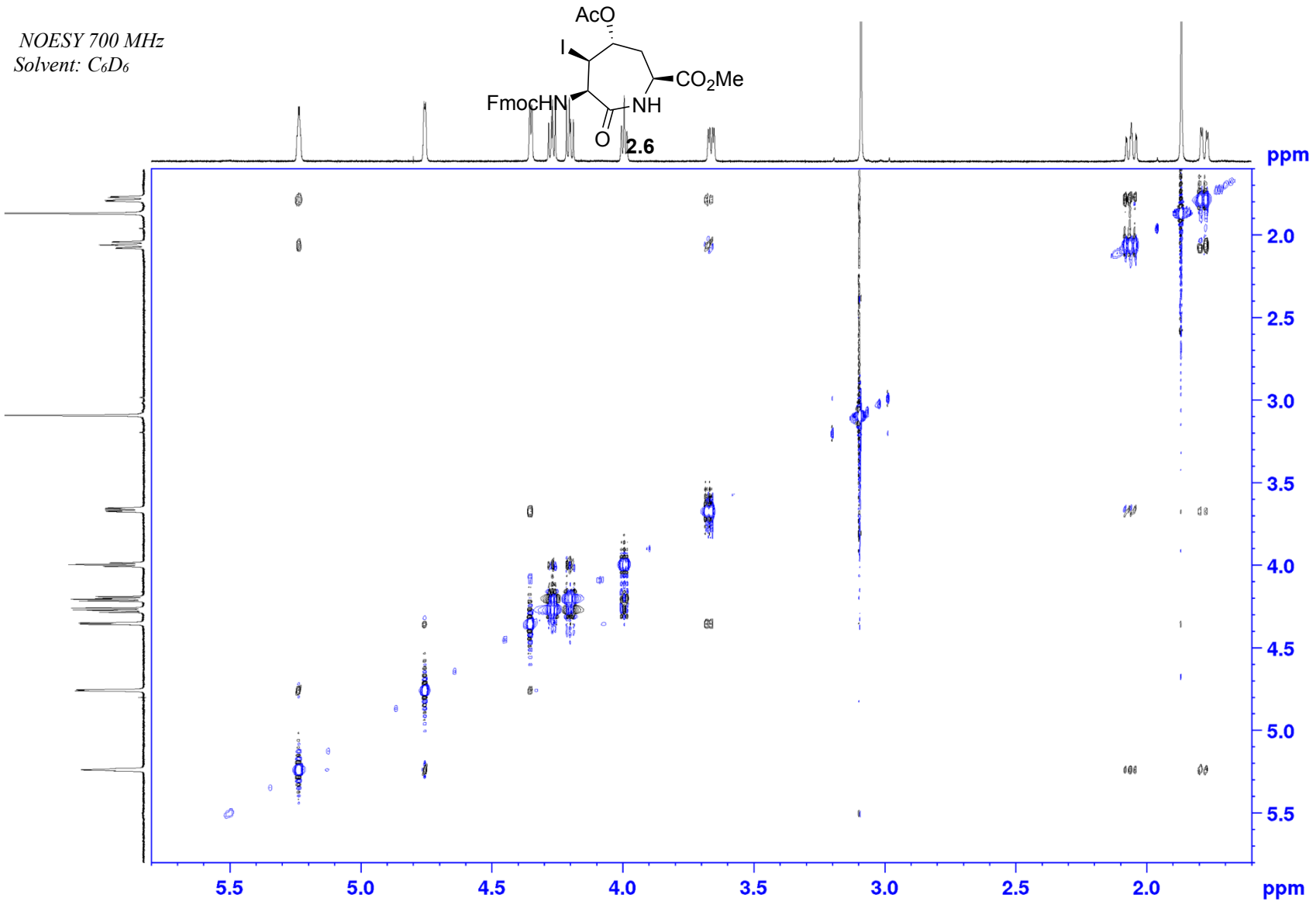
NOESY 700 MHz
Solvent: C6D6
AcO
I
CO2Me
FmocHN
NH
O
2.6
ppm
2.0
2.5
3.0
3.5
4.0
4.5
5.0
5.5
5.5
5.0
4.5
4.0
3.5
3.0
2.5
2.0
ppm

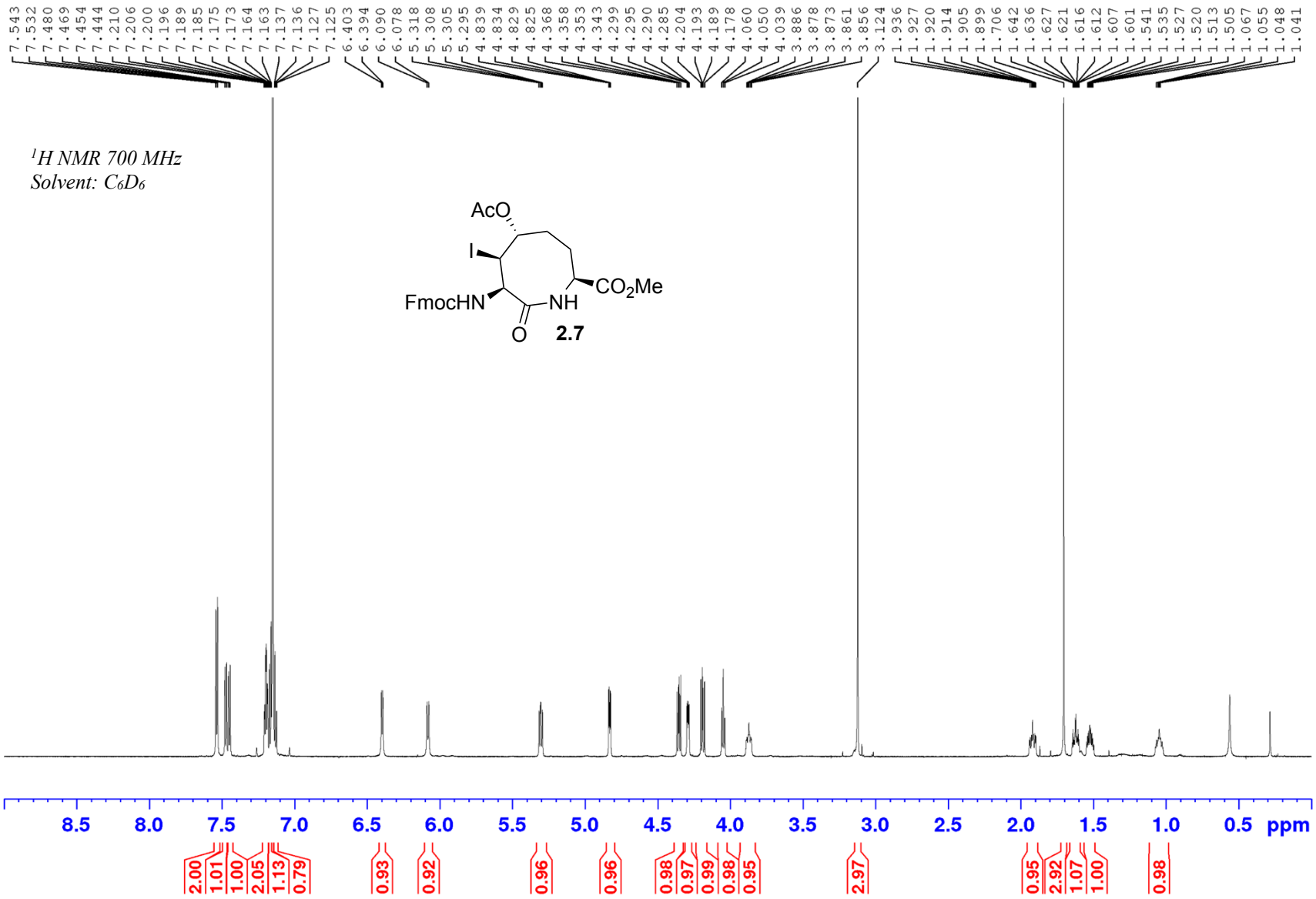
7.543 7.532 7.480 7.469 7.454 7.444 7.210 7.206 7.200 7.196 7.189 7.185 7.175 7.173 7.164 7.163 7.137 7.136 7.127 7.125
6.403 6.394 6.090 6.078 5.318 5.308 5.305 5.295 4.839 4.834 4.829 4.825 4.368 4.358 4.353 4.343 4.299 4.295 4.290 4.285 4.204 4.193 4.189 4.178 4.060 4.050 4.039 3.886 3.878 3.873 3.861 3.856 3.124
1.936 1.927 1.920 1.914 1.905 1.899 1.706 1.642 1.636 1.627 1.621 1.616 1.612 1.607 1.601 1.541 1.535 1.527 1.520 1.513 1.505 1.067 1.055 1.048 1.041
1H NMR 700 MHz
Solvent: C6D6
AcO
I
FmocHN
NH
CO2Me
O
2.7
8.5 8.0 7.5 7.0 6.5 6.0 5.5 5.0 4.5 4.0 3.5 3.0 2.5 2.0 1.5 1.0 0.5 ppm
2.00 1.01 1.00 2.05 1.13 0.79 0.93 0.92 0.96 0.96 0.98 0.97 0.99 0.98 0.95 2.97 0.95 2.92 1.07 1.00 0.98

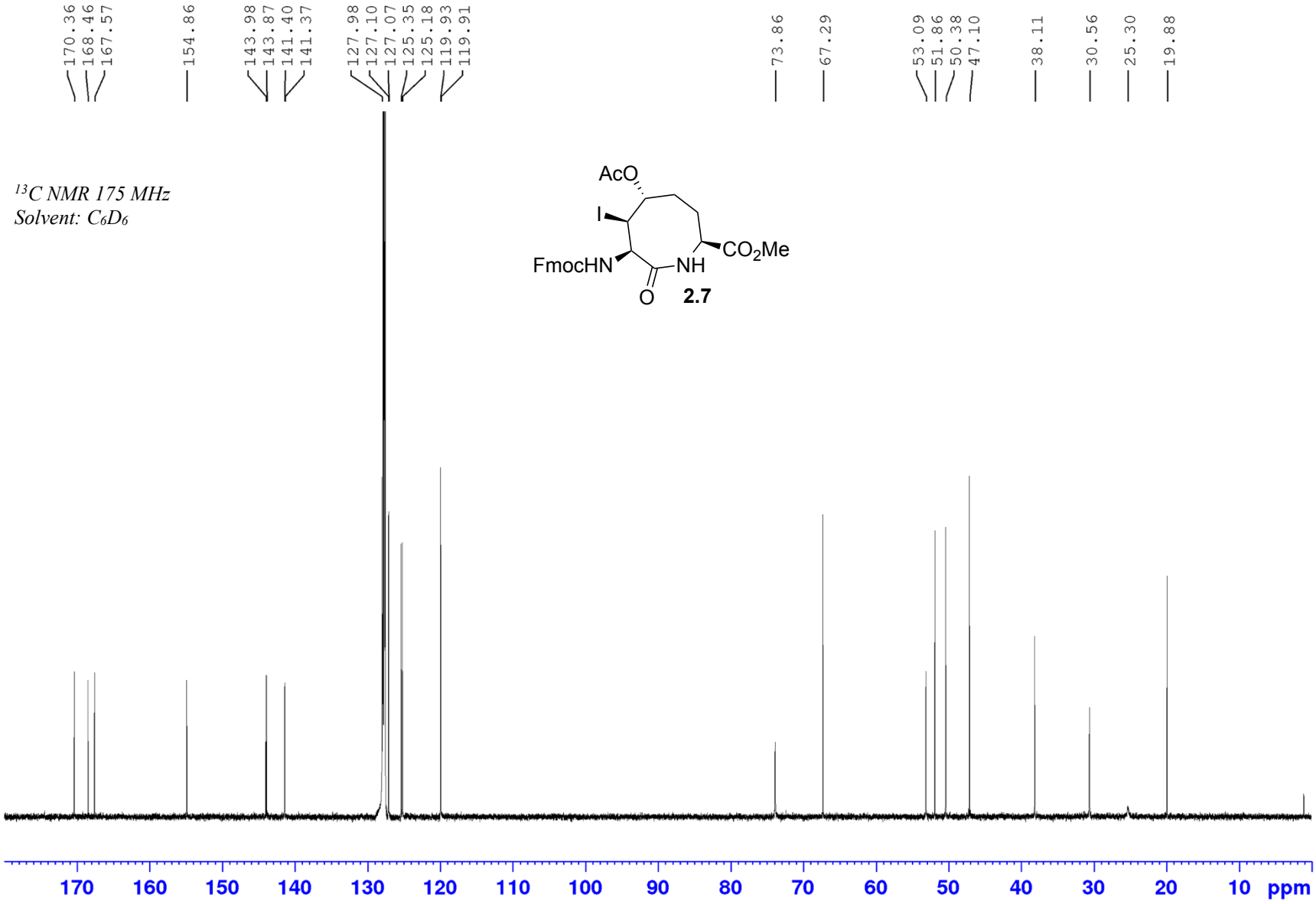
170.36
168.46
167.57
154.86
143.98
143.87
141.40
141.37
127.98
127.10
127.07
125.35
125.18
119.93
119.91
73.86
67.29
53.09
51.86
50.38
47.10
38.11
30.56
25.30
19.88
13C NMR 175 MHz
Solvent: C6D6
AcO
I
FmocHN
NH
CO2Me
O
2.7
170
160
150
140
130
120
110
100
90
80
70
60
50
40
30
20
10
ppm

COSY 700 MHz
Solvent: C_6D_6

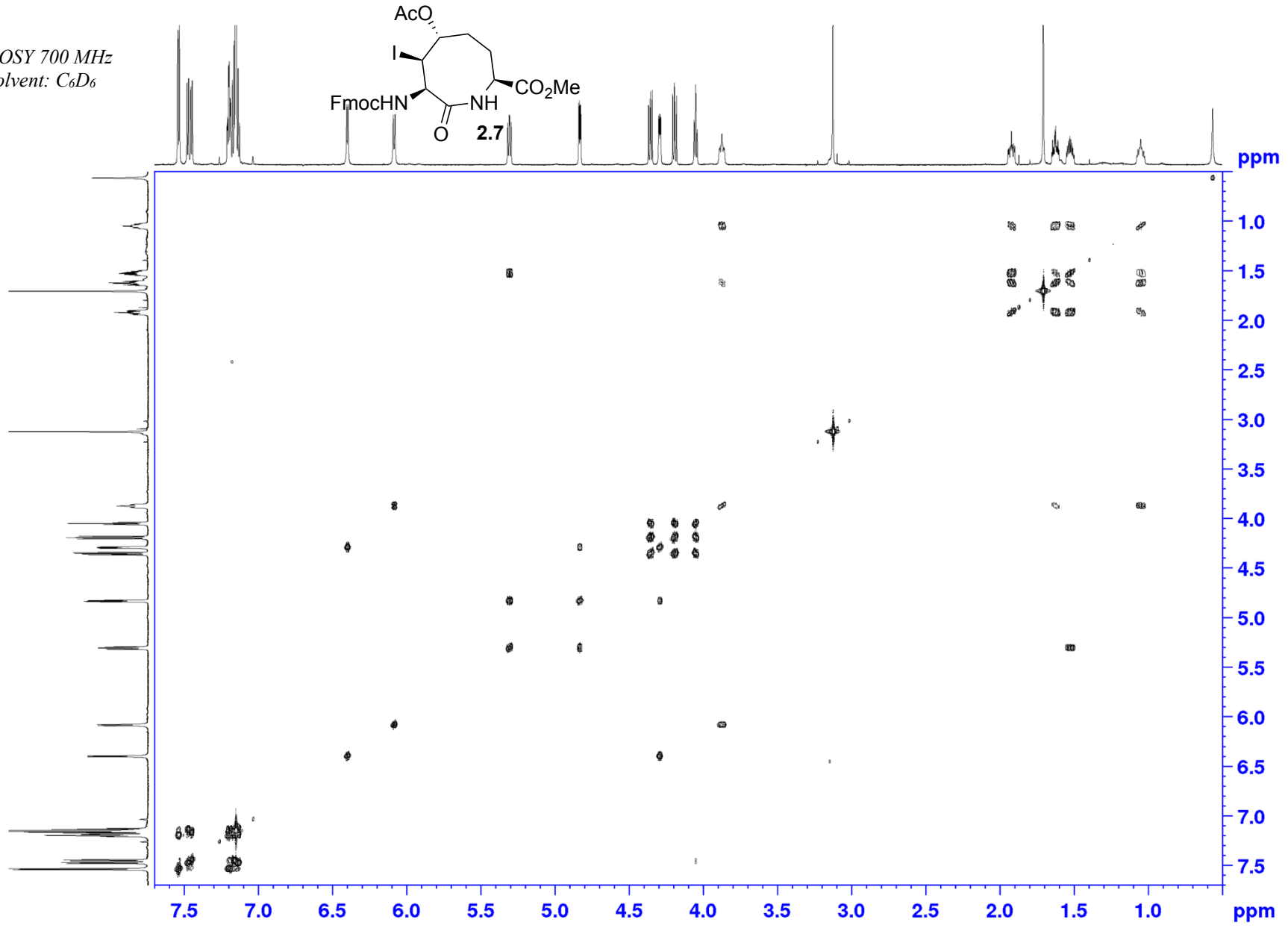

DEPT 175 MHz
Solvent: C_6D_6

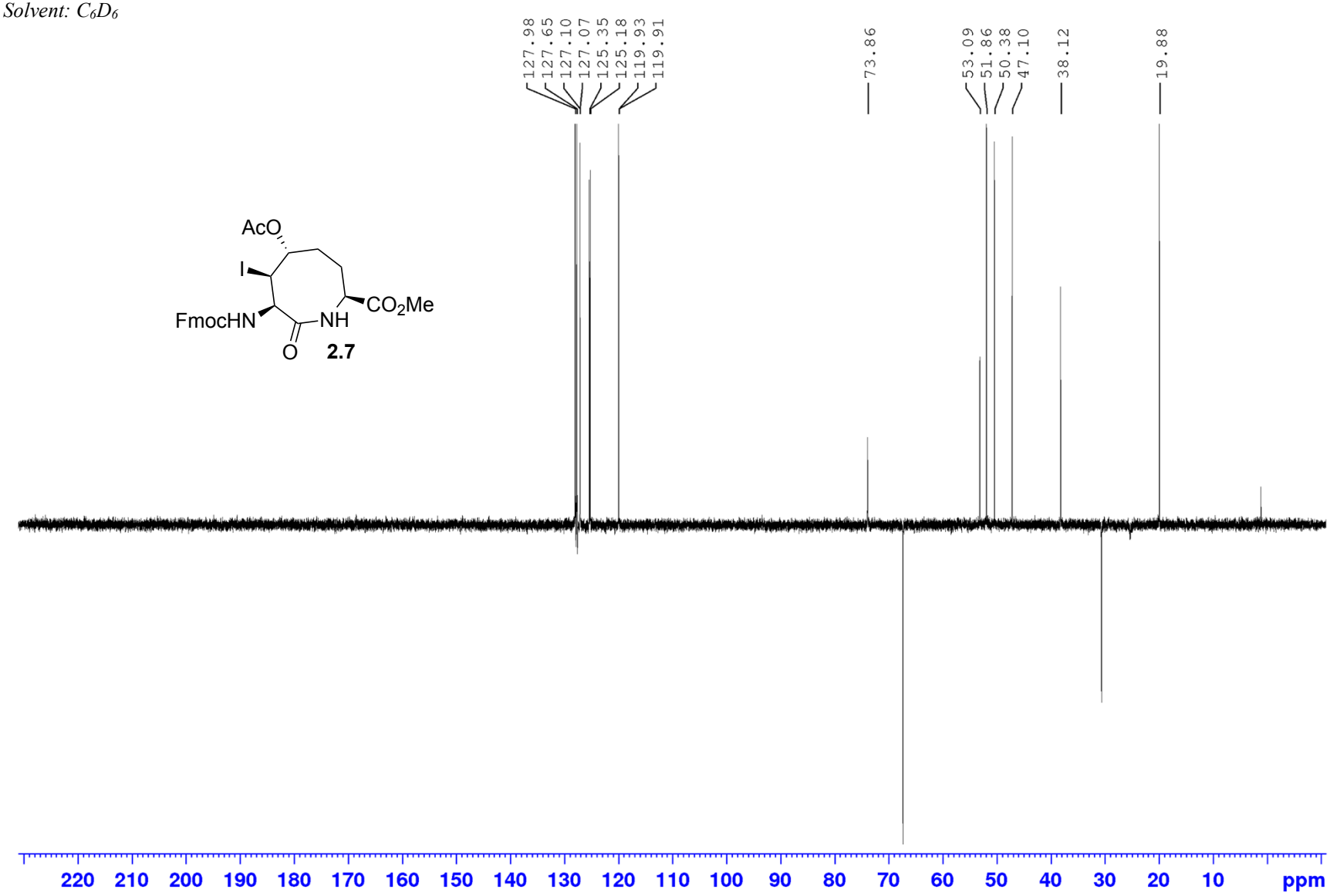

HSQC 175 MHz
Solvent: C_6D_6

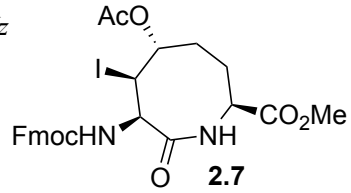

2.7

NOESY 700 MHz
Solvent: C_6D_6

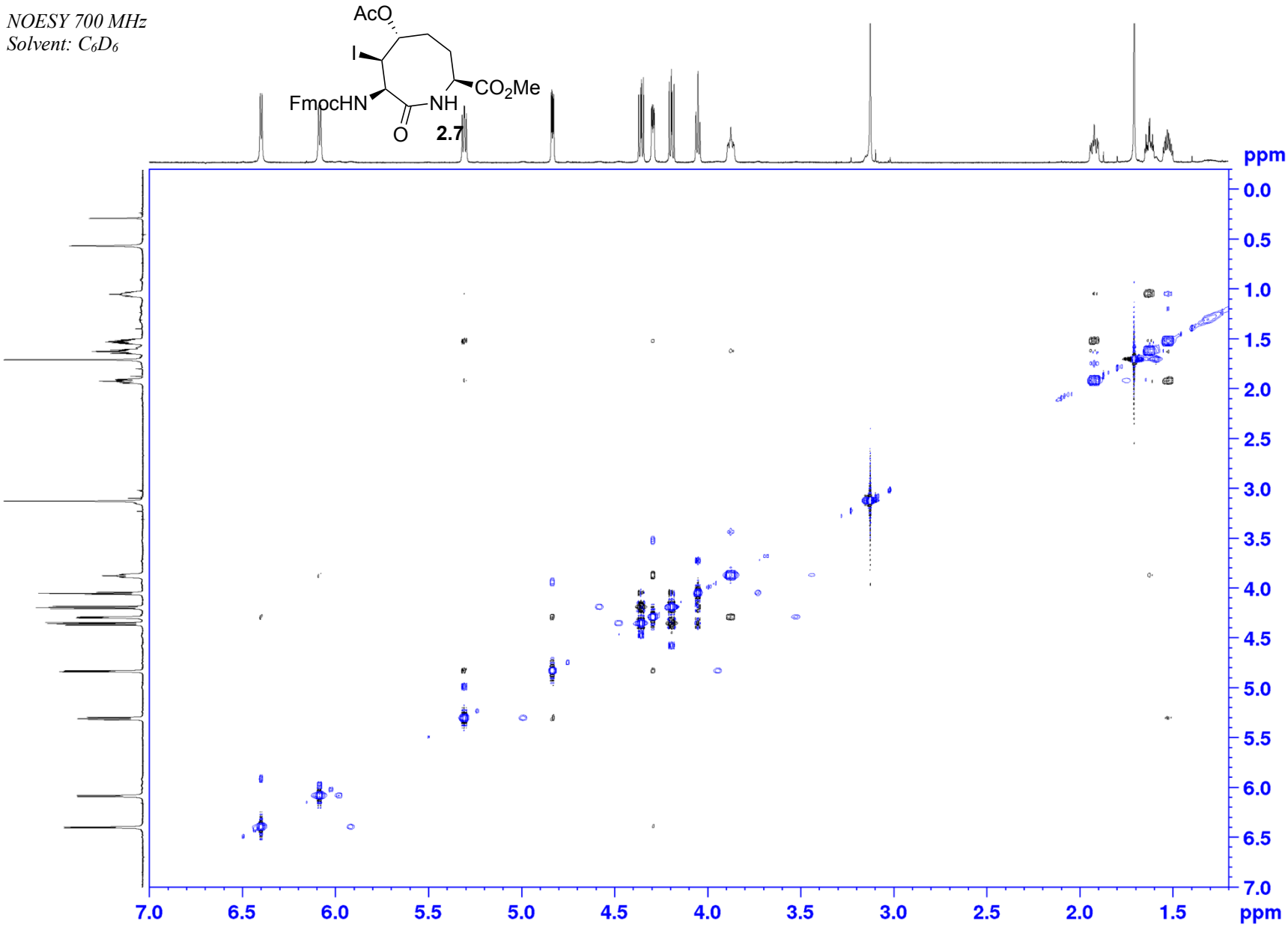

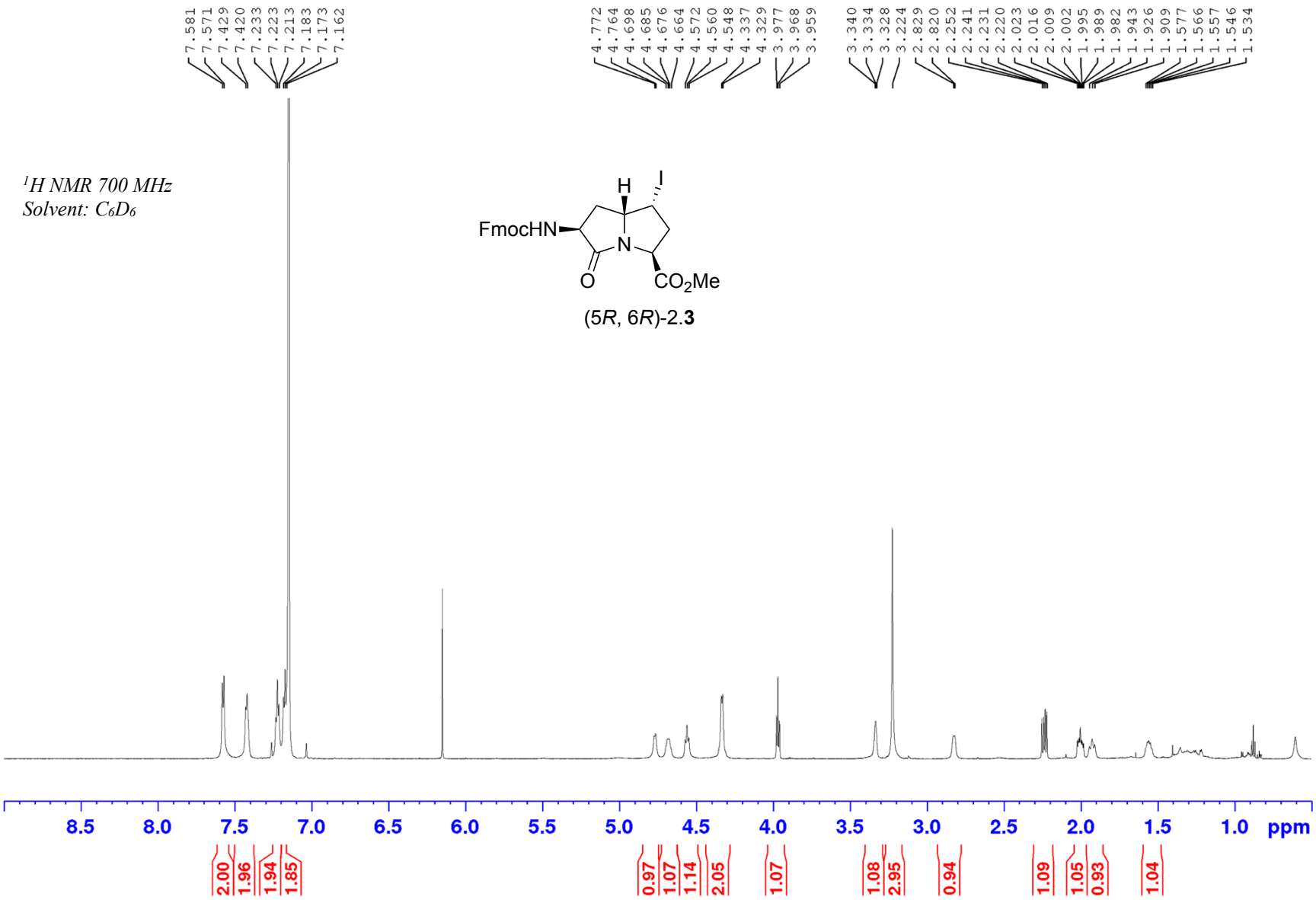
7.581
7.571
7.429
7.420
7.233
7.223
7.213
7.183
7.173
7.162
4.772
4.764
4.698
4.685
4.676
4.664
4.572
4.560
4.548
4.337
4.329
3.977
3.968
3.959
3.340
3.334
3.328
3.224
2.829
2.820
2.252
2.241
2.231
2.220
2.023
2.016
2.009
2.002
1.995
1.989
1.982
1.943
1.926
1.909
1.577
1.566
1.557
1.546
1.534
1H NMR 700 MHz
Solvent: C6D6
H
I
FmocHN
N
O
CO2Me
(5R, 6R)-2.3
8.5
8.0
7.5
7.0
6.5
6.0
5.5
5.0
4.5
4.0
3.5
3.0
2.5
2.0
1.5
1.0
ppm
2.00
1.96
1.94
1.85
0.97
1.07
1.14
2.05
1.07
1.08
2.95
0.94
1.09
1.05
0.93
1.04

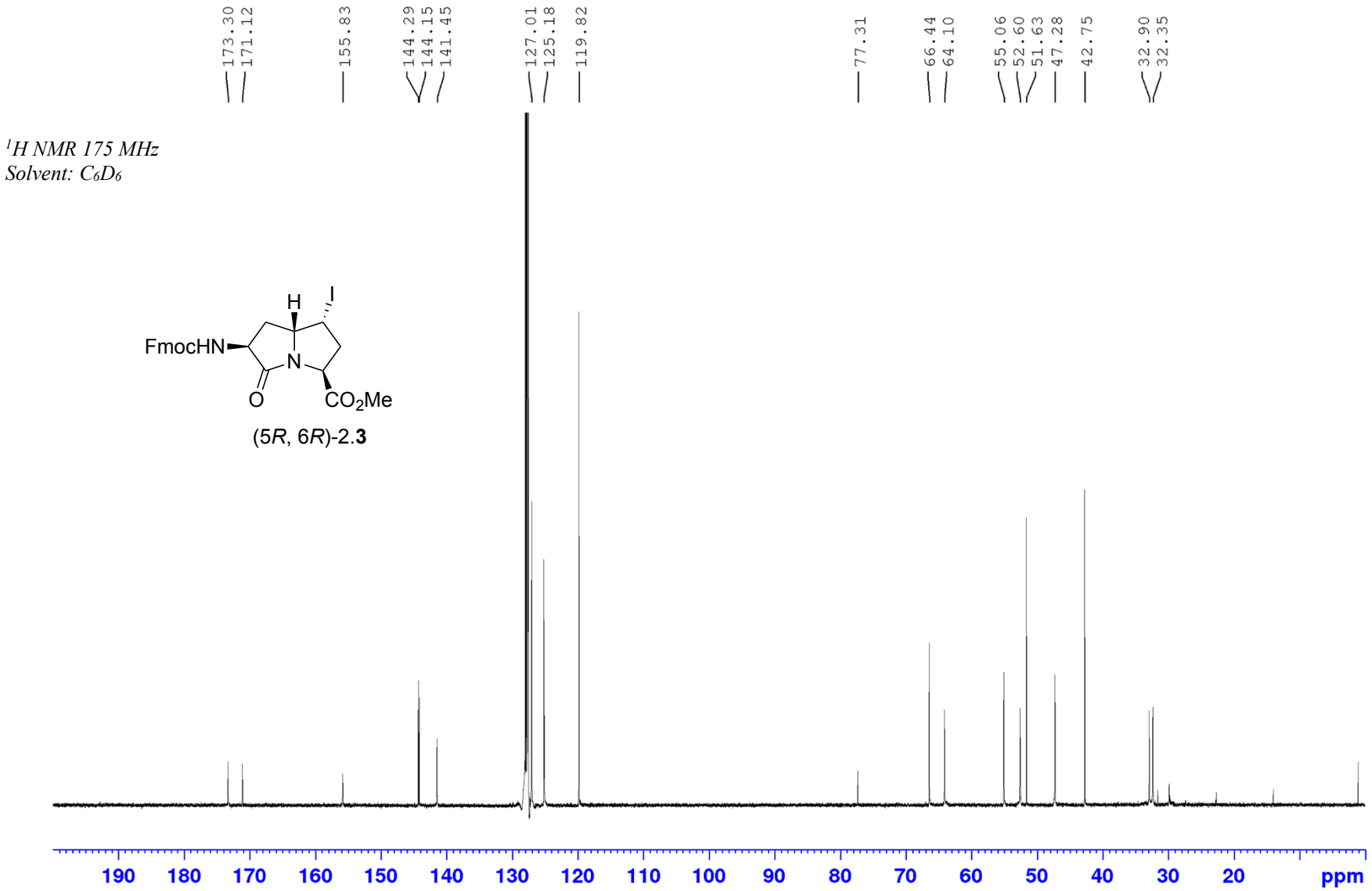

[1]H NMR 175 MHz
Solvent: C_6D_6

(5*R*, 6*R*)-2.**3**

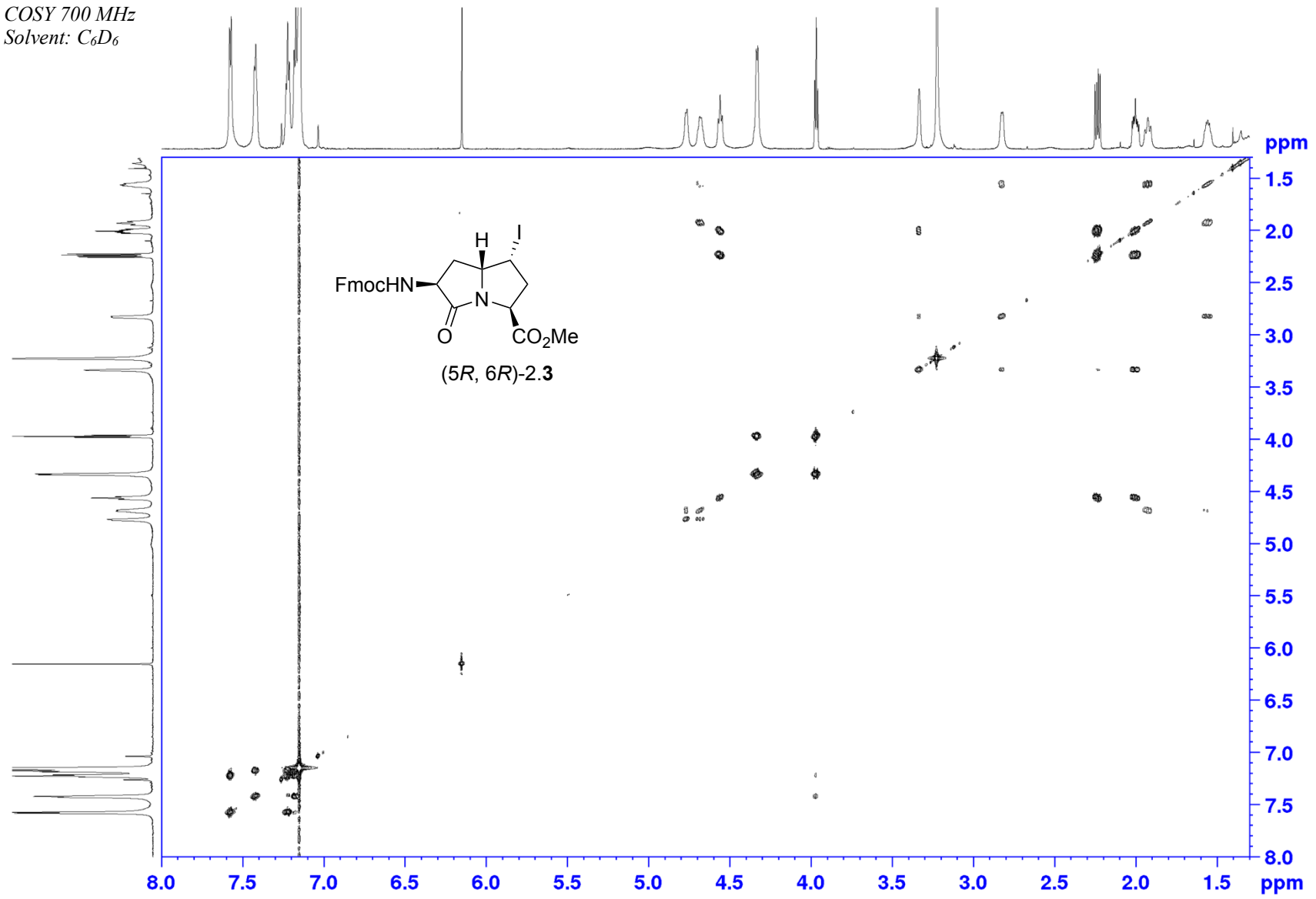
COSY 700 MHz
Solvent: C6D6
H
I
FmocHN
N
O
CO2Me
(5R, 6R)-2.3
ppm
1.5
2.0
2.5
3.0
3.5
4.0
4.5
5.0
5.5
6.0
6.5
7.0
7.5
8.0
8.0
7.5
7.0
6.5
6.0
5.5
5.0
4.5
4.0
3.5
3.0
2.5
2.0
1.5
ppm

DEPT 175 MHz
Solvent: C_6D_6

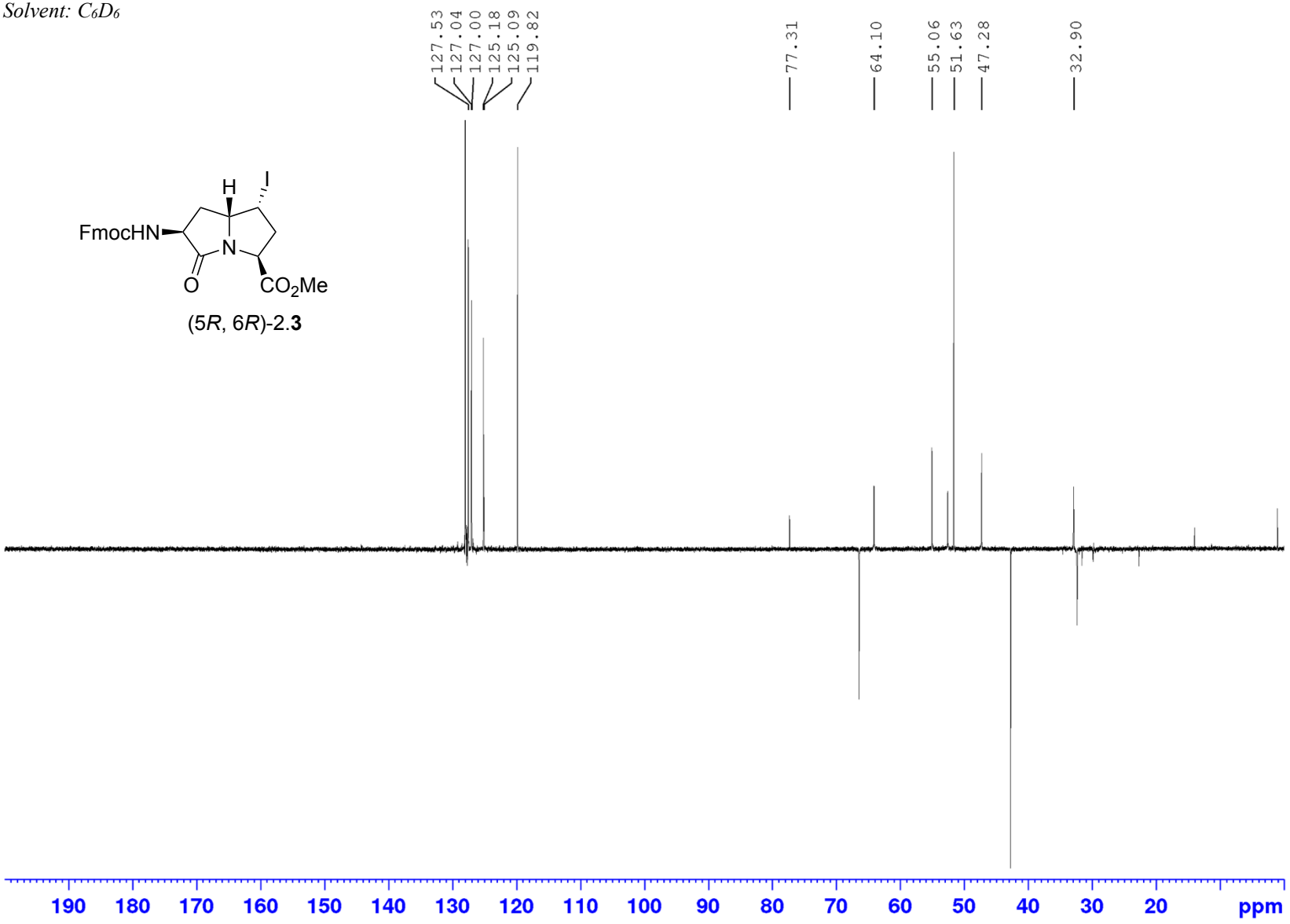

(5*R*, 6*R*)-2.**3**

HSQC 175 MHz
Solvent: C_6D_6

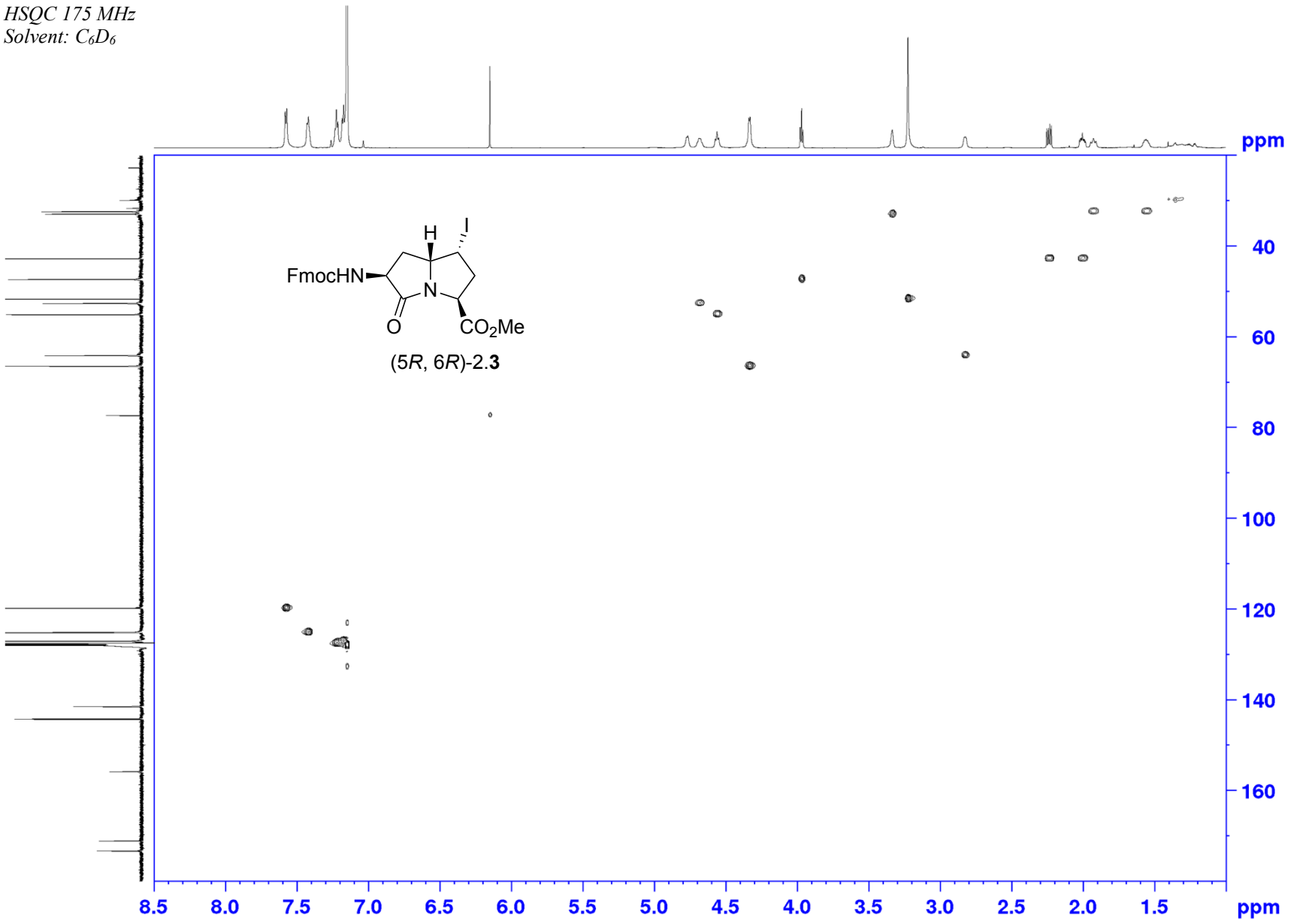

NOESY 700 MHz
Solvent: C_6D_6

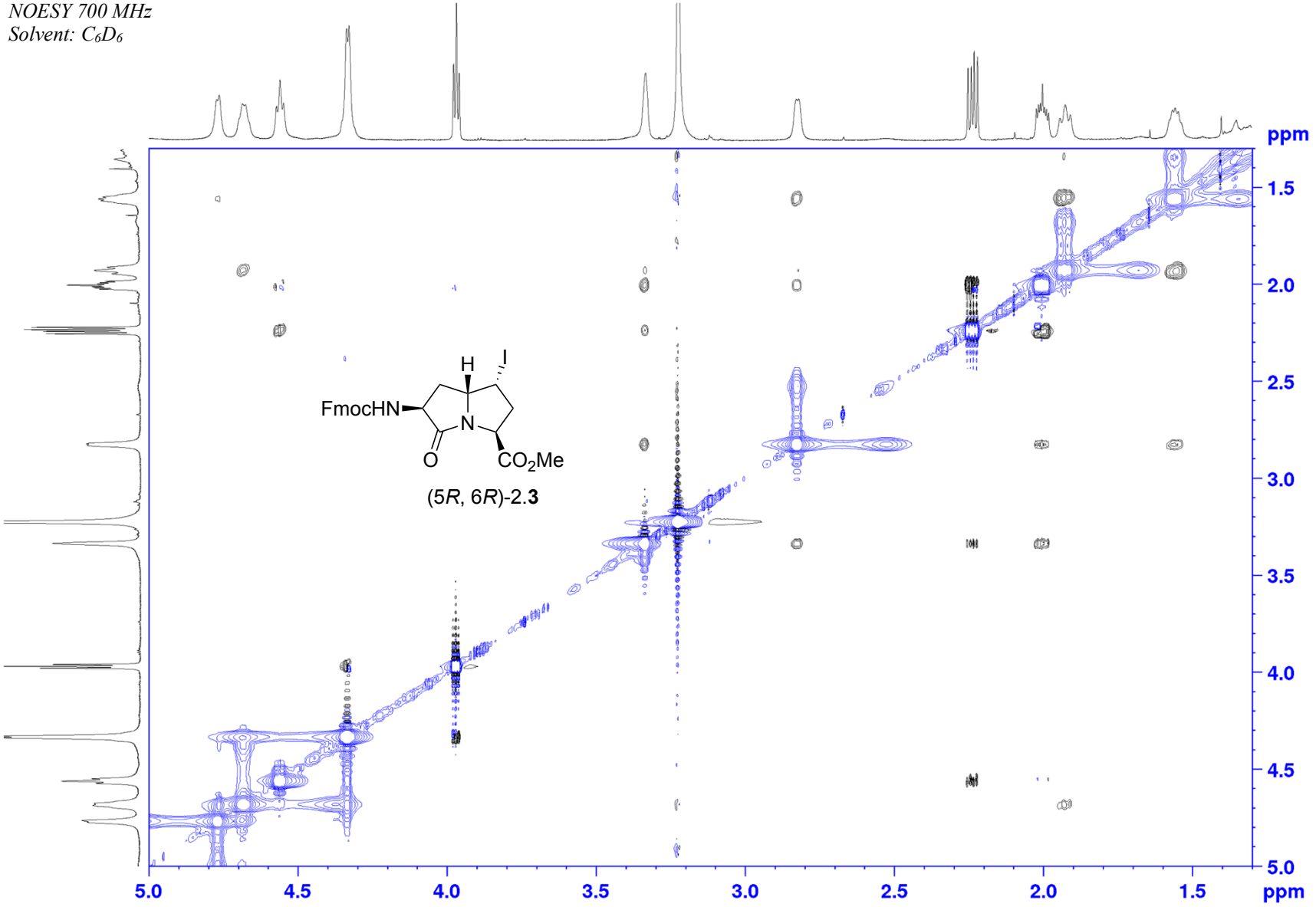

(5*R*, 6*R*)-2.**3**

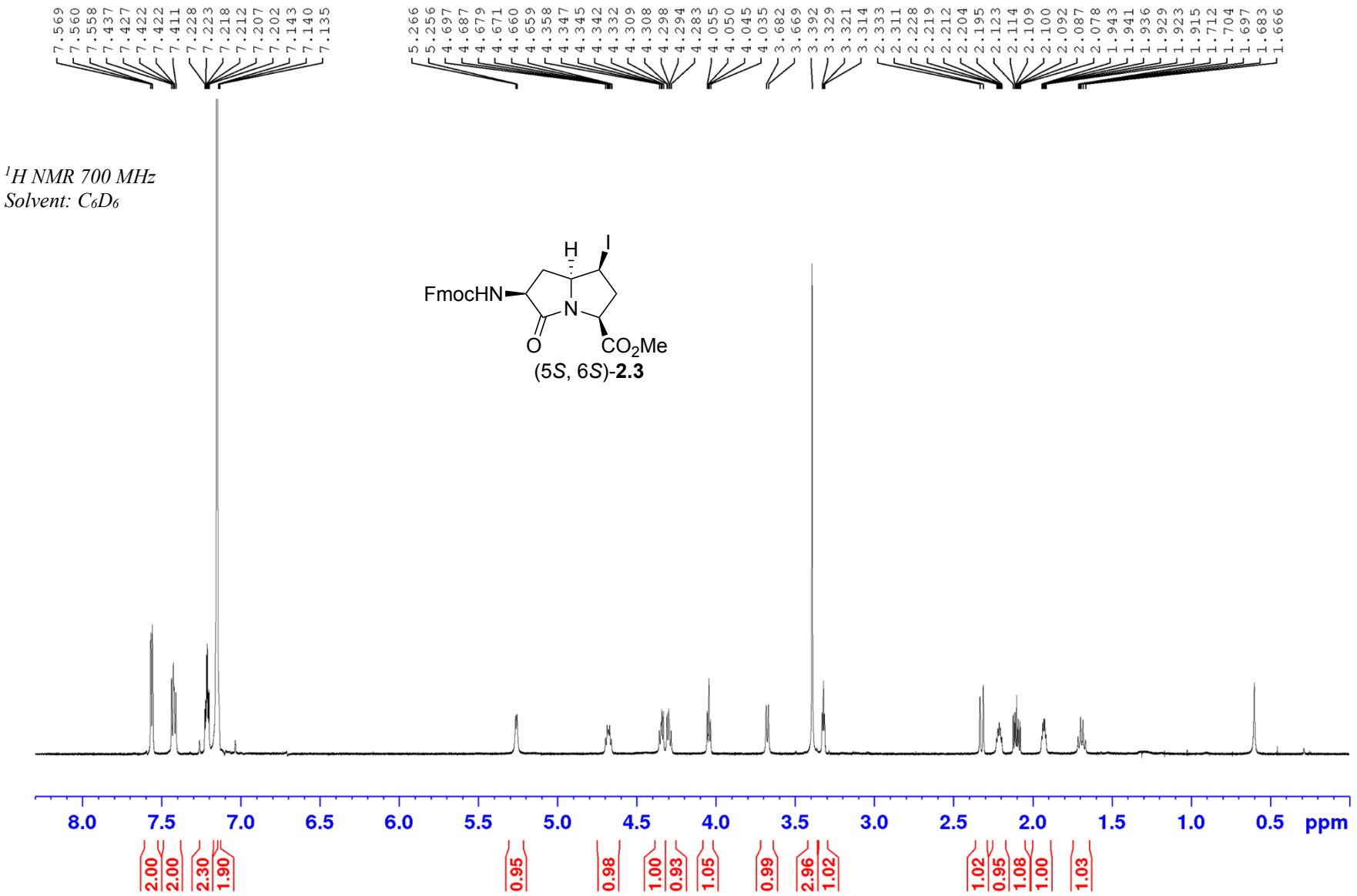

^{1}H NMR 700 MHz
Solvent: C_6D_6

(5*S*, 6*S*)-**2.3**

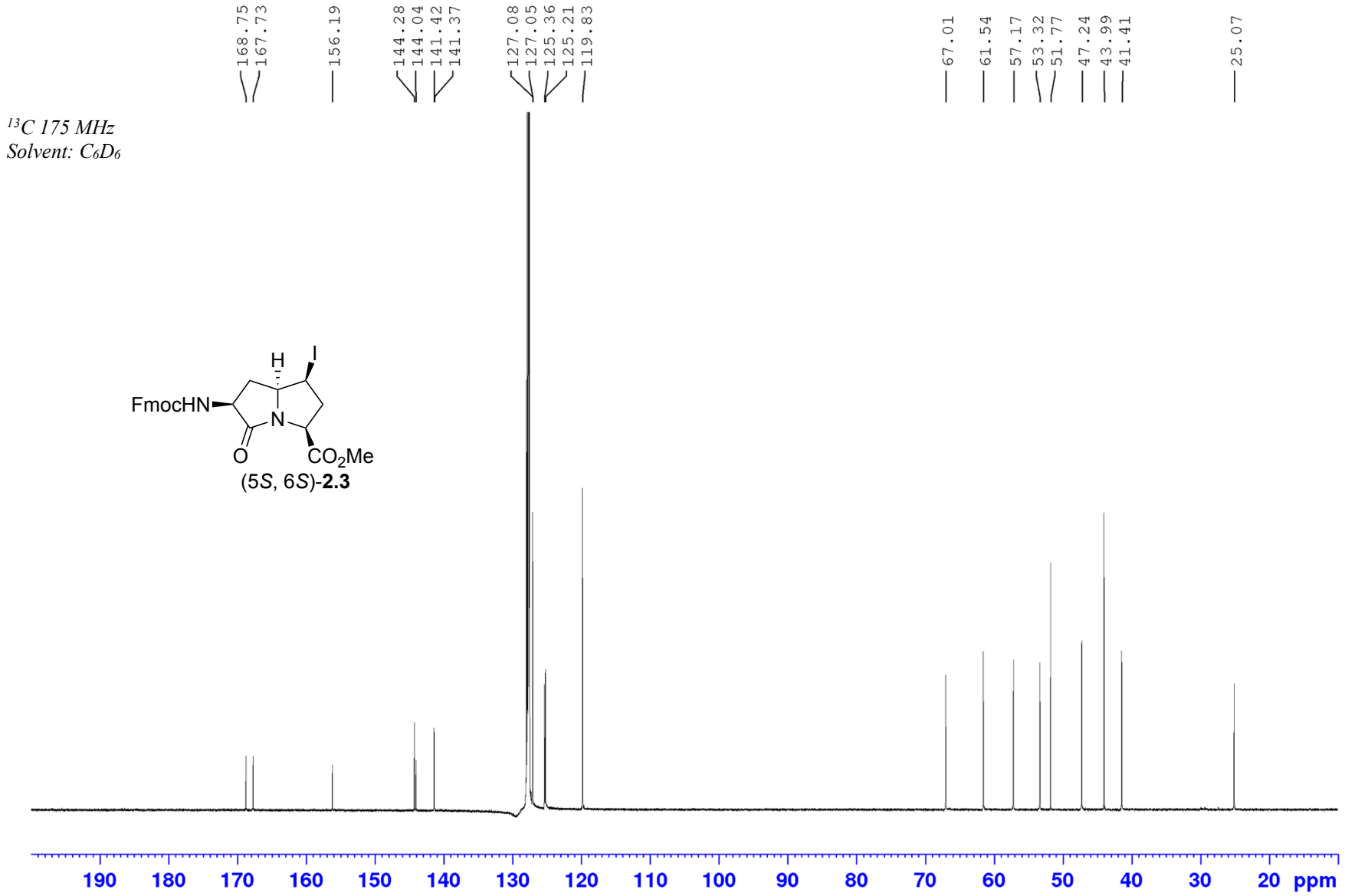
168.75
167.73
156.19
144.28
144.04
141.42
141.37
127.08
127.05
125.36
125.21
119.83
67.01
61.54
57.17
53.32
51.77
47.24
43.99
41.41
25.07
13C 175 MHz
Solvent: C6D6
H
I
FmocHN
N
O
CO2Me
(5S, 6S)-2.3
190
180
170
160
150
140
130
120
110
100
90
80
70
60
50
40
30
20
ppm

COSY 700 MHz
Solvent: C_6D_6

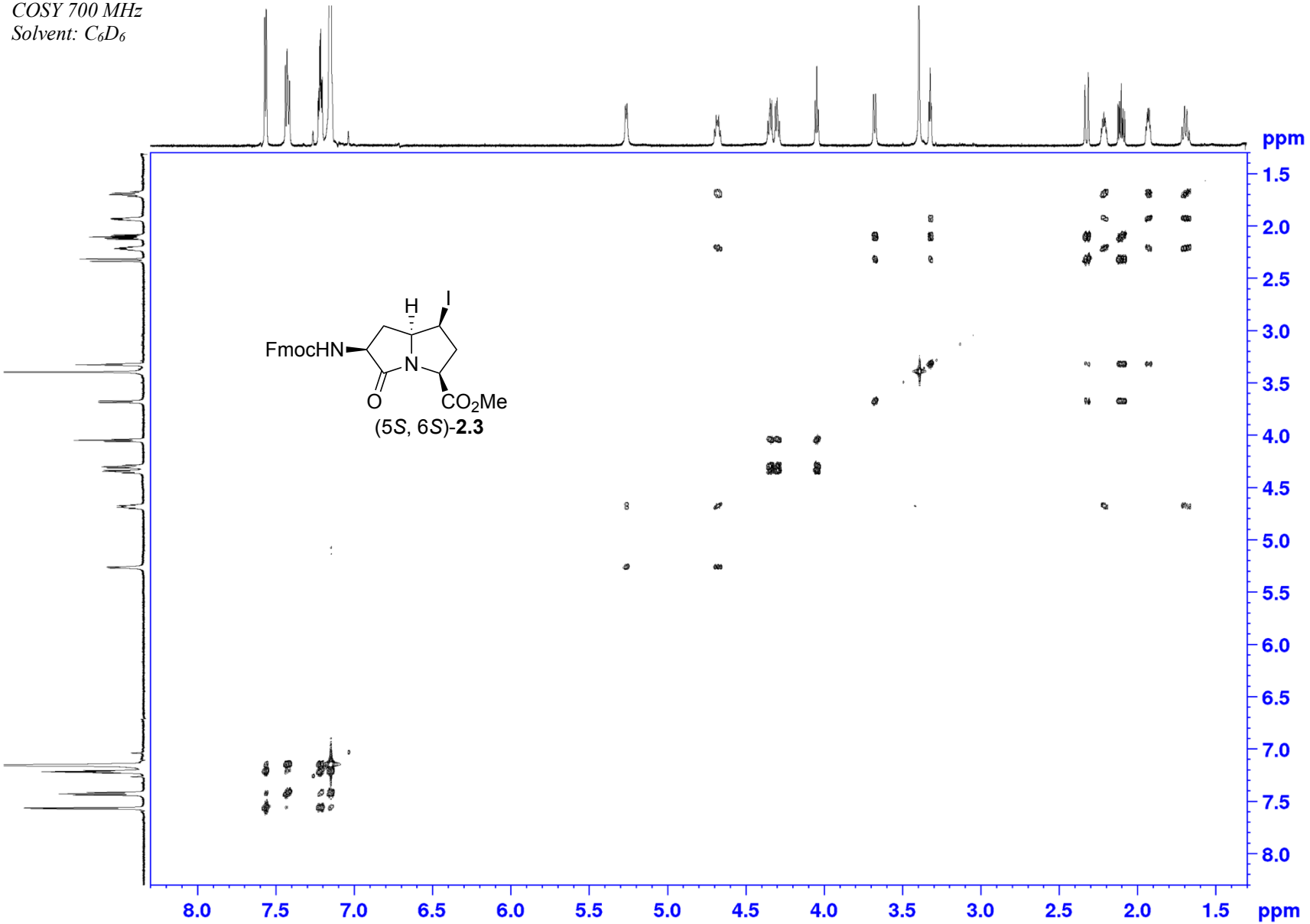

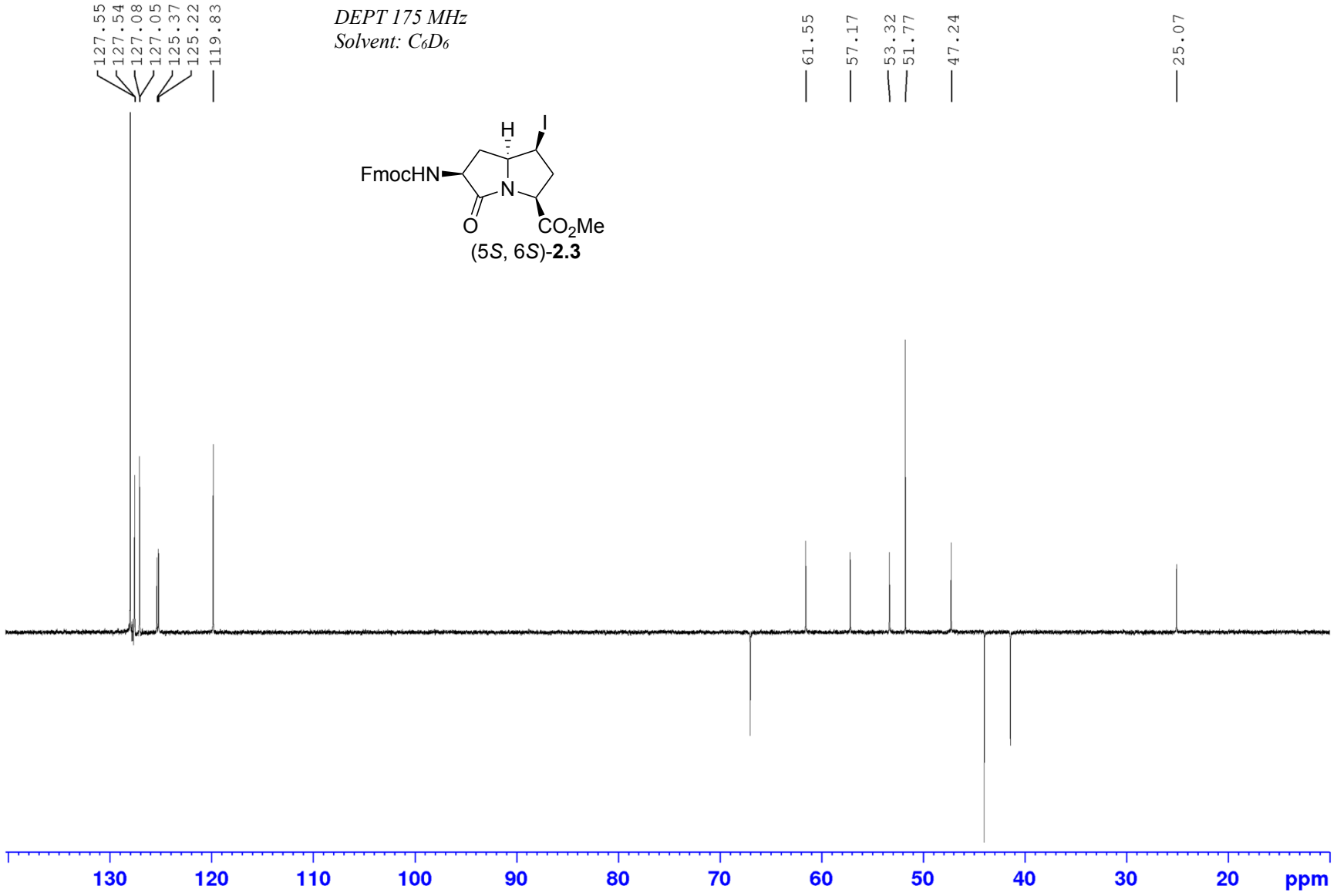
127.55
127.54
127.08
127.05
125.37
125.22
119.83
61.55
57.17
53.32
51.77
47.24
25.07
DEPT 175 MHz
Solvent: C6D6
H
I
FmocHN
N
O
CO2Me
(5S, 6S)-2.3
130
120
110
100
90
80
70
60
50
40
30
20
ppm

HSQC 175 MHz
Solvent: C_6D_6

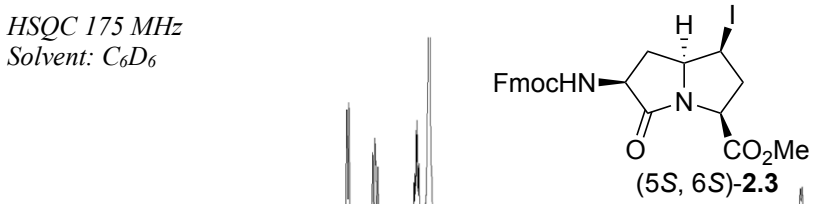

(5*S*, 6*S*)-**2.3**

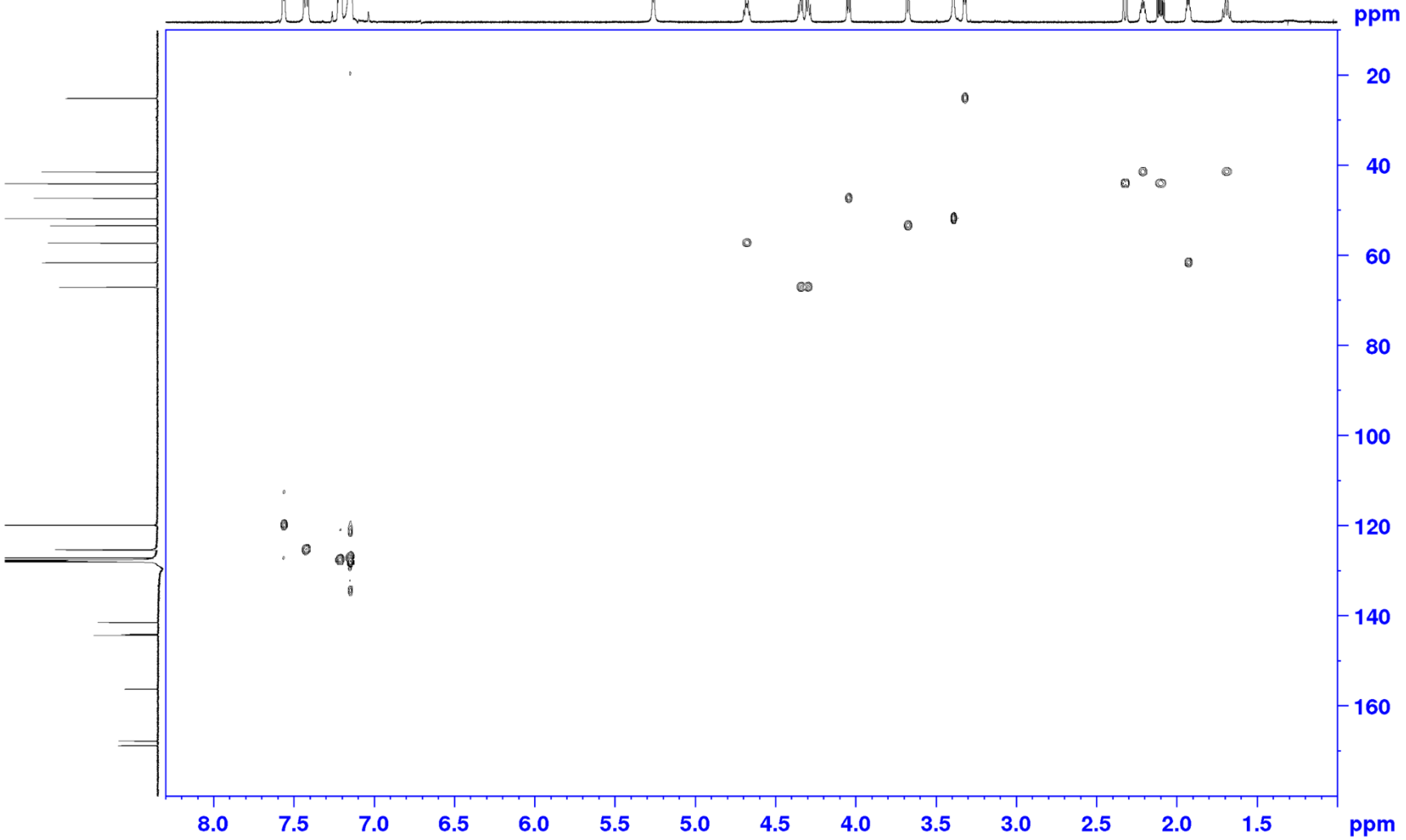

NOESY 700 MHz
Solvent: C_6D_6

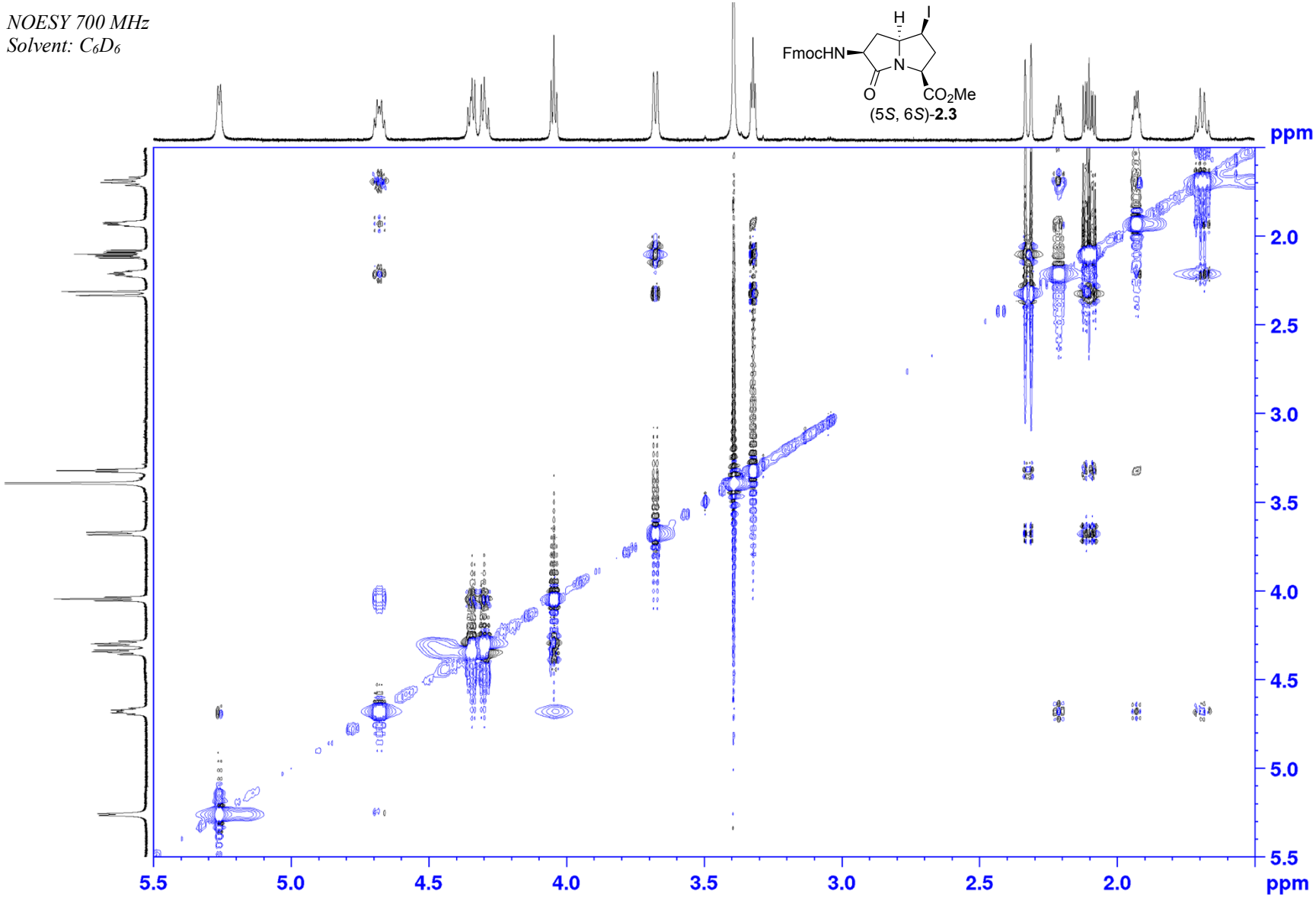

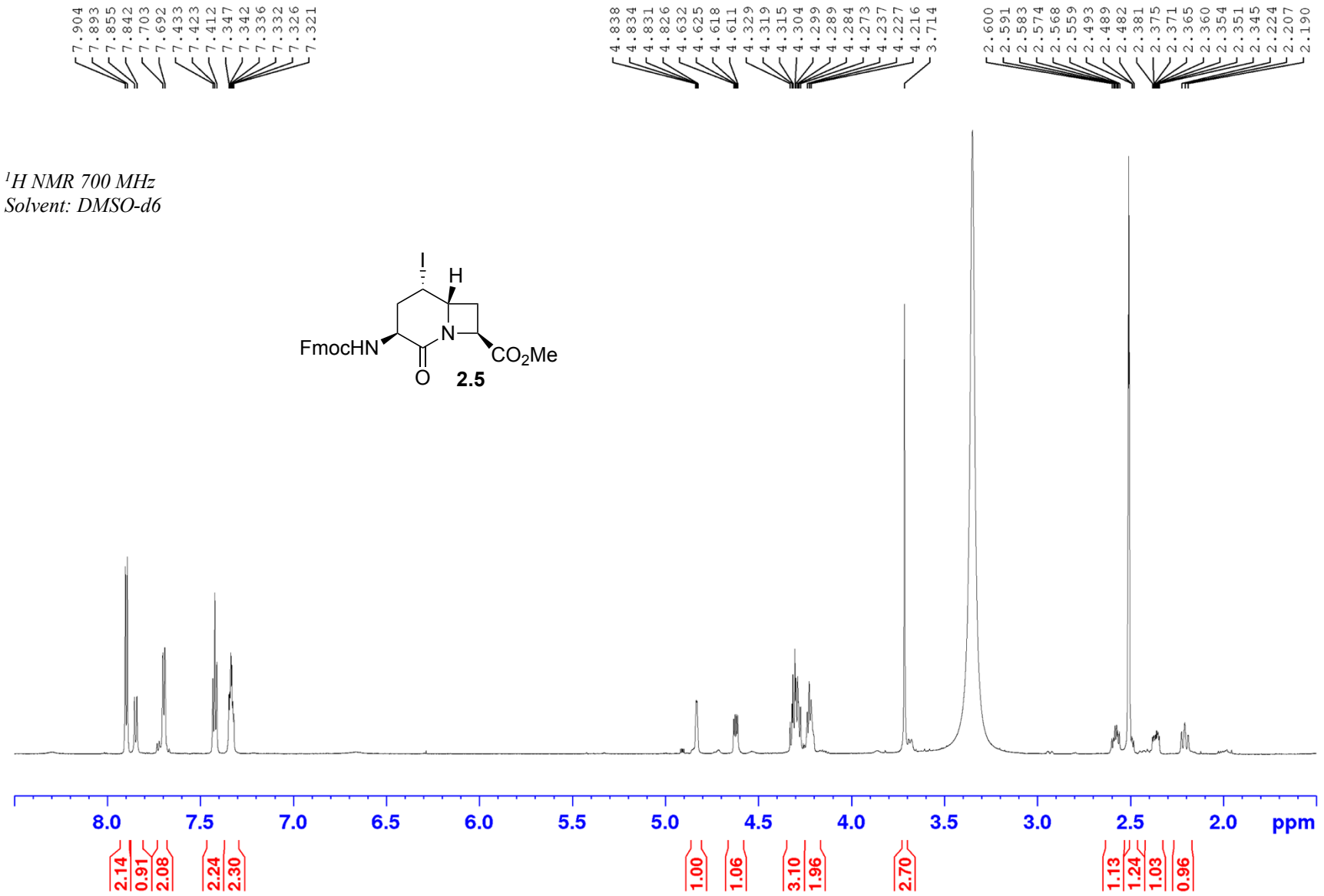
7.904
7.893
7.855
7.842
7.703
7.692
7.433
7.423
7.412
7.347
7.342
7.336
7.332
7.326
7.321
4.838
4.834
4.831
4.826
4.632
4.625
4.618
4.611
4.329
4.319
4.315
4.304
4.299
4.289
4.284
4.273
4.237
4.227
4.216
3.714
2.600
2.591
2.583
2.574
2.568
2.559
2.493
2.489
2.482
2.381
2.375
2.371
2.365
2.360
2.354
2.351
2.345
2.224
2.207
2.190
1H NMR 700 MHz
Solvent: DMSO-d6
I
H
N
FmocHN
CO2Me
O
2.5
8.0
7.5
7.0
6.5
6.0
5.5
5.0
4.5
4.0
3.5
3.0
2.5
2.0
ppm
2.14
0.91
2.08
2.24
2.30
1.00
1.06
3.10
1.96
2.70
1.13
1.24
1.03
0.96

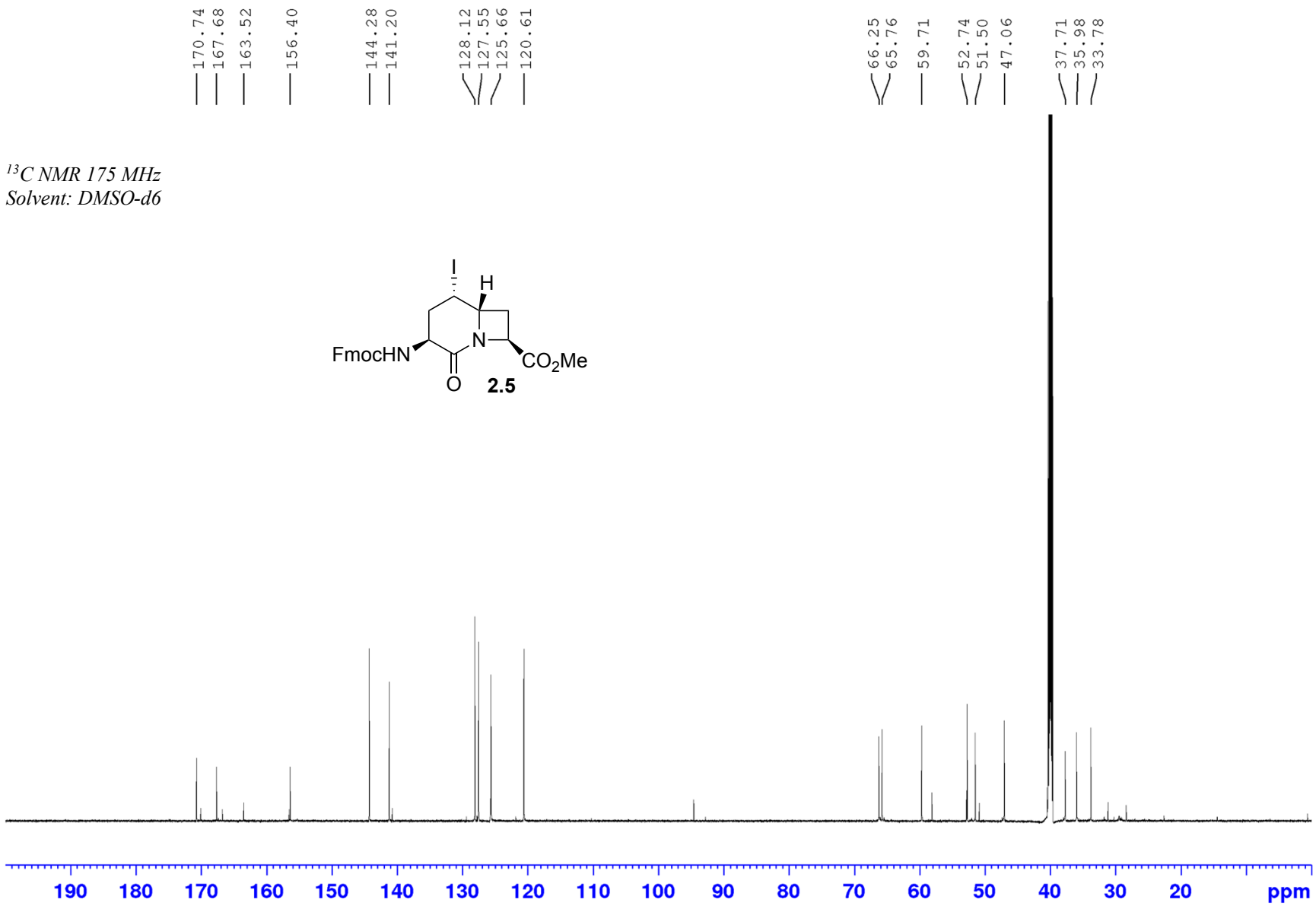
170.74
167.68
163.52
156.40
144.28
141.20
128.12
127.55
125.66
120.61
66.25
65.76
59.71
52.74
51.50
47.06
37.71
35.98
33.78
13C NMR 175 MHz
Solvent: DMSO-d6
I
H
N
FmocHN
CO2Me
O
2.5
190
180
170
160
150
140
130
120
110
100
90
80
70
60
50
40
30
20
ppm

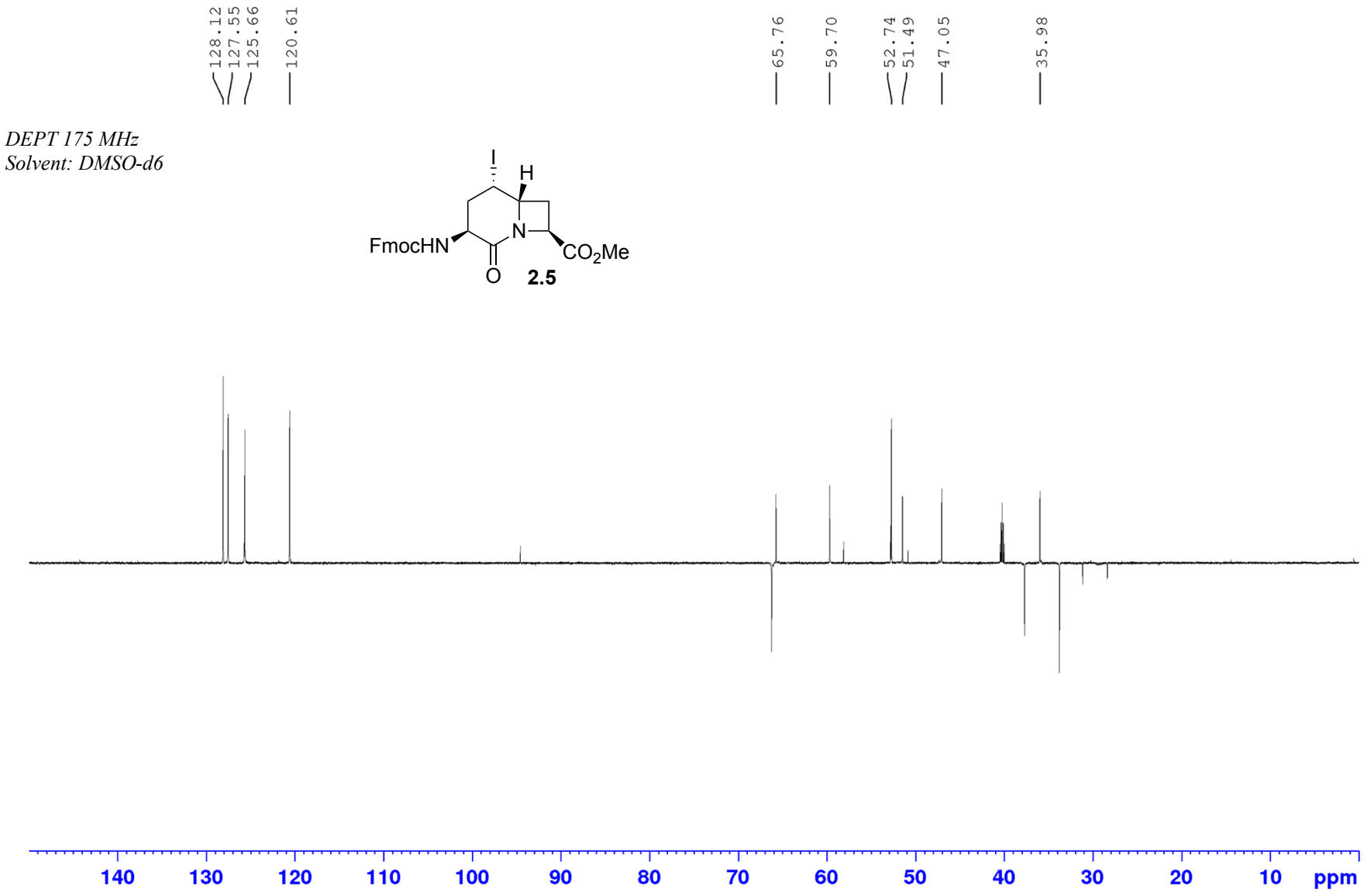
128.12
127.55
125.66
120.61
65.76
59.70
52.74
51.49
47.05
35.98
DEPT 175 MHz
Solvent: DMSO-d6
I
H
N
FmocHN
CO2Me
O
2.5
140
130
120
110
100
90
80
70
60
50
40
30
20
10
ppm

COSY 700 MHz
Solvent: DMSO-d6

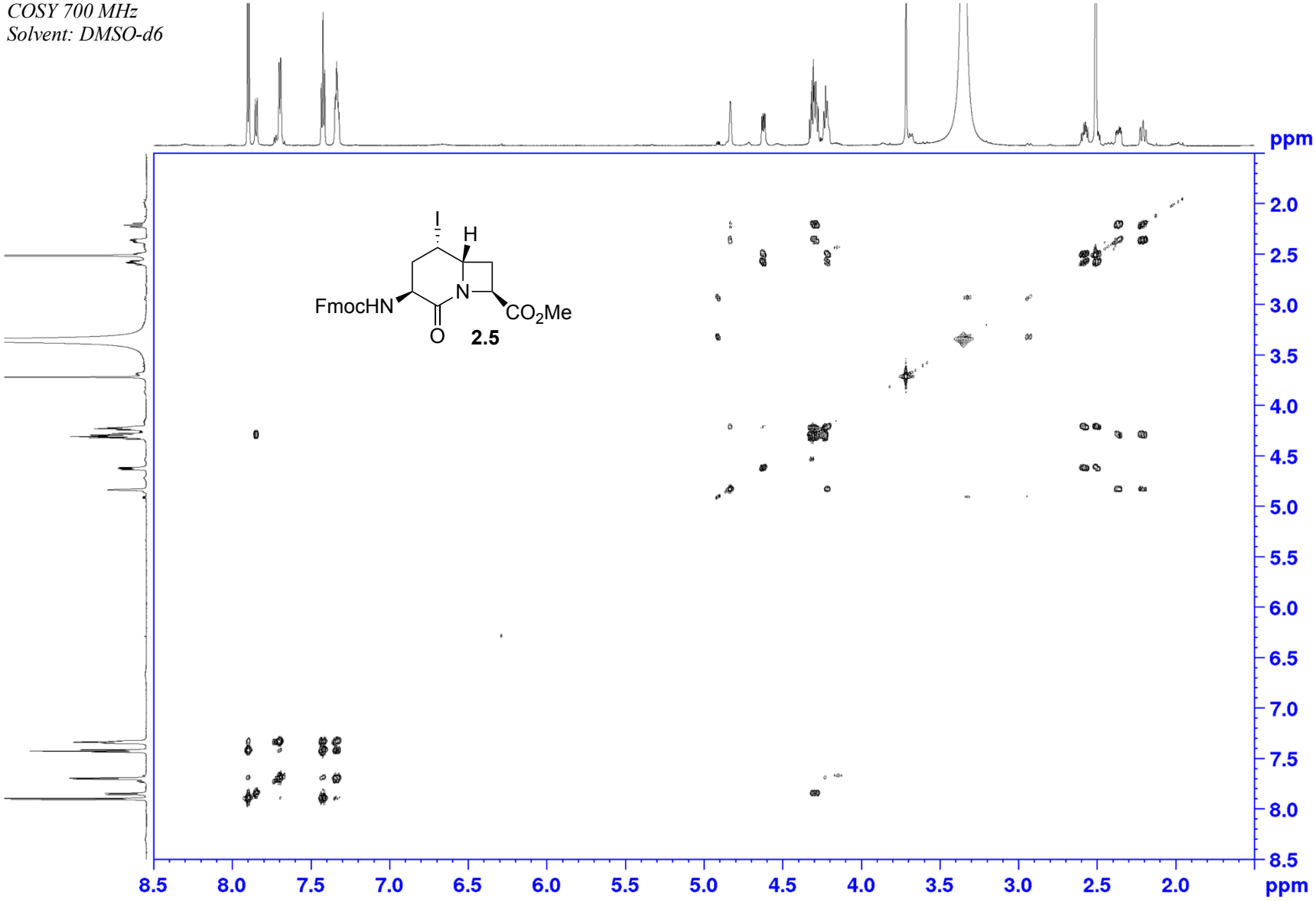

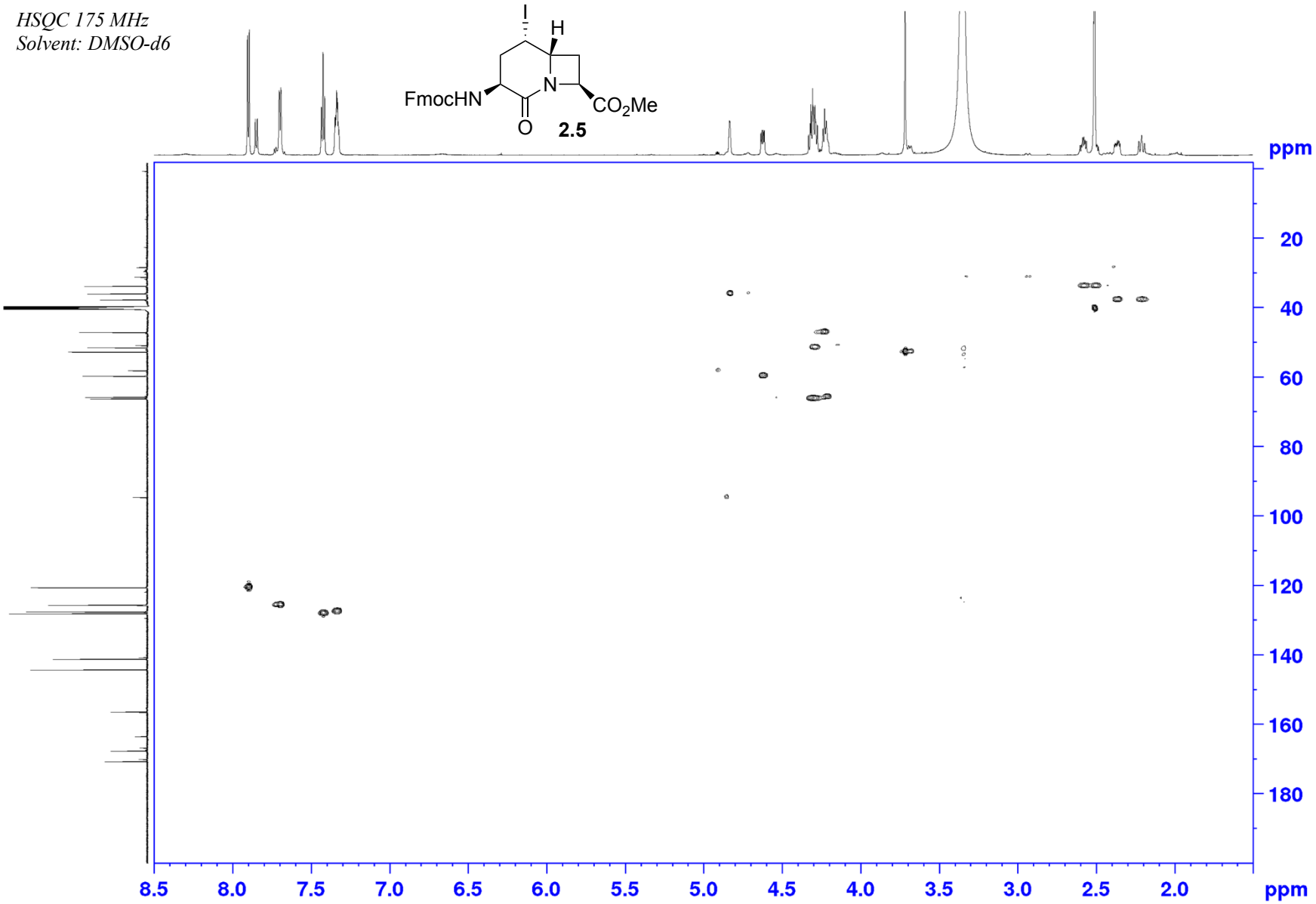
HSQC 175 MHz
Solvent: DMSO-d6
I
H
FmocHN
N
CO2Me
O
2.5
ppm
20
40
60
80
100
120
140
160
180
8.5
8.0
7.5
7.0
6.5
6.0
5.5
5.0
4.5
4.0
3.5
3.0
2.5
2.0
ppm

NOESY 700 MHz
Solvent: DMSO-d6

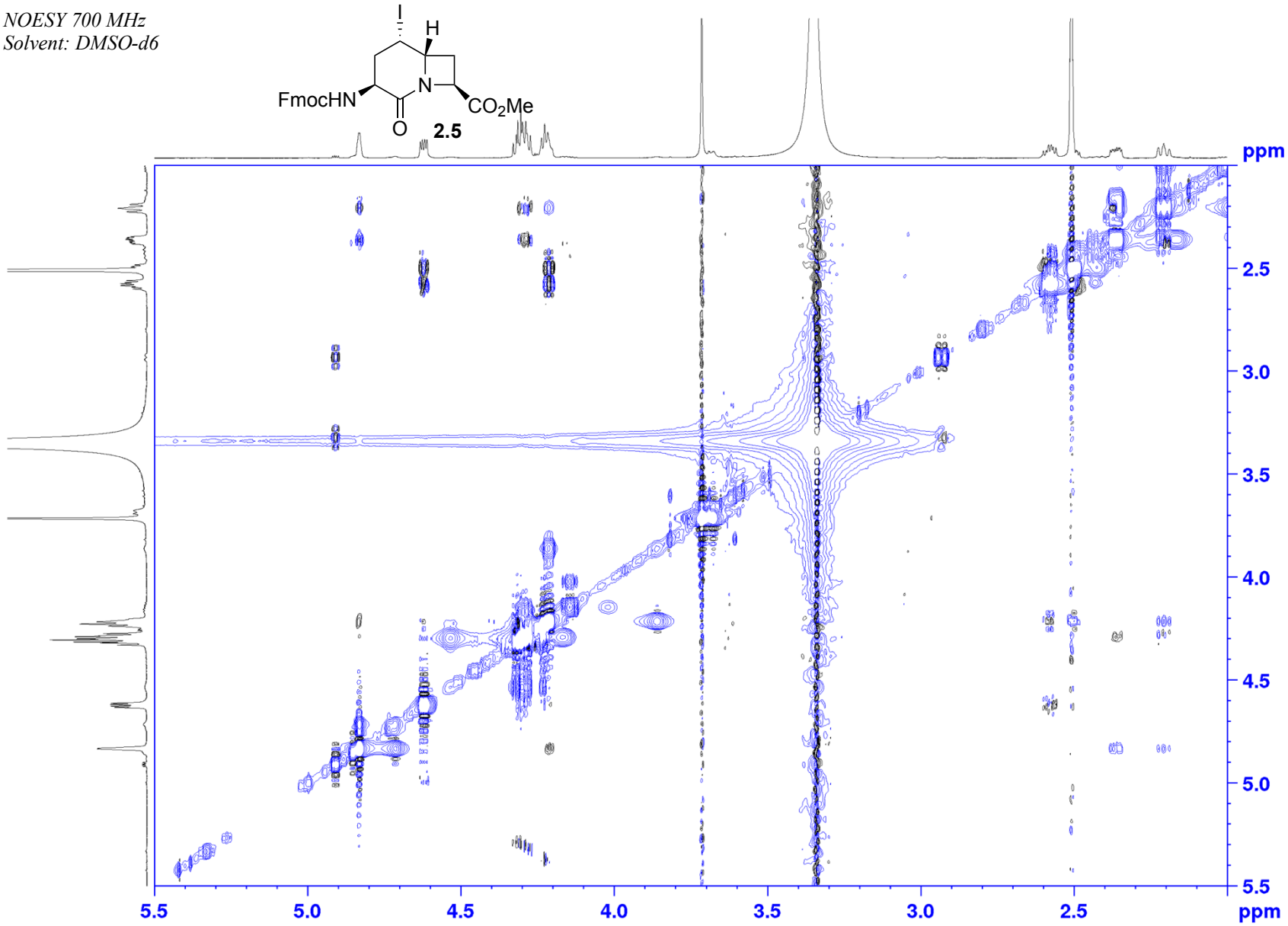

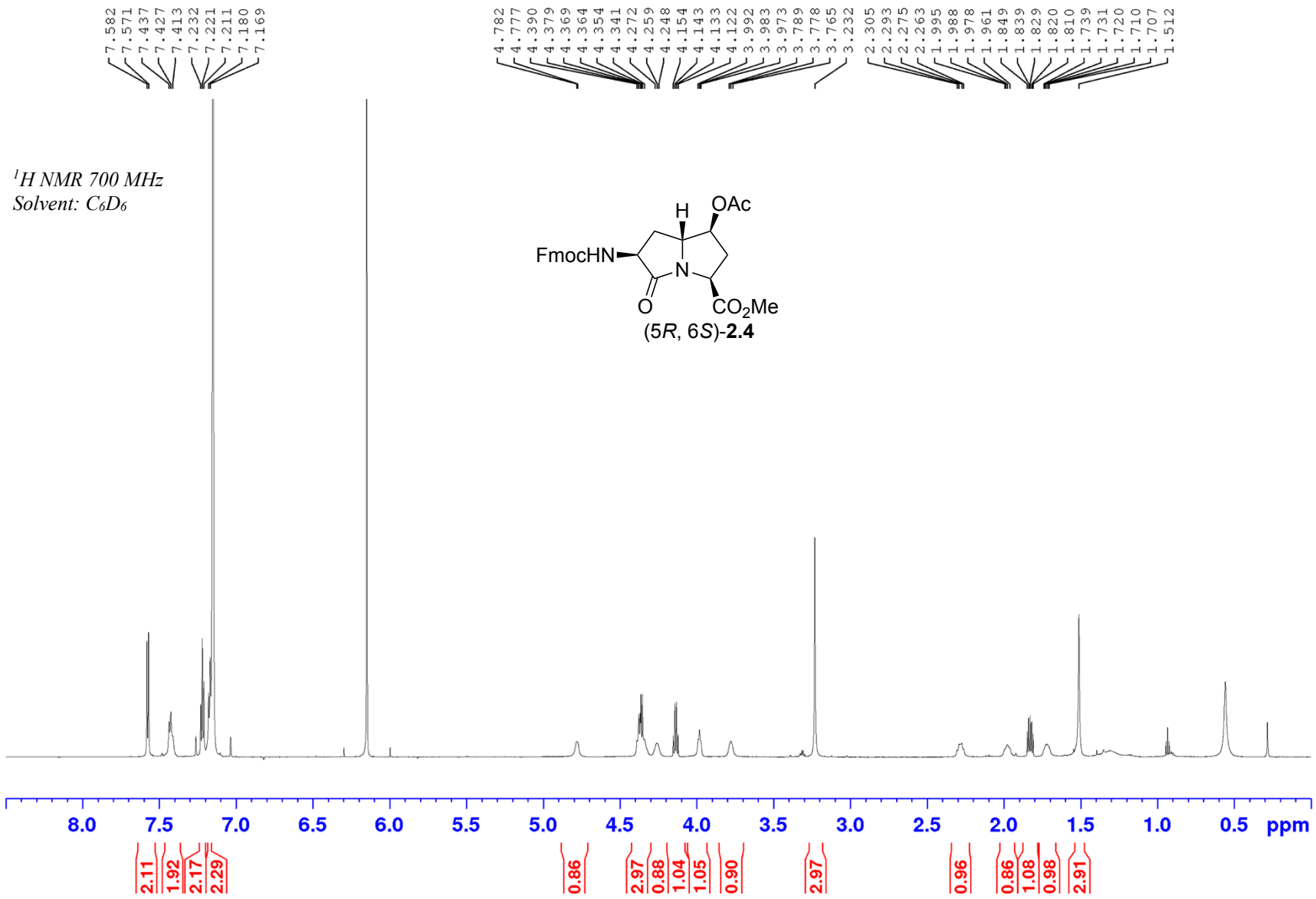
7.582
7.571
7.437
7.427
7.413
7.232
7.221
7.211
7.180
7.169
4.782
4.777
4.390
4.379
4.369
4.364
4.354
4.341
4.272
4.259
4.248
4.154
4.143
4.133
4.122
3.992
3.983
3.973
3.789
3.778
3.765
3.232
2.305
2.293
2.275
2.263
1.995
1.988
1.978
1.961
1.849
1.839
1.829
1.820
1.810
1.739
1.731
1.720
1.710
1.707
1.512
^{1}H NMR 700 MHz
Solvent: C_6D_6
H
OAc
FmocHN
N
O
CO_2Me
(5*R*, 6*S*)-**2.4**
8.0
7.5
7.0
6.5
6.0
5.5
5.0
4.5
4.0
3.5
3.0
2.5
2.0
1.5
1.0
0.5
ppm
2.11
1.92
2.17
2.29
0.86
2.97
0.88
1.04
1.05
0.90
2.97
0.96
0.86
1.08
0.98
2.91

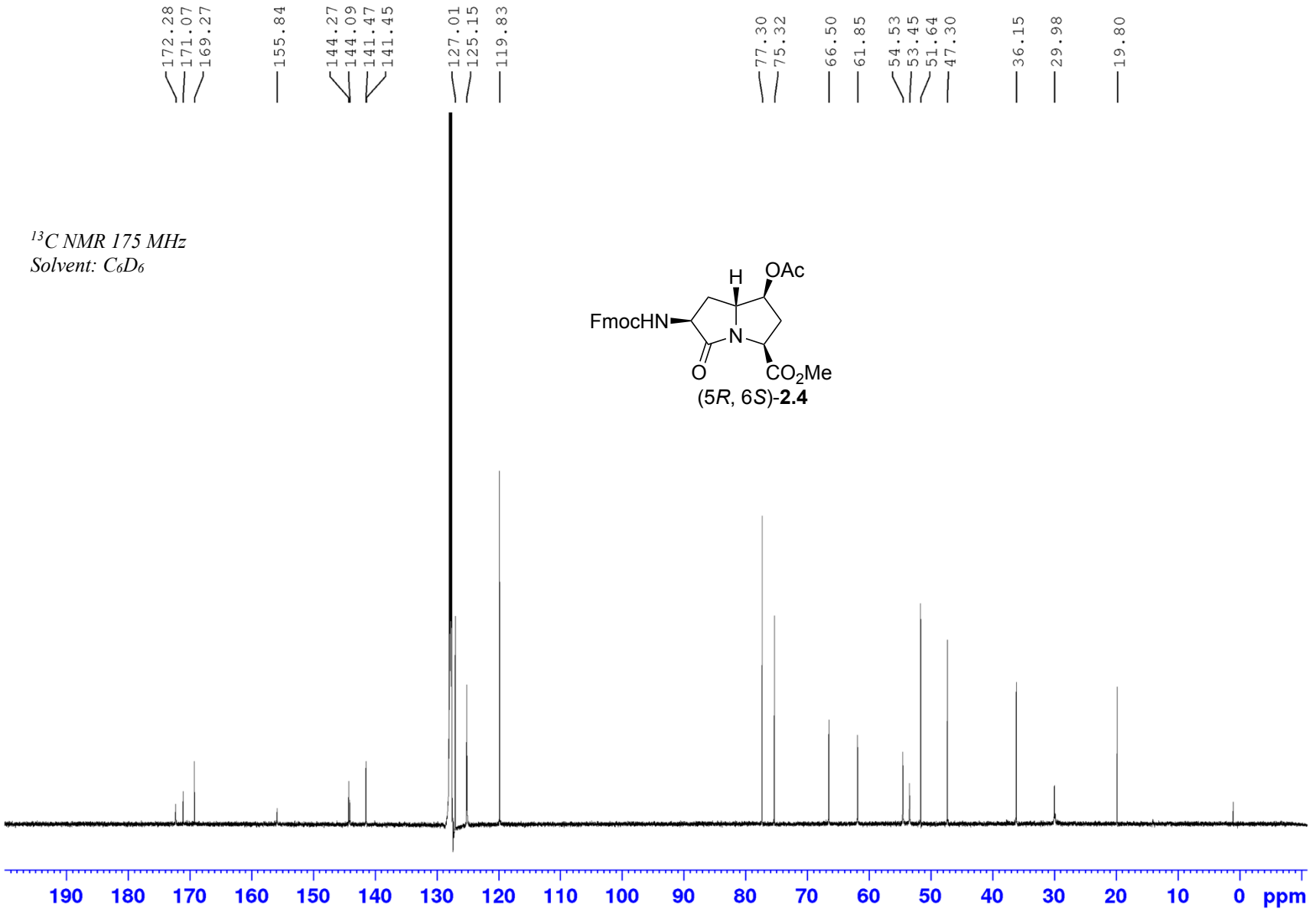
172.28
171.07
169.27
155.84
144.27
144.09
141.47
141.45
127.01
125.15
119.83
77.30
75.32
66.50
61.85
54.53
53.45
51.64
47.30
36.15
29.98
19.80
13C NMR 175 MHz
Solvent: C6D6
H
OAc
FmocHN
N
O
CO2Me
(5R, 6S)-2.4
190 180 170 160 150 140 130 120 110 100 90 80 70 60 50 40 30 20 10 0 ppm

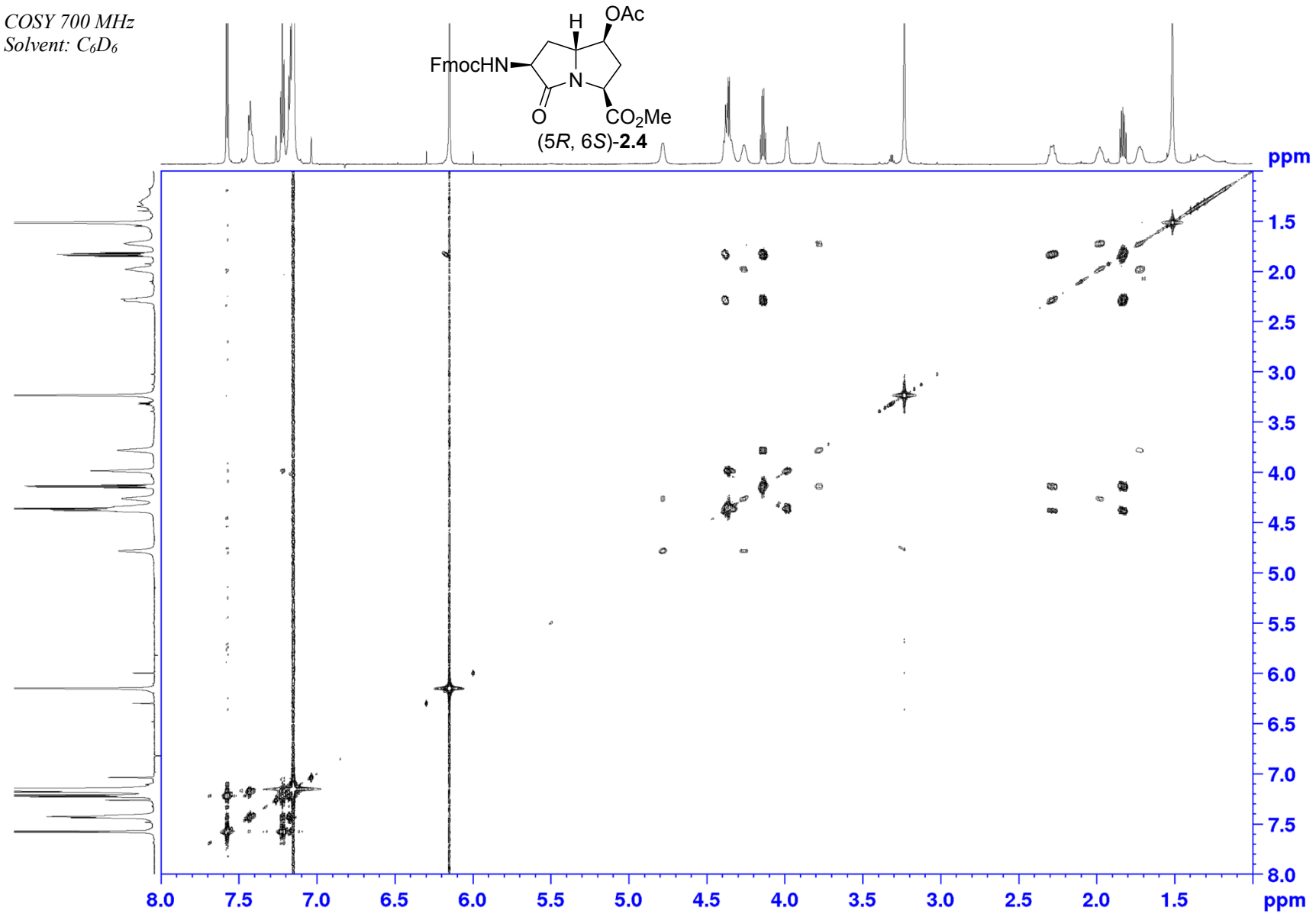
COSY 700 MHz
Solvent: C6D6
H
OAc
FmocHN
N
O
CO2Me
(5R, 6S)-2.4
ppm
1.5
2.0
2.5
3.0
3.5
4.0
4.5
5.0
5.5
6.0
6.5
7.0
7.5
8.0
8.0
7.5
7.0
6.5
6.0
5.5
5.0
4.5
4.0
3.5
3.0
2.5
2.0
1.5
ppm

DEPT 175 MHz
Solvent: C_6D_6

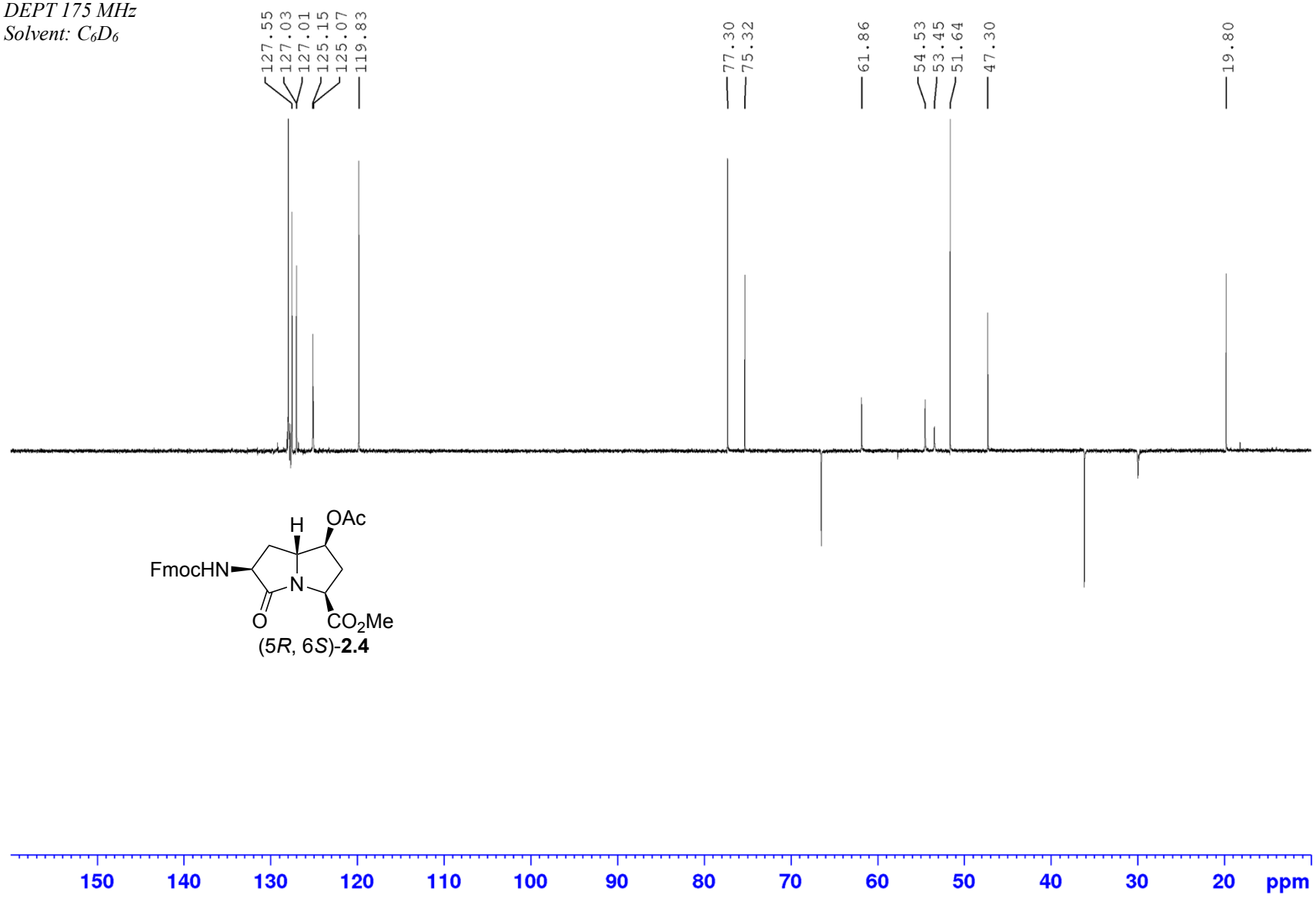

(5*R*, 6*S*)-**2.4**

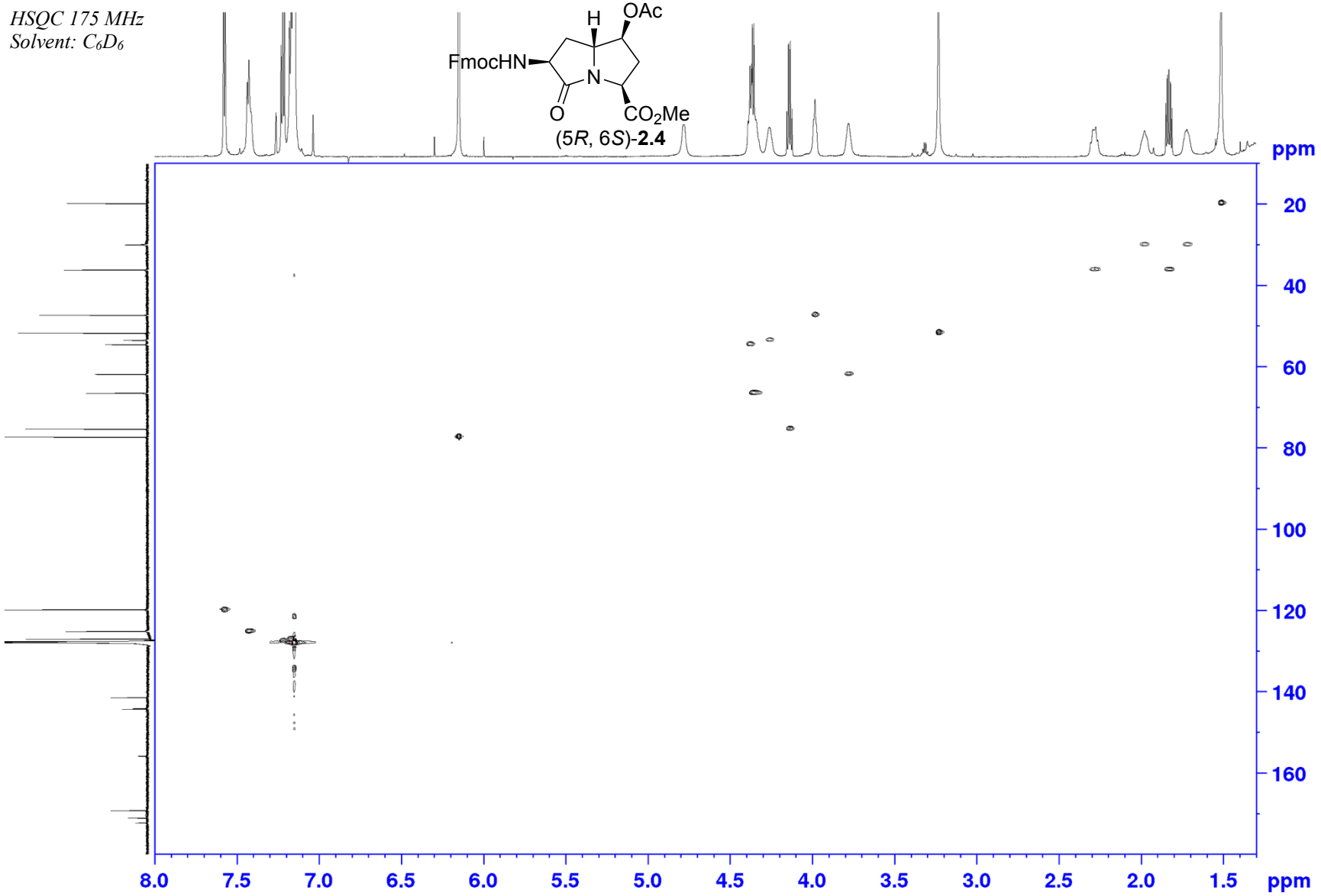
HSQC 175 MHz
Solvent: C6D6
H
OAc
FmocHN
N
O
CO2Me
(5R, 6S)-2.4
ppm
20
40
60
80
100
120
140
160
8.0
7.5
7.0
6.5
6.0
5.5
5.0
4.5
4.0
3.5
3.0
2.5
2.0
1.5
ppm

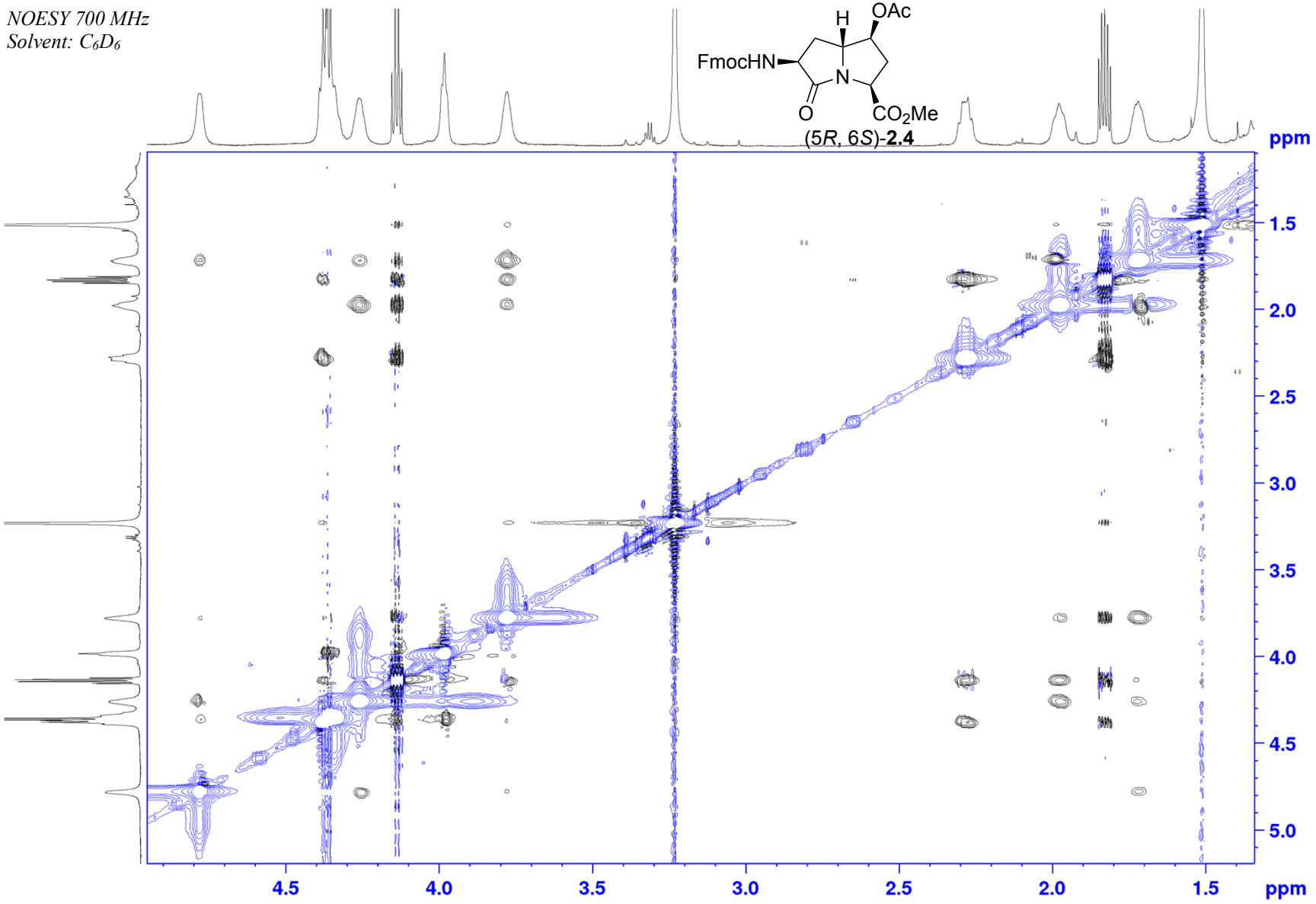
NOESY 700 MHz
Solvent: C6D6
H
OAc
FmocHN
N
O
CO2Me
(5R, 6S)-2.4
ppm
1.5
2.0
2.5
3.0
3.5
4.0
4.5
5.0
4.5
4.0
3.5
3.0
2.5
2.0
1.5
ppm

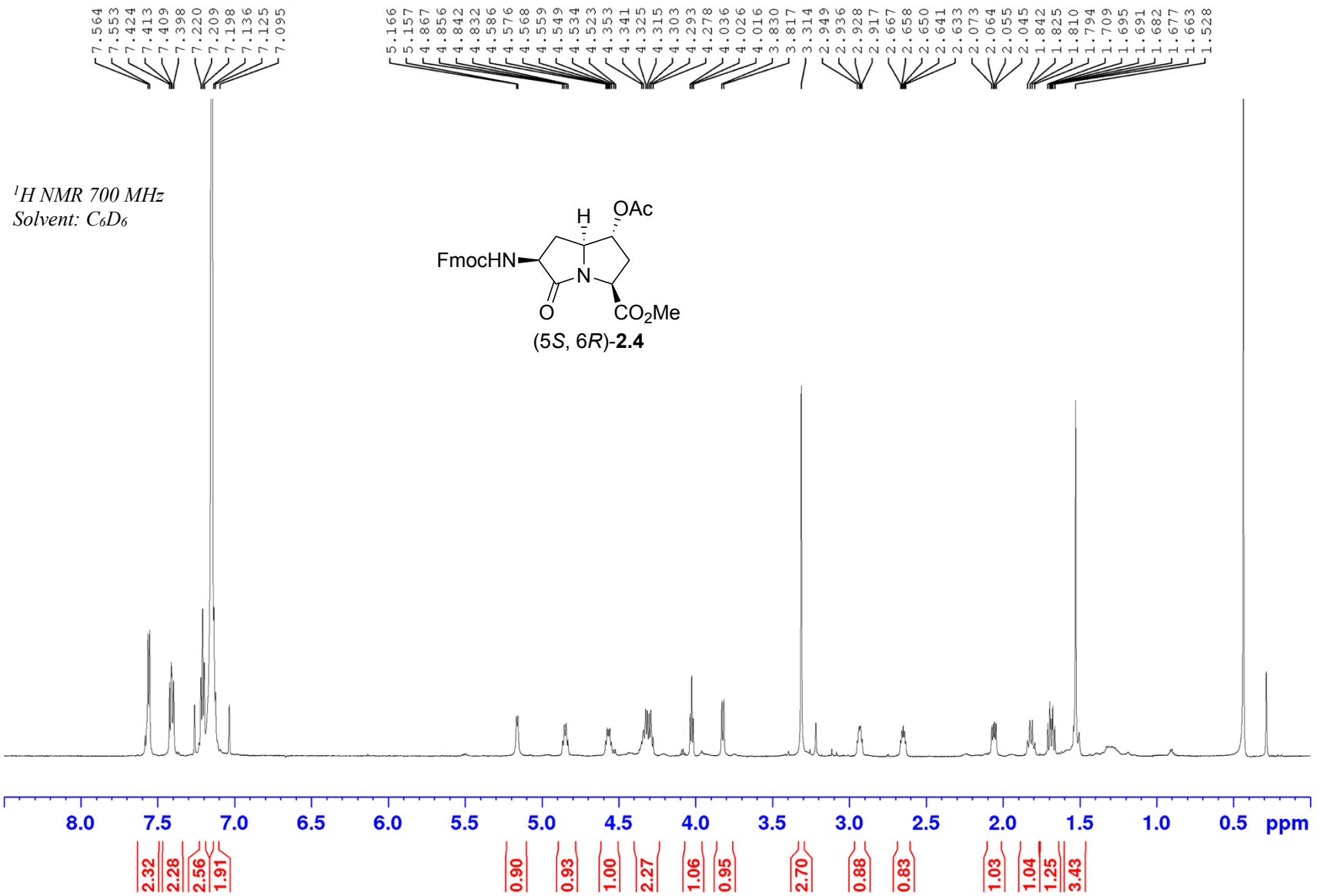
7.564
7.553
7.424
7.413
7.409
7.398
7.220
7.209
7.198
7.136
7.125
7.095
5.166
5.157
4.867
4.856
4.842
4.832
4.586
4.576
4.568
4.559
4.549
4.534
4.523
4.353
4.341
4.325
4.315
4.303
4.293
4.278
4.036
4.026
4.016
3.830
3.817
3.314
2.949
2.936
2.928
2.917
2.667
2.658
2.650
2.641
2.633
2.073
2.064
2.055
2.045
1.842
1.825
1.810
1.794
1.709
1.695
1.691
1.682
1.677
1.663
1.528
1H NMR 700 MHz
Solvent: C6D6
H
OAc
FmocHN
N
O
CO2Me
(5S, 6R)-2.4
8.0
7.5
7.0
6.5
6.0
5.5
5.0
4.5
4.0
3.5
3.0
2.5
2.0
1.5
1.0
0.5
ppm
2.32
2.28
2.56
1.91
0.90
0.93
1.00
2.27
1.06
0.95
2.70
0.88
0.83
1.03
1.04
1.25
3.43

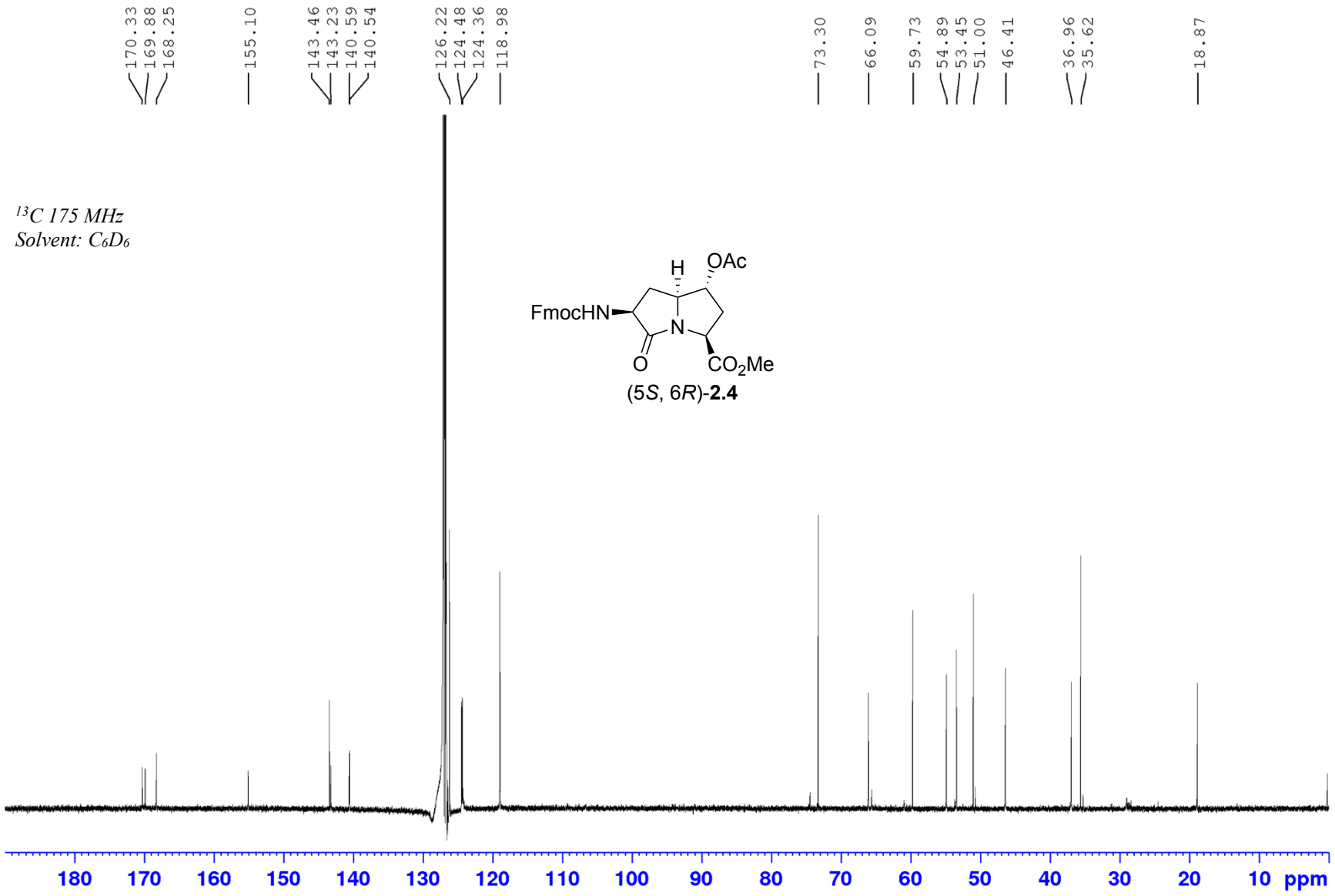
170.33
169.88
168.25
155.10
143.46
143.23
140.59
140.54
126.22
124.48
124.36
118.98
73.30
66.09
59.73
54.89
53.45
51.00
46.41
36.96
35.62
18.87
13C 175 MHz
Solvent: C6D6
H
OAc
FmocHN
N
O
CO2Me
(5S, 6R)-2.4
180
170
160
150
140
130
120
110
100
90
80
70
60
50
40
30
20
10
ppm

COSY 700 MHz
Solvent: C_6D_6

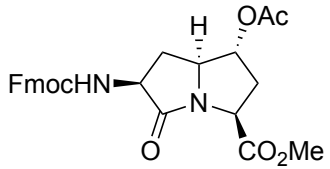

(5*S*, 6*R*)-**2.4**

HSQC 175 MHz
Solvent: C_6D_6

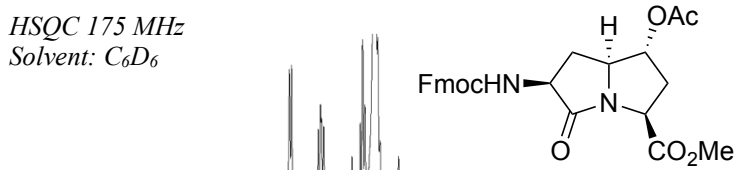

(5*S*, 6*R*)-**2.4**

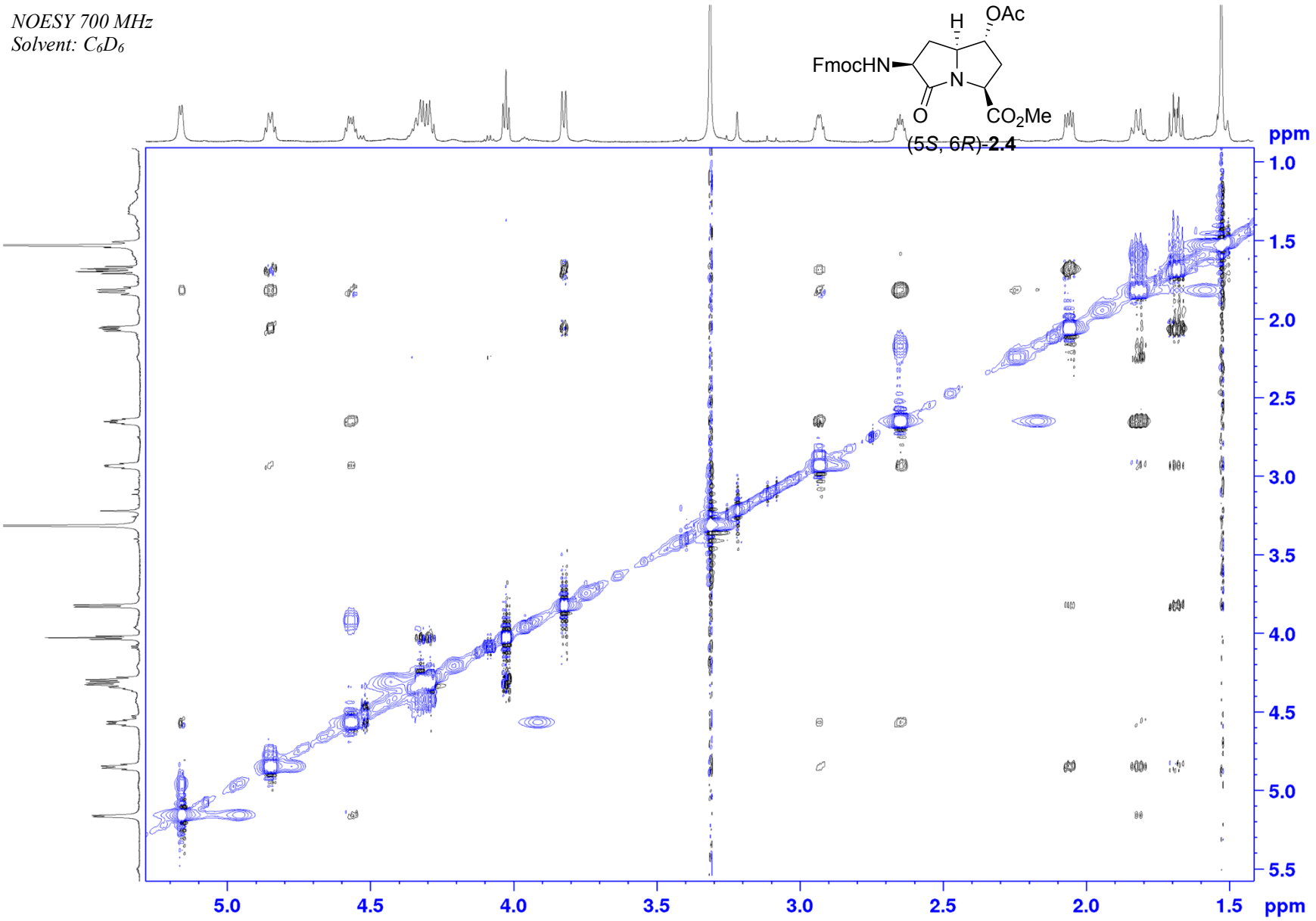
NOESY 700 MHz
Solvent: C6D6
H
OAc
FmocHN
N
O
CO2Me
(5S, 6R)-2.4
ppm
1.0
1.5
2.0
2.5
3.0
3.5
4.0
4.5
5.0
5.5
5.0
4.5
4.0
3.5
3.0
2.5
2.0
1.5
ppm

8.166
7.805
7.794
7.654
7.644
7.446
7.436
7.425
7.365
7.355
7.344
7.122
7.115
6.353
6.342
6.330
6.287
6.279
5.755
5.749
5.742
5.736
4.461
4.451
4.285
4.276
4.267
3.924

^{1}H NMR 700 MHz
Solvent: $CDCl_3$

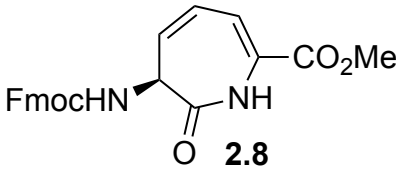

2.8

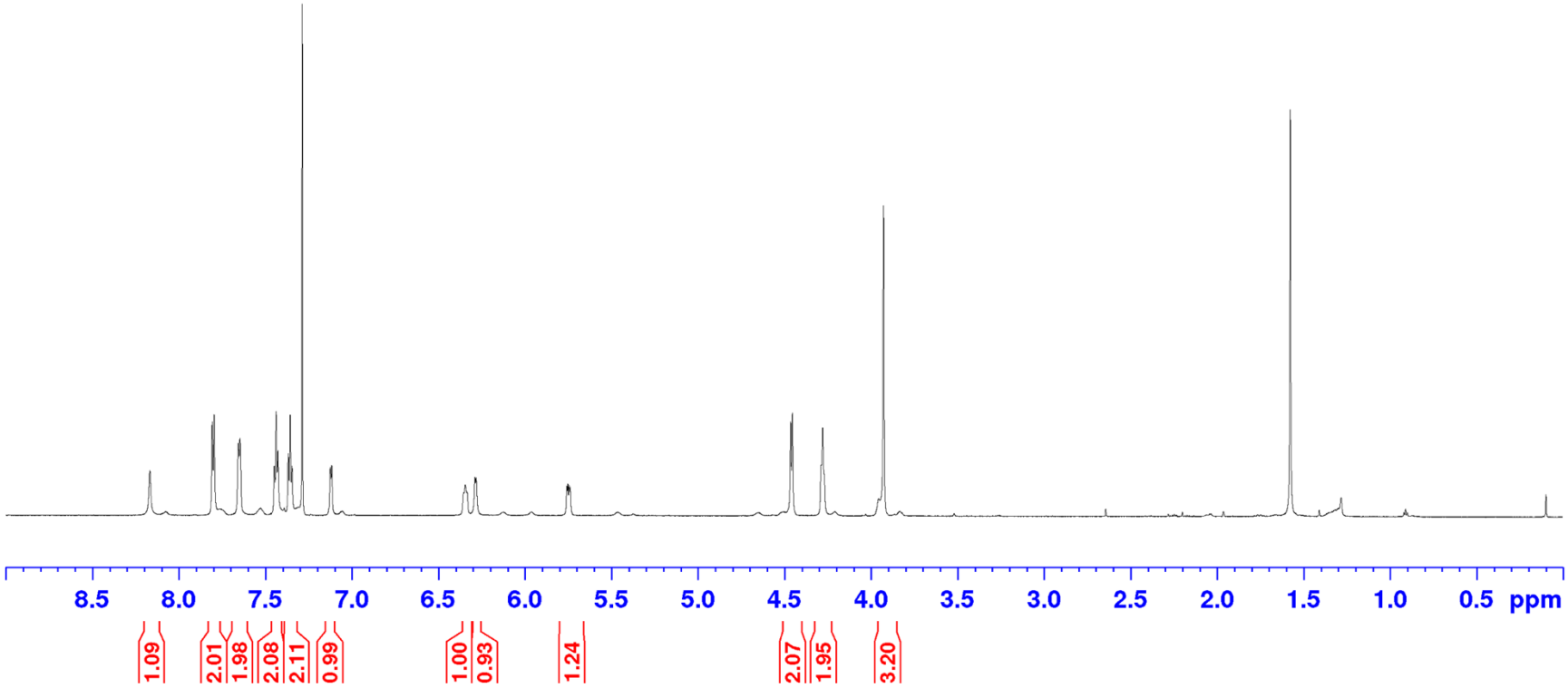

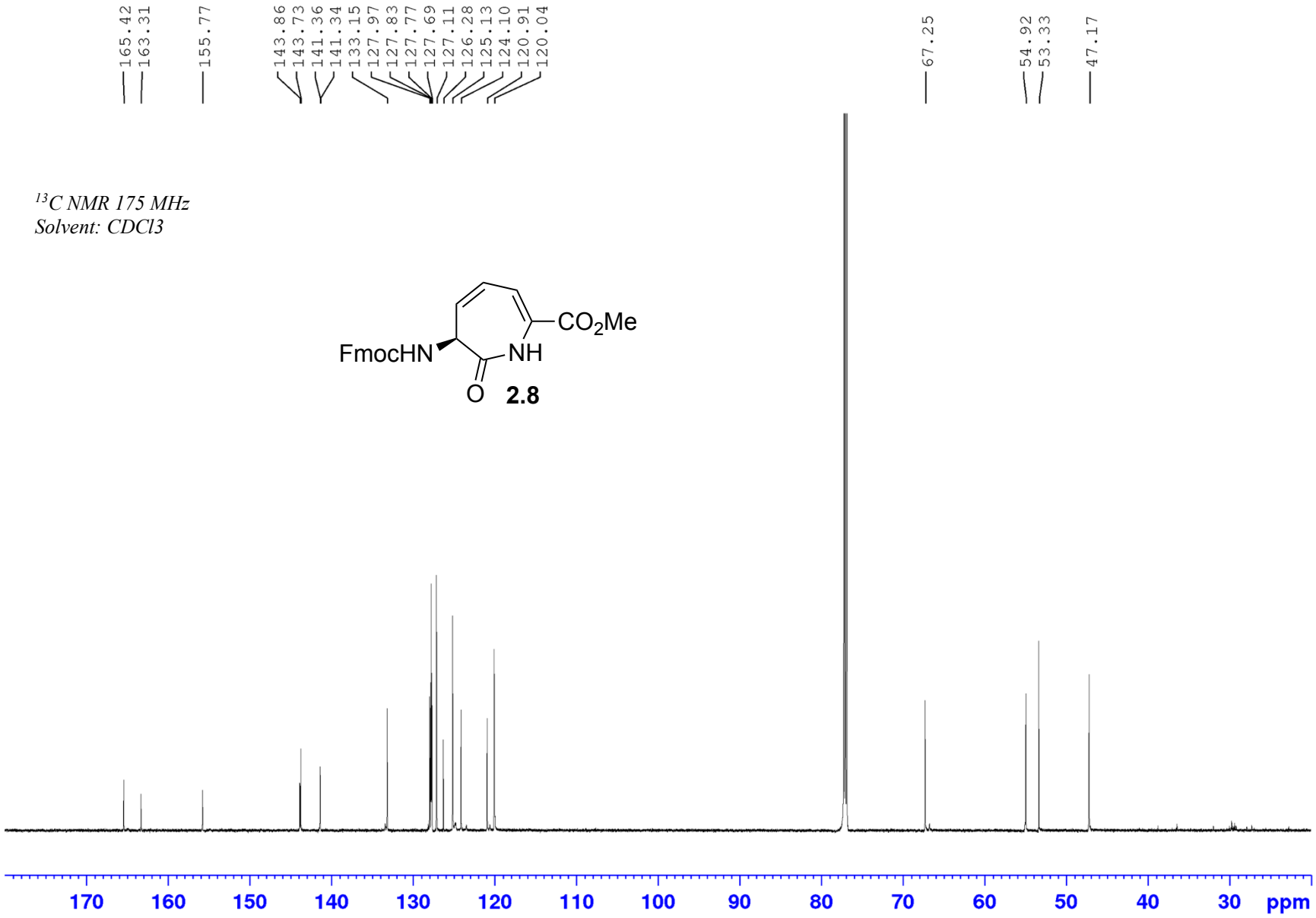
165.42
163.31
155.77
143.86
143.73
141.36
141.34
133.15
127.97
127.83
127.77
127.69
127.11
126.28
125.13
124.10
120.91
120.04
67.25
54.92
53.33
47.17
13C NMR 175 MHz
Solvent: CDCl3
CO2Me
FmocHN
NH
O
2.8
170
160
150
140
130
120
110
100
90
80
70
60
50
40
30
ppm

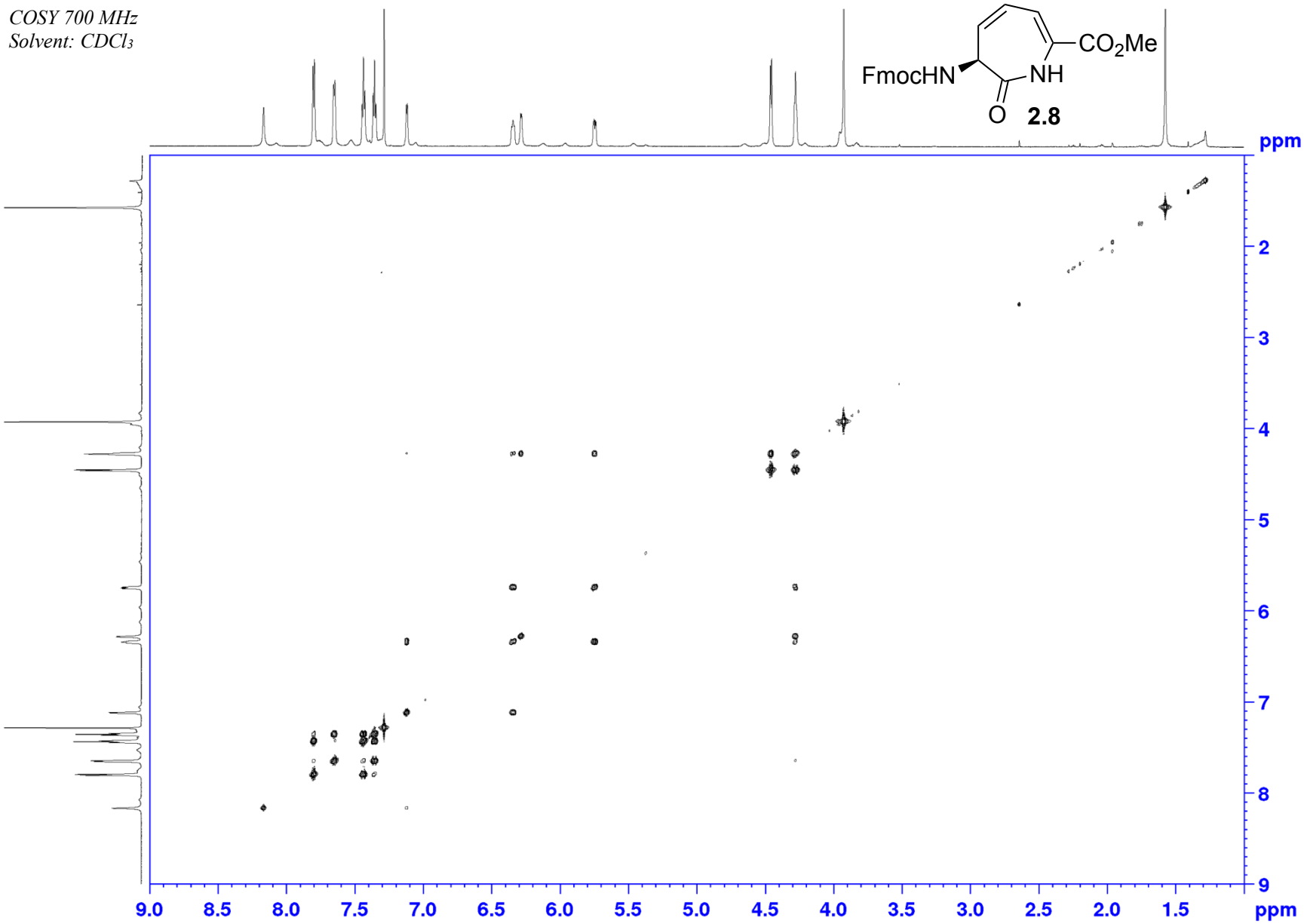
COSY 700 MHz
Solvent: CDCl3
FmocHN
NH
CO2Me
O
2.8
ppm
9.0
8.5
8.0
7.5
7.0
6.5
6.0
5.5
5.0
4.5
4.0
3.5
3.0
2.5
2.0
1.5
ppm
2
3
4
5
6
7
8
9

DEPT 175 MHz
Solvent: $CDCl_3$

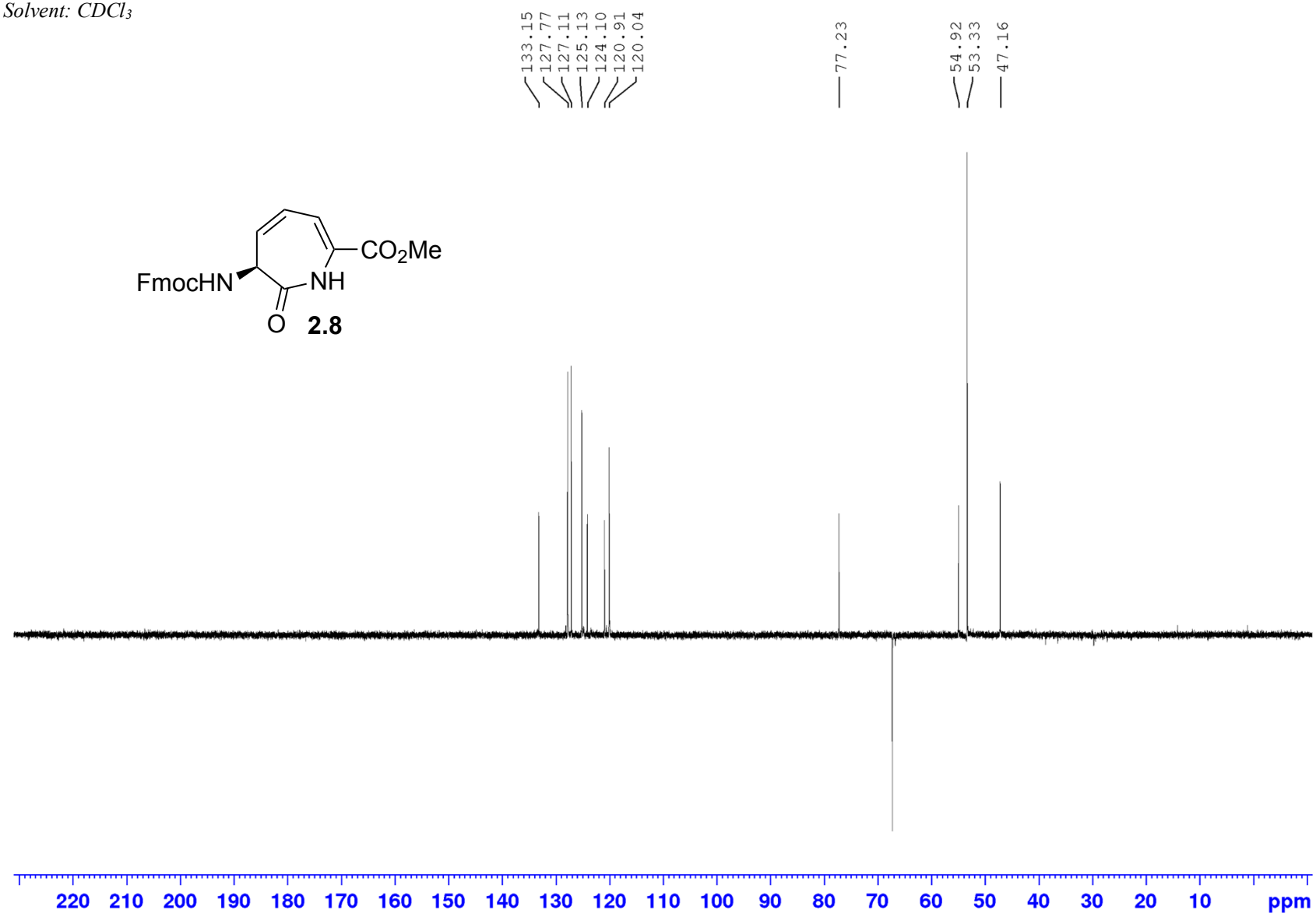

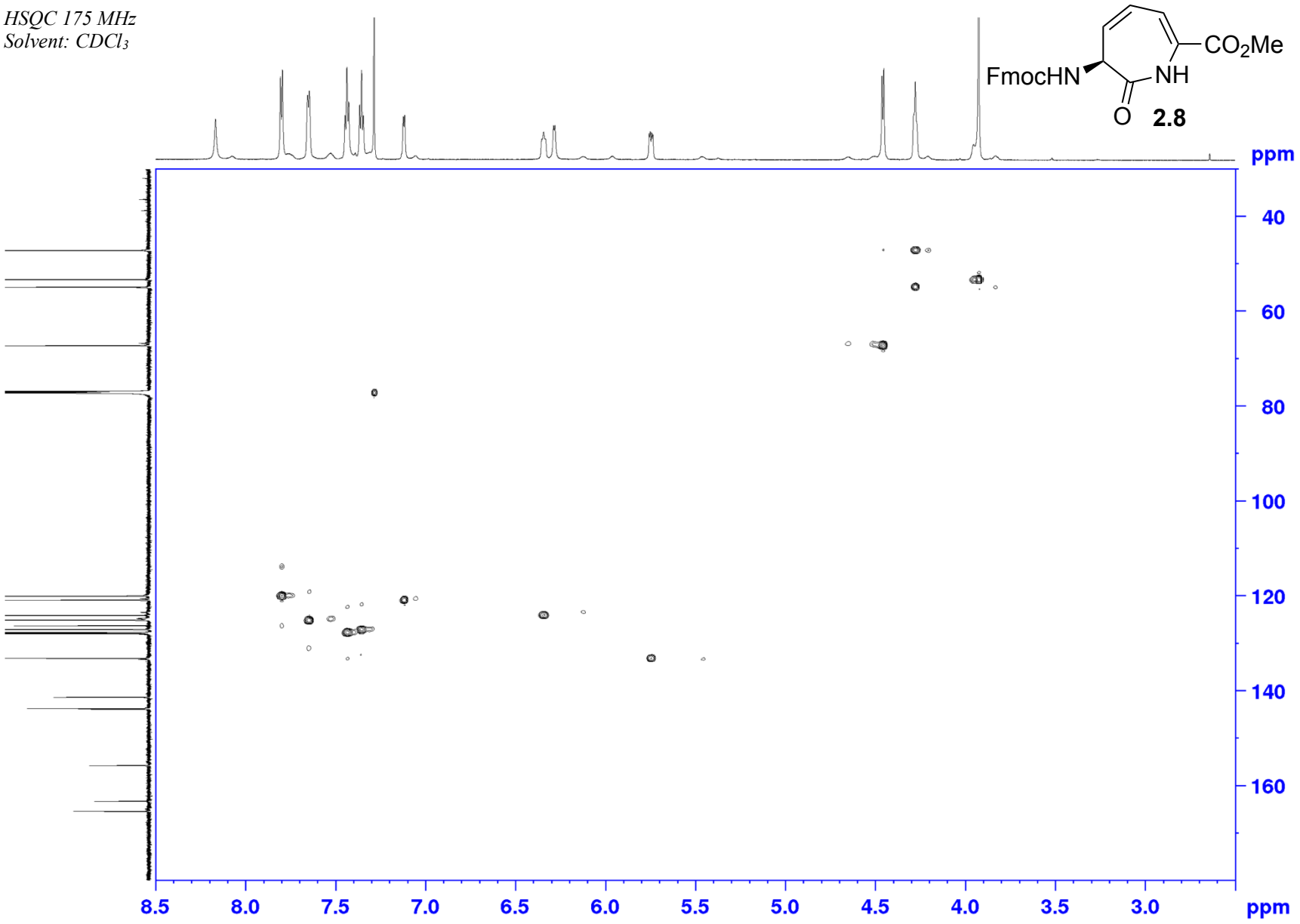
HSQC 175 MHz
Solvent: CDCl3
FmocHN
NH
O
CO2Me
2.8
ppm
40
60
80
100
120
140
160
8.5
8.0
7.5
7.0
6.5
6.0
5.5
5.0
4.5
4.0
3.5
3.0
ppm

^{1}H NMR 500 MHz
Solvent: $CDCl_3$

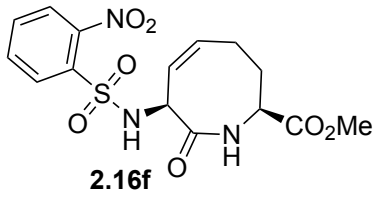

2.16f

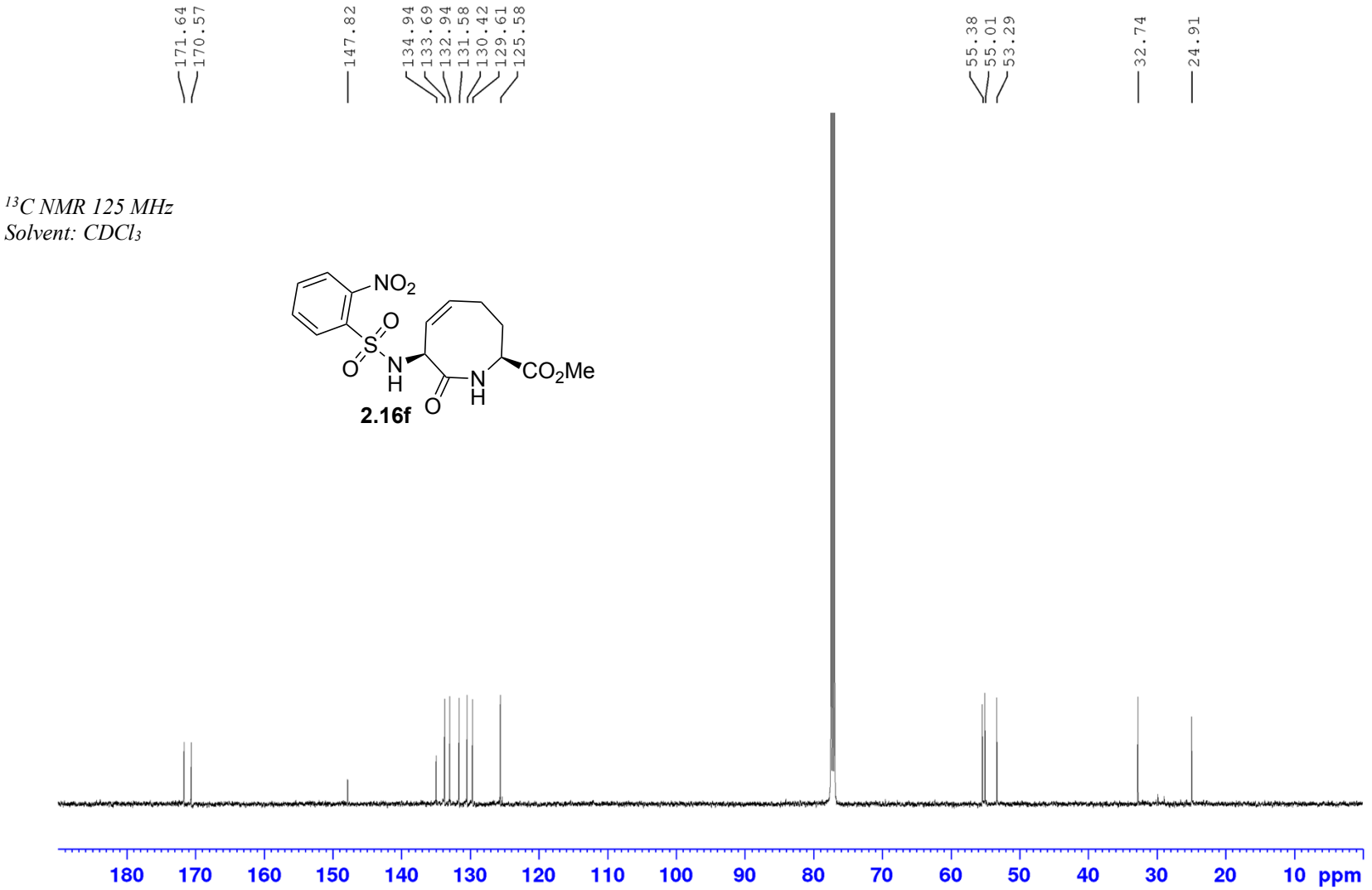

^{13}C NMR 125 MHz
Solvent: $CDCl_3$

2.16f

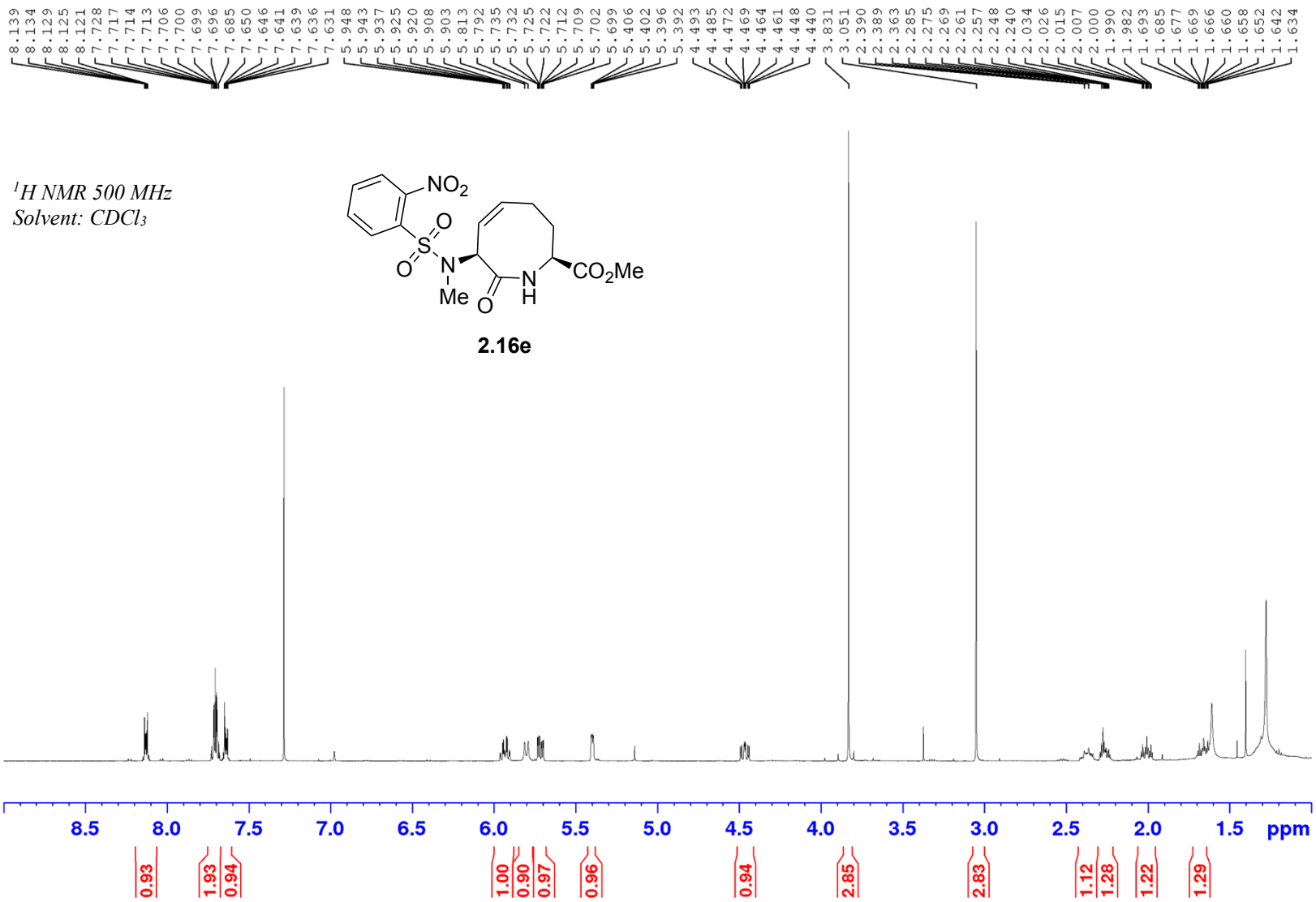
8.139
8.134
8.129
8.125
8.121
7.728
7.717
7.714
7.713
7.706
7.700
7.699
7.696
7.685
7.650
7.646
7.641
7.639
7.636
7.631
5.948
5.943
5.937
5.925
5.920
5.908
5.903
5.813
5.792
5.735
5.732
5.725
5.722
5.712
5.709
5.702
5.699
5.406
5.402
5.396
5.392
4.493
4.485
4.472
4.469
4.464
4.461
4.448
4.440
3.831
3.051
2.390
2.389
2.363
2.285
2.275
2.269
2.261
2.257
2.248
2.240
2.034
2.026
2.015
2.007
2.000
1.990
1.982
1.693
1.685
1.677
1.669
1.666
1.660
1.658
1.652
1.642
1.634
1H NMR 500 MHz
Solvent: CDCl3
NO2
O
S
O
N
Me
O
N
H
CO2Me
2.16e
8.5
8.0
7.5
7.0
6.5
6.0
5.5
5.0
4.5
4.0
3.5
3.0
2.5
2.0
1.5
ppm
0.93
1.93
0.94
1.00
0.90
0.97
0.96
0.94
2.85
2.83
1.12
1.28
1.22
1.29

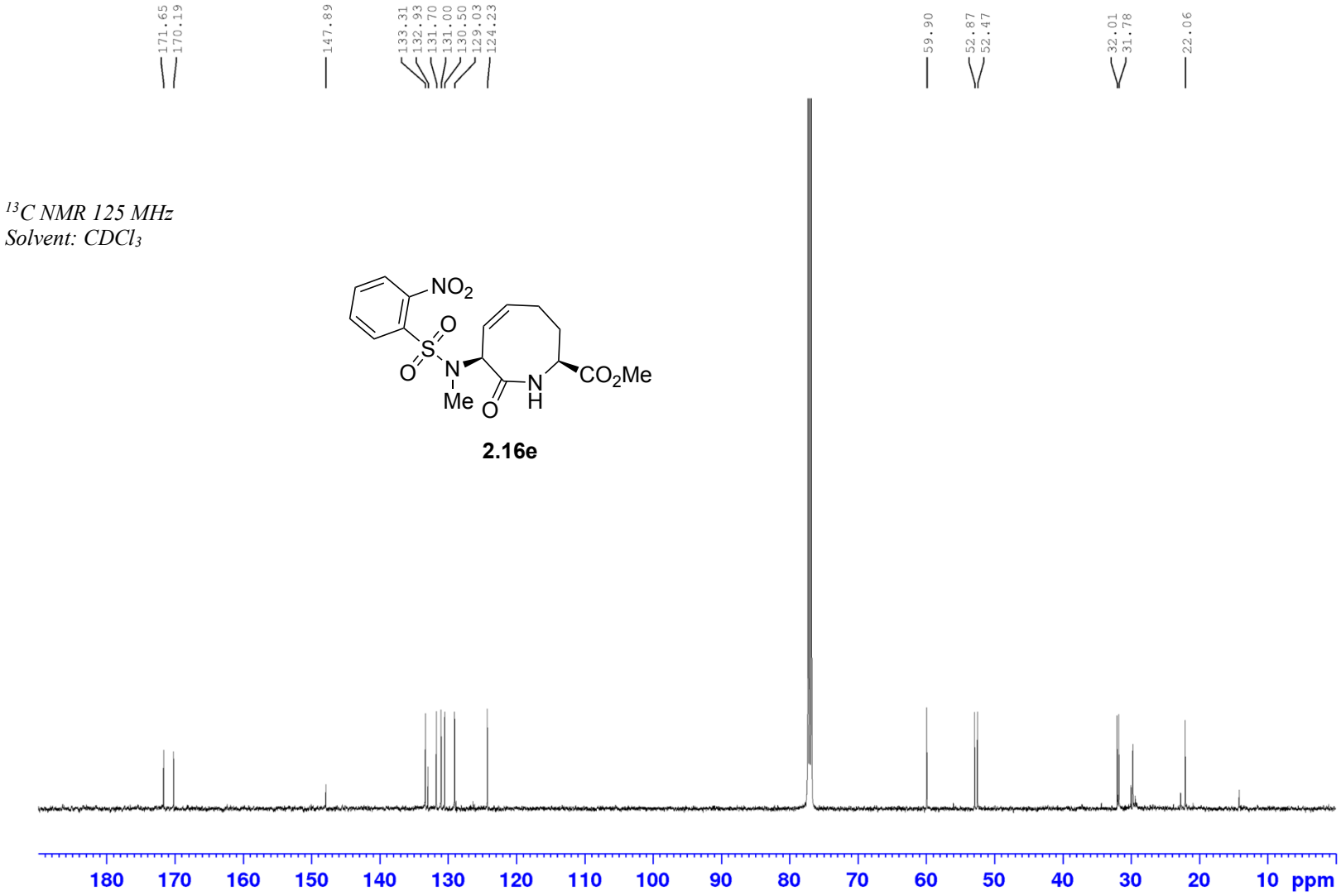

^{13}C NMR 125 MHz
Solvent: $CDCl_3$

2.16e

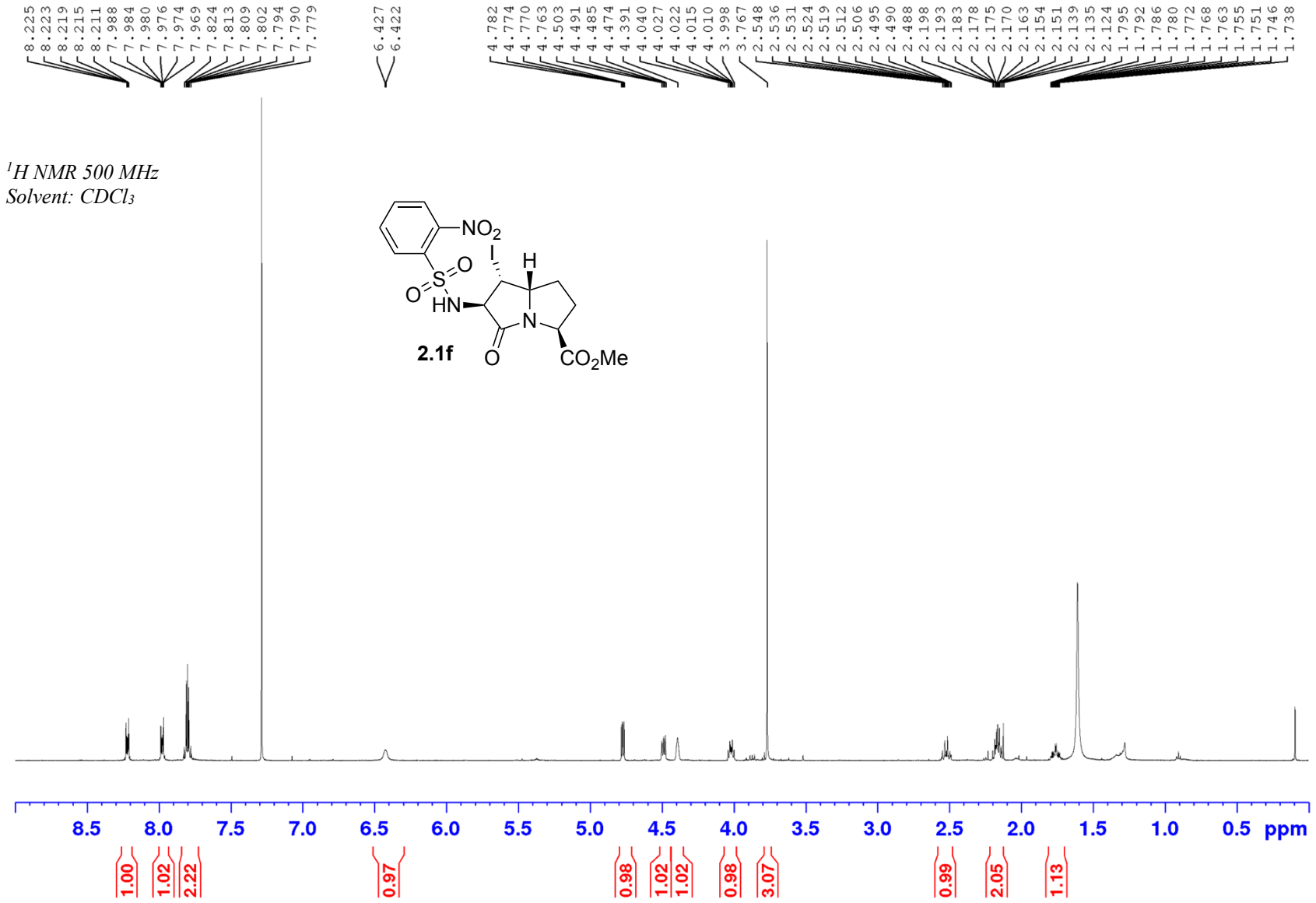
8.225
8.223
8.219
8.215
8.211
7.988
7.984
7.980
7.976
7.974
7.969
7.824
7.813
7.809
7.802
7.794
7.790
7.779
6.427
6.422
4.782
4.774
4.770
4.763
4.503
4.491
4.485
4.474
4.391
4.040
4.027
4.022
4.015
4.010
3.998
3.767
2.548
2.536
2.531
2.524
2.519
2.512
2.506
2.495
2.490
2.488
2.198
2.193
2.183
2.178
2.175
2.170
2.163
2.154
2.151
2.139
2.135
2.124
1.795
1.792
1.786
1.780
1.772
1.768
1.763
1.755
1.751
1.746
1.738
1H NMR 500 MHz
Solvent: CDCl3
NO2
I
H
O
S
O
HN
N
O
CO2Me
2.1f
8.5
8.0
7.5
7.0
6.5
6.0
5.5
5.0
4.5
4.0
3.5
3.0
2.5
2.0
1.5
1.0
0.5
ppm
1.00
1.02
2.22
0.97
0.98
1.02
1.02
0.98
3.07
0.99
2.05
1.13

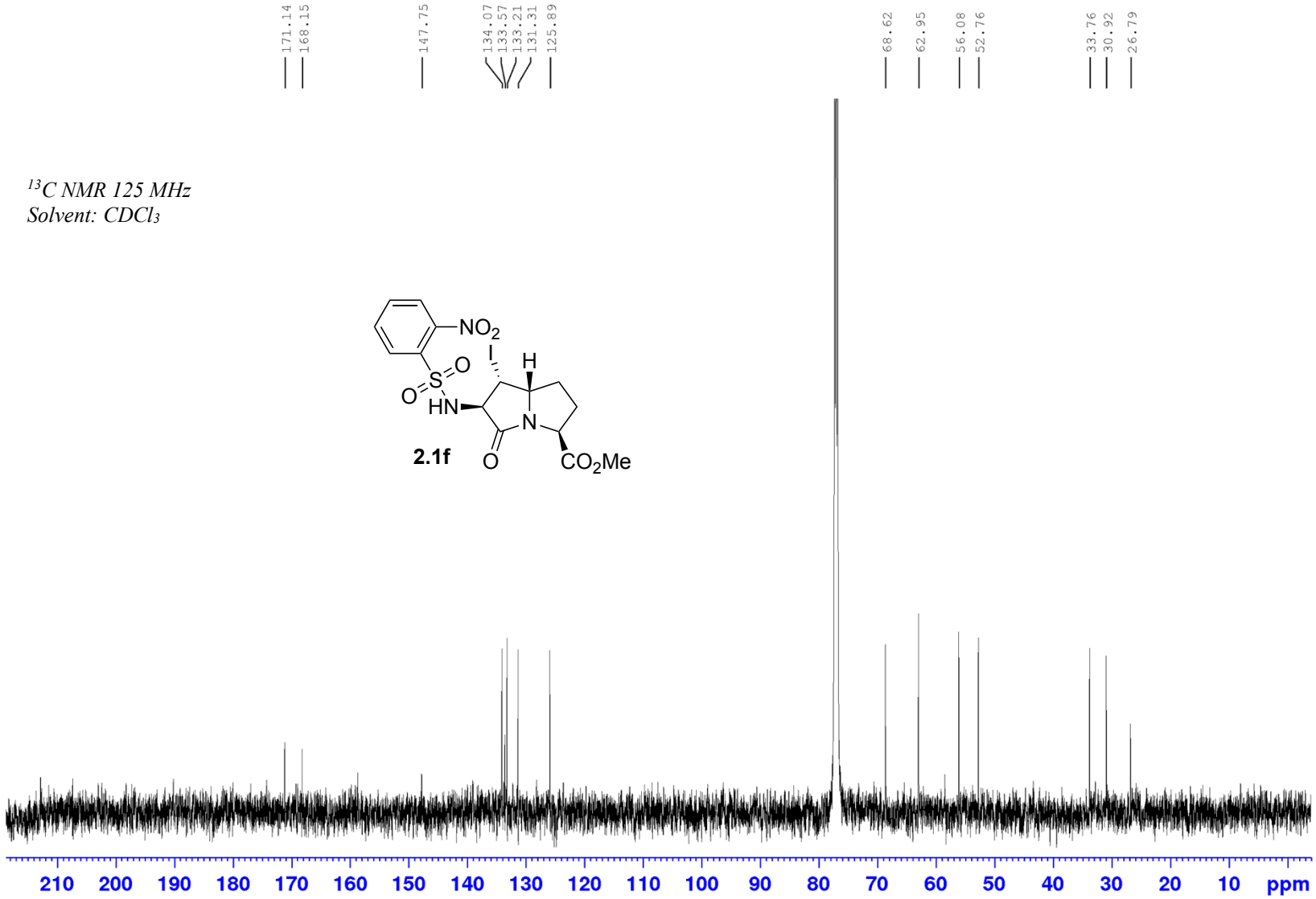
171.14
168.15
147.75
134.07
133.57
133.21
131.31
125.89
68.62
62.95
56.08
52.76
33.76
30.92
26.79
^{13}C NMR 125 MHz
Solvent: $CDCl_3$
NO_2
I
H
O
S
O
HN
N
O
CO_2Me
2.1f
210 200 190 180 170 160 150 140 130 120 110 100 90 80 70 60 50 40 30 20 10 ppm

COSY 500 MHz
Solvent: $CDCl_3$

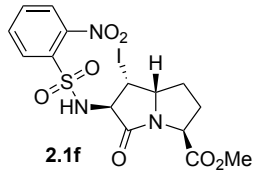

2.1f

DEPT NMR 125 MHz
Solvent: $CDCl_3$

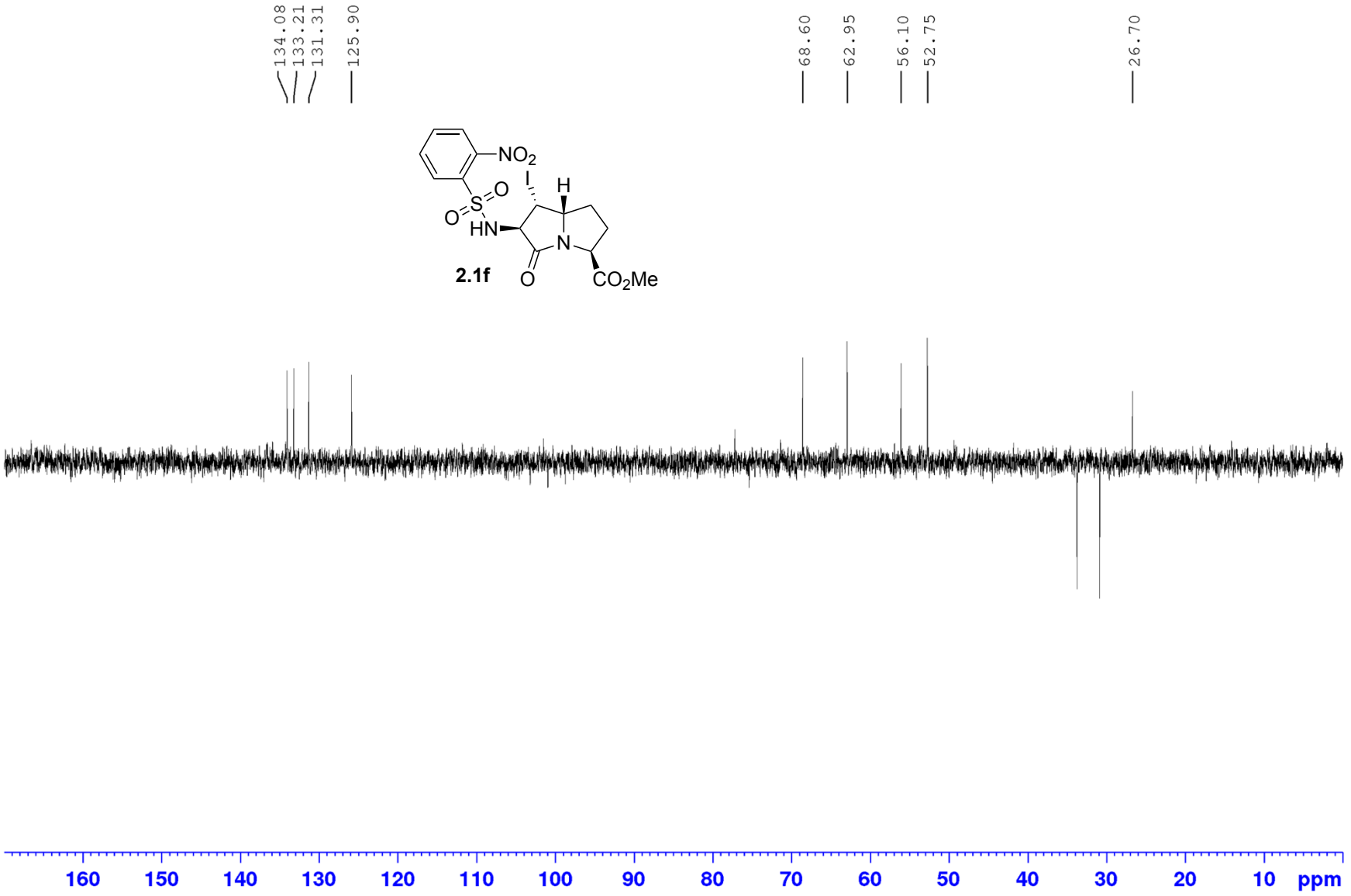

NOESY NMR 500 MHz
Solvent: $CDCl_3$

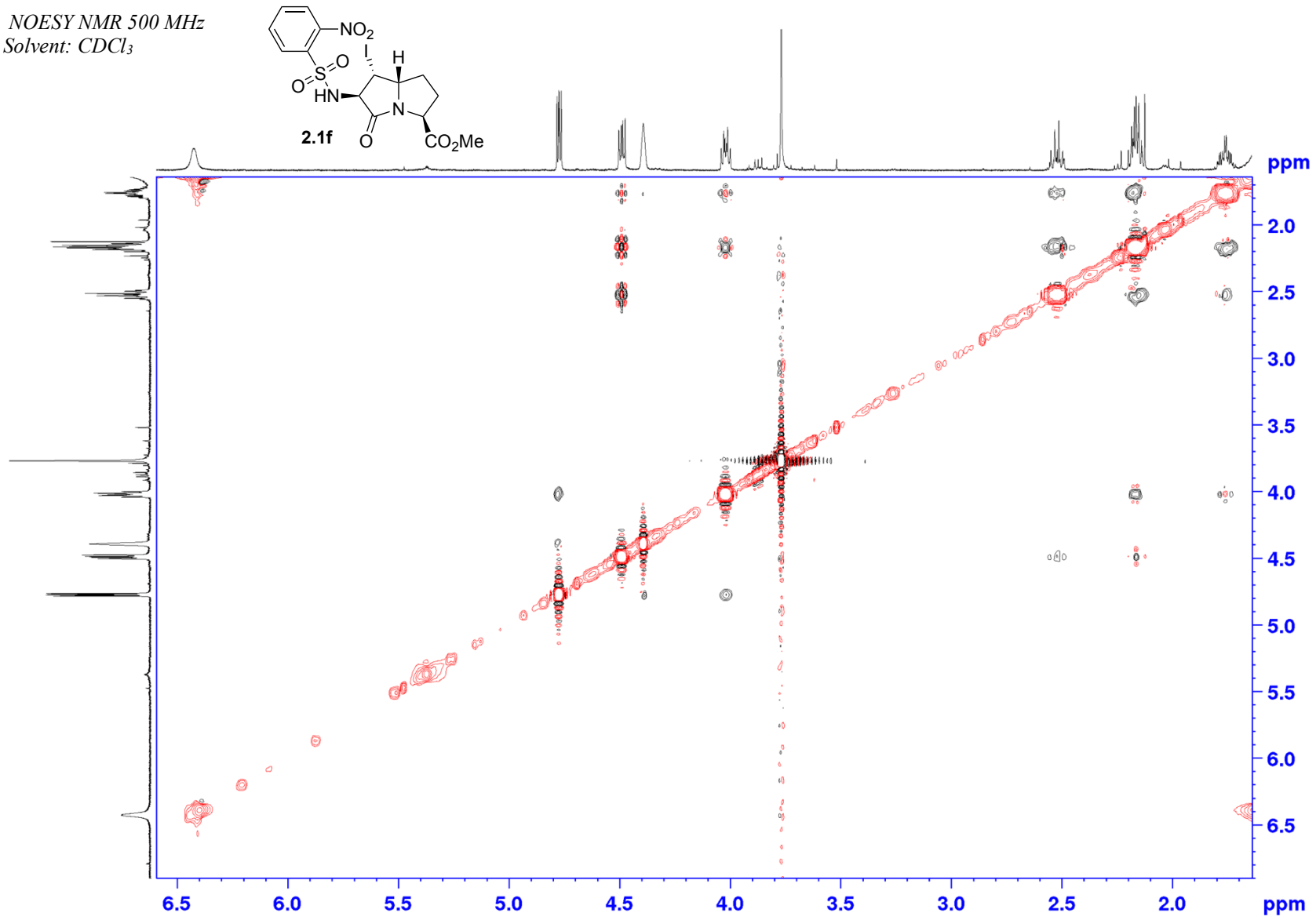

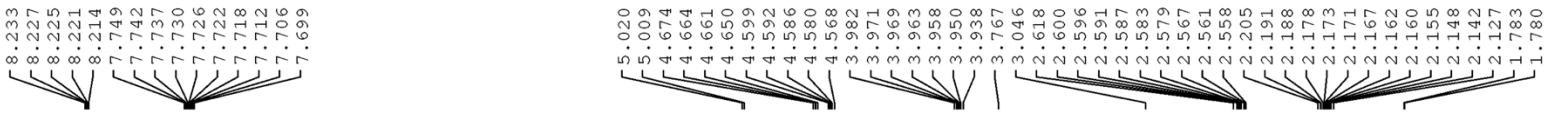

^{1}H NMR 500 MHz
Solvent: $CDCl_3$

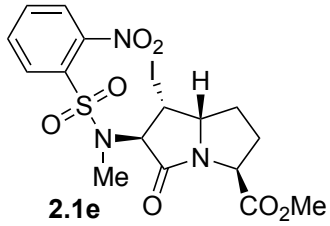

2.1e

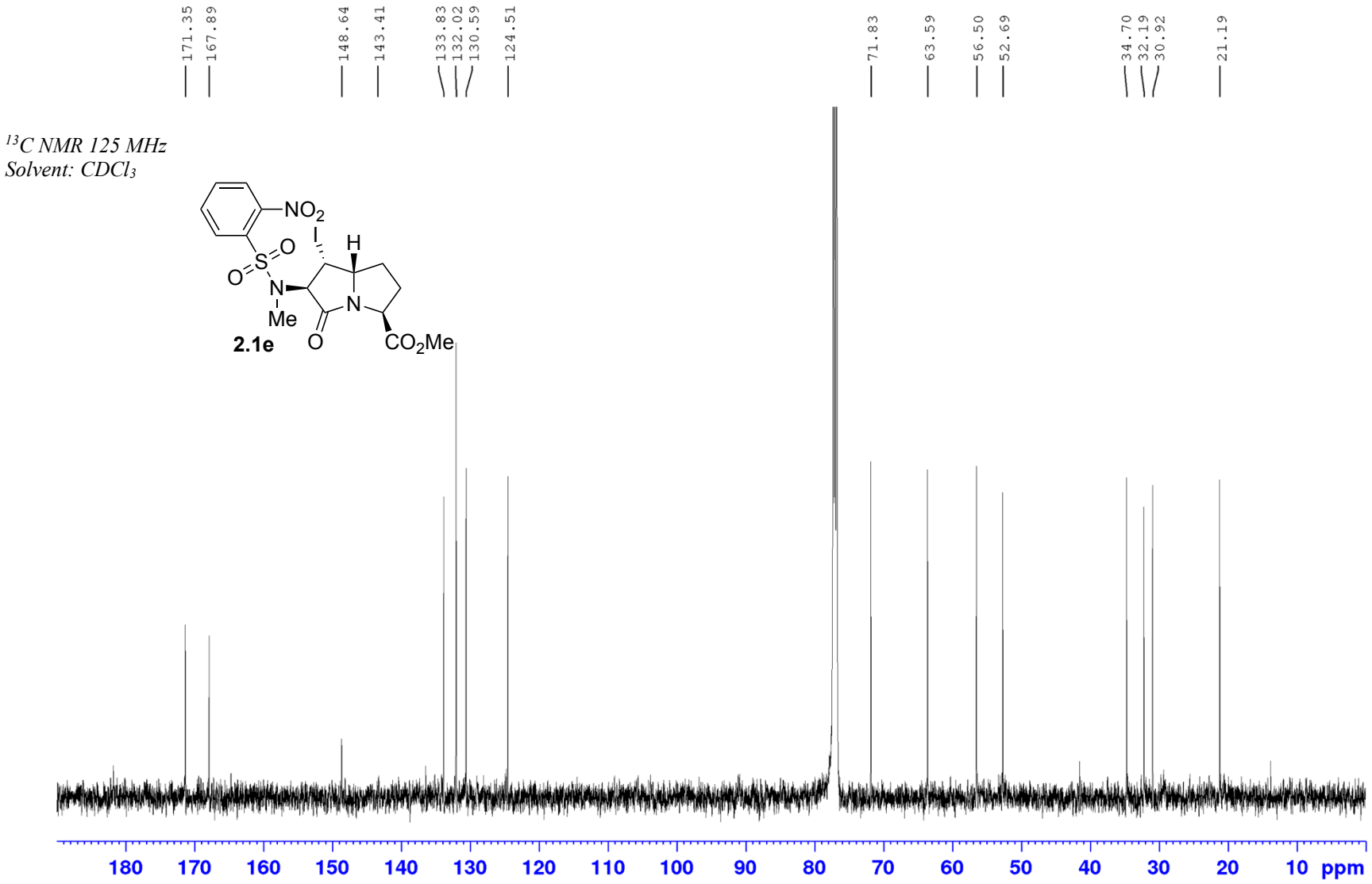

^{13}C NMR 125 MHz
Solvent: $CDCl_3$

2.1e

COSY 500 MHz
Solvent: $CDCl_3$

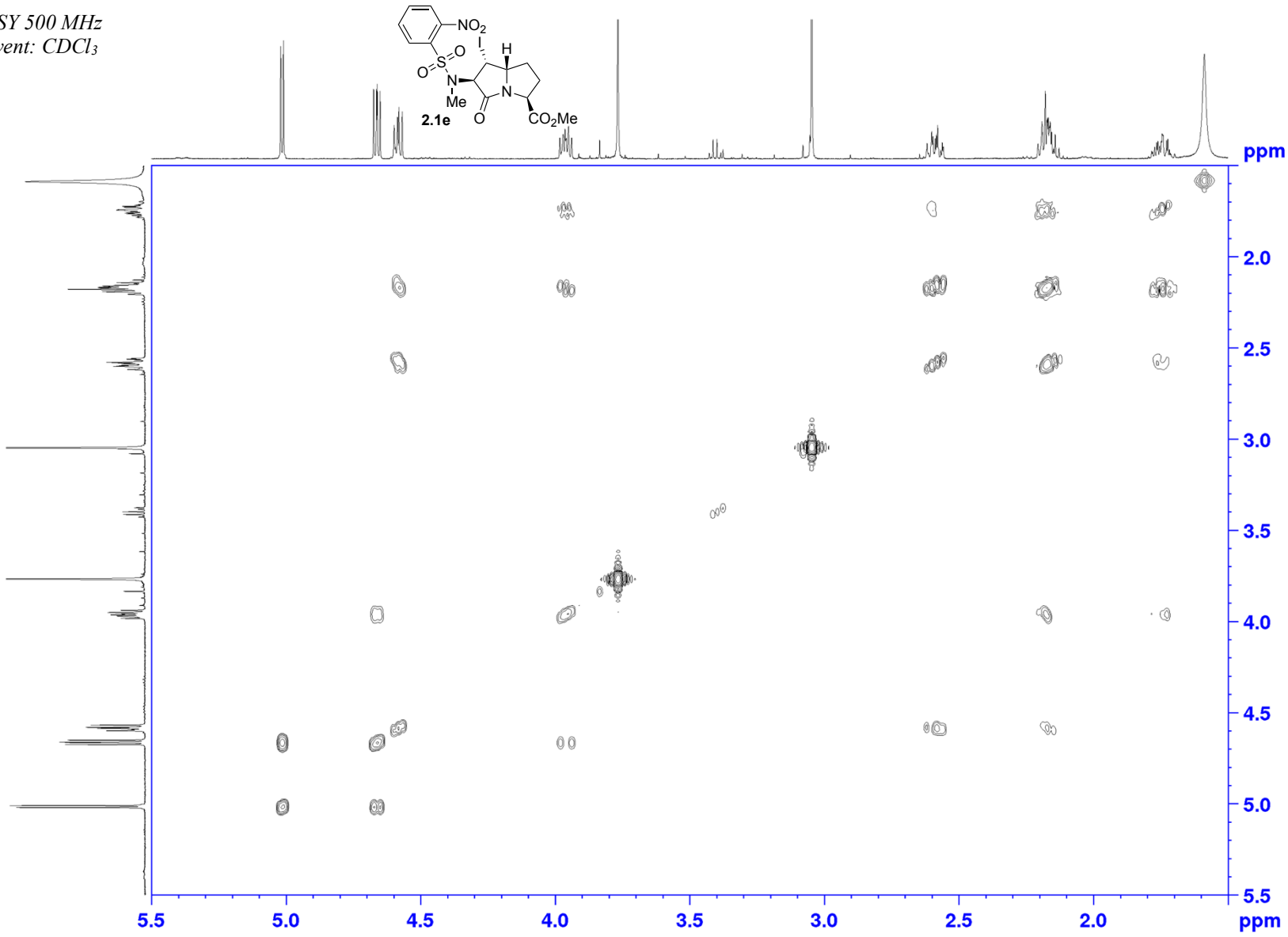

DEPT NMR 125 MHz
Solvent: $CDCl_3$

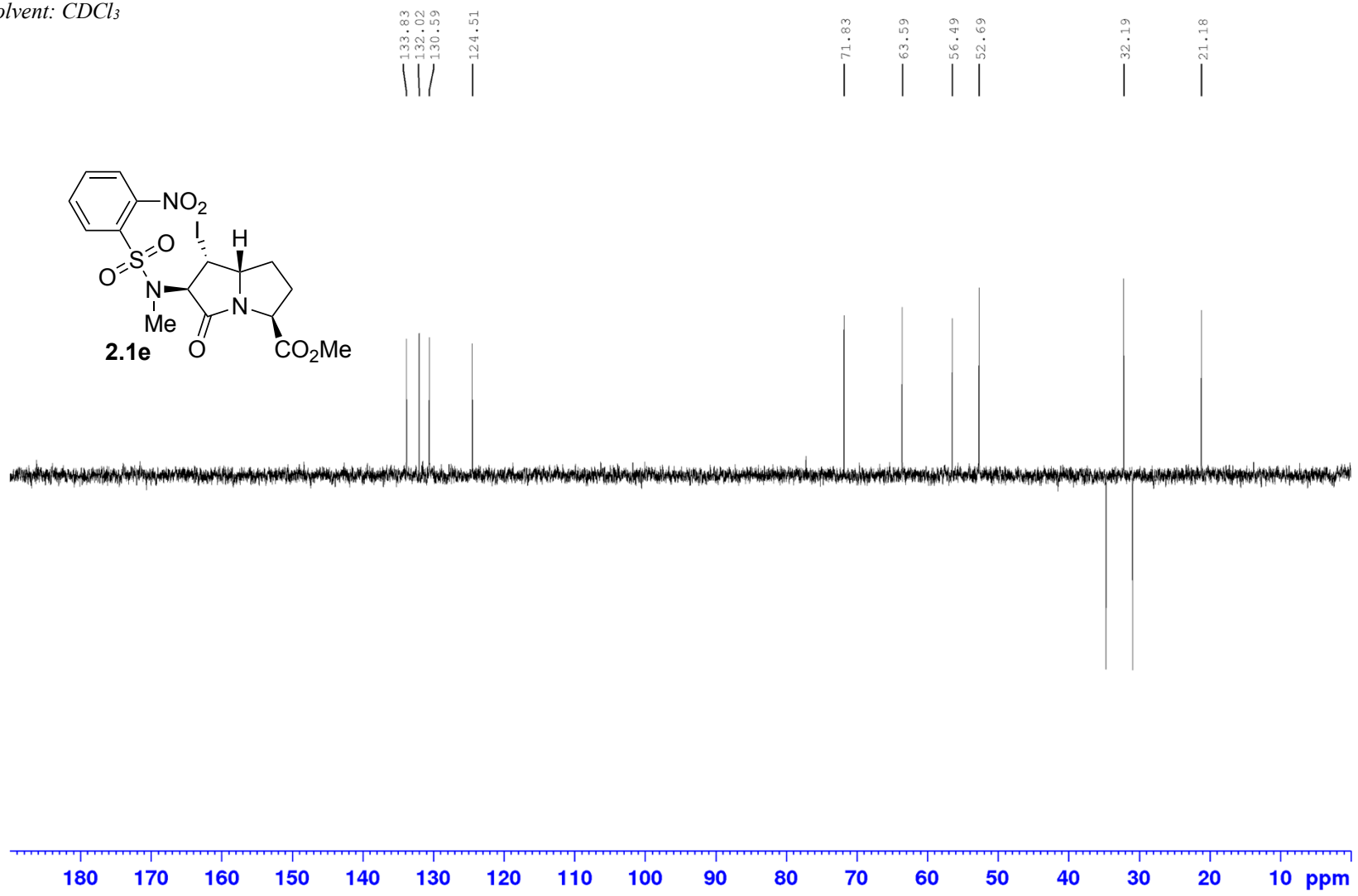

HSQC NMR 125 MHz
Solvent: $CDCl_3$

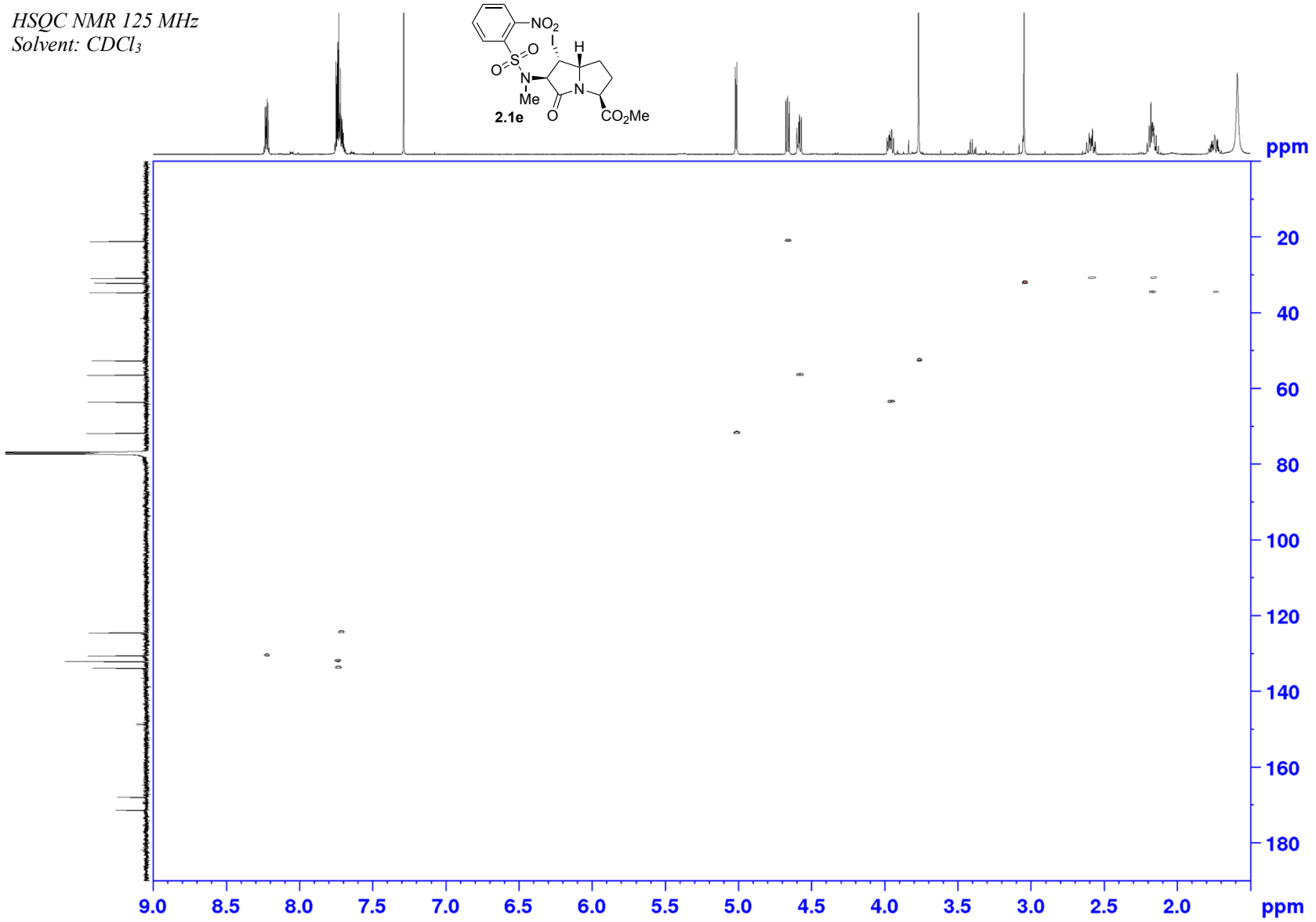

NOESY NMR 500 MHz
Solvent: $CDCl_3$

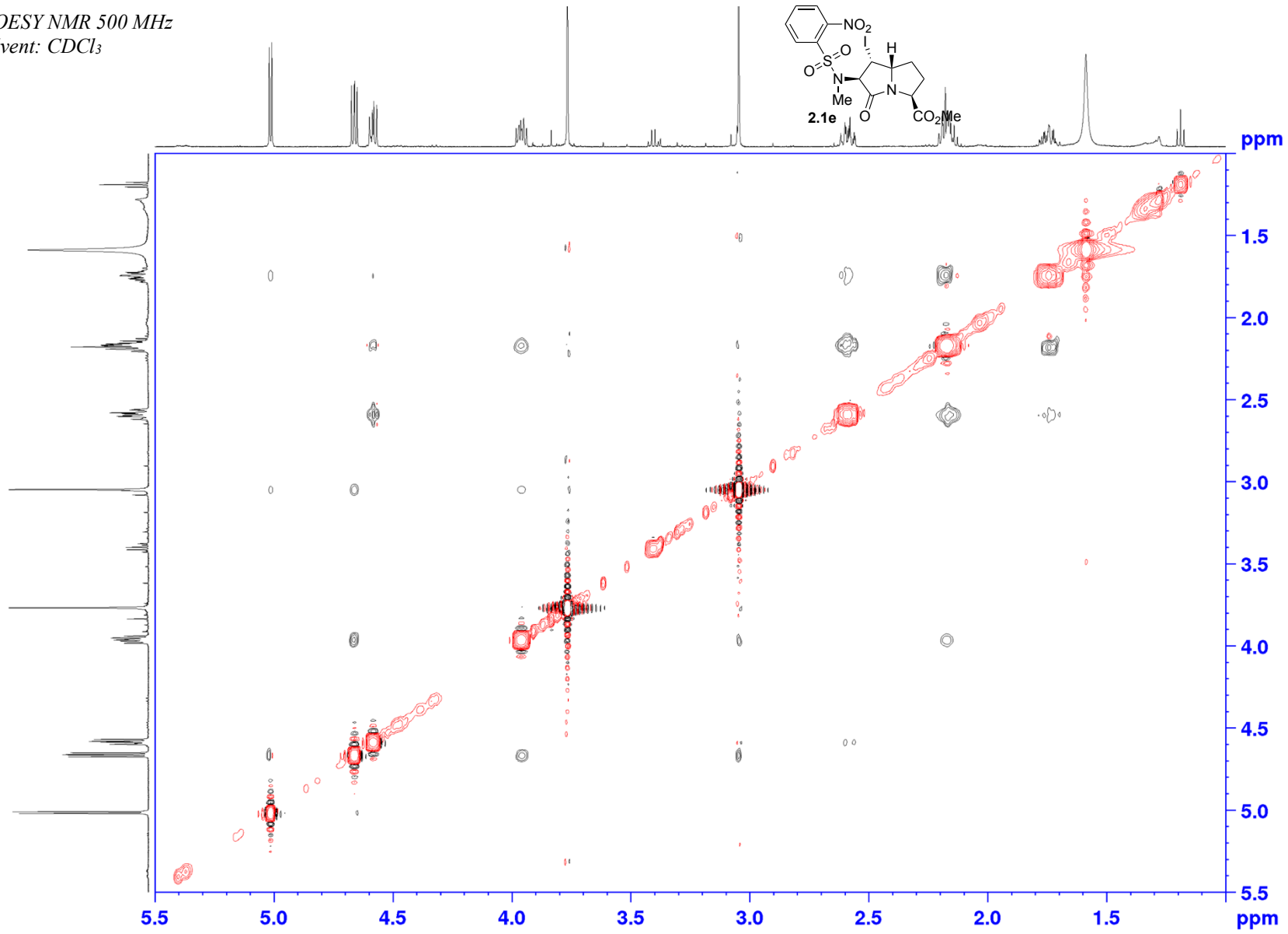

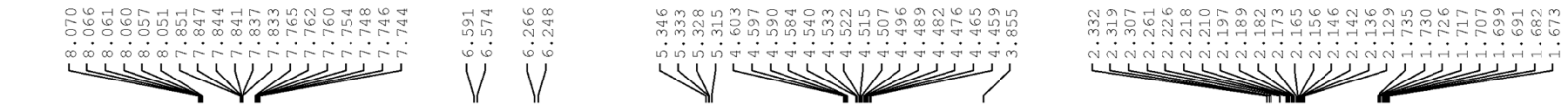

^{1}H NMR 500 MHz
Solvent: $CDCl_3$

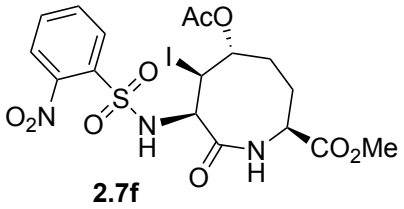

2.7f

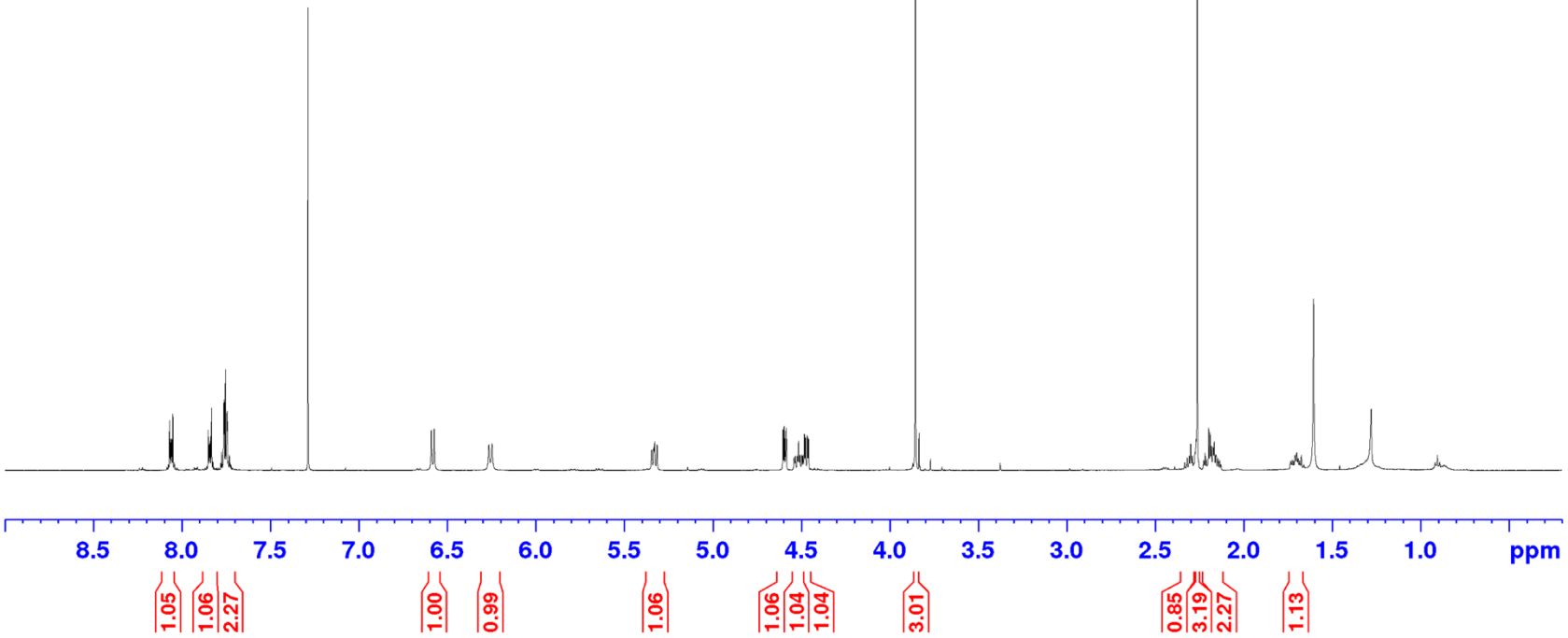

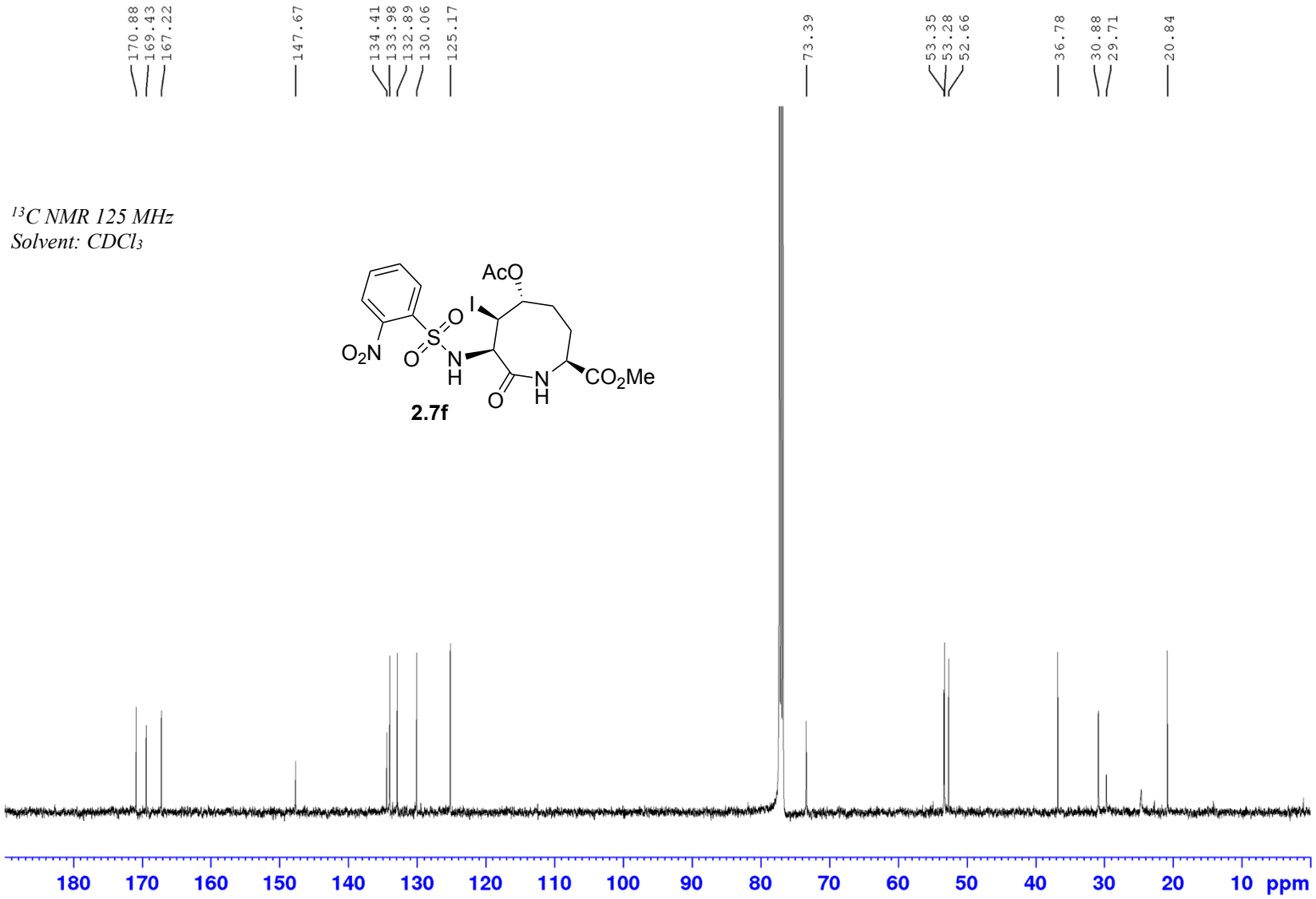
170.88
169.43
167.22
147.67
134.41
133.98
132.89
130.06
125.17
73.39
53.35
53.28
52.66
36.78
30.88
29.71
20.84
13C NMR 125 MHz
Solvent: CDCl3
AcO
I
O
S
O
O2N
N
H
N
H
O
CO2Me
2.7f
180
170
160
150
140
130
120
110
100
90
80
70
60
50
40
30
20
10
ppm

COSY 500 MHz
Solvent: $CDCl_3$

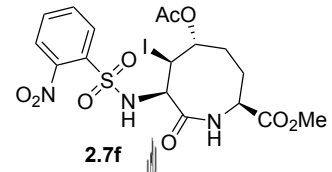

2.7f

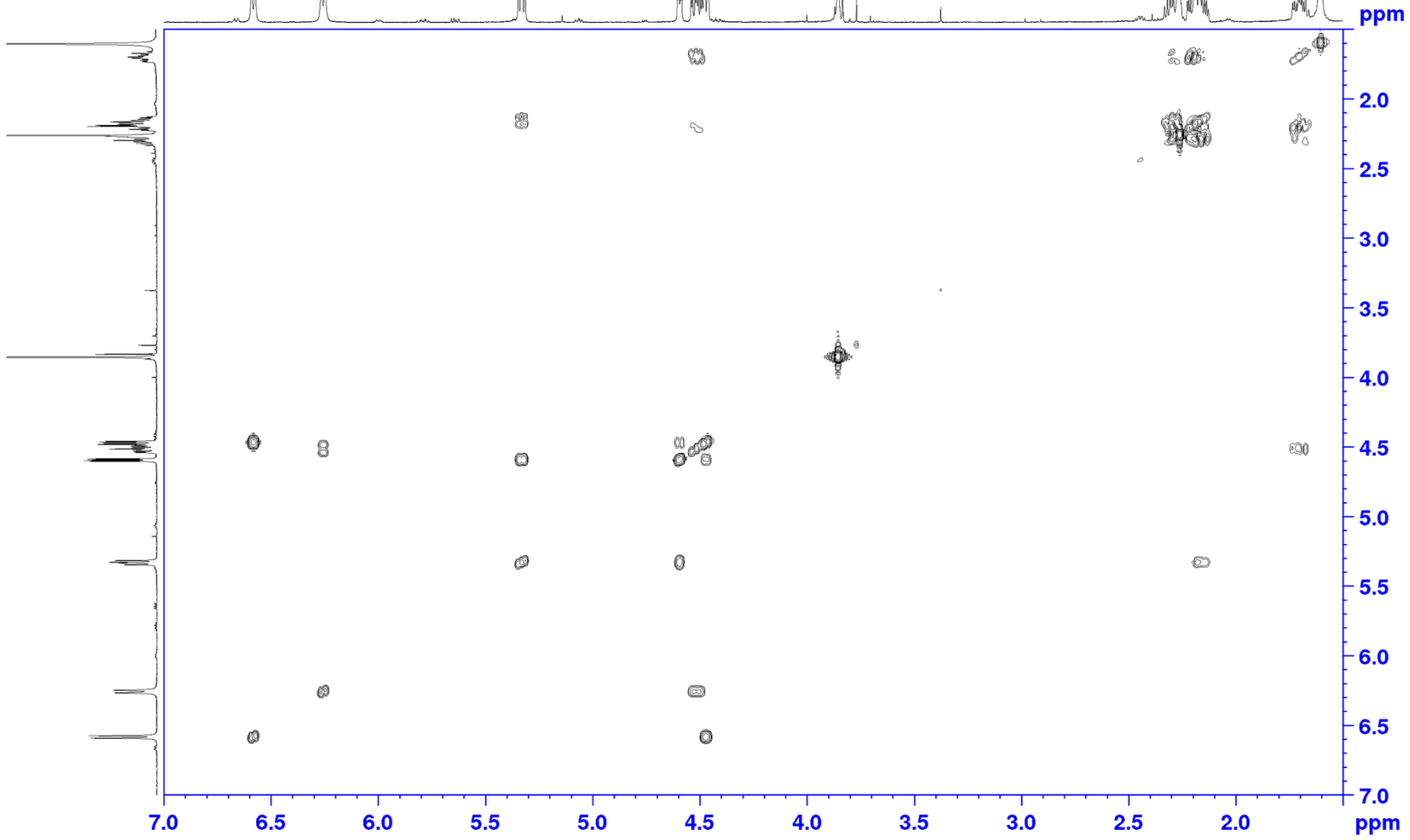

HSQC NMR 125 MHz
Solvent: $CDCl_3$

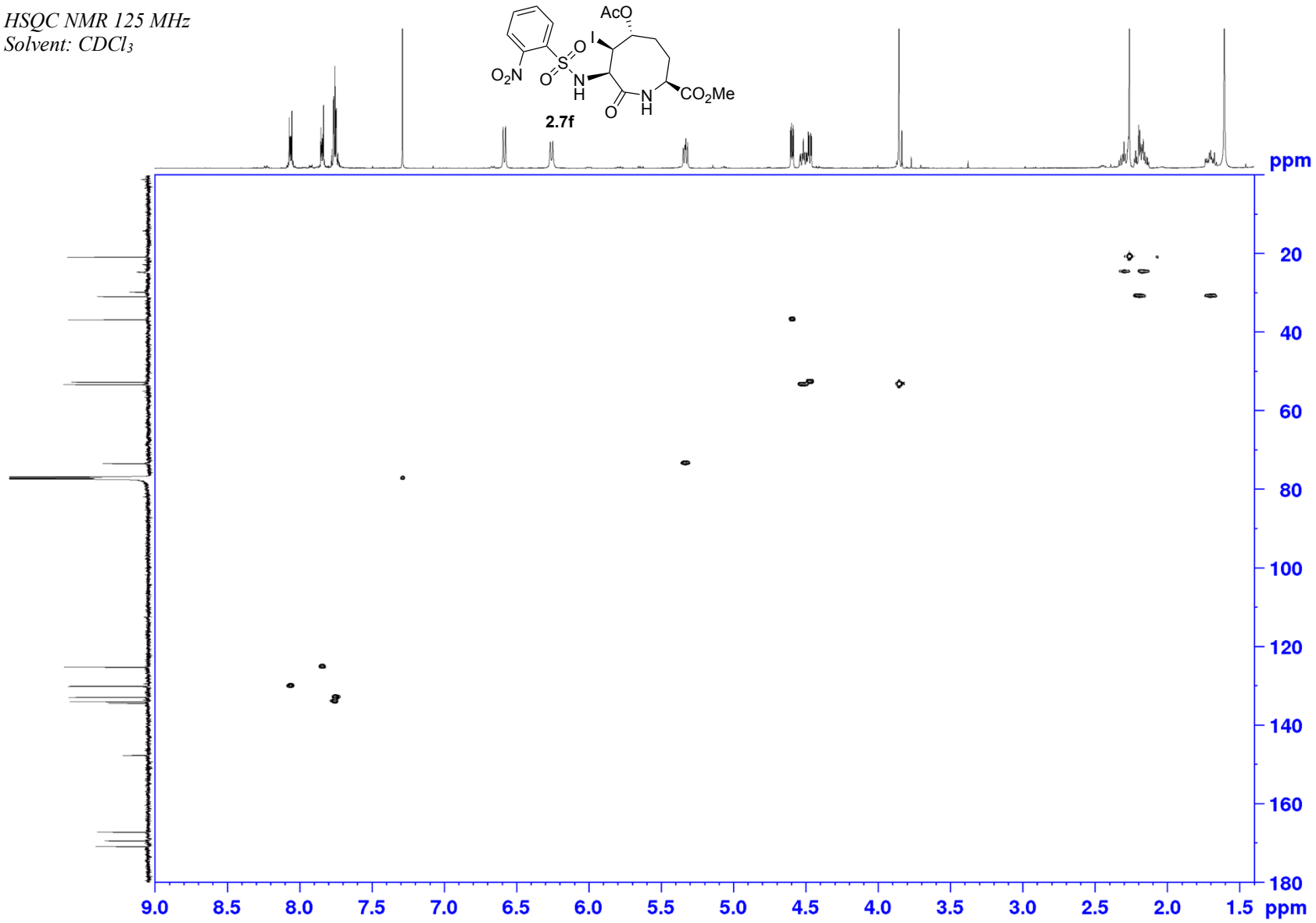

NOESY NMR 500 MHz
Solvent: $CDCl_3$

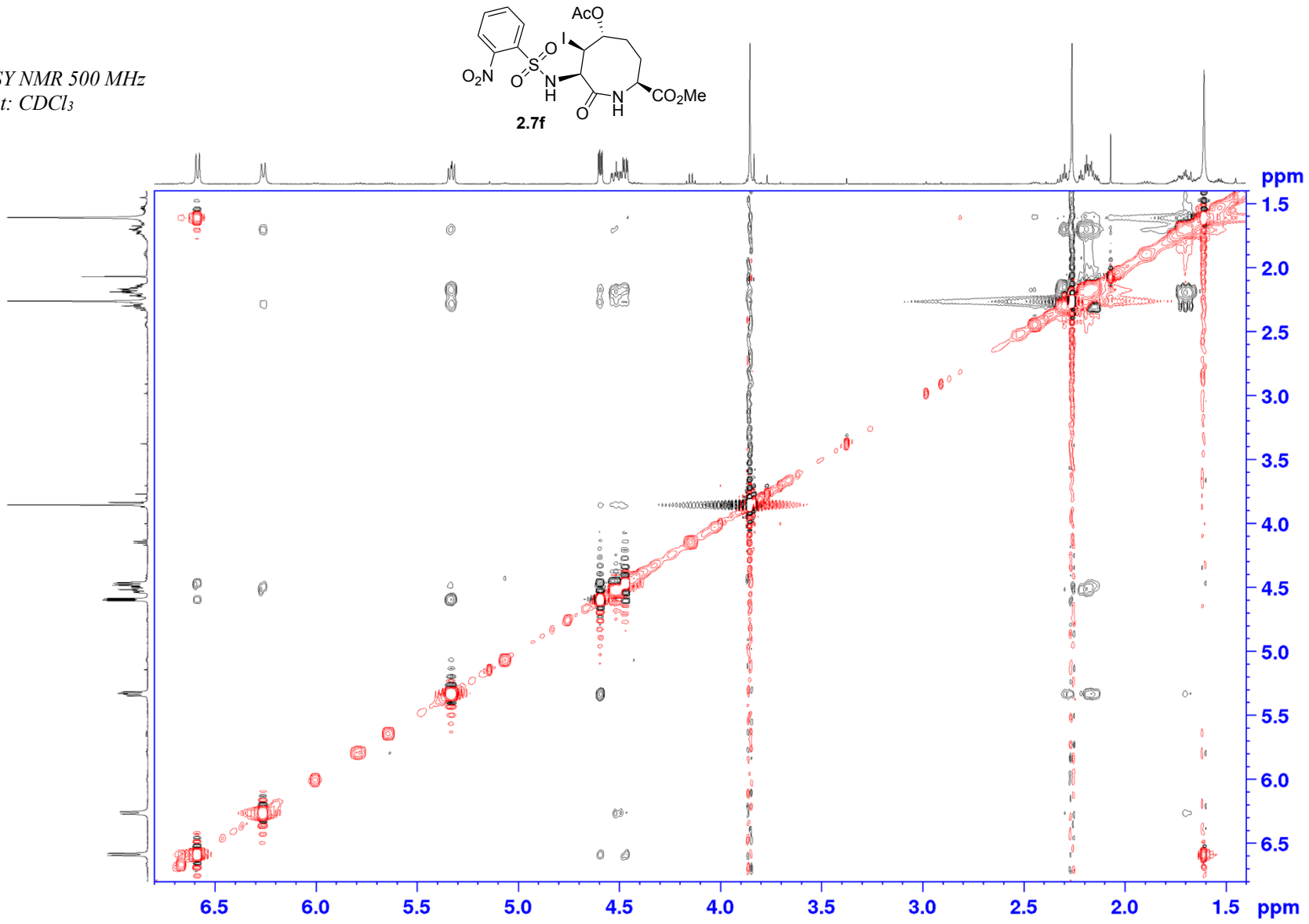

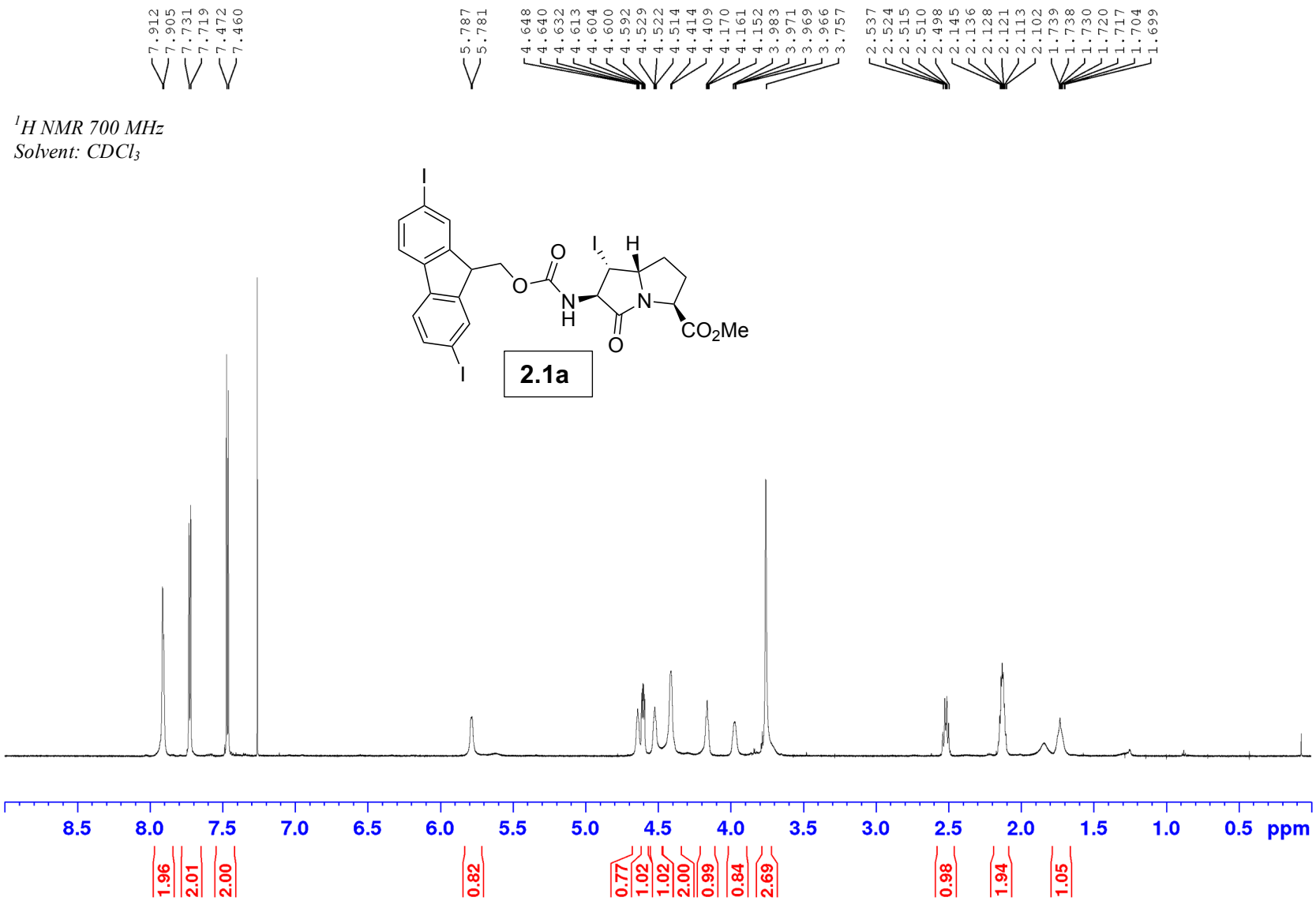

^{1}H NMR 700 MHz
Solvent: $CDCl_3$

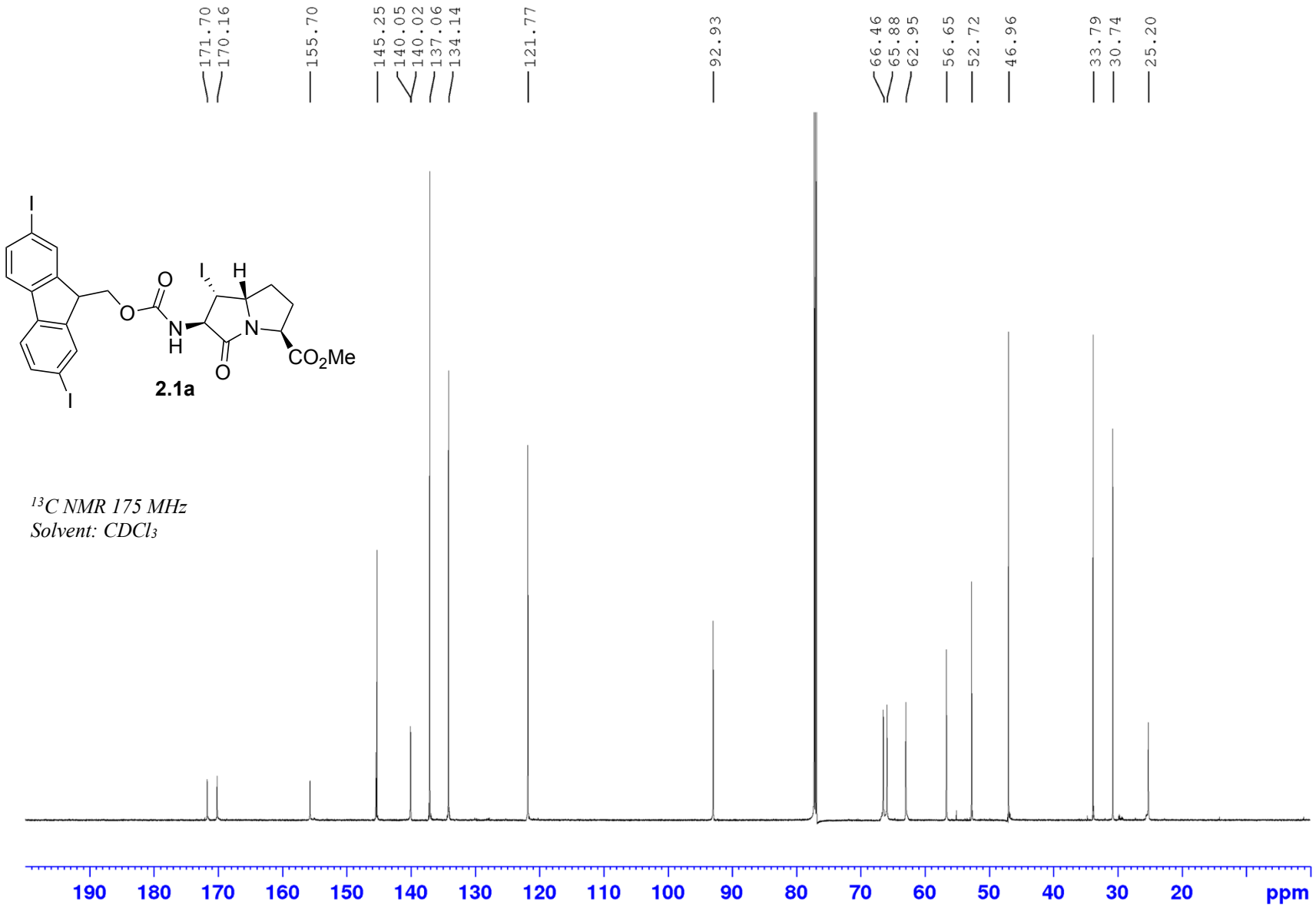
171.70
170.16
155.70
145.25
140.05
140.02
137.06
134.14
121.77
92.93
66.46
65.88
62.95
56.65
52.72
46.96
33.79
30.74
25.20
I
O
O
N
H
I
H
N
O
CO2Me
I
2.1a
13C NMR 175 MHz
Solvent: CDCl3
190
180
170
160
150
140
130
120
110
100
90
80
70
60
50
40
30
20
ppm

DEPT 175 MHz
Solvent: $CDCl_3$

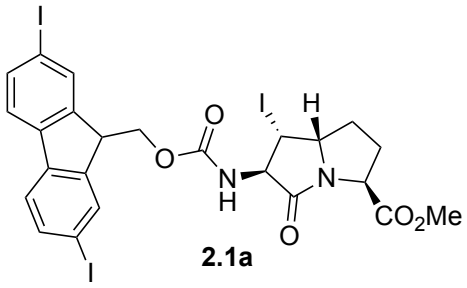

2.1a

COSY 700 MHz
Solvent: $CDCl_3$

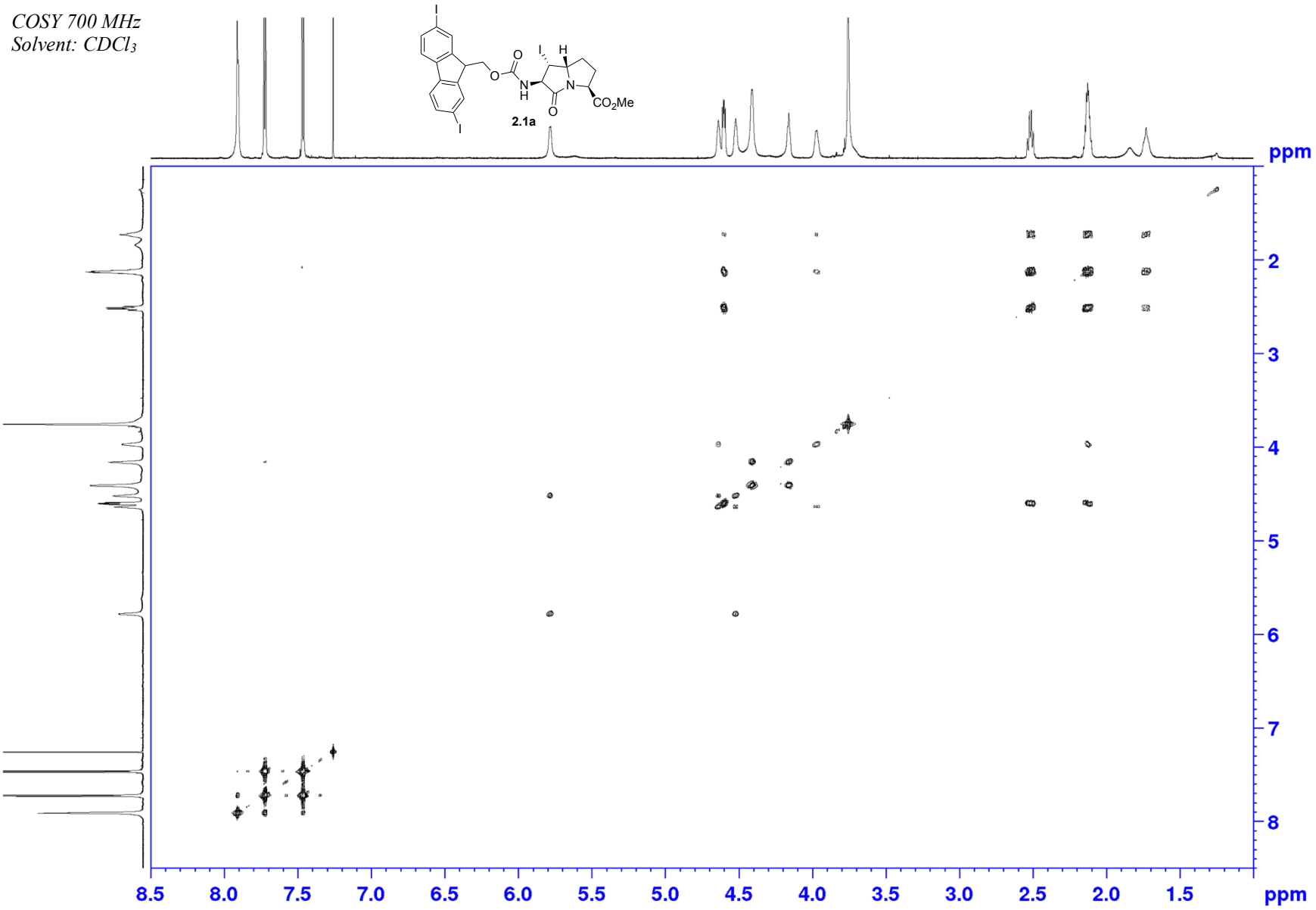

HSQC 175 MHz
Solvent: $CDCl_3$

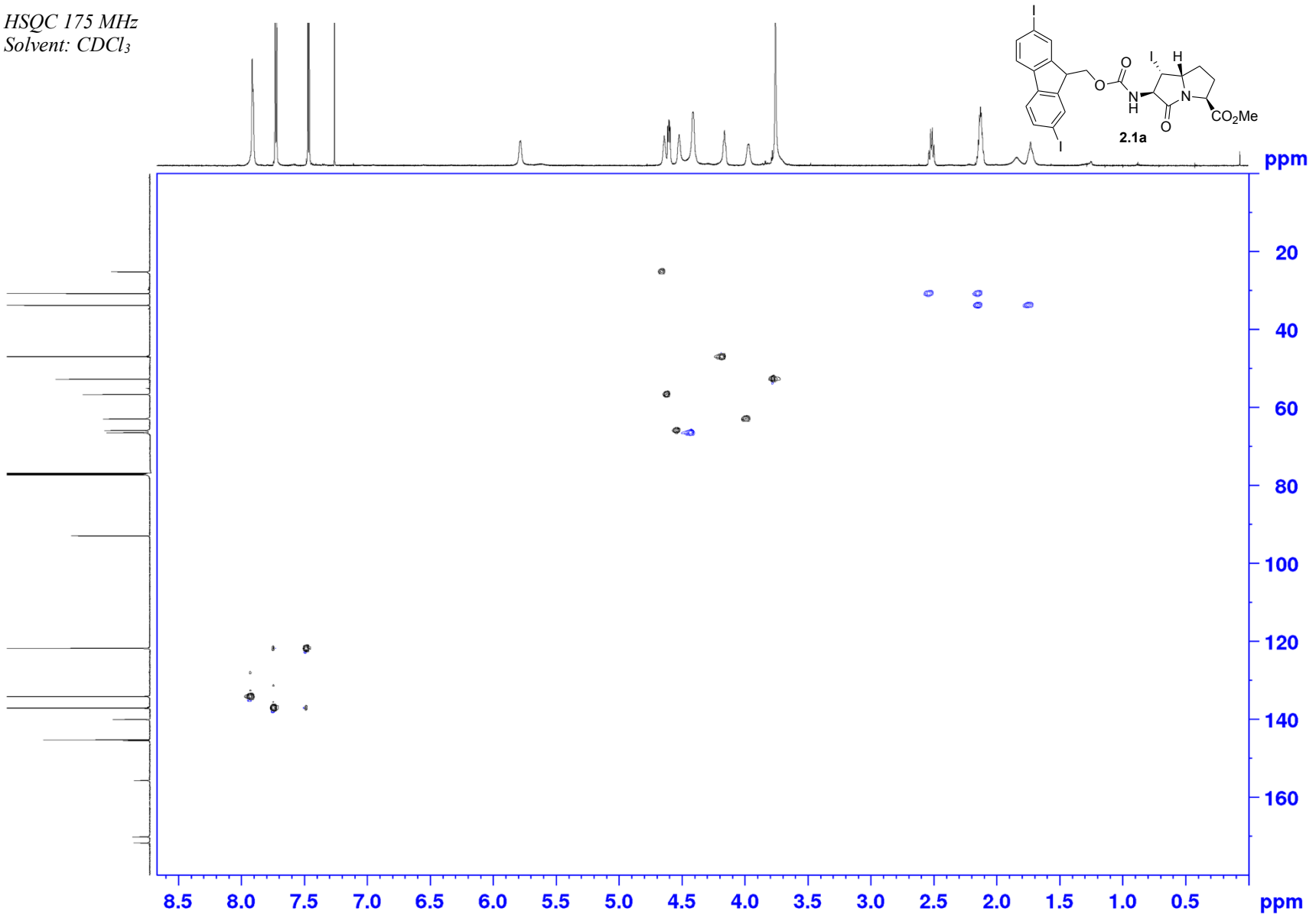

NOESY 700 MHz
Solvent: $CDCl_3$

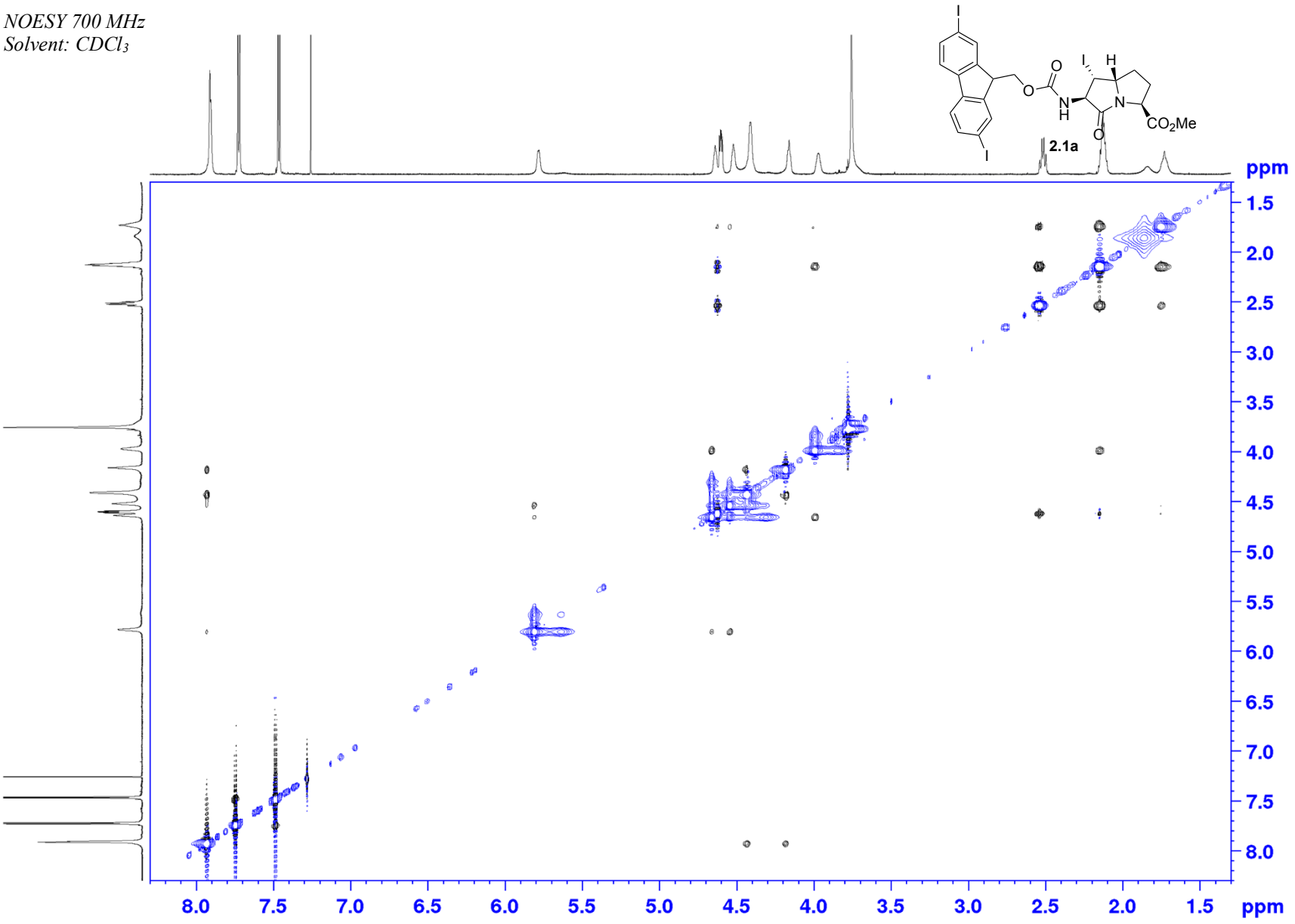

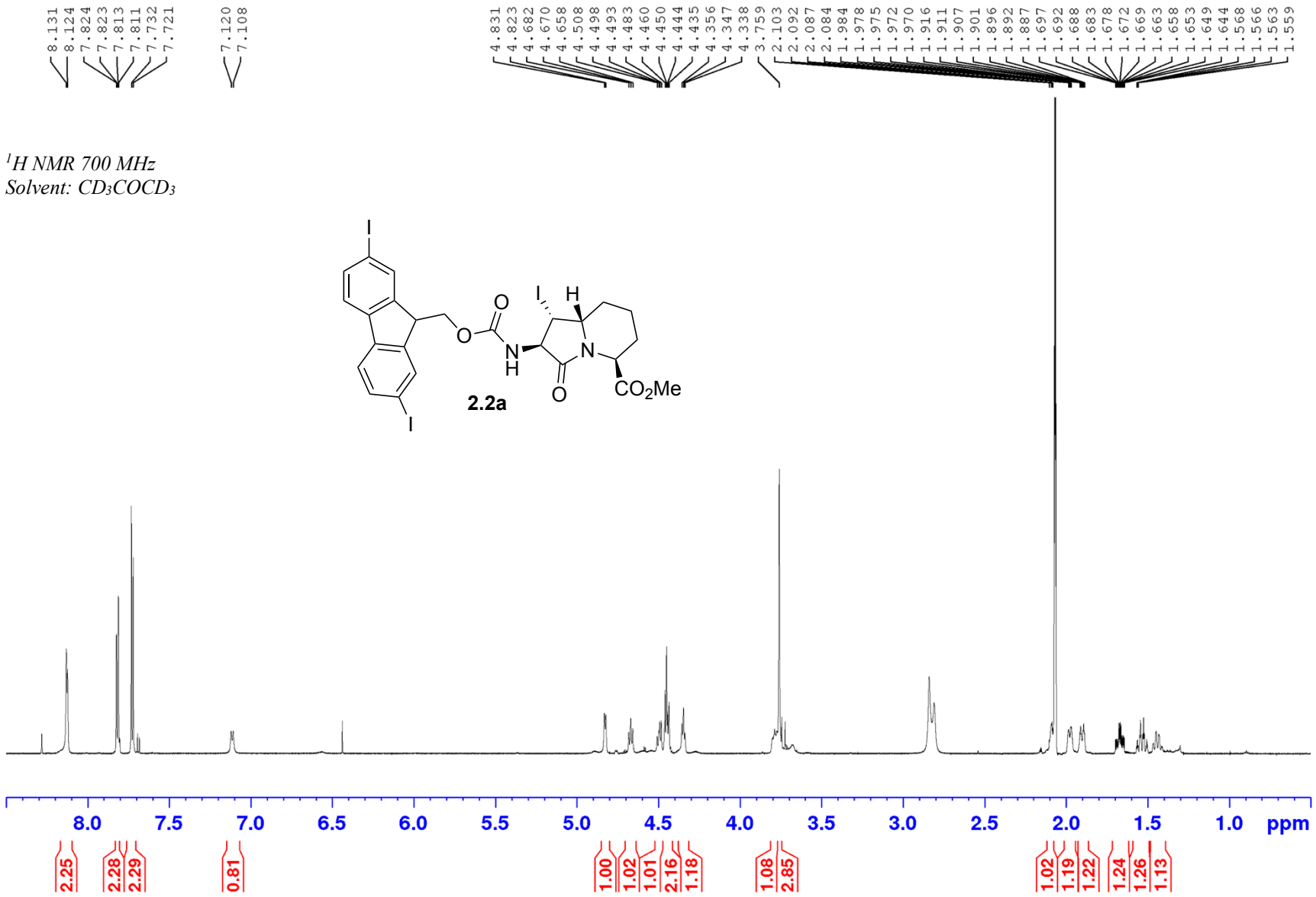

[1]H NMR 700 MHz
Solvent: CD_3COCD_3

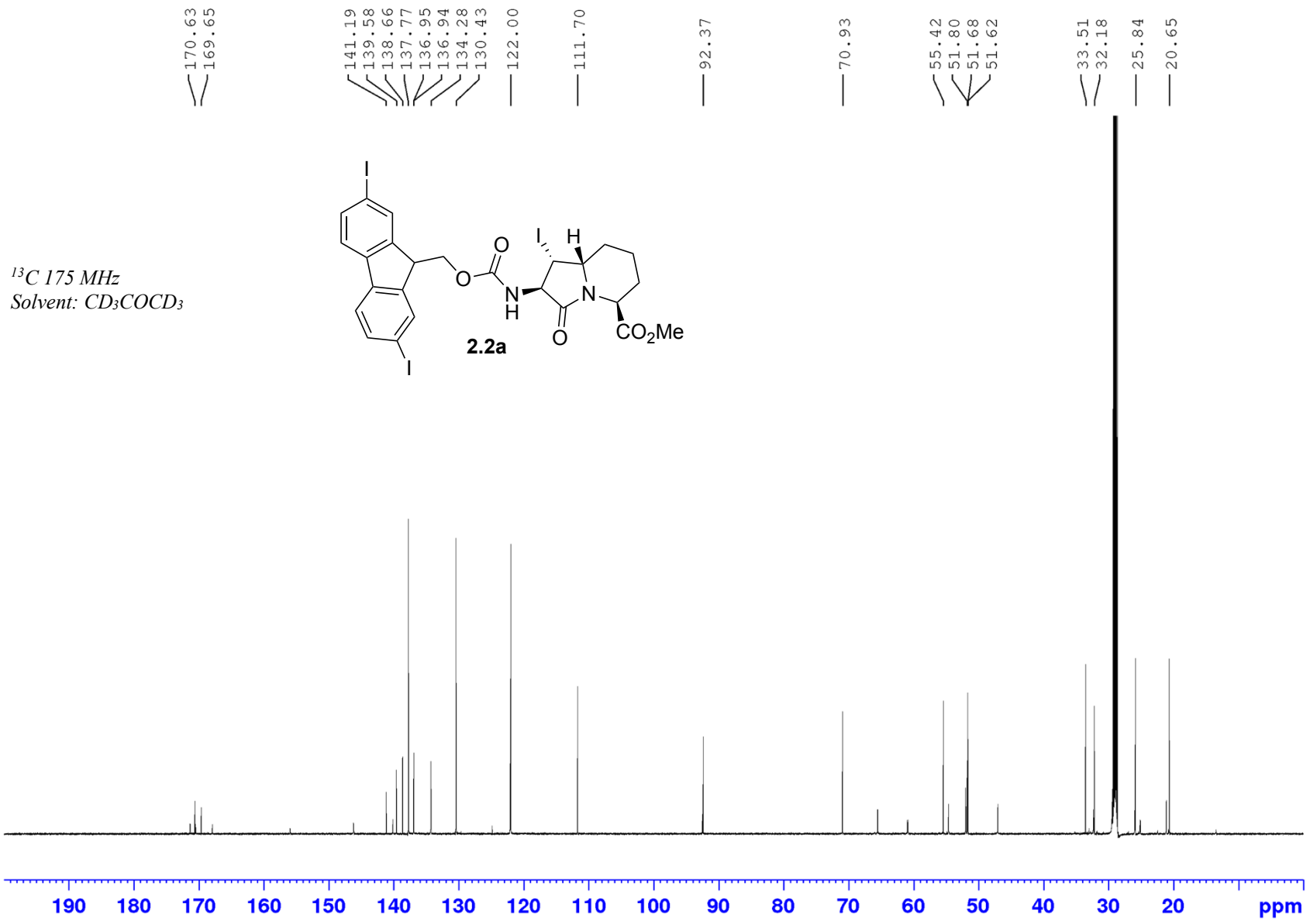
170.63
169.65
141.19
139.58
138.66
137.77
136.95
136.94
134.28
130.43
122.00
111.70
92.37
70.93
55.42
51.80
51.68
51.62
33.51
32.18
25.84
20.65
13C 175 MHz
Solvent: CD3COCD3
2.2a
190
180
170
160
150
140
130
120
110
100
90
80
70
60
50
40
30
20
ppm

COSY 700 MHz
Solvent: CD_3COCD_3

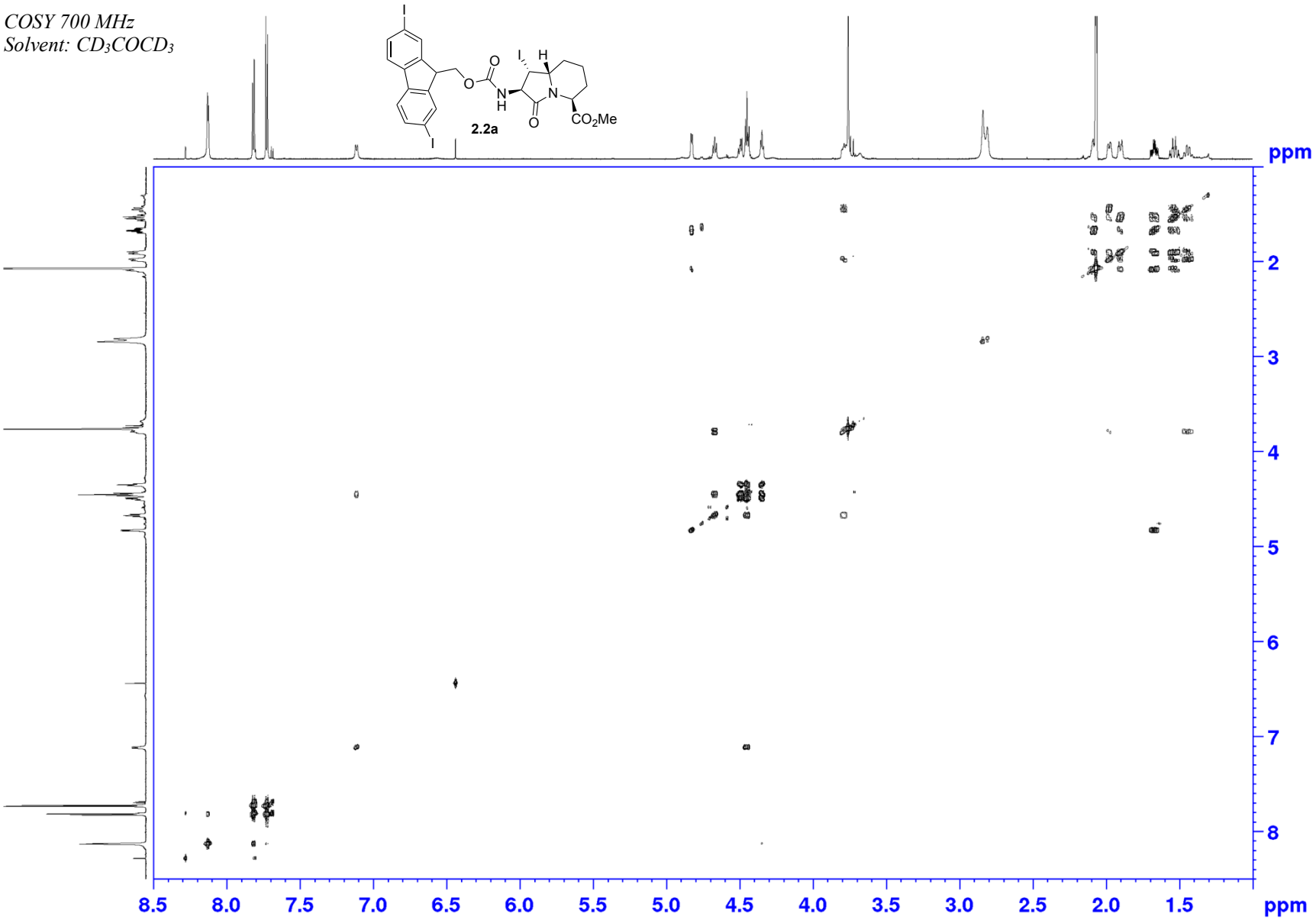

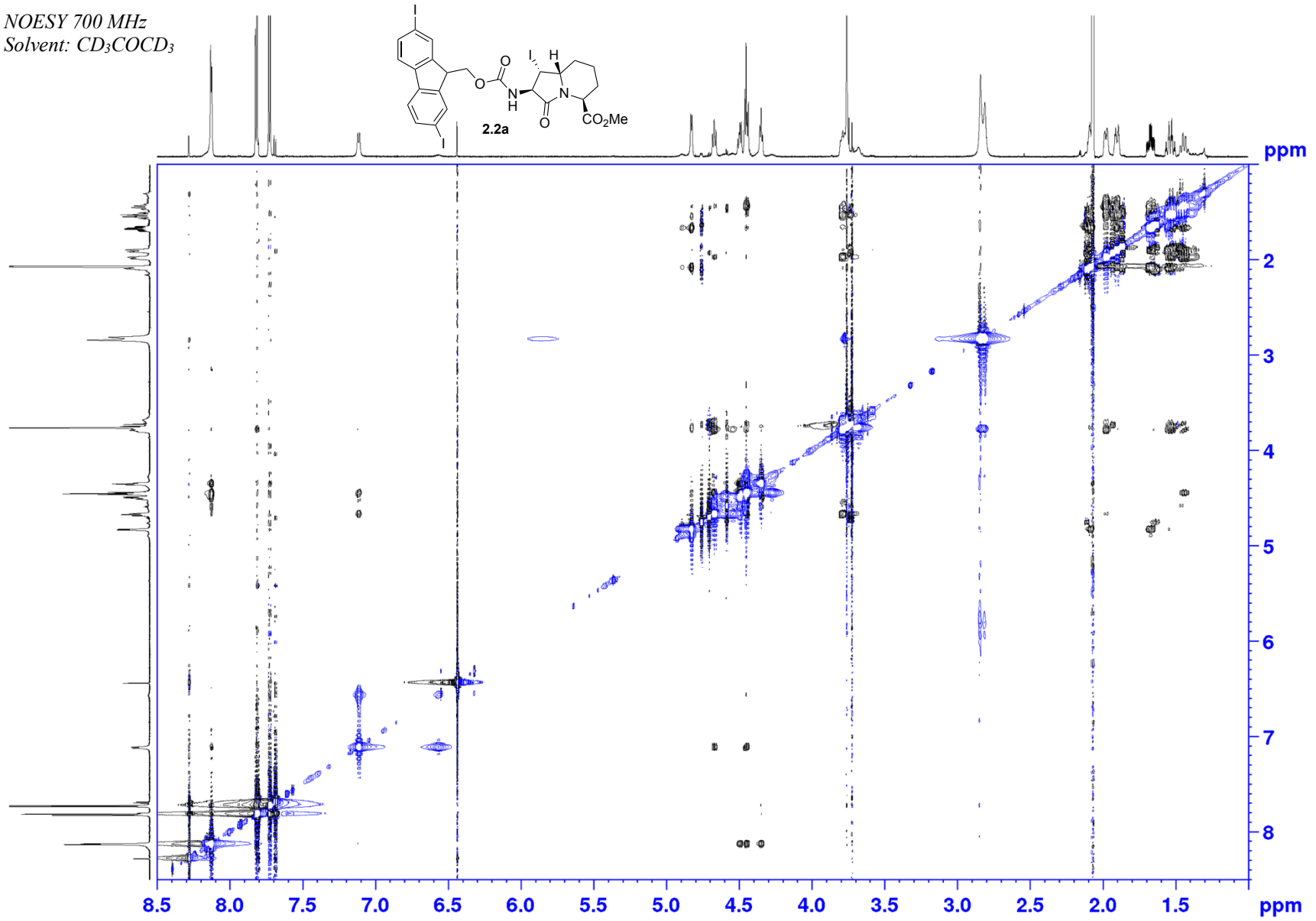
NOESY 700 MHz
Solvent: CD3COCD3
2.2a
ppm
8.5
8.0
7.5
7.0
6.5
6.0
5.5
5.0
4.5
4.0
3.5
3.0
2.5
2.0
1.5
ppm

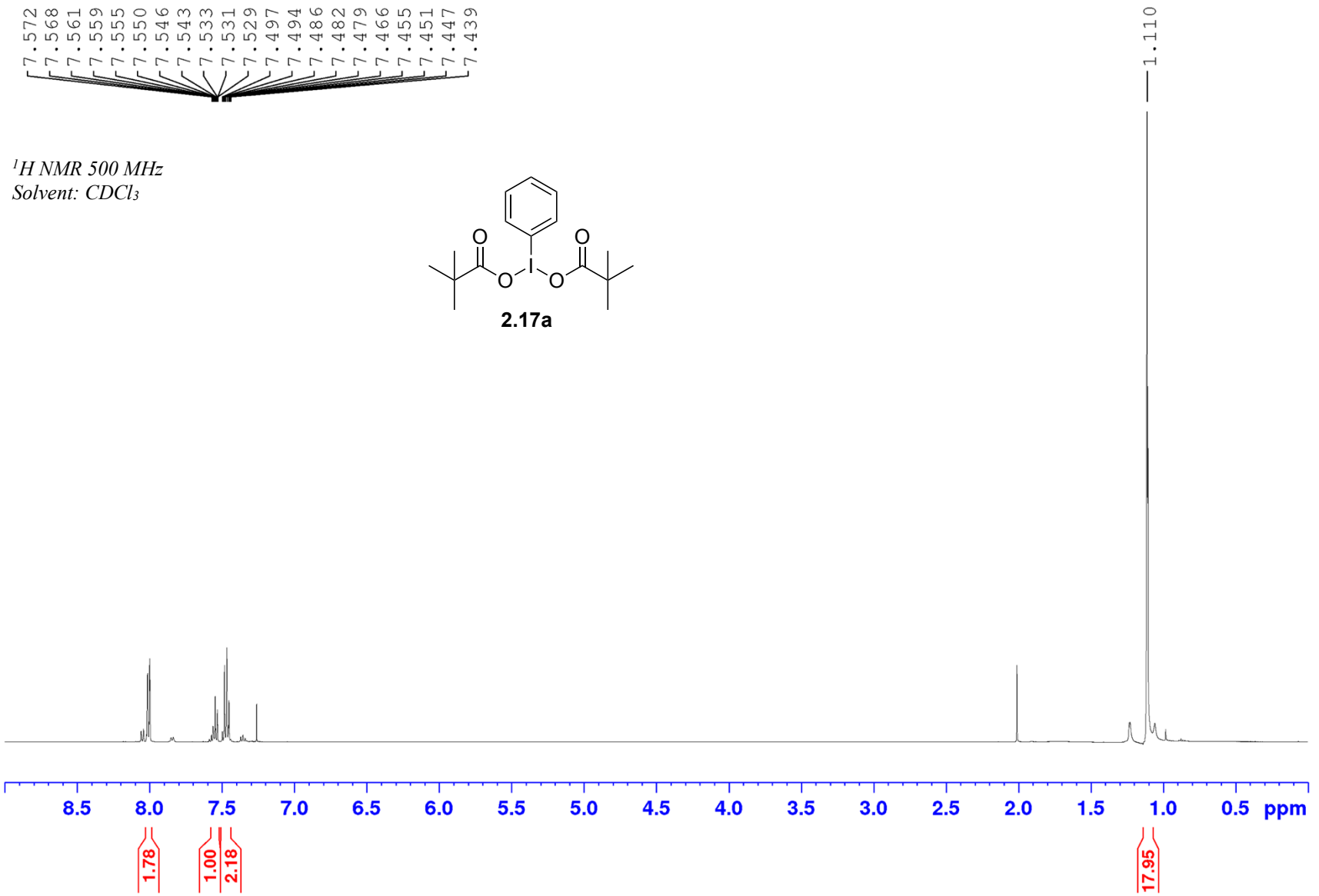

^{1}H NMR 500 MHz
Solvent: $CDCl_3$

2.17a

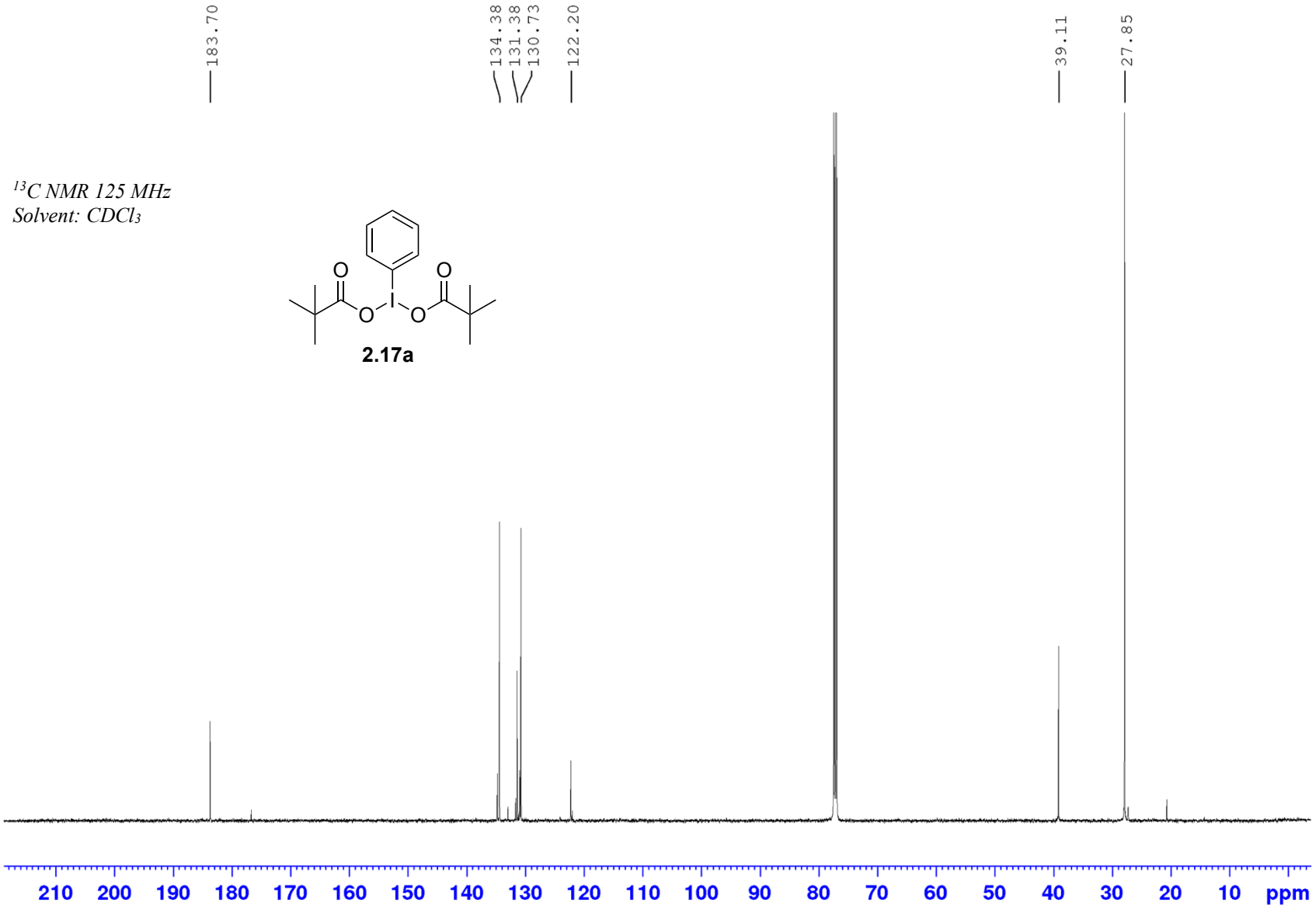
183.70
134.38
131.38
130.73
122.20
39.11
27.85
13C NMR 125 MHz
Solvent: CDCl3
O
O
I
O
O
2.17a
210 200 190 180 170 160 150 140 130 120 110 100 90 80 70 60 50 40 30 20 10 ppm

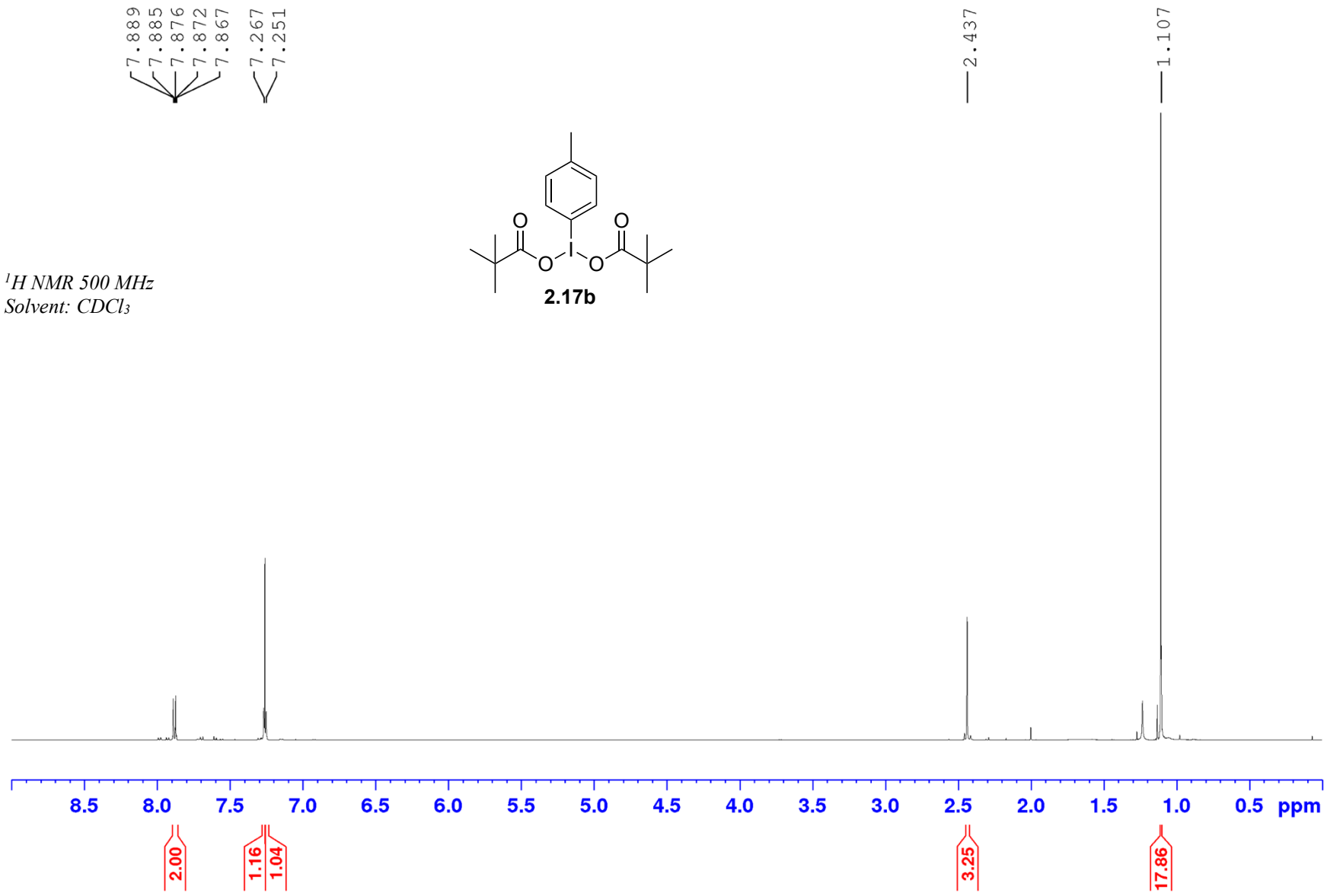
7.889
7.885
7.876
7.872
7.867
7.267
7.251
2.437
1.107
O
O
O
O
I
2.17b
[1]H NMR 500 MHz
Solvent: CDCl3
8.5
8.0
7.5
7.0
6.5
6.0
5.5
5.0
4.5
4.0
3.5
3.0
2.5
2.0
1.5
1.0
0.5
ppm
2.00
1.16
1.04
3.25
17.86

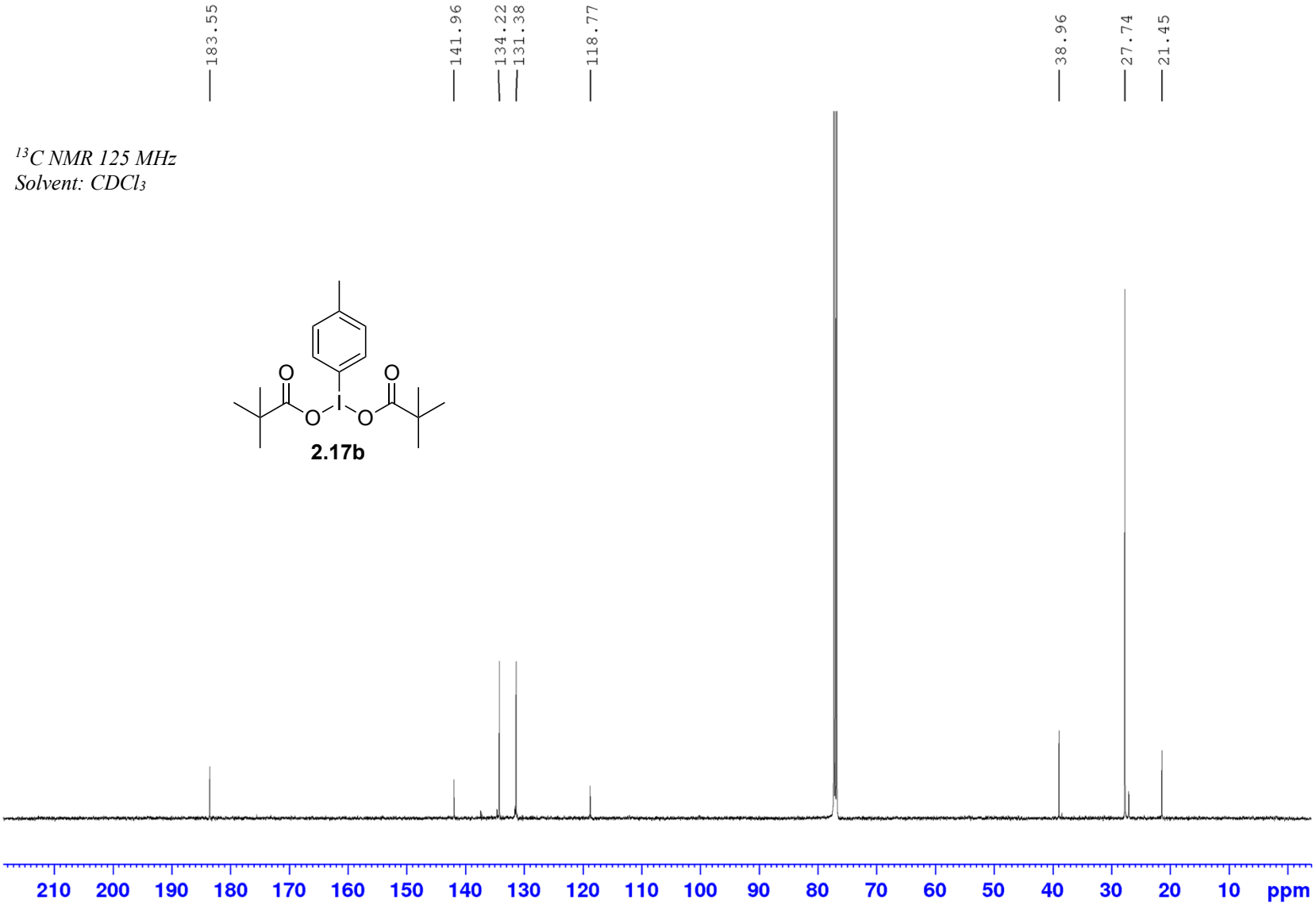
183.55
141.96
134.22
131.38
118.77
38.96
27.74
21.45
13C NMR 125 MHz
Solvent: CDCl3
2.17b
210 200 190 180 170 160 150 140 130 120 110 100 90 80 70 60 50 40 30 20 10 ppm

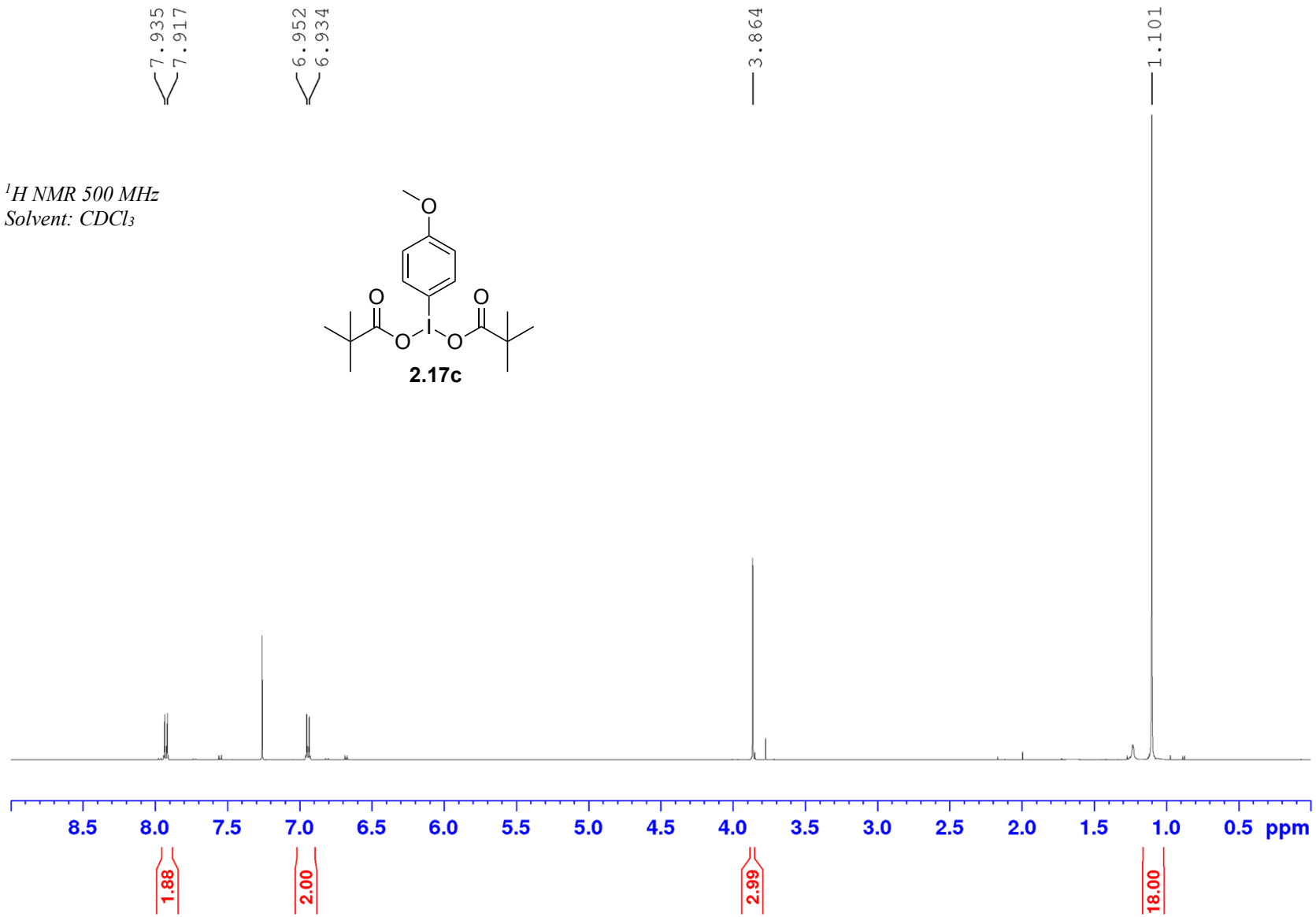
7.935
7.917
6.952
6.934
3.864
1.101
^1H NMR 500 MHz
Solvent: $CDCl_3$
O
O
O
I
O
O
2.17c
8.5
8.0
7.5
7.0
6.5
6.0
5.5
5.0
4.5
4.0
3.5
3.0
2.5
2.0
1.5
1.0
0.5
ppm
1.88
2.00
2.99
18.00

^{13}C NMR 125 MHz
Solvent: $CDCl_3$

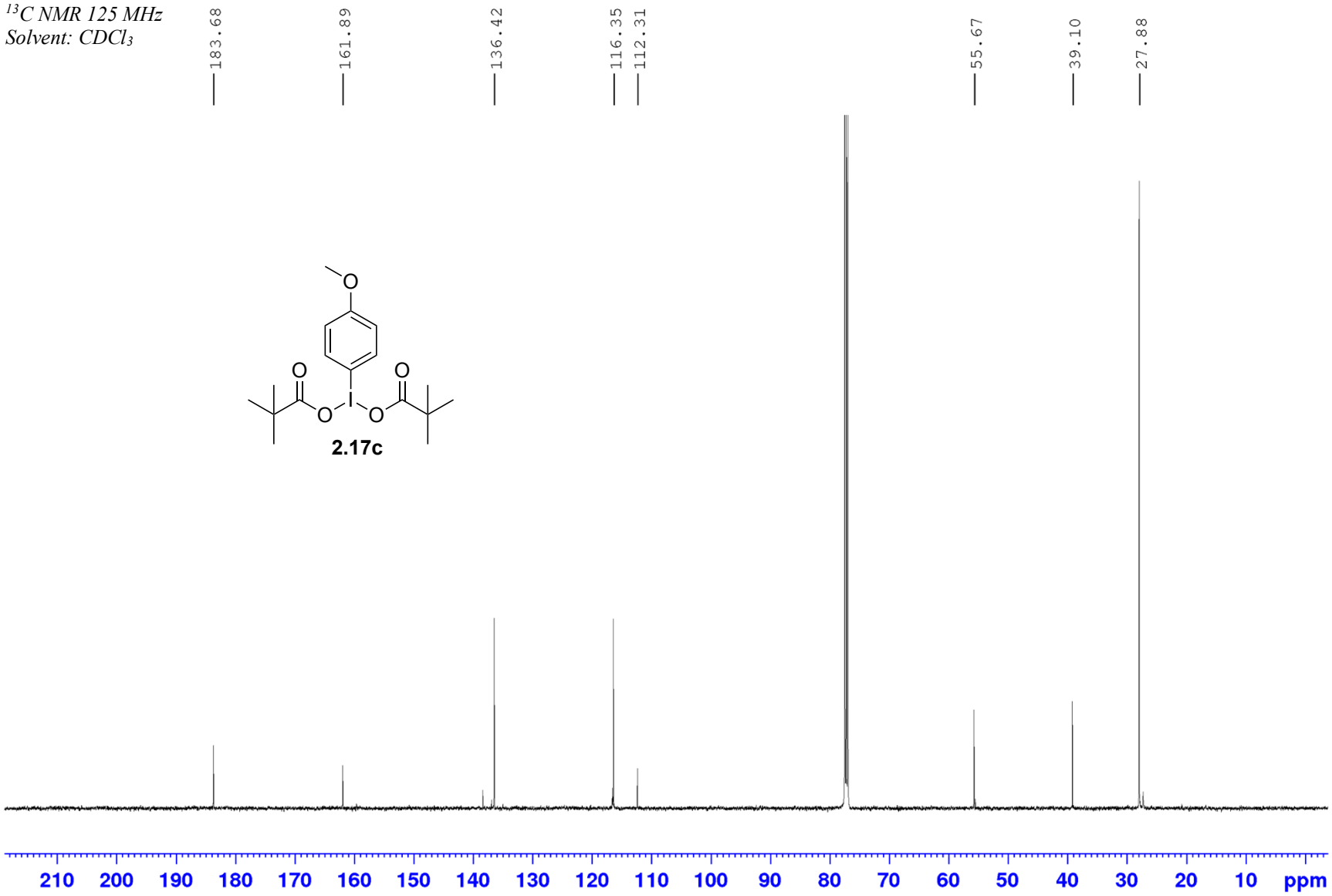

^{1}H NMR 500 MHz
Solvent: $CDCl_3$

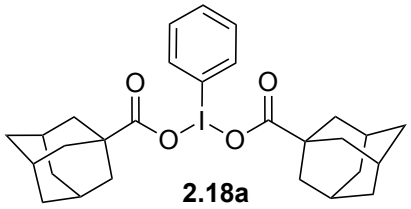

2.18a

^{13}C NMR 125 MHz
Solvent: $CDCl_3$

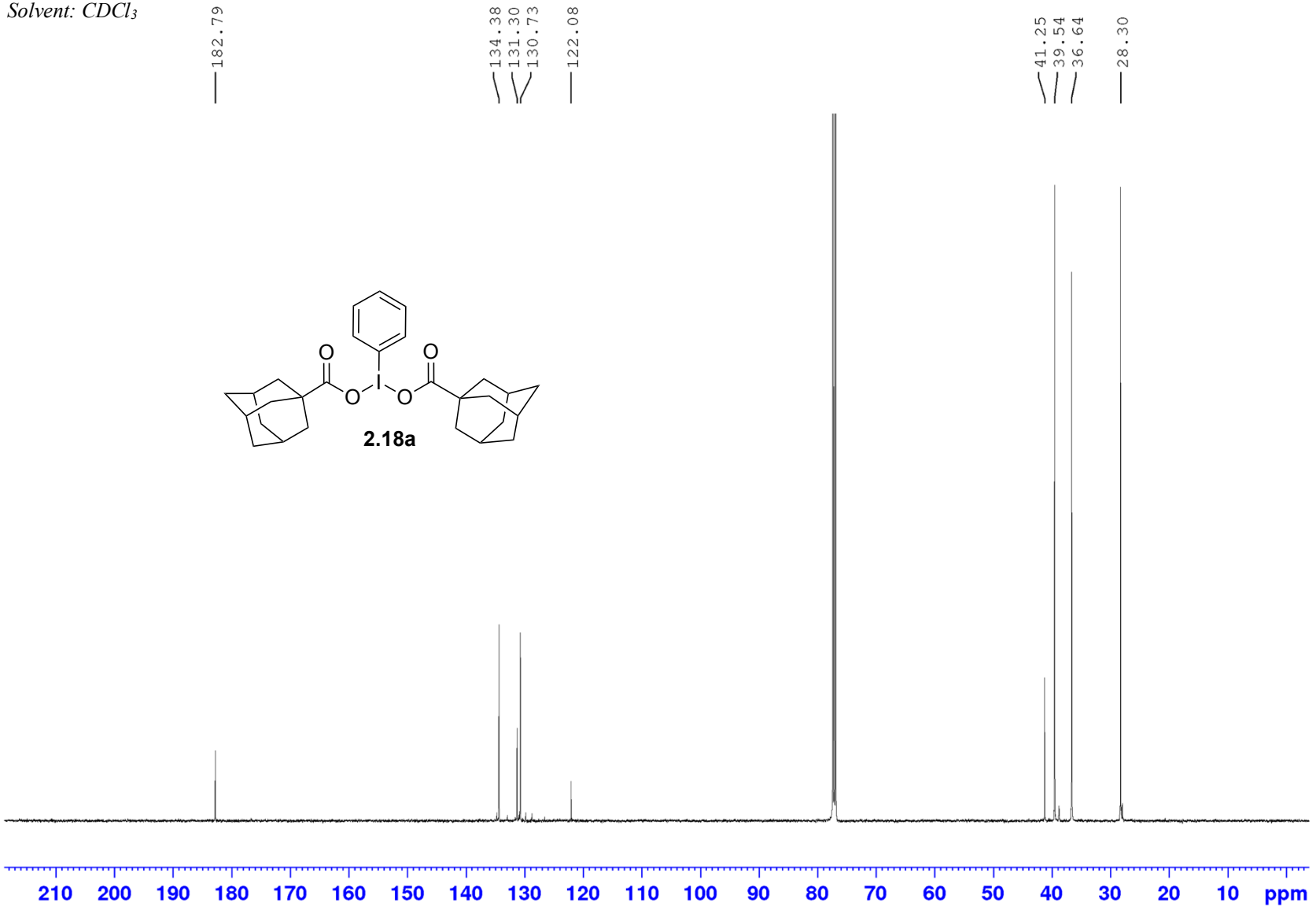

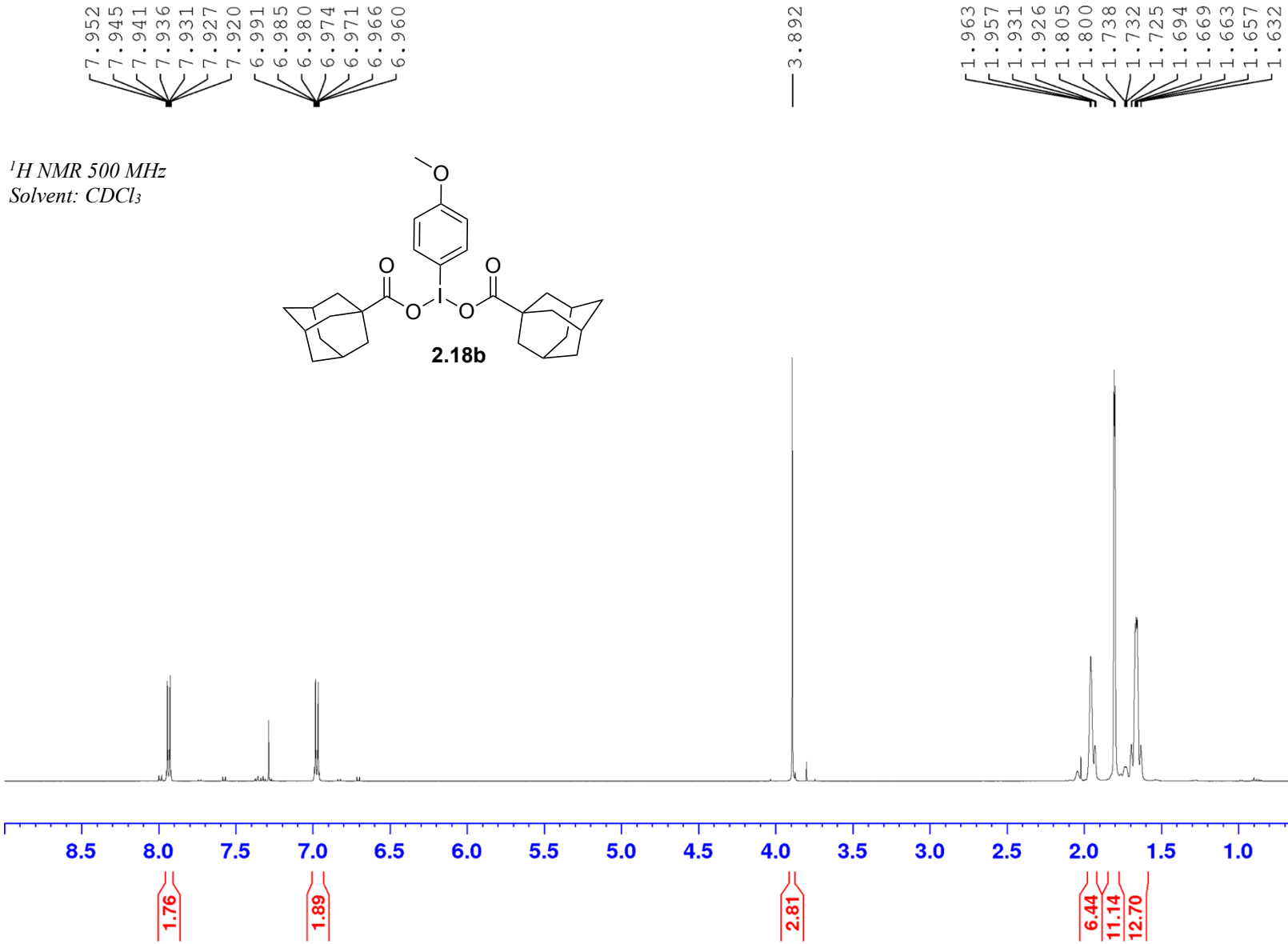
7.952
7.945
7.941
7.936
7.931
7.927
7.920
6.991
6.985
6.980
6.974
6.971
6.966
6.960
3.892
1.963
1.957
1.931
1.926
1.805
1.800
1.738
1.732
1.725
1.694
1.669
1.663
1.657
1.632
1H NMR 500 MHz
Solvent: CDCl3
2.18b
8.5
8.0
7.5
7.0
6.5
6.0
5.5
5.0
4.5
4.0
3.5
3.0
2.5
2.0
1.5
1.0
0.5
ppm
1.76
1.89
2.81
6.44
11.14
12.70

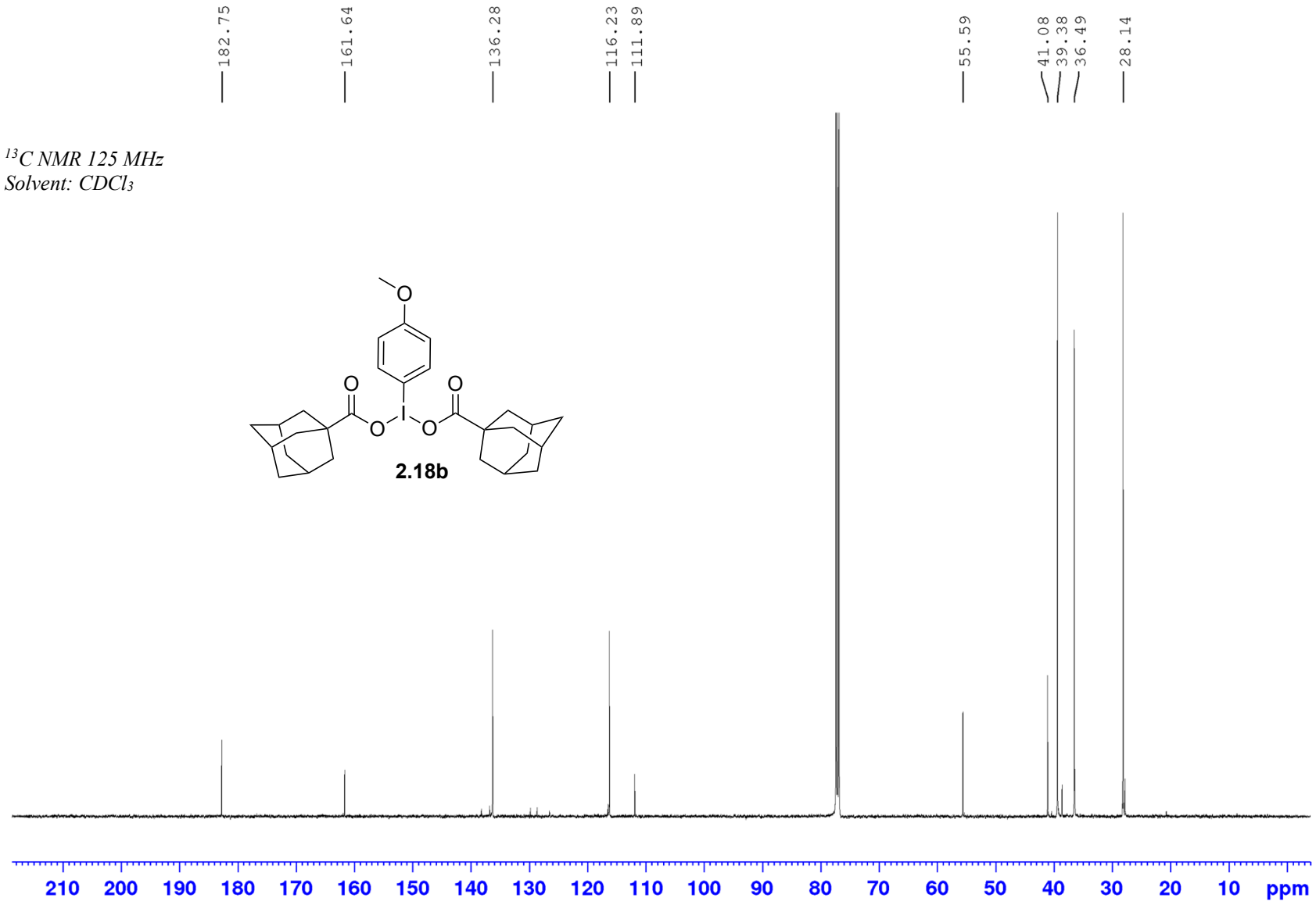
182.75
161.64
136.28
116.23
111.89
55.59
41.08
39.38
36.49
28.14
13C NMR 125 MHz
Solvent: CDCl3
O
O
O
I
O
O
2.18b
210 200 190 180 170 160 150 140 130 120 110 100 90 80 70 60 50 40 30 20 10 ppm

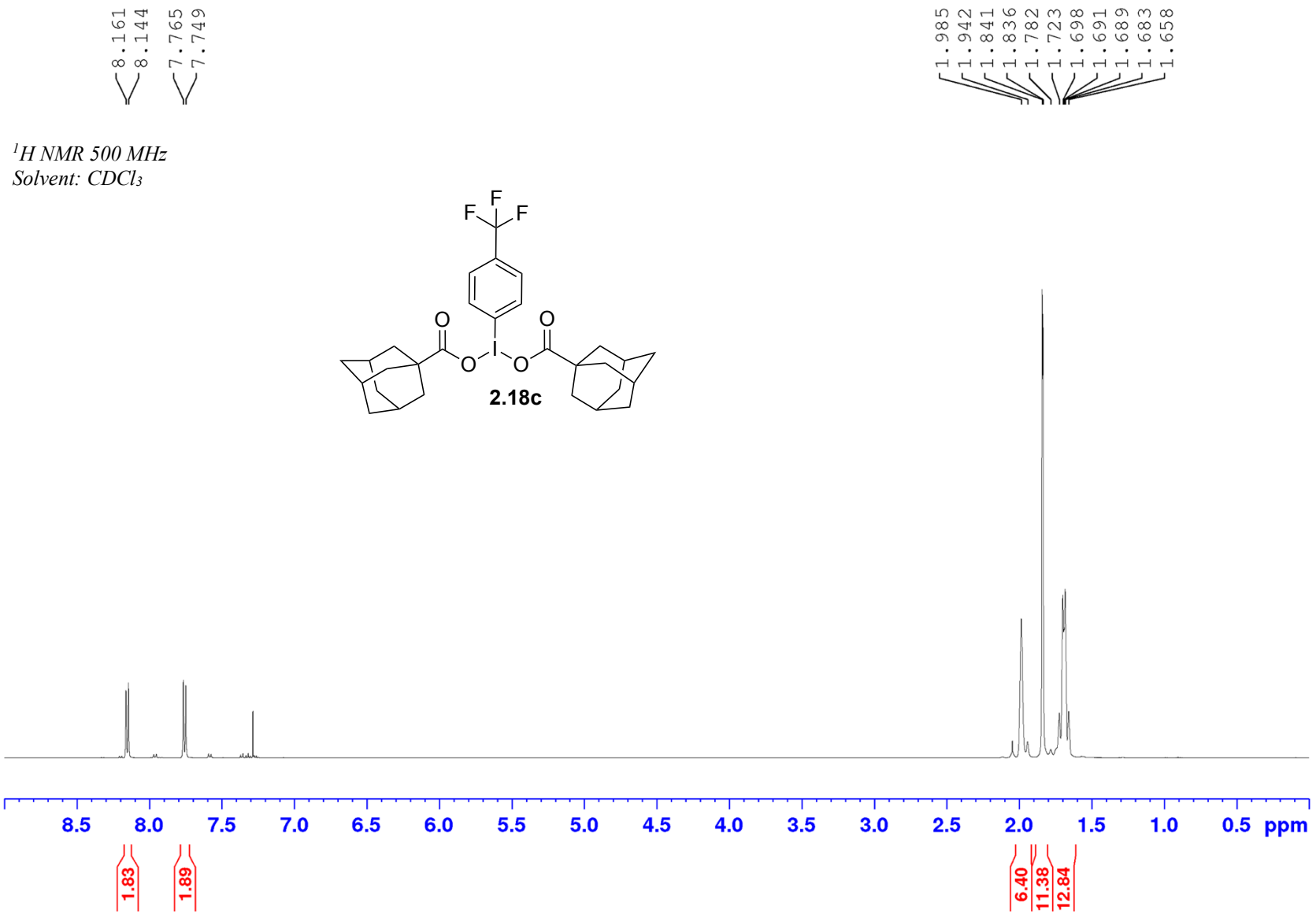

^{1}H NMR 500 MHz
Solvent: $CDCl_3$

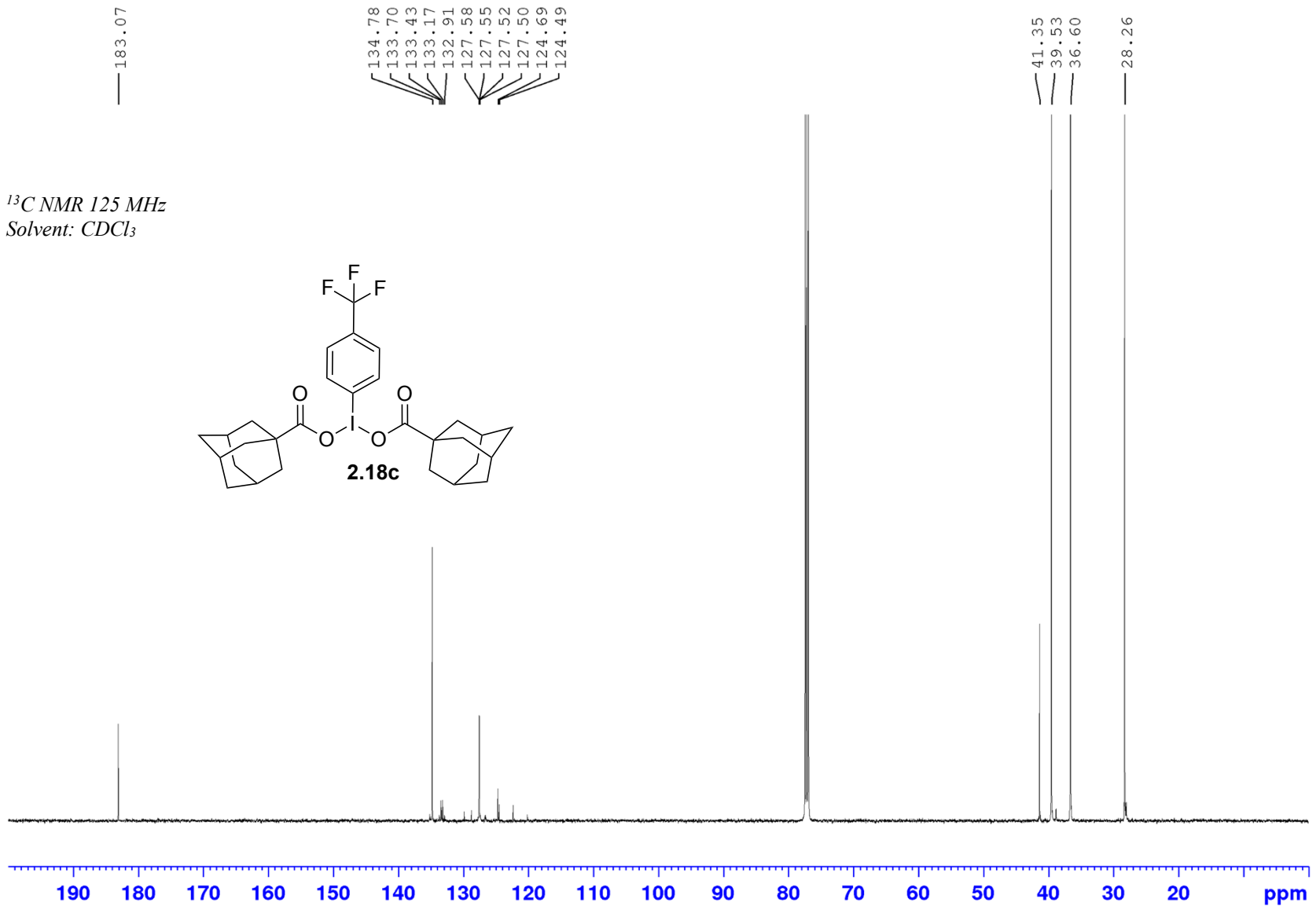
183.07
134.78
133.70
133.43
133.17
132.91
127.58
127.55
127.52
127.50
124.69
124.49
41.35
39.53
36.60
28.26
13C NMR 125 MHz
Solvent: CDCl3
F
F
F
O
O
O
O
I
2.18c
190
180
170
160
150
140
130
120
110
100
90
80
70
60
50
40
30
20
ppm

^{1}H and ^{13}C spectra of hypervalent(III)iodine derivatives and controls referenced to CD_3CN 1.94 ppm and 1.32 ppm respectiviely .

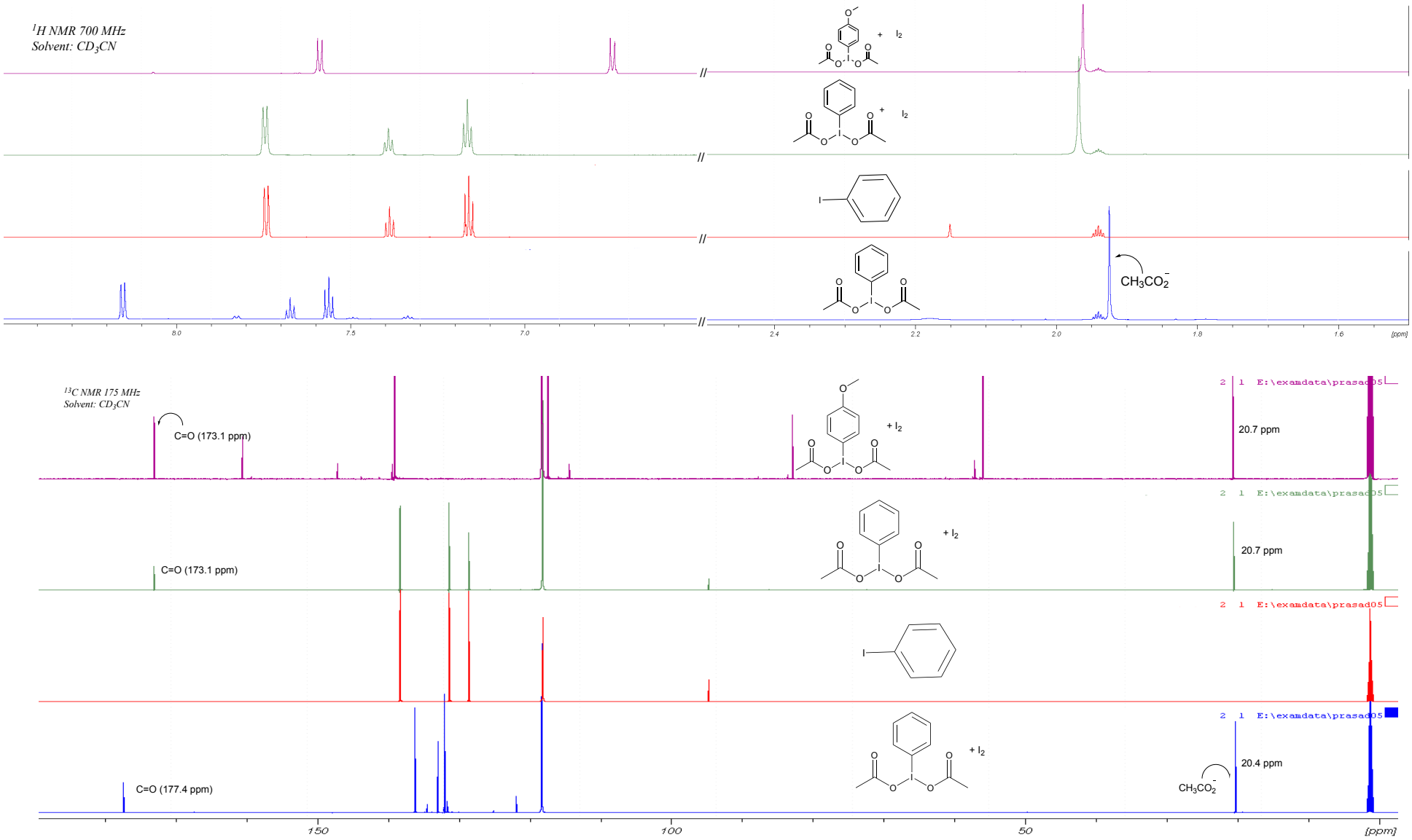

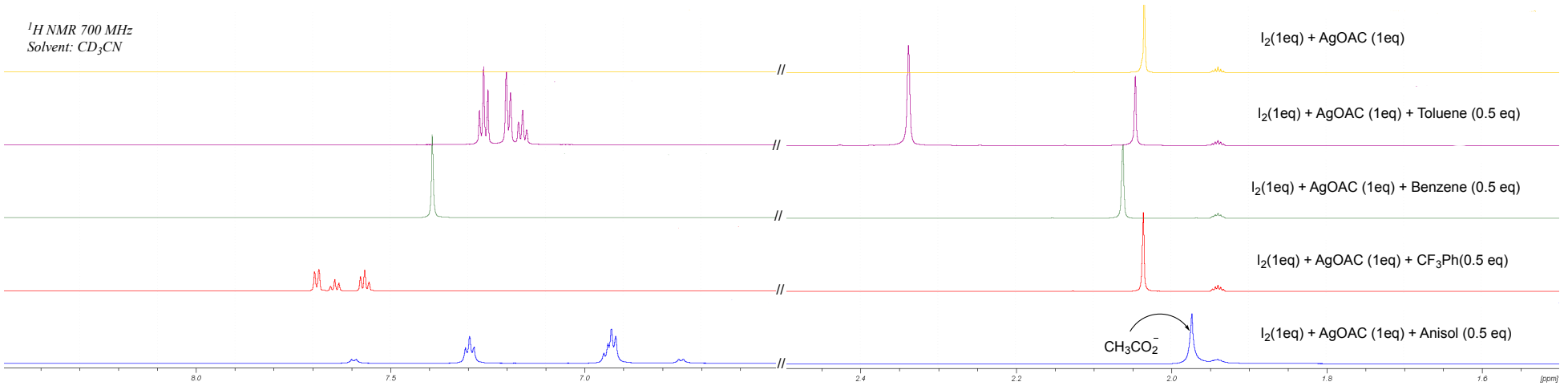
^{1}H NMR 700 MHz
Solvent: CD_3CN
I_2(1eq) + AgOAC (1eq)
I_2(1eq) + AgOAC (1eq) + Toluene (0.5 eq)
I_2(1eq) + AgOAC (1eq) + Benzene (0.5 eq)
I_2(1eq) + AgOAC (1eq) + CF_3Ph(0.5 eq)
I_2(1eq) + AgOAC (1eq) + Anisol (0.5 eq)
$CH_3CO_2^-$
8.0
7.5
7.0
2.4
2.2
2.0
1.8
1.6
[ppm]

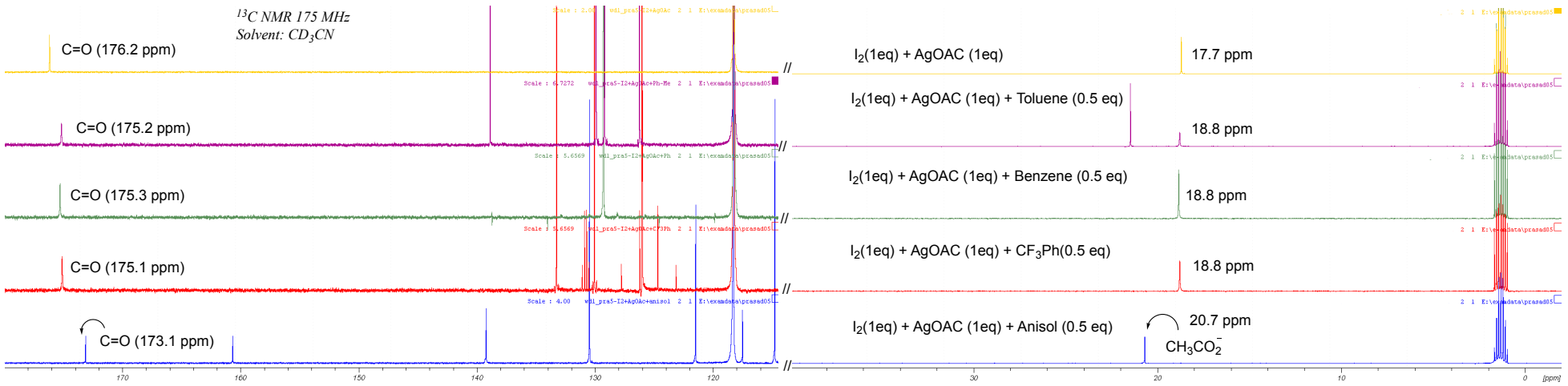
^{13}C NMR 175 MHz
Solvent: CD_3CN
C=O (176.2 ppm)
C=O (175.2 ppm)
C=O (175.3 ppm)
C=O (175.1 ppm)
C=O (173.1 ppm)
I_2(1eq) + AgOAC (1eq)
17.7 ppm
I_2(1eq) + AgOAC (1eq) + Toluene (0.5 eq)
18.8 ppm
I_2(1eq) + AgOAC (1eq) + Benzene (0.5 eq)
18.8 ppm
I_2(1eq) + AgOAC (1eq) + CF_3Ph(0.5 eq)
18.8 ppm
I_2(1eq) + AgOAC (1eq) + Anisol (0.5 eq)
20.7 ppm
$CH_3CO_2^-$
170
160
150
140
130
120
30
20
10
0
[ppm]

Spectral data for Article 2.

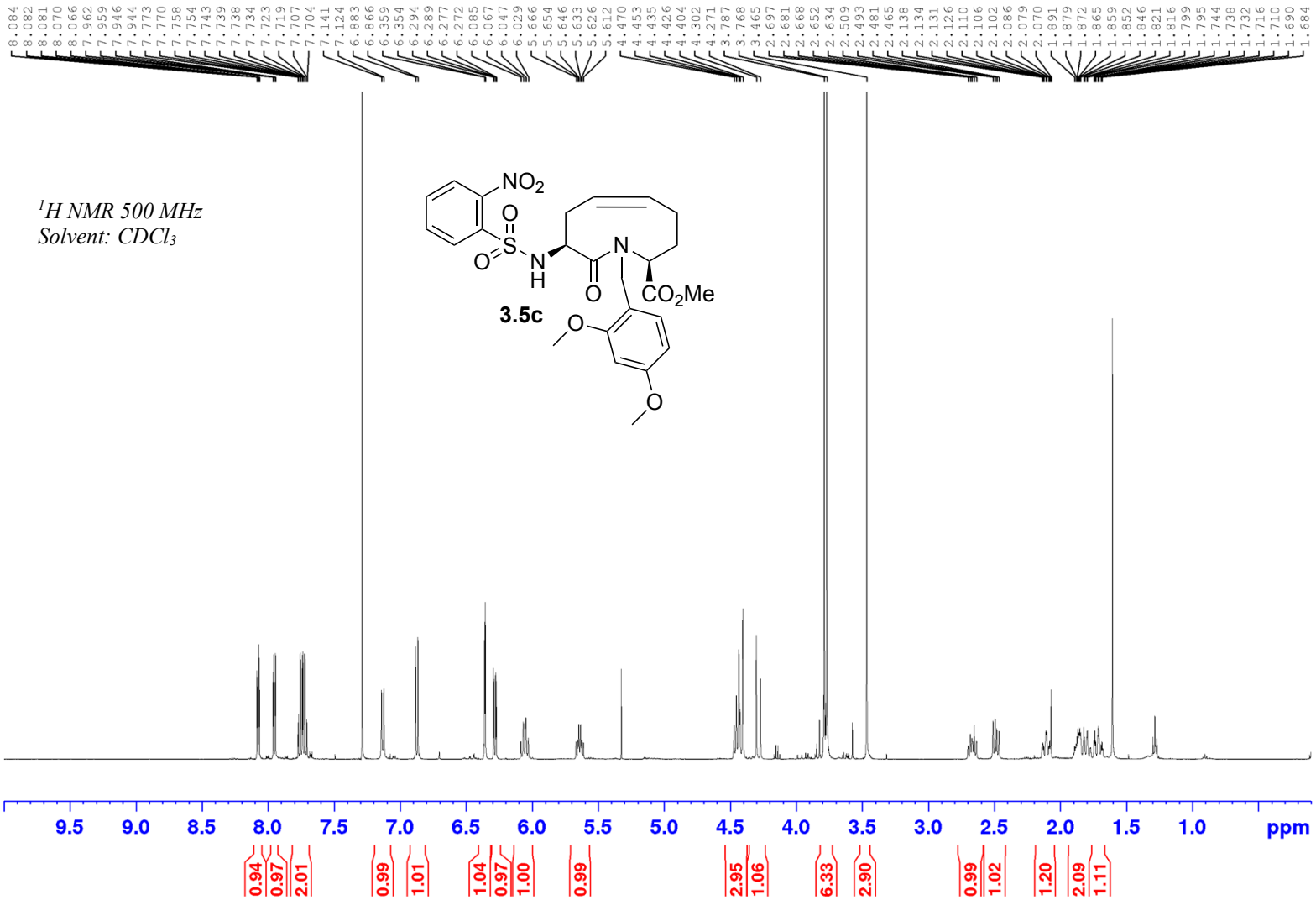
8.084
8.082
8.081
8.070
8.066
7.962
7.959
7.946
7.944
7.773
7.770
7.758
7.754
7.743
7.739
7.738
7.734
7.723
7.719
7.707
7.704
7.141
7.124
6.883
6.866
6.359
6.354
6.294
6.289
6.277
6.272
6.085
6.067
6.047
6.029
5.666
5.654
5.646
5.633
5.626
5.612
4.470
4.453
4.435
4.426
4.404
4.302
4.271
3.787
3.768
3.465
2.697
2.681
2.668
2.652
2.634
2.509
2.493
2.481
2.465
2.138
2.134
2.131
2.126
2.110
2.106
2.102
2.086
2.079
2.070
1.891
1.879
1.872
1.865
1.859
1.852
1.846
1.821
1.816
1.799
1.795
1.744
1.738
1.732
1.716
1.710
1.690
1.684
1H NMR 500 MHz
Solvent: CDCl3
NO2
O
S
O
N
H
O
N
O
CO2Me
3.5c
O
O
9.5
9.0
8.5
8.0
7.5
7.0
6.5
6.0
5.5
5.0
4.5
4.0
3.5
3.0
2.5
2.0
1.5
1.0
ppm
0.94
0.97
2.01
0.99
1.01
1.04
0.97
1.00
0.99
2.95
1.06
6.33
2.90
0.99
1.02
1.20
2.09
1.11

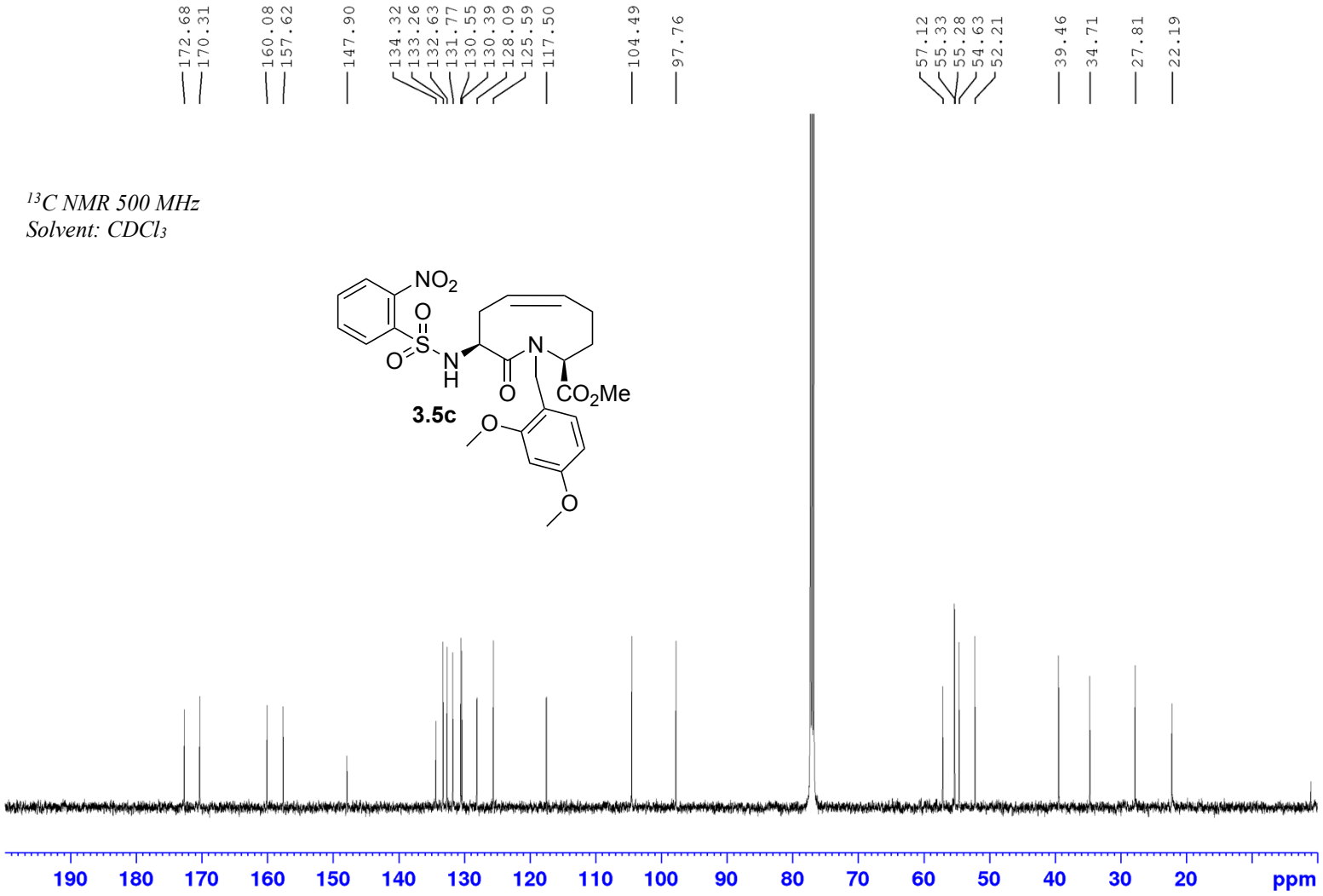
172.68
170.31
160.08
157.62
147.90
134.32
133.26
132.63
131.77
130.55
130.39
128.09
125.59
117.50
104.49
97.76
57.12
55.33
55.28
54.63
52.21
39.46
34.71
27.81
22.19
13C NMR 500 MHz
Solvent: CDCl3
NO2
O
S
O
N
H
O
N
CO2Me
3.5c
O
O
190
180
170
160
150
140
130
120
110
100
90
80
70
60
50
40
30
20
ppm

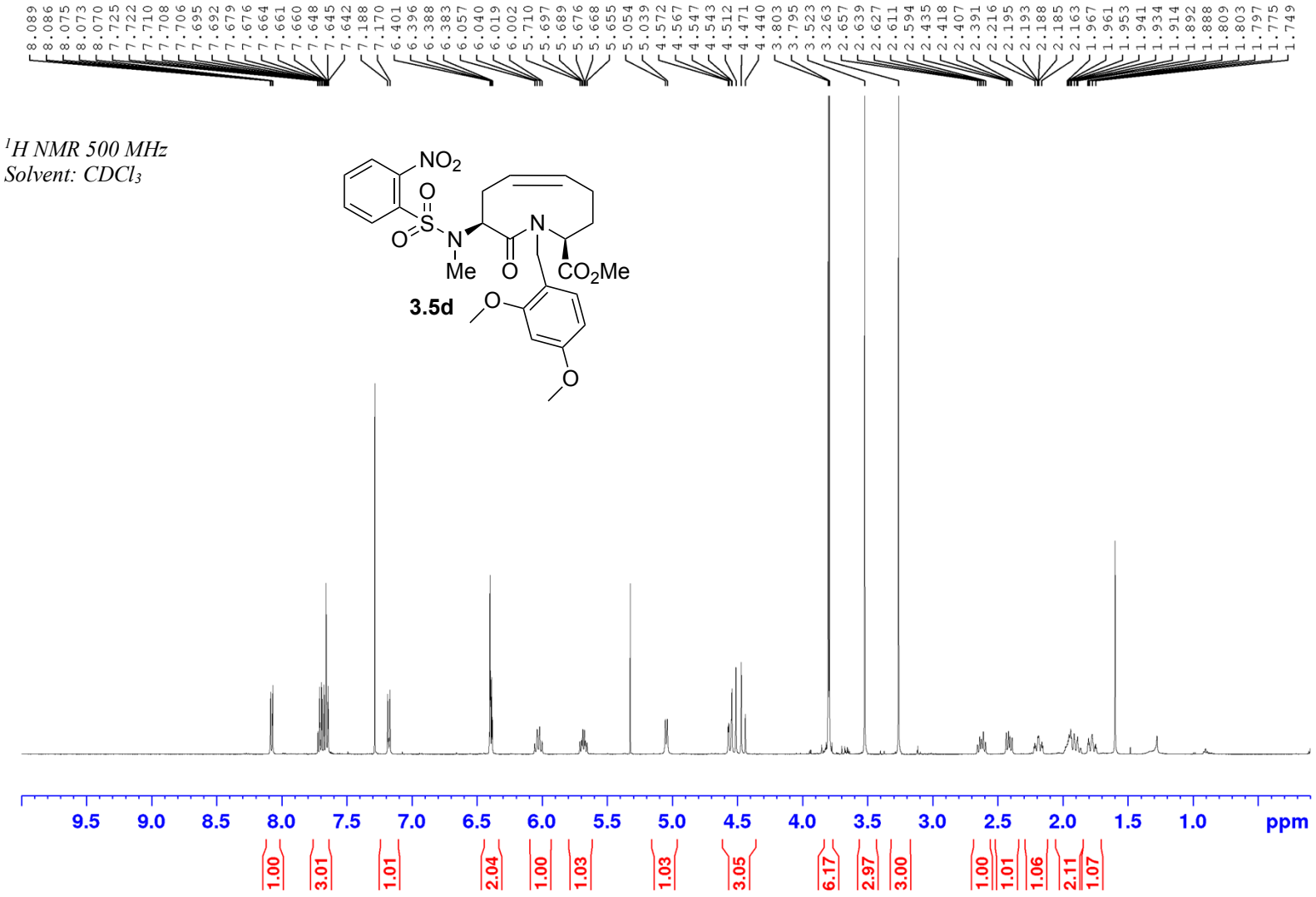
8.089
8.086
8.075
8.073
8.070
7.725
7.722
7.710
7.708
7.706
7.695
7.692
7.679
7.676
7.664
7.661
7.660
7.648
7.645
7.642
7.188
7.170
6.401
6.396
6.388
6.383
6.057
6.040
6.019
6.002
5.710
5.697
5.689
5.676
5.668
5.655
5.054
5.039
4.572
4.567
4.547
4.543
4.512
4.471
4.440
3.803
3.795
3.523
3.263
2.657
2.639
2.627
2.611
2.594
2.435
2.418
2.407
2.391
2.216
2.195
2.193
2.188
2.185
2.163
1.967
1.961
1.953
1.941
1.934
1.914
1.892
1.888
1.809
1.803
1.797
1.775
1.749
1H NMR 500 MHz
Solvent: CDCl3
NO2
O
S
O
N
Me
O
N
O
CO2Me
O
O
3.5d
9.5
9.0
8.5
8.0
7.5
7.0
6.5
6.0
5.5
5.0
4.5
4.0
3.5
3.0
2.5
2.0
1.5
1.0
ppm
1.00
3.01
1.01
2.04
1.00
1.03
1.03
3.05
6.17
2.97
3.00
1.00
1.01
1.06
2.11
1.07

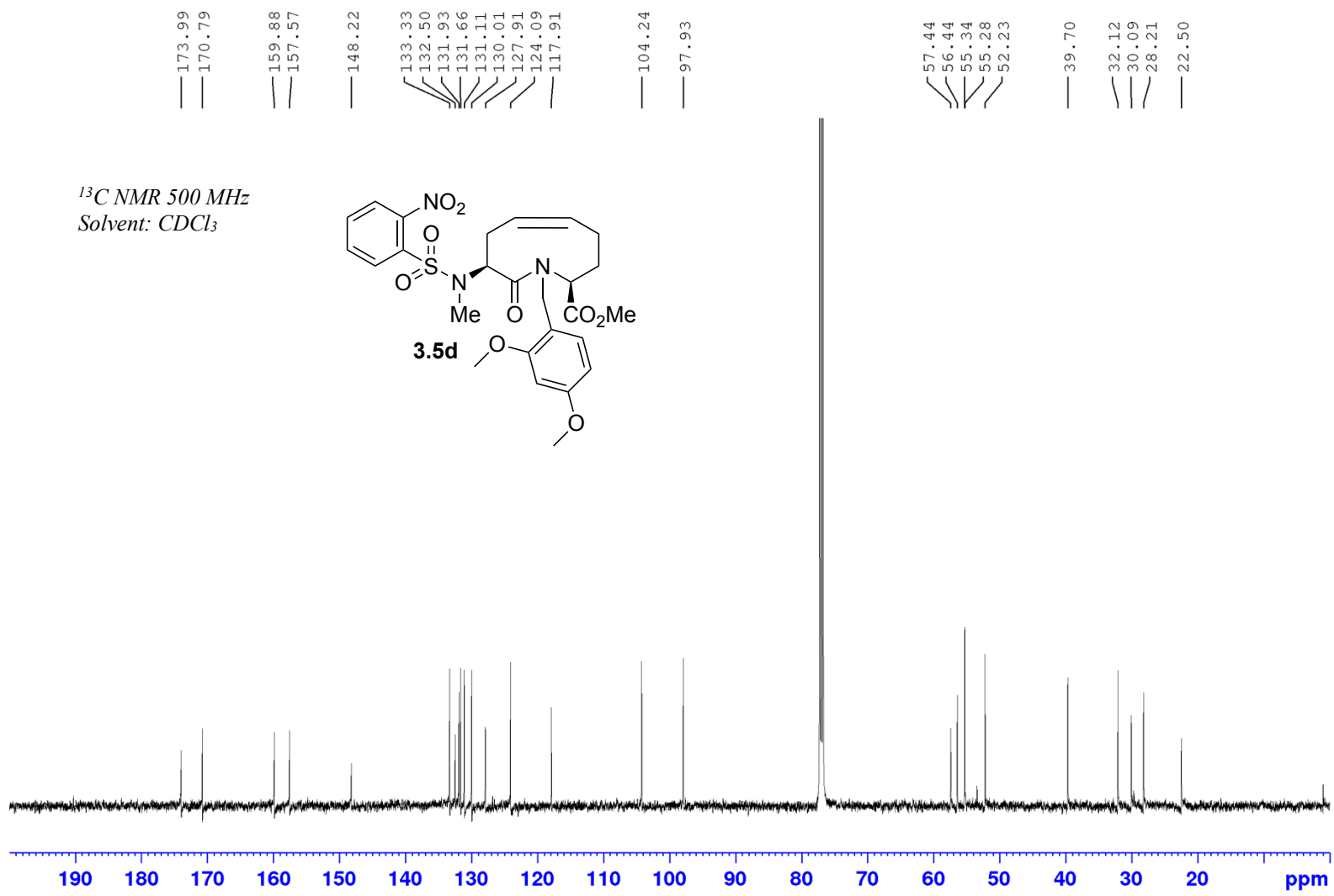
173.99
170.79
159.88
157.57
148.22
133.33
132.50
131.93
131.66
131.11
130.01
127.91
124.09
117.91
104.24
97.93
57.44
56.44
55.34
55.28
52.23
39.70
32.12
30.09
28.21
22.50
13C NMR 500 MHz
Solvent: CDCl3
NO2
O
S
O
N
Me
O
N
CO2Me
O
O
3.5d
190
180
170
160
150
140
130
120
110
100
90
80
70
60
50
40
30
20
ppm

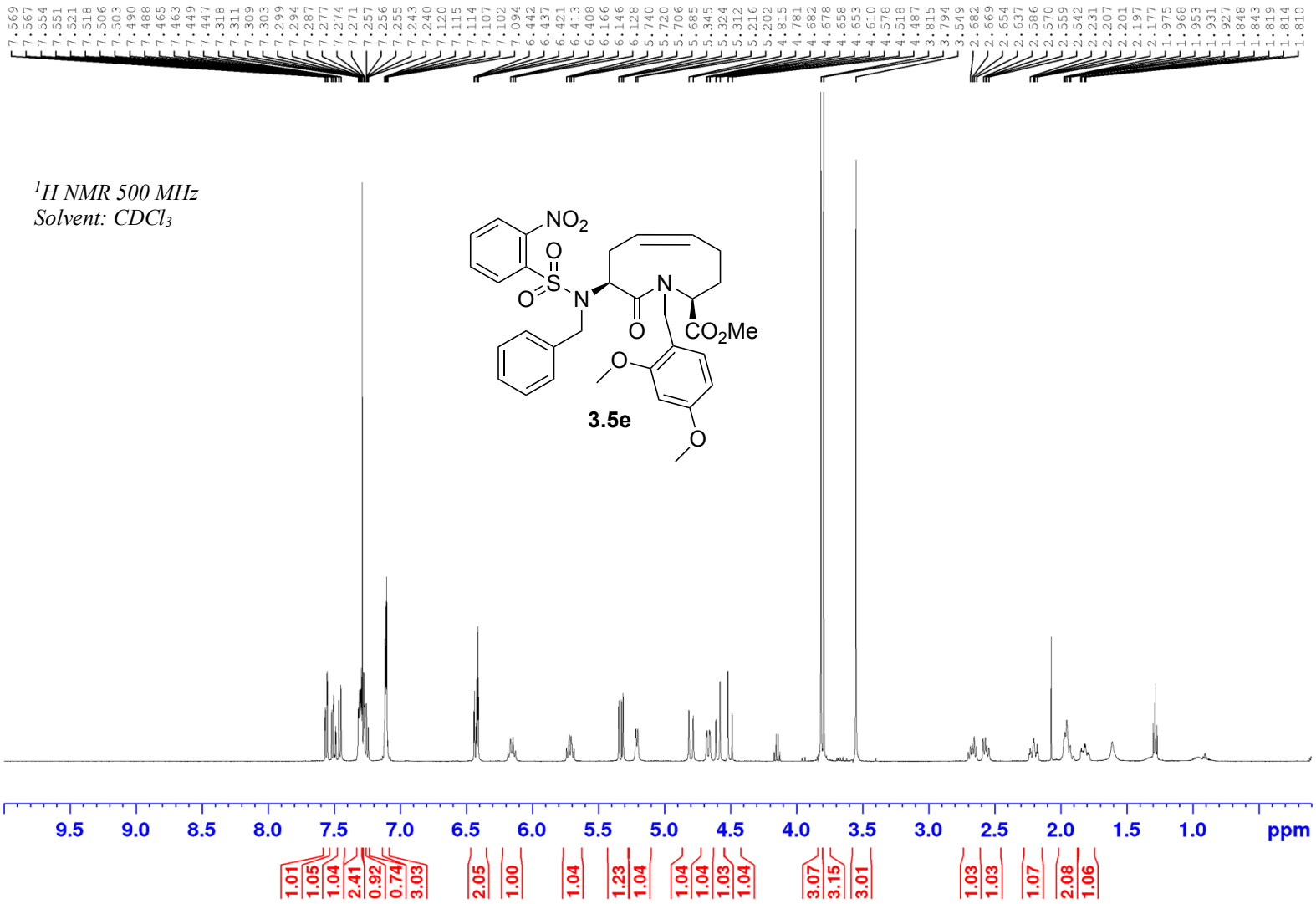
7.569
7.567
7.554
7.551
7.521
7.518
7.506
7.503
7.490
7.488
7.465
7.463
7.449
7.447
7.318
7.311
7.309
7.303
7.299
7.294
7.287
7.277
7.274
7.271
7.257
7.256
7.255
7.243
7.240
7.120
7.115
7.114
7.107
7.102
7.094
6.442
6.437
6.421
6.413
6.408
6.166
6.146
6.128
5.740
5.720
5.706
5.685
5.345
5.324
5.312
5.216
5.202
4.815
4.781
4.682
4.678
4.658
4.653
4.610
4.578
4.518
4.487
3.815
3.794
3.549
2.682
2.669
2.654
2.637
2.586
2.570
2.559
2.542
2.231
2.207
2.201
2.197
2.177
1.975
1.968
1.953
1.931
1.927
1.848
1.843
1.819
1.814
1.810
1H NMR 500 MHz
Solvent: CDCl3
NO2
O
S
O
N
O
N
O
CO2Me
O
O
3.5e
9.5
9.0
8.5
8.0
7.5
7.0
6.5
6.0
5.5
5.0
4.5
4.0
3.5
3.0
2.5
2.0
1.5
1.0
ppm
1.01
1.05
1.04
2.41
0.92
0.74
3.03
2.05
1.00
1.04
1.23
1.04
1.04
1.04
1.03
1.04
3.07
3.15
3.01
1.03
1.03
1.07
2.08
1.06

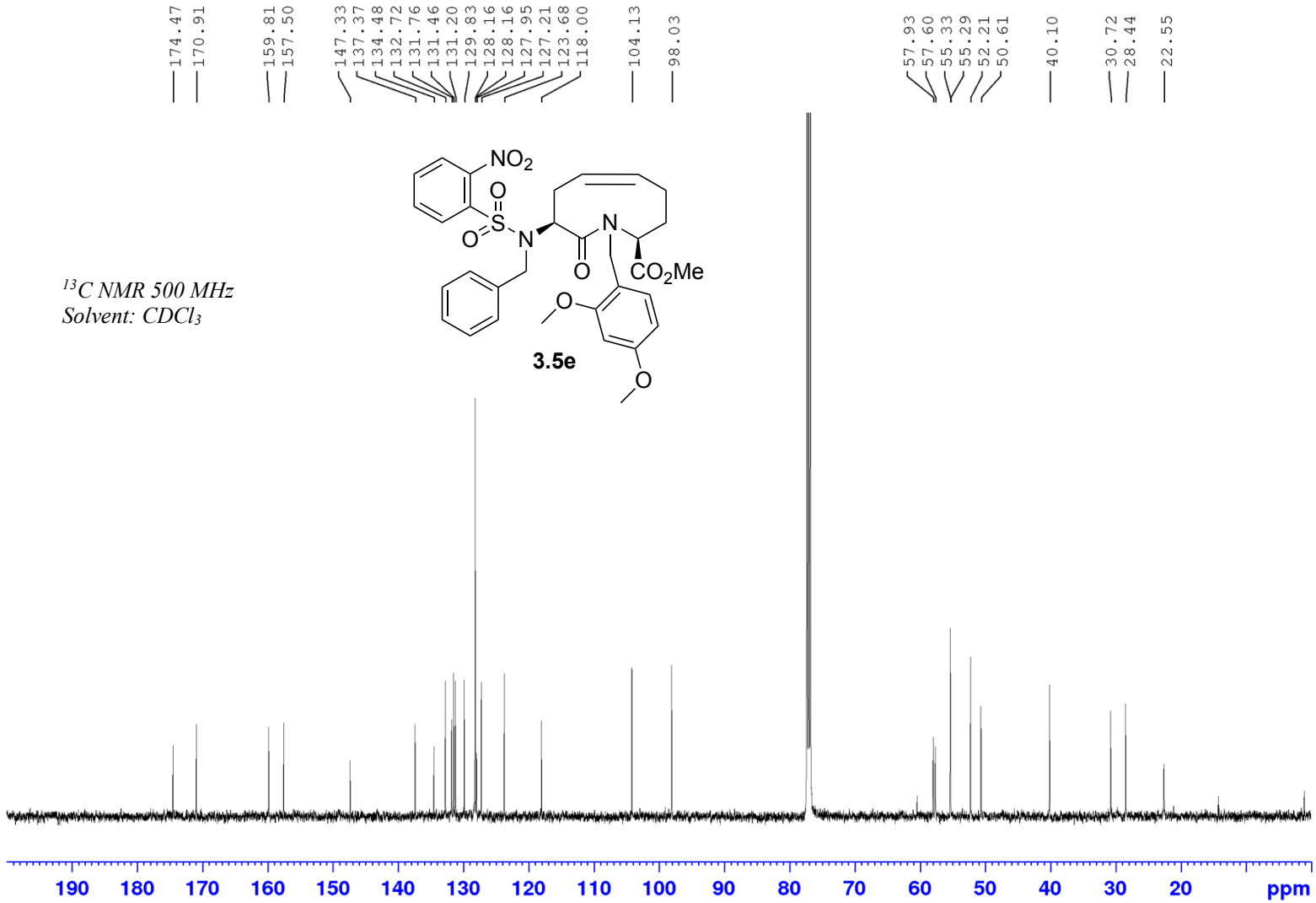
174.47
170.91
159.81
157.50
147.33
137.37
134.48
132.72
131.76
131.46
131.20
129.83
128.16
128.16
127.95
127.21
123.68
118.00
104.13
98.03
57.93
57.60
55.33
55.29
52.21
50.61
40.10
30.72
28.44
22.55
NO2
O
S
O
N
N
O
CO2Me
O
O
3.5e
13C NMR 500 MHz
Solvent: CDCl3
190
180
170
160
150
140
130
120
110
100
90
80
70
60
50
40
30
20
ppm

^{1}H NMR 500 MHz
Solvent: $CDCl_3$

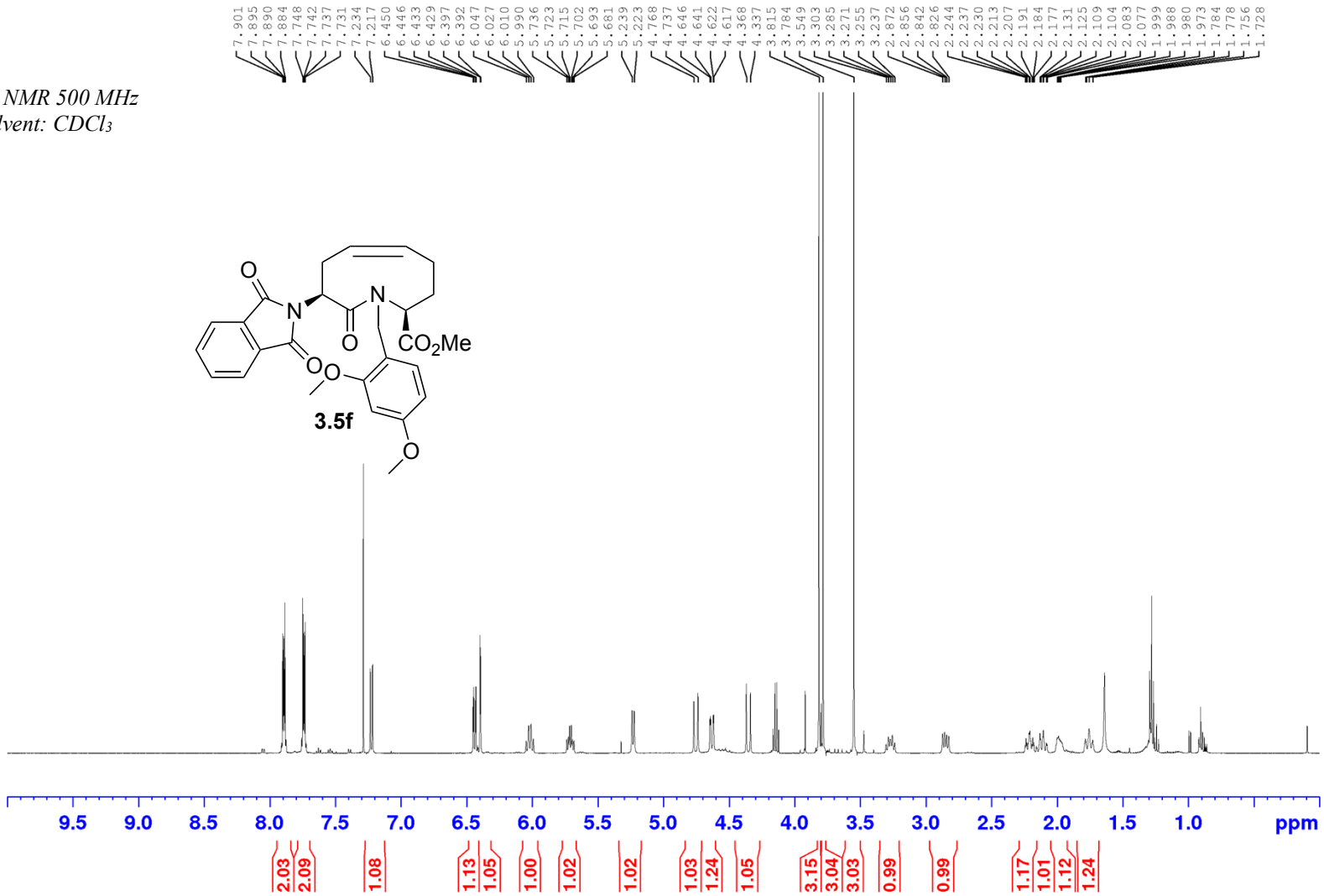

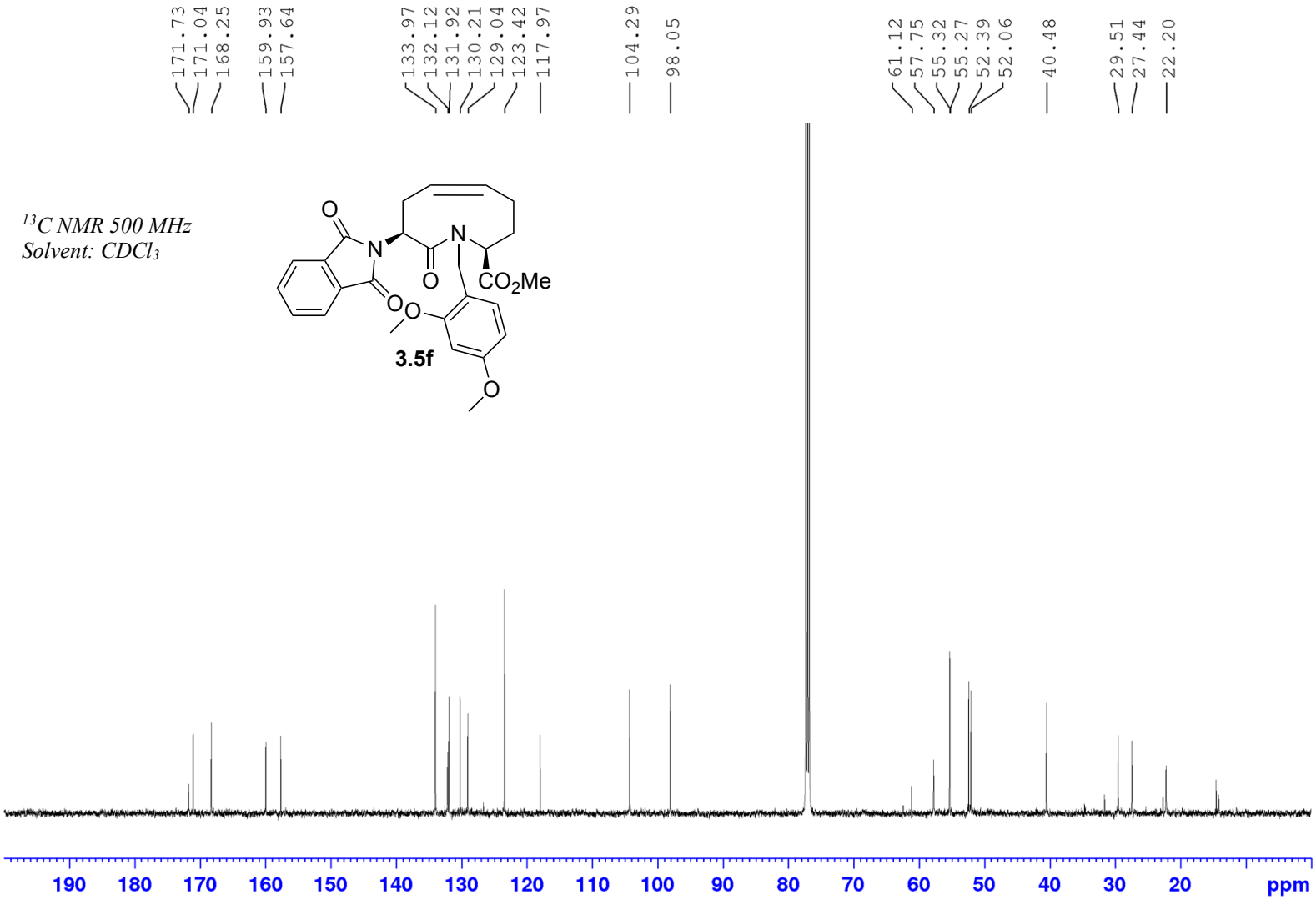
171.73
171.04
168.25
159.93
157.64
133.97
132.12
131.92
130.21
129.04
123.42
117.97
104.29
98.05
61.12
57.75
55.32
55.27
52.39
52.06
40.48
29.51
27.44
22.20
13C NMR 500 MHz
Solvent: CDCl3
3.5f
190
180
170
160
150
140
130
120
110
100
90
80
70
60
50
40
30
20
ppm

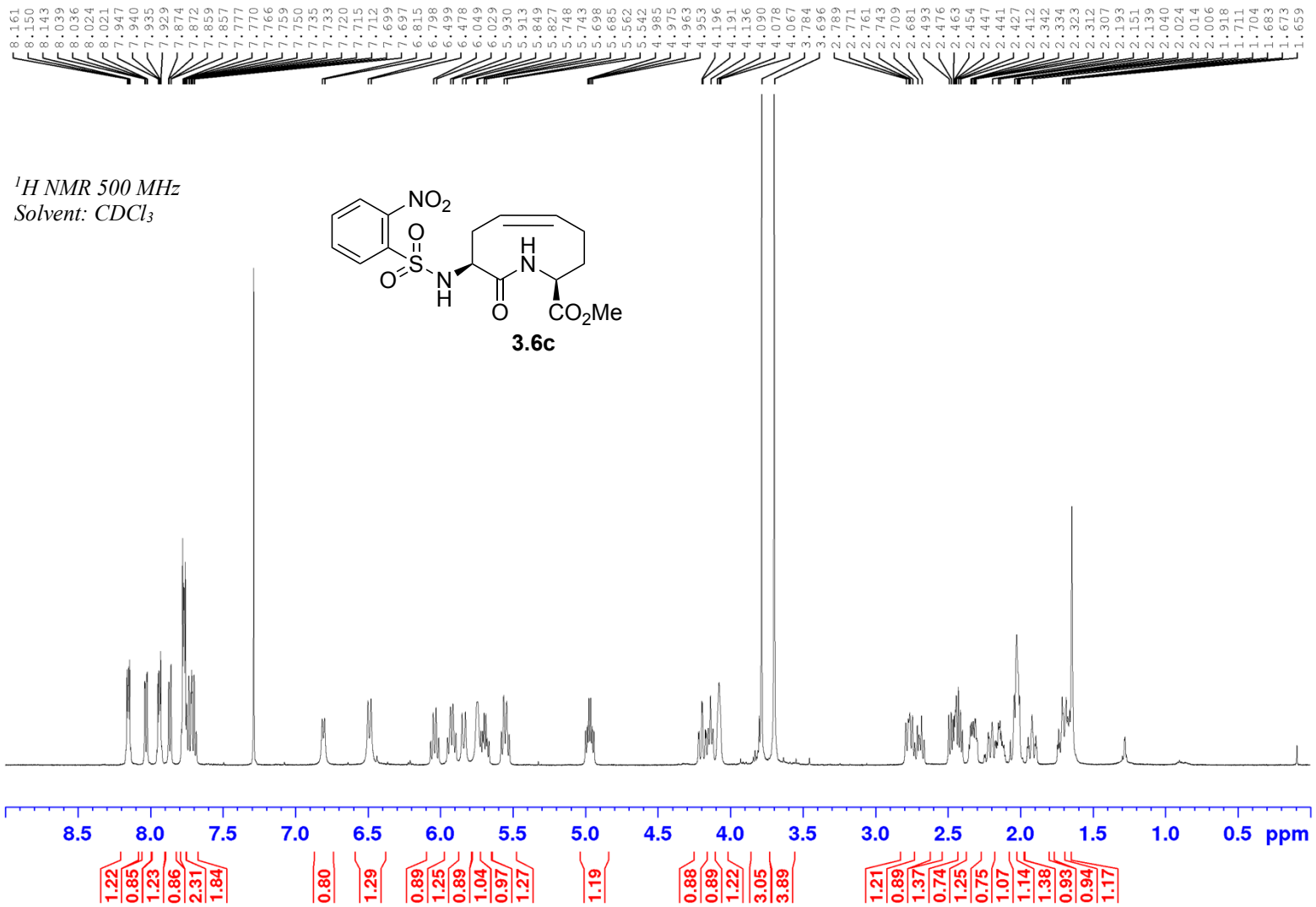
8.161
8.150
8.143
8.039
8.036
8.024
8.021
7.947
7.940
7.935
7.929
7.874
7.872
7.859
7.857
7.777
7.770
7.766
7.759
7.750
7.735
7.733
7.720
7.715
7.712
7.699
7.697
6.815
6.798
6.499
6.478
6.049
6.029
5.930
5.913
5.849
5.827
5.748
5.743
5.698
5.685
5.562
5.542
4.985
4.975
4.963
4.953
4.196
4.191
4.136
4.090
4.078
4.067
3.784
3.696
2.789
2.771
2.761
2.743
2.709
2.681
2.493
2.476
2.463
2.454
2.447
2.441
2.427
2.412
2.342
2.334
2.323
2.312
2.307
2.193
2.151
2.139
2.040
2.024
2.014
2.006
1.918
1.711
1.704
1.683
1.673
1.659
1H NMR 500 MHz
Solvent: CDCl3
NO2
O
S
O
N
H
H
N
O
CO2Me
3.6c
8.5
8.0
7.5
7.0
6.5
6.0
5.5
5.0
4.5
4.0
3.5
3.0
2.5
2.0
1.5
1.0
0.5
ppm
1.22
0.85
1.23
0.86
2.31
1.84
0.80
1.29
0.89
1.25
0.89
1.04
0.97
1.27
1.19
0.88
0.89
1.22
3.05
3.89
1.21
0.89
1.37
0.74
1.25
0.75
1.07
1.14
1.38
0.93
0.94
1.17

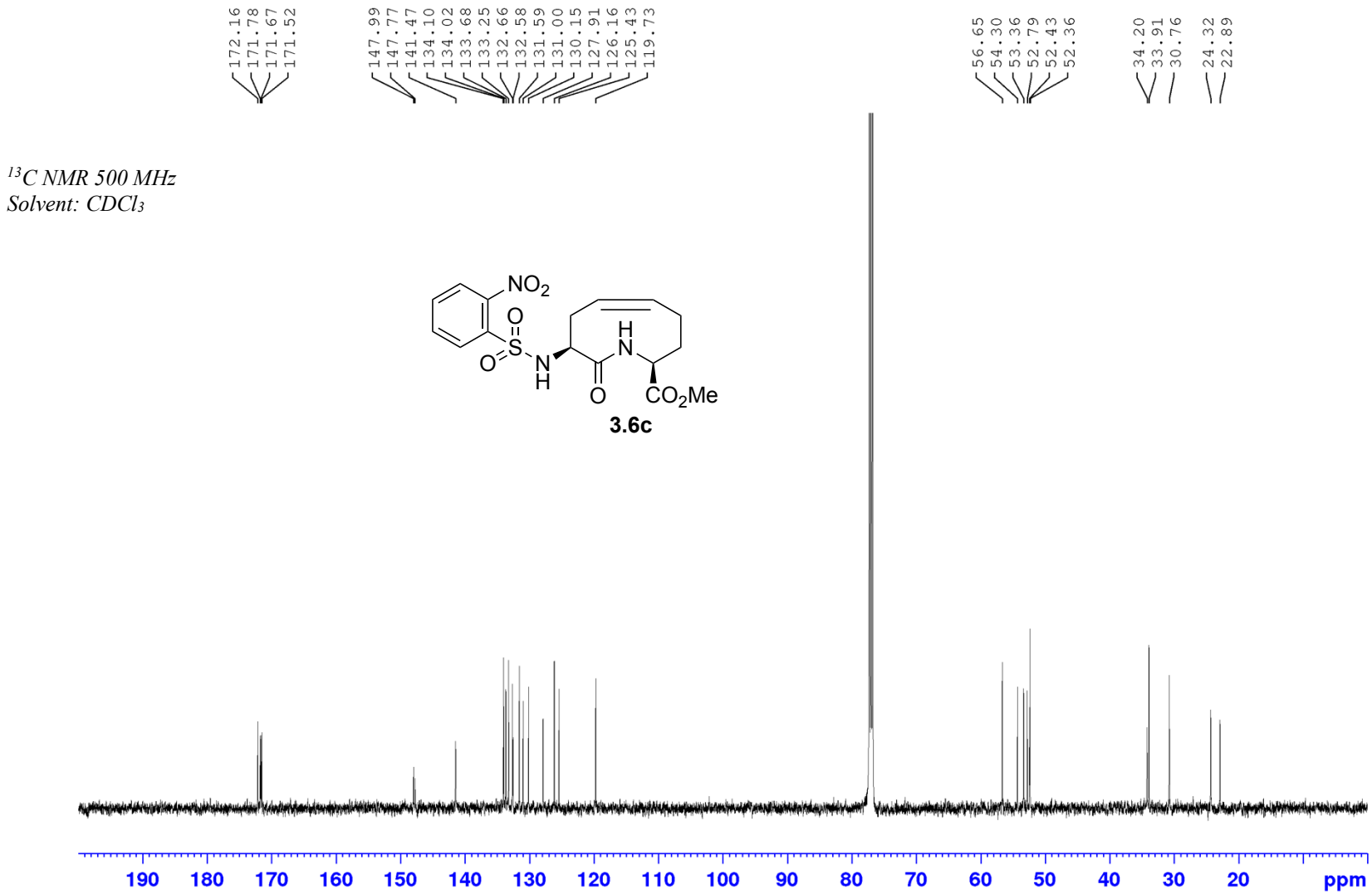

^{13}C NMR 500 MHz
Solvent: $CDCl_3$

3.6c

^{1}H NMR 500 MHz
Solvent: $CDCl_3$

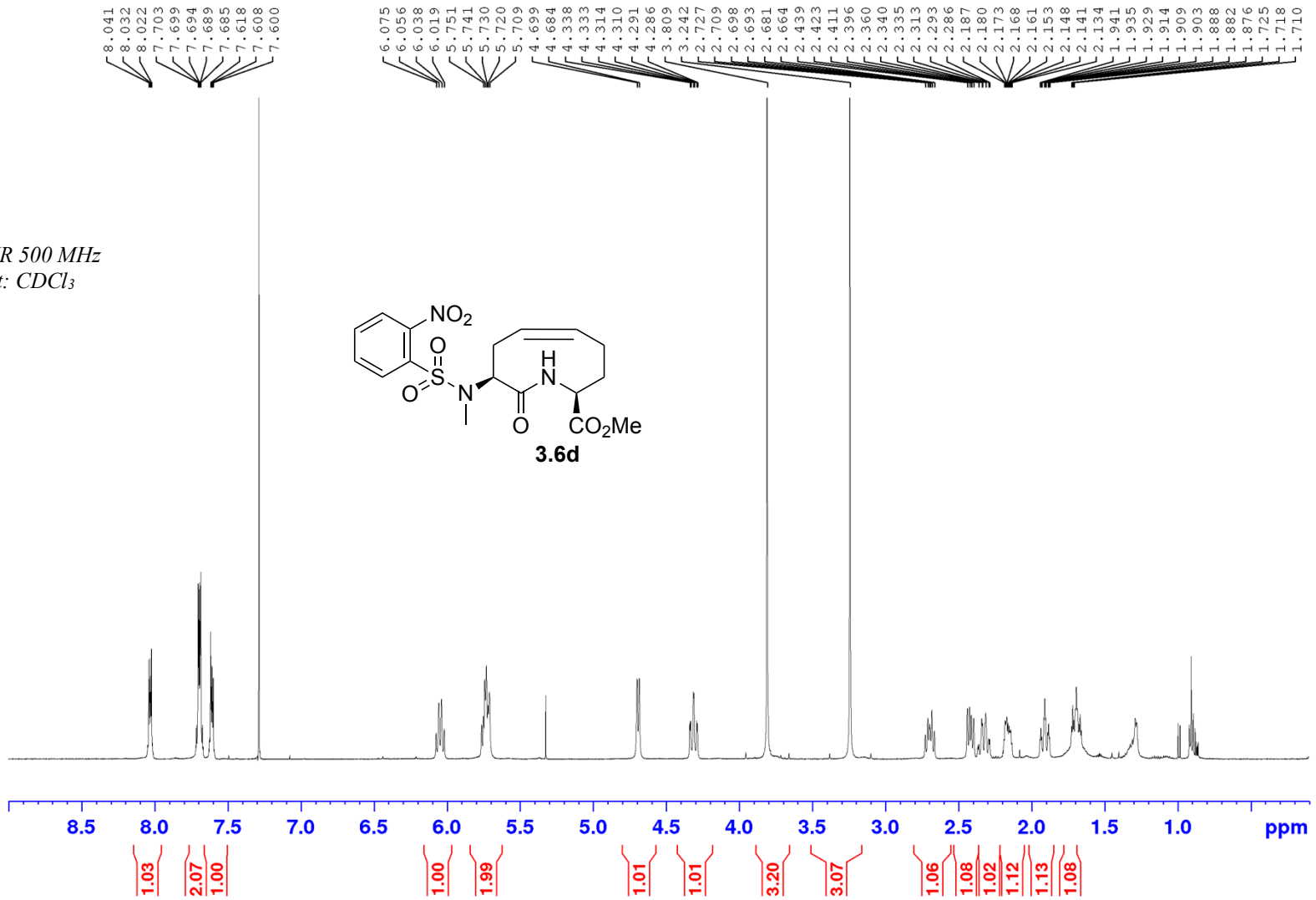

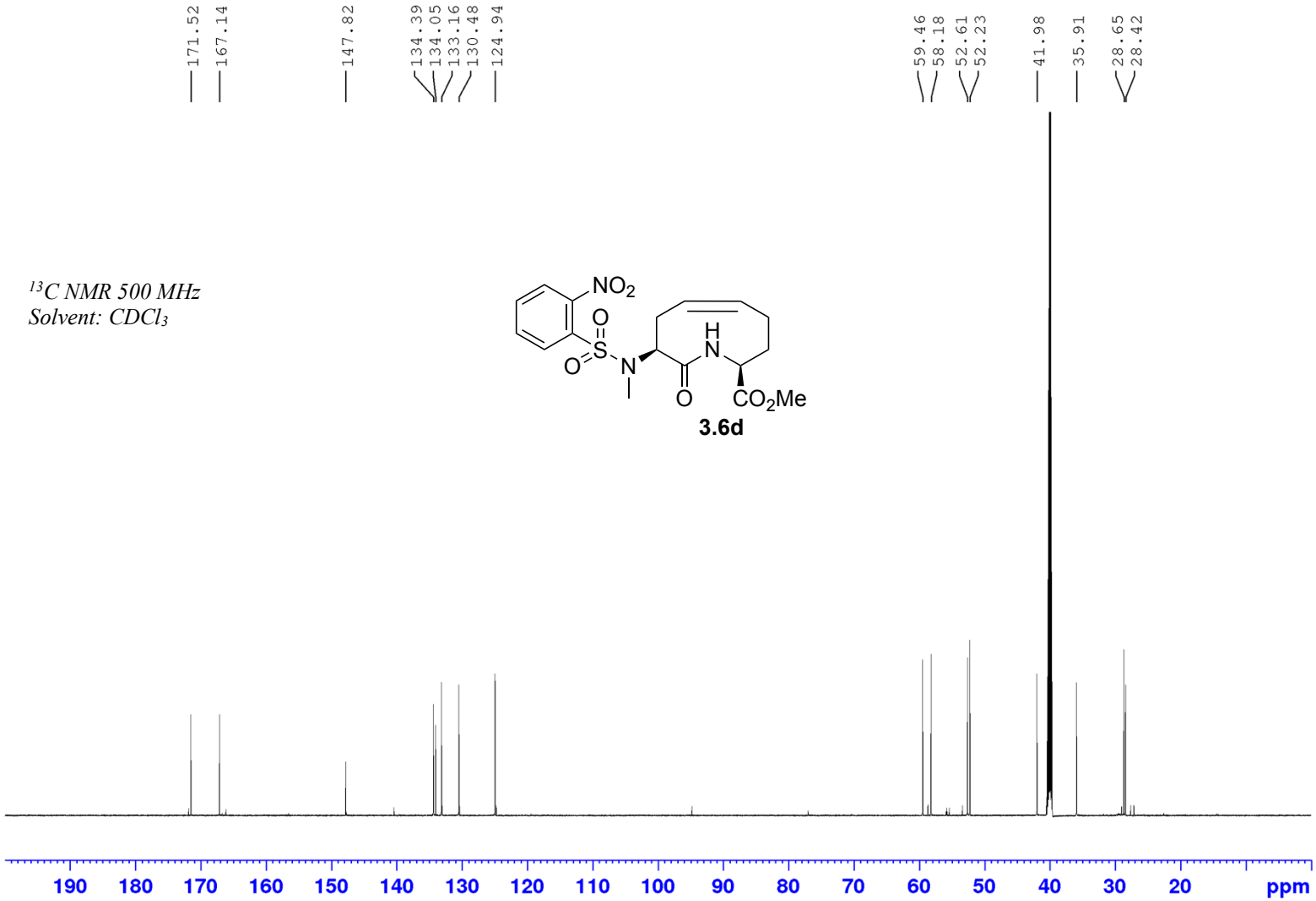
171.52
167.14
147.82
134.39
134.05
133.16
130.48
124.94
59.46
58.18
52.61
52.23
41.98
35.91
28.65
28.42
13C NMR 500 MHz
Solvent: CDCl3
NO2
O
O
S
N
H
N
O
CO2Me
3.6d
190
180
170
160
150
140
130
120
110
100
90
80
70
60
50
40
30
20
ppm

[1]H NMR 500 MHz
Solvent: $CDCl_3$

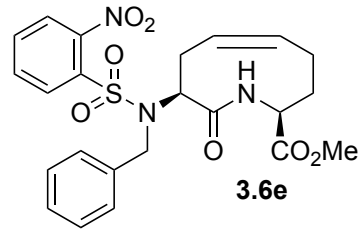

3.6e

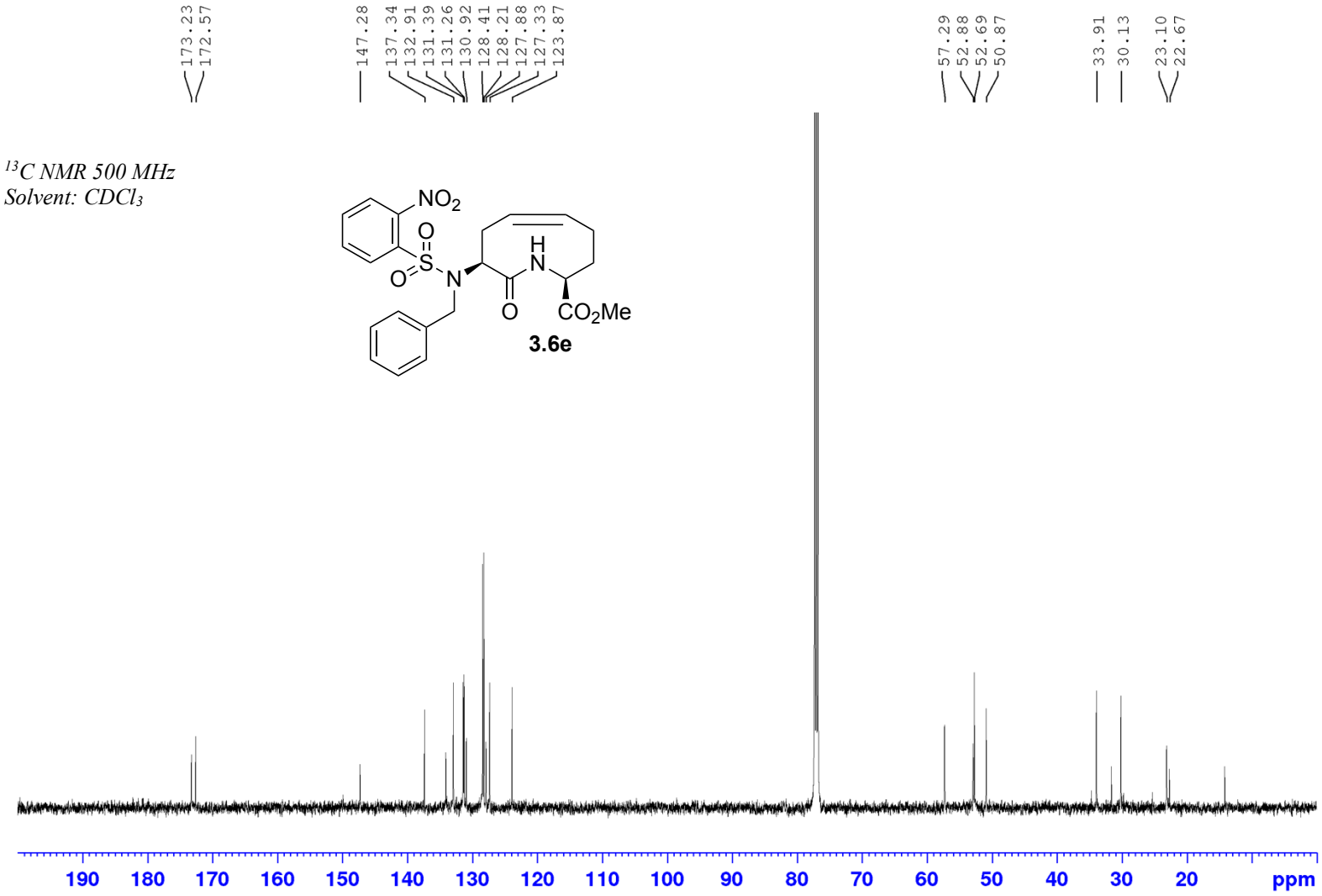
173.23
172.57
147.28
137.34
132.91
131.39
131.26
130.92
128.41
128.21
127.88
127.33
123.87
57.29
52.88
52.69
50.87
33.91
30.13
23.10
22.67
13C NMR 500 MHz
Solvent: CDCl3
NO2
O
S
O
N
H
N
O
CO2Me
3.6e
190
180
170
160
150
140
130
120
110
100
90
80
70
60
50
40
30
20
ppm

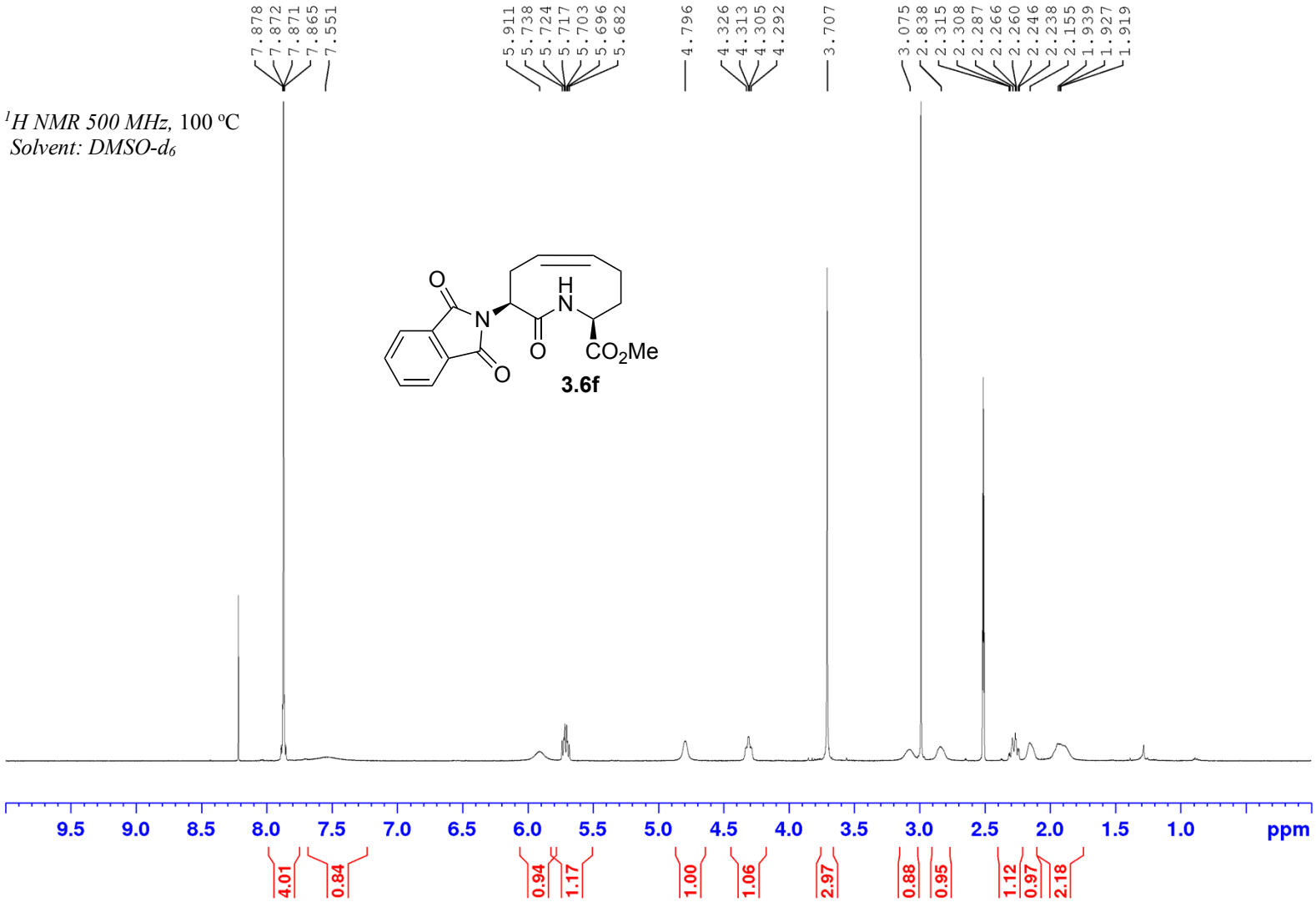
7.878
7.872
7.871
7.865
7.551
5.911
5.738
5.724
5.717
5.703
5.696
5.682
4.796
4.326
4.313
4.305
4.292
3.707
3.075
2.838
2.315
2.308
2.287
2.266
2.260
2.246
2.238
2.155
1.939
1.927
1.919
1H NMR 500 MHz, 100 ºC
Solvent: DMSO-d6
O
N
O
H
N
O
CO2Me
O
3.6f
9.5
9.0
8.5
8.0
7.5
7.0
6.5
6.0
5.5
5.0
4.5
4.0
3.5
3.0
2.5
2.0
1.5
1.0
ppm
4.01
0.84
0.94
1.17
1.00
1.06
2.97
0.88
0.95
1.12
0.97
2.18

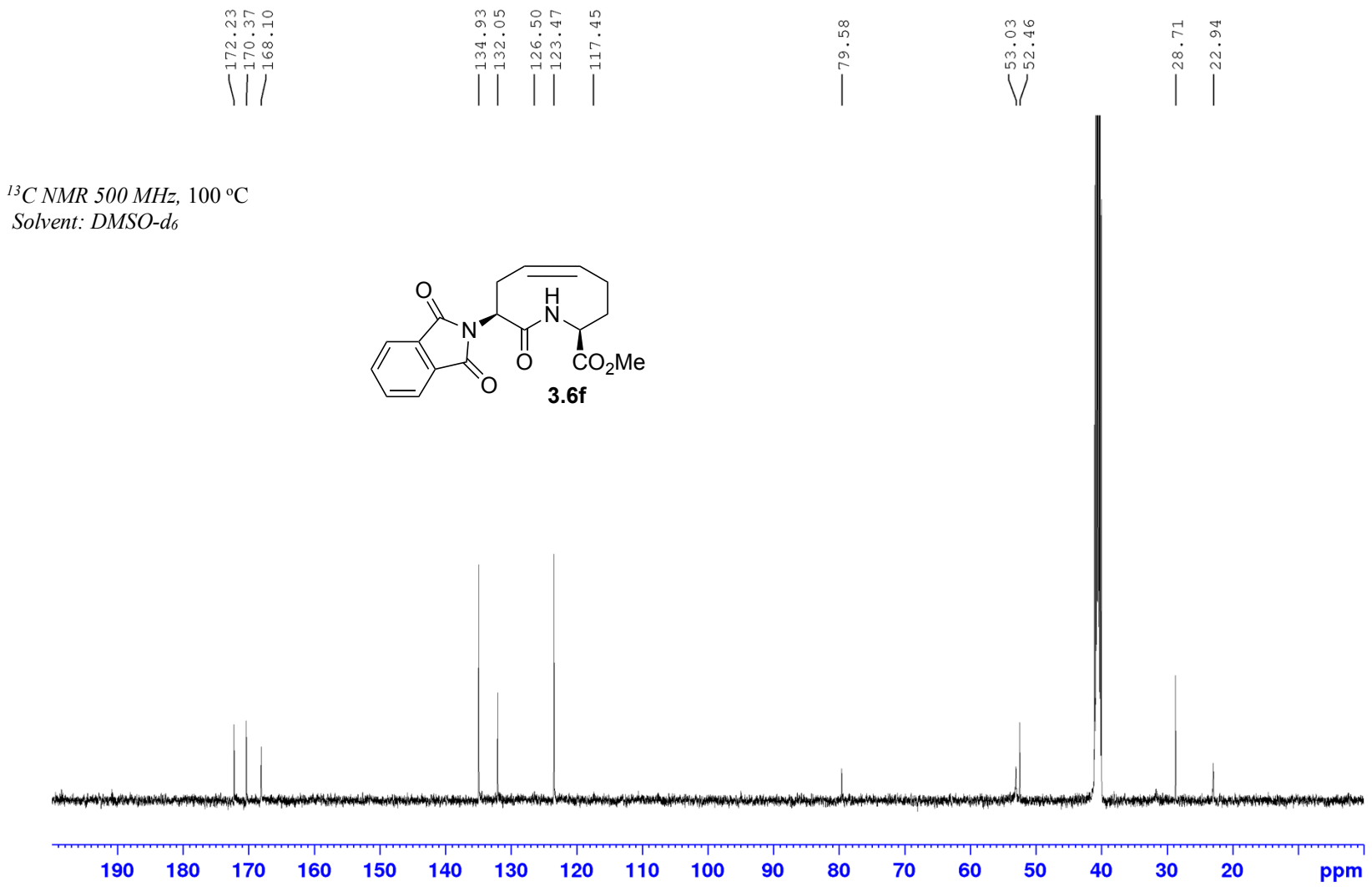
172.23
170.37
168.10
134.93
132.05
126.50
123.47
117.45
79.58
53.03
52.46
28.71
22.94
13C NMR 500 MHz, 100 °C
Solvent: DMSO-d6
O
N
O
O
H
N
O
CO2Me
3.6f
190
180
170
160
150
140
130
120
110
100
90
80
70
60
50
40
30
20
ppm

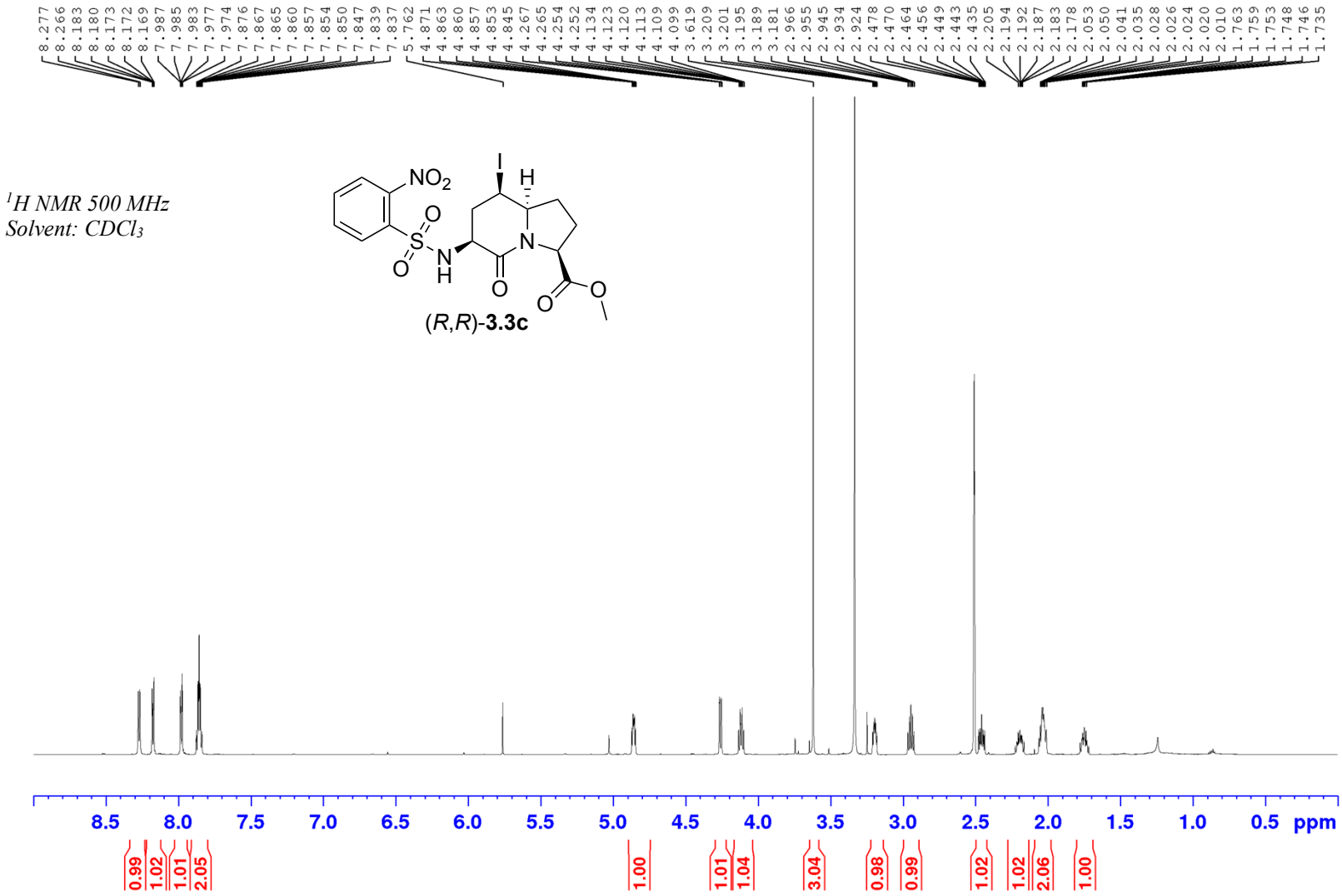

[1]H NMR 500 MHz
Solvent: $CDCl_3$

(*R*,*R*)-**3.3c**

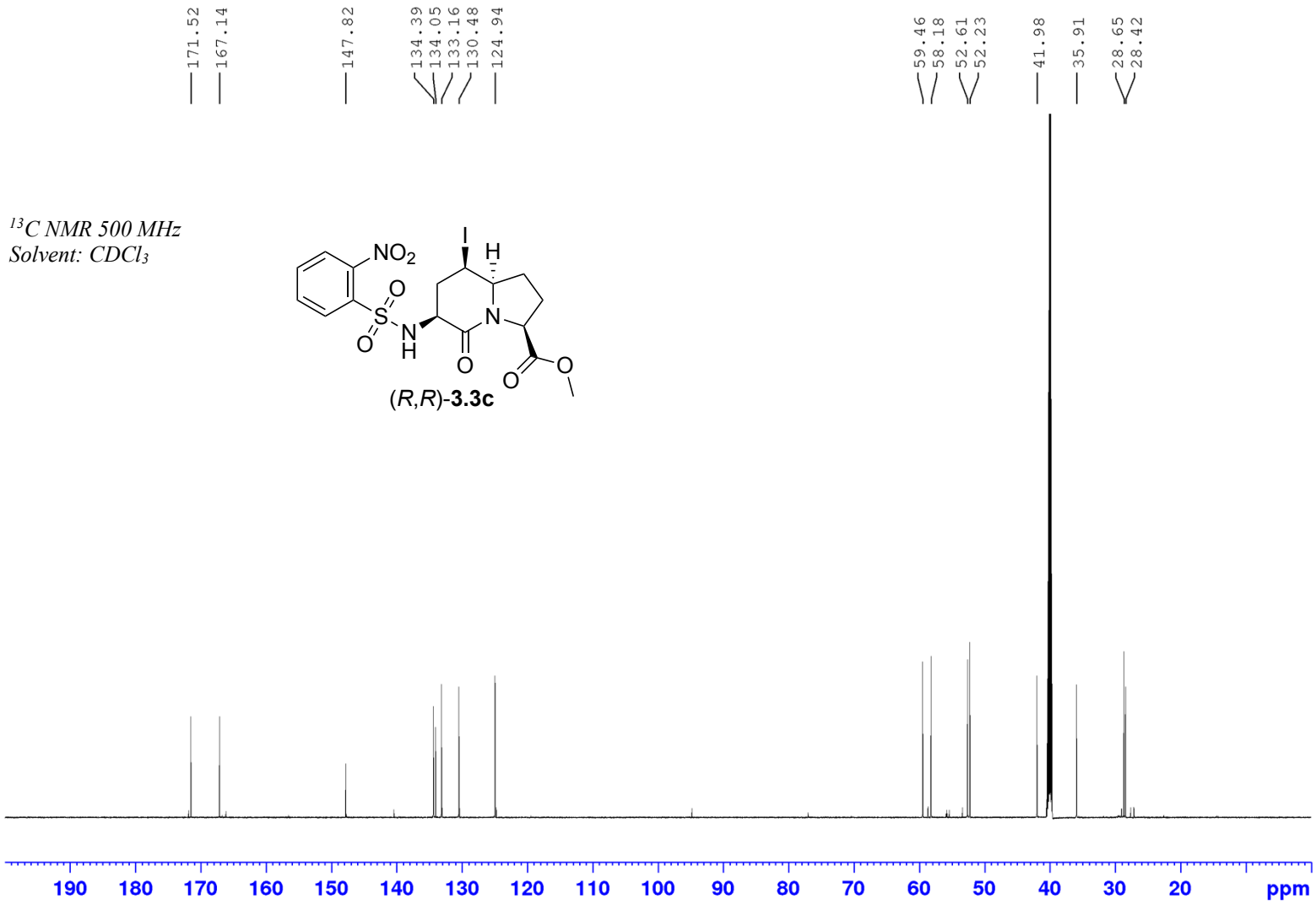
171.52
167.14
147.82
134.39
134.05
133.16
130.48
124.94
59.46
58.18
52.61
52.23
41.98
35.91
28.65
28.42
13C NMR 500 MHz
Solvent: CDCl3
NO2
I
H
O
S
O
N
H
N
O
O
O
O
(R,R)-3.3c
190
180
170
160
150
140
130
120
110
100
90
80
70
60
50
40
30
20
ppm

COSY 500 MHz
Solvent: $CDCl_3$

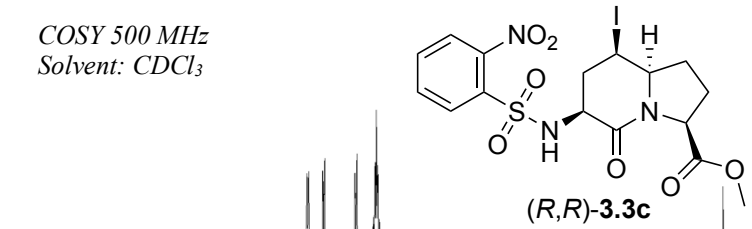

(*R*,*R*)-**3.3c**

HSQC 500 MHz
Solvent: $CDCl_3$

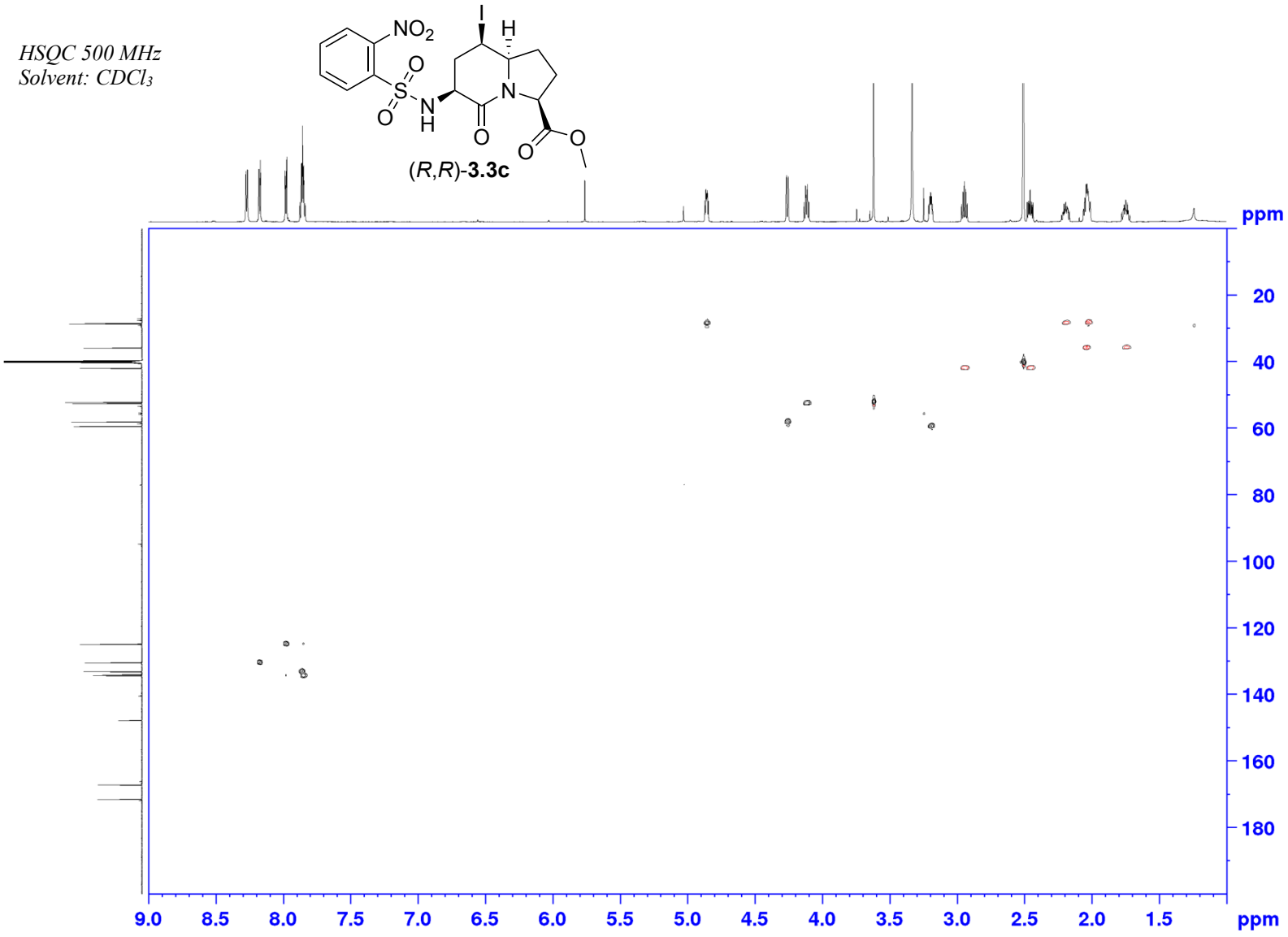

NOESY 500 MHz
Solvent: $CDCl_3$

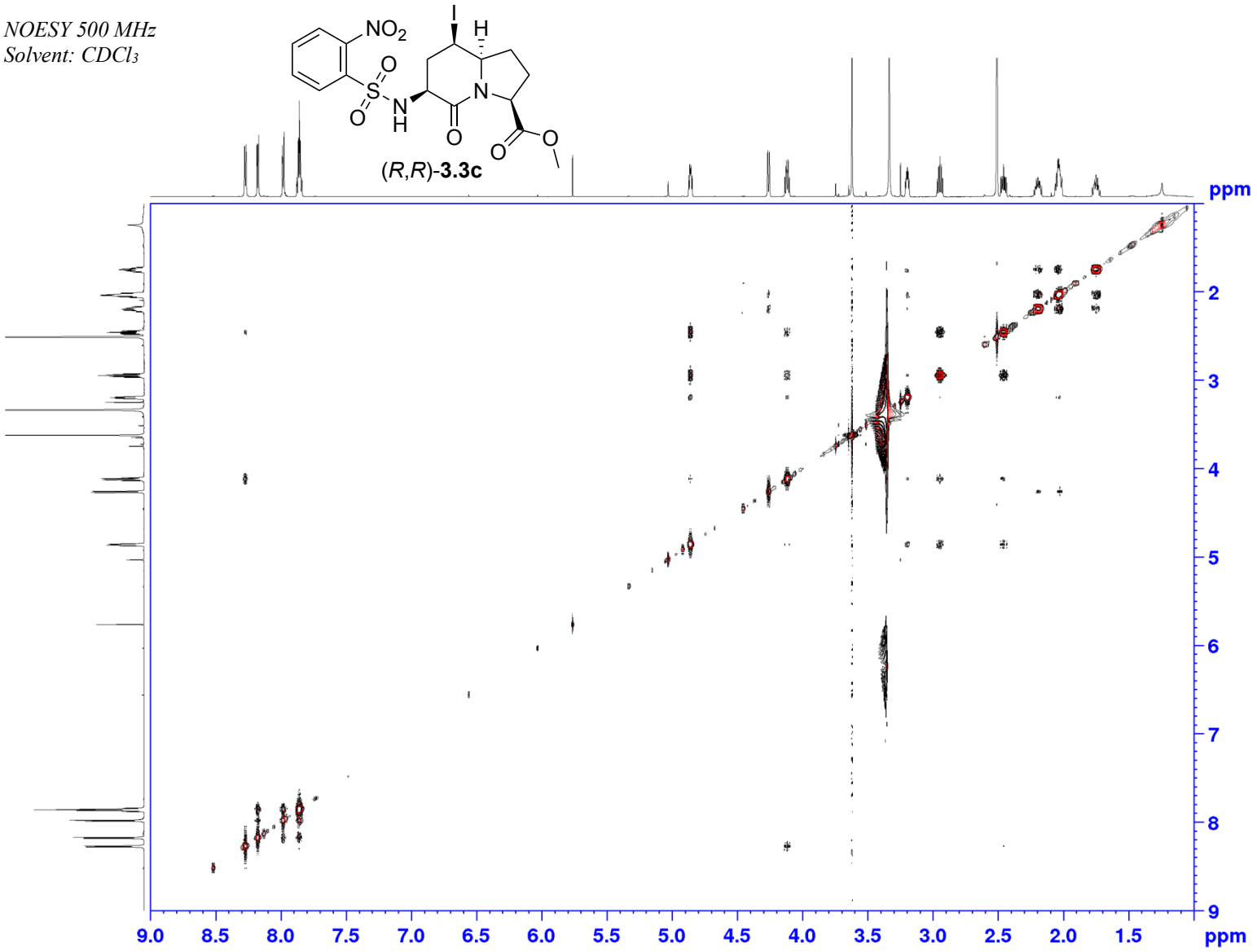

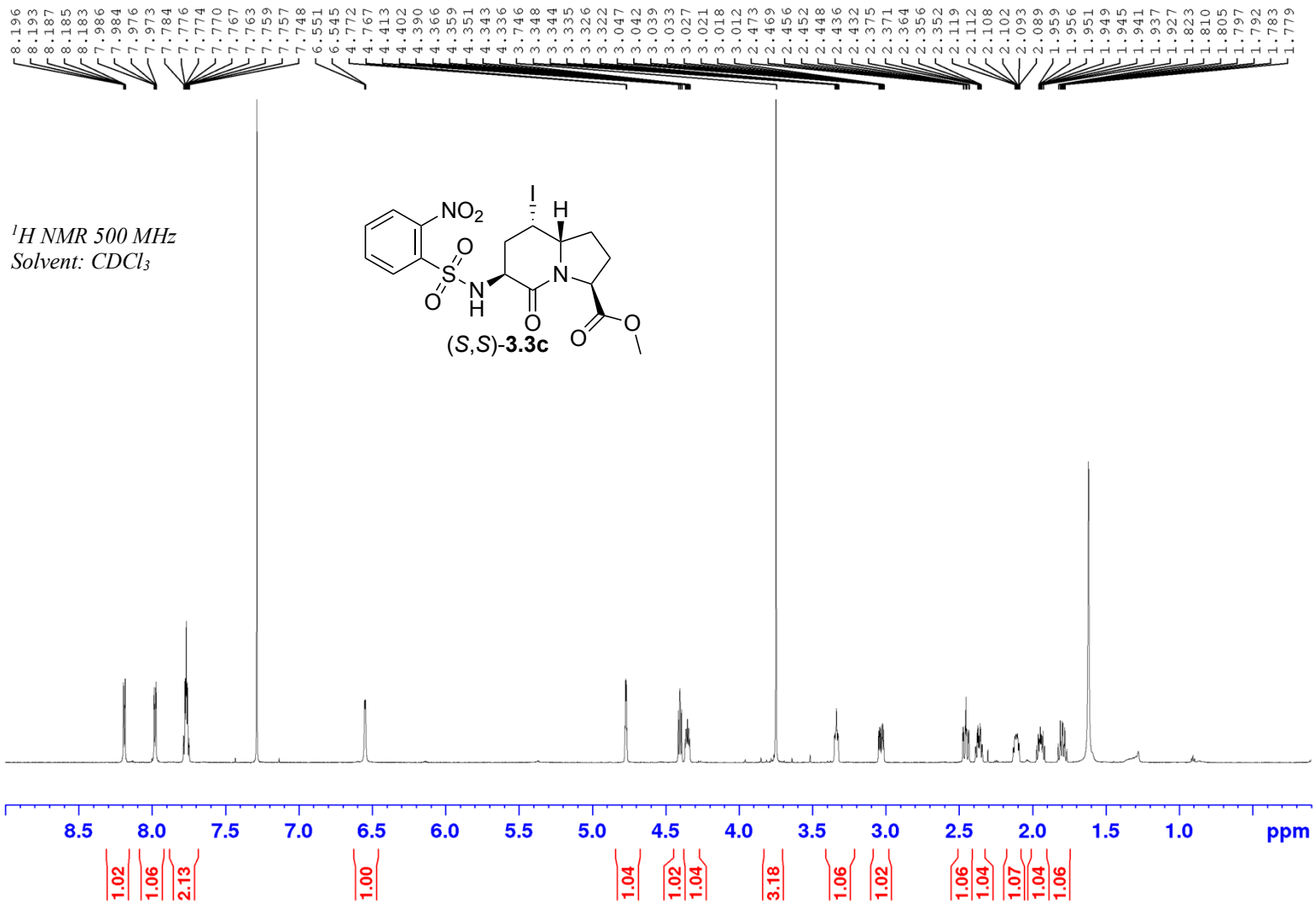
8.196
8.193
8.187
8.185
8.183
7.986
7.984
7.976
7.973
7.784
7.776
7.774
7.770
7.767
7.763
7.759
7.757
7.748
6.551
6.545
4.772
4.767
4.413
4.402
4.390
4.366
4.359
4.351
4.343
4.336
3.746
3.348
3.344
3.335
3.326
3.322
3.047
3.042
3.039
3.033
3.027
3.021
3.018
3.012
2.473
2.469
2.456
2.452
2.448
2.436
2.432
2.375
2.371
2.364
2.356
2.352
2.119
2.112
2.108
2.102
2.093
2.089
1.959
1.956
1.951
1.949
1.945
1.941
1.937
1.927
1.823
1.810
1.805
1.797
1.792
1.783
1.779
1H NMR 500 MHz
Solvent: CDCl3
NO2
O
S
O
N
H
I
H
N
O
O
O
(S,S)-3.3c
8.5
8.0
7.5
7.0
6.5
6.0
5.5
5.0
4.5
4.0
3.5
3.0
2.5
2.0
1.5
1.0
ppm
1.02
1.06
2.13
1.00
1.04
1.02
1.04
3.18
1.06
1.02
1.06
1.04
1.07
1.04
1.06

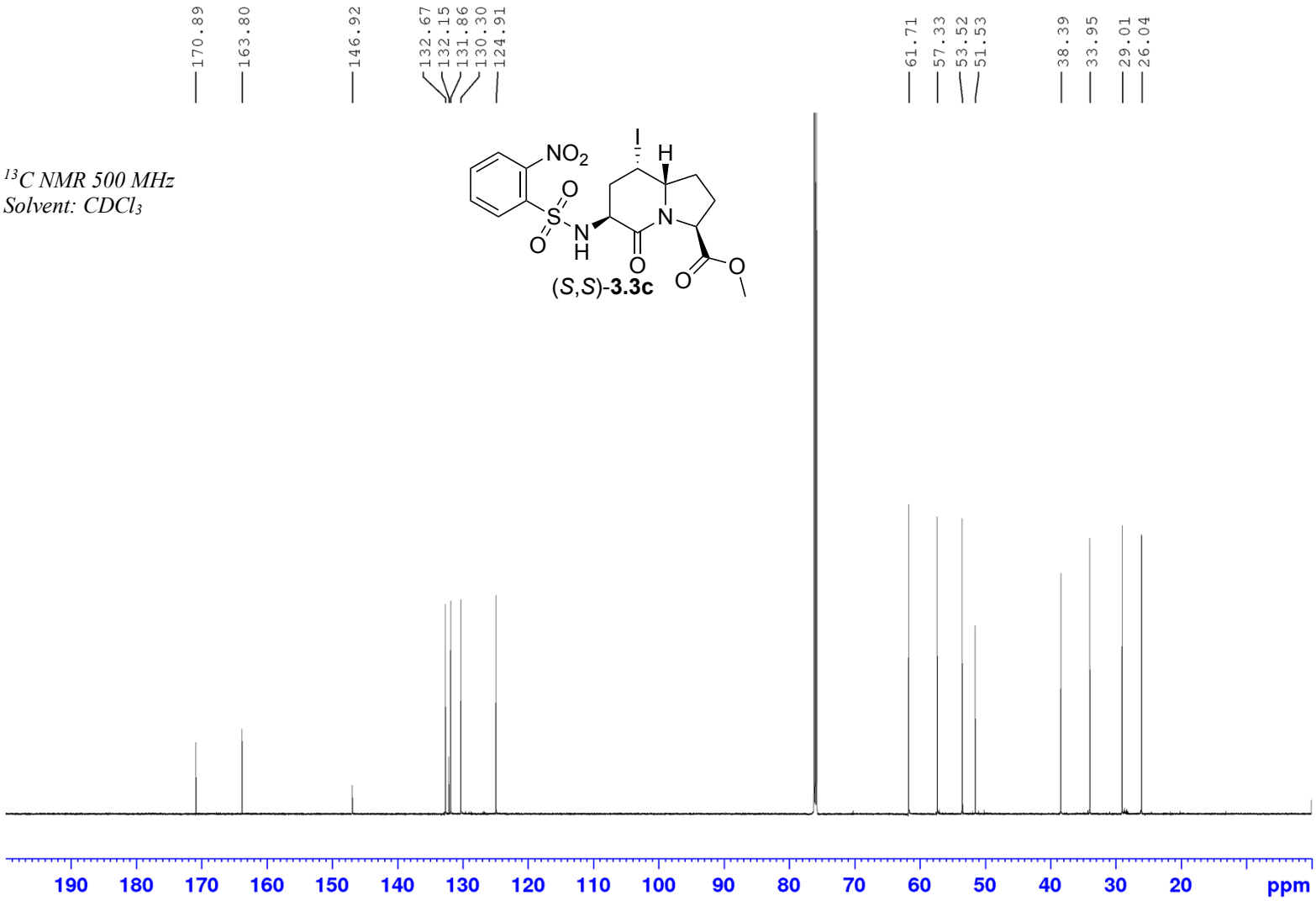
170.89
163.80
146.92
132.67
132.15
131.86
130.30
124.91
61.71
57.33
53.52
51.53
38.39
33.95
29.01
26.04
^{13}C NMR 500 MHz
Solvent: $CDCl_3$
NO_2
I
H
O
S
O
N
H
N
O
O
O
(S,S)-3.3c
190
180
170
160
150
140
130
120
110
100
90
80
70
60
50
40
30
20
ppm

COSY NMR 500 MHz
Solvent: $CDCl_3$

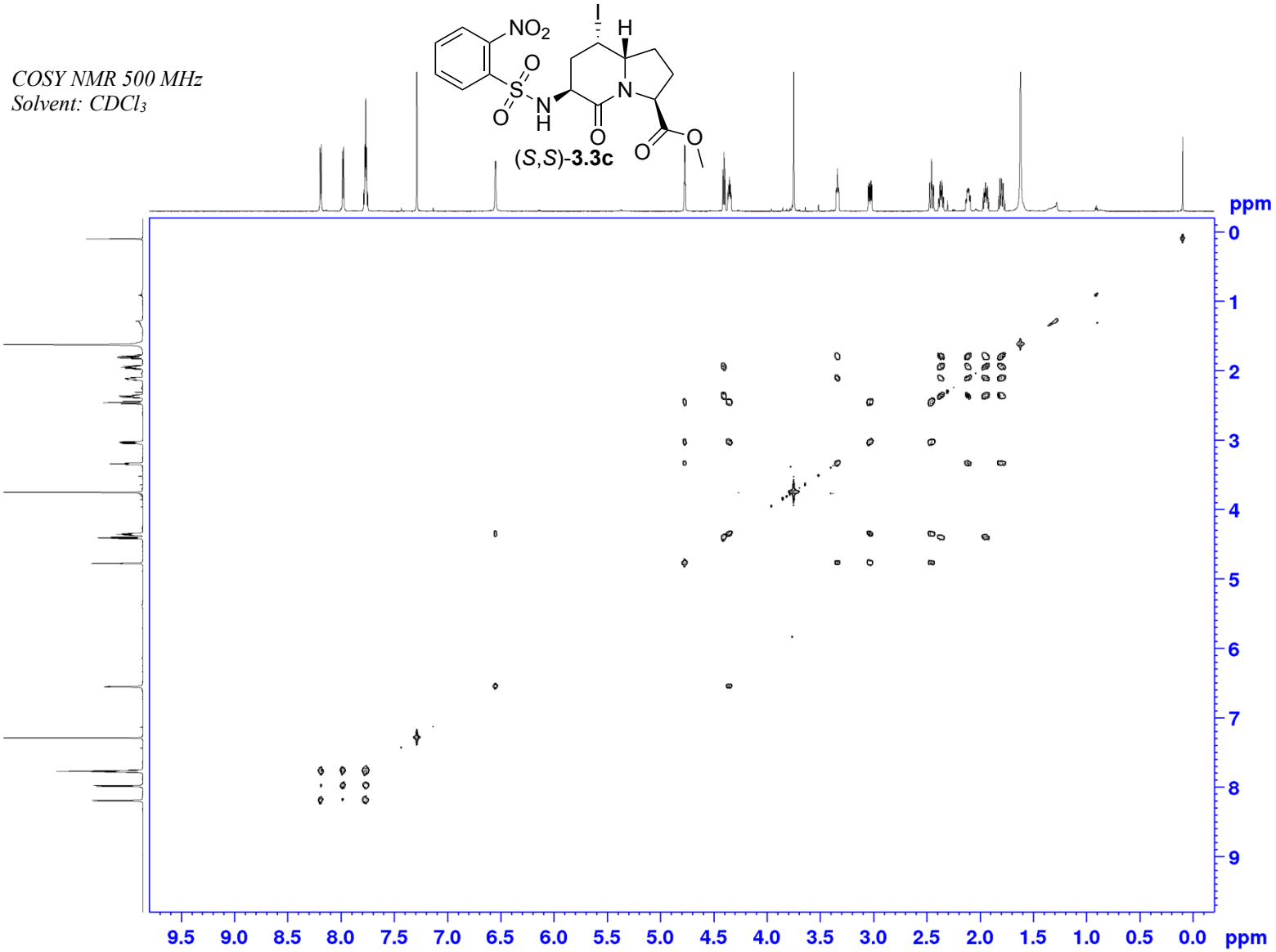

HSQC NMR 500 MHz
Solvent: $CDCl_3$

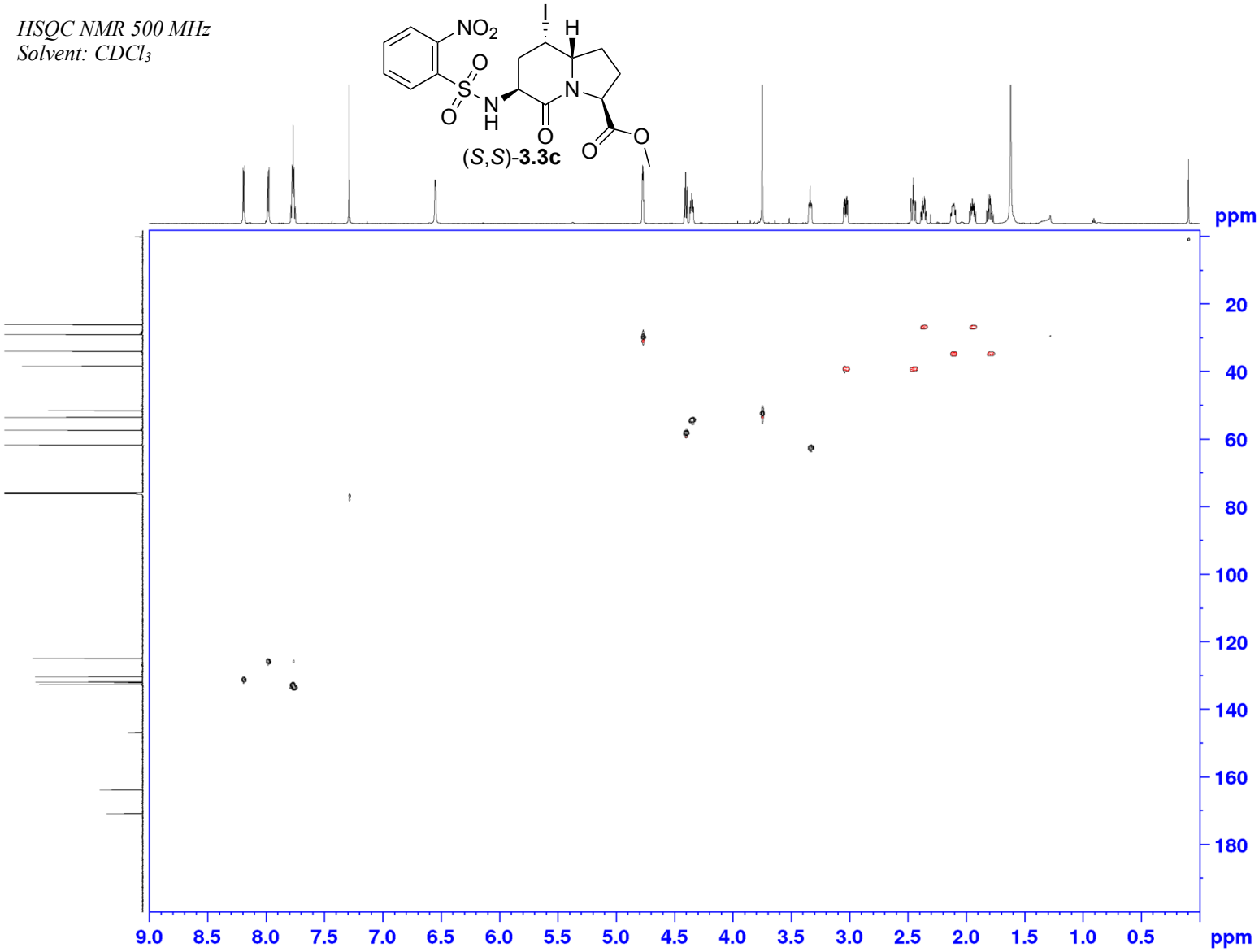

NOESY NMR 500 MHz
Solvent: $CDCl_3$

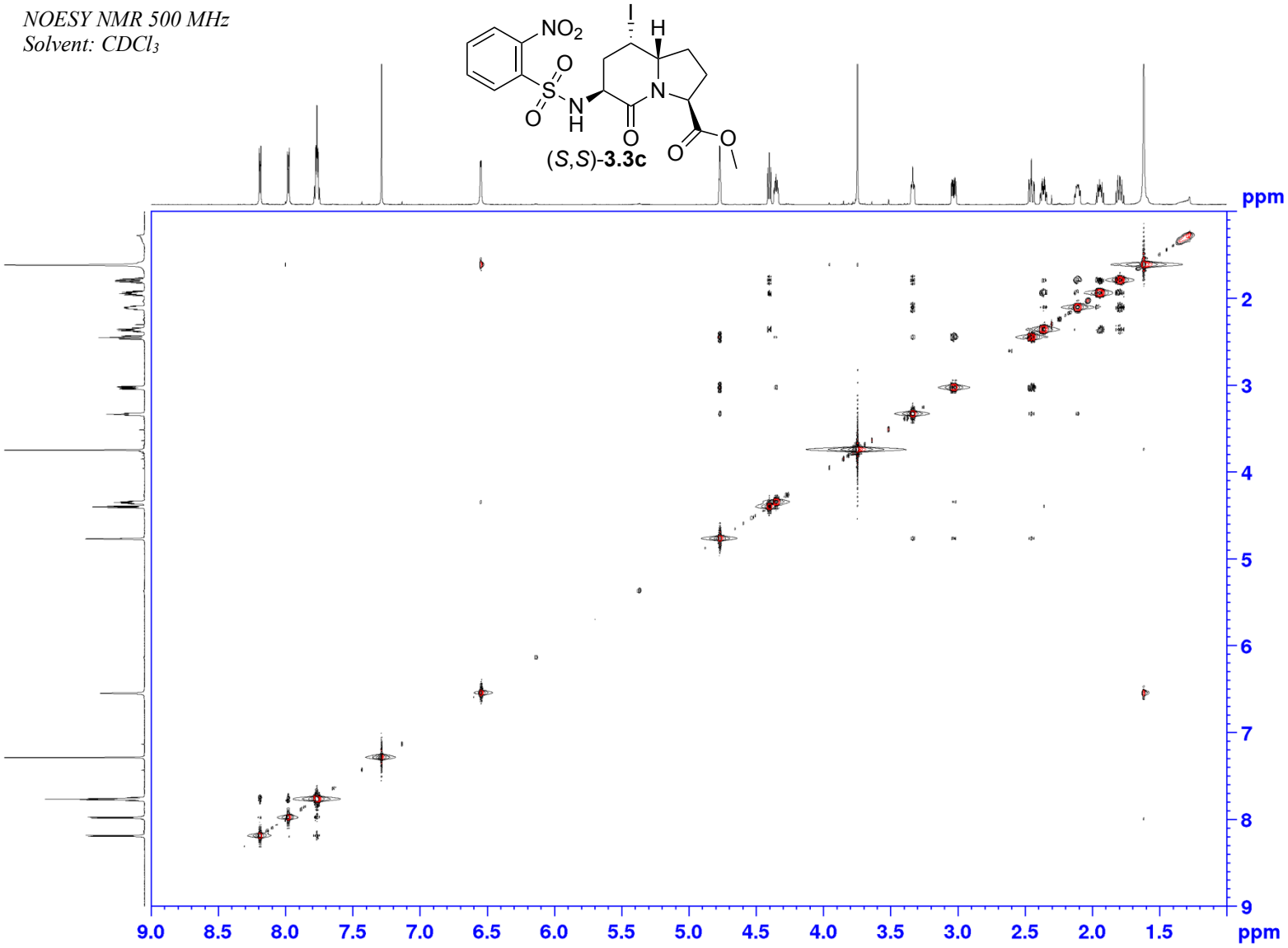

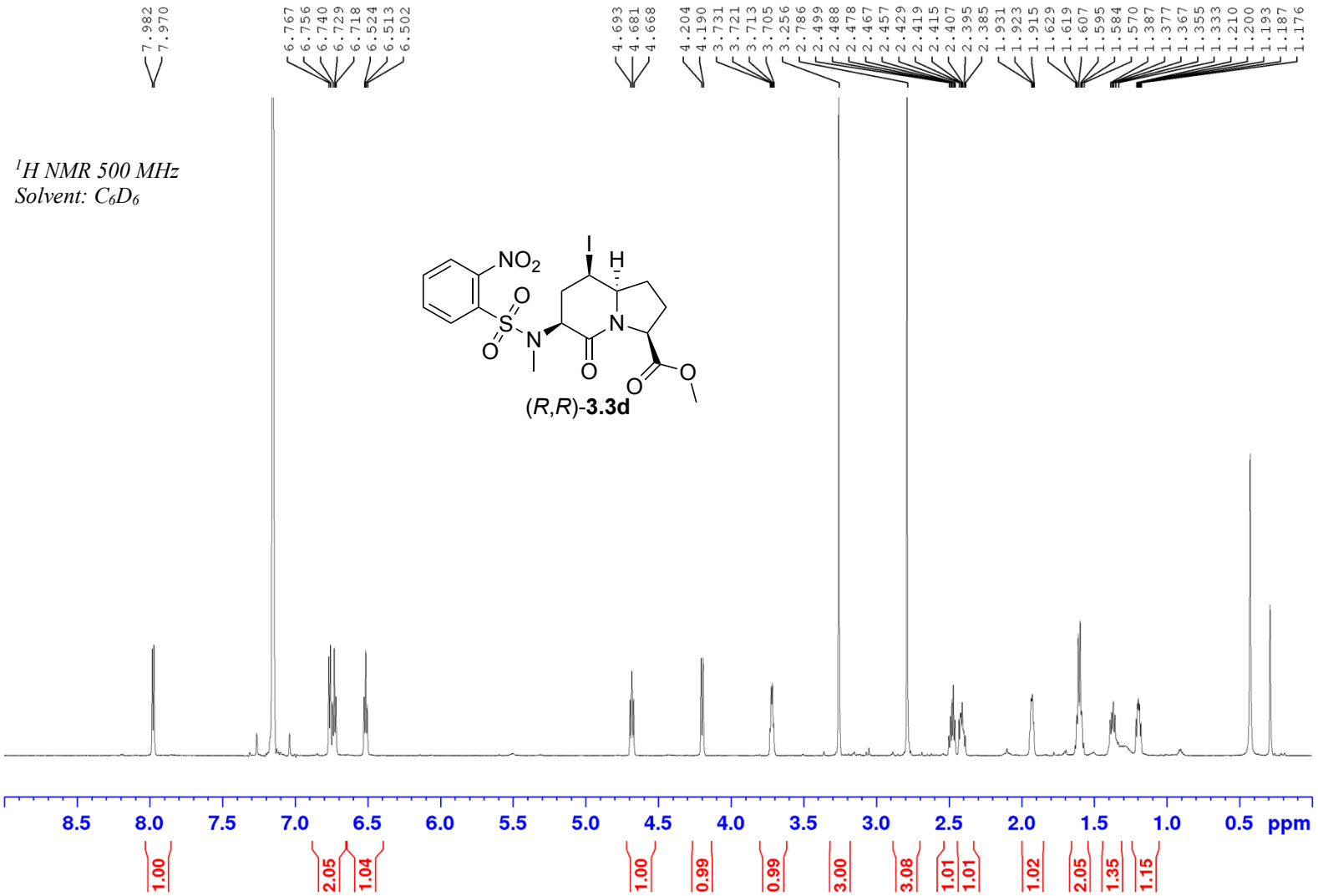
7.982
7.970
6.767
6.756
6.740
6.729
6.718
6.524
6.513
6.502
4.693
4.681
4.668
4.204
4.190
3.731
3.721
3.713
3.705
3.256
2.786
2.499
2.488
2.478
2.467
2.457
2.429
2.419
2.415
2.407
2.395
2.385
1.931
1.923
1.915
1.629
1.619
1.607
1.595
1.584
1.570
1.387
1.377
1.367
1.355
1.333
1.210
1.200
1.193
1.187
1.176
1H NMR 500 MHz
Solvent: C6D6
NO2
I
H
O
S
O
N
N
O
O
O
O
(R,R)-3.3d
8.5
8.0
7.5
7.0
6.5
6.0
5.5
5.0
4.5
4.0
3.5
3.0
2.5
2.0
1.5
1.0
0.5
ppm
1.00
2.05
1.04
1.00
0.99
0.99
3.00
3.08
1.01
1.01
1.02
2.05
1.35
1.15

^{13}C NMR 500 MHz
Solvent: C_6D_6

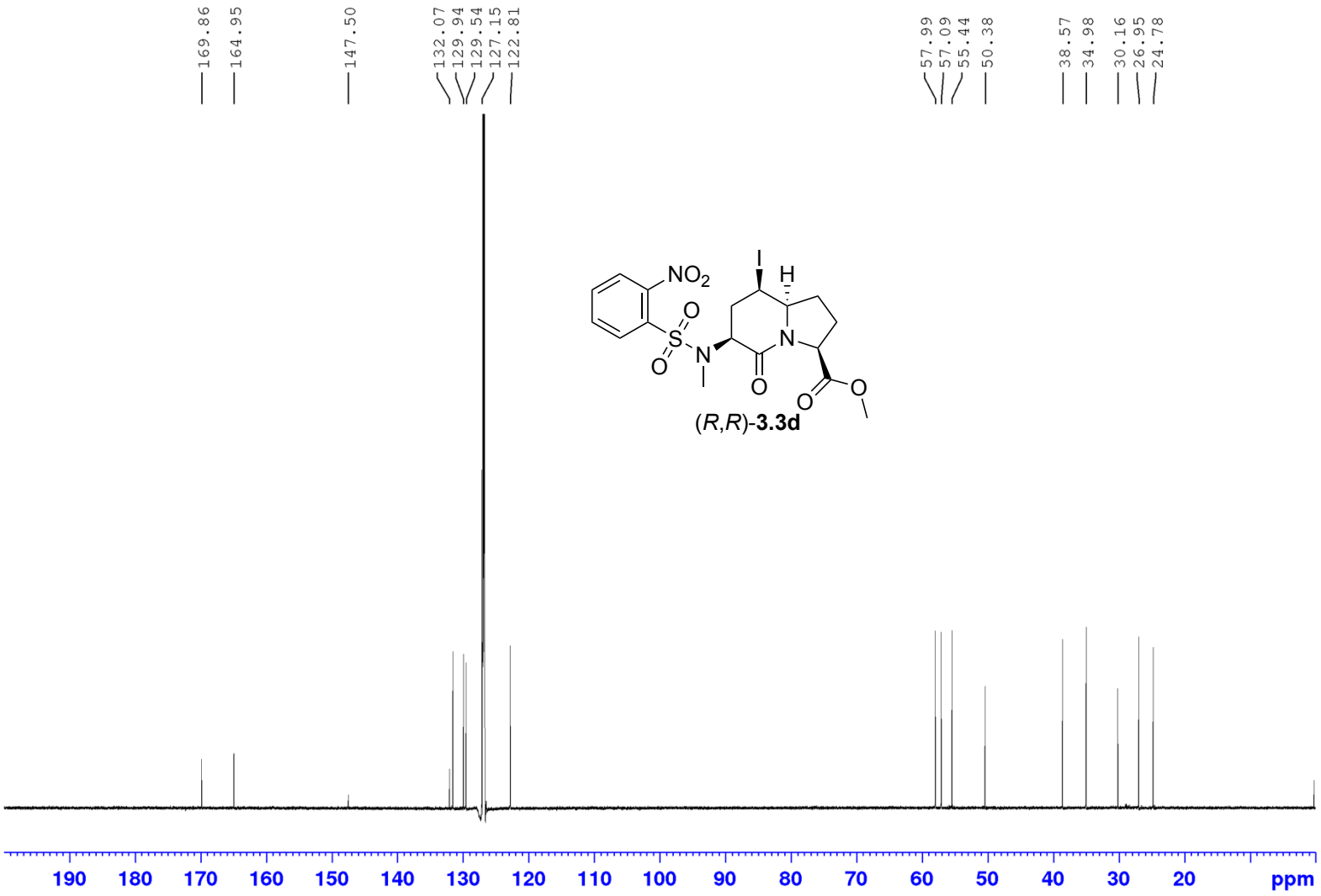

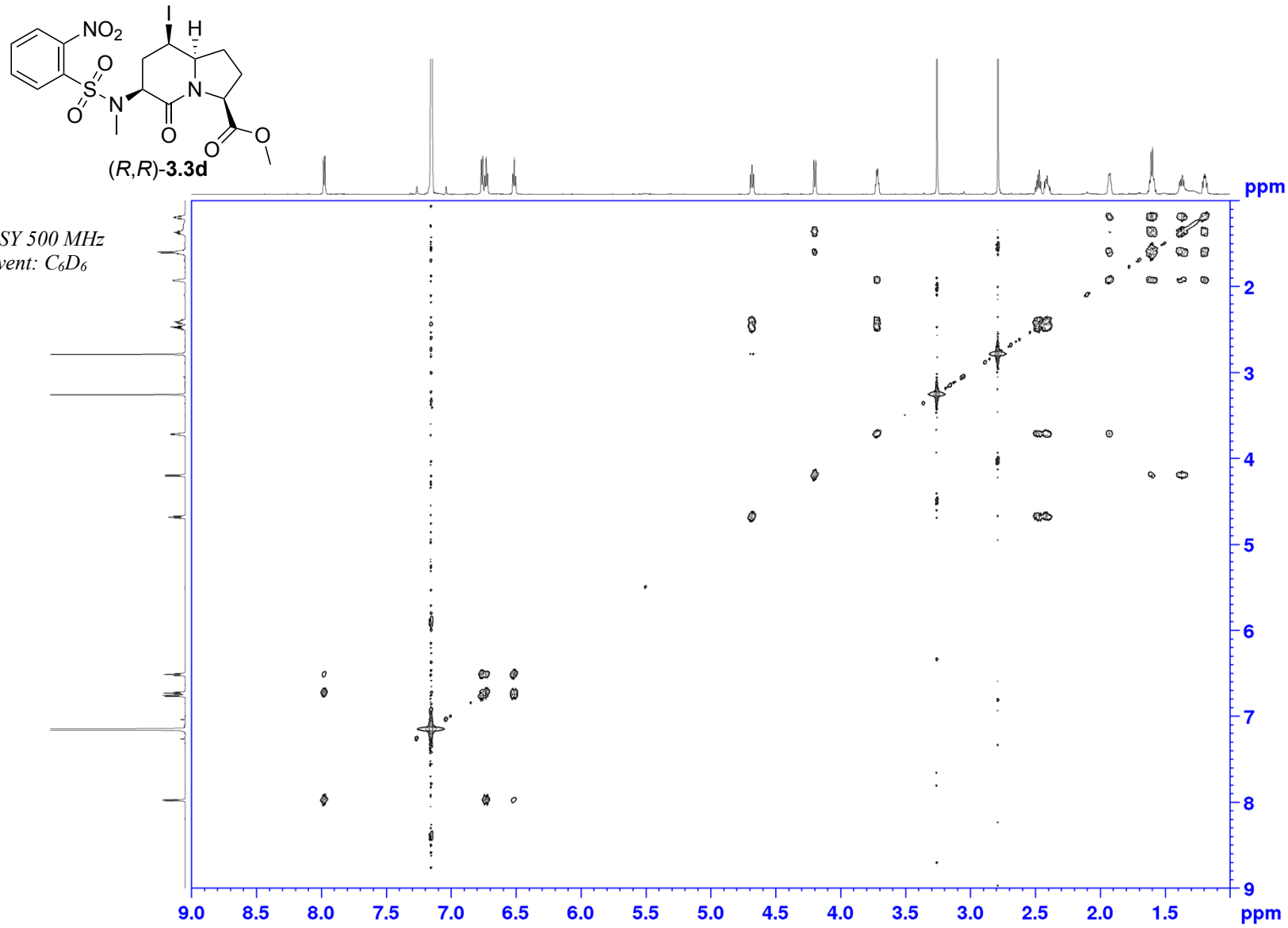
NO2
I
H
O
S
O
N
O
N
O
O
O
(R,R)-3.3d
COSY 500 MHz
Solvent: C6D6
ppm
2
3
4
5
6
7
8
9
9.0
8.5
8.0
7.5
7.0
6.5
6.0
5.5
5.0
4.5
4.0
3.5
3.0
2.5
2.0
1.5
ppm

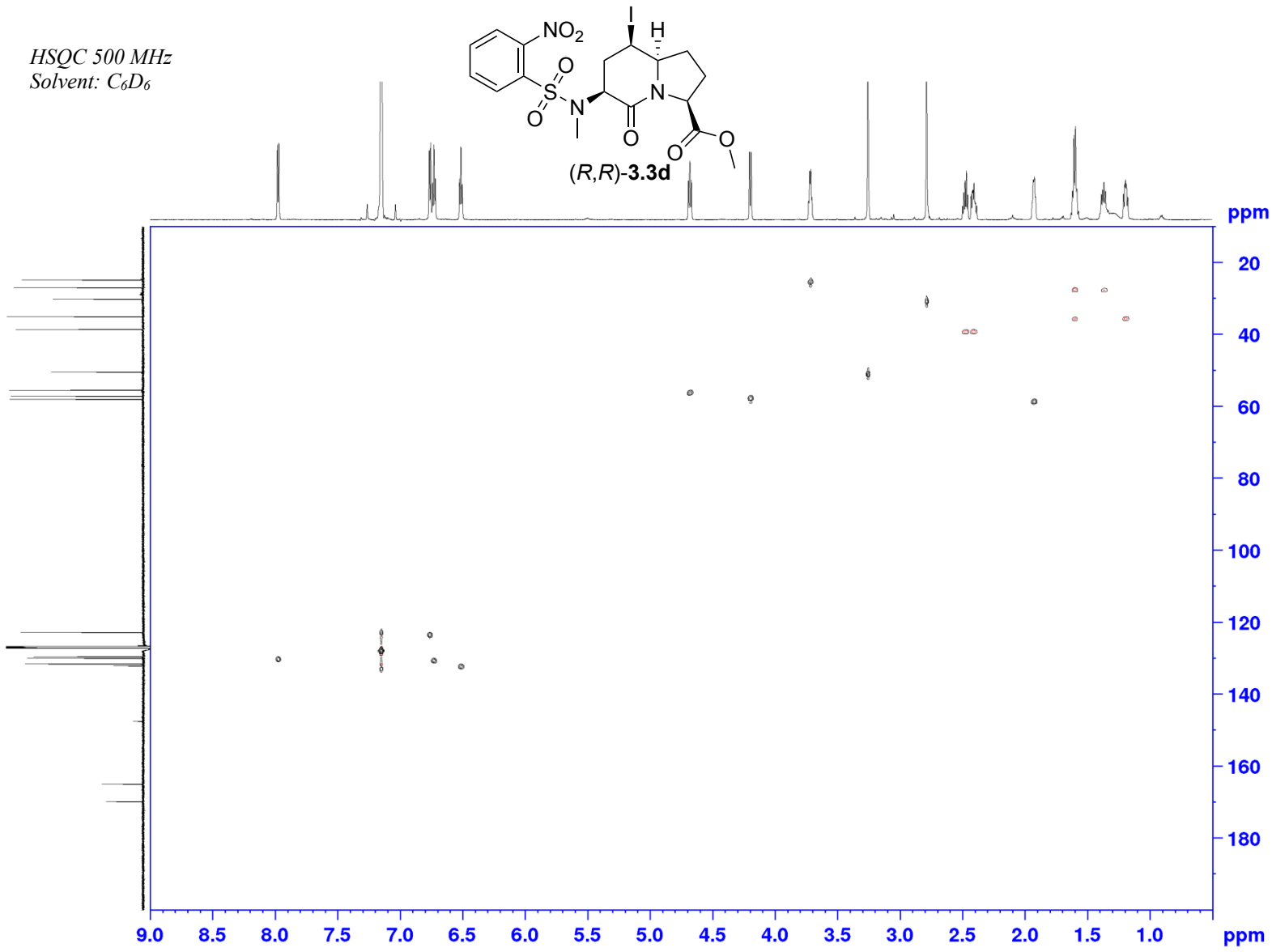
HSQC 500 MHz
Solvent: C6D6
NO2
O
S
O
N
H
N
O
O
O
(R,R)-3.3d
ppm
20
40
60
80
100
120
140
160
180
9.0
8.5
8.0
7.5
7.0
6.5
6.0
5.5
5.0
4.5
4.0
3.5
3.0
2.5
2.0
1.5
1.0
ppm

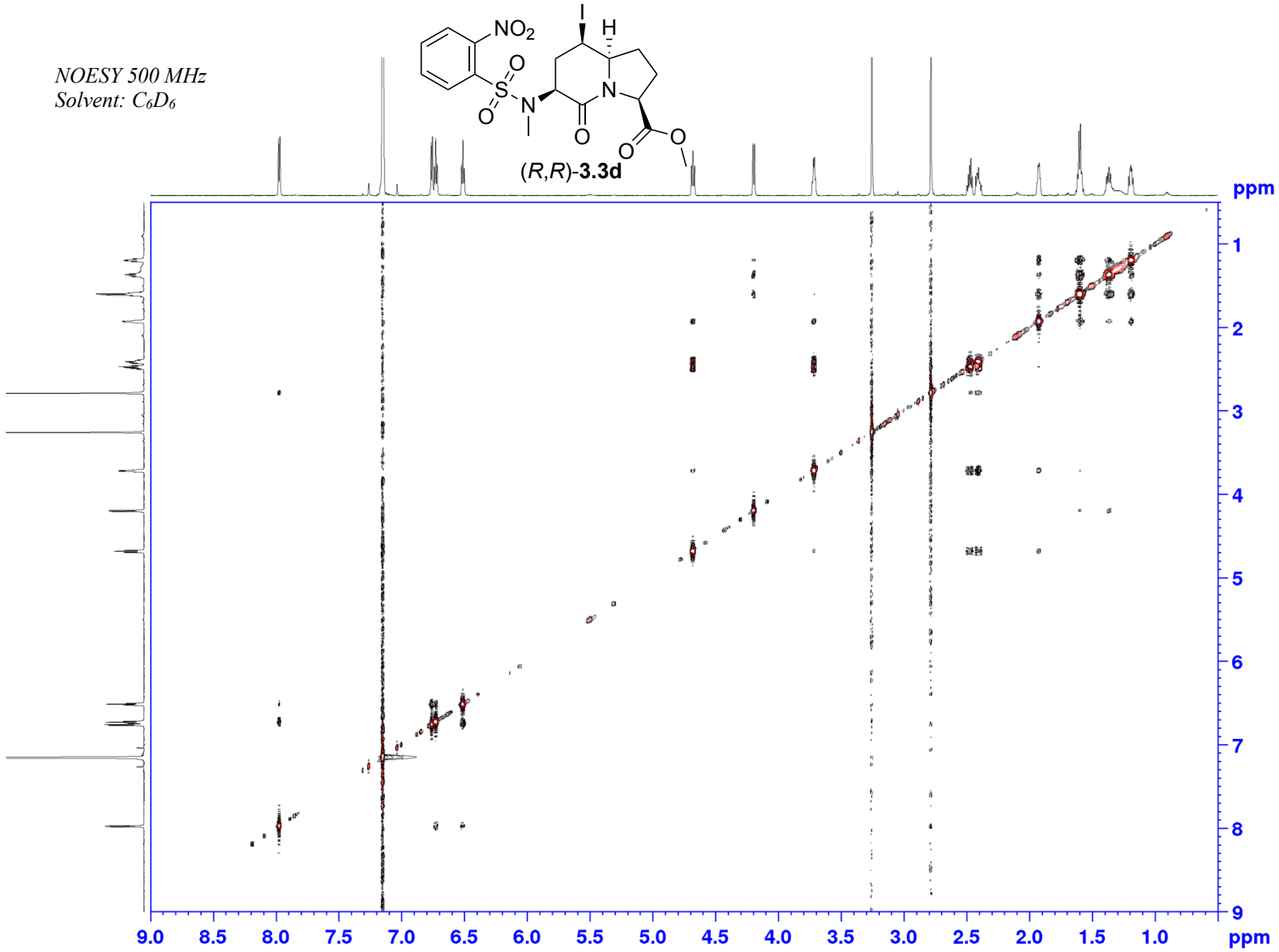
NOESY 500 MHz
Solvent: C6D6
NO2
O
S
O
N
I
H
N
O
O
O
(R,R)-3.3d
ppm
1
2
3
4
5
6
7
8
9
9.0
8.5
8.0
7.5
7.0
6.5
6.0
5.5
5.0
4.5
4.0
3.5
3.0
2.5
2.0
1.5
1.0
ppm

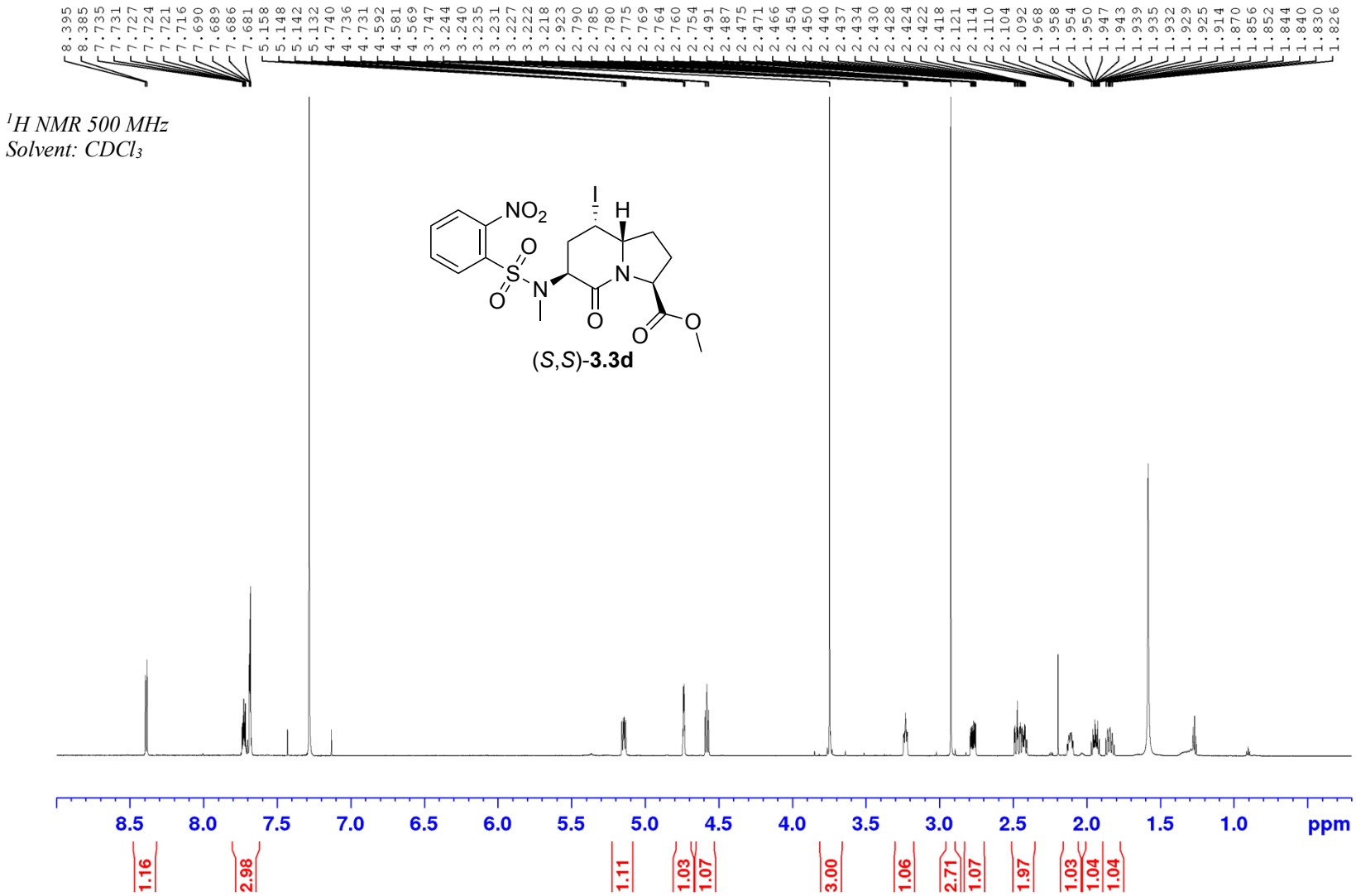
8.395
8.385
7.735
7.731
7.727
7.724
7.721
7.716
7.690
7.689
7.686
7.681
5.158
5.148
5.142
5.132
4.740
4.736
4.731
4.592
4.581
4.569
3.747
3.244
3.240
3.235
3.231
3.227
3.222
3.218
2.923
2.790
2.785
2.780
2.775
2.769
2.764
2.760
2.754
2.491
2.487
2.475
2.471
2.466
2.454
2.450
2.440
2.437
2.434
2.430
2.428
2.424
2.422
2.418
2.121
2.114
2.110
2.104
2.092
1.968
1.958
1.954
1.950
1.947
1.943
1.939
1.935
1.932
1.929
1.925
1.914
1.870
1.856
1.852
1.844
1.840
1.830
1.826
1H NMR 500 MHz
Solvent: CDCl3
NO2
I
H
S
O
O
N
N
O
O
O
O
(S,S)-3.3d
8.5
8.0
7.5
7.0
6.5
6.0
5.5
5.0
4.5
4.0
3.5
3.0
2.5
2.0
1.5
1.0
ppm
1.16
2.98
1.11
1.03
1.07
3.00
1.06
2.71
1.07
1.97
1.03
1.04
1.04

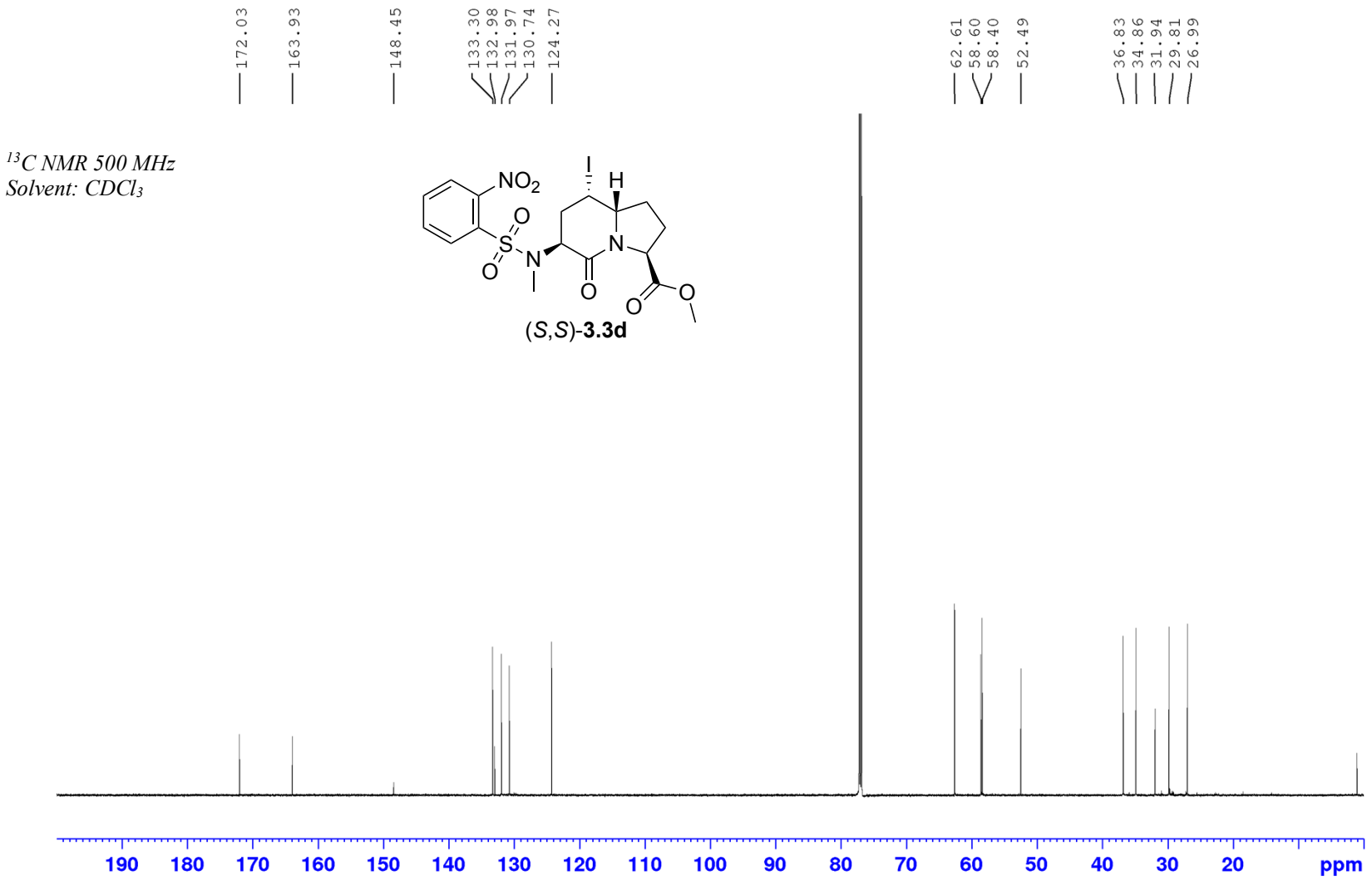
172.03
163.93
148.45
133.30
132.98
131.97
130.74
124.27
62.61
58.60
58.40
52.49
36.83
34.86
31.94
29.81
26.99
13C NMR 500 MHz
Solvent: CDCl3
NO2
I
H
O
S
N
O
N
O
O
O
(S,S)-3.3d
190
180
170
160
150
140
130
120
110
100
90
80
70
60
50
40
30
20
ppm

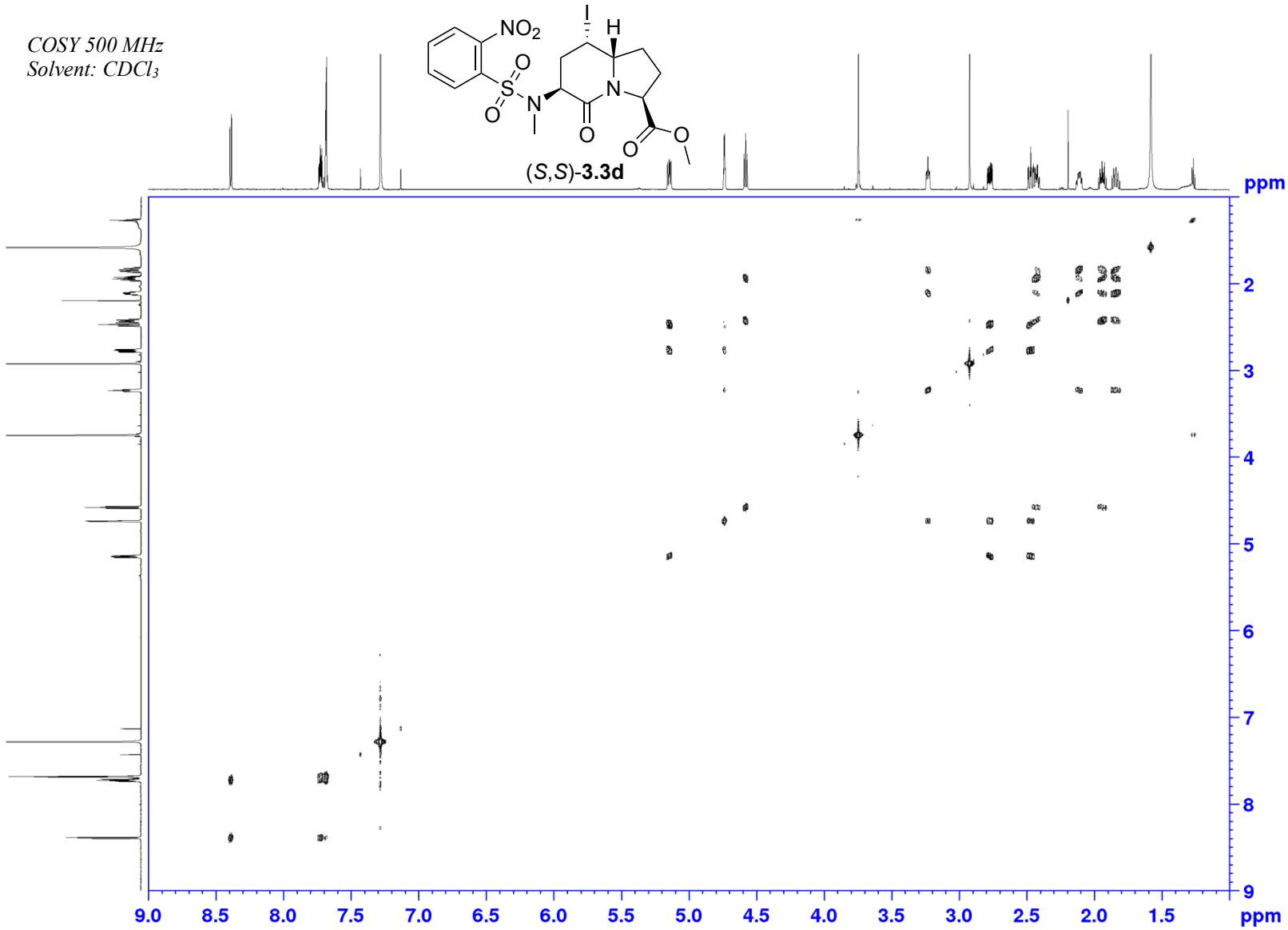
COSY 500 MHz
Solvent: CDCl3
NO2
O
S
O
N
I
H
N
O
O
O
(S,S)-3.3d
ppm
2
3
4
5
6
7
8
9
9.0
8.5
8.0
7.5
7.0
6.5
6.0
5.5
5.0
4.5
4.0
3.5
3.0
2.5
2.0
1.5
ppm

HSQC 500 MHz
Solvent: $CDCl_3$

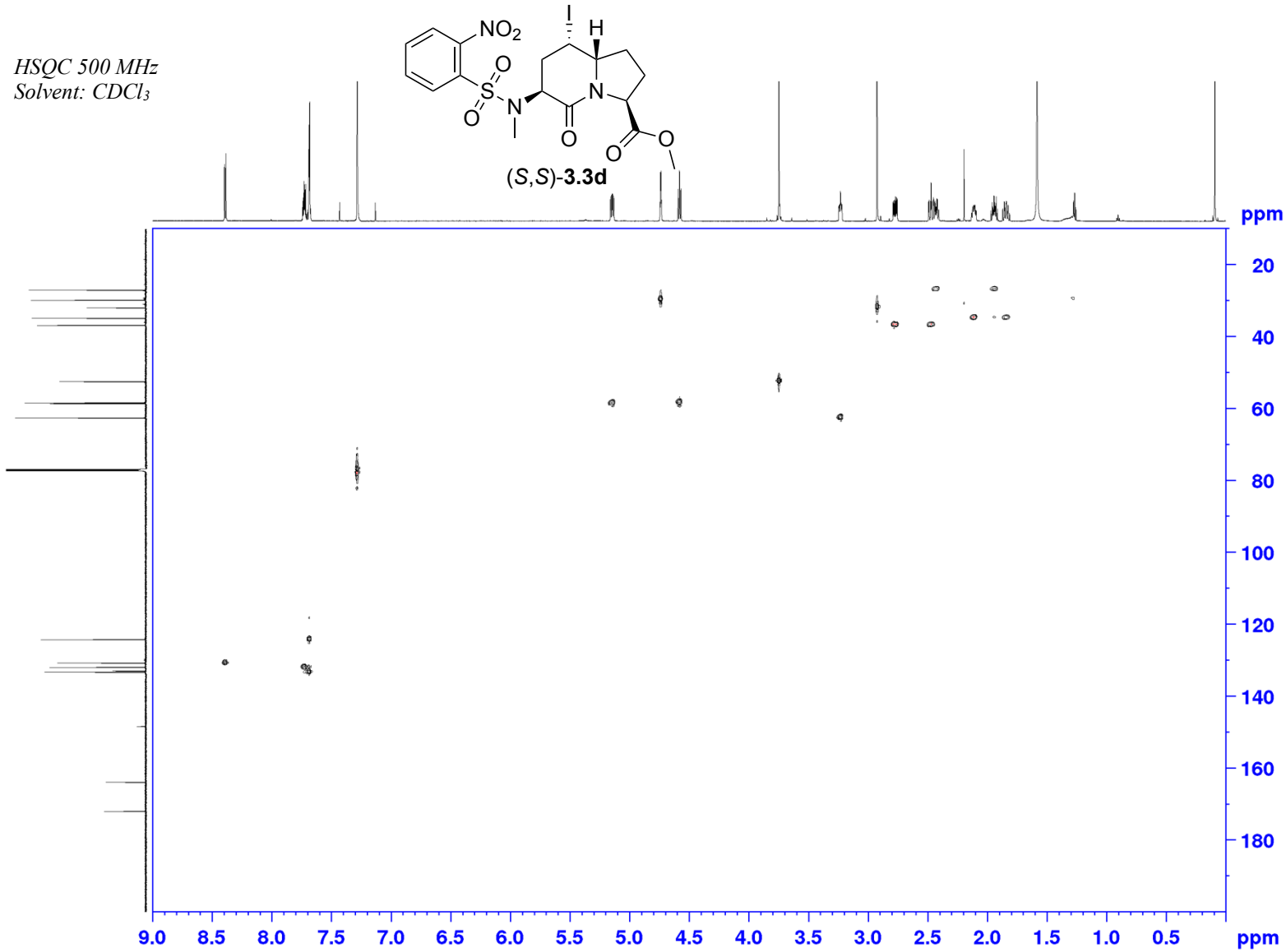

NOESY 500 MHz
Solvent: $CDCl_3$

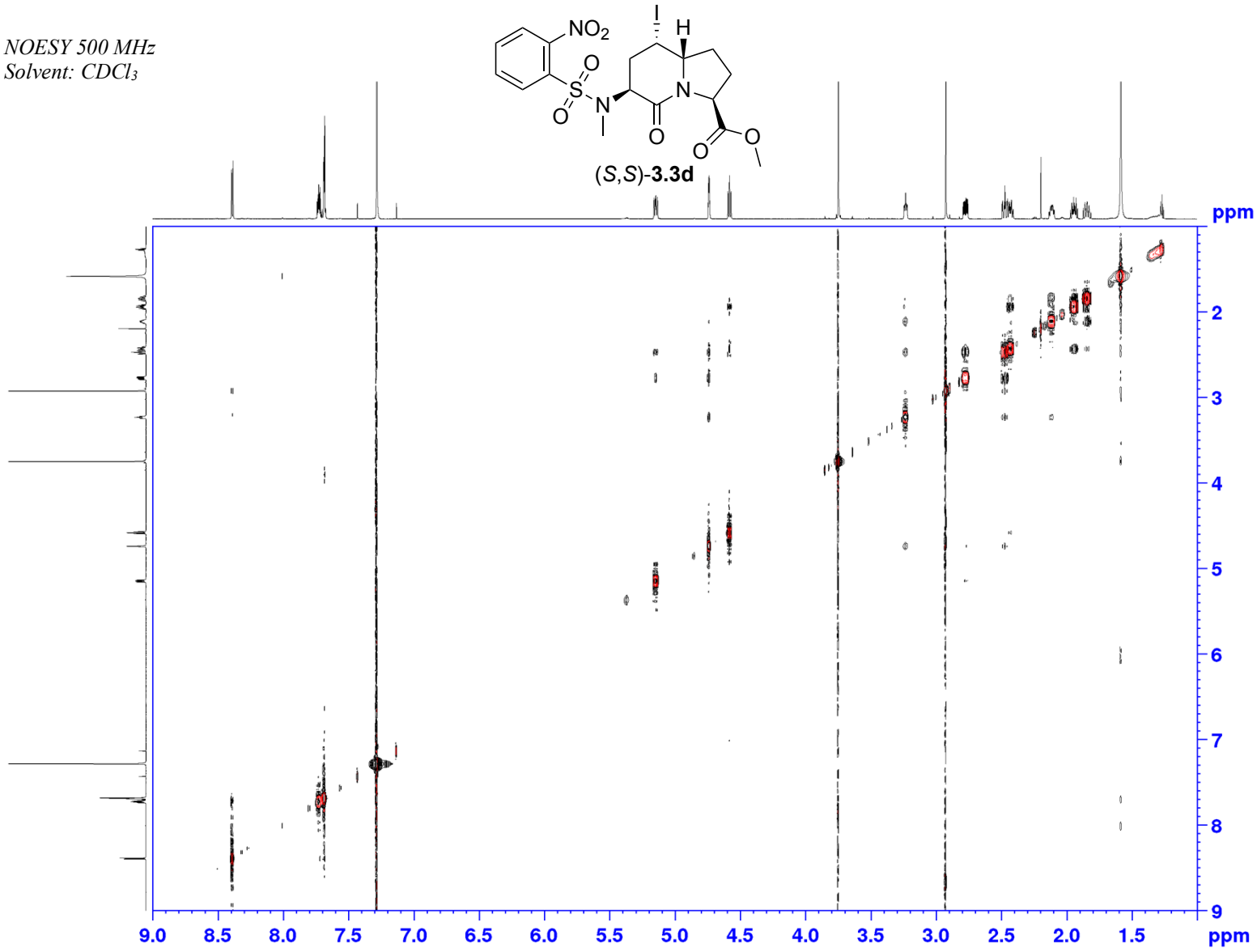

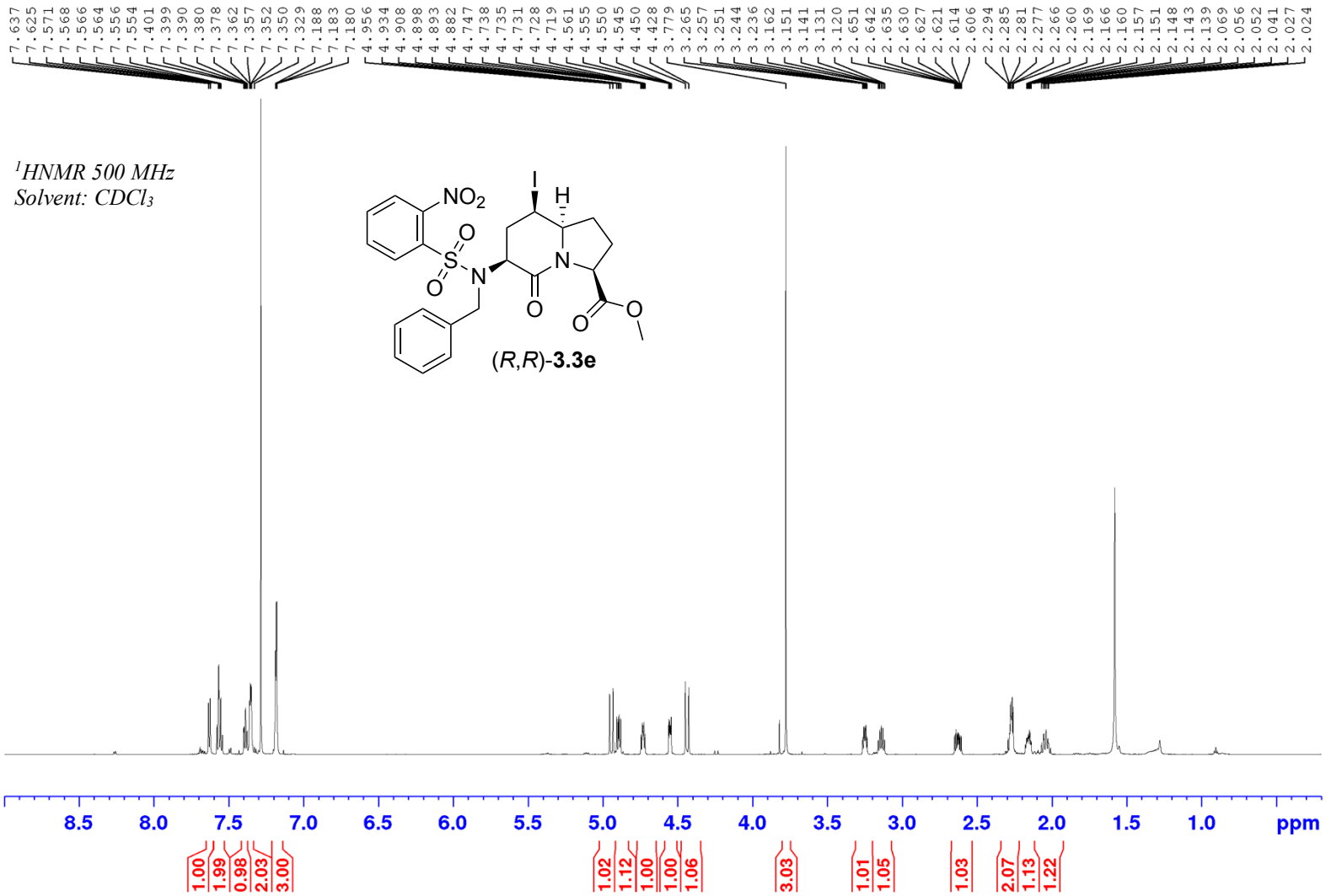
7.637
7.625
7.571
7.568
7.566
7.564
7.556
7.554
7.401
7.399
7.390
7.380
7.378
7.362
7.357
7.352
7.350
7.329
7.188
7.183
7.180
4.956
4.934
4.908
4.898
4.893
4.882
4.747
4.738
4.735
4.731
4.728
4.719
4.561
4.555
4.550
4.545
4.450
4.428
3.779
3.265
3.257
3.251
3.244
3.236
3.162
3.151
3.141
3.131
3.120
2.651
2.642
2.635
2.630
2.627
2.621
2.614
2.606
2.294
2.285
2.281
2.277
2.266
2.260
2.169
2.166
2.160
2.157
2.151
2.148
2.143
2.139
2.069
2.056
2.052
2.041
2.027
2.024
1HNMR 500 MHz
Solvent: CDCl3
NO2
I
H
O
S
O
N
N
O
O
O
O
(R,R)-3.3e
8.5
8.0
7.5
7.0
6.5
6.0
5.5
5.0
4.5
4.0
3.5
3.0
2.5
2.0
1.5
1.0
ppm
1.00
1.99
0.98
2.03
3.00
1.02
1.12
1.00
1.00
1.06
3.03
1.01
1.05
1.03
2.07
1.13
1.22

^{13}CNMR 500 MHz
Solvent: $CDCl_3$

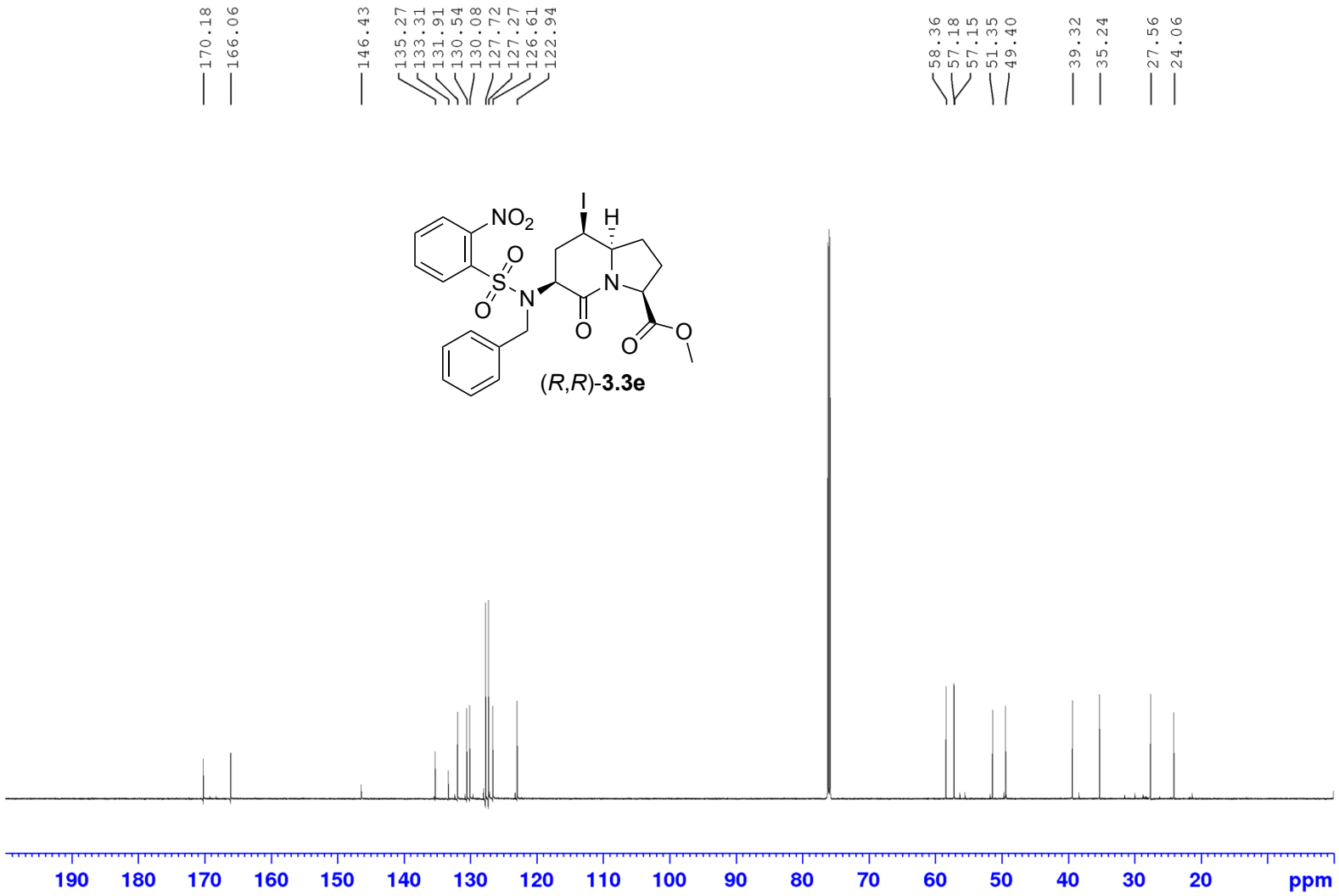

COSY 500 MHz
Solvent: $CDCl_3$

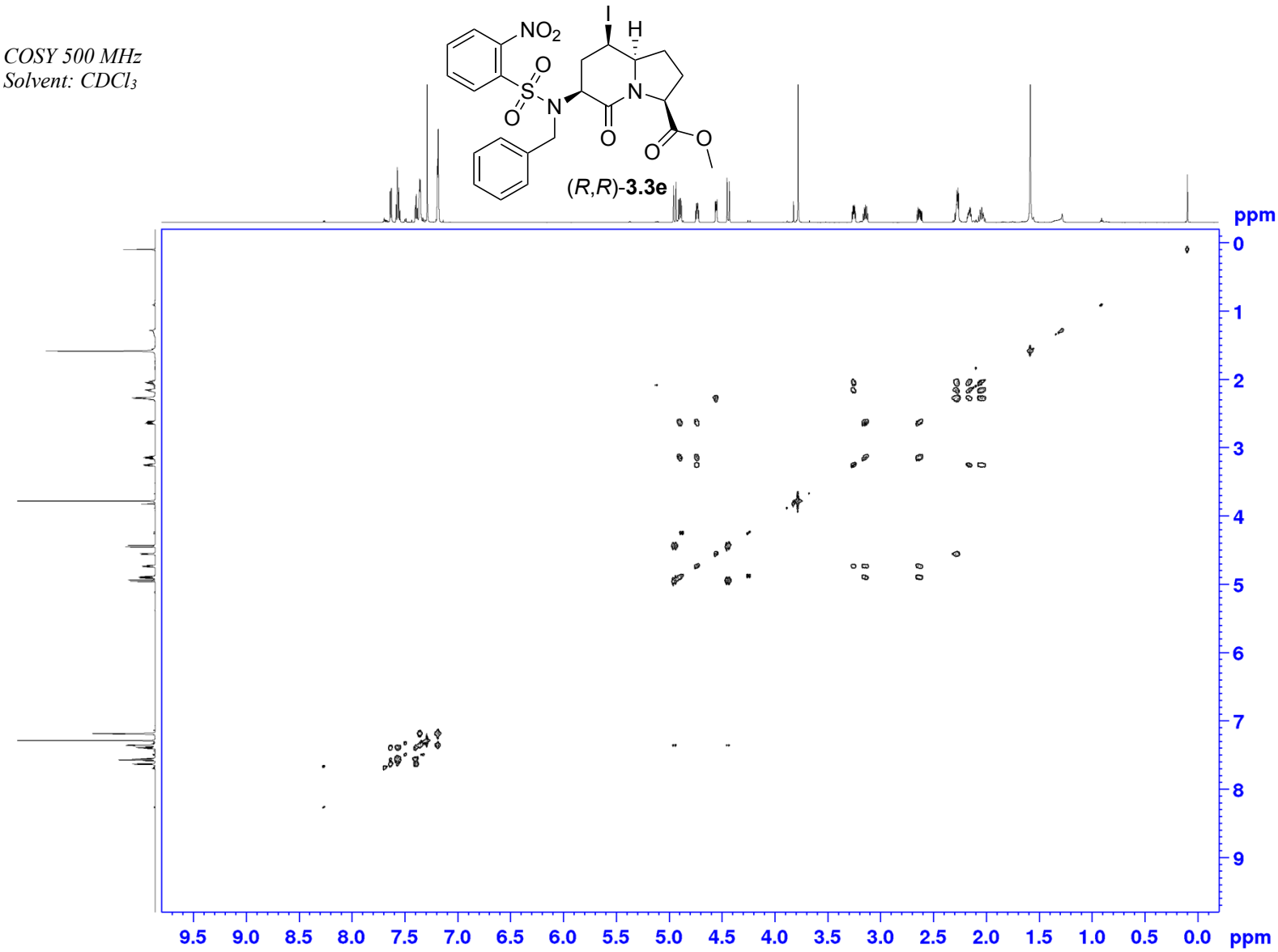

HSQC 500 MHz
Solvent: $CDCl_3$

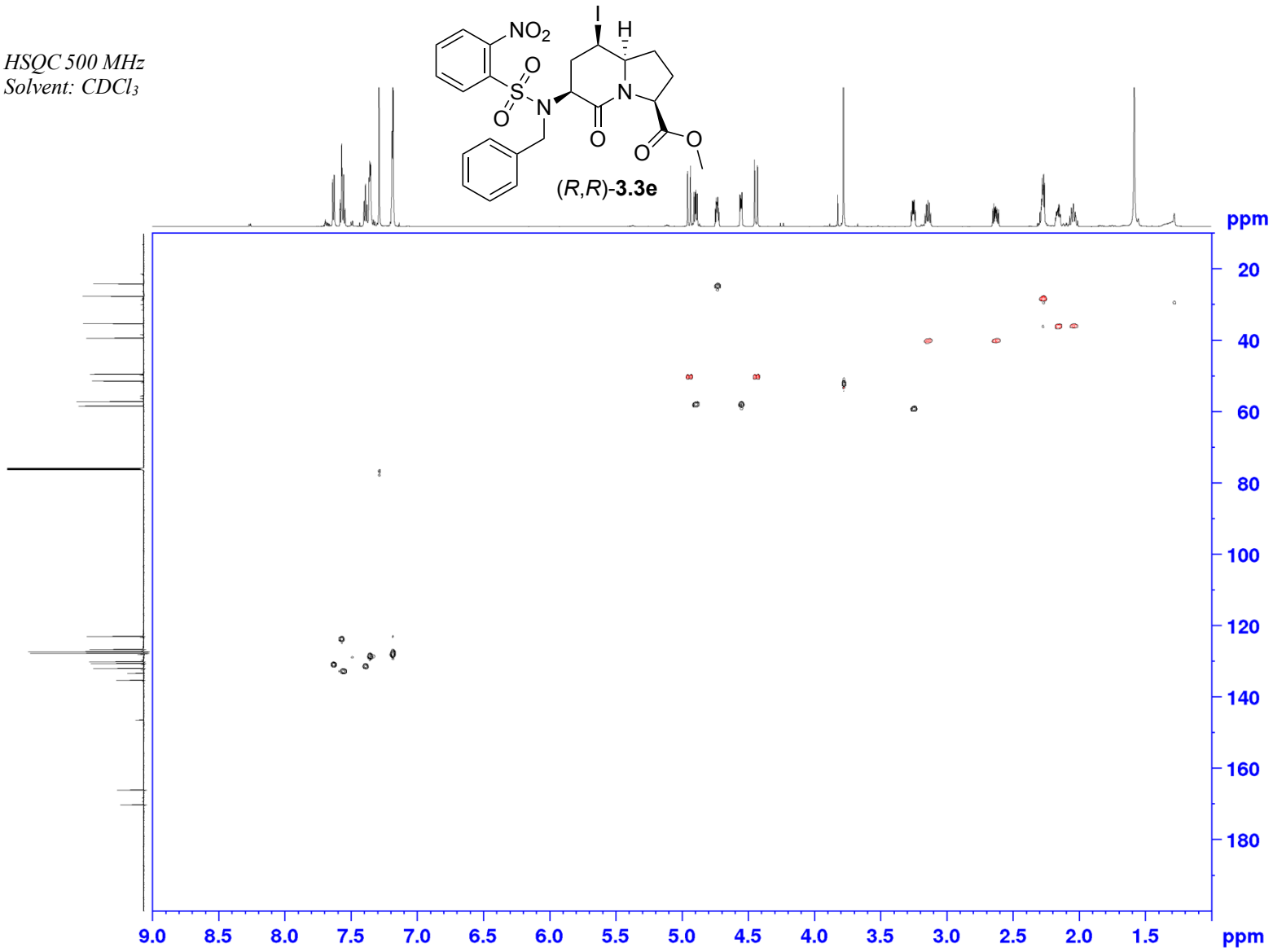

NOESY 500 MHz
Solvent: $CDCl_3$

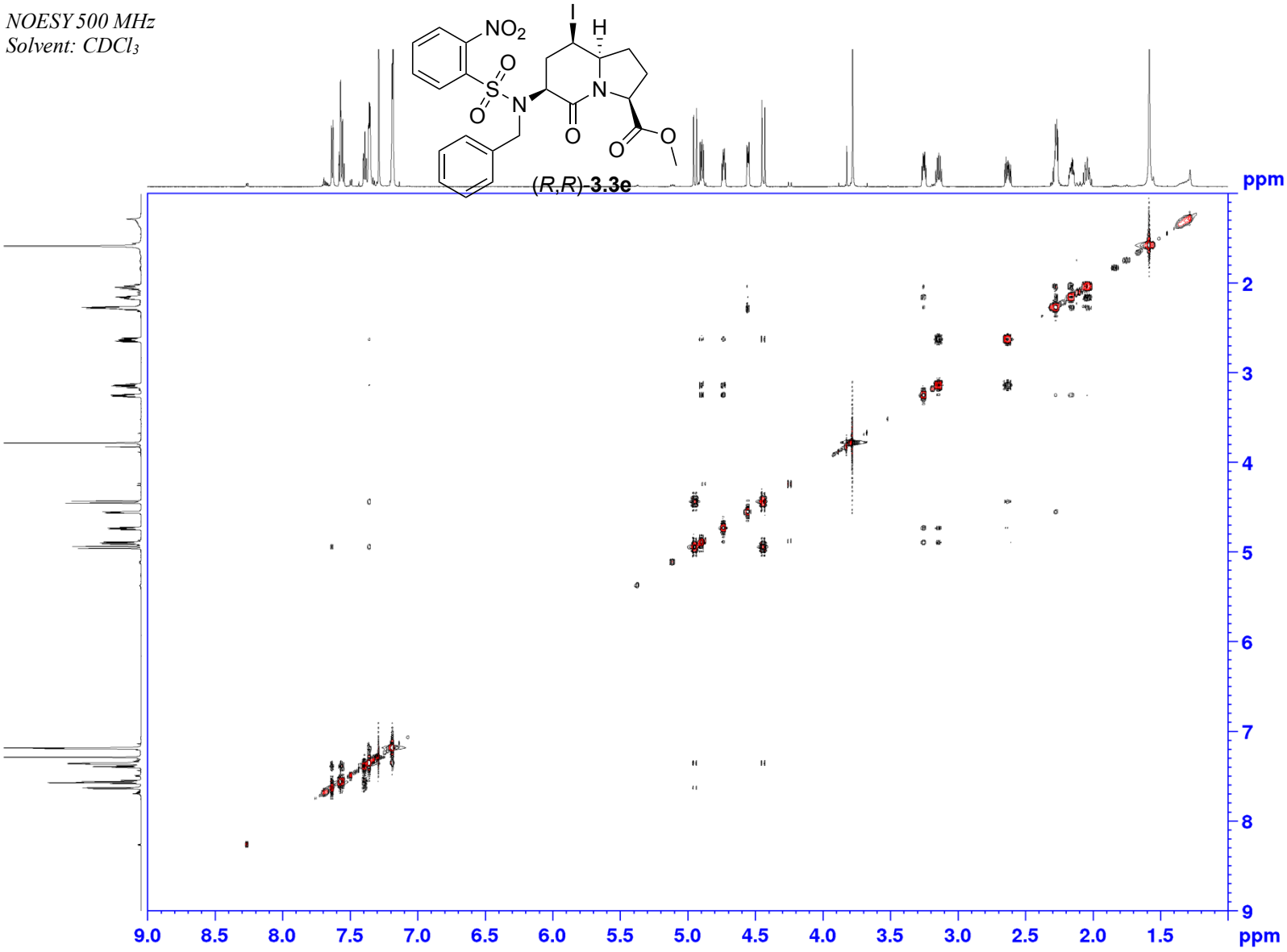

[1]H NMR 500 MHz
Solvent: CD_3OD

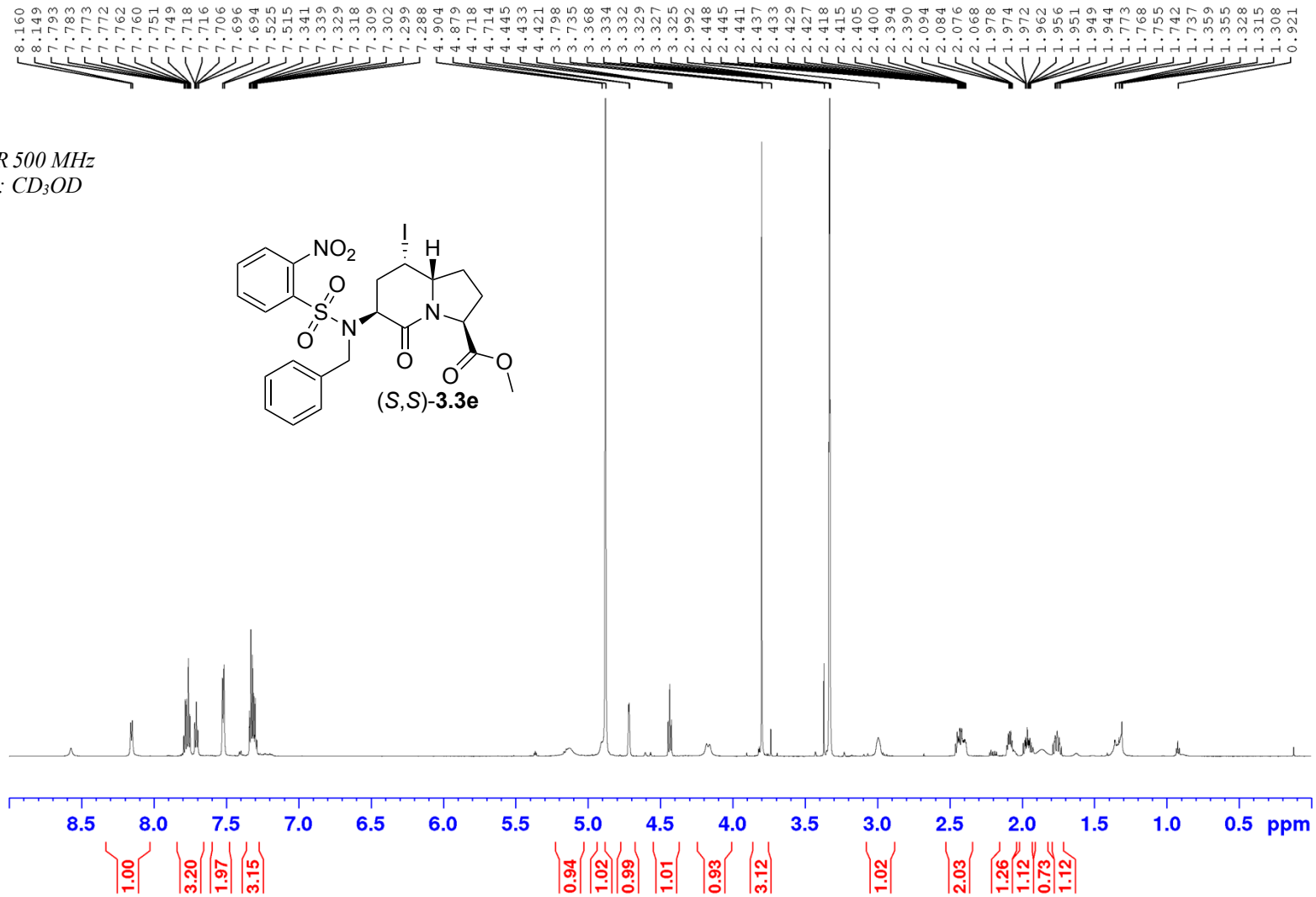

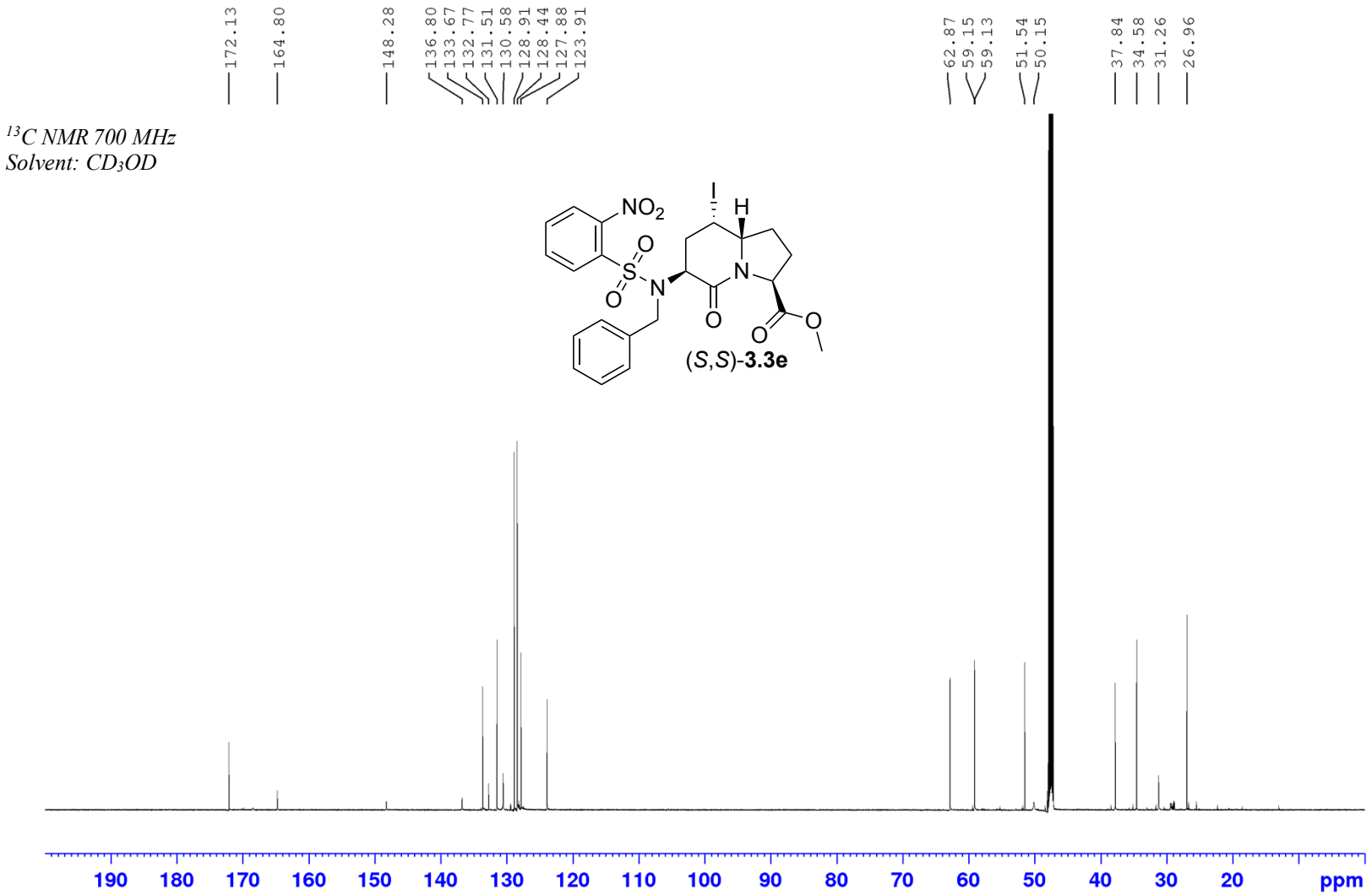
172.13
164.80
148.28
136.80
133.67
132.77
131.51
130.58
128.91
128.44
127.88
123.91
62.87
59.15
59.13
51.54
50.15
37.84
34.58
31.26
26.96
13C NMR 700 MHz
Solvent: CD3OD
NO2
I
H
O
S
O
N
N
O
O
O
O
(S,S)-3.3e
190
180
170
160
150
140
130
120
110
100
90
80
70
60
50
40
30
20
ppm

COSY 700 MHz
Solvent: CD_3OD

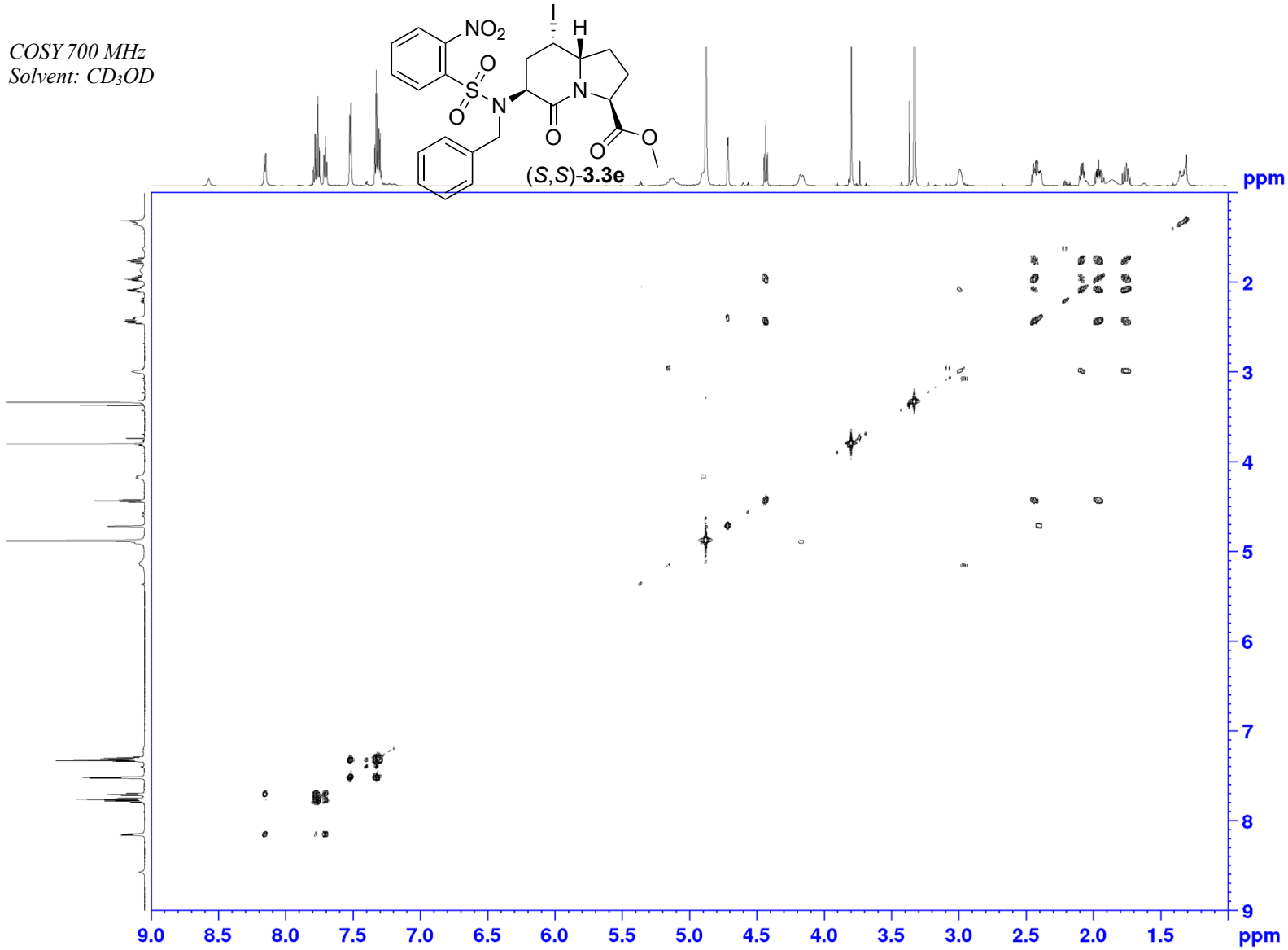

HSQC 700 MHz
Solvent: CD_3OD

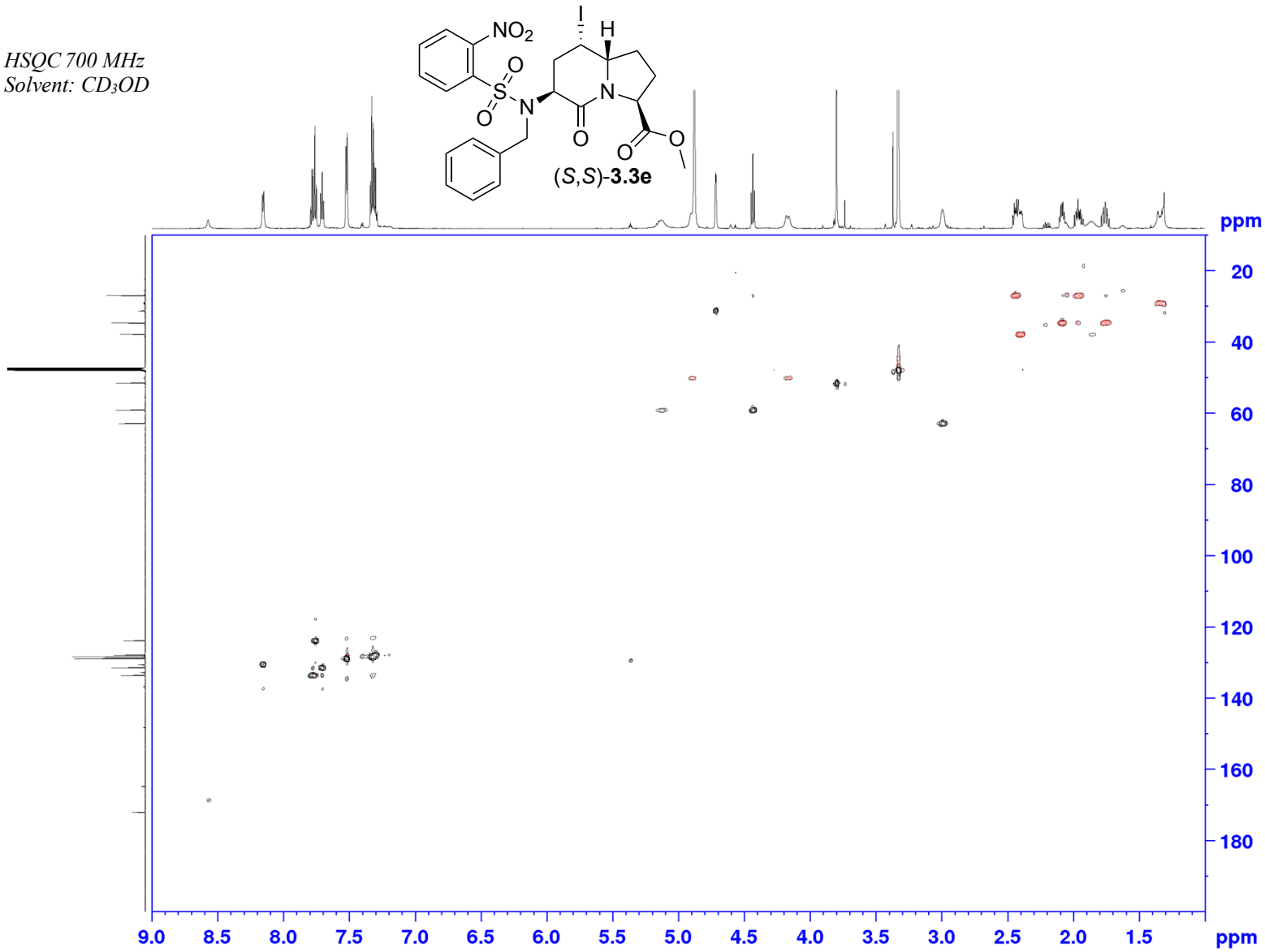

NOESY 700 MHz
Solvent: CD_3OD

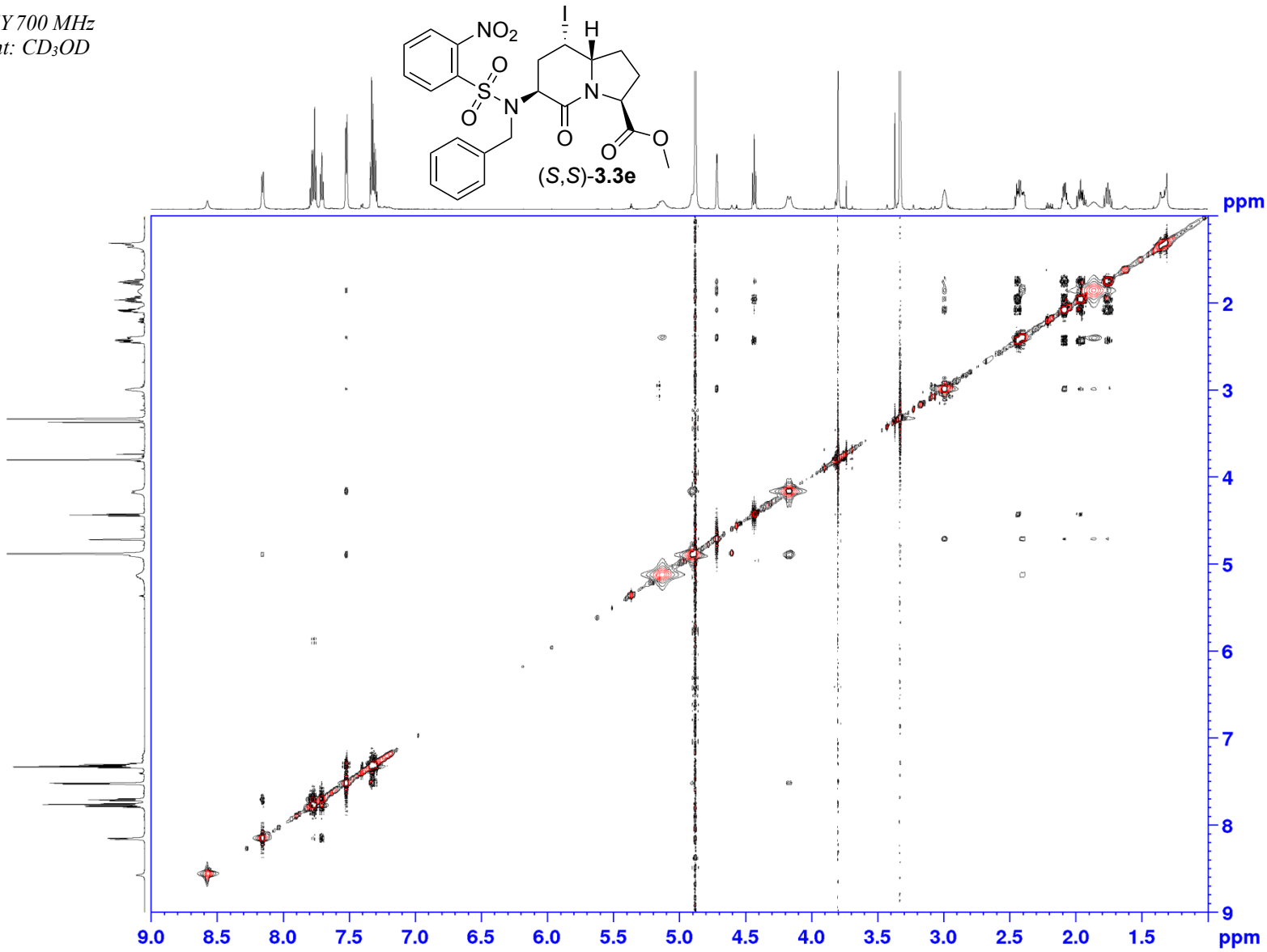

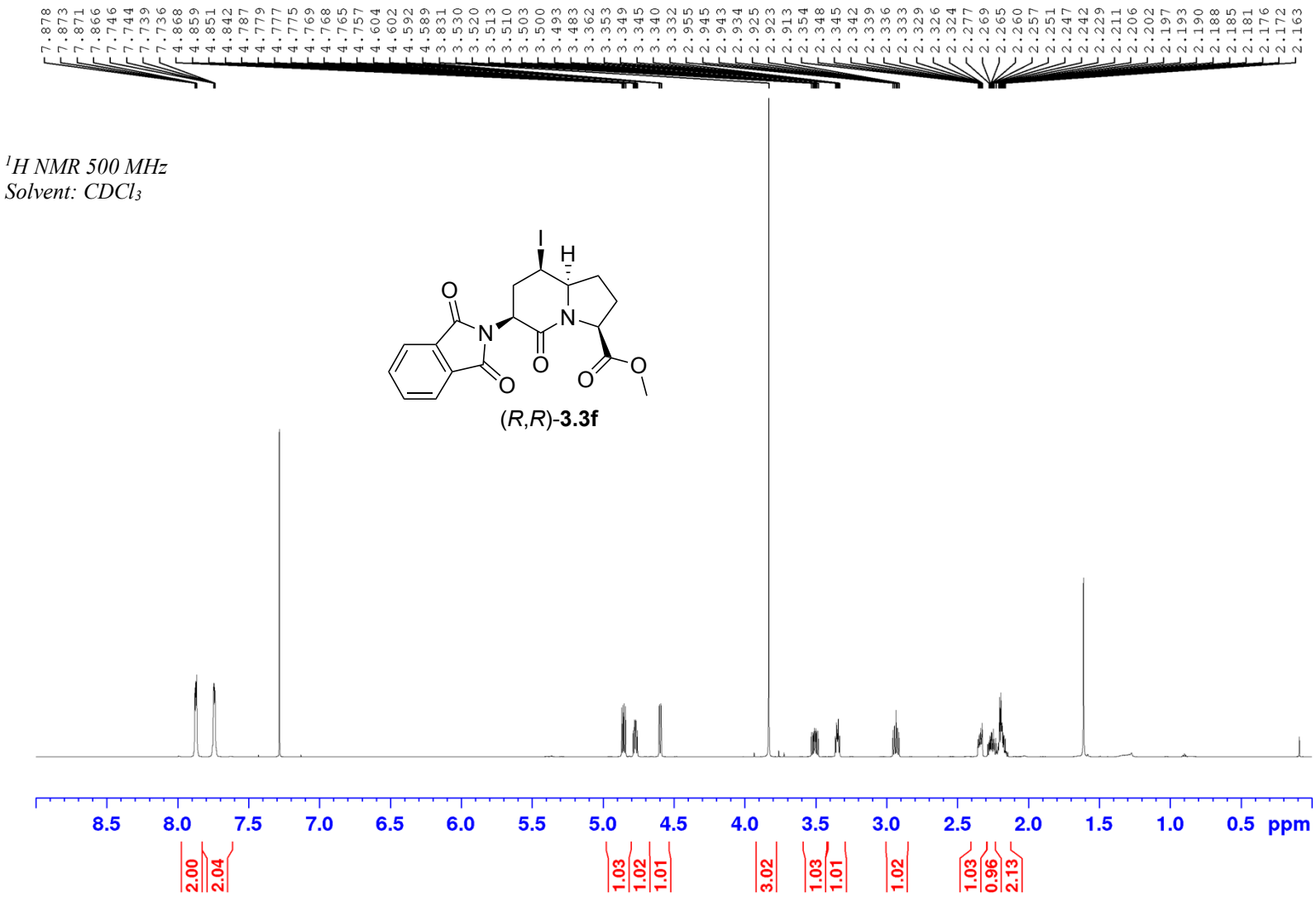

[1]H NMR 500 MHz
Solvent: $CDCl_3$

(*R*,*R*)-**3.3f**

^{13}C NMR 500 MHz
Solvent: $CDCl_3$

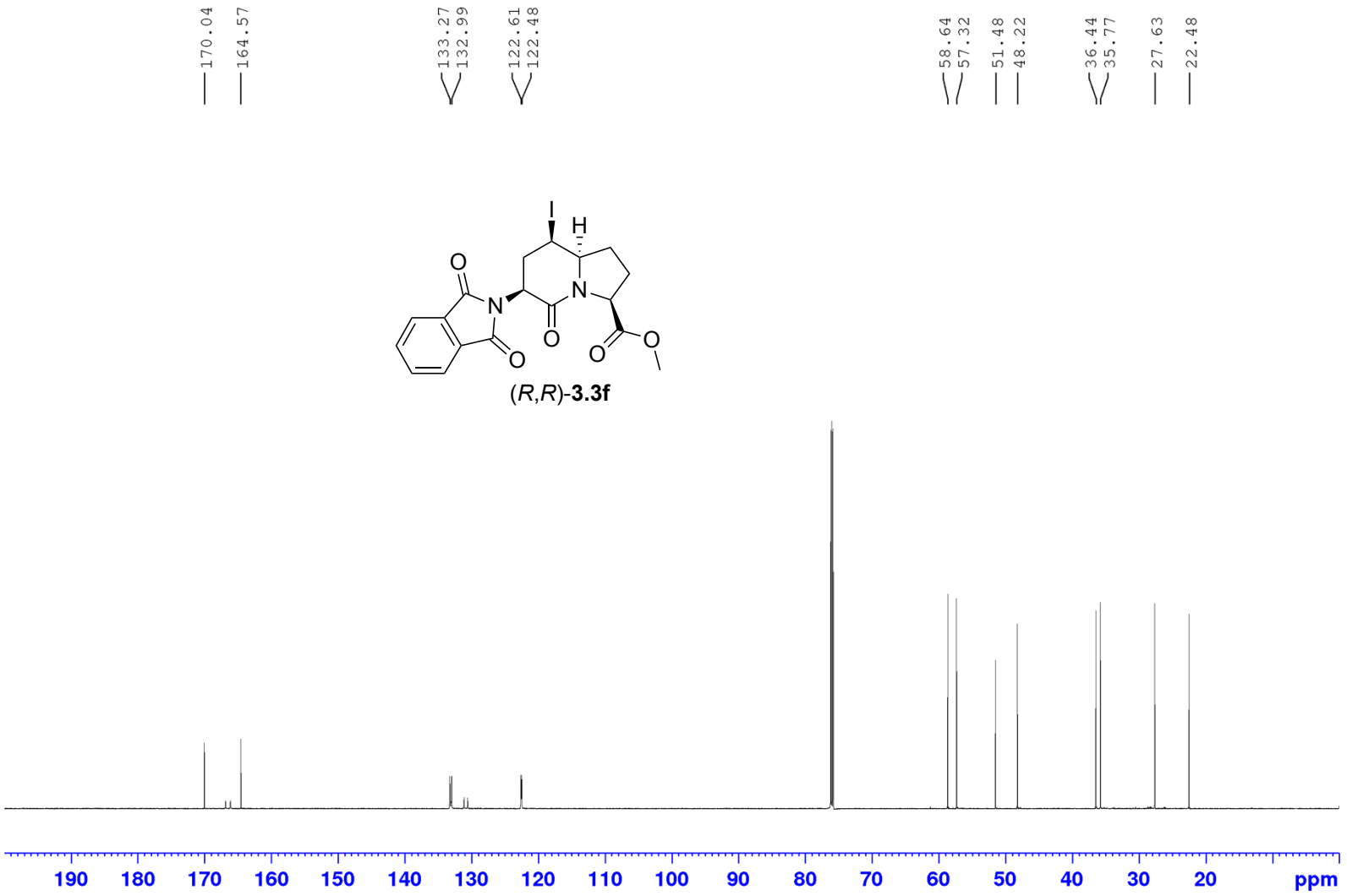

(*R*,*R*)-**3.3f**

COSY *500 MHz*
Solvent: $CDCl_3$

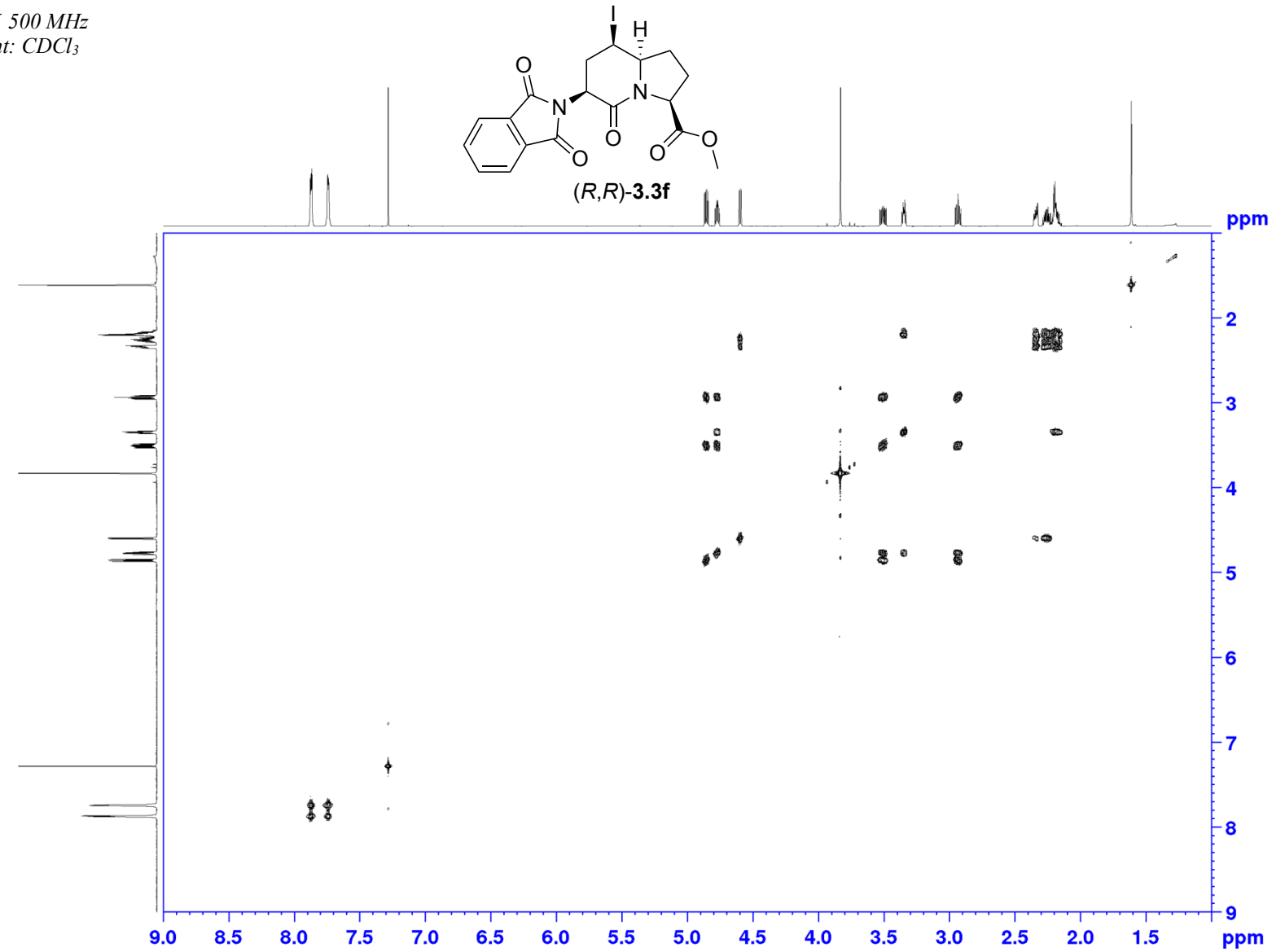

HSQC *500 MHz*
Solvent: $CDCl_3$

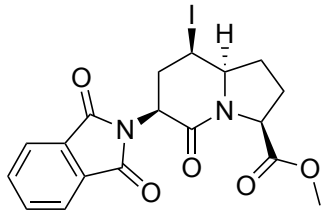

(*R*,*R*)-**3.3f**

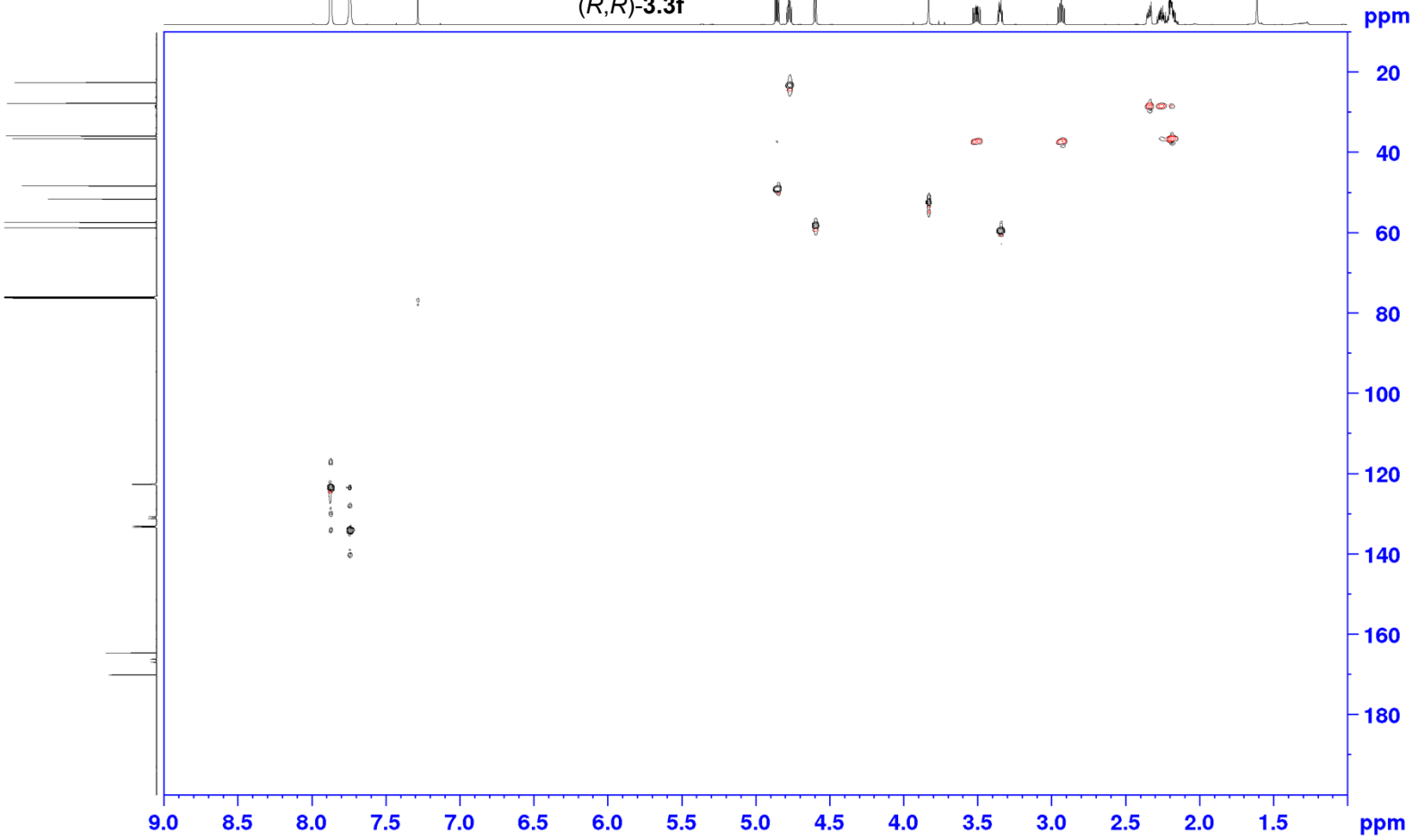

NOESY *500 MHz*
Solvent: $CDCl_3$

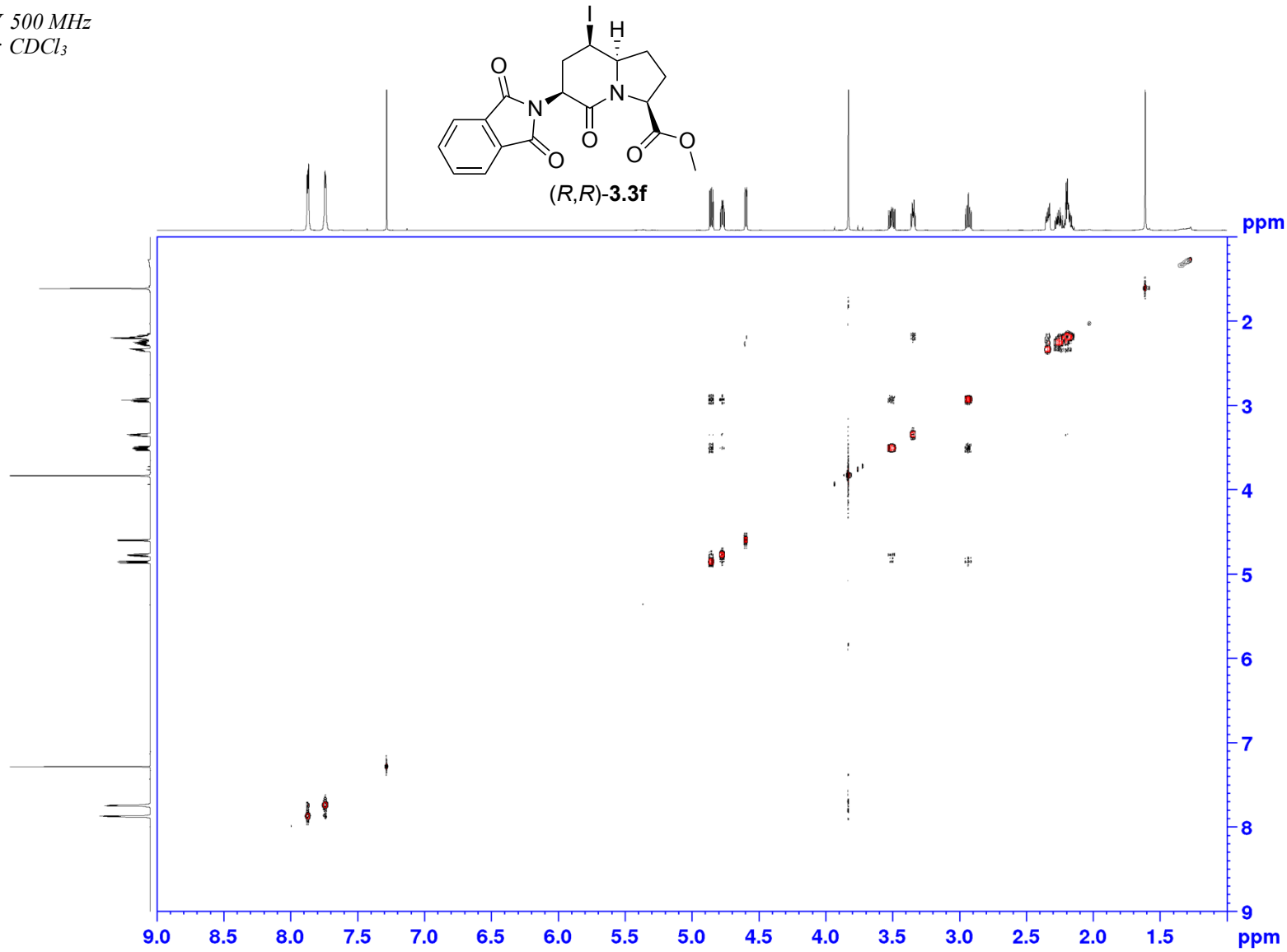

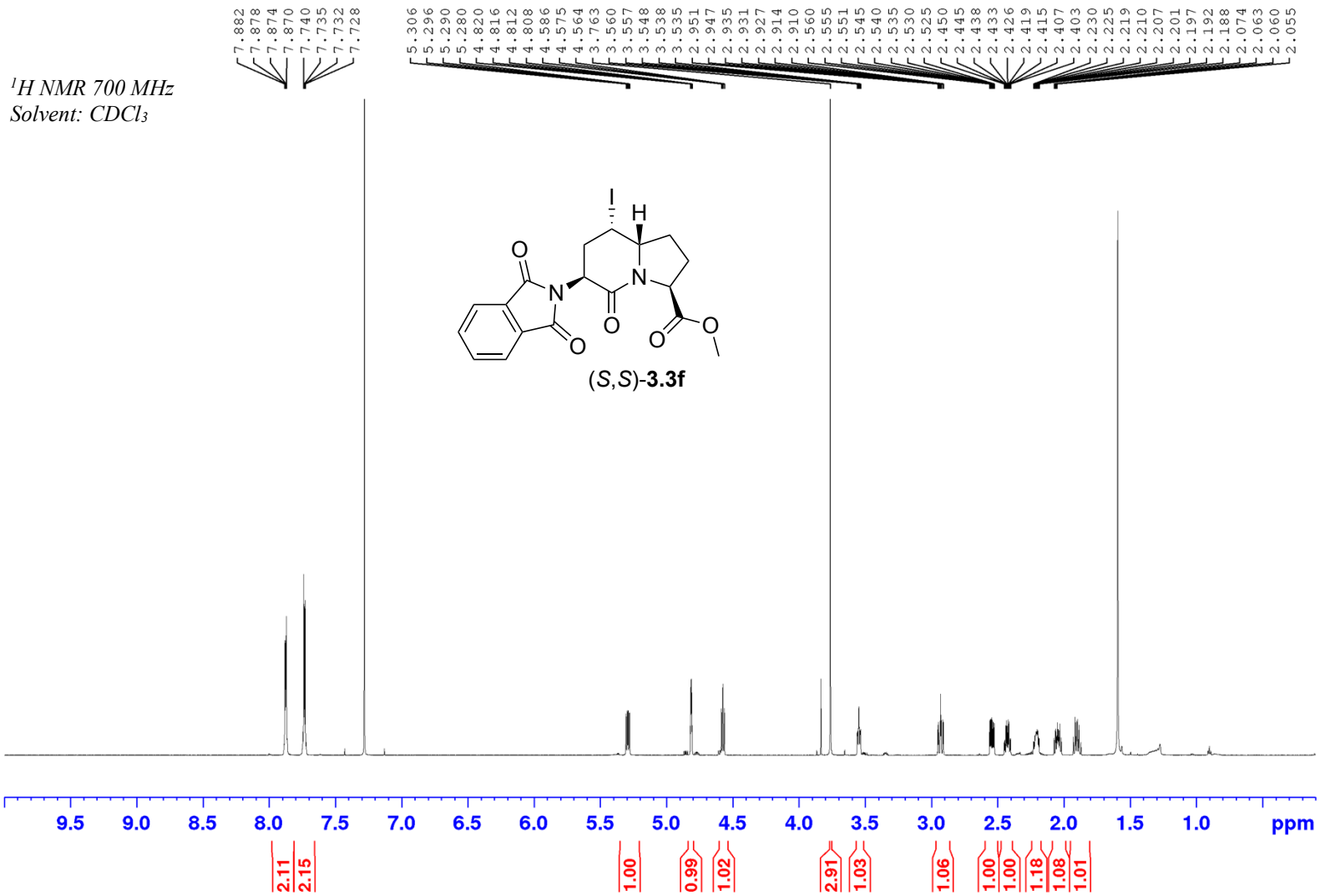
^{1}H NMR 700 MHz
Solvent: CDCl$_3$
7.882
7.878
7.874
7.870
7.740
7.735
7.732
7.728
5.306
5.296
5.290
5.280
4.820
4.816
4.812
4.808
4.586
4.575
4.564
3.763
3.560
3.557
3.548
3.538
3.535
2.951
2.947
2.935
2.931
2.927
2.914
2.910
2.560
2.555
2.551
2.545
2.540
2.535
2.530
2.525
2.450
2.445
2.438
2.433
2.426
2.419
2.415
2.407
2.403
2.230
2.225
2.219
2.210
2.207
2.201
2.197
2.192
2.188
2.074
2.063
2.060
2.055
(S,S)-3.3f
9.5
9.0
8.5
8.0
7.5
7.0
6.5
6.0
5.5
5.0
4.5
4.0
3.5
3.0
2.5
2.0
1.5
1.0
ppm
2.11
2.15
1.00
0.99
1.02
2.91
1.03
1.06
1.00
1.00
1.18
1.08
1.01

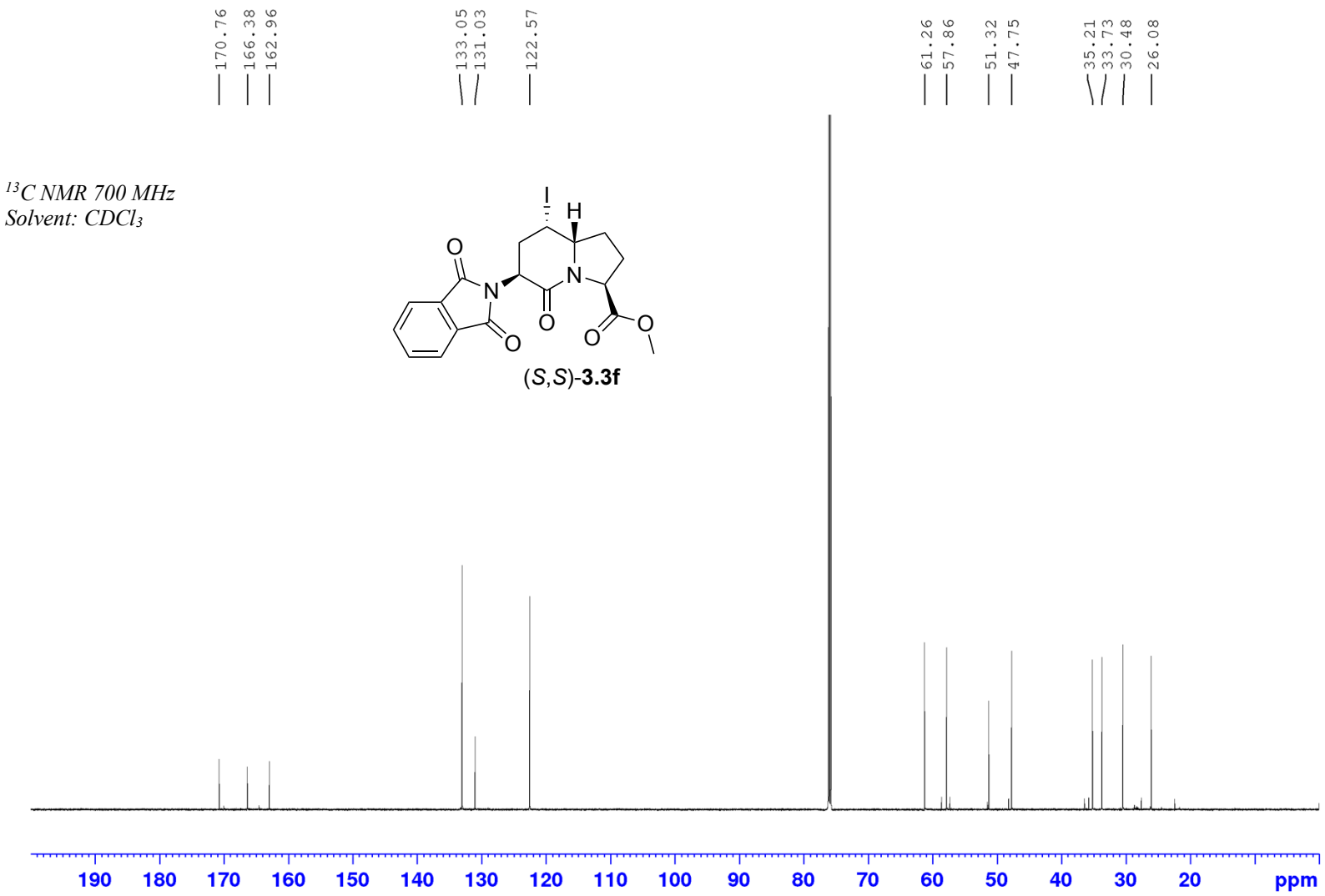
170.76
166.38
162.96
133.05
131.03
122.57
61.26
57.86
51.32
47.75
35.21
33.73
30.48
26.08
13C NMR 700 MHz
Solvent: CDCl3
(S,S)-3.3f
190
180
170
160
150
140
130
120
110
100
90
80
70
60
50
40
30
20
ppm

COSY 700 MHz
Solvent: $CDCl_3$

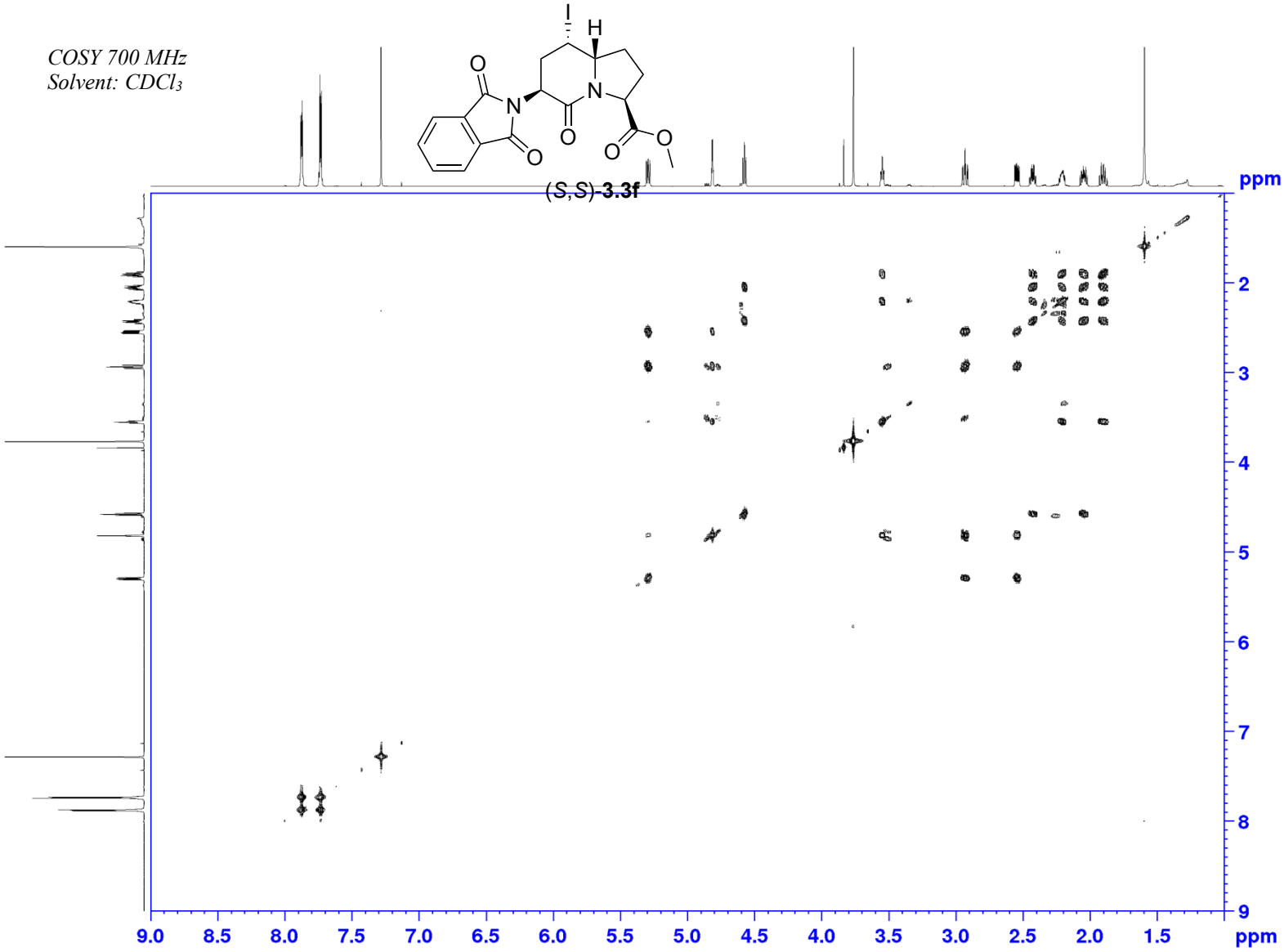

HSQC 700 MHz
Solvent: $CDCl_3$

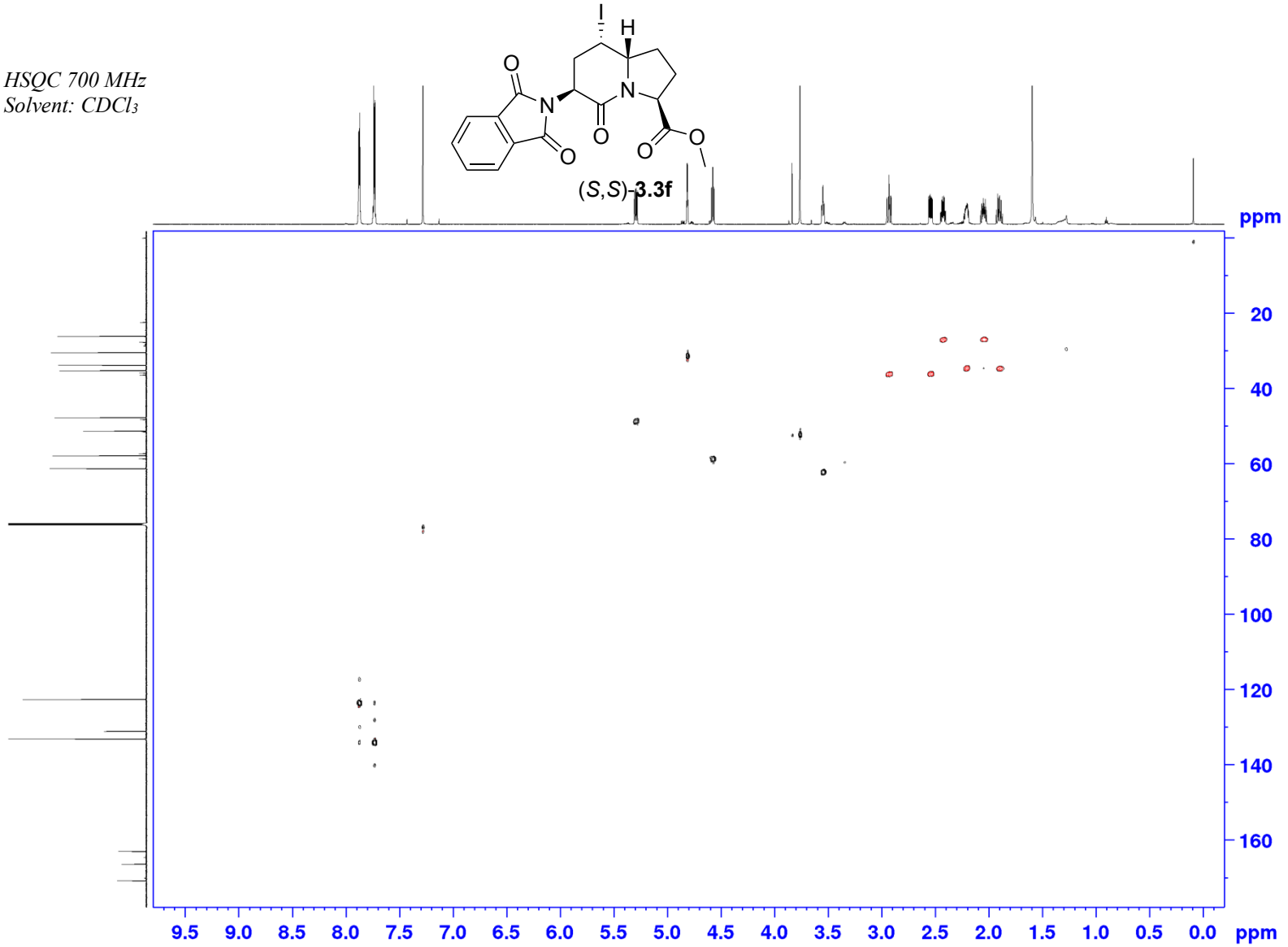

NOESY 700 MHz
Solvent: $CDCl_3$

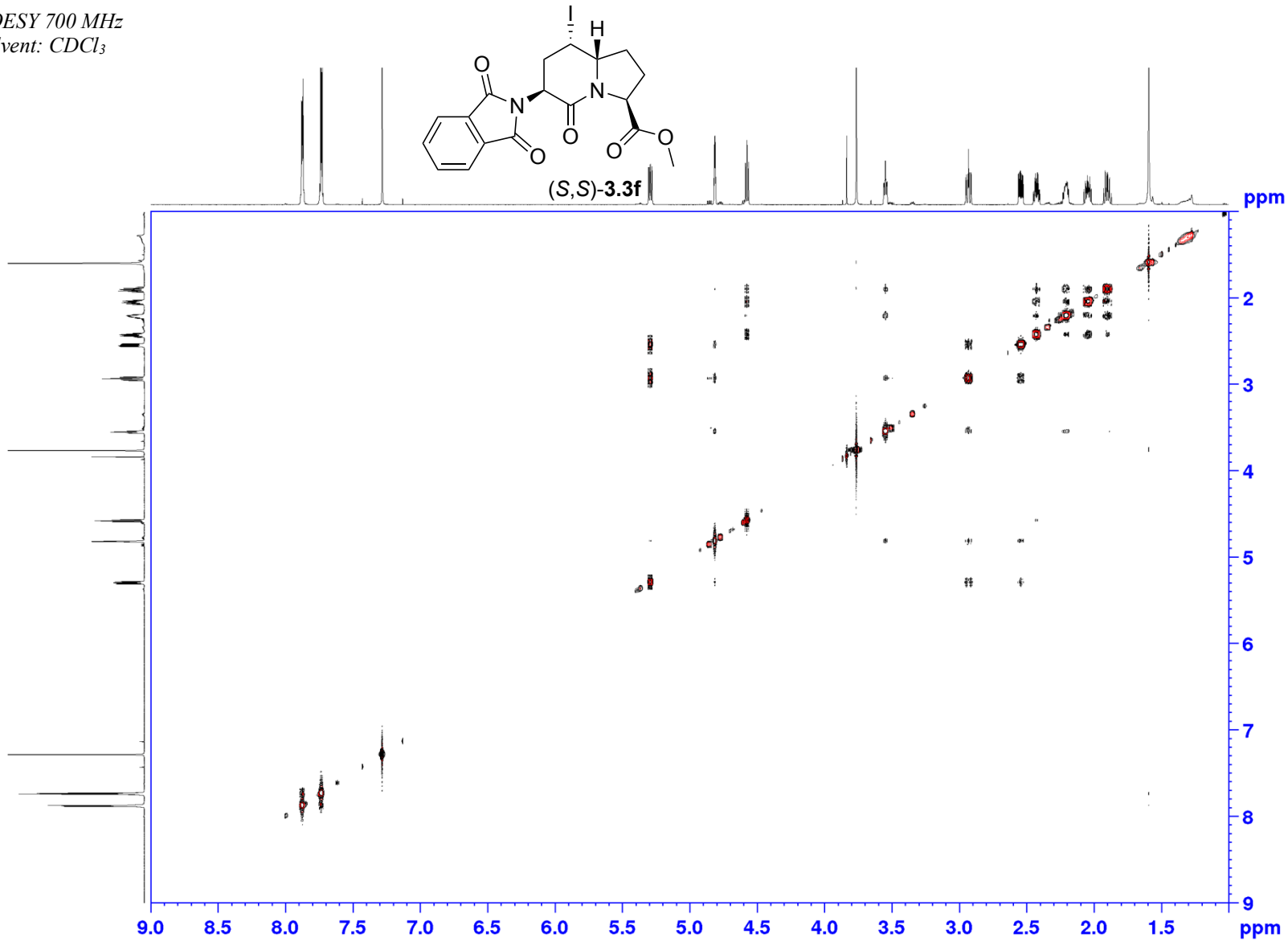

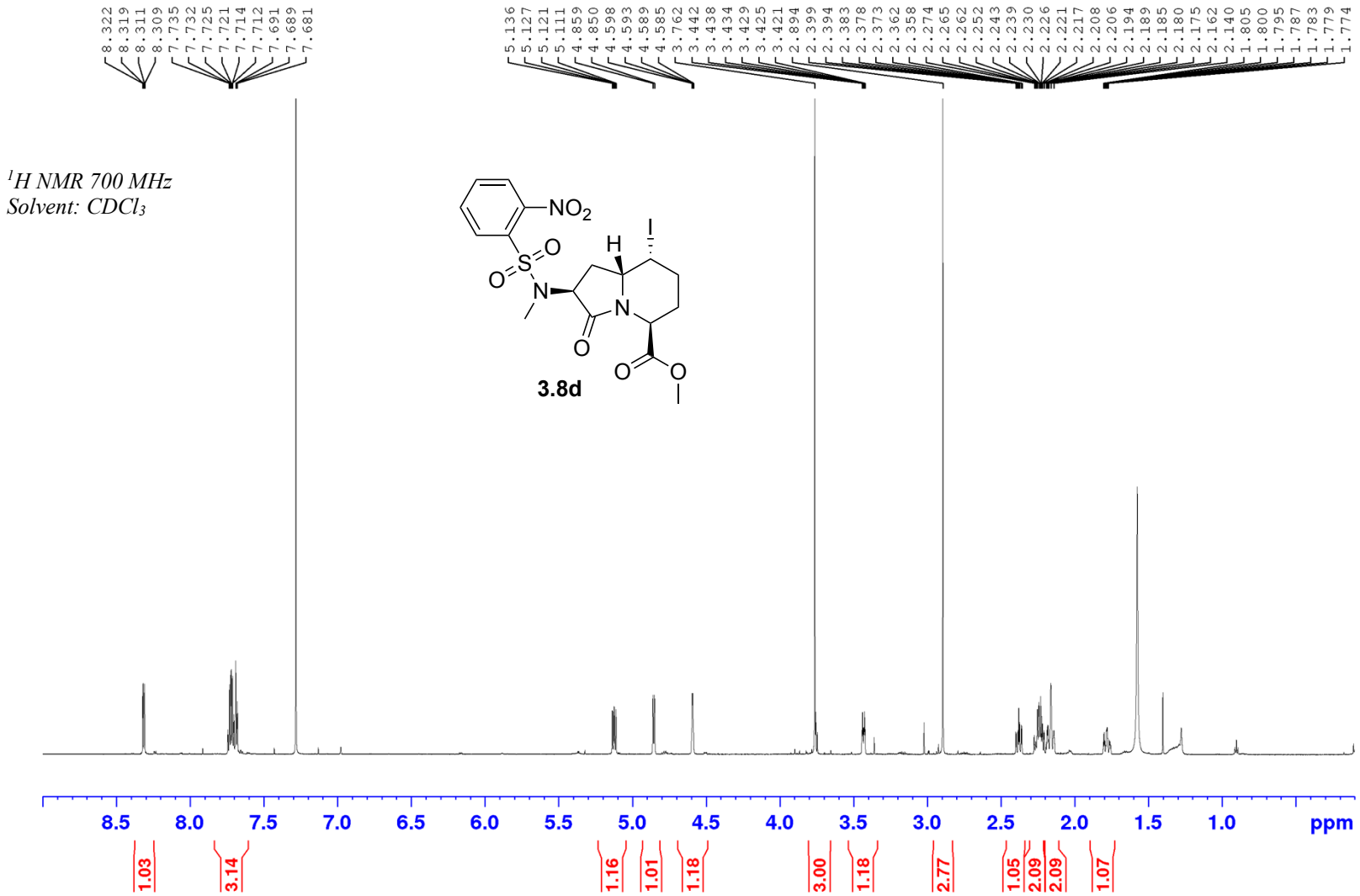
8.322
8.319
8.311
8.309
7.735
7.732
7.725
7.721
7.714
7.712
7.691
7.689
7.681
5.136
5.127
5.121
5.111
4.859
4.850
4.598
4.593
4.589
4.585
3.762
3.442
3.438
3.434
3.429
3.425
3.421
2.894
2.399
2.394
2.383
2.378
2.373
2.362
2.358
2.274
2.265
2.262
2.252
2.243
2.239
2.230
2.226
2.221
2.217
2.208
2.206
2.194
2.189
2.185
2.180
2.175
2.162
2.140
1.805
1.800
1.795
1.787
1.783
1.779
1.774
1H NMR 700 MHz
Solvent: CDCl3
NO2
S
O
O
N
H
I
N
O
O
O
3.8d
8.5
8.0
7.5
7.0
6.5
6.0
5.5
5.0
4.5
4.0
3.5
3.0
2.5
2.0
1.5
1.0
ppm
1.03
3.14
1.16
1.01
1.18
3.00
1.18
2.77
1.05
2.09
2.09
1.07

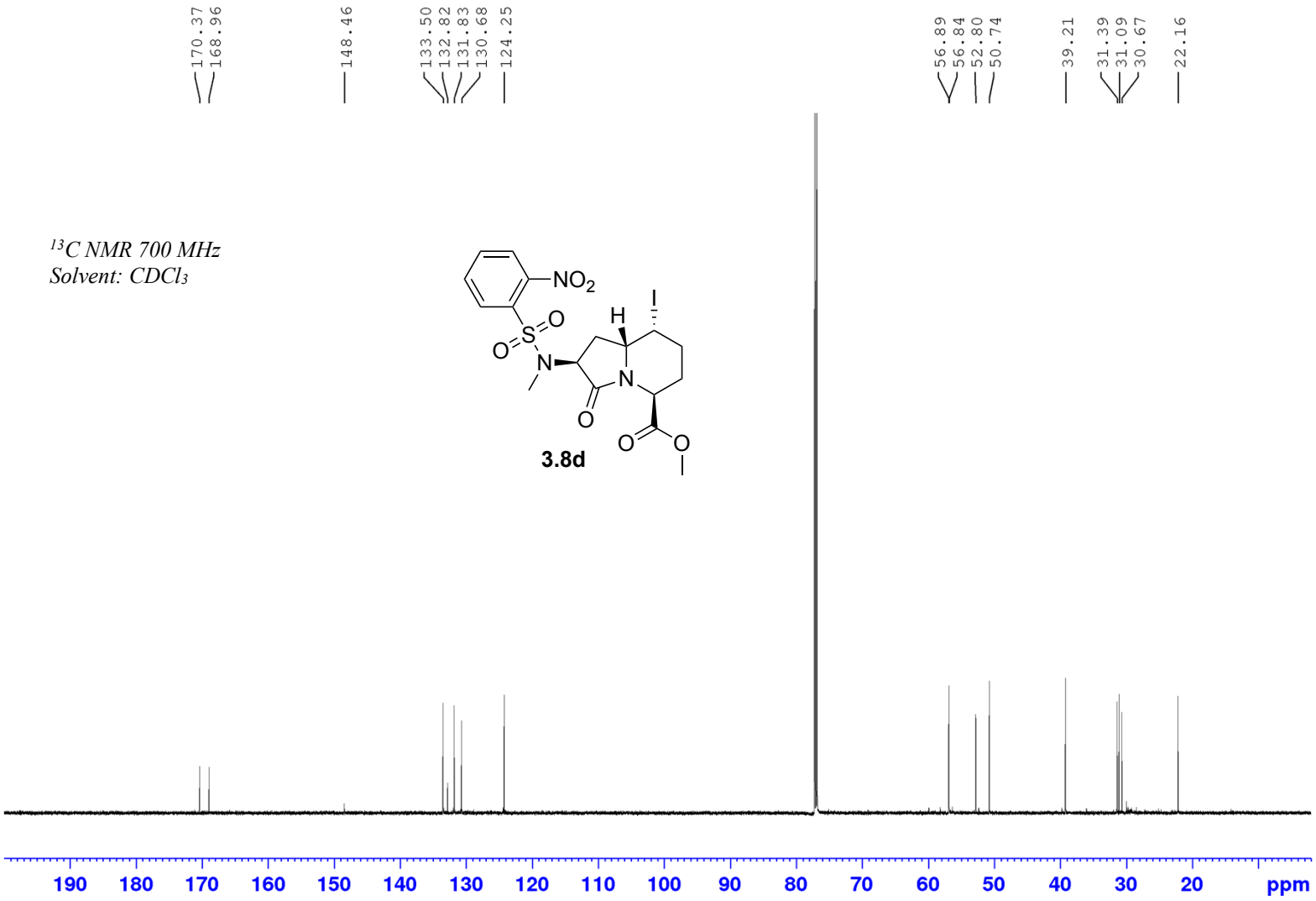
170.37
168.96
148.46
133.50
132.82
131.83
130.68
124.25
56.89
56.84
52.80
50.74
39.21
31.39
31.09
30.67
22.16
13C NMR 700 MHz
Solvent: CDCl3
NO2
S
O
O
N
H
I
N
O
O
O
3.8d
190
180
170
160
150
140
130
120
110
100
90
80
70
60
50
40
30
20
ppm

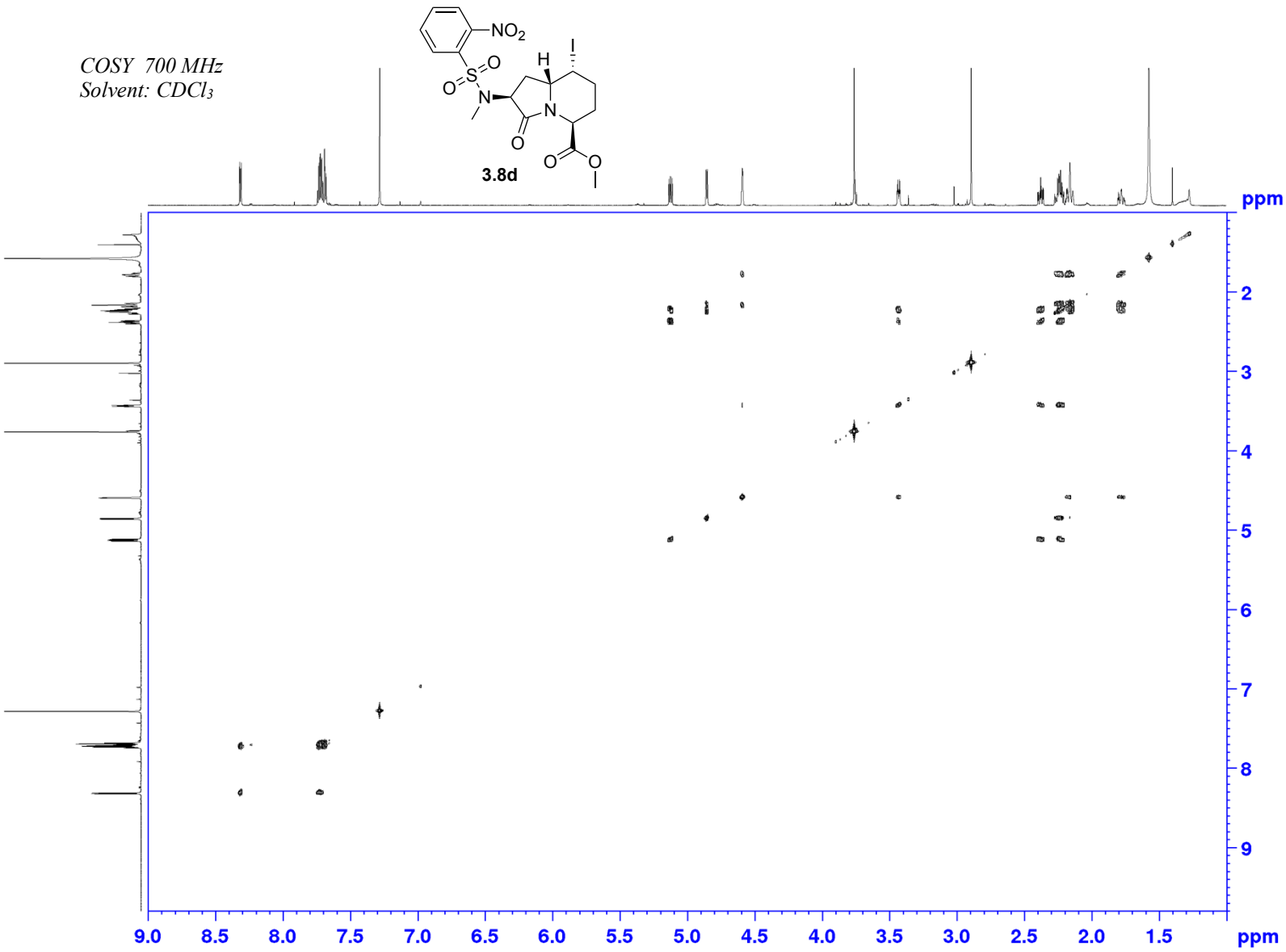
COSY 700 MHz
Solvent: CDCl3
NO2
S
O
O
N
H
I
N
O
O
O
O
3.8d
ppm
2
3
4
5
6
7
8
9
9.0
8.5
8.0
7.5
7.0
6.5
6.0
5.5
5.0
4.5
4.0
3.5
3.0
2.5
2.0
1.5
ppm

HSQC 700 MHz
Solvent: $CDCl_3$

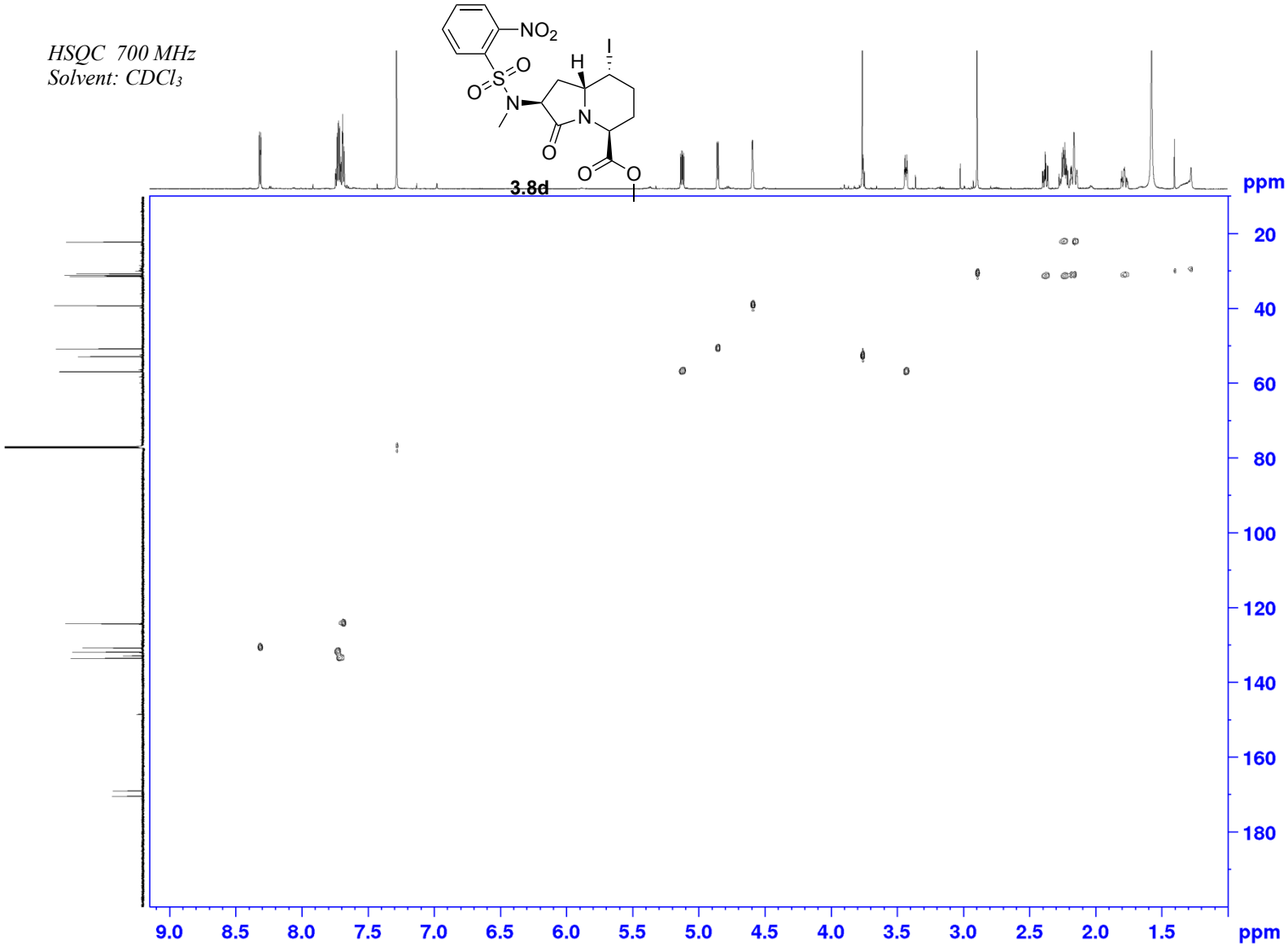

NOESY 700 MHz
Solvent: $CDCl_3$

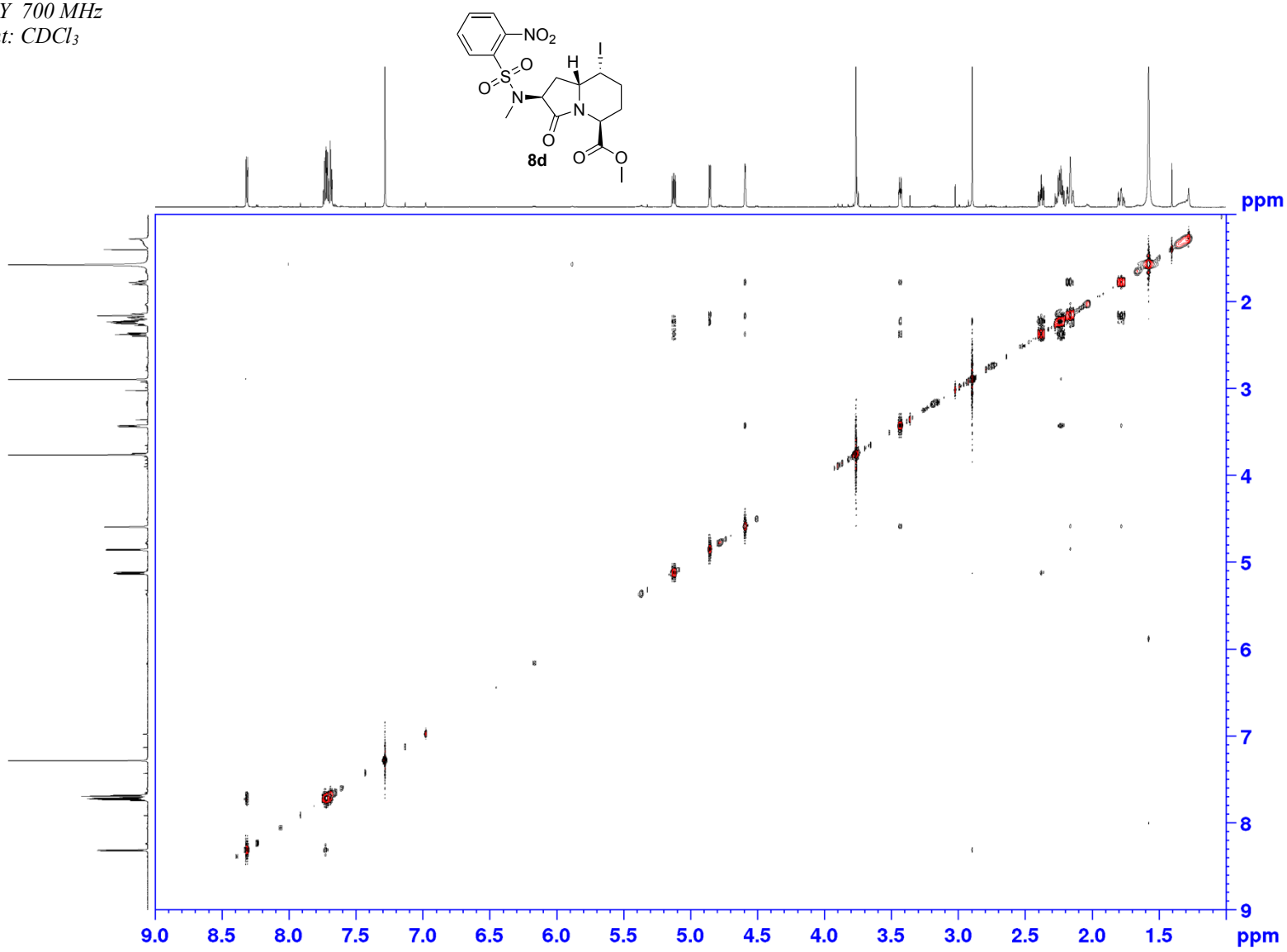

^{1}H NMR 700 MHz
Solvent: $CDCl_3$

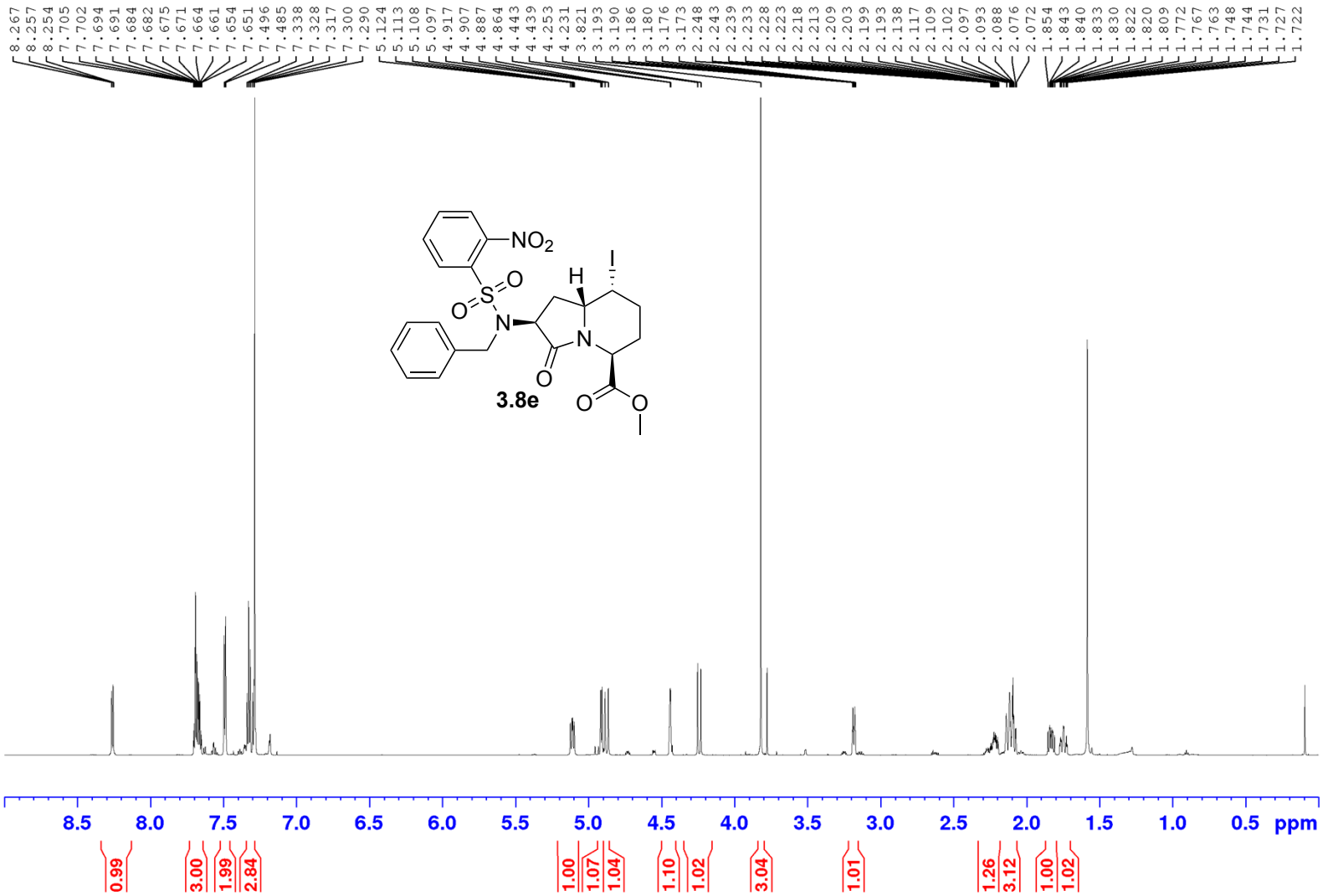

^{13}C NMR 700 MHz
Solvent: $CDCl_3$

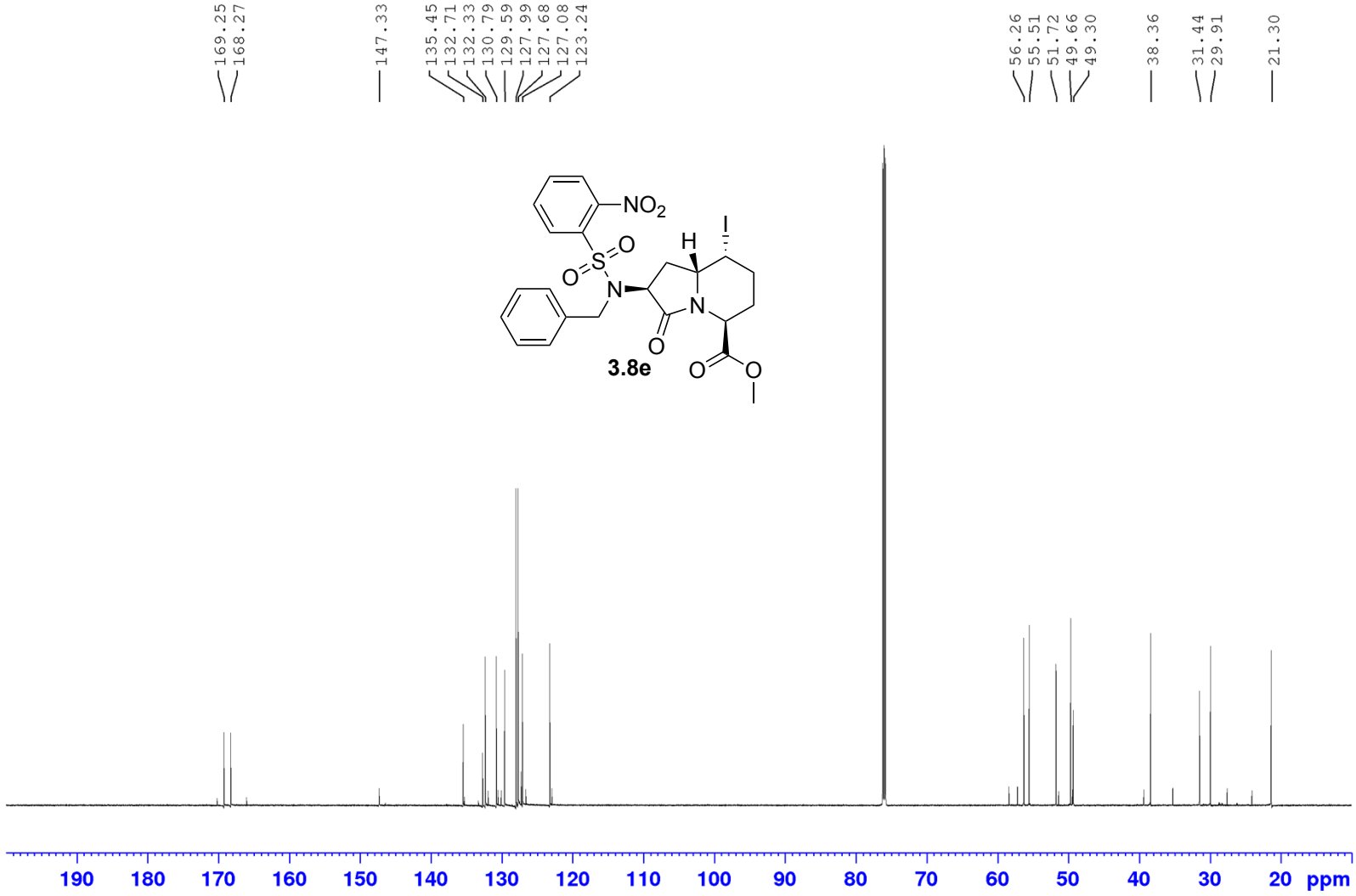

COSY 700 MHz
Solvent: $CDCl_3$

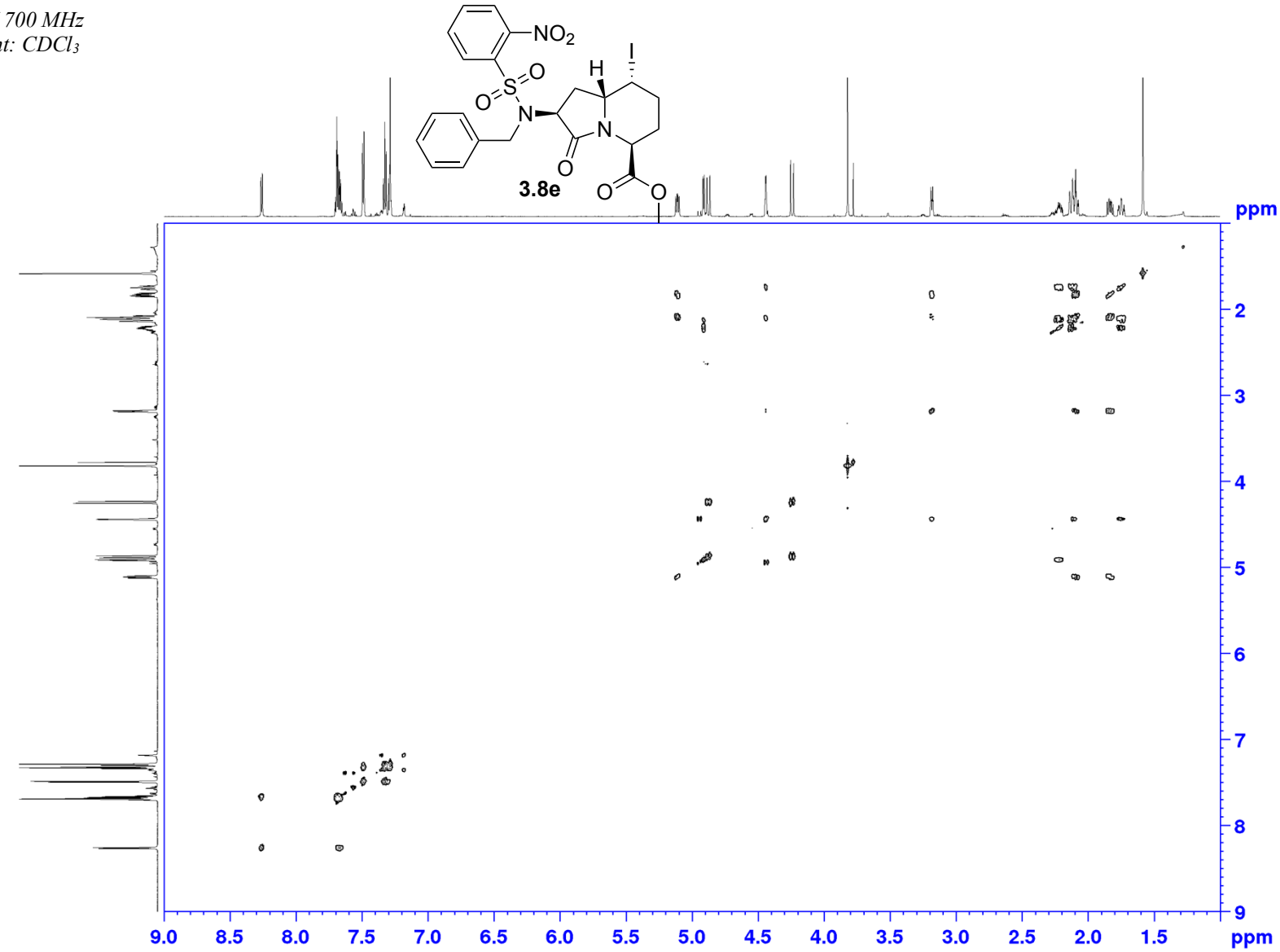

HSQC 700 MHz
Solvent: $CDCl_3$

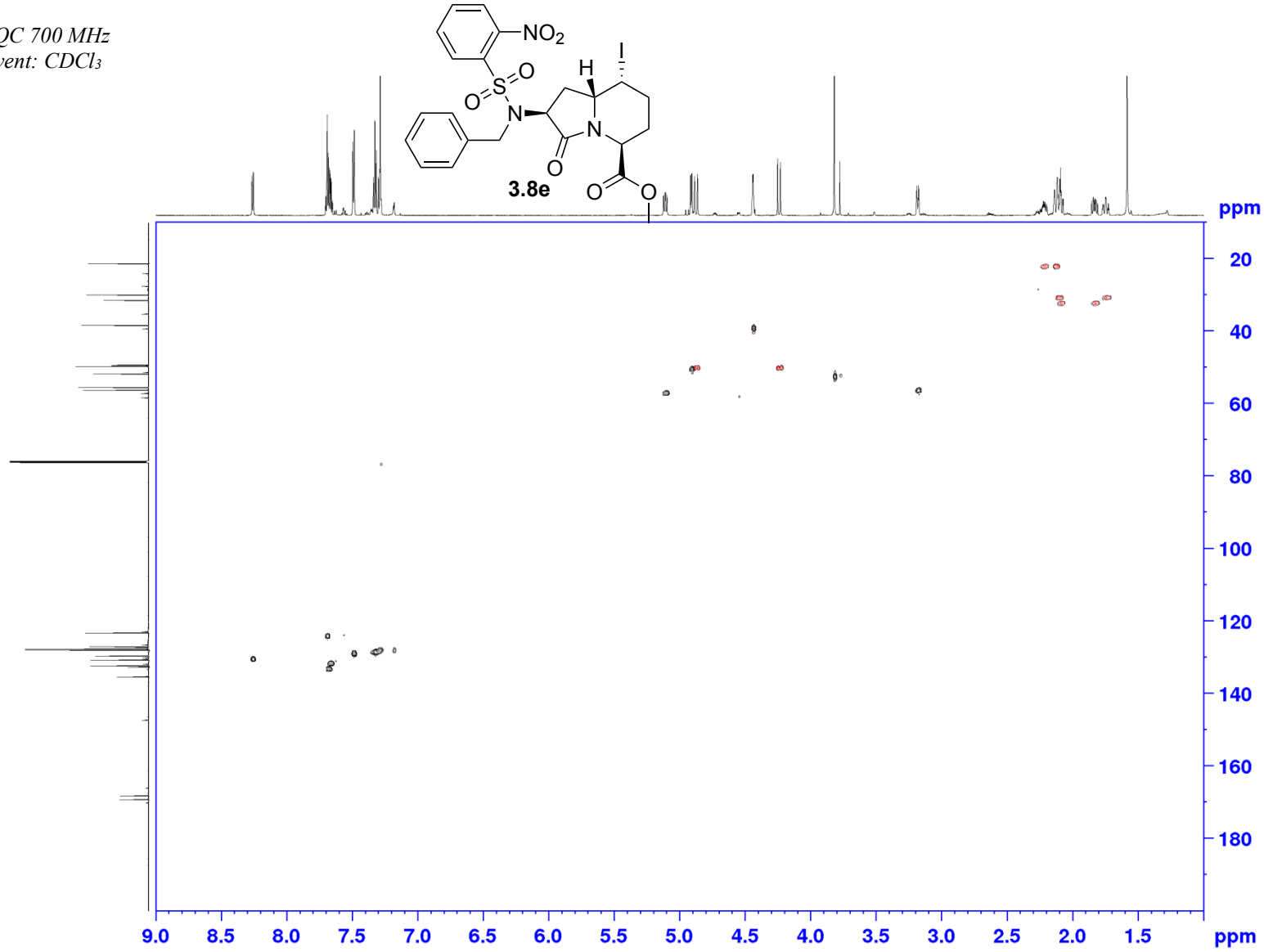

NOESY 700 MHz
Solvent: $CDCl_3$

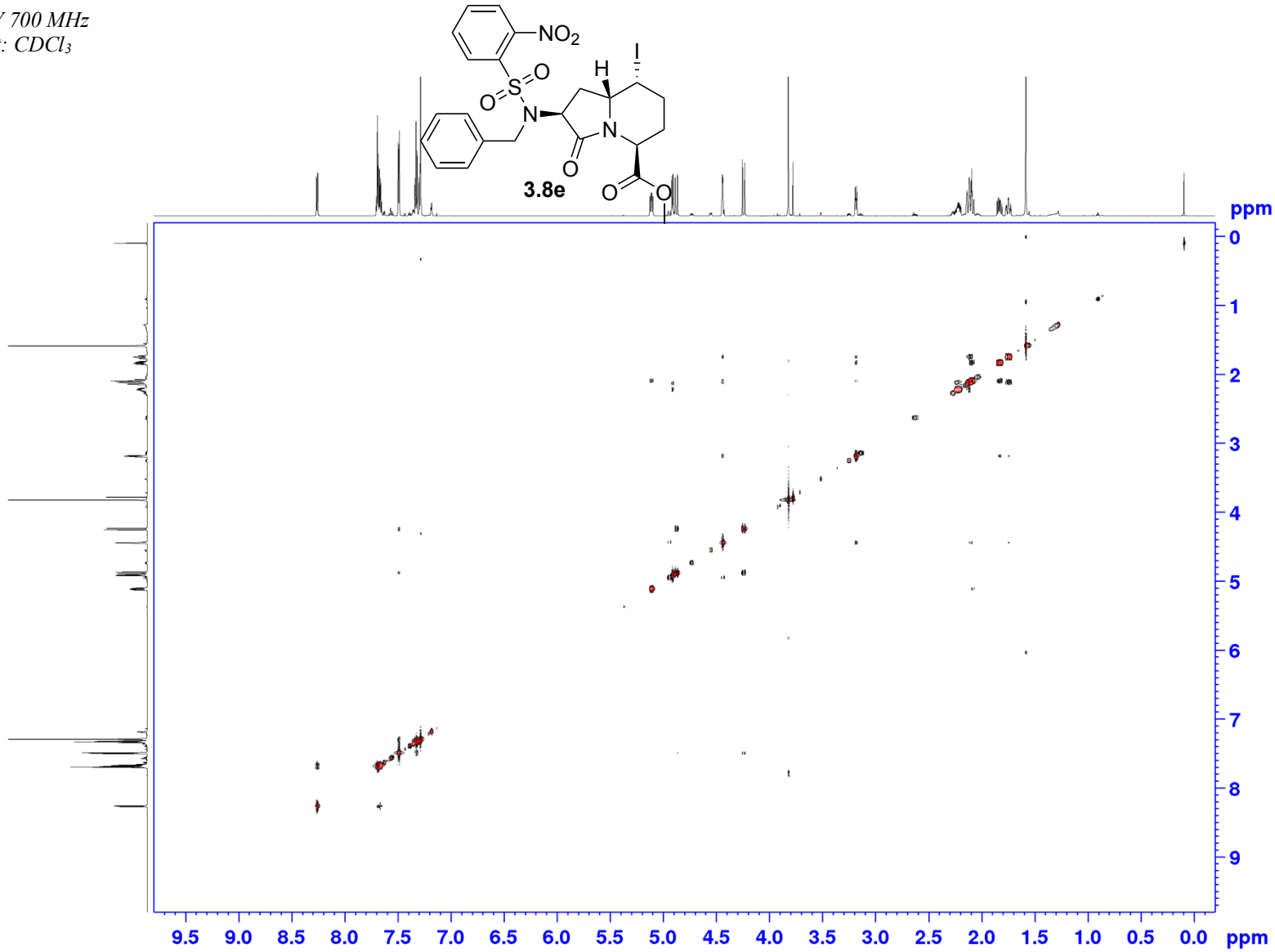

^{1}H NMR 700 MHz
Solvent: $CDCl_3$

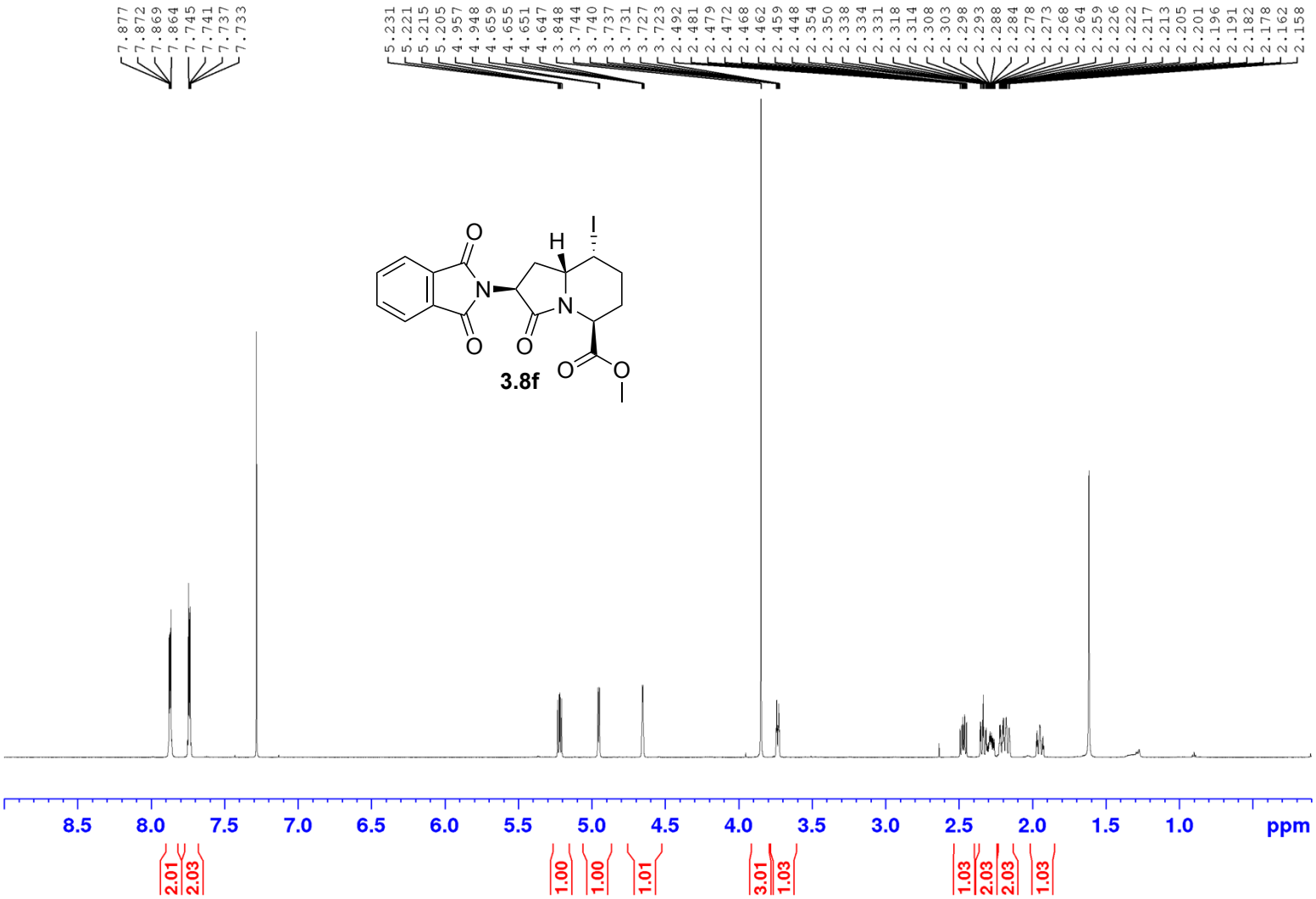

^{13}C NMR 700 MHz
Solvent: $CDCl_3$

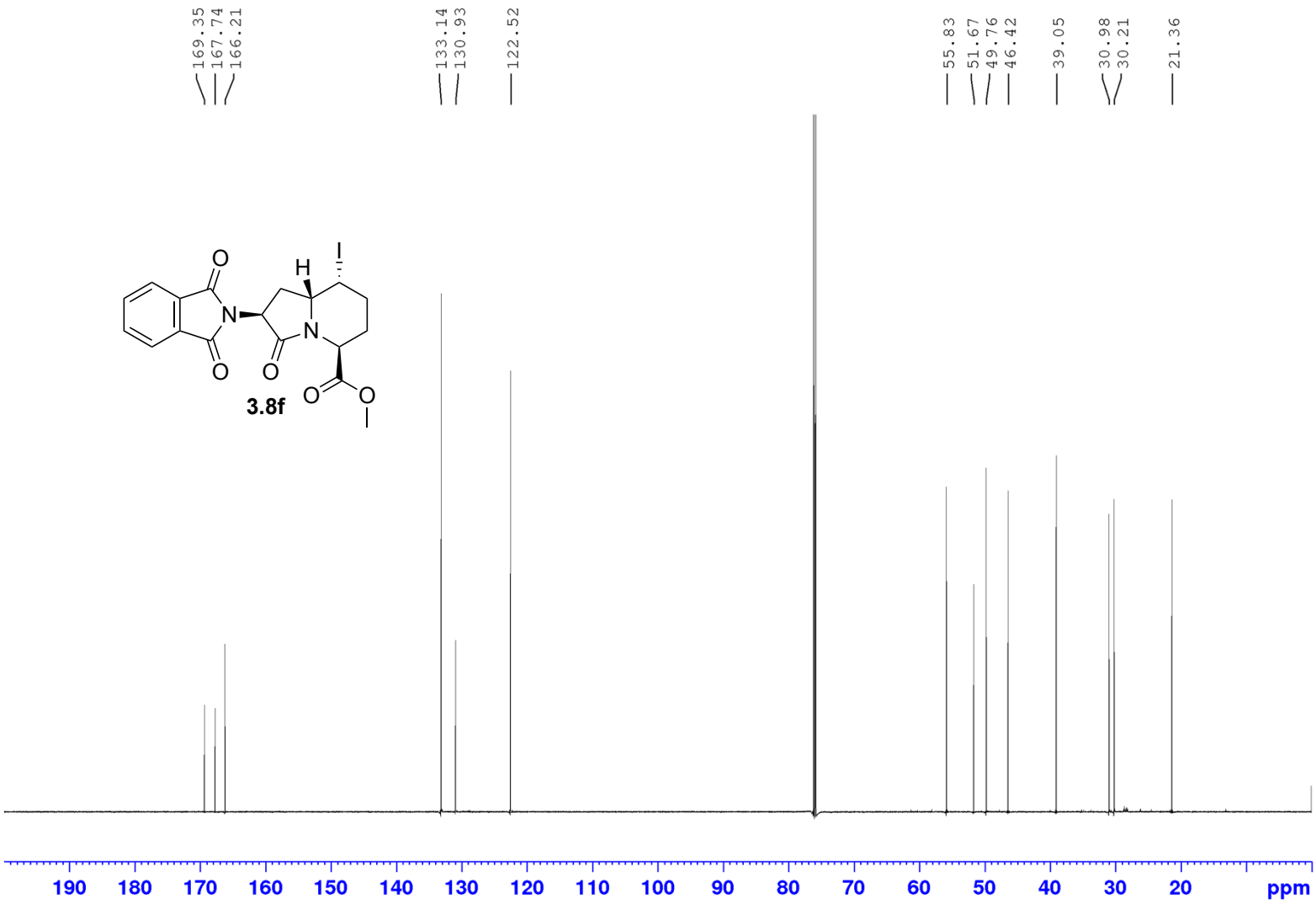

COSY 700 MHz
Solvent: $CDCl_3$

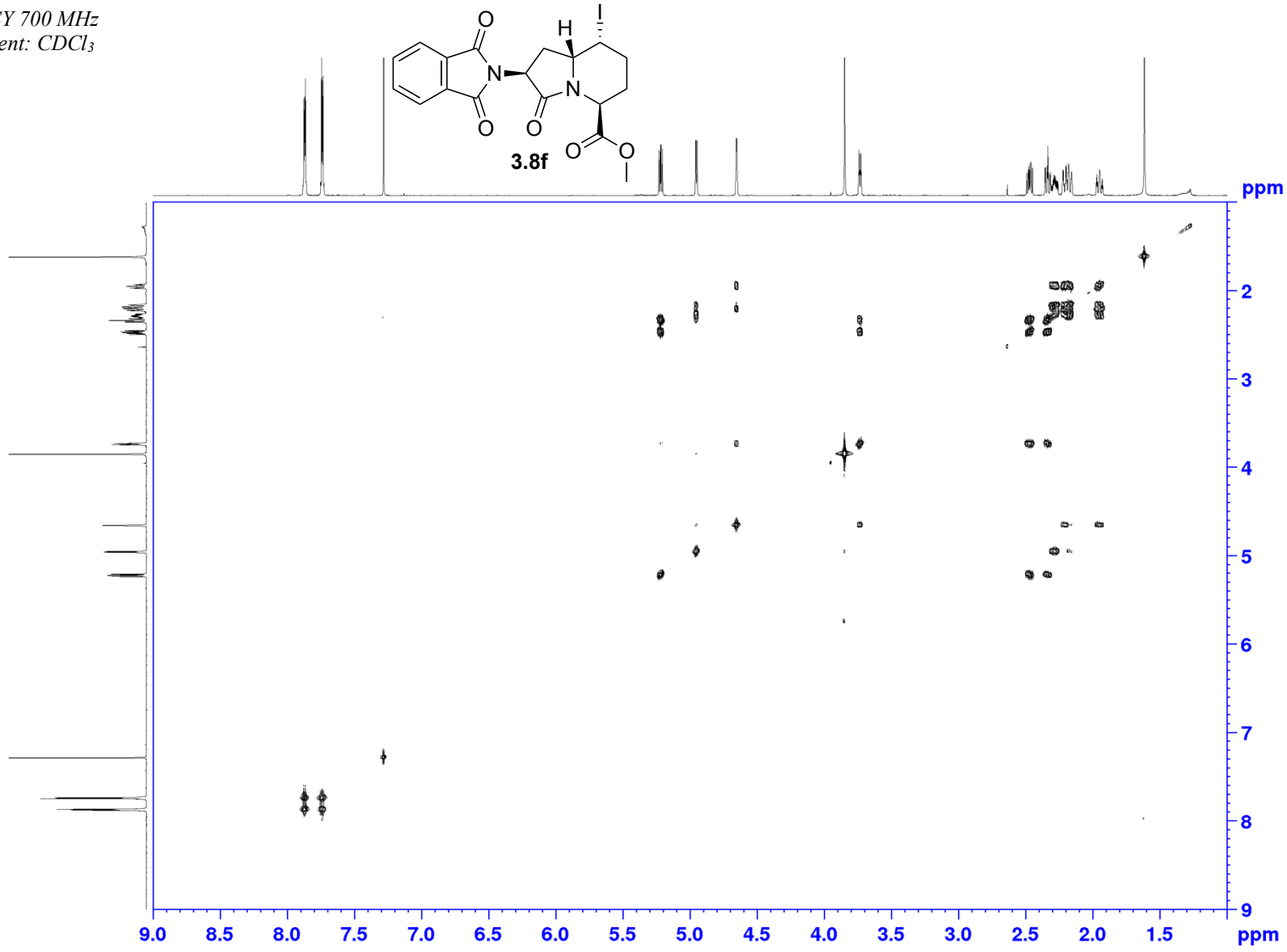

HSQC 700 MHz
Solvent: $CDCl_3$

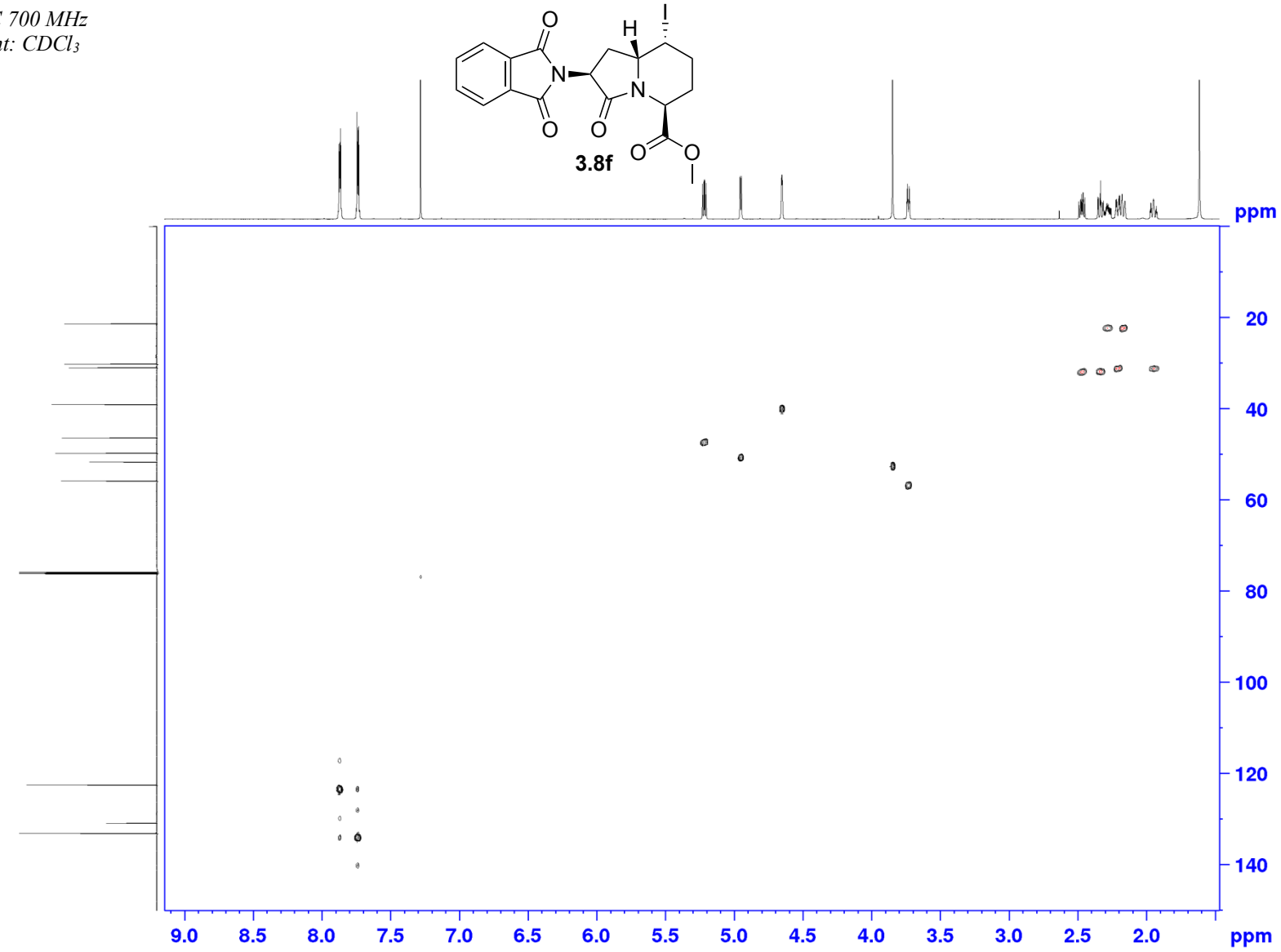

NOESY 700 MHz
Solvent: $CDCl_3$

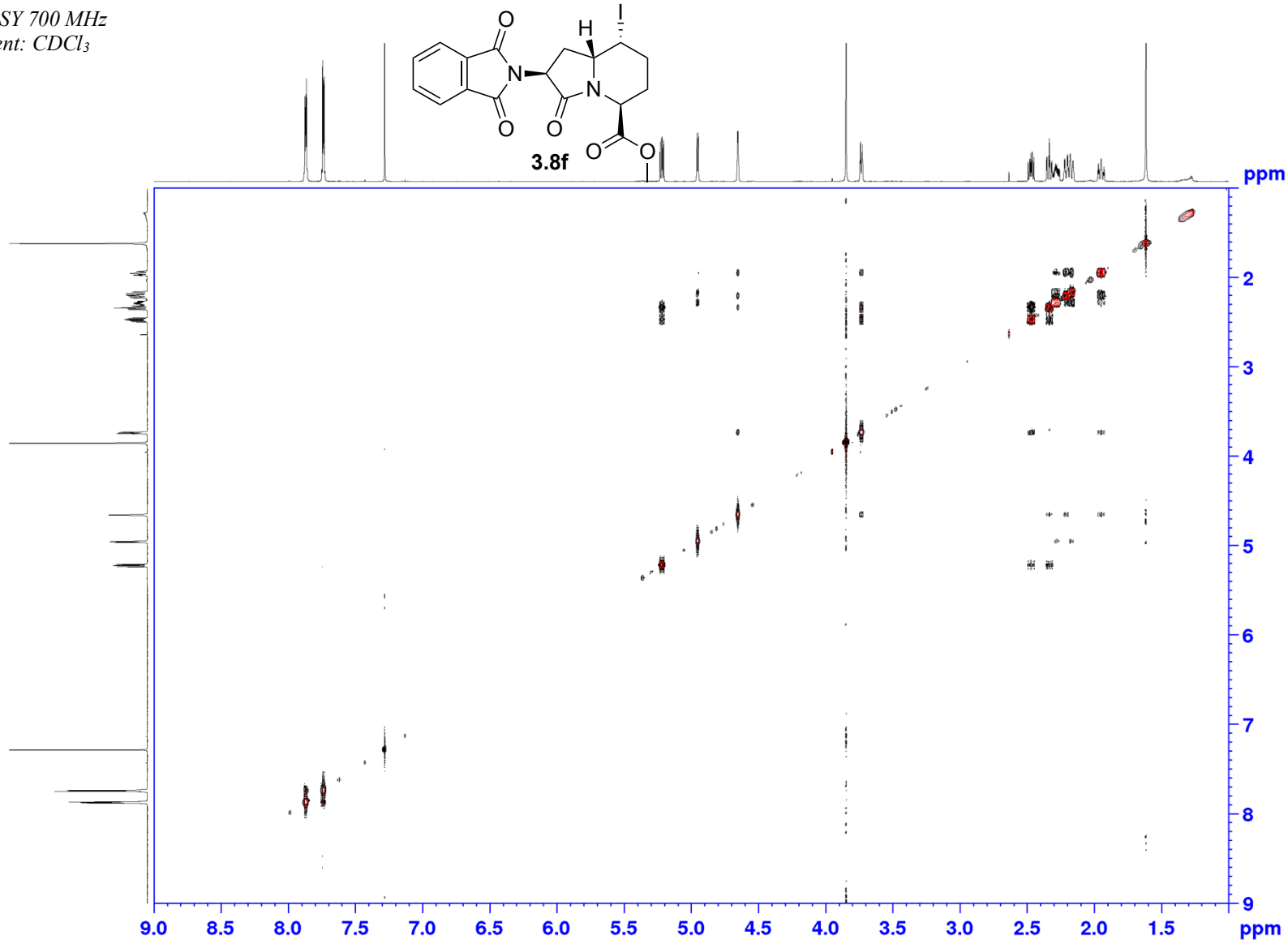

^{1}H NMR 500 MHz
Solvent: $CDCl_3$

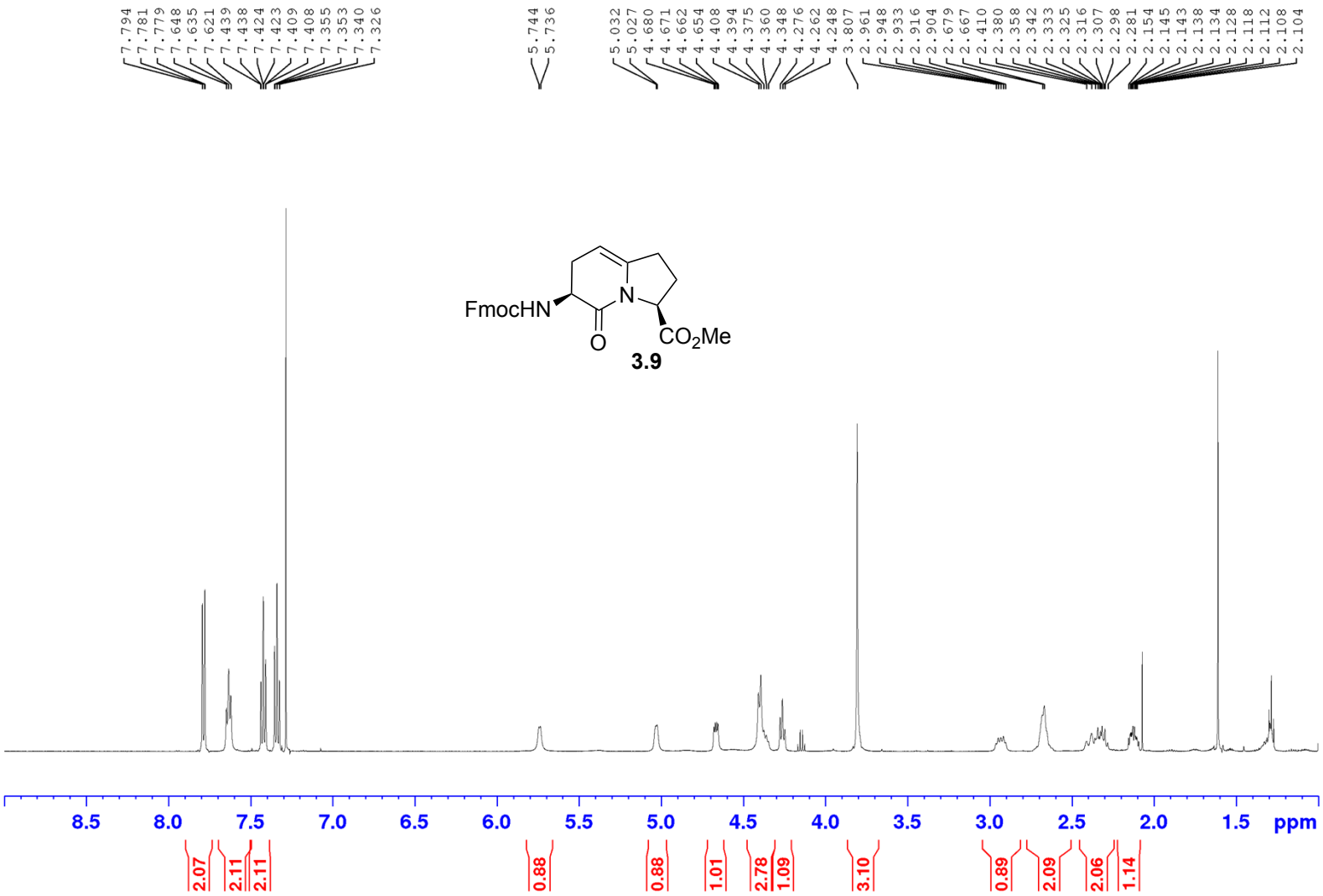

^{13}C NMR 500 MHz
Solvent: $CDCl_3$

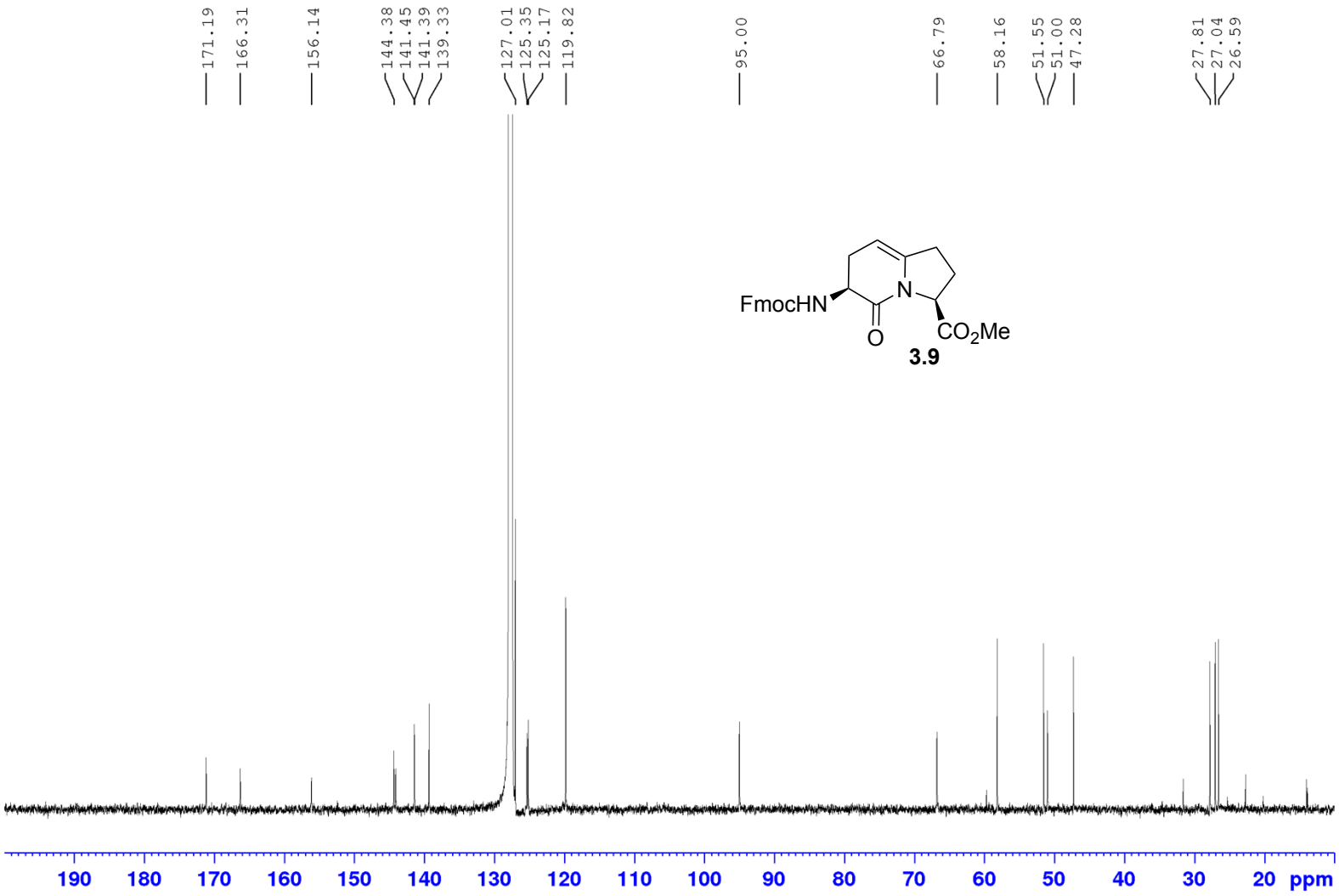

^{1}H NMR 500 MHz
Solvent: $CDCl_3$

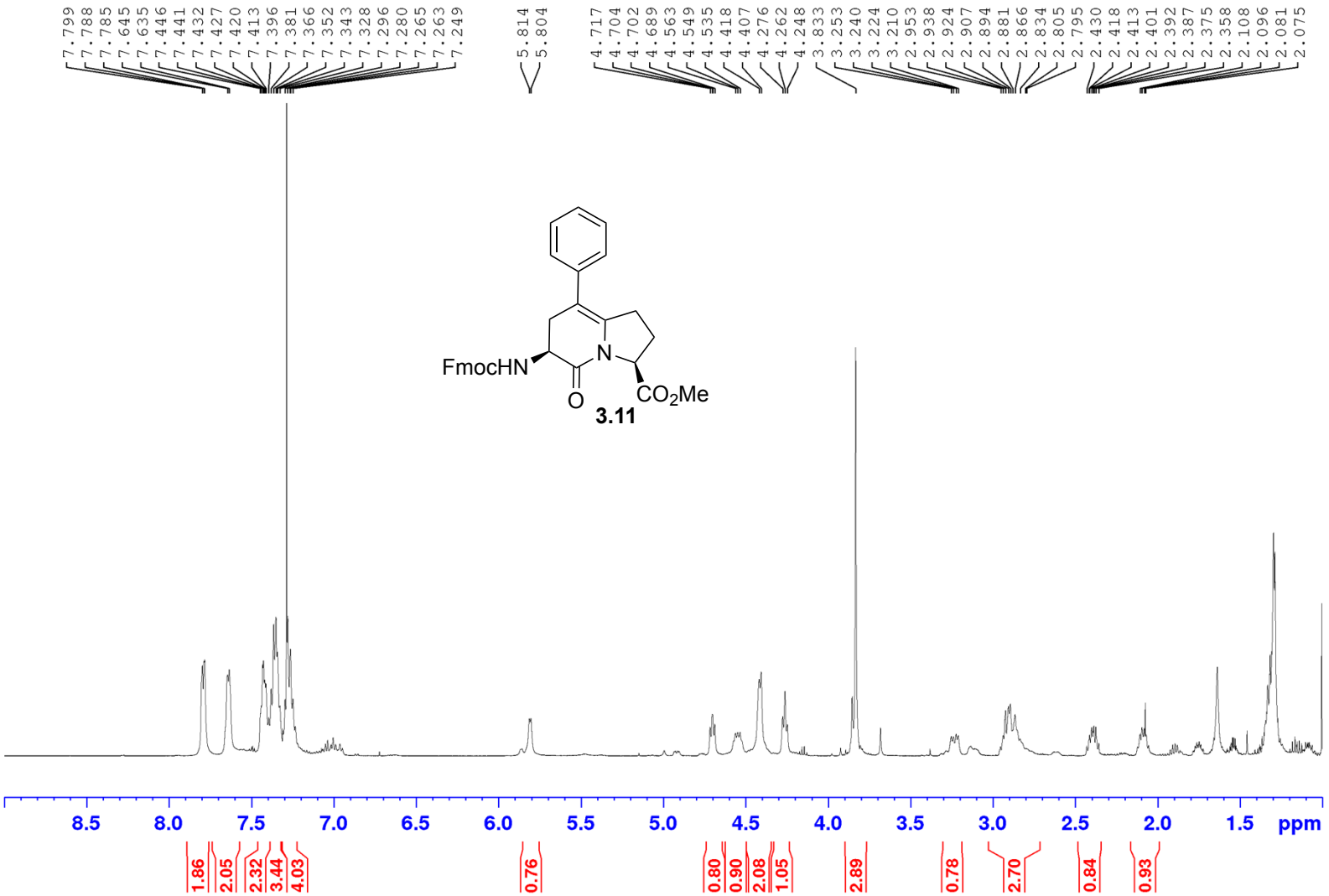

^{13}C NMR 500 MHz
Solvent: $CDCl_3$

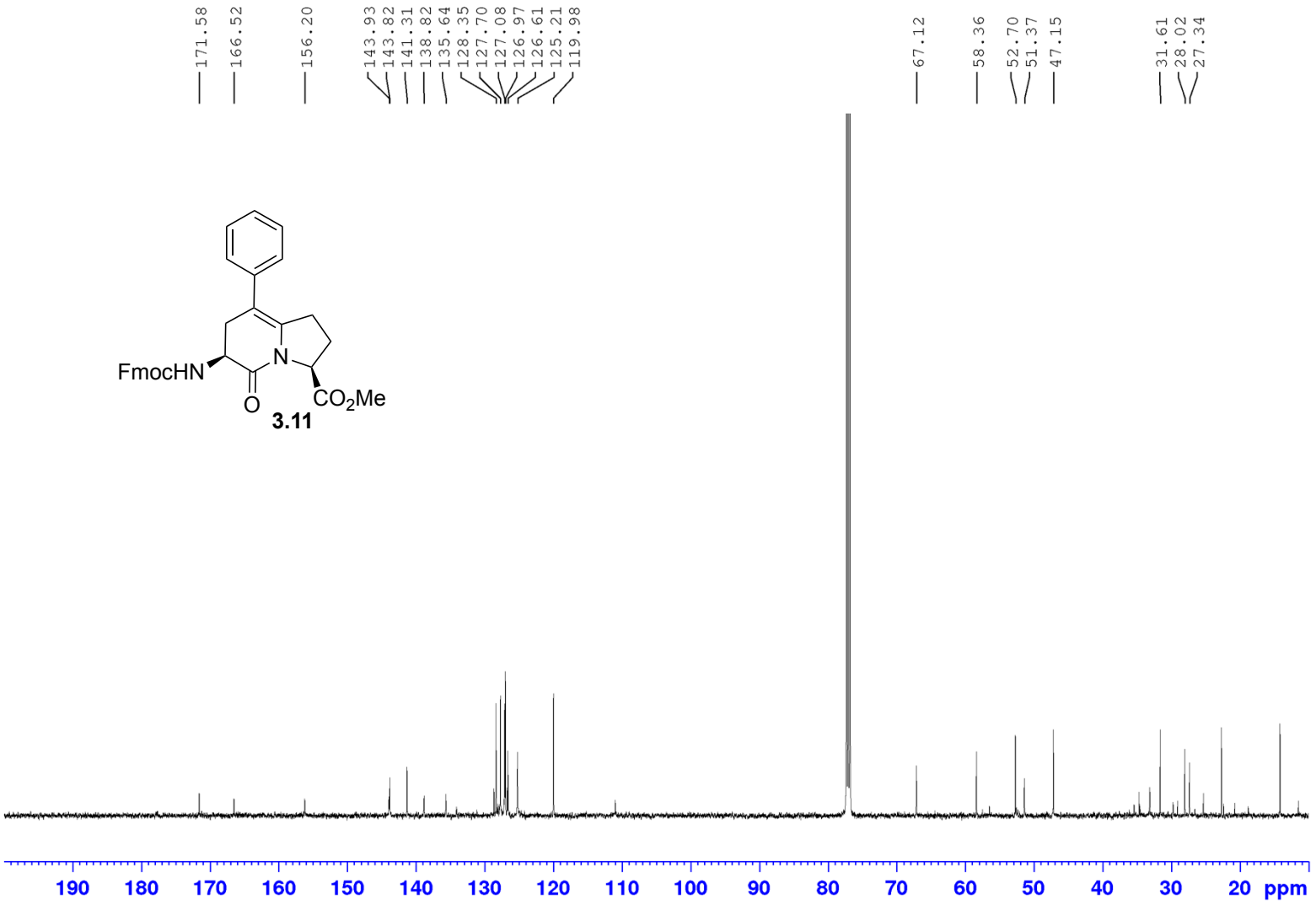

^{1}H NMR 700 MHz
Solvent: $CDCl_3$

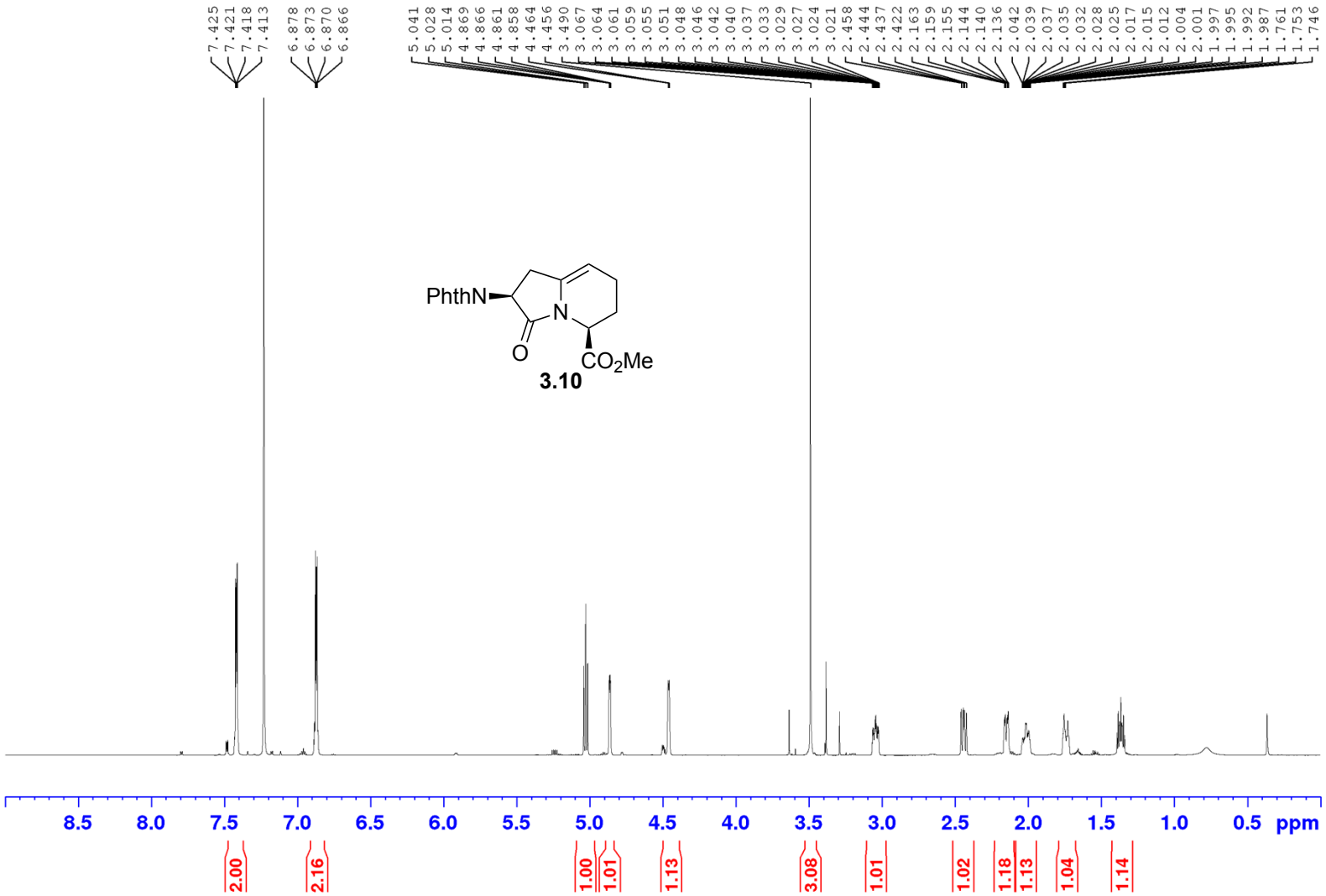

^{13}C NMR 700 MHz
Solvent: $CDCl_3$

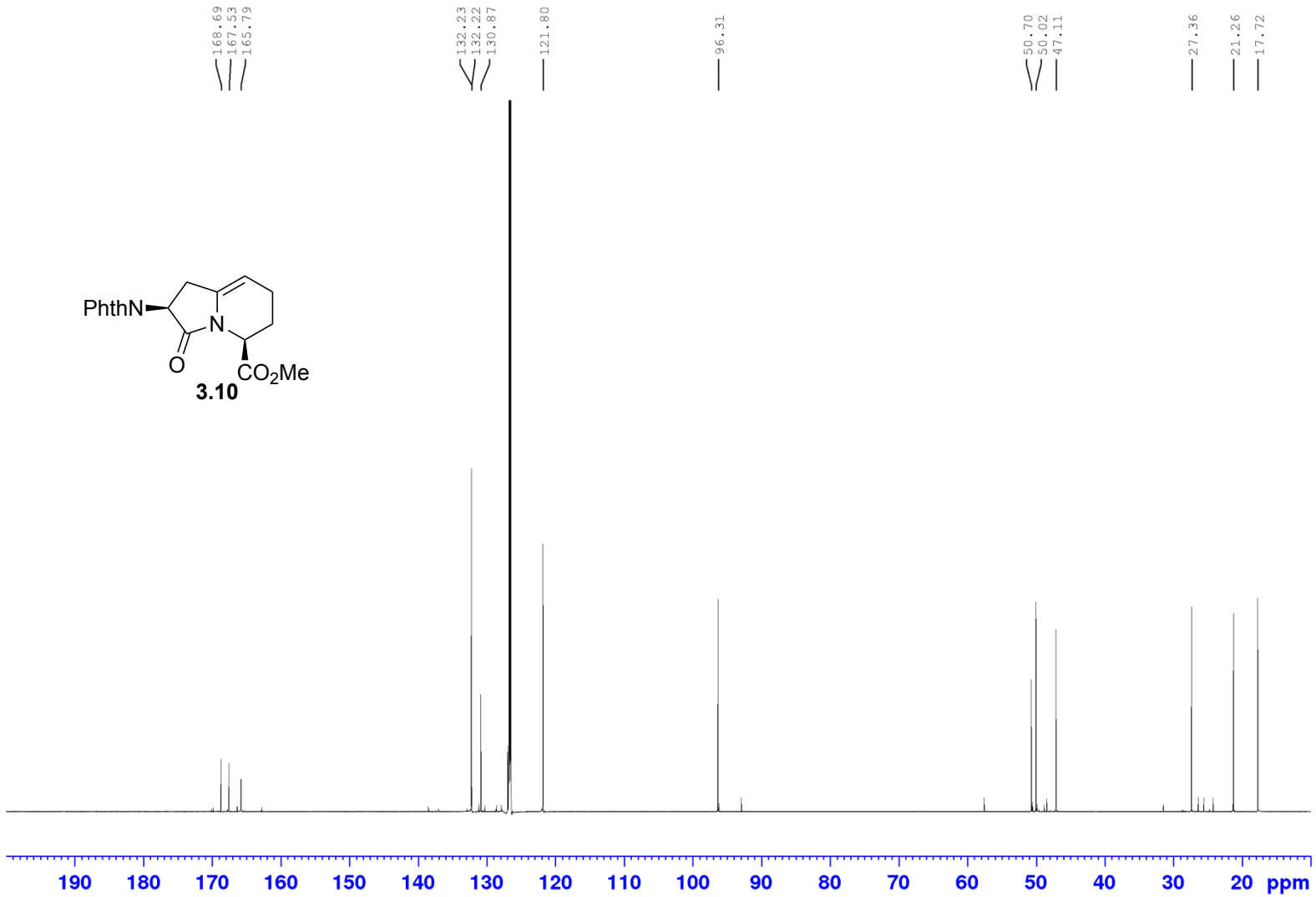

^{1}H NMR 700 MHz
Solvent: $CDCl_3$

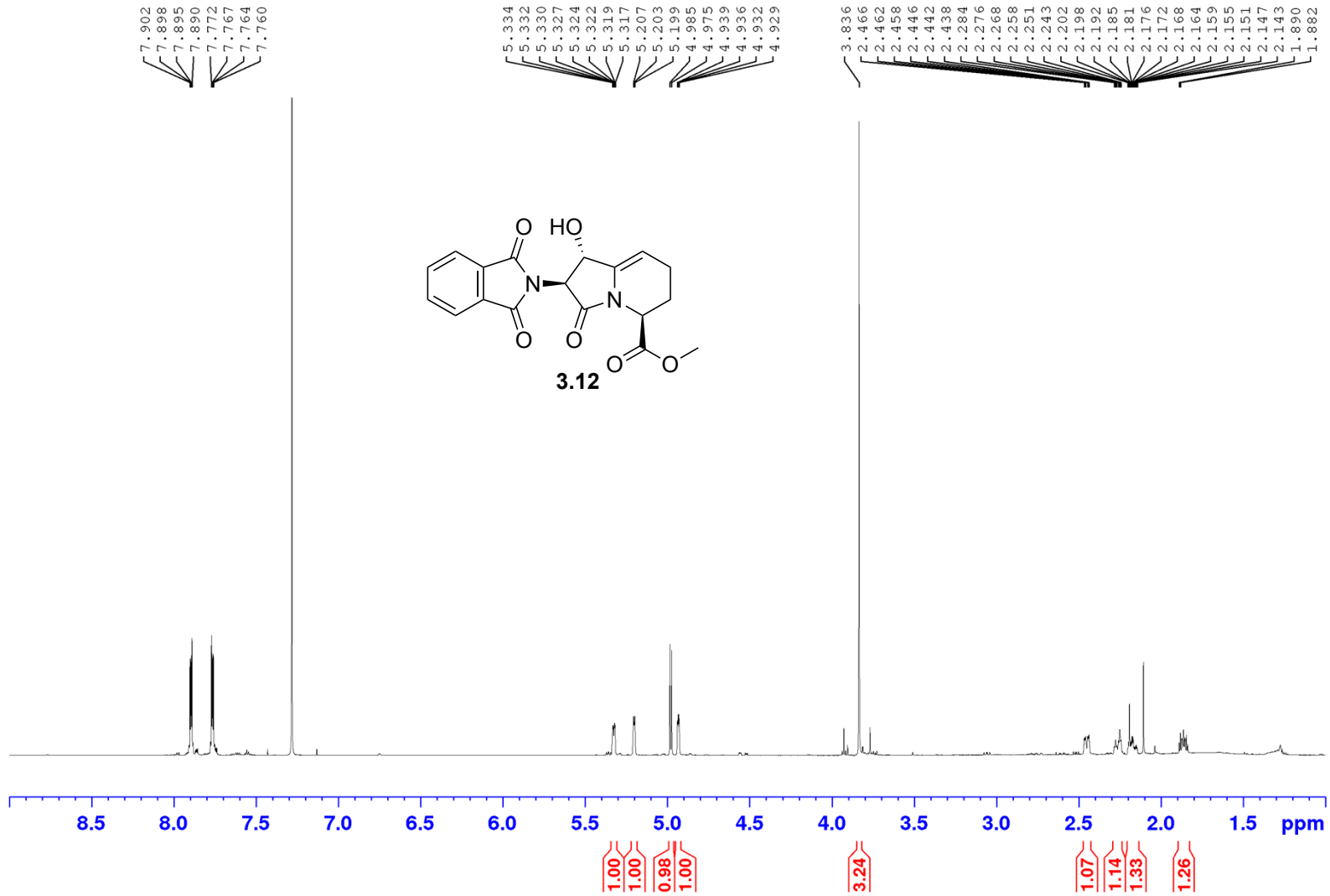

^{13}C NMR 700 MHz
Solvent: $CDCl_3$

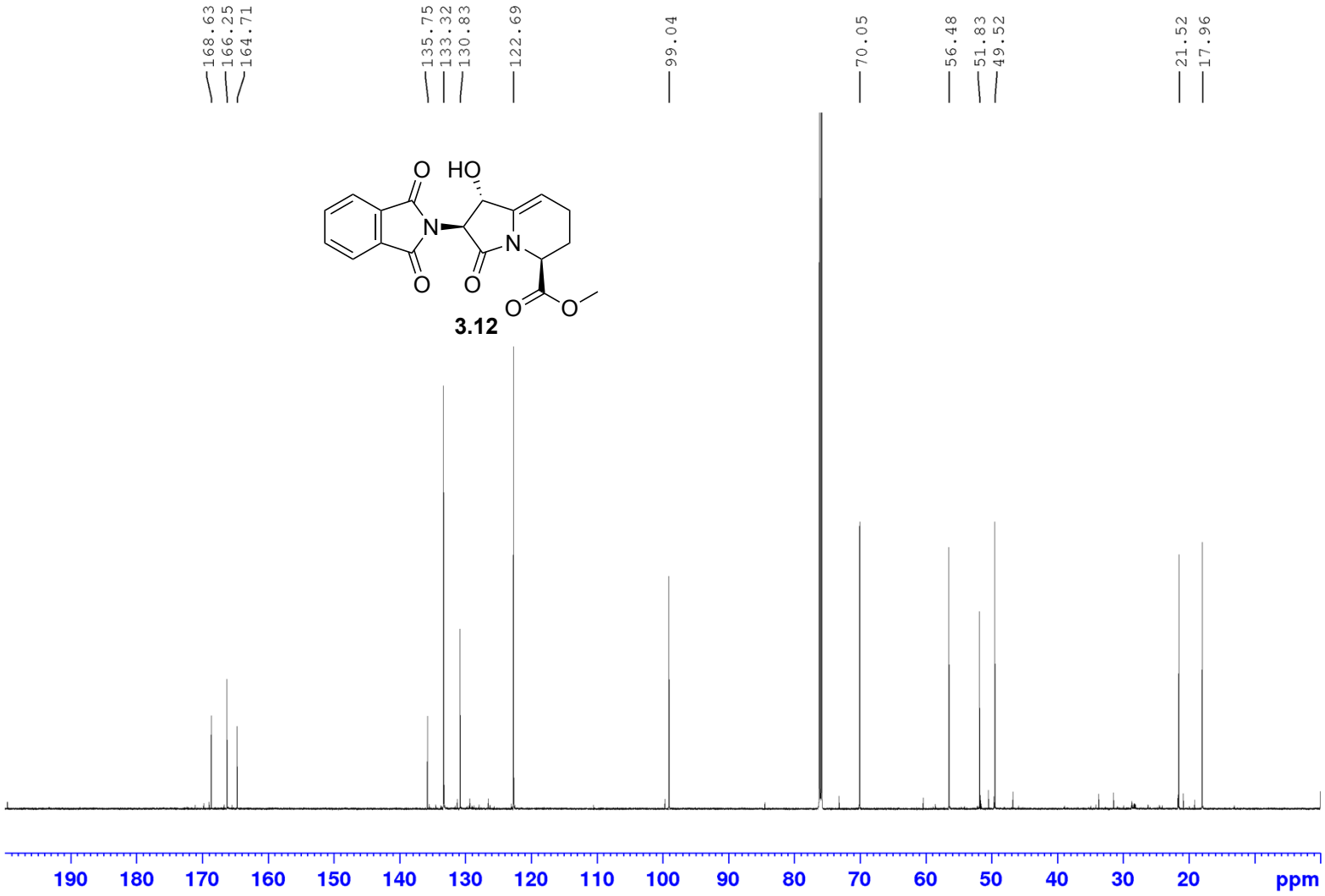

COSY 700 MHz
Solvent: $CDCl_3$

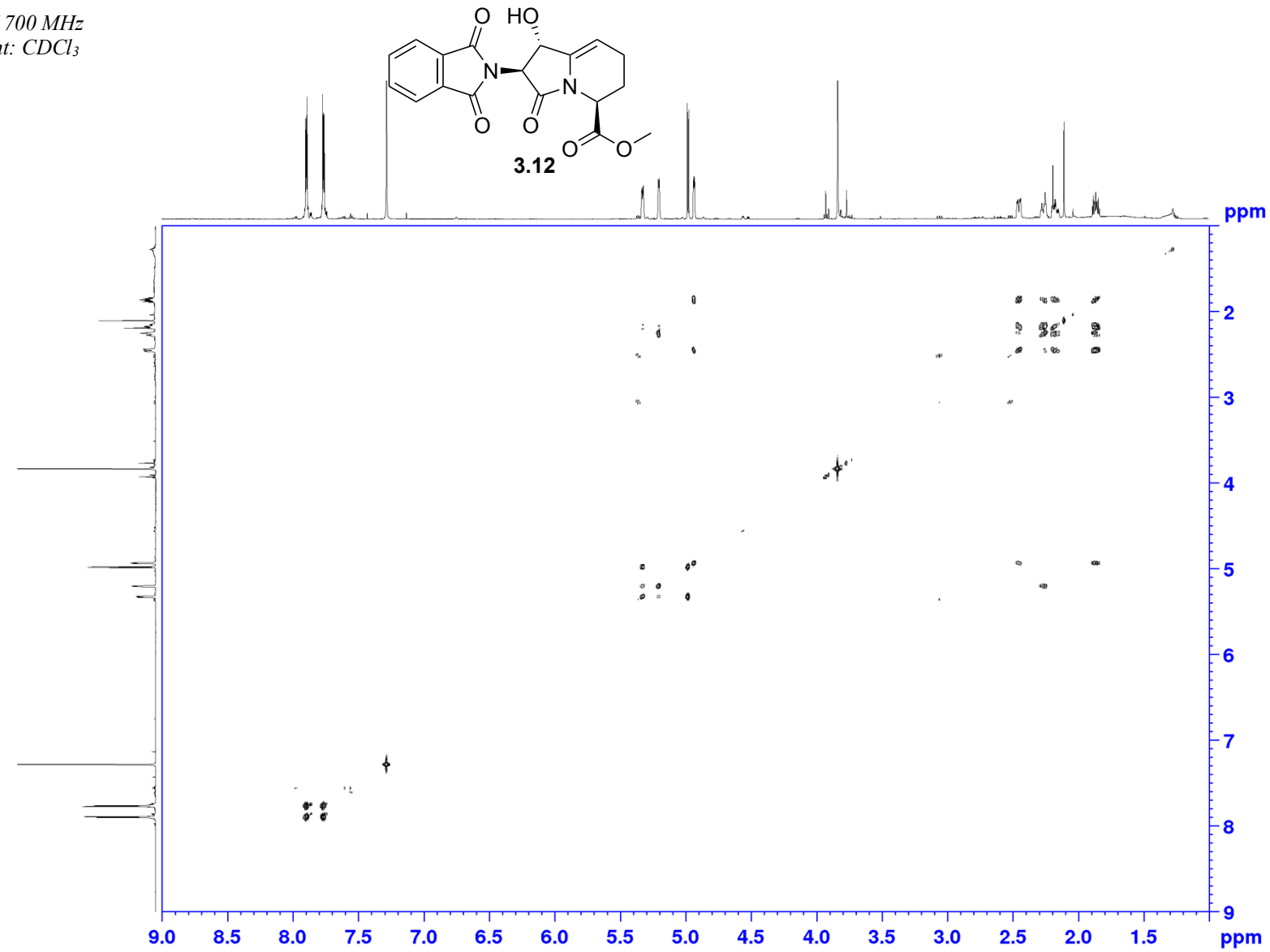

HSQC 700 MHz
Solvent: $CDCl_3$

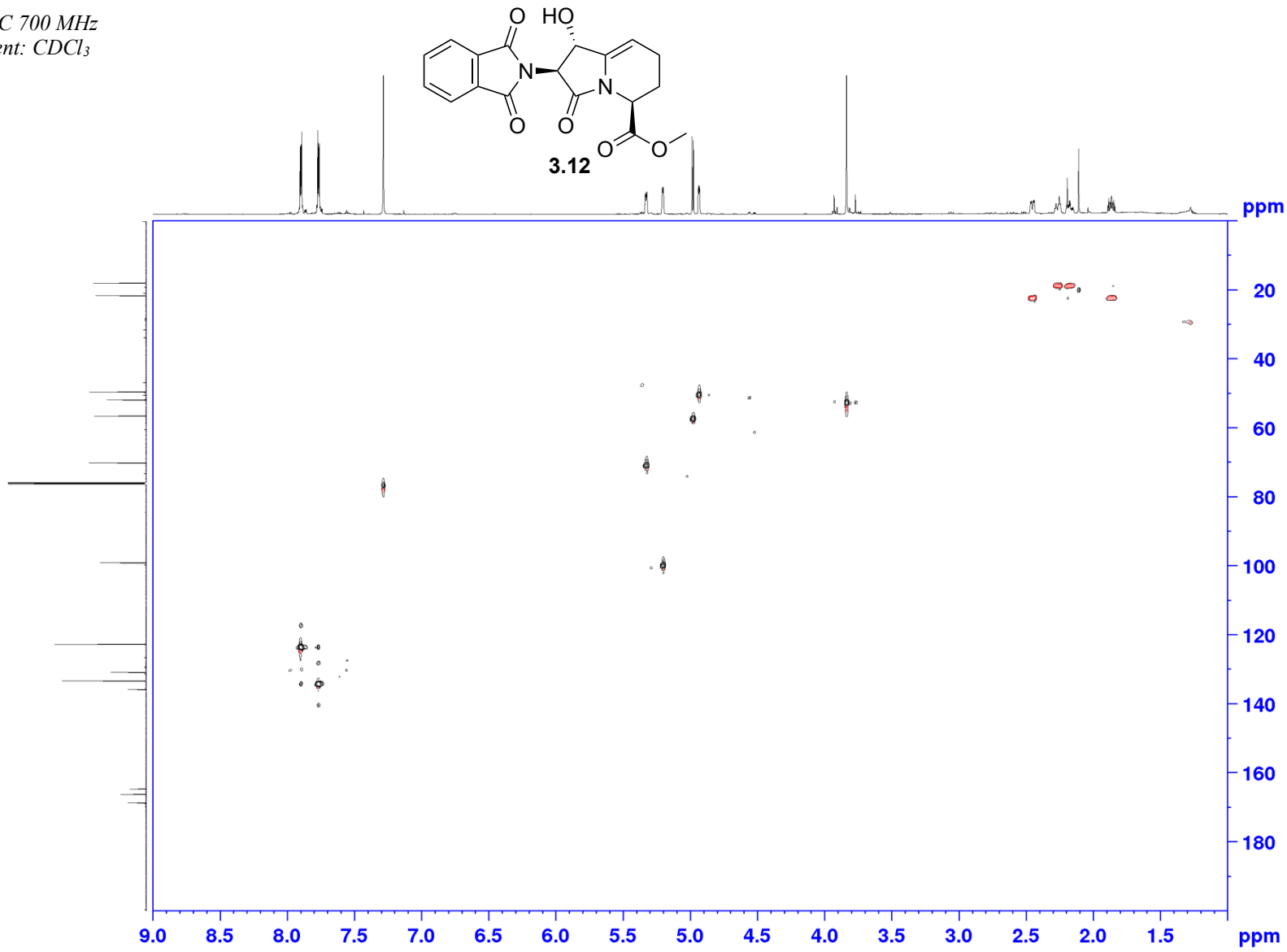

^{1}H NMR 700 MHz
Solvent: $CDCl_3$

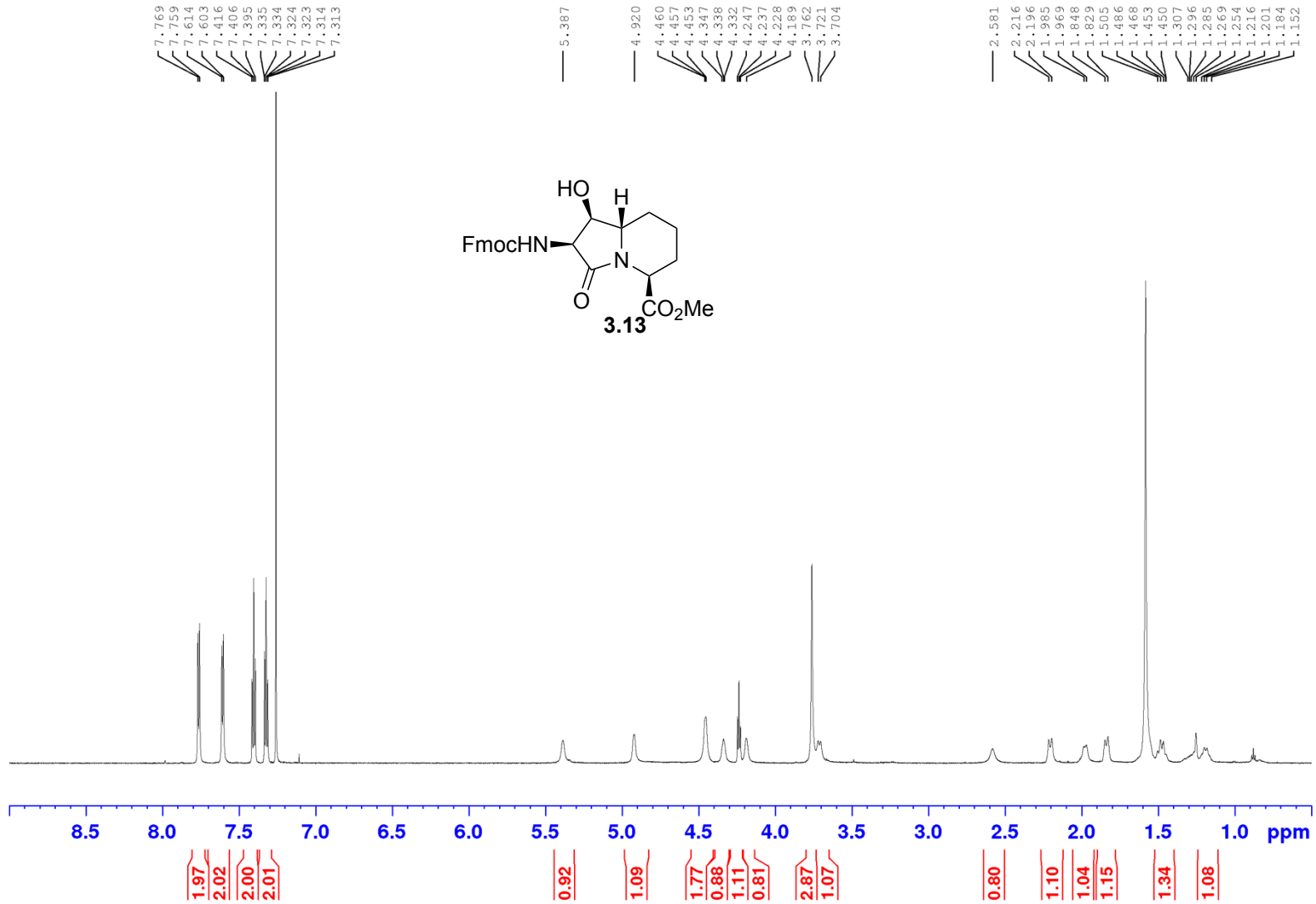

^{13}C NMR 700 MHz
Solvent: $CDCl_3$

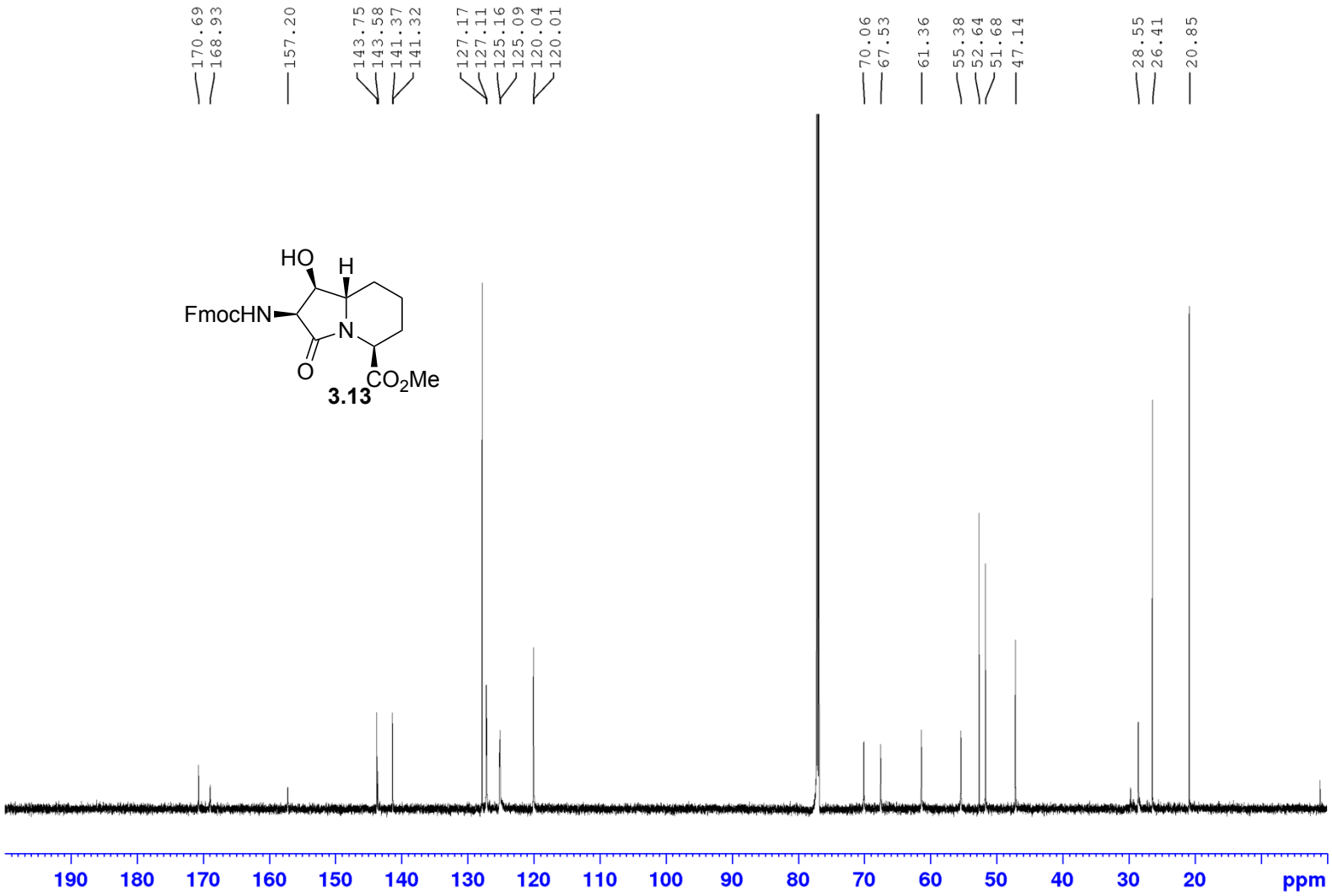

^{1}H NMR 700 MHz
Solvent: DMSO-d_6

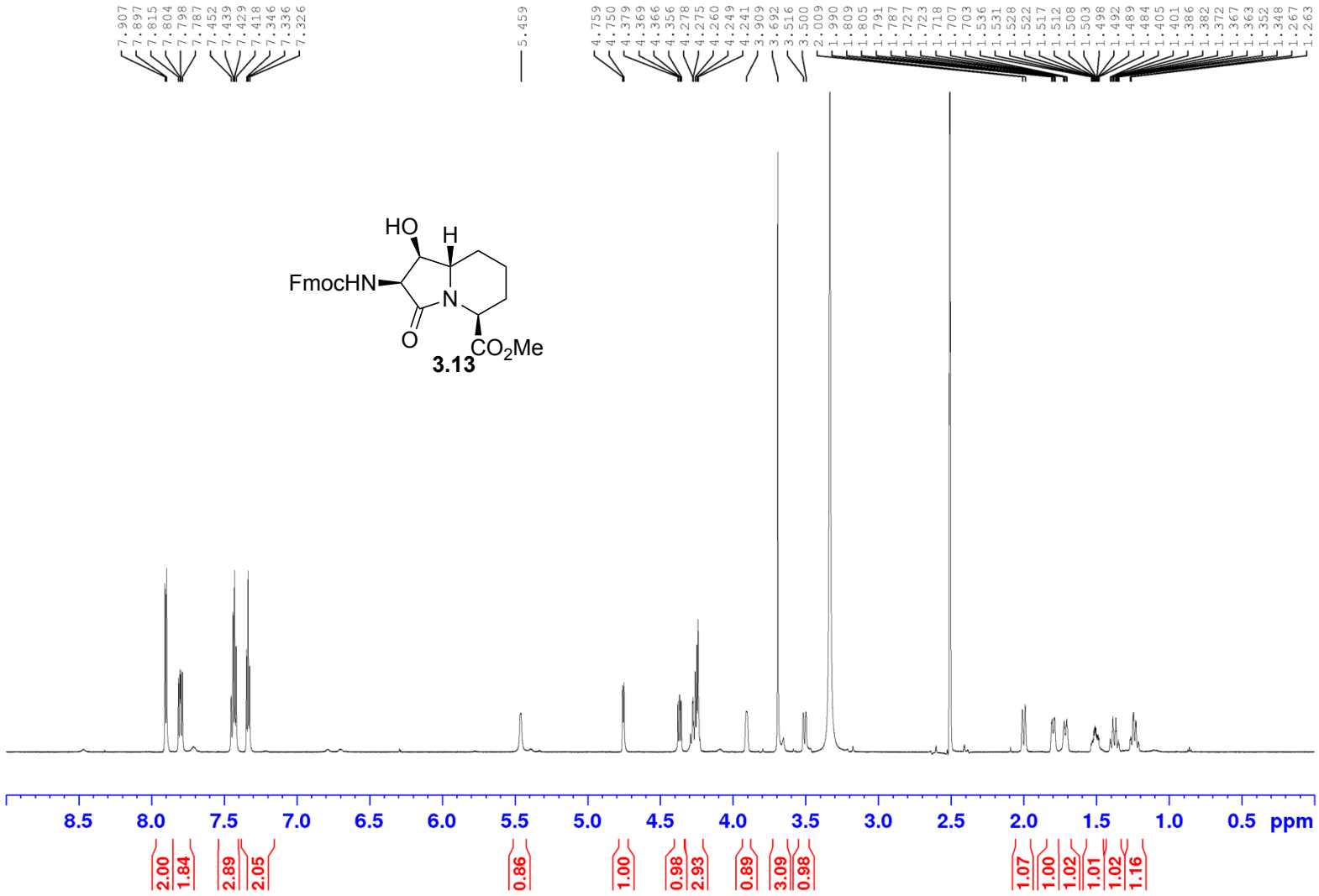

^{13}C NMR 700 MHz
Solvent: DMSO-d_6

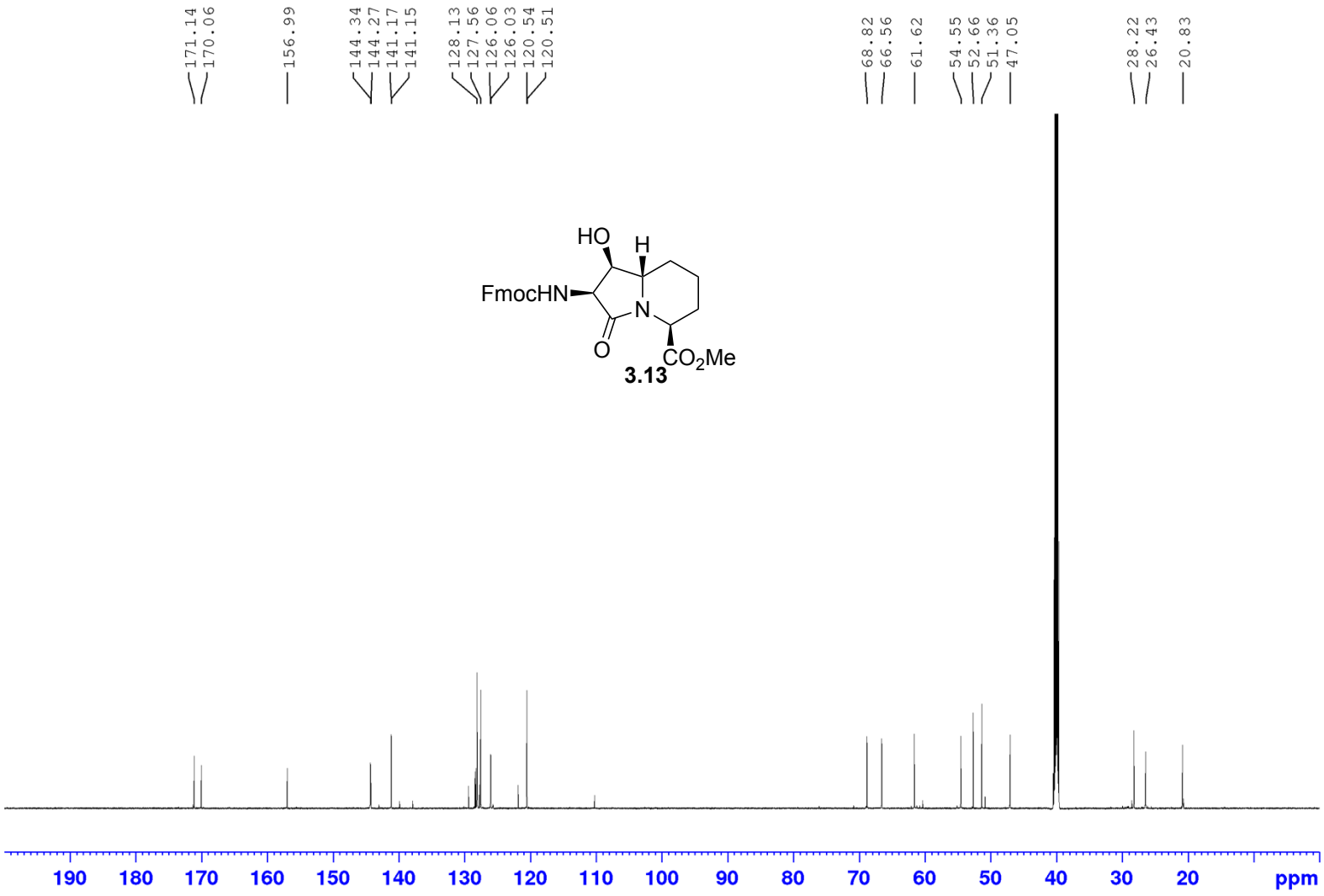

COSY 700 MHz
Solvent: DMSO-d_6

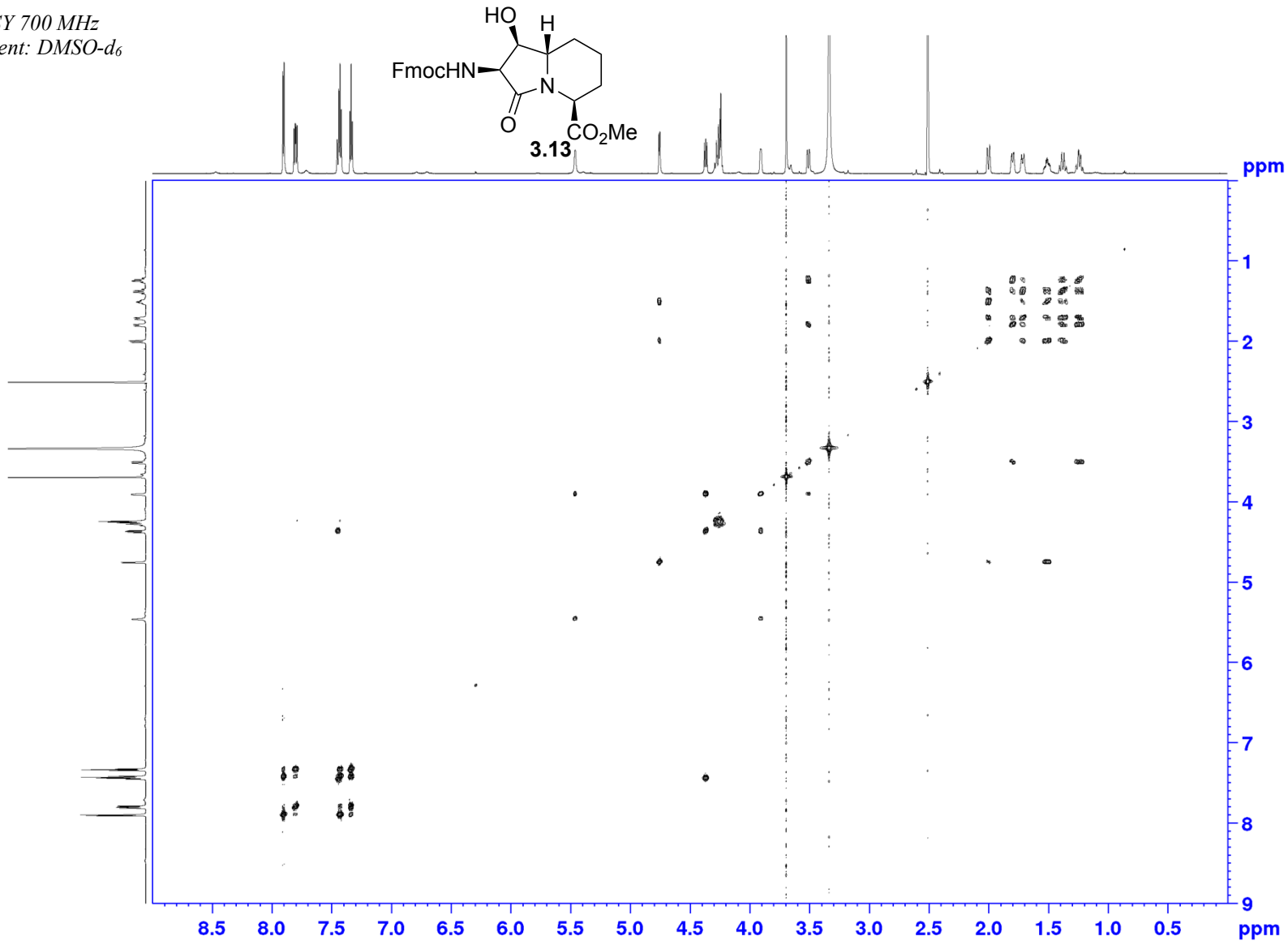

HSQC 700 MHz
Solvent: DMSO-d_6

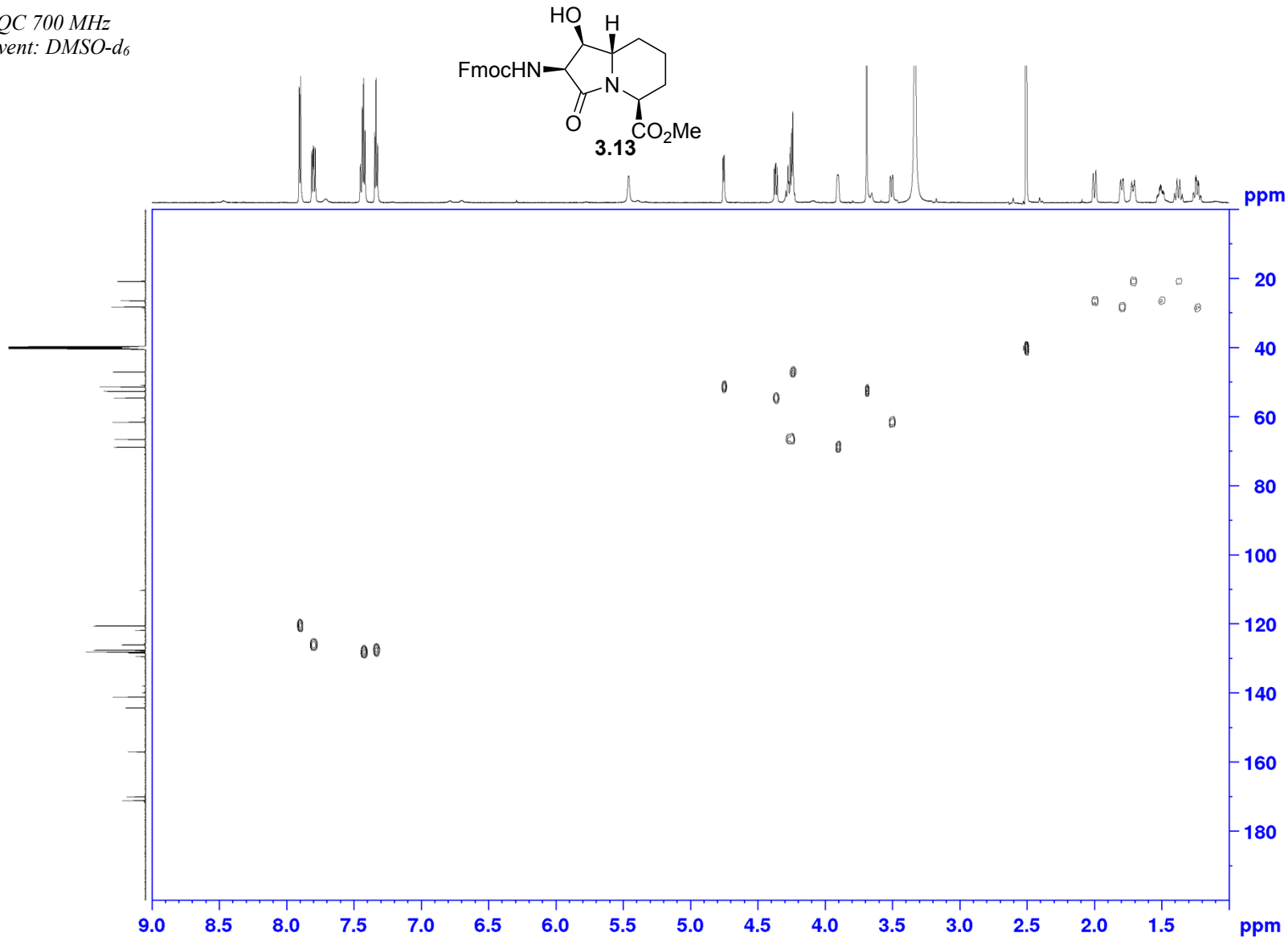

NOESY 700 MHz
Solvent: DMSO-d_6

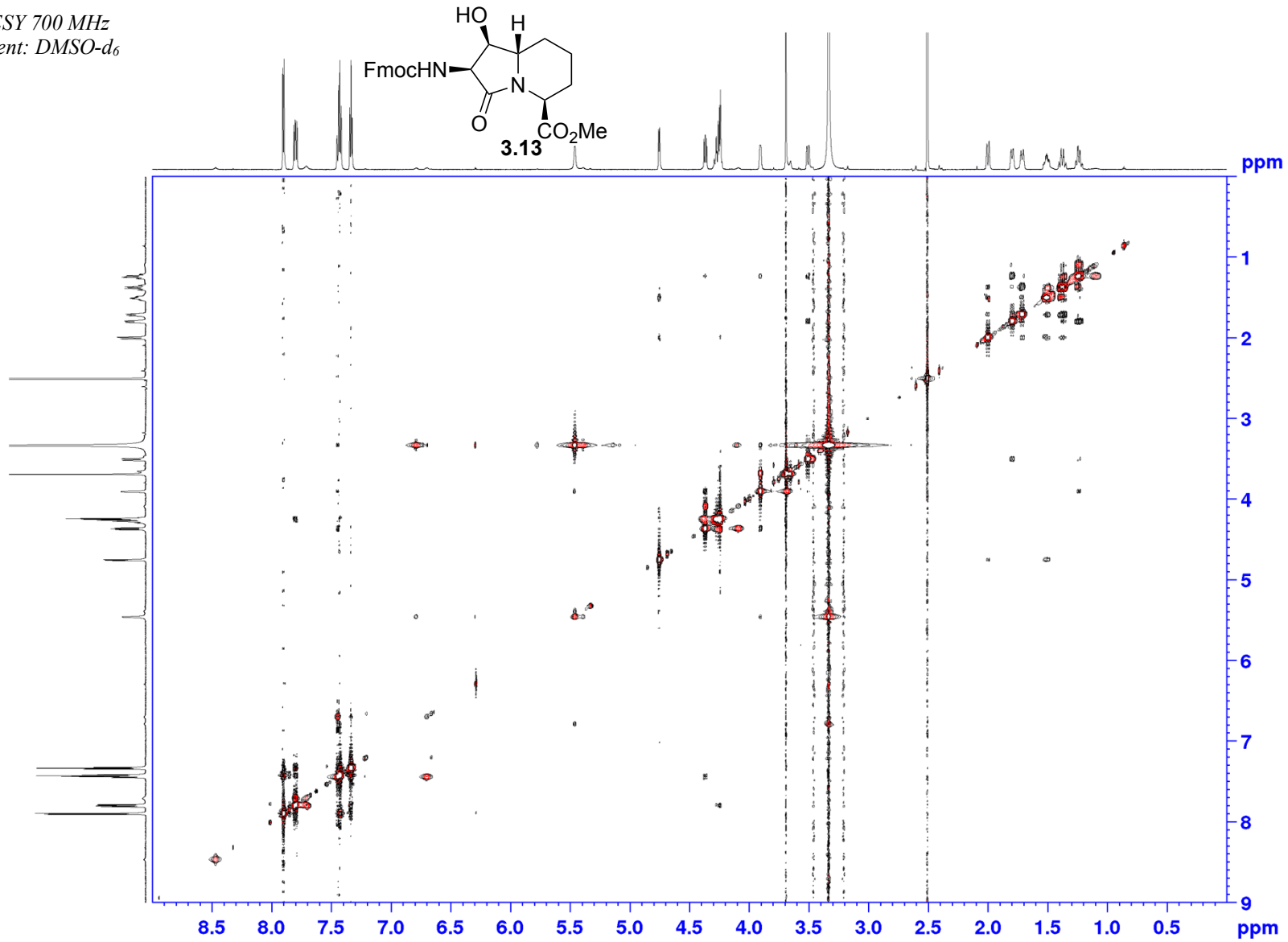

Spectral data for article 3

^{1}H NMR 700 MHz
Solvent: $CDCl_3$

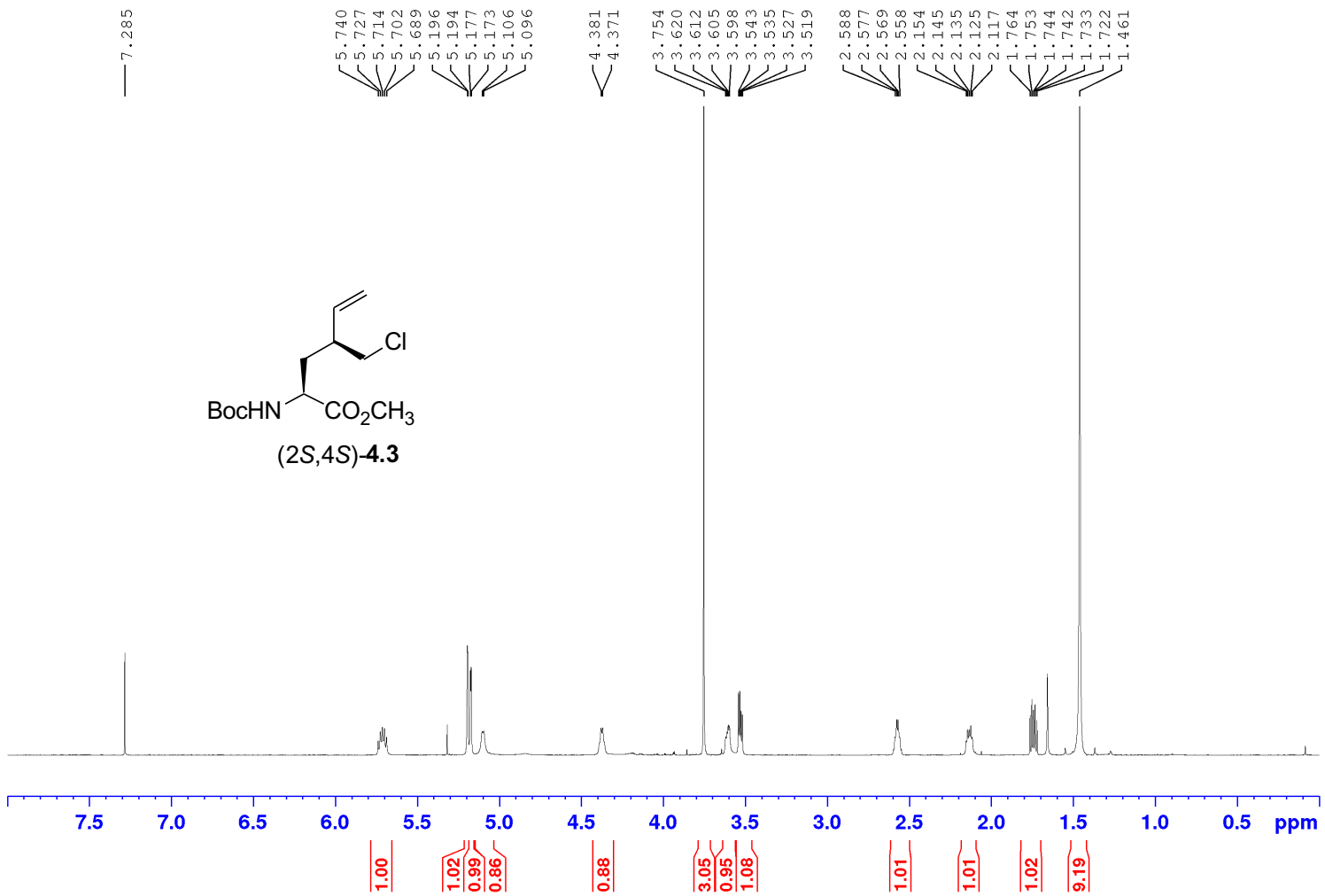

^{13}C NMR 175 MHz
Solvent: $CDCl_3$

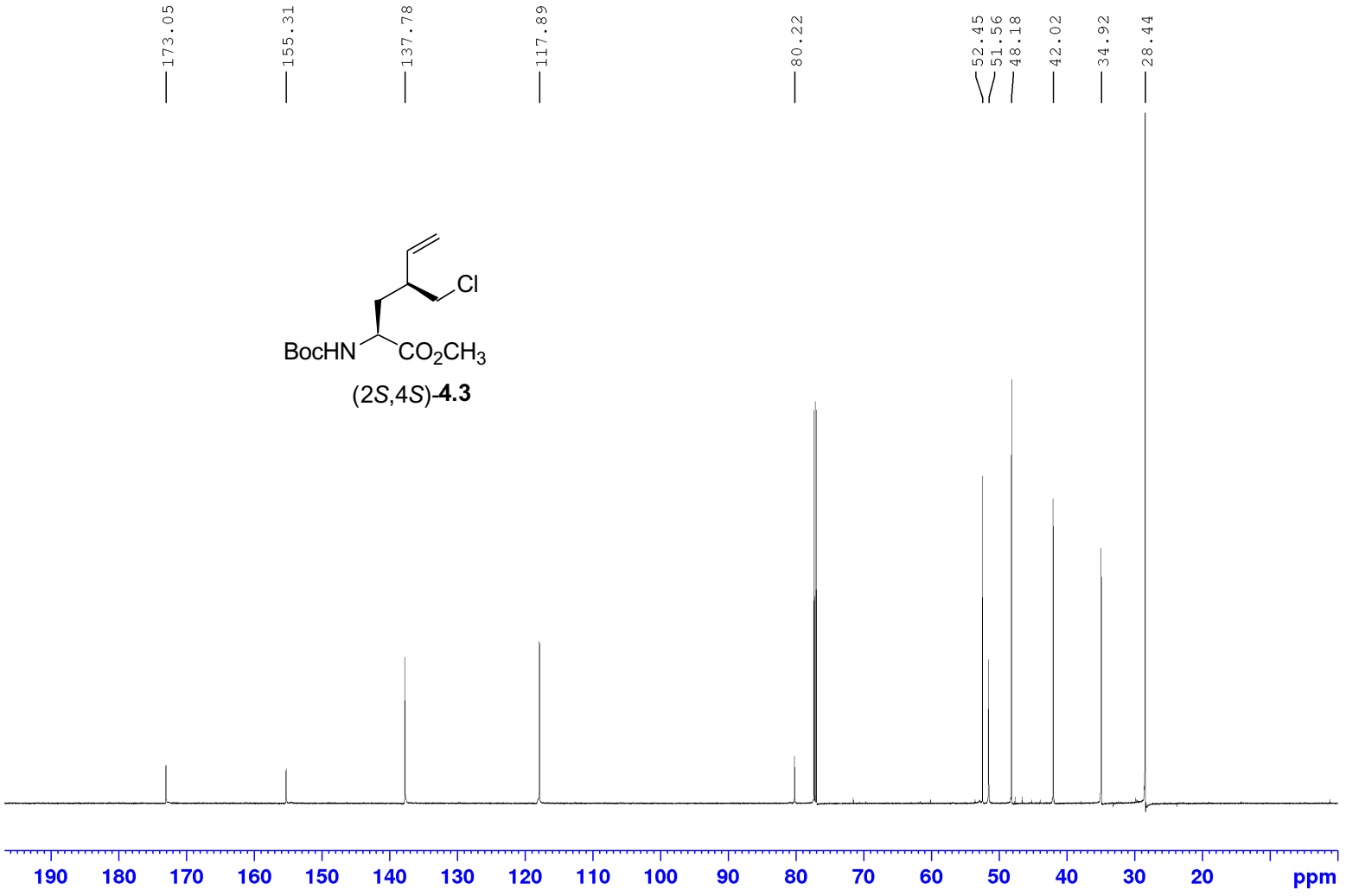

COSY 700 MHz
Solvent: $CDCl_3$

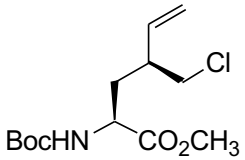

(2*S*,4*S*)-**4.3**

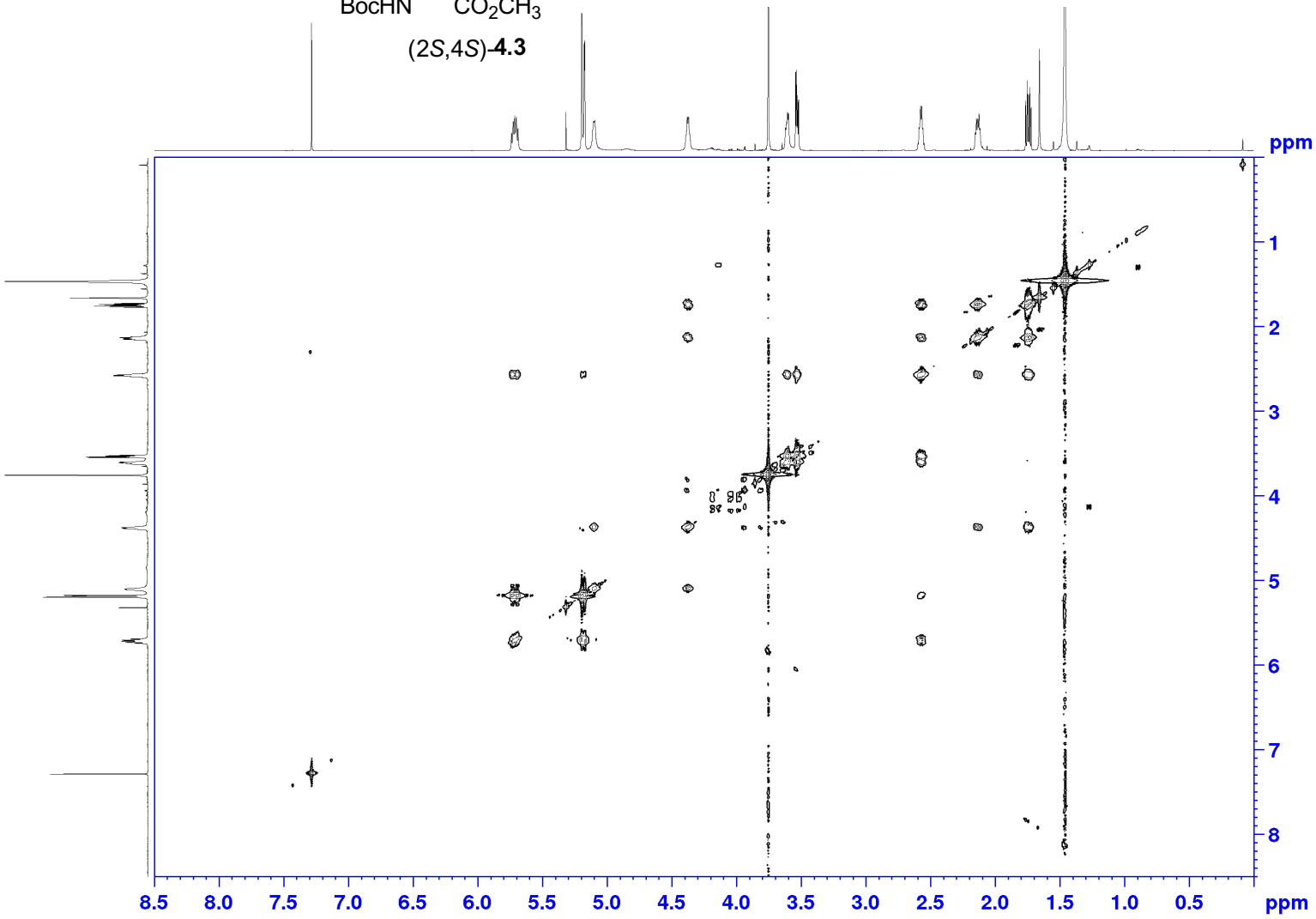

HSQC 700 MHz
Solvent: $CDCl_3$

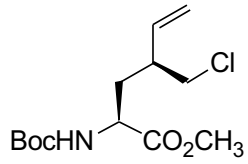

(2*S*,4*S*)-**4.3**

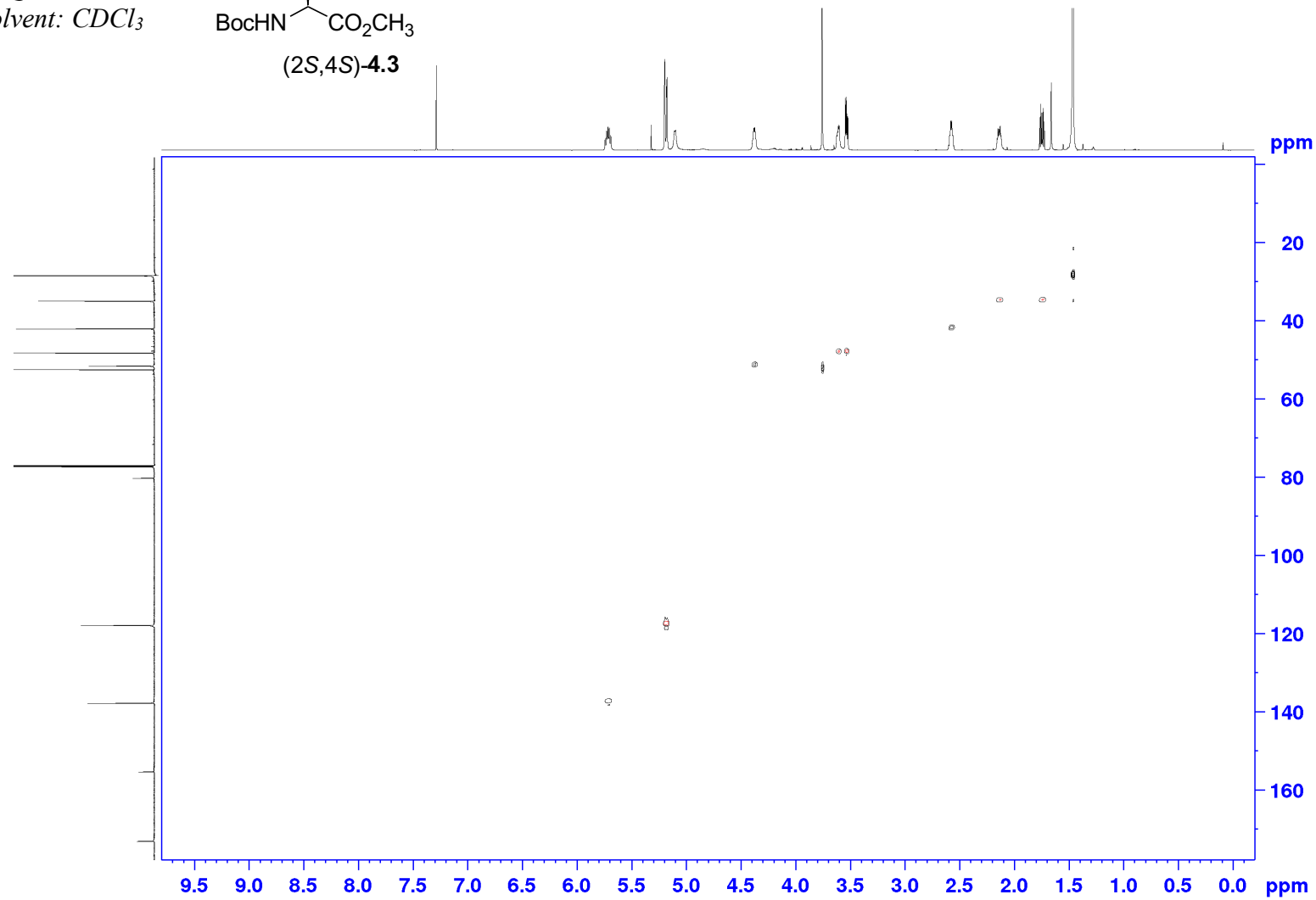

^{1}H NMR 700 MHz
Solvent: $CDCl_3$

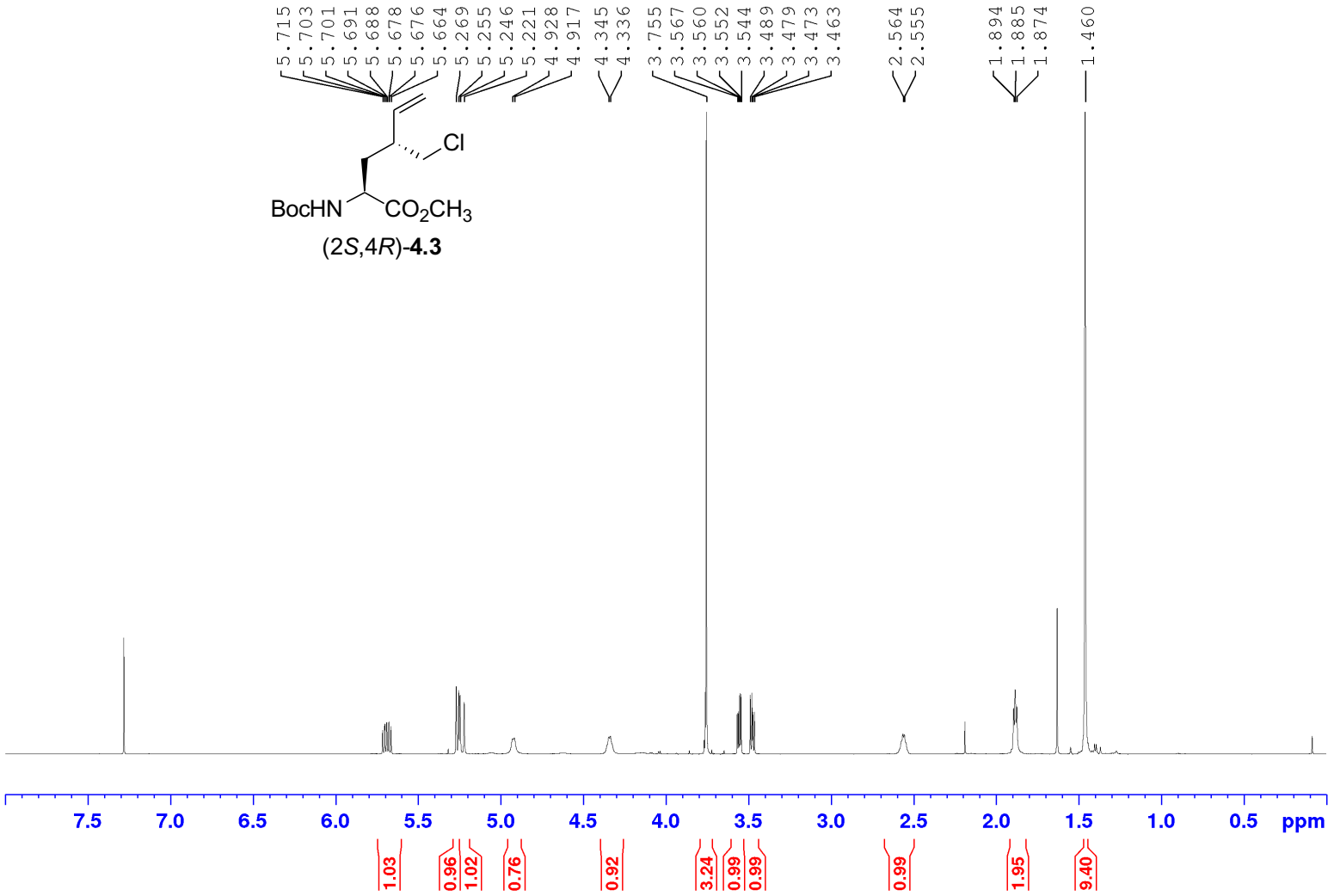

^{13}C NMR 175 MHz
Solvent: $CDCl_3$

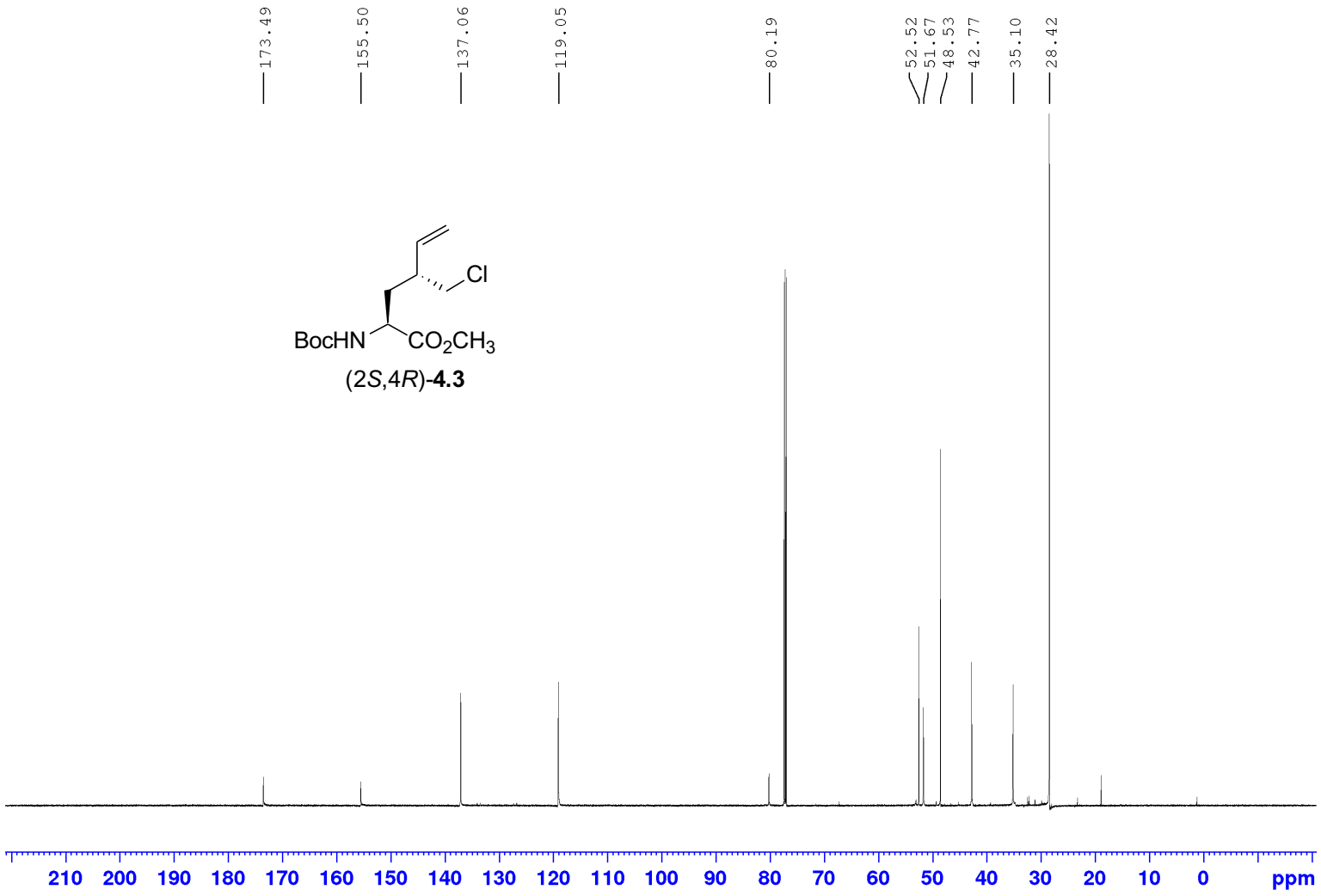

COSY NMR 700 MHz
Solvent: $CDCl_3$

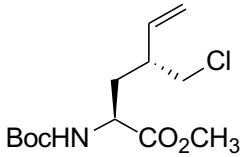

(2*S*,4*R*)-**4.3**

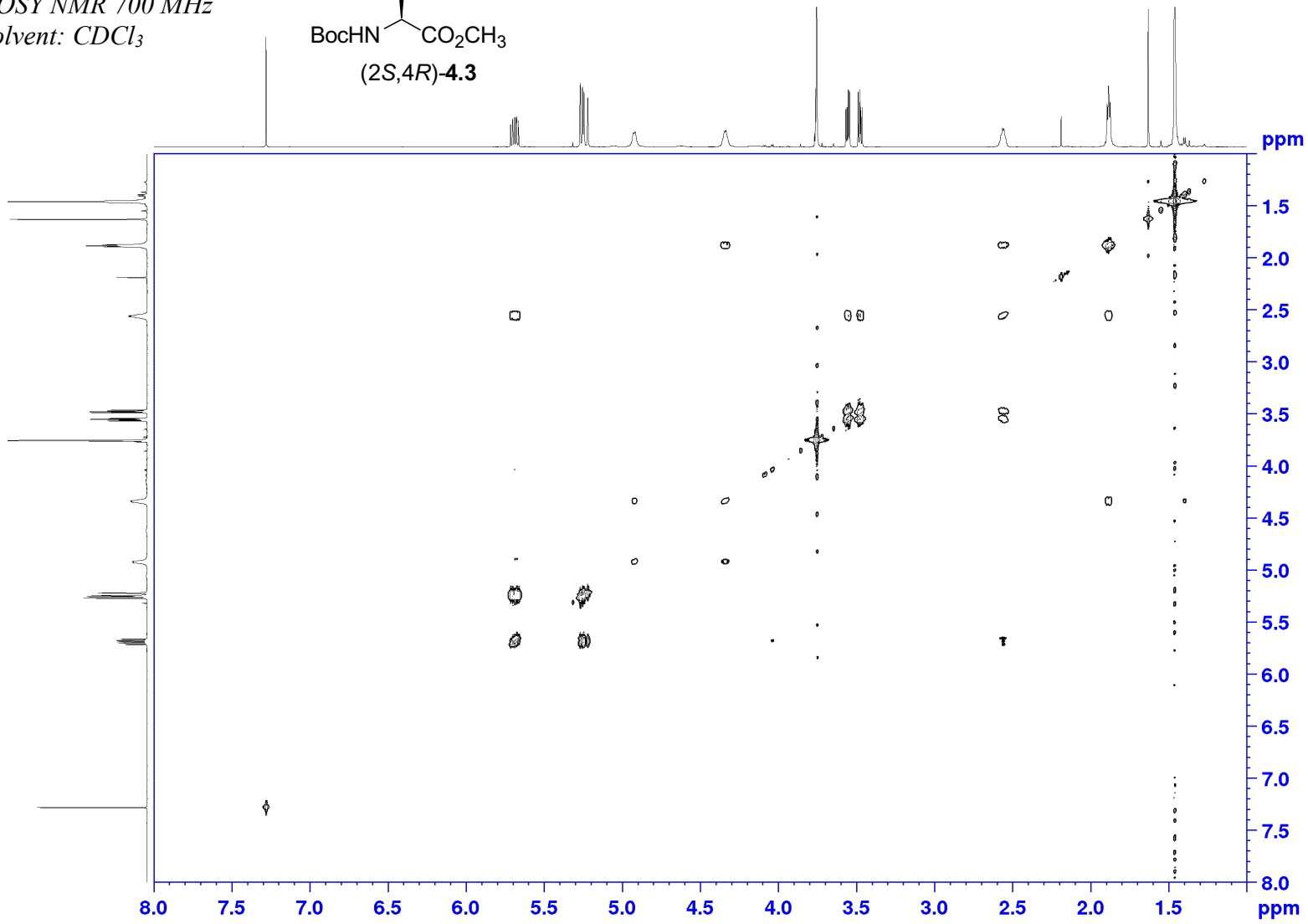

HSQC NMR 700 MHz
Solvent: $CDCl_3$

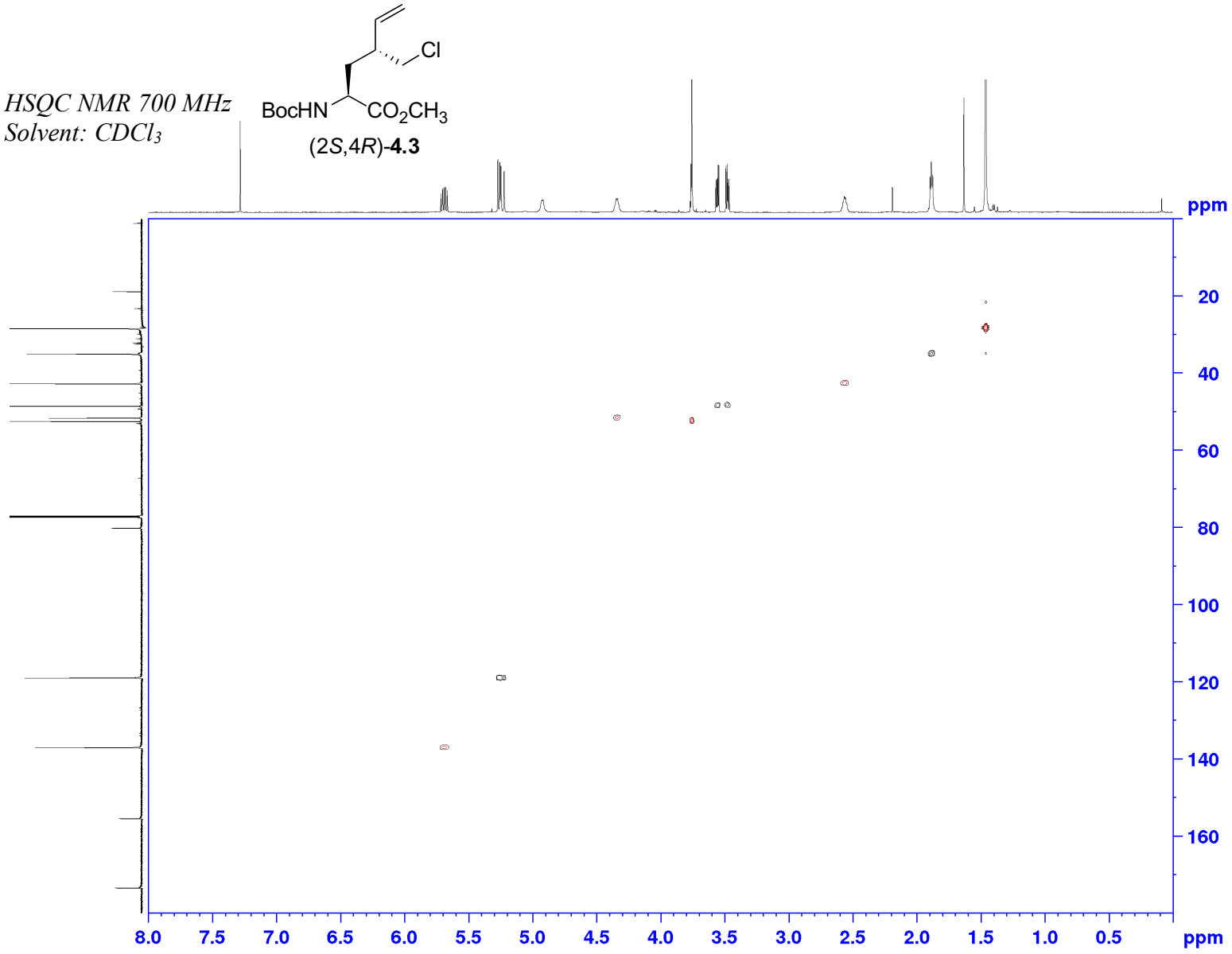

^{1}H NMR 700 MHz
Solvent: $CDCl_3$

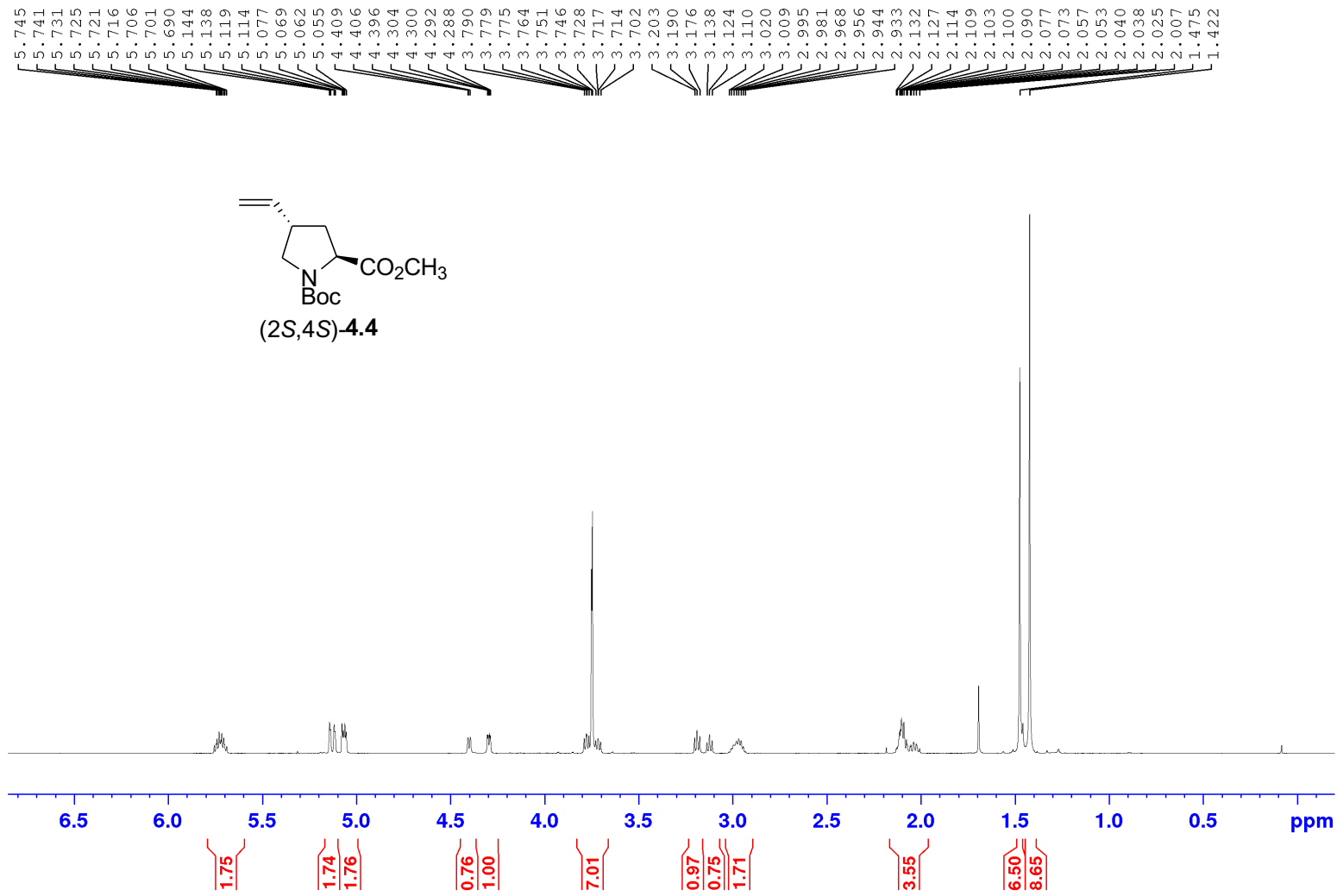

^{13}C NMR 175 MHz
Solvent: $CDCl_3$

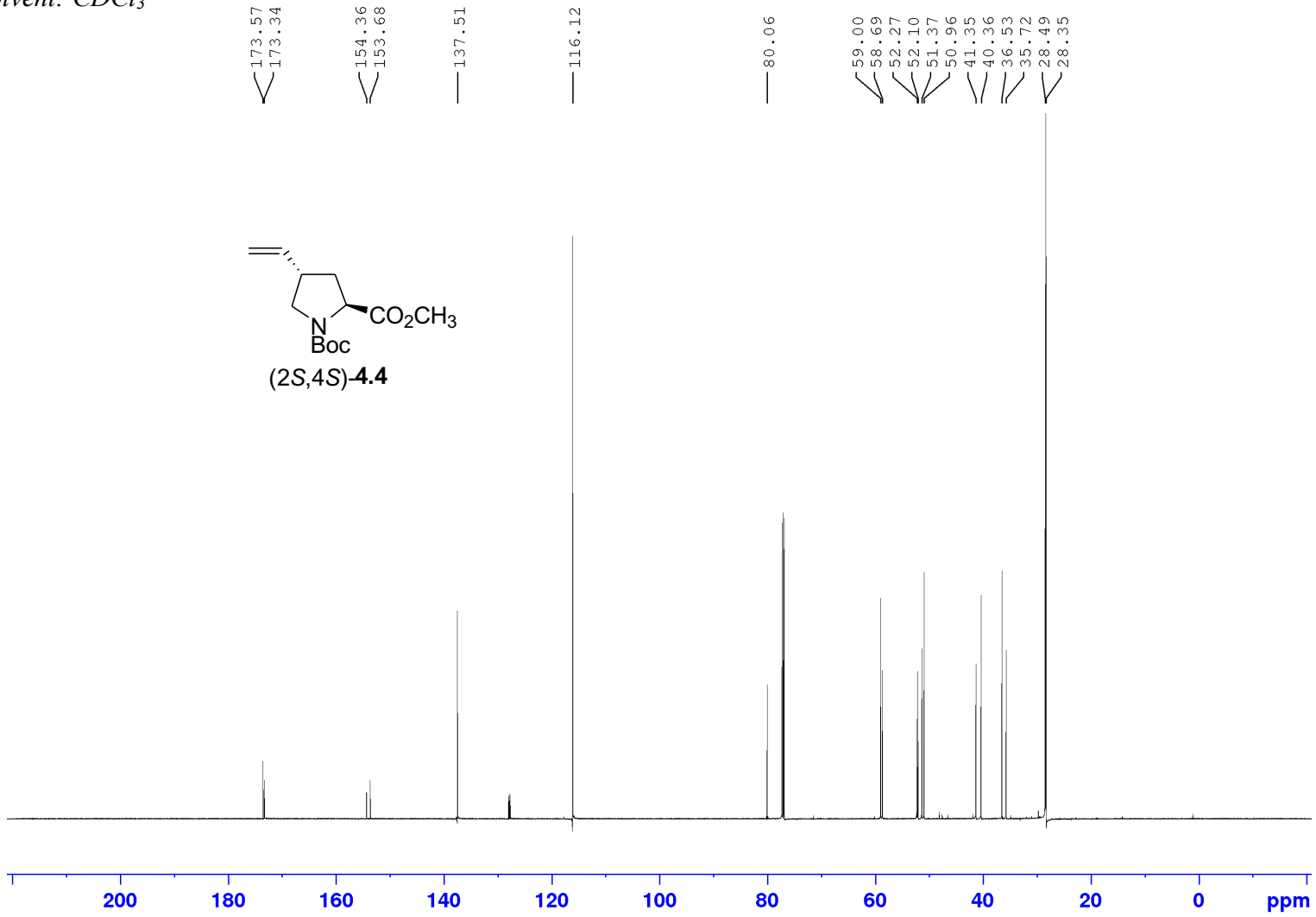

(2*S*,4*S*)-**4.4**

^{1}H NMR 500 MHz
Solvent: $CDCl_3$

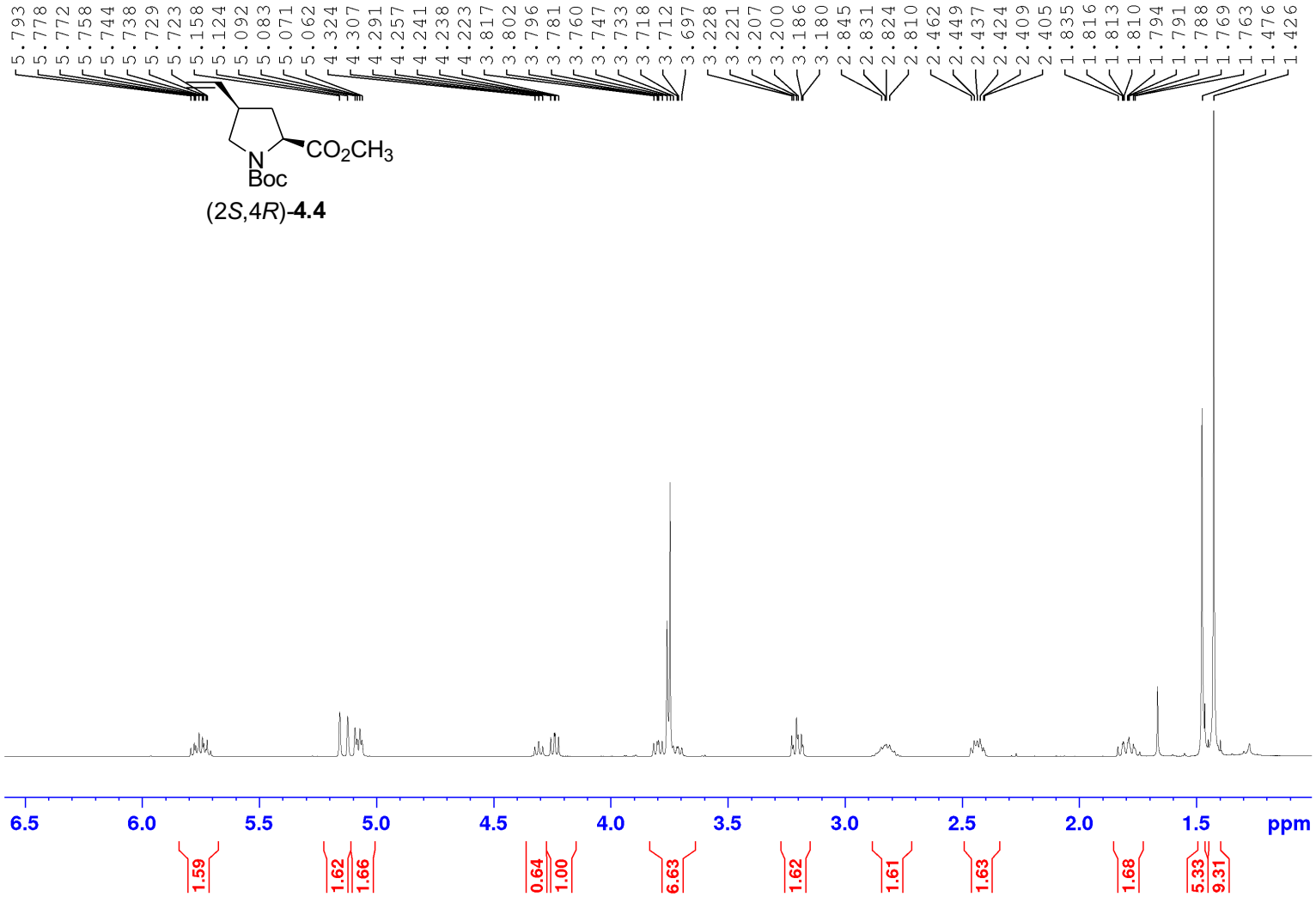

^{13}C NMR 125 MHz
Solvent: $CDCl_3$

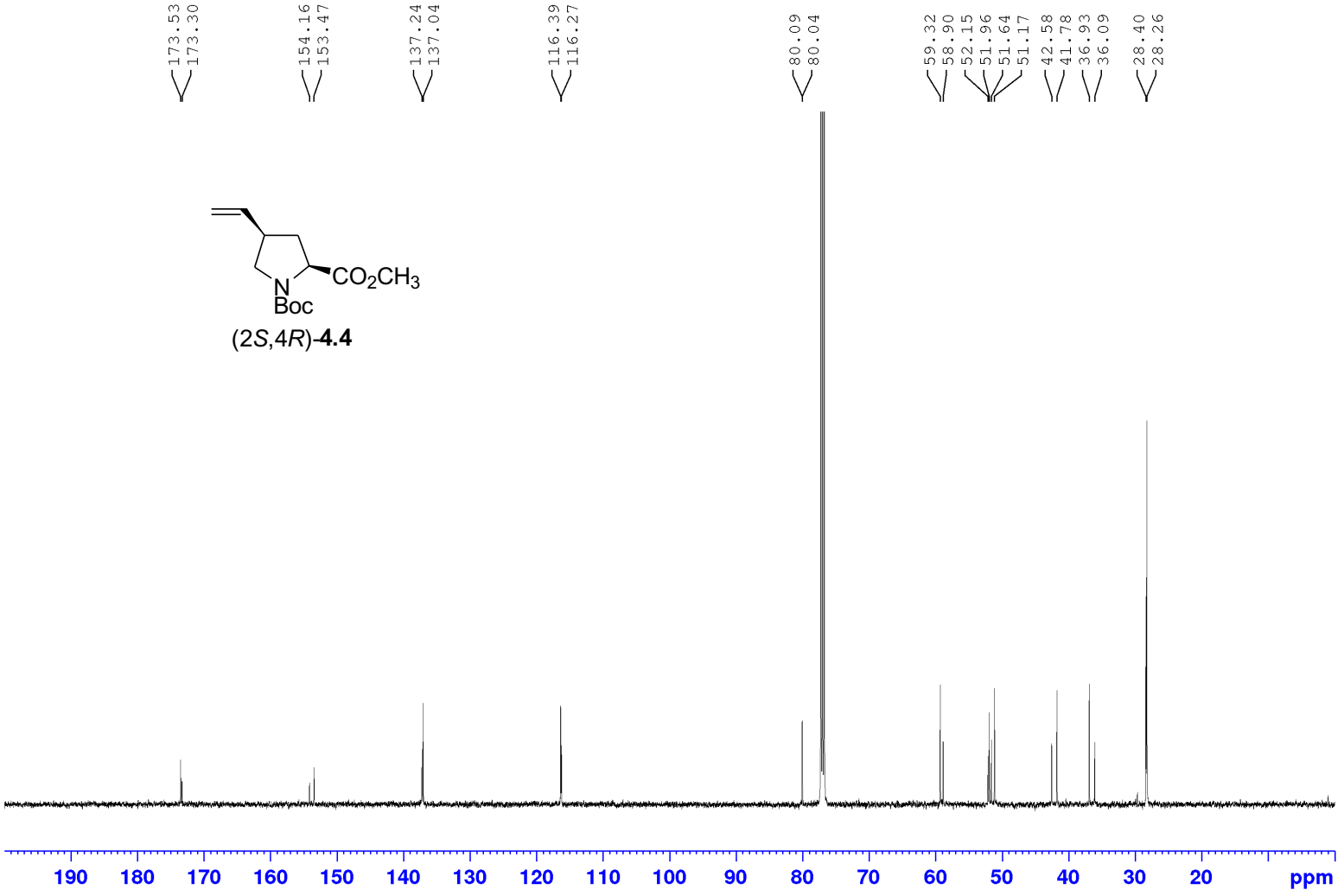

(2*S*,4*R*)-**4.4**

^{1}H NMR 400 MHz
Solvent: CD_3OD

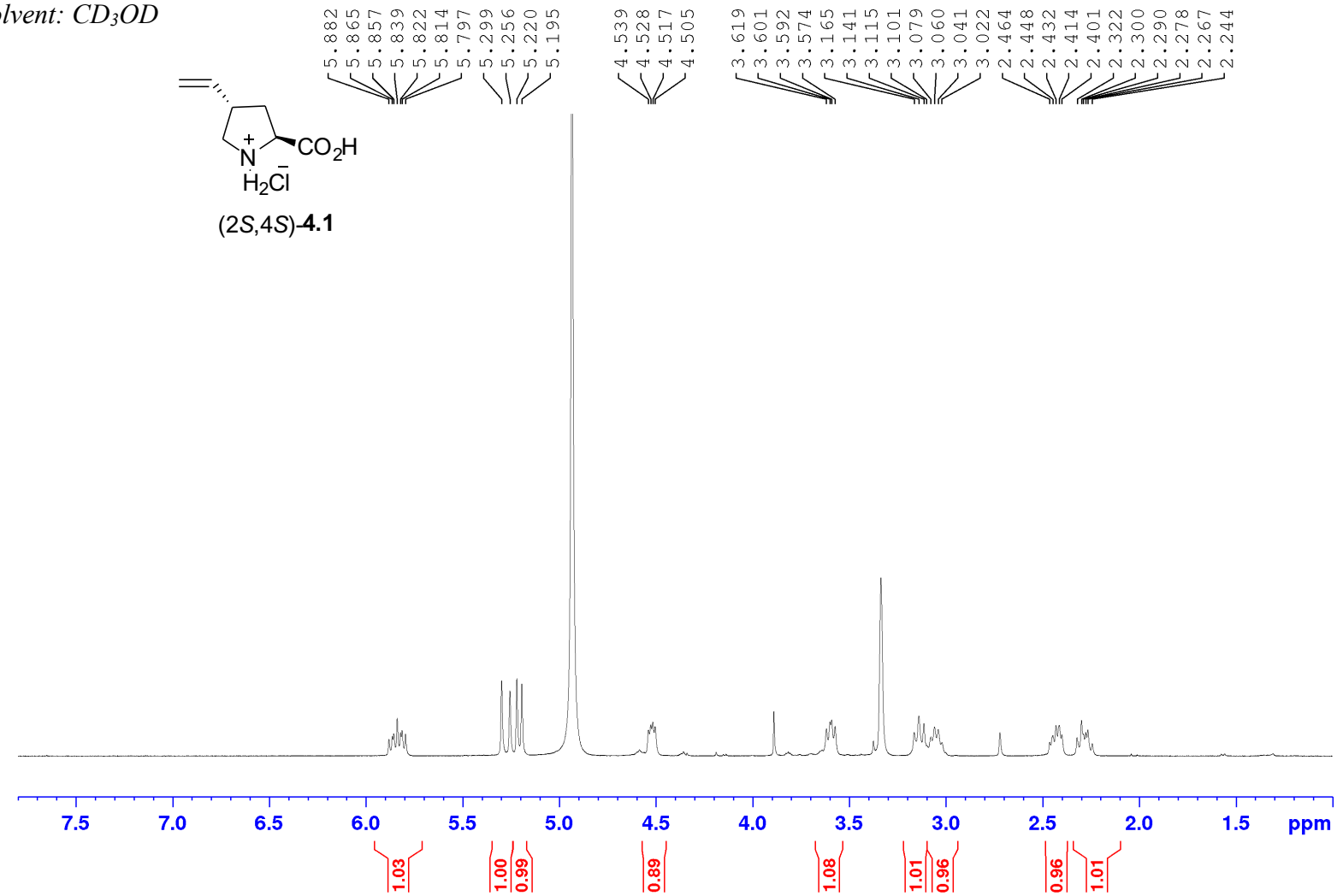

(2*S*,4*S*)-**4.1**

^{13}C NMR 125 MHz
Solvent: CD_3OD

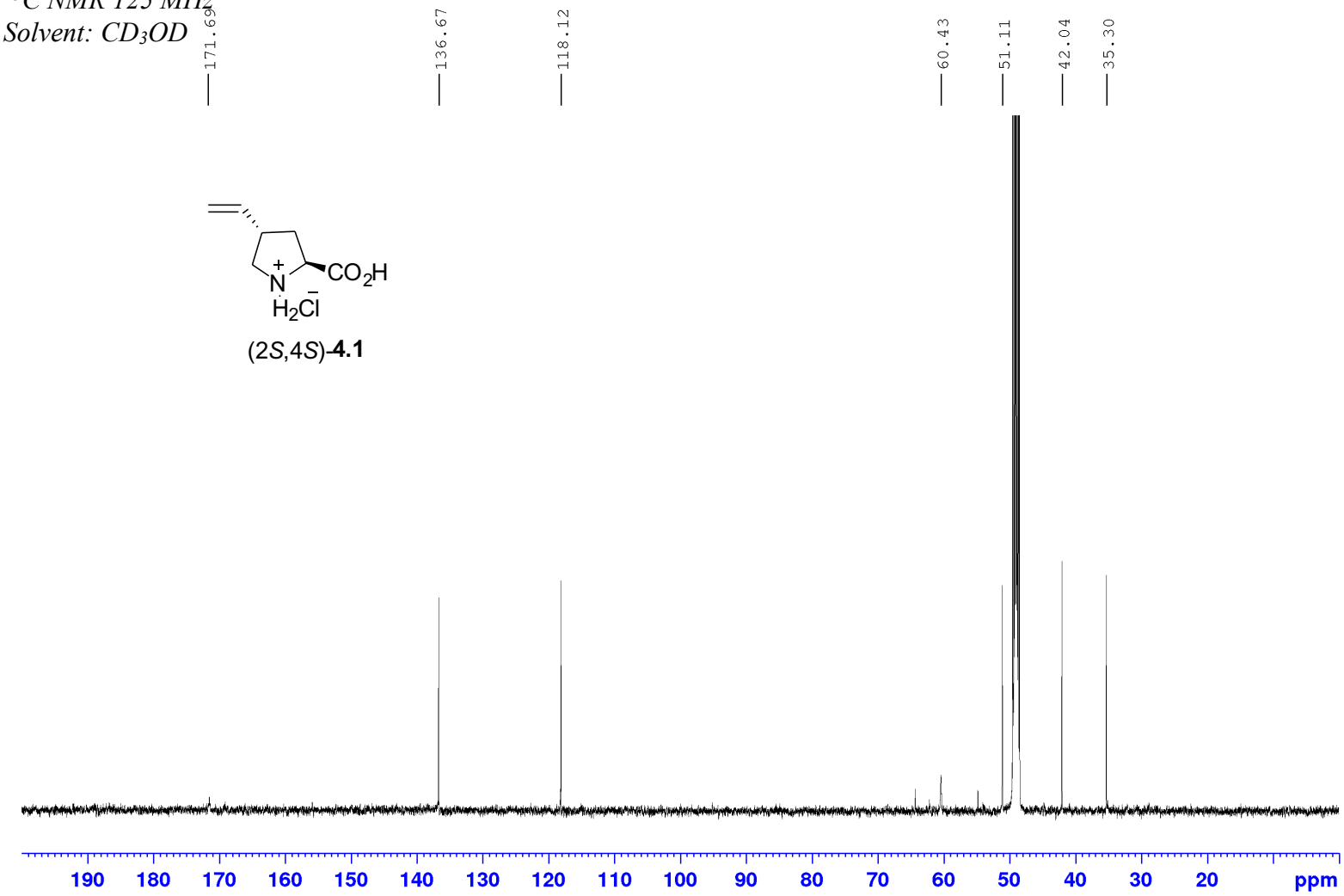

(2*S*,4*S*)-**4.1**

^{1}H NMR 400 MHz
Solvent: CD_3OD

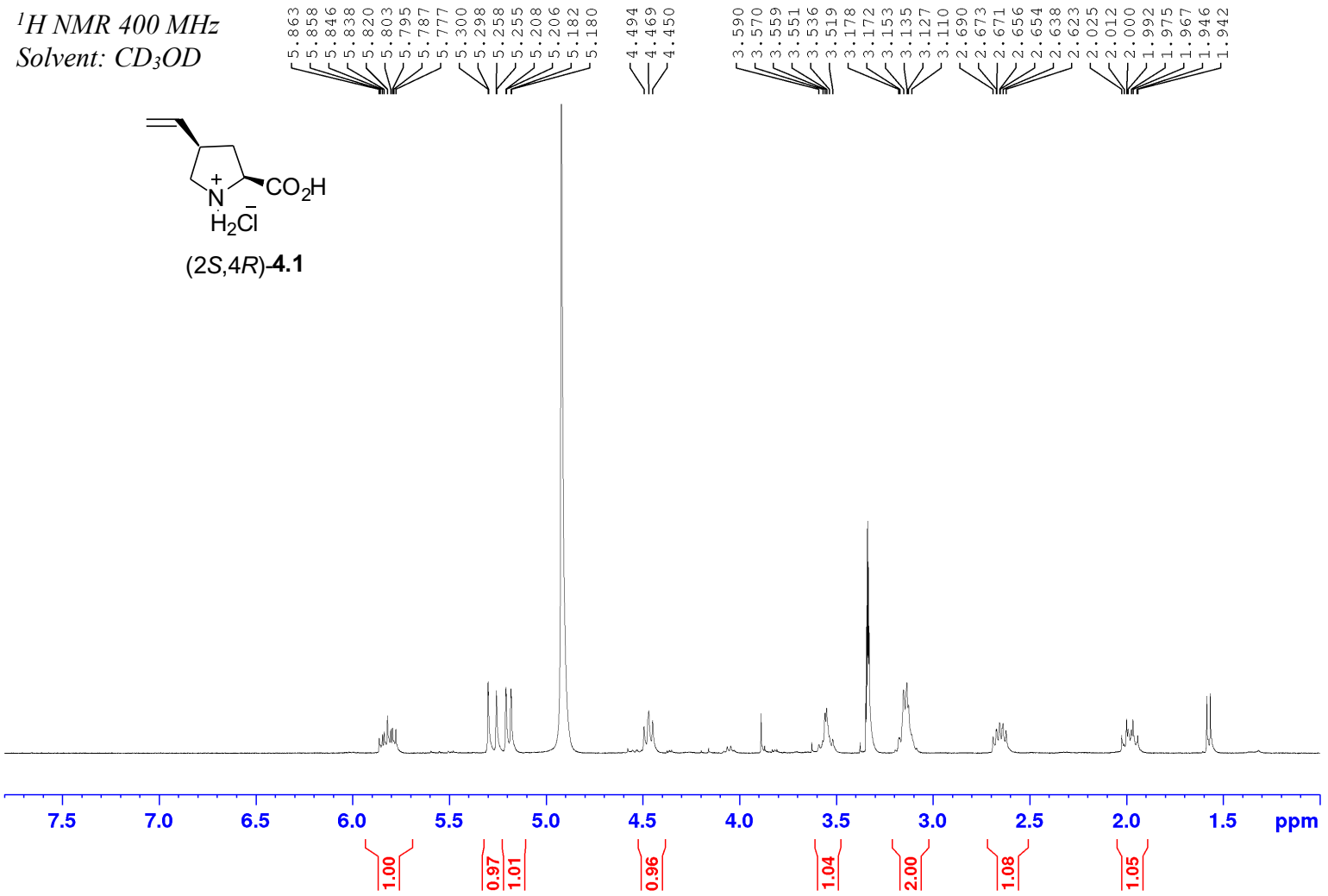

(2*S*,4*R*)-**4.1**

^{13}C NMR 125 MHz
Solvent: CD_3OD

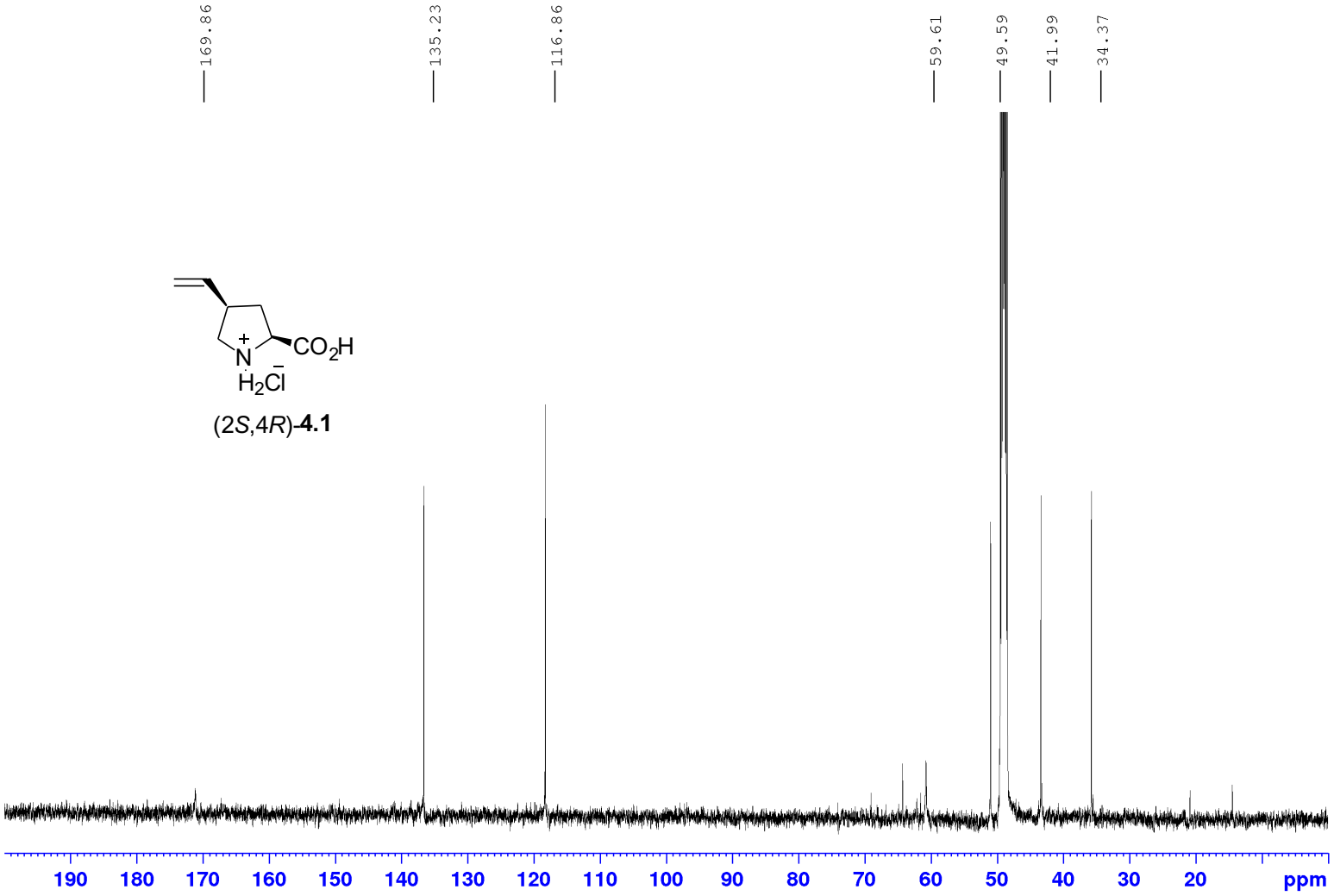

(2*S*,4*R*)-**4.1**

^{1}H NMR 500 MHz
Solvent: CD_3OD

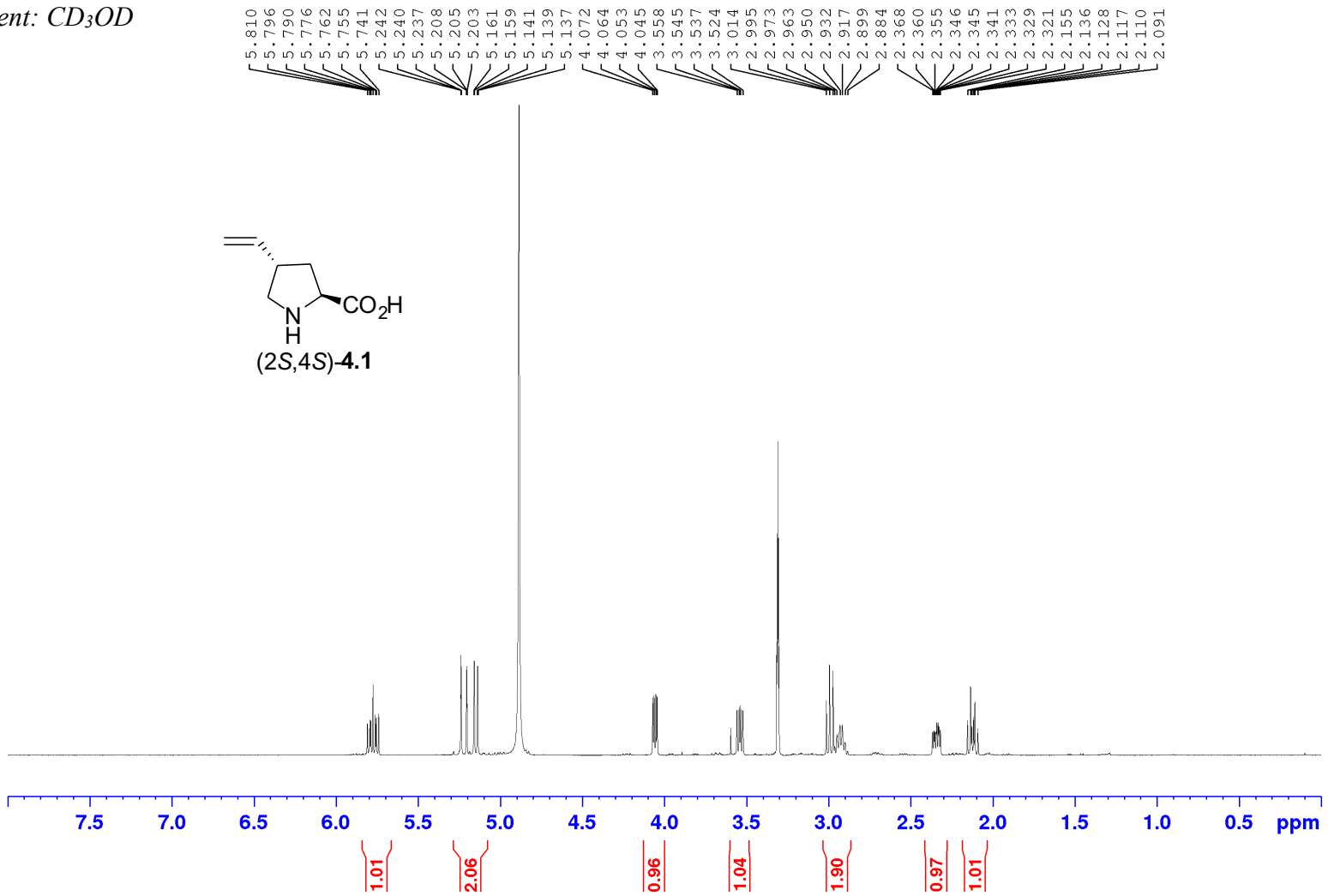

^{13}C NMR 125 MHz
Solvent: CD_3OD

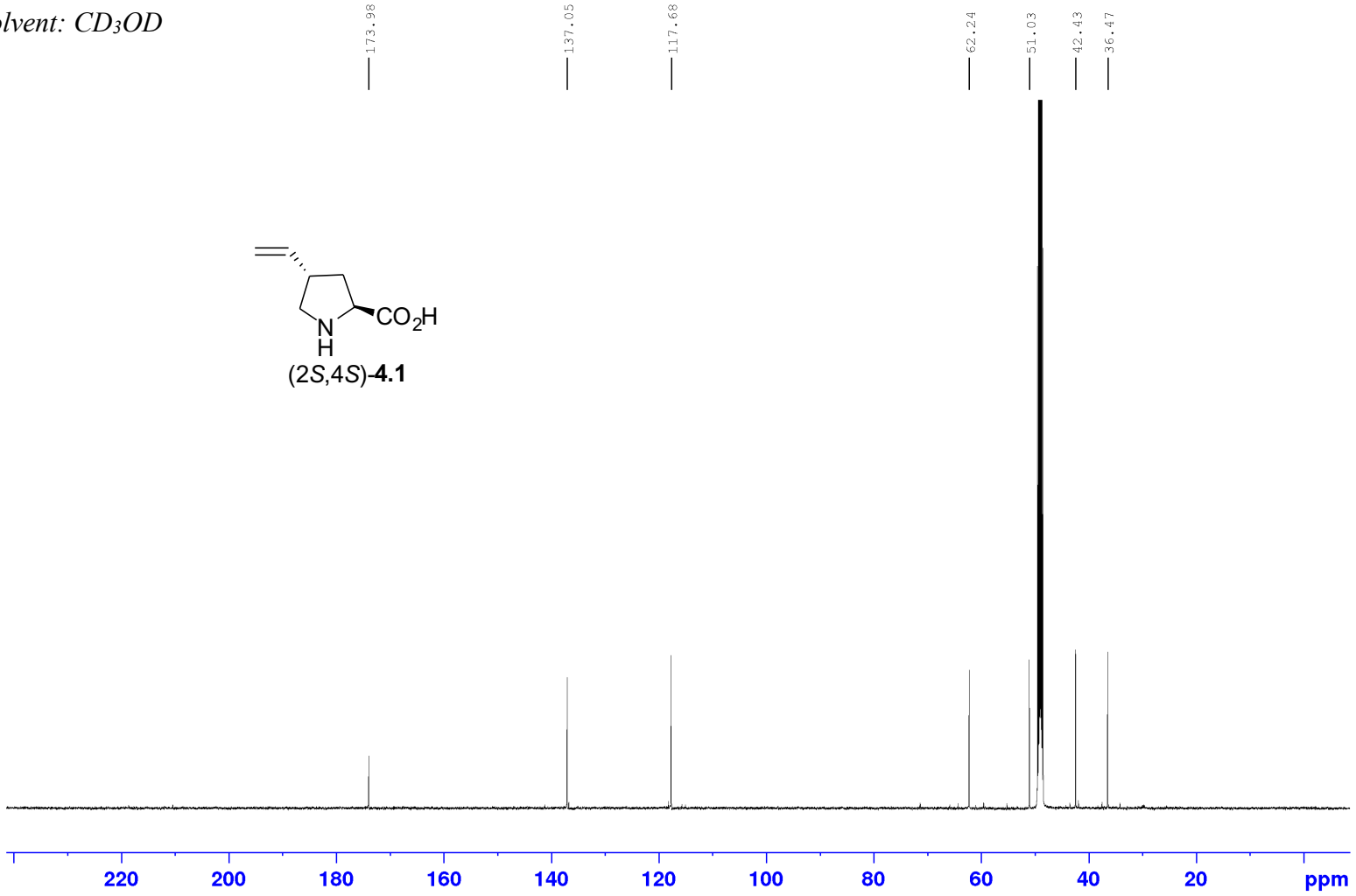

(2*S*,4*S*)-**4.1**

^{1}H NMR 500 MHz
Solvent: CD_3OD

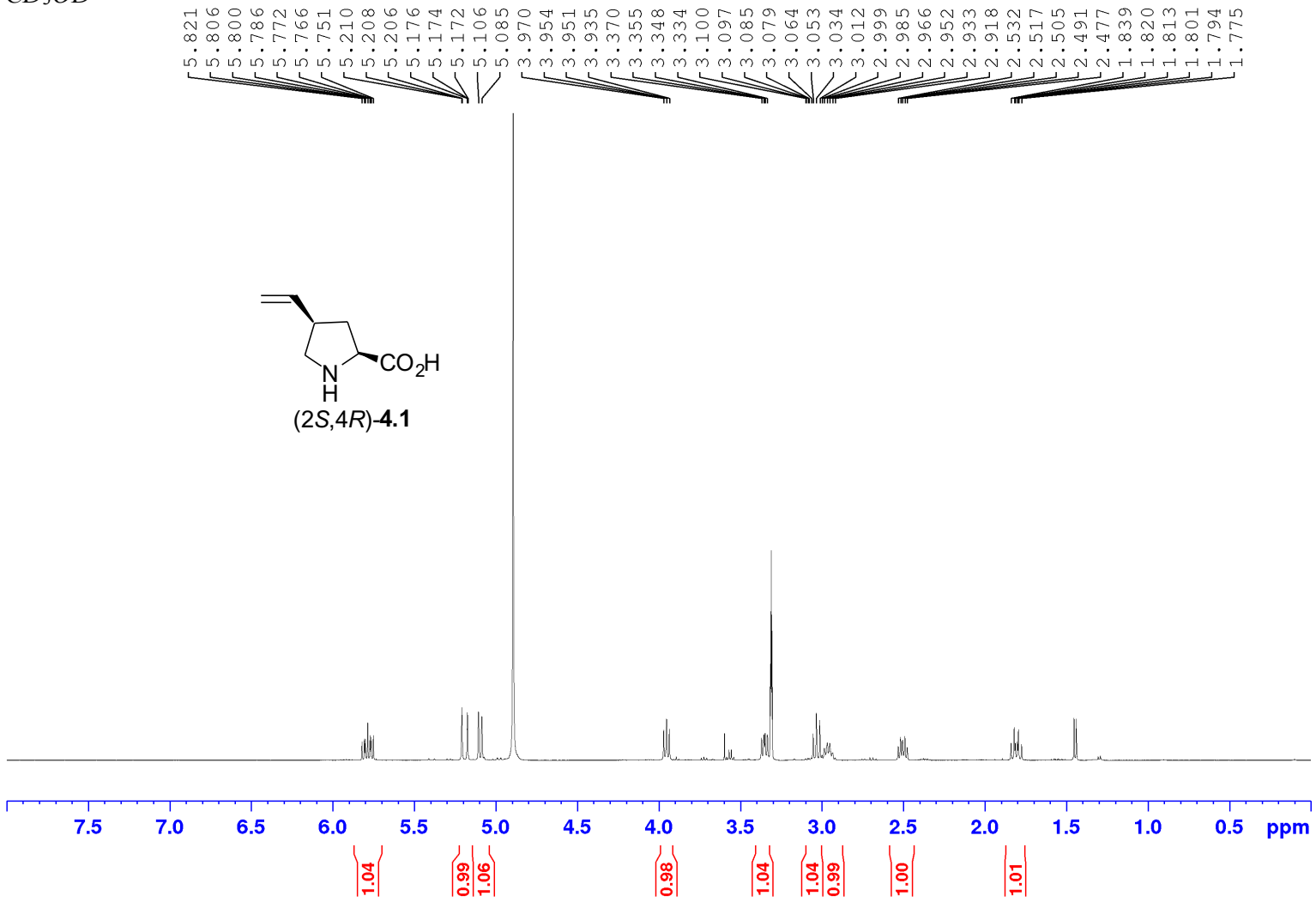

(2*S*,4*R*)-**4.1**

^{13}C NMR 125 MHz
Solvent: CD_3OD

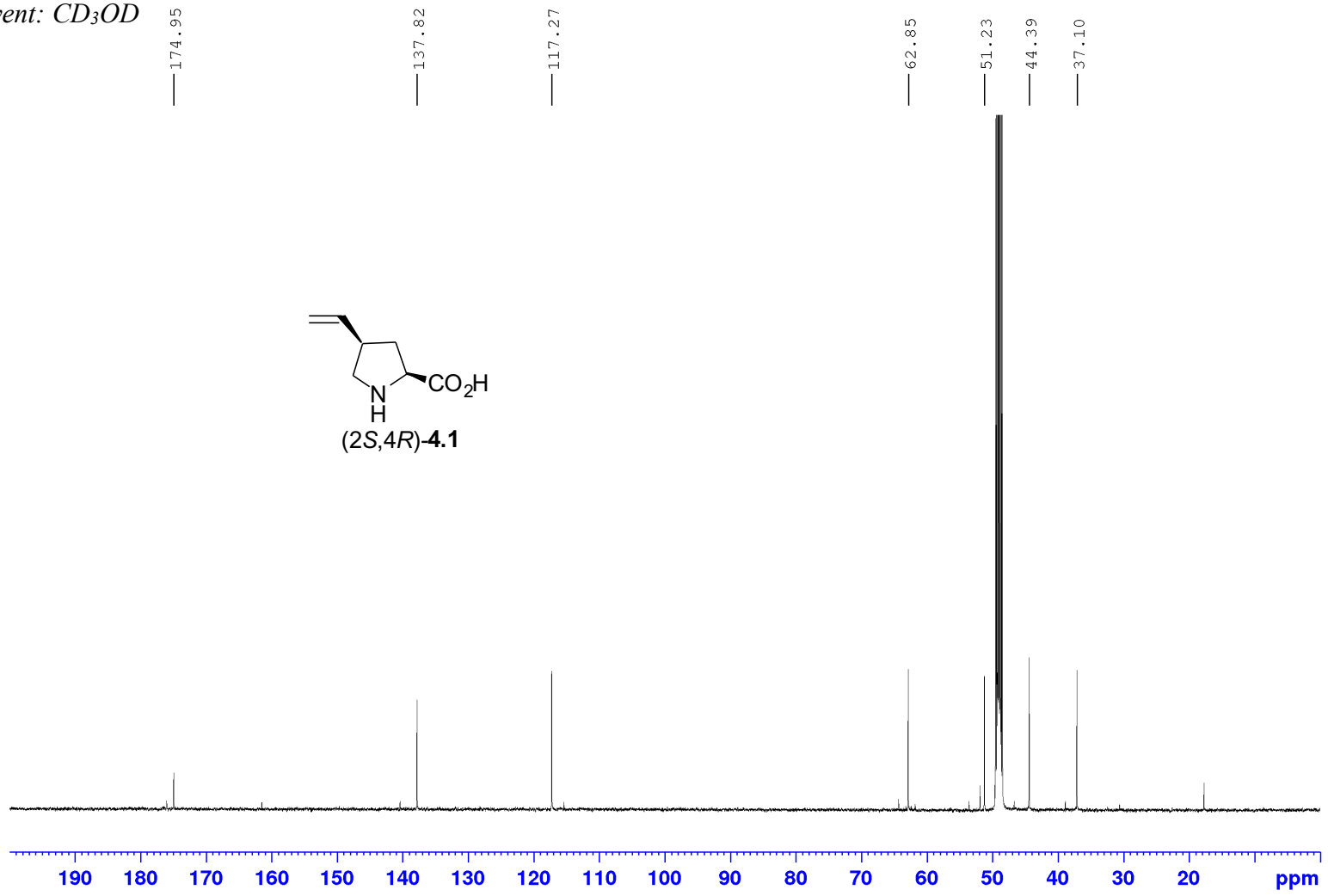

(2*S*,4*R*)-**4.1**

^{1}H NMR 500 MHz
Solvent: $CDCl_3$

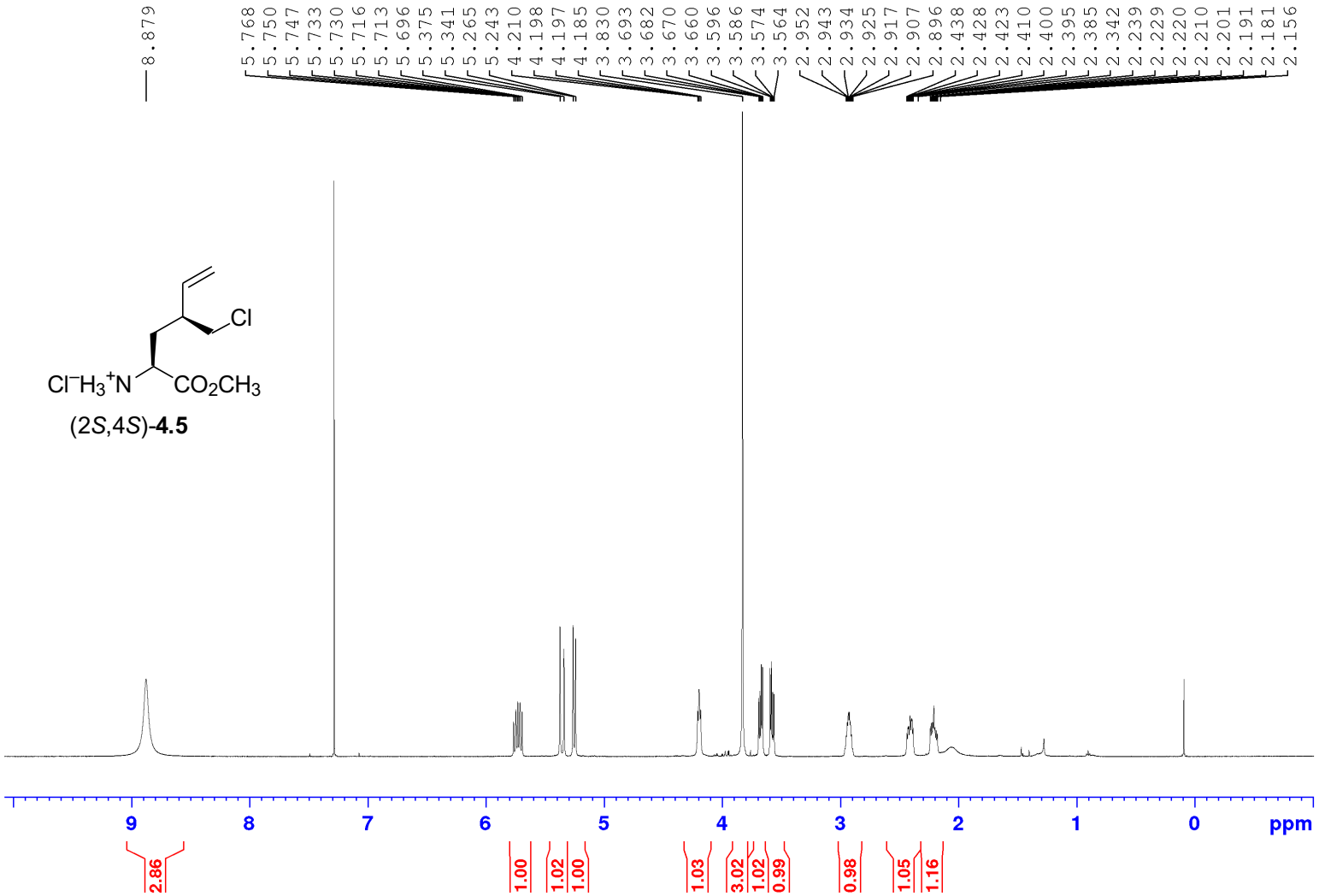

^{13}C NMR 125 MHz
Solvent: $CDCl_3$

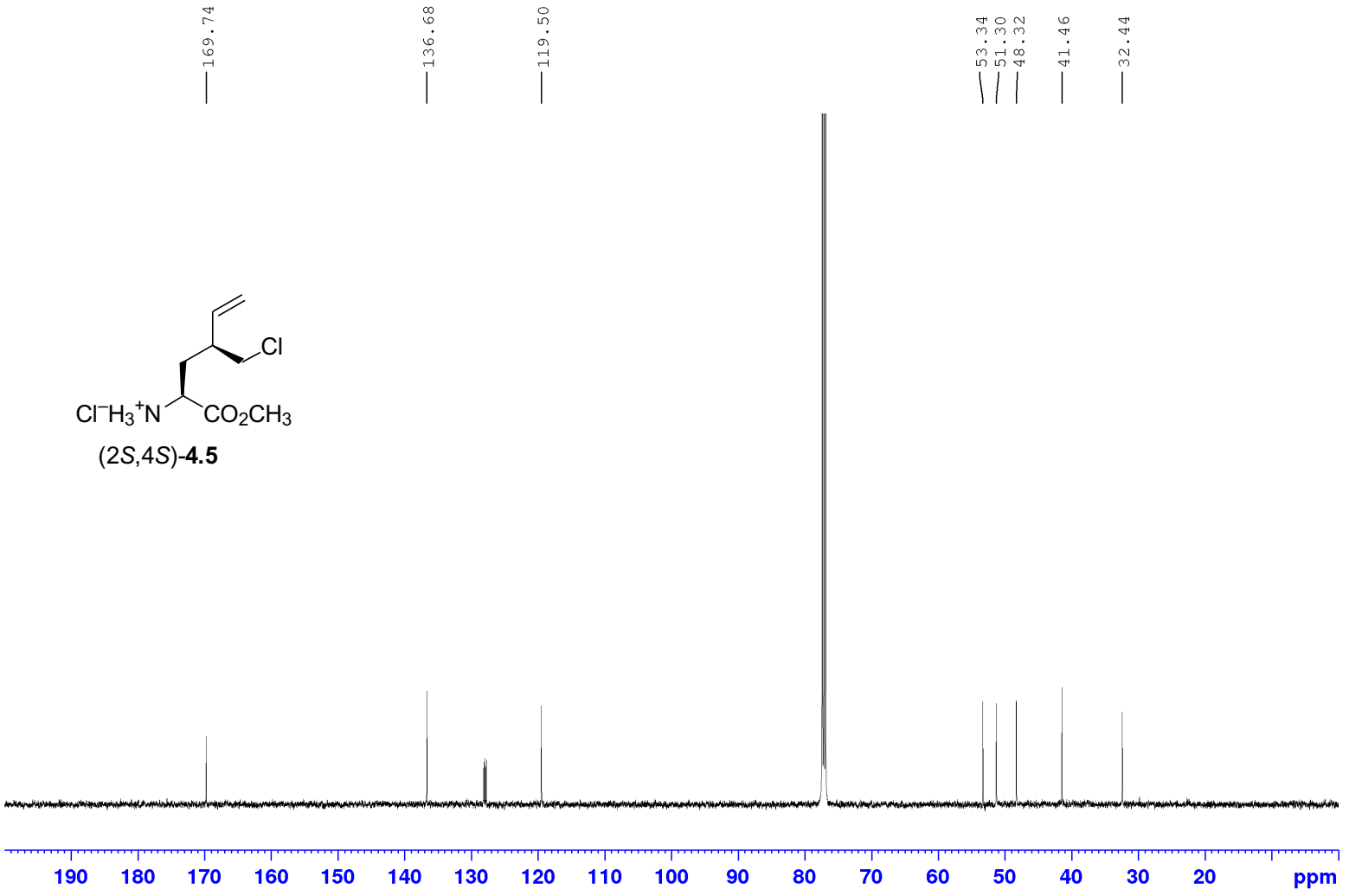

^{1}H NMR 500 MHz
Solvent: $CDCl_3$

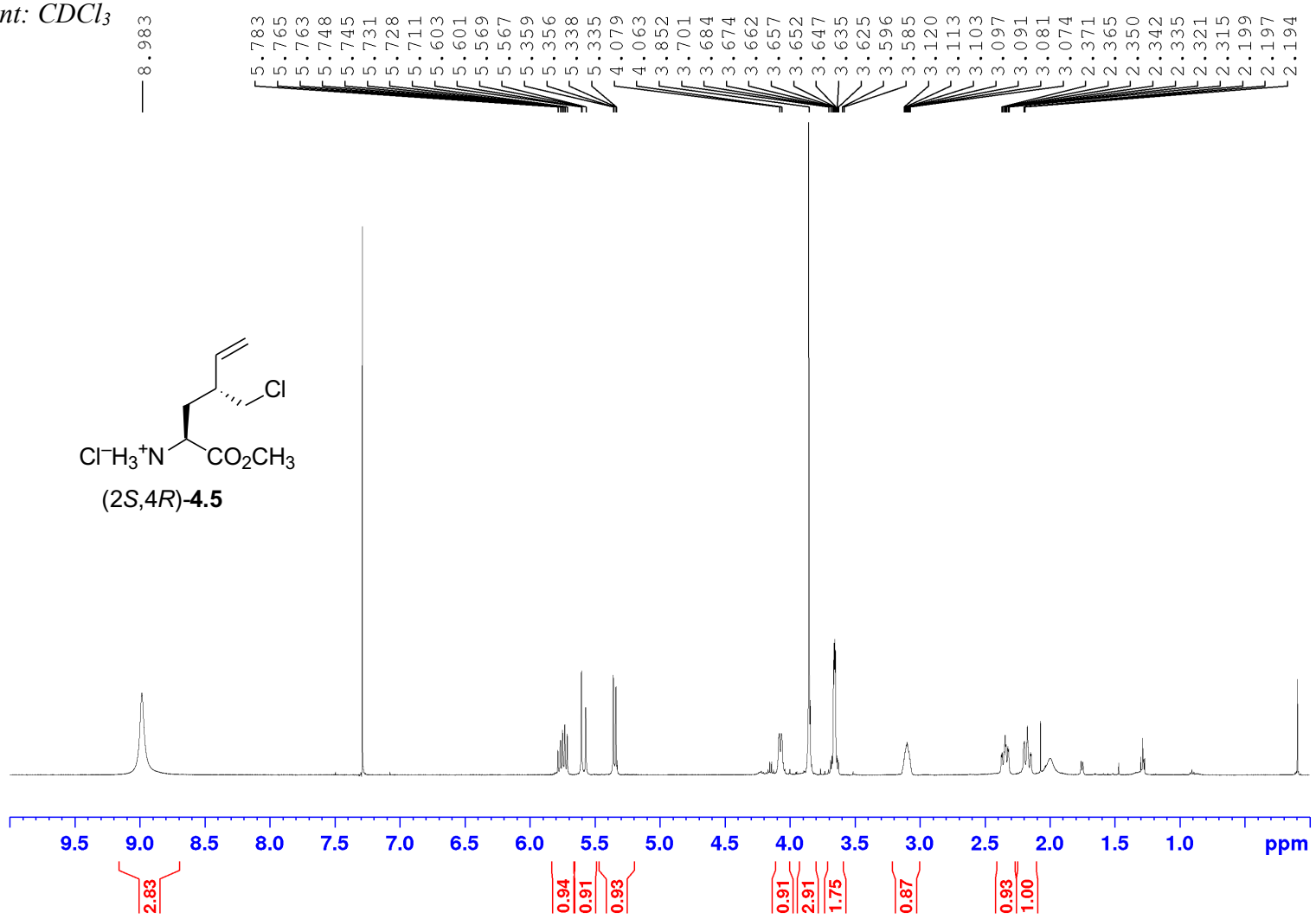

^{13}C NMR 125 MHz
Solvent: $CDCl_3$

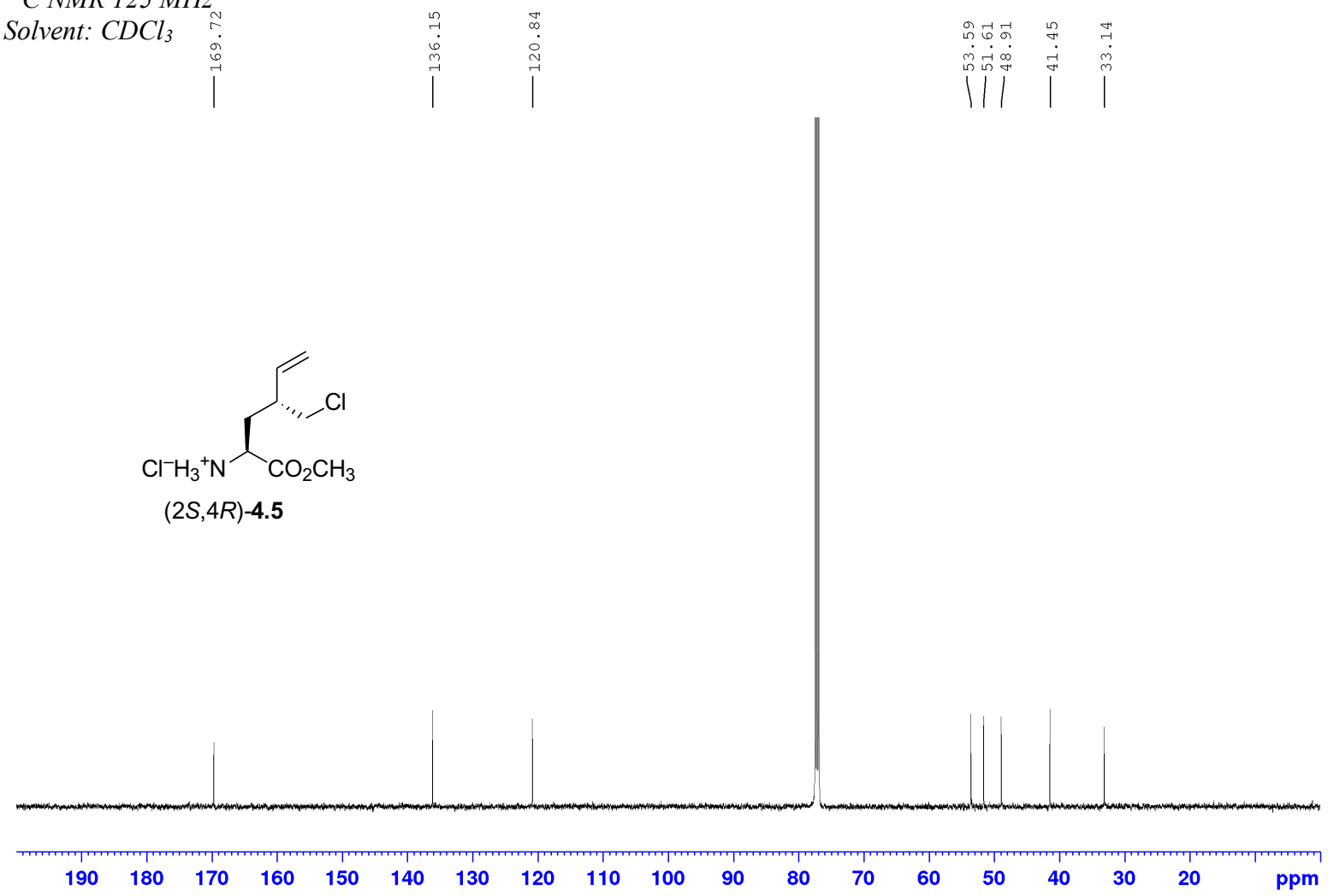

(2*S*,4*R*)-**4.5**

^{1}H NMR 500 MHz
Solvent: C_6D_6

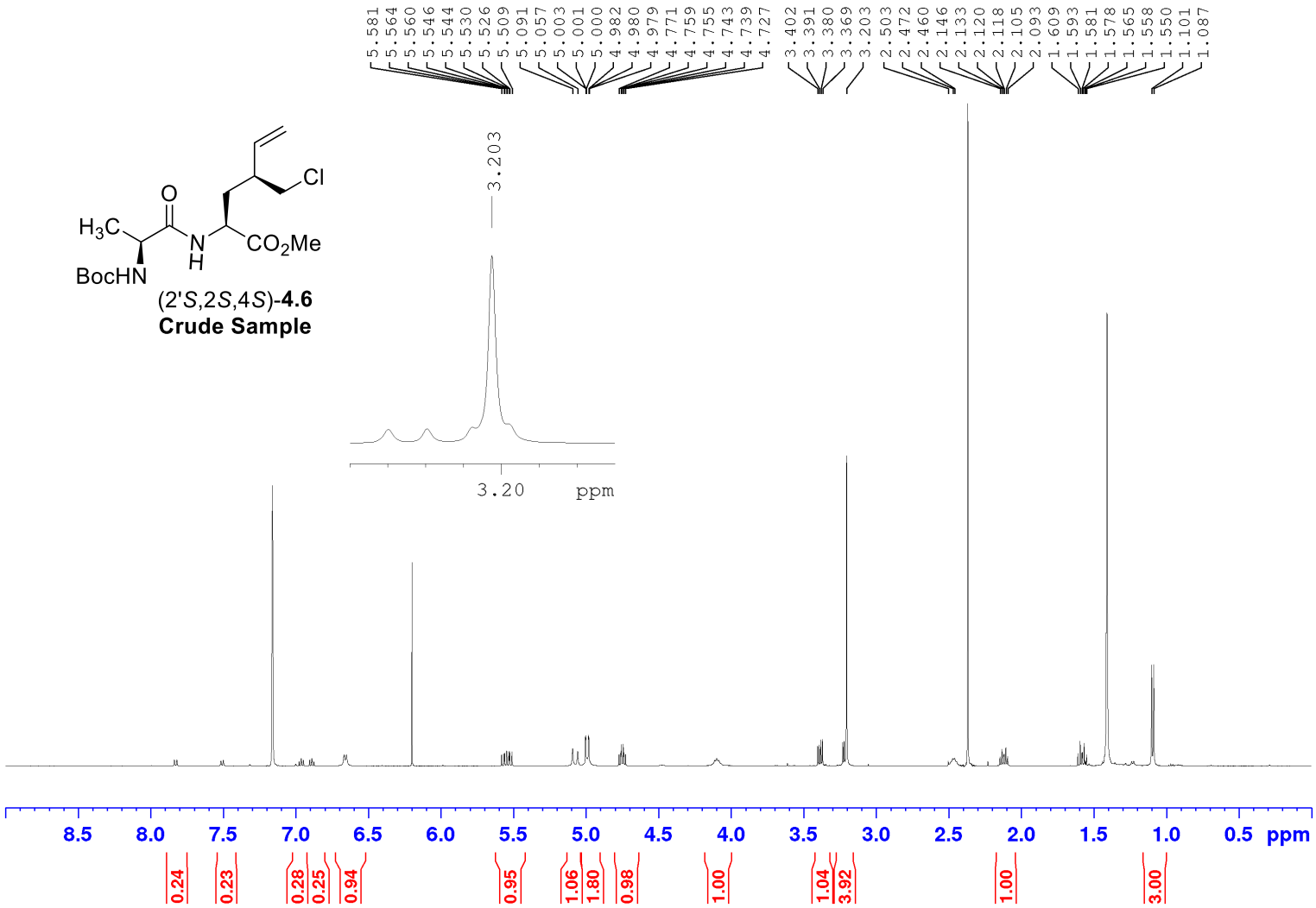

^{1}H NMR 500 MHz
Solvent: C_6D_6

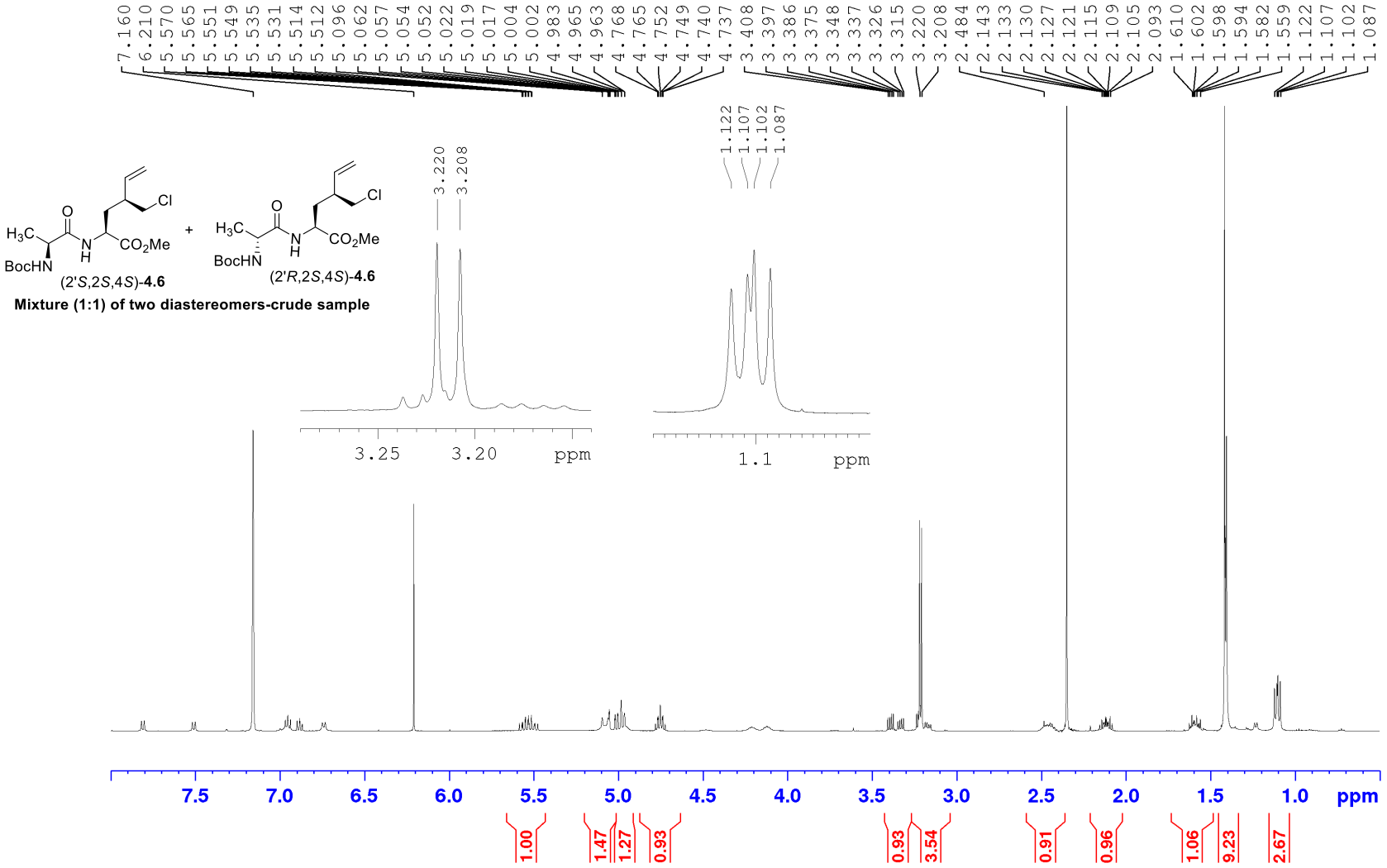

^{1}H NMR 500 MHz
Solvent: C_6D_6

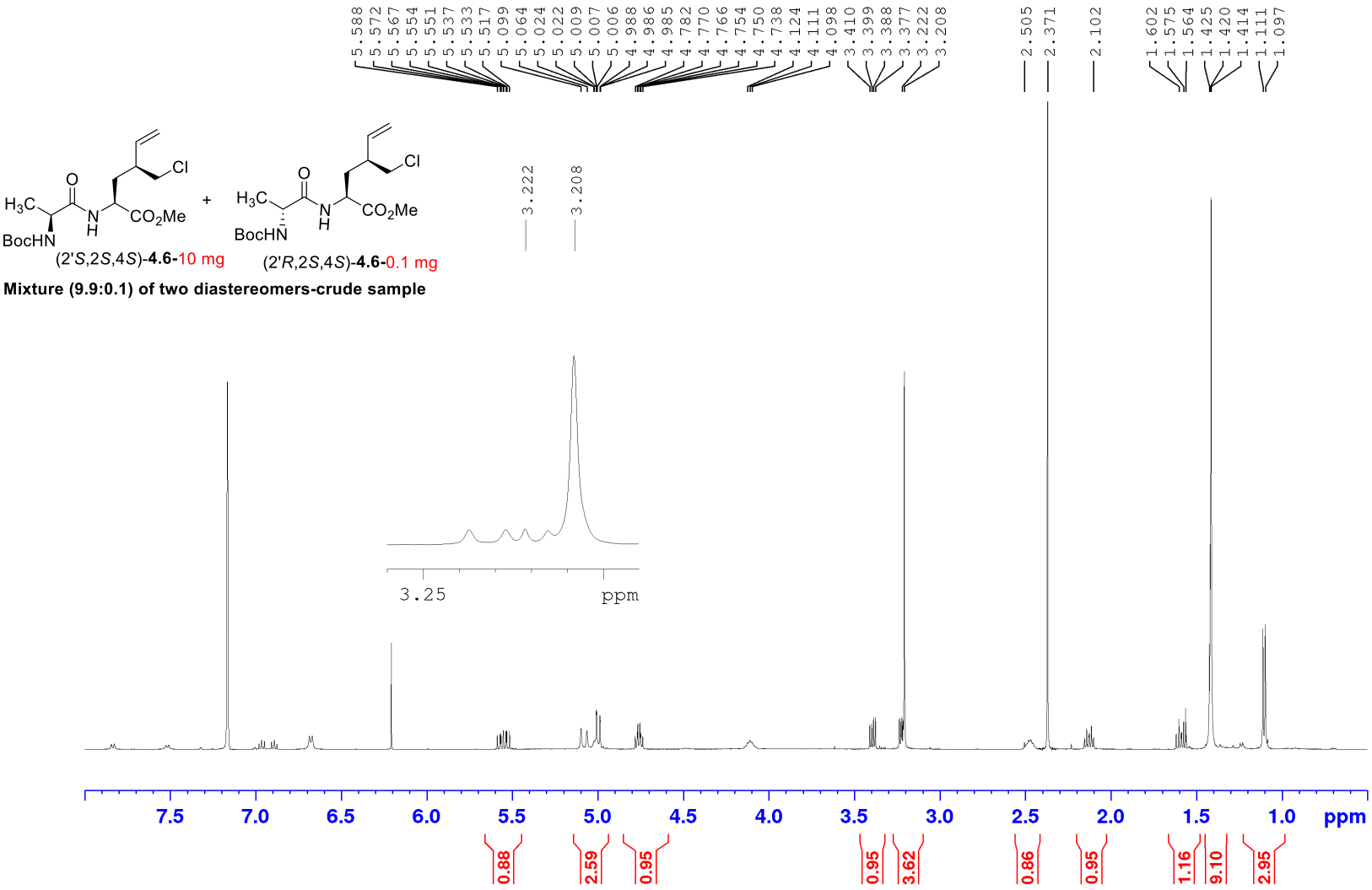

(2'*S*,2*S*,4*S*)-**4.6**-10 mg + (2'*R*,2*S*,4*S*)-**4.6**-0.1 mg

Mixture (9.9:0.1) of two diastereomers-crude sample

^{1}H NMR 500 MHz
Solvent: C_6D_6

Examination of the diastereotopic methyl ester at 3.208 and 3.222 ppm

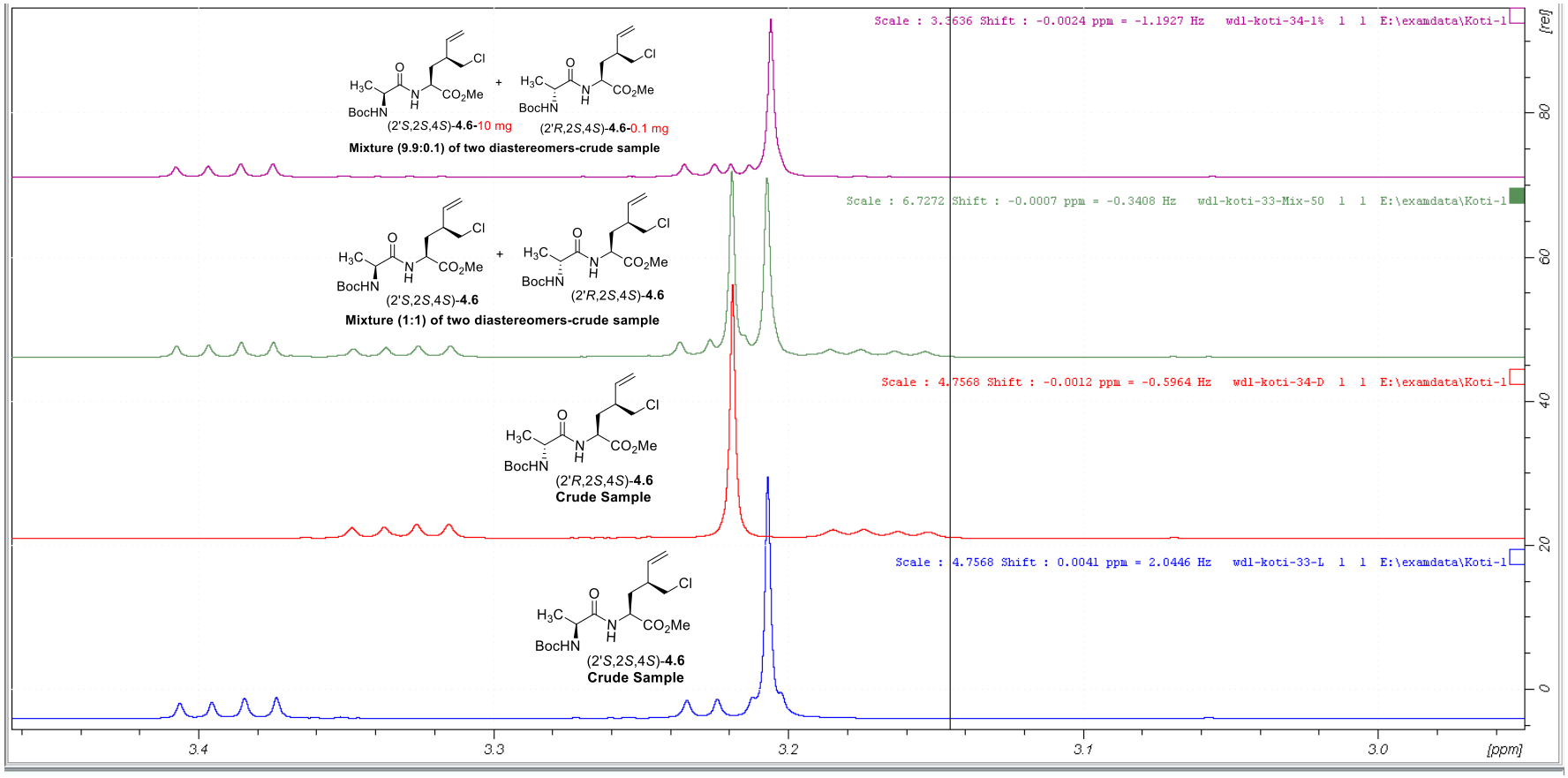

^{1}H NMR 400 MHz
Solvent: C_6D_6

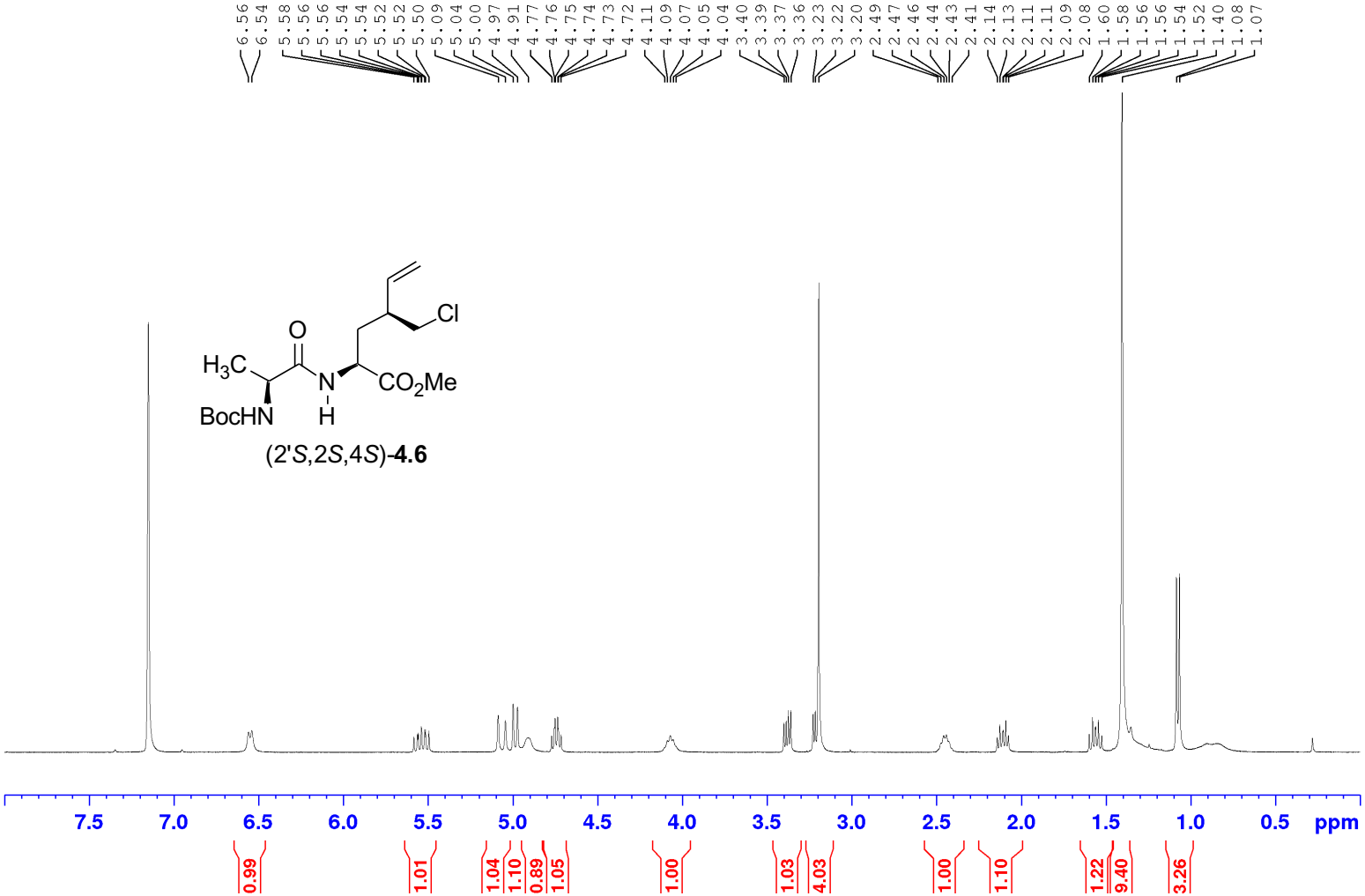

^{13}C NMR 100 MHz
Solvent: C_6D_6

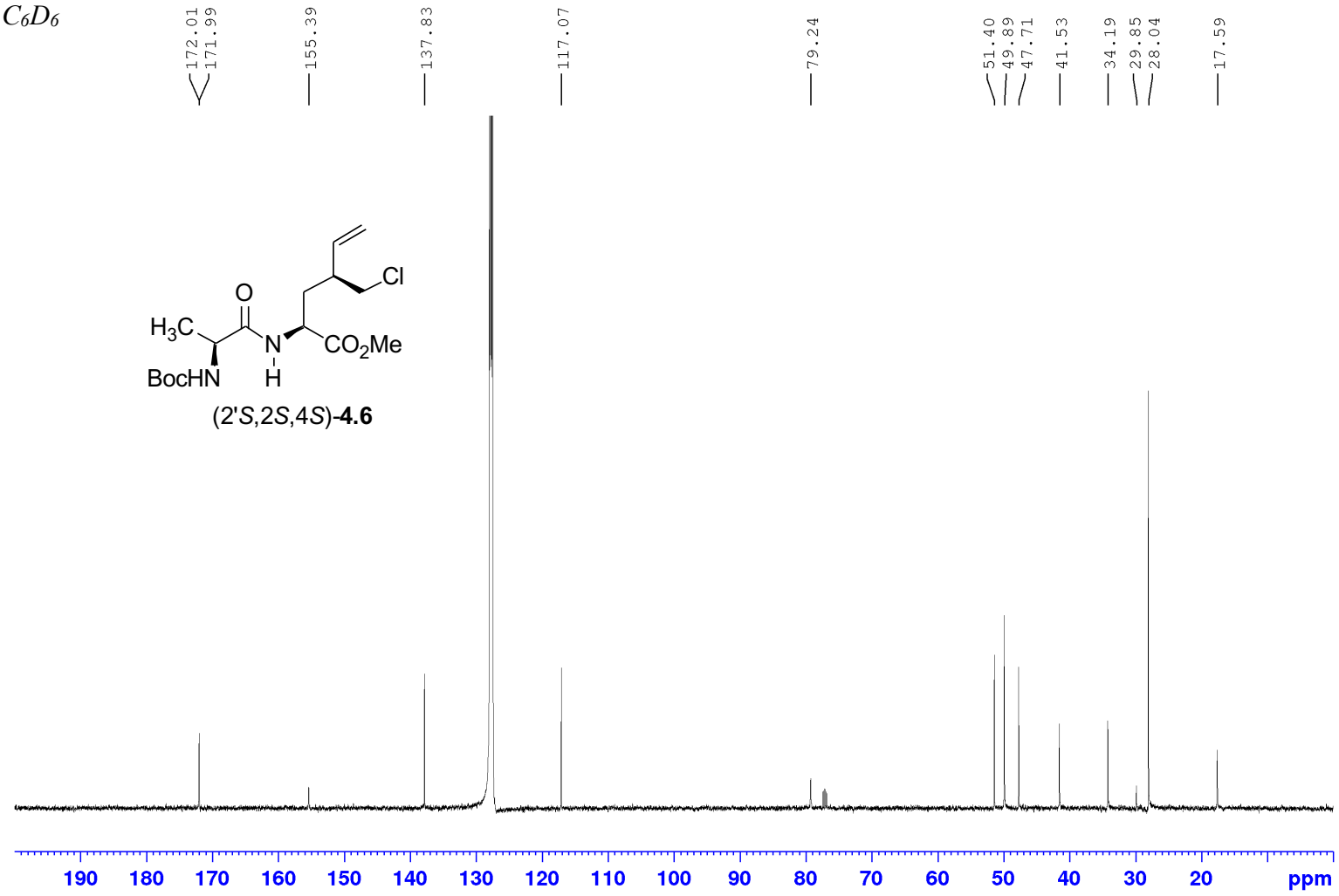

(2'*S*,2*S*,4*S*)-**4.6**

^{1}H NMR 400 MHz
Solvent: C_6D_6

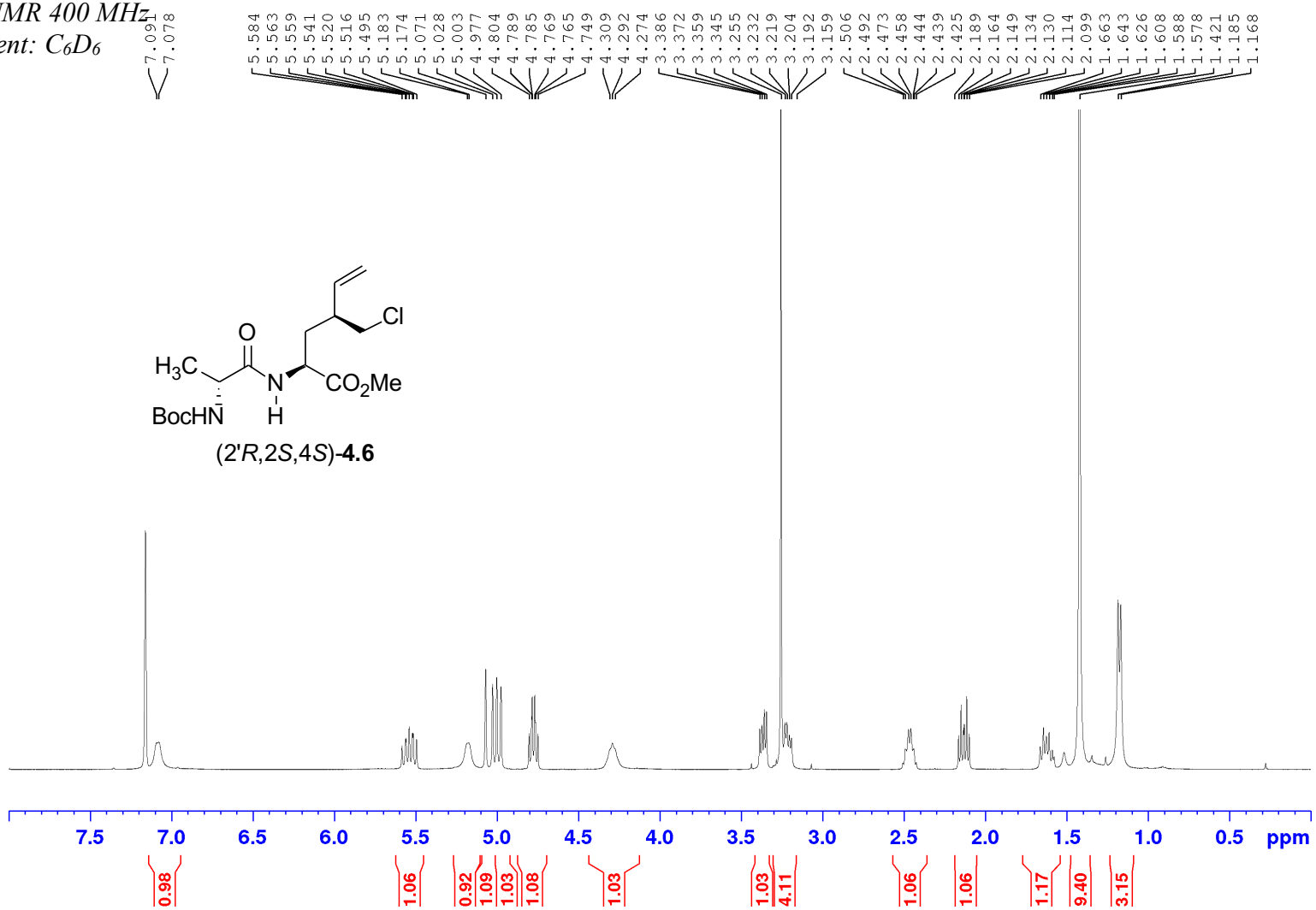

^{13}C NMR 100 MHz
Solvent: C_6D_6

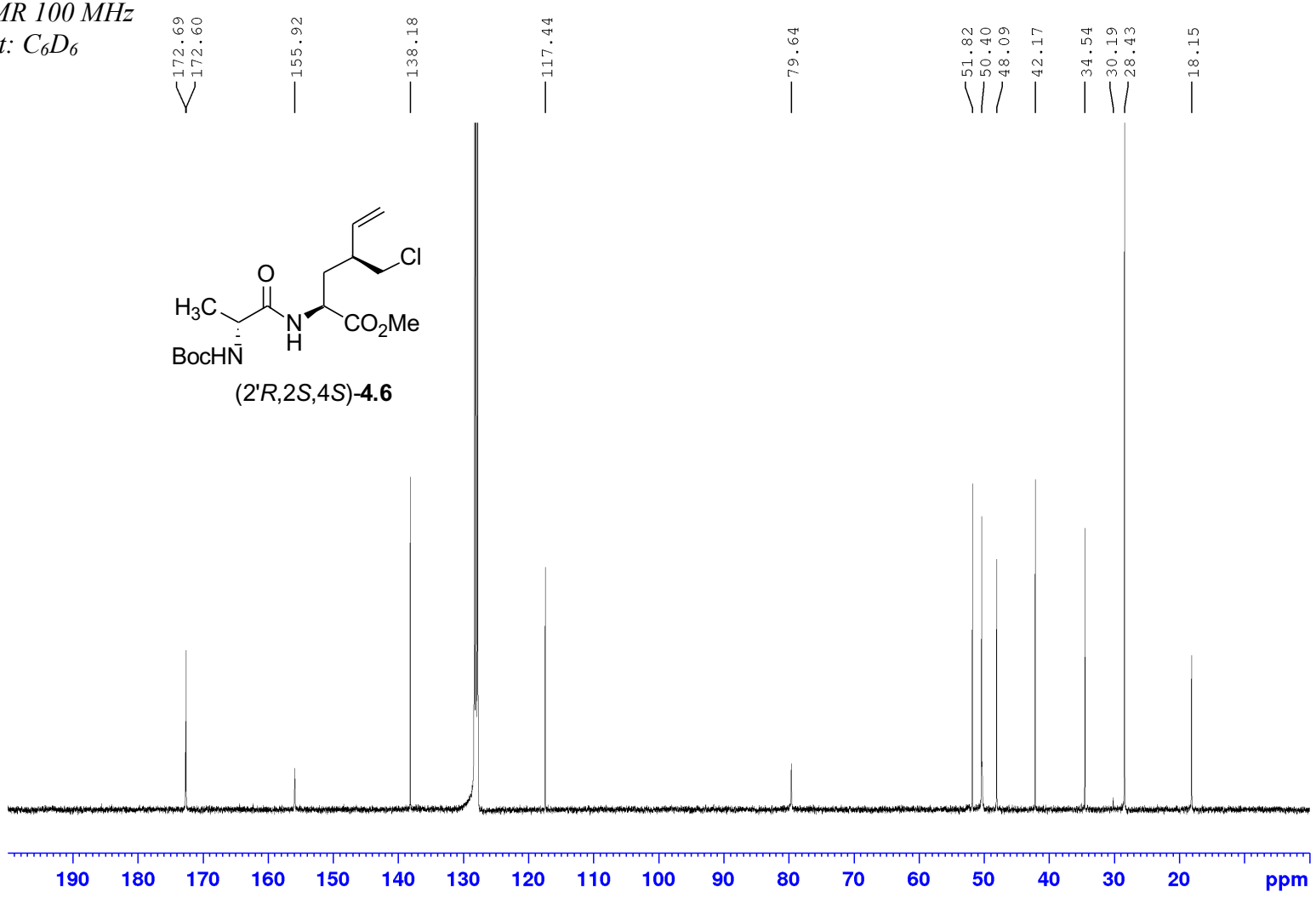

^{1}H NMR 500 MHz
Solvent: $CDCl_3$

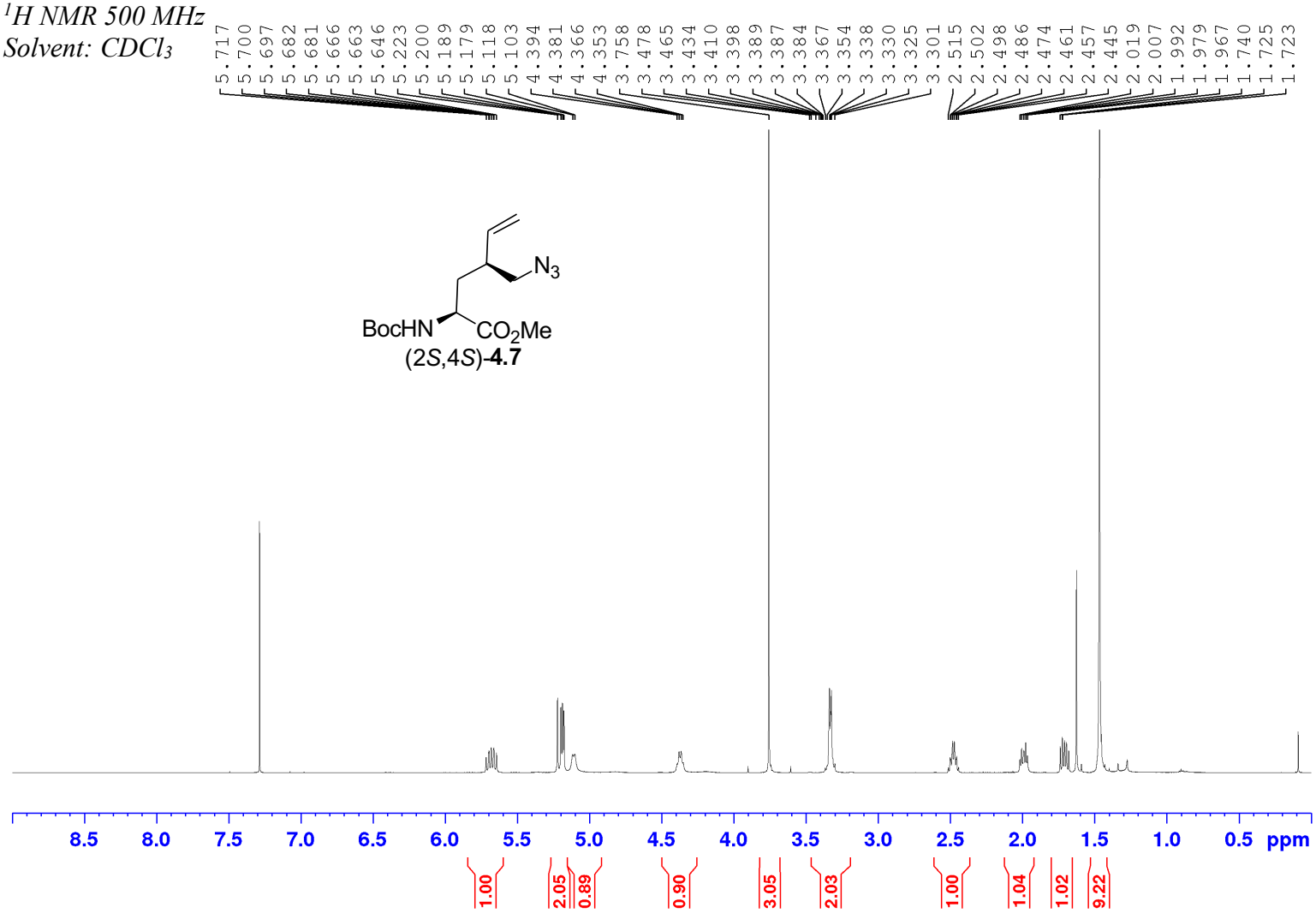

^{13}C NMR 125 MHz
Solvent: $CDCl_3$

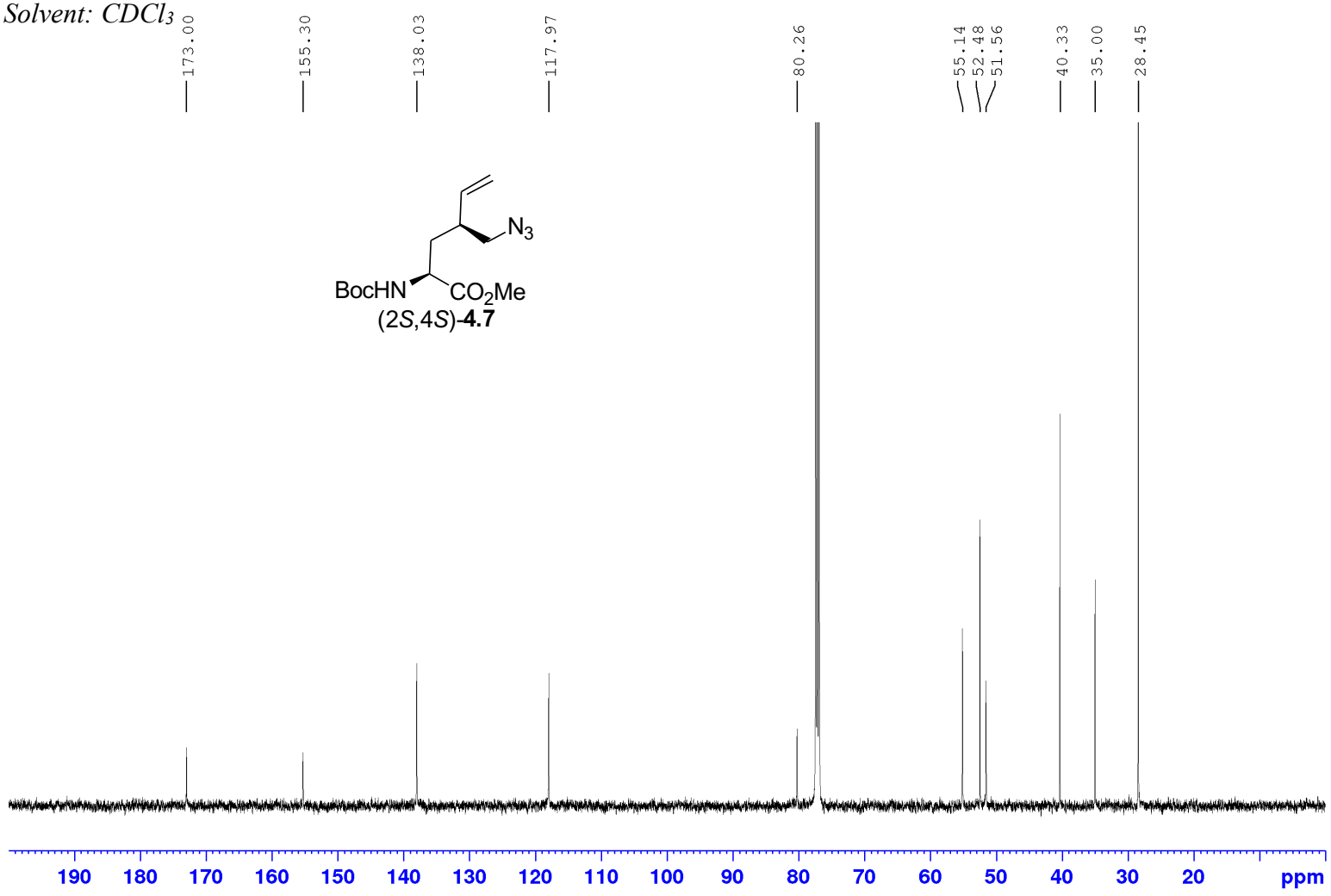

^{1}H NMR 500 MHz
Solvent: $CDCl_3$

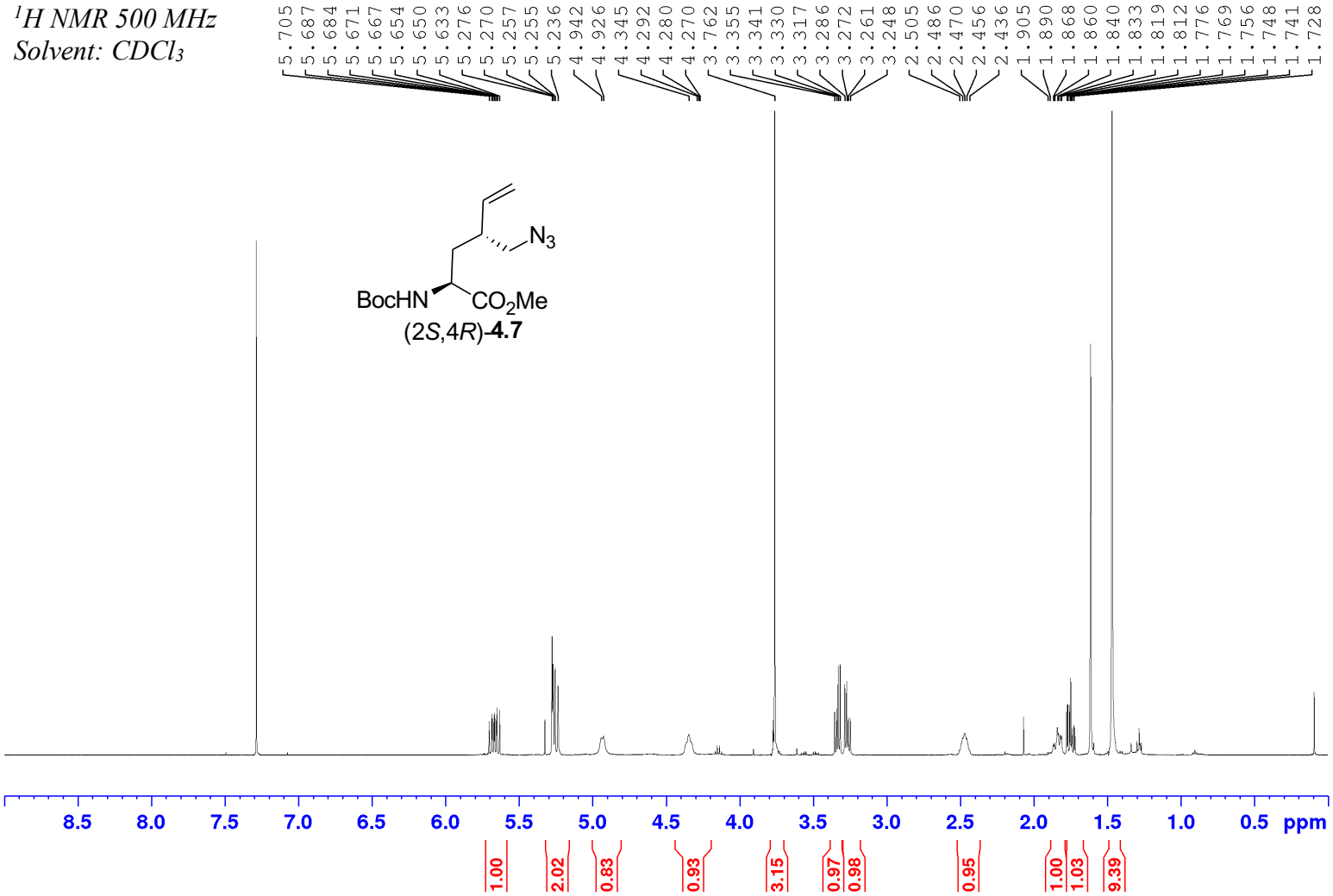

^{13}C NMR 125 MHz
Solvent: $CDCl_3$

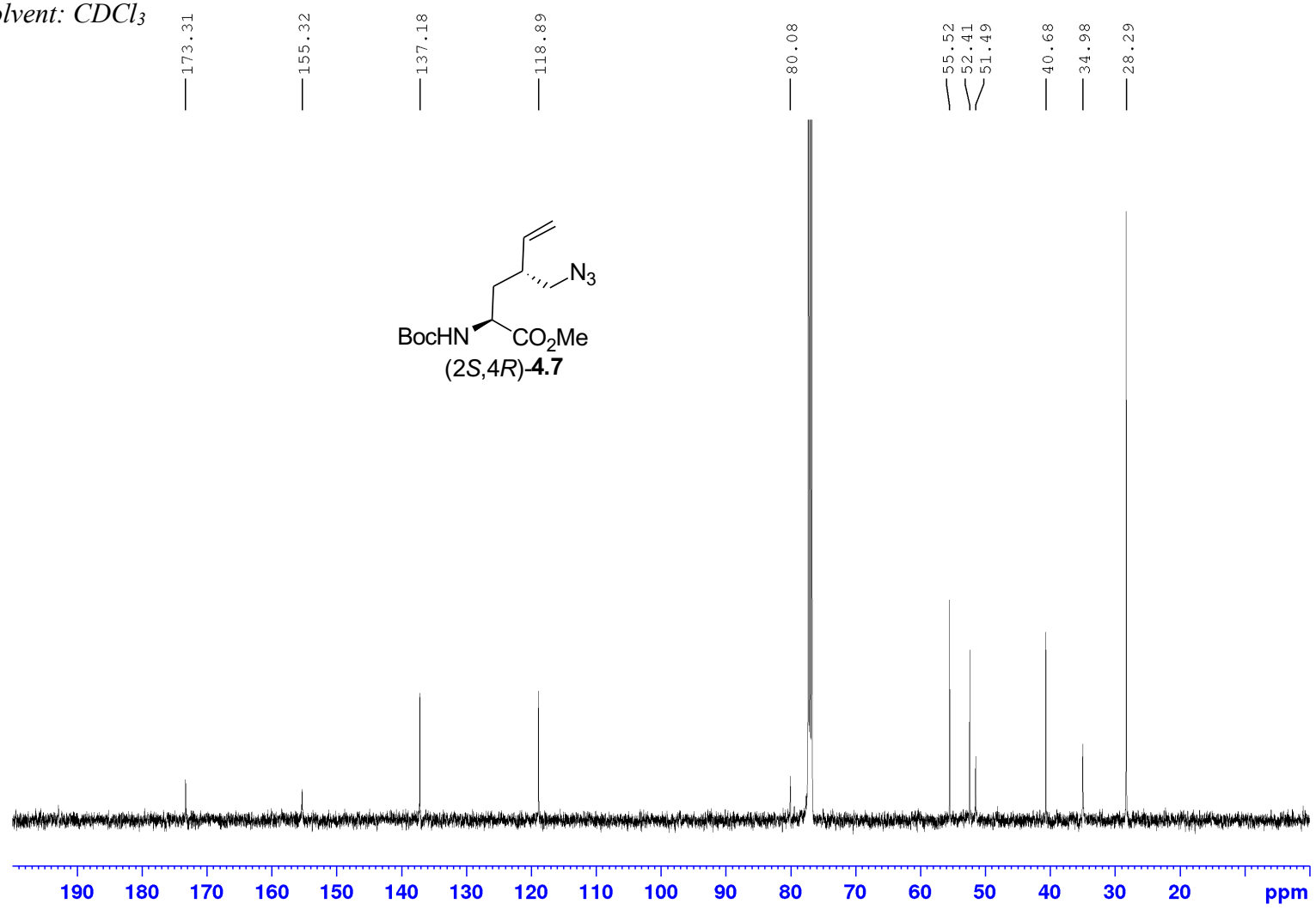

^{1}H NMR 500 MHz
Solvent: $CDCl_3$

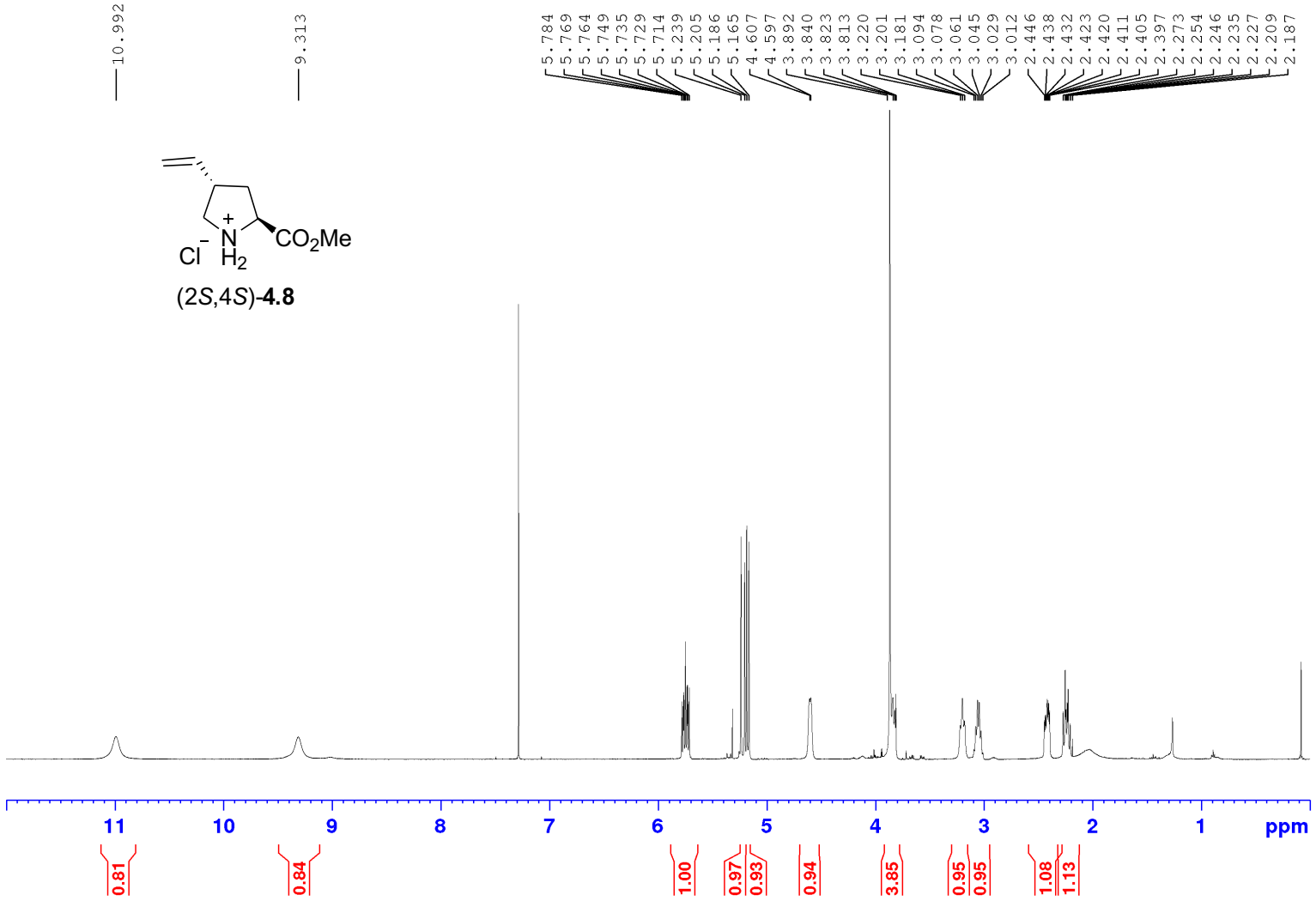

^{13}C NMR 125 MHz
Solvent: $CDCl_3$

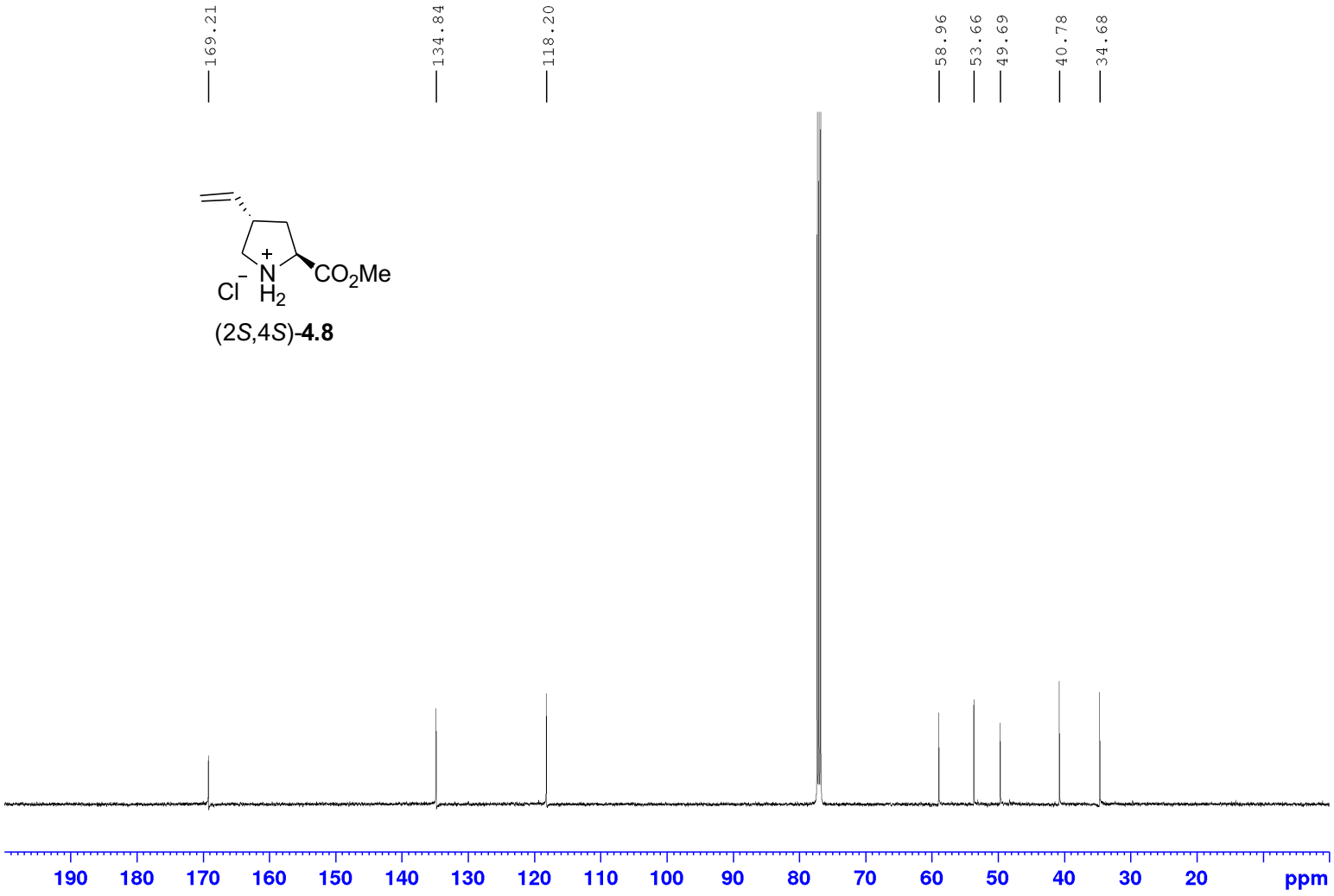

COSY NMR 500 MHz
Solvent: $CDCl_3$

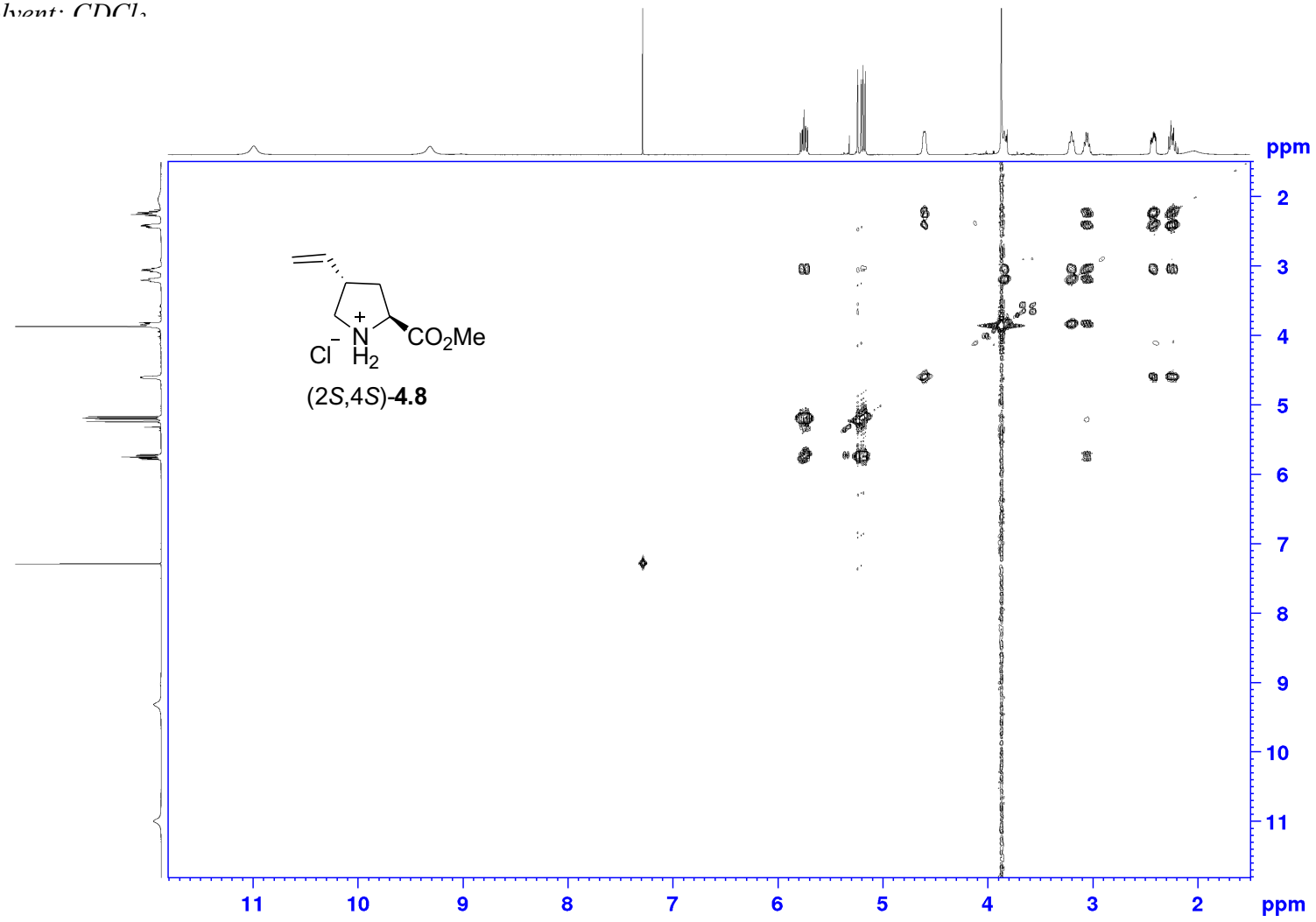

(2*S*,4*S*)-**4.8**

HSQC NMR 500 MHz
Solvent: $CDCl_3$

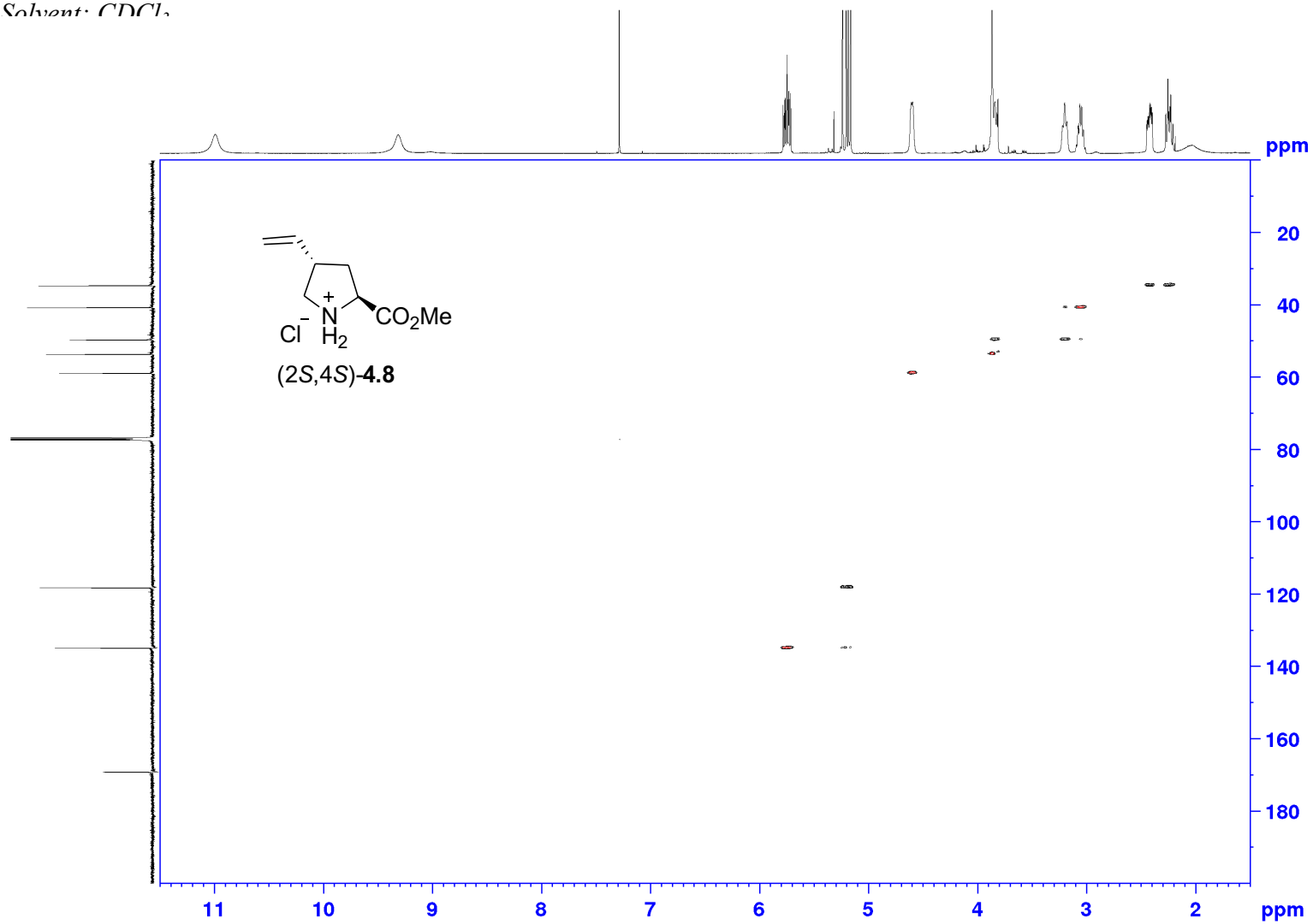

NOSEY NMR 500 MHz
Solvent: $CDCl_3$

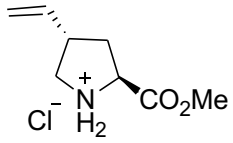

(2*S*,4*S*)-**4.8**

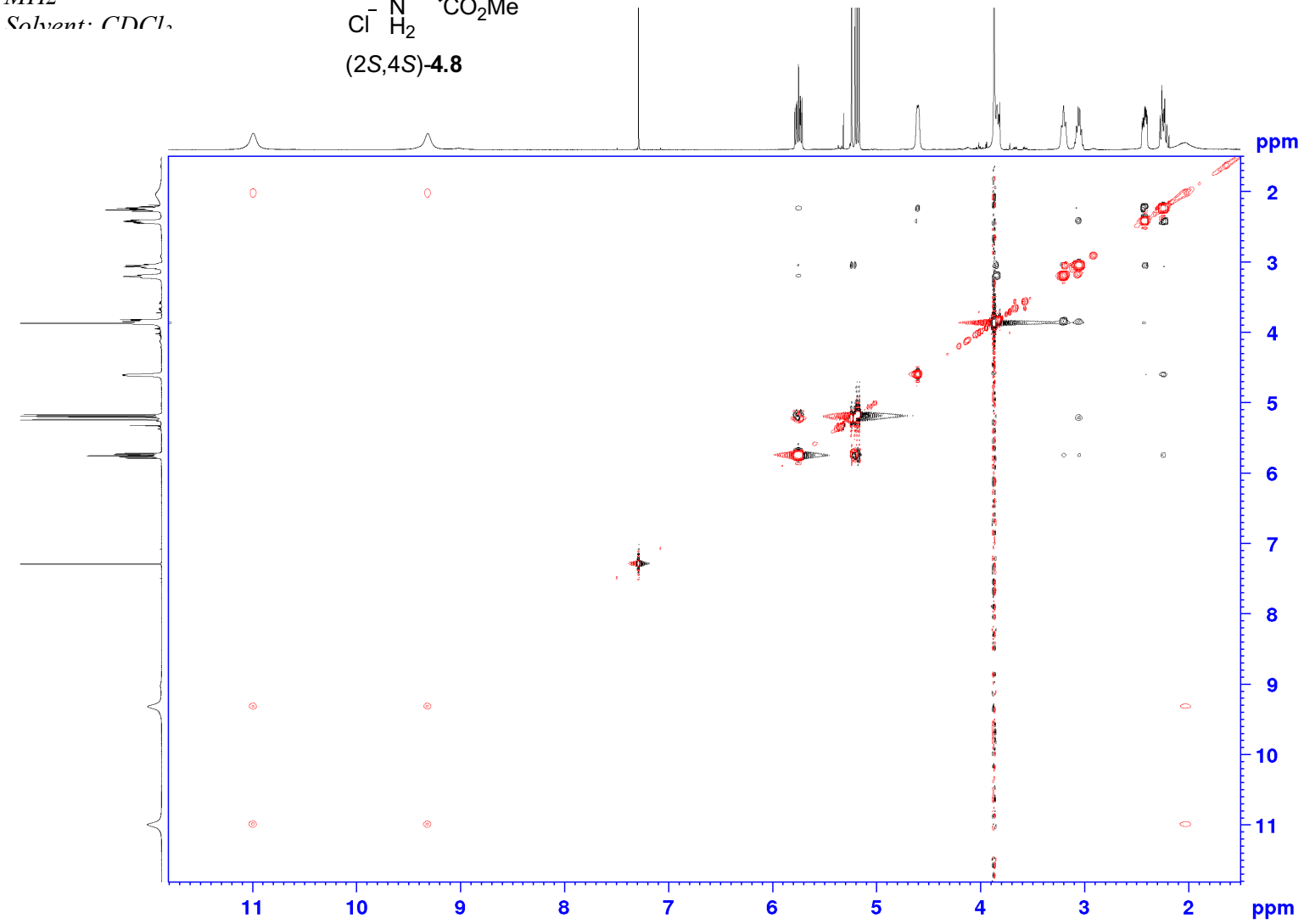

^{1}H NMR 500 MHz
Solvent: $CDCl_3$

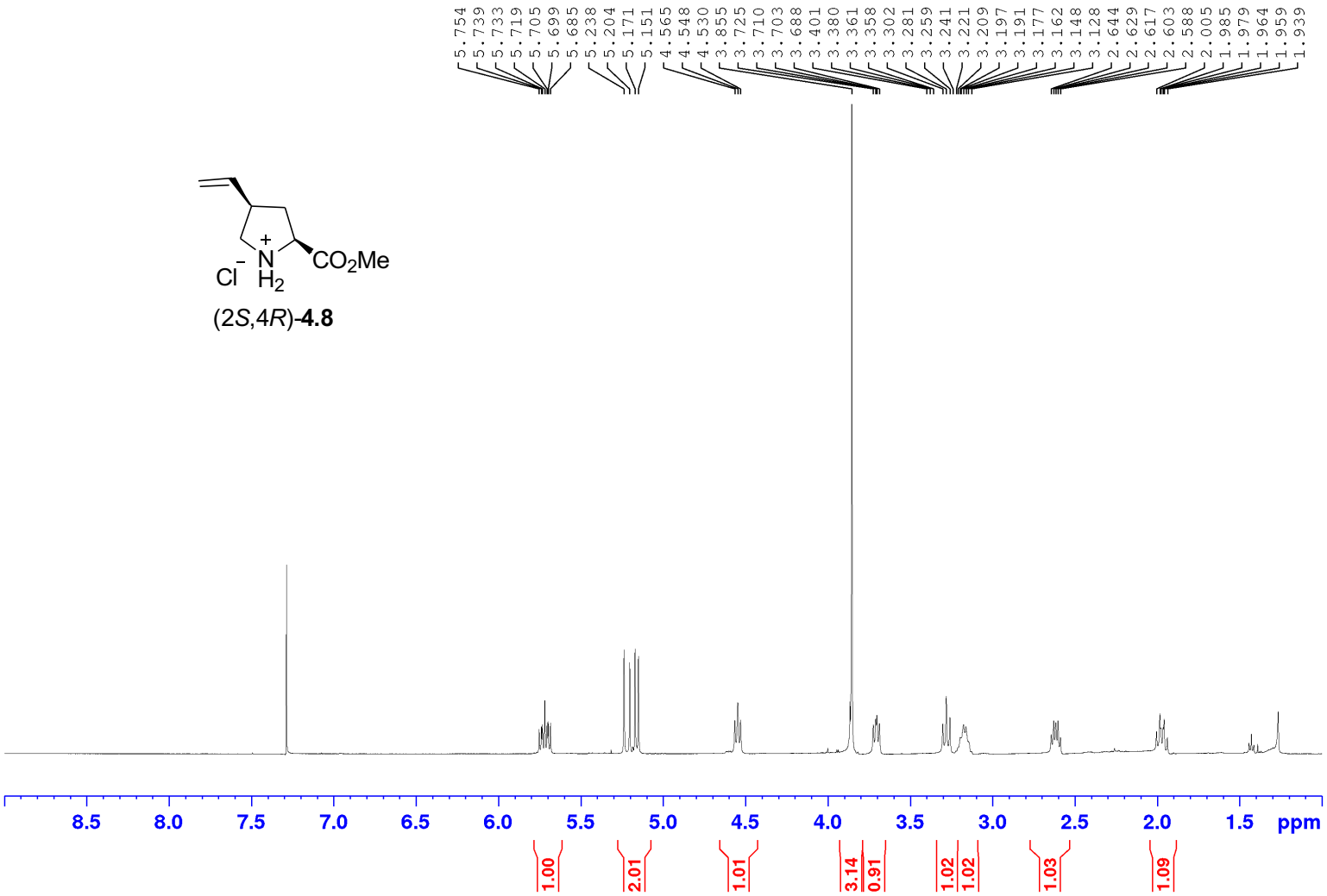

(2*S*,4*R*)-**4.8**

^{13}C NMR 125 MHz
Solvent: $CDCl_3$

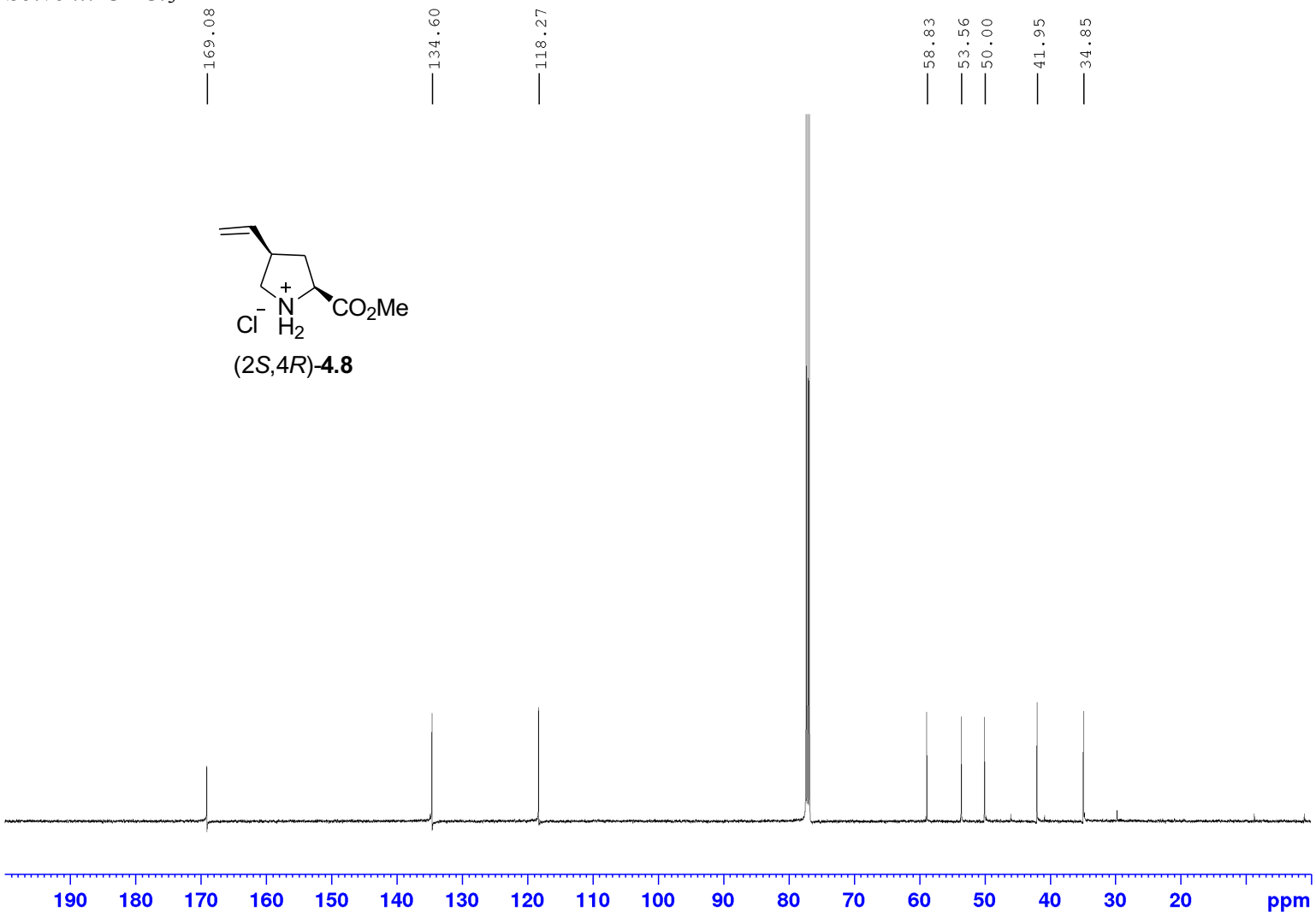

(2*S*,4*R*)-**4.8**

COSY NMR 500 MHz
Solvent: $CDCl_3$

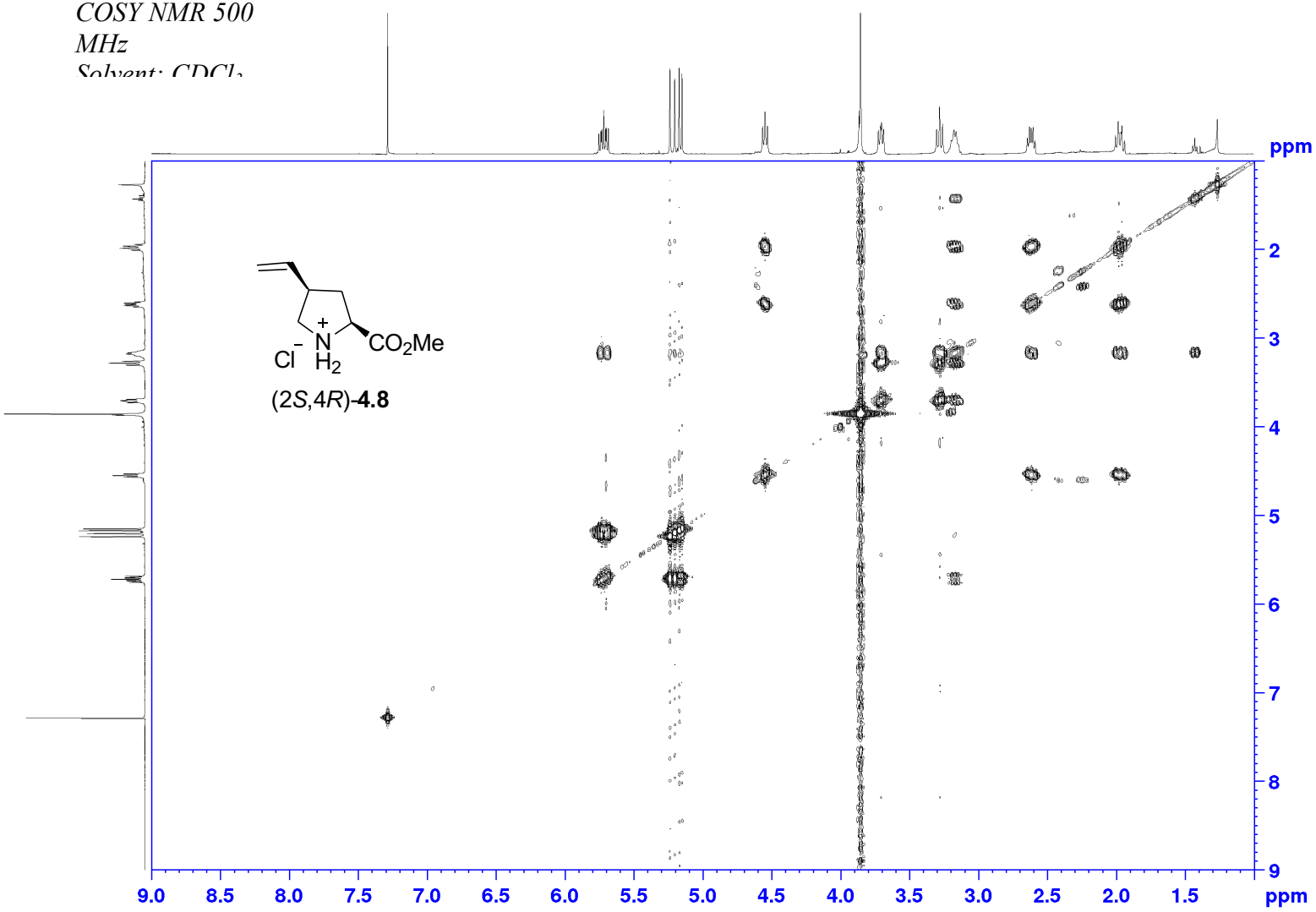

(2*S*,4*R*)-**4.8**

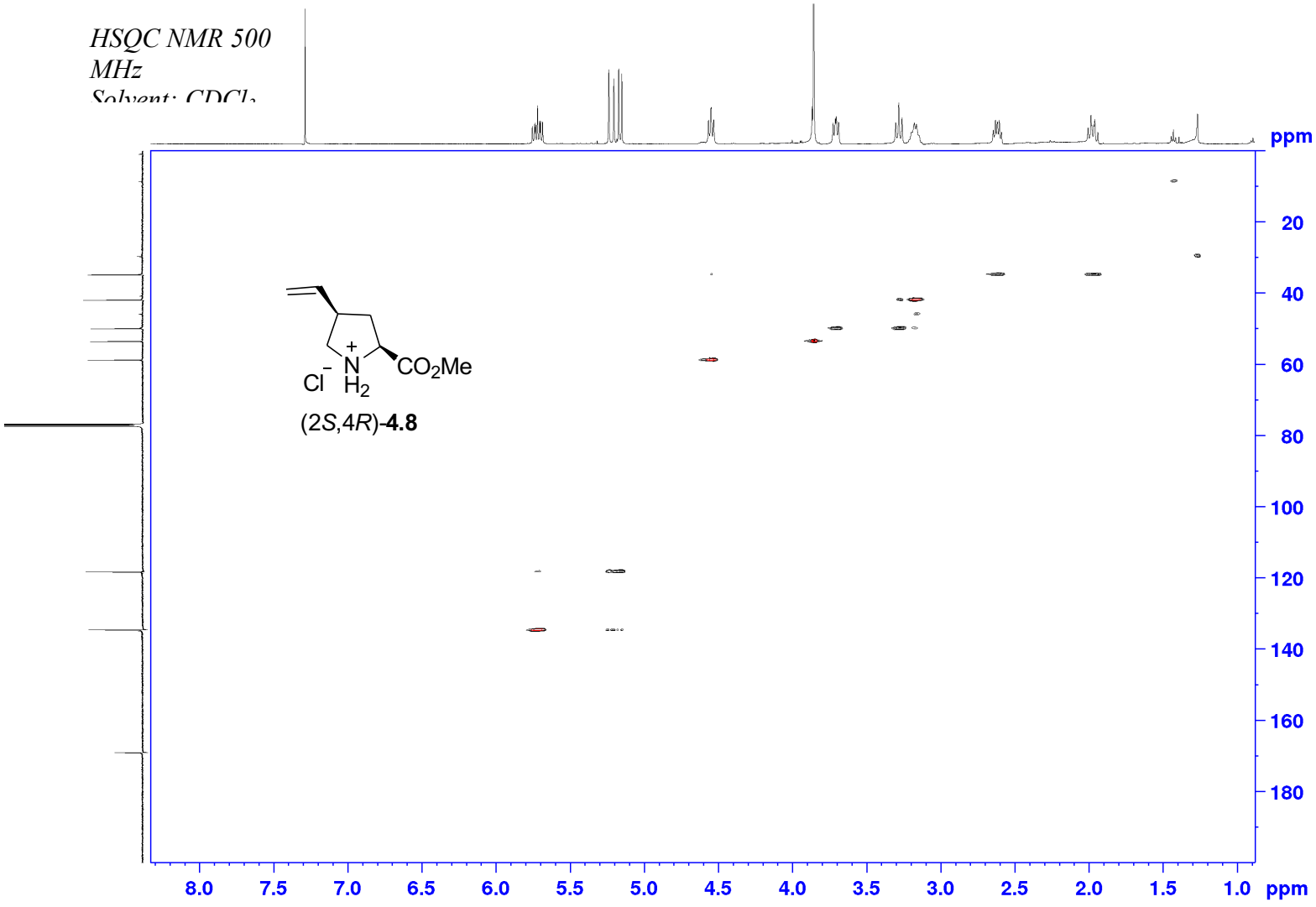
HSQC NMR 500
MHz
Solvent: CDCl3
ppm
20
40
60
80
100
120
140
160
180
8.0
7.5
7.0
6.5
6.0
5.5
5.0
4.5
4.0
3.5
3.0
2.5
2.0
1.5
1.0
ppm
Cl
N
H2
CO2Me
(2S,4R)-4.8

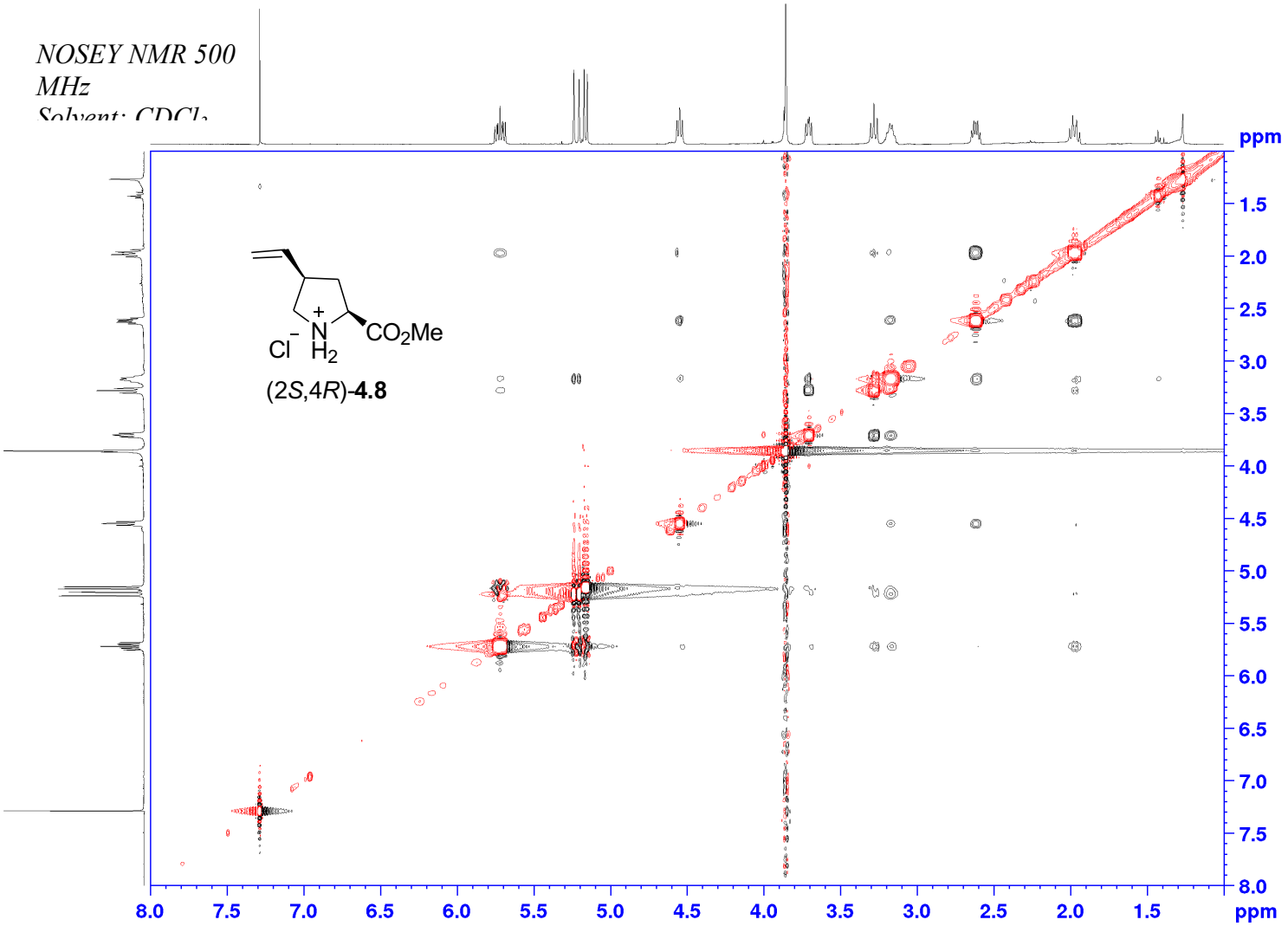
NOSEY NMR 500
MHz
Solvent: CDCl3
ppm
1.5
2.0
2.5
3.0
3.5
4.0
4.5
5.0
5.5
6.0
6.5
7.0
7.5
8.0
8.0
7.5
7.0
6.5
6.0
5.5
5.0
4.5
4.0
3.5
3.0
2.5
2.0
1.5
ppm
Cl⁻
N
H2
CO2Me
(2S,4R)-4.8

Spectral data for article 4

^{1}H NMR 700MHz
Solvent: CD_3OD

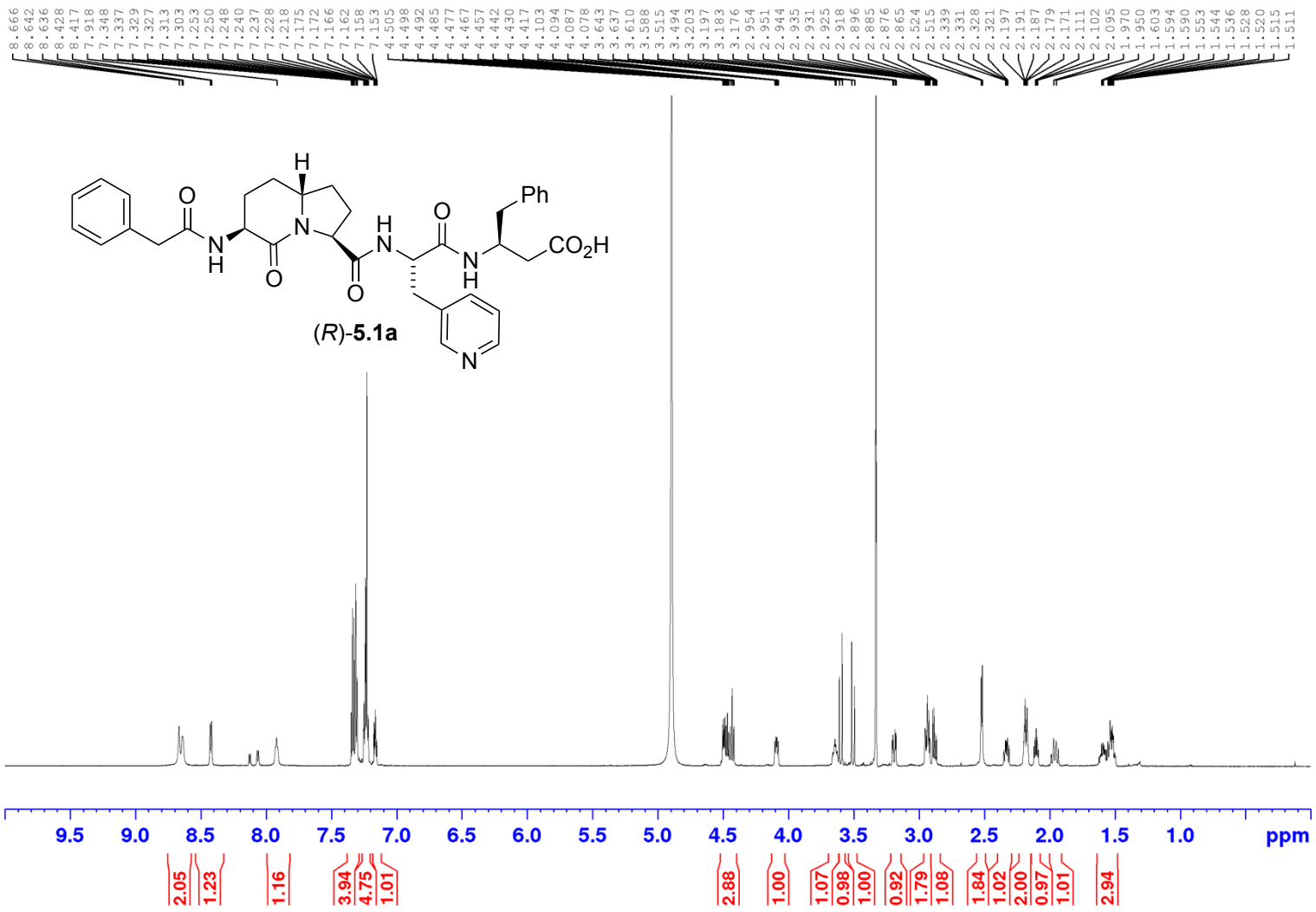

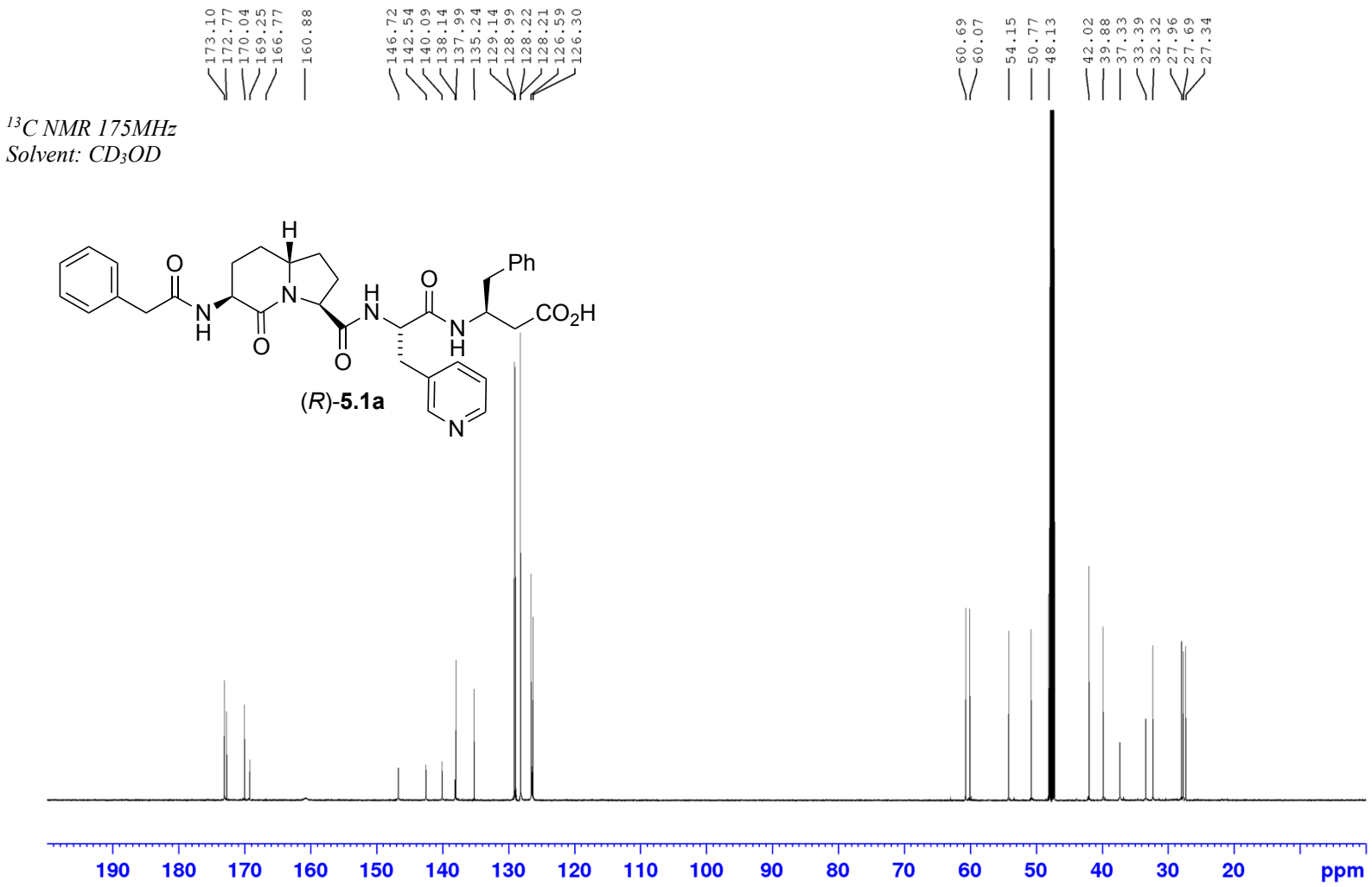
173.10
172.77
170.04
169.25
166.77
160.88
146.72
142.54
140.09
138.14
137.99
135.24
129.14
128.99
128.22
128.21
126.59
126.30
60.69
60.07
54.15
50.77
48.13
42.02
39.88
37.33
33.39
32.32
27.96
27.69
27.34
13C NMR 175MHz
Solvent: CD3OD
(R)-5.1a
190
180
170
160
150
140
130
120
110
100
90
80
70
60
50
40
30
20
ppm

^{1}H NMR 700MHz
Solvent: CD_3OD

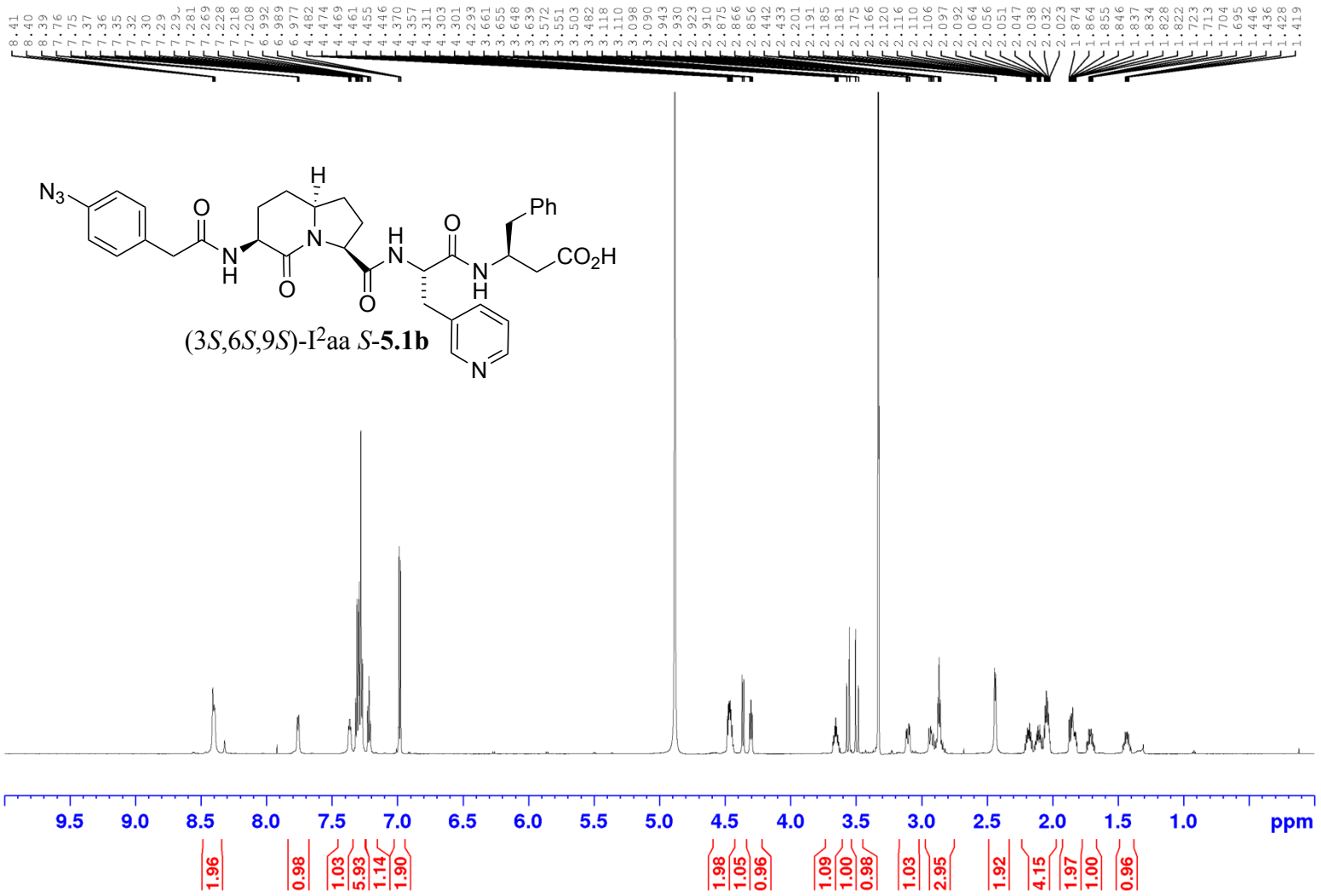

(3*S*,6*S*,9*S*)-I^{2}aa *S*-**5.1b**

^{13}C NMR 175MHz
Solvent: CD_3OD

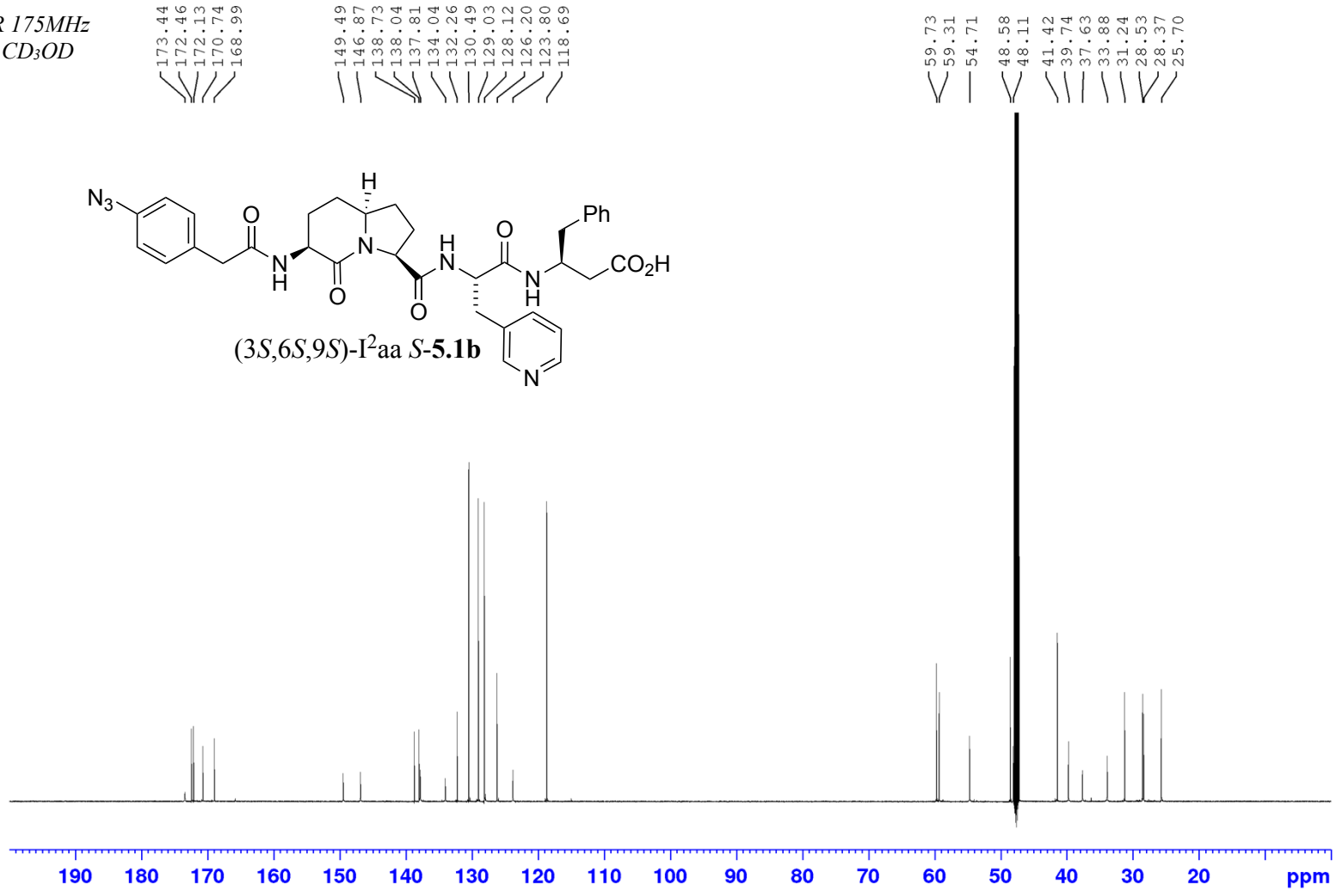

(3*S*,6*S*,9*S*)-I^{2}aa *S*-**5.1b**

^{1}H NMR 700MHz
Solvent: CD_3OD

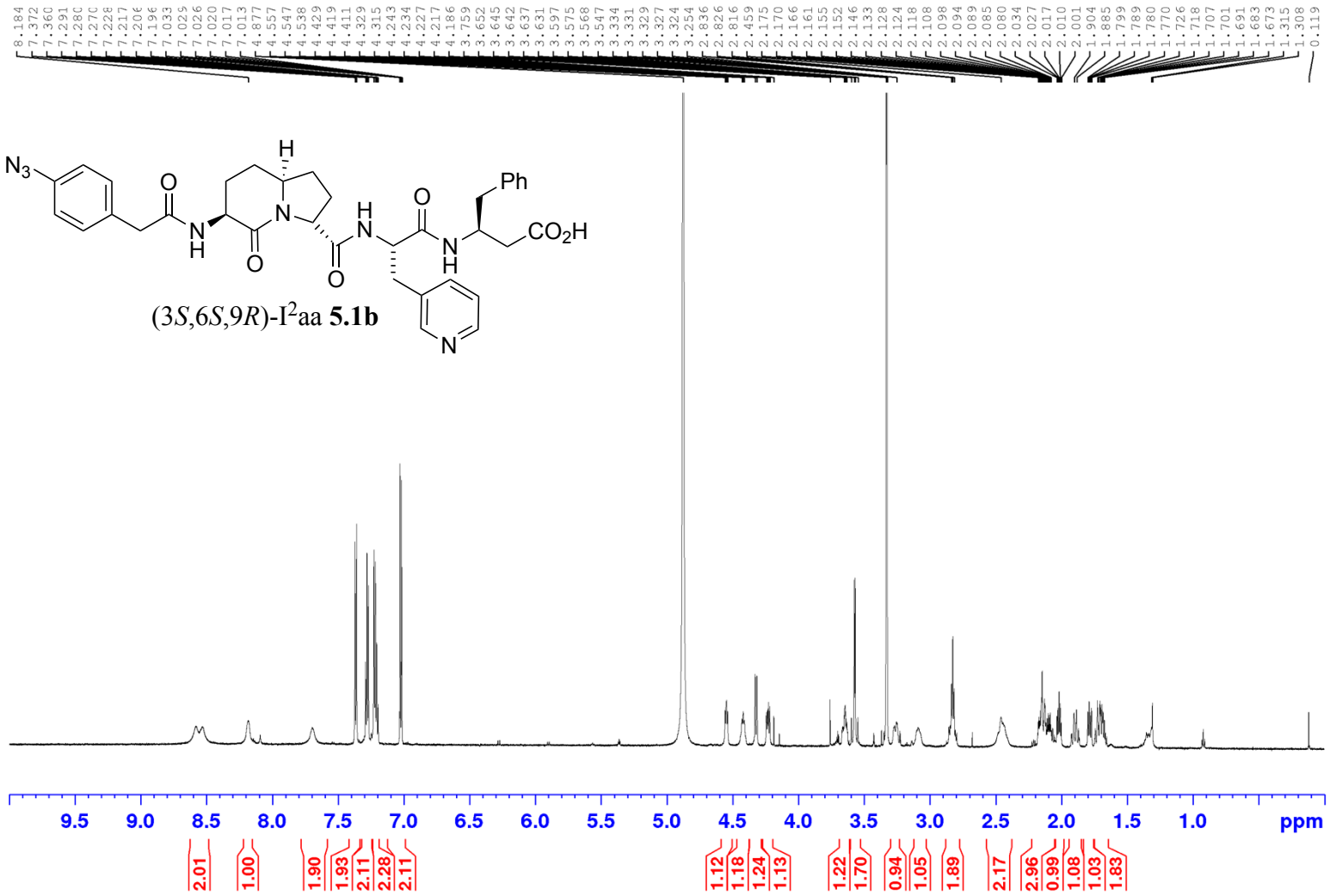

^{13}C NMR 175MHz
Solvent: CD_3OD

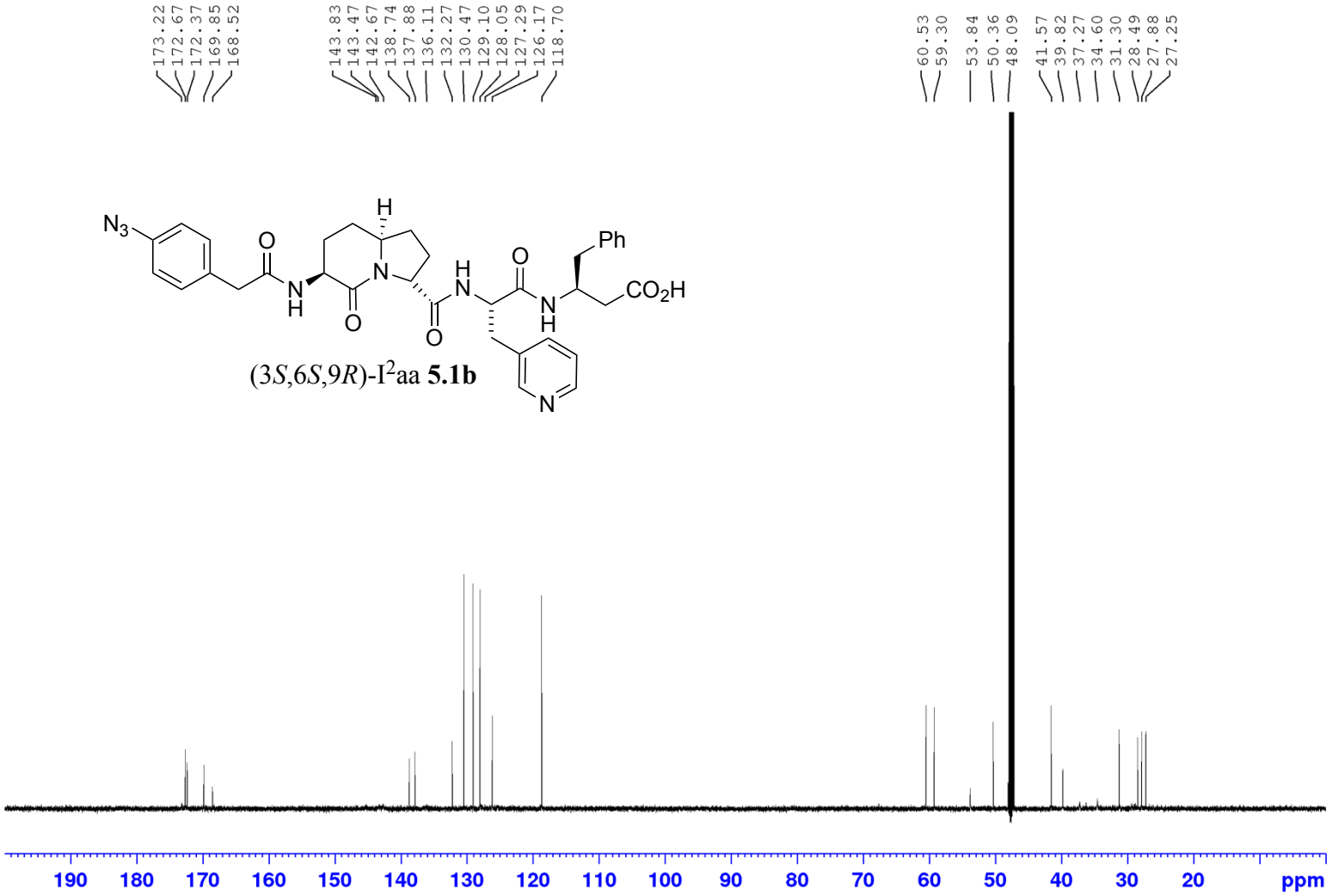

(3*S*,6*S*,9*R*)-I^{2}aa **5.1b**

^{1}H NMR 700MHz
Solvent: CD_3OD

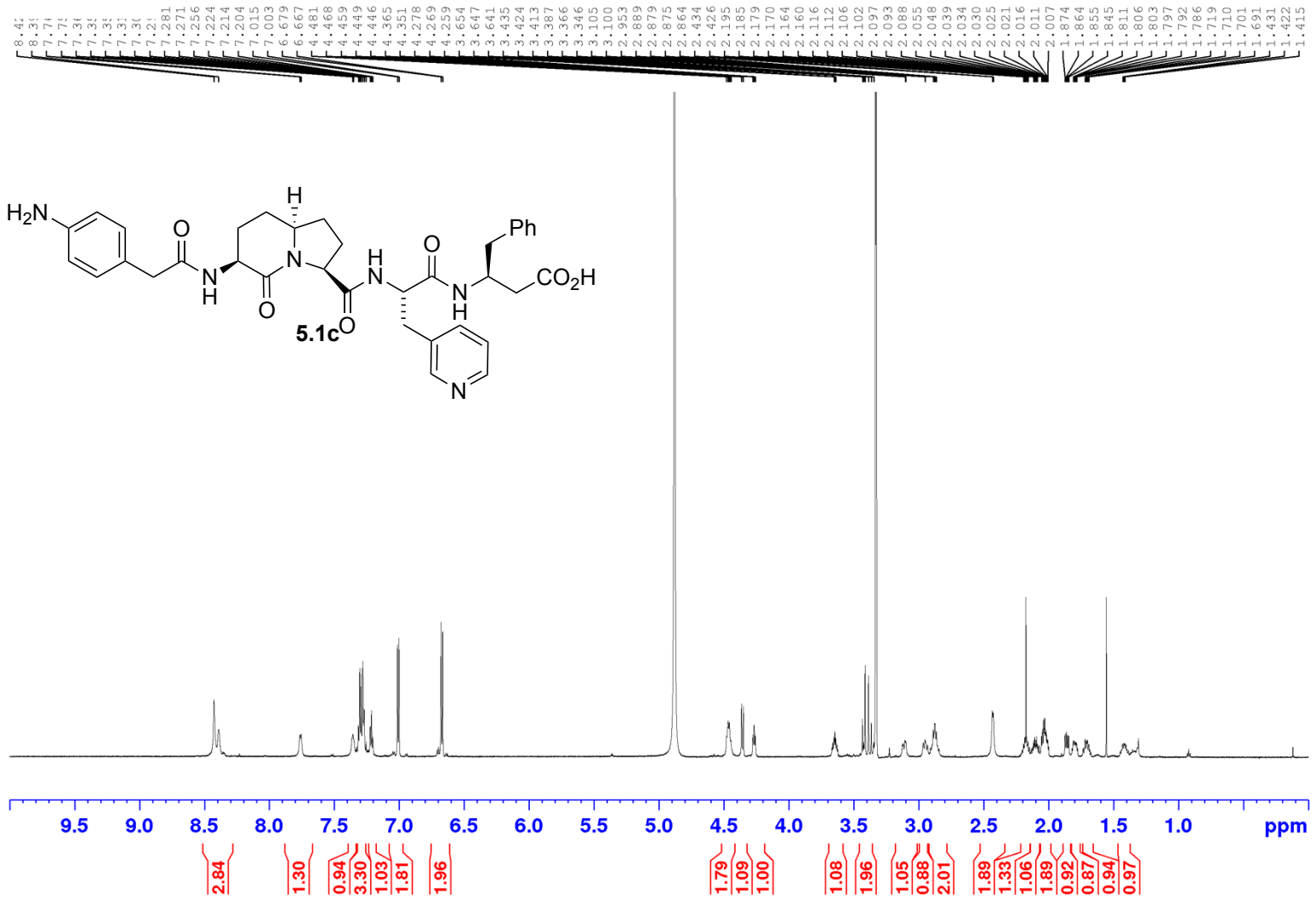

^{13}C NMR 175MHz
Solvent: CD_3OD

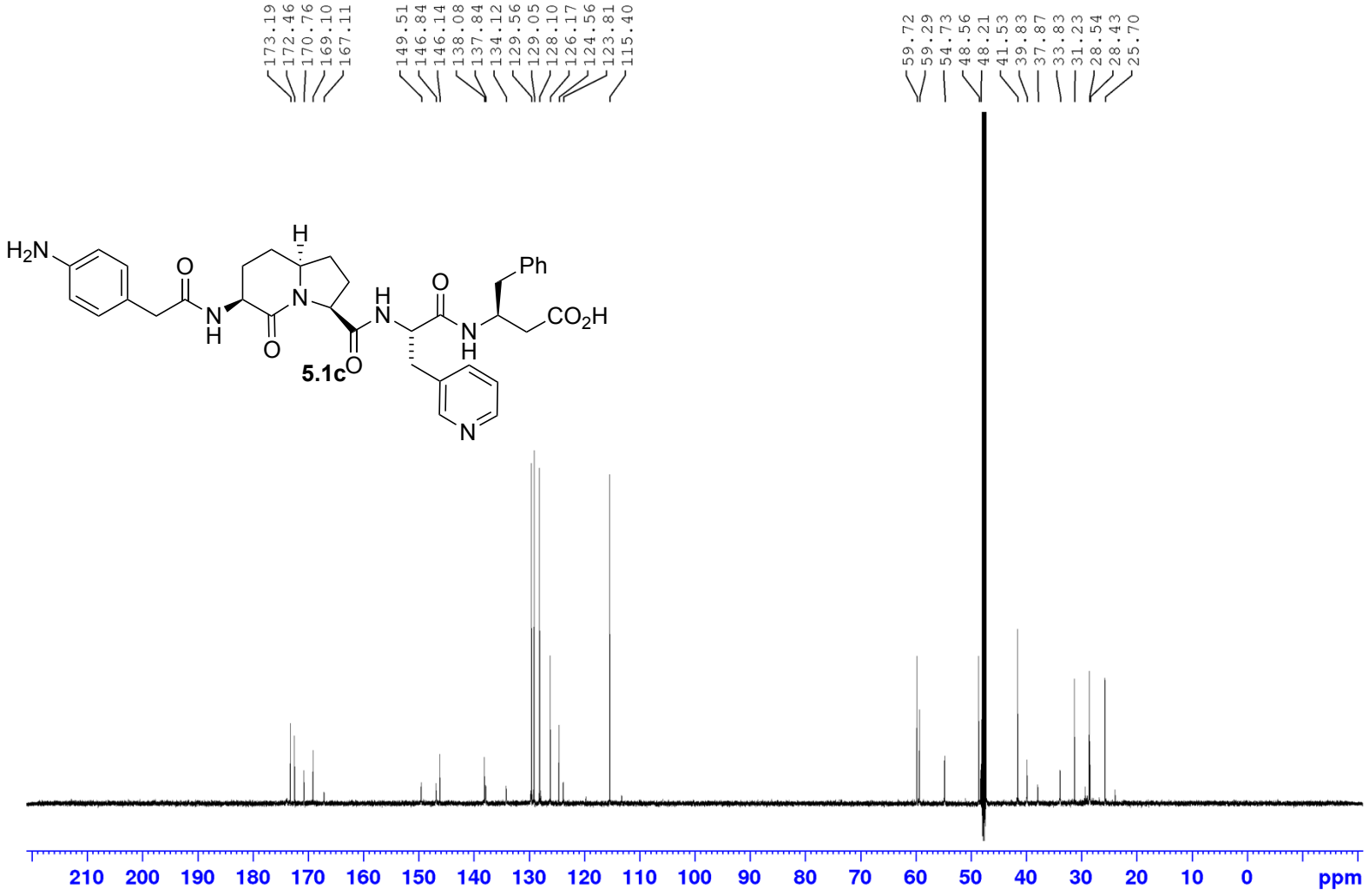

^{1}H NMR 700MHz
Solvent: CD_3OD

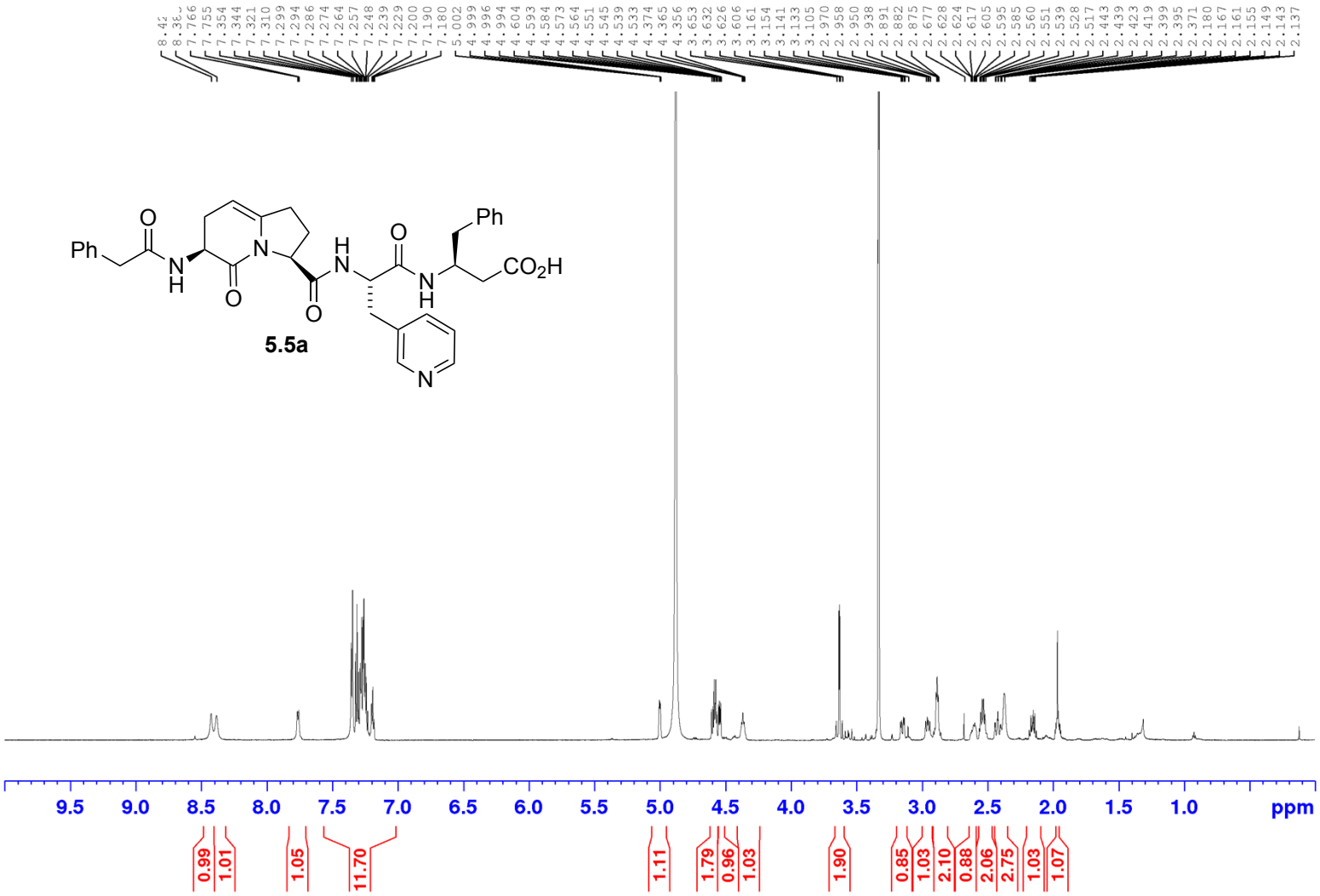

^{13}C NMR 175MHz
Solvent: CD_3OD

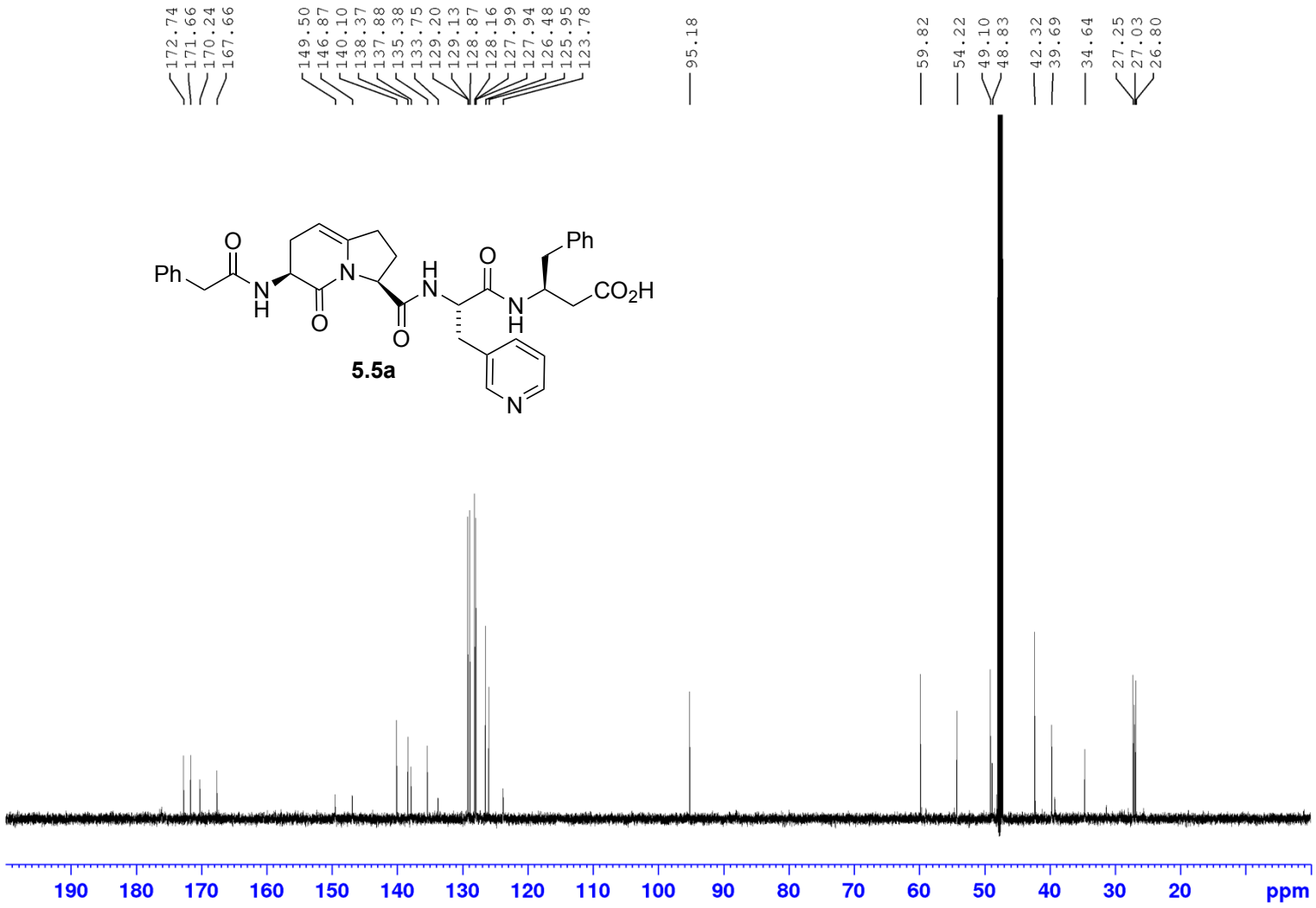

^{1}H NMR 700MHz
Solvent: CD_3OD

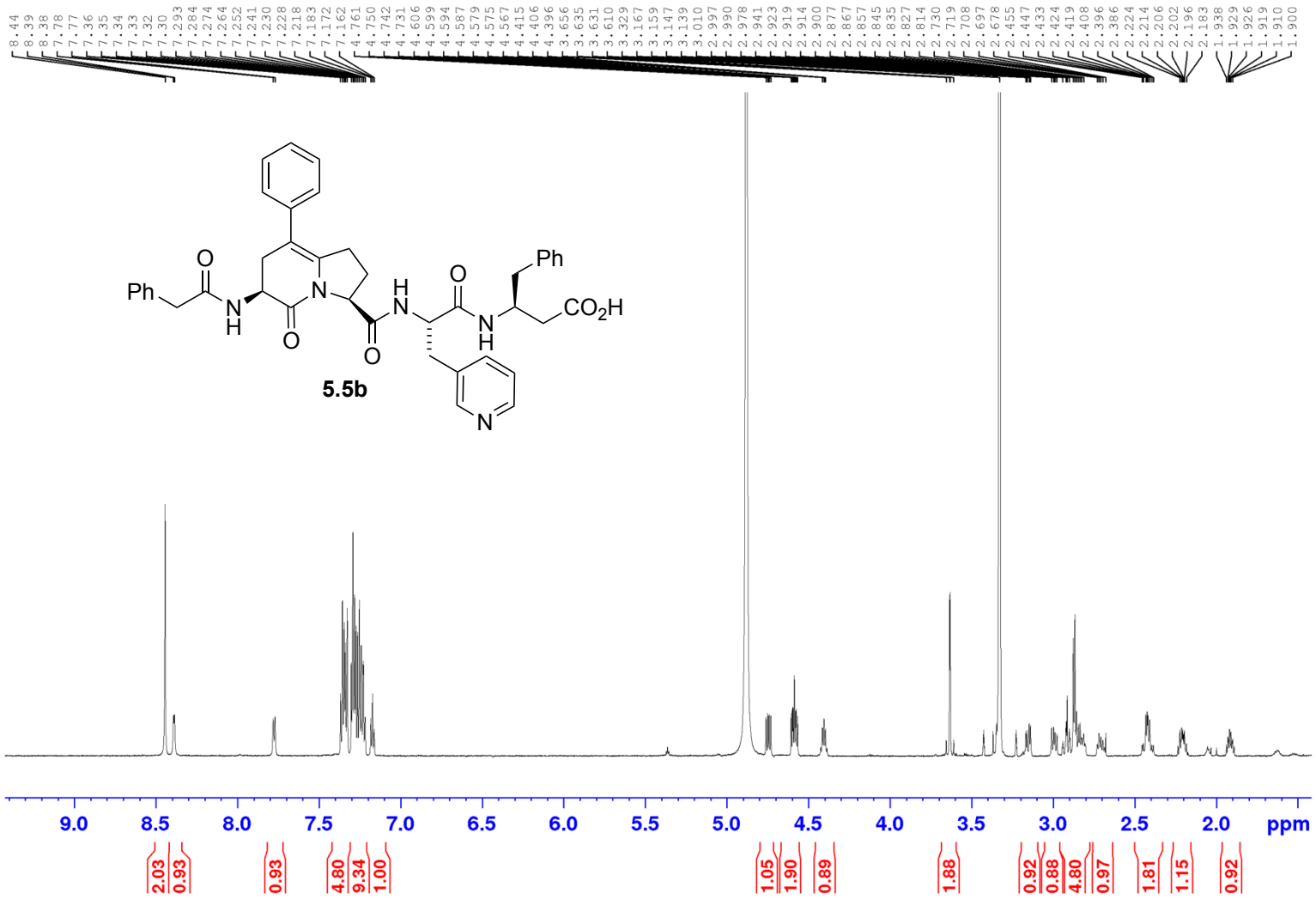

^{13}C NMR 175MHz
Solvent: CD_3OD

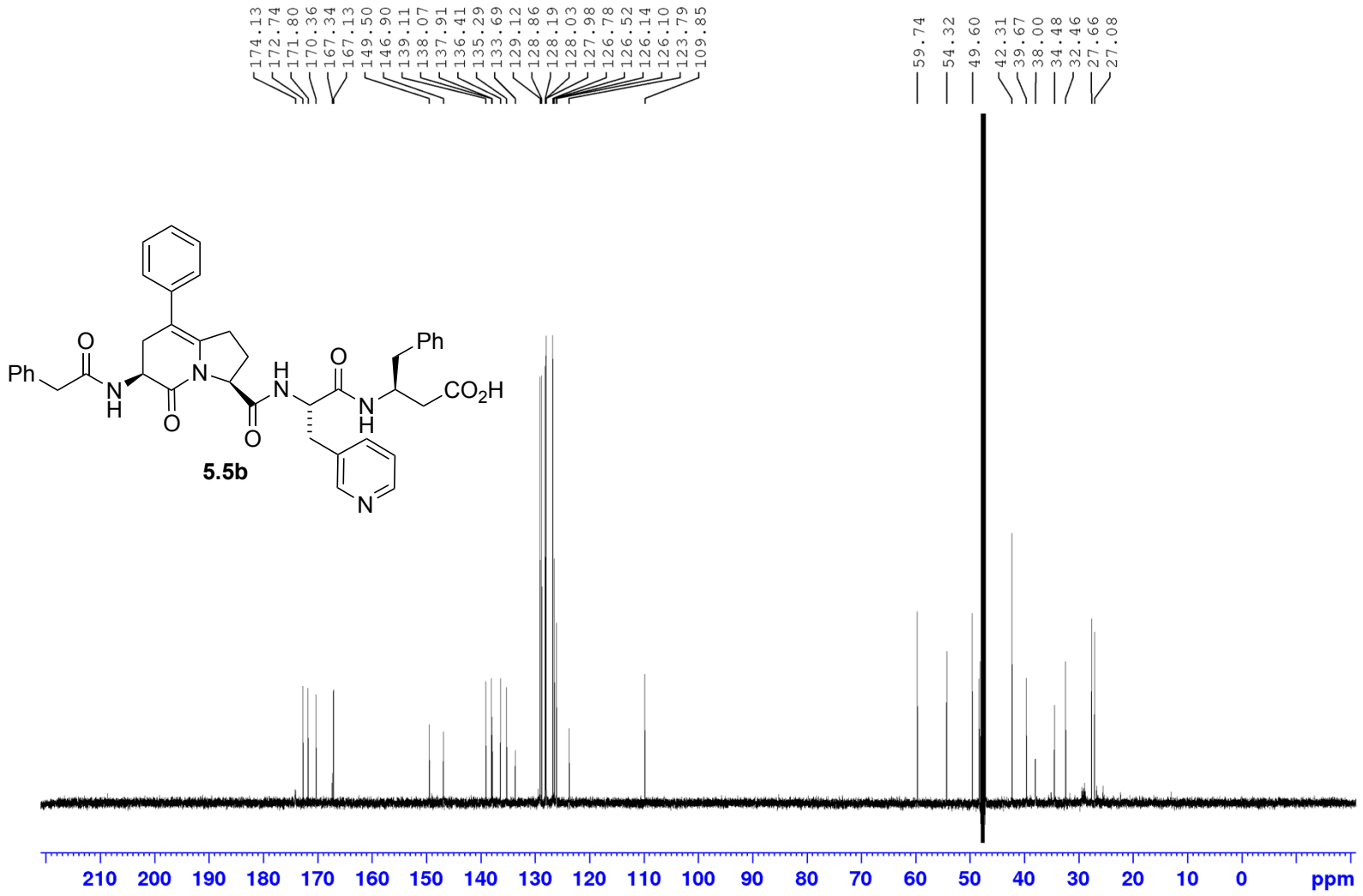

^{1}H NMR 700MHz
Solvent: CD_3OD

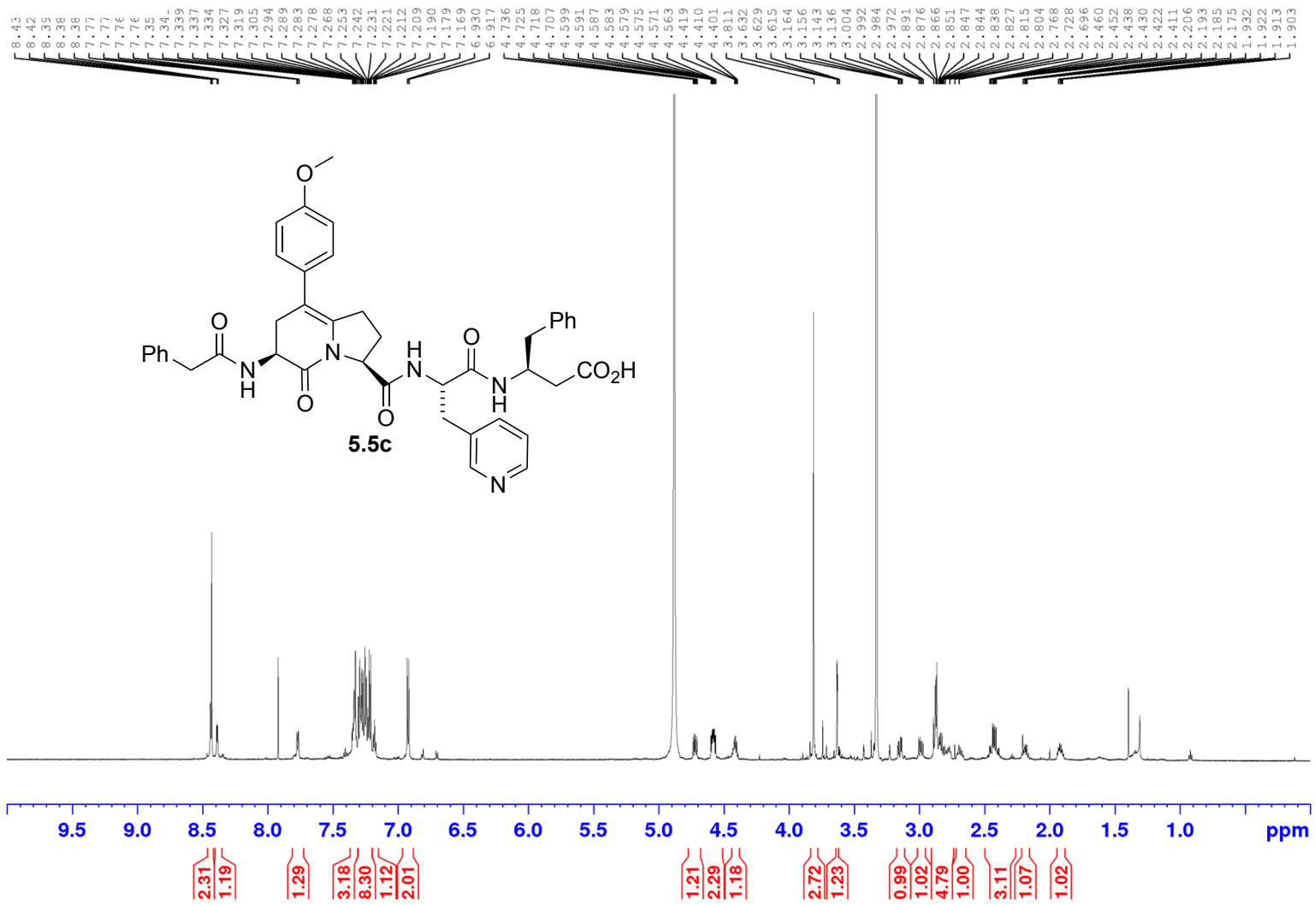

^{13}C NMR 175MHz
Solvent: CD_3OD

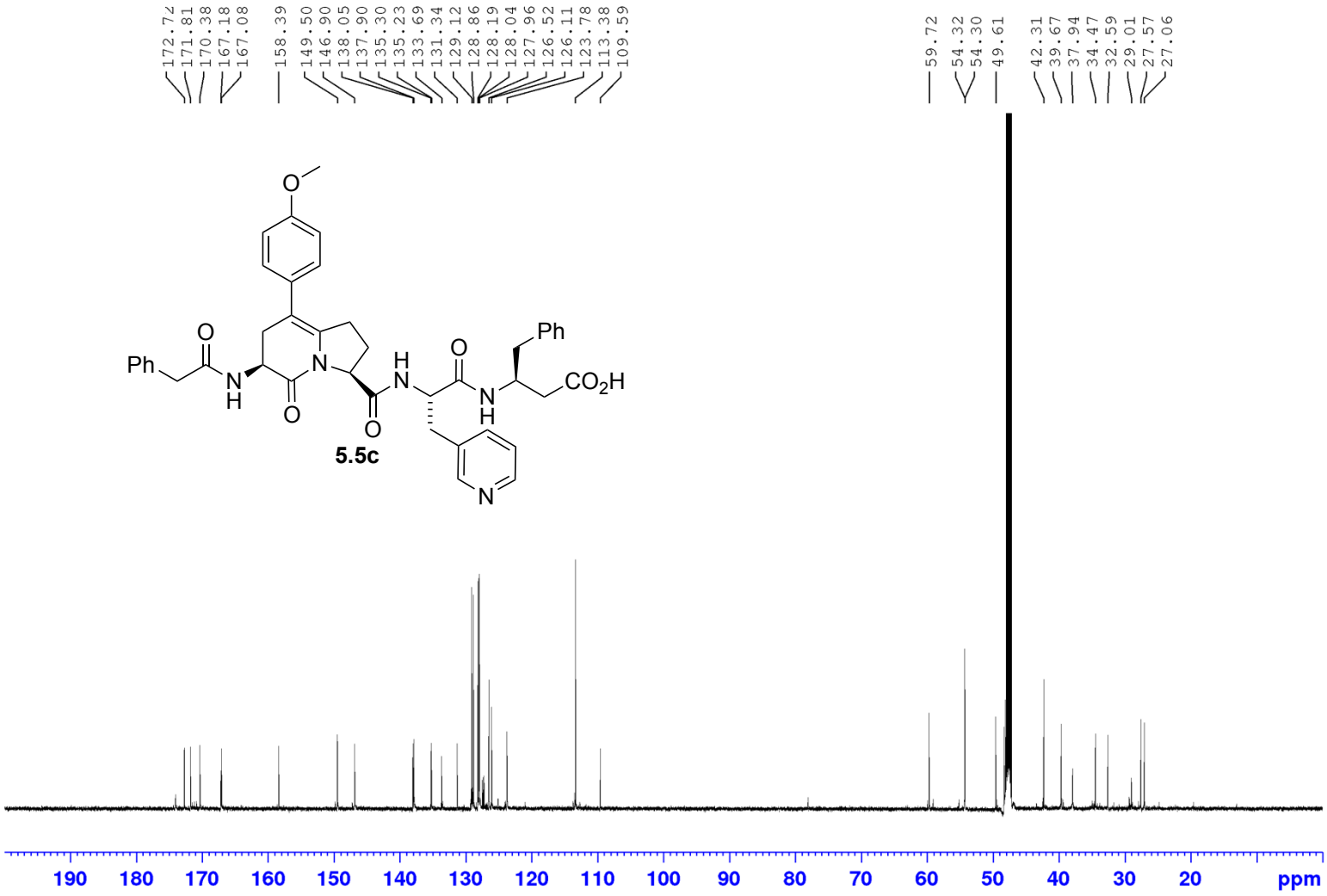

^{1}H NMR 700MHz
Solvent: CD_3OD

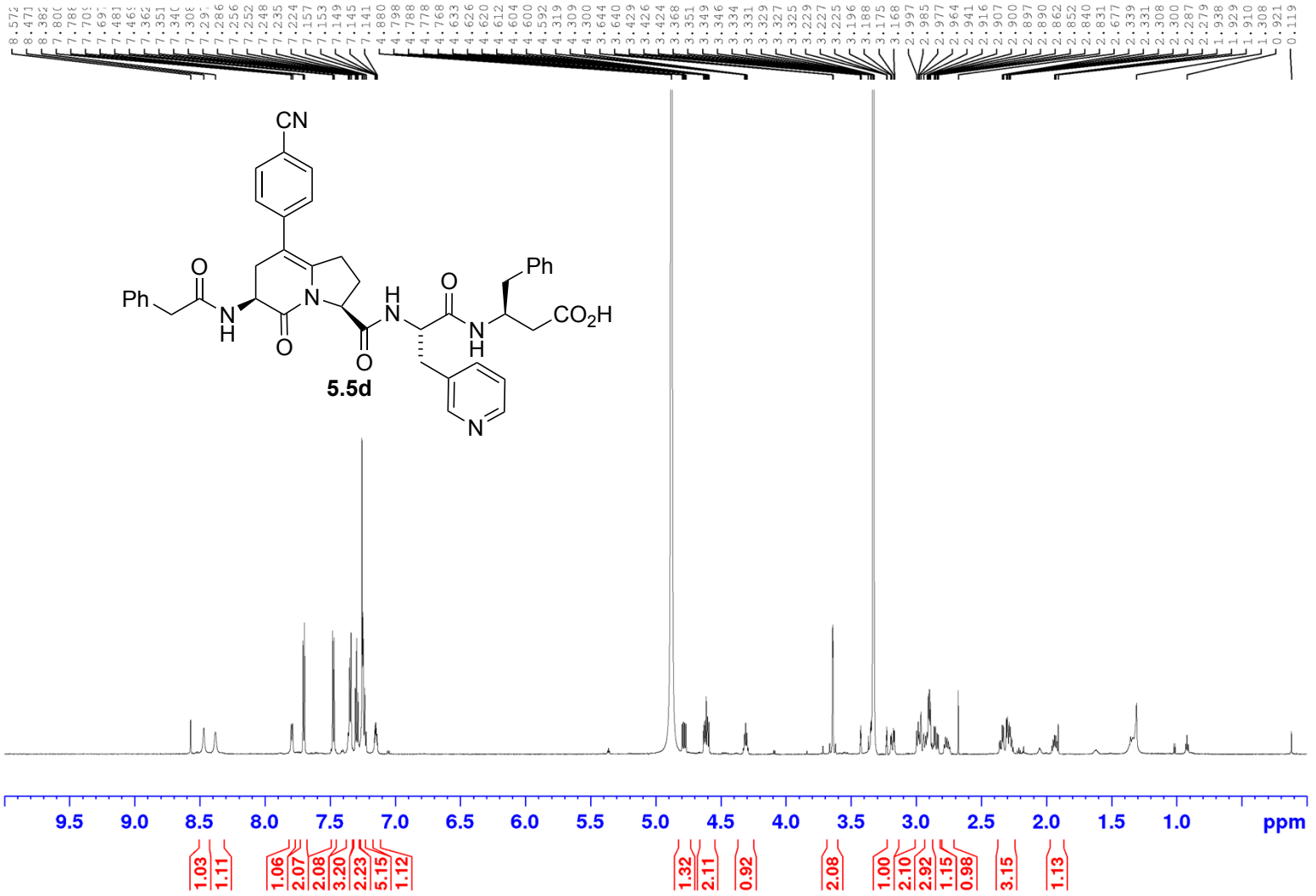

^{13}C NMR 175MHz
Solvent: CD_3OD

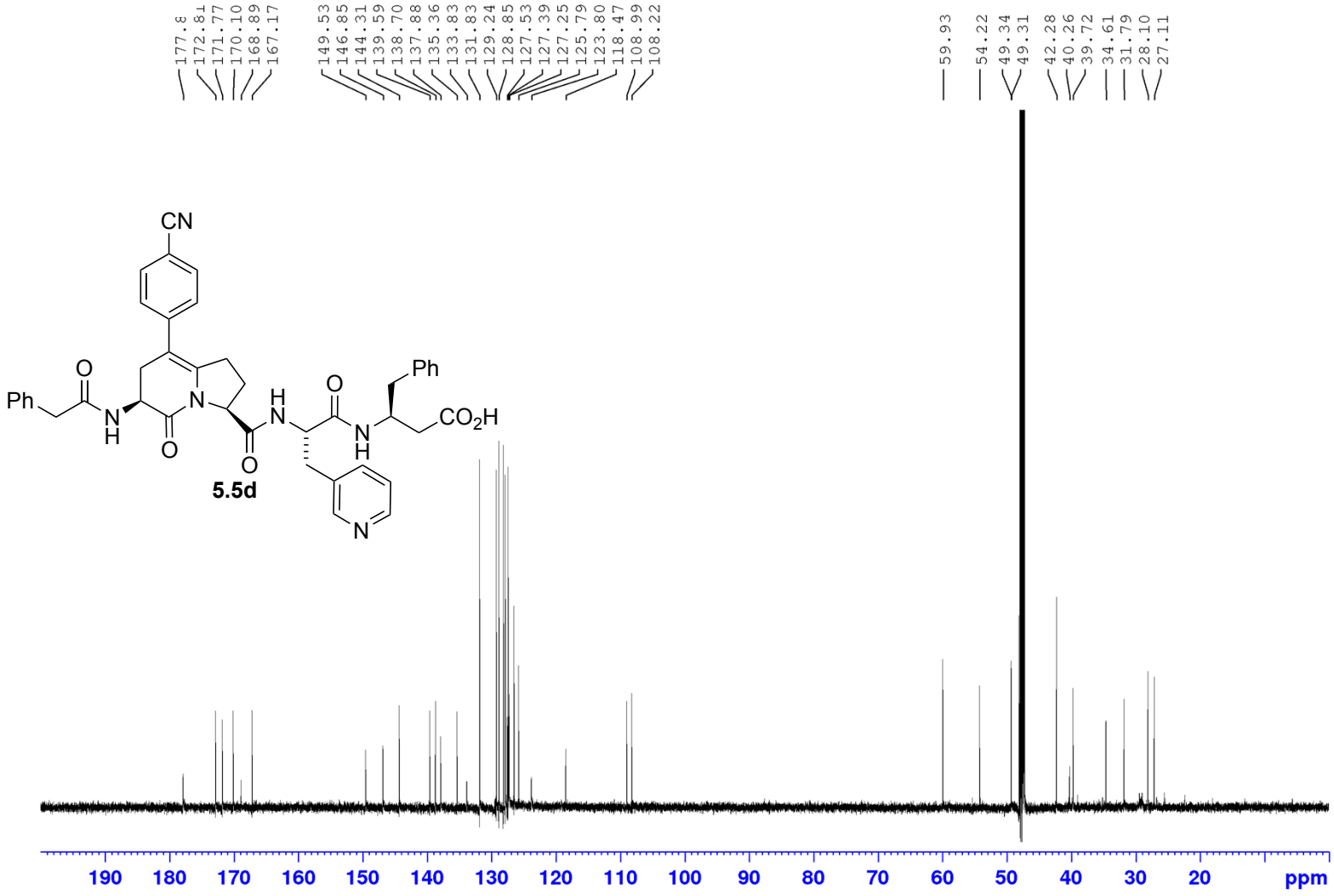

^{1}H NMR 700MHz
Solvent: CD_3OD

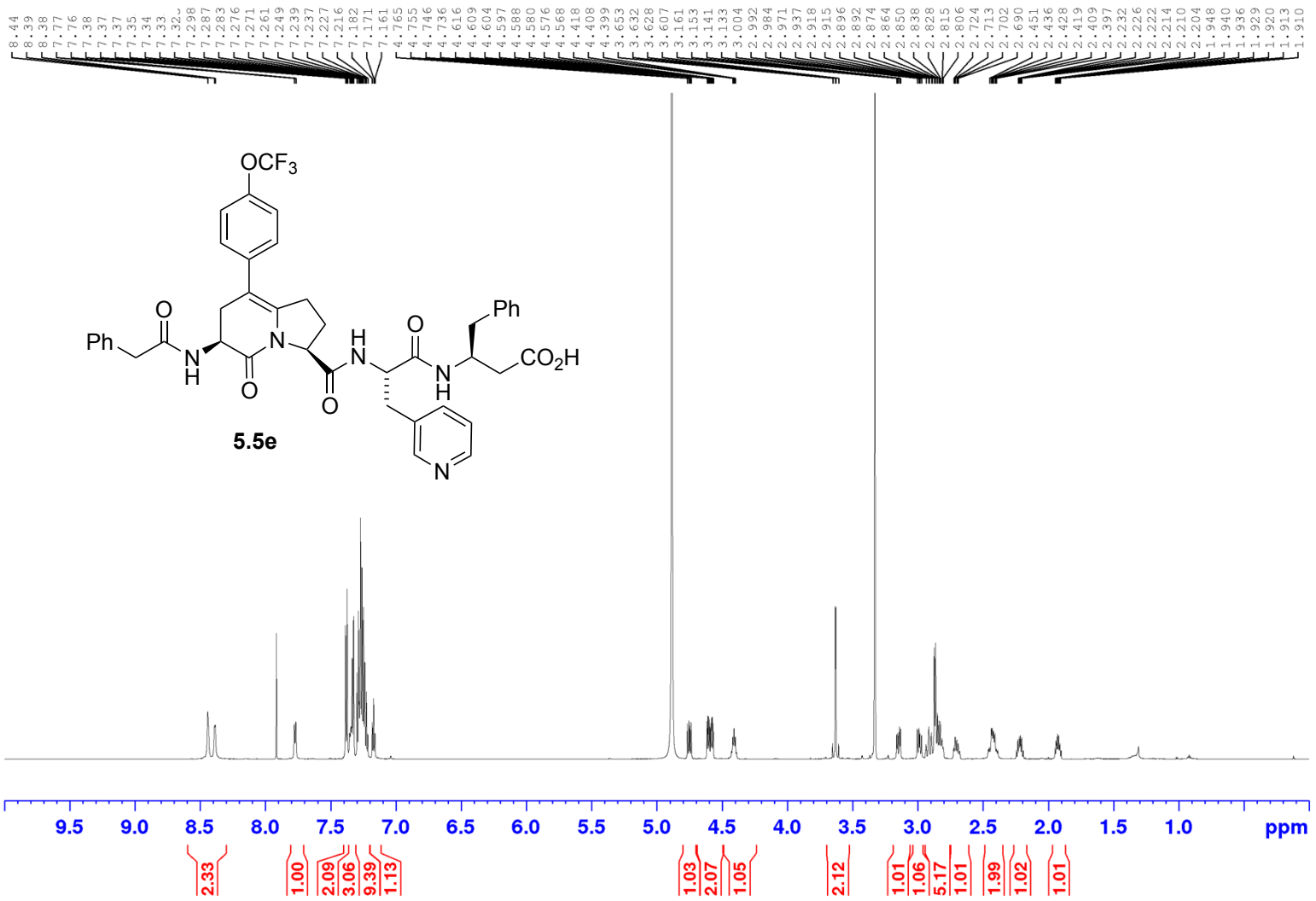

^{13}C NMR 175MHz
Solvent: CD_3OD

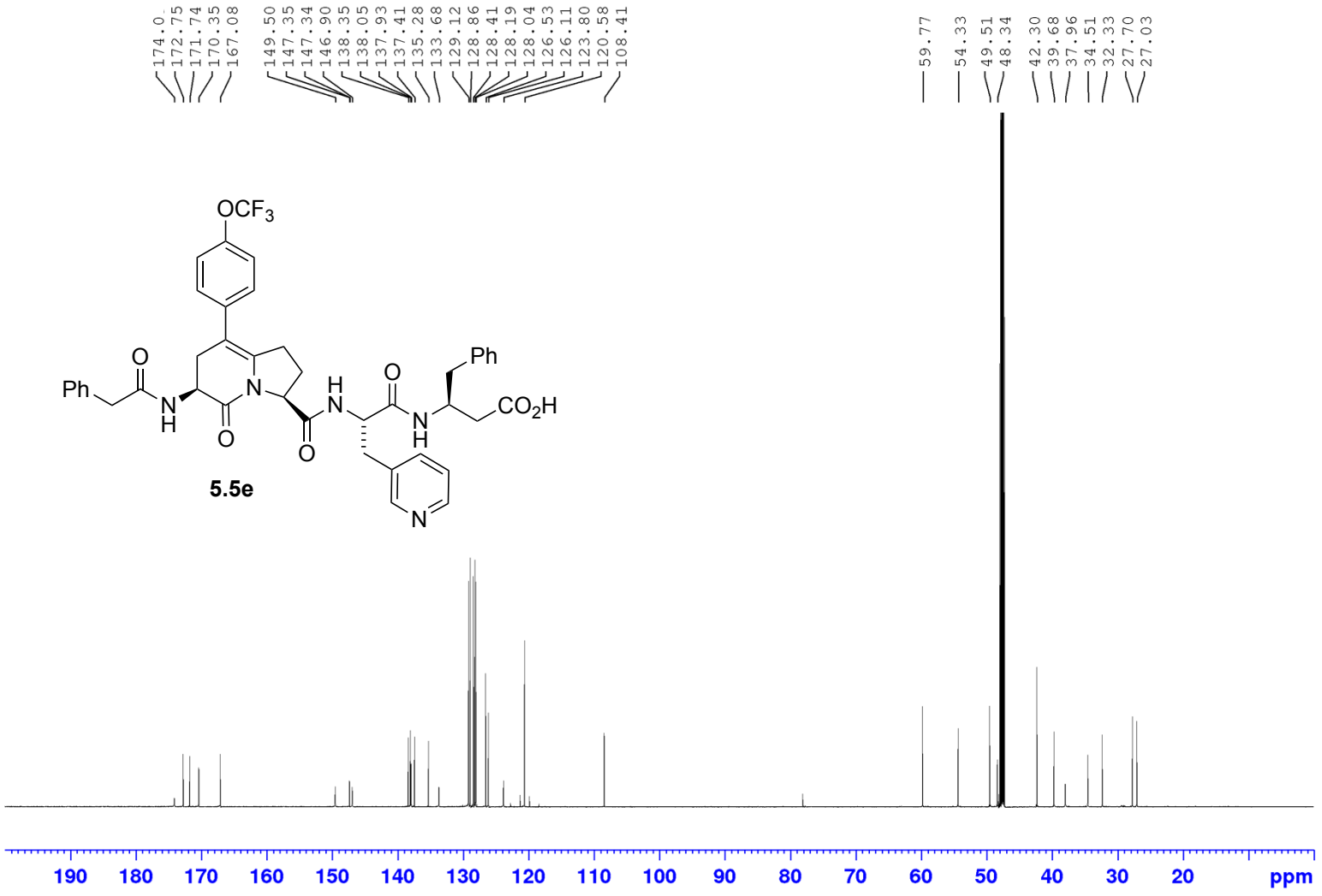

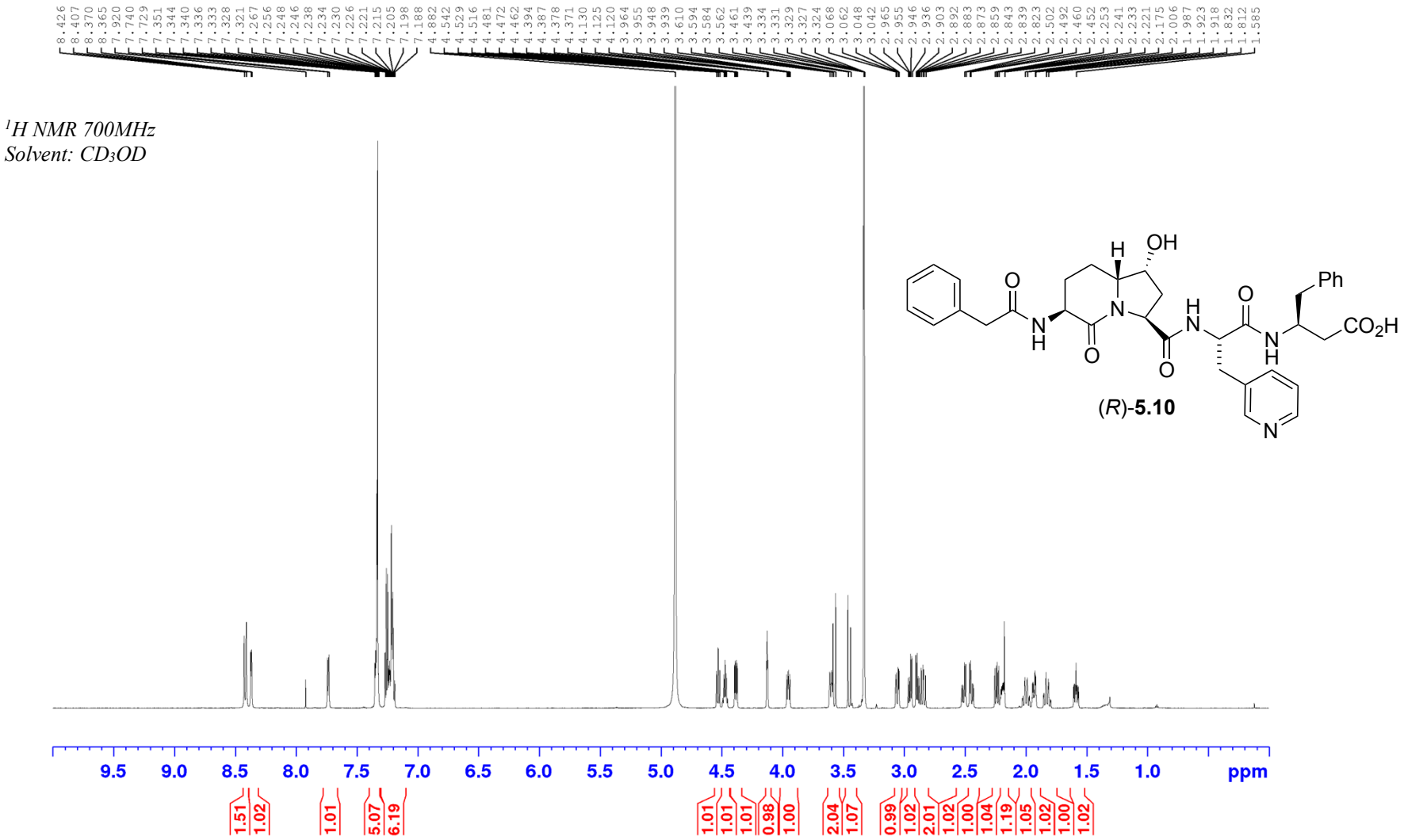

[1]H NMR 700MHz
Solvent: CD_3OD

(*R*)-**5.10**

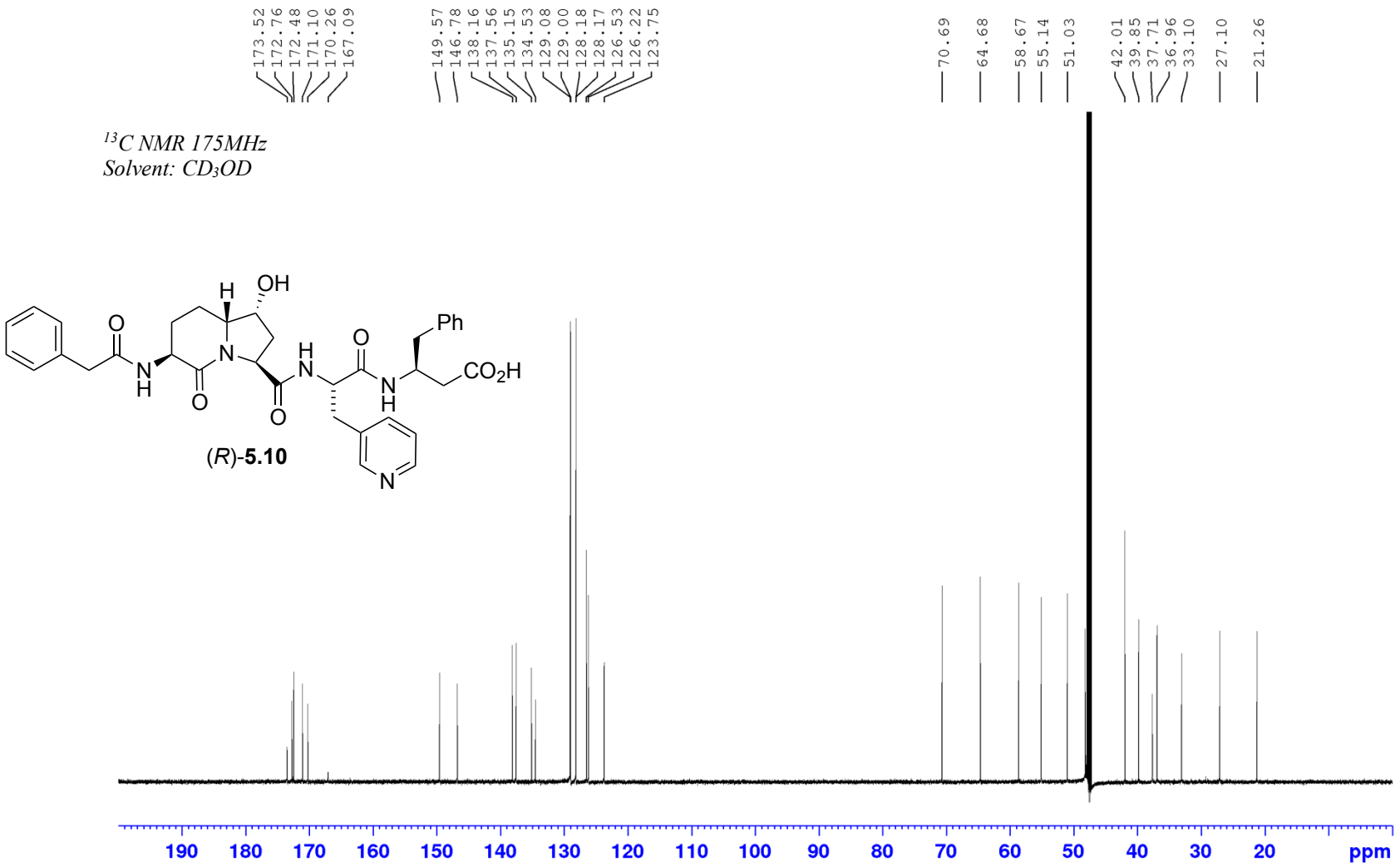

^{13}C NMR 175MHz
Solvent: CD_3OD

(*R*)-**5.10**

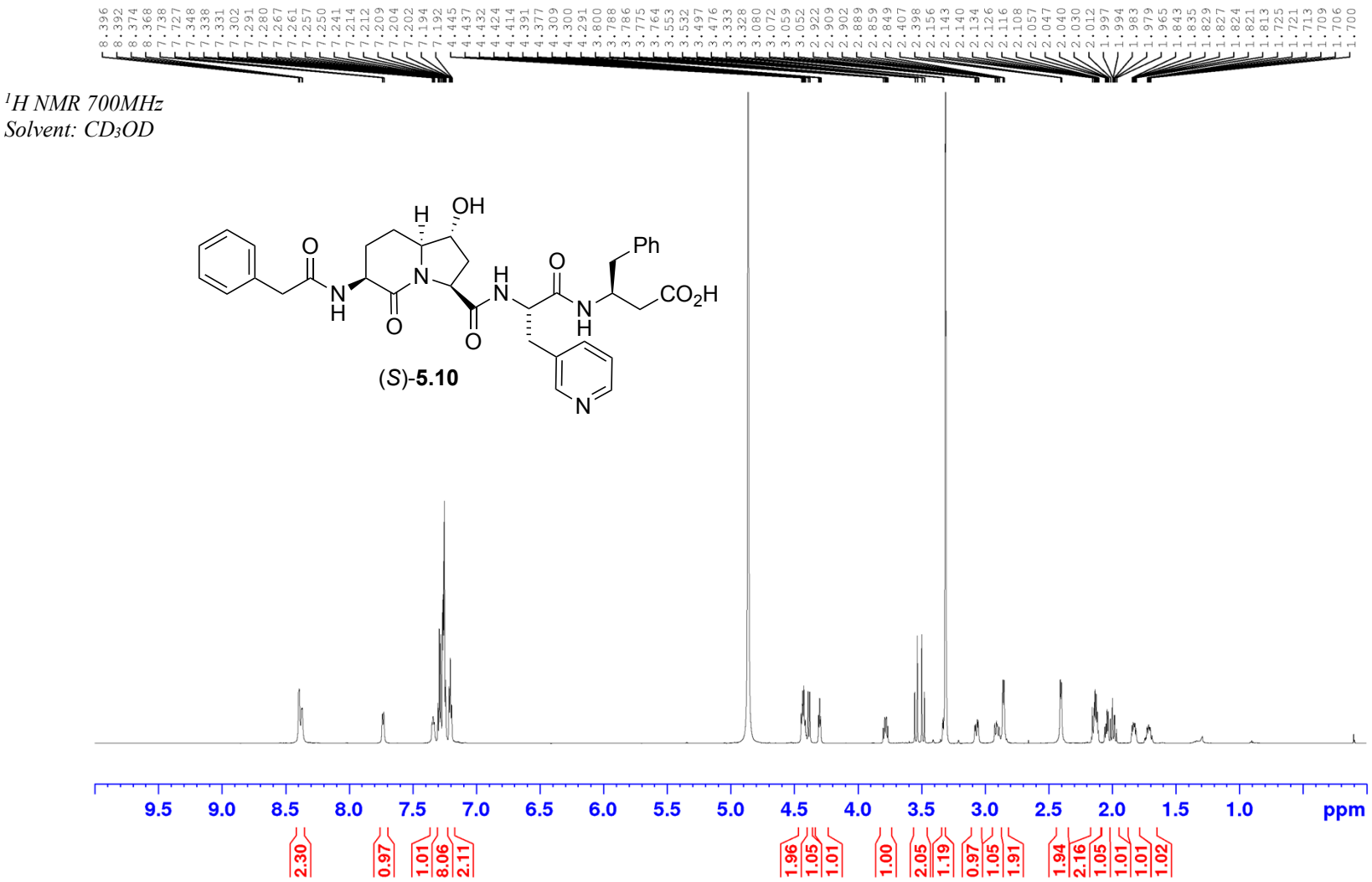

^{1}H NMR 700MHz
Solvent: CD_3OD

(*S*)-**5.10**

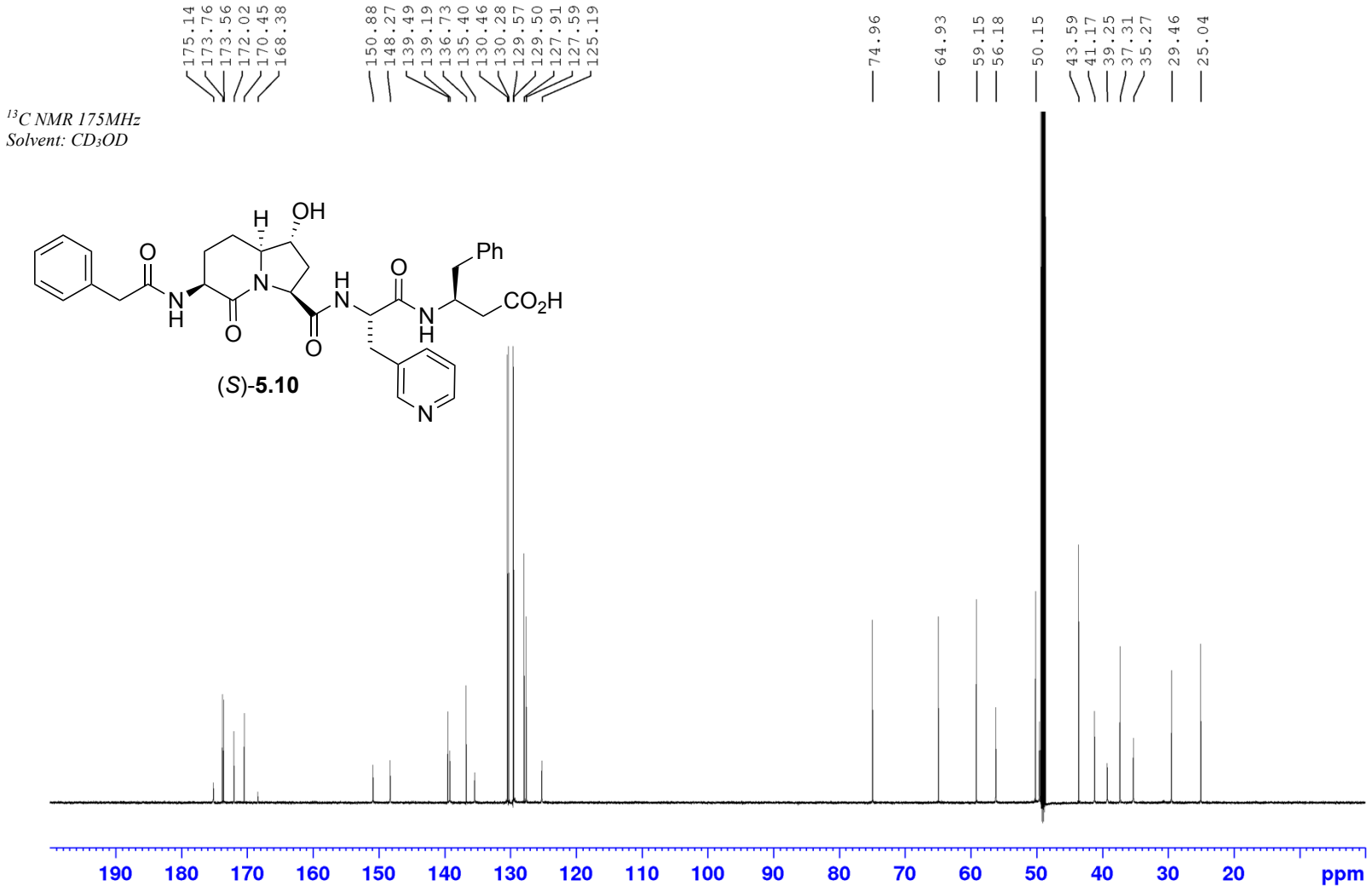

^{13}C NMR 175MHz
Solvent: CD_3OD

(*S*)-**5.10**

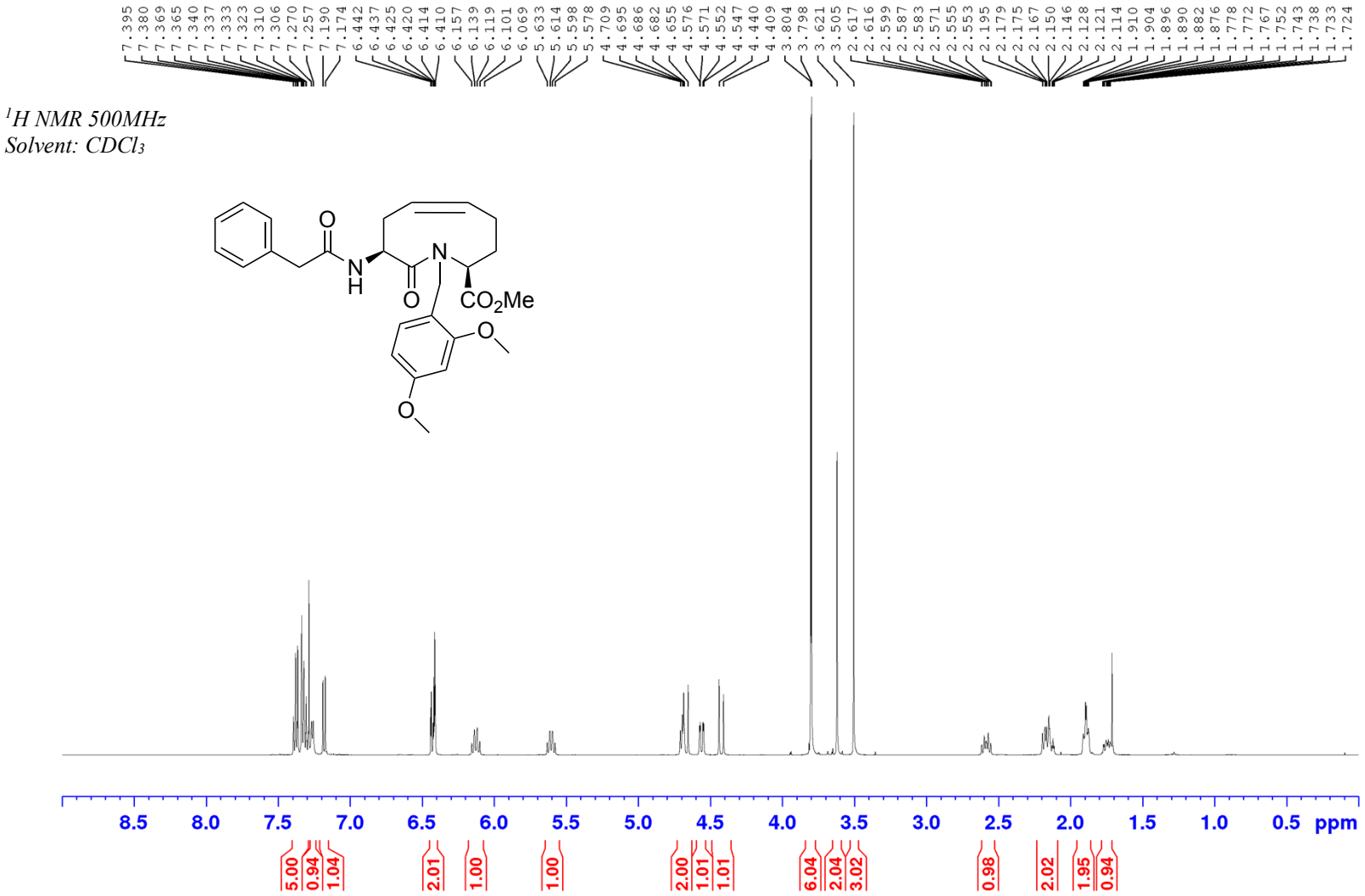
7.395
7.380
7.369
7.365
7.340
7.337
7.333
7.323
7.310
7.306
7.270
7.257
7.190
7.174
6.442
6.437
6.425
6.420
6.414
6.410
6.157
6.139
6.119
6.101
6.069
5.633
5.614
5.598
5.578
4.709
4.695
4.686
4.682
4.655
4.576
4.571
4.552
4.547
4.440
4.409
3.804
3.798
3.621
3.505
2.617
2.616
2.599
2.587
2.583
2.571
2.555
2.553
2.195
2.179
2.175
2.167
2.150
2.146
2.128
2.121
2.114
1.910
1.904
1.896
1.890
1.882
1.876
1.778
1.772
1.767
1.752
1.743
1.738
1.733
1.724
1H NMR 500MHz
Solvent: CDCl3
O
N
H
O
N
CO2Me
O
O
8.5
8.0
7.5
7.0
6.5
6.0
5.5
5.0
4.5
4.0
3.5
3.0
2.5
2.0
1.5
1.0
0.5
ppm
5.00
0.94
1.04
2.01
1.00
1.00
2.00
1.01
1.01
6.04
2.04
3.02
0.98
2.02
1.95
0.94

^{13}C NMR 125 MHz
Solvent: $CDCl_3$

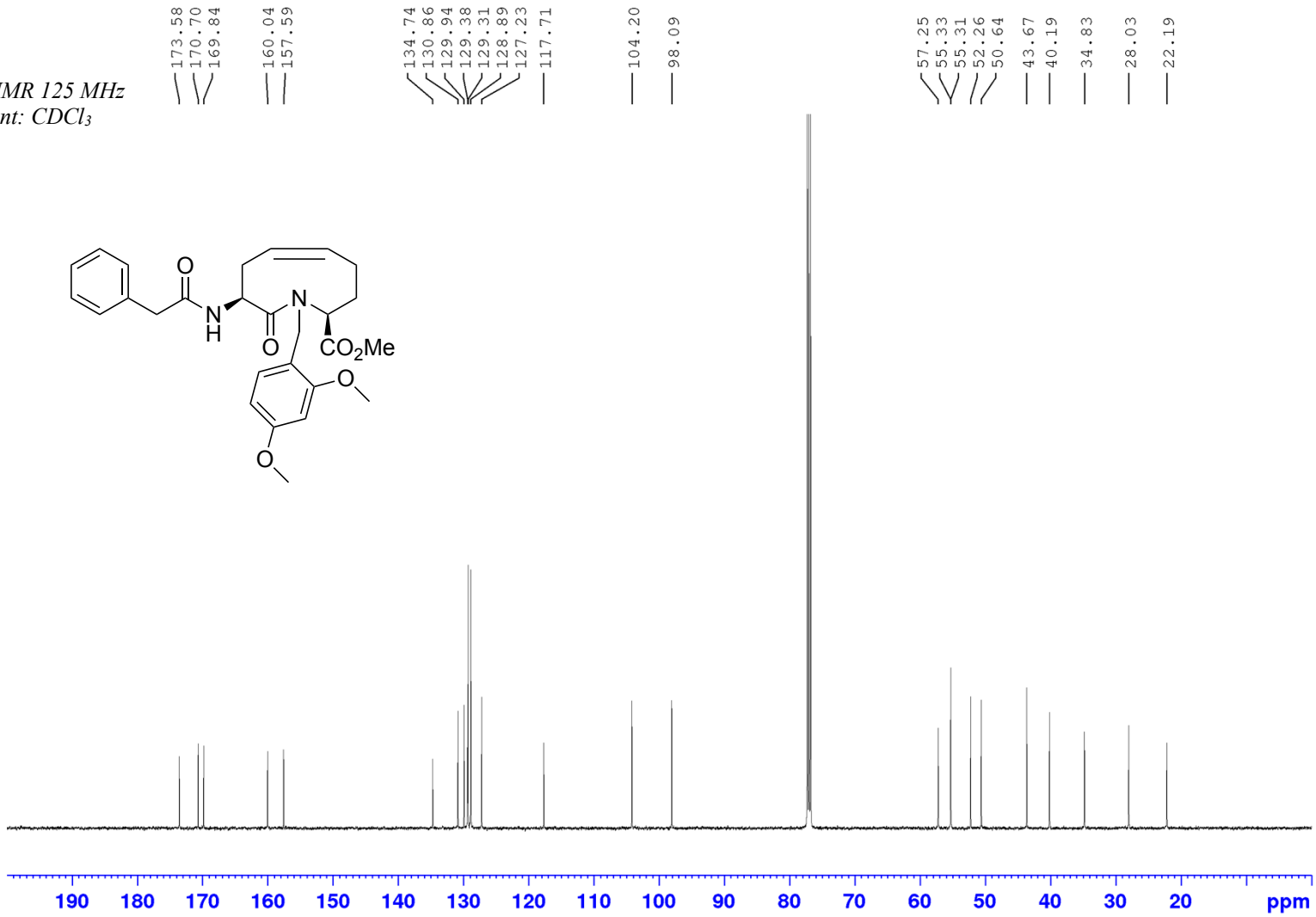

^{1}H NMR 500MHz
Solvent: $CDCl_3$

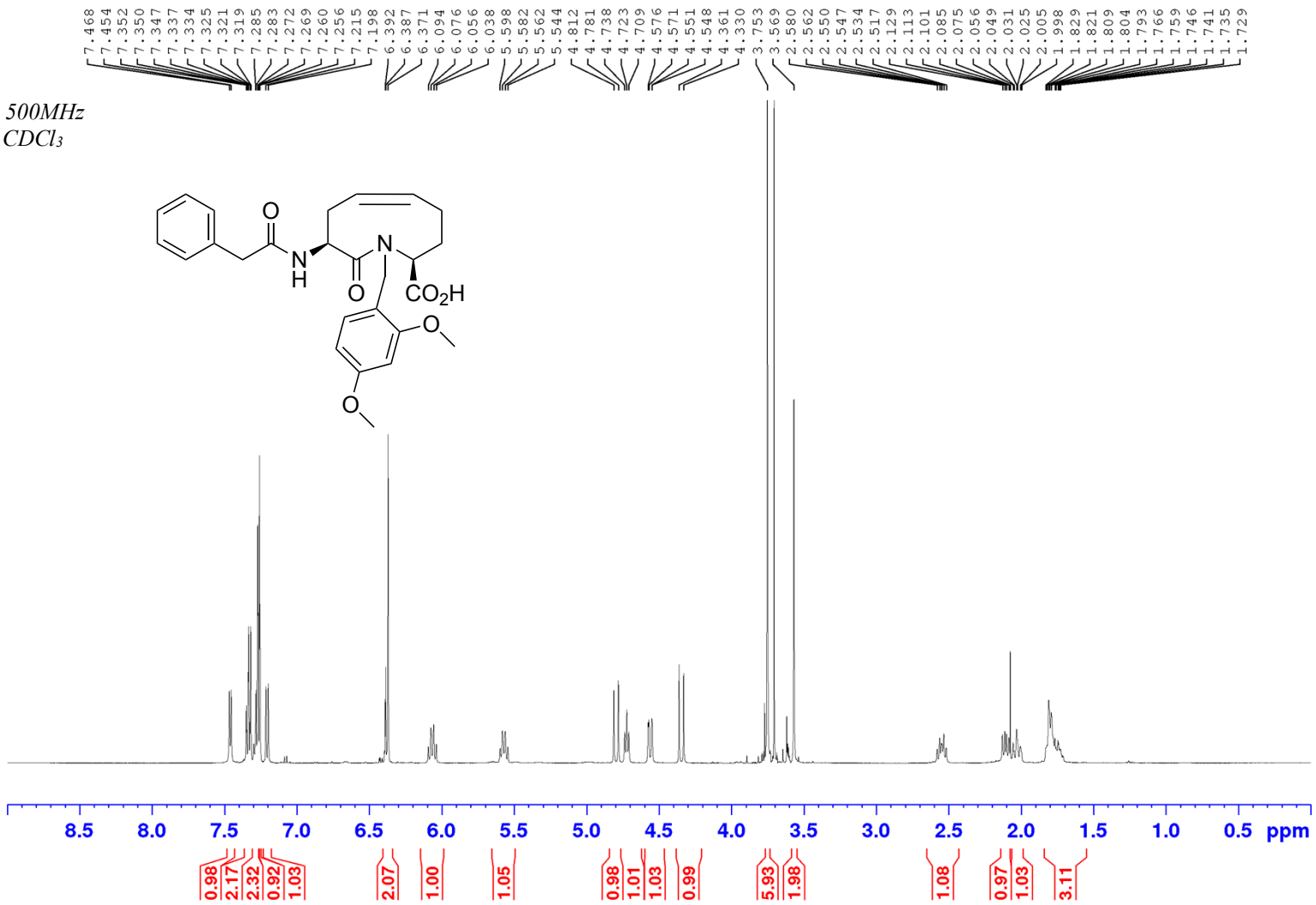

^{13}C NMR 125MHz
Solvent: $CDCl_3$

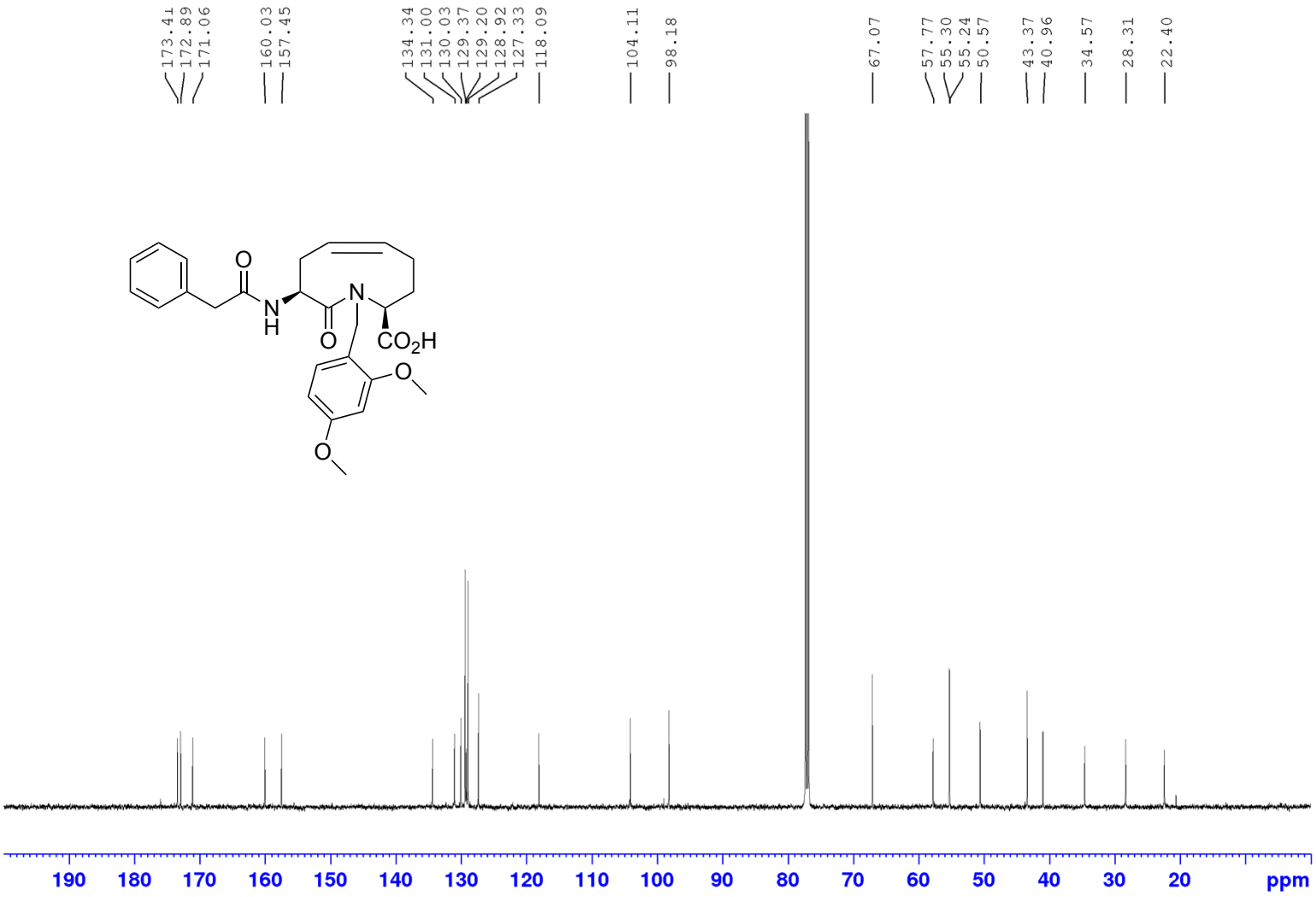

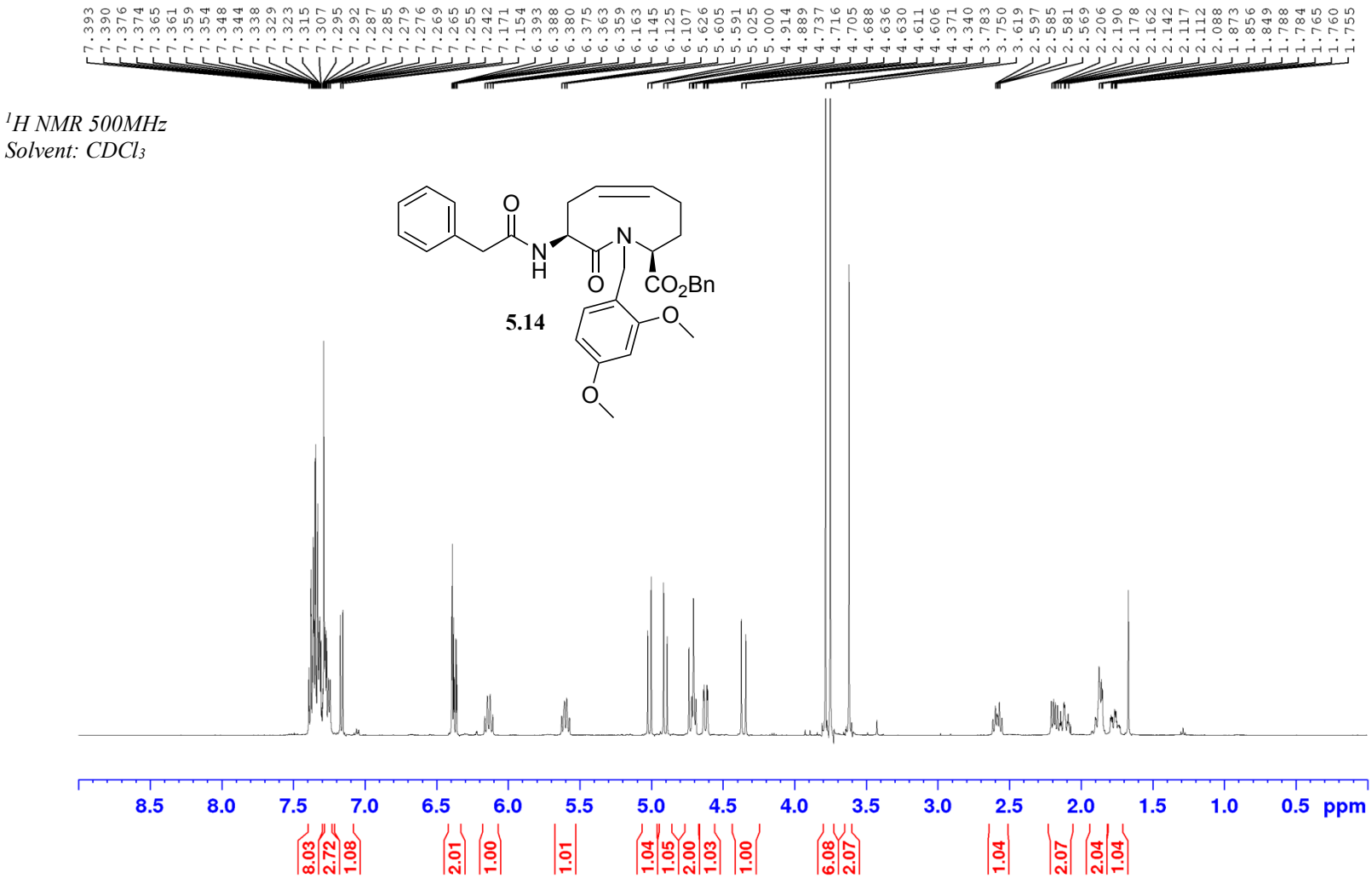

^{1}H NMR 500MHz
Solvent: $CDCl_3$

5.14

^{13}C NMR 500MHz
Solvent: $CDCl_3$

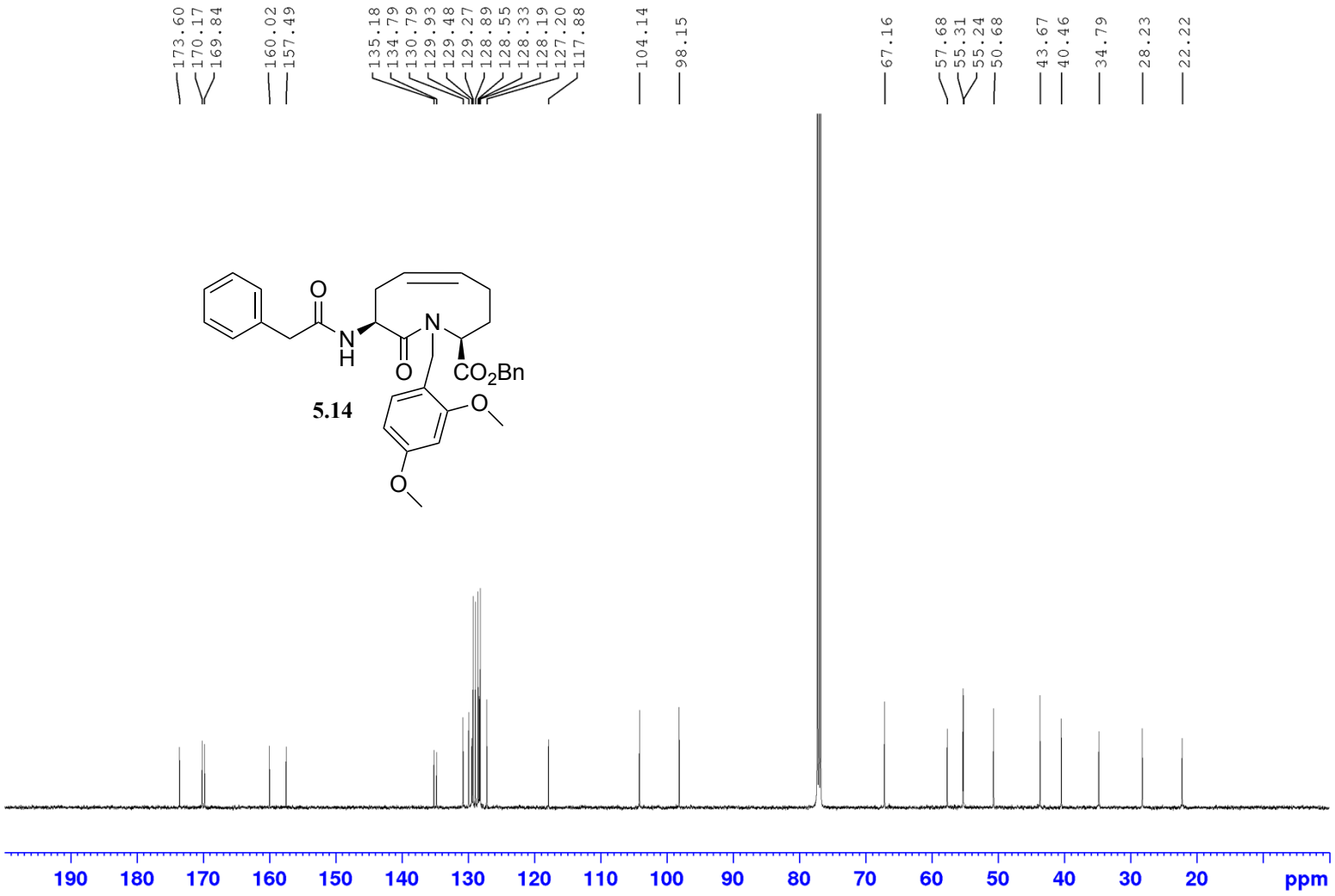

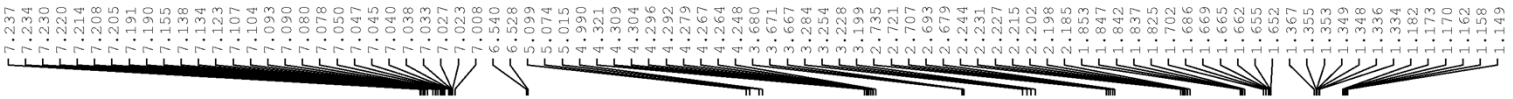

^{1}H NMR 500MHz
Solvent: C_6D_6

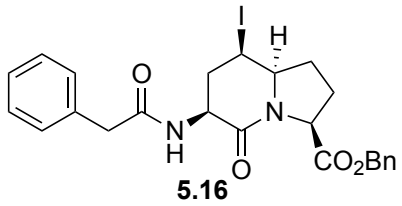

5.16

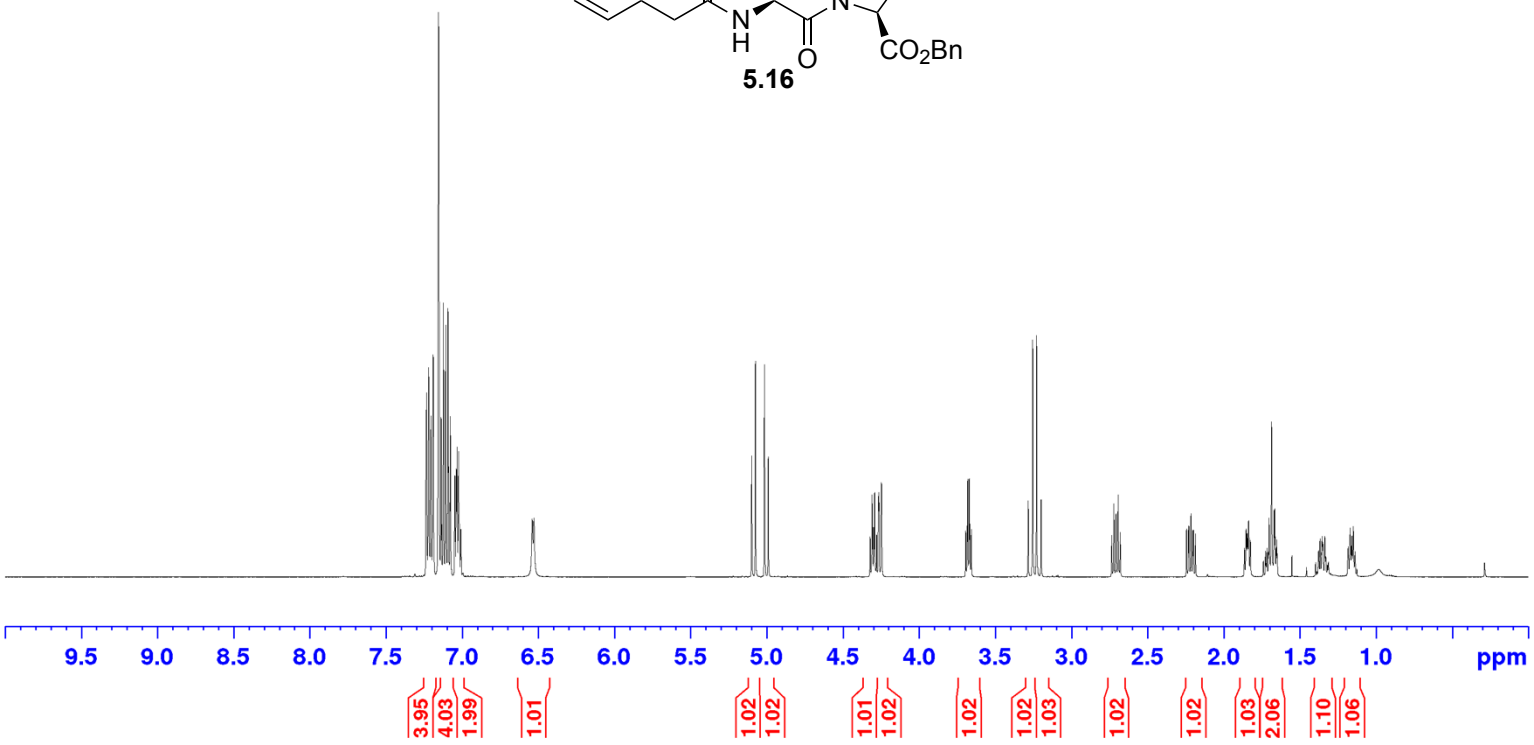

^{13}C NMR 125MHz
Solvent: C_6D_6

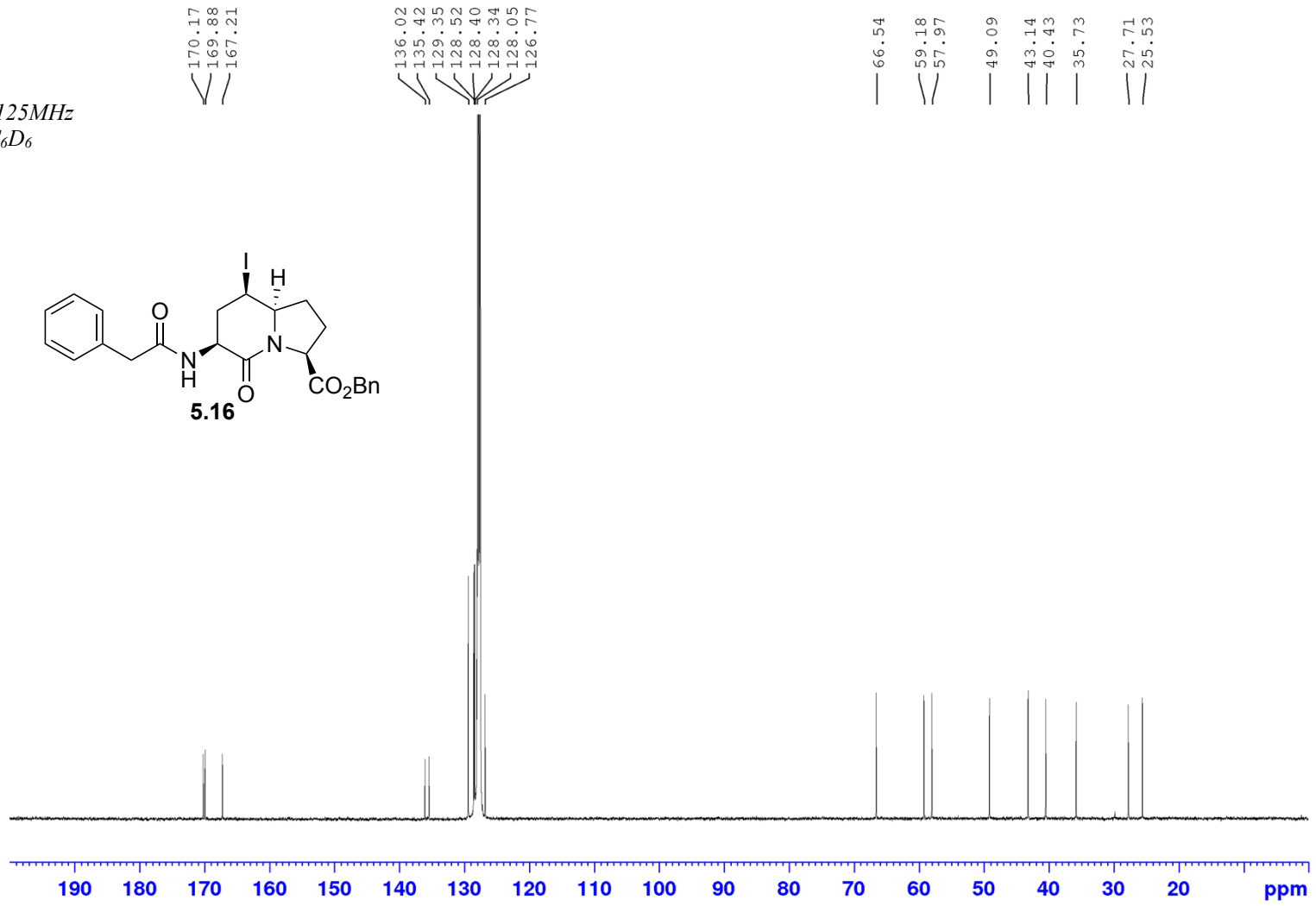

COSY 500MHz
Solvent: C_6D_6

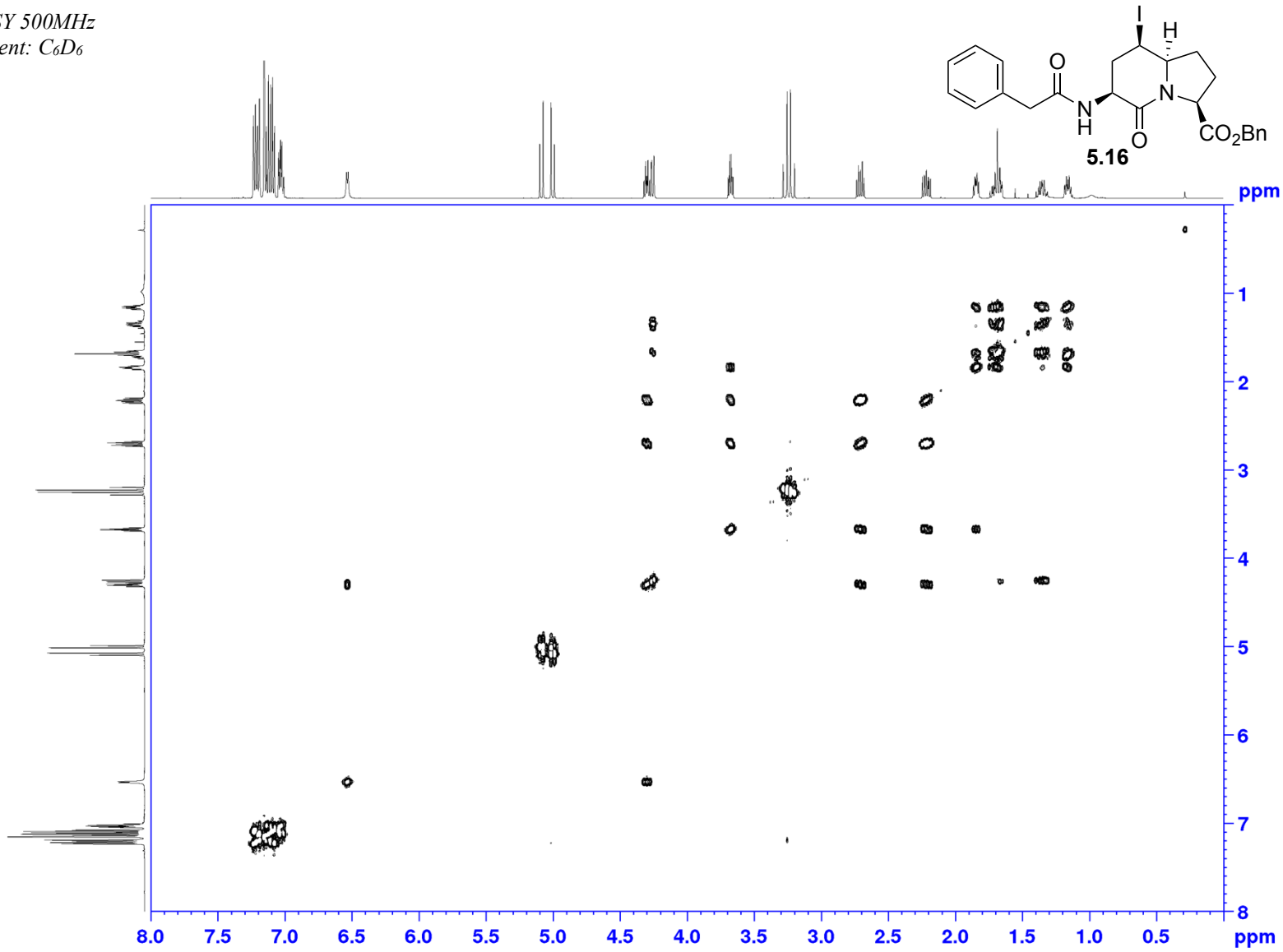

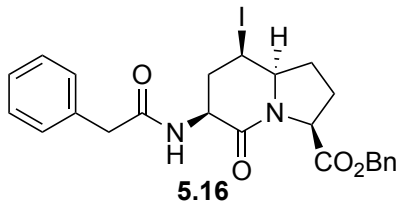

5.16

HSQC NMR 500MHz
Solvent: C_6D_6

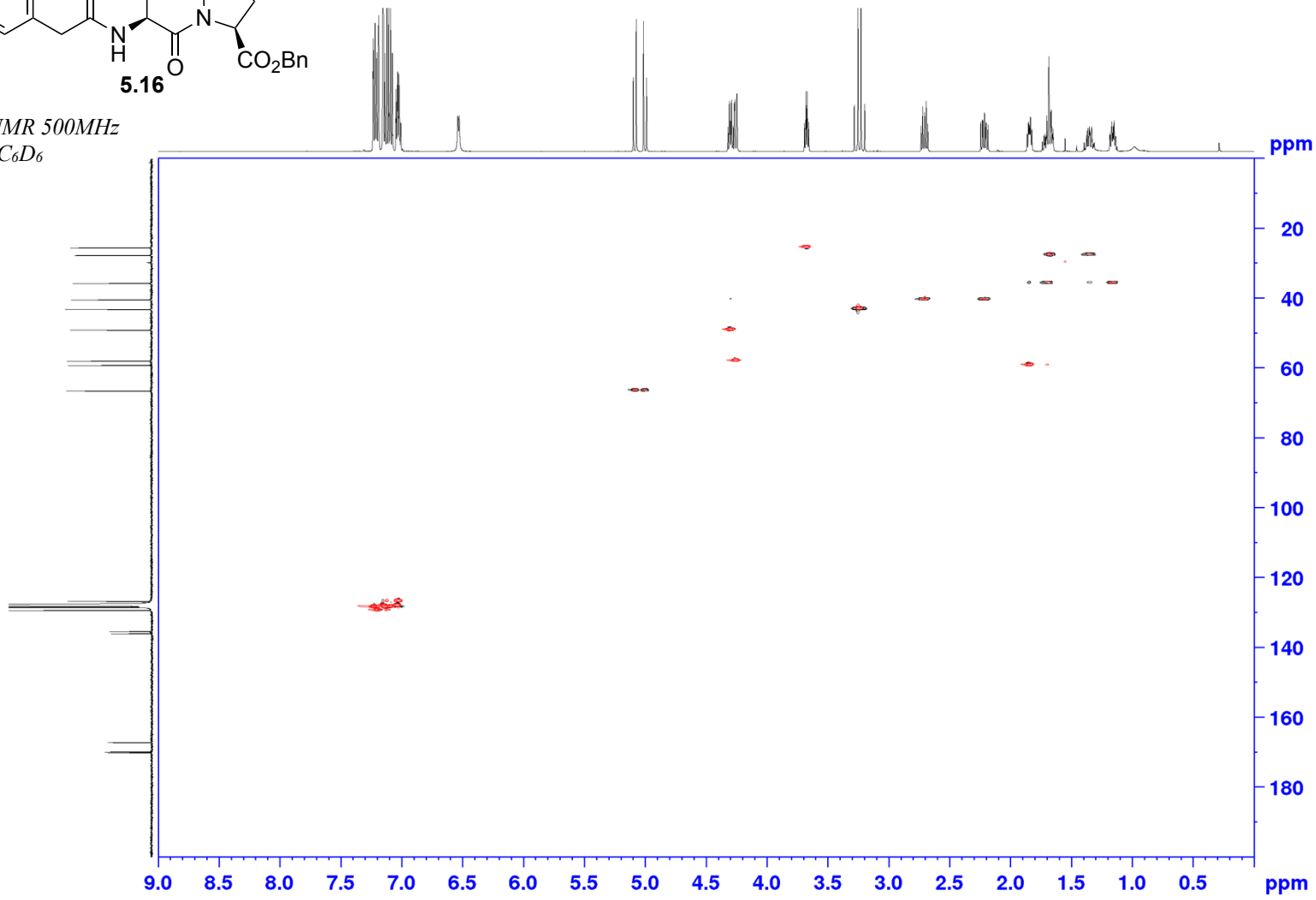

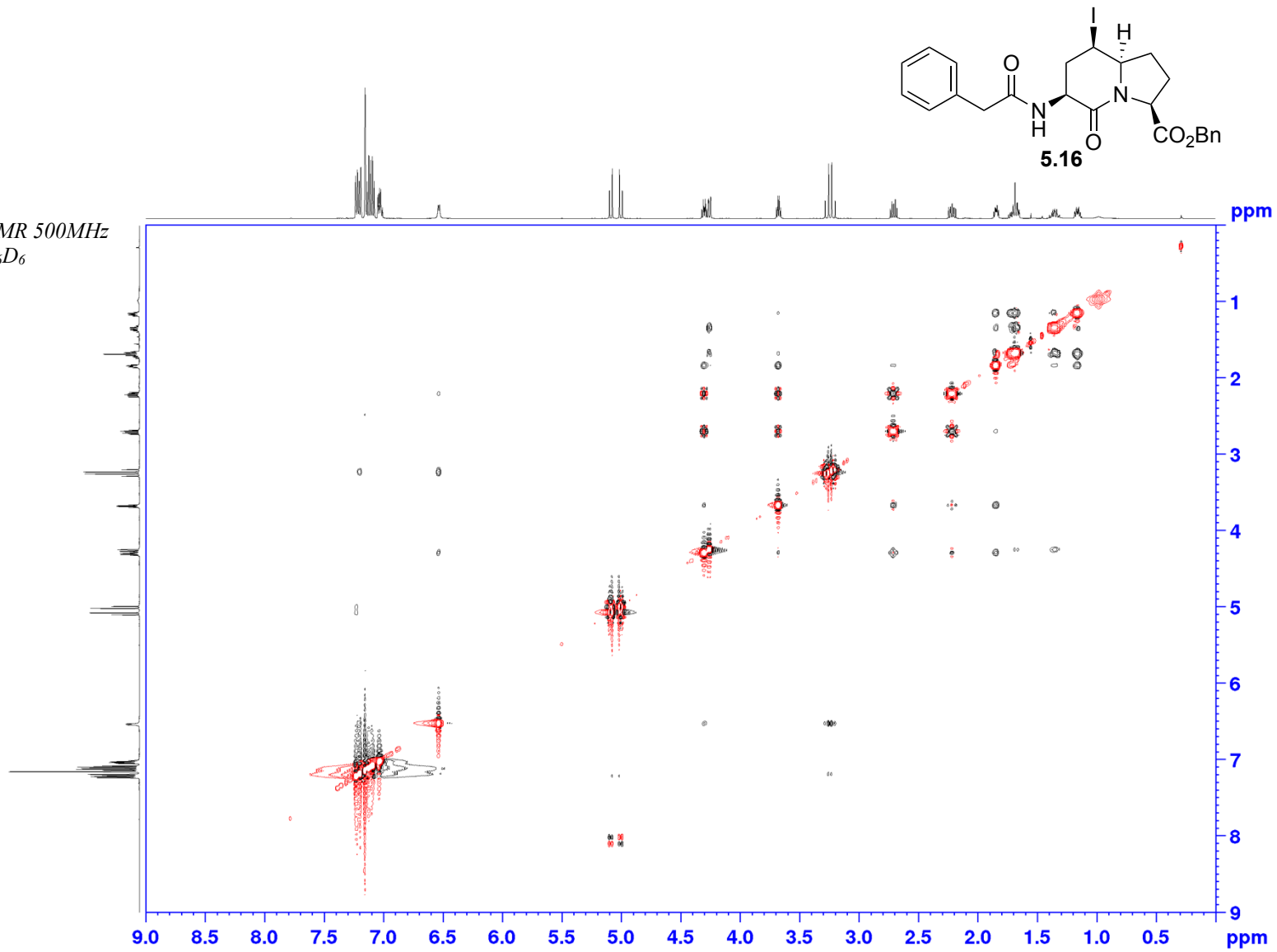

NOESY NMR 500MHz
Solvent: C_6D_6

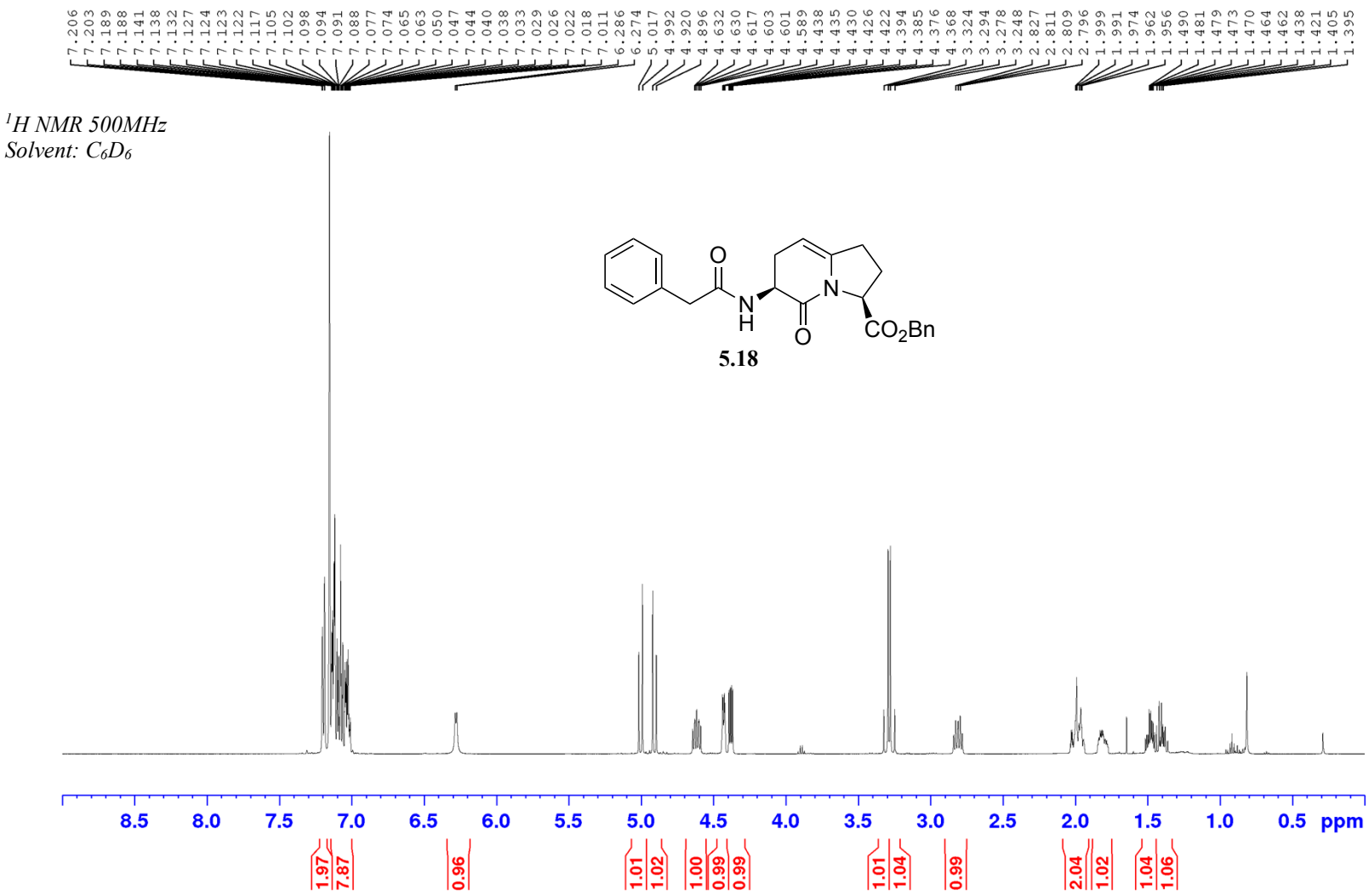
7.206
7.203
7.189
7.188
7.141
7.138
7.132
7.127
7.124
7.123
7.122
7.117
7.105
7.102
7.098
7.094
7.091
7.088
7.077
7.074
7.065
7.063
7.050
7.047
7.044
7.040
7.038
7.033
7.029
7.026
7.022
7.018
7.011
6.286
6.274
5.017
4.992
4.920
4.896
4.632
4.630
4.617
4.603
4.601
4.589
4.438
4.435
4.430
4.426
4.422
4.394
4.385
4.376
4.368
3.324
3.294
3.278
3.248
2.827
2.811
2.809
2.796
1.999
1.991
1.974
1.962
1.956
1.490
1.481
1.479
1.473
1.470
1.464
1.462
1.438
1.421
1.405
1.395
1H NMR 500MHz
Solvent: C6D6
O
N
H
O
N
CO2Bn
5.18
8.5
8.0
7.5
7.0
6.5
6.0
5.5
5.0
4.5
4.0
3.5
3.0
2.5
2.0
1.5
1.0
0.5
ppm
1.97
7.87
0.96
1.01
1.02
1.00
0.99
0.99
1.01
1.04
0.99
2.04
1.02
1.04
1.06

^{13}C NMR 125 MHz
Solvent: C_6D_6

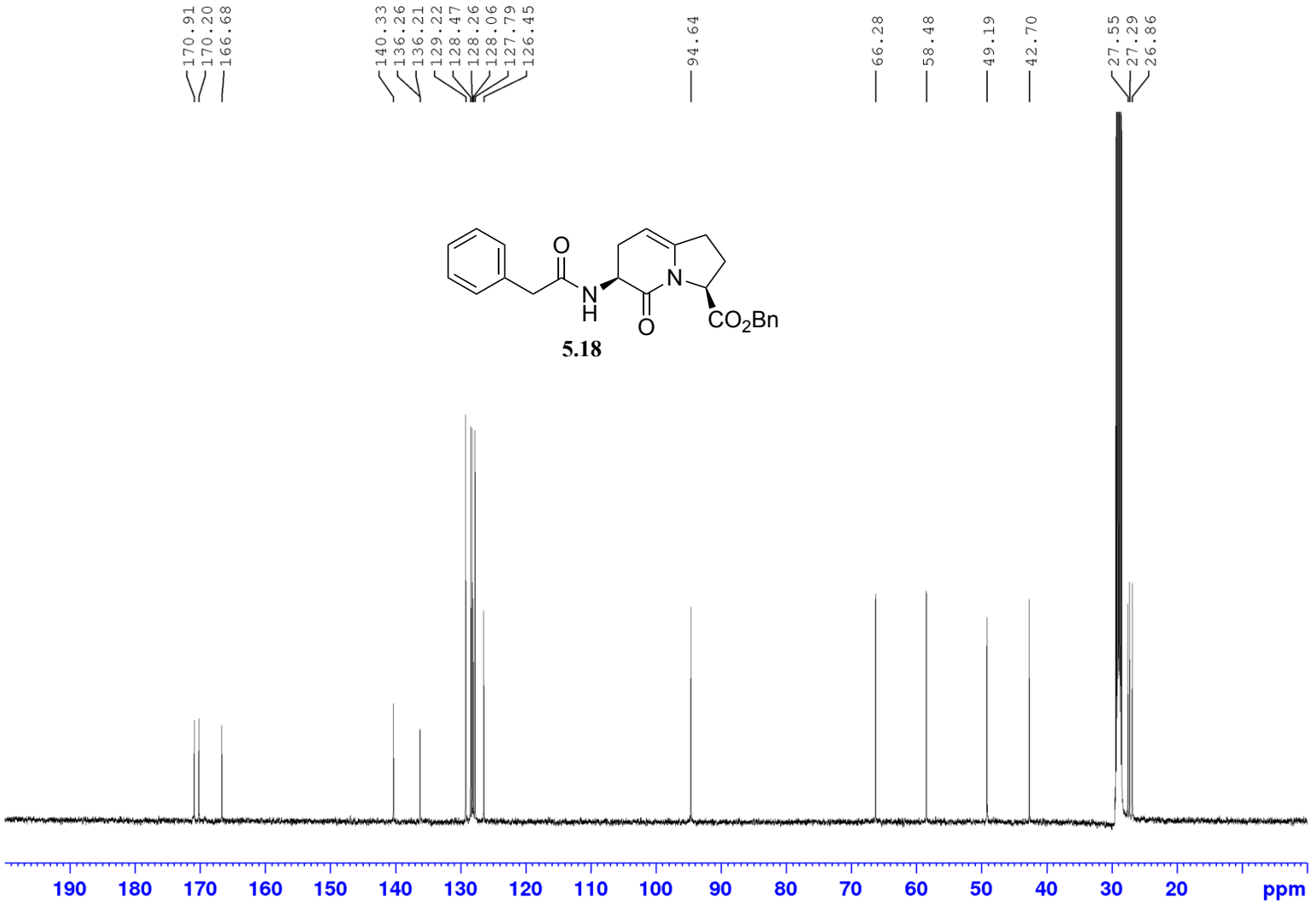

5.18

^{1}H NMR 500MHz
Solvent: $CDCl_3$

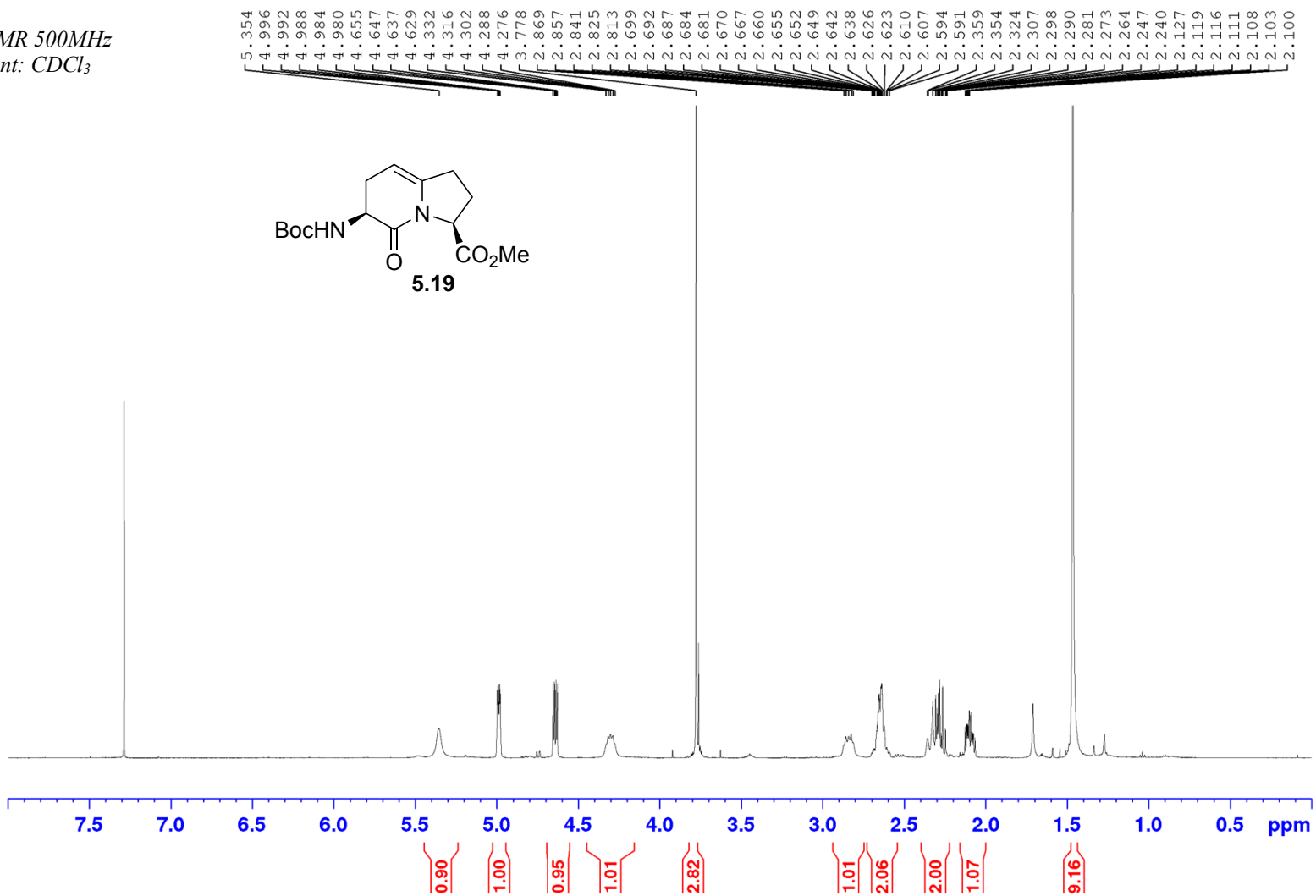

^{13}C NMR 125 MHz
Solvent: $CDCl_3$

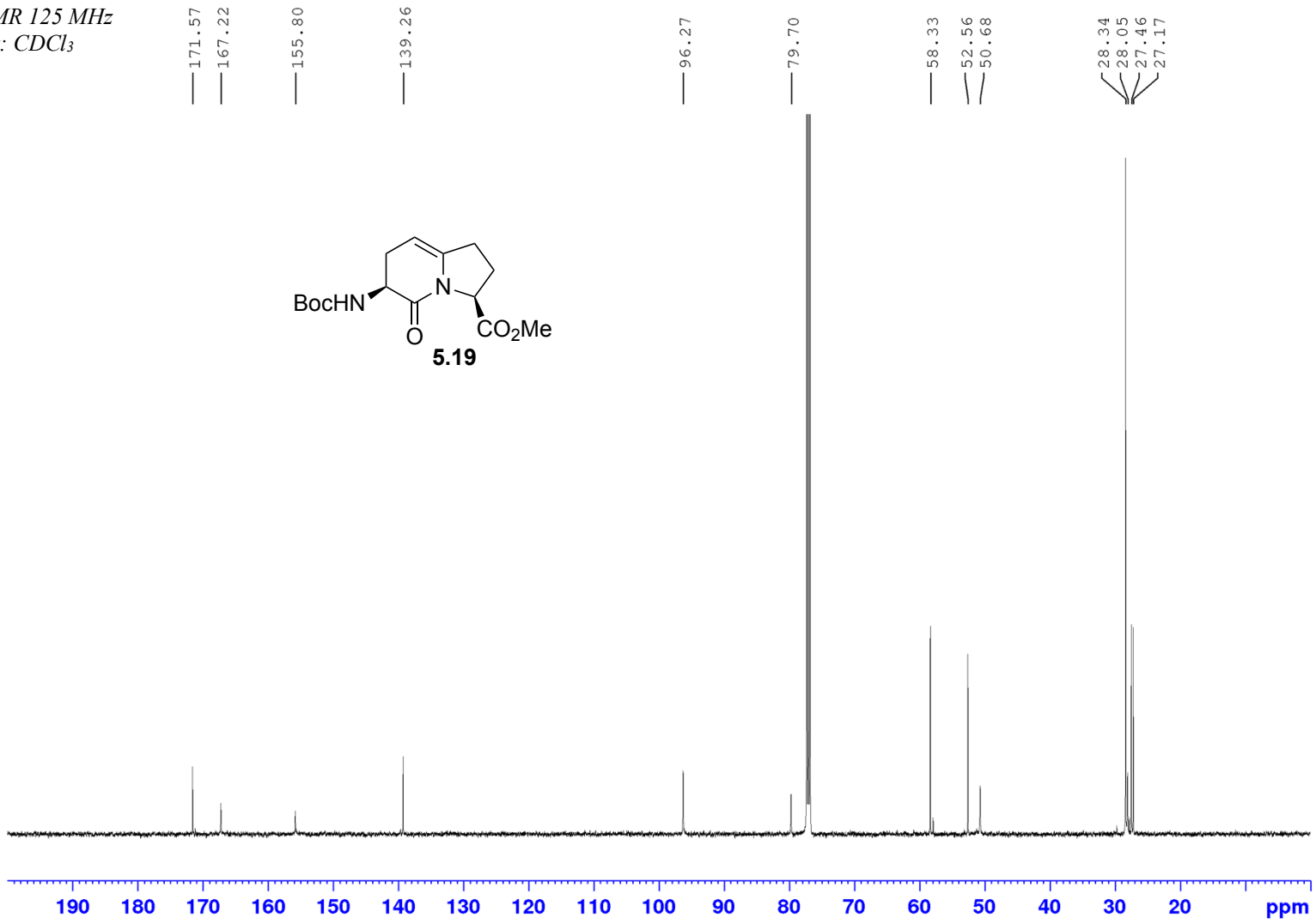

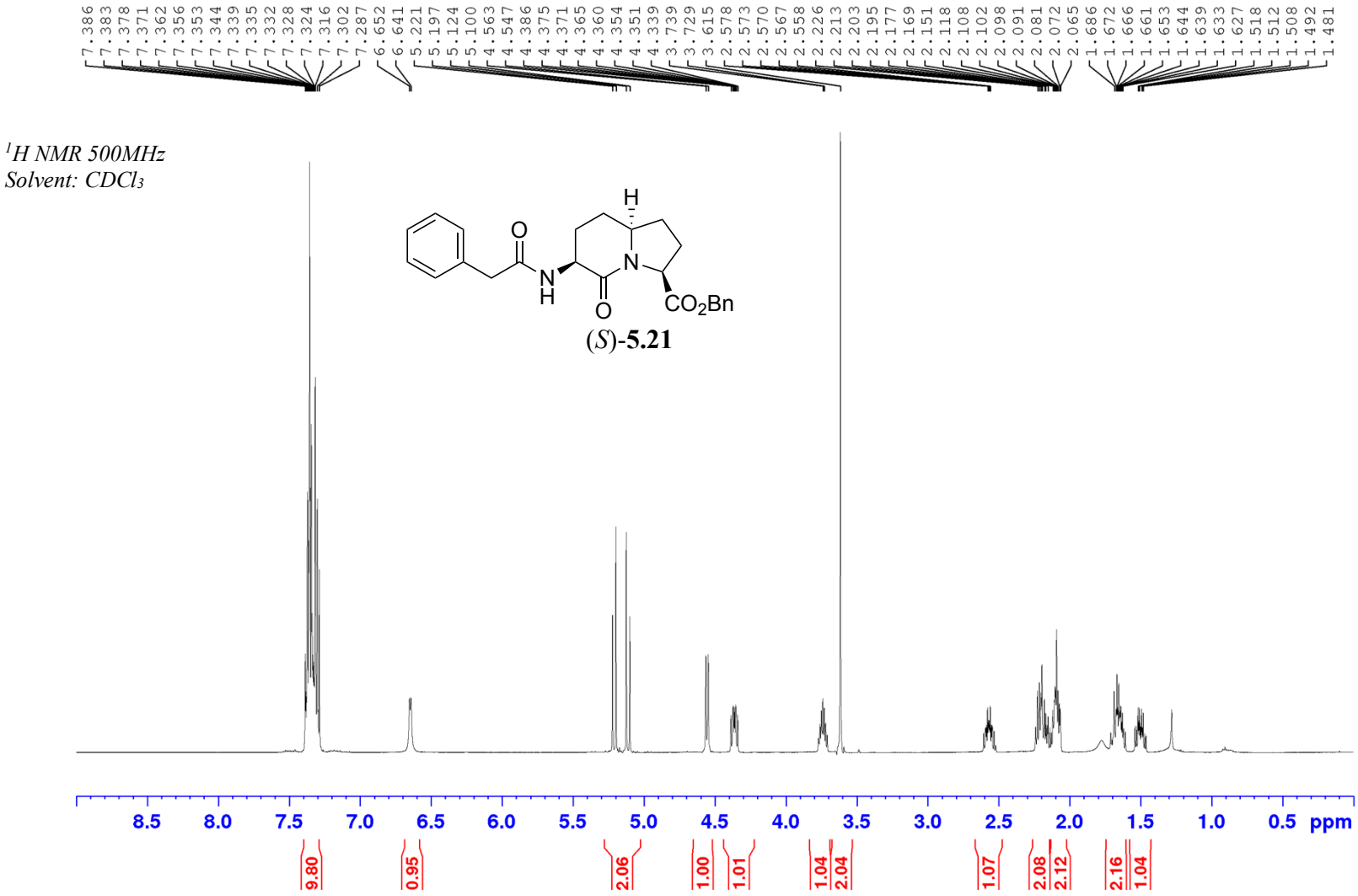

^{1}H NMR 500MHz
Solvent: $CDCl_3$

(*S*)-**5.21**

^{13}C NMR 125 MHz
Solvent: $CDCl_3$

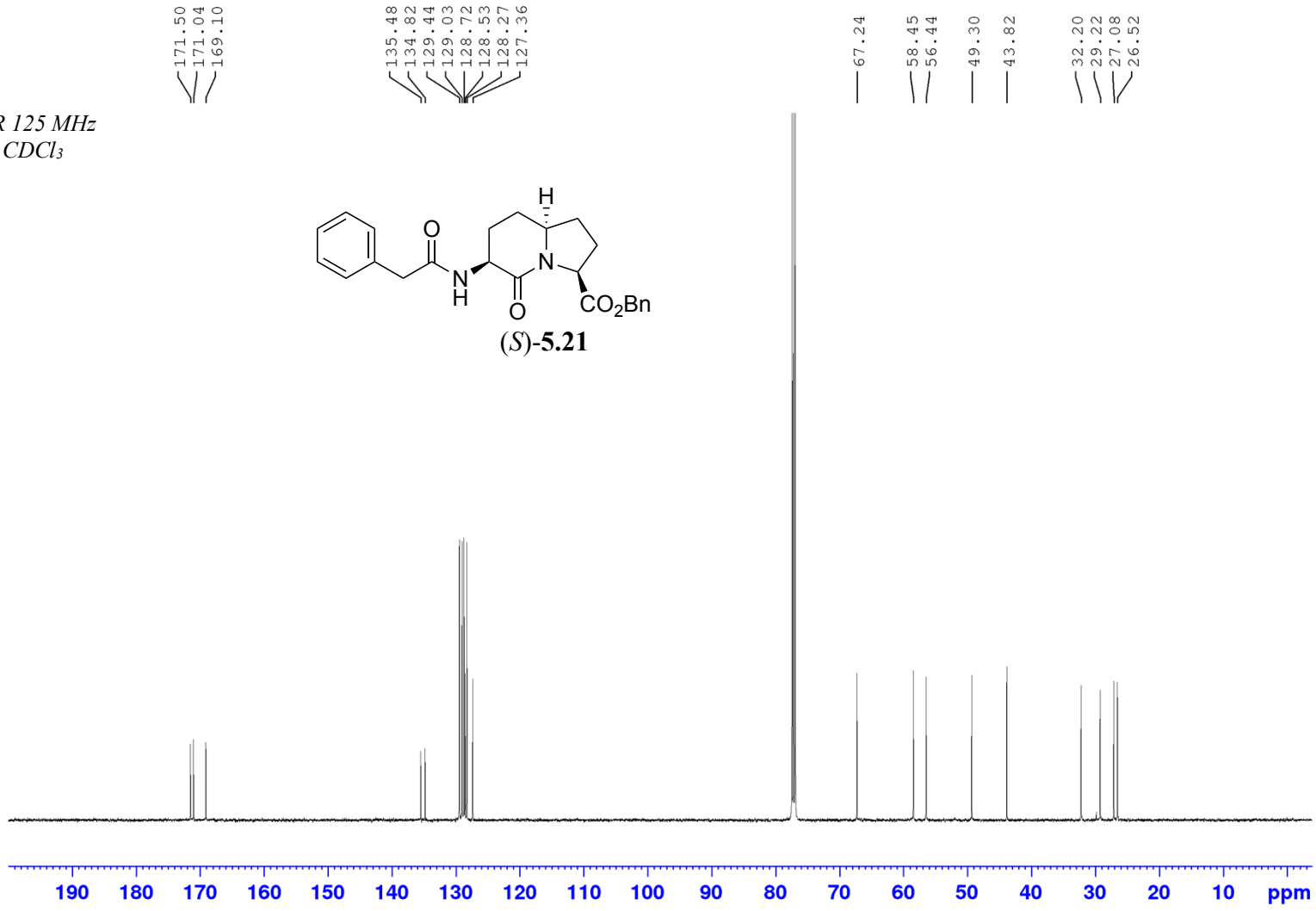

(*S*)-**5.21**

COSY NMR 500MHz
Solvent: $CDCl_3$

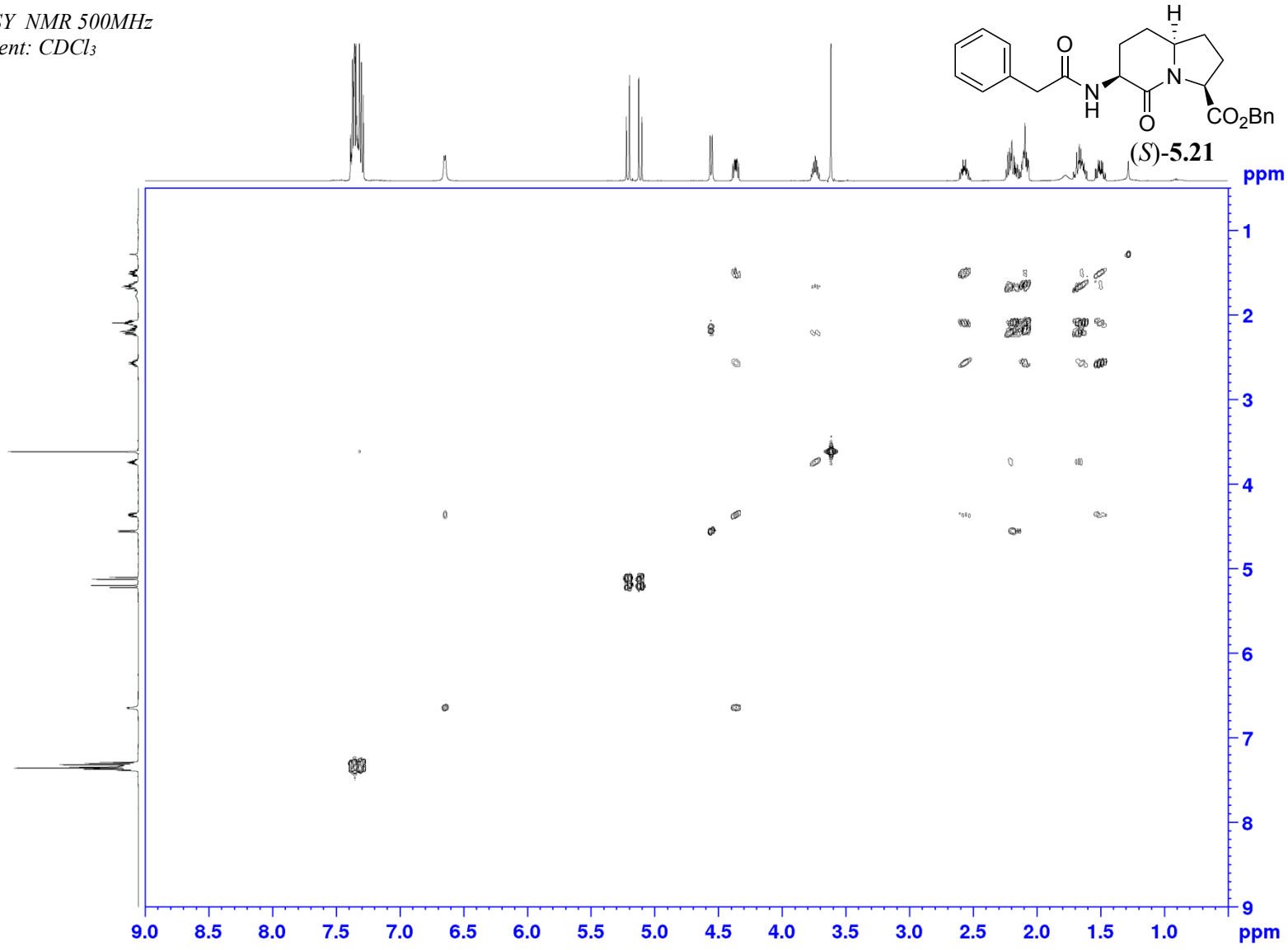

DEPT NMR 500MHz
Solvent: $CDCl_3$

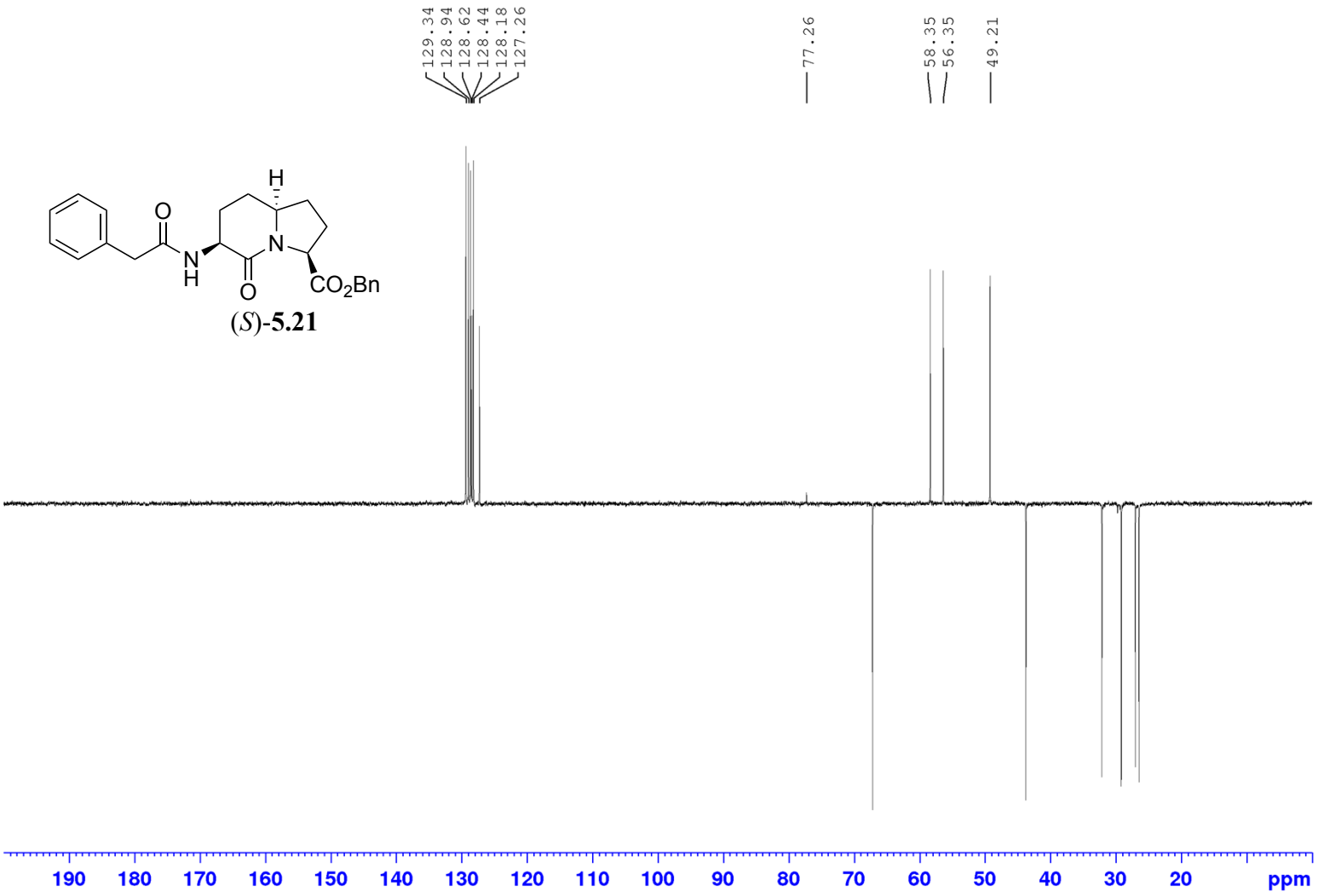

(*S*)-**5.21**

HSQC NMR 500MHz
Solvent: $CDCl_3$

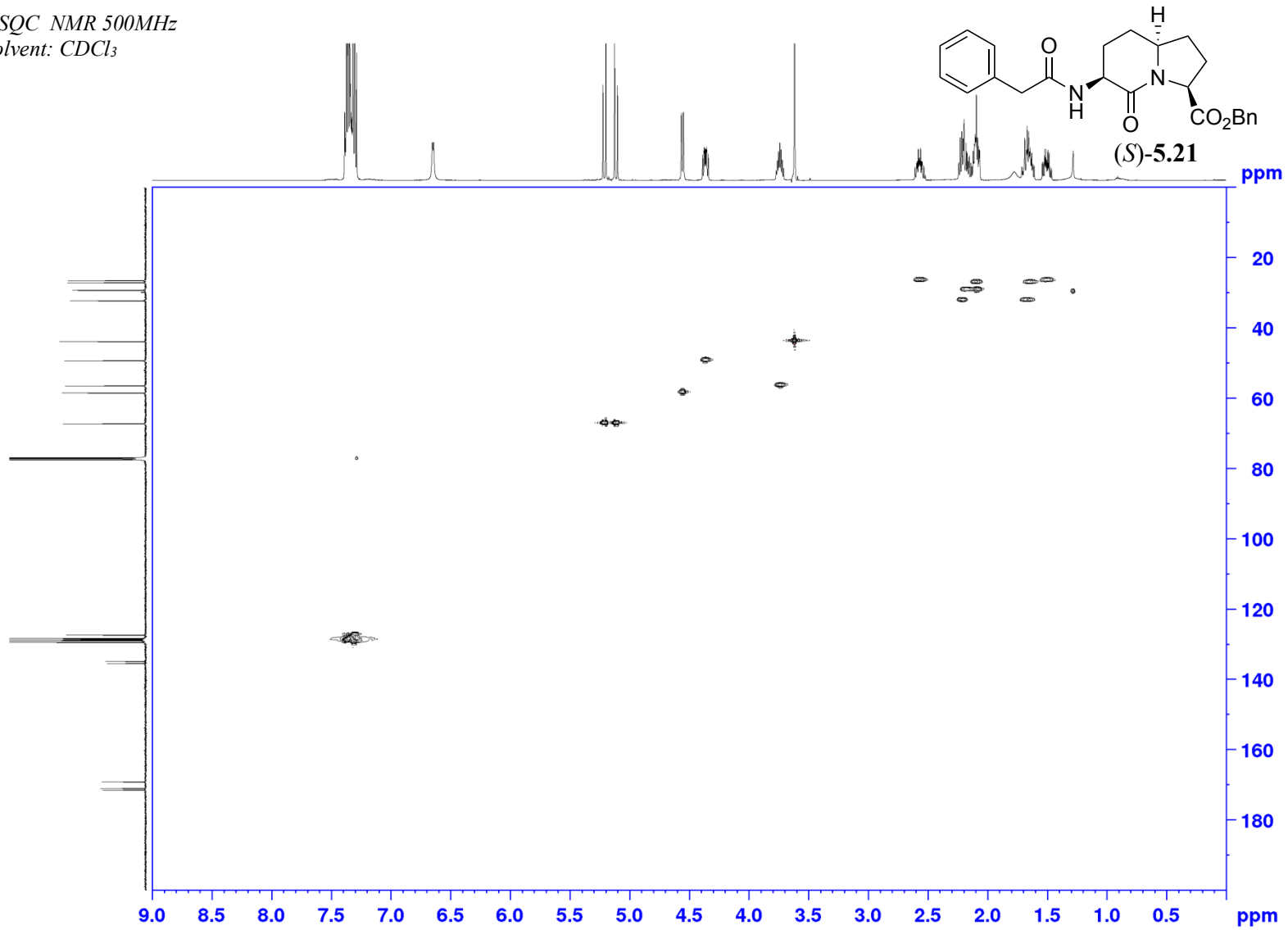

NOESY NMR 500MHz
Solvent: $CDCl_3$

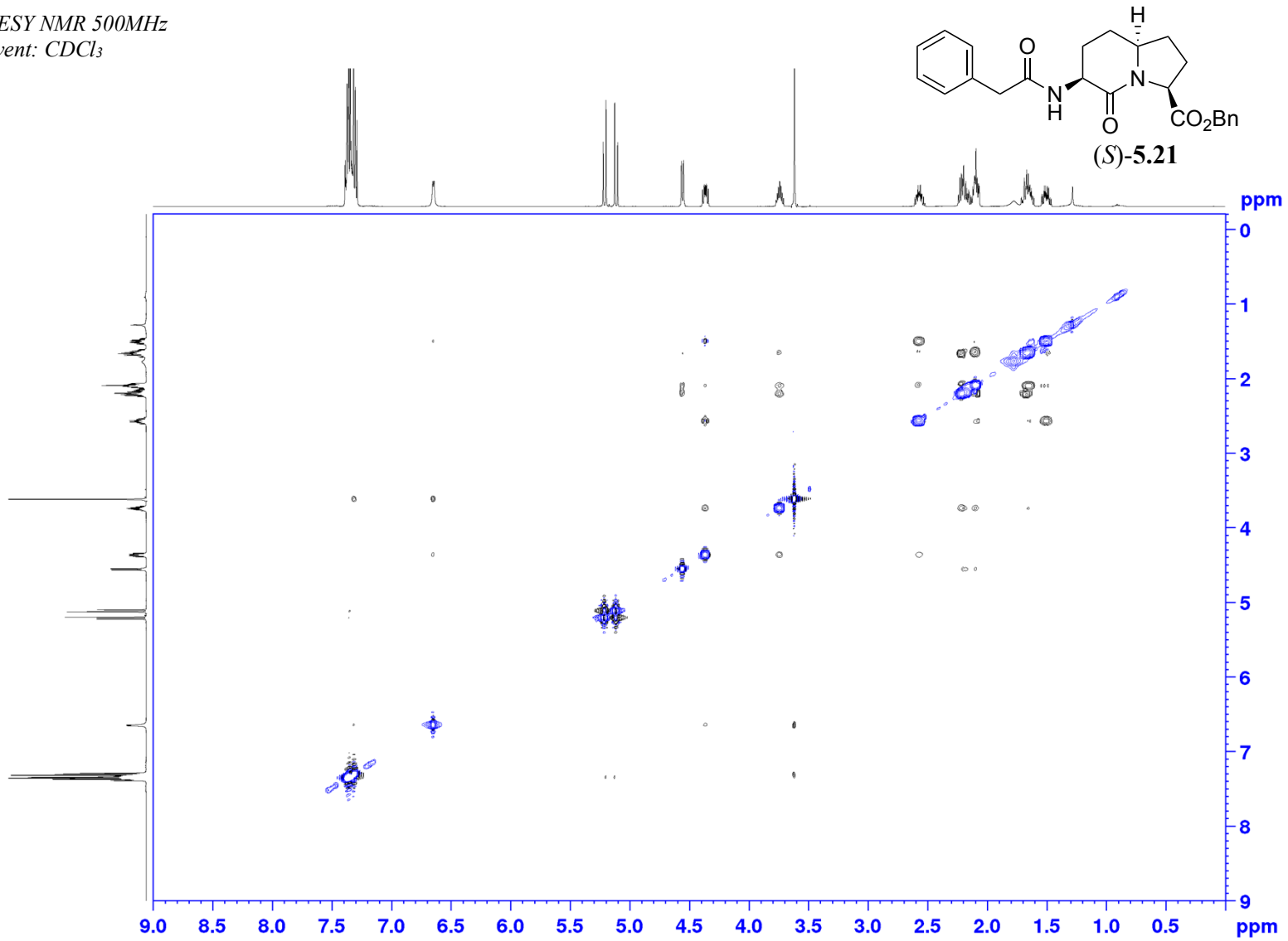

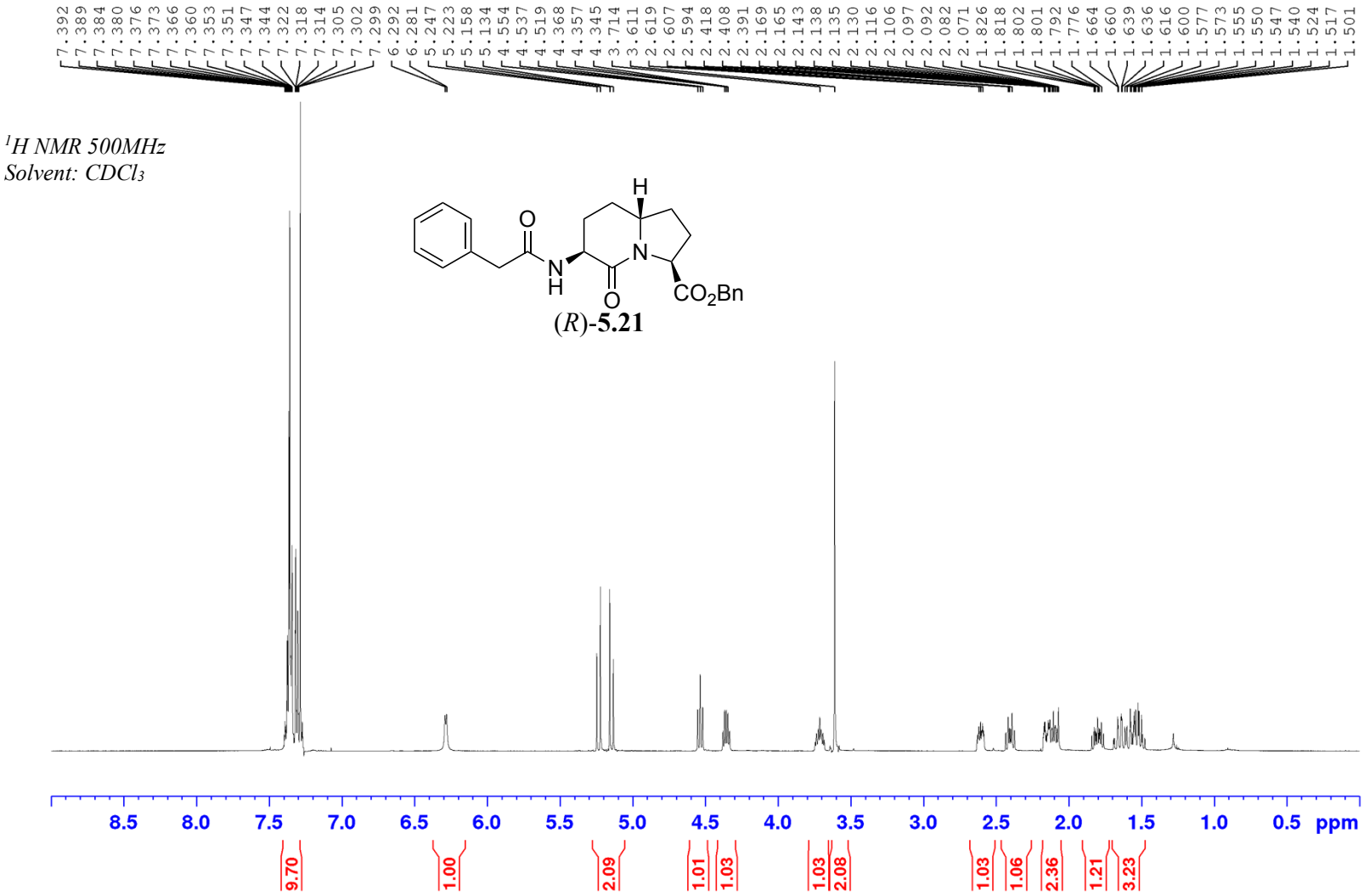
7.392
7.389
7.384
7.380
7.376
7.373
7.366
7.360
7.353
7.351
7.347
7.344
7.322
7.318
7.314
7.305
7.302
7.299
6.292
6.281
5.247
5.223
5.158
5.134
4.554
4.537
4.519
4.368
4.357
4.345
3.714
3.611
2.619
2.607
2.594
2.418
2.408
2.391
2.169
2.165
2.143
2.138
2.135
2.130
2.116
2.106
2.097
2.092
2.082
2.071
1.826
1.818
1.802
1.801
1.792
1.776
1.664
1.660
1.639
1.636
1.616
1.600
1.577
1.573
1.555
1.550
1.547
1.540
1.524
1.517
1.501
1H NMR 500MHz
Solvent: CDCl3
H
O
N
H
N
O
CO2Bn
(R)-5.21
8.5
8.0
7.5
7.0
6.5
6.0
5.5
5.0
4.5
4.0
3.5
3.0
2.5
2.0
1.5
1.0
0.5
ppm
9.70
1.00
2.09
1.01
1.03
1.03
2.08
1.03
1.06
2.36
1.21
3.23

^{13}C NMR 125 MHz
Solvent: $CDCl_3$

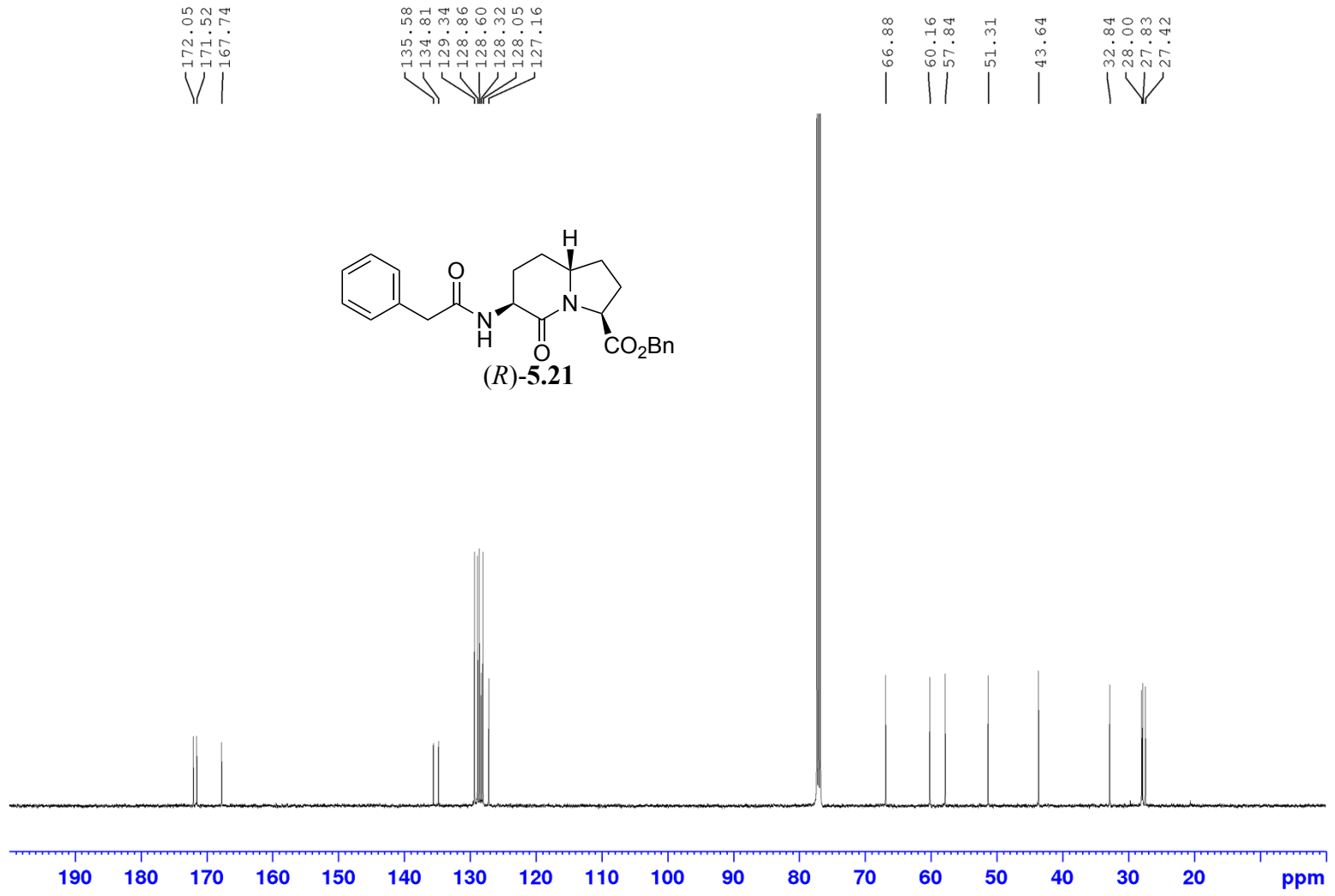

(*R*)-**5.21**

COSY NMR 500 MHz
Solvent: $CDCl_3$

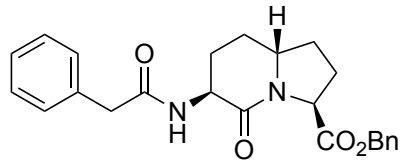

(*R*)-**5.21**

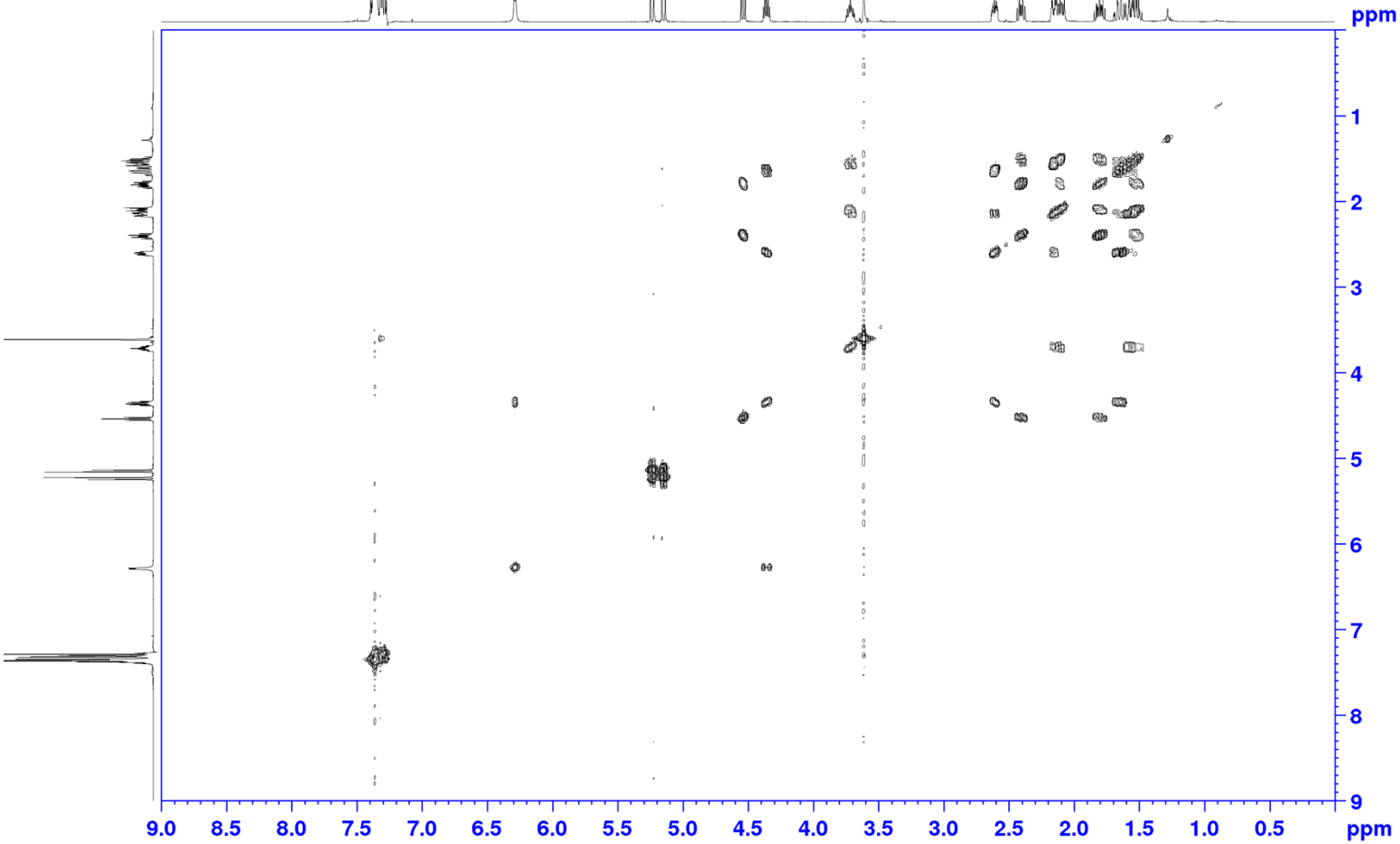

DEPT NMR 500 MHz
Solvent: $CDCl_3$

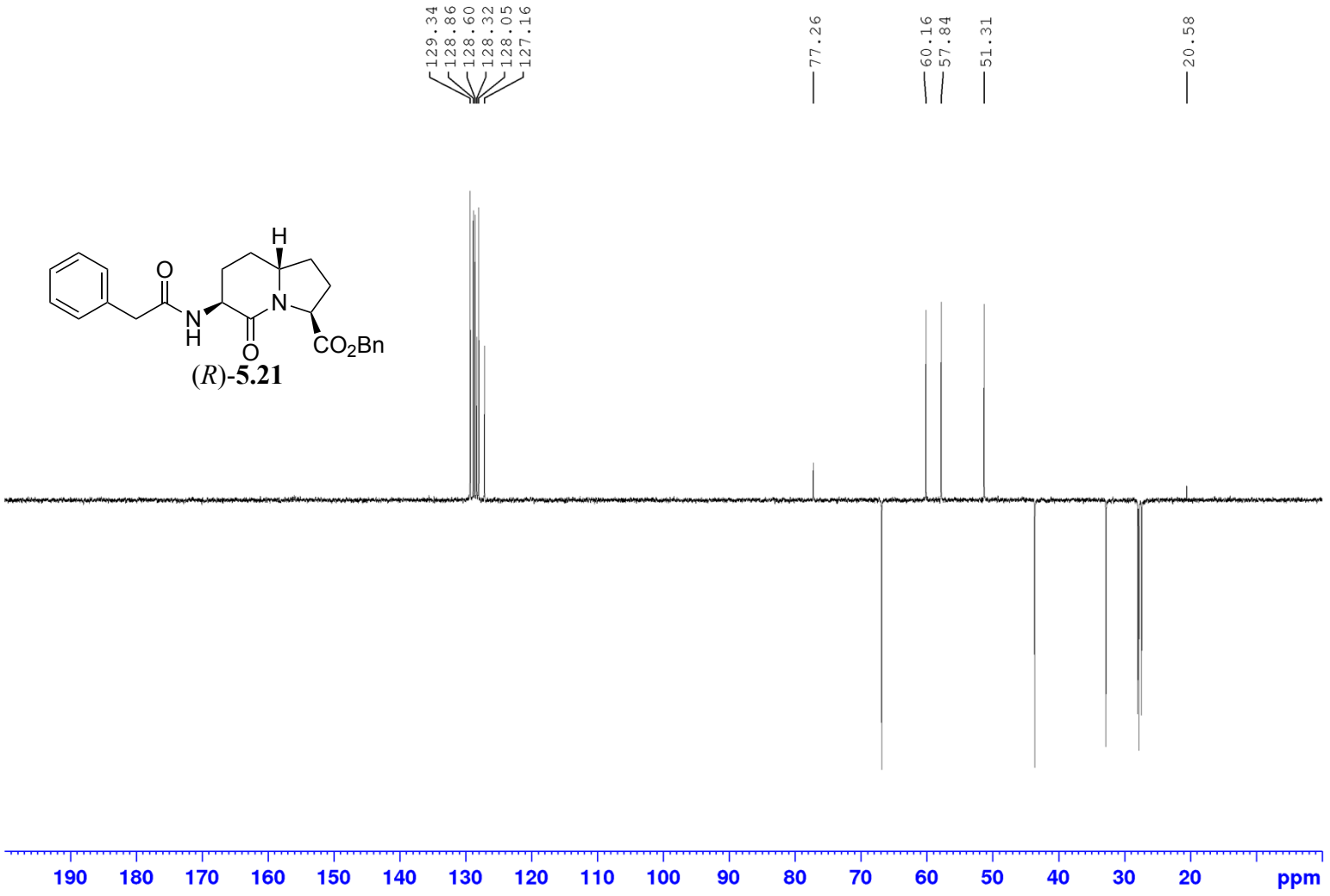

(*R*)-**5.21**

HSQC NMR 500 MHz
Solvent: $CDCl_3$

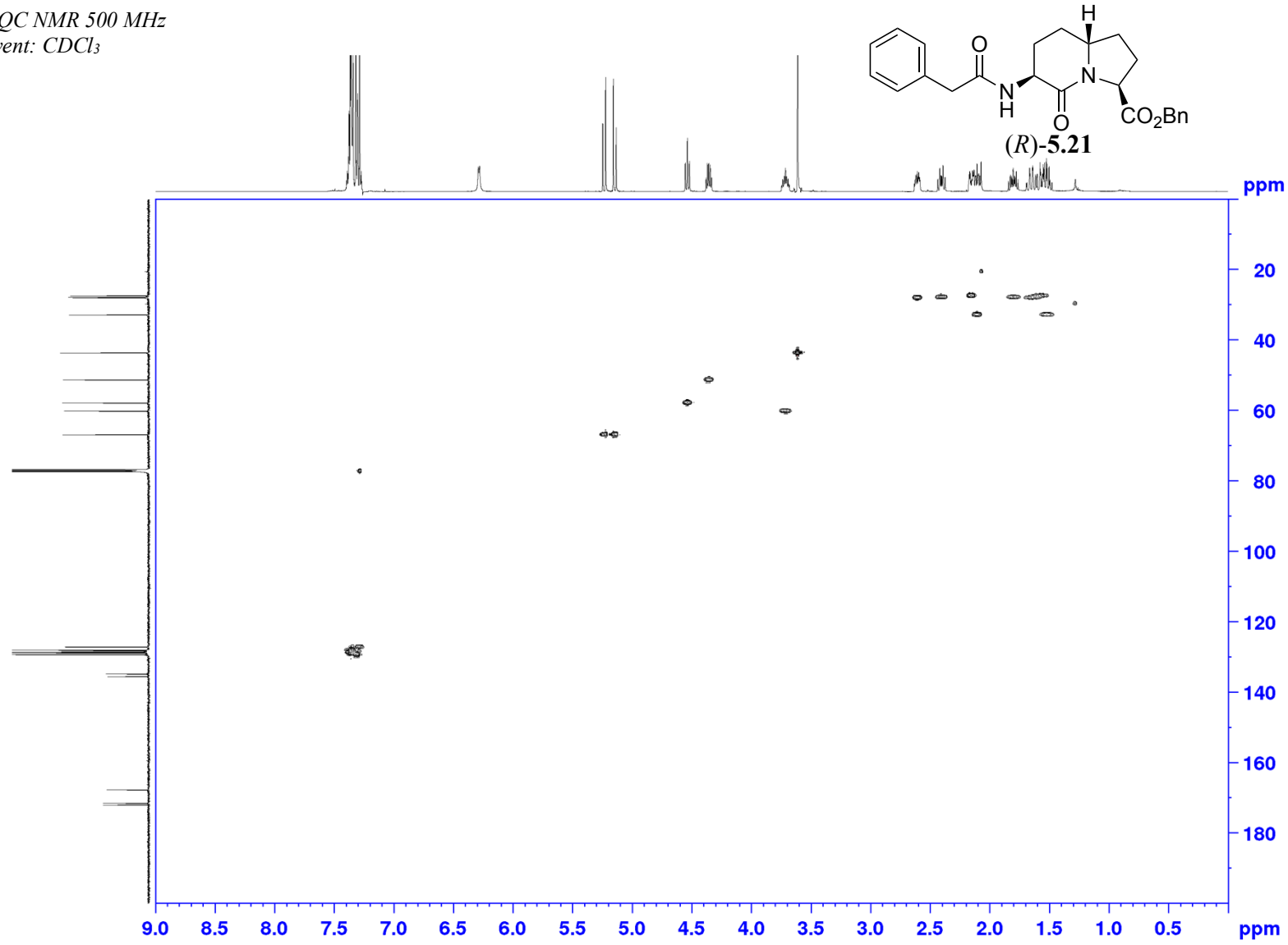

(*R*)-**5.21**

NOESY NMR 500 MHz
Solvent: $CDCl_3$

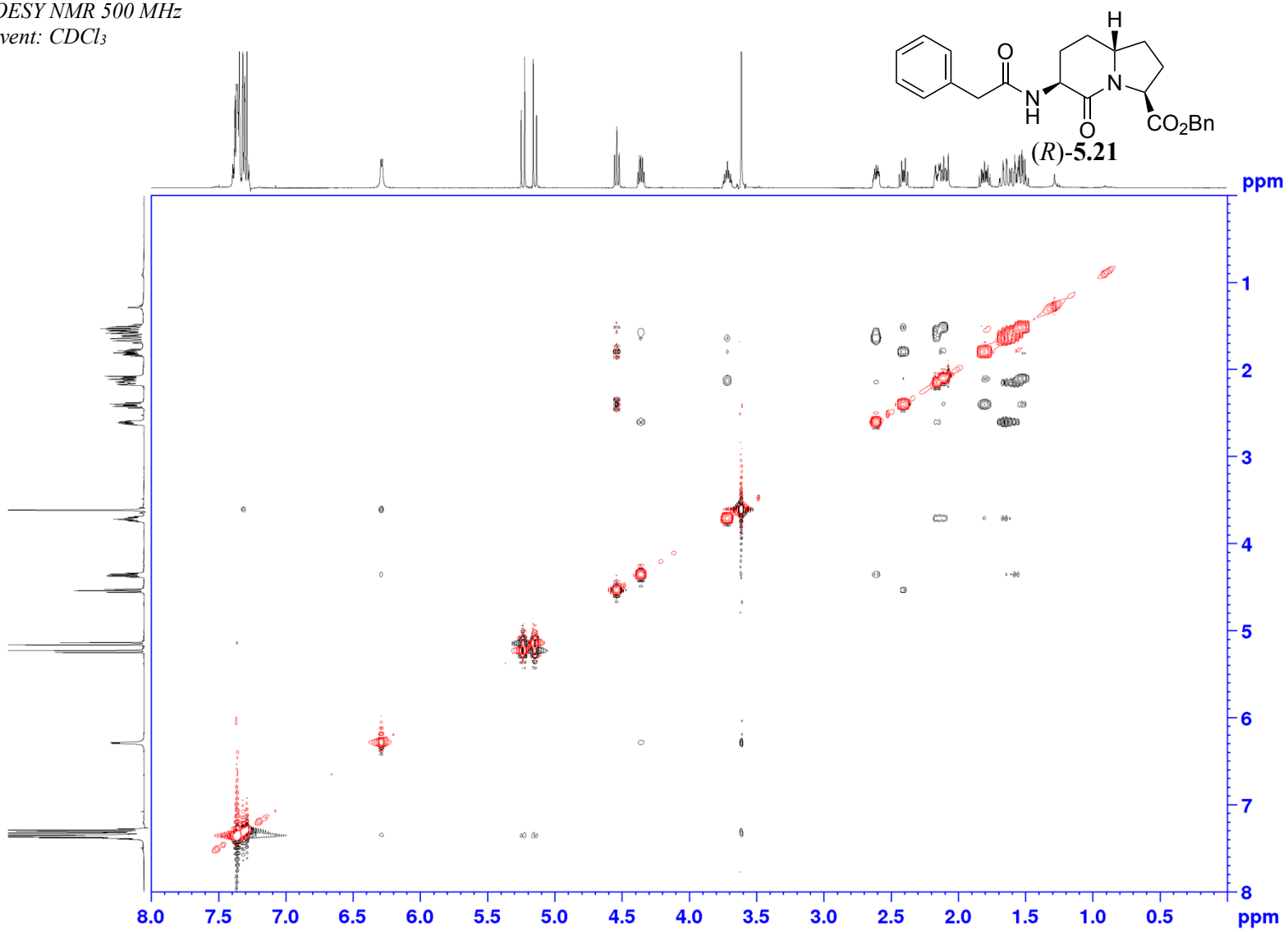

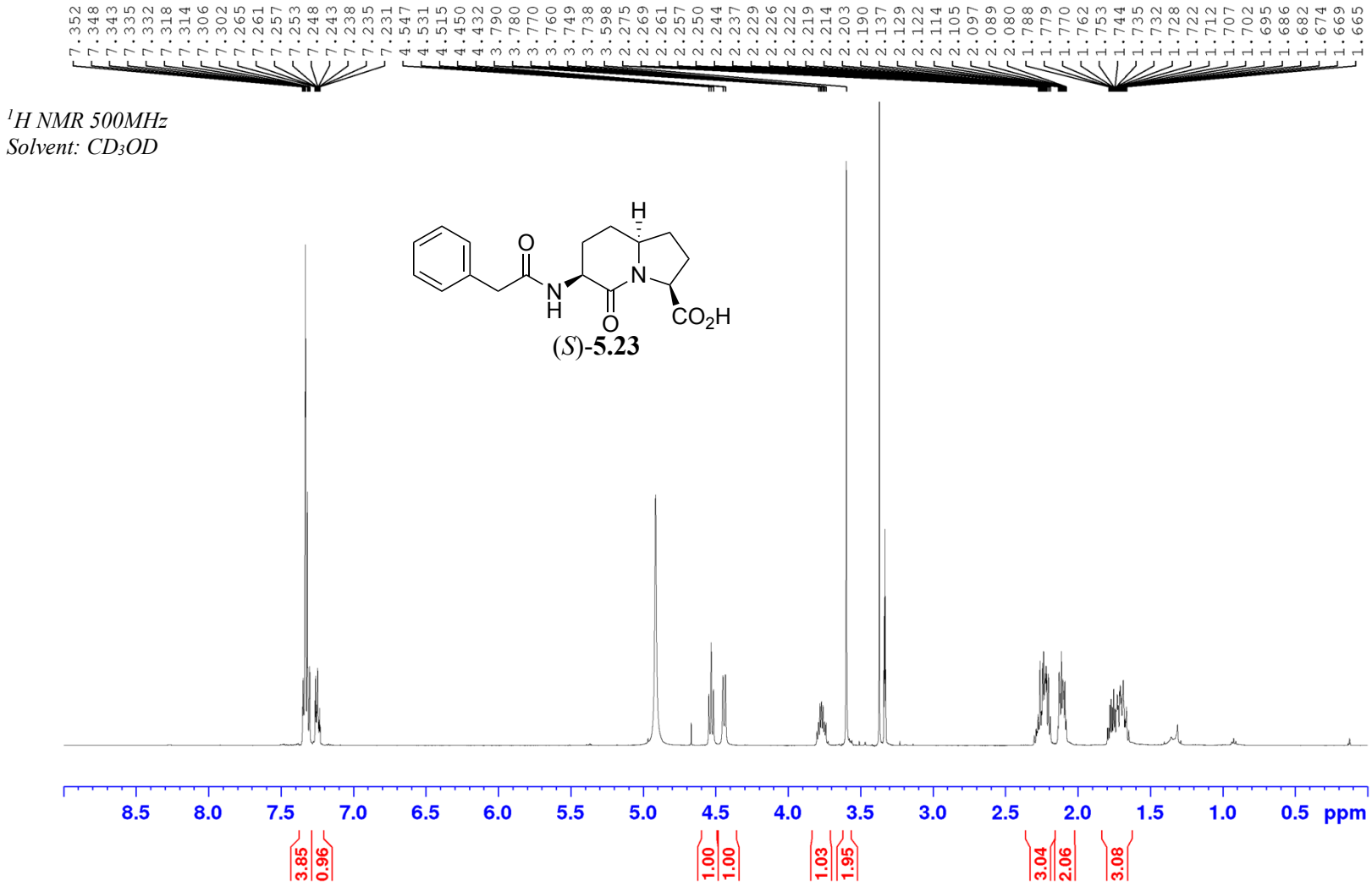

[1]H NMR 500MHz
Solvent: CD_3OD

(*S*)-**5.23**

^{13}C NMR 125MHz
Solvent: CD_3OD

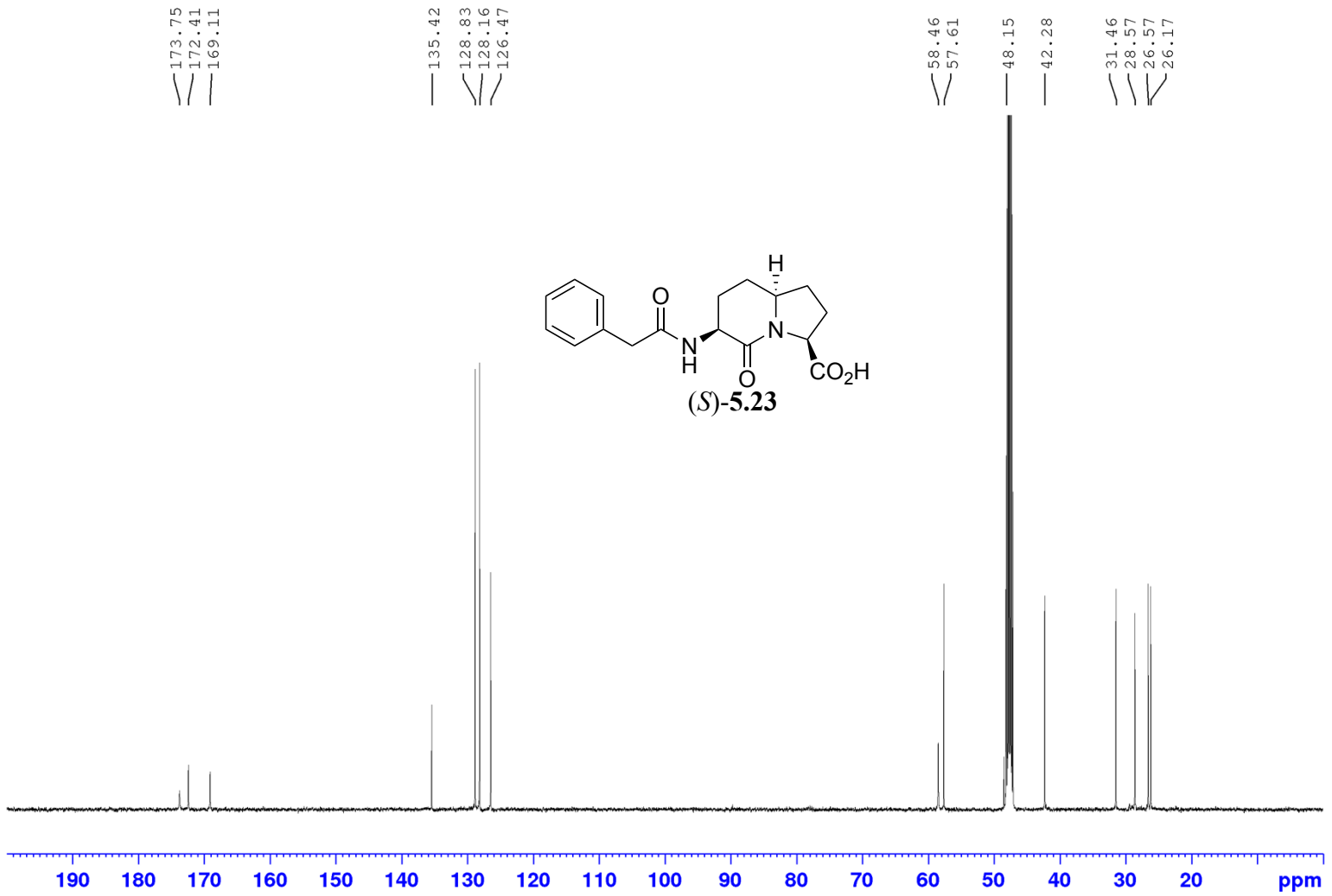

(*S*)-**5.23**

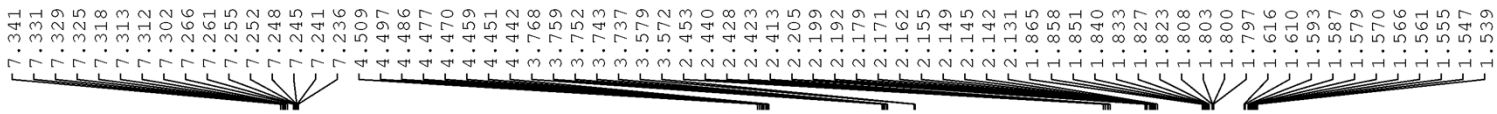

^{1}H NMR 500MHz
Solvent: CD_3OD

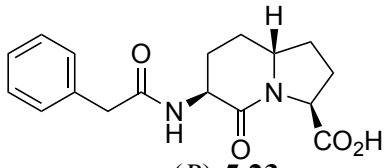

(*R*)-**5.23**

^{13}C NMR 125MHz
Solvent: CD_3OD

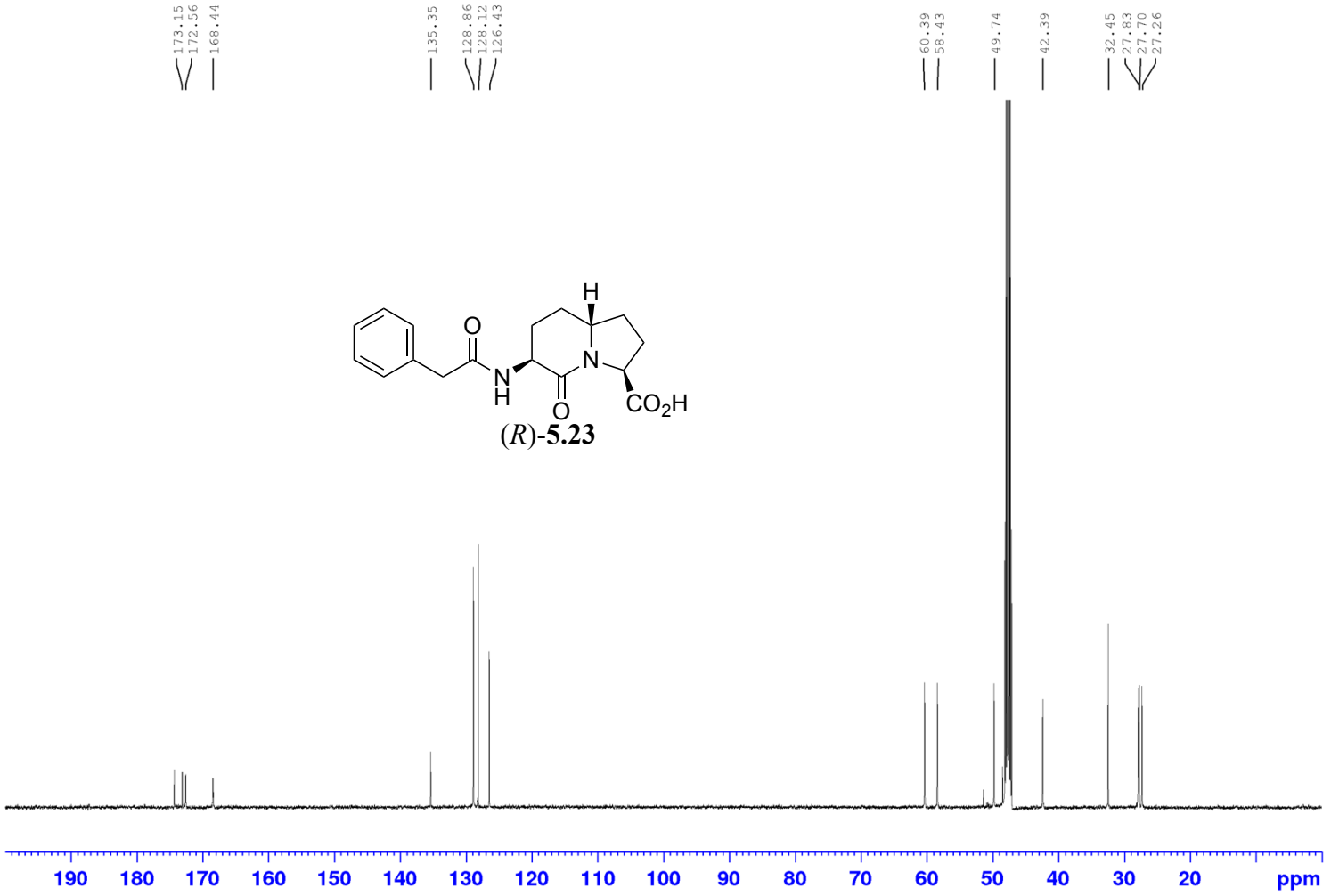

(*R*)-**5.23**

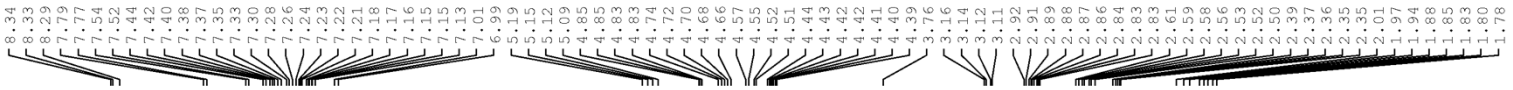

^{1}H NMR 400MHz
Solvent: $CDCl_3$

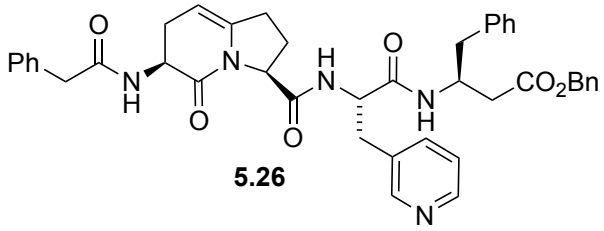

5.26

^{13}C NMR 125MHz
Solvent: CD_2Cl_2

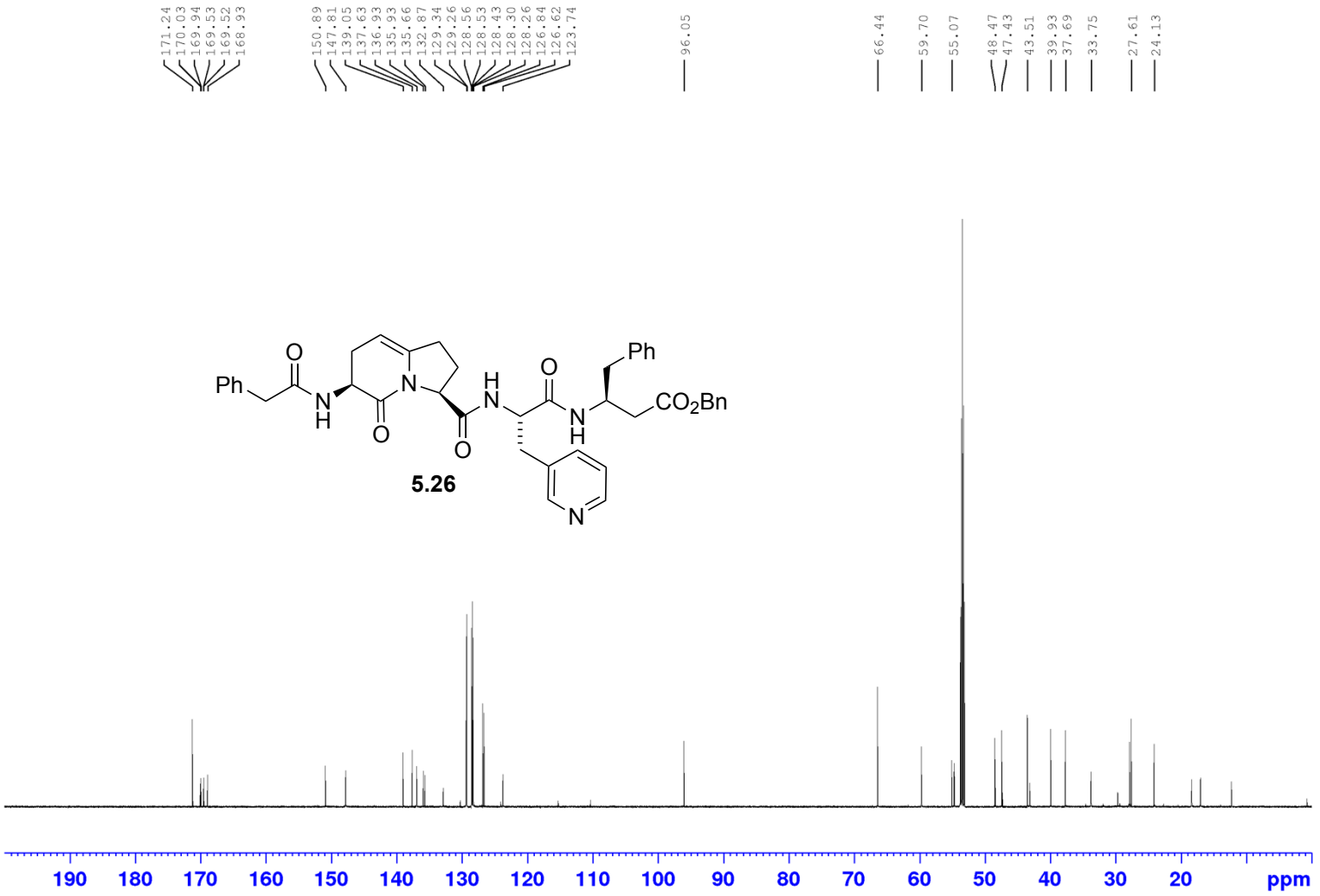

^{1}H NMR 500MHz
Solvent: $CDCl_3$

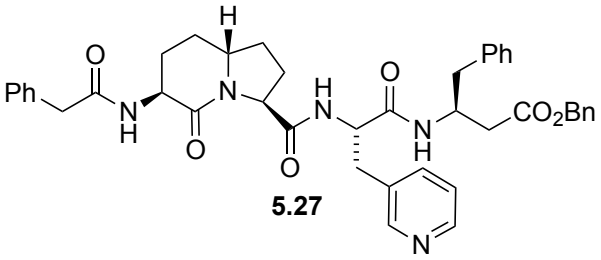

5.27

^{13}C NMR 125MHz
Solvent: $CDCl_3$

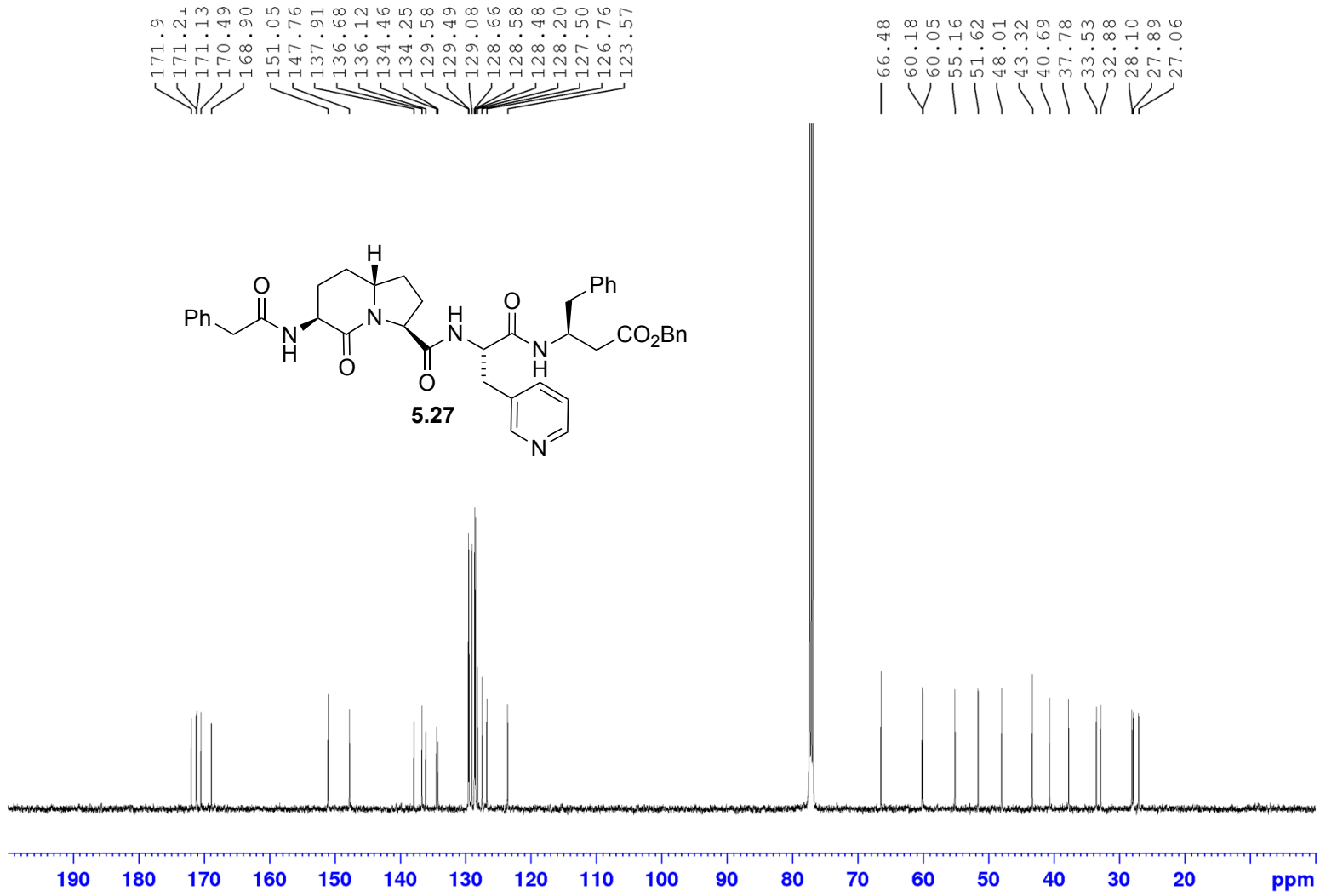

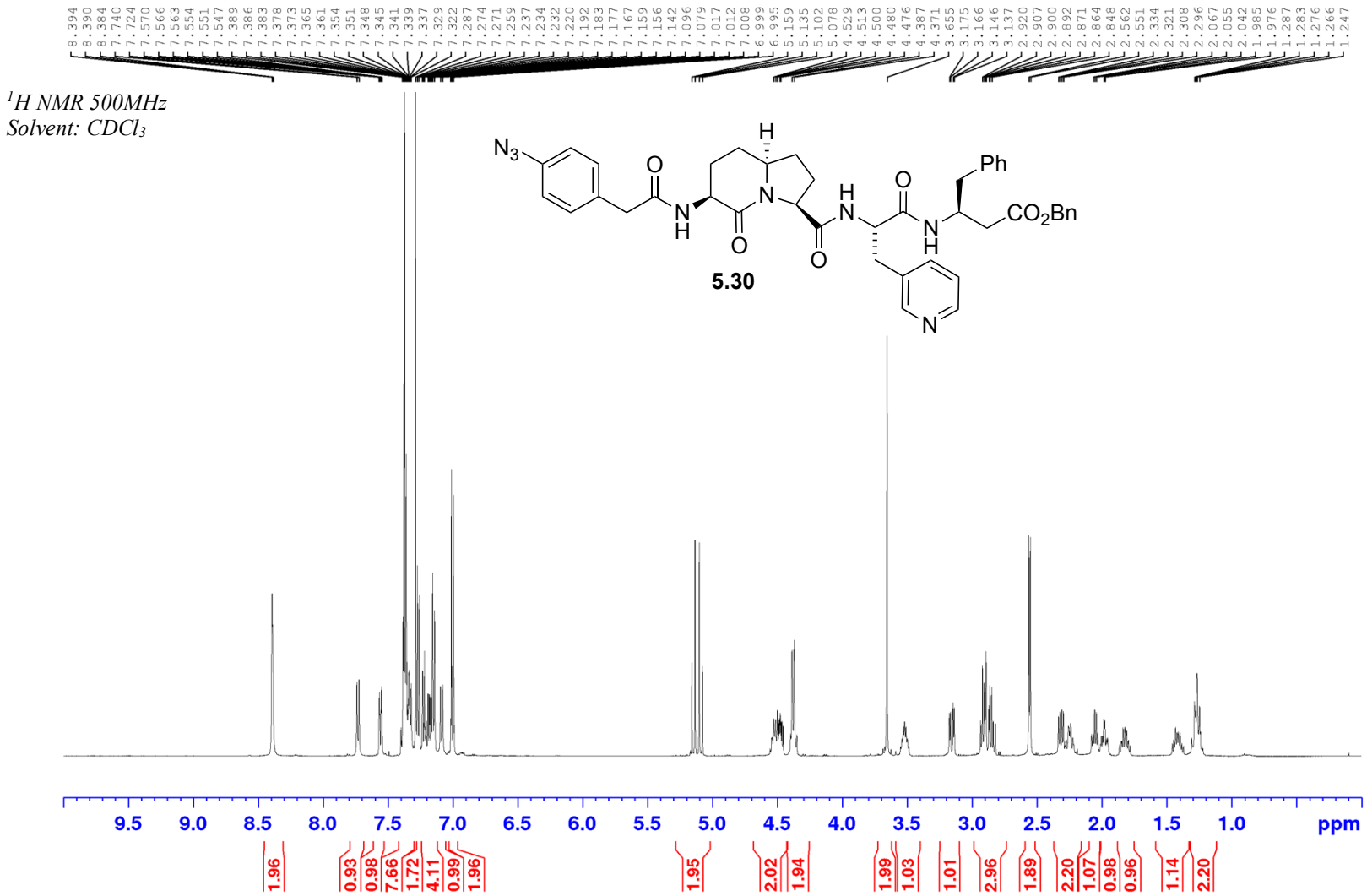
8.394
8.390
8.384
7.740
7.724
7.570
7.566
7.563
7.554
7.551
7.547
7.389
7.386
7.383
7.378
7.373
7.365
7.361
7.354
7.351
7.348
7.345
7.341
7.339
7.337
7.329
7.322
7.287
7.274
7.271
7.259
7.237
7.234
7.232
7.220
7.192
7.183
7.177
7.167
7.159
7.156
7.142
7.096
7.079
7.017
7.012
7.008
6.999
6.995
5.159
5.135
5.102
5.078
4.529
4.513
4.500
4.480
4.476
4.387
4.371
3.655
3.175
3.166
3.146
3.137
2.920
2.907
2.900
2.892
2.871
2.864
2.848
2.562
2.551
2.334
2.321
2.308
2.296
2.067
2.055
2.042
1.985
1.976
1.287
1.283
1.276
1.266
1.247
1H NMR 500MHz
Solvent: CDCl3
N3
O
H
N
O
N
H
O
H
N
O
N
H
Ph
CO2Bn
O
N
5.30
9.5
9.0
8.5
8.0
7.5
7.0
6.5
6.0
5.5
5.0
4.5
4.0
3.5
3.0
2.5
2.0
1.5
1.0
ppm
1.96
0.93
0.98
7.66
1.72
4.11
0.99
1.96
1.95
2.02
1.94
1.99
1.03
1.01
2.96
1.89
2.20
1.07
0.98
0.96
1.14
2.20

^{13}C NMR 125MHz
Solvent: $CDCl_3$

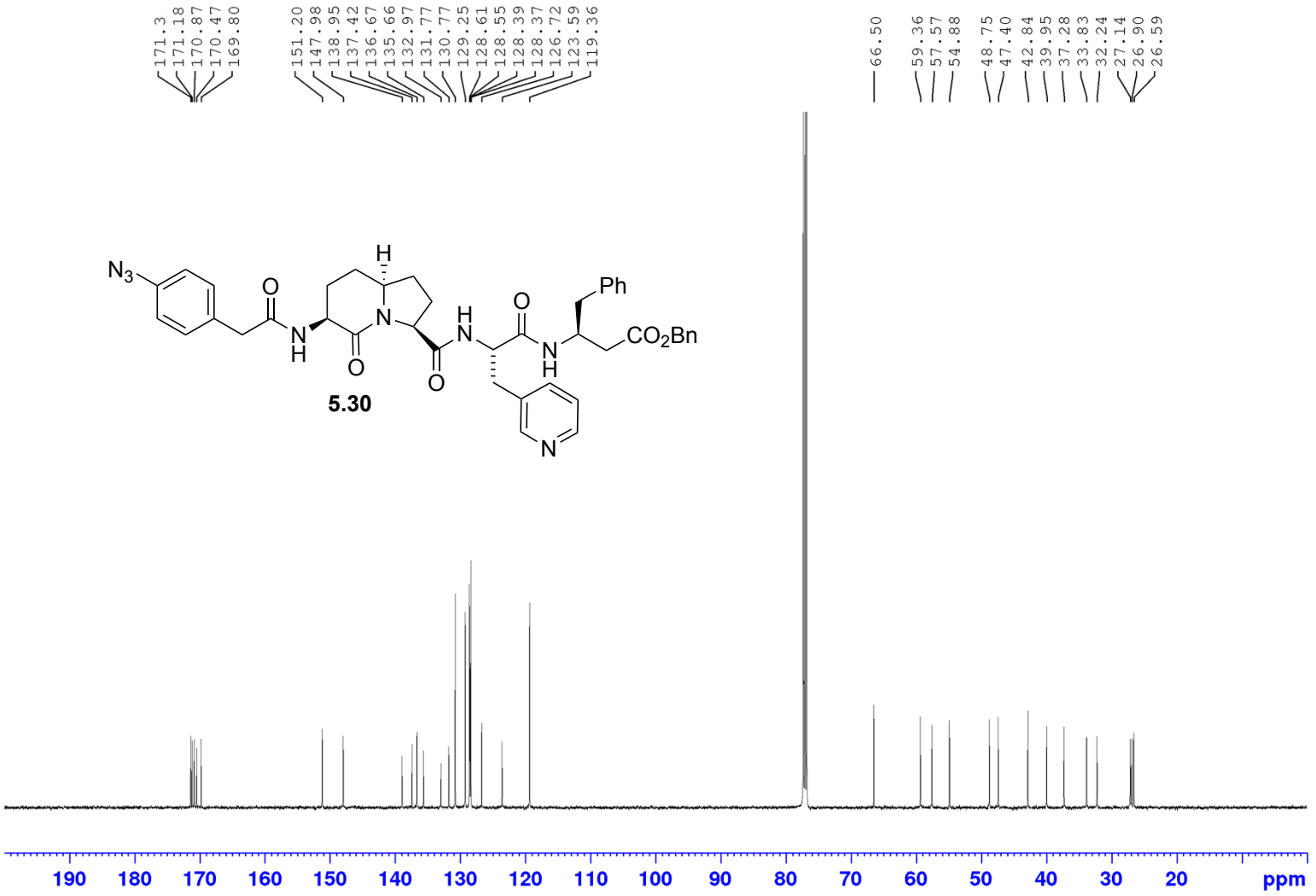

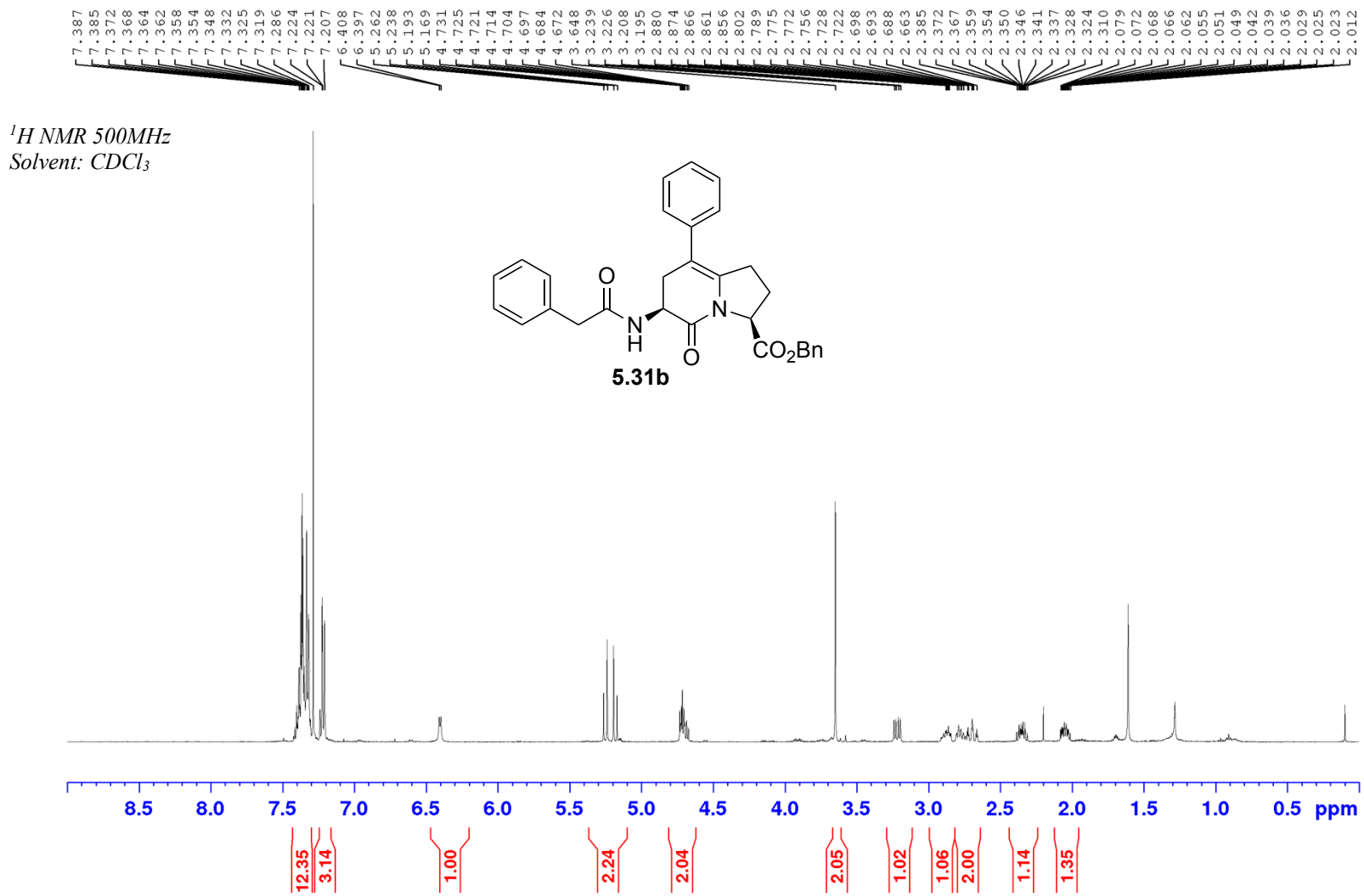
7.387
7.385
7.372
7.368
7.364
7.362
7.358
7.354
7.348
7.332
7.325
7.319
7.286
7.224
7.221
7.207
6.408
6.397
5.262
5.238
5.193
5.169
4.731
4.725
4.721
4.714
4.704
4.697
4.684
4.672
3.648
3.239
3.226
3.208
3.195
2.880
2.874
2.866
2.861
2.856
2.802
2.789
2.775
2.772
2.756
2.728
2.722
2.698
2.693
2.688
2.663
2.385
2.372
2.367
2.359
2.354
2.350
2.346
2.341
2.337
2.328
2.324
2.310
2.079
2.072
2.068
2.066
2.062
2.055
2.051
2.049
2.042
2.039
2.036
2.029
2.025
2.023
2.012
1H NMR 500MHz
Solvent: CDCl3
O
N
H
O
N
CO2Bn
5.31b
8.5
8.0
7.5
7.0
6.5
6.0
5.5
5.0
4.5
4.0
3.5
3.0
2.5
2.0
1.5
1.0
0.5
ppm
12.35
3.14
1.00
2.24
2.04
2.05
1.02
1.06
2.00
1.14
1.35

^{13}C NMR 125MHz
Solvent: $CDCl_3$

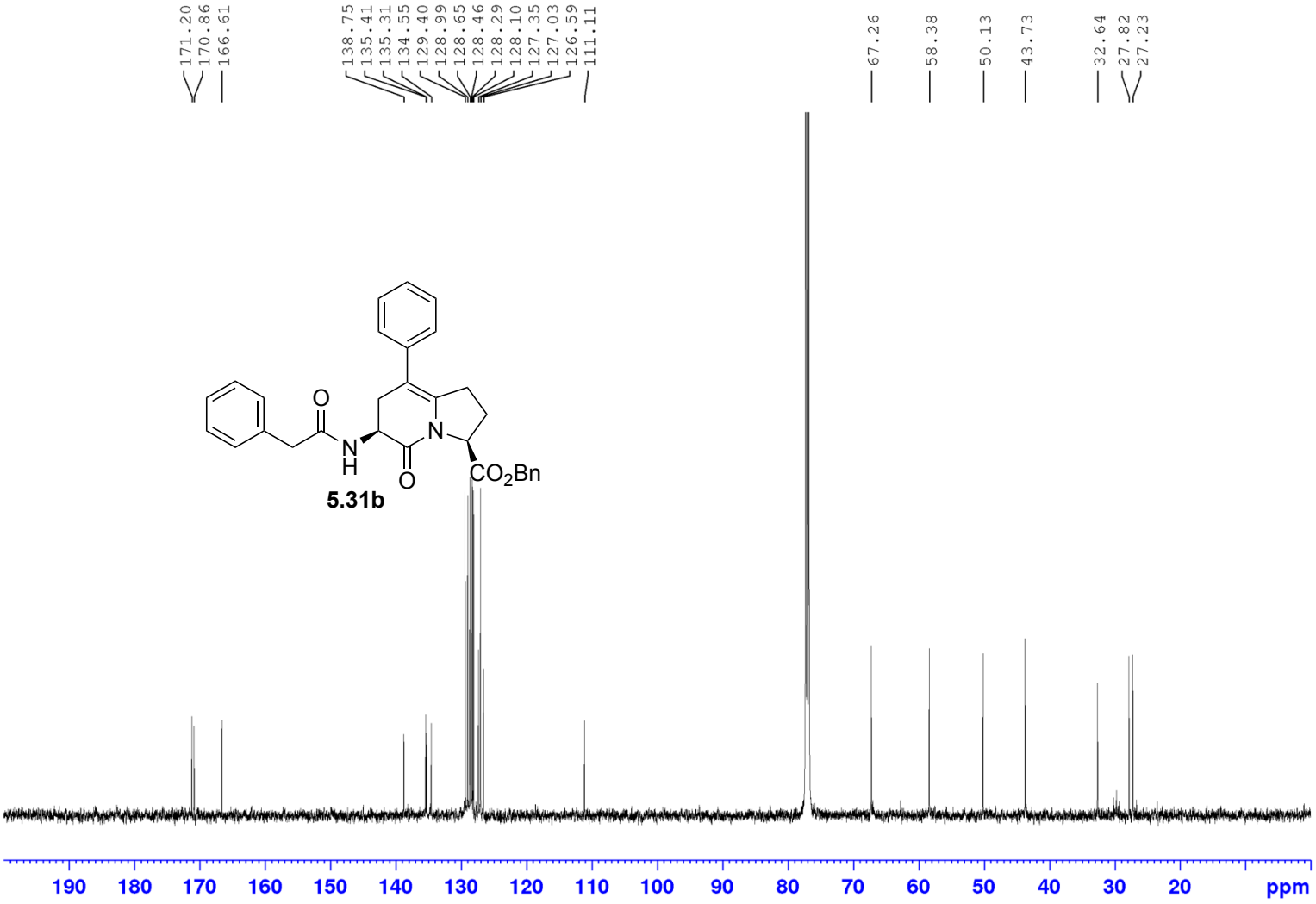

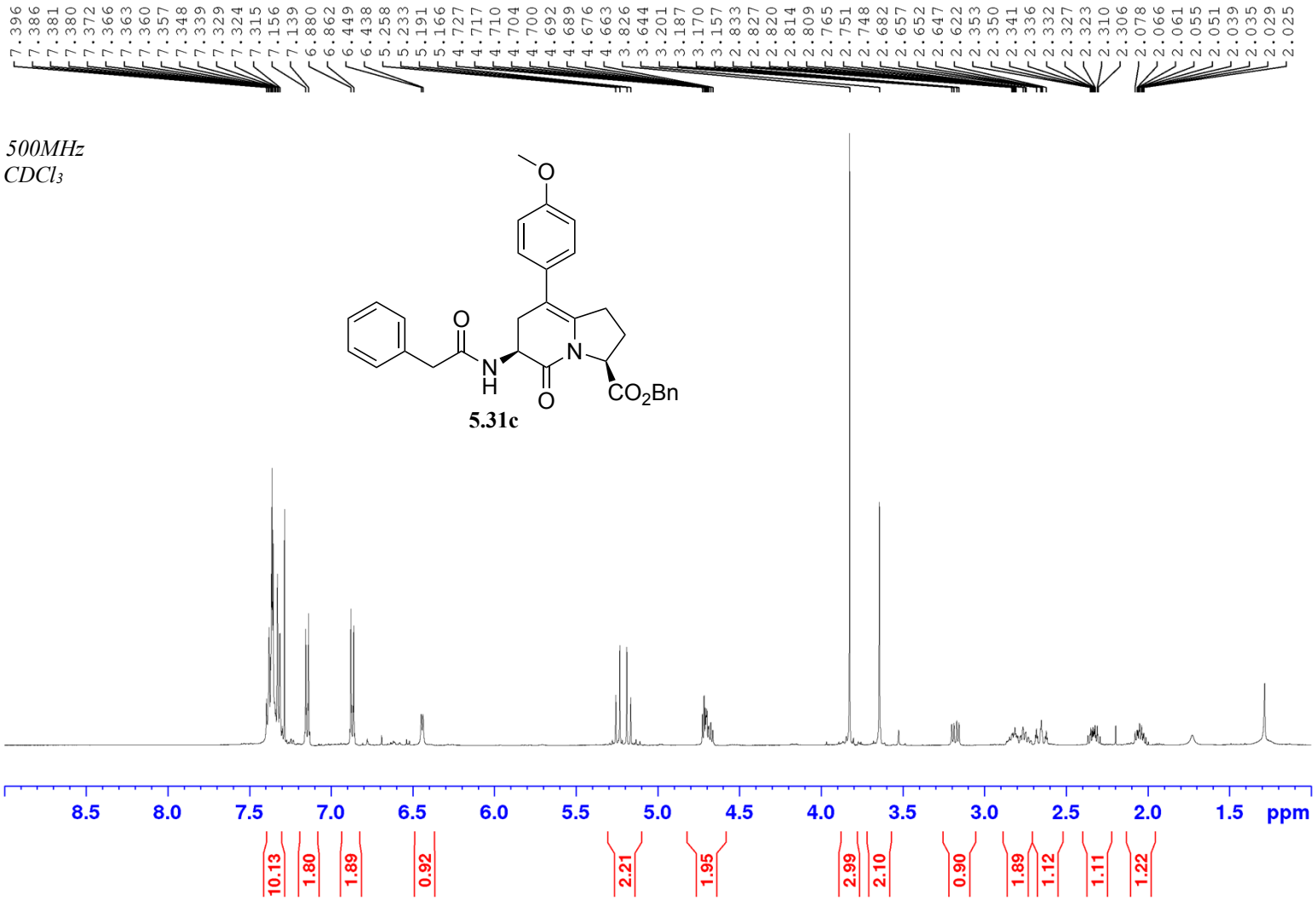

^{1}H NMR 500MHz
Solvent: $CDCl_3$

^{13}C NMR 125MHz
Solvent: $CDCl_3$

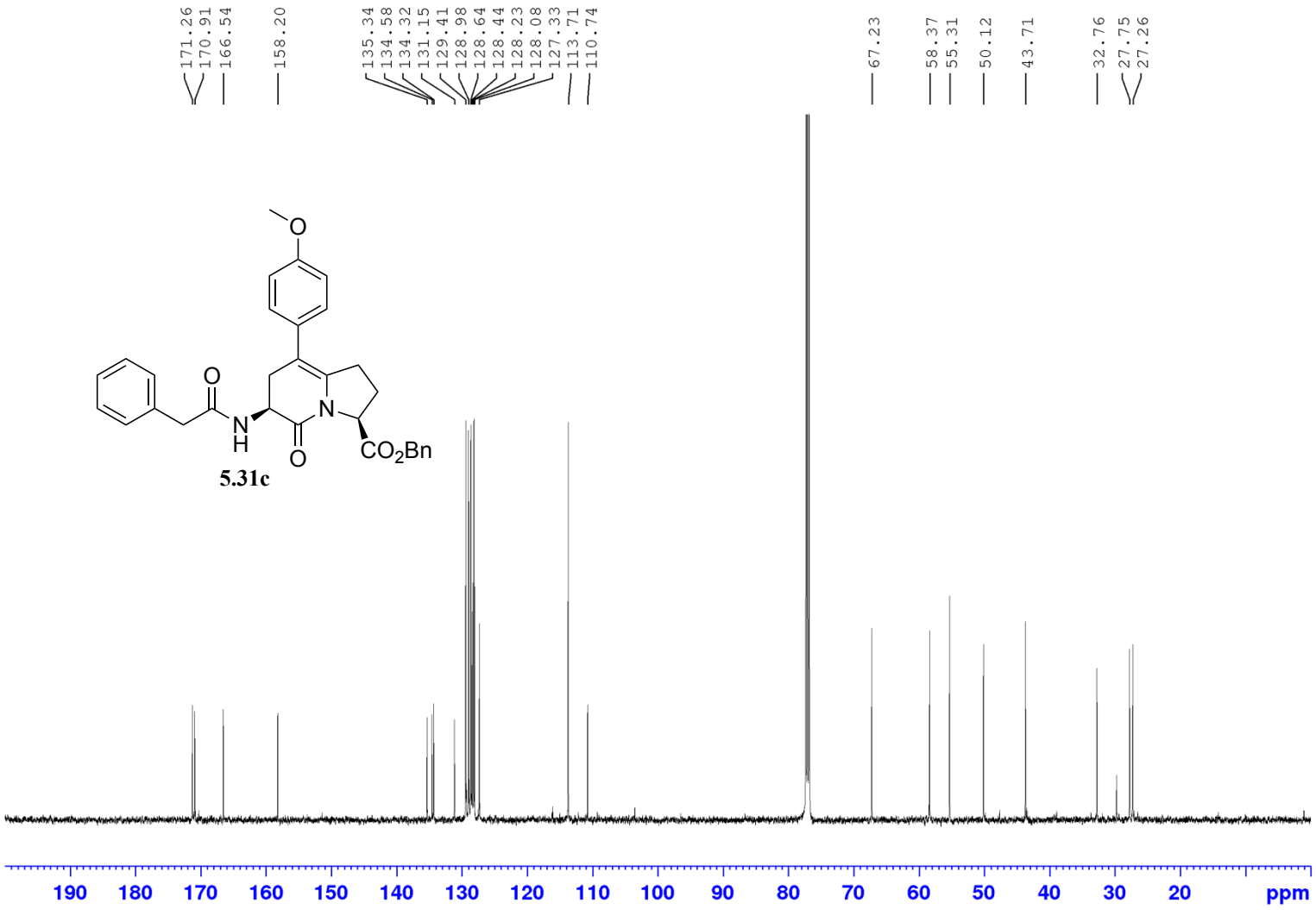

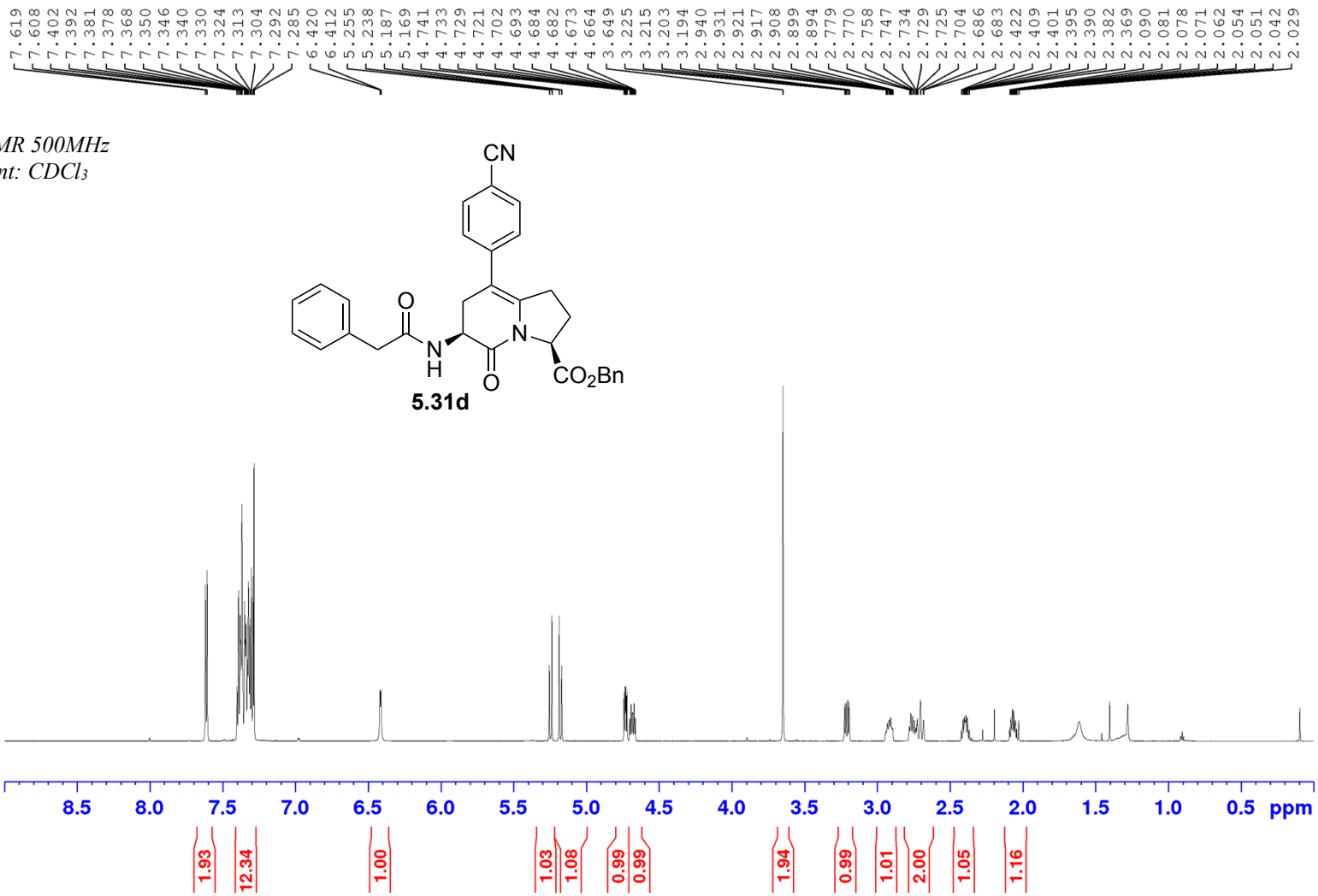

[1]H NMR 500MHz
Solvent: $CDCl_3$

^{13}C NMR 500MHz
Solvent: $CDCl_3$

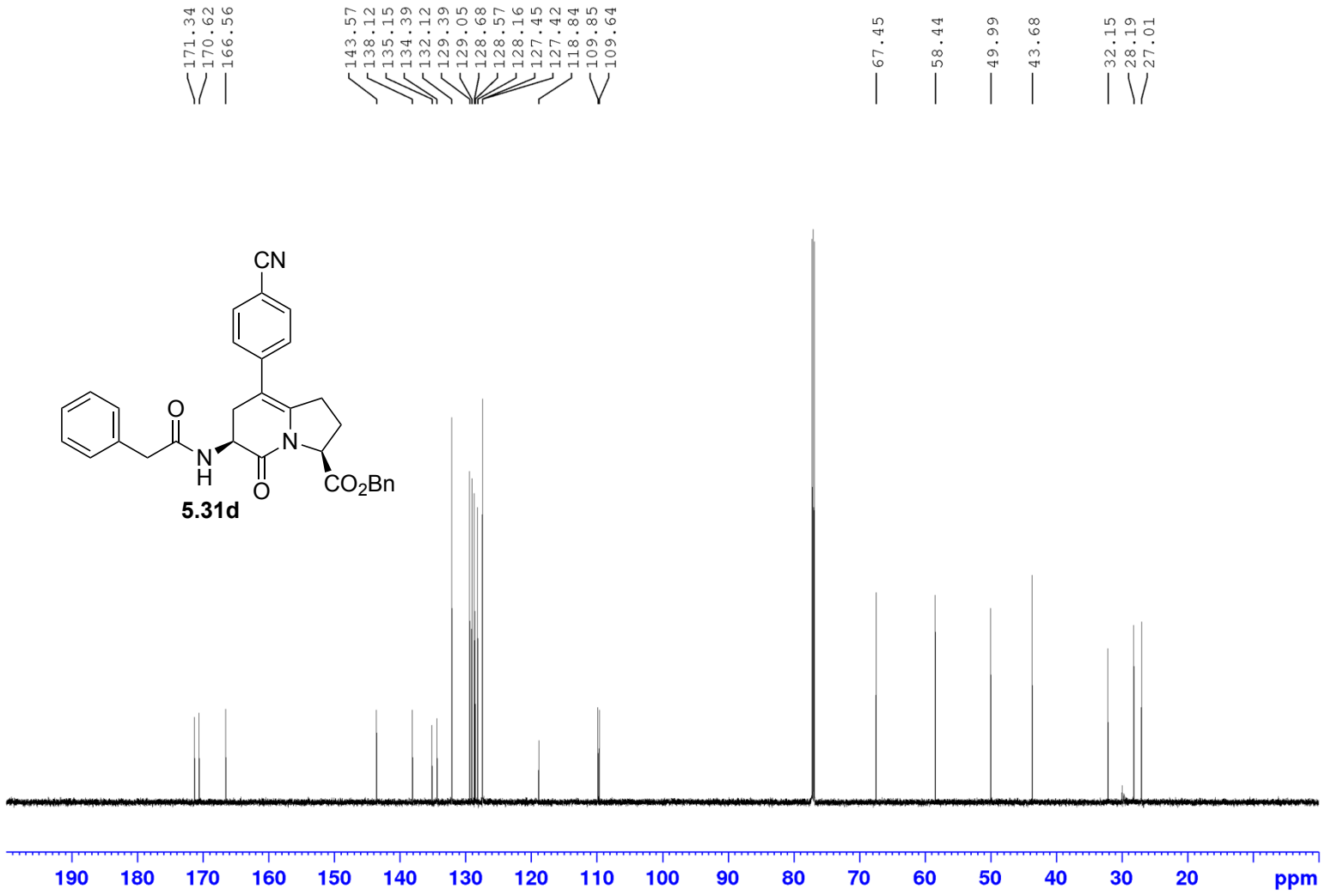

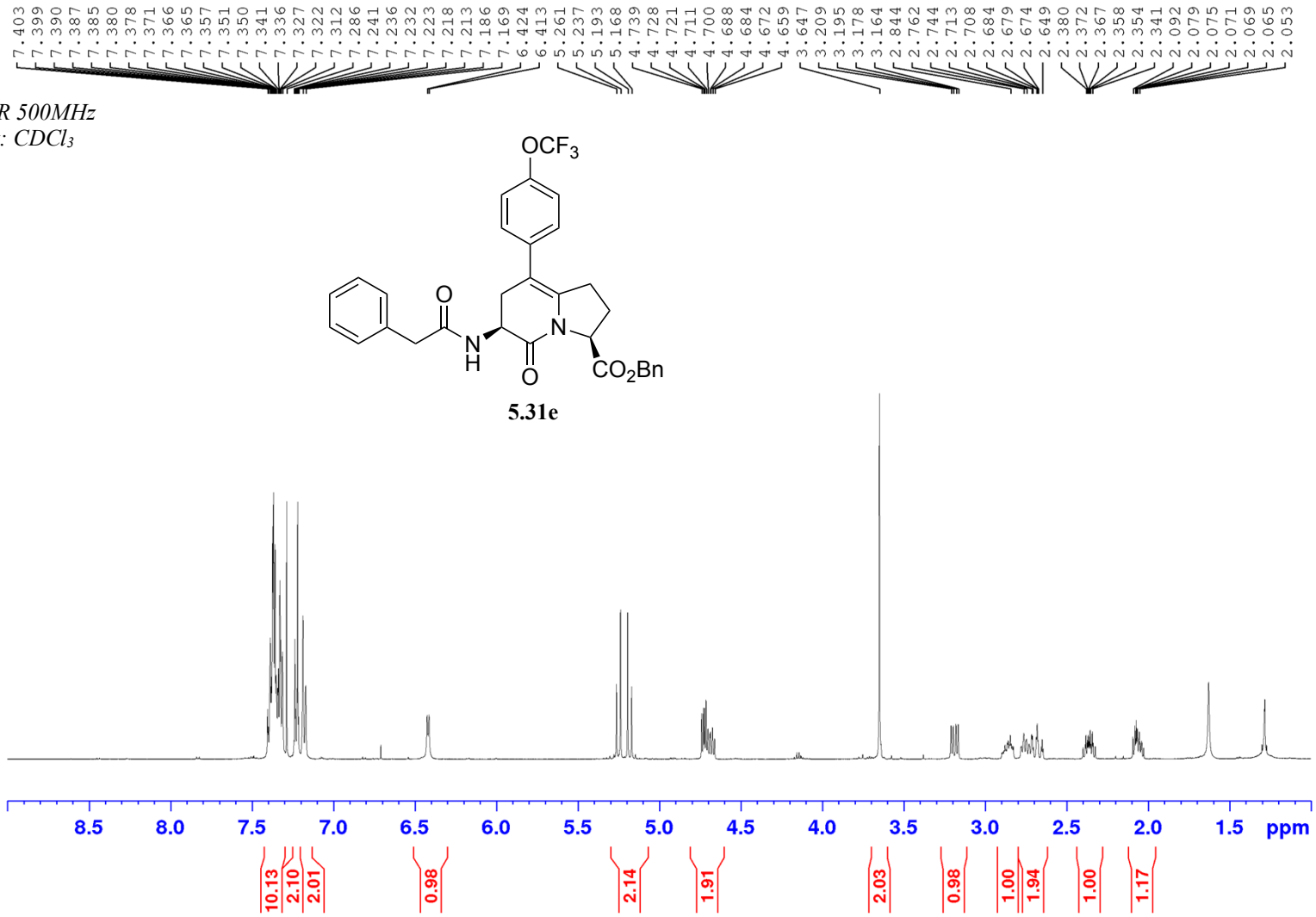

^{1}H NMR 500MHz
Solvent: $CDCl_3$

5.31e

^{13}C NMR 125MHz
Solvent: $CDCl_3$

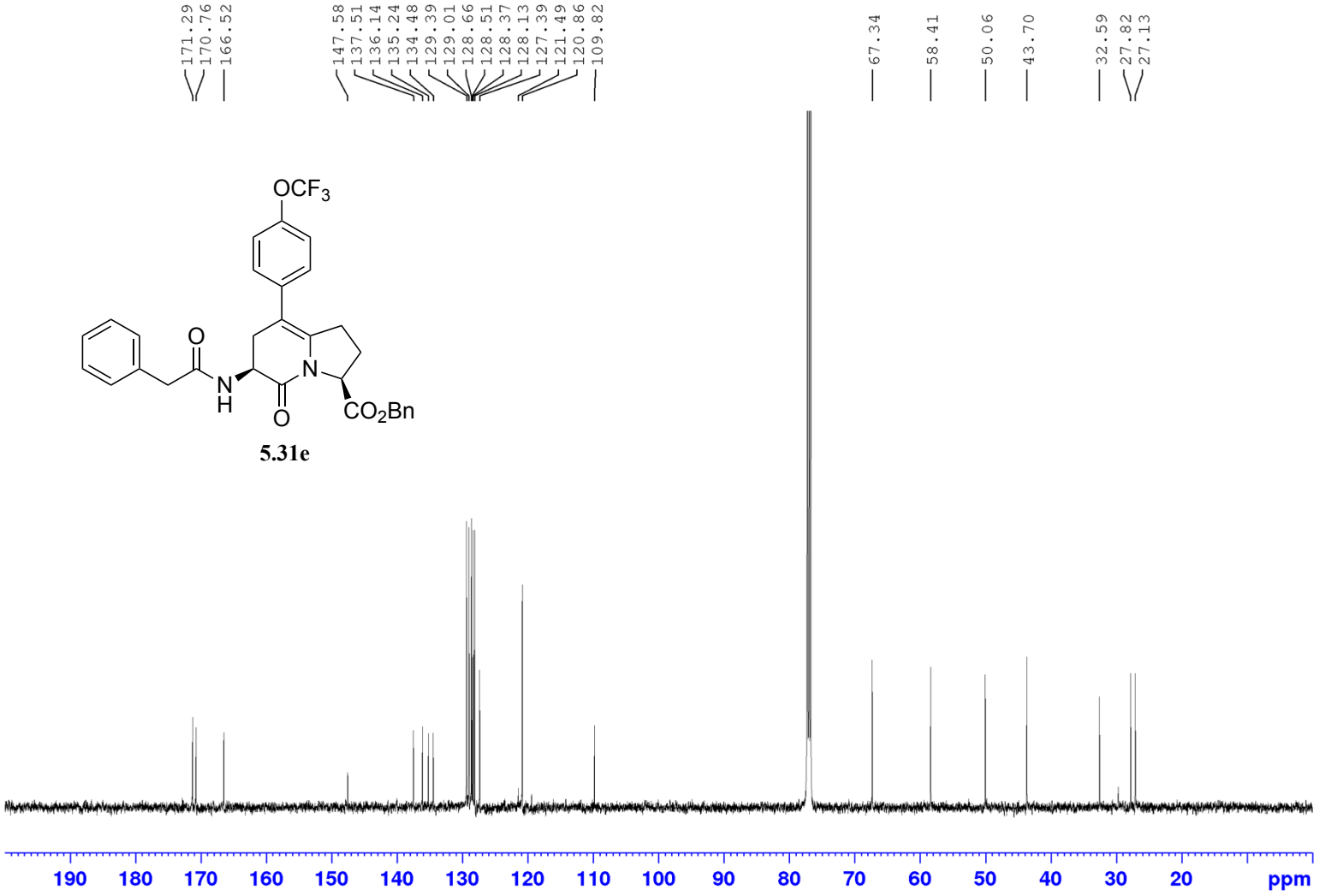

5.31e

[1]H NMR 700MHz
Solvent: CD_3OD

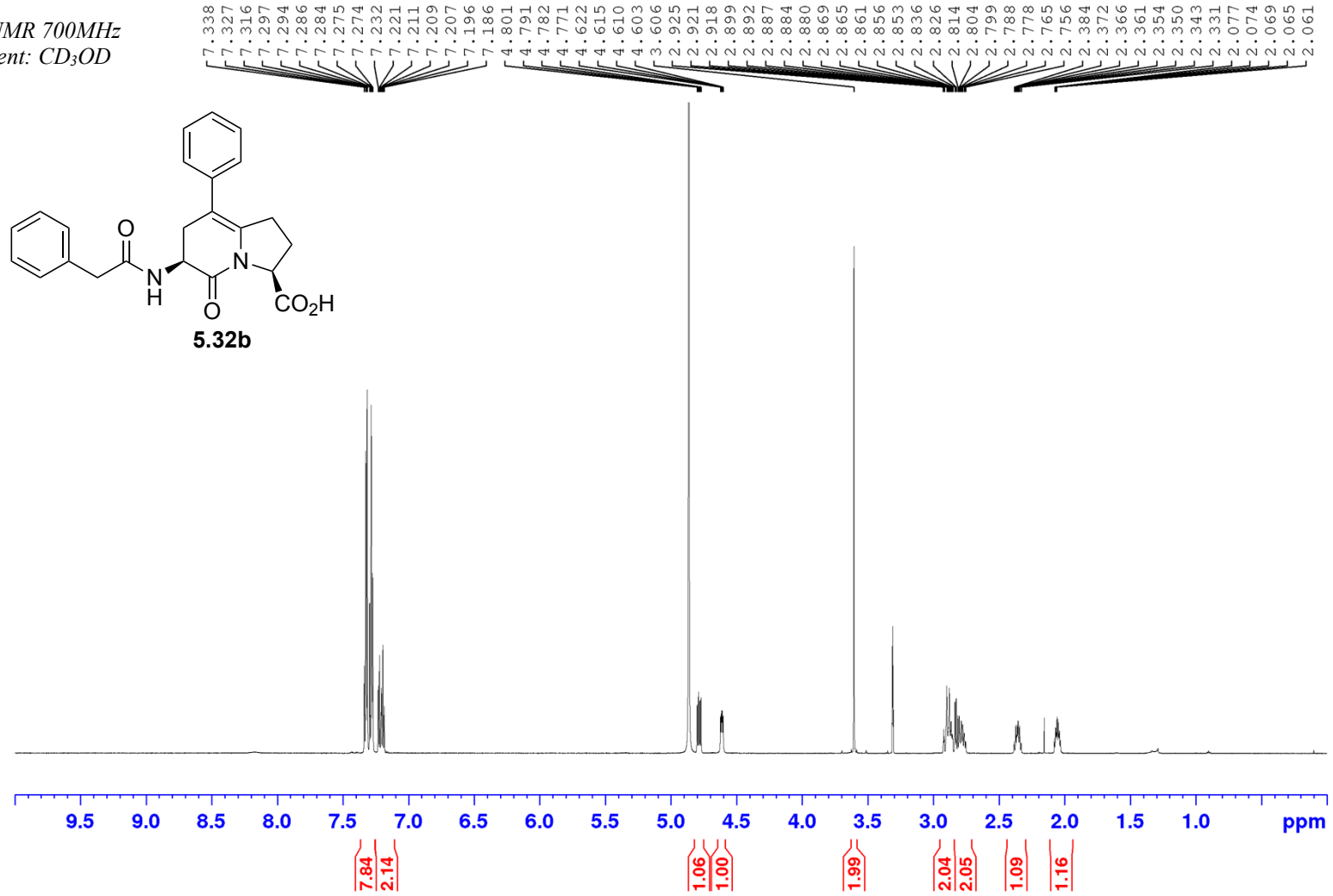

^{13}C NMR 175MHz
Solvent: CD_3OD

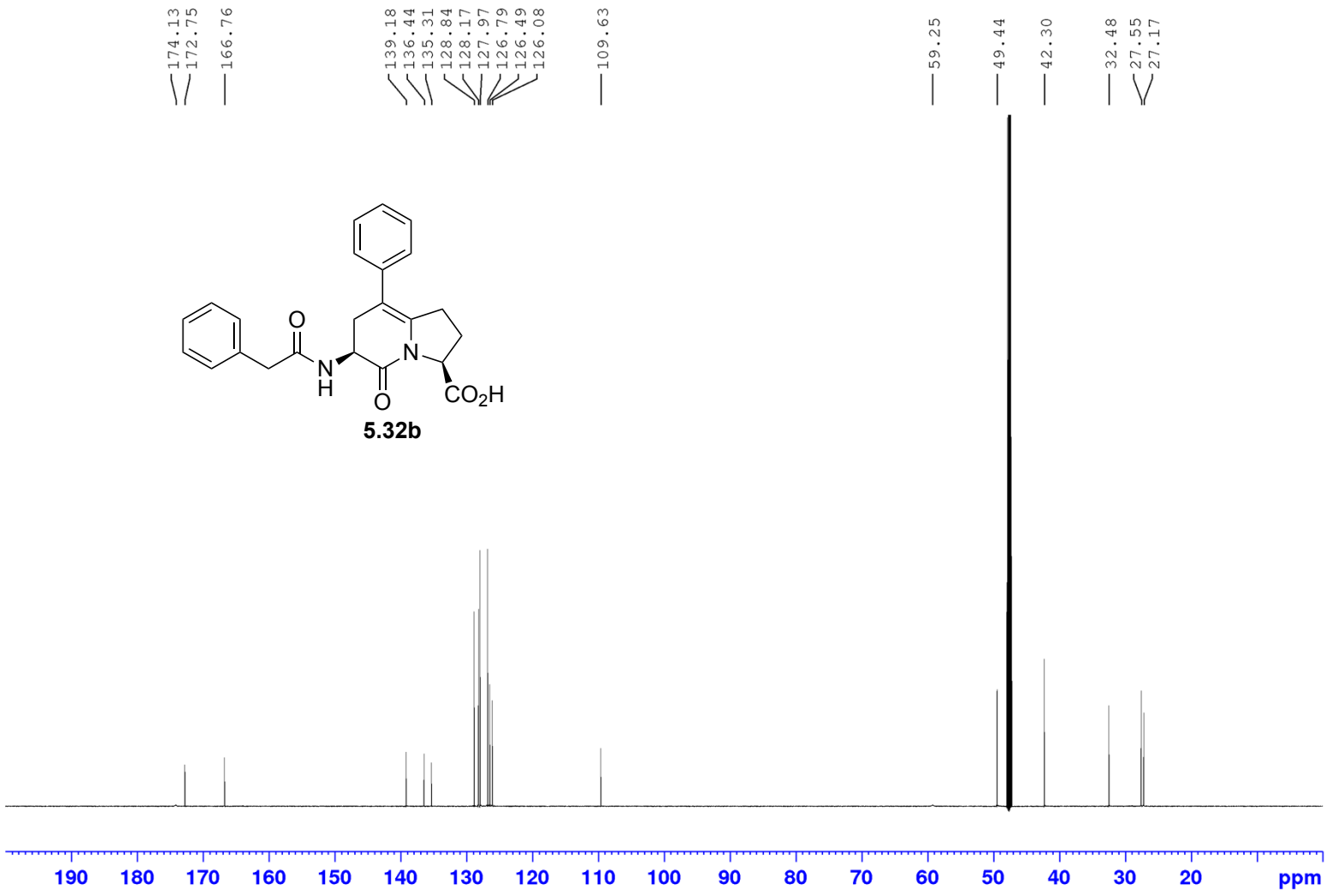

^{1}H NMR 700MHz
Solvent: CD_3OD

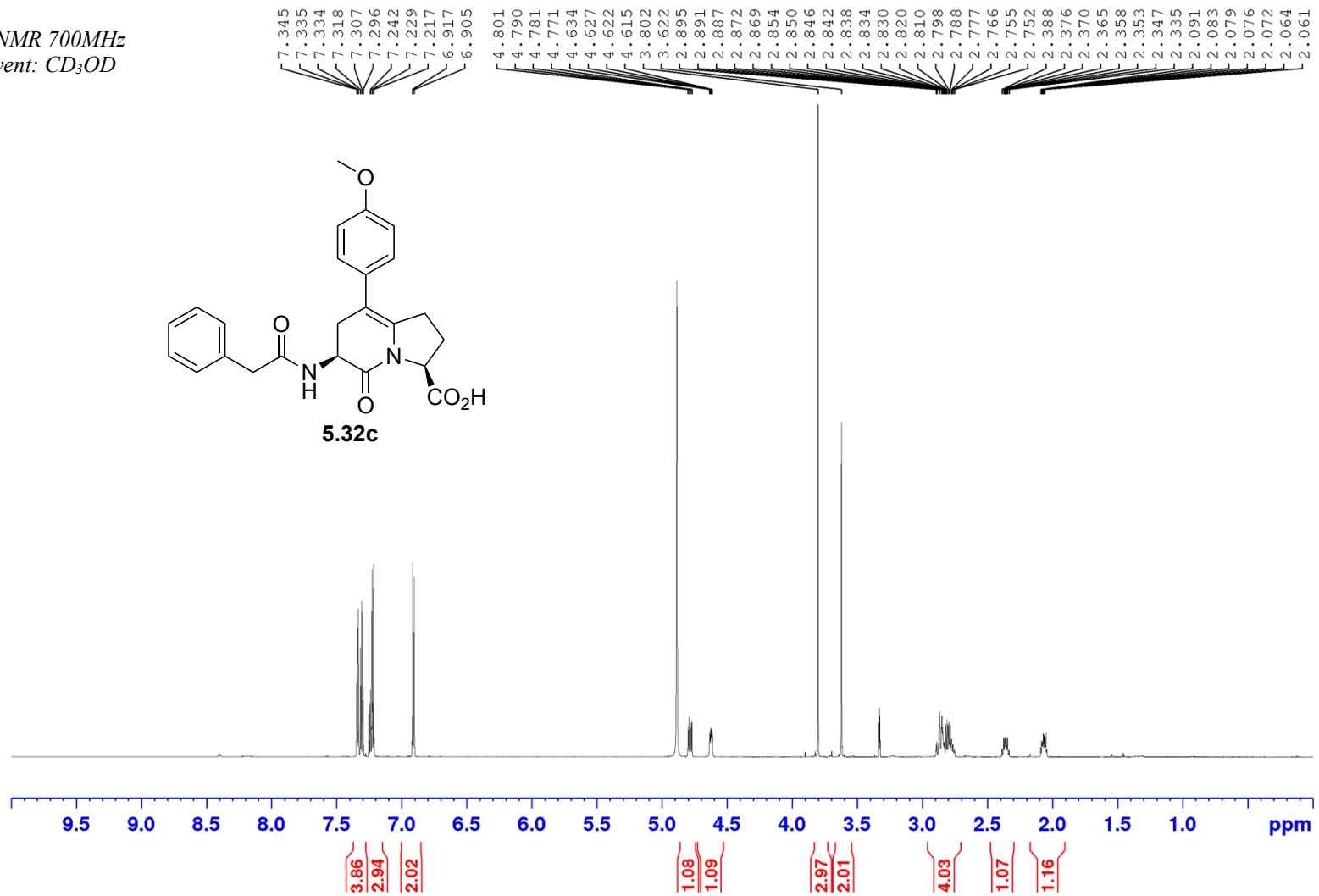

^{13}C NMR 175MHz
Solvent: CD_3OD

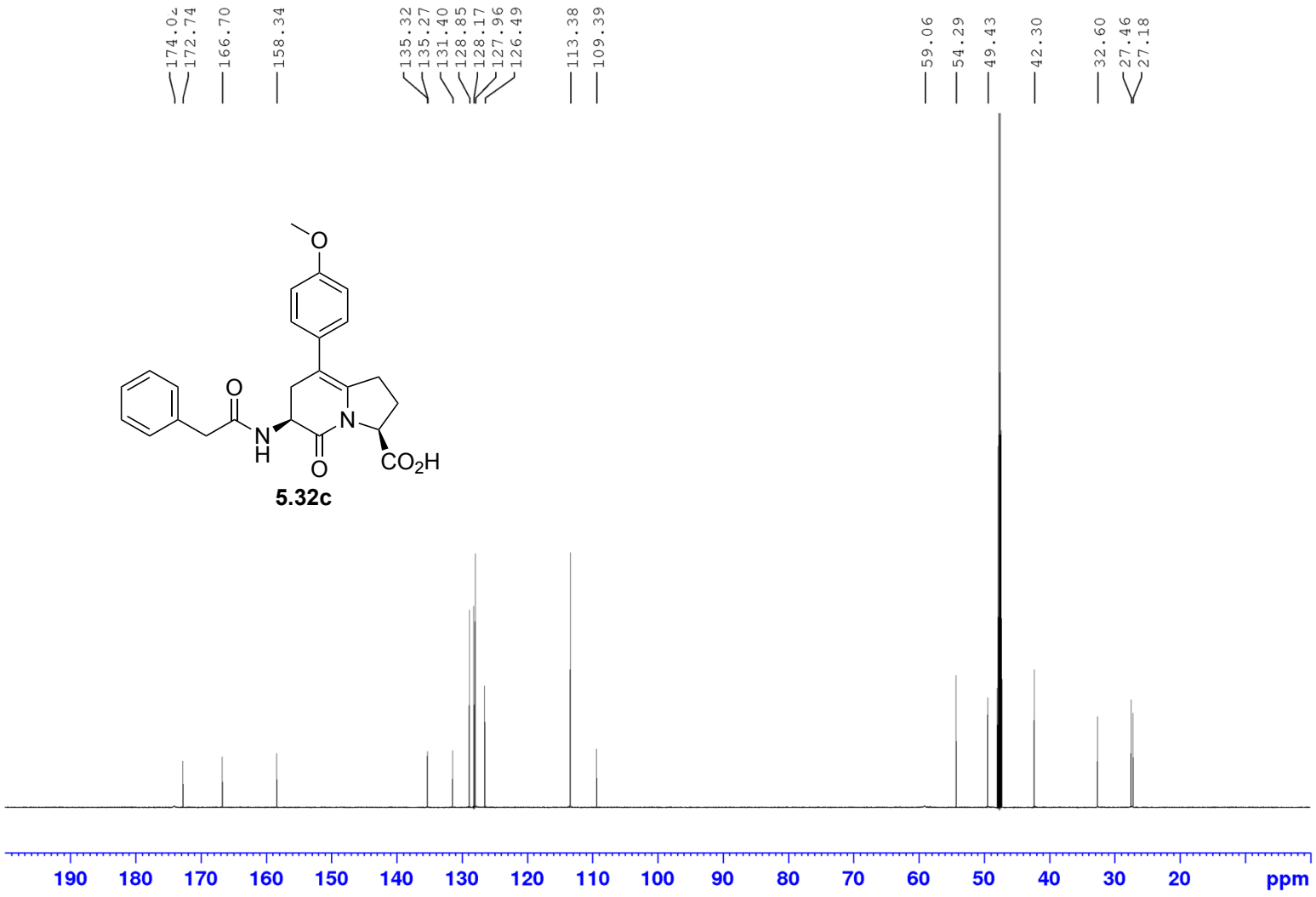

^{1}H NMR 700MHz
Solvent: CD_3OD

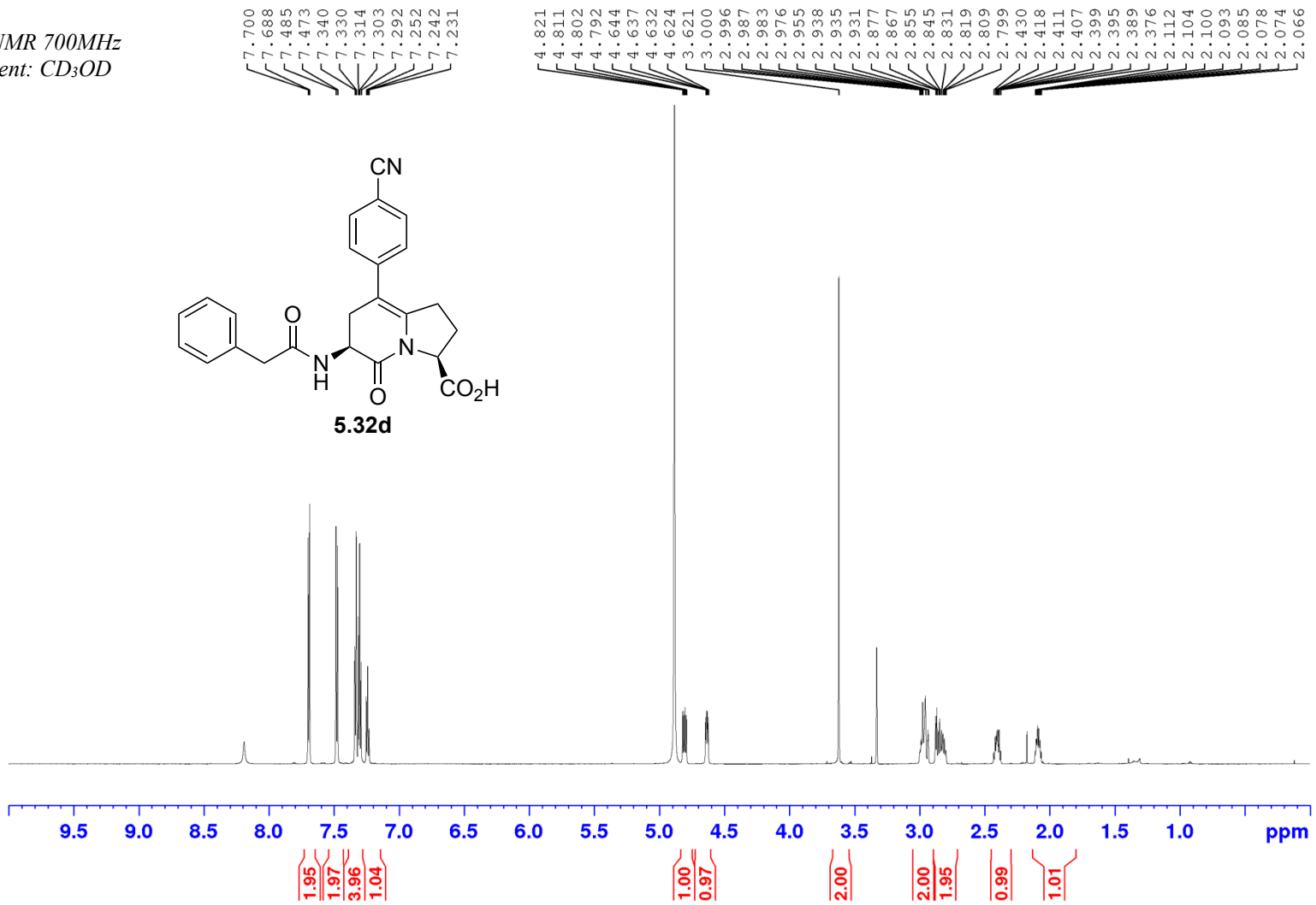

^{13}C NMR 175MHz
Solvent: CD_3OD

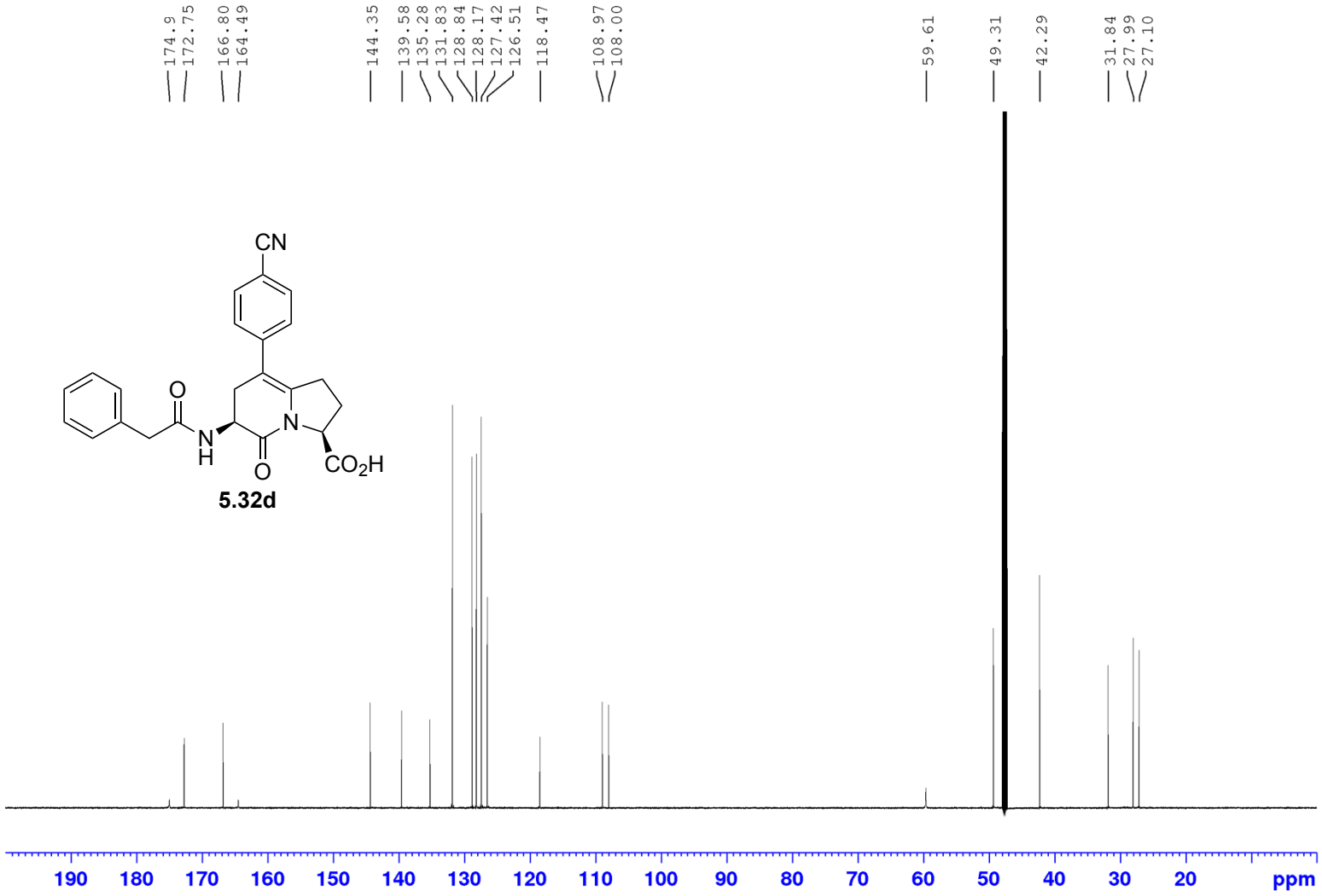

^{1}H NMR 700MHz
Solvent: CD_3OD

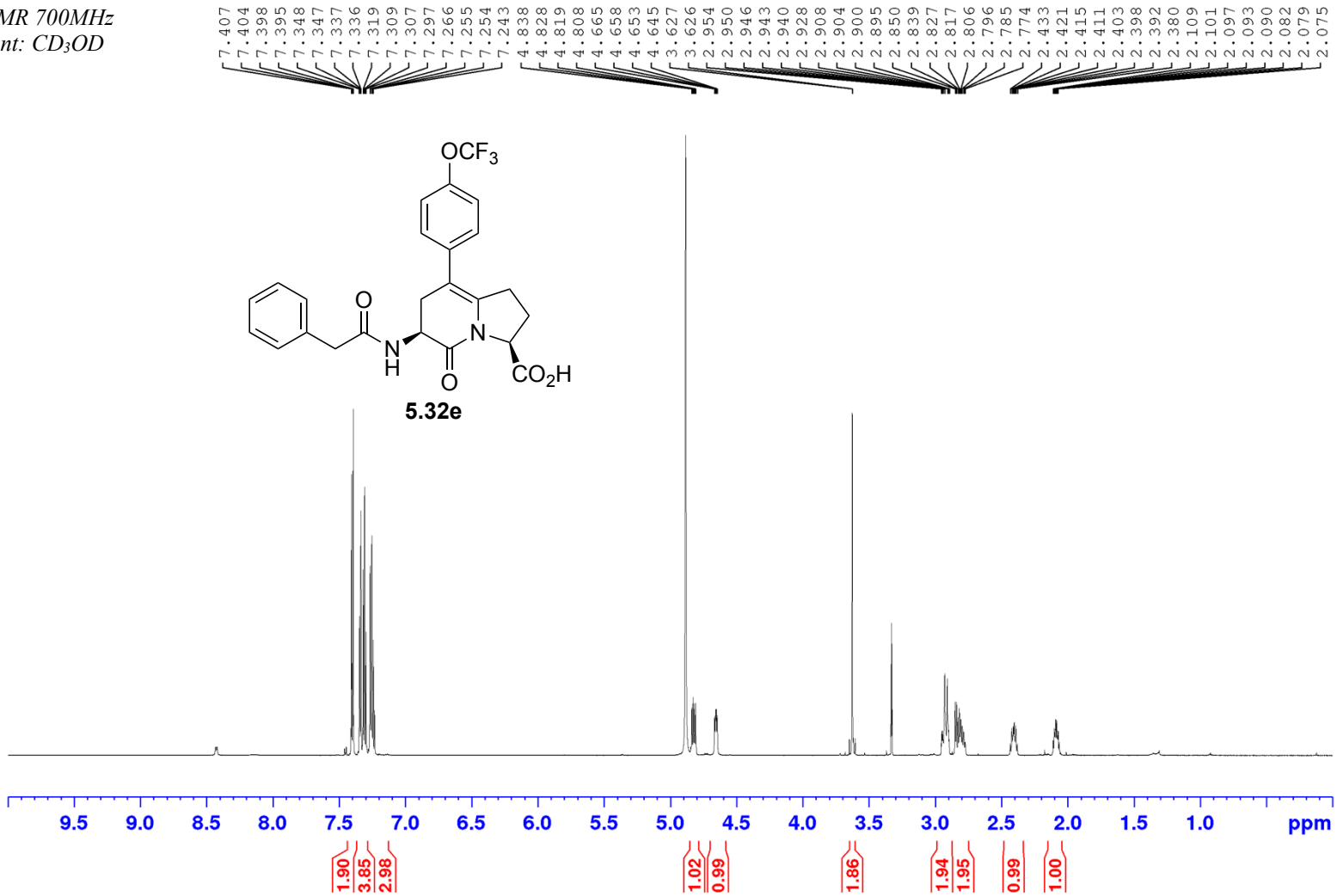

^{13}C NMR 175MHz
Solvent: CD_3OD

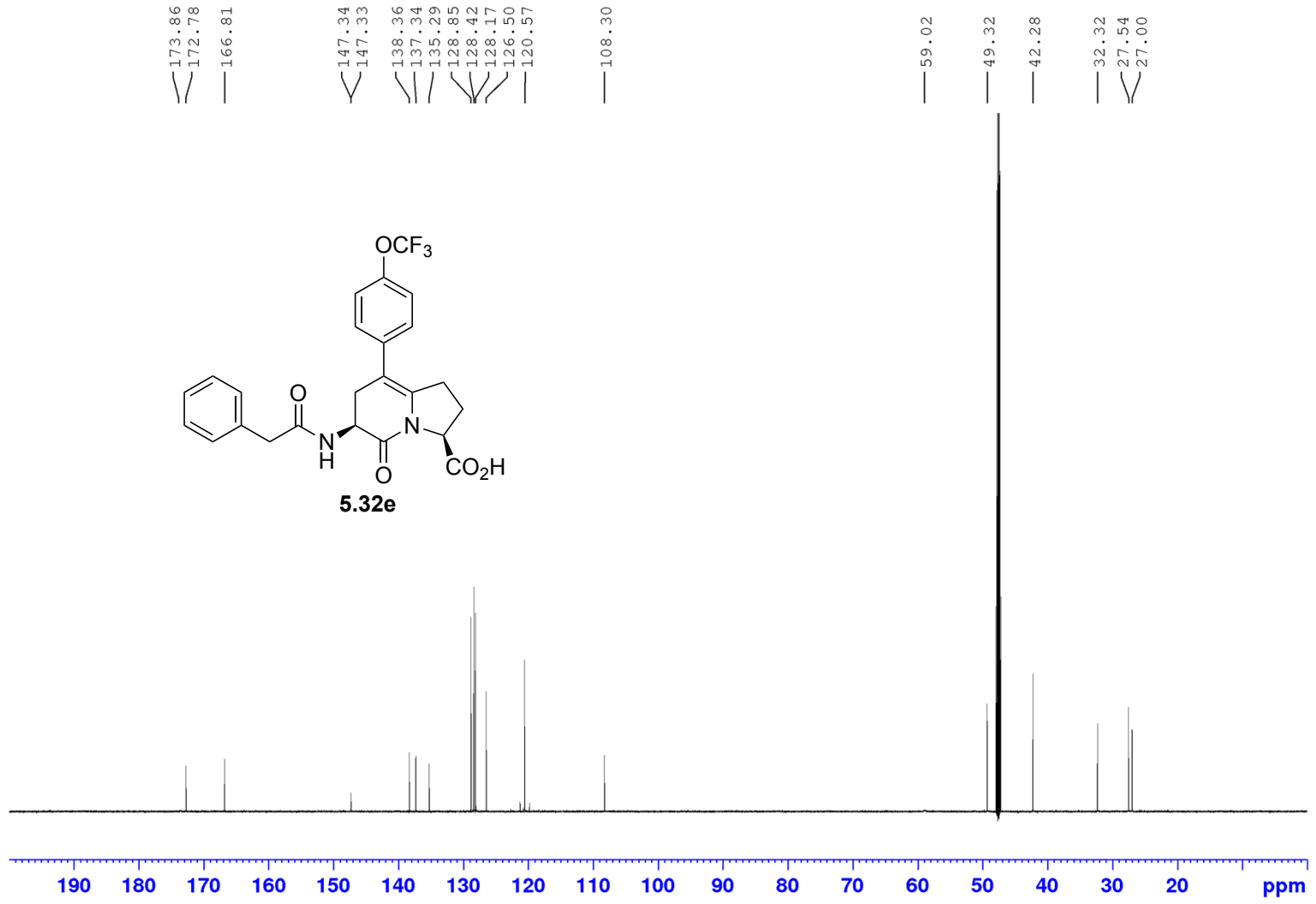

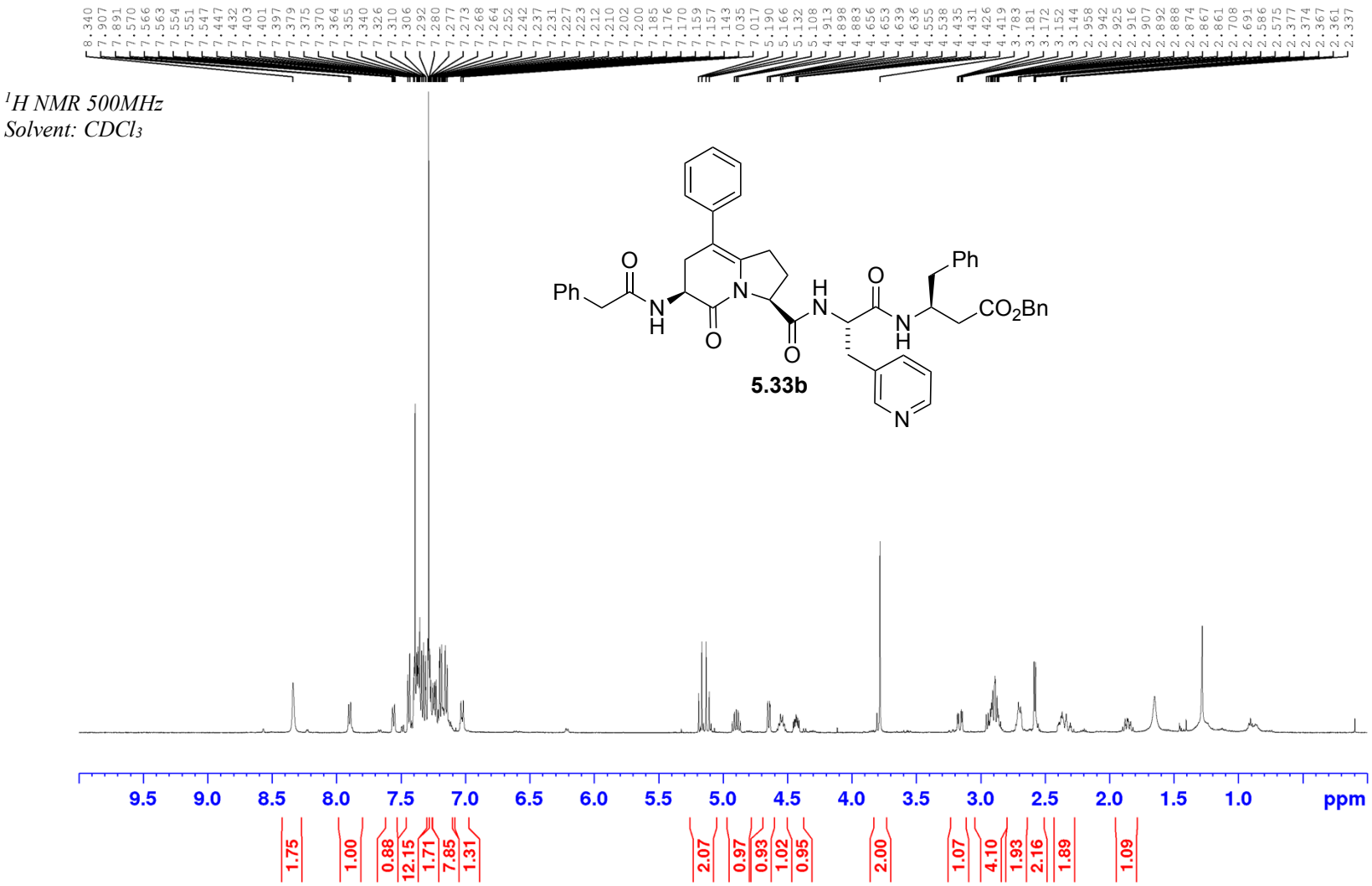

^{1}H NMR 500MHz
Solvent: $CDCl_3$

^{13}C NMR 125 MHz
Solvent: $CDCl_3$

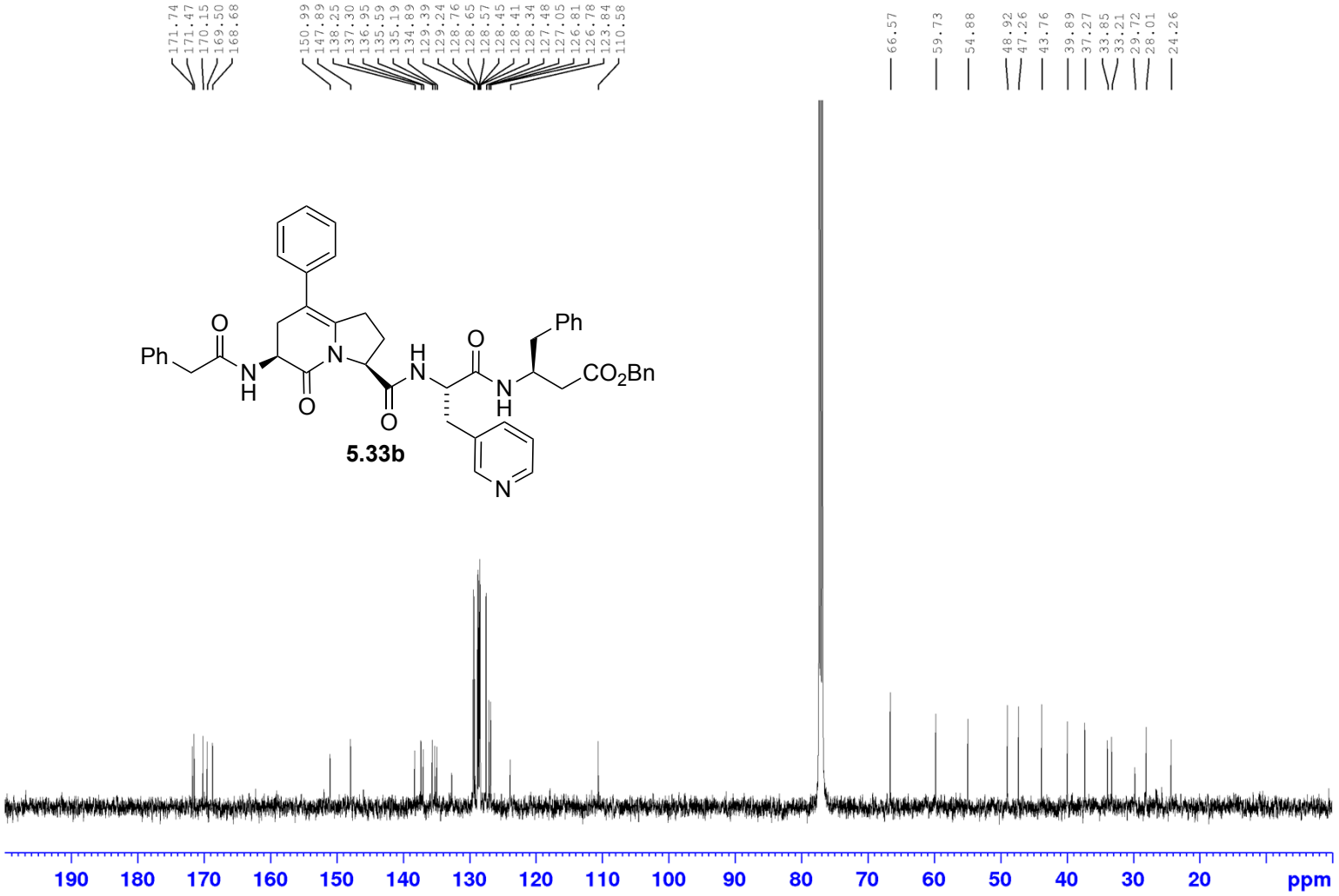

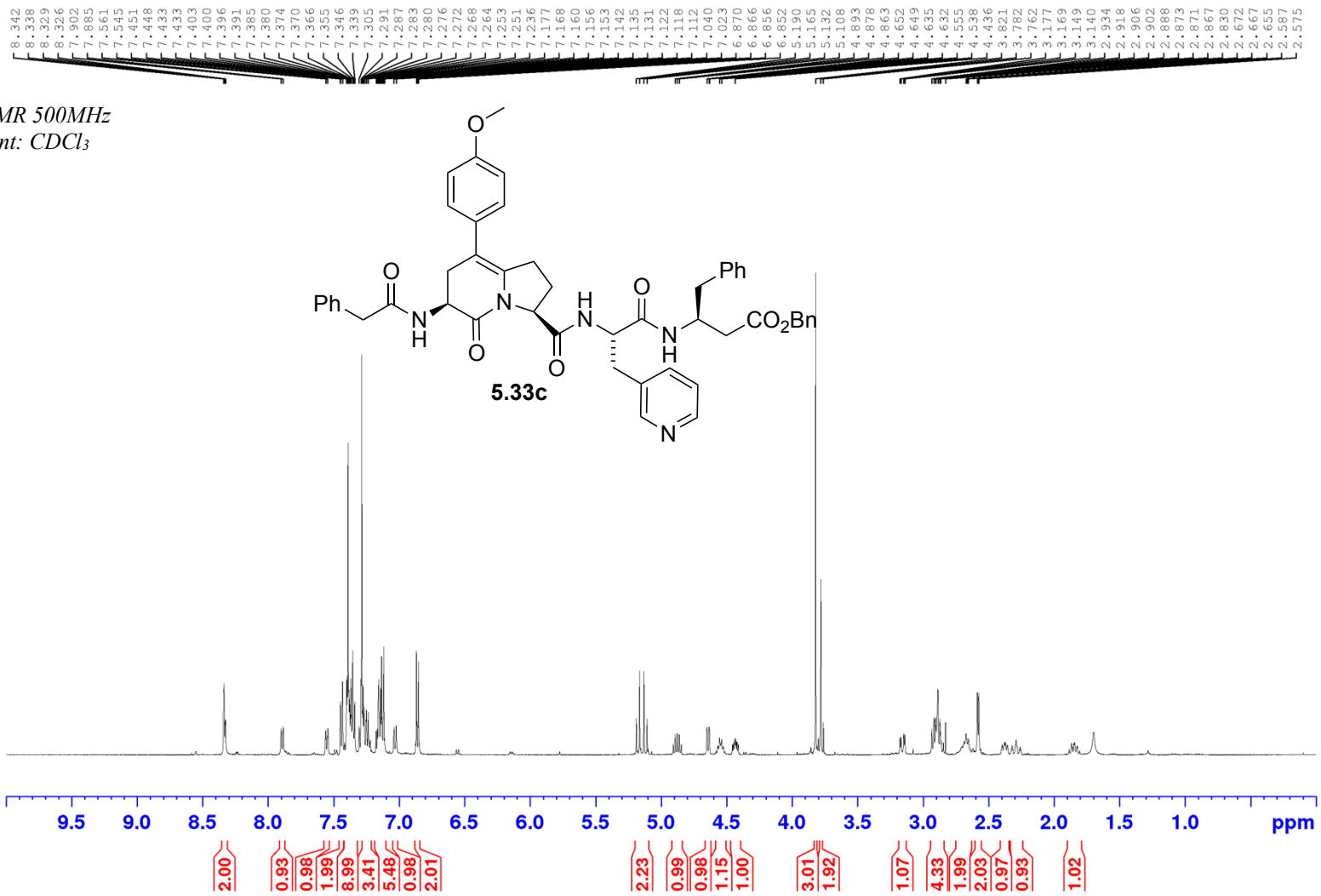

[1]H NMR 500MHz
Solvent: $CDCl_3$

^{13}C NMR 125MHz
Solvent: $CDCl_3$

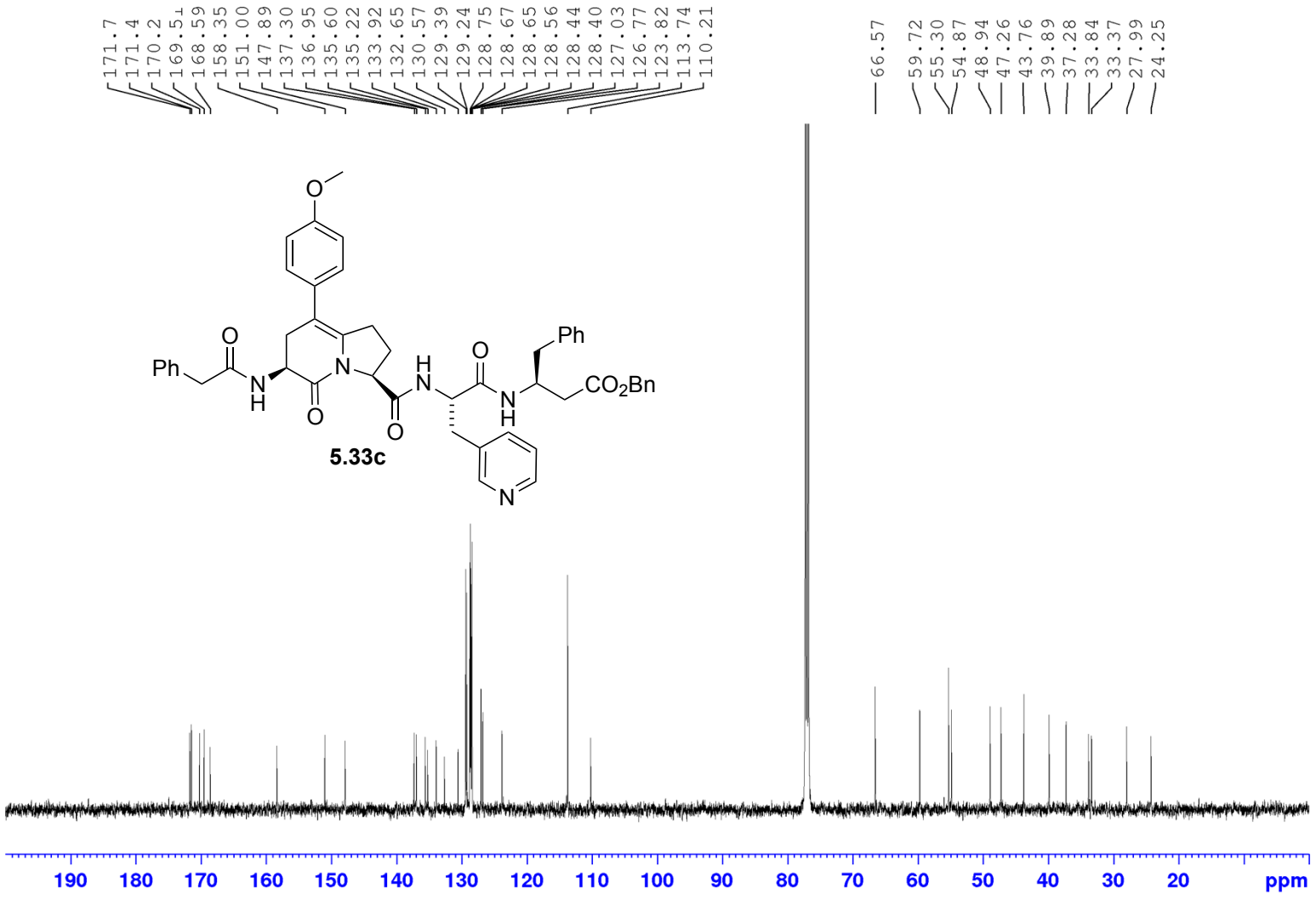

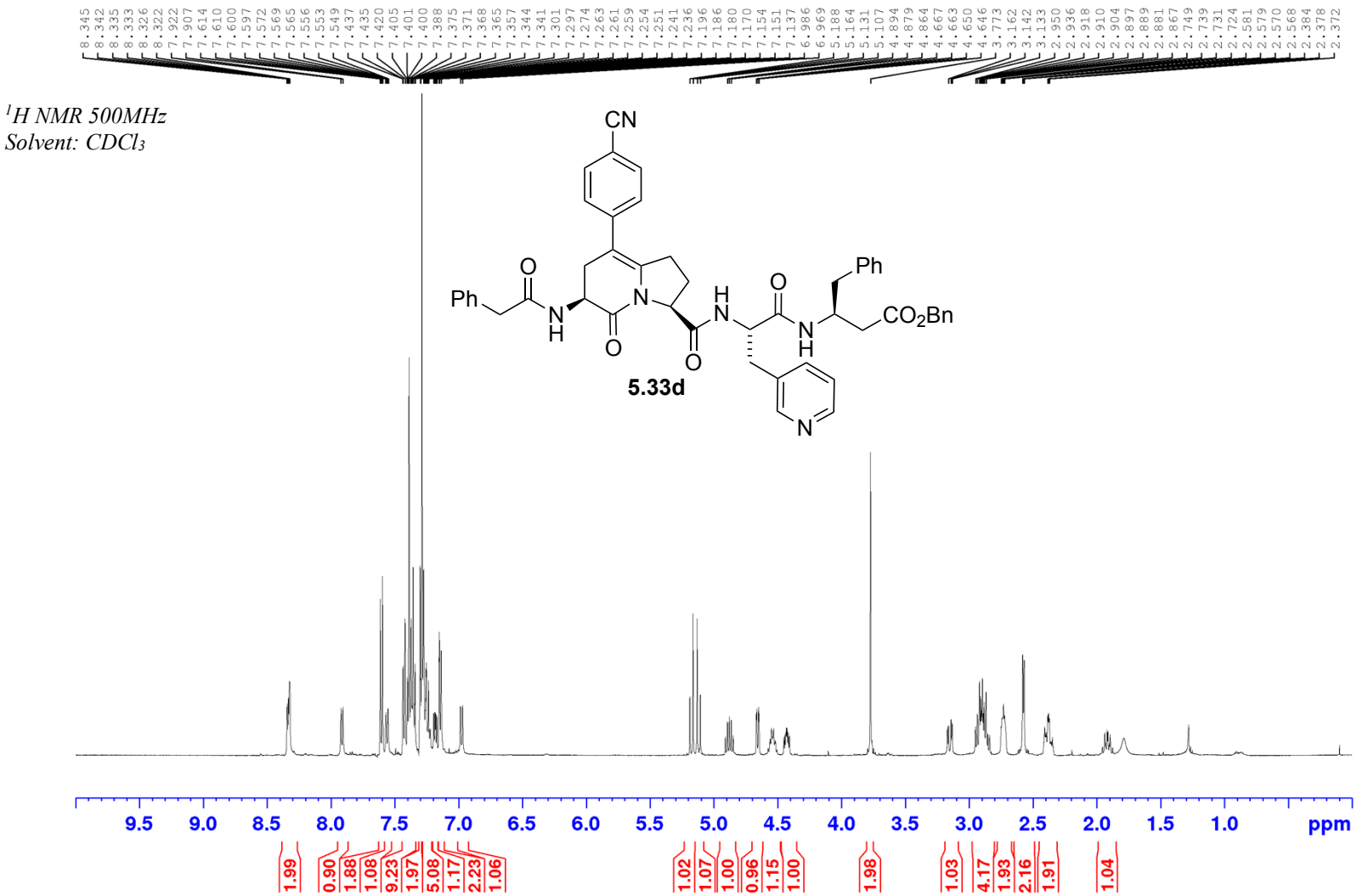
8.345
8.342
8.335
8.333
8.326
8.322
7.922
7.907
7.614
7.610
7.600
7.597
7.572
7.569
7.565
7.556
7.553
7.549
7.437
7.435
7.420
7.405
7.401
7.400
7.388
7.375
7.371
7.368
7.365
7.357
7.344
7.341
7.301
7.297
7.274
7.263
7.261
7.259
7.254
7.251
7.241
7.236
7.196
7.186
7.180
7.170
7.154
7.151
7.137
6.986
6.969
5.188
5.164
5.131
5.107
4.894
4.879
4.864
4.667
4.663
4.650
4.646
3.773
3.162
3.142
3.133
2.950
2.936
2.918
2.910
2.904
2.897
2.889
2.881
2.867
2.749
2.739
2.731
2.724
2.581
2.579
2.570
2.568
2.384
2.378
2.372
1H NMR 500MHz
Solvent: CDCl3
CN
Ph
O
N
H
N
O
O
H
N
O
N
H
Ph
CO2Bn
N
5.33d
9.5
9.0
8.5
8.0
7.5
7.0
6.5
6.0
5.5
5.0
4.5
4.0
3.5
3.0
2.5
2.0
1.5
1.0
ppm
1.99
0.90
1.88
1.08
9.23
1.97
5.08
1.17
2.23
1.06
1.02
1.07
1.00
0.96
1.15
1.00
1.98
1.03
4.17
1.93
2.16
1.91
1.04

^{13}C NMR 125MHz
Solvent: $CDCl_3$

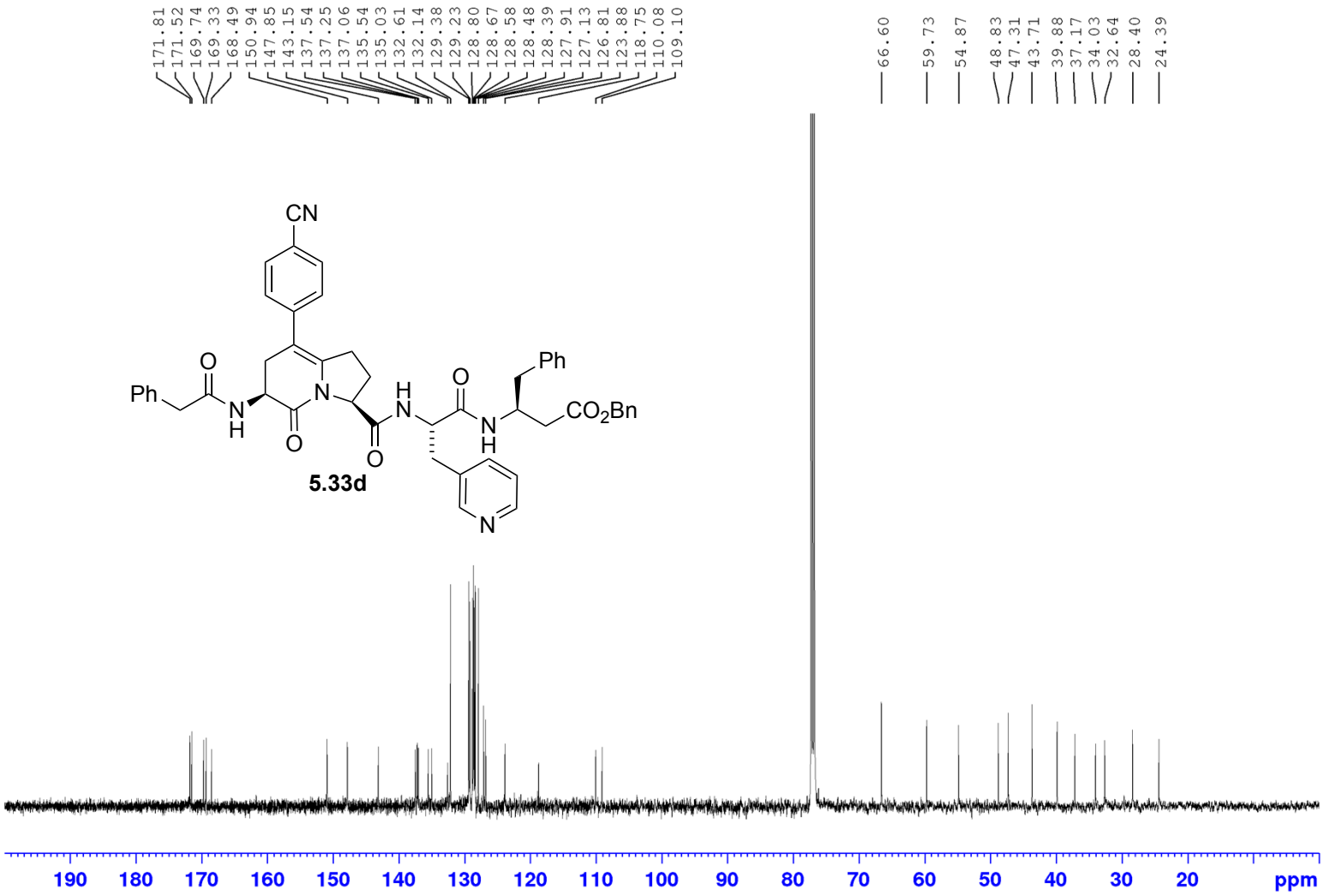

[1]H NMR 500MHz
Solvent: $CDCl_3$

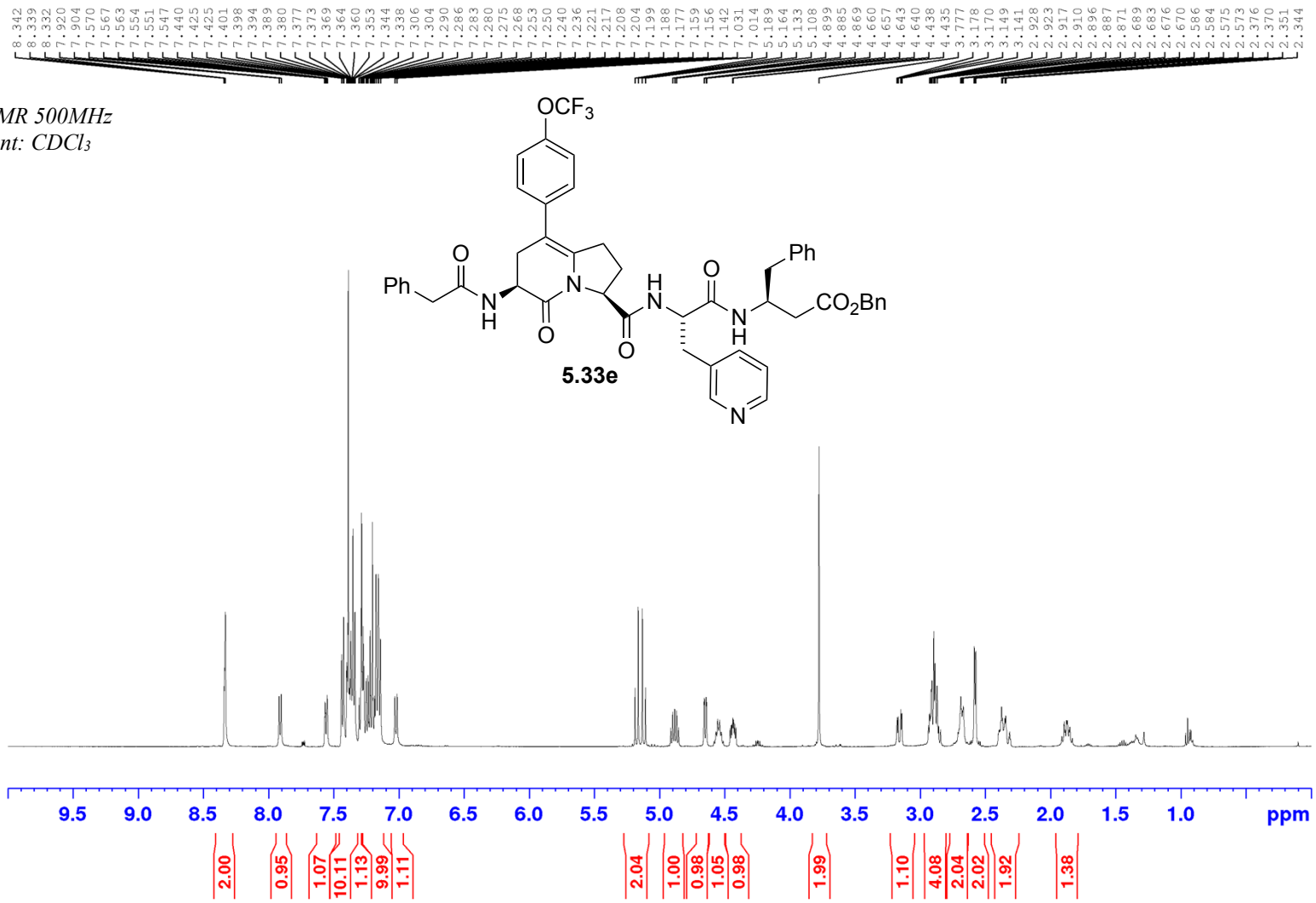

^{13}C NMR 125MHz
Solvent: $CDCl_3$

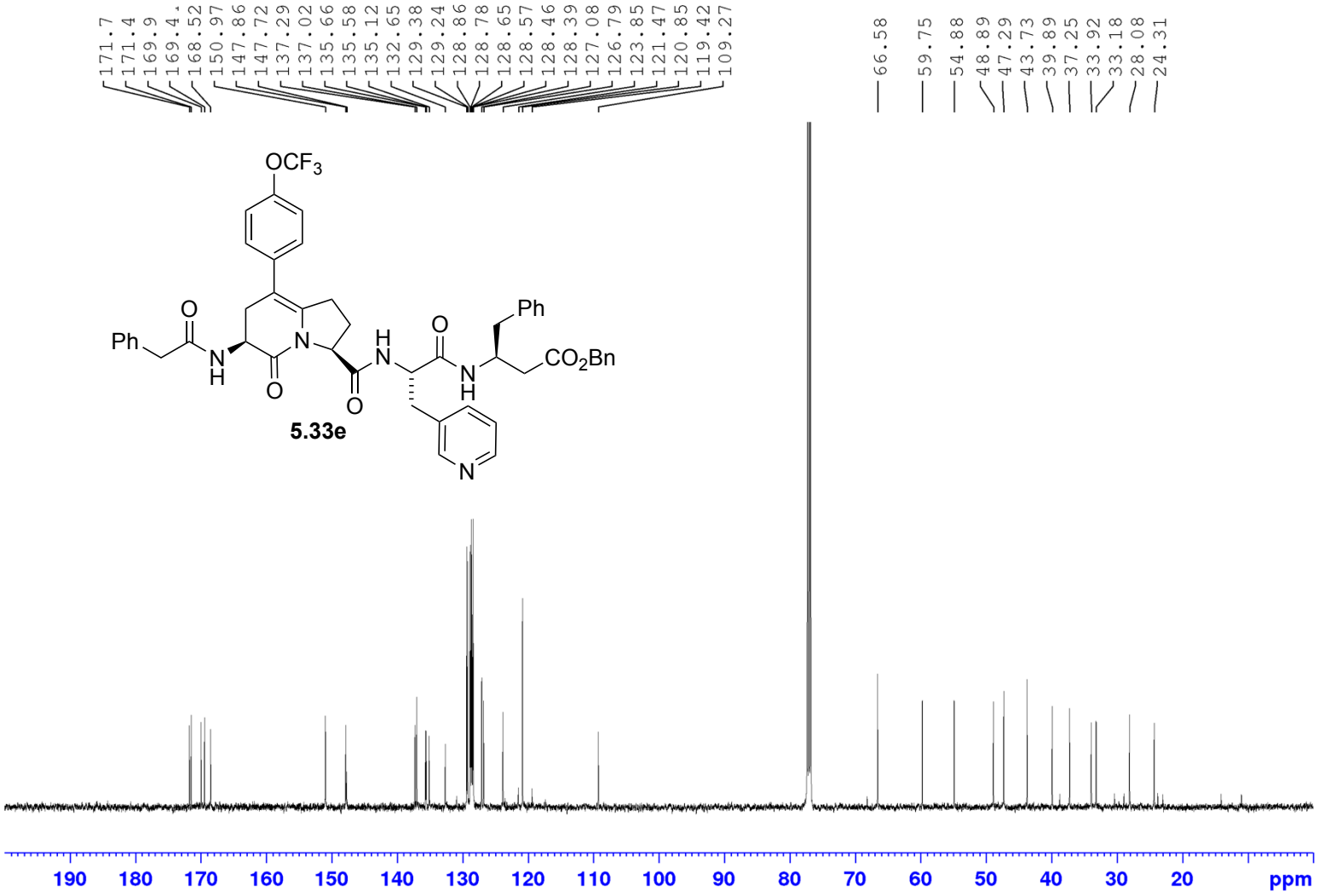

^{1}H NMR 700 MHz
Solvent: C_6D_6

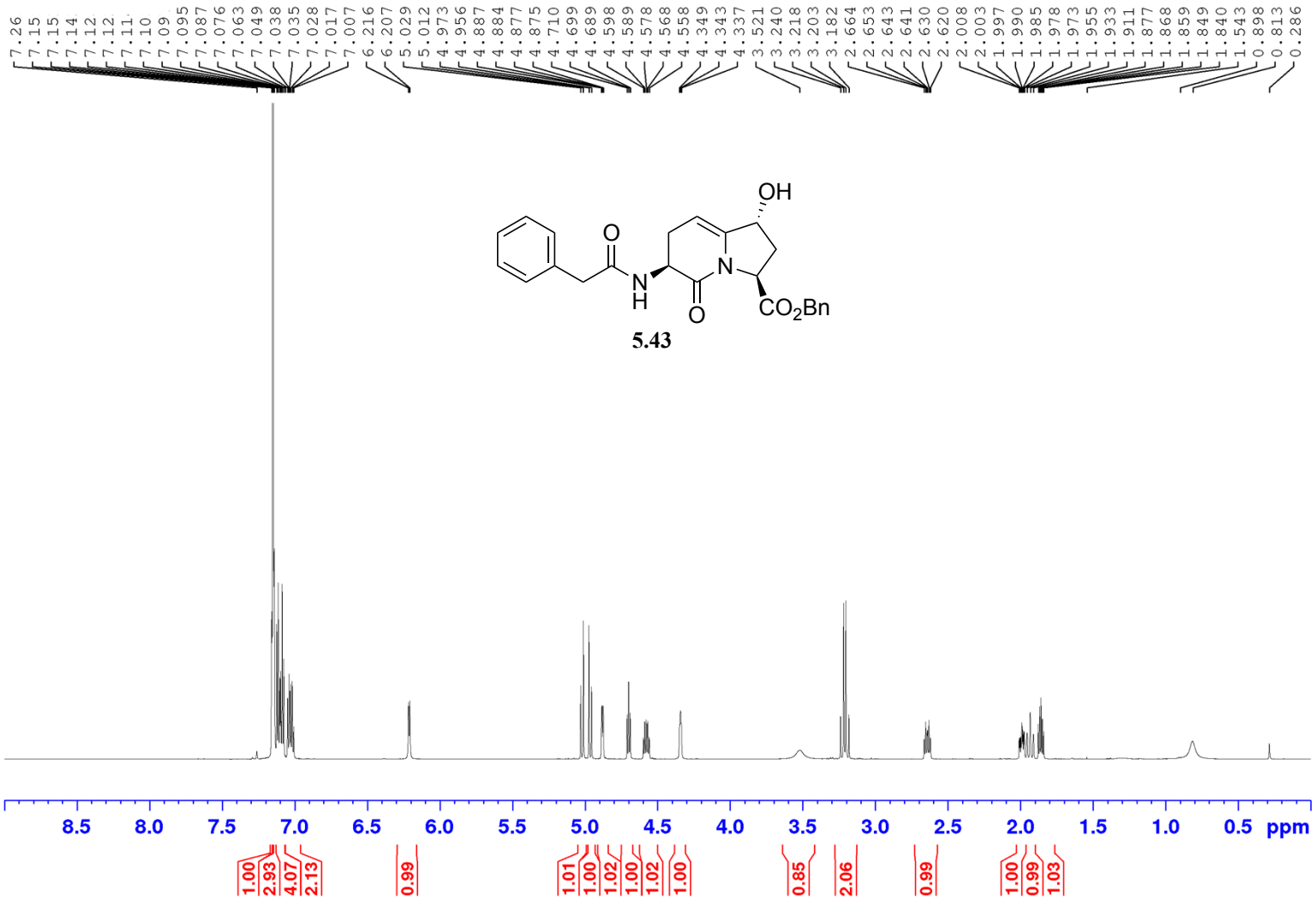

5.43

^{13}C NMR 175MHz
Solvent: C_6D_6

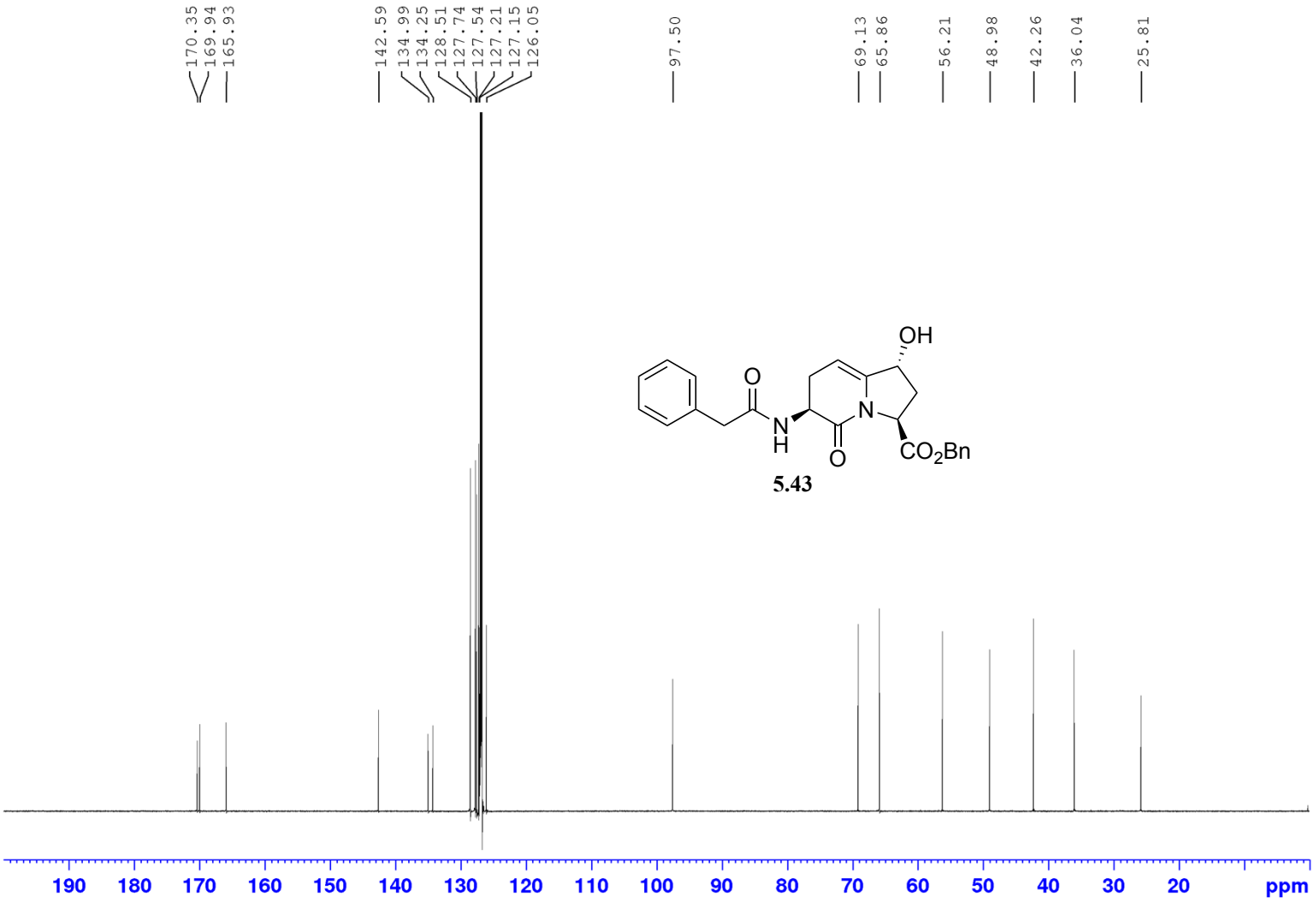

5.43

COSY NMR 700 MHz
Solvent: C_6D_6

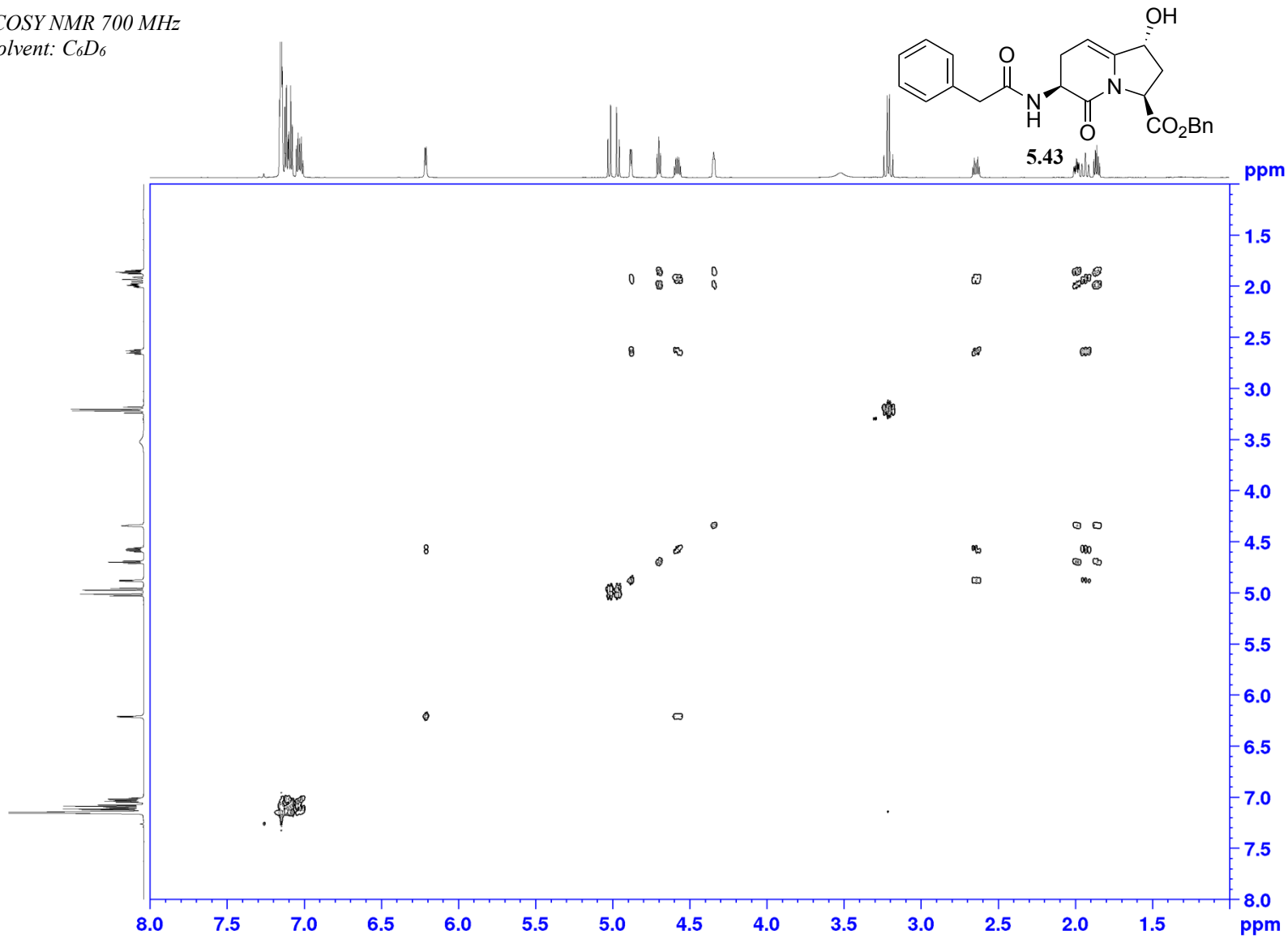

HSQC NMR 700 MHz
Solvent: C_6D_6

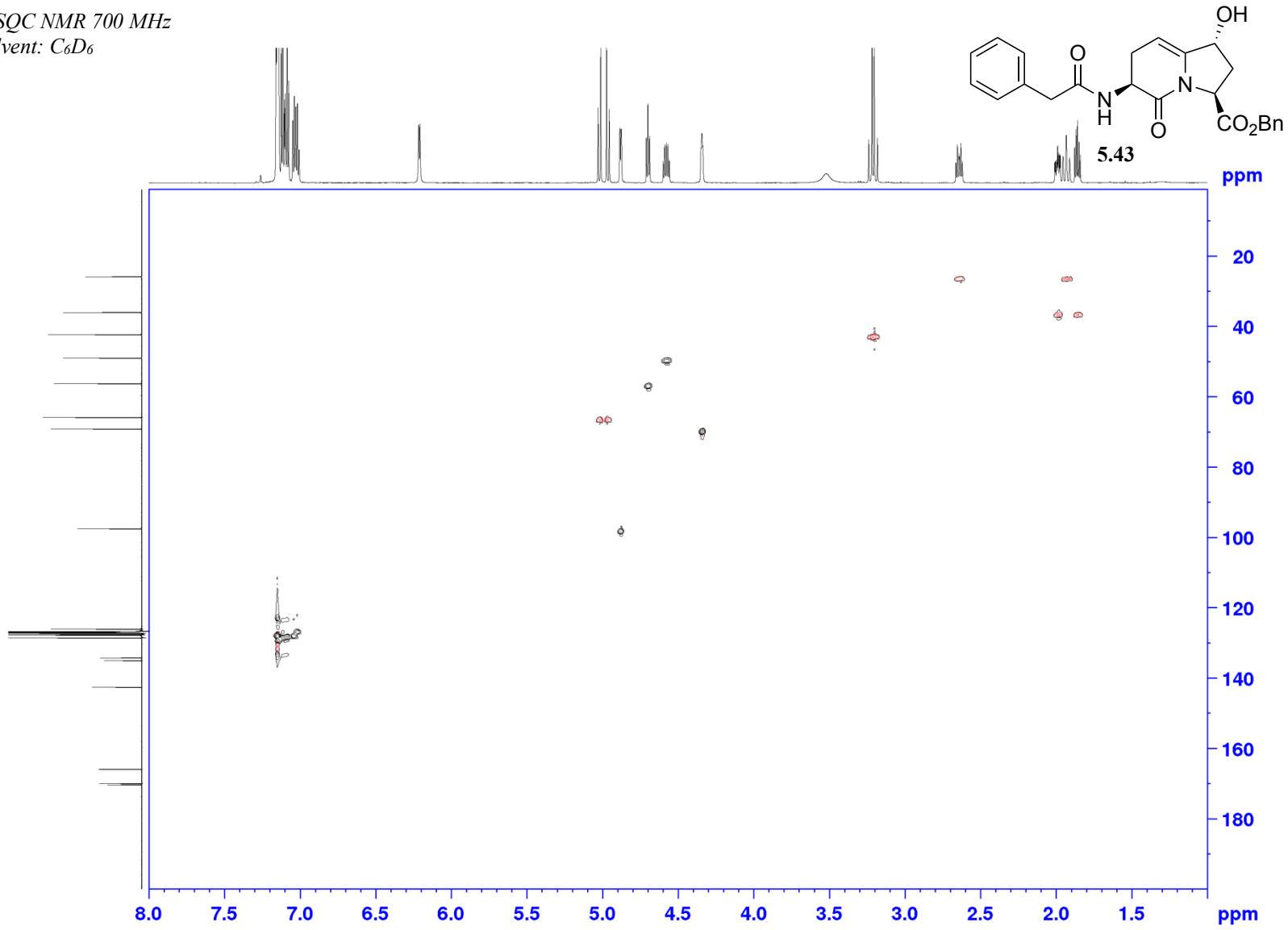

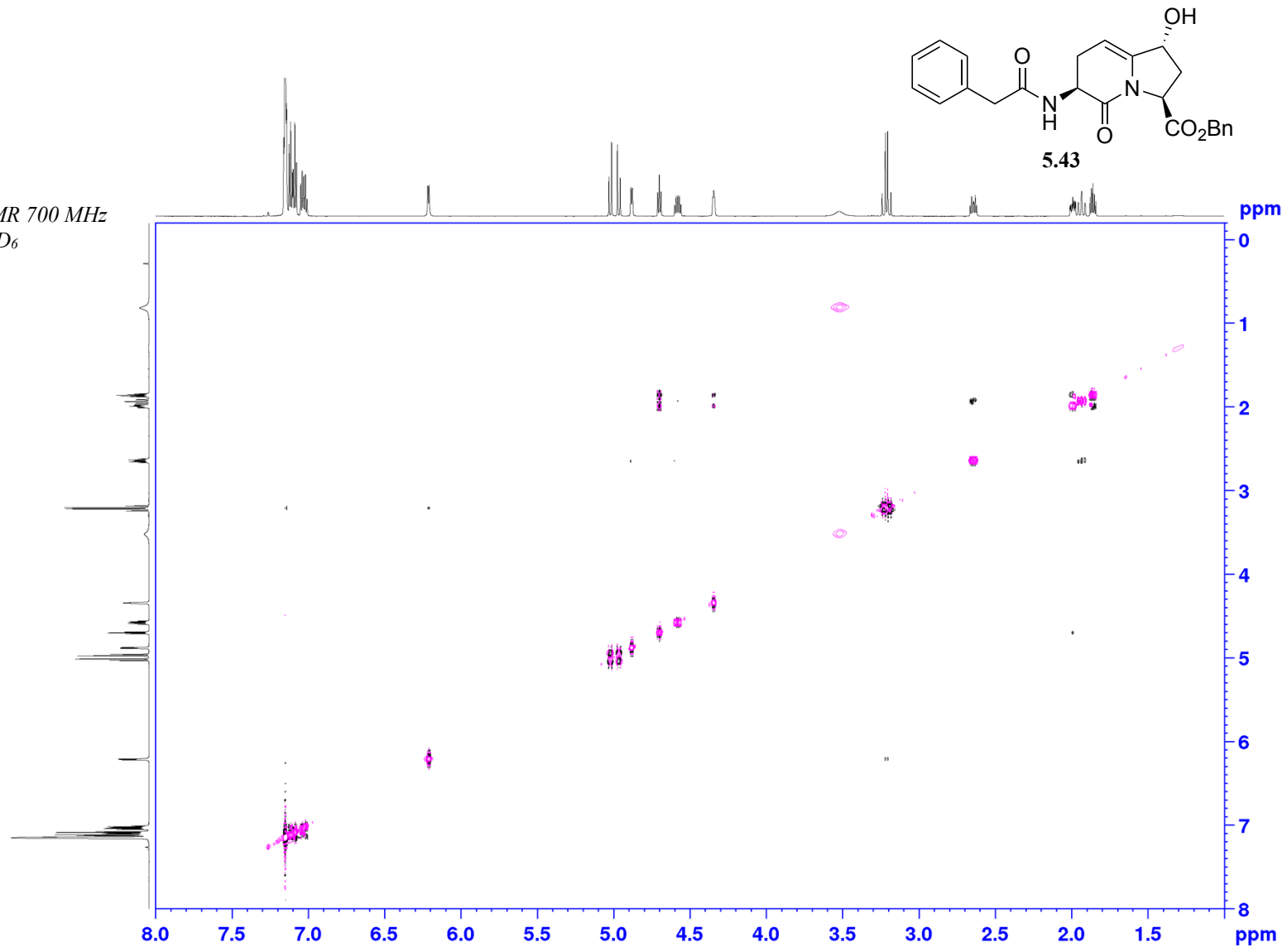
OH
O
N
H
N
O
CO2Bn
5.43
NOESY NMR 700 MHz
Solvent: C6D6
ppm
0
1
2
3
4
5
6
7
8
8.0
7.5
7.0
6.5
6.0
5.5
5.0
4.5
4.0
3.5
3.0
2.5
2.0
1.5
ppm

^{1}H NMR 700MHz
Solvent: CD_3COCD_3

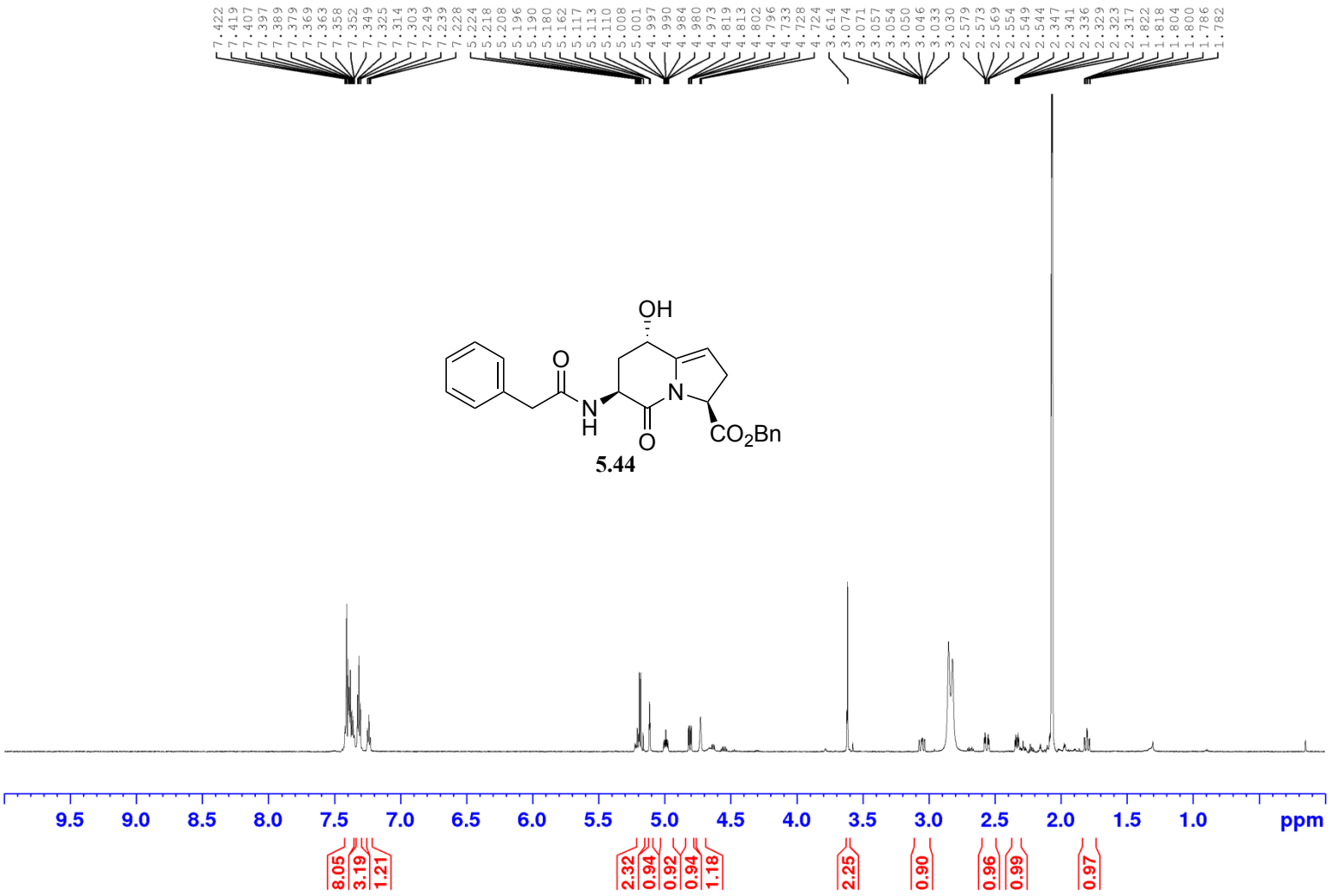

^{13}C NMR 700MHz
Solvent: CD_3COCD_3

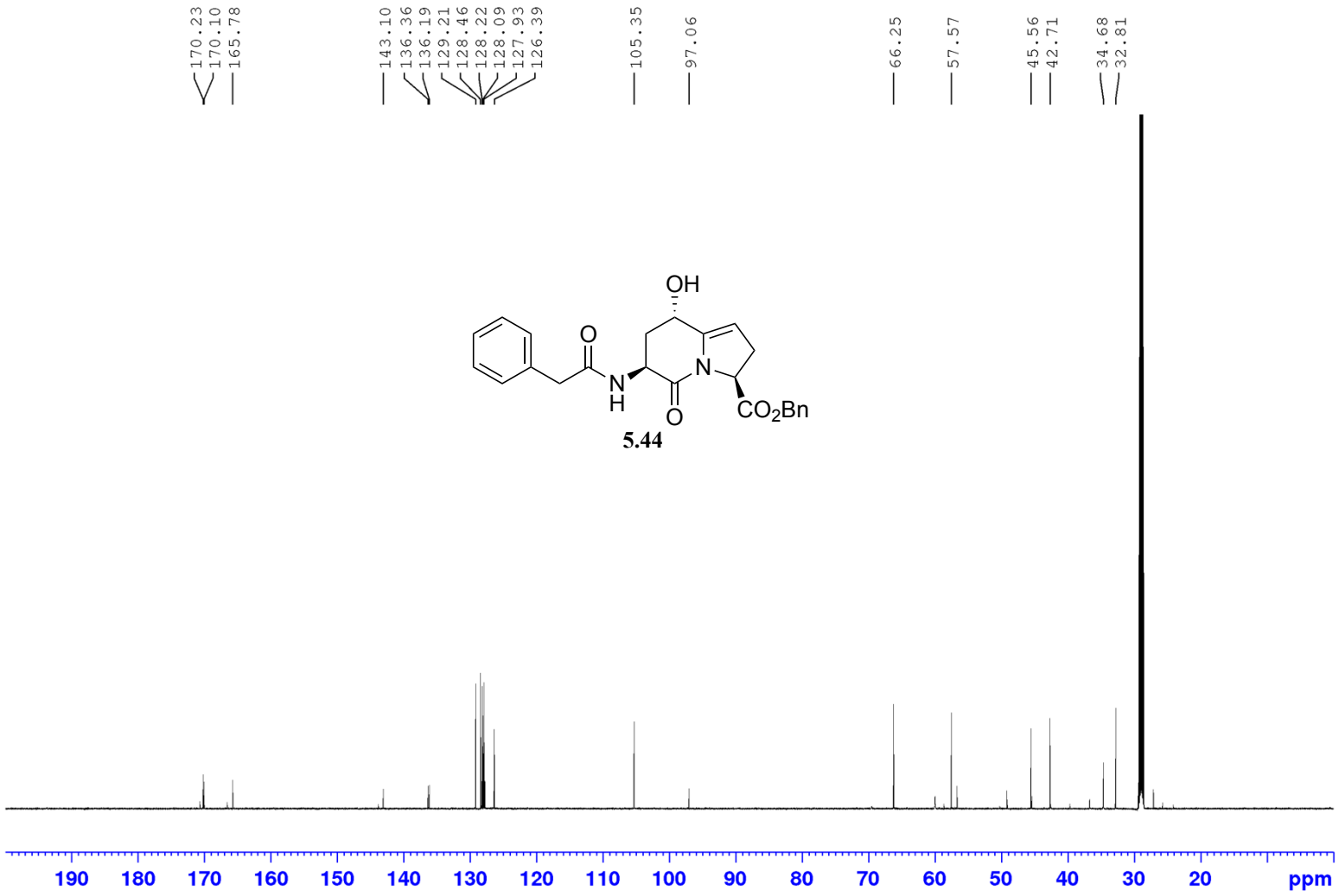

COSY 700MHz
Solvent: CD_3COCD_3

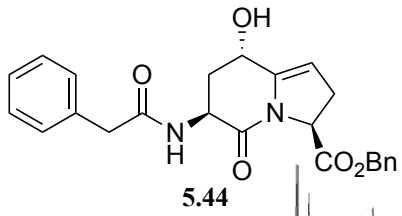

5.44

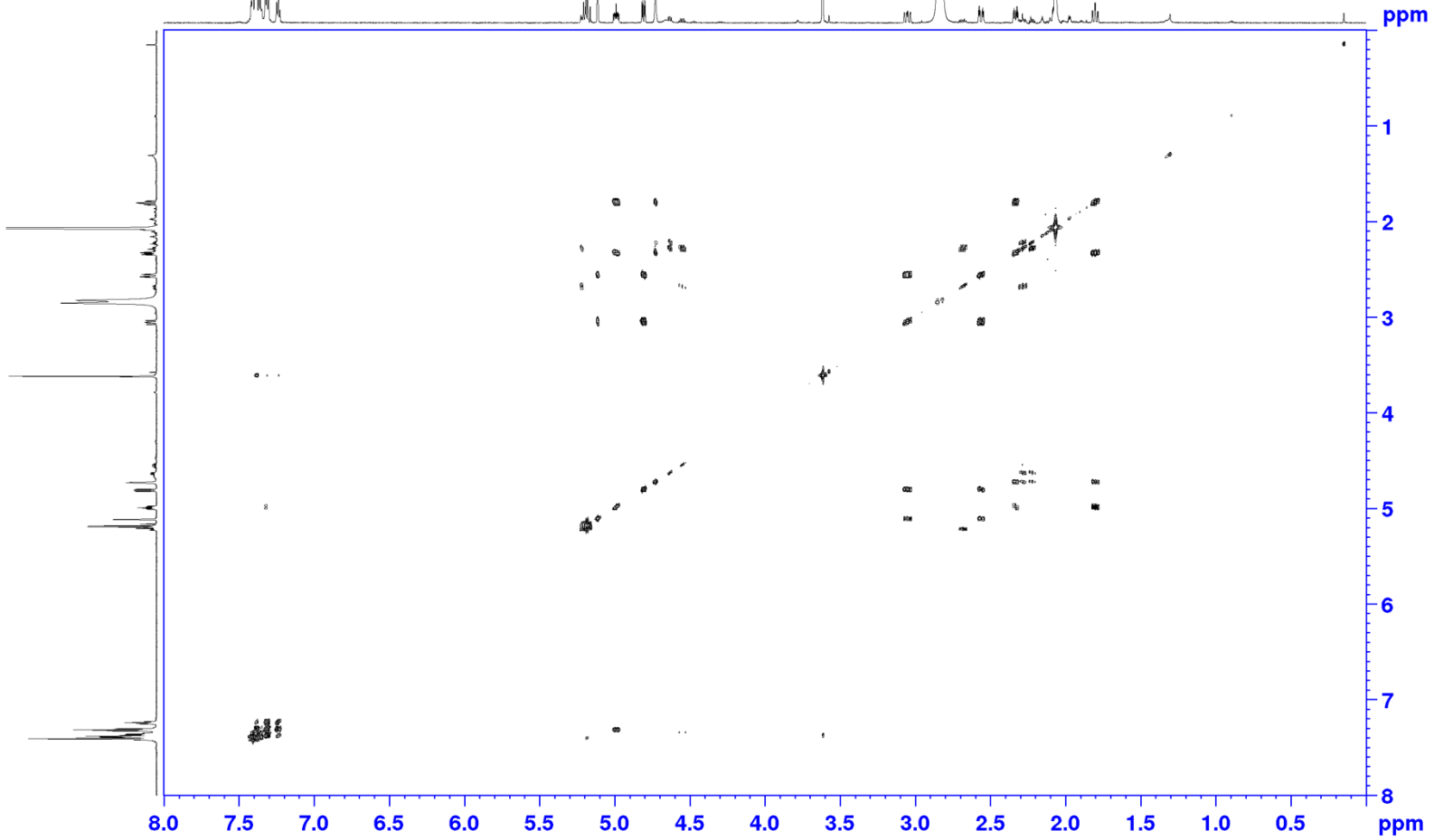

HSQC NMR 700MHz
Solvent: CD_3COCD_3

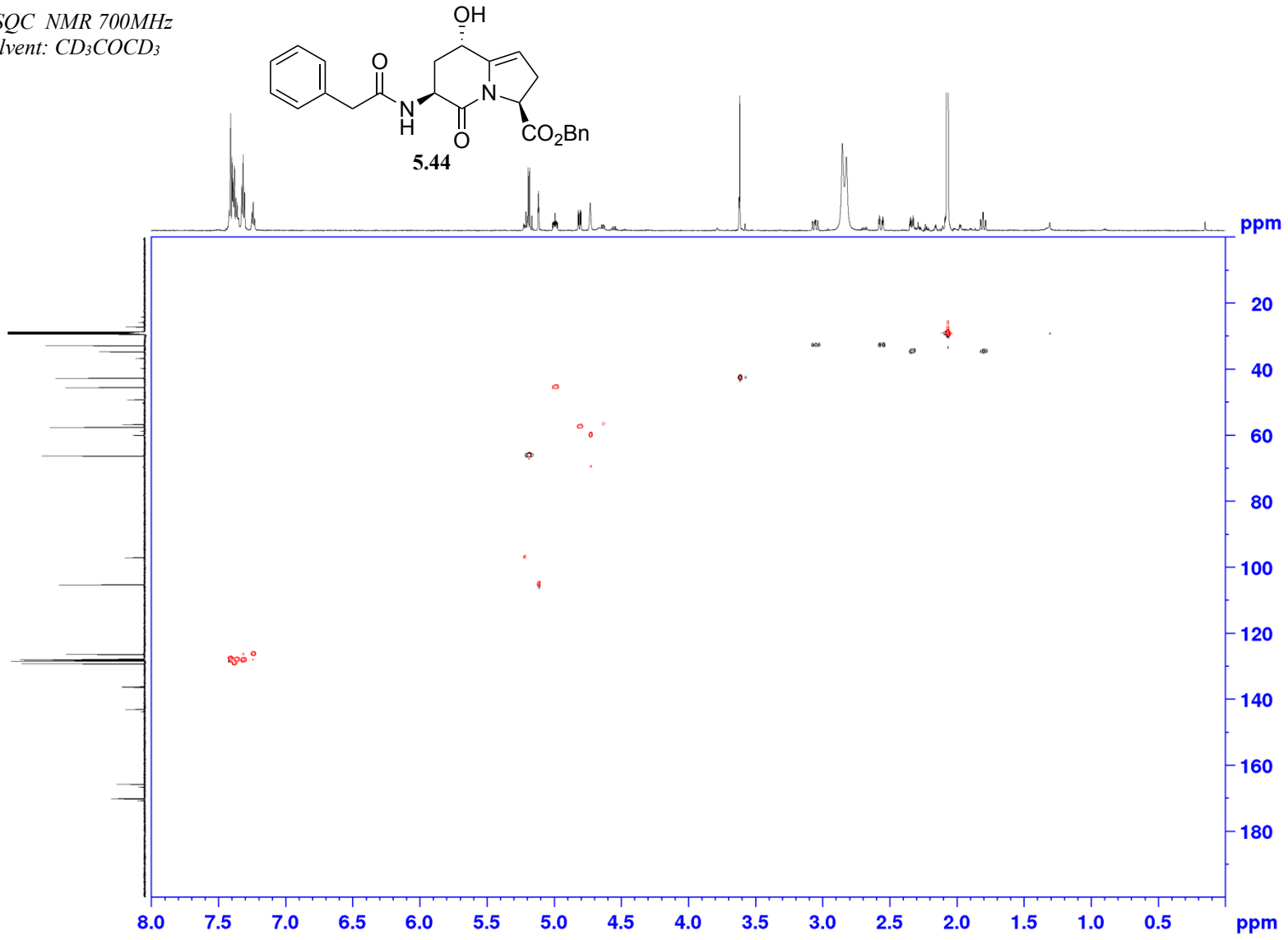

NOESY NMR 700MHz
Solvent: CD_3COCD_3

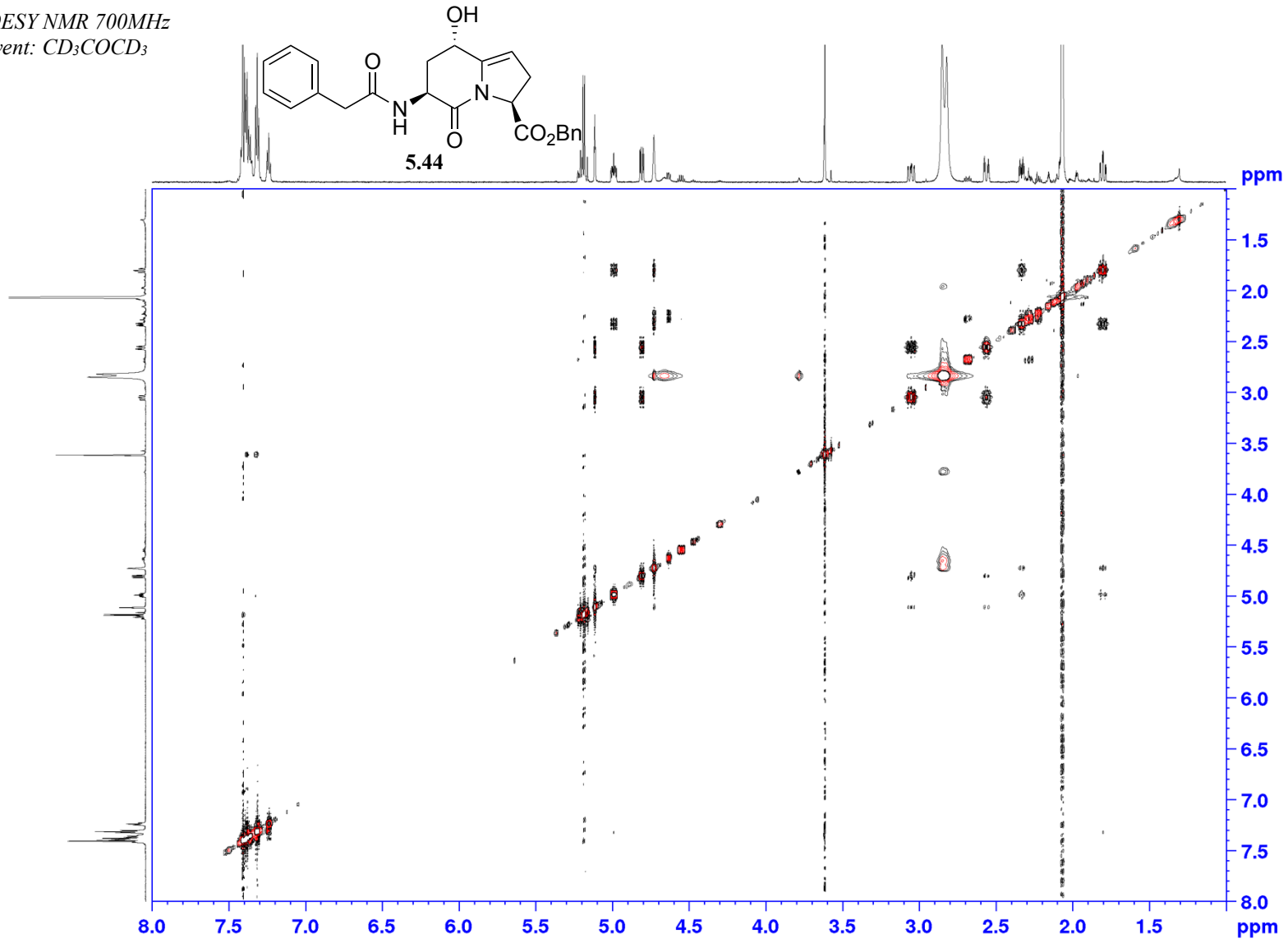

5.44

^{1}H NMR 700MHz
Solvent: $CDCl_3$

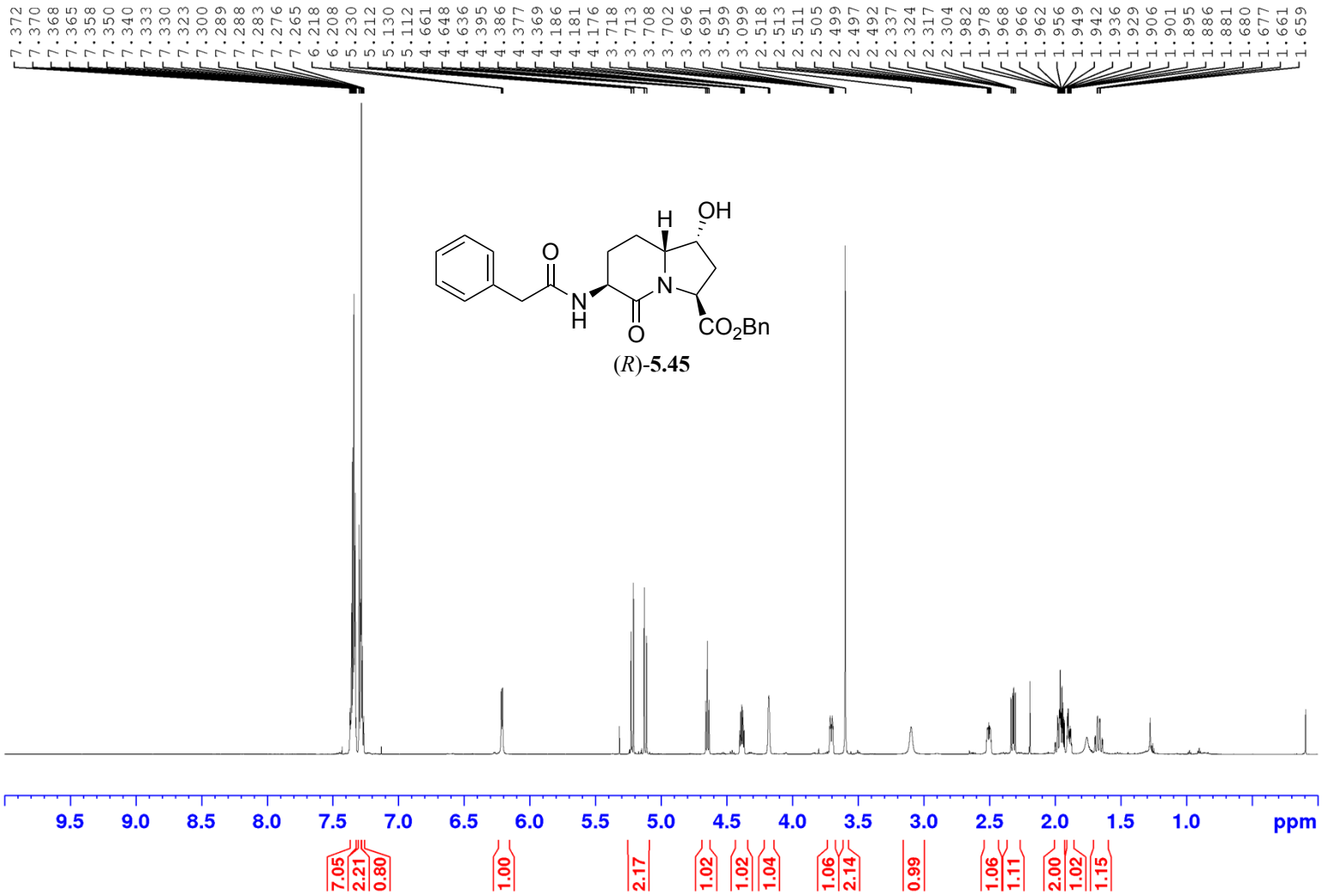

(*R*)-**5.45**

^{13}C NMR 175 MHz
Solvent: $CDCl_3$

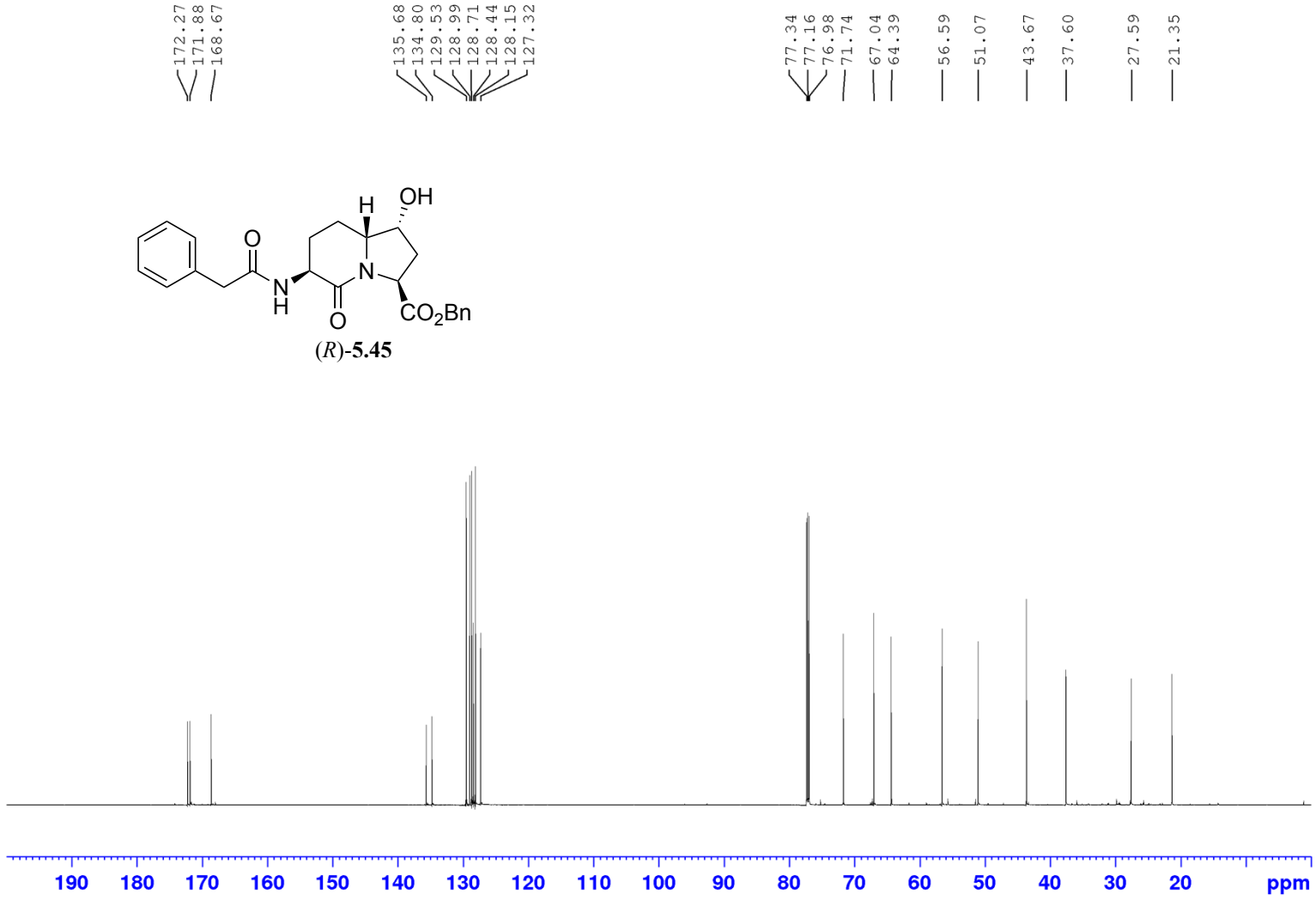

(*R*)-**5.45**

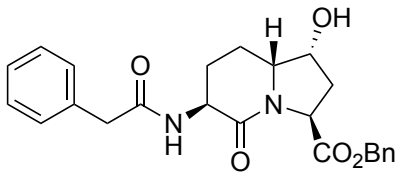

(*R*)-**5.45**

COSY NMR 700 MHz
Solvent: $CDCl_3$

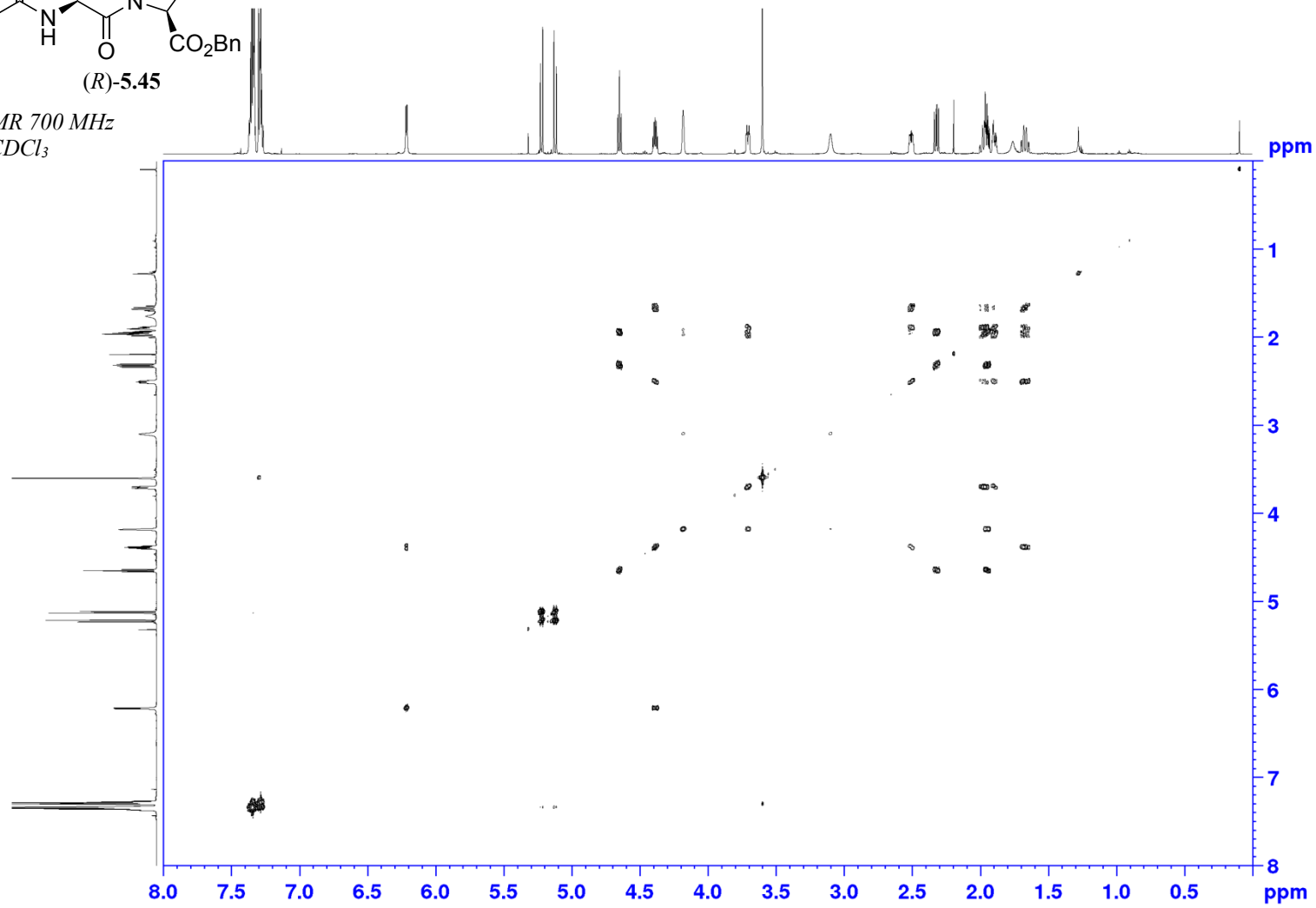

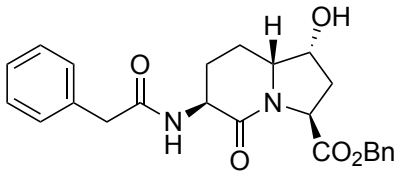

(*R*)-**5.45**

HSQC NMR 700 MHz
Solvent: $CDCl_3$

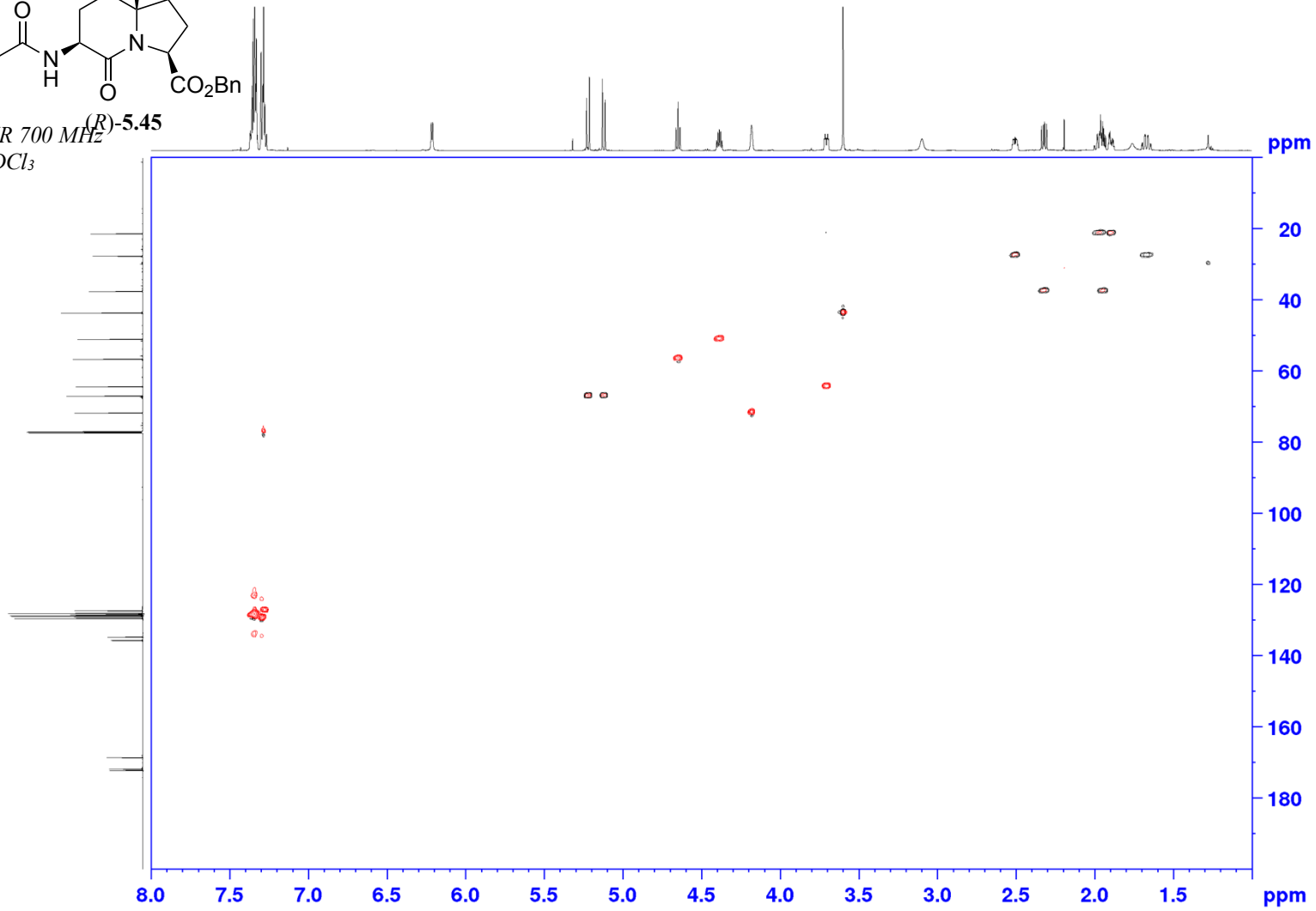

NOESY NMR 700 MHz
Solvent: $CDCl_3$

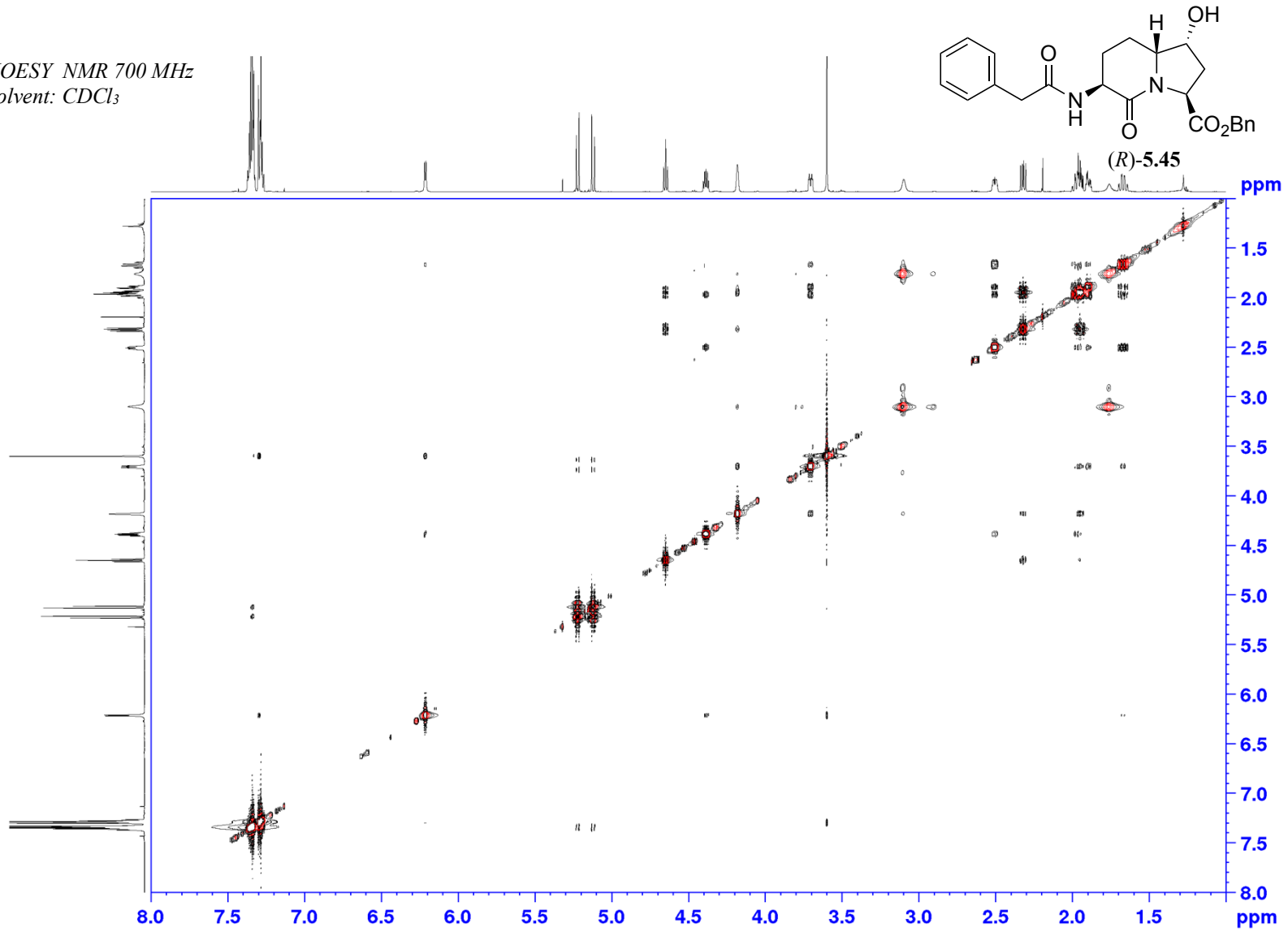

^{1}H NMR 700 MHz
Solvent: $CDCl_3$

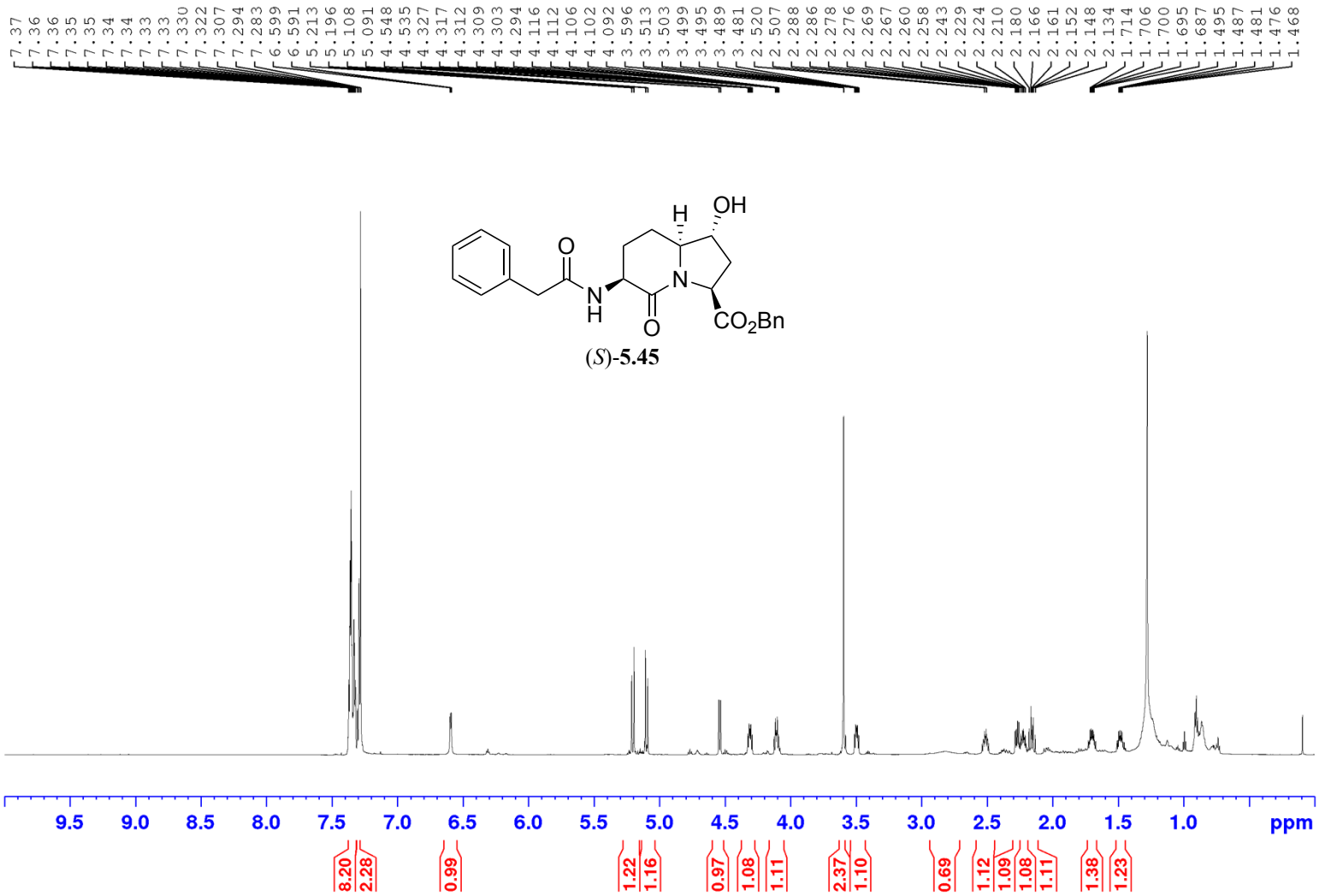

^{13}C NMR 700MHz
Solvent: $CDCl_3$

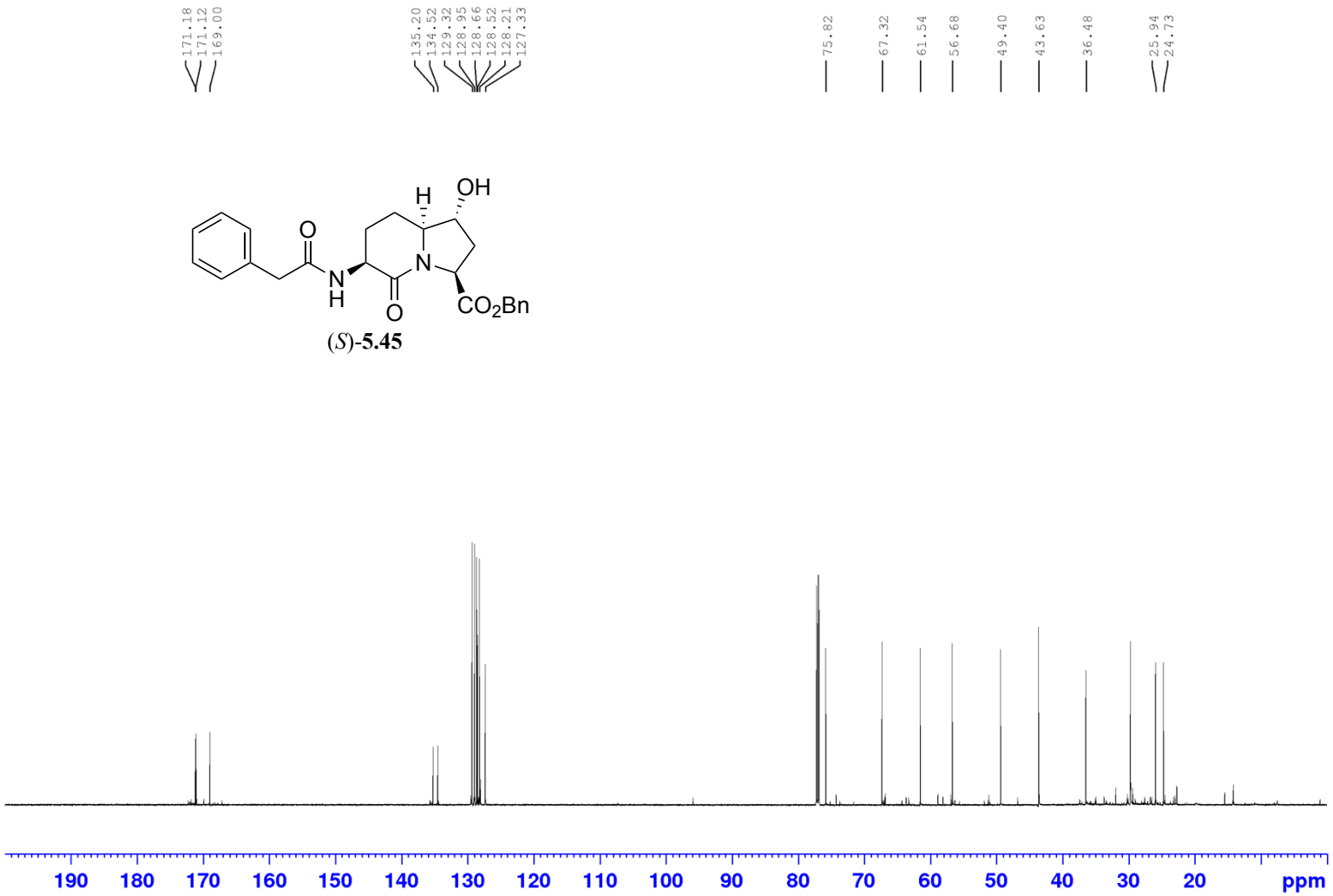

(*S*)-**5.45**

COSY NMR 700MHz
Solvent: $CDCl_3$

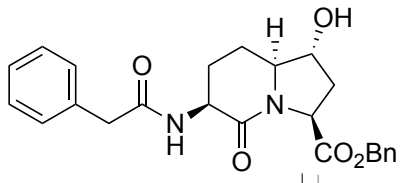

(*S*)-**5.45**

HSQC NMR 700MHz
Solvent: $CDCl_3$

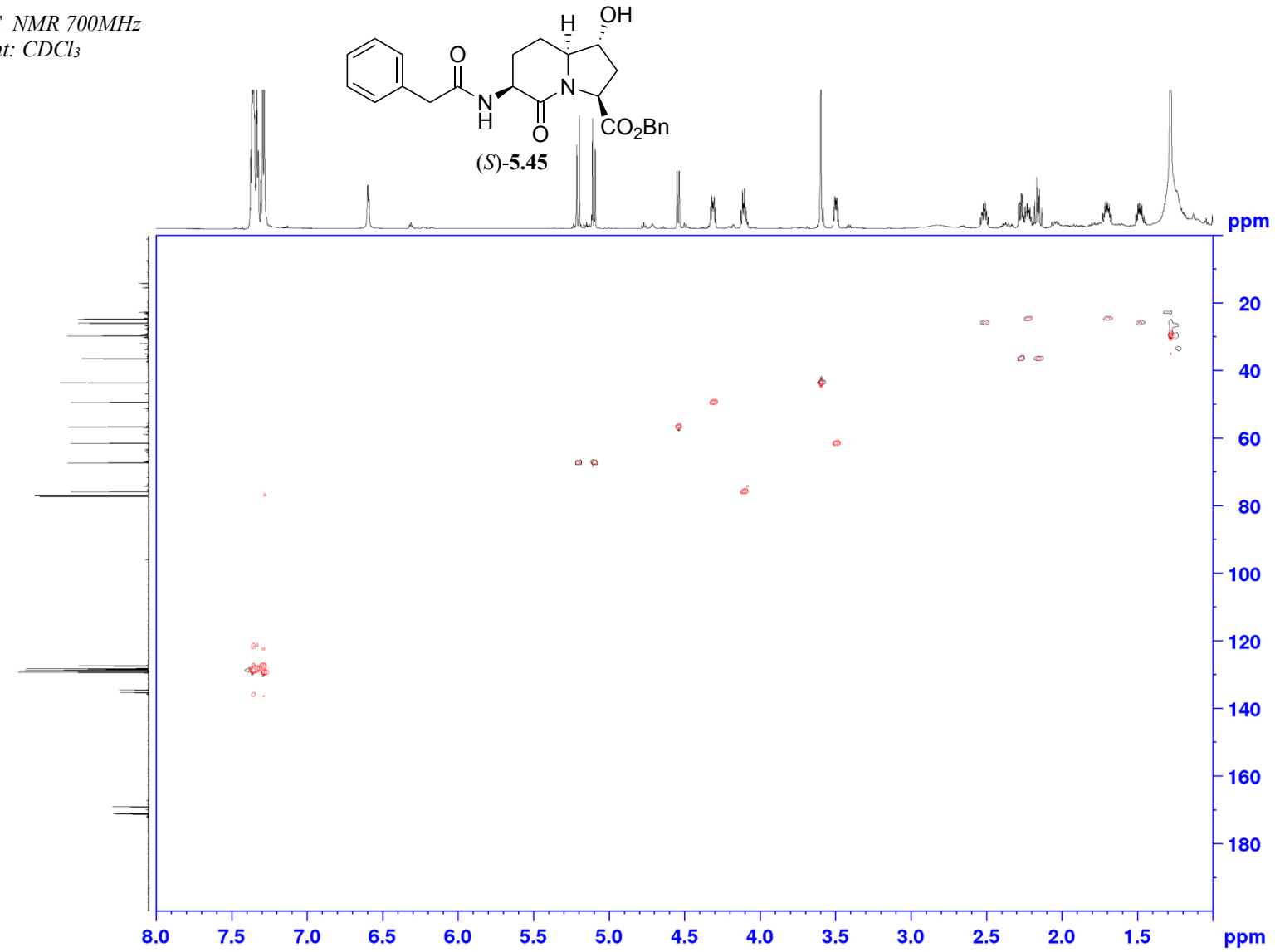

(*S*)-**5.45**

NOESY NMR 700MHz
Solvent: $CDCl_3$

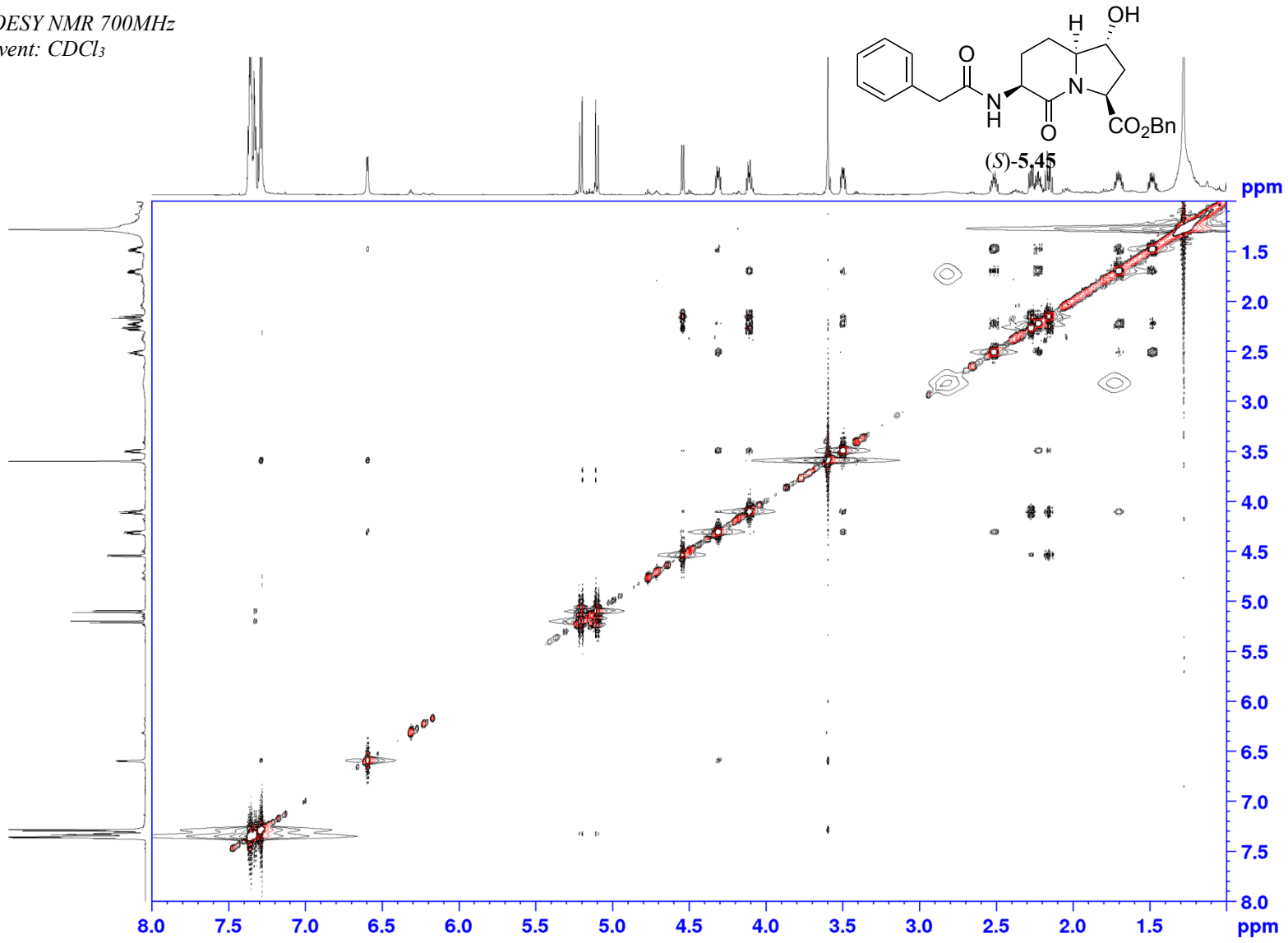

^{1}H NMR 500MHz
Solvent: CD_3OD

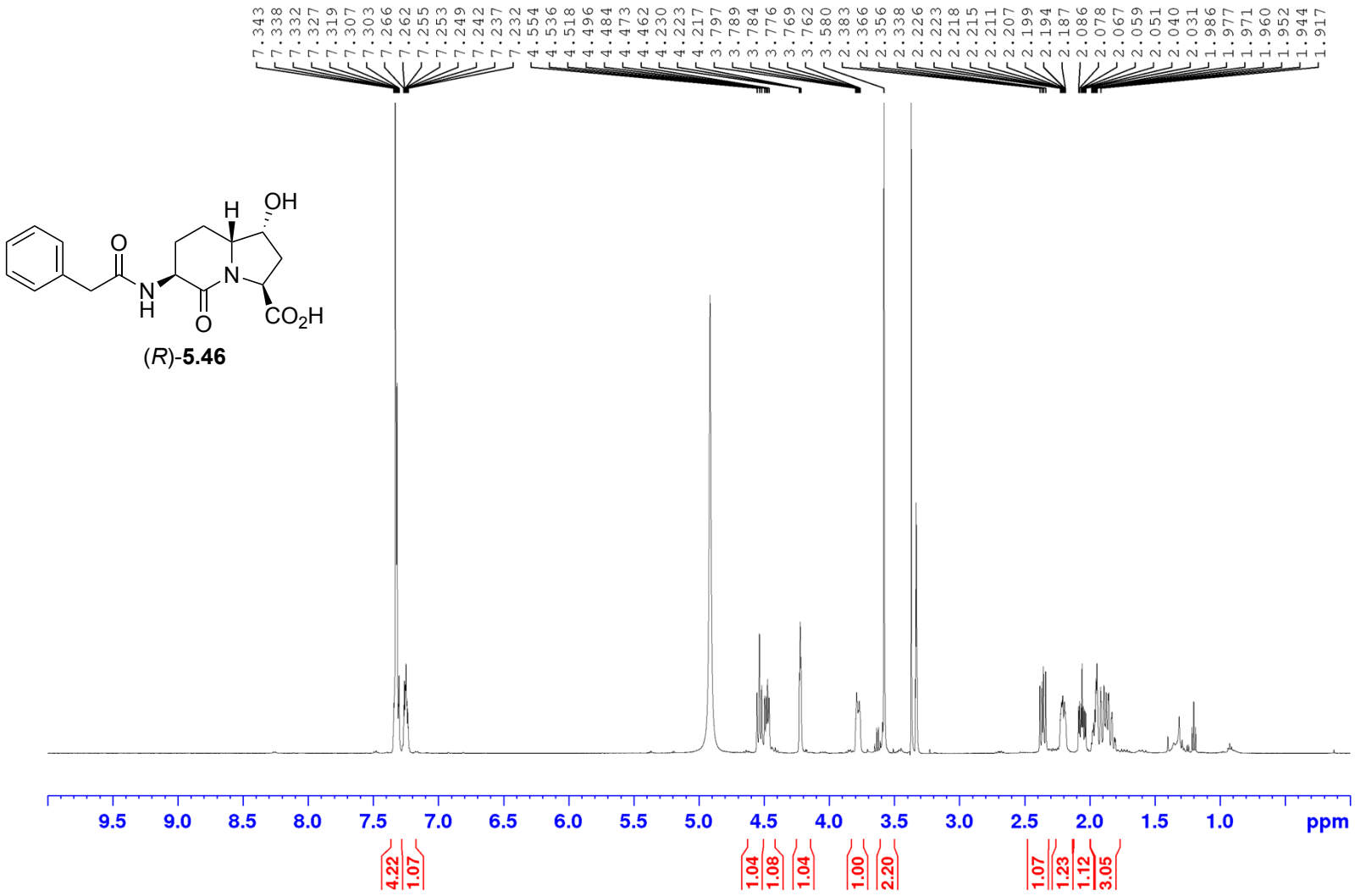

(*R*)-**5.46**

^{13}C NMR 500MHz
Solvent: CD_3OD

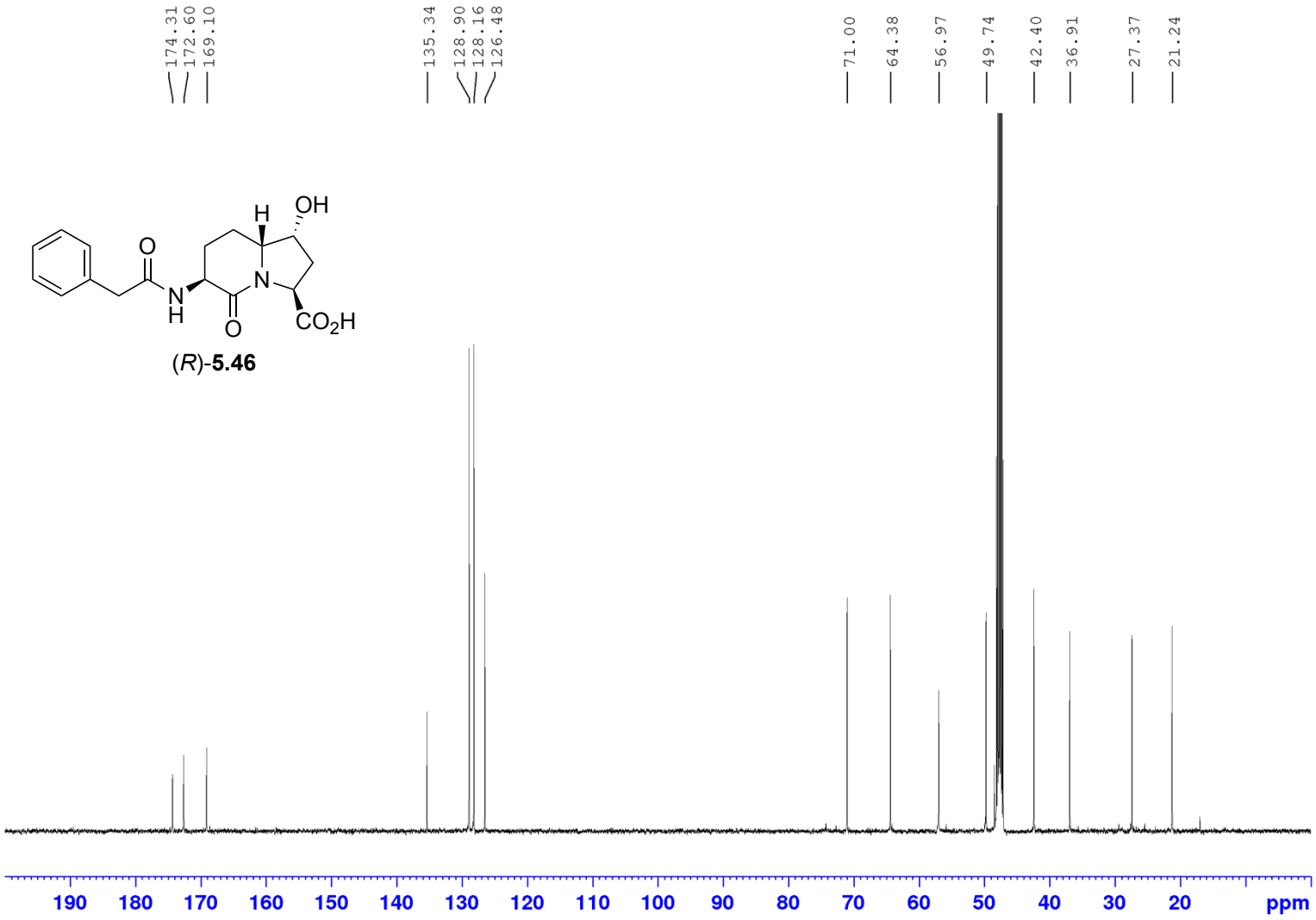

(*R*)-**5.46**

^1H NMR 500MHz
Solvent: $CDCl_3$

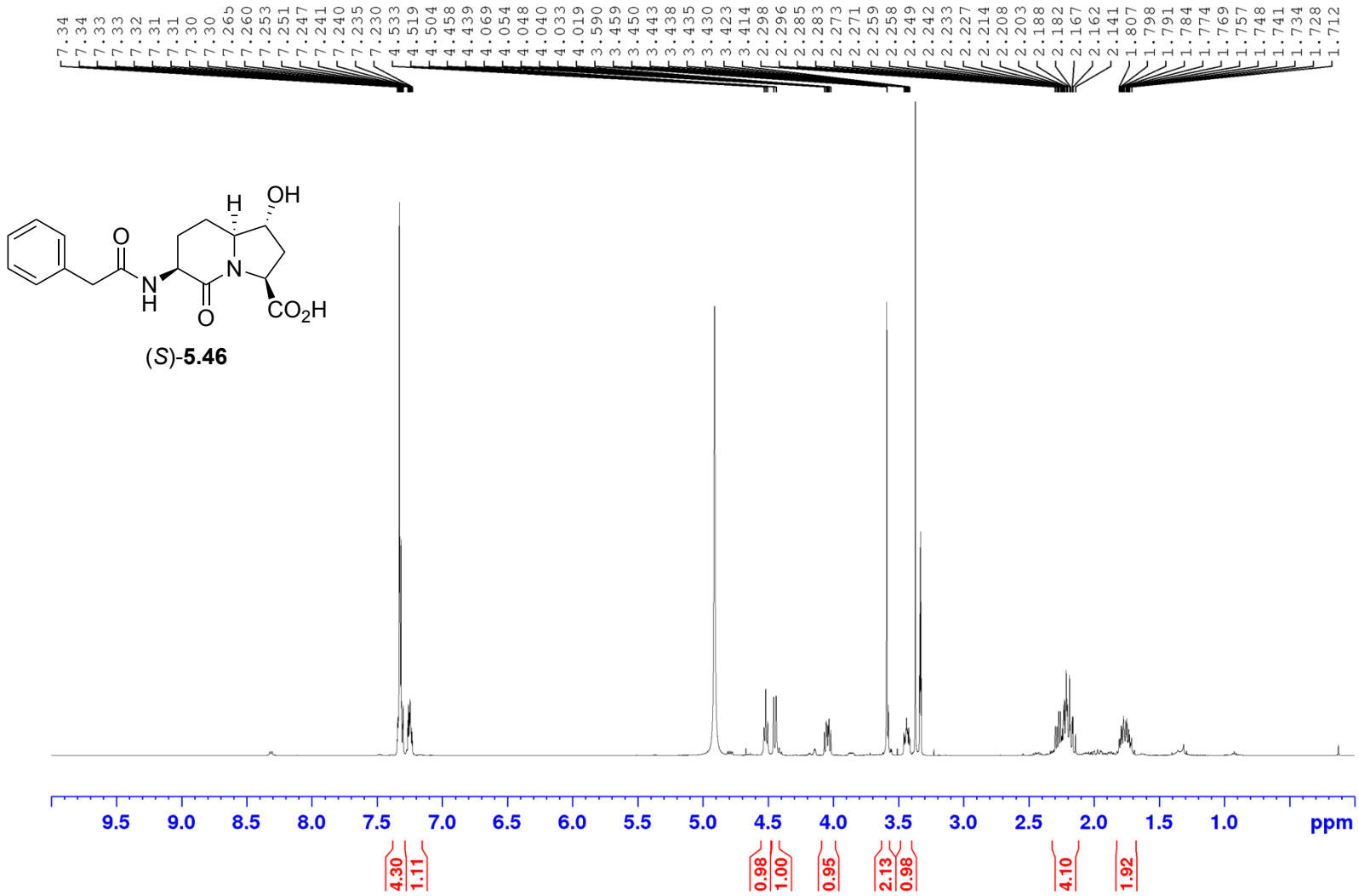

(*S*)-**5.46**

^{13}C NMR 125MHz
Solvent: $CDCl_3$

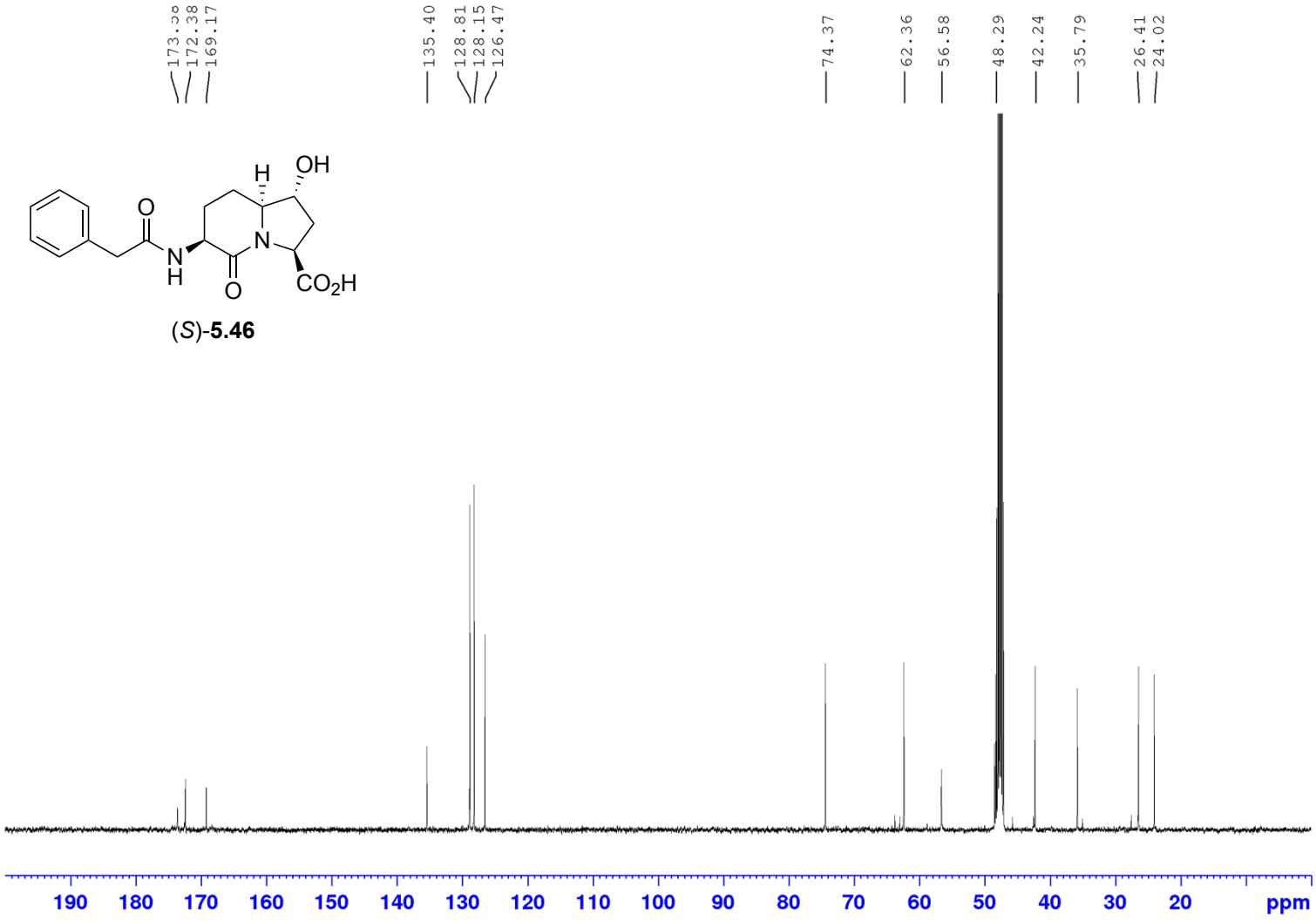

(*S*)-**5.46**

^1H NMR 700MHz
Solvent: $CDCl_3$

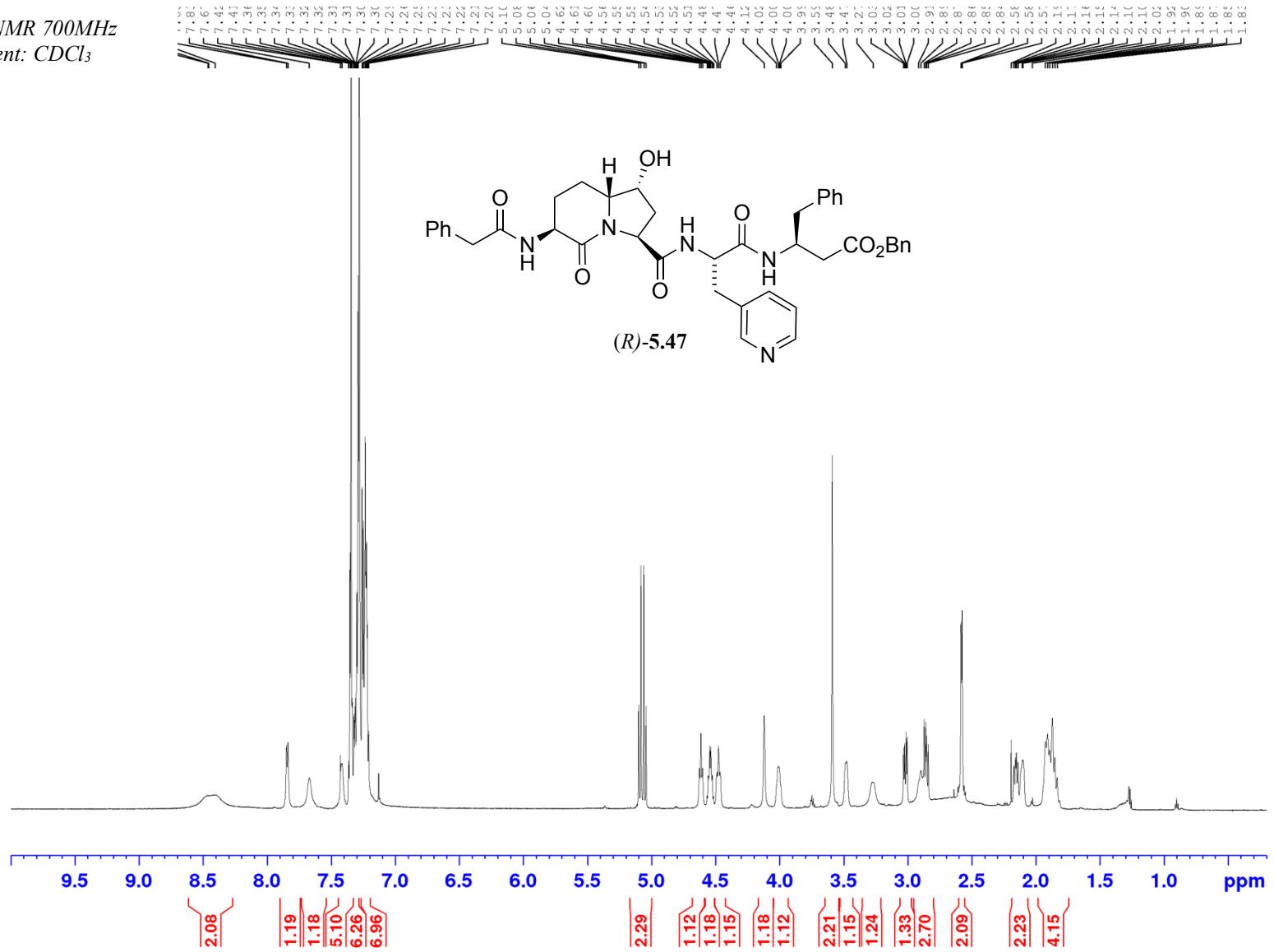

(*R*)-**5.47**

^{13}C NMR 175 MHz
Solvent: $CDCl_3$

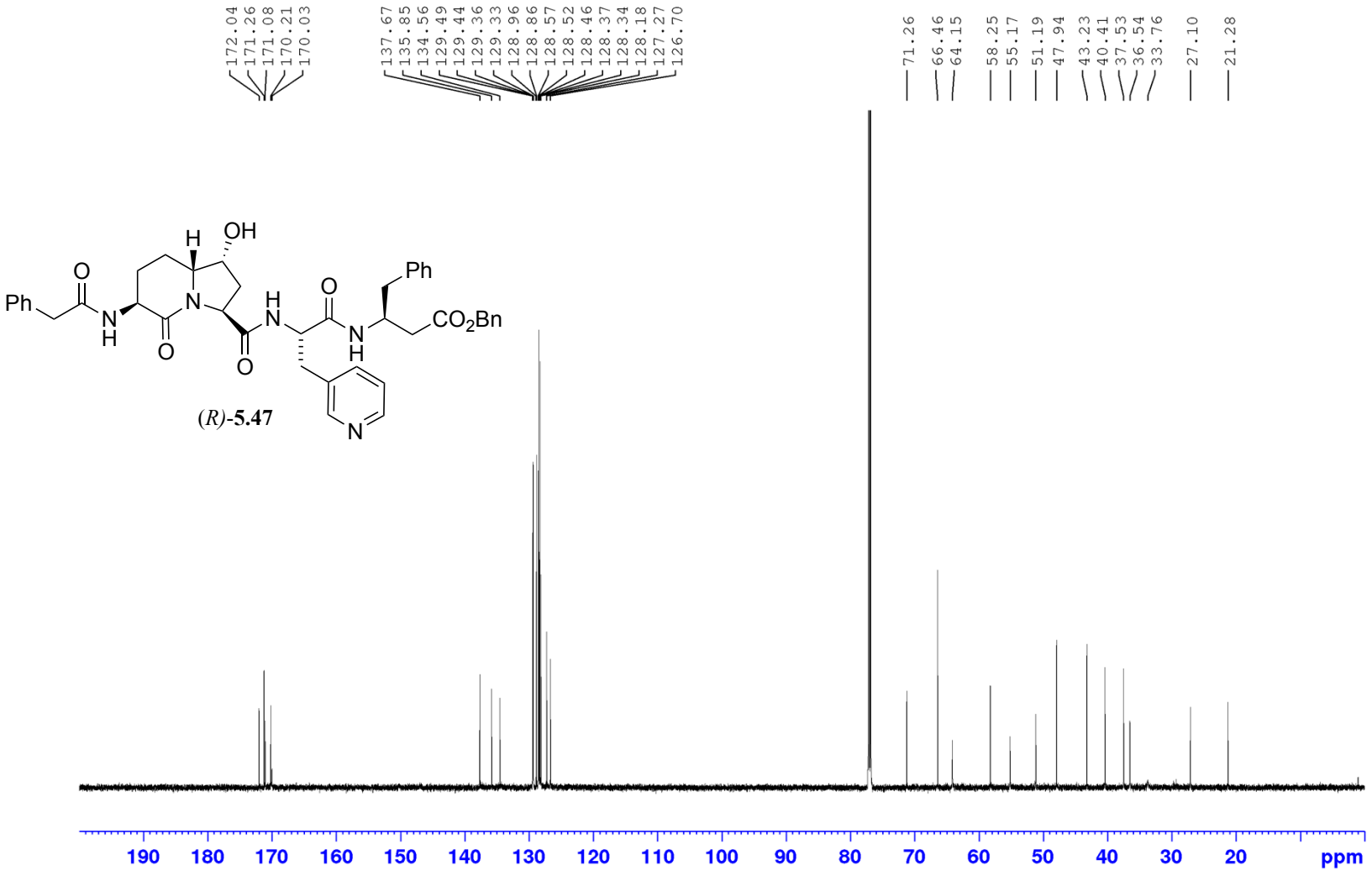

(*R*)-**5.47**

^{1}H NMR 700 MHz
Solvent: $CDCl_3$

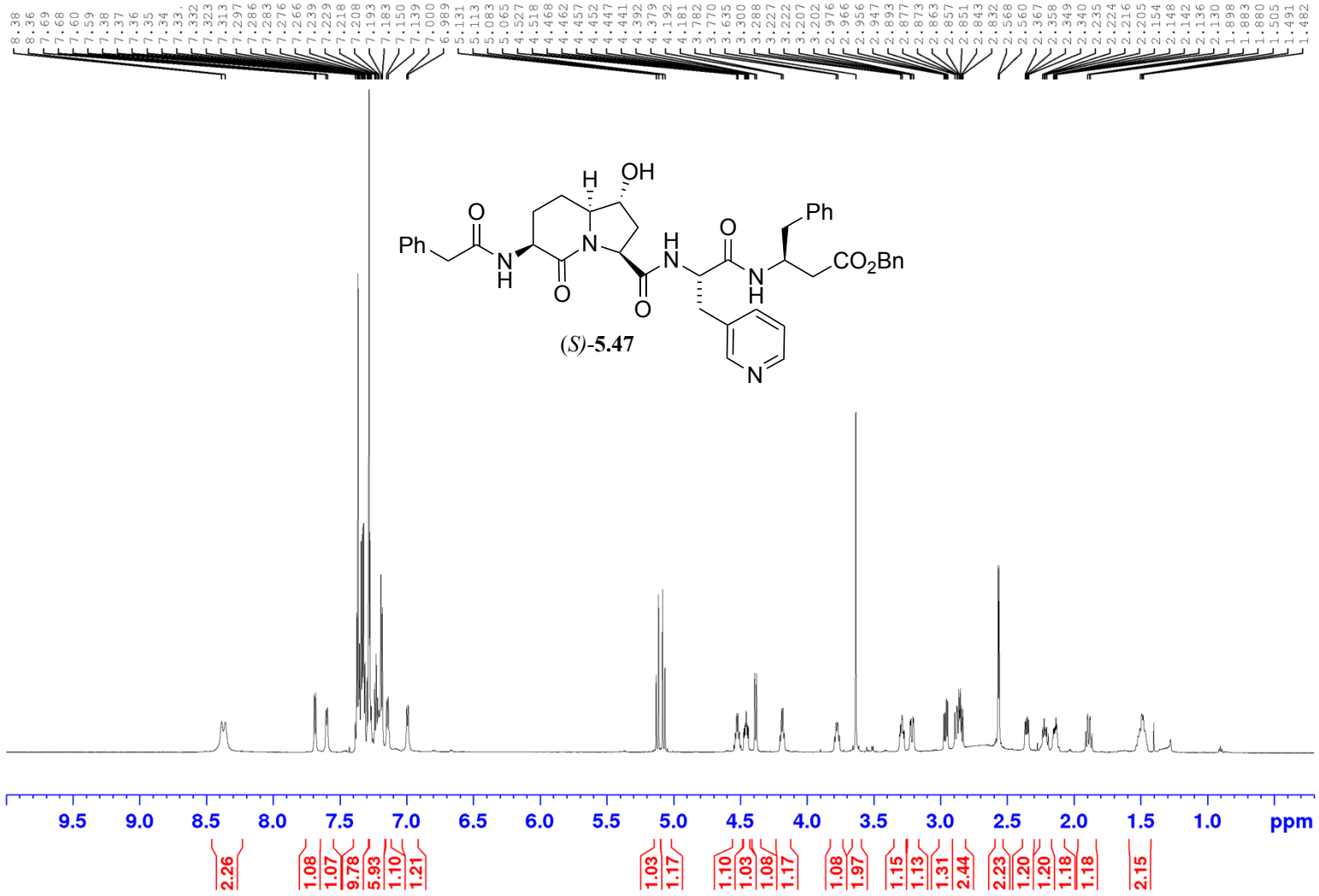

^{13}C NMR 175 MHz
Solvent: $CDCl_3$

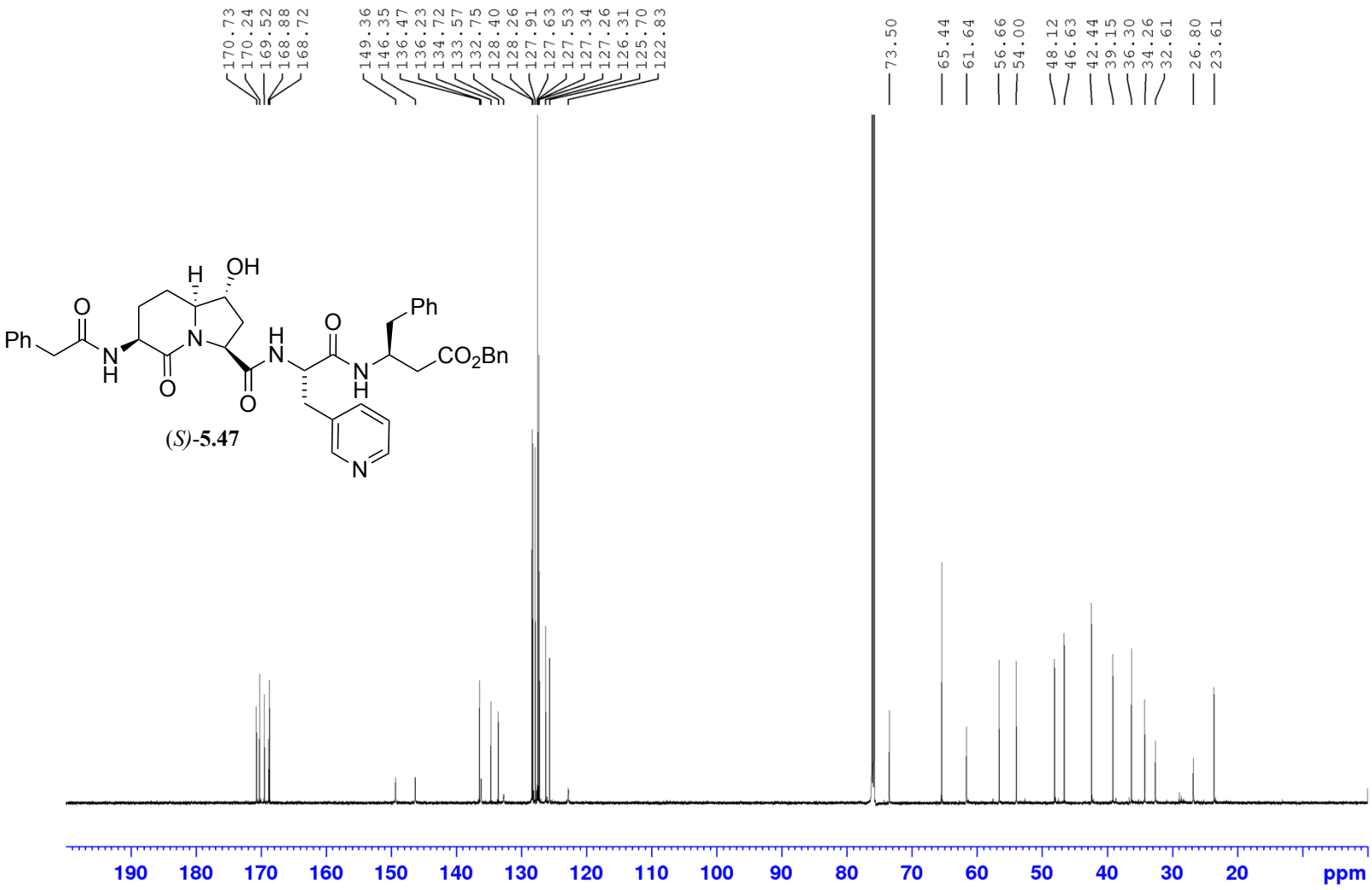

(*S*)-**5.47**

Ascertainment of purity by HPLC

Method F: Analytical HPLC, 50 to 90% MeOH [0.1% formic acid (FA)] in water (0.1% FA) over 14 min, flow rate of 0.5 mL/min on a on a Sunfire C18 analytical column (3.5 μm, 4.6 mm X 100 mm).

Method H: Analytical HPLC, 30 to 90% MeOH or MeCN[0.1% formic acid (FA)] in water (0.1% FA) over 14/15 min, flow rate of 0.5 mL/min on a on a Sunfire C18 analytical column (3.5 μm, 4.6 mm X 100 mm).

Method N: Analytical HPLC, 10 to 90% MeCN [0.1% formic acid (FA)] in water (0.1% FA) over 14 min, flow rate of 0.8 mL/min on a on XTerra ™ C18 column C18 (3.5 μm, 2.1 mm X 50mm)

Method O: Analytical HPLC, 30 to 95% MeOH [0.1% formic acid (FA)] in water (0.1% FA) over 14 min, flow rate of 0.8 mL/min on a on XTerra ™ C18 column C18 (3.5 μm, 2.1 mm X 50mm)

Method P: Analytical HPLC, 20 to 80% MeOH [0.1% formic acid (FA)] in water (0.1% FA) over 14 min, flow rate of 0.8 mL/min on a on XTerra ™ C18 column C18 (3.5 μm, 2.1 mm X 50mm)

Method H, *R*-**5.1**, Purity ≥ 96% (MeOH)

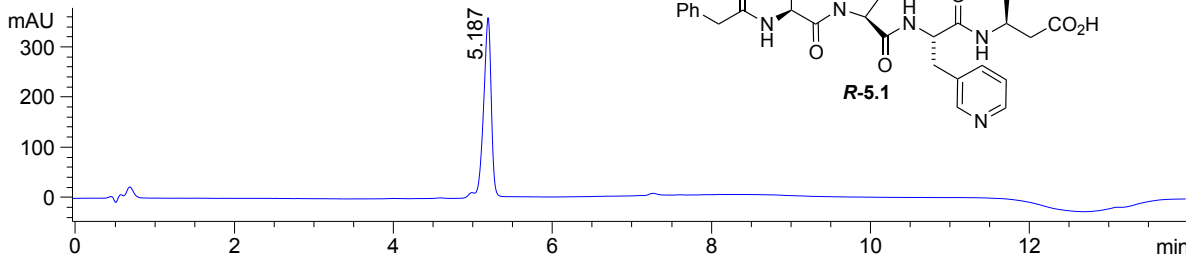

Method N, *R*-**1**, Purity ≥ 96% (ACN)

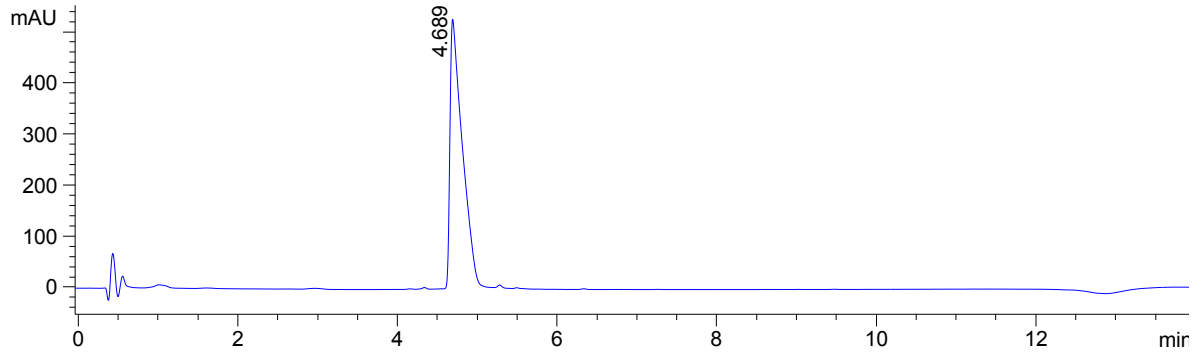

Method O, *S*-**5.1b**, Purity ≥ 96% (MeOH)-Major

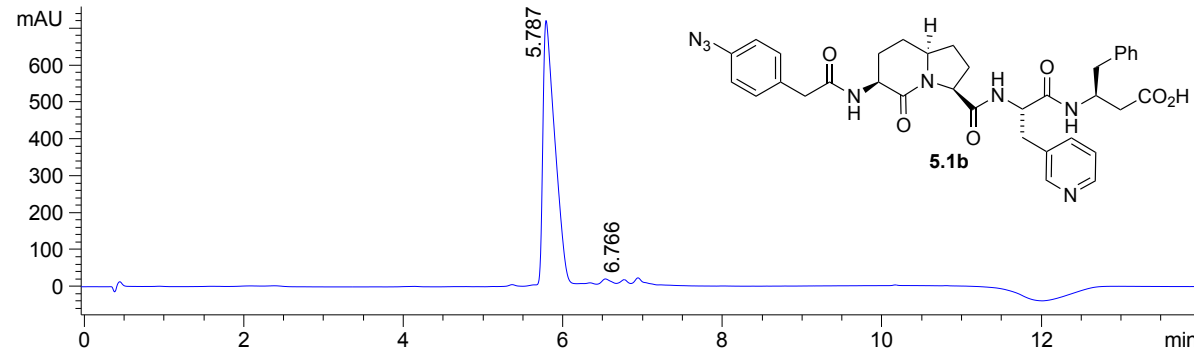

Method N, *S*-**5.1b**, Purity ≥ 96% (ACN)

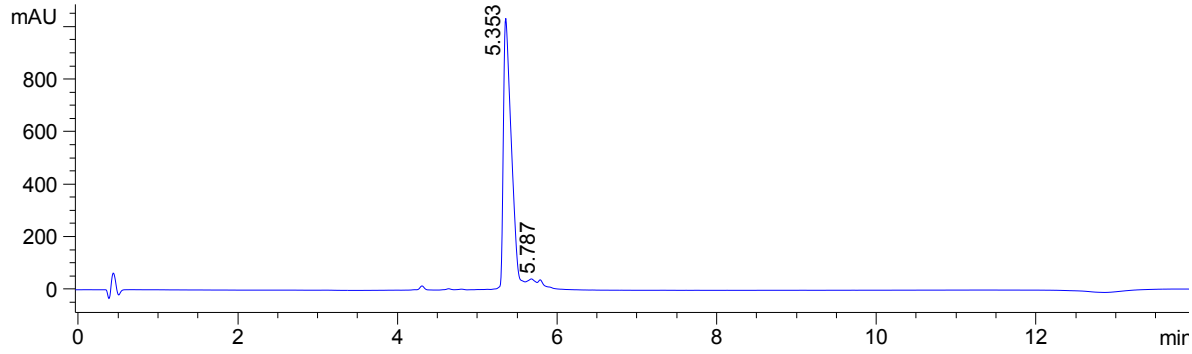

Method H, *S*-**5.1c**, Purity ≥ 96% (MeOH)

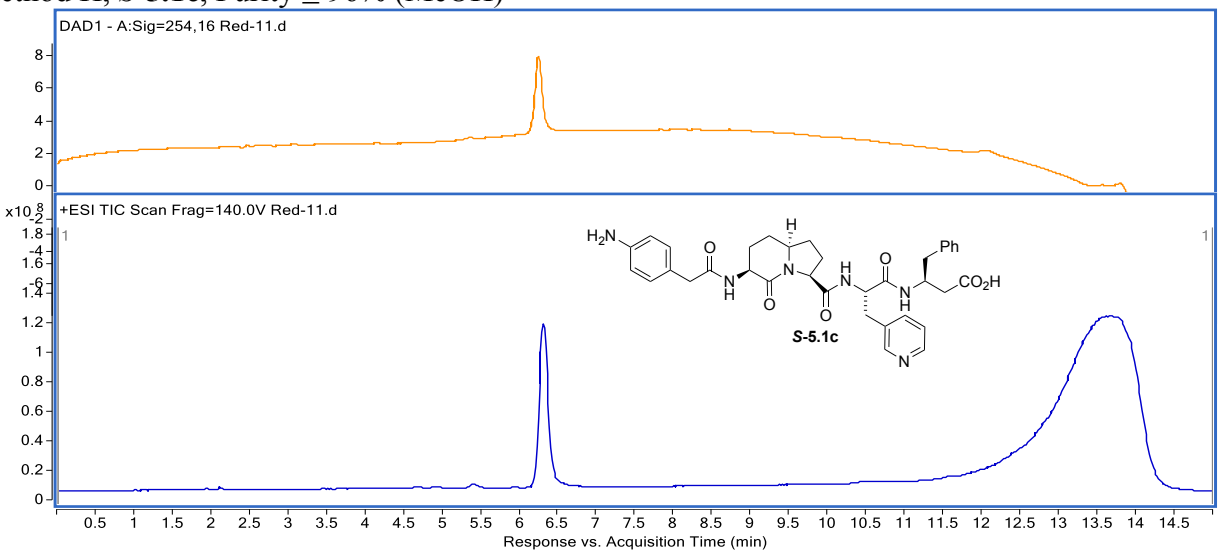

Method P, **5.5a**, Purity ≥ 96% (MeOH)

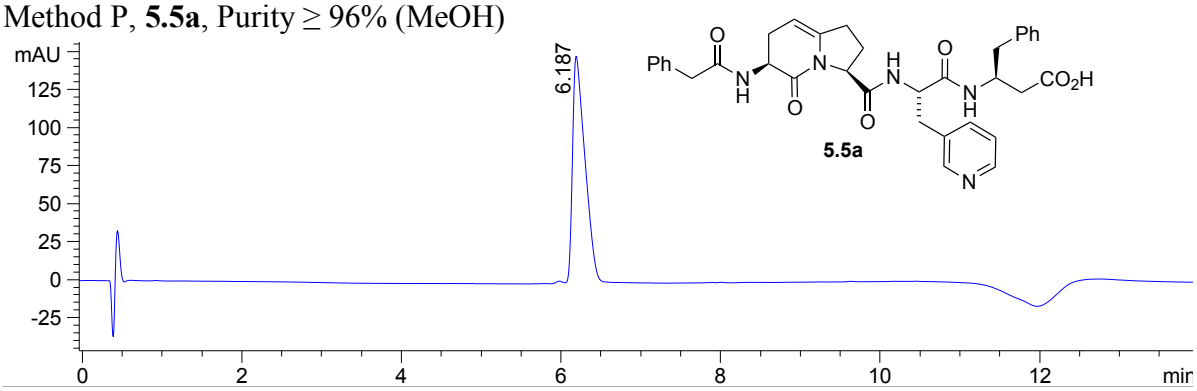

Method N, **5.5a**, Purity ≥ 96% (ACN)

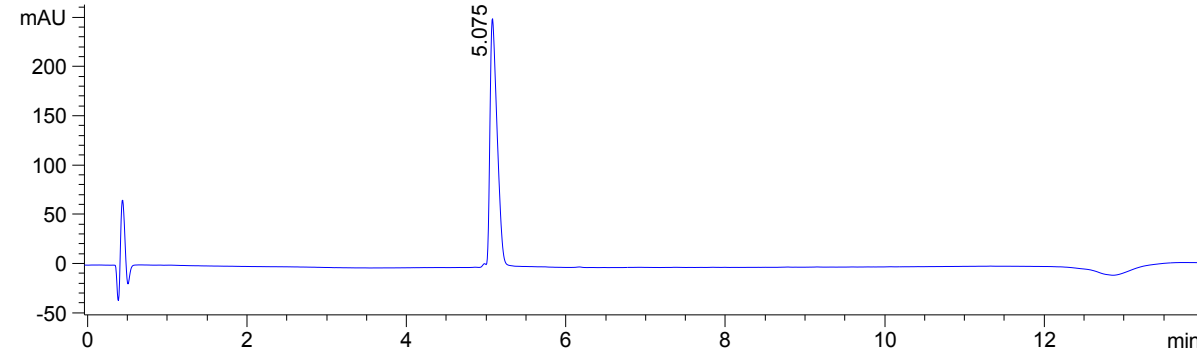

Method O, **5.5b**, Purity ≥ 96% (MeOH)

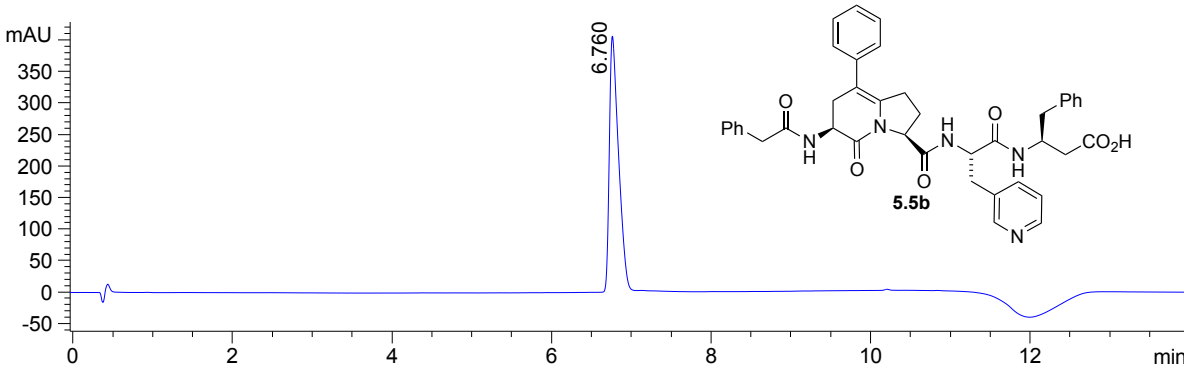

Method N, **5.5b**, Purity ≥ 96% (ACN)

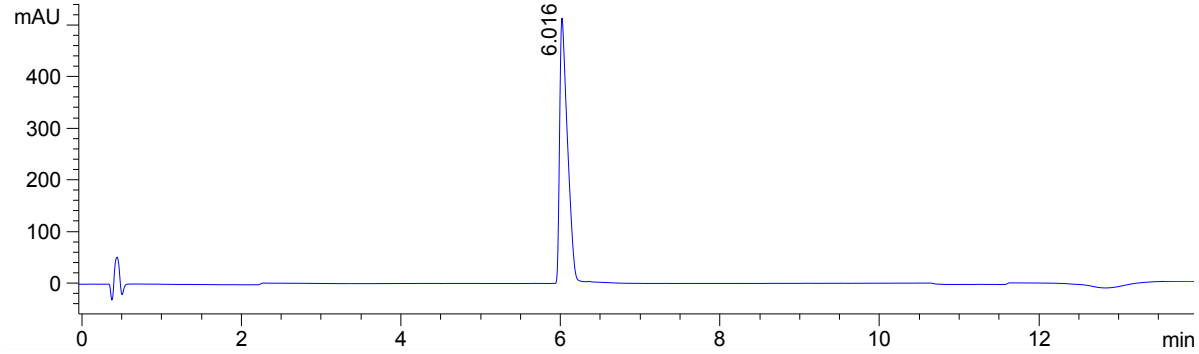

Method F, **5.5c**, Purity ≥ 96% (MeOH)

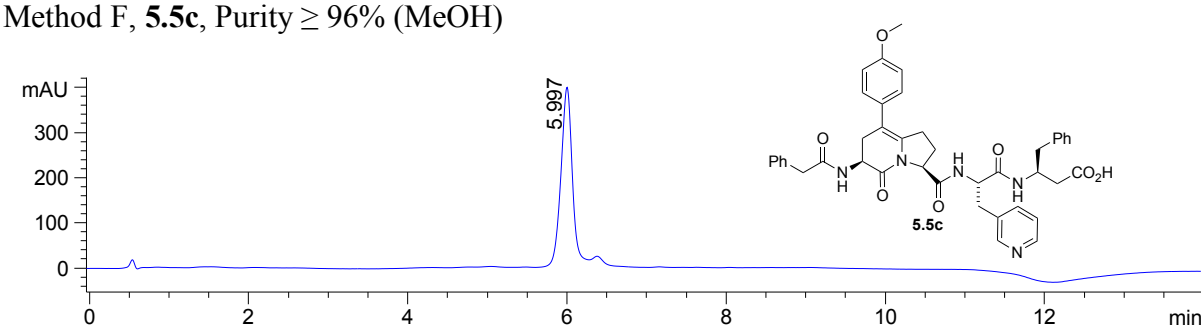

Method N, **5.5c**, Purity ≥ 96% (ACN)

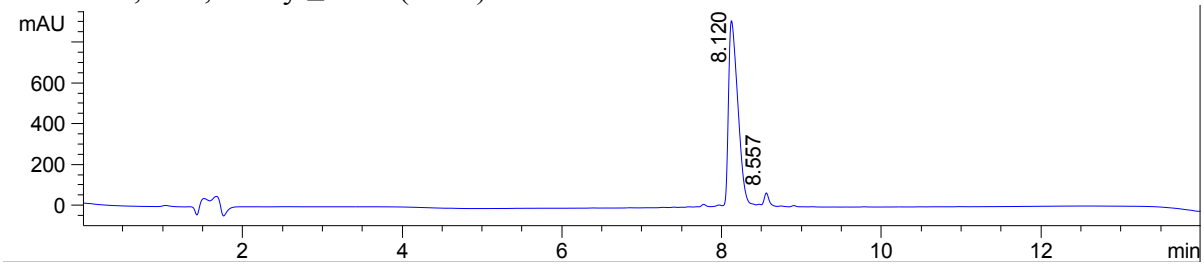

Method H, **5.5d**, Purity ≥ 96% (MeOH)

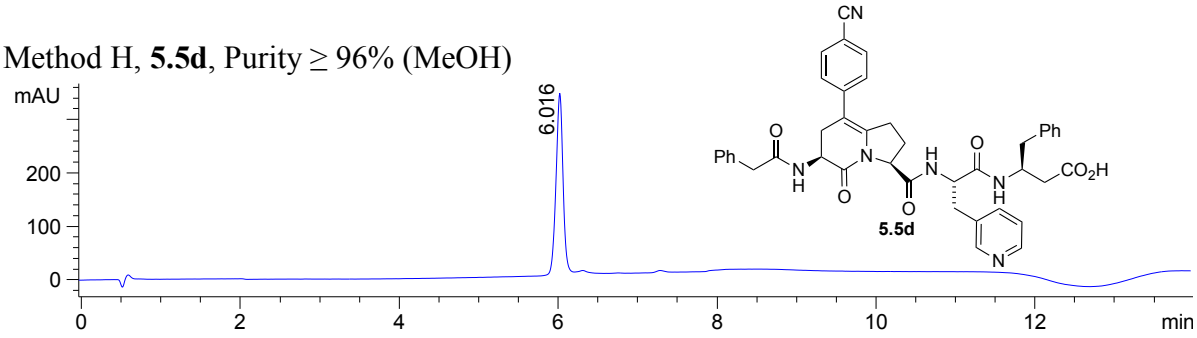

Method H, **5.5d** Purity ≥ 96% (ACN)

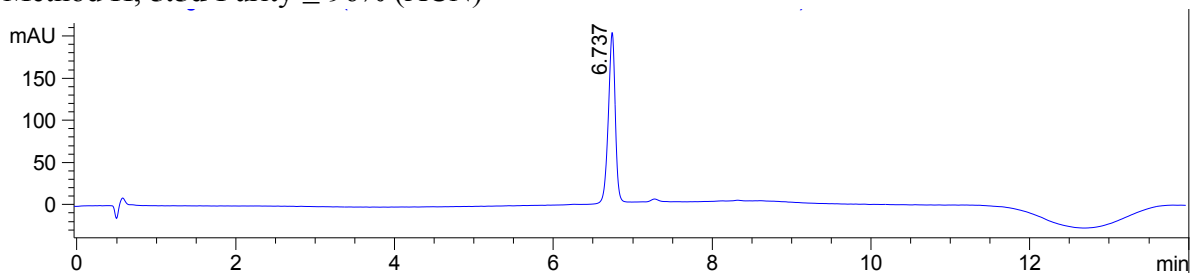

Method O, **5.5e**, Purity ≥ 96% (MeOH)

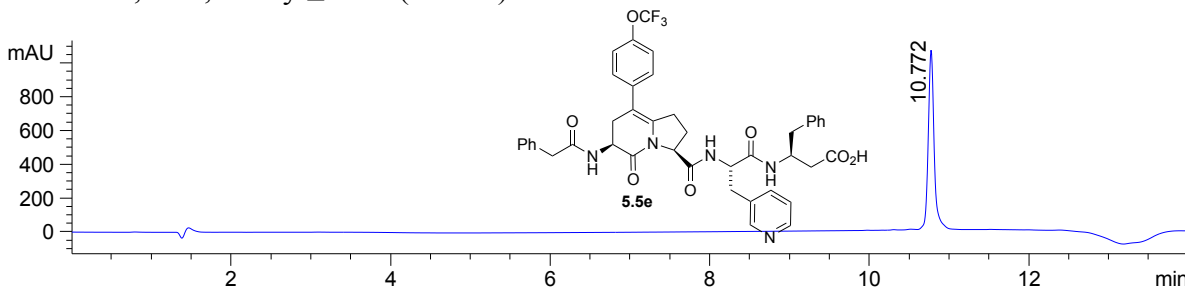

Method N, **5.5e**, Purity ≥ 96% (ACN)

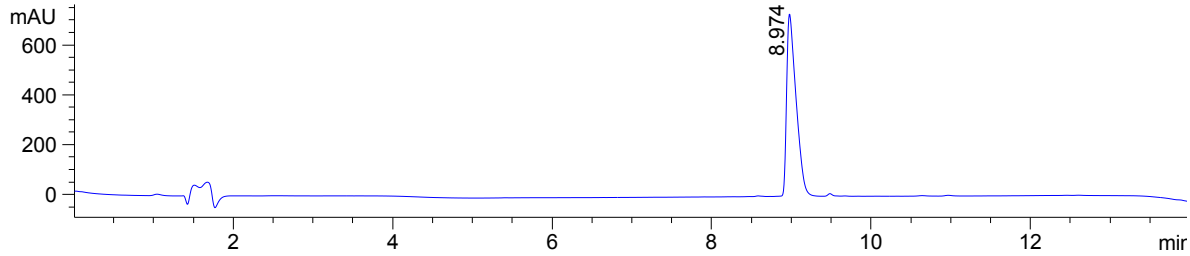

Method P, *R*-**5.10**, Purity ≥ 96% (MeOH)

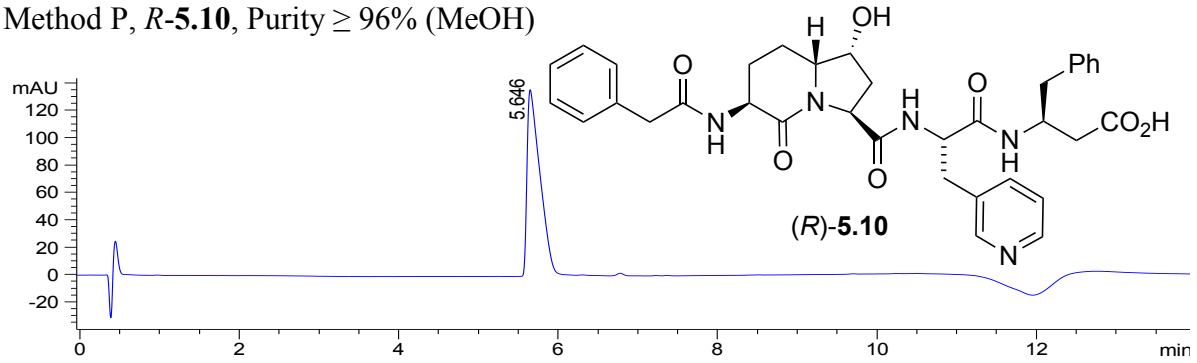

Method N, R-10, Purity ≥ 96% (ACN)

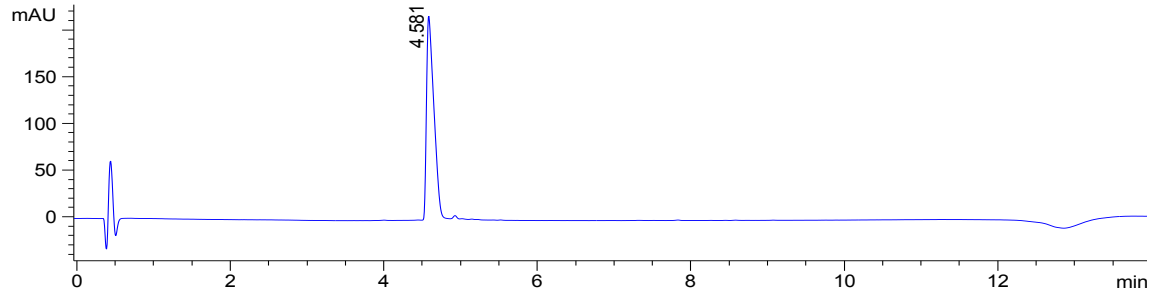

Method P, *S*-**5.10**, Purity ≥ 96% (MeOH)

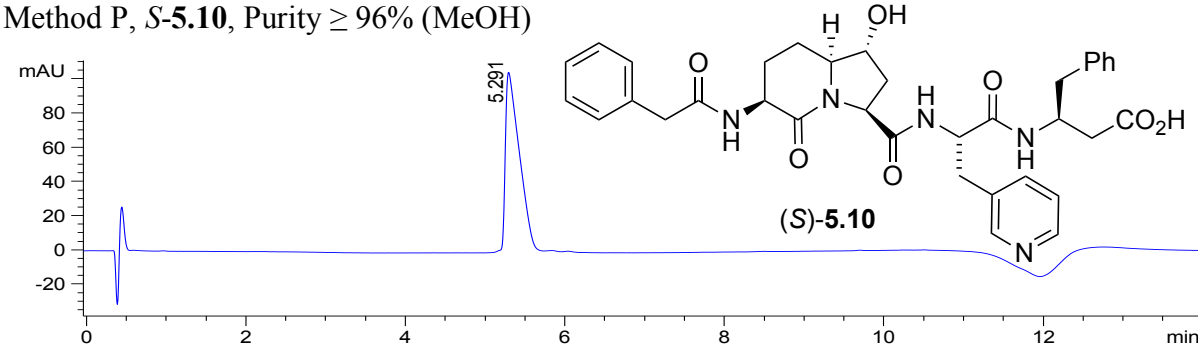

Method N, *S*-**5.10**, Purity ≥ 96% (ACN)